INTERNATIONAL DOCTORAL SCHOOL OF THE USC

Daniel
Marcos Atanes

PhD Thesis

# Ligand-controlled selective C–H borylations using Iridium catalysts

Santiago de Compostela, 2024

**Doctoral Programme in Chemical Science and Technology**

INTERNATIONAL DOCTORAL
SCHOOL OF THE USC

DOCTORAL THESIS

# LIGAND-CONTROLLED SELECTIVE C–H BORYLATIONS USING IRIDIUM CATALYSTS

Author

Daniel Marcos Atanes

Supervisor: José Luis Mascareñas Cid

Tutor: José Luis Mascareñas Cid

**PHD PROGRAMME IN CHEMICAL SCIENCE AND TECHNOLOGY**

SANTIAGO DE COMPOSTELA

2024

## Acknowledgements

This PhD thesis has been funded by the Spanish Ministry of Universities through the “Formación de Profesorado Universitario” program (FPU18/04495).

The Spanish Ministry of Universities also funded a predoctoral stay at UC Berkeley through the “Ayudas complementarias de movilidad destinadas a beneficiarios del programa de formación del profesorado universitario”. This stay was also funded by Fulbright Spain through a “Beca investigación Predoctoral Fulbright-Spain”.

This work has received financial support from Spanish grants (Grants PID2019-108624RB-I00, PID2022-137318OB-I00, SAF2016-76689-R funded by Agencia Estatal de investigación (AEI)), the Consellería de Cultura, Educación e Ordenación Universitaria (Grant ED431C 2017/19 and Grant ED431C 2021/25) the Instituto de Salud Carlos III (Grant IHRC22/00009) and the European Union (ERC-2103-AdG 340055, European Regional Development Fund-ERDF corresponding to the multiannual financial framework 2014-2020).

USC
UNIVERSIDADE DE SANTIAGO DE COMPOSTELA

Table of contents

USC
UNIVERSIDADE
DE SANTIAGO
DE COMPOSTELA

*1 Abbreviations and acronyms ..... 11*

*2 Resumo ..... 15*

*3 Summary ..... 27*

*4 Introduction ..... 37*

**4.1 Organic chemistry ..... 39**

**4.2 Organometallic catalysis ..... 40**

4.2.1 Historical overview ..... 40
4.2.2 Catalysis in organic chemistry ..... 42
4.2.3 Transition metal complexes in catalysis ..... 44
4.2.4 Cornerstone metal-catalyzed reactions in modern synthesis ..... 46

**4.3 Transition metal-promoted C–H functionalizations ..... 49**

4.3.1 Introduction to C–H functionalization ..... 49
4.3.2 Initial developments ..... 50
4.3.3 Mechanisms of transition metal-promoted C–H activations ..... 52

**4.4 Synthetic relevance of organoboron compounds ..... 54**

**4.5 Borylation of C–H bonds, preliminary examples ..... 55**

**4.6 Iridium-catalyzed C–H borylations of aromatic systems ..... 57**

4.6.1 Initial results, regioselectivity and mechanistic rational ..... 57
4.6.2 Monodentate ligands (L) ..... 60
4.6.3 Hemilabile ligands (L–L') ..... 63
4.6.4 Bidentate monoanionic ligands (L–X) ..... 66
4.6.5 Supramolecular control of the regioselectivity by using designed bidentate L–L ligands ..... 70

**4.7 Iridium-catalyzed borylations of alkyl C–H bonds ..... 86**

4.7.1 Bidentate neutral ligands (L–L) ..... 86
4.7.2 Monodentate ligands (L) ..... 89
4.7.3 Monoanionic bidentate ligands (L–X) ..... 90
4.7.4 Pincer L–L–X ligands ..... 93

*5 General objectives ..... 95*

*6 Methodology ..... 99*

**6.1 General experimental methodology ..... 101**

**6.2 General computational methodology ..... 103**

*7 Results and Discussion ..... 107*

**7.1 Towards the borylation of distal aromatic rings using ligand-directed supramolecular interactions ..... 109**

7.1.1 State of the art ..... 111
7.1.2 Objectives ..... 111
7.1.3 Results and discussion ..... 111
7.1.4 Conclusions ..... 124

**7.2 Ir-catalyzed *ortho*-borylation of benzamides using designed bipyridine ligands ..... 125**

7.2.1 Introduction ..... 127

USC UNIVERSIDADE DE SANTIAGO DE COMPOSTELA

7.2.2 Objective ..... 133
7.2.3 Results and discussion ..... 133
7.2.4 Conclusions ..... 166

**7.3 Ir-catalyzed selective borylation of $Csp^3$–H bonds in methylamides ..... 169**
7.3.1 Introduction ..... 171
7.3.2 Objectives ..... 172
7.3.3 Results and discussion ..... 172
7.3.4 Conclusions ..... 199

***8 Conclusions ..... 201***

***9 Bibliography ..... 205***

***10 Experimental section ..... 209***

**10.1 Experimental procedures for section *7.1*. ..... 211**
10.1.1 Synthesis of substrates ..... 211
10.1.2 Ligand synthesis ..... 213
10.1.3 General borylation procedure ..... 232
10.1.4 Synthesis of borylated products ..... 233

**10.2 Experimental procedures for section *7.2* ..... 237**
10.2.1 Kinetic studies at different temperatures ..... 237
10.2.2 Eyring plots and activation *para*meters ..... 244
10.2.3 NMR and HRMS studies of $[Ir(COD)Cl]_2$ and L28 complexes ..... 247
10.2.4 Kinetic Isotopic Effects (KIE) ..... 249
10.2.5 Synthesis of substrates ..... 251
10.2.6 Ligand synthesis ..... 279
10.2.7 General Procedure for *ortho*-Borylation ..... 297
10.2.8 Pre*para*tion of fungicide 41 ..... 319
10.2.9 Crystallographic data ..... 321

**10.3 Computational analysis for section *7.2* ..... 324**
10.3.1 Calculated structures for borylation pre-catalytic species ..... 324
10.3.2 Calculated structures for benzamide borylation with Ir(I) catalysts ..... 325
10.3.3 Calculated structures for benzamide borylation with ligand bipy and Ir(III) catalyst ..... 326
10.3.4 Calculated structures for benzamide borylation with ligand L27 and Ir(III) catalyst ..... 328
10.3.5 Calculated structures for benzamide borylation with ligand L46 and Ir(III) catalyst ..... 329
10.3.6 Calculated structures for benzamide borylation with ligand L47 and Ir(III) catalyst ..... 331
10.3.7 Quantum theory of atoms in molecules (QTAIM) analysis ..... 332
10.3.8 Natural Bond Orbital (NBO) analysis ..... 334
10.3.9 Energy Decomposition Analysis (EDA) ..... 335
10.3.10 Enthalpy-entropy compensation including quasiharmonic approximations to enthalpy and entropy ..... 336

**10.4 Experimental procedures for section *7.3* ..... 337**
10.4.1 Kinetic Isotope effects (KIE) ..... 337
10.4.2 Synthesis of substrates ..... 340
10.4.3 Ligand synthesis ..... 356
10.4.4 General procedure for N-Me borylation ..... 358

**10.5 Computational analysis for section *7.3* ..... 373**
10.5.1 Non-Covalent Interactions (NCI) analysis ..... 373
10.5.2 Energy Decomposition Analysis (EDA) ..... 374
10.5.3 Calculated structures for the borylation of 44a with bipy as ligand ..... 375
10.5.4 Calculated structures for the borylation of 44a with L27 as ligand ..... 376
10.5.5 Calculated structures for the borylation of 44a with L28 as ligand ..... 377

10.5.6 Minimum energy pathway (MEP) for *N,N*-diethylpropionamide (**44u**) borylation ..... 378
10.5.7 Minimum energy pathway (MEP) for *N,N*-dimethylisobutyramide (**44f**) borylation (N-$CH_3$ vs C-$CH_3$ positions) ..... 379
10.5.8 Minimum energy pathway (MEP) for *N,N*-dimethylhexylamide (**44a**) borylation following a rollover cyclometalation mechanism ..... 382
10.5.9 Calculated structures for borylation pre-catalytic species ..... 384

***11 Annexes ..... 387***

**11.1 Annex I: Selected NMR spectra ..... 389**
11.1.1 Selected spectra for molecules in section 7.1 ..... 391
11.1.2 Selected spectra for molecules in section 7.2 ..... 419
11.1.3 Selected spectra for molecules in section 7.3 ..... 493

**11.2 Annex II: Complete list of NMR spectra ..... 525**

**11.3 Annex III: Selected GC-MS chromatograms ..... 529**
11.3.1 Selected GC-MS chromatograms for reactions in section 7.1 ..... 531
11.3.2 Selected GC-MS chromatograms for reactions in section 7.2 ..... 535
11.3.3 Selected GC-MS chromatograms for reactions in section 7.3 ..... 537

**11.4 Annex IV: Exploring 3D models of relevant calculated structures ..... 539**

**11.5 Annex V: Relevant calculated structures ..... 543**

**11.6 Annex VI: List of publications ..... 547**

**11.7 Annex VII: Copyright permission ..... 551**

USC UNIVERSIDADE DE SANTIAGO DE COMPOSTELA

# 1 Abbreviations and acronyms

USC
UNIVERSIDADE
DE SANTIAGO
DE COMPOSTELA

**Ac:** Acetate
**Acac**: Acetylacetonate
**Ad:** Adamantyl
**Ar:** Aromatic ring
**Bcat:** Boron catecholate
**BCP**: Bond critical point
**BDE:** Bond dissociation energy
**Beg:** Boron ethyleneglycolate
**Bipy**: 2,2'-bipyridine
**Boc:** *tert*-Butyloxycarbonyl
**BOX**: bis-oxazoline
**Bpin**: Boron pinacolate
**brs:** Broad singlet
**Bu:** Butyl
**Bz:** Benzoyl
**cat:** Catalytic amount
**CBL**: chiral bidentate ligands
**CMD:** Concerted metalation-deprotonation
**COD:** 1,5-Cyclooctadiene
**COE**: Cyclooctene
**Cp**: cyclopentadienyl
**Cp***: pentamethylcyclopentadienyl
**CPME**: cyclopentylmethylether
**Cy:** Cyclohexyl
**d:** Doublet
**DCE**: 1,2-Dichloroethane
**DCM**: Dichloromethane
**dr:** Diastereoisomeric ratio
**DEPT**: Distortionless Enhancement by Polarization Transfer
**DFT**: Density functional theory
**DG:** Directing group
**DME**: Dimethoxyethane
**DMF**: *N*,*N*-Dimethylformamide
**DMSO**: Dimethyl sulfoxide
**dppe**: 1,4-Bis(diphenylphosphino)ethane
**dppf:** 1,1'-Ferrocenediyl-bis(diphenylphosphine)
**dtbpy:** 4,4'-Di-*tert*-butyl-2,2'-dipyridyl
**E:** Electrophile
**Ea**: Activation energy
**ee**: Enantiomeric excess
**equiv.**: Equivalent
**er**: Enantiomeric ratio
**ESI**: Electrospray
**Et**: Ethyl
**e⁻:** electron
**GC/MS**: Gas chromatography–mass spectrometry
**HFIP**: Hexafluoroisopropanol
**hυ:** light
**HMBC**: Heteronuclear Multiple Bond Correlation
**HRMS**: High resolution mass spectrometry
**HSQC**: Heteronuclear Single Quantum Correlation
**Ind:** Indenyl
**$^{i}$Pr**: Isopropyl
**J**: Coupling constant
**KIE:** Kinetic isotopic effect
**LA:** Lewis acid
**m:** Multiplet
**Me**: Methyl
**Mes**: Mesitylene
**MHz**: Megahertzs
**MOM:** Methoxymethyl ether
**$^{n}$Bu**: n-Butyl
**NCI**: Non-covalent interaction
**$^{n}$Hex**: n-Hexyl
**NMP**: N-methyl-2-pyrrolidone
**NMR**: Nuclear magnetic resonance
**Nu**: Nucleophile
**OA:** Oxidative addition
**Ph**: Phenyl
**phen**: 1,10-phenanthroline
**ppm:** parts per million

USC DE SANTIAGO

**PyOX**: Pyridine oxazoline
**q**: Quadruplet
**RDS**: Rate-determining step
**RE**: Reductive elimination
**rt**: Room temperature
**s**: Singlet
**t**: Triplet
**TBABr**: tetrabutyl ammonium bromide
**TBACl**: tetrabutyl ammonium chloride
**TBAI:** tetrabutyl ammonium iodide
**$^t$Bu:** *tert*-Butyl
**Tf:** Triflate
**THF**: Tetrahydrofuran
**TM**: Transition metal
**tmphen:** 3,4,7,8-Tetramethyl-1,10-phenanthroline
**TMS**: Trimethylsilyl
**TS:** Transition state

# 2 Resumo

USC
UNIVERSIDADE
DE SANTIAGO
DE COMPOSTELA

A química orgánica, pedra angular do mundo científico, xoga un papel fundamental en varios ámbitos da actividade humana. Como campo que se centra na síntese e transformación de moléculas orgánicas, revolucionou as industrias farmacéutica, agrícola e de materiais. A súa viaxe histórica é tan fascinante como indispensables as súas aplicacións modernas. A química orgánica non só se ocupa da creación de moléculas complexas senón que tamén pretende fomentar a sustentabilidade e a eficiencia nos procesos químicos.

Na síntese orgánica actual, a sustentabilidade é a principal prioridade. Os químicos están a desenvolver métodos máis ecolóxicos para reducir os residuos, conservar enerxía e aproveitar os recursos renovables. As reaccións catalíticas, especialmente as que implican complexos de metais de transición, están no centro destes avances. Os metais de transición, coas súas estruturas electrónicas únicas, permiten unha gama diversa de mecanismos organometálicos que son esenciais para a transformación eficiente e precisa das moléculas orgánicas. Por exemplo, as reaccións de acoplamento cruzado revolucionaron a síntese orgánica ao formar enlaces carbono-carbono e carbono-heteroátomo.

Os ligandos xogan un papel fundamental na modulación do comportamento dos catalizadores de metais de transición. Ao modificar meticulosamente o ambiente electrónico e estérico do centro metálico, os ligandos poden mellorar a reactividade, a selectividade e aumentar a estabilidade do sistema catalítico. Isto levou a avances significativos na eficiencia catalítica, o que permitiu aos químicos lograr un control preciso dos procesos sintéticos e resultou particularmente importante na síntese de moléculas complexas onde acadar altos niveis de selectividade adoita ser un reto crítico.

Outro descubrimento transformador na química orgánica moderna é o concepto de activación C–H. Os métodos sintéticos tradicionais adoitan requirir substratos pre-funcionalizados, engadindo pasos e residuos ao proceso global. Pola contra, a activación e funcionalización de enlaces C–H permite axilizar as vías sintéticas e reducir os residuos. Este enfoque non só simplifica a síntese de moléculas complexas, senón que tamén se aliña cos principios da química verde ao mellorar a economía global do átomo e a sustentabilidade dos procesos químicos.

A viaxe da activación C–H comezou a mediados do século XX, cos primeiros exemplos que mostraban transformacións estequiométricas empregando metais de transición. O traballo innovador de Shilov na década de 1960, sentou as bases para a funcionalización catalítica de enlaces C–H. Estudos posteriores, especialmente os de Bergman e Graham, avanzaron aínda máis o campo ao estudar aspectos cruciais do mecanismo de reacción, particularmente no contexto dos sistemas baseados en iridio. Estes esforzos culminaron no desenvolvemento de procesos catalíticos altamente

USC UNIVERSIDADE DE SANTIAGO DE COMPOSTELA

eficientes que se converteron en métodos fundamentais para a síntese orgánica moderna.

Unha das aplicacións máis empregadas da activación C–H é a borilación selectiva de sistemas aromáticos promovida por metais. Esta reacción permite a introdución de grupos de boro na posición menos obstaculizada de aneis aromáticos, creando intermediarios versátiles que poden ser funcionalizados aínda máis para construír estruturas moleculares complexas. A utilidade dos compostos que conteñen boro esténdese por varios campos, incluíndo a química medicinal, a ciencia dos materiais e os agroquímicos, facendo da borilación C–H unha ferramenta crítica no arsenal dos químicos sintéticos.

A reacción foi desenvolvida principalmente polo grupo do profesor John Hartwig e implica o uso dun precatalizador de Ir (normalmente $[Ir(OMe)(COD)]_2$ ou $[Ir(COD)Cl]_2$), $B_2pin_2$ como fonte de boro e unha 2,2'-bipiridina como ligando. Usando este sistema catalítico, o grupo de Hartwig demostrou con éxito a versatilidade desta reacción borilando unha ampla gama de arenos e heteroarenos cunha excelente eficiencia.

Non obstante, aínda que a reacción mostrou unha notable eficiencia, controlar a rexioselectividade resulta un importante reto. Os efectos estéricos do substrato dominaron a reacción, observándose o produto borilado na posición menos impedida estéricamente. Desde os artigos iniciais sobre a reacción de borilación C–H, numerosos grupos deseñaron ligandos con estruturas diversas para intentar acadar un control máis preciso sobre a rexioselectividade desta reacción. Varios grupos desenvolveron ligandos que permiten a coordinación dun grupo director do substrato e guían a reacción de borilación cara á posición *orto* deses grupos directores. Estes ligandos pódense dividir principalmente en tres categorías: ligandos monodentados (L), ligandos hemilábiles (L–L') ou ligandos monoaniónicos bidentados (L–X). Ademais, outros grupos desenvolveron ligandos para borilar selectivamente substratos aromáticos de maneira selectiva. Estes enfoques adoitan implicar o deseño de ligandos bifuncionais cun núcleo de 2,2'-bipiridina que se coordina co metal e un grupo de recoñecemento supramolecular que interactúa cun grupo funcional do substrato.

Nesta tese de doutoramento, describimos os nosos esforzos para activar de forma rexioselectiva enlaces C–H distais. Para abordar este desafío, propuxemos unha estratexia que emprega ligandos bifuncionais baseados en bipiridina equipados con estruturas que permitan establecer enlace de hidróxeno. O obxectivo central era deseñar ligandos que puidesen dirixir o catalizador de iridio cara ás posicións distais dos aneis aromáticos, permitindo a activación selectiva de enlaces C–H en sitios doutro xeito inaccesibles. A diferenza dos enfoques convencionais que dependen principalmente de grupos directores para lograr a selectividade, esta estratexia aproveita as interaccións non covalentes, especialmente os enlaces de hidróxeno, para controlar a

rexioselectividade. Ao empregar interaccións supramoleculares, este método ofrece o potencial de superar as limitacións dos métodos existentes e ampliar o alcance da química da borilación C–H.

Primeiro deseñamos e sintetizamos ligandos formados por 2,2'-bipiridinas substituídas en posición 5 con estruturas ríxidas de fenilo ou alquino que conectan o núcleo de bipiridina con grupos dadores de enlaces de hidróxeno, deseñados para establecer interaccións robustas entre o ligando e o sustrato, guiando o catalizador a sitios distais do anel aromático. Desafortunadamente, con substratos modelo como a N,N-dimetil-[1,1'-bifenil]-3-carboxamida, non observamos ningunha reactividade en condicións de borilación estándar, mesmo despois de analizar diferentes parámetros de reacción como a temperatura e o disolvente.

Para abordar este problema, a investigación cambiou a un substrato diferente, a N,N-dimetil-[1,1'-bifenil]-4-carboxamida, que presentaba unha reactividade lixeiramente mellorada. Porén, a reactividade aínda era moi pobre, o que suxire que a rixidez dos ligandos pode dificultar un aliñamento adecuado entre o catalizador e o substrato. Esta observación provocou un redeseño do ligando co obxectivo de aumentar a súa flexibilidade para mellorar as interaccións substrato-catalizador.

Polo tanto, realizamos a transición cara a deseños de ligandos máis flexibles, incorporando estruturas de éter para mellorar a flexibilidade conformacional que conectase o núcleo de 2,2'-bipiridina cos dadores de enlace de hidróxeno como a tiourea (**L3**), urea (**L4**) e escuaramida (**L5**). Os resultados con estes ligandos foron máis prometedores. Os ligandos **L4** e **L5**, en particular, mostraron unha reactividade significativamente mellorada, o que levou a maiores conversións nas reaccións de borilación. Sen embargo, a borilación distal prevista non se produciu. Pola contra, as reaccións produciron predominantemente produtos de borilación na posición *orto*, o que suxire que as interaccións supramoleculares pretendidas non guiaban a activación C–H. Non obstante, esta aparente selectividade á posición *orto* é bastante sorprendente para os ligandos neutros bidentados e foi estudiada posteriormente. Dado que as bipiridinas substituídas en 5 non deron os produtos desexados, estivemos motivados a modificar o patrón de substitución no núcleo de bipiridina para acadar o noso obxectivo de activación distal de C–H.

A continuación deseñamos e sintetizamos outros ligandos 2,2'-bipiridinas substituídas en posición 4 e 1,10-fenantrolinas substituídas en posición 5 con diferentes conectores entre os núcleos de bipiridina/fenantrolina e os grupos urea que actúan como dadores de enlaces de hidróxeno. Con estes ligandos, observamos a borilación distal en diferentes posicións do substrato N,N-dimetil-[1,1'-bifenil]-4-carboxamida. Os ligandos nos que os grupos urea atopábanse situados na posición *meta* no conector mostraron un aumento da borilación en *meta* no segundo anel aromático, mentres que os ligandos

USC DE COMPOSTELA

onde os grupos urea estaban situados na posición *para* no conector mostraron unha lixeira preferencia pola borilación na posición *para* do segundo anel aromático. Con estes resultados prometedores analizamos varias condicións de reacción para tentar mellorar os resultados. Non obstante, diminuir a temperatura de reacción ou o uso de *p*-xileno como disolvente non melloraron significativamente a selectividade ou a conversión da reacción. En xeral, os rendementos e rexioselectividades foron comparables aos obtidos ao usar 2,2'-bipiridina como ligando de control e, en particular, experimentos control con substratos que carecían dun sitio de recoñecemento de enlaces de hidróxeno deron resultados similares. Estes resultados indican que a borilación distal pode ser inherente ás características estéricas e electrónicas destes substratos de bifenilo, en lugar de implicar procesos impulsados por enlaces de hidróxeno. En xeral, isto destaca a complexidade de controlar a rexioselectividade desexada mediante interaccións supramoleculares.

A pesar deste foco inicial na consecución da borilación en posicións distais, a observación da borilación en posición *orto* coas bipiridinas substituídas en posición 5 foi intrigante e, polo tanto, decidimos seguir estudando esta selectividade inusual para ligandos neutros bidentados.

Inicialmente, investigamos a influencia dos substituíntes nos ligandos de 5-fenil-2,2'-bipiridina na borilación da N,N-dimetilbenzamida. Descubrimos que grupos doadores de electróns como -Me ou -OMe mostraban o mesmo patrón de rexioselectividade que a 2,2'-bipiridina. Non obstante, as bipiridinas substituídas con 5-fenilo mostraron unha lixeira preferencia pola *orto*-selectividade. As bipiridinas substituídas na posición 5 con grupos receptores de electróns melloraron a selectividade de *orto*borilación. Notablemente, o substituínte 5-$CF_3$ foi particularmente eficaz para levar a altos rendementos de produtos *orto*-mono-borilados. Probamos outros núcleos de ligando L–L, como quinolina-piridina ou piridina-oxazolina, que tamén favoreceron a orientación da reacción cara a posición *orto*, aínda que con velocidades de reacción e selectividades variables. Pola contra, os ligandos de bis-oxazolina non mostraron reactividade algunha. Ademais, investigamos algúns ligandos monodentados, que tamén mostraron unha preferencia pola selectividade *orto*, pero a reacción foi menos eficiente en comparación coa bipiridina substituída por 5-$CF_3$.

Todos estes resultados confirman que un ligando de 2,2'-bipiridina substituído por 5-$CF_3$ (**L27**) logra dirixir a borilación de benzamidas cara á posición *orto*, mentres que en ausencia do substituínte $CF_3$ (**bipy**) a orientación da reacción de borilación C–H é *meta* e *para*.

Analizamos diferentes disolventes e observamos que o uso de disolventes non polares (como hexano, ciclohexano, *p*-xileno, 1,4-dioxano ou dibutiléter) fixo diminuir a reactividade e produciu mesturas de produtos borilados en posicións *meta* e *para*. O uso

de disolventes polares (como THF, MeCN, EtOAc ou CPME) favoreceu, fortemente, a reacción de borilación en *orto*. Os disolventes haloxenados como o DCE inhibiron a reacción, mentres que os disolventes coordinadores (DMF ou DMSO) reduciron ou inhibiron a conversión.

Antes de afondar nos detalles mecanísticos, decidimos avaliar o alcance da reacción. O novo sistema catalítico coas bipiridinas substituídas con 5-$CF_3$ demostrou unha ampla aplicabilidade ao permitir efectivamente a *orto*-borilación dunha variedade diversa de derivados de benzamida, incluíndo substituíntes voluminosos no grupo amida, amidas cíclicas e heterocíclicas, amidas secundarias e varios substituíntes con heteroátomos como -OMe (amida de Weinreb).

A reacción mostrou unha notable versatilidade ao ser eficaz con benzamidas que levan diferentes substituíntes no anel aromático, incluíndo grupos doadores de electróns, grupos receptores de electróns e incluso halóxenos. Ademais, a reacción de *orto*-borilación é compatible con alcohois ou aminas non protexidos pero os rendementos son modestos. É importante destacar que os substratos con múltiples sistemas aromáticos tamén deron o produto de *orto*-borilación esperado en excelentes rendementos e rexioselectividade.

A reactividade deste sistema catalítico esténdese máis aló das benzamidas. Co benzoato de metilo e a acetofenona como substratos tamén observamos a reacción de borilación en *orto*, aínda que foi necesario o uso de temperaturas máis altas e tempos de reacción máis longos. A N-Me-tosilsulfonamida asimesmo reaccionou con éxito, producindo o produto esperado cun rendemento excelente. Ademáis, varias moléculas heterocíclicas (furanos, pirrois e tiofenos) foron igualmente boriladas satisfactoriamente. Notablemente, a reacción mostrou unha alta selectividade cara á posición *orto* das benzamidas, mesmo en presenza doutros grupos directores dentro da molécula. As reaccións de control con 2,2'-bipiridina en lugar do ligando modificado 5-$CF_3$-2,2'-bipiridina non conseguiron producir os produtos *orto*-borilados en ningún dos casos.

É importante destacar que as condicións de reacción suaves e a notable tolerancia a diversos grupos funcionais fan deste método unha opción ideal para a funcionalización en fase avanzada de moléculas complexas. Isto foi exemplificado pola funcionalización exitosa de varios derivados de moléculas farmacéuticamente relevantes. Finalmente, para demostrar a utilidade sintética do noso método, utilizamos esta reacción como un paso fundamental na síntese dun funxicida coñecido, mellorando a síntese previamente establecida.

Non obstante, substratos aromáticos sen grupos carbonilo non reaccionan nas mesmas condicións cando se usa o ligando 5-$CF_3$-2,2'-bipiridina. Isto suxire que a

USC UNIVERSIDADE DE SANTIAGO DE COMPOSTELA

presenza do grupo carbonilo no substrato é crucial tanto para a reactividade como para a rexioselectividade deste sistema catalítico.

Unha vez establecida a eficacia e a xeneralidade deste método, propuxémonos desentrañar o mecanismo que explique a *orto*-rexioselectividade recentemente observada. Inicialmente, exploramos mecanismos non canónicos, como un ciclo Ir(I)/Ir(III) ou a posibilidade de que o ligando 5-$CF_3$-2,2'-bipiridina puidese sufrir un proceso de ciclometalación e converterse nun ligando bidentado monoaniónico (L-X). Este proceso permitiría a coordinación do grupo carbonilo do substrato ao centro metálico antes do paso de activación C–H. Non obstante, os datos experimentais xunto cos cálculos de DFT descartaron estas vías alternativas, apoiando un mecanismo canónico Ir(III)/Ir(V).

A observación experimental de que o substituínte $CF_3$ no ligando de bipiridina necesita estar na posición 5 para que a reacción sexa selectiva cara á posición *orto* foi particularmente interesante. En experimentos con bipiridinas substituídas na posición 3 ou 4 con grupos $CF_3$, observamos o mesmo patrón de selectividade que coa 2,2'-bipiridina (borilación nas posicións *meta* e *para*, menos obstaculizadas). Esta observación suxeriu que a recén descuberta selectividade a *orto* non se debe unicamente ás características electrónicas dos ligandos.

A maiores, puidemos observar un complexo Ir catiónico entre $[Ir(COD)Cl]_2$ e o ligando de bipiridina substituído por 5-$CF_3$ mediante experimentos de RMN e MS que mostraron que o ligando permanecía coordinado co centro metálico a través dos átomos de N, mesmo despois de quentar a reacción de xeito prolongado. Finalmente, experimentos computacionais apoiaron aínda máis este feito, mostrando que a enerxía necesaria para a descoordinación dunha das piridinas era maior que a enerxía necesaria para a activación C–H.

Ademais, experimentos de efectos isotópicos cinéticos revelaron que o paso de activación C–H é o paso que limita a velocidade neste mecanismo, o que suxire un mecanismo Ir(III)/Ir(V) similar ao descrito para a borilación non dirixida usando 2,2'-bipiridina como ligando.

Dado o feito de que se atopou que a adición oxidante era o paso que determinaba a velocidade de reacción, realizamos unha análise computacional detallada deste paso, comparando a activación C–H en posicións *orto*, *meta* e *para,* usando como ligandos 2,2'-bipiridina e os ligandos bipiridina substituidos en posicións 3-, 4- e 5 por grupos $CF_3$. Este estudo corroborou o observado experimentalmente, xa que só cando o ligando era a 5-$CF_3$-2,2'-bipiridina prevalecía a vía da activación C–H en *orto*. Ademais, tamén exploramos as razóns subxacentes deste comportamento e descubrimos que a rexioselectividade está determinada por interaccións non covalentes entre o grupo

USC UNIVERSIDADE DE SANTIAGO DE COMPOSTELA

benzamida do substrato e o anel de bipiridina polarizado. Estas interaccións están presentes nos estados de transición calculados co ligando 5-$CF_3$-2,2'-bipiridina pero ausentes nos estados de transición co ligando 2,2'-bipiridina convencional.

Esta comprensión mecanística non só explicou os resultados experimentais, senón que tamén destacou o potencial de explotar interaccións non covalentes para controlar a rexioselectividade noutras reaccións de funcionalización C–H. Ademais, os cálculos DFT tamén revelaron un delicado equilibrio entre factores entálpicos e entrópicos. Aínda que a posición *orto* adoita estar desfavorecida coa 2,2'-bipiridina estándar debido a penalizacións estéricas e entrópicas, os ligandos substituídos por 5-$CF_3$ introducen unha estabilización entálpica substancial que fai que se favorezca esta vía de reacción.

Despois destes resultados, exploramos se os ligandos de bipiridina tamén poden funcionar como ligandos privilexiados para a borilación de enlaces C($sp^3$)–H; especialmente escollemos N-metilamidas como substratos debido ao éxito anterior que observamos coas benzamidas. Ademais, estes substratos teñen unha gran importancia porque atópanse habitualmente en moléculas bioloxicamente activas e teñen o potencial de introducir unha valiosa diversidade estrutural en obxectivos sintéticos.

Neste caso, a reacción usando a 2,2'-bipiridina convencional como ligando non se observou case ningún produto. Despois probamos ligandos con grupos doadores de electróns na posición 5 da bipiridina, o que tamén provocou unha formación mínima de produto. Non obstante, os grupos atractores de electróns como substituíntes mostraron resultados prometedores. Finalmente, descubrimos que a incorporación dun grupo -$CF_3$ na posición 5 do anel de piridina mellorou significativamente o rendemento da borilación do grupo metilo das metilamidas en comparación co ligando canónico bipiridina. Neste caso, o ligando simétrico 5,5'-bis$CF_3$-2,2'-bipiridina demostrou ser máis reactivo e efectivo, o que levou a unha conversión case completa. Como no caso das benzamidas aromáticas, outras bipiridinas que conteñen grupos $CF_3$ en posicions distintas á posición 5 foron menos eficaces nesta transformación e deron lugar a unha reactividade máis próxima ao ligando 2,2'-bipiridina.

Os ligandos de quinolina-piridina tamén deron resultados comparables a algúns grupos receptores de electróns, pero tiñan menor reactividade en comparación cos ligandos substituídos por 5-$CF_3$. Tamén probamos os ligandos de fenantrolina, descritos proviamente na borilación de substratos alquílicos, pero estes ligandos non presentaron ningunha conversión no sistema.

Unha selección de disolventes utilizando o ligando de mellor rendemento indicou que os disolventes etéreos, especialmente o THF, eran óptimos para lograr conversións

USC UNIVERSIDADE DE SANTIAGO DE COMPOSTELA

máis altas. Pola contra, disolventes fortemente coordinantes como NMP ou MeCN non lograron promover ningunha conversión medible.

Esta borilación selectiva de enlaces N-metilo en substratos N-metilamida estendeuse con éxito a unha gama máis ampla de substratos. Ademais, o proceso de borilación acomodou alquilamidas cíclicas con aneis de varios tamaños, incluíndo o adamantano, e mostrou tolerancia aos halóxenos e outros grupos funcionais como ureas ou incluso amidas secundarias. Isto demostra a versatilidade deste sistema catalítico. Notablemente, a reacción ocorre con éxito na posición N-Me mesmo cando os grupos aromáticos están presentes na molécula. Isto representa unha vantaxe significativa sobre as estratexias de borilación non dirixida, que adoitan activar preferentemente enlaces C–H aromáticos debido á súa maior reactividade intrínseca.

A utilidade do método demostrouse aínda máis na funcionalización na fase tardía de moléculas complexas, especialmente de intermediarios farmacéuticos. A capacidade de borilar selectivamente grupos metilo en presenza de grupos funcionais sensibles destaca a practicidade e robustez deste enfoque. Este nivel de selectividade e tolerancia aos grupos funcionais convérteo nunha ferramenta inestimable para modificar moléculas bioactivas, facilitando a rápida xeración de análogos estruturais para o descubrimento e desenvolvemento de fármacos.

Do mesmo xeito que cos sistemas aromáticos, realizouse unha exhaustiva investigación mecanicista para identificar os factores responsables da selectividade observada na borilación C($sp^3$)–H. Estudos computacionais similares e datos experimentais eliminaron mecanismos alternativos, como un ciclo Ir(I)/Ir(III) ou a ciclometalación do ligando, e apoiaron un mecanismo canónico Ir(III)/Ir(V).

Neste caso, os experimentos de efecto isotópico cinético revelaron que o paso de activación do enlace C–H inflúe significativamente na velocidade de reacción, pero tamén poden estar implicados outros pasos. Estudos recentes dos grupos de Hartwig e Sakaki arroxaron luz sobre as vías mecanísticas para a borilación C-H de substratos alquílicos. Non obstante, cada un destes estudos suxire un mecanismo lixeiramente diferente despois da activación do enlace C–H, que implica diferentes isomerizacións antes da etapa de eliminación redutora que produce o produto borilado.

Partindo destes precedentes, analizamos meticulosamente o perfil enerxético desta reacción e determinamos que a vía de menor enerxía implica a activación do enlace C–H, seguida dun proceso de isomerización que implica o reposicionamento de dous dos grupos borilo coordinados co átomo de iridio para cambiar entre dúas estruturas de bipiramidais pentagonais distintas. Este proceso culmina nunha eliminación redutora, levando á formación do produto desexado. Este mecanismo calculouse para a reacción cos ligandos que conteñen 5-$CF_3$ e para a 2,2'-bipiridina.

USC UNIVERSIDADE DE SANTIAGO DE COMPOSTELA

Aínda que as enerxías eran bastante similares, observamos que o paso de activación C-H requiría menor enerxía cos ligandos que conteñen 5-$CF_3$ en comparación coa 2,2'-bipiridina.

Unha vez calculado o mecanismo completo da reacción, observamos que o aumento da reactividade cando se usan ligandos que conteñen 5-$CF_3$ podería atribuírse ao paso de adición oxidante. Polo tanto, centrámonos na análise do paso de activación C-H tanto para os ligandos que conteñen os grupos 5-$CF_3$ como para o ligando 2,2'-bipiridina. Estudos computacionais revelaron que as interaccións non covalentes entre o anel polarizado do ligando bipiridina e o grupo carbonilo da alquilamida xogan un papel crucial na estabilización do estado de transición para a activación do enlace C–H N-metilo. Estas interaccións, semellantes ás comentadas no caso dos precursores aromáticos, están presentes exclusivamente cos ligandos que conteñen os grupos 5-$CF_3$ e non se observan no caso da reacción co ligando 2,2’-bipiridina.

A importancia destas interaccións non covalentes impulsadas pola dispersión, a pesar da súa relevancia a miúdo ignorada, fai fincapé na necesidade crucial de consideralas en futuras investigacións en varias reaccións químicas.

USC
UNIVERSIDADE DE SANTIAGO DE COMPOSTELA

# 3 Summary

USC
UNIVERSIDADE
DE SANTIAGO
DE COMPOSTELA

Organic chemistry, a cornerstone of the scientific world, plays a pivotal role in various domains of human endeavor. As a field that focuses on the synthesis and transformation of organic molecules, it has revolutionized the pharmaceutical, agricultural, and materials industries. Its historical journey is as fascinating as its modern applications are indispensable. Organic chemistry not only deals with the creation of complex molecules but also aims to foster sustainability and efficiency in chemical processes.

In today's organic synthesis, sustainability is the top priority. Chemists are developing greener methods to reduce waste, conserve energy, and harness renewable resources. Catalytic reactions, especially those involving transition metal complexes, are at the heart of these advancements. Transition metals, with their unique electronic structures, enable a diverse range of organometallic mechanisms which are essential for the efficient and precise transformation of organic molecules. For instance, cross-coupling reactions have revolutionized organic synthesis by forming carbon-carbon and carbon-heteroatom bonds.

Ligands play a pivotal role in modulating the behavior of transition metal catalysts. By meticulously designing the electronic and steric environment of the metal center, ligands can enhance reactivity, improve selectivity, and increase the stability of the catalytic system. This has led to significant advancements in catalytic efficiency, enabling chemists to achieve precise control over synthetic processes. This has been particularly impactful in the synthesis of complex molecules where achieving high levels of selectivity is often a critical challenge.

Another transformative discovery in modern organic chemistry is the concept of C–H activation. Traditional synthetic methods often required pre-functionalized substrates, adding steps and waste to the overall process. In contrast, the activation and functionalization of C–H bonds allows to streamline synthetic pathways and reducing waste. This approach not only simplifies the synthesis of complex molecules but also aligns with the principles of green chemistry by enhancing the overall atom economy and sustainability of chemical processes.

The journey of C–H activation commenced in the mid-20th century, with early examples showcasing stoichiometric transformations. A pivotal moment arrived with Shilov's groundbreaking work in the 1960s, which laid the groundwork for catalytic C–H functionalization. Subsequent studies, notably those by Bergman and Graham, further advanced the field by elucidating crucial aspects of the reaction mechanism, particularly in the context of iridium-based systems. These foundational efforts culminated in the development of highly efficient catalytic processes that have become integral to organic synthesis.

USC UNIVERSIDADE DE SANTIAGO DE COMPOSTELA

One of the most potent applications of C–H activation is the metal-promoted selective borylation of aromatic systems. This reaction enables the introduction of boron groups at the less hindered position on aromatic rings, creating versatile intermediates that can be further functionalized to construct intricate molecular structures. The utility of boron-containing compounds extends across various fields, including medicinal chemistry, materials science, and agrochemicals, making C–H borylation a critical tool in the synthetic chemist's arsenal.

The reaction was primarily developed by the group of Professor John Hartwig. It involves the use of an Ir precatalyst (usually $[Ir(OMe)(COD)]_2$ or $[Ir(COD)Cl]_2$), $B_2pin_2$ as the boron source, and a 2,2'-bipyridine as a ligand. Using this catalytic system, Hartwig's group has successfully demonstrated the versatility of this reaction by borylating a wide range of arenes and heteroarenes with excellent efficiency.

However, while the reaction exhibited remarkable efficiency, controlling the regioselectivity proved challenging. The steric effects of the substrate dominated the reaction, leading to the borylated product at the less hindered position. Since the initial reports on the C–H borylation reaction, numerous groups have designed ligands with diverse structures, enabling more precise control over the regioselectivity of C–H borylation. Several groups have developed ligands that allow the coordination of a directing group from the substrate and guide the borylation toward the *ortho* position of those directing groups. These ligands primarily fall into three categories: monodentate ligands (L), hemilabile ligands (L–L'), or bidentate monoanionic ligands (L–X). Additionally, other groups have developed ligands to selectively borylate arene substrates. These approaches often involve the design of bifunctional ligands with a 2,2'-bipyridine core that coordinates to the metal and a supramolecular recognition group that interacts with a functional group of the substrate.

In this PhD dissertation, we describe our efforts to regioselectively activate distal C–H bonds. To address this challenge, we proposed a ligand-directed strategy to achieve distal borylation using bifunctional bipyridine-based ligands equipped with hydrogen-bonding functionalities. The central goal was to design ligands that could direct the iridium catalyst to the distal positions on aromatic rings, enabling selective C–H activation at otherwise inaccessible sites. Unlike conventional approaches that primarily rely on directing groups to achieve selectivity, this strategy leverages non-covalent interactions—specifically hydrogen bonding—to control regioselectivity. By employing supramolecular interactions, this method offers the potential to overcome the limitations of existing methods and expand the scope of C–H borylation chemistry.

We first designed and synthesized ligands consisting of 5-substituted bipyridines with rigid phenyl or alkyne linkers connecting the bipyridine core to hydrogen-bonding groups, designed to establish robust hydrogen-bonding interactions, guiding the catalyst

USC DE COMPOSTELA

to distal sites on the aromatic ring. Unfortunately, with model substrates such as N,N-dimethyl-[1,1'-biphenyl]-3-carboxamide, we observed no conversion under standard borylation conditions, even after screening different reaction parameters like temperature and solvent.

To address this issue, the investigation shifted to a different substrate, N,N-dimethyl-[1,1'-biphenyl]-4-carboxamide, which exhibited slightly improved reactivity. However, the reactivity was still very poor, suggesting that the rigidity of the ligands may hinder a proper alignment between the catalyst and the substrate. This observation prompted a redesign of the ligand aimed at increasing its flexibility to enhance substrate-catalyst interactions.

Therefore, we transitioned toward more flexible ligand designs, incorporating ether linkers to enhance conformational flexibility, and with hydrogen-bonding moieties such as thiourea (**L3**), urea (**L4**), and squaramide (**L5**). The results with these ligands were more promising. In particular, ligands with a urea (**L4**) or squaramide (**L5**) group. Ligands **L4** and **L5**, in particular, showed significantly improved reactivity, leading to higher conversions in borylation reactions. However, the anticipated distal borylation did not occur. Instead, the reactions predominantly yielded *ortho*-borylated products, suggesting that the intended supramolecular interactions were not guiding the C–H activation. This apparent *ortho*-selectivity is quite surprising for bidentate neutral ligands. Given that the 5-substituted bipyridines did not yield the desired products, we were motivated to modify the substitution pattern in the bipyridine core to achieve our objective of distal C–H activation.

We next designed and synthesized other 4-substituted bipyridines and 5-substituted phenanthrolines with different aromatic linkers connecting the bipyridine/phenanthroline cores to the urea groups. With these ligands, we observed distal borylation at different positions of the substrate N,N-dimethyl-[1,1'-biphenyl]-4-carboxamide. Urea-containing ligands where the urea groups were positioned at the *meta* position in the linker exhibited increased *meta* borylation, while ligands where the urea groups were positioned at the *para* position in the linker showed a slight preference for *para* borylation. With these promising results in hand, we screened several reaction conditions in an attempt to improve the results. However, lowering the reaction temperature or using p-xylene as a solvent didn't significantly improve the selectivity or conversion of the reaction. Overall, these results were comparable to those obtained when using 2,2'-bipyridine as a control ligand and, notably, control experiments with substrates lacking a hydrogen bonding recognition site yielded similar outcomes. These findings indicate that distal borylation may be inherent to the steric and electronic characteristics of these biphenyl substrates, rather than involving hydrogen bonding-

USC UNIVERSIDADE DE SANTIAGO DE COMPOSTELA

driven processes. These results underscore the intricacies of controlling the desired regioselectivity through supramolecular interactions.

Despite this initial focus on achieving distal borylation, the observation of *ortho* borylation with the 5-substituted bipyridines was intriguing and therefore we were prompted to further study this unusual selectivity for bidentate neutral ligands.

Initially, we investigated the influence of substituents on 5-phenyl-2,2'-bipyridine ligands on the borylation of N,N-dimethylbenzamide. We discovered that electron-donating groups like -Me or -OMe exhibited the same regioselectivity pattern as the 2,2'-bipyridine. However, 5-phenyl substituted bipyridines displayed a slight preference for *ortho*-selectivity. Bipyridines substituted at position 5 with electron-withdrawing groups enhanced the *ortho*-borylation selectivity. Notably, the 5-$CF_3$ substituent was particularly effective in leading to high yields of *ortho*-mono-borylated products. We also tested other L–L ligand cores, such as quinoline-pyridine or pyridine-oxazoline frameworks, which also favored *ortho*-orientation, albeit with varying reaction rates and selectivities. In contrast, bis-oxazoline ligands exhibited no reactivity whatsoever. Furthermore, we investigated some monodentate ligands, which also showed a preference for *ortho* selectivity, but the reaction was less efficient compared to the 5-$CF_3$-substituted bipyridine.

All these results confirm that a 5-$CF_3$-substituted 2,2'-bipyridine ligand (**L27**) is *ortho*-directing, whereas in the absence of the $CF_3$ (**bipy**) substituent the orientation of the C–H borylation reaction is *meta* and *para*.

We screened different solvents and observed that using a 5-$CF_3$-2,2'-bipyridine ligand in non-polar solvents (such as hexane, cyclohexane, *p*-xylene, 1,4-dioxane or dibutylether) decreased reactivity and resulted in regioisomeric mixtures of *meta* and *para* borylation products. The use of polar solvents (such as THF, MeCN, EtOAc or CPME) favored, strongly the *ortho*-borylation process. Halogenated solvents such as DCE inhibited the reaction, while coordinating solvents (DMF or DMSO) reduced or inhibited conversion.

Before delving into the mechanistic details, assessing the scope of *ortho*-borylation was crucial. The novel catalytic system with the 5-$CF_3$-subtituted bipyridines demonstrated a broad applicability by effectively enabling the *ortho*-borylation of a diverse array of benzamide derivatives including bulky substituents in the amide group, cyclic and heterocyclic amides, secondary amides, and various heteroatom substituents such as -OMe (Weinreb amide).

The reaction exhibited remarkable versatility by being effective with benzamides bearing different substituents in the aromatic ring, including electron-donating groups, electron-withdrawing groups, and even halogens. Moreover, the *ortho*-borylation reaction is compatible with unprotected alcohols or amines but yields are modest. Importantly,

USC DE SANTIAGO DE COMPOSTELA

substrates with multiple aromatic systems also yielded the expected *ortho*-borylation product in excellent yields and regioselectivity.

The reactivity of this catalytic system extends beyond benzamides. Methylbenzoate and acetophenone underwent *ortho*-borylation, albeit at higher temperatures and longer reaction times. N-Me-tosylsulfonamide also reacted successfully, producing the anticipated product in excellent yield. This reaction surpasses the limitations of arene substrates, as several heterocyclic molecules were also successfully borylated. Notably, the reaction exhibited high selectivity toward the *ortho* position of benzamides, even in the presence of other prevalent directing groups within the molecule. Control reactions with 2,2'-bipyridine instead of the privileged 5-$CF_3$-2,2'-bipyridine ligand failed to yield the *ortho*-borylated products in all cases.

Importantly, the mild reaction conditions and remarkable tolerance of functional groups make this method an ideal choice for late-stage functionalization of complex molecules. This was exemplified by the successful functionalization of several drug derivatives. Finally, to demonstrate the synthetic utility of our method, we utilized this reaction as a pivotal step in the synthesis of a well-known fungicide, improving the previously reported synthesis.

However, aromatic substrates without carbonyl groups do not react under the same conditions when using the 5-$CF_3$-2,2'-bipyridine ligand. This suggests that the presence of the carbonyl group in the substrate is crucial for both the reactivity and the regioselectivity of this catalytic system.

Once the effectiveness and generality of this method were established, we set out to unravel the underlying mechanism for the newly observed *ortho*-regioselectivity. Initially, we explored non-canonical mechanisms, such as an Ir(I)/Ir(III) cycle or the possibility that the 5-$CF_3$-2,2'-bipyridine ligand could undergo a rollover cyclometalation process and function as a monoanionic bidentate L–X ligand, which are known to allow the coordination of the carbonyl moiety of the substrate before the C–H activation step. However, experimental data coupled with DFT calculations ruled out these alternative pathways, supporting a canonical Ir(III)/Ir(V) mechanism.

The experimental observation that the $CF_3$ substituent in the bipyridine ligand needs to be in the 5 position for the reaction to be selective towards the *ortho*-borylation was particularly intriguing. In experiments with 3- or 4- $CF_3$ substituted bipyridines, we observed the same selectivity pattern as with 2,2'-bipyridine (borylation at the less hindered *meta* and *para* positions). This observation strongly suggested that the newfound *ortho* selectivity was not solely due to the electronic characteristics of the ligands.

USC UNIVERSIDADE DE SANTIAGO DE COMPOSTELA

Furthermore, we were able to observe a cationic Ir complex between $[Ir(COD)Cl]_2$ and the 5-$CF_3$ substituted bipyridine ligand by NMR and MS experiments which showed that the ligand stayed coordinated to the metal center through the N atoms even after prolonged heating. Finally, computational experiments further supported this finding, showing that the energy required for the decoordination of one of the pyridines was higher.

Additionally, kinetic isotopic effect experiments revealed that the C–H activation step is the rate-limiting step in this mechanism, suggesting an Ir(III)/Ir(V) mechanism similar to the one described for undirected borylation using 2,2'bipyridine as a ligand.

Given that the C-H oxidative addition was found to be the rate-determining step, we conducted a detailed computational analysis of this step, comparing the *ortho*, *meta*, and *para* C–H activation for the reaction using as ligands 2,2'bipyridine and the 3-, 4-, and 5-$CF_3$ substituted ones. This study corroborated our experimental findings, as only when the ligand was the 5-$CF_3$-2,2'-bipyridine did the *ortho* pathway prevail. Furthermore, we also explored the underlying reasons for this behavior and discovered that the regioselectivity is determined by rare non-covalent interactions between the substrate's benzamide group and the polarized bipyridine ring. These interactions are present in the transition states calculated with the 5-$CF_3$-2,2'-bipyridine ligand but absent in the transition states with the conventional 2,2'-bipyridine ligand.

This mechanistic understanding not only explained the experimental results but also highlighted the potential of exploiting non-covalent interactions to control regioselectivity in other challenging C–H functionalization reactions. Additionally, the DFT calculations also revealed a delicate balance between enthalpic and entropic factors. While the *ortho* position is typically disfavored with standard 2,2'-bipyridine due to steric and entropic penalties, the 5-$CF_3$-substituted ligands introduce substantial enthalpic stabilization.

After these results we also explored whether bipyridine ligands can also work as privileged ligands for the borylation of $C(sp^3)$–H bonds, specially we chose N-methylamides as substrates due to the previous success we observed with benzamides. Additionally, these substrates hold great significance because they are commonly found in biologically active molecules and have the potential to introduce valuable structural diversity in synthetic targets.

In this case, the reaction using the conventional 2,2'bipyridine as a ligand yielded almost no product. We then tested ligands with electron-donating groups at the 5-position of the bipyridine, which also resulted in minimal product formation. However, electron-withdrawing groups as substituents showed promising results. Ultimately, we discovered that the incorporation of a -$CF_3$ group at the 5-position of the pyridine ring significantly enhanced the yield of the borylation of the methyl group of methyl amides compared to the canonical ligand bipyridine. In this instance, the symmetric 5,5'-bis$CF_3$-

2,2'-bipyridine ligand proved to be more reactive and effective, leading to almost complete conversion. As in the case of the aromatic benzamides, other $CF_3$ containing bipyridines were less effective in this transformation and resulted in reactivity closer to the 2,2'-bipyridine ligand.

Quinoline-pyridine ligands also yielded results comparable to some electron-withdrawing groups but had lower reactivity compared to the 5-$CF_3$ substituted ligands. We also tested phenanthroline ligands, which are known to borylate alkylic substituents, did not exhibit any conversion in the system.

A solvent screening using the best-performing ligand indicated that ethereal solvents, particularly THF, were optimal for achieving higher conversions. In contrast, strongly coordinating solvents such as NMP or MeCN failed to promote any measurable conversion.

The success of this selective borylation of methyl C–H bonds in methylamides was successfully extended to a broader range of substrates. Moreover, the borylation process accommodated cyclic alkyl amides of various ring sizes, including adamantane, and exhibited tolerance for halogens and other functional groups such as ureas or even secondary amides. This demonstrates the versatility of the optimal catalytic system. Notably, the reaction successfully occurs in the N-Me position even when aromatic groups are present in the molecule. This represents a significant advantage over undirected borylation strategies, which often preferentially activate aromatic C–H bonds due to their higher intrinsic reactivity.

The method's utility was further demonstrated in the late-stage functionalization of complex molecules, particularly pharmaceutical intermediates. The ability to selectively borylate methyl groups in the presence of sensitive functional groups highlights the practicality and robustness of this approach. This level of selectivity and functional group tolerance makes it an invaluable tool for modifying bioactive molecules, facilitating the rapid generation of structural analogs for drug discovery and development.

As with aromatic systems, a comprehensive mechanistic investigation was conducted to identify the factors responsible for the observed selectivity in C($sp^3$)–H borylation. Similar computational studies and experimental data eliminated alternative mechanisms, such as an Ir(I)/Ir(III) cycle or the ligand rollover cyclometalation, and supported a canonical Ir(III)/Ir(V) mechanism.

In this case, kinetic isotopic effect experiments revealed that the C-H activation step significantly influences the reaction rate, but other steps may also be involved. Recent studies by Hartwig's and Sakaki's groups have shed light on the mechanistic pathways for the C-H borylation of alkylic substrates. However, each of these studies

USC UNIVERSIDADE DE SANTIAGO DE COMPOSTELA

suggests a slightly different mechanism after the C–H activation, involving different isomerizations prior to the reductive elimination step that yields the borylated product.

Building on these findings, we have meticulously analyzed the energy profile of this reaction and determined that the lowest energy pathway involves C-H activation, followed by an isomerization process involving the repositioning of two boryl groups coordinated to the iridium atom to switch between two distinct pentagonal bipyramidal structures. This process culminates in a reductive elimination, leading to the formation of the desired product. This mechanism was computed for the 5-$CF_3$-containing ligands and for the 2,2'-bipyridine as a ligand. While the energies were quite similar, we observed that the C-H activation step required lower energy with the 5-$CF_3$-containing ligands compared to the 2,2'-bipyridine.

Once we had calculated the complete mechanism of the reaction and observed that the increased reactivity when using the 5-$CF_3$-containing ligands might be attributed to the oxidative addition step, we focused on analyzing the C–H activation step for both the 5-$CF_3$-containing ligands and the 2,2'-bipyridine ligand. Computational studies revealed that non-covalent interactions between the polarized ring of the bipyridine ligand and the carbonyl group of the alkyl amide play a crucial role in stabilizing the transition state for methyl C–H activation. These interactions, similar to those discussed in the case of aromatic precursors, are exclusively present with the 5-$CF_3$-containing ligands and are absent in the case of the reaction with the 2,2'-bipyridine ligand.

The significance of these dispersion-driven non-covalent interactions, despite their often-overlooked importance, emphasizes the crucial need to consider them in future investigations across various chemical reactions.

USC
UNIVERSIDADE DE SANTIAGO DE COMPOSTELA

# 4 Introduction

USC
UNIVERSIDADE
DE SANTIAGO
DE COMPOSTELA

## 4.1 Organic chemistry

In simple terms, Chemistry is defined as the branch of science that studies the nature, properties, and composition of matter, as well as its transformations. Throughout human history, chemistry has played a crucial role in shaping the world around us, from the development of life-saving pharmaceuticals to the creation of sustainable materials.[1] Due to its involvement in so many aspects of human history and its ability to interface seamlessly with other sciences, chemistry is often referred to as the "central science", making its study essential for the progress of society.[2]

Among the numerous branches of chemistry, organic chemistry has played a pivotal role in shaping the modern world. Specifically, organic synthesis, the science of constructing organic molecules through chemical processes, is at the heart of many advancements in pharmaceutical, agricultural, and material science.[3] As these industries seek more sustainable practices, organic chemists face new challenges: developing greener, more efficient methodologies that minimize waste and reduce energy consumption.

The discipline, integral to chemistry, has evolved significantly since its beginning. Historically, organic synthesis began with the synthesis of urea by Friedrich Wöhler in 1828, which debunked the theory of vitalism and paved the way for the development of numerous synthetic methods. Over the course of the twentieth century, the scope and precision of organic synthesis expanded significantly, and today synthetic chemists can tackle the construction of molecules with remarkable level of complexity. Nowadays, organic synthesis has become indispensable across various fields and industries, enabling the production of essential drugs, crop protection agents, and innovative materials, among others.[4] Examples of complex molecules synthesized using the tools of organic synthesis are depicted in Figure *1*.[5]

---

[1] Morris, P. J. T. *"The matter factory : a history of the chemistry laboratory"*. **2015.**

[2] a) Balaban, A. T.; Klein, D. J. *Scientometrics* **2006,** *69,* 615–637., b) Brown, T. E.; LeMay, H. E. H.; Bursten, B. E.; Murphy, C.; Woodward, P. *"Chemistry: the central science"*. Pearson Education, **2014.**, c) Comte, A.; Bridges, J. H. *"A general view of positivism"*. Tráubner and co, **1865.**, d) van Brakel, J.; Vermeeren, H. *Philosophy Research Archives* **1981,** *7,* 501–552.

[3] Ferrie, C.; Florance, C. *"Organic Chemistry for Babies"*. Sourcebooks, Incorporated, **2018.**

[4] Wentrup, C. *Eur. J. Org. Chem.* **2022,** e202101492.

[5] a) Atanes, N.; Castedo, L.; Guitian, E.; Saa, C.; Saa, J. M.; Suau, R. *J. Org. Chem.* **1991,** *56,* 2984–2988., b)Evans, D. A.; Kaldor, S. W.; Jones, T. K.; Clardy, J.; Stout, T. J. *J. Am. Chem. Soc.* **1990,** *112,* 7001–7031., c) Funk, R. L.; Vollhardt, K. P. C. *J. Am. Chem. Soc.* **1979,** *101,* 215–217., d) Nicolaou, K. C.; Yang, Z.; Liu, J. J.; Ueno, H.; Nantermet, P. G.; Guy, R. K.; Claiborne, C. F.; Renaud, J.; Couladouros, E. A.; Paulvannan, K.; Sorensen, E. J. *Nature* **1994,** *367,* 630–634., e) Schmitt; Johnston; Christensen *J. Org. Chem.* **1980,** *45,* 1142–1148., f) Woodward, R. B.; Cava, M. P.; Ollis, W. D.; Hunger, A.; Daeniker, H. U.; Schenker, K. *J. Am. Chem. Soc.* **1954,** *76,* 4749–4751.

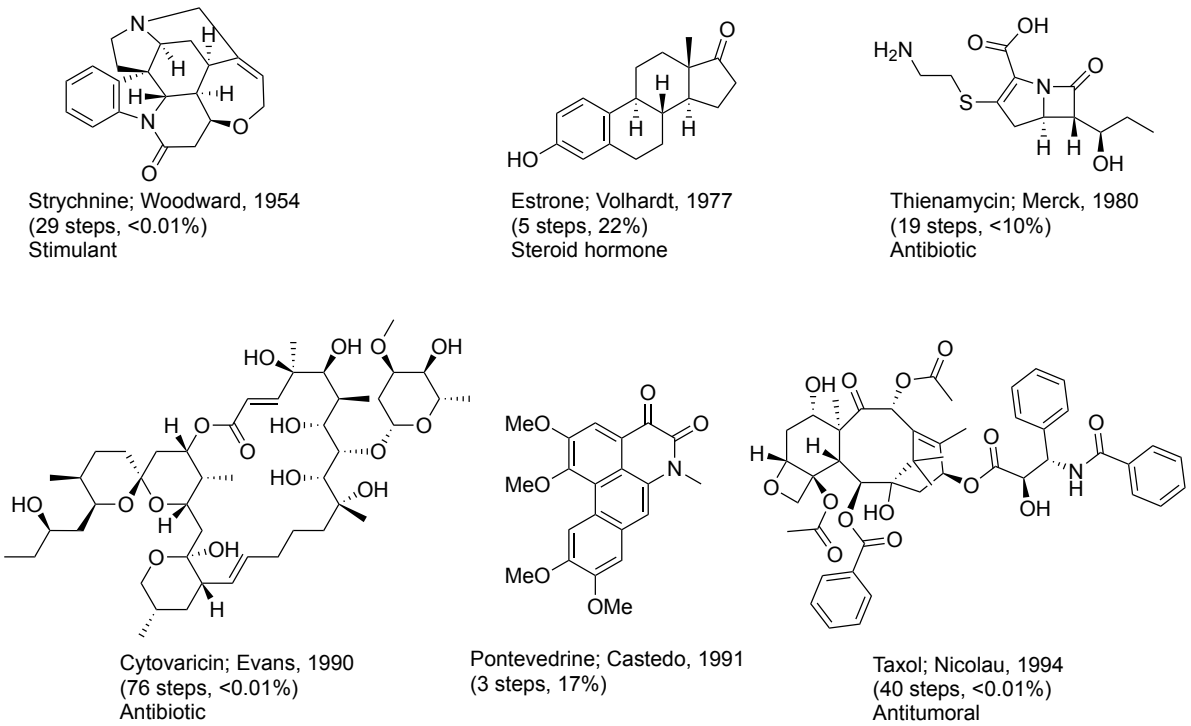



**Figure *1*** Examples of classic total syntheses, their number of steps and total yield.

In the 21st century, modern organic synthesis faces new challenges and has shifted the traditional focus of merely creating molecules to doing so in a more efficient and sustainable manner.[6] This shift prioritizes developing greener processes that reduce environmental impact while ensuring economic viability. Key goals for sustainability in chemistry include the use of renewable feedstocks, implementing energy-efficient processes, minimizing the number of steps and the production of waste. In this context, the discovery of catalytic reactions is especially relevant because of their intrinsic atom economy. Among the different types of catalysts those based on transition metal complexes are extremely attractive, in great part because they work via organometallic mechanisms, which provide many reaction alternatives.

## 4.2 Organometallic catalysis

### 4.2.1 Historical overview

The unique electronic properties of transition metal complexes, particularly their ability to form stable coordination bonds with organic substrates and participate in redox cycles, have made them indispensable in a wide range of catalytic applications. Indeed, transition metal catalysis based on organometallic chemistry is behind some of the most powerful synthetic methodologies available today.

USC UNIVERSIDADE DE SANTIAGO

[6] Tanja Gaich; Phil S. Baran *J. Org. Chem.* **2010,** *75,* 4657–4673.

The origins of organometallic chemistry can be traced back to the early 18th century. In 1706, Johann Jacob Diesbach, a Berlin-based paint maker, accidentally discovered Prussian blue ($Fe_4[Fe(CN)_6]_3 \cdot xH_2O$), an iron-cyanide complex, that became one of the earliest examples of an organometallic complex. This compound, still used today both as a pigment and as an antidote for thallium and cesium poisonings, set the stage for future explorations into metal-organic interactions.[7]

The 19th century witnessed more deliberate efforts to synthesize organometallic compounds. A major breakthrough occurred with the discovery of Zeise's salt ($K[PtCl_3(C_2H_4)] \cdot H_2O$) in 1830, the first metal-alkene complex, which provided insights into π-bonding between metals and organic molecules.[8] This discovery laid the groundwork for the Dewar–Chatt–Duncanson model, that explains the chemical bonding in transition-metal alkene complexes.[9]

In the mid-19th century, Edward Frankland reported the metalation of alkyl compounds to generate the first organometallic alkyl compounds such as $ZnEt_2$, $HgEt_2$, $SnEt_4$ or $BMe_3$.[10] These reactive compounds were employed by other researchers such as Friedel and Crafts to prepare other main-group organometallic complexes such as organochlorosilanes from the reactions of $SiCl_4$ with $ZnR_2$.[11]

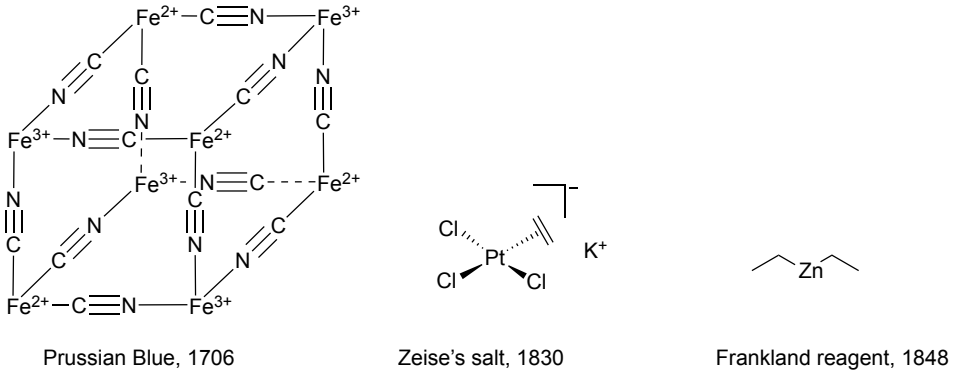



**Figure *2*** Molecular structures of early organometallic compounds.

The field of organometallic chemistry experienced a surge in progress at the turn of the 20th century. One of the most significant advances was the Grignard reaction, discovered by Victor Grignard in 1900. This reaction, which involves the oxidative addition of magnesium to organic halides, enabled the formation of organomagnesium

[7] Kraft, A. *"The History of Prussian Blue";* Jenny Stanford Publishing: **2019;** pp 1–26.
[8] a) Jarvis, J. A. J.; Kilbourn, B. T.; Owston, P. G. *Acta Cryst. B* **1971,** *27,* 366–372., b) Zeise, &.; William Christopher *Ann. Phys.* **1831,** *97,* 497–541.
[9] Mingos, D. M. P. *"Recent Developments in Theoretical Organometallic Chemistry";* Academic Press: **1977;** pp 1–51.
[10] a) Frankland, E. *Phil. Trans. R. Soc.* **1852,** *142,* 417–444., b) Frankland, E. *Justus Liebigs Ann. Chem.* **1862,** *124,* 129–157.
[11] Friedel, C.; Crafts, J. M. *Justus Liebigs Ann. Chem.* **1863,** *127,* 28–32.

compounds (RMgX) which could be used to alkylate carbonyl derivatives.[12] The Grignard reagent became a cornerstone of organic synthesis, offering a powerful tool for constructing carbon-carbon bonds.[13]

These early discoveries, from the synthesis of Prussian blue to the development of the Grignard reagent, laid the groundwork for modern organometallic chemistry and catalysis, and their synthetic application.[14]

### 4.2.2 Catalysis in organic chemistry

The invention and development of catalytic methods represents a primary scientific and technological challenge. By virtue of accelerating chemical reactions and reducing waste, catalytic technologies can have an enormous economic and environmental impact.

Although the term "catalysis" was first introduced by Swedish chemist Jöns Jacob Berzelius in 1835,[15] the concept was initially described by Elizabeth Fulhame in 1794 in her book "*An Essay on Combustion with a View to a New Art of Dying and Painting, wherein the Phlogistic and Antiphlogistic Hypotheses are Proved Erroneous*".[16] In her experiments, she documented the reduction of metal salts in organic solvents (such as ethers and alcohols) by various reducing agents, including hydrogen gas, sulfur, and phosphorus. One key discovery was that small amounts of water accelerated the reduction of metal salts, allowing the reactions to occur more quickly and at lower temperatures.

In a catalytic process, a catalyst increases the rate of a reaction without altering the overall standard Gibbs energy change. In a system where **A** is transformed into **B**, the rate of conversion depends on the activation energy or the "height" of the energy barrier. The addition of a catalyst lowers the activation energy by providing an alternative pathway for the reaction, thereby accelerating the process (Figure *3*).

[12] Victor Grignard *Compt. Rend.* **1900,** *130,* 1322–1324.
[13] Dietmar Seyferth *Organometallics* **2009,** *28,* 1598–1605.
[14] Astruc, D. *"Organometallic Chemistry and Catalysis"*. Springer, **2007.**
[15] Jöns Jacob Berzelius *Ann. Chim. Phys.* **1836,** *61,* 146–151.
[16] Elizabeth Fulhame. *"An essay on combustion, with a view to a new art of dying and painting. Wherein the phlogistic and antiphlogistic hypotheses are proven erroneous".* **1794.**

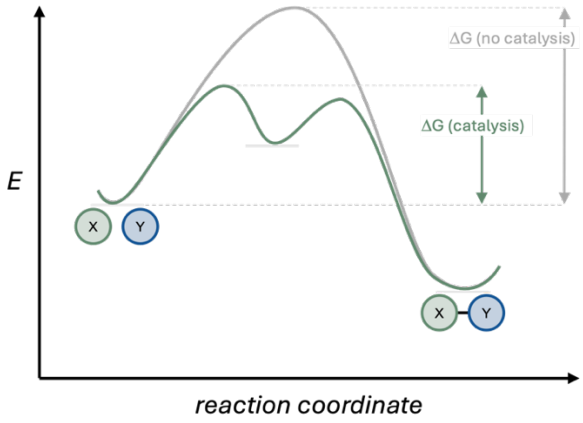



**Figure *3*** Energy profile of uncatalyzed vs catalyzed reactions.

There are various types of classifications for catalytic processes, depending on the nature of the catalyst: organic (organocatalysis),[17] inorganic,[18] organometallic,[19] and biocatalysis.[20] They can also be classified based on the mechanism, such as acid-base (Lewis[21] and Brønsted[22]), phase transfer,[23] redox, or light-promoted reactions. Another method of classification is by the phase of the reaction mixture: homogeneous or heterogeneous catalysis (Figure *4*).

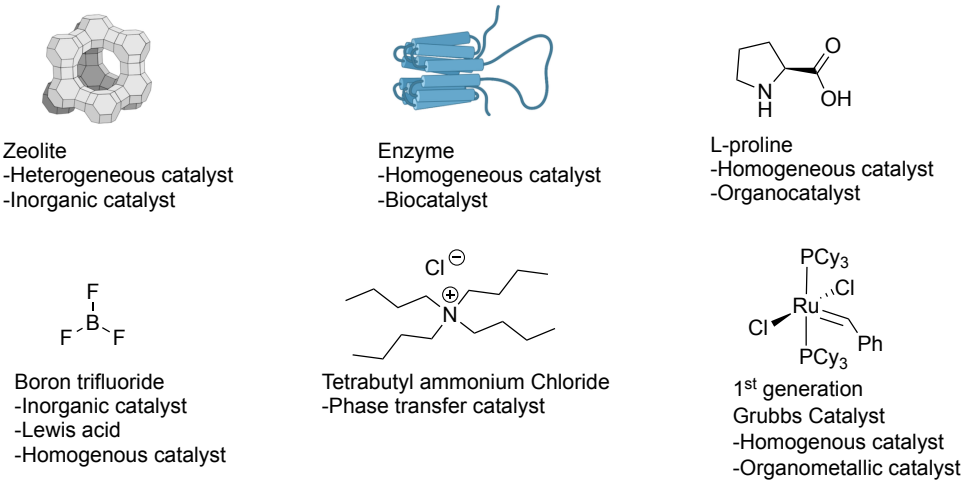



**Figure *4*** Examples of different catalysts.

[17] a) Dalko, P. I. *"Comprehensive Enantioselective Organocatalysis"*. **2013.**, b) Macmillan, D. W. C. *Nature* **2008,** *455,* 304–308., c) Mukherjee, S.; Yang, J. W.; Hoffmann, S.; List, B. *Chem. Rev.* **2007,** *107,* 5471–5569.

[18] Lichen Liu; Avelino Corma *Chem. Rev.* **2018,** *118,* 4981–5079.

[19] Hartwig, J. F. *"Organotransition metal chemistry : from bonding to catalysis"*. **2010.**

[20] Bell, E. L.; Finnigan, W.; France, S. P.; Green, A. P.; Hayes, M. A.; Hepworth, L. J.; Lovelock, S. L.; Niikura, H.; Osuna, S.; Romero, E.; Ryan, K. S.; Turner, N. J.; Flitsch, S. L. *Nat Rev Methods Primers* **2021,** *1*

[21] Vedejs, E.; Denmark, S. E. *"Lewis base catalysis in organic synthesis"*. **2016.**

[22] Yu, J.; Shi, F.; Gong, L. *Acc. Chem. Res.* **2011,** *44,* 1156–1171.

[23] Marcos, M.; Castro, J. L.; Castedo, L.; Riguera, R. *Tetrahedron* **1986,** *42,* 649–653.

### 4.2.3 Transition metal complexes in catalysis

Transition metal complexes can present exceptional properties as catalytic species owing to their coordination versatility, which allows the introduction of different ligands, and the possibility of the metals to cycle among different redox states. The organometallic mechanistic profiles of these complexes can be broadly categorized into inner or outer-sphere processes.

In inner-sphere processes, the substrate directly interacts with the metal center within the coordination sphere of ligands. The metal facilitates the reaction through steps like oxidative addition, reductive elimination, migratory insertion, and β-hydride elimination. For instance, in an oxidative addition, the metal center inserts into a bond (typically a C–H or C–X bond), increasing its oxidation state and creating a metal-substrate intermediate. During these processes, the substrate forms a temporary intermediate with the metal, enabling the desired chemical transformation (Figure *5*, **A**).

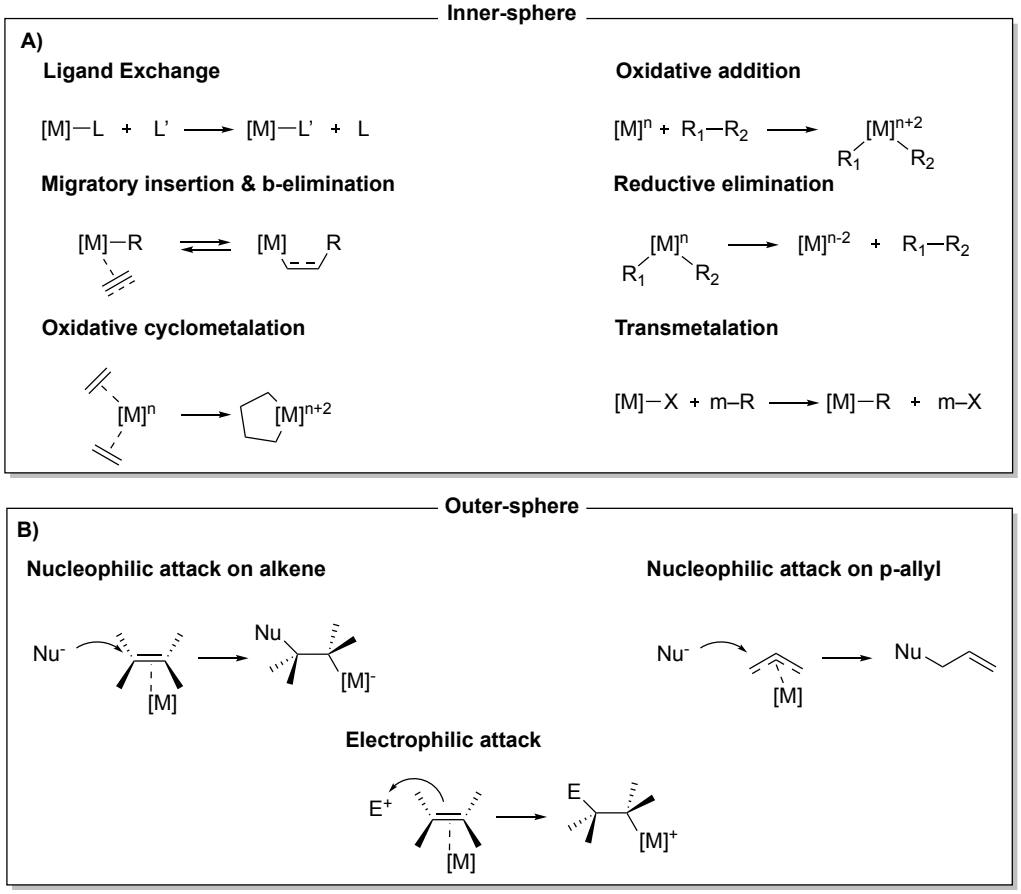



**Figure *5*** Elementary steps of organometallic reactions for inner- (**A**) and outer- (**B**) sphere mechanisms.

On the other hand, outer-sphere processes entails a coordination of the substrate to the metal, which triggers its reactivity with external reactants, usually nucleophiles or electrophiles, that are not directly bound to the metal center (Figure *5*, **B**).

USC UNIVERSIDADE DE SANTIAGO DE COMPOSTELA

The catalytic power of transition metals is not solely determined by the metal itself but also by the ligands that surround it. By altering the electronic and steric environment around the metal, ligands can modulate the reactivity, selectivity, and stability of the catalytic complex.[24]

Electronically, ligands influence the metal's ability to participate in key mechanistic steps by either donating or withdrawing electron density to the metal, thus altering the metal's reactivity and redox ability. Sterically, ligands can block certain reaction sites or channels, thereby guiding substrates to react in a specific orientation, which enhances selectivity. This is particularly important in asymmetric processes.[25]

Moreover, ligands contribute to the reactivity/stability balance of the catalytic system, ensuring that the metal complex remains active under the reaction conditions. Stabilizing ligands prevent decomposition, improve tolerance to air and moisture, and extend the operational lifespan of the catalyst.[26] This robustness is essential for developing sustainable and economically viable catalytic processes. Examples of ligands commonly used in transition metal catalysis are shown in Figure *6*.

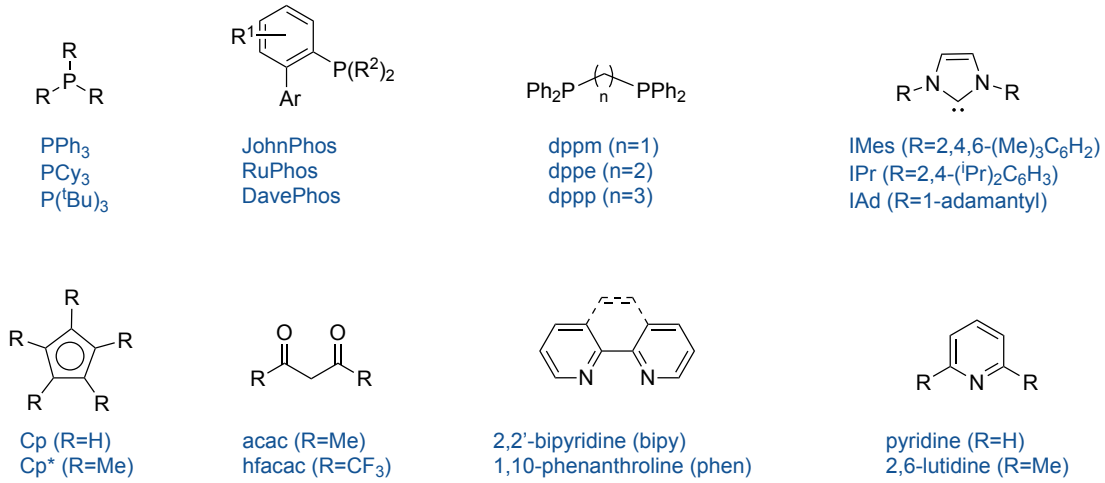



**Figure 6** Examples of common ligands employed in transition-metal catalyzed reactions.

Transition metal complexes are thus highly adaptable systems that can be fine-tuned to optimize their performance in different types of catalytic applications. The broad range of transition metals with different characteristics, great variety of ligands together with the possibility of using different type of organometallic mechanistic steps make of transition metal catalysis one of the more powerful and versatile tools available for synthetic chemists to device catalytic reactions.[27]

[24] Berrisford, D. J.; Bolm, C.; Sharpless, K. B. *Angew. Chem. Int. Ed.* **1995,** *34,* 1059–1070.
[25] Durand, D. J.; Fey, N. *Acc. Chem. Res.* **2021,** *54,* 837–848.
[26] Ferenc Joó. *"Aqueous Organometallic Catalysis".* **2001.**
[27] Nakazawa, H.; Koe, J. *"Organometallic chemistry".* **2021.**

### 4.2.4 Cornerstone metal-catalyzed reactions in modern synthesis

One of the more relevant types of metal-catalyzed reactions was devised in the early 1970s and involve cross-coupling processes (Figure *7*).[28] These transformations, usually based on Pd(0)-catalysts, enable the formation of carbon-carbon bonds with remarkable precision, and revolutionized the synthesis of complex organic molecules. These reactions have become indispensable tools not only in academic research but also in large-scale industrial applications, particularly in pharmaceutical and chemical industries.

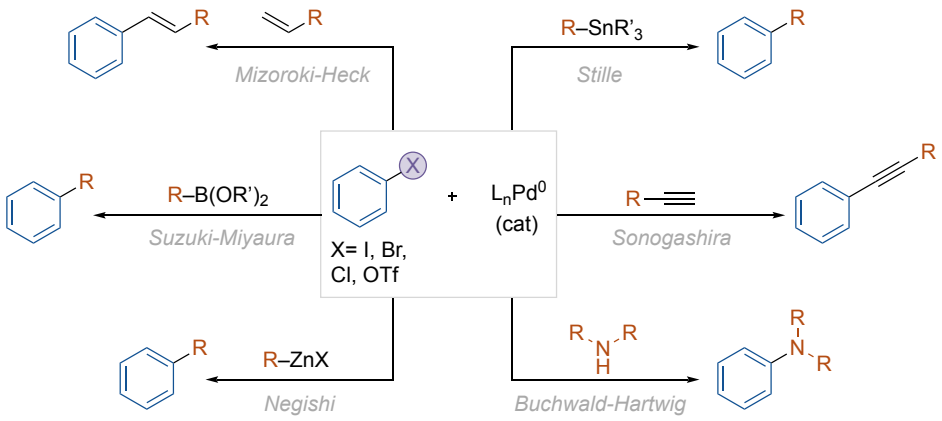



**Figure *7*** Pd(0)-catalyzed cross-coupling reactions.

In these reactions, the catalytic cycle typically begins with an oxidative addition step, where the Pd(0) complex inserts into the aryl halide bond forming the metalated intermediate **II** in Figure *8*. This is followed by transmetalation, where an organometallic reagent transfers its organic group to the palladium complex to give intermediate **III'**. Finally, reductive elimination releases the desired product and regenerates the active Pd(0) catalyst, completing the cycle. Alternatively, the complex resulting from the oxidative addition can add to unsaturated moiety, to generate a palladium intermedium **III** that evolves by beta-hydride elimination, in a Heck-like process (Figure *8*).

Beyond the laboratory, organometallic catalysts have played a critical role in developing large-scale industrial processes. One prominent example is the Monsanto process, which uses a rhodium-based catalyst (cis-$[Rh(CO)_2I_2]^-$) to catalyze the carbonylation of methanol into acetic acid. This process was later improved by the Cativa process, which employs an iridium-based catalyst and allowed improved results.

USC UNIVERSIDADE DE SANTIAGO

[28] de Meijere; Diederich, F. *"Metal-Catalyzed Cross-Coupling Reactions"*. Wiley-VCH, **2004.**

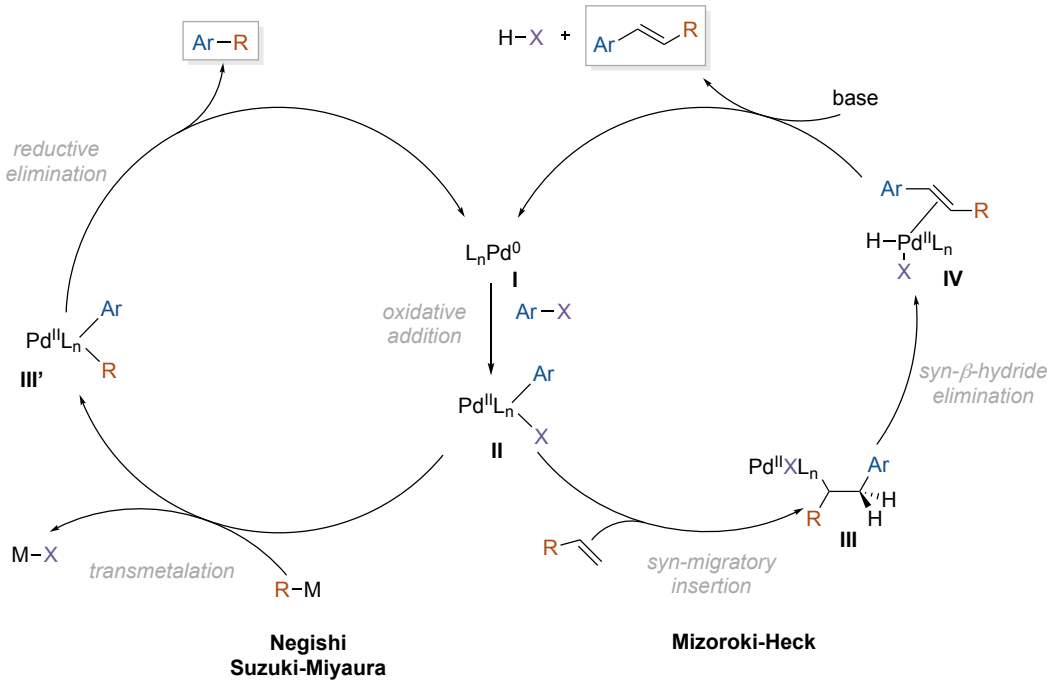



**Figure *8*** General catalytic cycles for Mizoroki-Heck, Negishi and Suzuki Miyaura reactions.

Other industrial applications include the Wacker process, which among other allows to oxidize ethylene to acetaldehyde using palladium chloride and copper chloride, and the Ziegler-Natta catalysts, responsible for producing polyethylene and polypropylene, the most widely used plastics today. Additionally, hydroformylation, or the production of aldehydes from alkenes, is another key industrial process reliant on transition metal catalysts, particularly cobalt (BASF-oxo, Exxon and Shell processes) and rhodium (Union Carbide and Ruhrchemie/Rhone–Poulenc processes) complexes.[29]

Since its inception, organometallic chemistry and catalysis has continuously pushed the boundaries of both academic and industrial chemistry. Its impact is evident in the number of Nobel Prizes awarded to chemists in the field, from Victor Grignard to Akira Suzuki.

Organometallic catalysis has not only transformed the way chemists approach molecular synthesis but has also opened the door to more sustainable and efficient processes. By leveraging the unique properties of transition metals, these catalytic reactions continue to be at the forefront of modern chemical research.As we look toward even more innovative methods, such as C–H functionalization, the potential for creating complex molecules in a simpler, greener manner becomes increasingly evident.

[29] a) Colacot, T. J.; Sivakumar, V. *"Organometallics in process chemistry"*. **2019.**, b) Colacot, T. J.; Johansson Seechurn, C. C. C.; Grubbs, R. H. *"Organometallic chemistry in industry"*. **2020.**

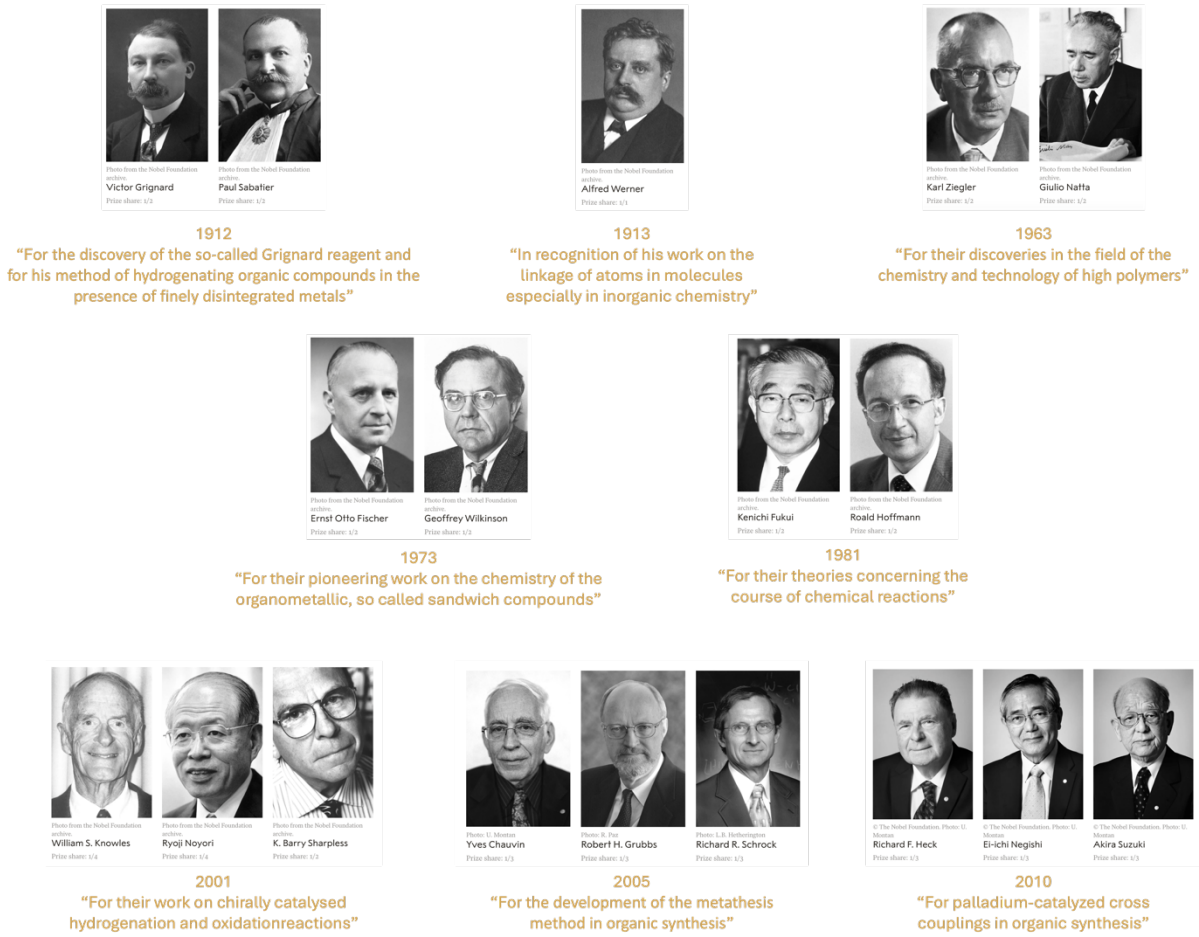
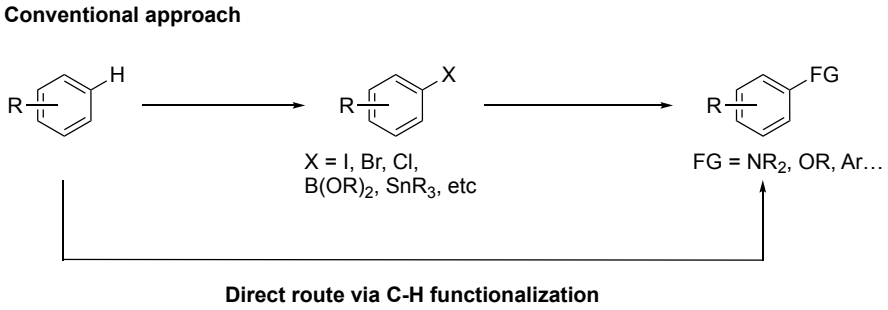



**Figure 9** Nobel prizes awarded to organometallic chemistry.

## 4.3 Transition metal-promoted C–H functionalizations

### 4.3.1 Introduction to C–H functionalization

Building on the power of organometallic catalysis, modern synthetic chemists are exploring new methodologies that could allow more direct processes for molecular construction and manipulation. One such approach is based on the development of transition metal-catalyzed C–H functionalizations, which offers a groundbreaking way to transform abundant and native C–H bonds into valuable functional groups.[30] The advantages of a direct functionalization of C–H bonds is outlined in *Scheme 1* for the case of aromatic systems.




**Scheme *1*** Example of C–H functionalization expediting organic synthesis.

This strategy not only allows to streamline synthetic processes but also aligns perfectly with the goals of green chemistry by reducing waste and improving atom economy.[31] One of the benefits of this technology derives from the possibility of using highly abundant hydrocarbons feedstocks as substrates.[32]

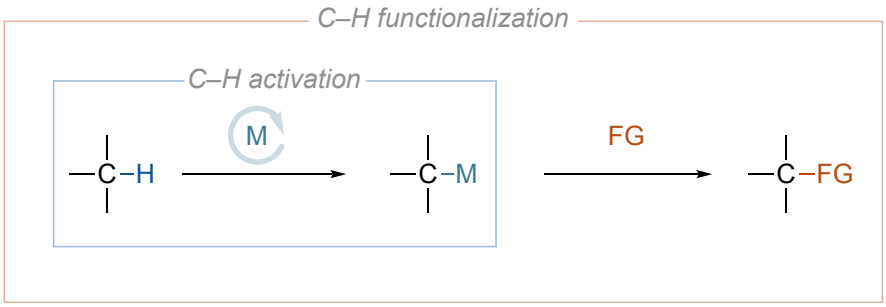
Metal-promoted C–H activations refer to the process in which the interaction of a transition metal complex with C–H bonds in alkanes, alkenes, or arenes, results in the formation of a metal-carbon bond. Importantly, this definition excludes reactions such as Friedel-Crafts alkylations, metal-oxo/H-atom abstraction, and metallonitrene/metallocarbene reactions, which are part of a broader category known as "C–H functionalization" (Scheme *2*).

---

[30] a) Bergman, R. G. *Nature* **2007,** *446,* 391–393., b) Godula, K.; Sames, D. *Science* **2006,** *312,* 67–72., c) Goldberg, K. I.; Goldman, A. S.; Meeting, A. C. S. *"Activation and Functionalization of C-H Bonds".* American Chemical Society, **2004.**, d) Labinger, J. A.; Bercaw, J. E. *Nature* **2002,** *417,* 507–514., e) Rogge, T.; Kaplaneris, N.; Chatani, N.; Kim, J.; Chang, S.; Punji, B.; Schafer, L. L.; Musaev, D. G.; Wencel-Delord, J.; Roberts, C. A.; Sarpong, R.; Wilson, Z. E.; Brimble, M. A.; Johansson, M. J.; Ackermann, L. *Nat Rev Methods Primers* **2021,** *1,* 1–31.

[31] a) Dalton, T.; Faber, T.; Glorius, F. *ACS Cent. Sci.* **2021,** *7,* 245–261., b) Gensch; Hopkinson; Glorius; Wencel-Delord *Chem. Soc. Rev.* **2016,** *45,* 2900–2936., c) Wencel-Delord, J.; Glorius, F. *Nature Chem* **2013,** *5,* 369–375.

[32] a) Crabtree, R. H. *J. Chem. Soc., Dalton Trans.* **2001,** 2437–2450., b) Hartwig, J. F. *J. Am. Chem. Soc.* **2016,** *138,* 2–24.




**Scheme *2*** Formal definitions of C–H activation and C–H functionalization.

### 4.3.2 Initial developments

The ability to directly activate C–H bonds without the need for pre-functionalized substrates marked a major milestone in organic synthesis. Early developments in this field, often limited to stoichiometric processes, laid the groundwork for modern catalytic methods.

The first relevant breakthrough in the area saw the light in 1963, when Kleiman and Dubeck reported the cyclometalation of diazobenzene using $Cp_2Ni$ to give the corresponding nickelacycle (Scheme *3*).[33]

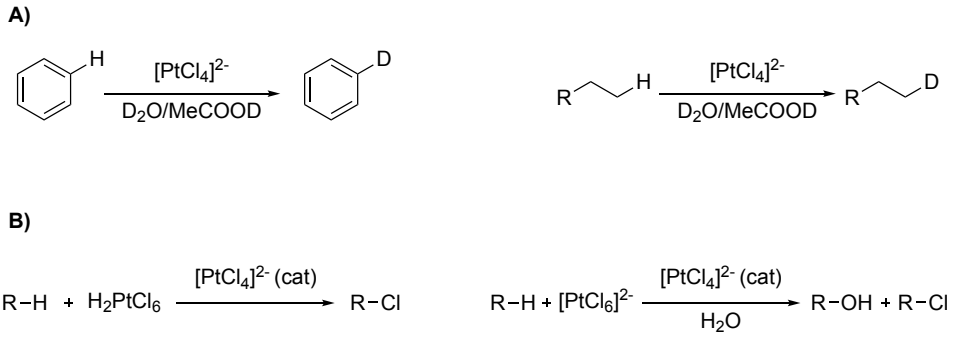



**Scheme *3*** Cyclometalation of diazobenzene via stoichiometric C–H activation.

The first evidence of catalytic C–H activation was reported in 1969 by Alexander Shilov and co-workers. They observed H-D exchange in aromatic systems when Pt(II) salts, such as $K_2PtCl_4$, were used in $D_2O$ (Scheme *4* **A**).[34]

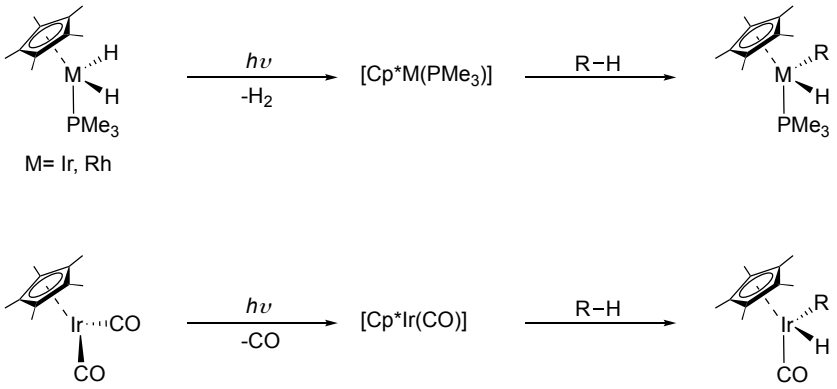
This reaction, unaffected by electronic properties of substituents, was proposed to involve an oxidative addition step. Shilov's team extended this work to functionalize alkanes into alkyl halides and alcohols using Pt(II) and Pt(IV) salts as oxidants, though the stoichiometric requirement for Pt(IV) limited its practical application (Scheme *4* **B**).[35]

[33] Kleiman, J. P.; Dubeck, M. *J. Am. Chem. Soc.* **1963,** *85,* 1544–1545.
[34] Gol'dshleger, N. F.; Tyabin, M. B.; Shilov, A. E.; Shteinman, A. A. *Zh. Fiz. Khim.* **1969,** *43,* 2174.
[35] a) Alexander E. Shilov; Georgiy B. Shul'pin *Chem. Rev.* **1997,** *97,* 2879–2932., b) Gol'Dshleger, N. F.; Es'Kova, V.; Shilov, A. E.; Shteinman, A. A. *Zh.Fiz.Khim* **1972,** *46,* 1353–1354.




**Scheme *4*** **A**) H/D exchange of hydrocarbons catalyzed by Pt(II) salts. **B**) C–H activation and functionalization by Pt(II) salts.

In 1983, Robert Bergman[36] and William Graham[37] independently developed a transition-metal-mediated intermolecular C–H activation of alkanes based on an oxidative addition to Cp*–iridium(I) complexes such as [Cp*IrH$_2$(PMe$_3$)] (Bergman's group) and [Cp*Ir(CO)$_2$] (Graham's group). The analogous rhodium complex [Cp*RhH$_2$(PMe$_3$)] was also reported.[38] These complexes undergo a photolytic loss of dihydrogen or CO to generate a reactive 16-electron intermediate, which then undergoes an oxidative addition of the hydrocarbon solvent to form [Cp*(L)M(H)(R)] *(*Scheme 5).




**Scheme *5*** Early examples of C–H activation at Cp*Ir and Cp*Rh complexes.

Competition experiments of C–H activation with these Cp*Ir and Cp*Rh complexes revealed general trends in reaction rates that align better with a preference for forming stronger metal-carbon bonds, rather than to react with weaker C–H bonds. This is illustrated by the faster activation of stronger sp$^2$ C–H bonds compared to sp$^3$ C–H bonds. Additionally, between different types of sp$^3$ C–H bonds, the rate of primary C–H

[36] a) Andrew H. Janowicz; Robert G. Bergman *J. Am. Chem. Soc.* **1983,** *105,* 3929–3939., b) Janowicz, A. H.; Bergman, R. G. *J. Am. Chem. Soc.* **1982,** *104,* 352–354.

[37] James K. Hoyano; Alexander D. McMaster; William A. G. Graham *J. Am. Chem. Soc.* **1983,** *105,* 7190–7191.

[38] a) Jones, W. D.; Feher, F. J. *J. Am. Chem. Soc.* **1984,** *106,* 1650–1663., b) Periana, R. A.; Bergman, R. G. *Organometallics* **1984,** *3,* 508–510.

bond activation was found to be 10-50 times faster than the activation of secondary C–H bonds (Figure *10*).[39]

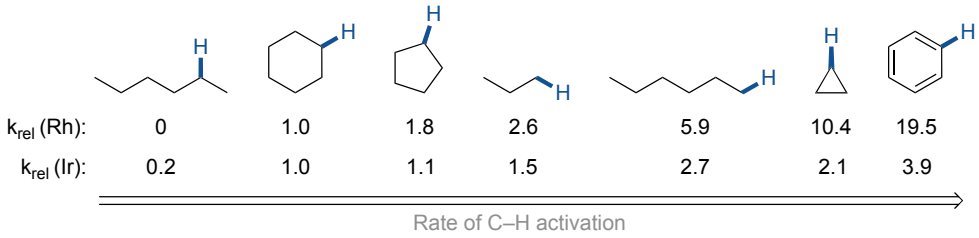



**Figure *10*** Relative rates of C–H activation with Cp*Ir and Cp*Rh complexes

### 4.3.3 Mechanisms of transition metal-promoted C–H activations

Following these early key developments, researchers sought to understand the underlying mechanisms that govern this type of metal-promoted C–H activations. The study of these mechanisms has been crucial in optimizing the efficiency and selectivity of ensuing catalytic processes, allowing for more predictable and controlled transformations. The C–H activation mechanisms depend on the metal center, ancillary ligands and reaction conditions; a summary of these mechanisms is depicted in Figure *11*.[40]

One of the mechanisms involves an oxidative addition to the metal complexes, which is common for low-valent, electron-rich and coordinatively unsaturated transition metals (e.g., Rh, Ir, Ru, Pt). The metal center inserts into the C–H bond, increasing its oxidation state by two units, resulting in a metal-hydride and metal-carbon bond (Figure *11* **A**).

Other mechanistic option is a σ-bond *meta*thesis, typically observed with early transition metals, such as lanthanides or actinides, with $d^0$ or $d^0f^n$ configurations. In this process, there is a concerted exchange between a metal-hydride and a C–H bond, without a change in the metal's oxidation state (Figure *11* **B**).

Another common process relies on single electron transfer processes (SET). This process can be considered to occur in two steps. First the homolytic cleavage of the C–H bond forms a metal-hydride species and a carbon-centered radical. Then, the recombination of the radical with the metal center generates the metal-carbon bond, forming an oxidized alkyl/aryl-hydride metal complex (Figure *11* **C**).

[39] a) Jones, W. D.; Hessell, E. T. *J. Am. Chem. Soc.* **1993,** *115,* 554–562., b) Jones, W. D.; Feher, F. J. *Organometallics* **1983,** *2,* 562–563.
[40] a) Balcells, D.; Clot, E.; Eisenstein, O. *Chem. Rev.* **2010,** *110,* 749–823., b) Boutadla, Y.; Davies, D. L.; Macgregor, S. A.; Poblador-Bahamonde, A. I. *Dalton Trans.* **2009,** 5820–5831., c) Gallego, D.; Baquero, E. A. *Open Chemistry* **2018,** *16,* 1001–1058., d) Roudesly, F.; Oble, J.; Poli, G. *Journal of Molecular Catalysis A: Chemical* **2017,** *426,* 275–296.

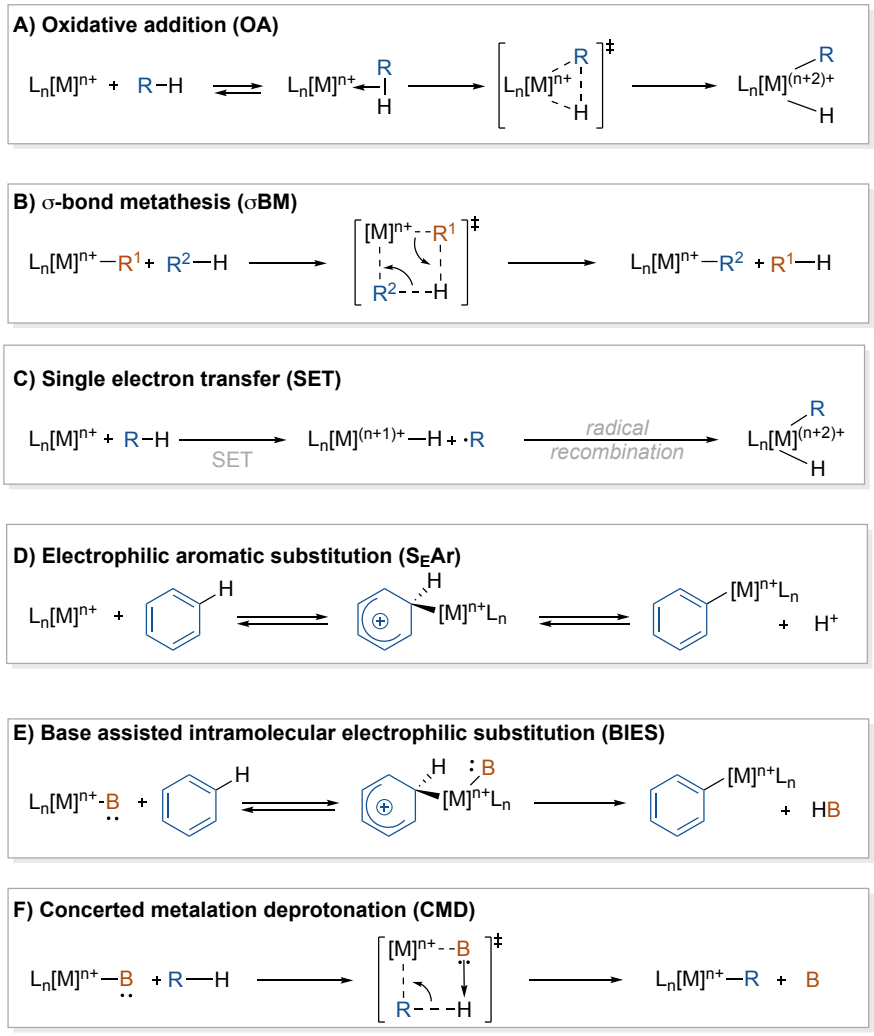



**Figure *11*** Outline of different mechanisms for C–H activations by a metal complex.

When a late transition metal is in a high oxidation state and the substrate has a relatively electron-rich π-component, a metalation mechanism based on an electrophilic substitution can occur. This mechanism involves the formation of delocalized cationic intermediates (e.g., the Wheland intermediate in aromatic systems), followed by proton loss, to yield the metal-carbon bond (Figure *11* **D**). In the case where the base is in the coordination sphere of the metal center, this mechanism is also known as a base-assisted intramolecular electrophilic-type substitution (Figure *11* **E**).

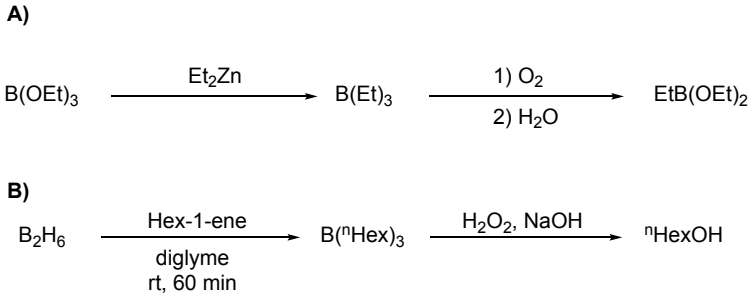
Closely related to the electrophilic substitution mechanism is the so-called concerted metalation deprotonation (CMD) mechanism, which involves the deprotonation of the C–H bond by a base, typically coordinated to the metal center, while the metal simultaneously coordinates to the carbon atom through a cyclic transition state (Figure *11* **F**). This mechanism is most often invoked in reactions catalyzed by Pd(II), Rh(III), and Ru(II) for the selective activation of C–H bonds adjacent to heteroatoms or π-systems that act as directing groups.

USC UNIVERSIDADE DE SANTIAGO DE COMPOSTELA

## 4.4 Synthetic relevance of organoboron compounds

Organoboron derivatives have been and still are among the most versatile reactants in organic chemistry. The synthesis of the first organoboron compounds was reported in 1860 by Frankland and Duppa,[41] who successfully prepared triethyl borane and diethyl ethylborate (Scheme *6* **A**).

Almost a century later, significant progress was made when Brown developed the hydroboration of alkenes using diborane to synthesize trialkylboranes.[42] The resulting borane compounds could be oxidized to alcohols using alkaline peroxide, providing a new synthetic route to alcohols (*Scheme 6* **B**).




**Scheme *6*** Early synthesis and transformations of organoboron compounds.

Twenty years after Brown's discovery, Suzuki and Miyaura described a groundbreaking reaction in which organoboron compounds were cross-coupled with organohalides under palladium (Pd) catalysis, to form $Csp^2$–$Csp^2$ bonds.[43] This reaction, now known as the Suzuki-Miyaura coupling, has become a fundamental transformation in organic synthesis.

Since that discovery, new methods for transformations of C–B bonds have been developed, highlighting the importance of organoboron compounds as versatile intermediates in organic synthesis. These transformations include amination, etherification, thiolation, fluorination, homologation, alkylation, cyanation, or carboxylation, among others (Figure *12*).[44]

[41] Frankland, E.; Duppa, B. F. *Justus Liebigs Ann. Chem.* **1860,** *115,* 319–322.
[42] Brown, H.; Rao, B. C. *J. Org. Chem.* **1957,** *22,* 1136–1137.
[43] a) Miyaura, N.; Suzuki, A. *J. Chem. Soc., Chem. Commun.* **1979,** 866–867., b) Miyaura, N.; Yamada, K.; Suzuki, A. *Tetrahedron Lett.* **1979,** *20,* 3437–3440.
[44] Whiting, A.; Fernández, E. *"Synthesis and Application of Organoboron Compounds".* Springer International Publishing, **2015.**

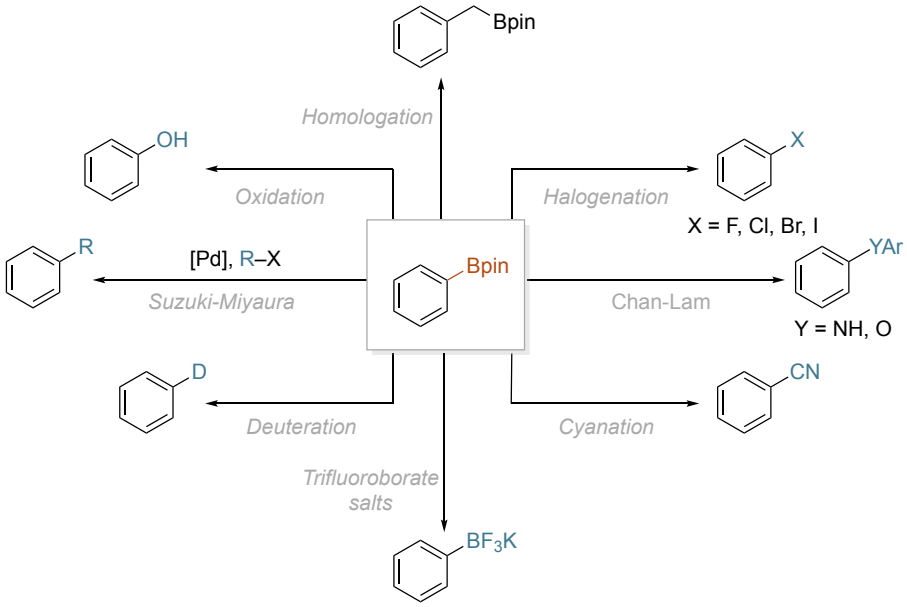


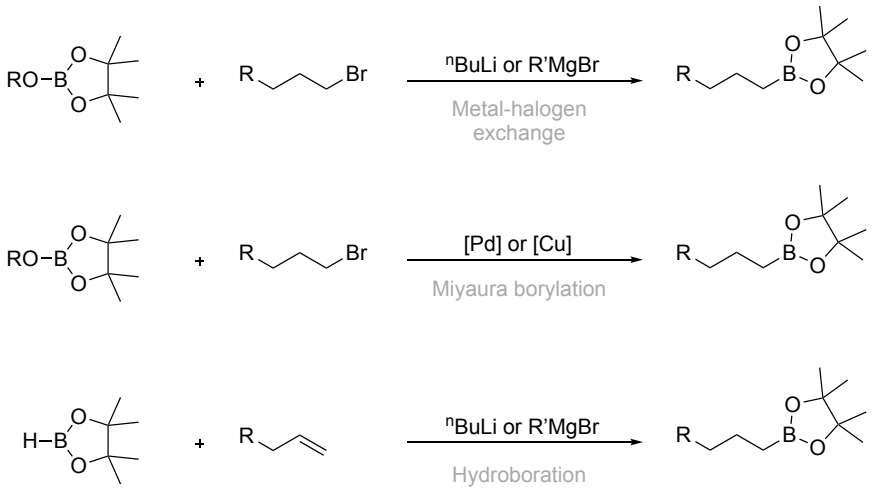

**Figure *12*** Synthetic utility of borylated arenes.

Several organoboron derivatives can participate in these reactions, including boranes, boronic acids, boronate esters, borinic acids, borinic esters, boroxines, and trifluoroborates. Among these, boronate esters are particularly valuable due to their easy handling, and usually good solubility properties. Compared to their organometallic counterparts like organostannanes, organozincs, and organocopper reagents, organoboron compounds offer advantages in terms of stability, ready access, lower toxicity, and more controlled reactivity.

## 4.5 Borylation of C–H bonds, preliminary examples

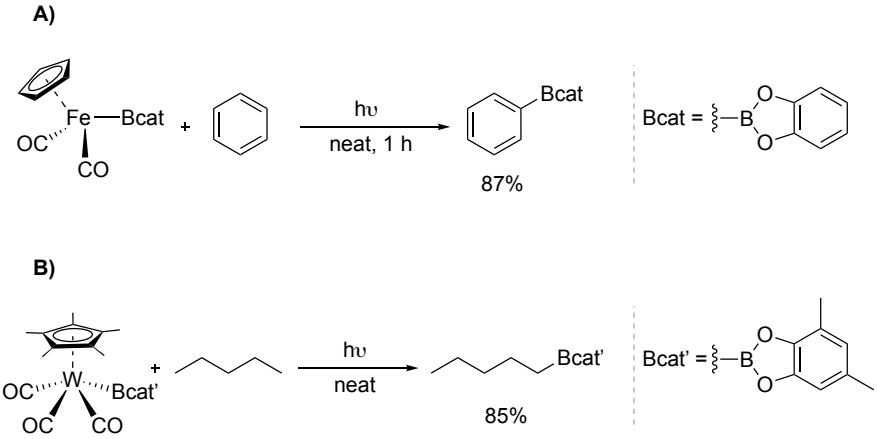
Among the various applications of C–H functionalization reactions, the direct transformation of C–H bonds into C–boron derivatives has emerged as a game-changing technique. Unlike earlier methods such as metal-halogen exchange, hydroboration or Miyaura borylation, which rely on organohalides and multistep transformations (Scheme *7*), C–H borylation offers a more sustainable and direct route to organoboron products without the use of hazardous halogenated reactants.

USC UNIVERSIDADE DE SANTIAGO DE COMPOSTELA




**Scheme *7*** Some methods for the synthesis of organoboranes.

Early metal-promoted C–H borylation processes were often restricted to stoichiometric transformations. Therefore, in 1995 Waltz and Hartwig demonstrated that photochemically generated low-valent Fe, Mn, and Re boryl complexes could convert aryl and vinyl C–H bonds into useful carbon–boron bonds (Scheme *8* A).[45] In 1997, they further discovered that low-valent tungsten boryl complexes could react with alkanes to form alkylboronate esters in high yield (Scheme *8* B).[46]




**Scheme *8*** Early metal-promoted C–H borylation processes.

In 1999, Hartwig and coworkers reported for the first time a catalytic borylation of alkanes with $B_2pin_2$ as boron source, and a rhenium complex as catalyst.[47] The same year, Smith and Maleczka showed that Cp*Ir($PMe_3$)H(Bpin) (Bpin = pinacolboryl) could catalyze the borylation of benzene using pinacolborane as borylating agent (HBpin).[48] Despite the reaction exhibited poor efficiency, achieving only three turnovers after five days of heating at 150 °C, this report triggered many other developments in the field. In the year 2000, the

[45] Waltz, K. M.; He, X.; Muhoro, C.; Hartwig, J. F. *J. Am. Chem. Soc.* **1995,** *117,* 11357–11358.
[46] Waltz, K. M.; Hartwig, J. F. *Science* **1997,** *277,* 211–213.
[47] Chen, H.; Hartwig, J. F. *Angew. Chem. Int. Ed.* **1999,** *38,* 3391–3393.
[48] Iverson, C. N.; Smith, M. R. *J. Am. Chem. Soc.* **1999,** *121,* 7696–7697.

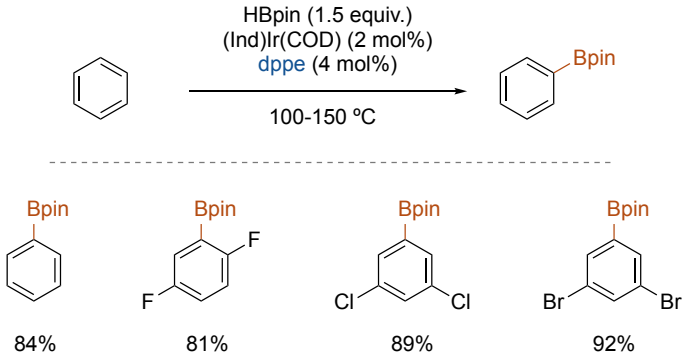
same authors, as well as Hartwig and coworkers, reported a rhodium-catalyzed version of these processes.[49]

Currently, the scope of metal-promoted catalytic C–H borylations includes a wide range of substrate classes, such as aryl, benzylic, and primary, secondary, or tertiary alkyl C–H bonds. While there are reactions promoted by complexes with different transition metals, iridium (Ir)[50] has proven to be the more effective metal for C–H borylation processes, not only because of its electronic characteristics, but also because of its coordination and redox versatility. In many cases the reactions are guided by directing groups present in the substrates.

## 4.6 Iridium-catalyzed C–H borylations of aromatic systems

### 4.6.1 Initial results, regioselectivity and mechanistic rational

Following the initial 1999 report, Smith III and Maleczka advanced C–H borylations of aromatic systems by employing a catalytic system based on (Ind)Ir(COD) combined with a bisphosphine ligand (Scheme *9*).[51]




**Scheme *9*** Aryl C-H borylation catalyzed by an Ir-bisphosphine complex.

This new catalytic approach delivered faster reaction rates and demonstrated broader functional group compatibility than the rhodium-catalyzed process. The regioselectivity of the reaction was primarily influenced by the steric properties of the arene substrate, as seen in the selective borylation at the 5-position of 1,3-disubstituted arenes. This selectivity, which contrasted with traditional electrophilic aromatic substitution (EAS), provided a more direct route to synthesizing 1,3,5-trisubstituted arenes. Despite these advances, the requirement for high temperatures (100-150 °C) and neat conditions remained as limitations.

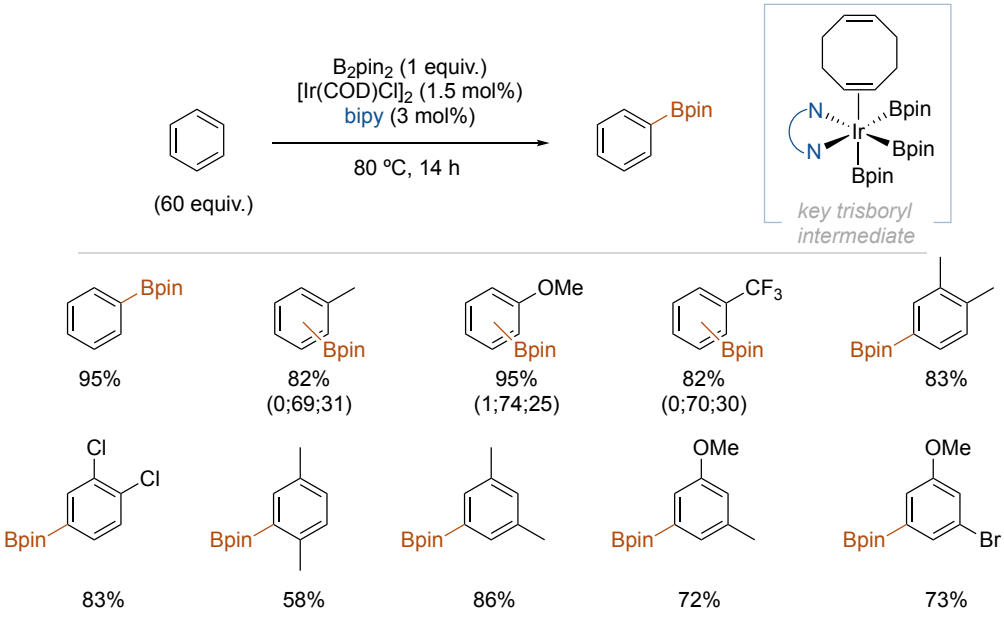
---

[49] a) Chen, H.; Schlecht, S.; Semple, T. C.; Hartwig, J. F. *Science* **2000,** *287,* 1995–1997., b) Cho, J.; Iverson, C. N.; Smith, M. R. *J. Am. Chem. Soc.* **2000,** *122,* 12868–12869.

[50] a) Alvarez, L. W.; Alvarez, W.; Asaro, F.; Michel, H. V. *Science* **1980,** *208,* 1095–1108., b) Payne, D. *Nat. Chem.* **2016,** *8,* 392–392., c) Tennant, S. *Phil. Trans. R. Soc. Lon* **1804,** *94,* 411–418.

[51] Cho, J.; Tse, M. K.; Holmes, D.; Maleczka, R. E.; Smith, M. R. *Science* **2002,** *295,* 305–308.

Around the same time, Ishiyama, Miyaura, Hartwig, and co-workers developed a more efficient aryl C–H borylation of simple arenes using $B_2pin_2$ as borylating reagent. Their system utilized catalysts derived from $[Ir(COD)Cl]_2$ or $[Ir(OMe)(COD)]_2$ in combination with 2,2'-bipyridine (**bipy**) or 4,4'-di-*tert*-butylbipyridine (**dtbpy**) as bidentate neutral ligands ( L–L).[52] Importantly, they identified a trisboryl intermediate as the resting state of the catalyst (Scheme *10*). This new catalytic system proved more efficient, operating at relatively lower temperatures (80 °C) and demonstrating superior activity compared to phosphine-based ligands. Additionally, further investigations revealed that this catalytic system allowed the reactions to proceed in other solvents, a notable improvement over the neat arene conditions required by the earlier Smith and Maleczka system.




**Scheme *10*** Iridium-catalyzed arene C-H borylation with a bipyridine ligand. The regioisomeric mixtures refer to *ortho*/*meta*/*para* proportions. Yields based on $B_2pin_2$

The mechanistic studies suggested the formation of a Ir(III) tris-boryl species $[Ir(bipy)(COE)(Bpin)_3]$ as the pre-assembled catalyst entering the catalytic cycle (Figure *13*, Intermediate **I**). The rate-determining step (RDS) was found to be the oxidative addition of this Ir(III) species into the C($sp^2$)–H bond, forming an Ir(V) intermediate (**III**). Isotopic labeling and kinetic studies revealed a substantial primary kinetic isotope effect, with the overall reaction rate being first order in arene, zero order in $B_2pin_2$, and half order in the catalyst.[53]

[52] a) Ishiyama, T.; Takagi, J.; Ishida, K.; Miyaura, N.; Anastasi, N. R.; Hartwig, J. F. *J. Am. Chem. Soc.* **2002a,** *124,* 390–391., b) Ishiyama, T.; Takagi, J.; Hartwig, J. F.; Miyaura, N. *Angew. Chem. Int. Ed.* **2002b,** *41,* 3056–3058.

[53] Boller, T. M.; Murphy, J. M.; Hapke, M.; Ishiyama, T.; Miyaura, N.; Hartwig, J. F. *J. Am. Chem. Soc.* **2005,** *127,* 14263–14278.

Computational studies by Sakaki further supported this mechanism.[54] After reductive elimination of the borylated product, the $B_2pin_2$ would undergo an oxidative addition to regenerate an active Ir(III) tris-boryl complex (**II**).

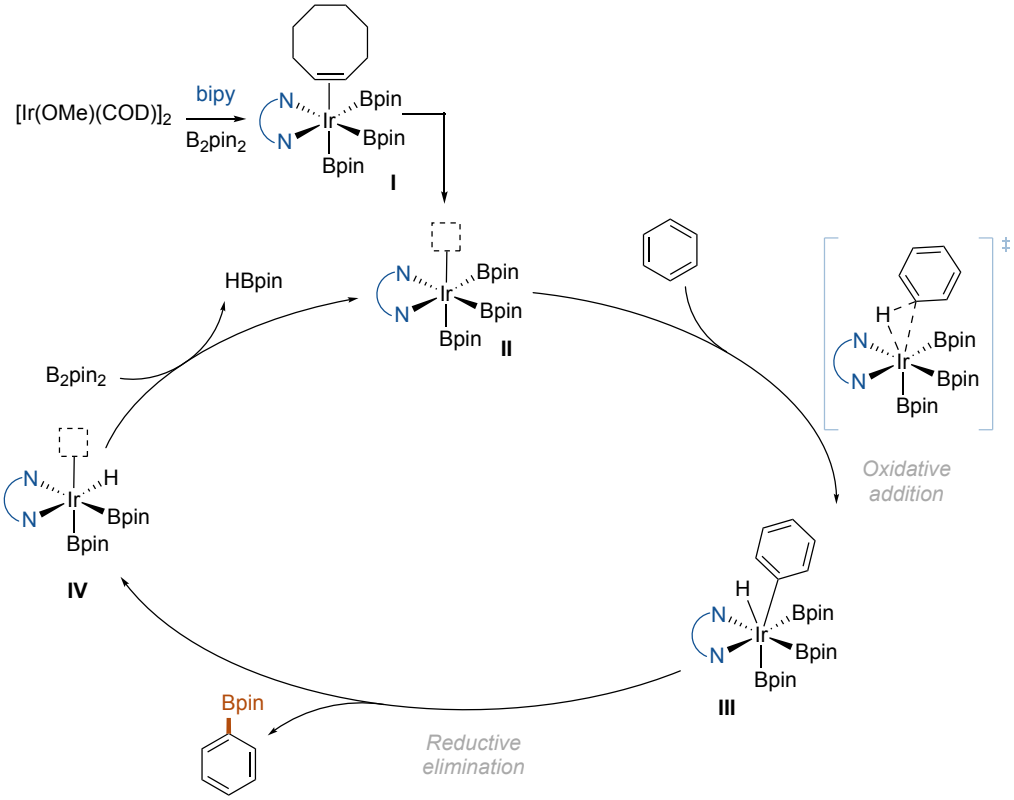


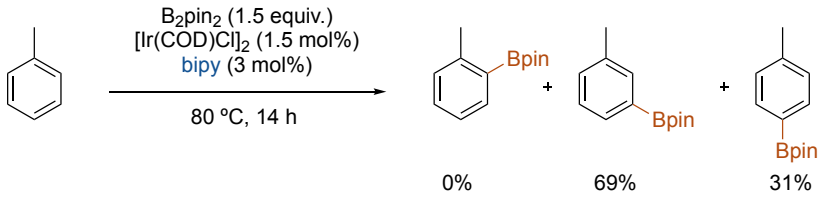

**Figure *13*** Mechanistic outline of the aromatic C–H borylation process. N-N refers to a 2,2'-bipyridine type ligand (L–L).

After these key developments, various research groups focused on developing new ligands that could further enhance the reactivity and tune the regioselectivity. In these iridium-catalyzed C–H borylations (CHBs) based on the use of bidentate neutral L–L type of ligands such as 2,2'-bipyridines or 1-10-phenanthrolines, the regioselectivity is generally governed by steric effects.[55]

For example, in the case of a monosubstituted arene like toluene, the reaction typically yields a statistical ratio of 2:1 for *meta* and *para* borylated products (Scheme *11*).[52]

[54] Hitoshi Tamura; Hideki Yamazaki; Hirofumi Sato; Shigeyoshi Sakaki *J. Am. Chem. Soc.* **2003,** *125,* 16114–16126.

[55] Caldeweyher, E.; Elkin, M.; Gheibi, G.; Johansson, M.; Sköld, C.; Norrby, P.; Hartwig, J. F. *J. Am. Chem. Soc.* **2023,** *145,* 17367–17376.

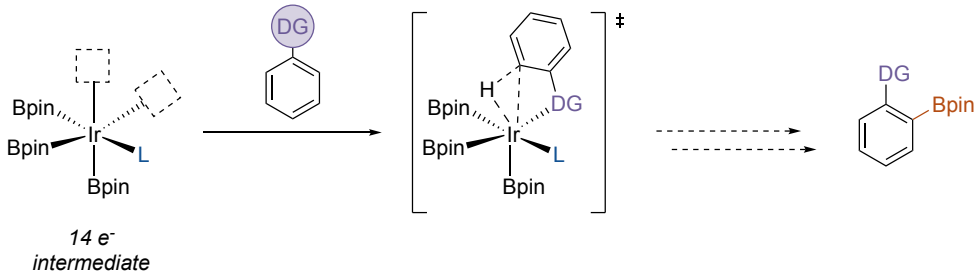



**Scheme *11*** Regioselectivity of an Ir-catalyzed borylation using bipyridine (**bipy**) as ligand.

### 4.6.2 Monodentate ligands (L)

A major and ongoing endeavor in this powerful chemistry is the development of strategies for leveraging the presence of a directing group and thus controlling the regioselectivity. One of these strategies is based on the use of monodentate (L) instead of bidentate neutral ligands.

By adjusting the stoichiometry, monodentate ligands provide complexes with two vacant coordination sites, which can coordinate with a directing group (DG) of the substrate (Scheme *12*). This coordination, not only facilitates the C-H activation, but also directs it to the *ortho* position.[56]




**Scheme *12*** Monodentate ligand coordination with Ir metal and C–H borylation.

The mechanism is analogous to the one described for canonical L–L ligands but begins with a 14-electron iridium complex with two vacant coordination sites (Intermediate **II,** *Figure 14*). At this stage, a directing group in the substrate coordinates to the metal center, forming Intermediate **III**.

Subsequently, oxidative addition occurs to the ortho C-H bond, leading to the formation of the cyclometallated intermediate (**IV**). This species then undergoes reductive elimination, ultimately yielding the expected borylated product.[57]

[56] Xu, L.; Wang, G.; Zhang, S.; Wang, H.; Wang, L.; Liu, L.; Jiao, J.; Li, P. *Tetrahedron* **2017,** *73,* 7123–7157.
[57] Jover, J.; Maseras, F. *Organometallics* **2016,** *35,* 3221–3226.

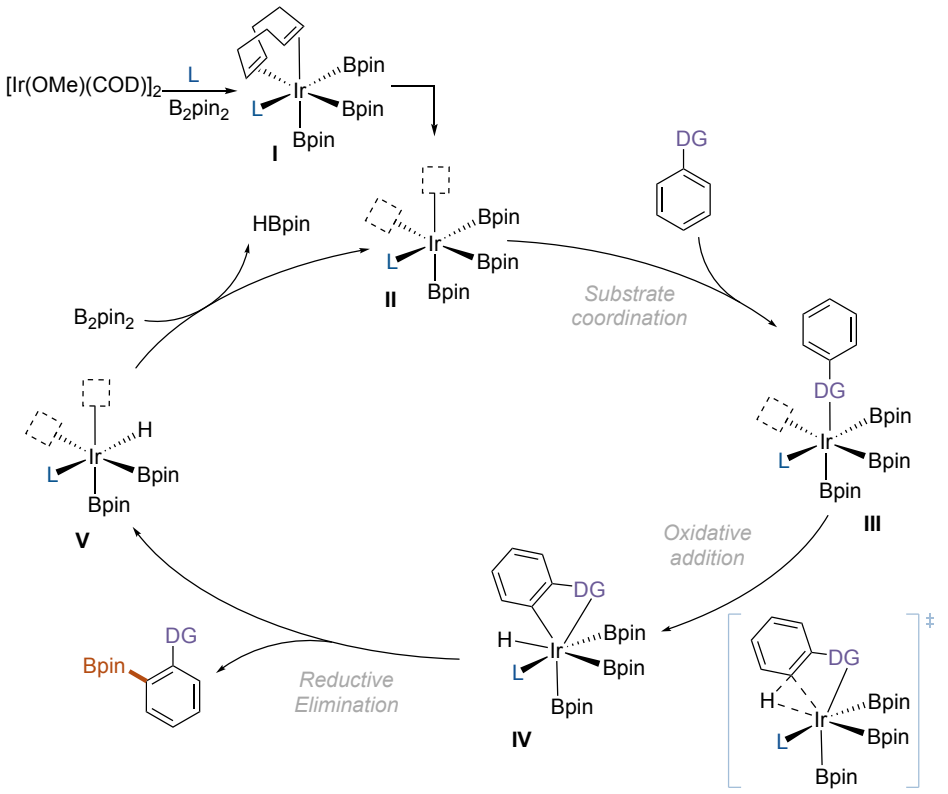
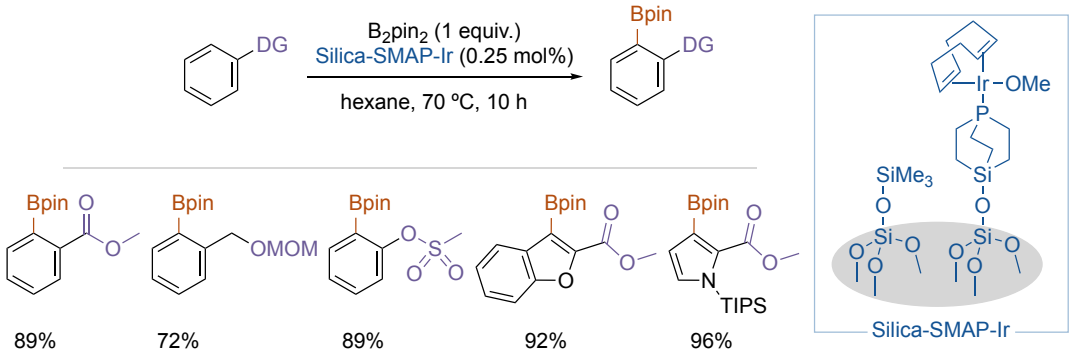



**Figure *14*** General mechanism for Ir borylations using monodentate neutral ligands (L).

The Sawamura group pioneered an innovative approach for *ortho*- C–H borylations of aromatic systems using a heterogeneous iridium catalytic system in combination with a monodentate phosphine ligand embedded within a silica framework (Scheme *13*). The method is now widely recognized as Sawamura's borylation or Ir-SMAP.[58]

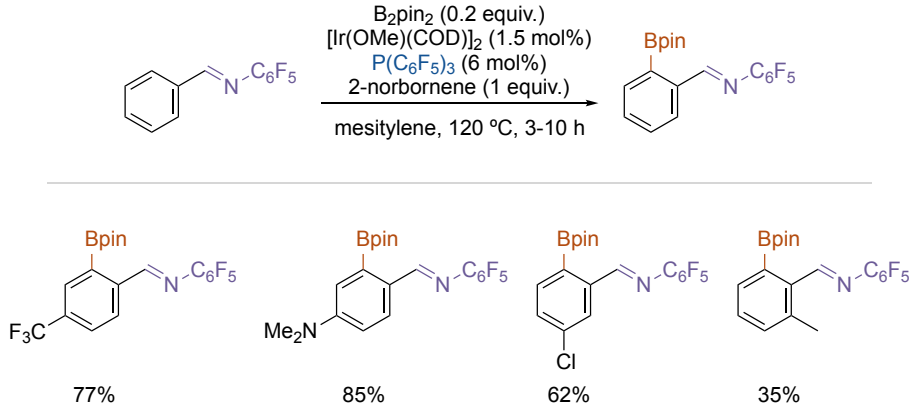



**Scheme *13*** Sawamura's solid supported Silica SMAP *ortho*-borylation.

Despite the impressive activity of the catalysts, and the good *ortho*-selectivity, the synthesis of this catalytic system is complex, involving multiple challenging steps, which restricts a broad adoption.

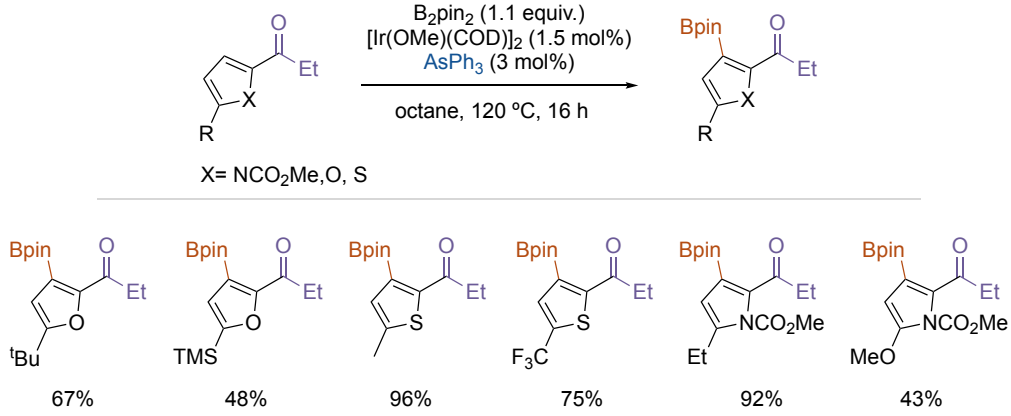
[58] a) Kawamorita, S.; Ohmiya, H.; Hara, K.; Fukuoka, A.; Sawamura, M. *J. Am. Chem. Soc.* **2009,** *131,* 5058–5059., b) Kawamorita, S.; Ohmiya, H.; Sawamura, M. *J. Org. Chem.* **2010,** *75,* 3855–3858., c) Konishi, S.; Kawamorita, S.; Iwai, T.; Steel, P. G.; Marder, T. B.; Sawamura, M. *Chem. Asian J.* **2014,** *9,* 434–438., d) Yamazaki, K.; Kawamorita, S.; Ohmiya, H.; Sawamura, M. *Org. Lett.* **2010,** *12,* 3978–3981.

The Ishiyama's group focused on developing appropriately designed electron-deficient phosphines as ligands, assuming that they would coordinate iridium in monodentate manner. Their research led to the development of a catalytic system that enabled highly selective *ortho*-borylations of a variety of arenes. By employing $[Ir(COD)(OMe)]_2$ in combination with $P(C_6F_5)_3$, and an excess of arene substrate, they were able to obtain *ortho*-borylated products, although the reaction required elevated temperatures (Scheme *14*).[59]




**Scheme *14*** Ishiyama electron-deficient phosphines borylation. Yields based on $B_2pin_2$.

The same group also explored alternative monodentate ligands such as $AsPh_3$,[60] which allowed a good control of the regioselectivity in the borylation of carbonyl-substituted heterocycles, expanding the range of substrates suitable for iridium-catalyzed borylations (Scheme *15*).

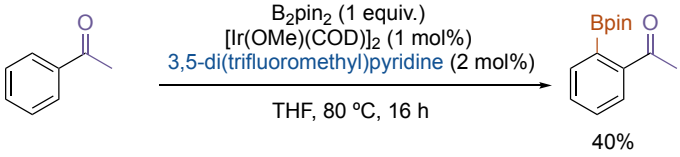



**Scheme *15*** Ito and Ishiyama borylation using $AsPh_3$ as iridium ligand.

More recently, in 2019, Smith III and co-workers patented an approach that employs 3,5-di(trifluoromethyl)pyridine as monodentate ligands for selective *ortho* iridium-catalyzed C–H borylations in substrates with carbonyl directing groups (Scheme *16*).

[59] Sasaki, I.; Amou, T.; Ito, H.; Ishiyama, T. *Org. Biomol. Chem.* **2014,** *12,* 2041–2044.
[60] Sasaki, I.; Taguchi, J.; Hiraki, S.; Ito, H.; Ishiyama, T. *Chem. Eur. J.* **2015,** *21,* 9236–9241.

They obtained excellent regioselectivity, although the reaction yields were modest.[61]

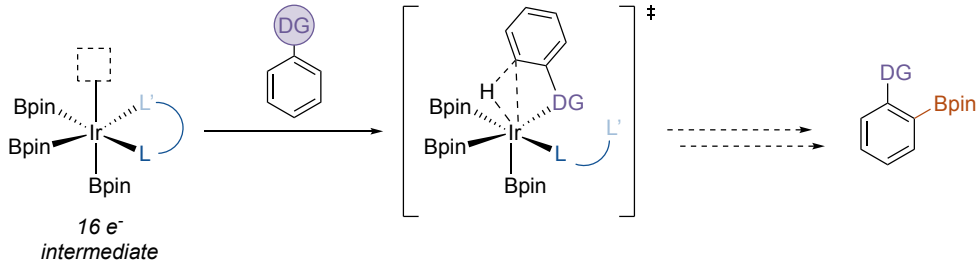



**Scheme *16*** Carbonyl-directed borylations using electron-deficient pyridines as ligands.

Despite these successful examples, the above strategy presents important limitations associated to the difficulty of avoiding the coordination of two ligands to the iridium center, which hampers the effect of the directing group and therefore compromises the reactivity and regiocontrol.

### 4.6.3 Hemilabile ligands (L–L')

Hemilabile ligands are employed as a solution to address the issue of multicoordination of several monodentate ligands to the iridium, which harms the reactivity and especially the regioselectivity. Hemilabile ligands typically consist of a strong donor, such as a pyridine ring, that coordinates tightly to the iridium center, paired with a secondary donor, such as an amine, which can easily dissociate to create an open coordination site (Scheme *17*).




**Scheme *17*** Hemilabile ligand coordination with Ir metal and C–H borylation.

These ligands present a hybrid behavior between bidentate and monodentate ligands. The proposed catalytic cycle starts with a 16 $e^-$ intermediate (**II**) which can coordinate to the directing group in the substrate generating a stable 18 $e^-$ intermediate (III). In this complex the more labile ligand L' can dissociate from the Ir center to yield an intermediate like **IV**, that presents a vacant for the oxidative addition of the closest C–H bond, generating the cyclometalated intermediate **V** (Figure *15*) Finally, reductive elimination would generate the desired product and the hemilabile ligand would again coordinate to the iridium with both L groups to regenerate the active catalytic species.[62]

[61] Smith III, M. R.; Maleczka, R. E.; Li, H.; Jayasundara, C. R. K.; Oppenheimer, J.; Sabasovs, D. .,US20190062350A1**,2019.**

[62] Haldar, C.; Hoque, M. E.; Chaturvedi, J.; Hassan, M. M. M.; Chattopadhyay, B. *Chem. Commun.* **2021,** *57,* 13059–13074.

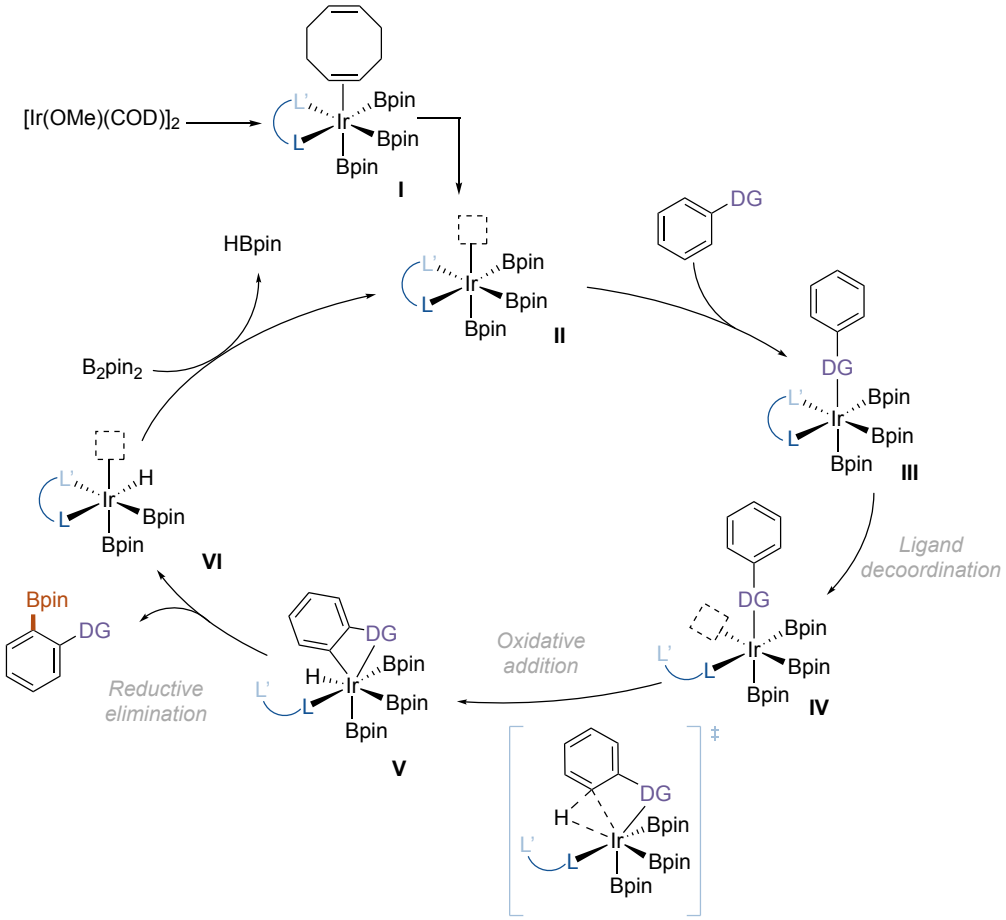
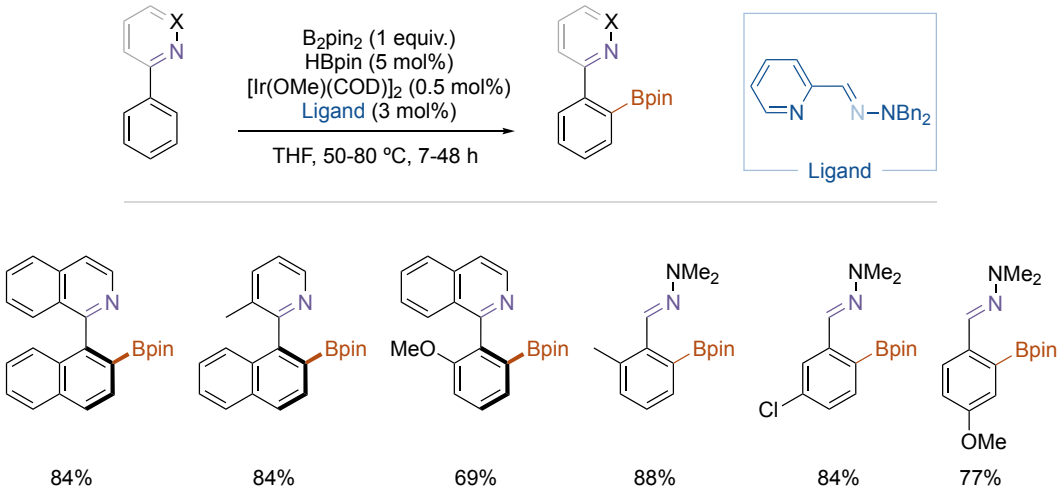



**Figure *15*** Proposed mechanism for C–H borylation using hemilabile ligands.

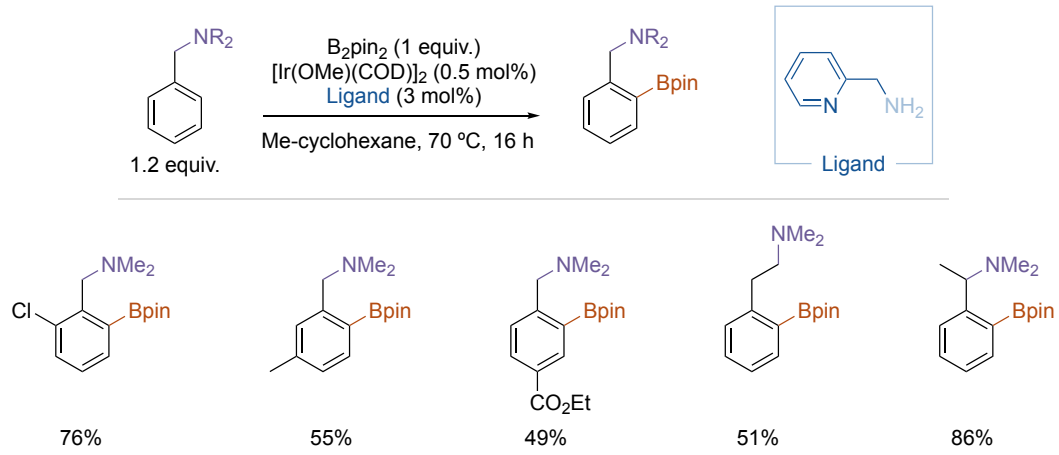
The Fernández and Lasaletta group made significant contributions in this topic by utilizing pyridine N,N-dimethyl hydrazones as hemilabile ligands (Scheme *18*).




**Scheme *18*** Borylation with hemilabile ligands developed by Fernández and Lasaletta.

With this new ligand they were able to optimize the regioselectivity in the borylation of 2-aryl pyridines and aryl hydrazones, obtaining the corresponding *ortho*-borylated products with good yields.[63]

The Clark's group contributed to this concept by using picolylamine as a hemilabile ligand, successfully achieving selective *ortho*-borylation in benzylamines when using a slight excess of substrate (Scheme *19*). However, this method was limited in scope, as no borylated products were obtained when applied to substrates with other directing groups.[64]



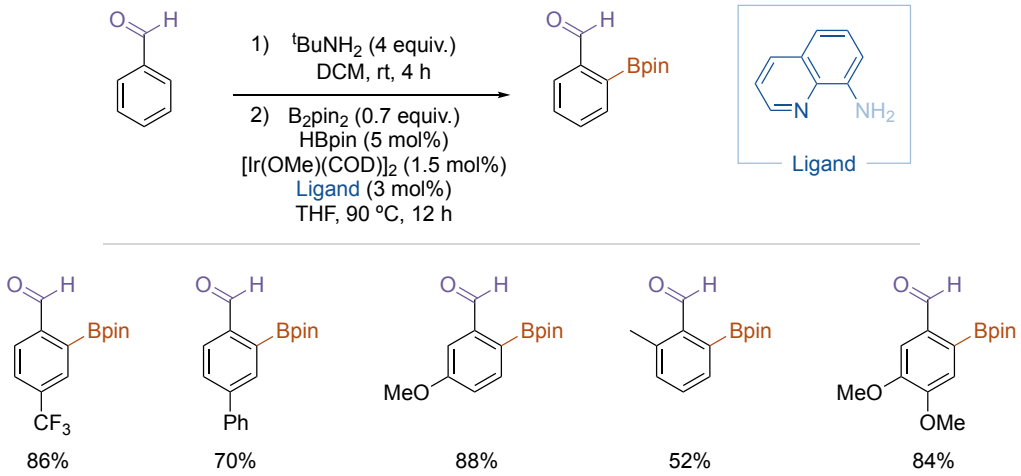

**Scheme *19*** Borylation with picolylamine ligands developed by Clark and coworkers.

More recently, Chattopadhyay and colleagues expanded the use of hemilabile ligands, demonstrating that with 8-aminoquinoline it is possible to achieve the *ortho*-selective borylation of aromatic aldehydes (Scheme *20*). The reaction requires the use of *tert*-butylamine as additive to generate a transition imine directing group.[65]

[63] a) López-Rodríguez, R.; Ros, A.; Fernández, R.; Lassaletta, J. M. *J. Org. Chem.* **2012,** *77,* 9915–9920., b) Ros, A.; Estepa, B.; López-Rodríguez, R.; Álvarez, E.; Fernández, R.; Lassaletta, J. M. *Angew. Chem. Int. Ed.* **2011,** *50,* 11724–11728., c) Ros, A.; López-Rodríguez, R.; Estepa, B.; Álvarez, E.; Fernández, R.; Lassaletta, J. M. *J. Am. Chem. Soc.* **2012,** *134,* 4573–4576.

[64] a) Hale, L. V. A.; McGarry, K. A.; Ringgold, M. A.; Clark, T. B. *Organometallics* **2015,** *34,* 51–55., b) Roering, A. J.; Hale, L. V. A.; Squier, P. A.; Ringgold, M. A.; Wiederspan, E. R.; Clark, T. B. *Org. Lett.* **2012,** *14,* 3558–3561.

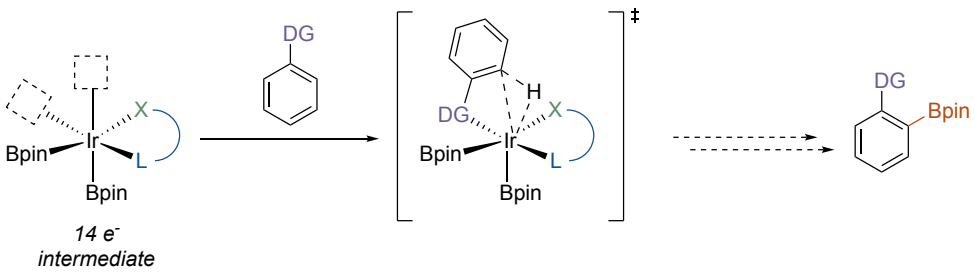
[65] Bisht, R.; Chattopadhyay, B. *J. Am. Chem. Soc.* **2016,** *138,* 84–87.




**Scheme *20*** Borylation reactions using 8-aminoquinoline ligands.

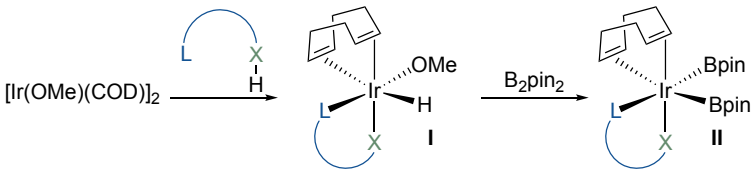
## 4.6.4 Bidentate monoanionic ligands (L–X)

Another type of ligands capable of generating 14-electron Iridium(III) intermediates and therefore allow directed borylation processes, are bidentate ligands based on an anionic and a neutral moiety (L–X), because they allow the generation of two vacant sites in the iridium complex (Scheme *21*).




**Scheme *21*** Directed *ortho*-borylation using a monoanionic bidentate ligand (L–X)

In most cases, the monoanion ligand is generated by oxidative addition of a Si–H or B–H bond to an Ir(I) precatalyst. This process produces an Ir(III)–H complex **I**, that after reaction with $B_2pin_2$ generates the catalytically active bisboryl complex **II** (Scheme *22*).




**Scheme *22*** Monoanionic bidentate ligand precursor (X is usually B or Si).

In this 14-electron intermediate, the iridium center has two vacant coordination sites. These open sites allow the complex to coordinate a directing group from the substrate to give intermediate **III** (Figure *16*), which is the one involved in the C–H activation to give the cyclometalated intermediate **IV**. After the oxidative addition, the complex undergoes reductive elimination, yielding the desired borylated product.

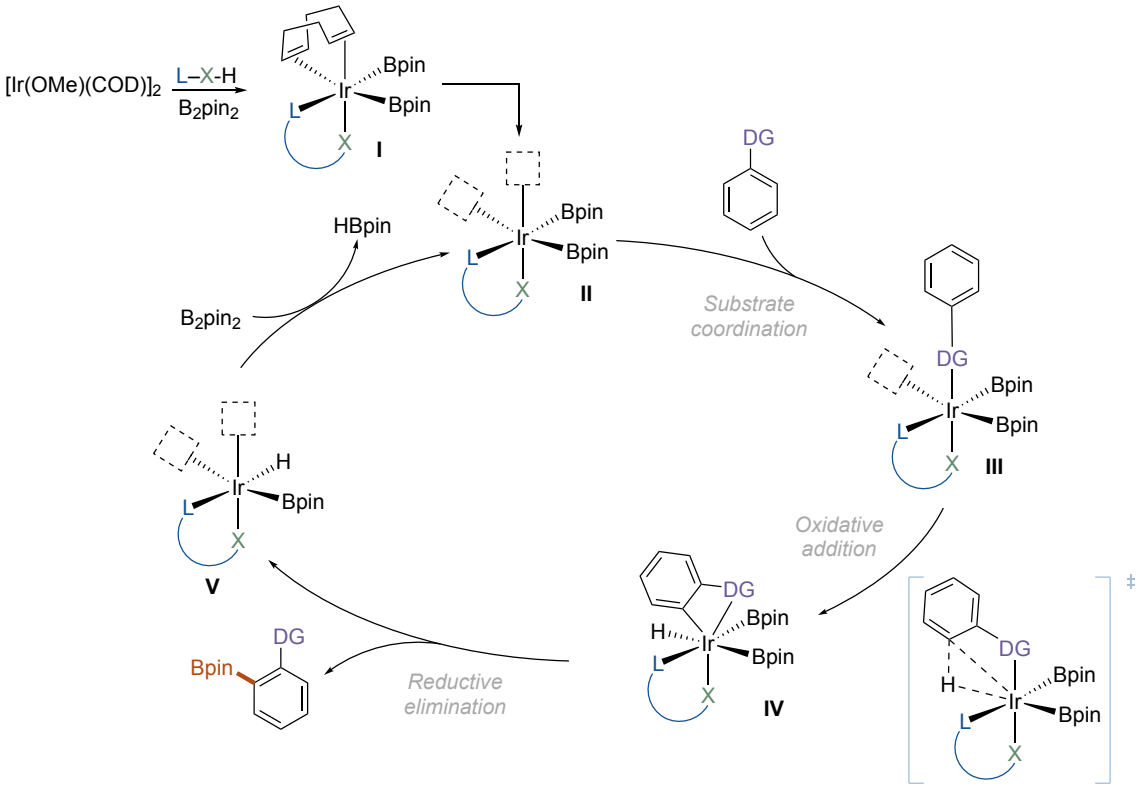
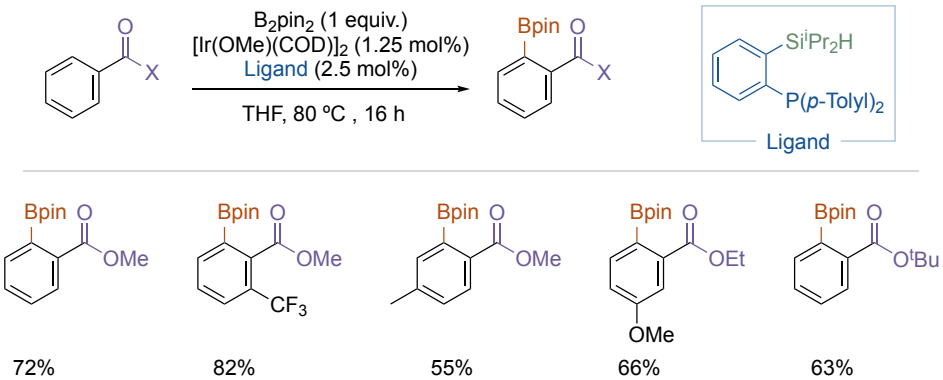



**Figure *16*** General mechanism for C–H borylation using monoanionic bidentate ligands.

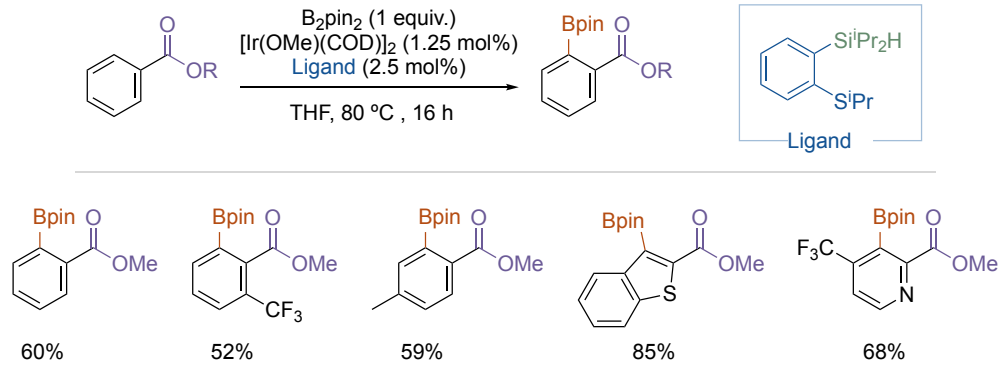
Several groups have developed C–H borylation reactions based on this type of ligands. In 2014, Smith III's group demonstrated that phosphine silane moieties can be used as ligand precursors in the *ortho*-C–H borylation of aromatic ester substrates.[66] The reaction starts by oxidative addition of the Si–H bond of the silane to the Ir(I) complex, to generate the active catalyst, that proceeds through the previously described mechanism to yield the corresponding *ortho*-borylated products.




**Scheme *23*** *Ortho* C-H borylation developed by Smith III and coworkers based on the use a P-Si bidentate ligand.

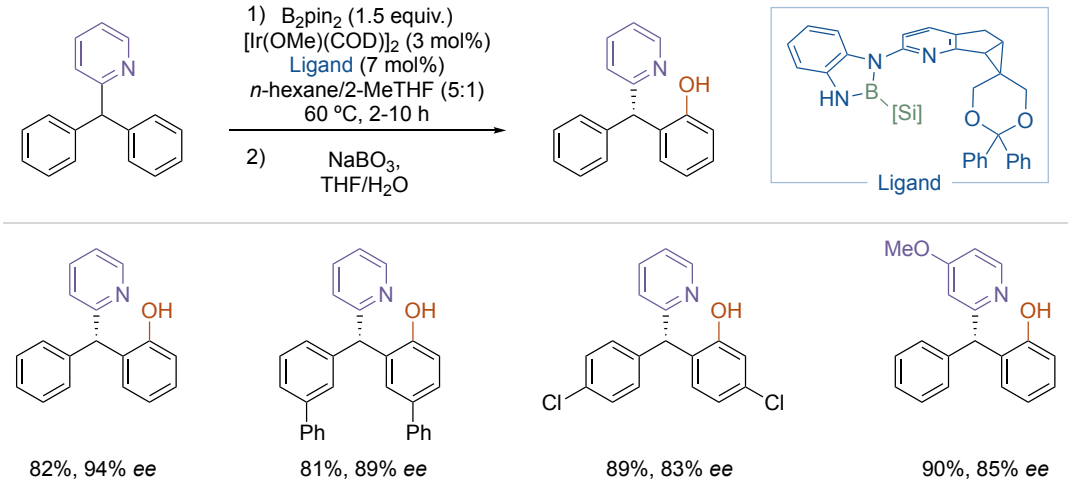
[66] Ghaffari, B.; Preshlock, S. M.; Plattner, D. L.; Staples, R. J.; Maligres, P. E.; Krska, S. W. K.; Maleczka, R. E.; Smith III, M. R. *J. Am. Chem. Soc.* **2014,** *136,* 14345–14348.

Building on the same concept and ligand geometry, Pengfei Li's group introduced a modified ligand featuring a sulfur moiety in place of phosphine, which rendered the ligand air-stable.[67] This modification enabled the successful *ortho*-borylation of a wide range of esters, albeit with moderate yields.




**Scheme *24*** *Ortho* borylations based on the use of S-Si bidentate ligands.

The same group also reported a pyridine sylilborane ligand precursor that allows the *ortho*-borylation of a wide variety of substrates equipped with pyridine directing groups.[68] Building on that concept they developed a chiral ligand which allowed to obtain highly enantioselective iridium-catalyzed C–H borylation of diaryl(2-pyridyl)methanes.[69]

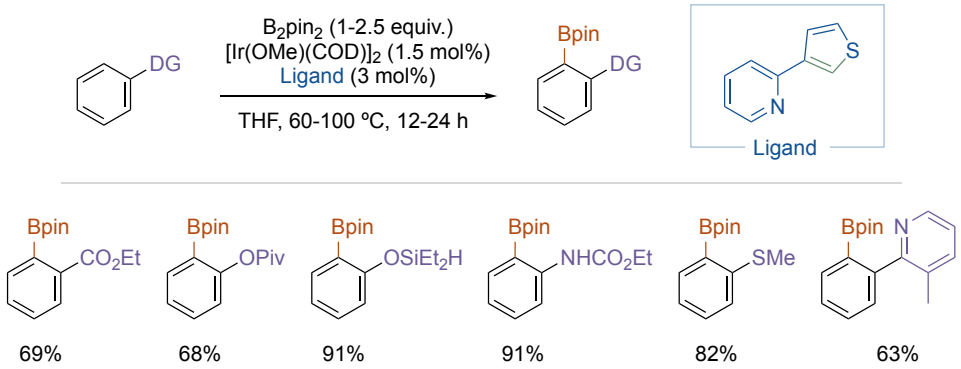



**Scheme *25*** Enantioselective *ortho* borylations using a chiral B-N ligand.

In 2021, the Chattopadhyay's group introduced a stable iridium complex that used a pyridyl-thienyl derivative as ligand (Scheme *26*). This system exploited the acidity of the $C_2$–H bond in thiophene to generate the required L–X (nitrogen-carbon) ligand by oxidative addition to the iridium pre catalyst. The reaction shows a good scope, allowing the

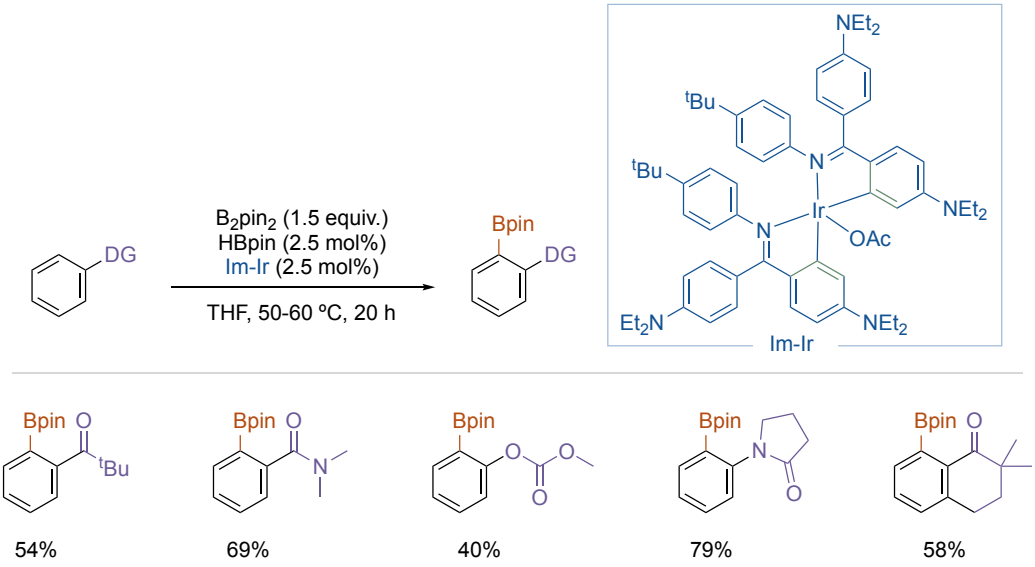
[67] Jiao, J.; Nie, W.; Song, P.; Li, P. *Org. Biomol. Chem.* **2021,** *19,* 355–359.
[68] Wang, G.; Liu, L.; Wang, H.; Ding, Y.; Zhou, J.; Mao, S.; Li, P. *J. Am. Chem. Soc.* **2017,** *139,* 91–94.
[69] Song, P.; Hu, L.; Yu, T.; Jiao, J.; He, Y.; Xu, L.; Li, P. *ACS Catal.* **2021,** *11,* 7339–7349.

selective *ortho*borylation of a wide variety of substrates exhibiting different directing groups.[70]




**Scheme *26*** *Ortho*-borylation of aromatic esters using a nitrogen-carbon bidentate monoanionic ligand formed in situ through a C-H activation of the thiophene moiety.

In 2024, Joanna Wencel-Delord's group employed high-throughput screening techniques to explore a variety of preformed C–N ligands, leading to the discovery of an air-stable iridium (III) precatalyst featuring two triarylimine ligands (Scheme *27*). This bis-cyclometallated iridium complex undergoes initial activation with HBpin, followed by the elimination of one of the cyclometallated imines, generating the active catalyst. This system showed consistent *ortho*-selectivity in the C–H borylation of benzamide substrates and proved versatile across a broad range of directing groups.[71]



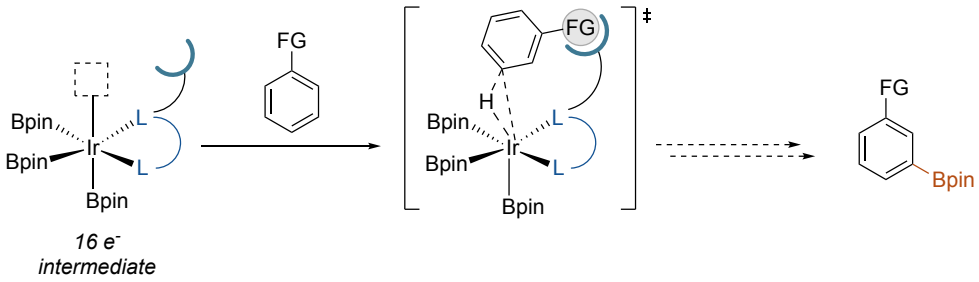

**Scheme *27*** *Ortho*borylation using precatalysts with triarylimine ligands.

[70] Hoque, M. E.; Hassan, M. M. M.; Chattopadhyay, B. *J. Am. Chem. Soc.* **2021,** *143,* 5022–5037.
[71] Zakis, J. M.; Messinis, A. M.; Ackermann, L.; Smejkal, T.; Wencel-Delord, J. *Adv. Synth. Catal.* **2024,** *366,* 2292–2304.

### 4.6.5 Supramolecular control of the regioselectivity by using designed bidentate L–L ligands

Most of the above reactions allow to control the *ortho*-regioselectivity in the borylation reaction because of a direct coordination of a donor, directing group of the substrate to a vacant coordination site of the iridium catalyst. Changing the regioselectivity from *ortho*- to *meta*- and/or *para*- represents a considerable challenge.

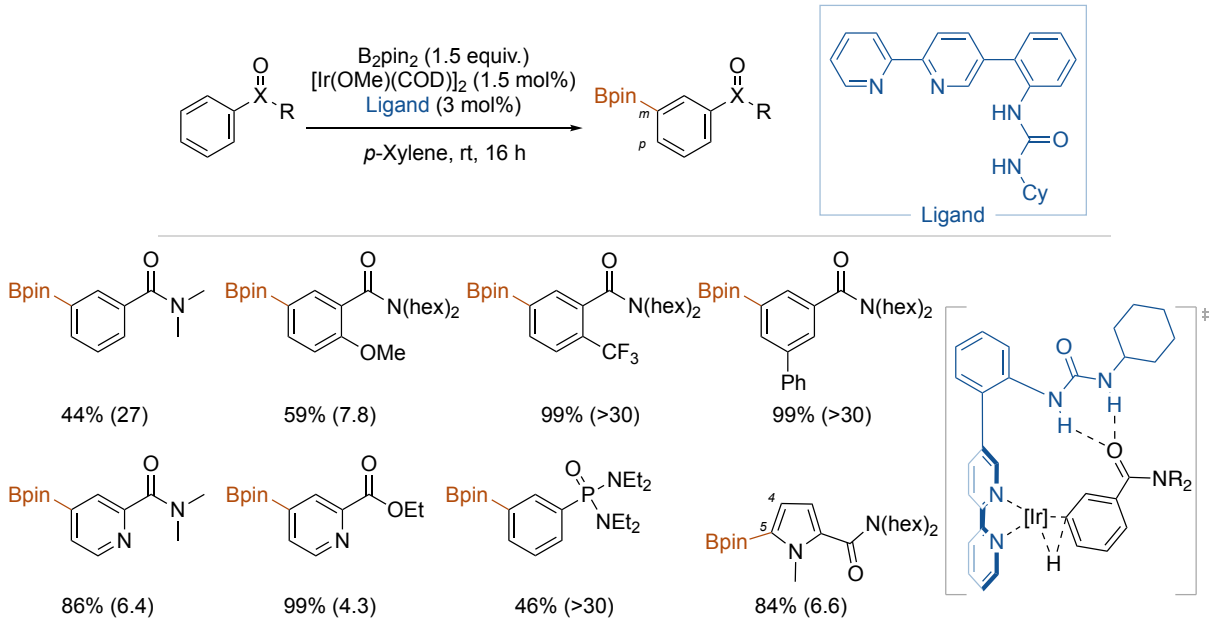
Several research groups have addressed this challenge making L–L ligands equipped with specific functional groups capable of establishing outer-sphere supramolecular interactions with the substrate (Scheme *28*). As a result, these modified ligands can fine-tune the regioselectivity of the reaction, while preserving the reactivity provided by the bidentate neutral ligands.




**Scheme *28*** Outer sphere directed C-H borylations guided by non-covalent interactions between ligand and the substrate.

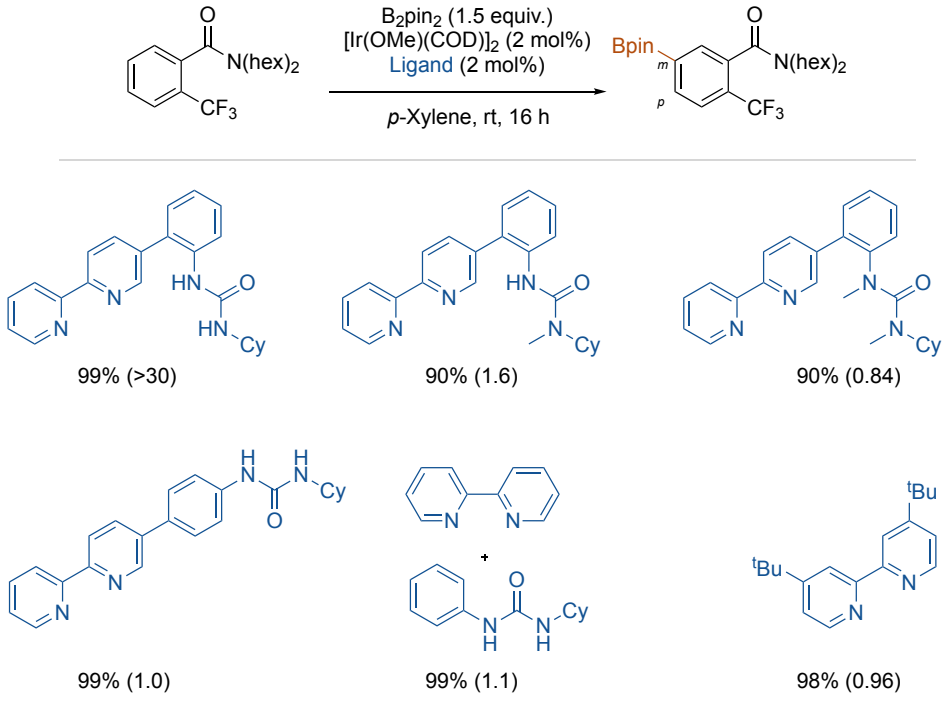
Kanai and Kuninobu pioneered this approach by developing a bipyridine ligand with a urea moiety, which is able to promote *meta*-selective CHB in benzamides and related substrates. This selectivity was suggested to arise from the establishment of hydrogen bond interactions between the urea and the carbonyl acceptor of the substrates, as outlined in the proposed transition state structure in Scheme *29*.[72]

[72] a) Kuninobu, Y.; Ida, H.; Nishi, M.; Kanai, M. *Nature Chem* **2015,** *7,* 712–717., b) Lu, X.; Yoshigoe, Y.; Ida, H.; Nishi, M.; Kanai, M.; Kuninobu, Y. *ACS Catal.* **2019,** *9,* 1705–1709., c) Wang, J.; Torigoe, T.; Kuninobu, Y. *Org. Lett.* **2019,** *21,* 1342–1346.



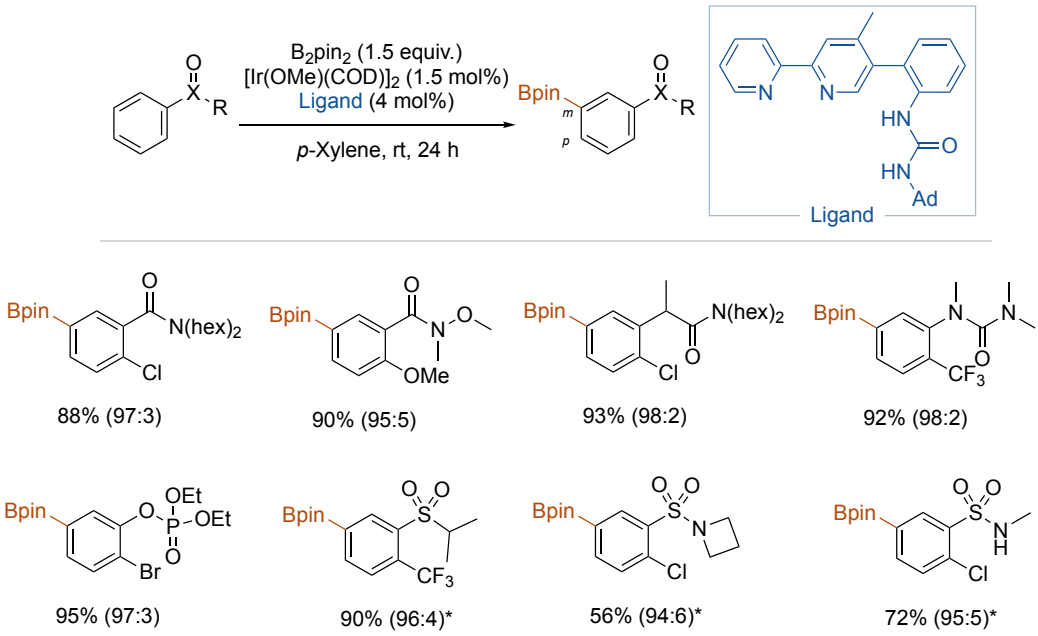

**Scheme *29*** *Meta* selective borylation guided by out sphere H-bonding interactions. Ratio *meta/para* in parenthesis.

As depicted in Scheme *30*, the *meta/para* ratio decreased when using N-Me protected ureas reverting to the ratio obtained when using **dtbpy** as ligand and confirming the relevance of the proposed interaction.




**Scheme *30*** Control experiments with designed ligands confirming the relevance of the proposed H-bonding interaction. Ratio *meta/para* in parenthesis.

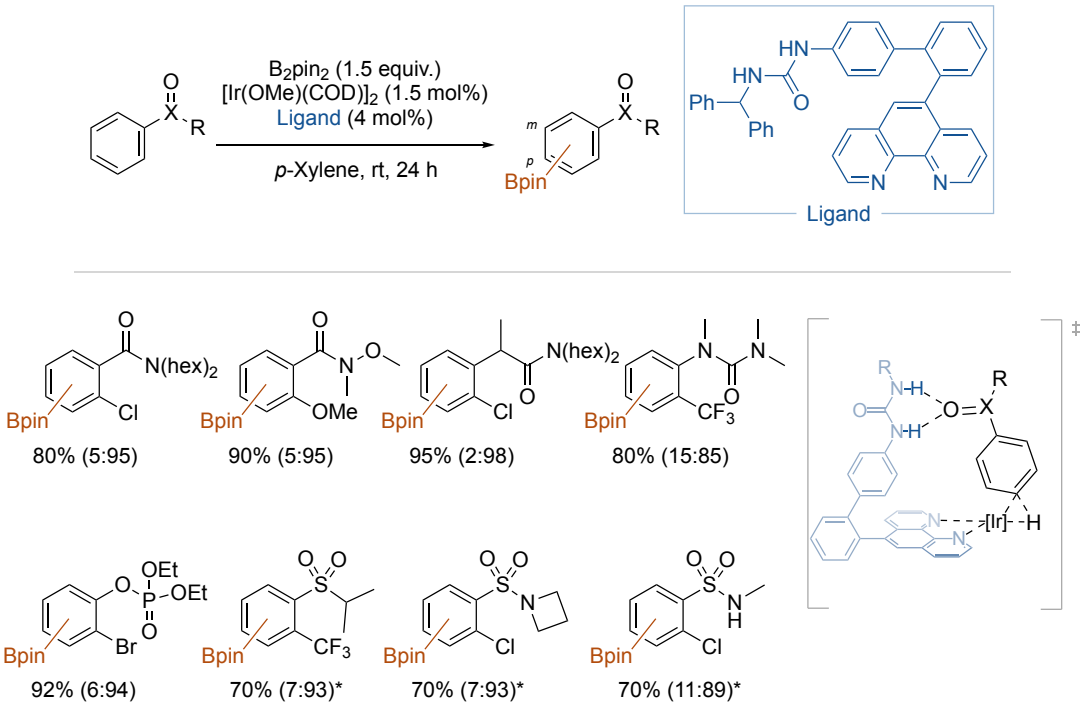
The Liang's group developed a related *meta*-selective borylation method using a urea-based bipyridine ligand similar to that of Kanai's (Scheme *31*).[73] With this system, they successfully achieved *meta*-selective borylation across various aromatic substrates, including amides, ureas, phosphonates, and sulfonamides. Their work highlighted the considerable versatility of this ligand scaffold, demonstrating its adaptability to different substrate geometries and functional groups.




**Scheme *31*** *Meta* selective borylation guided by H-bonds expanded to other substrates. *Cy instead of Ad as the urea substituent. Ratio *meta*/*para* in parenthesis.

Liang and colleagues also expanded the approach for *para*-borylation of related arene substrates, by using computationally designed phenanthroline ligands featuring a urea pendant, as shown in Scheme *32*. The *para* selectivity was explained in terms of a transition state that precisely locates the iridium at the right distance for the *para* C-H activation.

[73] a) Chang, W.; Chen, Y.; Lu, S.; Jiao, H.; Wang, Y.; Zheng, T.; Shi, Z.; Han, Y.; Lu, Y.; Wang, Y.; Pan, Y.; Yu, J.; Houk, K. N.; Liu, F.; Liang, Y. *Chem* **2022,** *8,* 1775–1788., b) Wang, Y.; Chang, W.; Qin, S.; Ang, H.; Ma, J.; Lu, S.; Liang, Y. *Angew. Chem. Int. Ed.* **2022,** *61,* e202206797.

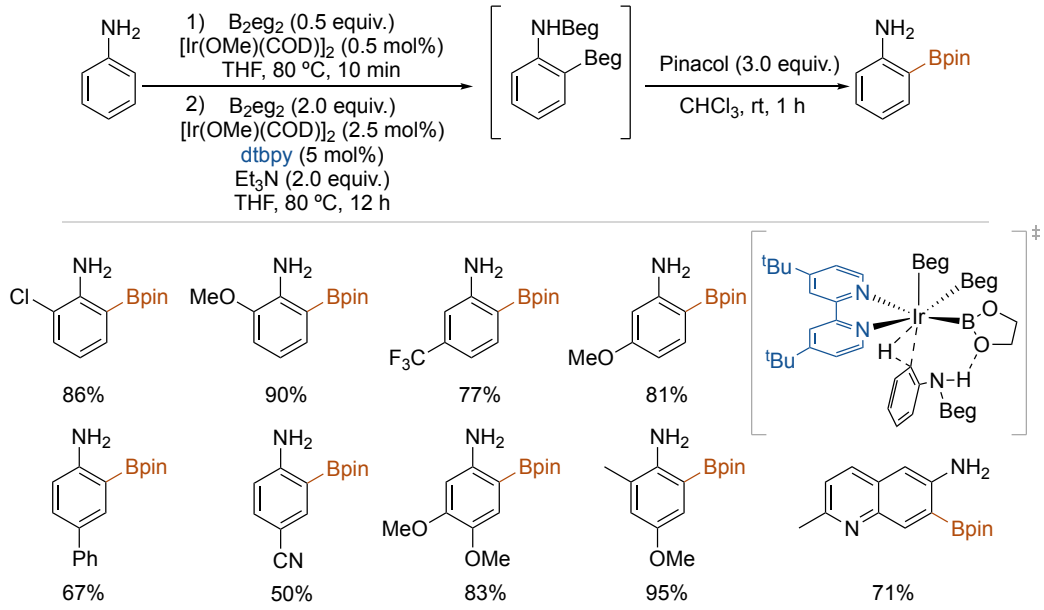



**Scheme *32*** *Para* selective borylation guided by H-bonds and outline of the proposed TS to control regioselectivity. Ratio *meta*/*para* in parenthesis.

In 2018, Chattopadhyay and colleagues reported a distinct approach involving hydrogen-bond interactions to achieve *ortho*-selective borylation of protected anilines.[74] They observed that non-covalent interactions between the NH group of the substrate and the oxygen atom from boronate ligands on the iridium center were key in guiding the reaction's regioselectivity.

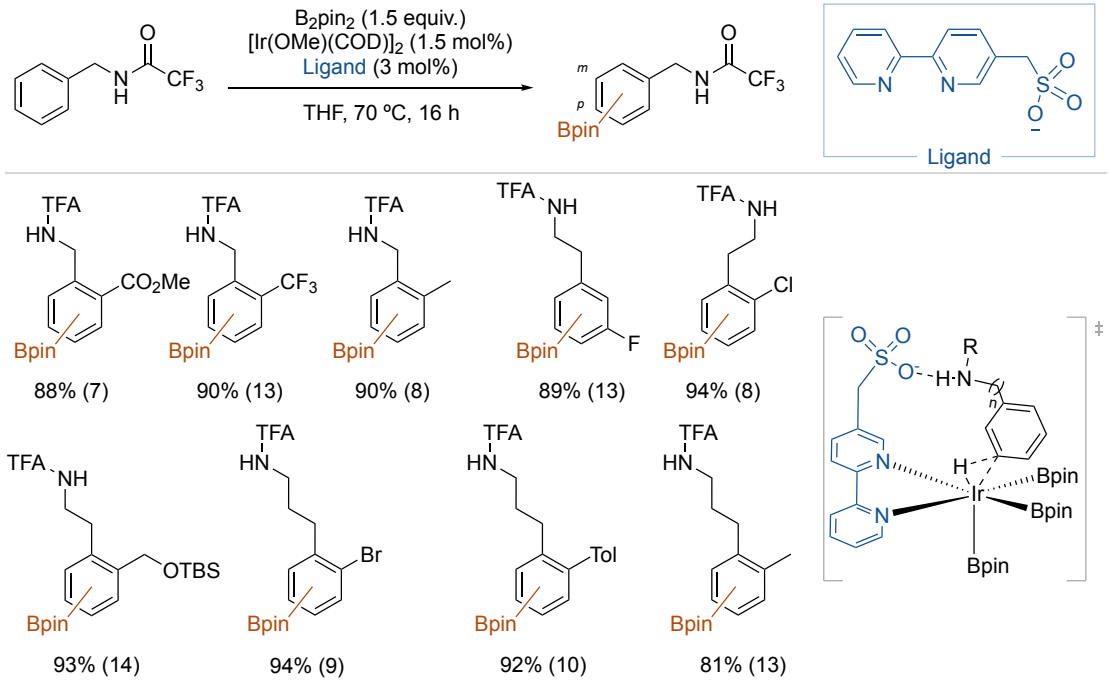
To harness this interaction, the team initially protected the aniline with a boronate ethylene glycol ester (Beg), which facilitated the desired non-covalent bonding. They then used $B_2eg_2$ as the boron source, which, due to its smaller steric bulk compared to $B_2pin_2$, allowed a better interaction with the substrate. This methodology allowed the researchers to effectively achieve *ortho*-selective borylation across a diverse range of anilines (Scheme *33*).

[74] Smith, M. R.; Bisht, R.; Haldar, C.; Pandey, G.; Dannatt, J. E.; Ghaffari, B.; Maleczka, R. E.; Chattopadhyay, B. *ACS Catal.* **2018,** *8,* 6216–6223.




**Scheme *33*** *Ortho*-borylation of anilines, and outline of the proposed TS showing key out sphere interactions to control regioselectivity.

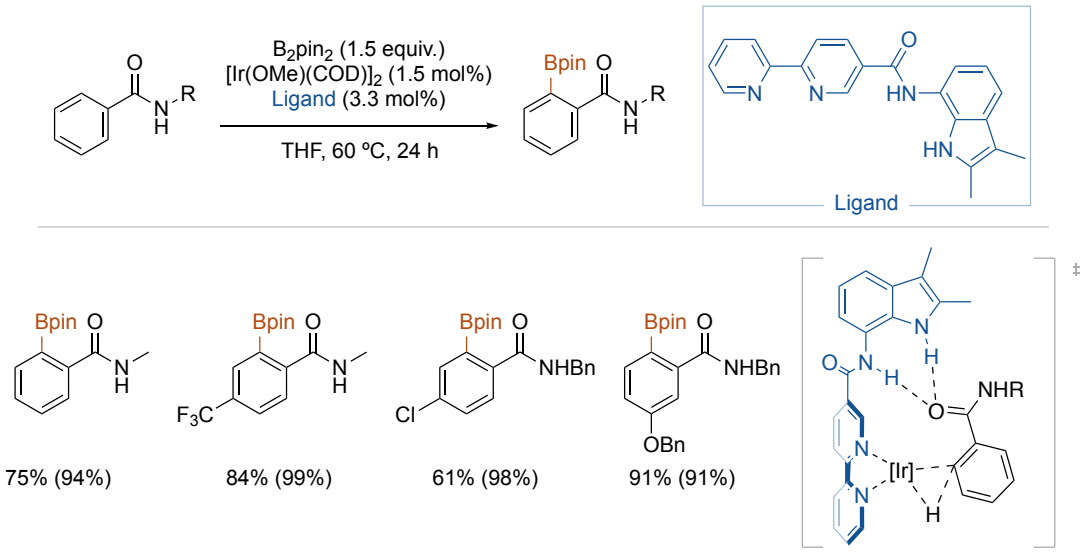
Phipps and his team have been very active in the field, developing a variety of hydrogen bond-based strategies that rely on the presence of an anionic sulfonate group in a bipyridine ligand.[75] The sulfonate group establishes hydrogen-bond interactions with benzyl-amine-derived amides, which allows to direct the borylation of the *meta* position.




**Scheme *34*** Phipps *meta* borylation guided by H-bond interactions and outline of the proposed TS. Ratio *meta*/*para* in parenthesis.

[75] Davis, H. J.; Genov, G. R.; Phipps, R. J. *Angew. Chem. Int. Ed.* **2017,** *56,* 13351–13355.

In 2019, Reek's group developed a bipyridine ligand containing an indole amide, which facilitated the *ortho*-borylation of secondary amides with exceptional regioselectivity.[76] The indole amide group functions as an H-bond donor, forming non-covalent interactions with the substrate's carbonyl group. These interactions specifically guide the C–H activation towards the *ortho* position, ensuring highly selective *ortho*-borylation of the substrate (Scheme *35*).

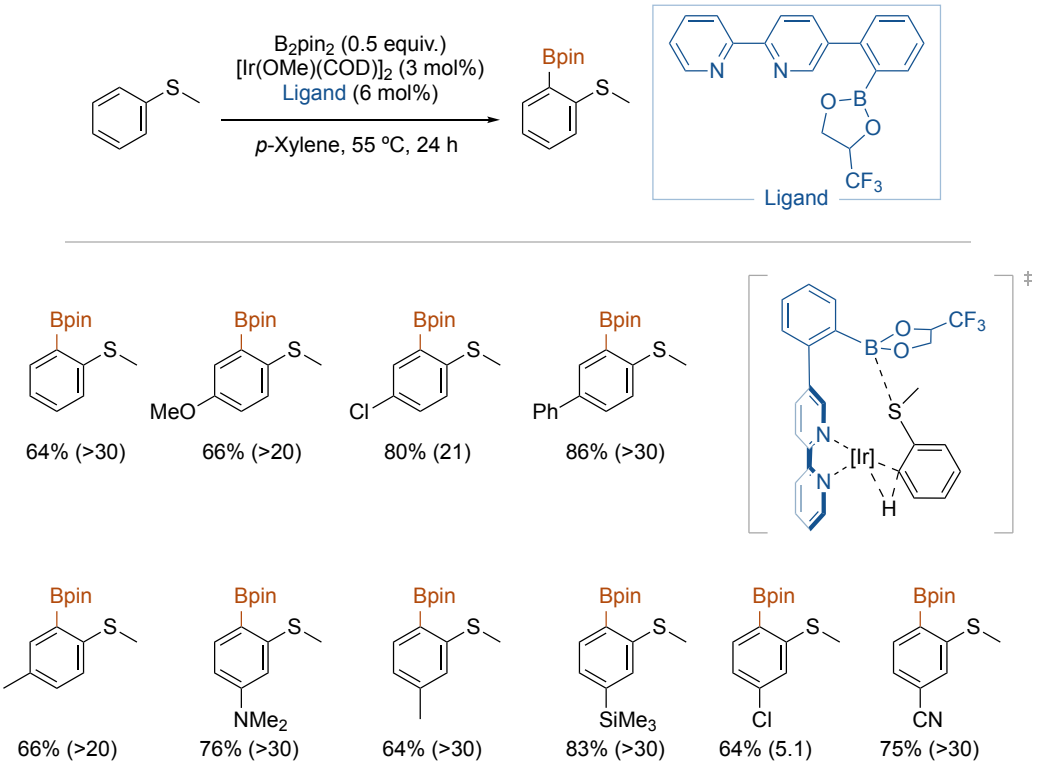



**Scheme *35*** H-bond directed *ortho* borylation of secondary amides developed by Reek's group and outline of the proposed TS to control regioselectivity. *Ortho* % in parenthesis.

Beyond hydrogen bonding, research groups have explored Lewis acid-base interactions to achieve regioselective C–H borylations of aromatic systems. Notably, in 2017, Kanai's group developed a strategy for *ortho*-selective borylation of thioanisole derivatives by employing a bipyridine ligand modified with a boronate ester.[77] The boron atom of this group effectively interacts with the sulfur atom of the substrate, facilitating selective *ortho*-borylation.

The Lewis acid–base interaction in this system is robust enough to counteract the steric repulsion that typically arises between the catalytically active iridium-boryl complex and substituents on the substrate. This approach allowed for high *ortho* selectivity and exhibited notable tolerance for various functional groups, highlighting its potential versatility for selective borylation of thioanisole derivatives and similar substrates (Scheme *36*).

[76] Bai, S.; Bheeter, C. B.; Reek, J. N. H. *Angew. Chem. Int. Ed.* **2019,** *58,* 13039–13043.
[77] Li, H. L.; Kuninobu, Y.; Kanai, M. *Angew. Chem. Int. Ed.* **2017,** *56,* 1495–1499.

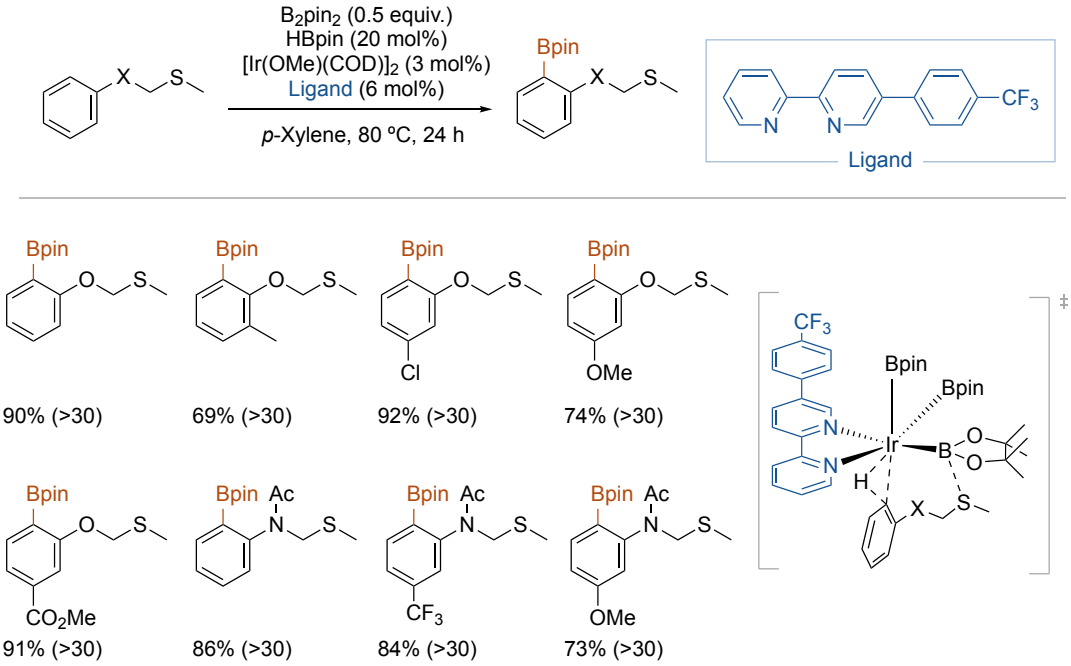



**Scheme *36*** Kanai *ortho* borylation of thioanisoles guided by Lewis acid-base interactions and outline of the proposed TS showing key interactions to control regioselectivity. Ratio *ortho*/others in parenthesis.

The Kuninobu's group also leveraged a Lewis acid-base interaction to achieve *ortho*-selective borylation, targeting phenol and aniline derivatives containing a methylthio group at the α-position relative to the oxygen or nitrogen atom.[78] In this approach, they employed a bipyridine ligand substituted with an electron-withdrawing group to further enhance the non-covalent contacts.

The interaction between the sulfur atom on the substrate and one of the Bpin ligands in the iridium complex seems to be key for the desired selectivity. This interaction directs the borylation selectively to the *ortho* position, providing an effective and precise method for modifying phenol and aniline derivatives with excellent regioselectivity.

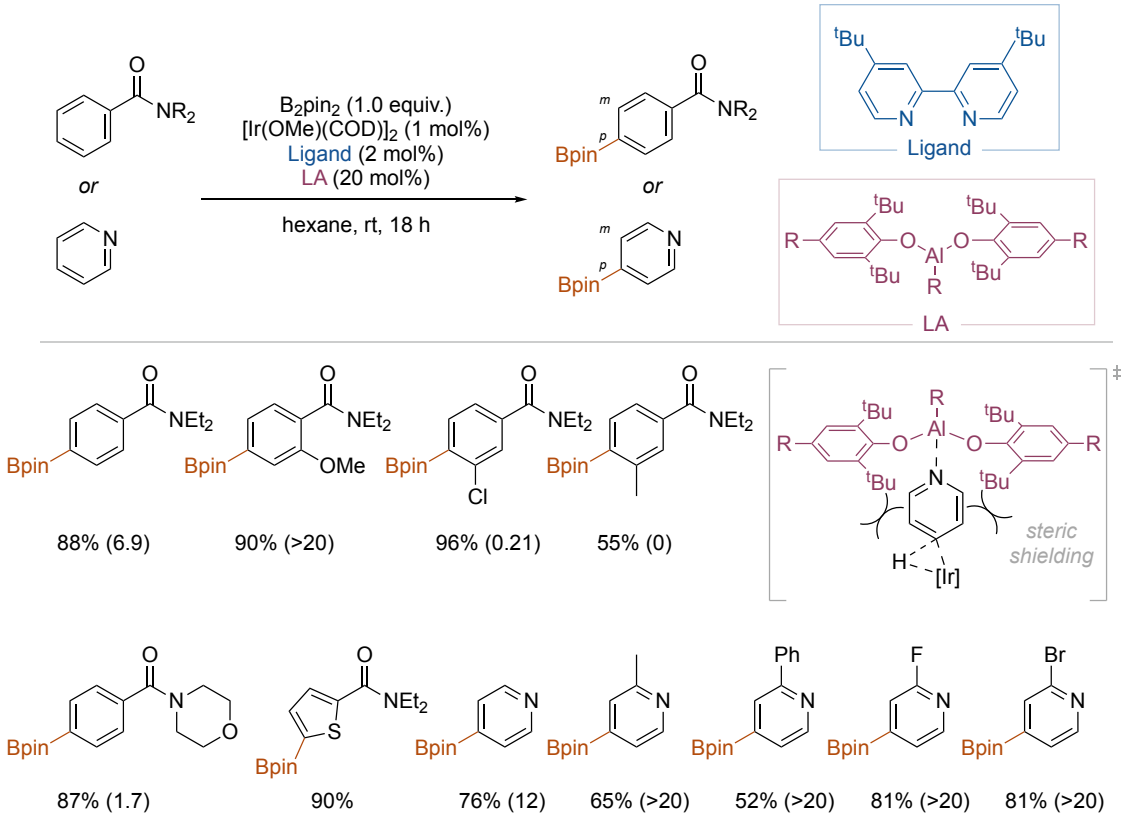
[78] Li, H.; Kanai, M.; Kuninobu, Y. *Org. Lett.* **2017,** *19,* 5944–5947.




**Scheme *37*** Kuninobu *ortho* borylation of thioethers guided by Lewis acid-base interactions and outline of the proposed TS to control regioselectivity. Ratio *ortho*/others in parenthesis.

A different approach has been used by Nakao and co-workers who were able to develop a *para*-selective borylation of benzamides and pyridines relying on a cooperative mechanism involving an aluminum site. A bulky aluminum alkoxide unit acts as a Lewis acid, and coordinates to the carbonyl (benzamides) or the pyridyl nitrogen (pyridine) of the substrates (Scheme *38*).

The steric repulsion between the bulky aluminum site and the iridium catalyst enables precise control over regioselectivity, directing borylation to the *para* position. The method demonstrated a significant functional group tolerance, including compatibility with Lewis-basic groups, without compromising regioselectivity. However, it didn't work well with *meta*-substituted benzamides; in these cases the substrate-controlled regioselectivity dominates, leading to *meta*-borylation rather than the intended *para* product.

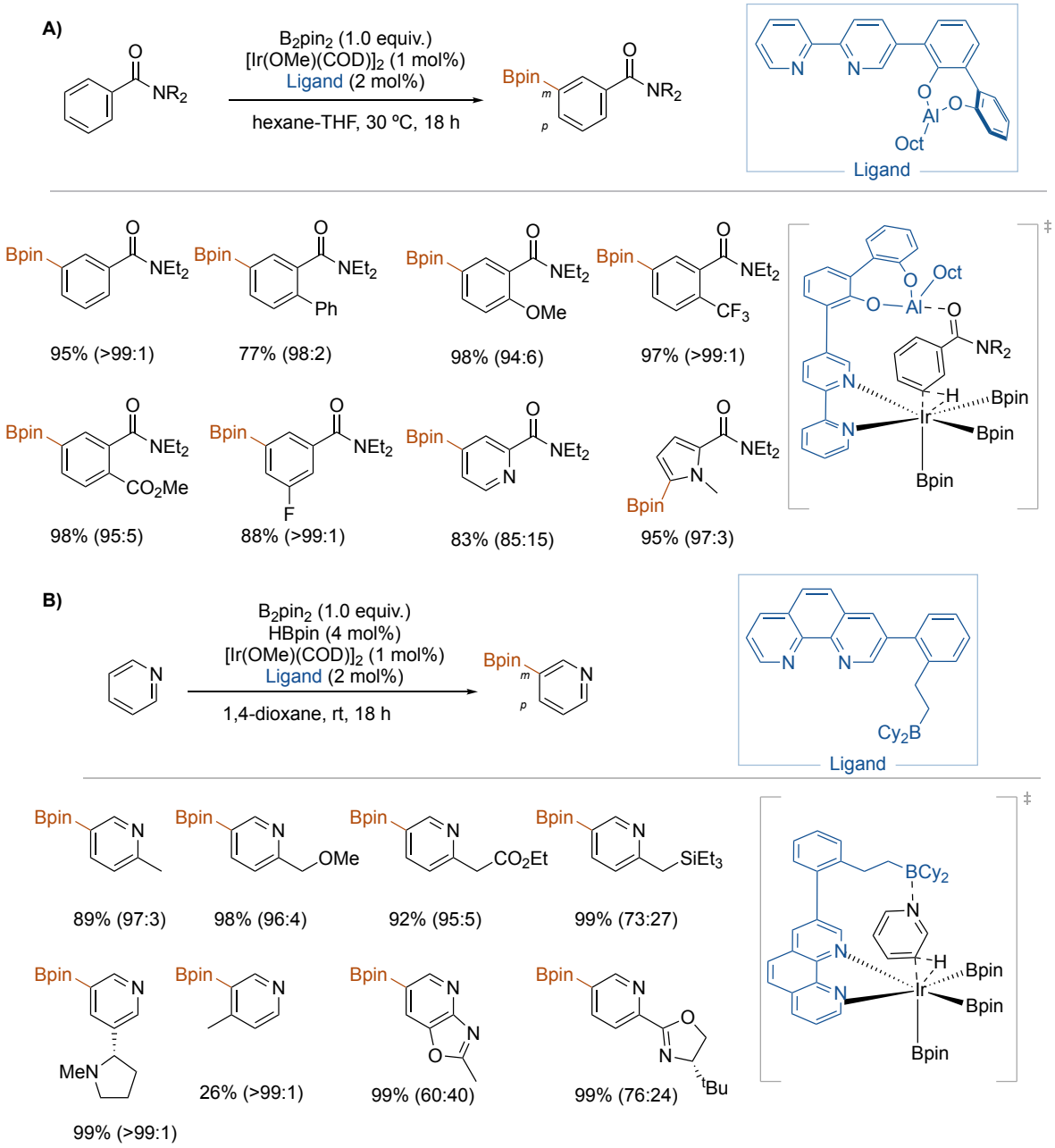



**Scheme *38*** *Para* borylation of benzamides and pyridines and rational proposed for explaining the regioselectivity. Ratio *para*/others in parenthesis.

The same group later reported a *meta*-selective C–H borylation of benzamides and pyridines by directly incorporating an aluminum or boron derivative into the ligand. Here, a strategically positioned aluminum or boron moiety coordinates with the Lewis-basic carbonyl group in benzamides or the $sp^2$-hybridized nitrogen in pyridines, positioning the iridium center near the desired $C_3$-position for borylation (Scheme *39*).[79]

Similar to their previous approach, this method also tolerates a wide array of functional groups, maintaining excellent selectivity and reactivity even in the presence of Lewis-basic moieties.

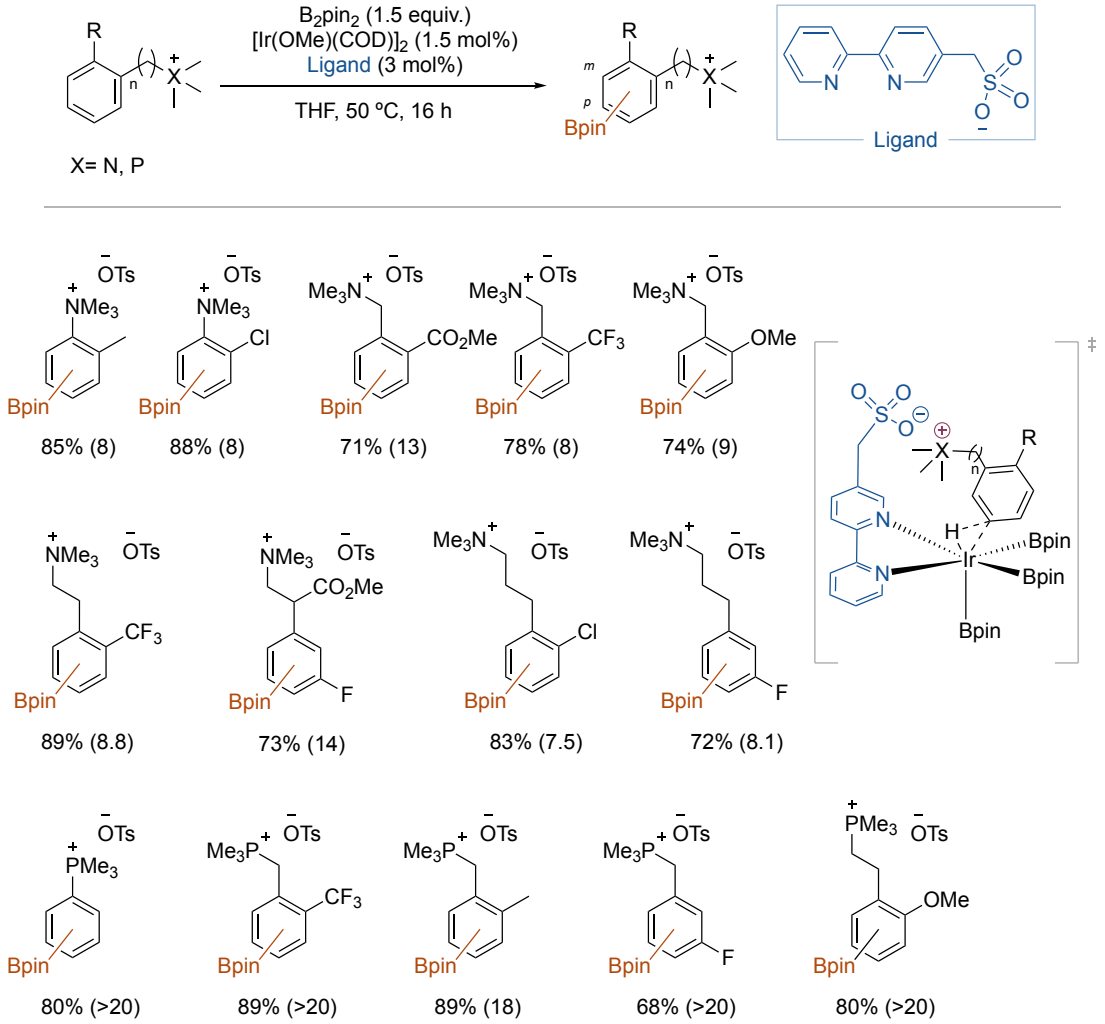
[79] Yang, L.; Uemura, N.; Nakao, Y. *J. Am. Chem. Soc.* **2019,** *141,* 7972–7979.




**Scheme *39*** *Meta*-borylation of benzamides (**A**) and of pyridines (**B**) and outline of the proposed TSs that explain the regioselectivities. Ratio *meta*/others in parenthesis.

Ion-pairing interactions can also be harnessed for similar types of selectivities, as demonstrated by Phipps and coworkers. Incorporating an anionic sulfonate group into a bipyridine ligand creates a recognition site that interacts with cationic substrates, such as quaternary ammonium and phosphonium salts, which allows to attain selective C–H borylation at the *meta* position (Scheme *40*).[80]

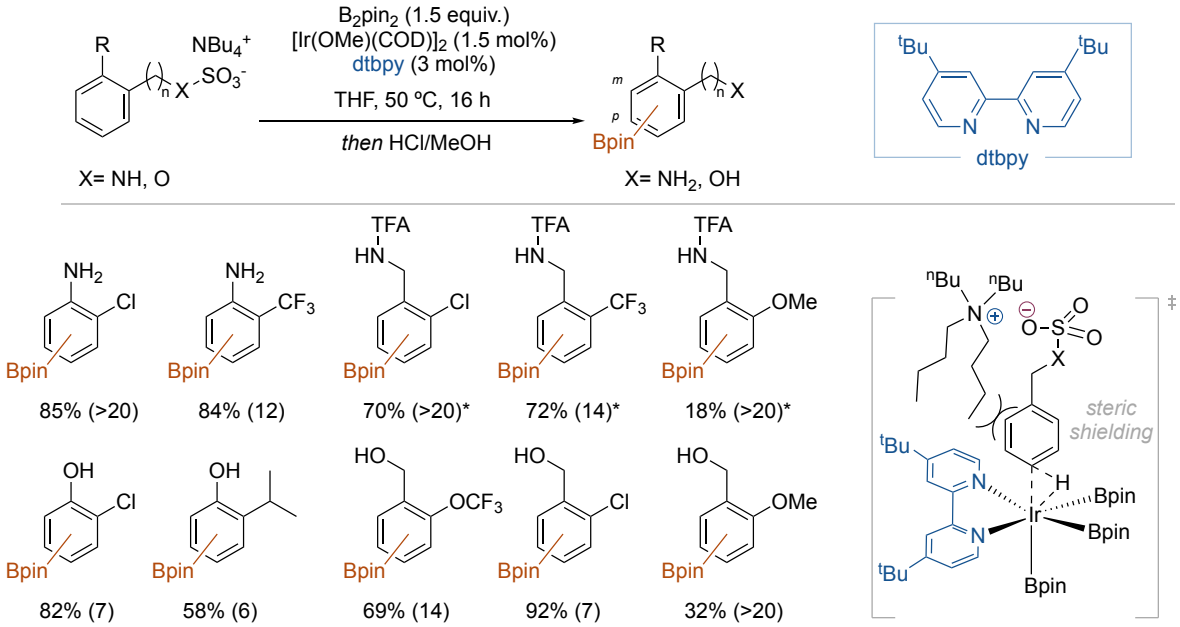
[80] a) Davis, H. J.; Mihai, M. T.; Phipps, R. J. *J. Am. Chem. Soc.* **2016,** *138,* 12759–12762., b) Lee, B.; Mihai, M. T.; Stojalnikova, V.; Phipps, R. J. *J. Org. Chem.* **2019,** *84,* 13124–13134., c) Mihai, M. T.; Davis, H. J.; Genov, G. R.; Phipps, R. J. *ACS Catal.* **2018,** *8,* 3764–3769.




**Scheme *40*** Phipps *meta* selective borylation guided by ion-pair interactions. Ratio *meta*/others in parenthesis

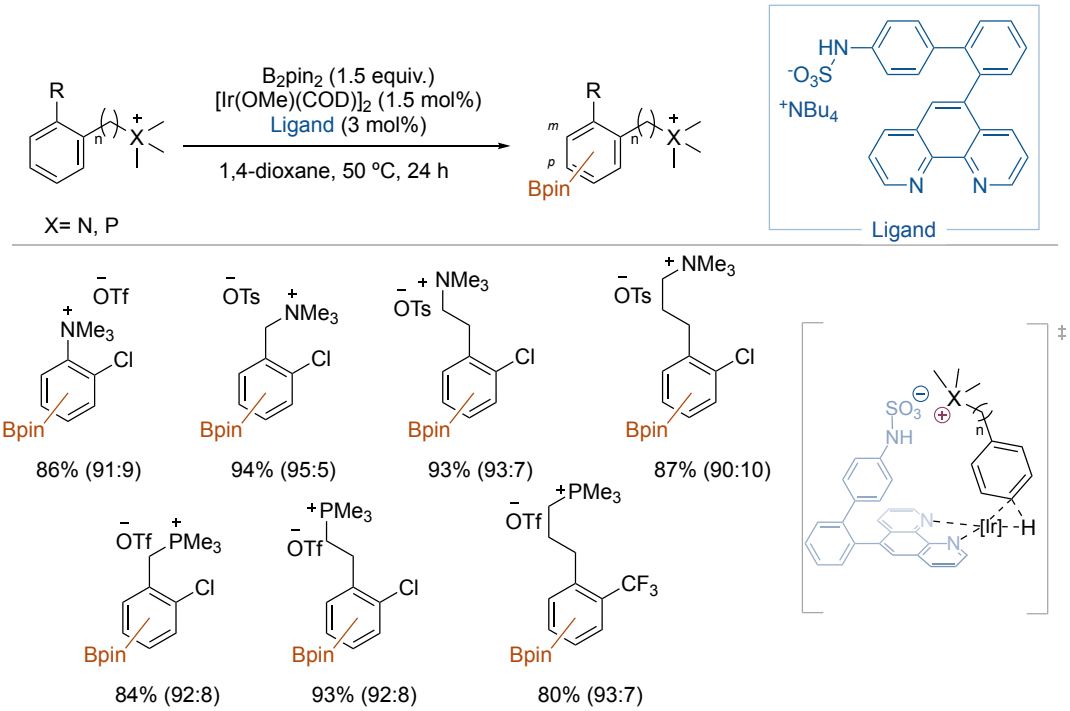
This group also developed a related but different strategy, also based on ion pairing of sulfates tethered to the substrates, but using tetraalkyl ammonium counter-cations and standard **bipy** ligands.[81] The extended alkyl chains on these cations provide steric shielding for the *ortho* and *meta* positions, leaving only the *para* position accessible, which enables highly selective *para*-borylation with excellent regioselectivity (Scheme *41*).

[81] Mihai, M. T.; Williams, B. D.; Phipps, R. J. *J. Am. Chem. Soc.* **2019,** *141,* 15477–15482.




**Scheme *41*** *Para* selective borylation guided by ion-pair interactions with external bulky ammonium cations. Ratio *para*/others in parenthesis**.** *Treated with TFAA after sulfonate deprotection.

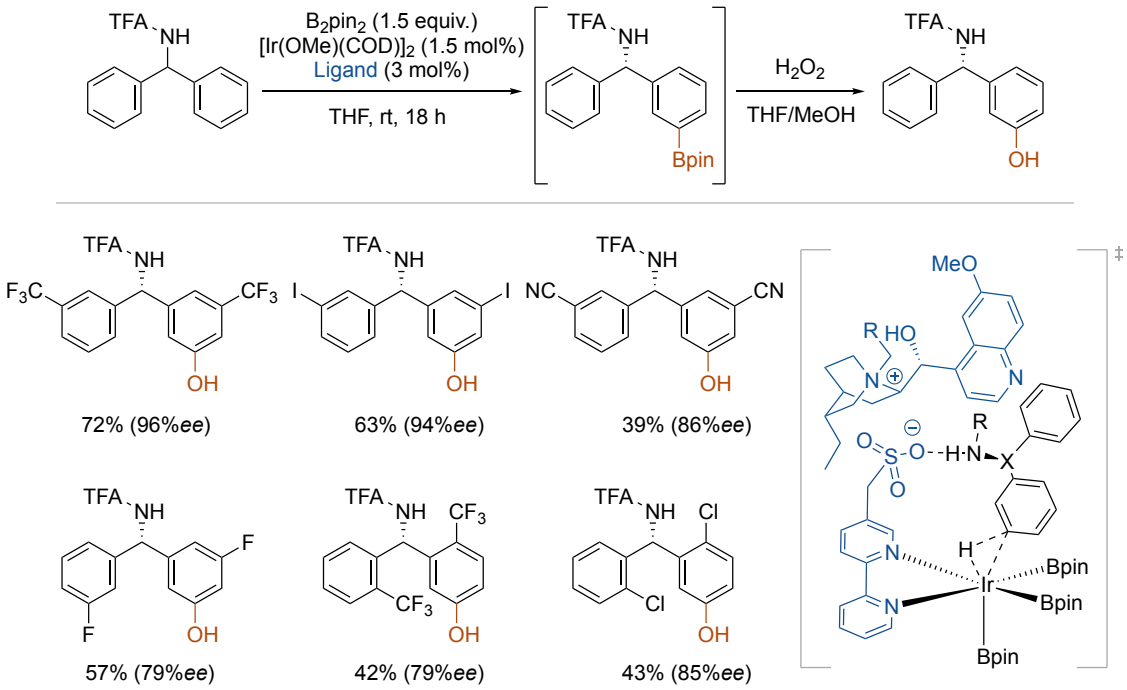
Related non-covalent contacts were reported by Liang and coworkers for a *para*-C–H borylation of aromatic systems equipped with ammonium or phosphonium units (Scheme *42*).[82]




**Scheme *42*** Liang *para* selective borylation guided by ion pair interactions. Ratio *para*/others in parenthesis.

[82] Lu, S.; Zheng, T.; Ma, J.; Deng, Z.; Qin, S.; Chen, Y.; Liang, Y. *Angew. Chem. Int. Ed.* **2022,** *61,* e202201285–n/a.

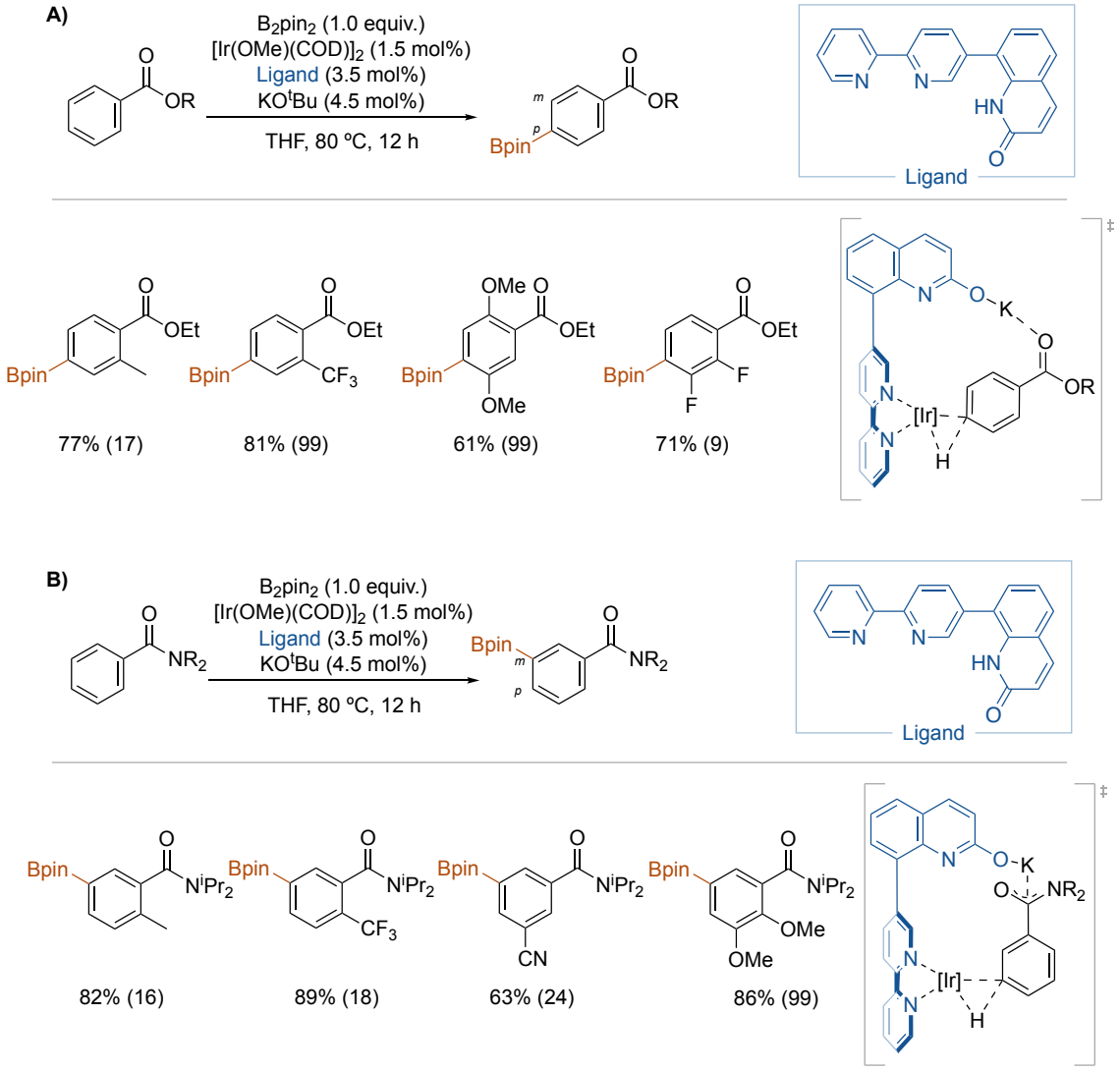
A very relevant extension of the non-covalent strategy based on ion-pair interactions was also developed by the Phipps group and entails the use of chiral cations to generate asymmetric in the C–H borylation reaction. The approach was used to desymmetrize benzhydrylamides and was proposed to work thanks to the formation of ion-pair assemblies like indicated in the Scheme *43*.




**Scheme *43*** Enantioselective *meta*-borylation exploiting ion-pair interactions with a chiral cation.

Chattopadhyay and colleagues further expanded the field of supramolecularly-controlled iridium-catalyzed C–H borylations by employing outer-sphere O-$K^+$---O ion-pairing interactions between an L-shaped bipyridine ligand beating a quinolone moiety and aryl esters or amides. In this approach, the quinolone moiety of the ligand forms non-covalent interactions with the carbonyl group of aromatic esters, steering the C–H borylation toward the *para* position (Scheme *44* A).[83] Conversely, for aromatic amides, the ligand interacts with the delocalized π system of the amide group, promoting *meta*-selective C–H borylation (Scheme *44* B).[84]

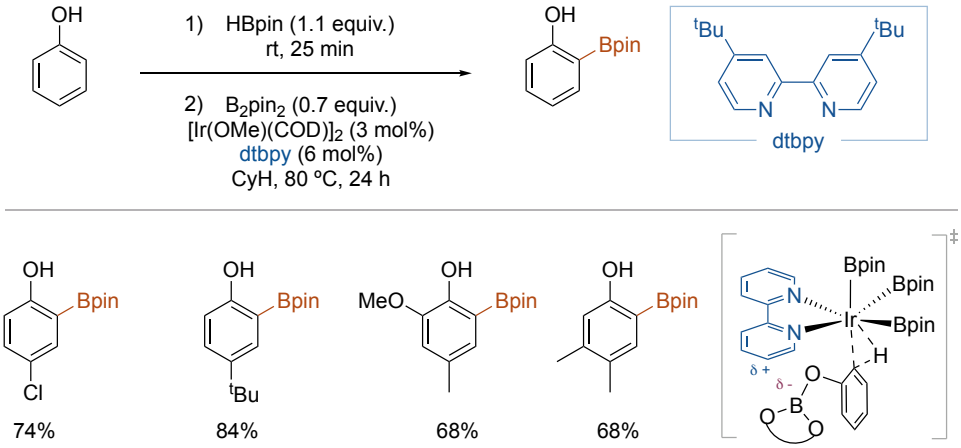
[83] Hoque, M. E.; Bisht, R.; Haldar, C.; Chattopadhyay, B. *J. Am. Chem. Soc.* **2017,** *139,* 7745–7748.
[84] Bisht, R.; Hoque, M. E.; Chattopadhyay, B. *Angew. Chem. Int. Ed.* **2018,** *57,* 15762–15766.




**Scheme *44* A)** *Para* borylation of esters guided by ion pair interactions. Ratio *para*/others in parenthesis **B)** *Meta* borylation of amides guided by ion pair interactions. Ratio *meta*/others in parenthesis**.**

Malezcka, Singleton and Smith III found an interesting *ortho*-directing effect in phenolic substrates, suggested to occur because of a non-covalent electrostatic interaction between a Bpin-oxygen unit and a **dtbpy** ligand (Scheme *45*).[85]

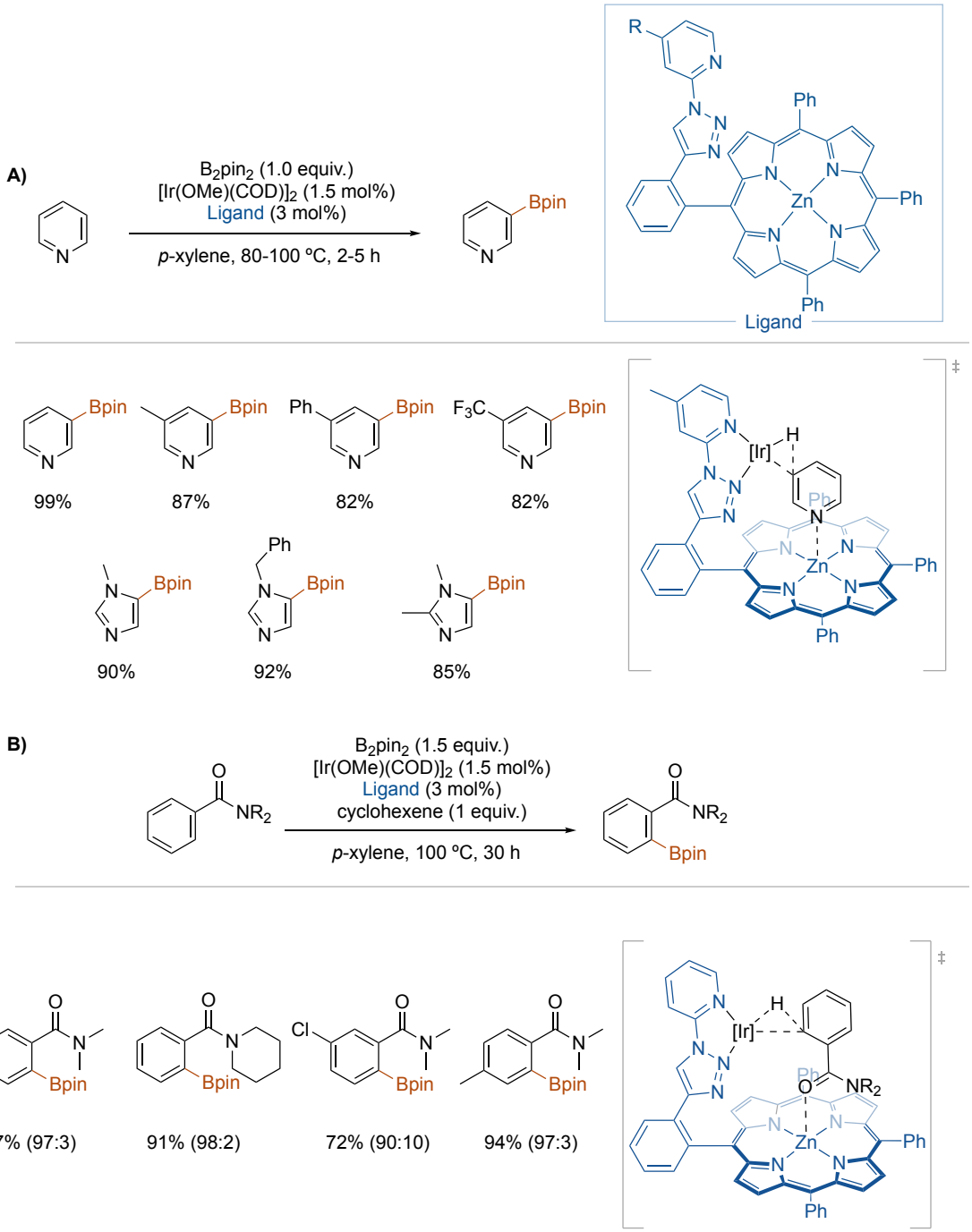
[85] Chattopadhyay, B.; Dannatt, J. E.; Andujar-De Sanctis, I. L.; Gore, K. A.; Maleczka, R. E.; Singleton, D. A.; Smith III, M. R. *J. Am. Chem. Soc.* **2017,** *139,* 7864–7871.




**Scheme *45*** *Ortho* borylation of phenols guided by electrostatic interactions.

In 2021, Doria and co-workers introduced a novel porphyrin-derived ligand for the Ir-catalyzed $C_3$-selective borylation of pyridines and heteroarenes (Scheme *46* A) and the *ortho* C–H borylation of benzamides (Scheme *46* B).[86] This ligand, featuring a Zn-incorporated porphyrin unit and a pyridyl triazole unit, facilitated a selective borylation by allowing weak secondary interactions between the pyridine nitrogen atom or the amide carbonyl and the Zn atom.

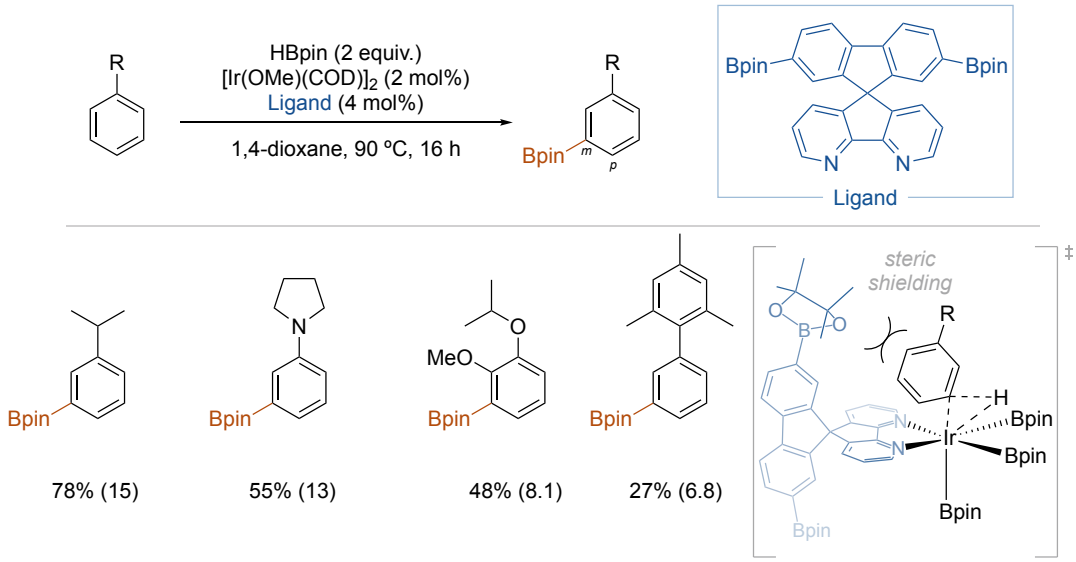
[86] a) Trouvé, J.; Zardi, P.; Al-Shehimy, S.; Roisnel, T.; Gramage-Doria, R. *Angew. Chem. Int. Ed.* **2021,** *60,* 18006–18013., b) Trouvé, J.; Rajeshwaran, P.; Tomasini, M.; Perennes, A.; Roisnel, T.; Poater, A.; Gramage-Doria, R. *ACS Catal.* **2023,** *13,* 7715–7729., c) Trouvé, J.; Delahaye, V.; Tomasini, M.; Rajeshwaran, P.; Roisnel, T.; Poater, A.; Gramage-Doria, R. *Chem. Sci.* **2024,** *15,* 11794–11806.




**Scheme *46*** **A)** Doria *meta* selective borylation of pyridines guided by secondary interactions. Ratio *meta*/others in parenthesis. **B)** Doria *ortho* selective borylation of benzamides guided by secondary interactions. Ratio *ortho*/others in parenthesis

In addition to non-covalent contacts, it is possible to use steric effects to control the regioselectivity in C–H borylation reactions. Therefore, Ilies and co-workers developed a *meta*-selective borylation strategy using a spiro bidentate 4,5-diazafluorenone ligand (Scheme *47*). This system allowed for a high *meta*-selectivity when a Bpin group was incorporated into the ligand. The authors attributed this remote selectivity to the steric effects induced by the ligand environment, a hypothesis

supported by DFT calculations, which indicated that ligand-induced steric shielding favored *meta*-selective borylation.[87]




**Scheme *47*** Ilies *meta* selective borylation guided by steric shielding. Ratio *meta*/others in parenthesis.

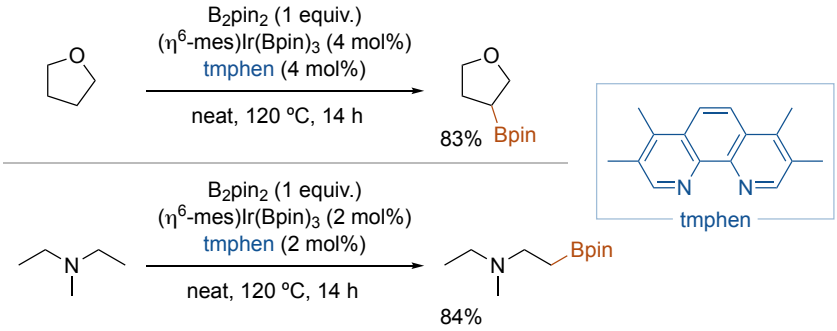
## 4.7 Iridium-catalyzed borylations of alkyl C–H bonds

Considering the successful outcomes of the above iridium-catalyzed borylations of aromatic C($sp^2$)–H bonds, a significant attention has also been turned to the more challenging task of borylating alkyl C–H bonds. This challenge is a consequence of the lower reactivity of this type of C($sp^3$)–H bonds, and the usually larger number of competing positions compared to those available in aromatic systems. Nonetheless, in recent years there have been substantial advances in the area, most of them resulting from the use of specific iridium ligands.

### 4.7.1 Bidentate neutral ligands (L–L)

In 2012, Liskey and Hartwig demonstrated that mixing a specific Ir (I) complex with 3,4,7,8-tetramethyl-1,10-phenanthroline (**tmphen**) results in a highly active catalyst for the undirected C–H borylation of alkyl C–H bonds, although the reaction requires high temperatures and the use of neat substrates (without solvent).[88] Remarkably, they found that C–H bonds beta to oxygen or nitrogen atoms in ethers and amines are more reactive than other C–H bonds in these molecules. This regioselectivity, at least in the case of the acyclic amines, has been explained in terms of steric reasons, but this is not very clear.

[87] Ramadoss, B.; Jin, Y.; Asako, S.; Ilies, L. *Science* **2022,** *375,* 658–663.
[88] a) Larsen, M. A.; Oeschger, R. J.; Hartwig, J. F. *ACS Catal.* **2020,** *10,* 3415–3424., b) Li, Q.; Liskey, C. W.; Hartwig, J. F. *J. Am. Chem. Soc.* **2014,** *136,* 8755–8765., c) Liskey, C. W.; Hartwig, J. F. *J. Am. Chem. Soc.* **2012,** *134,* 12422–12425.




**Scheme *48*** Borylation of the alkyl C-H bonds in ethers and amines using tmphen as ligand.

The mechanism proposed for the C($sp^3$)–H borylation is analogous to the one described for aromatic C–H bonds. The catalytically active species is the Ir(III) tris-boryl Ir(tmphen)$(Bpin)_3$ (**II**, Figure *17*). The rate-determining step (RDS) was found to be the oxidative addition of this Ir(III) species into the C($sp^3$)–H bond, forming an Ir(V) species (**III**). After reductive elimination of the borylated product, the $B_2pin_2$ undergoes an oxidative addition to regenerate the active Ir(III) tris-boryl complex.

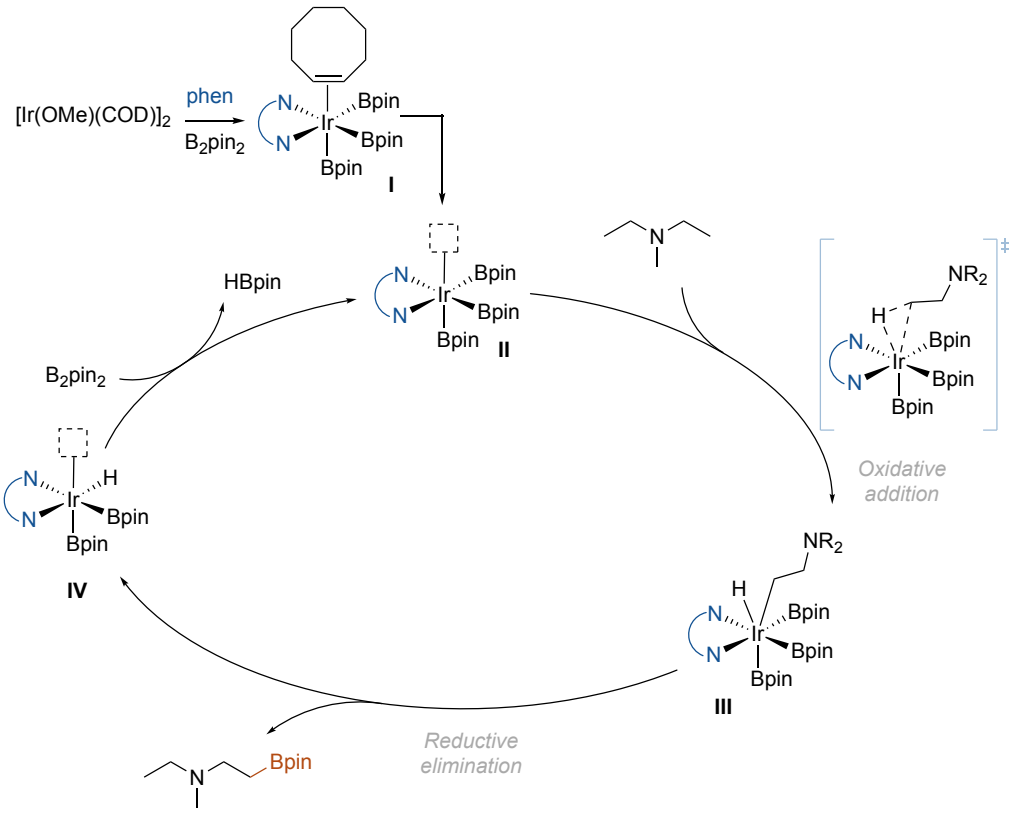
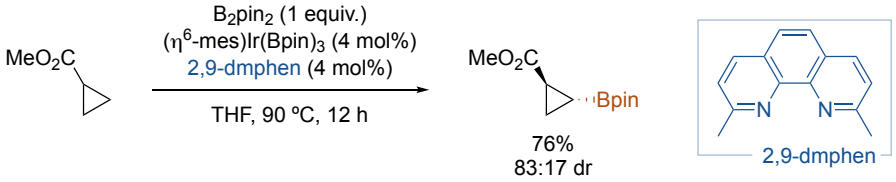



**Figure *17*** General mechanism for the C–H borylation of alkyl substrates.

Later on it was shown that using as ligand the 2,9-dimethylphenanthroline (**2,9-dmphen**) improved reactivity, and therefore it is possible to perform the borylation of monosubstituted cyclopropanes by using THF as solvent, although an excess of substrate

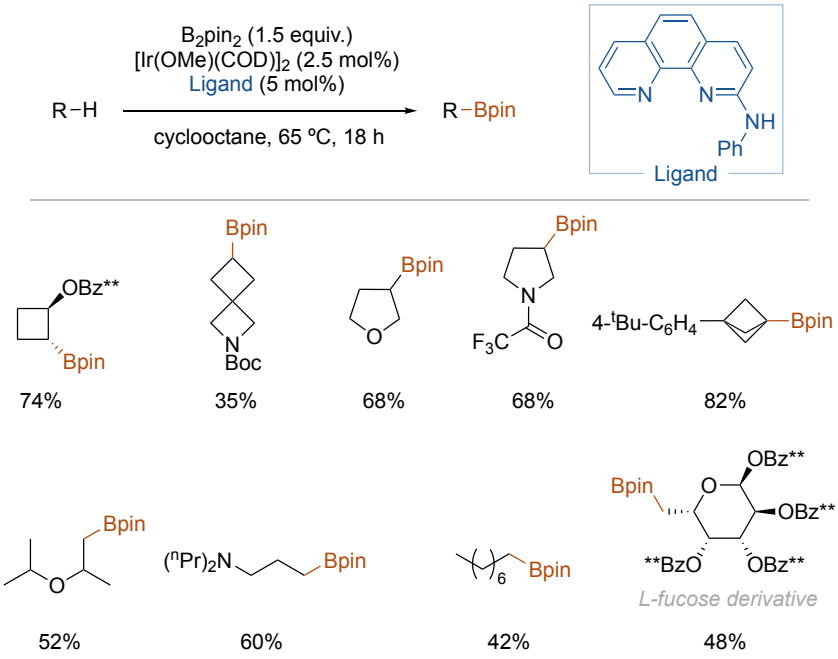
USC UNIVERSIDADE DE SANTIAGO DE COMPOSTELA

relative to $B_2pin_2$ was still required. The reaction proceeded with an excellent diastereoselectivity for the trans isomer.[89]




**Scheme *49*** Borylation of cyclopropanes using 2,9-dmphen as ligand.

The Hartwig's group later discovered that other ligands based on 2-substituted phenanthrolines, (2-Me and 2-NHPh phenanthrolines) enabled the borylation of a variety of aliphatic substrates under milder conditions, and without the need to use a large excess of substrate, obtaining the borylated products in the less sterically hindered positions (Scheme *50*).[90]




**Scheme *50*** Borylation of alkyl C-H bonds using 2-NHPh-phen as ligand

While the reaction was proposed to follow the standard mechanism, recent studies suggest that the rate-limiting step in the proposed mechanism might be an isomerization of the iridium-hydride intermediate ($Ir(Bpin)_3(R)(H)$, Figure *18*) resulting from oxidative addition, rather than the C–H activation. This is supported by DFT computational studies using bicyclopropane as a substrate and **tmphen** as the ligand. The simulations indicate that the rate-limiting step is not the C–H activation but an

[89] Liskey, C. W.; Hartwig, J. F. *J. Am. Chem. Soc.* **2013,** *135,* 3375–3378.
[90] a) Oeschger, R.; Su, B.; Yu, I.; Ehinger, C.; Romero, E.; He, S.; Hartwig, J. *Science* **2020,** *368,* 736–741., b) Yu, I. F.; Manske, J. L.; Diéguez-Vázquez, A.; Misale, A.; Pashenko, A. E.; Mykhailiuk, P. K.; Ryabukhin, S. V.; Volochnyuk, D. M.; Hartwig, J. F. *Nat. Chem.* **2023,** *15,* 685–693., c) Yu, I. F.; D'Angelo, K. A.; Hernandez-Mejías, A. D.; Cheng, N.; Hartwig, J. F. *J. Am. Chem. Soc.* **2024,** *146,* 7124–7129.

isomerization where the Ir complex adopts a pentagonal-bipyramidal conformation. In this conformation, the hydride is nearly coplanar with the phenanthroline ligand and two boryl groups, which facilitates the following RE step.

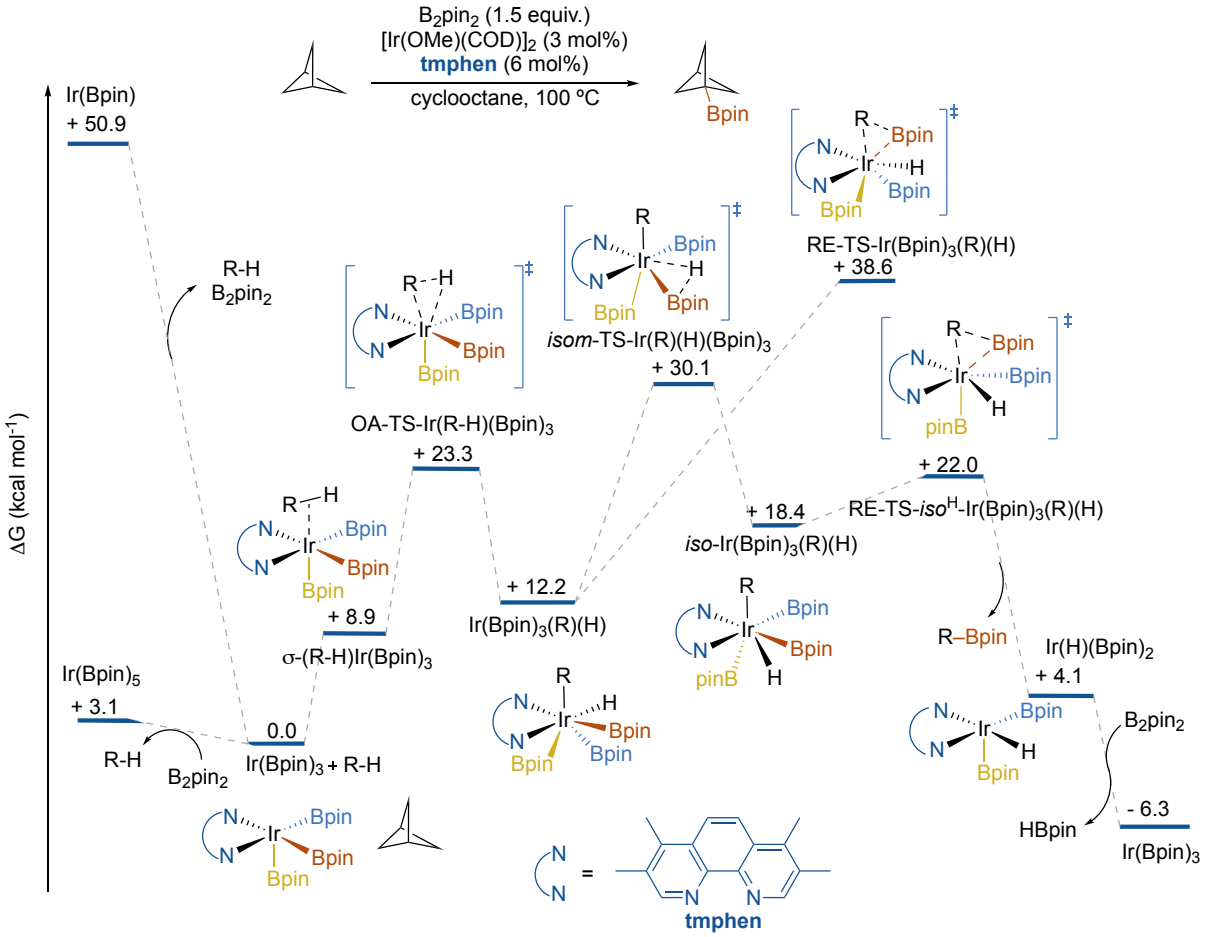



**Figure *18*** Results of a DFT study on the borylation of BCPs using **tmphen** as the ligand where the rate determining step is the isomerization of the $Ir(Bpin)_3(R)(H)$ intermediate to *isom*-TS-$Ir(R)(H)(Bpin)_3$.

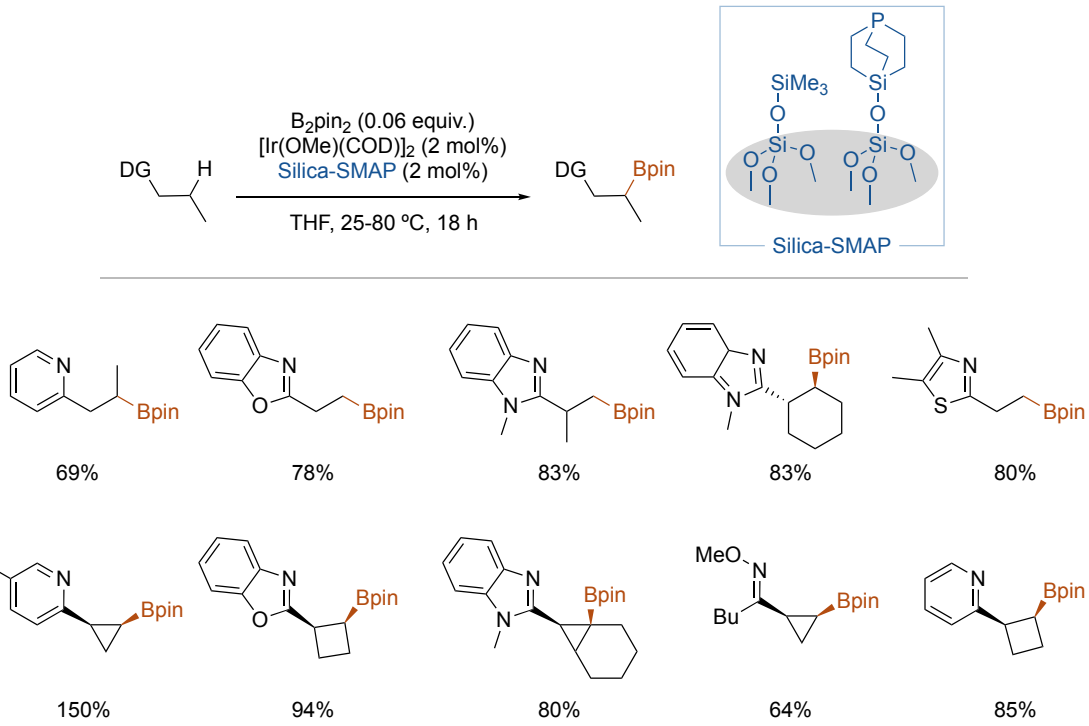
## 4.7.2 Monodentate ligands (L)

As in the case of aromatic systems, the presence of a directing group in the substrate can accelerate the reaction and allow a better control of the regioselectivity. Leveraging this directing group effect requires that the iridium catalyst present two vacant coordination sites, so that the directing group (DG) can coordinate to the metal and guide the C–H activation. As in the case of the aromatic systems, this would be possible by using monodentate instead of bidentate neutral ligands.

Therefore, Sawamura and coworkers applied their Ir-SMAP system (Iridium Silica-Monophosphine) for the borylation of aliphatic substrates containing strong coordinating directing groups such as pyridines or 1,3-azoles. In general, they obtained good yields and

USC UNIVERSIDADE DE SANTIAGO DE COMPOSTELA

regioselectivities, although an excess of the substrate was required (Scheme *51*).[91] They also applied the reaction to the C–H borylation of small, tense carbocycles like cyclopropanes and cyclobutanes.[92] sites. These sites allow the coordination of nitrogen atoms of the directing group, favoring C–H borylation.




**Scheme *51*** Directed C-H borylation of alkyl groups catalyzed by Ir bound to an immobilized phosphine. Yields based on $B_2pin_2$.

### 4.7.3 Monoanionic bidentate ligands (L–X)

As in the case of the aromatic C–H borylations, monoanionic L–X ligands have also been used for the C–H borylation of aliphatic substrates.

Despite being bidentate, the monoanionic character of the ligand allows for the coordination of a directing group present in the substrate to the metal center, as indicated in the previous section. The ligand precursor (either a silane or a sylilborane) evolves by oxidative addition to form the corresponding metal hydride (**I**, Figure *19*). Coordination of the directing group of the substrate to the resulting bisboryl intermediate facilitates the C–H activation at a specific position. Finally, a reductive elimination yields the borylated product.

[91] a) Iwai, T.; Murakami, R.; Harada, T.; Kawamorita, S.; Sawamura, M. *Adv. Synth. Catal.* **2014,** *356,* 1563–1570., b) Murakami, R.; Iwai, T.; Sawamura, M. *Synlett* **2016,** *27,* 1187–1192.
[92] Murakami, R.; Tsunoda, K.; Iwai, T.; Sawamura, M. *Chem. Eur. J.* **2014,** *20,* 13127–13131.

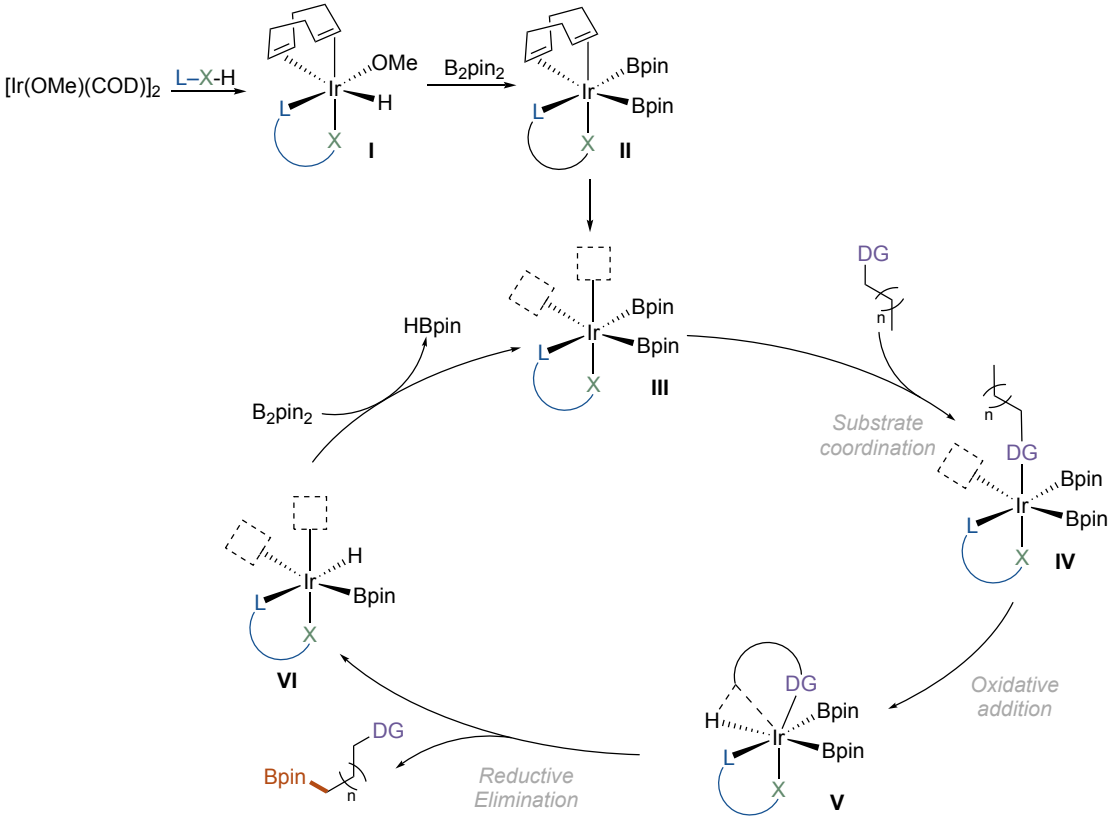
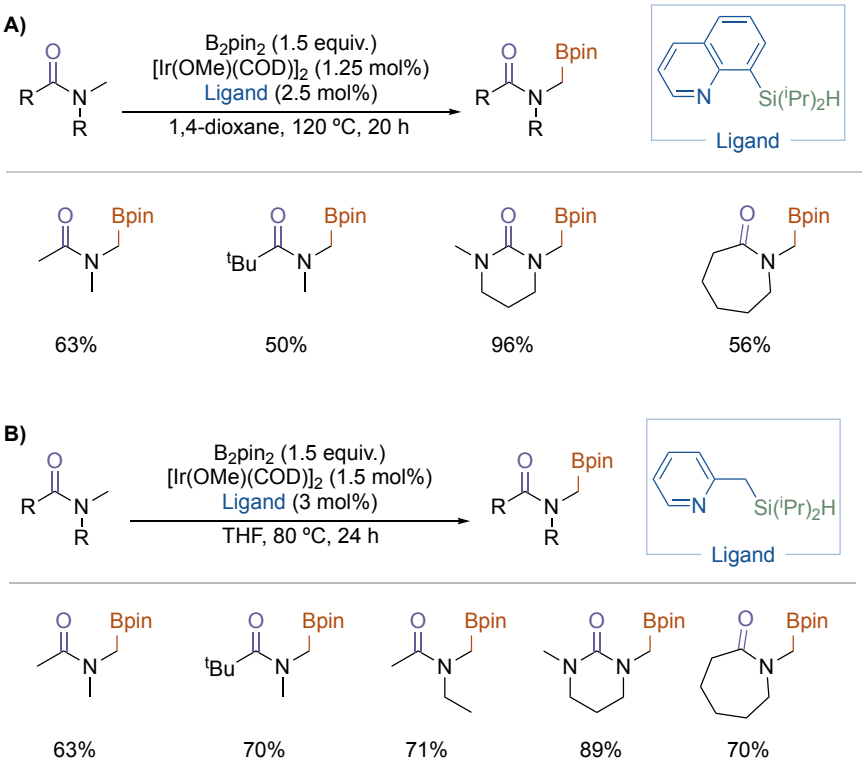



**Figure *19*** General mechanism for the alkyl C–H borylation using monoanionic bidentate ligands.

Examples of this type of reaction involving L–X type of ligands were reported by the groups of Clark (Scheme *52* **A**)[93] and Maleczka's (Scheme *52* **B**)[94] for the borylation of methylamides. The reactions, which were carried out with ligands consisting of a pyridine or quinoline moiety tethered to a silyl group, required high temperatures and presented a limited scope.

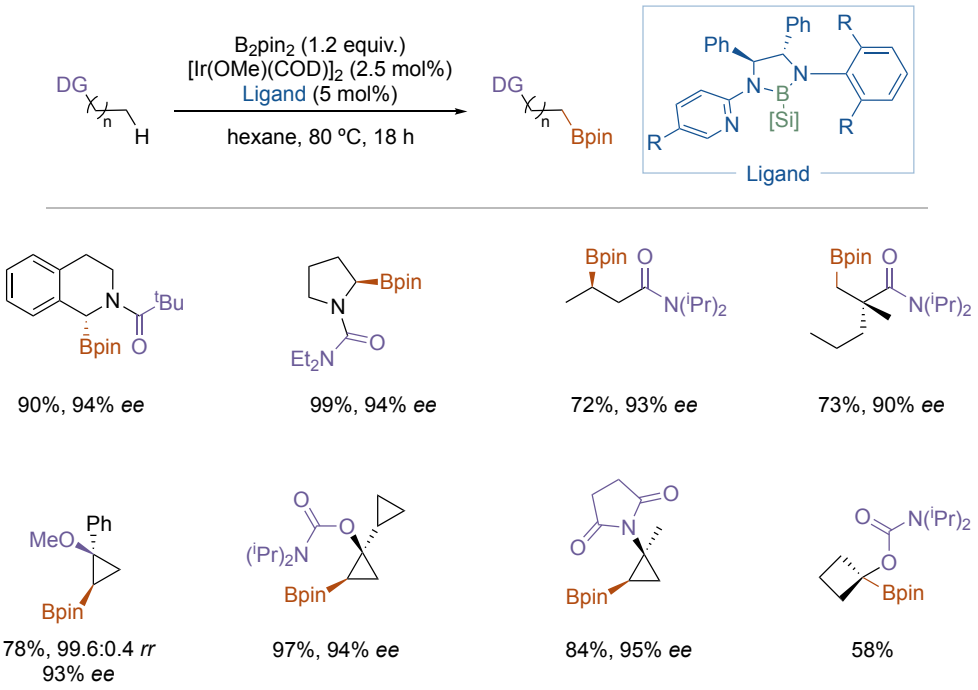
[93] Hyland, S. N.; Meck, E. A.; Tortosa, M.; Clark, T. B. *Tetrahedron Lett.* **2019,** *60,* 1096–1098.
[94] Dannatt, J. E.; Yadav, A.; Smith, M. R.; Maleczka, R. E. *Tetrahedron* **2022,** *109,* 132578.




**Scheme *52* A)** Borylation of N–Me position of amides using a quinoline-Si type of ligand developed by Clark's group. **B)** Related borylation developed by the group of Malezcka.

Similarly, the group of Senmiao Xu's group developed L–X type of ligands incorporating both a pyridine and aminoborane moiety. This unique ligand structure enabled the selective functionalization of diverse alkyl C–H bonds at the β-position of a variety of substrates with different directing groups (benzothiazoles, imines, amides, and ethers). Importantly, they also designed enantioselective versions of these ligands, that led to highly enantioselective C–H borylations of alkyl substrates.[95]

[95] a) Chen, X.; Chen, L.; Zhao, H.; Gao, Q.; Shen, Z.; Xu, S. *Chin. J. Chem.* **2020,** *38,* 1533–1537., b) Du, R.; Liu, L.; Xu, S. *Angew. Chem. Int. Ed.* **2021,** *60,* 5843–5847., c) Du, R.; Xu, S. *Sci. China Chem.* **2024**, d) Gao, Q.; Xu, S. *Angew. Chem. Int. Ed.* **2023,** *62,* e202218025., e) Shi, Y.; Gao, Q.; Xu, S. *J. Am. Chem. Soc.* **2019,** *141,* 10599–10604., f) Shi, Y.; Yang, Y.; Xu, S. *Angew. Chem. Int. Ed.* **2022,** *61,* e202201463., g) Xie, T.; Chen, L.; Shen, Z.; Xu, S. *Angew. Chem. Int. Ed.* **2023,** *62,* e202300199., h) Yang, Y.; Chen, J.; Shi, Y.; Liu, P.; Feng, Y.; Peng, Q.; Xu, S. *J. Am. Chem. Soc.* **2024,** *146,* 1635–1643., i) Zou, X.; Li, Y.; Ke, Z.; Xu, S. *ACS Catal.* **2022,** *12,* 1830–1840.

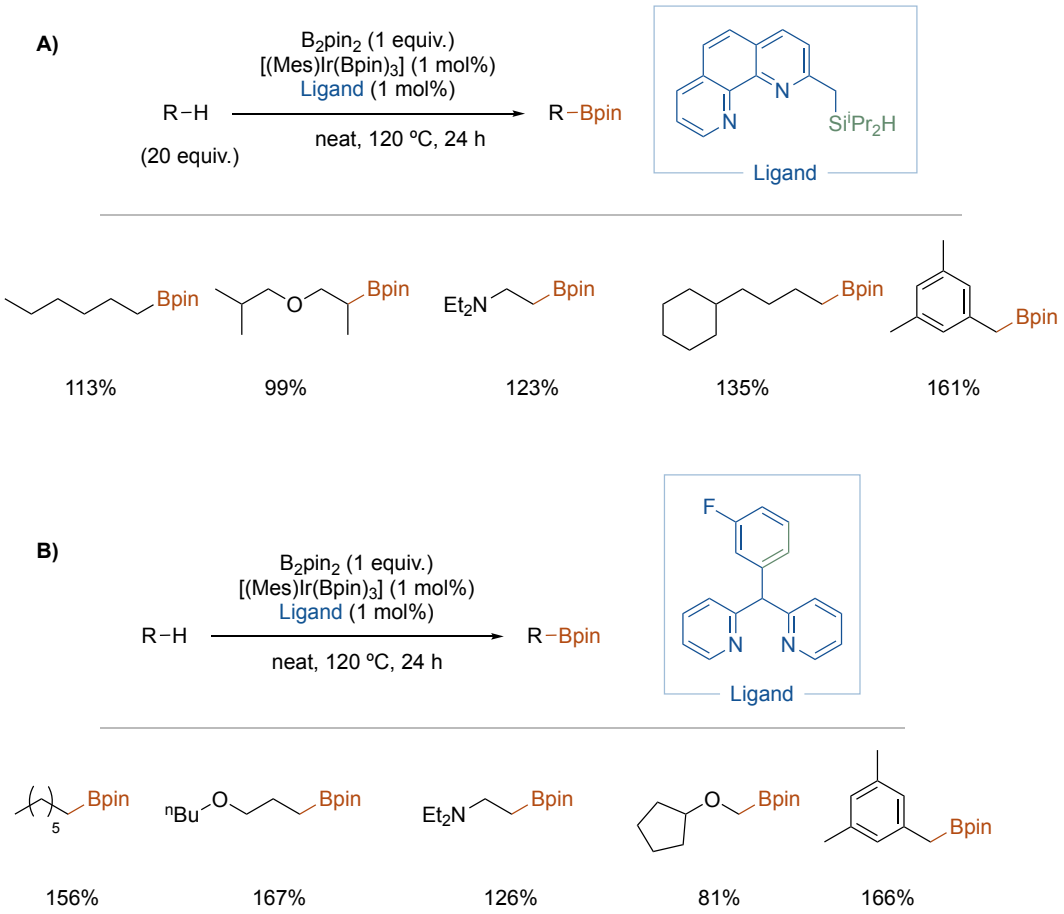



**Scheme *53*** Xu enantioselective borylation of alkyl bonds using CBL.

### 4.7.4 Pincer L–L–X ligands

Pincer ligands, where Ir is coordinated to two pyridines and an additional carbon or silicon atom, have also been sporadically used for alkyl C–H borylations. Therefore, the Kuninobu (Scheme *54* A)[96] and Schley (Scheme *54* B)[97] groups, developed undirected borylation of various hydrocarbon solvents using this type of ligands, though high temperatures and excess substrate were required.

[96] Kawazu, R.; Torigoe, T.; Kuninobu, Y. *Angew. Chem. Int. Ed.* **2022,** *61,* e202202327.
[97] a) Jones, M. R.; Fast, C. D.; Schley, N. D. *J. Am. Chem. Soc.* **2020,** *142,* 6488–6492., b) Jones, M. R.; Schley, N. D. *Synlett* **2021,** *32,* 845–850.




**Scheme *54* A)** Borylation of alkyl bonds using a N–N–Si ligand developed by Kuninobu's group. **B)** Borylation of alkyl bonds using a N–N–C ligand developed by Schley's group.

Overall, all the previous results confirm the relevance and recent progress in C–H borylation reactions, that has transformed the technology from a simple curiosity to a powerful and sustainable tool in synthetic organic chemistry.[98] It is crucial to remember that the resulting C–B bonds are highly versatile and can be elaborated through various methods, such as oxidation, halogenation, Suzuki-Miyaura, or Chan-Lam couplings (Figure *12*). Despite the advances, there are yet many challenges to be approached, especially with regards to reaching new types of regioselectivities, obtaining a better understanding on the mechanisms and the role of ligands and developing enantioselective versions.

USC UNIVERSIDADE DE SANTIAGO

[98] Yu, I. F.; Wilson, J. W.; Hartwig, J. F. *Chem. Rev.* **2023,** *123,* 11619–11663.

# 5 General objectives

USC
UNIVERSIDADE
DE SANTIAGO
DE COMPOSTELA

The goal of this PhD thesis is the development of novel strategies for performing regioselective iridium-catalyzed C–H borylations leveraging on non-covalent interactions with newly designed ligands.

The first section will focus on the preparation of bifunctional bipyridine and phenanthroline ligands functionalized with urea or squaramide groups, designed for achieving iridium catalyzed regioselective C–H borylations at the distal ring of biphenyl systems. This is a goal that has not yet been achieved using previously described strategies.

The second section aimed at the performing *ortho*-borylations in aryl carboxamides and derivatives using readily accessible bidentate neutral L–L bipyridine ligands. This requires the design of very specific ligands modified at the 5-position of the pyridine rings. As indicated in the introduction, L–L ligands tend to give *meta* and *para* products, and therefore harnessing them for *ortho* orientation is intriguing.

Finally, the last section was focused on the borylation of non-aromatic systems, specifically alkylamides, also using L–L ligands, something that has not been demonstrated in previous work.

USC
UNIVERSIDADE DE SANTIAGO DE COMPOSTELA

# 6 Methodology

USC
UNIVERSIDADE
DE SANTIAGO
DE COMPOSTELA

## 6.1 General experimental methodology

Unless specified otherwise, all commercially available reagents and solvents were used as received. Reactions were conducted in dry solvents unless otherwise stated. Procedures for the synthesis of precursors were performed under a dry nitrogen atmosphere using vacuum-line and standard Schlenk techniques. Chemicals were purchased from Sigma Aldrich, Alfa Aesar, TCI, Fluorochem, Apollo Scientific or BLDpharm and used without further purification. Dry solvents were directly purchased from Sigma Aldrich or Across Organics (Extra Dry over Molecular Sieves) and used without further purification. Catalytic reactions were carried out with THF from a solvent purification system (MBraun, SPS-5) stored over Molecular Sieves.

Reaction mixtures were stirred using Teflon-coated magnetic stir bars. The abbreviation "rt" refers to reactions carried out approximately between 21-25 °C. Temperature was maintained using Thermowatch-controlled heating blocks. Thin-layer chromatography (TLC) was performed on pre-coated silica gel F254 plates and components were visualized by observation under UV light and/or by treating the plates with $KMnO_4$ or *p*-anisaldehyde followed by heating. Flash chromatography was carried out on silica gel (40-63 μm) or using a Büchi Pure Chromatography system.

Concentration refers to the removal of volatile solvents via distillation using a rotary evaporator Büchi R-210 equipped with a thermostated bath B-491, a vacuum regulator V-850, followed by residual solvent removal under high vacuum.

NMR data was collected at room temperature or at 258 K at the CiQUS facility of the University of Santiago de Compostela on a Varian Mercury 300 MHz spectrometer and at the CACTI facility of the University of Vigo on a Bruker Advance DPX400 MHz, a Bruker NEO 400 MHz or a Bruker AVANCE DPX600 MHz spectrometer. Data are represented as follows: chemical shift, multiplicity (s = singlet, d = doublet, t = triplet, q = quartet, m = multiplet, br = broad signal, bs = broad singlet, dd = doublet of doublets, dt = doublet of triplets, dq = doublet of quartets, td = triplet of doublets, ddd = doublet of doublet of doublets, ddt = doublet of doublet of triplets, dtd = doublet of triplet of doublets, tt = triplet of triplets, pd = pentuplet of doublets, h=hexaplet dqd = doublet of quartets of doublets), coupling constants in Hertz (Hz). The chemical shifts for protons (δ) are reported in parts per million downfield from tetramethylsilane and are referenced to residual protium in the NMR solvent ($CHCl_3$ δ = 7.26 ppm, DMSO-$d_6$ δ = 2.5 ppm, MeOD δ = 3.3 ppm, $(CD_3)_2CO$ δ = 2.05 ppm, THF-d8 δ =3.58, 1.72 ppm). Chemical shifts for carbon are reported in parts per million downfield from tetramethylsilane and are referenced to the carbon resonances of the solvent ($CDCl_3$ δ = 77.16 ppm, DMSO-$d_6$ δ = 39.52 ppm, MeOD δ = 49.0 ppm, $(CD_3)_2CO$ δ = 29.84 ppm). In the $^{13}C$ NMR spectra of the borylated products, the carbon connected with the boron atom was not always observed due to quadrupolar relaxation. The chemical shifts for fluor (δ) are reported in parts per million

relative to trichlorofluoromethane. The chemical shifts for boron (δ) are reported in parts per million relative to $BF_3{\cdot}OEt_2$. The chemical shifts for nitrogen (δ) are reported in parts per million relative to liquid $NH_3$ at 25 ºC. NMR spectra were analyzed using MestreNova© NMR data processing software (www.mestrelab.com).

High Resolution Mass Spectra (HRMS) were performed at the CACTI facility of the University of Vigo on a Bruker TIMS-TOF or a SOLARIX XR FT-ICR-MS 7T. Samples were prepared by adding a spray solution of 70:29.9:0.1 (v/v/v) $CH_3OH$/water/formic acid or 70:29.9:0.1 (v/v/v) $CH_3CN$/water/formic acid to a solution of the sample. M+Na masses of borylated products were obtained after diluting an aliquot in a saturated solution of NaCl in MeOH/$CH_2Cl_2$ 1:3 (v/v). Mass spectrometry data was analyzed using Bruker DataAnalysis Version 5.1 data processing software.

GC/MS analysis (CI) were performed on an Agilent 5977B GC/MSD equipped with a 30 m HP-5MS column. Method: Initial temperature = 70 ˚C for 3 min, then 30 ºC/min to 300 ºC and hold for 8 min. Data was processed using Agilent MassHunter Qualitative Analysis 10.0 software.

In the supporting information we have included copies of only some representative GC/MS chromatograms.

The X-ray intensity data were measured at the Unidade de Raios X, RIAIDT, in the CACTUS facility of the University of Santiago de Compostela on a Bruker D8 VENTURE PHOTON-III C14 κ-geometry diffractometer system equipped with a Incoatec IμS 3.0 microfocus sealed tube (Cu Kα, λ = 1.54178 Å) and a multilayer mirror monochromator.

USC
UNIVERSIDADE DE SANTIAGO DE COMPOSTELA

## 6.2 General computational methodology

Full geometry optimizations and transition structure (TS) searches were carried out with Gaussian 16 [99] using the M06 hybrid functional,[100] the 6-31G(d)[101] basis set and the LANL2DZ[102] effective core potential for Ir, with ultrafine integration grids. The possibility of different conformations was considered for all structures. All stationary points were characterized by a frequency analysis performed at the same level used in the geometry optimizations from which thermal corrections were obtained at 298.15 K. The quasiharmonic approximations reported by Head-Gordon et al. and Grimme et al. were applied using GoodVibes[103] to replace the rigid-rotor harmonic oscillator (RRHO) approximation for the calculation of the vibrational contribution to enthalpy[104] and entropy,[105] respectively. Scaled frequencies were not considered. Mass-weighted intrinsic reaction coordinate (IRC) calculations were carried out using the Hessian-based predictor-corrector integrator scheme by Hratchian and Schlegel[106] in order to ensure that the TSs indeed connected the appropriate reactants and products. Single-point energies were calculated on the optimized geometries using different DFT functionals (M06,[100] ωB97x-D,[107] B3LYP[108] and B3LYP-D3 featuring Grimme's dispersion correction[109] with Becke-Johnson damping) and basis sets (6-311G(2d,p)[110] and 6-311++G(2d,p)[111]) together with the SDD[112] effective core potential for Ir, with ultrafine integration grids. Bulk solvent effects in tetrahydrofuran were considered implicitly through the integral equation

---

[99] M. J. Frisch, G. W. Trucks, H. B. Schlegel, G. E. Scuseria, M. A. Robb, J. R. Cheeseman, G. Scalmani, V. Barone, G. A. Petersson, H. Nakatsuji, X. Li, M. Caricato, A. V. Marenich, J. Bloino, B. G. Janesko, R. Gomperts, B. Mennucci, H. P. Hratchian, J. V. Ortiz, A. F. Izmaylov, J. L. Sonnenberg, D. Williams-Young, F. Ding, F. Lipparini, F. Egidi, J. Goings, B. Peng, A. Petrone, T. Henderson, D. Ranasinghe, V. G. Zakrzewski, J. Gao, N. Rega, G. Zheng, W. Liang, M. Hada, M. Ehara, K. Toyota, R. Fukuda, J. Hasegawa, M. Ishida, T. Nakajima, Y. Honda, O. Kitao, H. Nakai, T. Vreven, K. Throssell, J. A. Montgomery Jr., J. E. Peralta, F. Ogliaro, M. J. Bearpark, J. J. ; Heyd, E. N. Brothers, K. N. Kudin, V. N. Staroverov, T. A. Keith, R. Kobayashi, J. Normand, K. Raghavachari, A. P. Rendell, J. C. Burant, S. S. Iyengar, J. Tomasi, M. Cossi, J. M. Millam, M. Klene, C. Adamo, R. Cammi, J. W. Ochterski, R. L. Martin, K. Morokuma, O. Farkas, J. B. Foresman, D. J. Fox, Gaussian 16, Revision C.01. Gaussian, Inc., Wallingford CT, **2016**.

[100] Zhao; Truhlar *Theor Chem Account* **2008,** *120,* 215–241.

[101] a) Hariharan, P. C.; Pople, J. A. *Theoret. Chim. Acta* **1973,** *28,* 213–222., b) Hehre, W. J.; Ditchfield, R.; Pople, J. A. *J. Chem. Phys.* **1972,** *56,* 2257–2261.

[102] Hay, P. J.; Wadt, W. R. *J. Chem. Phys.* **1985,** *82,* 299–310.

[103] Luchini, G.; Alegre-Requena, J. V.; Funes-Ardoiz, I.; Paton, R. S. *F1000Research* **2020,** *9,* 291.

[104] Li, Y.; Gomes, J.; Mallikarjun Sharada, S.; Bell, A. T.; Head-Gordon, M. *J. Phys. Chem. C* **2015,** *119,* 1840–1850.

[105] Grimme, S. *Chem. Eur. J.* **2012,** *18,* 9955–9964.

[106] a) Hratchian, H. P.; Schlegel, H. B. *J. Chem. Theory Comput.* **2005,** *1,* 61–69., b) Hratchian, H. P.; Schlegel, H. B. *J. Chem. Phys.* **2004,** *120,* 9918–9924.

[107] Chai, J.; Head-Gordon, M. *Phys. Chem. Chem. Phys.* **2008,** *10,* 6615–6620.

[108] Becke, A. D. *J. Chem. Phys.* **1993,** *98,* 5648–5652.

[109] Grimme, S.; Ehrlich, S.; Goerigk, L. *J. Comput. Chem.* **2011,** *32,* 1456–1465.

[110] Krishnan, R.; Binkley, J. S.; Seeger, R.; Pople, J. A. *J. Chem. Phys.* **1980,** *72,* 650–654.

[111] Clark, T.; Chandrasekhar, J.; Spitznagel, G. W.; Schleyer, P. V. R. *J. Comput. Chem.* **1983,** *4,* 294–301.

[112] Andrae, D.; Häußermann, U.; Dolg, M.; Stoll, H.; Preuß, H. *Theoret. Chim. Acta* **1990,** *77,* 123–141.

formalism IEF-PCM[113] and SMD[114] polarizable continuum models. Gibbs free energies (ΔG) were used for the discussion on the relative stabilities of the considered structures unless otherwise stated. Free energies calculated using the gas phase standard state concentration (1 atm = 1/24.5 M) were converted to reproduce the standard state concentration in solution (1 M) by adding or subtracting 1.89 kcal $mol^{-1}$ for bimolecular additions and decompositions, respectively. In general, the lowest energy conformer for each calculated stationary point was considered in the discussion of calculated selectivity. Cartesian coordinates, electronic energies, entropies, enthalpies, Gibbs free energies, and lowest frequencies of the calculated structures are summarized in the experimental section.

2D/1H Kinetic isotopic effects (KIE) were calculated at 298 K using Kinisot.py program[115] on the Gaussian output files corresponding to the lowest-energy optimized minima and transition states. The program diagonalizes the mass-weighted Hessian matrices to obtain harmonic vibrational frequencies and Bigeleisen-Mayer Reduced Isotopic Partition Function Ratios. The lowest six normal modes (translations and rotations) were not projected out. The one-dimensional tunnelling correction (Bell infinite-*para*bola model) was not used. Different scaling factors for vibrational frequencies in the range between 0.9 and 1.1 were tested.

Non-covalent interaction (NCI) analysis was performed with NCIPLOT3[116] using the promolecular density in the intermolecular mode. The NCI methodology is based on the analysis of the electron density (ρ) and its reduced density gradient (s). By mapping ρ and s on a three-dimensional grid centered on the molecule of interest, NCIs can be identified as the grid points in which ρ and s fall under a given threshold. Additionally, the sign of the second eigenvalue of the Hessian of ρ allows differentiation between van der Waals interactions, strong attractive interactions such as hydrogen bonds, and steric clashes. Non-covalent interactions were represented as isosurfaces of s (isovalue = 0.28), color-coded according to the interaction type (red: steric clashes, green: van der Waals, blue: strong attractive interactions). In all cases, only van der Waals interactions appear (green isosurfaces).

Topology analysis of the electron density were performed within the framework of Bader's quantum theory of atoms in molecules (QTAIM)[117] using Multiwfn 3.8.[118]

---

[113] a) Scalmani, G.; Frisch, M. J. *J. Chem. Phys.* **2010,** *132,* 114110., b) Tomasi, J.; Mennucci, B.; Cammi, R. *Chem. Rev.* **2005,** *105,* 2999–3094.
[114] Marenich, A. V.; Cramer, C. J.; Truhlar, D. G. *J. Phys. Chem. B* **2009,** *113,* 6378–6396.
[115] R. Paton, Patonlab/Kinisot: V2.0.1. **2022**. https://doi.org/10.5281/ZENODO.6831009**.**
[116] a) Contreras-García, J.; Johnson, E. R.; Keinan, S.; Chaudret, R.; Piquemal, J.; Beratan, D. N.; Yang, W. *J. Chem. Theory Comput.* **2011,** *7,* 625–632., b) Johnson, E. R.; Keinan, S.; Mori-Sánchez, P.; Contreras-García, J.; Cohen, A. J.; Yang, W. *J. Am. Chem. Soc.* **2010,** *132,* 6498–6506.
[117] Bader, R. F. W. *Chem. Rev.* **1991,** *91,* 893–928.
[118] Lu, T.; Chen, F. *J. Comput. Chem.* **2012,** *33,* 580–592.

Pairwise second-order perturbation energies (E2)[119] were calculated through a Natural Bond Orbital/Natural Localized Molecular Orbital (NBO/NLMO) analysis using the NBO 7.0 program[120] and Gaussian 16 as an interface. These attractive interactions were estimated by means of the localized σ, π, n, σ*and π* valence orbitals.

Electrostatic (Eelec), exchange (Eex), repulsion (Erep), polarization (Epol), electron correlation (Ecorr, which implicitly accounts for dispersion for the M06 functional) and desolvation (Edesol) contributions to interaction energies (Eint) between the catalyst and the substrate were calculated through the Generalized Kohn-Sham Energy Decomposition Analysis (GKS-EDA)[121] as implemented in the XEDA program[122] based in GAMESS 2021 R2.[123]

[119] a) Reed, A. E.; Curtiss, L. A.; Weinhold, F. *Chem. Rev.* **1988,** *88,* 899–926., b) Weinhold, F. *Natural Bond Orbital Methods* **1998***, 3*, 1792–1811.

[120] NBO 7.0. E. D. Glendening, J. K. Badenhoop, A. E. Reed, J. E. Carpenter, J. A. Bohmann, C. M. Morales, P. Karafiloglou, C. R. Landis, and F. Weinhold, Theoretical Chemistry Institute, University of Wisconsin, Madison, WI (**2018**).

[121] Su, P.; Tang, Z.; Wu, W. *WIREs Comput Mol Sci.* **2020,** *10,* e1460.

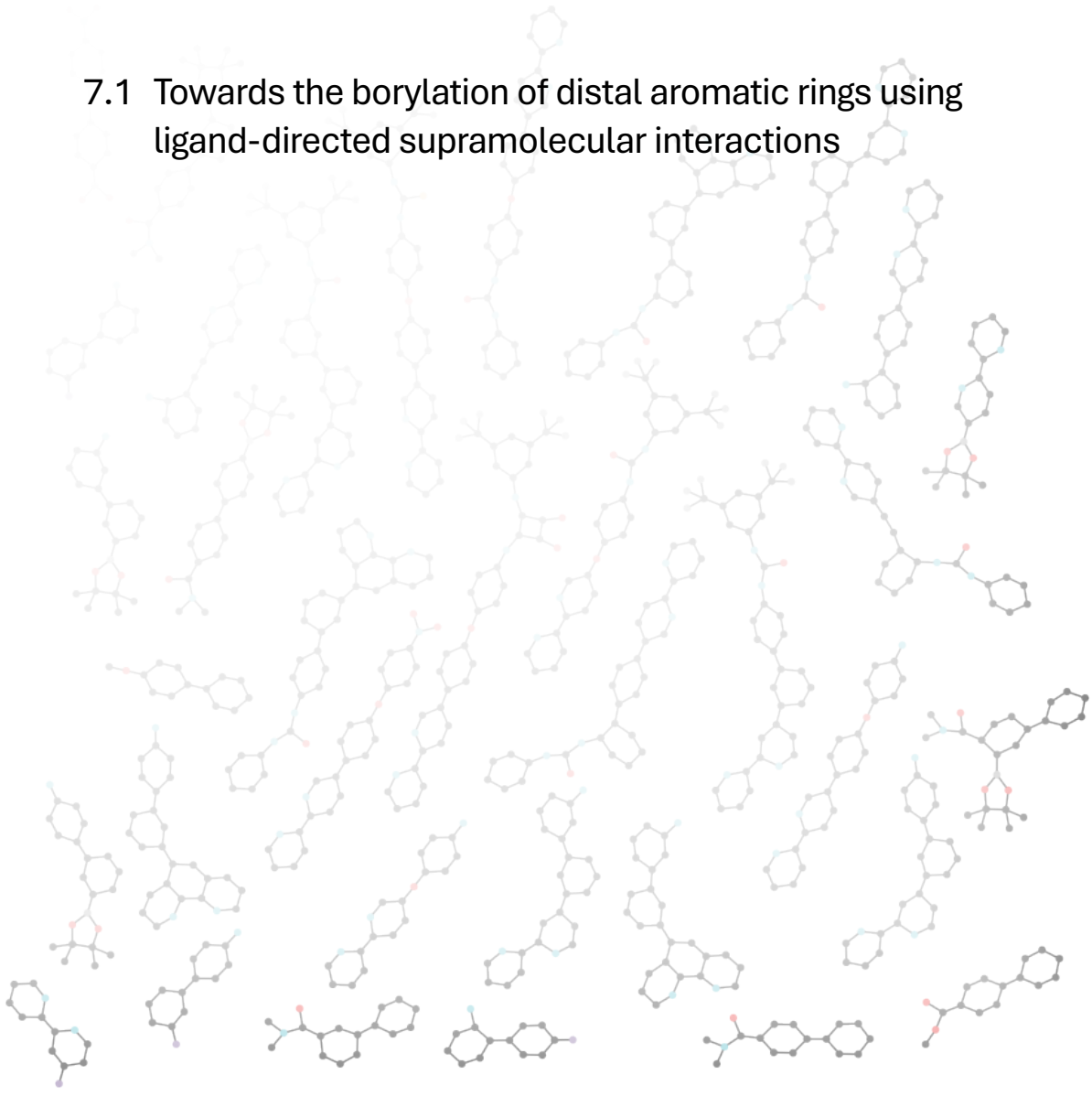
[122] Tang, Z.; Song, Y.; Zhang, S.; Wang, W.; Xu, Y.; Wu, D.; Wu, W.; Su, P. *J. Comput. Chem.* **2021,** *42,* 2341–2351.

[123] Barca, G. M. J.; Bertoni, C.; Carrington, L.; Datta, D.; De Silva, N.; Deustua, J. E.; Fedorov, D. G.; Gour, J. R.; Gunina, A. O.; Guidez, E.; Harville, T.; Irle, S.; Ivanic, J.; Kowalski, K.; Leang, S. S.; Li, H.; Li, W.; Lutz, J. J.; Magoulas, I.; Mato, J.; Mironov, V.; Nakata, H.; Pham, B. Q.; Piecuch, P.; Poole, D.; Pruitt, S. R.; Rendell, A. P.; Roskop, L. B.; Ruedenberg, K.; Sattasathuchana, T.; Schmidt, M. W.; Shen, J.; Slipchenko, L.; Sosonkina, M.; Sundriyal, V.; Tiwari, A.; Galvez Vallejo, J. L.; Westheimer, B.; Włoch, M.; Xu, P.; Zahariev, F.; Gordon, M. S. *J. Chem. Phys.* **2020,** *152,* 154102.

# 7 Results and Discussion

USC
UNIVERSIDADE
DE SANTIAGO
DE COMPOSTELA

## 7.1 Towards the borylation of distal aromatic rings using ligand-directed supramolecular interactions



### 7.1.1 State of the art

As outlined in the introduction, significant progress has been made in developing methods to control the reactivity and regioselectivity in iridium-catalyzed C–H borylation reactions. In the case of aromatic substrates, several methods for controlling *ortho*-, *meta*- or *para*- selectivity have been developed. Remarkably, there are not reports on the selective borylation of aromatic rings distal to that bearing the directing functional group.

This represents a relevant goal, as it would allow to expand the possibilities for the postfunctionalization of polyaromatic substrates, although it is highly challenging. Considering the significant progress in the use of out-sphere, supramolecular interactions to guide regioselective borylations, it seems reasonable to envision that appropriately designed ligands could allow a selective functionalization of rings distal to a functional group controlling the molecular recognition process.

### 7.1.2 Objectives

On the above grounds, we proposed as the initial objective of this PhD thesis the design of ligands for the selective borylation of distal aromatic rings in biphenyl systems bearing a functional directing group in one of the rings. This would require the design and synthesis of tailored bipyridine or phenanthroline ligands that can introduce selective supramolecular contacts to precisely locate the iridium catalyst near the C–H bond that will be activated.

Considering the work of Kanai on *meta*-selective borylations controlled by hydrogen bonds (Scheme *29*), we focused on bipyridine ligands that feature urea or squaramide groups and thereby can form hydrogen bonds with carbonyl or carboxy functional groups present in the substrates.

### 7.1.3 Results and discussion

The initial experiments in this project were conducted in collaboration with Dr. Cristian Vidal. To guide the design of the ligand, we took as reference the original work from Kanai and Kuninobu's, and expanded the linker between the bipyridine and the urea moieties so that we can target the activation of the distal ring.[72] This design strategy led us to the ligands indicated in Figure *20*, exhibiting a phenyl ring or an alkyne linker between the bipyridine core and the urea moiety.

USC UNIVERSIDADE DE SANTIAGO DE COMPOSTELA

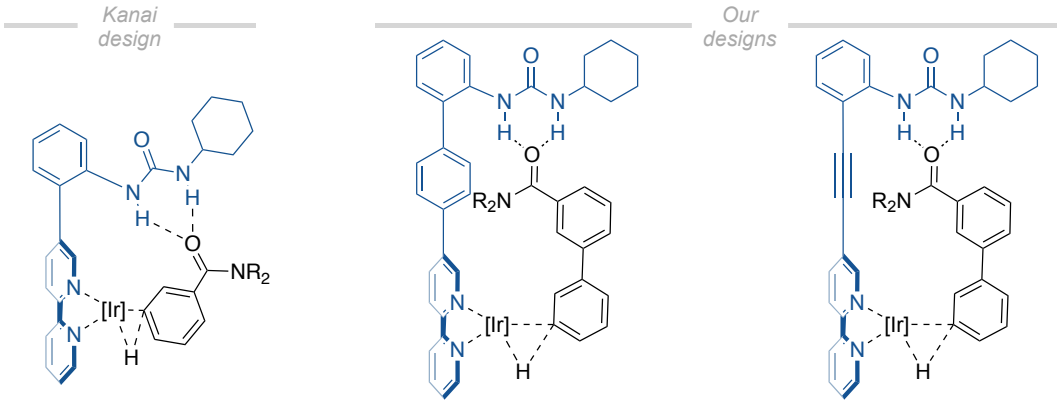
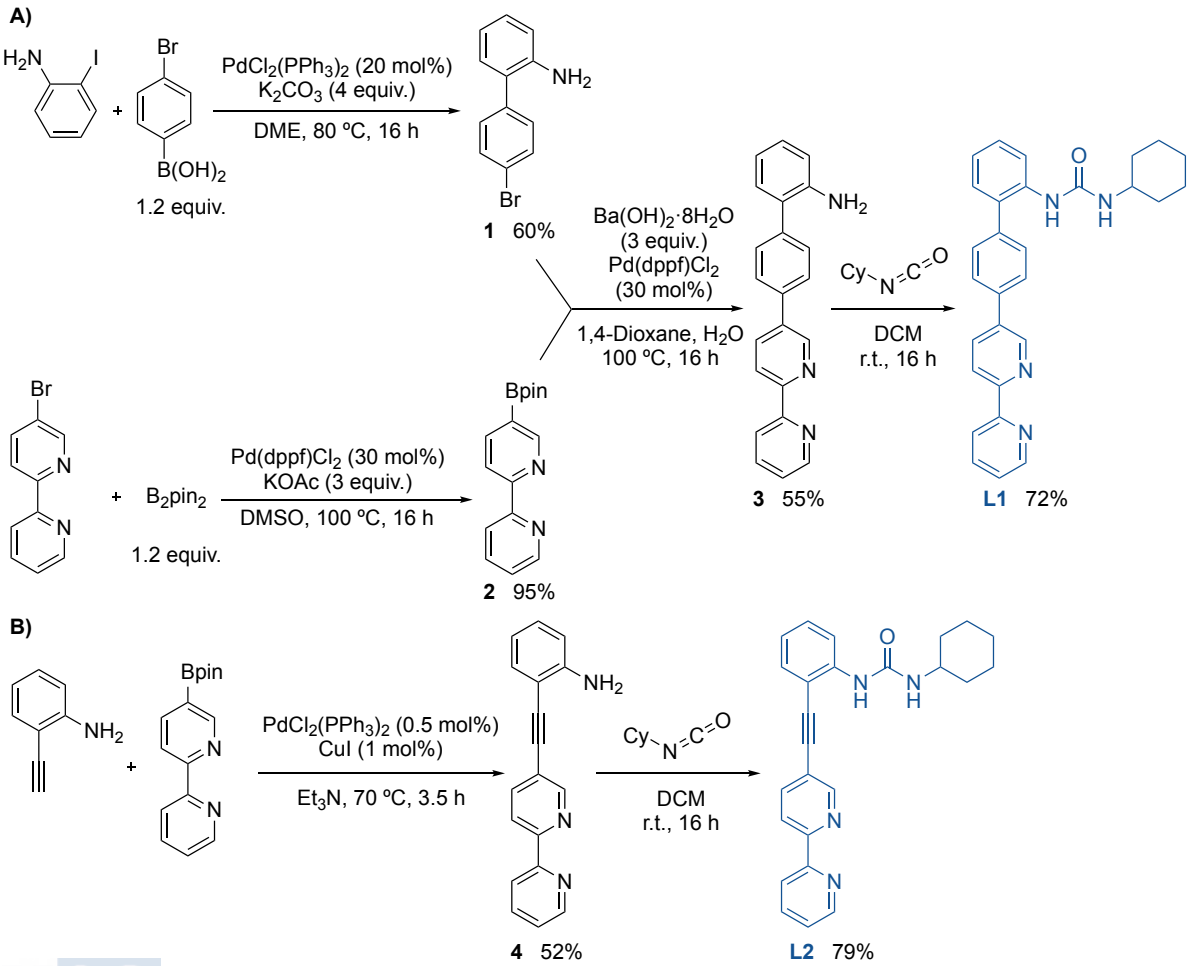



**Figure *20*** Original designs for the distal C–H borylation of biphenyls.

These ligands were synthesized by coupling the 5-bromo-2,2'-bipyridine to the amine linker moiety via a Suzuki or a Sonogashira coupling, to give either bipyridines **3** or **4** (*Scheme 55*). Subsequently, reaction with the corresponding isocyanate resulted in the formation of the desired urea equipped ligands **L1** and **L2** (Scheme *55*, see experimental part for details).

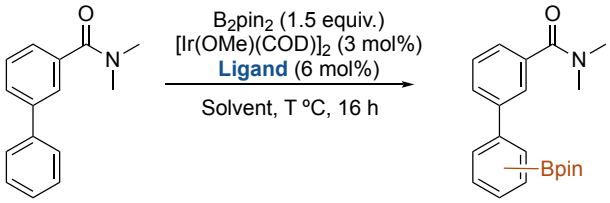



**Scheme *55*** Synthesis of **L1** (24% overall yield) and **L2** (39% overall yield).

Our initial borylation experiments were performed by treating the substrate N,N-dimethyl-[1,1'-biphenyl]-3-carboxamide (**5**) with $B_2pin_2$ (1.5 equiv.), $[Ir(OMe)COD]_2$ (3 mol %), and our custom ligands (6 mol %) in *p*-xylene or THF, at room temperature overnight. NMR and GC/MS analysis of the crude reaction mixture revealed the absence of any borylation products (Table *1*).

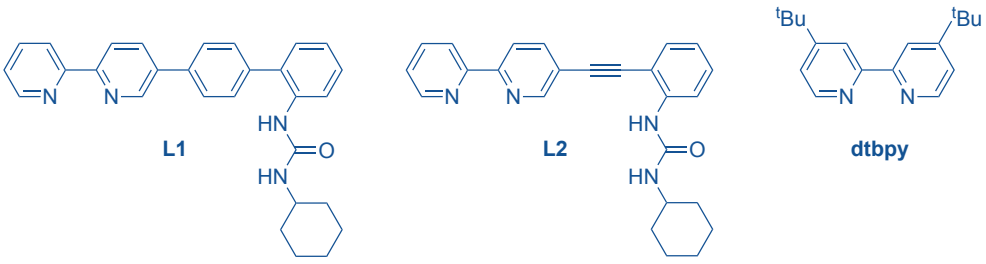
As a control, we performed the experiment using 4,4'-di-*tert*-butyl-2,2'-bipyridine (**dtbpy**) as ligand. Nevertheless, we still didn't detect any borylated products, even when the reaction temperature was raised to 80 ºC (Table *1*).

**Table *1*** First borylation experiments.




**5**

| Ligand | Solvent | Temperature ºC | **5** (SM, %) |
|---|---|---|---|
| **L1** | *p*-xylene | rt | 100 |
| **L1** | THF | rt | 100 |
| **L2** | *p*-xylene | rt | 100 |
| **L2** | THF | rt | 100 |
| **dtbpy** | *p*-xylene | rt | 100 |
| **dtbpy** | *p*-xylene | 80 | 100 |



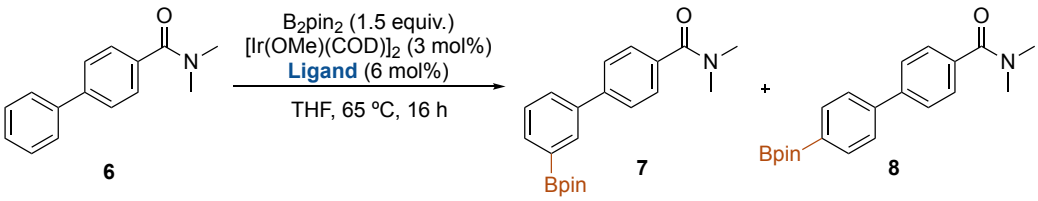

With these results, we wondered if the substrate's geometry was the reason for the lack of reactivity. Therefore, we decided to switch to N,N-dimethyl-[1,1'-biphenyl]-4-carboxamide (**6**) as a model substrate. We applied similar conditions to those described by Reek and coworkers[76] for the borylation of benzamide: $B_2pin_2$ (1.5 equiv.), $[Ir(OMe)COD]_2$ (3 mol%), 2,2'-bipyridine (**bipy**, 6 mol%) in THF at 65 ºC overnight. In this case, we observed the formation of two distinct borylated products by GC-MS. These products were later confirmed through independent synthesis (see the experimental part) to be the *meta* and *para* borylated products **7** and **8** (Table *2*, entry 1)

USC UNIVERSIDADE DE SANTIAGO DE COMPOSTELA

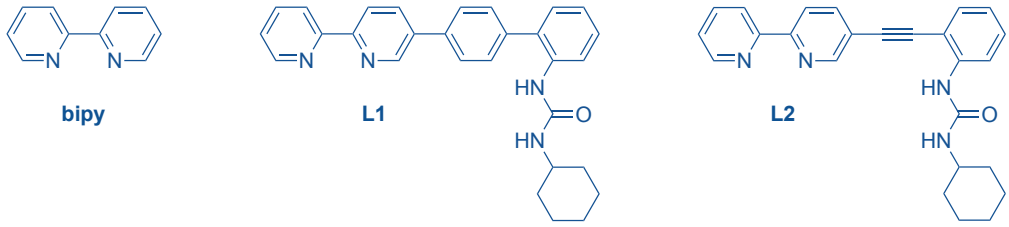
We then moved to our custom ligands. The experiment with the ligand bearing the phenyl linker **L1** showed a 8% conversion, but the reaction produced both products **7** and **8** in almost the same ratio as the control reaction with **bipy**. Furthermore, using the ligand containing the alkyne linker (**L2**) we observed no reactivity (Table *2*).

It's important to note, as mentioned in the footnote of the table, that the percentages were calculated from the integrals of the starting materials and products in the GC/MS chromatogram as these were essentially the only products detected in the analysis along with $B_2pin_2$. This type of relative quantification will be used in all other tables of the thesis manuscript, unless otherwise specified.

**Table *2*** Ligand screening




| Ligand | **6** (SM, %) | **7** (*meta*, %) | **8** (*para*, %) | Ratio **7/8** |
|---|---|---|---|---|
| **bipy** | 34 | 43 | 23 | 1.9 |
| **L1** | 92 | 5.4 | 2.6 | 2 |
| **L2** | 100 | 0 | 0 | 0 |




Note: The percentage was calculated considering the integrals of GC/MS peaks. **6**, **7** and **8** are essentially the only products detected in the analysis.

We then hypothesized that these designed ligands might be too rigid to successfully adapt to the transition state geometry required for a selective distal borylation. Therefore, we designed new, more flexible ligands that incorporated an ether moiety into the linker and have different H-bond recognition moieties such as thiourea (**L3**), urea (**L4**) or squaramide (**L5**) (Figure *21*).

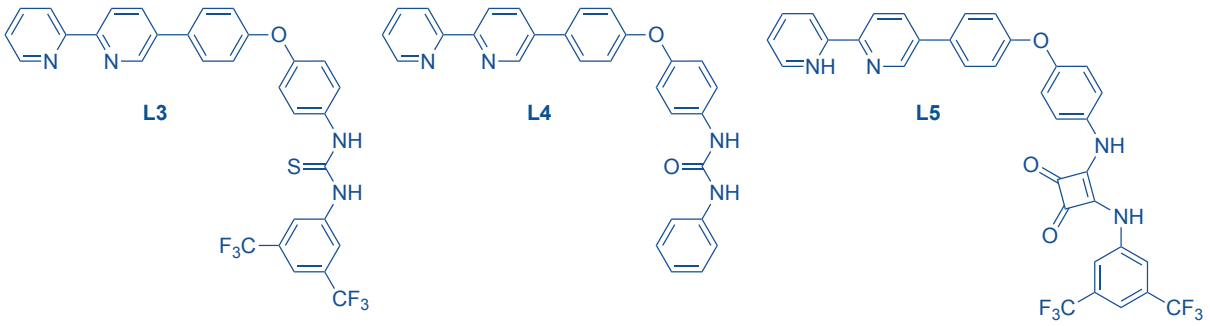
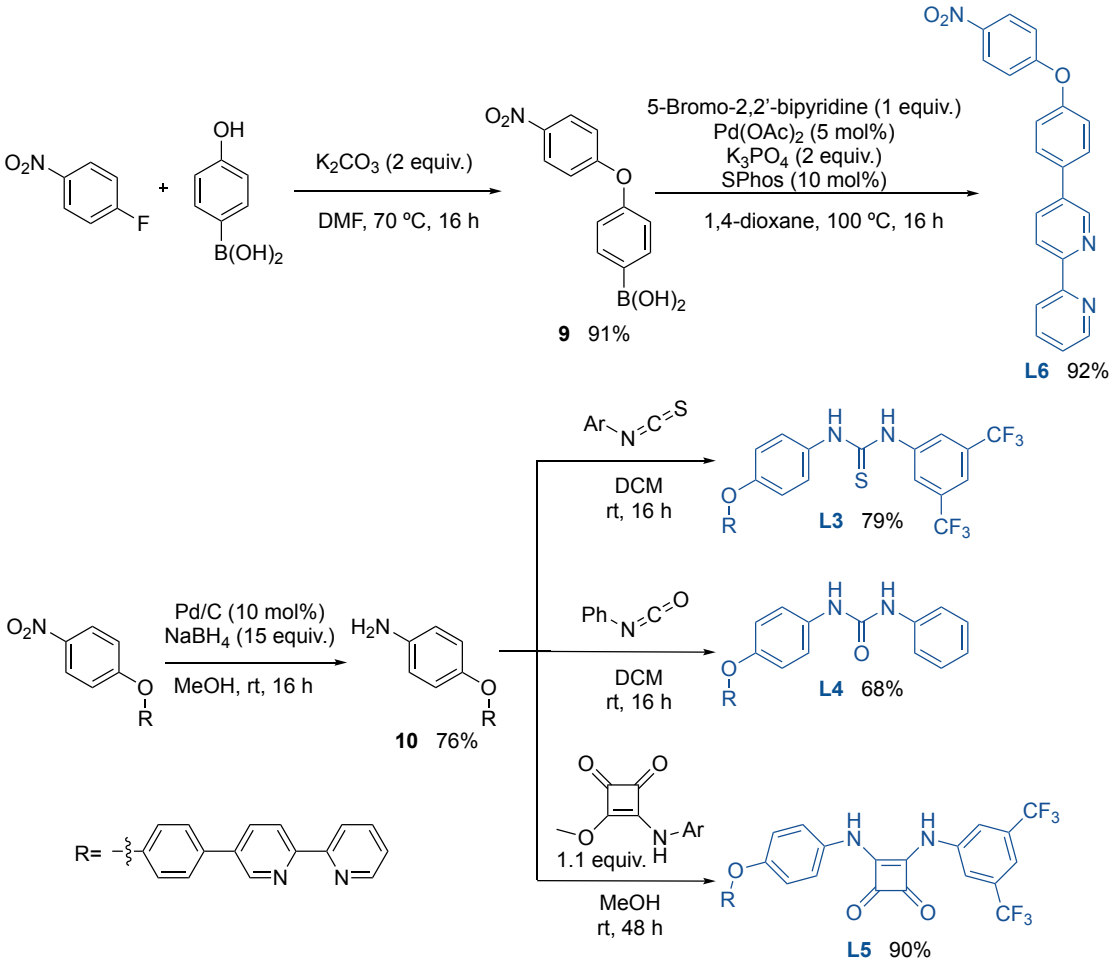



**Figure *21*** New designs for the distal C–H borylation of biphenyls.

These ligands were made by using a $S_NAr$ to build the diphenylether skeleton (**9**), followed by a Suzuki coupling to install the bipyridine core (**L6**) and the incorporation of the supramolecular recognition moiety (urea, thiourea, or squaramide) by reducing the -$NO_2$ group and reacting the resulting amine (**10**) with the corresponding isocyanate or squarate (**L3**-**L5**) (Scheme *56*, and experimental section).




**Scheme *56*** Synthesis of ligands **L3**-**L6.**

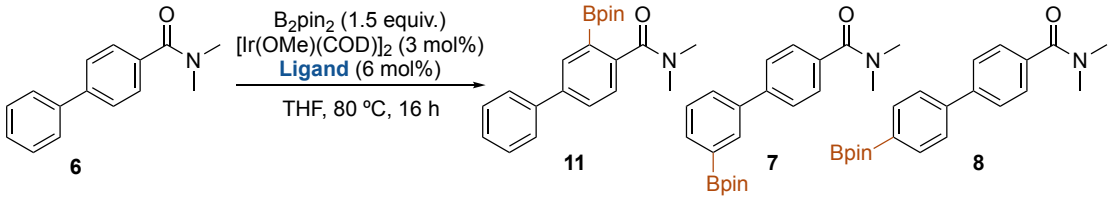
With these ligands at hand, we tested them in the borylation reaction using the standard reaction conditions, in THF but at a higher temperature of 80 ºC (Table *3*).

USC UNIVERSIDADE DE SANTIAGO DE COMPOSTELA

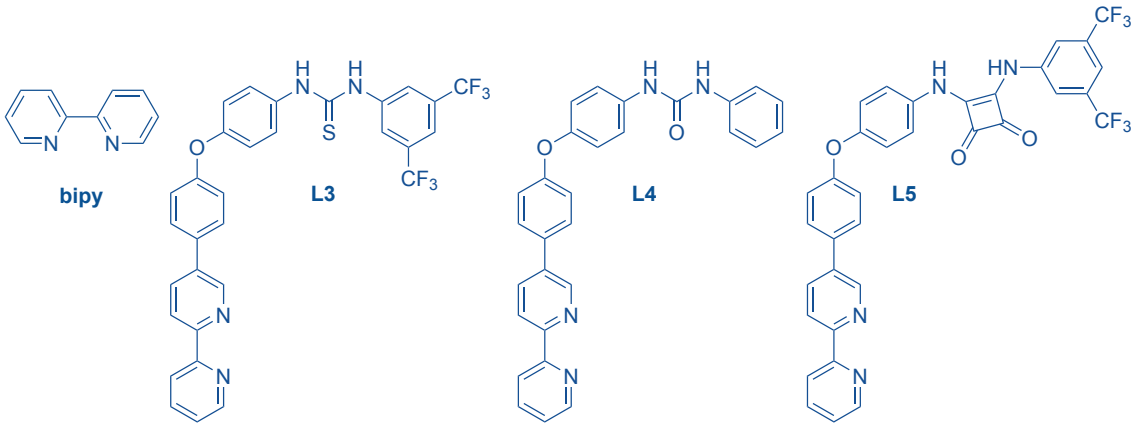
As shown in this table, the bipy showed almost full conversion towards meta and para products while thiourea-containing ligand (**L3**) failed to yield any conversion, likely because the sulfur poisoning of the Ir catalyst. In contrast, the urea (**L4**) and squaramide (**L5**) ligands demonstrated remarkable conversion and a surprising selectivity for *ortho*-borylation (**11**), which was an unexpected outcome considering that the ligands were specifically designed for the remote (distal) borylation.

This surprising and appealing result called for further investigation (see the subsequent section of the thesis).

**Table *3*** Ligand screening.




| Ligand | **6** (SM, %) | **11** (*ortho*, %) | **7+8** (*meta+para*, %) |
|---|---|---|---|
| **bipy** | 0 | 0 | 100 |
| **L3** | 100 | 0 | 0 |
| **L4** | 6 | 92 | 2 |
| **L5** | 16 | 71 | 13 |




Note: The percentage was calculated considering the integrals of GC/MS peaks. **6**, **7**, **8** and **11** are essentially the only products detected in the analysis.

At this point, and considering our initial objective, we reached out to computational chemist Dr. Gonzalo Jiménez Osés and his group, to refine our designs. These studies led to a newly designed ligand that might lead to borylated product at the *meta* position of the distal aromatic ring as the calculated energy barrier for the oxidative addition with the new ligand (22.8 kcal $mol^{-1}$) is significantly lower than the barrier for the oxidative addition of a C–H bond of benzene using **bipy** as a ligand (26.4 kcal $mol^{-1}$) (Figure *22*).

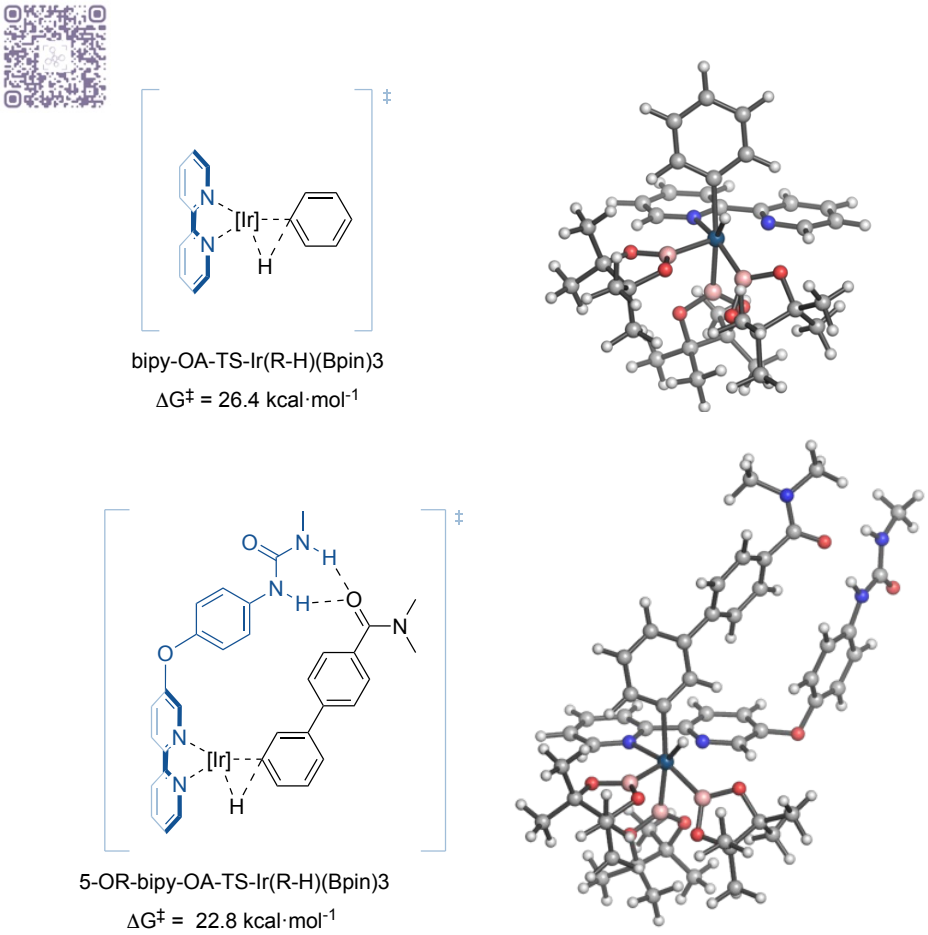
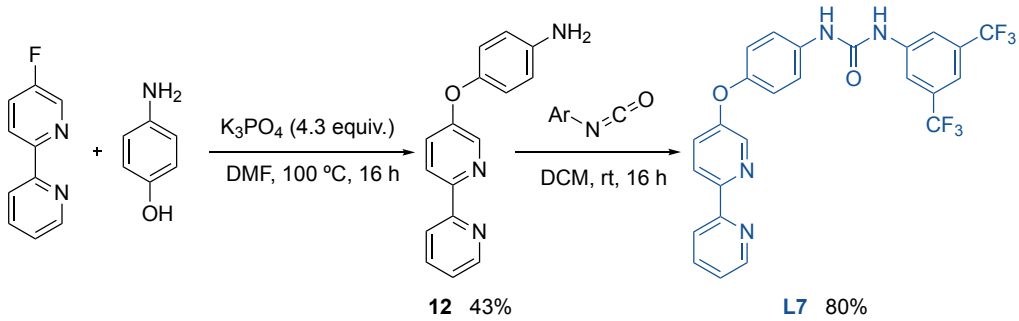



**Figure *22*** Computationally designed ligands for distal C-H activation. To see an interactive model of the calculated structures visit https://danielmarcosatanes.github.io/DMA_thesis-viewer/ or scan the QR code.

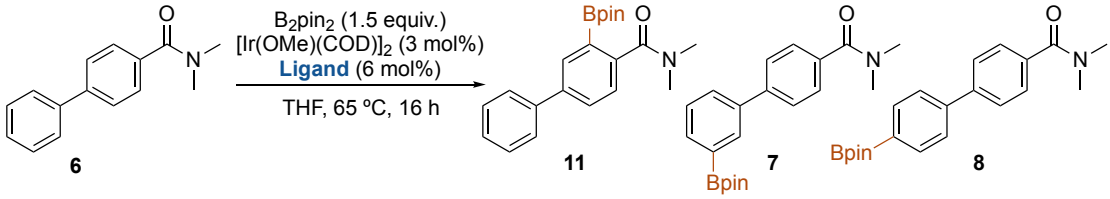
We successfully synthesized the computationally designed ligand **L7** with the urea moiety using a $S_NAr$ reaction to install the ether into the bipyridine core followed by a reaction with the isocyanate to obtain the urea ligand (Scheme *57*).



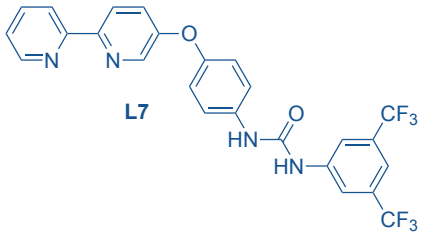

**Scheme *57*** Synthesis of ligands **L7** (34% overall yield).

Unfortunately, when tested in borylation reactions, we found that the ligand **L7** led to a reduced reactivity under the same reaction conditions as before. Notably, it maintained complete selectivity for proximal *ortho*-borylation. Modifying the solvent enhanced the conversion rates, but the regioselectivity remained predominantly *ortho* (Table *4*).

**Table *4*** Solvent screening using **L7** as ligand.




| **Solvent** | **6** (SM, **%**) | **11** (*ortho*, %) | **7+8** (*meta*+*para*, %) |
|---|---|---|---|
| THF | 82 | 18 | 0 |
| *p*-Xylene | 53 | 31 | 16 |
| CpOMe | 9 | 82 | 9 |




Note: The percentage was calculated considering the integrals of GC/MS peaks. **6**, **7**, **8** and **11** are essentially the only products detected in the analysis.

We then investigated whether altering the 5-substitution of the bipyridine ligand could alter the regioselectivity towards the distal aromatic ring. Inspired by Liang's work with phenanthrolines,[73] we designed 4-substituted bipyridines and 5-substituted phenanthroline ligands that were computationally optimized for borylation at either the *meta* or *para* positions at the distal aromatic ring of the biphenyl amide (Figure *23*).

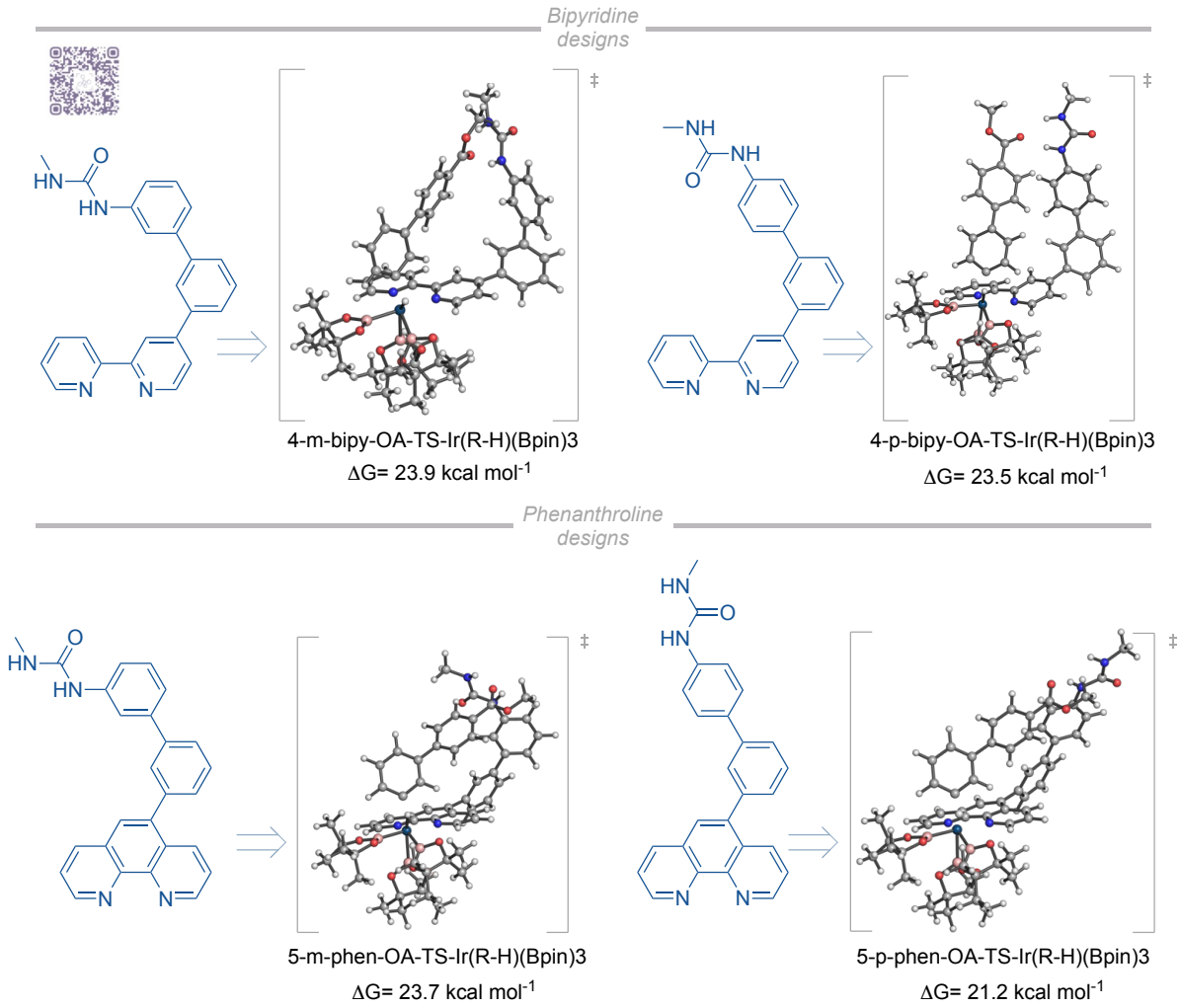
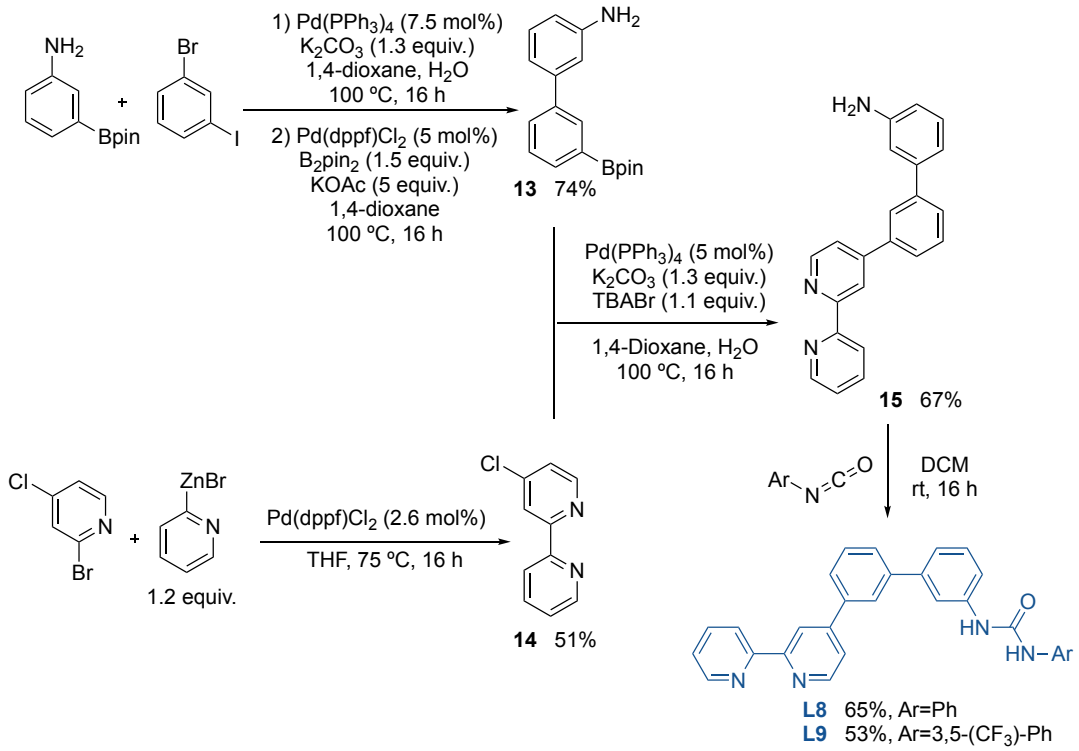


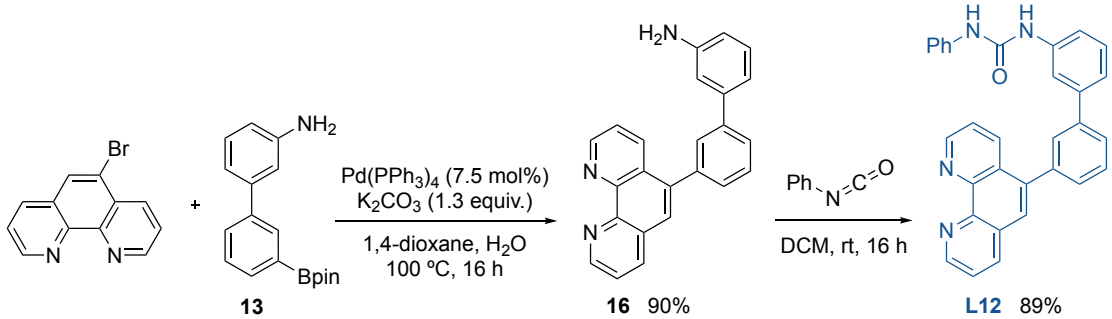

**Figure *23*** Computationally designed bipyridine and phenanthroline ligands for distal C–H activation of biphenyls. To see an interactive model of the calculated structures visit https://danielmarcosatanes.github.io/DMA_thesis-viewer/ or scan the QR code.

The experiments were conducted in collaboration with TFG student Maria Puente. These bipyridine ligands were synthesized in a similar manner to the previous ones, using a cross-coupling reaction to obtain the biphenyl amine linker (**13**). On the other hand, the 4-substituted bipyridine was synthesized through a Negishi coupling (**14**). Subsequently the two fragments were joined together via another cross-coupling reaction obtaining the bipyridine with the amino linker (**15**). Finally, the supramolecular recognition moiety was installed by reaction with the corresponding isocyanate (Scheme *58* showcases the synthesis of **L8** and **L9**; **L10** and **L11** were obtained in an analogous manner).




**Scheme *58*** Synthesis of bipyridine ligands **L8** and **L9**.

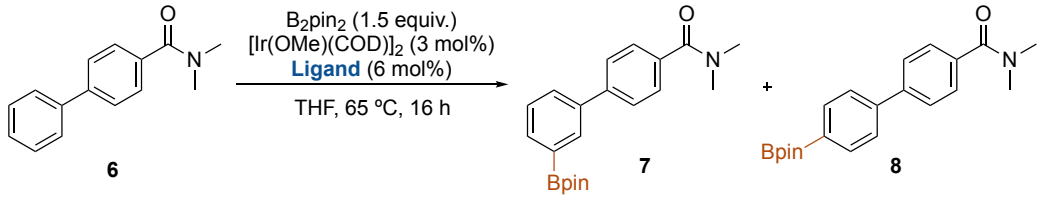
Phenanthroline ligands were synthesized in a similar manner, beginning with the 5-bromo-phenanthroline. This approach facilitated a streamline synthesis involving consecutive Suzuki couplings to obtain the phenanthroline attached to the corresponding linker (**16**). Finally, the desired ligand was obtained by reacting the amino containing phenanthroline with the isocyanate (Scheme *59*, represents the synthesis of **L12**; **L13** was synthesized in an analogous manner).



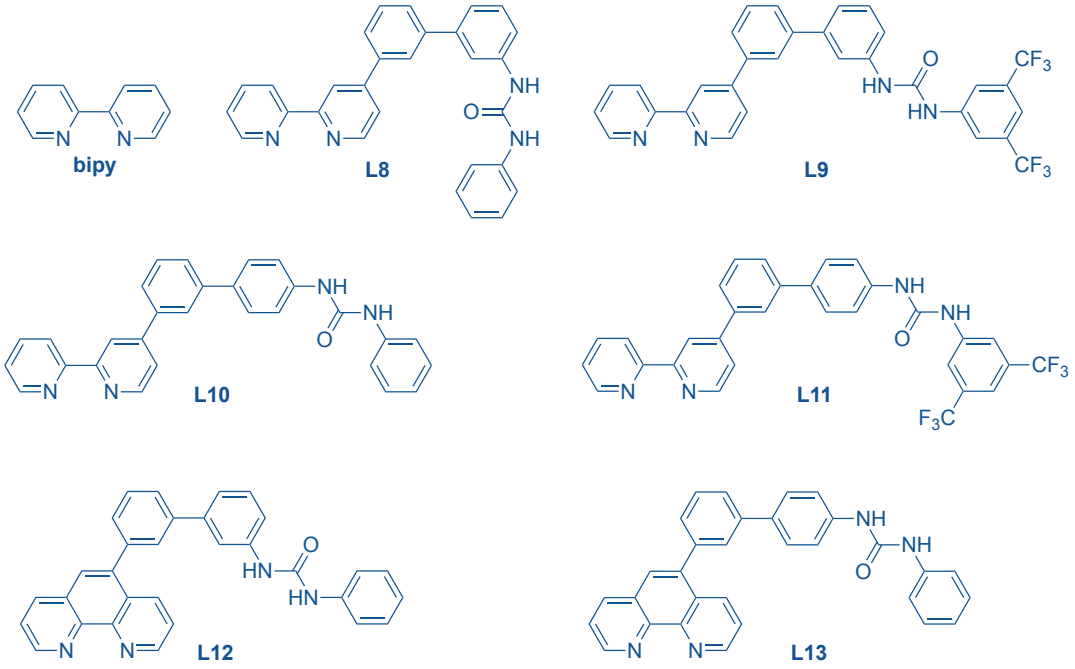

**Scheme *59*** Synthesis of phenanthroline ligand **L12.**

Once we synthesized these novel ligands, we used them under our standard reaction conditions. Remarkable, in these cases we did not observe *ortho*-borylation, but only the selective formation of *meta* and *para* borylation on the remote aromatic ring (Table *5*).

**Table *5*** Ligand screening.




| Ligand | **6** (SM, %) | **7** (*meta*, %) | **8** (para, %) | Ratio 7/8 |
|---|---|---|---|---|
| bipy | 34 | 43 | 23 | 1.9 |
| L8 | 23 | 56 | 21 | 2.66 |
| L9 | 17 | 52 | 31 | 1.67 |
| L10 | 4 | 53 | 43 | 1.23 |
| L11 | 5 | 51 | 43 | 1.18 |
| L12 | 15 | 55 | 29 | 1.9 |
| L13 | 4 | 66 | 33 | 2 |




Note: Percentages of starting material and products were determined by GC/MS analysis.

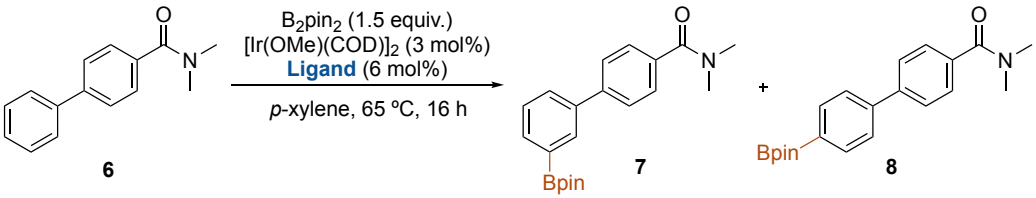
Interestingly, ligands with the urea group positioned in the *meta* position on the second aromatic ring (**L8** and **L9**) exhibited a significant increase in *meta* borylation (**7**), resulting in a *meta*-to-*para* ratio of 2.9:1. Conversely, ligands with the urea group positioned in the *para* position (**L10** and **L11**) displayed only a slight preference for *para* borylation (**8**), with a *meta*/*para* ratio of 1.2:1.

Based on these results, we aimed to enhance hydrogen bonding and improve the selectivity of the ligands by lowering the reaction temperature. However, we observed no reactivity at room temperature, even when using the control ligand 2,2'-bipyridine. We

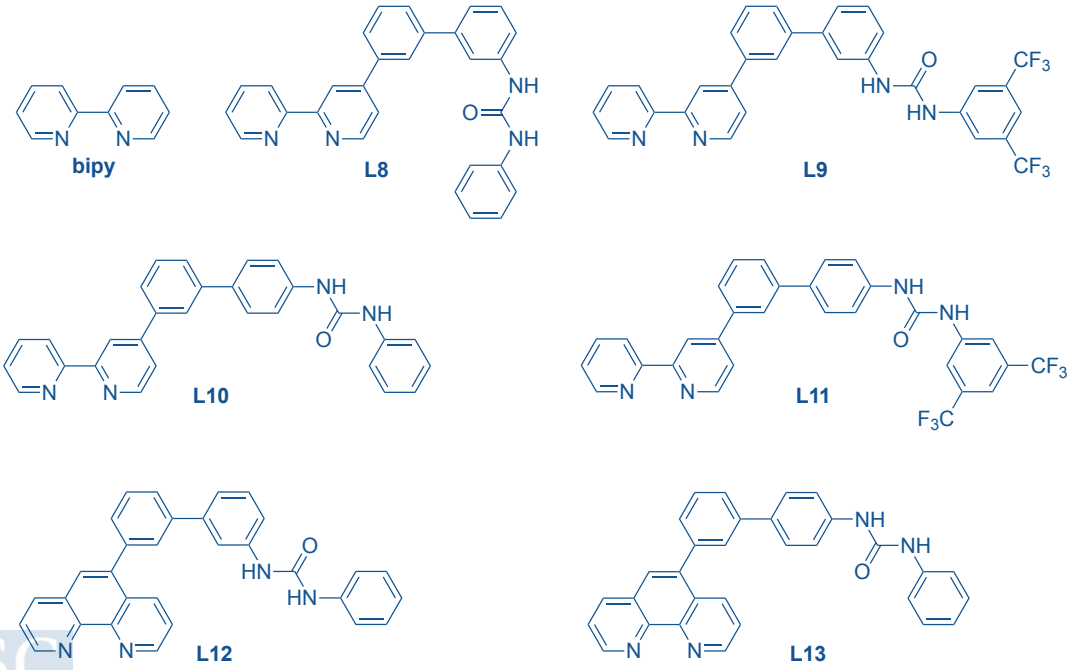
also tested other apolar solvents, such as hexane, in an attempt to promote hydrogen bonding interactions, but this approach proved unsuccessful as no conversion was observed, likely due to the poor solubility of the reaction components.

When we switched to *p*-xylene as the solvent, we observed excellent reactivity. However, the selectivity remained almost identical to that seen when using 2,2'-bipyridine as ligand (Table *6*). These findings suggest that while *p*-xylene enhances reactivity, it does not substantially affect the regioselectivity compared to the control ligand.

**Table *6*** Ligand screening



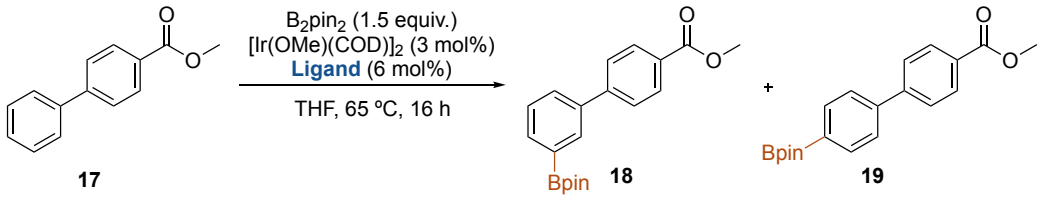

| Ligand | **6** (SM, %) | 7 (*meta*, %) | **8** (*para*, %) | **Ratio 7/8** |
|---|---|---|---|---|
| **bipy** | 1 | 41 | 57 | 0.72 |
| **L8** | 2 | 43 | 56 | 0.77 |
| **L9** | 2 | 43 | 55 | 0.78 |
| **L10** | 4 | 49 | 46 | 1.07 |
| **L11** | 7 | 52 | 41 | 1.27 |
| **L12** | 7 | 56 | 36 | 1.57 |
| **L13** | 1 | 41 | 58 | 0.71 |



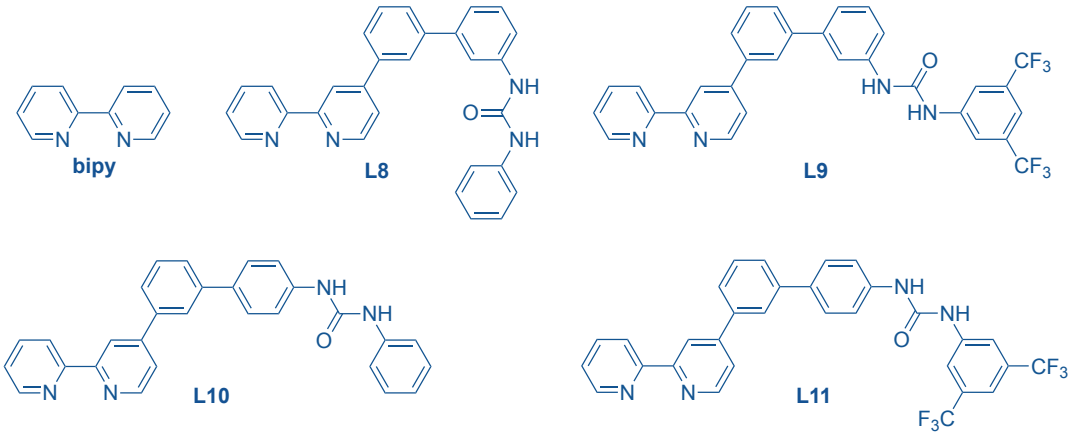

Note: Percentages of starting material and products were determined by GC/MS analysis.

Additionally, we tested these ligands on other substrates containing carbonyl groups, such as esters (**17**), and observed similar results to those obtained with the previous precursor biphenylamide (Table *7*). In this case, the *meta*-to-*para* borylation ratio varied depending on the ligand, but we were still unable to obtain a high degree of regioselectivity in the transformation.

**Table *7*** Ligand screening




| Ligand | **17** (SM, %) | **18** (*meta*, %) | **19** (*para*, %) | Ratio 18/19 |
|---|---|---|---|---|
| **bipy** | 14 | 51 | 35 | 1.45 |
| **L8** | 61 | 25 | 14 | 1.78 |
| **L28** | 2 | 48 | 50 | 0.96 |
| **L10** | 29 | 47 | 33 | 1.42 |
| **L11** | 17 | 48 | 35 | 1.37 |

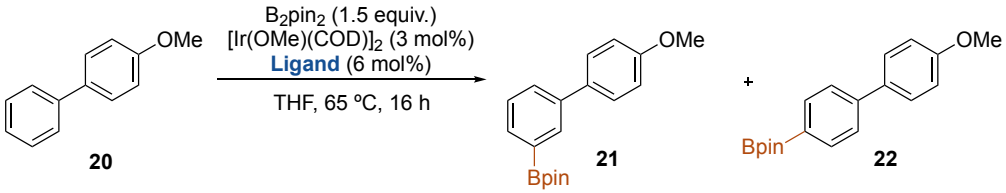



Note: Percentages of starting material and products were determined by GC/MS analysis.

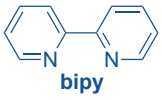
These results prompted us to investigate whether the carbonyl group was essential for the observed reactivity. As a control, we carried out the borylation of *p*-methoxybiphenyl (**20**) using both the standard 2,2'-bipyridine and the urea-containing ligand **L10**. In both cases, we observed com*para*ble regioselectivity and product distribution to that obtained with the carboxyl containing precusors **6** and **17** (Table *8*). This suggests that the regioselectivity is inherent to the substrate's structure and may not depend on the desired supramolecular interaction with the carbonyl moiety.

USC UNIVERSIDADE DE SANTIAGO DE COMPOSTELA

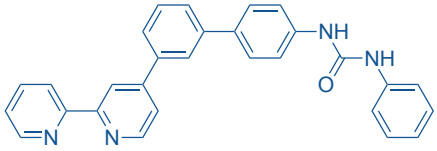
**Table *8*** Ligand screening




| Ligand | **20** (SM, %) | **21** (*meta*, %) | **22** (*para*, %) | **Ratio 21/22** |
|---|---|---|---|---|
| **bipy** | 14 | 50 | 36 | 1.38 |
| **L10** | 21 | 49 | 30 | 1.63 |




bipy




L10

Note: Percentages of starting material and products were determined by GC/MS analysis.

## 7.1.4 Conclusions

In this section, we explored the potential of supramolecular interactions, particularly hydrogen bonding, to achieve regioselective C–H borylations of biphenyl systems using iridium-based catalysts. Our approach involved designing bifunctional ligands that incorporated urea, thiourea, or squaramide recognition sites to guide the borylation process at remote positions on the distal aromatic ring.

While we successfully synthesized a series of ligands, the results of the borylations were inconsistent. For instance, when using bipyridine ligands containing a phenyl substituent at the 5 position of the pyridine, and p-phenylbenzamide as the substrate, we observed *ortho*-borylation products instead of the desired distal borylation.

Computational studies led us to design other ligands, such as 4-substituted bipyridines or 5-substituted phenanthrolines. Using these ligands, we observed mixtures of borylated products at the distal ring, with slightly higher *meta* than *para* regioselectivities. These results were similar to those obtained when using 2,2'-bipyridine as a control ligand. However, control experiments with substrates that lacked a H-bond recognition site yielded similar outcomes.

These findings suggest that the distal borylation is intrinsic to the steric and electronic characteristics of these biphenyl substrates rather than involving hydrogen bonding-directed processes. Overall, the results underscore the complexity of controlling regioselectivity through supramolecular interactions.

Nonetheless, the observation of *ortho* borylation with the 5-substituted systems prompted us to delve deeper into these processes.

## 7.2 Ir-catalyzed *ortho*-borylation of benzamides using designed bipyridine ligands

USC
UNIVERSIDADE DE SANTIAGO DE COMPOSTELA

This section includes work published in Angewandte Chemie International edition as: *Angew. Chem. Int. Ed*. **2023**, 62, e202214510*; Angew. Chem*. **2023**, *135*, e202214510.

DOI: 10.1002/anie.202214510

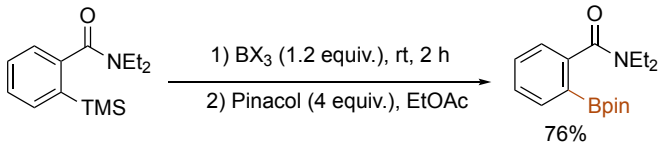
USC
UNIVERSIDADE DE SANTIAGO DE COMPOSTELA

## 7.2.1 Introduction

The above mentioned discovery of *ortho*-borylations of phenylbenzamide using bipyridine ligands containing a phenyl substituent at the 5 position of the pyridine is intriguing and highly interesting both, because of the intrinsic mechanistic reasons that could explain such regioselectivity using an L–L type of ligand, and also because the synthetic relevance of building *ortho*-functionalized benzamides in a selective manner.

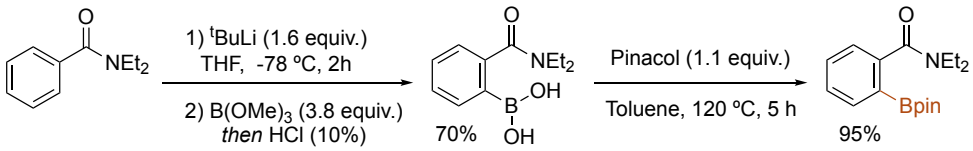
### *7.2.1.1 Transition-metal free ortho-borylation*

One of the earliest methods for obtaining *ortho*borylated benzamides involves an indirect three step process consisting of the *ortho*-metalation of a benzamide substrate using a lithium reagent, followed by ipso-borodesilylation upon treatment with $BCl_3$ or $BBr_3$, and treatment with pinacol to yield the *ortho*-boronpinacolate product.[124]




**Scheme *60*** *Ortho*-borylation of amides via borodesilylation.

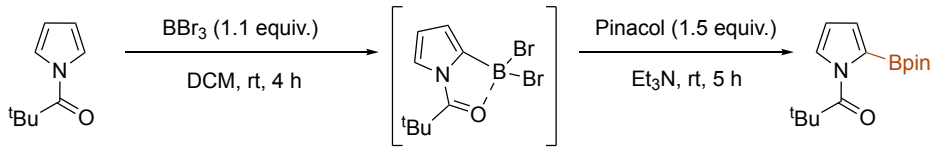
A similar approach involves the reaction of the *ortho*-lithium intermediate with a trialkyl borate, followed by hydrolysis and transesterification of the boronic acid to form the boronate pinacol ester.[125] While these methods are reliable, they entail several steps and requires the stoichiometric use of *sec*-BuLi or *tert*-BuLi, which raises significant safety concerns, and limits the compatibility with sensitive functional groups in the molecule.




**Scheme *61*** Alternative sequence for the *ortho*-borylation of amides.

Another method involves electrophilic borylation of amides using $BBr_3$. In this case, chelation between the boron atom and the carbonyl oxygen drives the regioselective *ortho* functionalization. Subsequent treatment with pinacol yields the desired *ortho*-borylated product. Unfortunately, this strategy is only useful with very specific electron rich heteroaromatic precursors.[126]

[124] Zhao, Z.; Snieckus, V. *Org. Lett.* **2005,** *7,* 2523–2526.
[125] Lahore, S.; Narkhede, U.; Merlini, L.; Dallavalle, S. *J. Org. Chem.* **2013,** *78,* 10860–10866.
[126] Wang, Z.; Chen, X.; Wu, L.; Wong, J. J.; Liang, Y.; Zhao, Y.; Houk, K. N.; Shi, Z. *Angew. Chem. Int. Ed.* **2021,** *60,* 8500–8504.




**Scheme *62*** Metal-free electrophilic *ortho*-borylation of amides.

### *7.2.1.2 Transition-metal-catalyzed ortho-borylation*

As extensively discussed in the introduction, C-H borylation reactions promoted by transition metal catalysts, especially iridium complexes, represents a particularly attractive technology to obtain aromatic borylated products. Achieving *ortho* selectivity in this type of reactions is challenging, although it has been achieved using monodentate, and especially L–X type of ligands. The effectiveness of these strategies hinges on the ability to generate iridium boryl intermediates with two vacant coordination sites. These intermediates facilitate the coordination of the amide directing group and subsequent activation of the *ortho* C–H bond, leading to *ortho* selectivity.

Herein we provide a brief revision of examples for the *ortho*-borylation of benzamides, although many of them had also been included in the general introduction (section 4.6).

As previously commented, in 2008, Sawamura's group was the first to report a regioselective *ortho*-borylation of benzamides, in their case using an Iridium heterogeneous catalyst (Figure *24*, **A**). They developed Silica-SMAP, a silica-supported, caged, compact phosphine ligand that enabled *ortho*-borylation of a wide variety of functionalized arenes. However, they only include one example involving aromatic amides.[58]

In 2015, Ito and Ishiyama introduced a system for the *ortho*-borylation of heterocyclic ketones, esters, and amides using an Ir catalyst and $AsPh_3$ as ligand (Figure *24*, **B**). Although the mechanism remains unclear, it appears that the monodentate nature of $AsPh_3$ allows the substrate's directing group to coordinate with the Ir center, leading to the formation of *ortho*-borylated products. While they mentioned a broad scope, their focus was on electron-rich heteroaromatic substrates, and they only provided two examples involving aromatic amides.[60]

In 2019, Smith III and coworkers filed a patent application showcasing the effectiveness of monodentate pyridine ligands in achieving selective Iridium-catalyzed C–H borylation. Specifically, using 2-methoxypyridine they could obtain the *ortho*-borylated product of N,N-dimethylbenzamide with good conversion and excellent selectivity (Figure *24*, **C**). Although the method seemed promising the scope was also very limited and only one aromatic amide was included in the scope.[61]

USC UNIVERSIDADE DE SANTIAGO DE COMPOSTELA

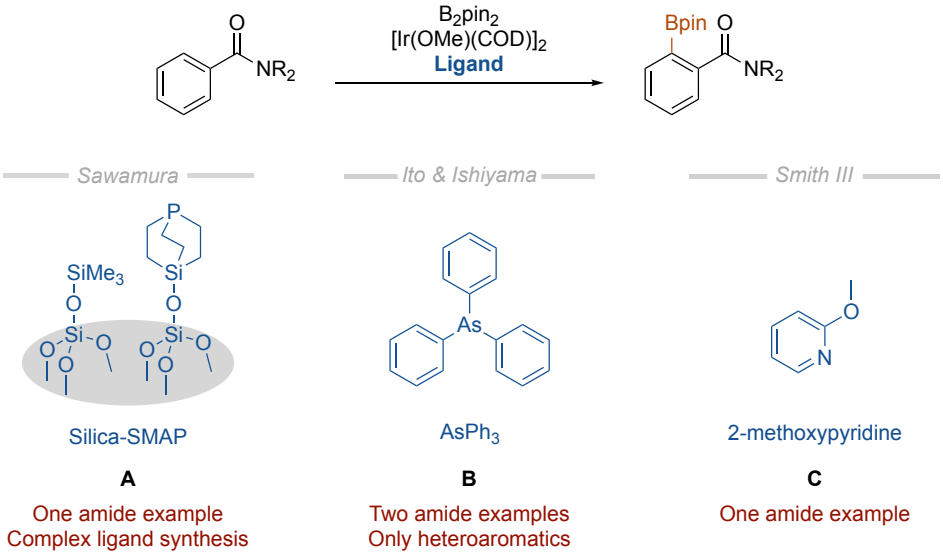



**Figure *24*** Monodentate ligands used for *ortho*-borylation of aromatic amides.

Beyond monodentate ligands, researchers have also explored bidentate monoanionic L–X ligands, which facilitate the reaction via a bisboryl intermediate. In these systems, two coordination sites on the Ir catalyst remain open: one for the substrate's directing group and another for oxidative addition of the C-H bond. These ligands have demonstrated high efficacy in directing *ortho*-borylation processes.

Among the more common L–X ligands are silicon-based bidentate ligands with Si–P (Figure *25*, **A**)[66] and Si–S structures (Figure *25*, **B**),[67] where the silyl group behaves as a monoanionic ligand. The catalytically active bisboryl intermediate is generated through sigma-bond *meta*thesis of the Si–H bond with a boryl group, producing an Si–Ir species. The electron-donating nature of these ligands generates an electron-rich metal center with increased nucleophilicity. Again, the methodology presented a rather limited scope, especially with respect to benzamides, and additional problems of functional group compatibility owing to the coordination unsaturated nature of the iridium reagents.

Another class of L–X ligands are based on the use of C–N structures. Therefore, in 2021, Chattopadhyay's group reported an air-stable iridium complex containing an anionic ligand based on a pyridyl-thienyl moiety.[70] This ligand takes advantage of the high acidity of the $C_2$–H bond of the thiophene ring to form a cyclometallated complex, that will work as an iridium L–X ligand, facilitating *ortho*-borylation across a broad range of substrates bearing different directing groups (DG), including benzamides. However, this system exhibits a quite high reactivity and thus presents challenges for the functionalization of complex molecules exhibiting other functional groups (Figure *25*, **C**).

In 2024, Joanna Wencel-Delord's group employed high-throughput screening of various related C–N ligands to discover an air-stable Iridium (III) precatalyst containing two triarylimine groups.[71] This bis-cyclometallated iridium complex undergoes activation with HBpin, followed by the elimination of one cyclometallated imine to form the active

catalyst. This system showed consistent regioselectivity in *ortho*-borylation of several benzamide substrates (Figure *25*, **D**).

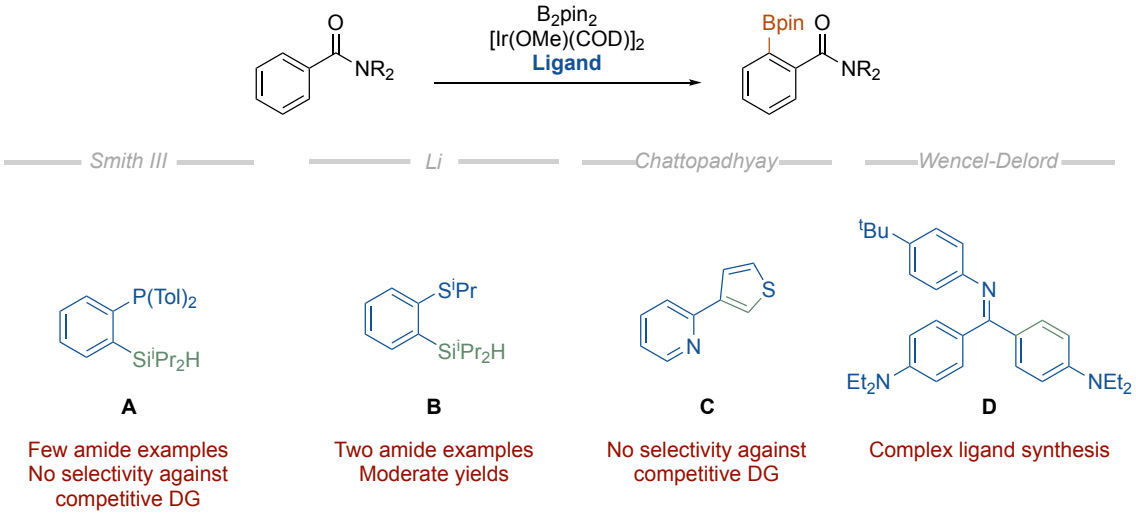



**Figure *25*** Monoanionic bidentate ligands used for *ortho*-borylation of aromatic amides.

As commented before, L–L type of ligands like 2,2'-bipyridine (**bipy**) fail to coordinate directing groups and promote the C-H activation of a substrate because the iridium contains only one vacant site. However, in 2019, the Reek's group demonstrated that this type of ligands could be used for *ortho*-borylation processes provided they can engage in intermolecular interactions with the substrate. Specifically, they designed a bipyridine ligand featuring an indole amide which enabled the *ortho*-borylation of secondary amides with remarkable regioselectivity. They explained the result in terms of the establishment of hydrogen bonding interactions between the indole N–H and the carbonyl group of the substrate. These interactions effectively direct the C–H activation towards the *ortho* position, ensuring high selectivity in the borylation process. Despite its efficiency, this method presented some limitations in terms of scope, and for instance it was limited to secondary benzamides (Figure *26*).[76]

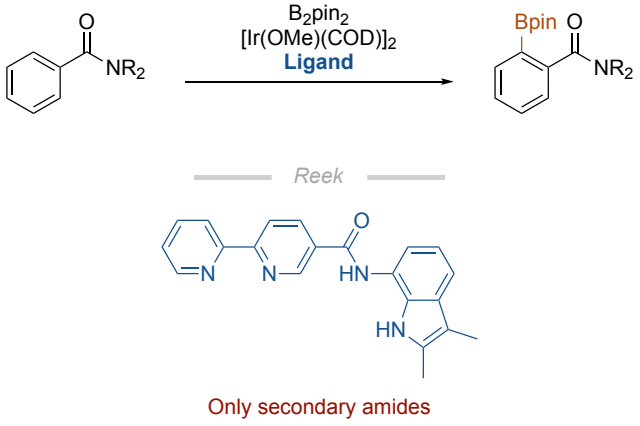
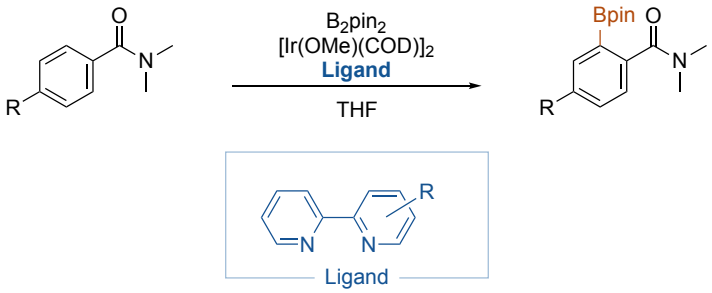



**Figure *26*** Supramolecular ligand used for *ortho*-borylation of aromatic amides.

## 7.2.2 Objective

Therefore, despite there were some precedents, at the beginning of our work the number of reports on the *ortho*-borylation of benzamides was very limited, and the methods presented a scarce scope. The surprising results obtained with L–L type ligands like **L4** (Table *3*), that led to the majoritarian formation of *ortho*-borylated products in biphenylcarboxamides, prompted us to further dig into this transformation. In particular, we aimed at confirming this reactivity with simpler benzamides, and discovering efficient L–L bipyridine ligands that could lead to more efficient and robust conversions.




**Scheme *63*** *Ortho*-borylation of benzamides with bipyridine-type of ligands.

In addition, we also aimed at developing a mechanistic rationale that could explain the surprising *ortho*-regioselectivity. As previously mentioned, these types of ligands tend to facilitate sterically controlled processes, resulting in preferred *meta* and *para* orientations.

## 7.2.3 Results and discussion

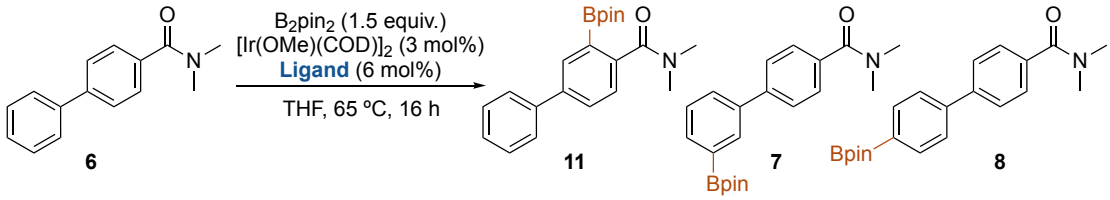
### *7.2.3.1 Reaction optimization and scope*

Before starting a detailed analysis of the influence of different ligands, we first needed to confirm that 2,2'-bipyridine ligands with a phenyl substitution at the 5 position of one of the pyridines yield a significantly higher proportion of the *ortho*-borylated product compared to standard 2,2'-bipyridine with no substitution (Table 9). Indeed, with ligand **L4** we obtained a 92/2 ratio of *ortho* versus *para*+*meta* products (94% conversion).

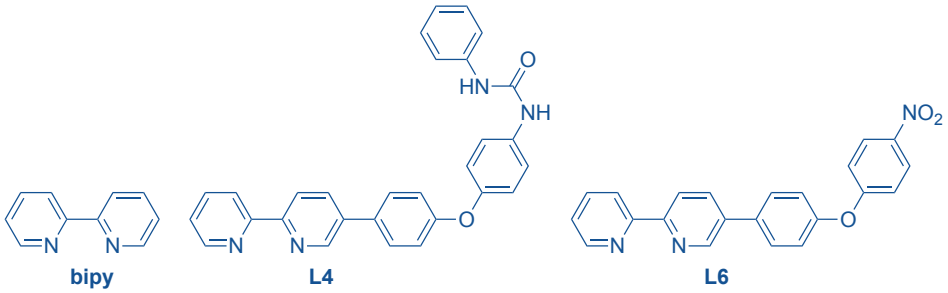
To test if this result is somewhat influenced by the establishments of H-bonds with the urea moiety, we tested the same process with ligand **L6** which contains a -$NO_2$ group instead of the urea. Remarkably, using this ligand we also obtained the *ortho*-borylated product as the major isomer, discarding the involvement of H-bonds in guiding the regioselectivity, as well as the electronic influence of the terminal ring.

USC UNIVERSIDADE DE SANTIAGO DE COMPOSTELA

**Table 9** *Ortho*-borylation results of *N*,*N*-dimethyl-[1,1'-biphenyl]-4-carboxamide (**6**).




| Ligand | **6** (SM, %) | **11** (*ortho*, %) | **7+8** (meta +para, %) |
|---|---|---|---|
| **bipy** | 37 | 0 | 63 |
| **L4** | 6 | 92 | 2 |
| **L6** | 7 | 63 | 29 |




Notes: Percentages of starting material and products were determined by GC/MS analysis. *Meta* and *para* isomers are described together as they were not isolated.

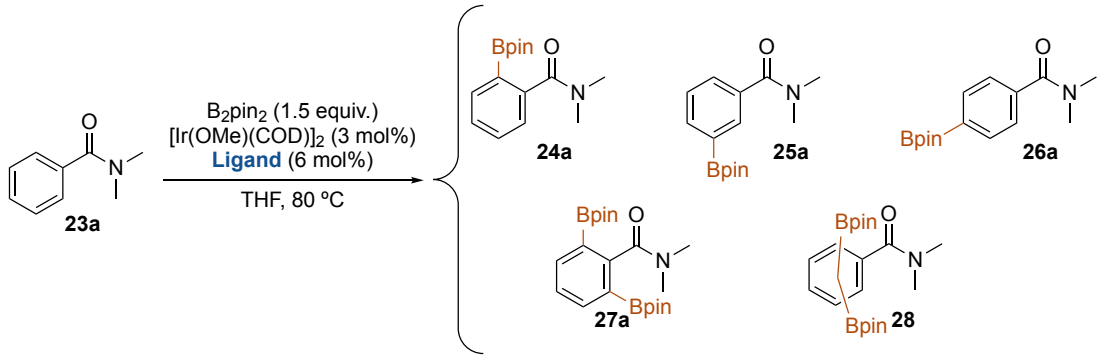
To further investigate the *ortho*-borylation and simplify the system eliminating the bias of a biphenyl system, we applied this ligand to *N,N*-dimethylbenzamide (**23a**) (Table 10). The reaction was carried out with **23a** (1 equiv.) $B_2pin_2$ (1.5 equiv.), $[Ir(OMe)COD]_2$ (3 mol%), ligand (6 mol%) in THF at 80 ºC for 3 h, and the products were analyzed by GC-MS. By comparing our results with previously reported data, we were able to identify the *meta* and *para*-borylated products. Furthermore, we successfully isolated and characterized the *ortho*-borylated product. Additionally, we also detected traces of diborylated products by GC-MS.

Therefore, when using ligand **L6**, we observed complete conversion of benzamide **23a**, with the major formation of the *ortho*-borylated product (**24a**), although we also observed a significant amount of *meta* and *para*-borylation, as well as diborylation side products.

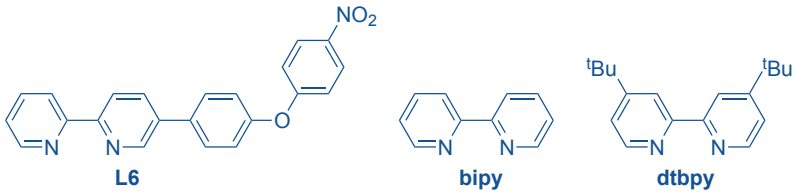
Importantly, using other common L–L ligands, such as 2,2'-bipyridine (**bipy**) and 4,4'-di-*tert*-butyl-2,2'-bipyridine (**dtbpy**), we observed full conversion to give a mixture of only *meta* and *para* mono and diborylated products (Table 10). This indicated that the substitution of the bipyridine ligand was critical for obtaining *ortho*-substituted products.

USC UNIVERSIDADE DE SANTIAGO DE COMPOSTELA

**Table 10** First borylation results and controls using **bipy** and **dtbpy** as ligands.

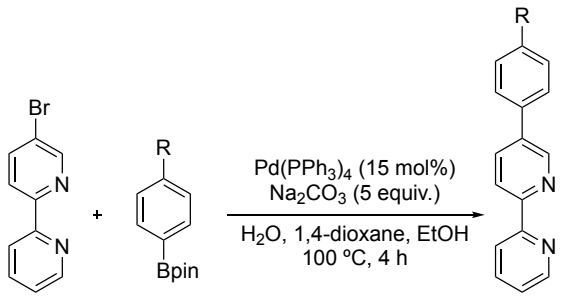



| Ligand | **23a** (SM, %) | **24a** (*ortho*, %) | **25a+26a** (meta +para, %) | **27a** (*di-ortho*, %) | **28** (*di*, %) |
|---|---|---|---|---|---|
| **L6** | 0 | 45 | 55 | 0 | 0 |
| **bipy** | 1 | 0 | 65 | 0 | 34 |
| **dtbpy** | 0 | 0 | 48 | 0 | 52 |




Notes: Percentages of starting material and products were determined by GC/MS analysis. *Meta* and *para* isomers are described together as they were not isolated.

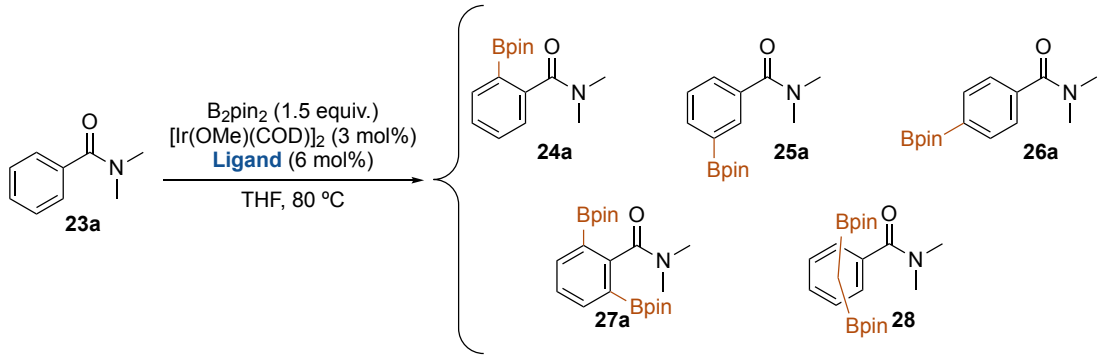
These results confirmed the exceptionality of the 5-phenyl substituted bipyridine ligands and called for a detailed exploration of the effect of other substituents in this pyridine position. Initially, we explored bipyridines with electron-donating groups (EDGs) attached to the extra phenyl ring at the 5-position. These ligands were synthesized by cross-coupling reactions between the 5-bromo-2,2'-bipyridine and the corresponding phenylboronic ester (Scheme *64*).



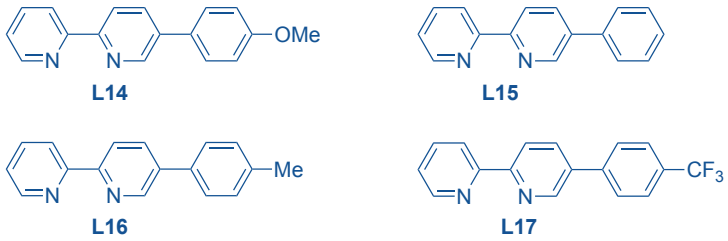

**Scheme *64*** General synthesis of 5-phenyl-2,2'-bypiridine ligands.

The borylation reaction was assayed using standard conditions. As can be deduced from Table 11, using ligands **L14**, **L15** and **L16** we obtained mixtures of mono- and diborylated products, with relatively low proportions of *ortho*-borylation. Curiously, when the phenyl substituent of the pyridine ring contains electron-withdrawing *p*-$CF_3$ group (**L17**), the *ortho* selectivity was substantially improved (Table 11).

**Table 11** Screening of 5-phenyl-2,2'-bipyridine ligands **L14**-**L17**.

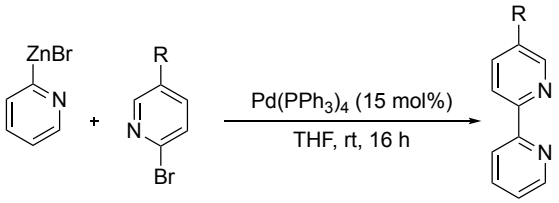



| Ligand | **23a** (SM, %) | **24a** (*ortho*, %) | **25a+26a** (meta +para, %) | **27a** (*di-ortho*, %) | **28** (*di*, %) |
|---|---|---|---|---|---|
| **L14** | 1 | 11 | 35 | 0 | 53 |
| **L15** | 1 | 14 | 39 | 0 | 53 |
| **L16** | 1 | 11 | 49 | 0 | 38 |
| **L17** | 2 | 42 | 14 | 4 | 38 |




Notes: Percentages of starting material and products were determined by GC/MS analysis. *Meta* and *para* isomers are described together as they were not isolated.

At this point, it was necessary to assay ligands that contain other substituents than aryls at the pyridine moiety. Therefore, we prepared these ligands using a Negishi coupling between the 2-pyridyl zinc bromide and functionalized 2-bromopyridines (Scheme *65*, See the experimental section for details).

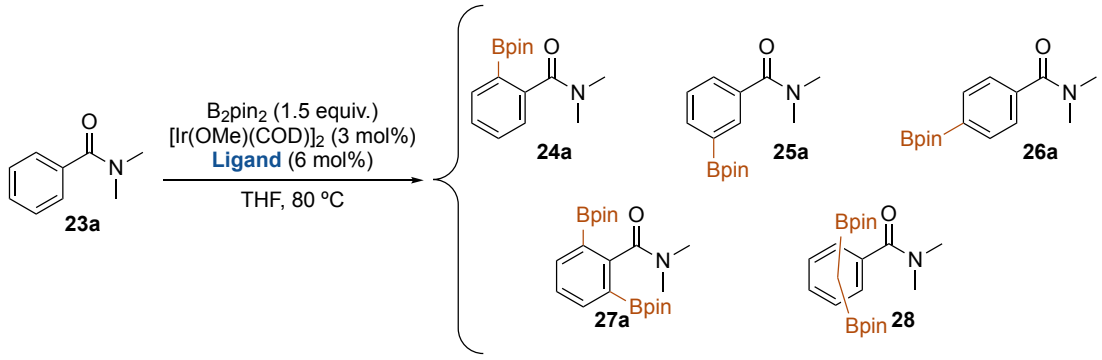



**Scheme *65*** General synthesis of 5-substituted 2,2'-bipyridine ligands.

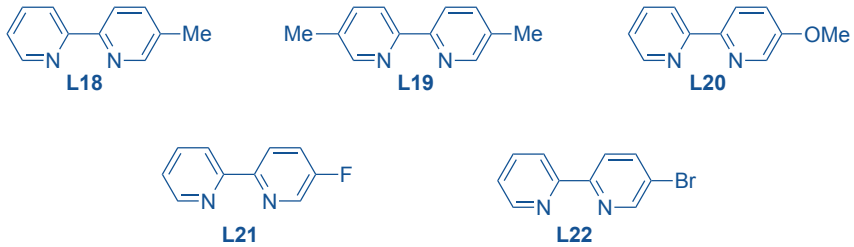
With these type of ligands at hand, we evaluated their ability to direct the *ortho* borylation under the same reaction conditions as before. The incorporation of EDG groups such as -Me (**L18** and **L19**) and -OMe (**L20**) at the 5-position of the ligands resulted in a reduced proportion of *ortho* borylation, with results rather similar to those obtained with the parent 2,2'-bipyridine. Notably, the use of halogenated bipyridines like **L21** and **L22** led to small improvements in *ortho* selectivity (Table 12).

USC UNIVERSIDADE DE SANTIAGO DE COMPOSTELA

**Table 12** Screening of 2,2'-bipyridine ligands equipped with EDG substituents at position 5.




| Ligand | **23a** (SM, %) | **24a** (*ortho*, %) | **25a+26a** (meta +para, %) | **27a** (*di-ortho*, %) | **28** (*di*, %) |
|---|---|---|---|---|---|
| **L18** | 1 | 4 | 58 | 0 | 37 |
| **L19** | 0 | 0 | 49 | 0 | 51 |
| **L20** | 0 | 7 | 52 | 10 | 31 |
| **L21** | 1 | 4 | 50 | 0 | 45 |
| **L22** | 13 | 12 | 63 | 0 | 12 |




Notes: Percentages of starting material and products were determined by GC/MS analysis. Meta and para isomers are described together as they were not isolated.

On the other hand, ligands with EWG at the 5-position, such as -CN (**L23**), -$C_6F_5$ (**L24**), -COMe (**L25**) or -$CO_2$Me (**L26**), resulted in better regiocontrol to favor the *ortho*-borylated product. However, some proportion of *meta* and *para* borylated byproducts were still observed (Table 13).

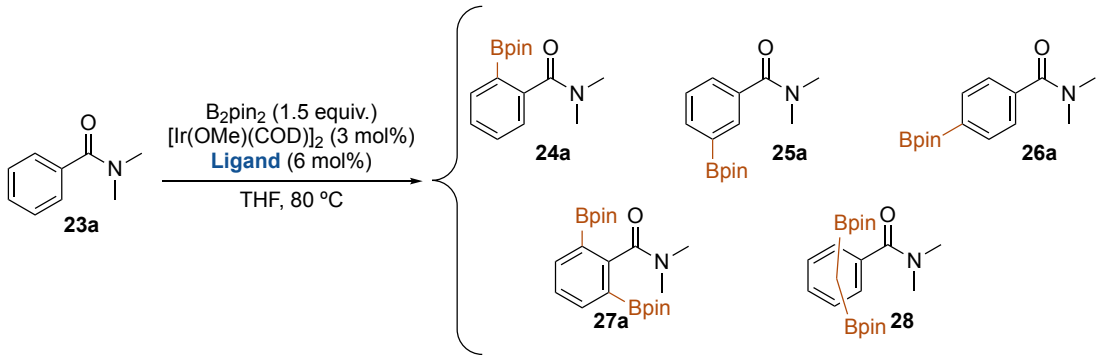
More relevant was the discovery that ligand **L27**, which contained a $CF_3$ substituent, exhibited remarkable *ortho*-selectivity, although, the *ortho*-diborylated product was the major one. By reducing the temperature from 80 to 65 ºC, and shortening the reaction time to 1.5 hours, a 90% yield of the desired *ortho* mono-borylated product **24a** was obtained. Interestingly, a symmetric ligand with two $CF_3$ substituents at both 5-positions (**L28**) yielded similar results but exhibited a greater tendency to form the diborylated derivative (Table 13).

In line with these results, the ligand **L29** with perfluorinated propyl chain (-$C_3F_7$) also demonstrated good *ortho* selectivity. Conversely, **L30** with a $CHF_2$ substituent was less selective, resulting in significant amounts of *meta* and *para* borylation.

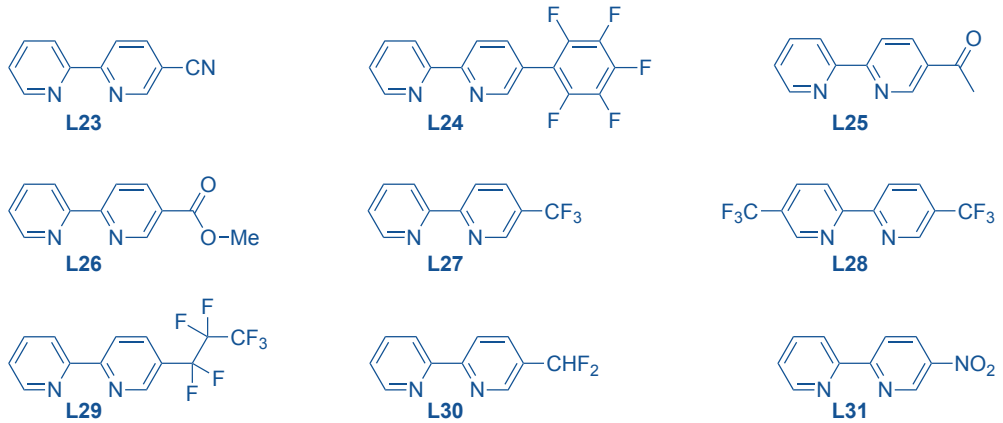
USC UNIVERSIDADE DE SANTIAGO DE COMPOSTELA

Interestingly, despite the $NO_2$ group being a strong EWG, using ligand **L31** we did not observe a good *ortho* regiocontrol, and behaved similarly to 2,2'-bipyridine (**bipy**).

**Table 13** Screening of 2,2'-bipyridine ligands with 5-EWG substituents.




| Ligand | **23a** (SM, %) | **24a** (*ortho*, %) | **25a+26a** (meta +para, %) | **27a** (*di-ortho*, %) | **28** (*di*, %) |
|---|---|---|---|---|---|
| **L23** | 1 | 46 | 6 | 9 | 38 |
| **L24** | 1 | 49 | 4 | 19 | 28 |
| **L25** | 0 | 34 | 6 | 0 | 60 |
| **L26** | 2 | 60 | 19 | 0 | 20 |
| **L27** | 0 | 20 | 0 | 80 | 0 |
| **L27** [a] | 3 | 90 | 0 | 7 | 0 |
| **L28** | 0 | 19 | 0 | 81 | 0 |
| **L28** [a] | 0 | 80 | 0 | 20 | 0 |
| **L29** | 0 | 62 | 0 | 38 | 0 |
| **L30** | 0 | 28 | 40 | 10 | 19 |
| **L31** | 0 | 1 | 57 | 0 | 42 |

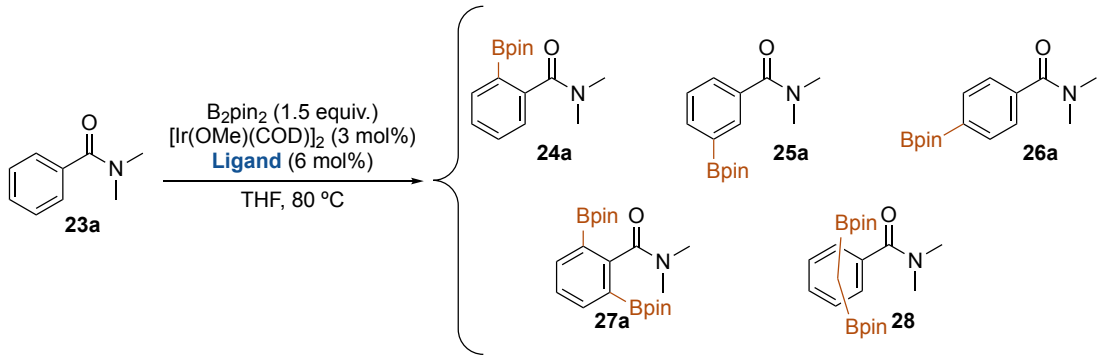



Notes: Percentages of starting material and products were determined by GC/MS analysis. *Meta* and *para* isomers are described together as they were not isolated.[a] 65 °C for 1.5 h.

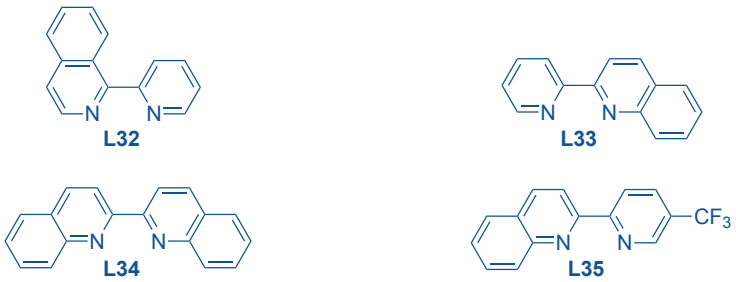
All these results suggest an amazing effect of a $CF_3$ substituent at the 5-position of the bipyridine. At this point it was pertinent to gain more information about the relevance of the bipyridine core, and therefore made a variety of new ligands with modifications in this skeleton. The synthesis is described in the supporting information.

Fusing a phenyl ring to one pyridine to give a quinoline-pyridine framework leads to ligands that also led to a substantial *ortho* orientation (**L32**-**L35**), though the reaction was slower compared to that with 5-$CF_3$-bipyridine (**L27**) (Table 14).

**Table 14** Screening of pyridine-quinoline ligands.




| Ligand | **23a** (SM, %) | **24a** (*ortho*, %) | **25a+26a** (meta +para, %) | **27a** (*di-ortho*, %) | **28** (*di*, %) |
|---|---|---|---|---|---|
| **L32** | 5 | 95 | 0 | 0 | 0 |
| **L33** | 0 | 100 | 0 | 0 | 0 |
| **L34** | 0 | 96 | 0 | 4 | 0 |
| **L35** | 0 | 54 | 0 | 46 | 0 |

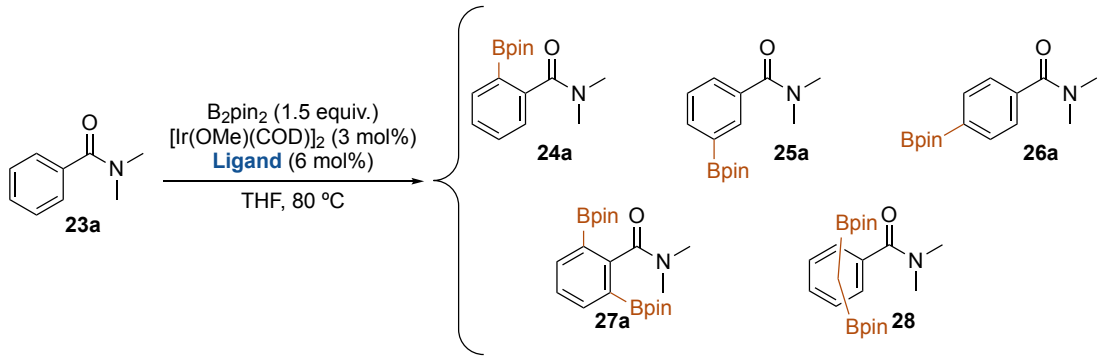



Notes: *Meta* and *para* isomers are described together as they were not isolated. Conversion and proportion of products were determined by GC/MS analysis.

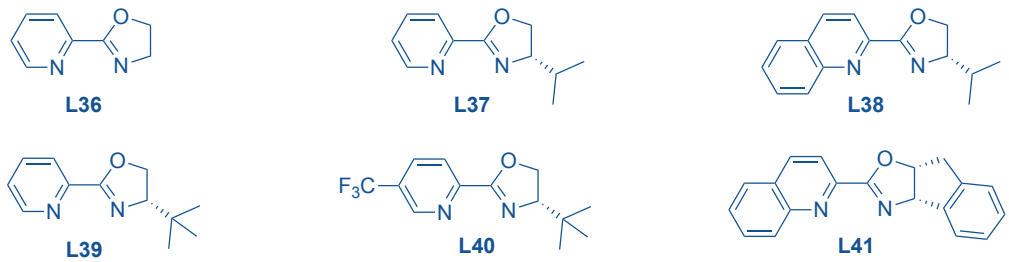
Pyridine-oxazoline ligands (PyOx) like **L36**-**L41**, also gave *ortho*-borylated products, but mixed with other isomers (Table 15). Chiral quinoline-oxazoline ligand **L38**, **L41** are quite appealing because they also orient in *ortho*, and might find utility in asymmetric reactions, for instance in desymetrization processes.

USC UNIVERSIDADE DE SANTIAGO DE COMPOSTELA

**Table 15** Screening of pyridine-oxazoline ligands.




| Ligand | **23a** (SM, %) | **24a** (*ortho*, %) | **25a+26a** (meta +para, %) | **27a** (*di-ortho*, %) | **28** (*di*, %) |
|---|---|---|---|---|---|
| **L36** | 0 | 22 | 51 | 0 | 27 |
| **L37** | 55 | 11 | 34 | 0 | 0 |
| **L38** | 40 | 60 | 0 | 0 | 0 |
| **L39** | 25 | 69 | 6 | 0 | 0 |
| **L40** | 43 | 16 | 41 | 0 | 0 |
| **L41** | 26 | 73 | 1 | 0 | 0 |

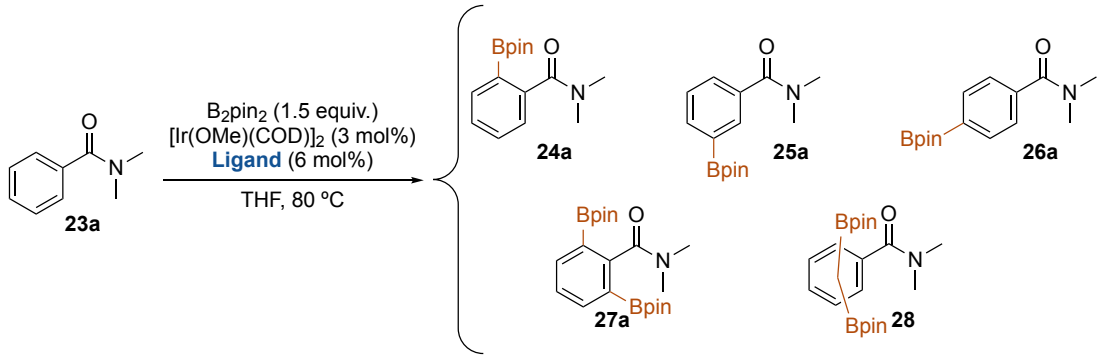



Notes: *Meta* and *para* isomers are described together as they were not isolated. Conversion and proportion of products were determined by GC/MS analysis.

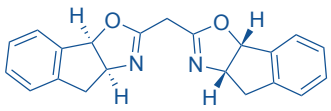
On the other hand, bis-oxazoline ligands (BOX, **L42**, **L43**) showed no reactivity, failing to promote the reaction entirely (Table 16). Finally, the reaction was also tested with monodentate ligands such as electron-deficient phosphines (**L44**) and pyridines (**L45**) (Table 16), known to facilitate *ortho*-borylation by promoting direct coordination of the carbonyl group to the metal.[127] As expected, these ligands led to the desired *ortho*-borylated product (**24a**), (adding 1 equivalent with respect to iridium), but the reaction was slower and much less efficient than with the $CF_3$ containing bipyridine **L27**.

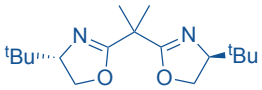
[127] Sasaki, I.; Amou, T.; Ito, H.; Ishiyama, T. *Org. Biomol. Chem.* **2014,** *12,* 2041–2044.

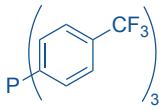
**Table 16** Screening of bis-oxazoline ligands and monodentate ligands.

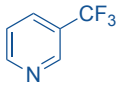



| Ligand | **23a** (SM, %) | **24a** (*ortho*, %) | **25a+26a** (meta +para, %) | **27a** (*di-ortho*, %) | **28** (*di*, %) |
|---|---|---|---|---|---|
| L42 | 100 | 0 | 0 | 0 | 0 |
| L43 | 100 | 0 | 0 | 0 | 0 |
| L44 | 25 | 75 | 0 | 0 | 0 |
| L45 | 54 | 46 | 0 | 0 | 0 |


L42


L43


L44

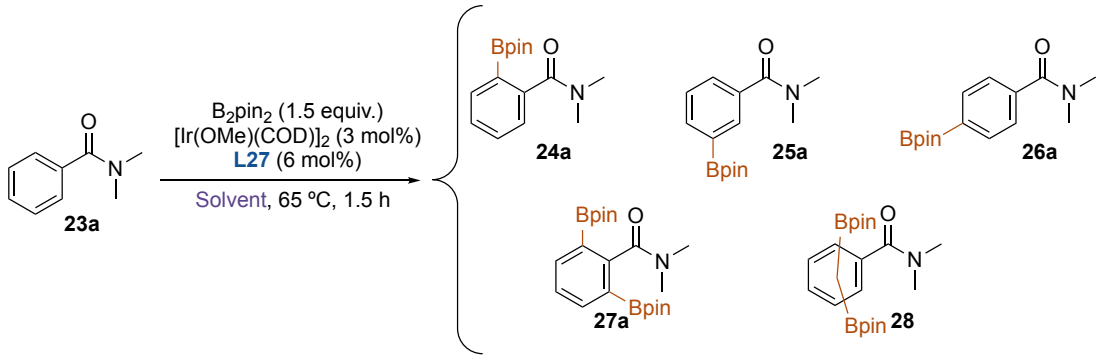

L45

Notes: Meta and para isomers are described together as they were not isolated. Conversion and proportion of products were determined by GC/MS analysis.

The fact that bidentate neutral L–L ligands could promote the *ortho*-borylation process led us to start to consider the existence of non-covalent interactions in the reaction, which might be highly affected by the solvent used. Therefore, we screened several solvents under the above standard conditions (Table *17*). Non-polar hydrocarbon solvents like hexane or cyclohexane significantly decreased the reactivity and, notably, led to regioisomeric mixtures of products. Weakly polar ethereal solvent such as dibutyl ether, produced a vastly different result compared with the more polar THF, with *meta* and *para* borylated products being the major products. Aromatic solvents like *p*-xylene also led to poor conversion and mixtures of regioisomers.

Polar solvents such as cyclopentylmethylether or MeCN predominantly afforded *ortho*-borylation, although with reduced conversion. Conversely, halogenated solvents such as DCE resulted in almost no conversion. The addition of small amounts of polar but highly coordinating solvents like DMSO or DMF (10 equiv.) were detrimental for the reaction in THF, either reducing conversion (DMSO), or completely inhibiting the process (DMF).

**Table *17*** Screening of solvents for *ortho*-borylation.




| Solvent | **23a** (SM, %) | **24a** (*ortho*, %) | **25a+26a** (*meta*+*para*, %) | **27a** (*di-ortho,* %) | **28** (di, %) |
|---|---|---|---|---|---|
| THF | 0 | 90 | 0 | 7 | 0 |
| *p*-Xylene | 55 | 23 | 19 | 3 | 0 |
| Cyclohexane | 33 | 9 | 64 | 1 | 2 |
| DCE | 95 | 5 | 0 | 0 | 0 |
| Dibutyl ether | 33 | 13 | 59 | 1 | 2 |
| 1,4-Dioxane | 42 | 27 | 28 | 1 | 2 |
| Hexane | 37 | 21 | 38 | 1 | 3 |
| MeCN | 49 | 51 | 0 | 0 | 0 |
| THF+ DMF (10 equiv.) | 62 | 38 | 0 | 2 | 0 |
| THF+ DMSO (10 equiv.) | 100 | 0 | 0 | 0 | 0 |
| Chlorobenzene | 100 | 0 | 0 | 0 | 0 |
| EtOAc | 62 | 22 | 16 | 0 | 0 |
| DME | 85 | 15 | 0 | 0 | 0 |
| HFIP | 100 | 0 | 0 | 0 | 0 |
| $C_6F_6$ | 100 | 0 | 0 | 0 | 0 |
| CPME | 9 | 81 | 1 | 9 | 0 |
| 1,3-Dioxolane | 11 | 89 | 0 | 0 | 0 |

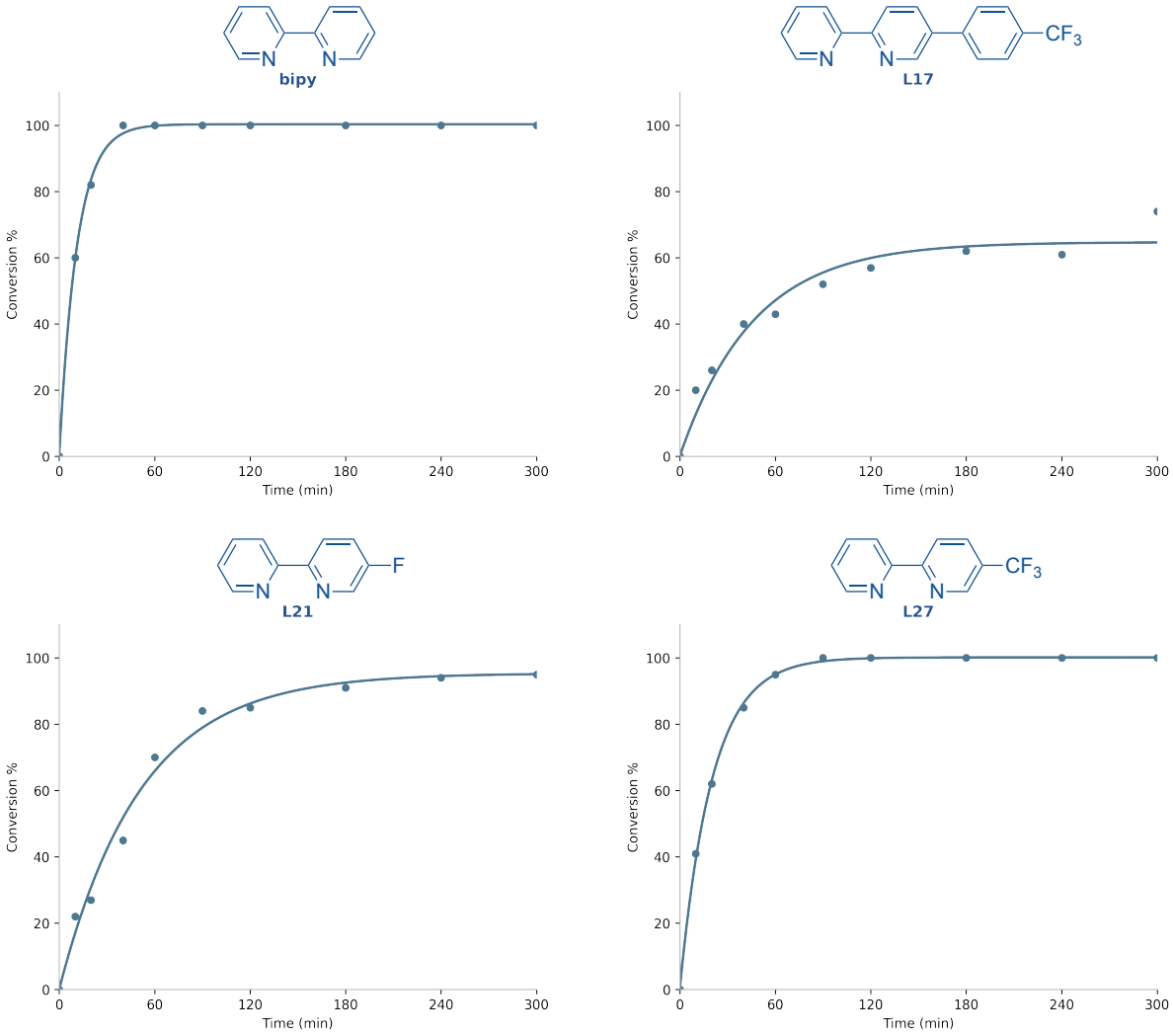
[a] The reaction was performed at 0.2 M. [b] *Meta* and *para* isomers are described together as they were not isolated. Note: Percentages of starting material and products were obtained by GC/MS analysis.

After all this screening of ligands and solvents, the optimal conditions for the *ortho* borylation using **L27** as ligand consists of heating a 1 equiv. of benzamide (**23a**), 1.5 equiv. of $B_2pin_2$, 3 mol% $[Ir(OMe)(COD)]_2$ and 6 mol% of **L27** in THF (0.2 M) at 65 °C. After 1.5 hours, the isolated yield of the desired product **24a** was 83%, with only a 7% yield of the

USC UNIVERSIDADE DE SANTIAGO DE COMPOSTELA

diborylated byproduct (**27a**) (as measured by GC/MS), and without the presence of other regioisomers.

A control reaction using 2,2'-bipyridine (**bipy**) instead of **L27** as ligand, under the same conditions, revealed a faster process to give a mixture of *meta* and *para* borylated products (Figure *27*). Fluor-containing ligands **L17** (-Ph-$CF_3$), **L21** (-F), **L27** (-$CF_3$), and **L28** (bis –$CF_3$) and others with EWG at the 5-position, such as **L23** (-CN) and **L24** (-$C_6F_5$) led to slower kinetics. We also conducted a time-course study with an electron-deficient phosphine ligand **L44**, and found that the reaction was slower compared to **L27** (58% yield after 1.5 hours).



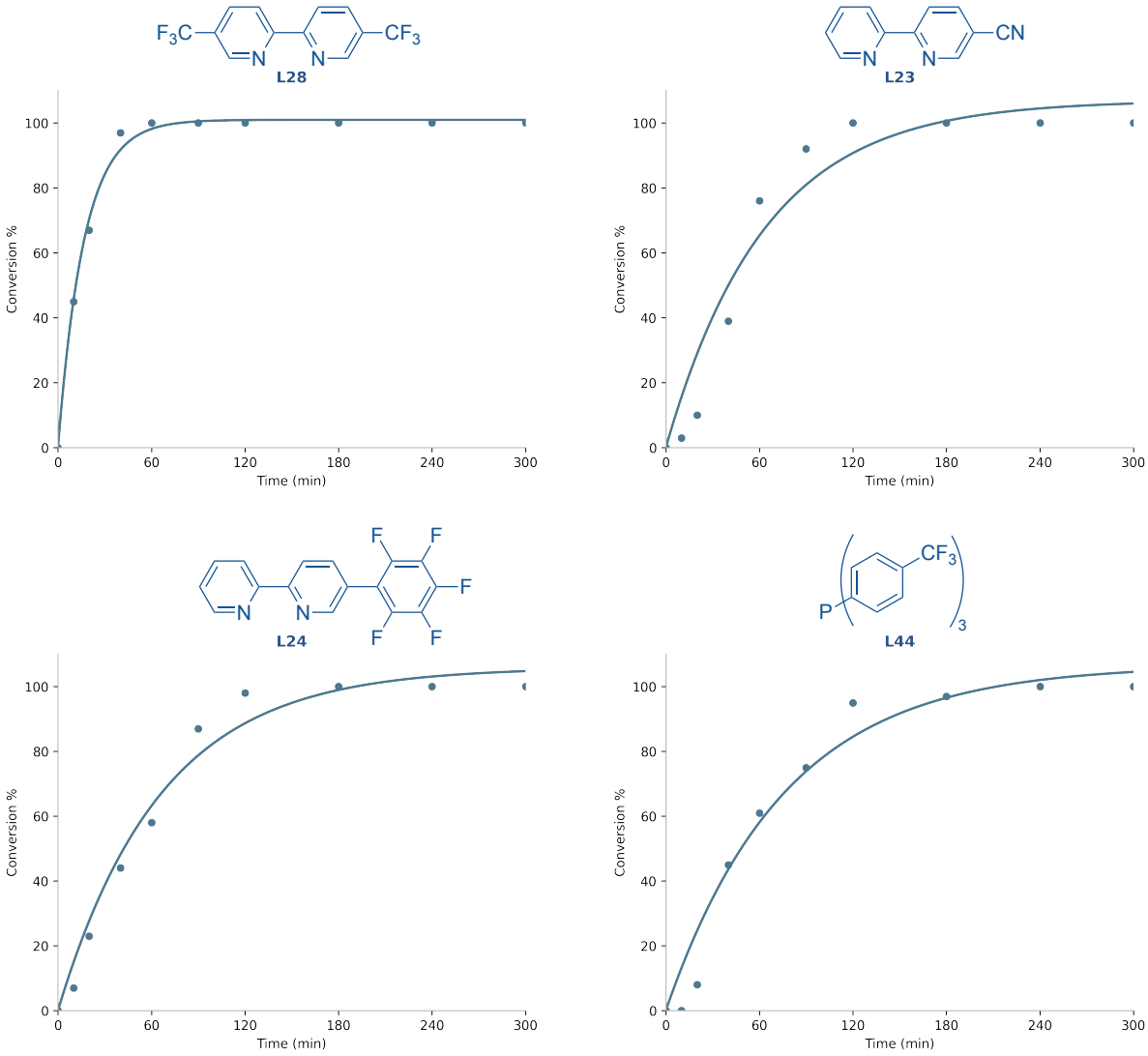



**Figure *27*** Qualitative kinetic conversion of **23a** with ligands **bipy**, **L17**, **L21**, **L27**, **L28**, **L23**, **L24**, and **L44**. Percentages of starting material and products were obtained by GC/MS analysis.

We also investigated the amount of mono- and di-borylated products formed with the trifluoromethyl-containing ligands **L27** and **L28** under optimized conditions. With **L27**, the reaction achieved complete conversion after 90 minutes, predominantly producing mono-borylated products with minimal di-borylation. Conversely, the bis-$CF_3$ substituted ligand (**L28**) exhibited complete conversion after just 40 minutes. However, it produced a higher percentage of diborylated side products (15%) compared to **L27** (<5%) (Figure *28*).

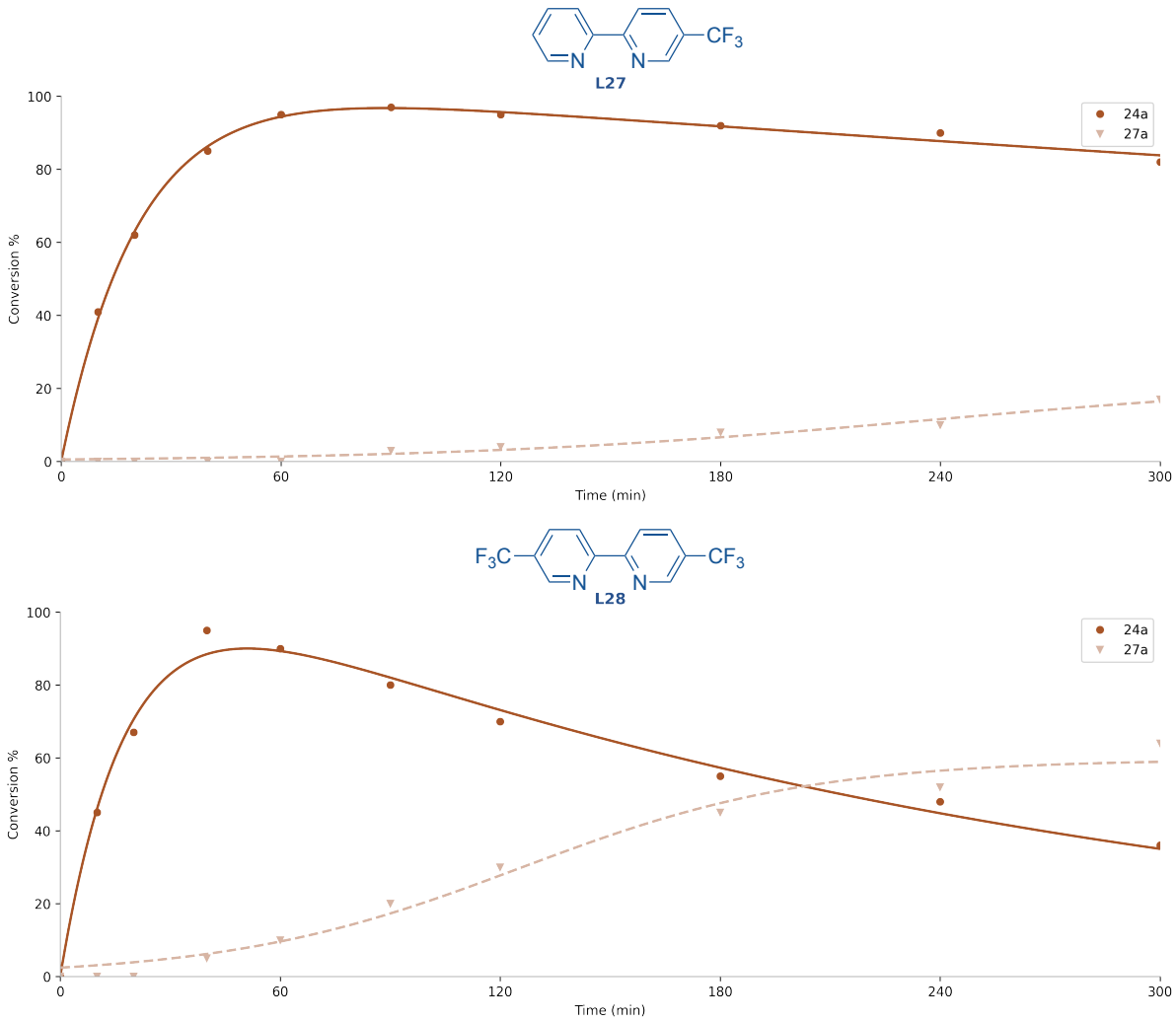



**Figure *28*** Percentage of *ortho* **24a** (solid lines) and di-*ortho*-borylated **27a** products (dashed lines) over time with ligands **L27** and **L28**. Percentages of each product were obtained by GC/MS analysis.

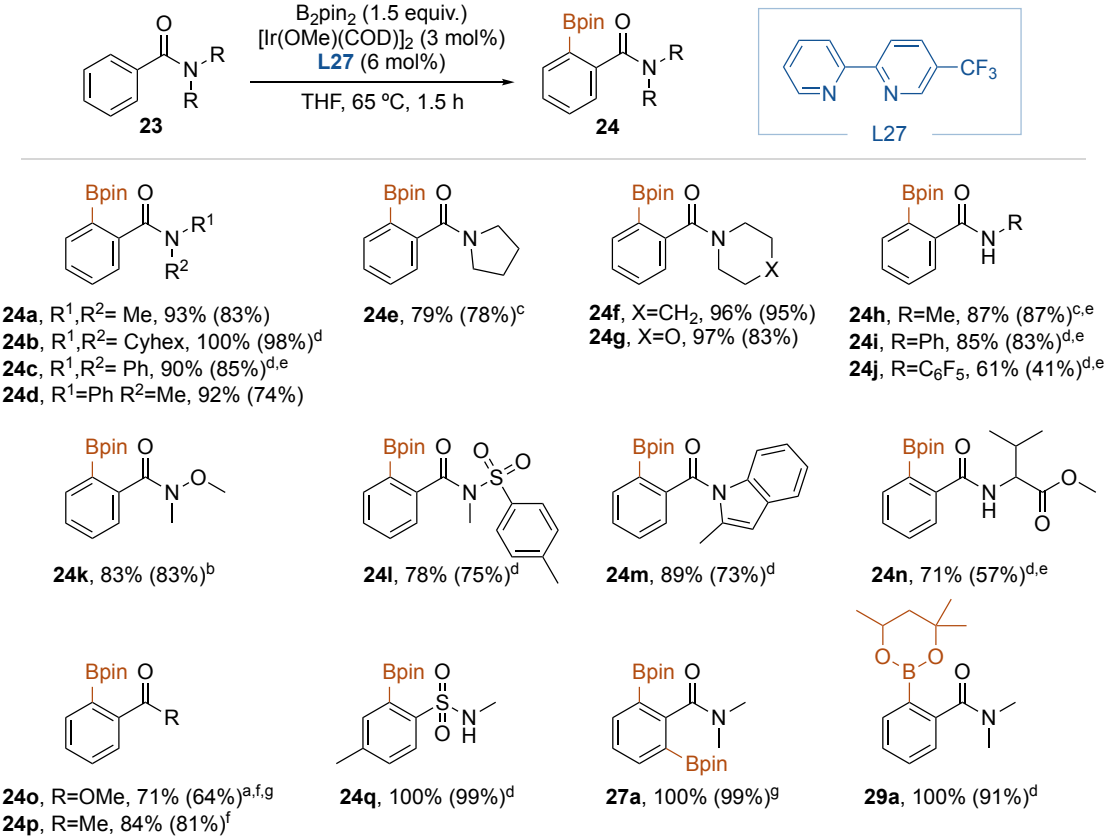
Before going into more mechanistic details, it was crucial to assess whether the *ortho*-borylation could be applied to a broader range of substrates. Encouragingly, many other tertiary amides underwent the transformation successfully (Scheme *66*). *Ortho* monoborylated products **24a-24g** were obtained in high yields with excellent regioselectivity, as no other mono-borylated byproducts were observed when **L27** was employed as a ligand. As expected, using **bipy** instead of **L27**, we did not detect *ortho*-borylated products, but only mixtures of other regioisomers (Scheme *67*).

The results obtained with amides featuring phenyl substituent on the nitrogen atom are quite significant in terms of chemoselectivity, owing to the potential functionalization of two aryl rings. When the standard 2,2'-bipyridine ligand (**bipy**) was employed, we observed a mixture of *meta* and *para* substituted products on the benzamide ring, along with partial borylation of the N-phenyl substituent (Scheme *67*). In contrast, the use of **L27** as a ligand delivered complete chemoselectivity, exclusively

USC UNIVERSIDADE DE SANTIAGO DE COMPOSTELA

functionalizing the benzamide phenyl ring, yielding products **24c** or **24d** in excellent yields (Scheme 66).

The *ortho*-borylation reaction is also effective with secondary amides, as evidenced by the good yields obtained of the *ortho*-borylated products (**24h**-**24j**). Similar to tertiary benzamides, substrates containing additional phenyl rings are selectively borylated in the benzamide moiety, provided that ligand **L27** (bipy-$CF_3$) is used in the reaction.



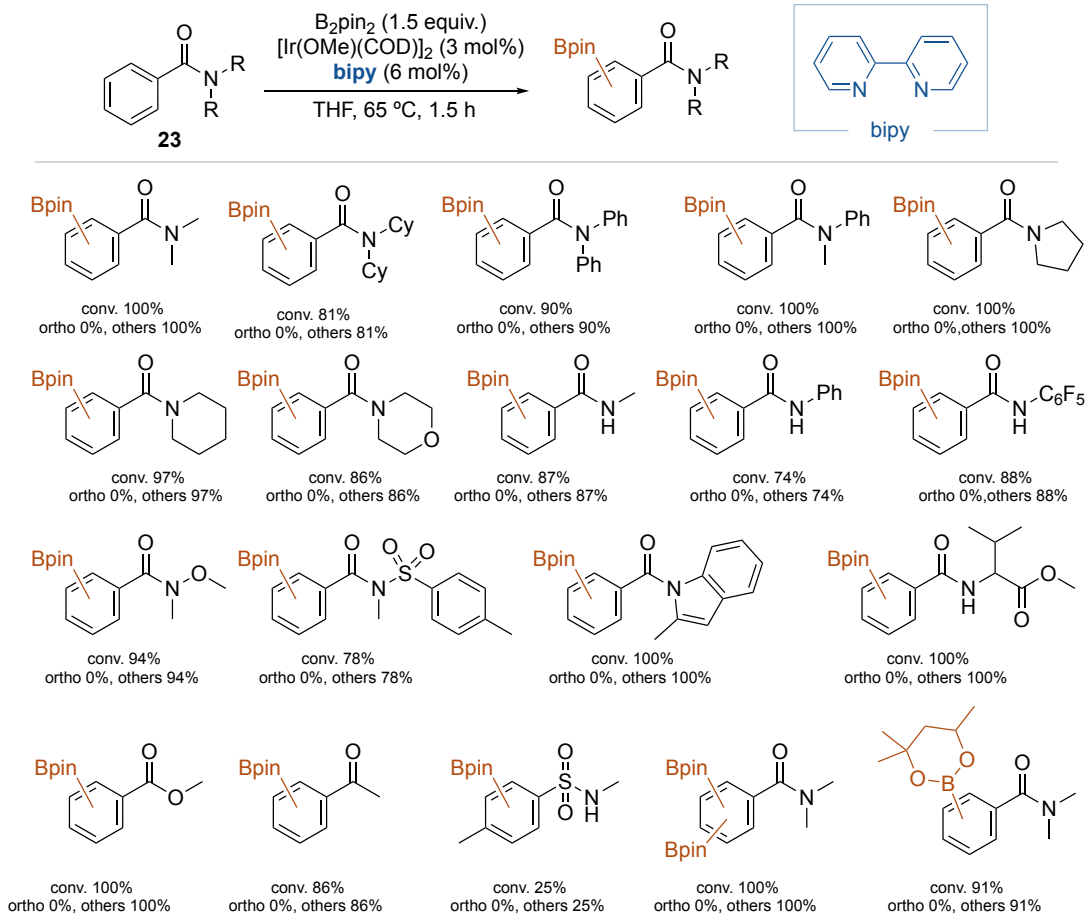

**Scheme 66** *Ortho*-borylation of benzamides and related precursors using mono $CF_3$ bearing ligand **L27**; Note: $^1$H-NMR yield of *ortho*-borylated products using $CH_2Br_2$ as IS (mean value of 3 parallel reactions) are given. Isolated yield described between parenthesis. The difference between NMR yield and isolated yield can be attributed to the well-known decomposition of the Bpin moiety during chromatographic purification. [a] Reaction time 1h. [b] Reaction time 2 h. [c] Reaction time 4 h. [d] Reaction time 24 h. [e] Reaction temperature 80 ºC. [f] Reaction temperature 100 ºC. [g] Bis-$CF_3$ ligand **L28** was used. Note: only traces of diborylated products were detected.

Notably, a $C_6F_5$ substituent at the nitrogen atom slowed down the reaction, suggesting an important role of the stereoelectronic properties of the amide on the reaction rate. Other heteroatom substituents at the nitrogen such as -OMe (Weinreb amide) or -$SO_2$R, are compatible with the catalytic process, yielding products **24k** and **24l** in good yield with no other borylation products detected. The same chemoselectivity was observed with a substrate featuring an indole derivative (**24m**). Furthermore, the amino acid derivative **24n** was also produced with high selectivity, pointing towards the potential

of the method for late-stage functionalization of short peptides containing benzamide substituents (Scheme *66*).

Overall, these results confirm the robustness of the *ortho*-borylation reaction, with its efficiency partially associated to the electron-donor characteristics of the benzamide. Control reactions with some of the aforementioned substrates using **bipy** instead of **L27** as ligand, failed to give the *ortho*-borylated products (Scheme *67*).

The reaction is not restricted to the use of $B_2pin_2$ as the borylating agent; using bis(hexyleneglycolato)diboron, we obtained the expected product in excellent yield (**29a**). Aditionally, *ortho*-diborylated product **27a** can be obtained using **L28** and excess of $B_2pin_2$ with very good yield (Scheme *66*).




**Scheme *67*** Borylation of benzamides and related precursors using **bipy** as ligand. Note: Reaction conditions for each substrate are the same as described in Scheme *66*. Conversions and percentages of products were determined by GC/MS analysis.

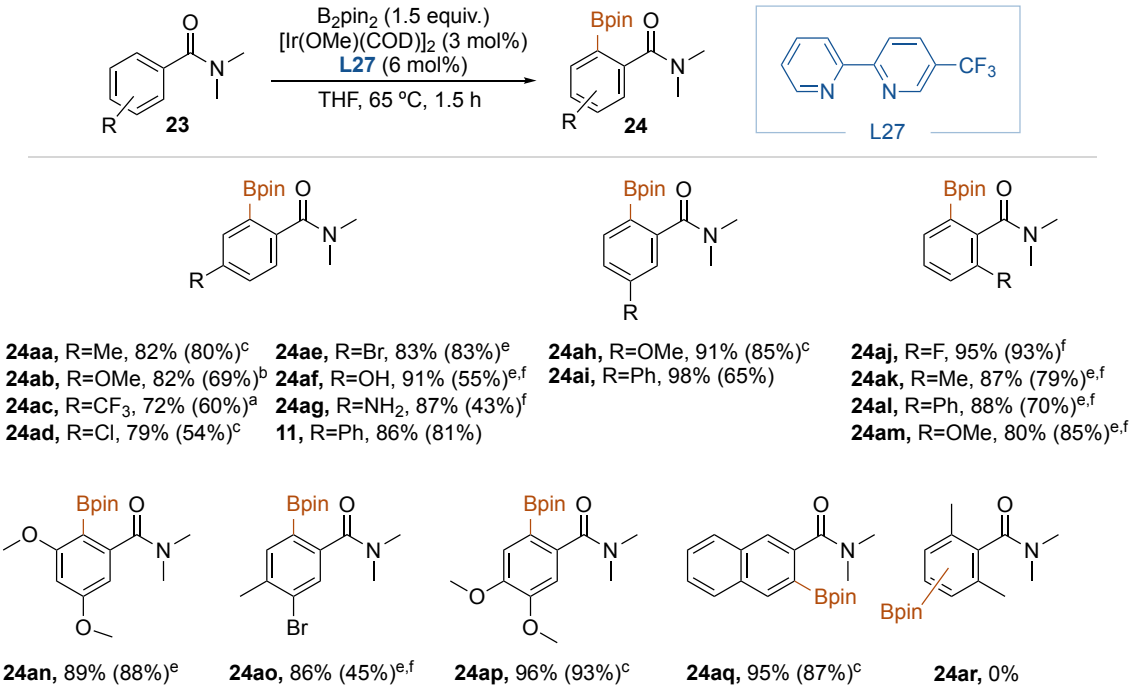
The observed reactivity extends beyond benzamides. For example methylbenzoate and acetophenone underwent *ortho*-borylation, yielding products **24o** and **24p**, respectively; however it was necessary to use higher temperatures and longer reaction times. Additionally, *N*-Me-tosylsulfonamide also reacted successfully,

USC UNIVERSIDADE DE SANTIAGO DE COMPOSTELA

producing the expected product **24q** in excellent yield. Notably, no *ortho*-borylation was observed when 2,2'-bipyridine (**bipy**) was used as a ligand (Scheme *67*).

The *ortho*-borylation reaction was also found to be effective with benzamides bearing different substituents at the aryl ring. As shown in Scheme *68*, substrates with EDGs like -Me, -OMe, or EWG such as -$CF_3$ at the *para* position react to yield the anticipated products (**24aa-24ac**) in good yields. Even halogen substituents, including -Cl and -Br, which are known to be sensitive to organometallic reagents, are also tolerated. Notably, the reaction can proceed in the presence of unprotected alcohols or amines (products **24af** and **24ag**), although isolated yields are modest due to partial decomposition during chromatographic purification.

In line with previous results, when the standard 2,2'-bipyridine ligand (**bipy**) was used, we observed generally lower conversions and never detected any *ortho*-borylation (Scheme *69*).

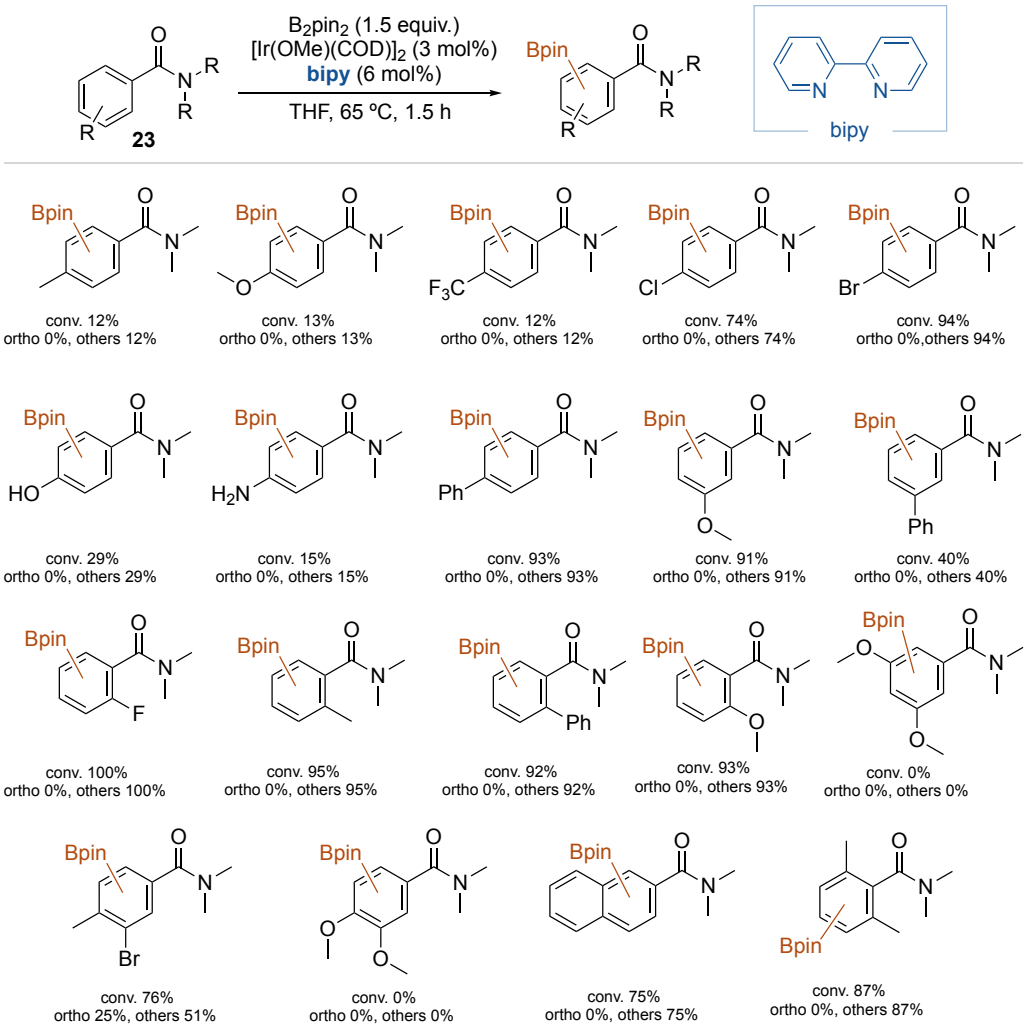



**Scheme *68*** *Ortho*-borylation of substituted benzamides. Note: $^1$H-NMR yield of *ortho*-borylated products using $CH_2Br_2$ as IS (mean value of 3 parallel reactions) are given, isolated yield described between parenthesis. The difference between NMR yield and isolated yield can be attributed to the well-known decomposition of the Bpin moiety during chromatographic purification. [a] Reaction time 1h. [b] Reaction time 1.25 h. [c] Reaction time 2 h. [d] Reaction time 4 h. [e] Reaction time 24 h. [f] Reaction temperature 80 °C. Note: only traces of diborylated products were detected.

*Meta*-substituted benzamides also react to produce *ortho*-borylated products at the less hindered position (**24ah** and **24ai**). Substrates with *ortho* substituents, which are typically challenging to functionalize, react efficiently to give the expected products (**24aj**, **24ak**, **24al** and **24am**) in excellent yields.

USC UNIVERSIDADE DE SANTIAGO DE COMPOSTELA

Disubstituted benzamides also afford the expected *ortho* borylated products (**24an-24ap**). Using the standard 2,2'-bipyridine ligand (**bipy**) instead of **L27**, resulted in poor conversions for many of these substrates, likely due to steric hinderance, and produced mixtures of *meta*-substituted products (Scheme *69*). For instance, 3,5-dimethoxy-*N,N*-dimethylbenzamide failed to react using **bipy** as ligand (no conversion after 1.5 h at 65 ºC, Scheme *69*), but high yields of the expected product (**24an**) were obtained with **L27**. Extended aromatic systems also undergo *ortho*-borylation exclusively at the amide's *ortho* position without forming any other borylated side product (**11, 24ai, 24al, 24aq**).



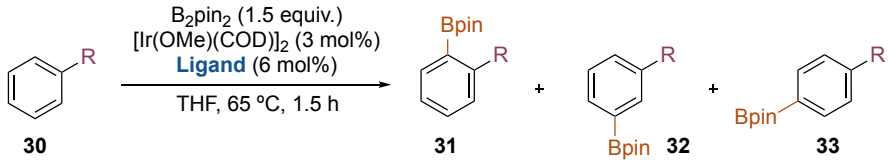

**Scheme 69** Borylation of substituted benzamides using **bipy** as ligand. Note: Reaction conditions for each substrate are the same as described in *Scheme 68*. Conversions and percentages of products were determined by GC/MS analysis

Interestingly, treatment of 2,6-dimethyl-*N,N*-dimethylbenzamide (*ortho*-disubstituted amide) under standard conditions using **L27** as ligand led to no conversion. However, using **bipy**, a mixture of *meta* and *para*-borylated products was observed. This result confirms the intrinsic lower reactivity of the catalyst when **L27** is used.

USC DE SANTIAGO DE COMPOSTELA

Other aromatic substrates lacking the carbonyl group, such as anisole or toluene remained essentially unchanged under standard reaction conditions with **L27**, but reacted under the same conditions (65 °C, 1.5 h) when **bipy** was used,[52] to give *meta*/*para* borylation products (See the *Supporting Information*). Forcing a little the reaction in presence of **L27** to 100 °C triggered the reactivity, yielding the same regioisomers as with **bipy**. These results confirm that with **L27** the reaction is chemoselective (only substrates bearing a substituted carbony like directing group work), and regioselective (*ortho* orientation).

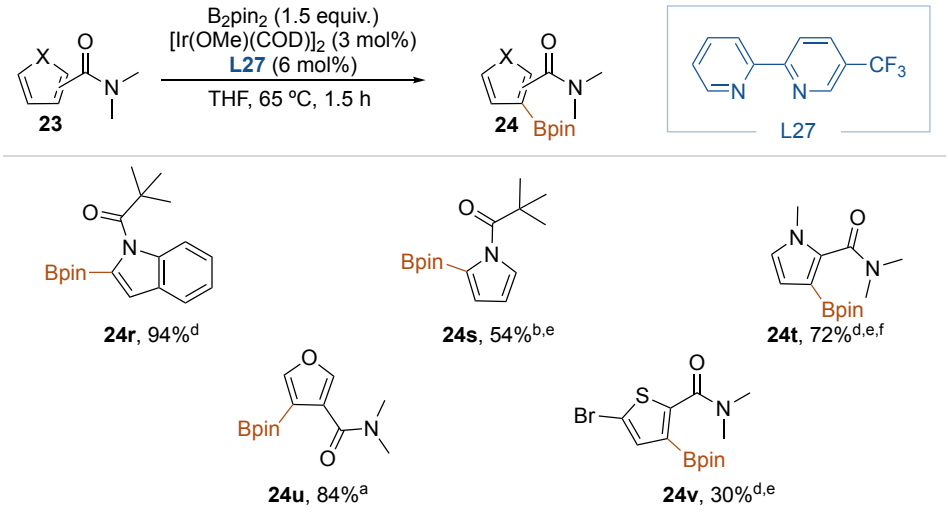
**Table *18*** Control reactions using Toluene and Anisole as substrate.




| R | Temperature (°C) | Ligand | **30** (SM, %) | **31** (*ortho*, %) | **32 +33** (*meta*+*para*, %) |
|---|---|---|---|---|---|
| –Me | 65 | **bipy** | 33 | 0 | 67 |
| | 65 | **L27** | 100 | 0 | 0 |
| | 100 | **L27** | 94 | 0 | 6 |
| –OMe | 65 | **bipy** | 21 | 0 | 79 |
| | 65 | **L27** | 100 | 0 | 0 |

Note: Percentage of products and starting materials were determined by GC/MS analysis. Identification of products was based on previous literature reports.

Next, we evaluated the applicability of our *ortho* borylation technology to challenging heterocyclic substrates containing amide functionalities. As illustrated in Scheme *70*, the reaction proceeds with excellent yields on various heterocycles such as indoles (**24s**), pyrroles (**24t** and **24u**), furans (**24v**), and even thiophenes (**24w**).

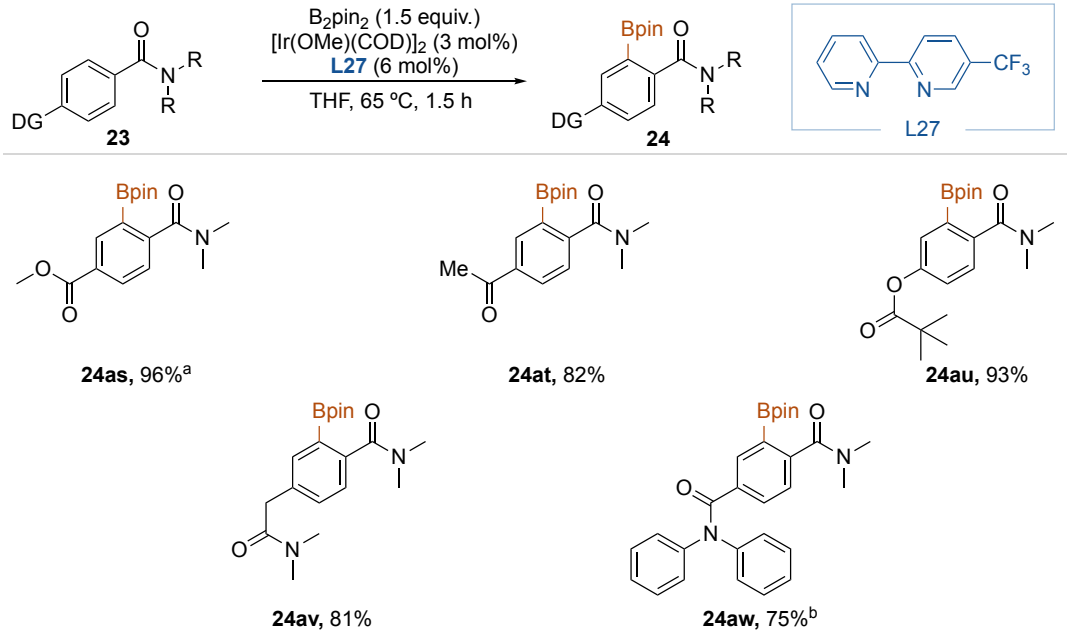



**Scheme *70*** *Ortho*-borylation of heterocycles. Note: Isolated yields are given in all the cases. [a] Reaction time 15 min. [b] Reaction time 1 h. [c] Reaction time 2 h. [d] Reaction time 24 h. [e] Reaction temperature 80 °C. [f] Ligand **L28** was used.

These results confirm a highly regio- and chemoselective transformation, with the substituted amide acting as a key reaction-promoting, and *ortho*-directing group. Consistent with the predominant directing effect of the amide, an aryl precursor featuring both ester and amide groups in relative *para* positions yielded exclusively the product **24as**, mono-borylated *ortho* to the amide moiety (Scheme *71*).

Similarly, benzamides containing *para*-methyl ketone or pivaloyl substituents, produced the desired products **24at** and **24au** in good yields, respectively. In all cases, the amide functionality effectively overrides other directing effects, ensuring a regioselective borylation. Not surprisingly, the regio-directing properties of the benzamide group also prevail in an internal competition with phenylacetamide (**24av**).

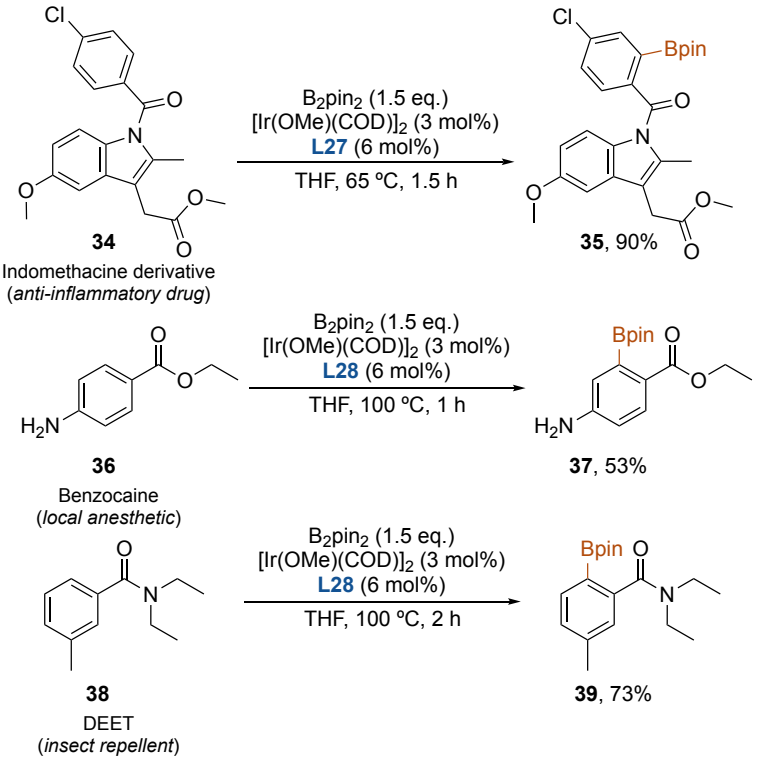
We also tested a substrate exhibiting competing dimethyl and diphenyl amides, demonstrating an excellent regioselectivity in the *ortho* -borylation to the dimethyl amide (**24aw**).




**Scheme *71*** *Ortho*-borylation of of substrates with competing DGs (directing group). Note: Isolated yields are given in all the cases. [a] Reaction time 2 h. [b] Reaction time24 h.

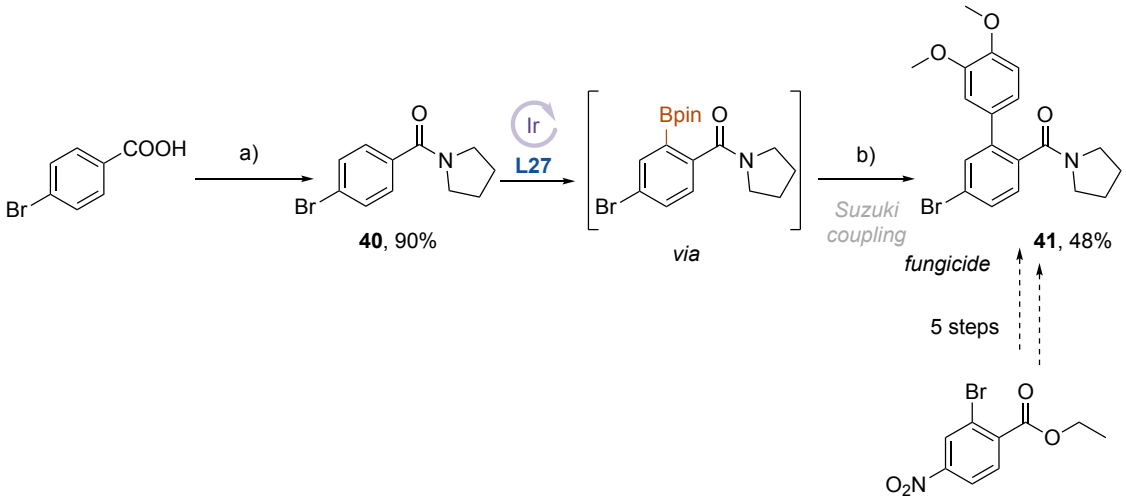
This reaction also allows a late-stage modification of complex, biorelevant substrates, such as an indomethacine derivative (**34**), benzocaine (**36**), and the insect repellent DEET (**38**), which were successfully borylated with excellent selectivity using **L27** or **L28** as iridium ligands (Scheme *72*).

USC UNIVERSIDADE DE SANTIAGO DE COMPOSTELA




**Scheme *72*** Borylation of biologically-relevant molecules. Note: Isolated yields are given in all the cases.

Finally, the synthetic utility of our method was demonstrated by its application in a three-step synthesis of fungicide **41**. The patented synthesis of this product involves five steps starting from ethyl 2-bromo-4-nitrobenzoate. Using our *ortho* borylation technology, the product can be obtained in good yield (43% overall), in only two synthetic operations (Scheme *73*). After converting the acid into the amide, the *ortho* aromatic ring can be introduced in a one-pot reaction involving the borylation and a subsequent *in situ* coupling reaction with 3,4(dimethoxy)iodobenzene.




**Scheme *73*** Three step-synthesis of fungicide **41**. a) $(COCl)_2$ (1.5 equiv.),DMF, DCM, 0 °C to rt, 2 h; then pyrrolidine 0 °C to rt, 16 h; b) $B_2pin_2$ (1.5 equiv.), $[Ir(OMe)(COD)]_2$ (3 mol %), **L27** (6 mol %), THF, 65 °C,1.5 h; then $H_2O$, degassed, and $Pd(PPh_3)_4$, $K_2CO_3$, 3,4(dimethoxy)iodobenzene, 100 °C, 16 h. (For full details see experimental section)

Overall, the $CF_3$-containing ligand **L27** allows the iridium-catalyzed chemo- and resioselective borylation of a diverse range of substrates, providing the more general approach for the *ortho*borylation of benzamide derivatives described to date.

### *7.2.3.2 Mechanistic insights*

After establishing the scope of the reaction, we turned our attention to further understand the mechanistic reasons behind the observed selectivity using the 5-trifluoromethylated ligands **L27** and **L28**.

The general accepted mechanism for the borylation reaction when using 2,2'-bipyridine as ligand, involves a catalytic cycle with Ir(III) and Ir(V) intermediates, and a rate determining oxidative addition of the C–H bond to the metal. Using benzamides as substrates this mechanism is consistent with the experimental observation of *meta/para* borylations, owing to steric reasons (Figure *29*).

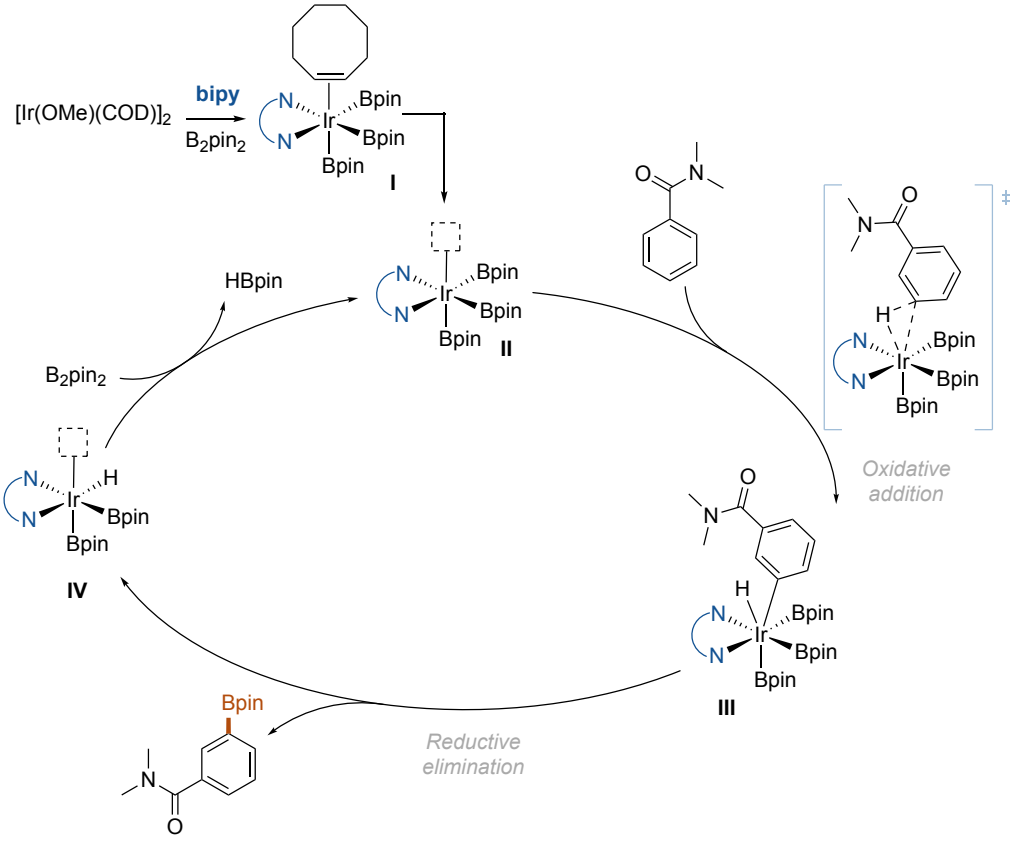



**Figure *29*** General mechanism for the Ir-catalyzed borylation of arenes using 2,2'-bipyridine as ligand applied to dimethylbenzamide.

To explain the impressive effect of the $CF_3$ substituents at the 5-position of the pyridines in the ligand, we initially considered alternative mechanisms. Firstly, we hypothesized that electron-deficient bipyridine ligands like **L27** might promote the formation of Ir(I) complexes, potentially shifting the catalytic process from the typical Ir(III)/Ir(V) cycle to one involving Ir(I)/Ir(III) intermediates (Figure *30*). This shift could facilitate the chelation of the amide directing group to the iridium center. However, both

experimental data and computational experiments, done in collaboration with the group of Dr. Gonzalo Jiménez-Osés, strongly suggest that this is not the case.

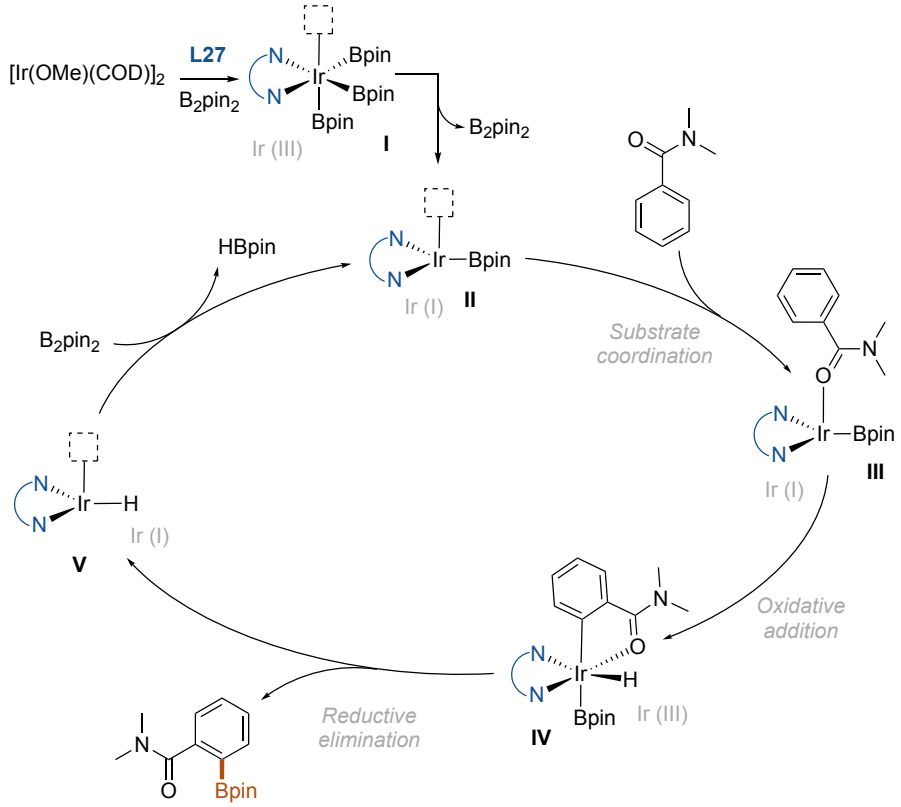
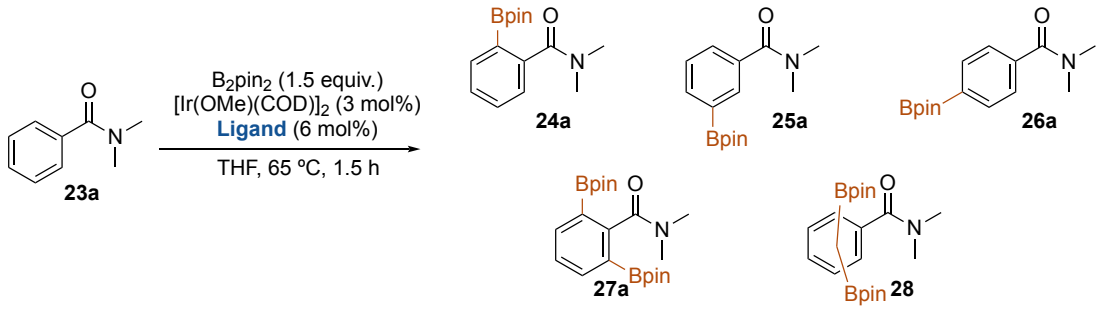



**Figure *30*** Possible Ir(I)/Ir(III) catalytic cycle for aromatic borylation.

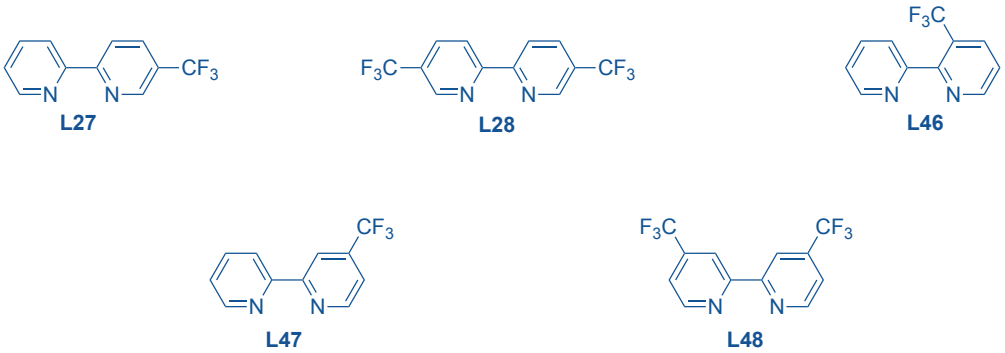
If this were the mechanism, ligands similar to **L27**, but with $CF_3$ at the 3- or 4-position of one of the pyridine rings should lead to similar results than the reaction with **L27**. However, when we performed the experiments with ligands **L46**, **L47** and **L48** we observed lower conversions, and the formation of *meta* and *para*-substituted products (Table 19).

This drastic change in reactivity and regioselectivity upon relocating the $CF_3$ groups from the *meta* to the *ortho* or *para* position in the bipyridine underscores that the critical factor for achieving selectivity is the presence of a $CF_3$ substituent at the 5-position of the bipyridine, rather than merely having an EWG at any position.

**Table 19** Regioselectivity changes depending on the position of the $CF_3$ substituents in the 2,2'-bipyridine core of the ligand.




| Ligand | **23a** (SM, %) | **24a** (*ortho*, %) | **25a+26a** (meta +para, %) | **27a** (*di-ortho*, %) | **28** (*di*, %) |
|---|---|---|---|---|---|
| **L27** | 3 | 90 | 0 | 7 | 0 |
| **L28** | 0 | 80 | 0 | 20 | 0 |
| **L46** | 95 | 5 | 0 | 0 | 0 |
| **L47** | 30 | 2 | 68 | 0 | 0 |
| **L48** | 36 | 0 | 64 | 0 | 0 |




Notes: Meta and para isomers are described together as they were not isolated. Conversion and proportion of products were determined by GC/MS analysis.

The viability of this mechanism was also explored computationally at 25 °C, using the $SMD_{THF}$/M06/6-311++G(2d,p)+SDD(Ir)//M06/6 31G(d) +LANL2DZ(Ir) method. We calculated the activation barriers for the oxidative addition step using model catalysts **bipy**_IrI_Bpin and **L27**_IrI_Bpin (Figure *31*), which feature one Bpin and a bidentate bipyridine ligand coordinated to the metal center. This unsaturated coordination would allow the carbonyl group of the substrate to coordinate to the iridium and act as a directing group (DG). However, the calculated activation energies for the formation of the C–H activated intermediates are notably high ($\Delta G^{\ddagger}$*ortho* = 48-51 kcal $mol^{-1}$), compared with the standard C-H activation ($\Delta G^{\ddagger}$ = 20-30 kcal $mol^{-1}$),[128] mainly because of the very unfavored release of $B_2pin_2$ from the 16-electron active catalyst (**bipy**_AC and **L27**_AC).

[128] Altus; Love *Commun Chem* **2021,** *4,* 1–11.

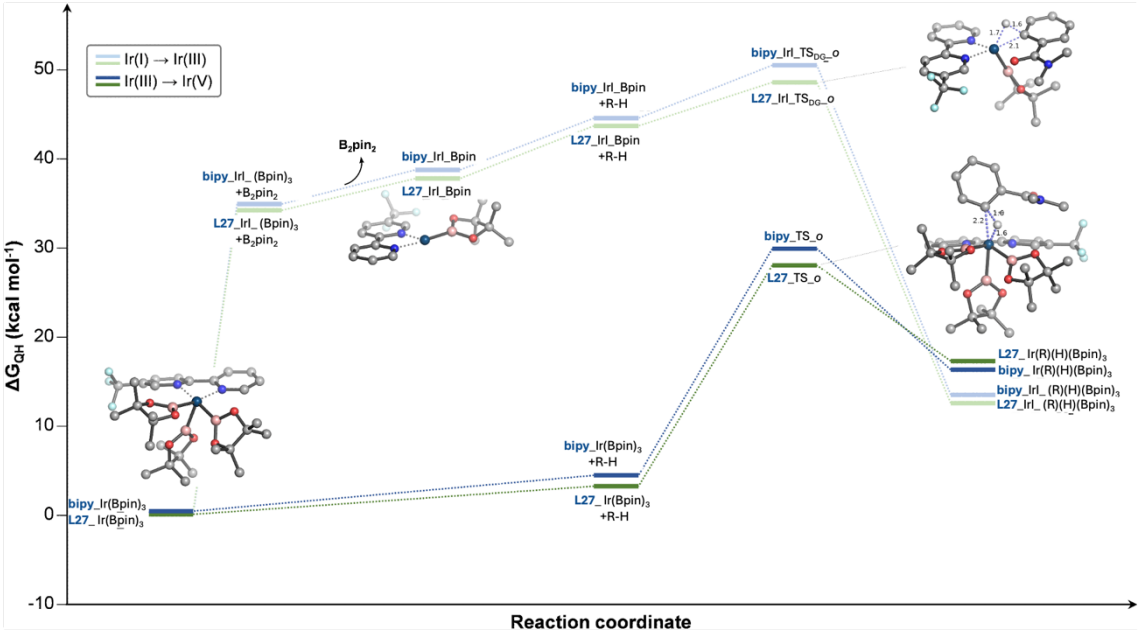



**Figure *31*** Minimum energy pathways (MEP) calculated with $SMD_{THF}$/M06/6-311++G(2d,p)+SDD(Ir)//M06/6-31G(d)+LANL2DZ(Ir) for the oxidative addition step between *N*,*N*-dimethylbenzamide (**23a**) and $Ir^{III}$(**bipy**)$(Bpin)_3$ or $Ir^{III}$(**L27**)$(Bpin)_3$ (*o* = *ortho* pathways only). Two possible mechanisms are compared: the canonical Ir(III) → Ir(V) involving a 16 $e^-$ active catalyst (AC), and an alternative Ir(I) → Ir(III) mechanism involving a 14 $e^-$ active catalyst (IrI_AC) after $B_2pin_2$ cleavage. The structures for the Ir(III) and Ir(I) active catalysts, and outer-sphere (TS for Ir(III)) and directing-group ($TS_{DG}$ for Ir(I)) transition states are shown. Non-reactive hydrogens have been omitted for clarity. Free energies relative to each lowest energy active catalyst (AC) ($\Delta G_{QH}$ in kcal $mol^{-1}$) are represented in the ordinate axis.

Given these computational results and the wide precedents supporting Ir (III)/Ir(V) mechanisms in this type of borylations,[53] and taking into account the experimental observations that electron deficient ligands with $CF_3$ groups in other positions of the bipyridine than *meta*, like **L46** and **L47**, behave like **bipy** rather than to **L27**, we can confidently exclude the Ir(I)/Ir(III) pathway to explain the observed reactivity and selectivity.

Another possible mechanism for the observed *ortho* selectivity could be based on **L27** acting as a hemilabile ligand, which would allow the formation of a catalytic 14-electron Ir(III) species that can directly coordinate with the amide carbonyl.

USC UNIVERSIDADE DE SANTIAGO DE COMPOSTELA

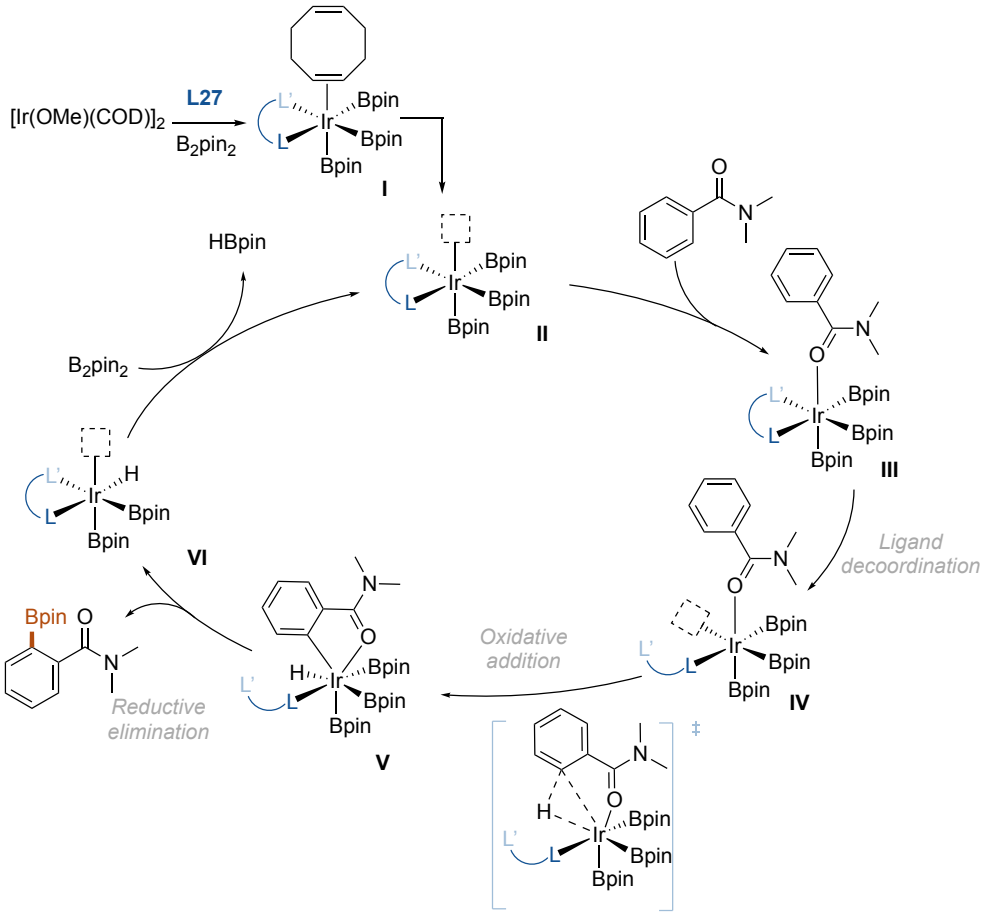



**Figure *32*** Possible mechanism if ligand **L27** acts as an hemilabile ligand.

However, the results when using the $CF_3$-containing ligands **L46** and **L47**, that might behave similarly than **L27** in this type of hemilabile behavior, are against this mechanistic proposal.

Additionally, our computational analysis indicated that de-coordinating the hemilabile ligand to produce intermediate **IV** presents a cost of 14-17 kcal $mol^{-1}$. Moreover, the activation barrier for the C–H activation step from this intermediate is very high ($\Delta G^{\ddagger}_{ortho}$ = 43-45 kcal $mol^{-1}$, Figure *33*).

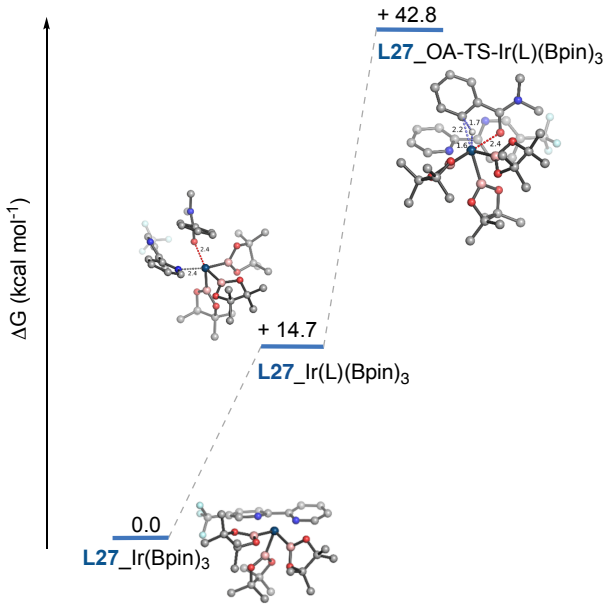



**Figure *33*** Minimum energy pathway (MEP) calculated with $SMD_{THF}$/M06/6-311++G(2d,p)+SDD(Ir)//M06/6-31G(d)+LANL2DZ(Ir) for the oxidative addition step between *N*,*N*-dimethylbenzamide (**23a**) and $Ir^{III}$(**L27**)$(Bpin)_3$. An alternative mechanism is considered which involves the de-coordination of one pyridine ring and the subsequent *ortho* C–H activation with the carbonyl group of the amide acting as a DG, directly coordinated to the Ir atom. Free energies relative to $(Ir(Bpin)_3$+R–H) ($\Delta G_{QH}$ in kcal $mol^{-1}$).

Another alternative could be based on the **L27** ligand undergoing a C-H activation to form an L–X type of ligand, which are known to allow the coordination of the carbonyl moiety of the substrate before the oxidative addition step (Figure *16*). However, the above commented difficulties for the decoordination of one of the pyridines also argues against this hypothesis.

Moreover, we performed some qualitative NMR experiments comparing the evolution of ligands **L28** and **bipy** upon treatment with stoichiometric amounts of the iridium precursor $[IrCODCl]_2$, and we observed the appearance of signals corresponding to a cationic complex (**42**), where the Ir is coordinated to the bipyridine via both N atoms.

Upon adding $B_2pin_2$ to this mixture, new signals corresponding to the bisboryl complex (**43**) emerged, which still featured Ir coordinated to the bipyridine through the two N atoms (Figure *34*). This provided further evidence that a rollover cyclometalation does not occur in this system.

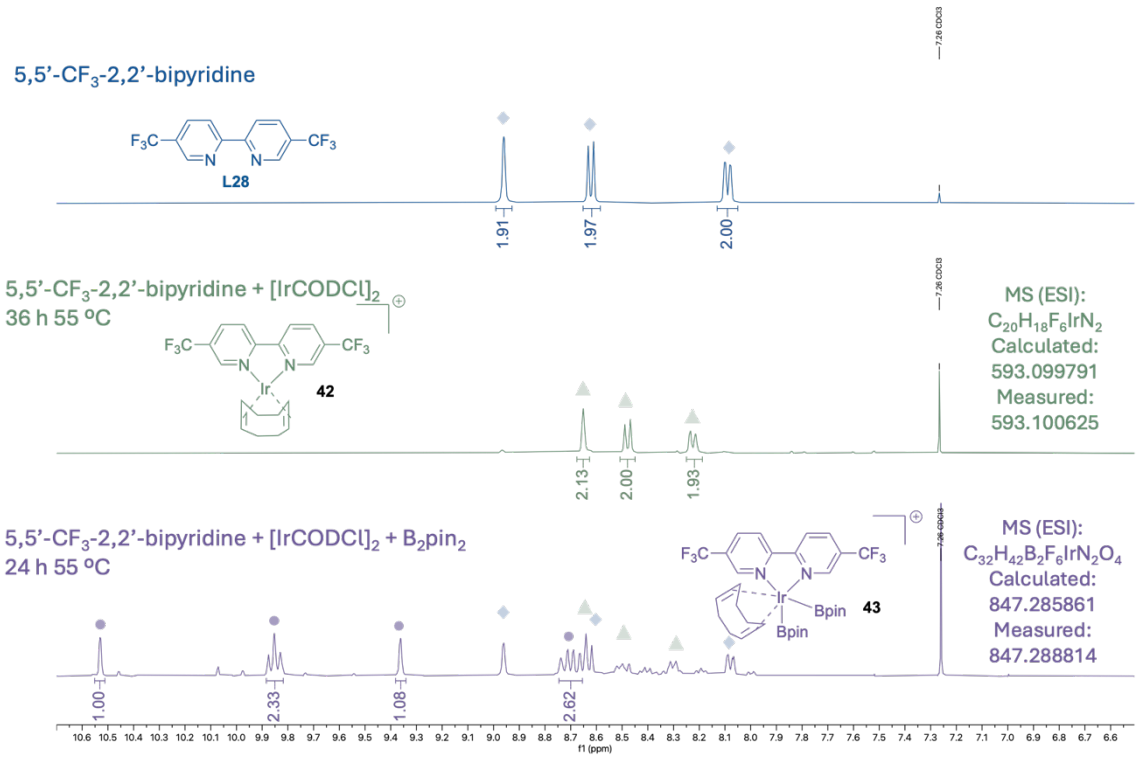



**Figure *34*** NMR and HRMS studies on the formation of Ir-**L28** complexes to analyze a possible rollover cyclometalation. Blue markers correspond to signals for **L28**, green markers to signals from complex **42** and purple markers to signals from complex **43**.

At this point, having discarded these alternative mechanisms, we made some kinetic studies comparing the behavior of **L27** versus **bipy**. Parallel kinetic experiments using *N,N*-dimethylbenzamide and its $d_5$-deuterated analogue as substrates, and with the trifluoromethylated ligand **L27** as ligand, allowed to measure a kinetic isotope effect (KIE) of 4.5. This value is similar to that obtained with **bipy**[53] and supports a classical mechanistic scenario where C–H activation is turnover-determining (Figure *35*). Therefore, the *ortho*-selectivity observed with **L27** is likely due to factors influencing the activation barrier of the C–H activation.

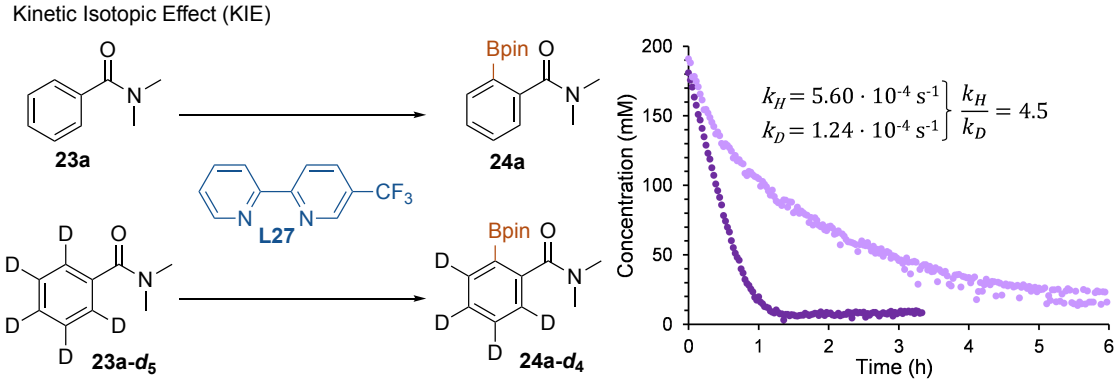



**Figure *35*** Kinetic isotope effect (KIE) determined from parallel reactions of substrates **23a** (dark purple) and **23a-d$_5$** (light purple).

The fact that the reactivity decreases when the amide is substituted with EWGs, and that harsher conditions are needed for borylation of esters and ketones, as well as the observation than substrates without carbonyl groups like toluene or anisole fail to react, suggests that the amide group plays a primary role in the C–H activation step. However, a direct interaction between the amide group and the iridium (III) atom is very improbable, as it would likely saturate the coordination sphere of the metal center, hindering the C–H activation process.

To try and discern the role of the amide in the C–H activation step, we conducted a detailed computational analysis of this step by considering all possible regioisomers (*ortho*, *meta* and *para*) as well as conformers of relevant stationary points for the reaction with ligands **bipy**, and the $CF_3$-substituted bipyridine isomeric ligands **L27** ($CF_3$ *meta* to the pyridine nitrogen), **L46** (*ortho*) and **L47** (*para*, Figure *36*). The analysis of the calculated transition state structures reveals that although the geometry of the lowest-energy *ortho* and *meta* TSs with ligands **bipy** and **L27** are almost identical (particularly the breaking C–H and forming Ir-C and Ir-H bonds, Figure *36*), their relative energies differ significantly.

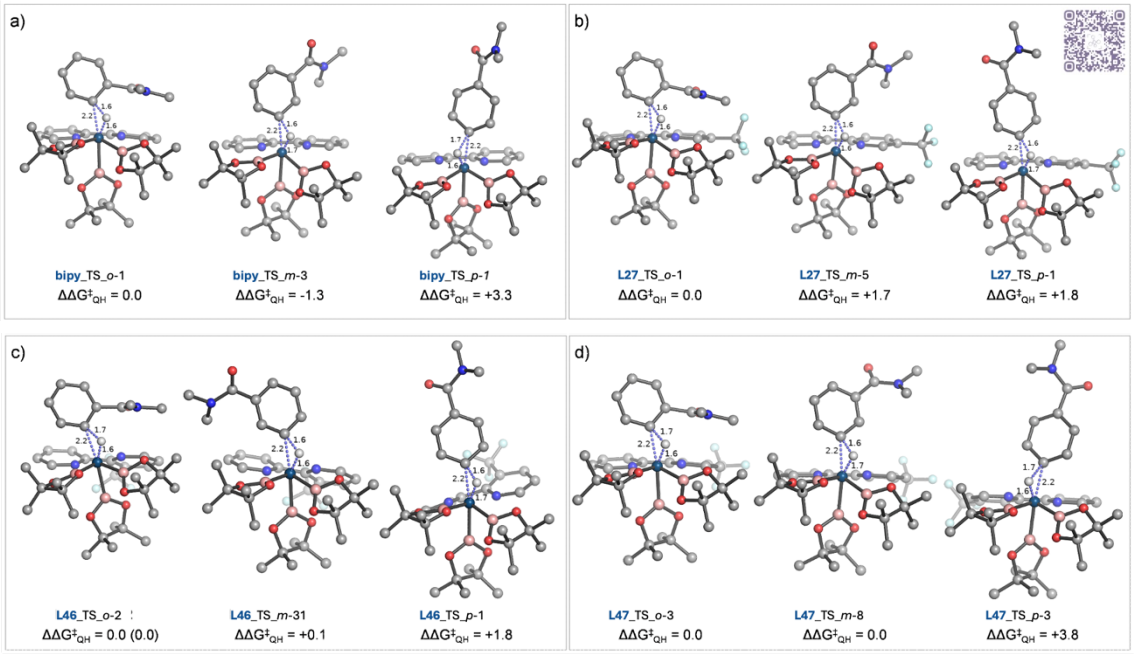
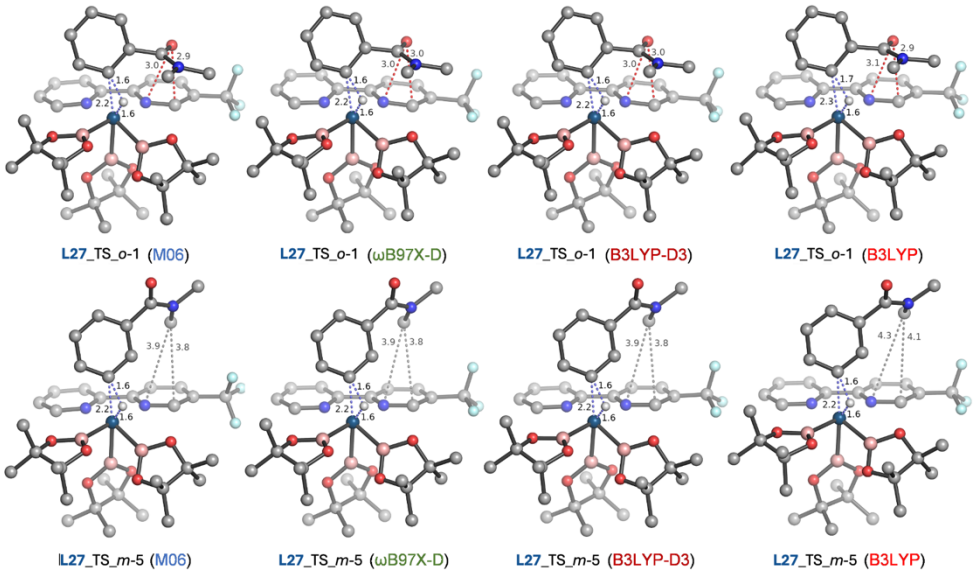



**Figure *36*** Low-energy outer-sphere transition states (TS) calculated for the oxidative addition step involving N,N-dimethylbenzamide (**23a**) and $Ir^{III}$(ligand)$(Bpin)_3$ (where ligand **bipy** (a), **L27** (b), **L46** (c), and **L47** (d) are used; o = *ortho*, m = *meta*, p = *para*). The relative activation free energies ($\Delta G^{\ddagger}_{QH}$) are given in kcal·mol$^{-1}$ and calculated using the $SMD_{THF}$/M06/6-311G(2d,p)+SDD(Ir)//M06/6-31G(d)+LANL2DZ(Ir) method. The metal-ligand and breaking/forming C–H, Ir–C, and Ir–H bonds are depicted as blue dashed lines, respectively. For clarity, non-reactive hydrogens have been excluded. To see an interactive model of the calculated structures visit https://danielmarcosatanes.github.io/DMA_thesis-viewer/ or scan the QR code.

However, it is important to note that the calculated activation barriers are highly sensitive to the theoretical method used (DFT functional, basis set, implicit solvation corrections and vibrational contribution to enthalpy and entropy) (Figure *37*).

USC DE SANTIAGO DE COMPOSTELA




| ΔΔG‡$_{o-m}$ (method) | | | |
|---|---|---|---|
| –5.0 (A1) | –6.0 (B1) | –5.9 (C1) | +1.8 (D1) |
| –5.0 (A2) | –5.6 (B2) | –4.8 (C2) | +2.9 (D2) |
| –2.0 (A3) | –2.7 (B3) | –2.5 (C3) | +5.0 (D3) |
| –2.7 (A4) | –3.6 (B4) | –3.4 (C4) | +4.1 (D4) |
| –1.7 (A5) | –2.0 (B5) | –1.1 (C5) | +6.5 (D5) |
| –2.5 (A6) | –2.9 (B6) | –2.0 (C6) | +5.6 (D6) |

| | Quantum mechanical method |
|---|---|
| A1 | M06/6-31G(d)+LANL2DZ (Ir) |
| A2 | M06/6-311++G(2d,p)+SDD (Ir)//M06/6-31G(d)+LANL2DZ (Ir) |
| A3 | SMD$_{THF}$/M06/6-31G(d)+LANL2DZ (Ir)//M06/6-31G(d)+LANL2DZ (Ir) |
| A4 | IEF-PCM$_{THF}$/M06/6-31G(d)+LANL2DZ (Ir)//M06/6-31G(d)+LANL2DZ (Ir) |
| A5 | SMD$_{THF}$/M06/6-311++G(2d,p)+SDD (Ir)//M06/6-31G(d)+LANL2DZ (Ir) |
| A6 | IEF-PCM$_{THF}$/M06/6-311++G(2d,p)+SDD (Ir)//M06/6-31G(d)+LANL2DZ (Ir) |
| B1 | ωB97X-D/6-31G(d)+LANL2DZ (Ir) |
| B2 | ωB97X-D/6-311++G(2d,p)+SDD (Ir)//ωB97X-D/6-31G(d)+LANL2DZ (Ir) |
| B3 | SMD$_{THF}$/ωB97X-D/6-31G(d)+LANL2DZ (Ir)//ωB97X-D/6-31G(d)+LANL2DZ (Ir) |
| B4 | IEF-PCM$_{THF}$/ωB97X-D/6-31G(d)+LANL2DZ (Ir)//ωB97X-D/6-31G(d)+LANL2DZ (Ir) |
| B5 | SMD$_{THF}$/ωB97X-D/6-311++G(2d,p)+SDD (Ir)//ωB97X-D/6-31G(d)+LANL2DZ (Ir) |
| B6 | IEF-PCM$_{THF}$/ωB97X-D/6-311++G(2d,p)+SDD (Ir)//ωB97X-D/6-31G(d)+LANL2DZ (Ir) |
| C1 | B3LYP-D3/6-31G(d)+LANL2DZ (Ir) |
| C2 | B3LYP-D3/6-311++G(2d,p)+SDD (Ir)//B3LYP-D3/6-31G(d)+LANL2DZ (Ir) |
| C3 | SMD$_{THF}$/B3LYP-D3/6-31G(d)+LANL2DZ (Ir)//B3LYP-D3/6-31G(d)+LANL2DZ (Ir) |
| C4 | IEF-PCM$_{THF}$/B3LYP-D3/6-31G(d)+LANL2DZ (Ir)//B3LYP-D3/6-31G(d)+LANL2DZ (Ir) |
| C5 | SMD$_{THF}$/B3LYP-D3/6-311++G(2d,p)+SDD (Ir)//B3LYP-D3/6-31G(d)+LANL2DZ (Ir) |
| C6 | IEF-PCM$_{THF}$/B3LYP-D3/6-311++G(2d,p)+SDD (Ir)//B3LYP-D3/6-31G(d)+LANL2DZ (Ir) |
| D1 | B3LYP/6-31G(d)+LANL2DZ (Ir) |
| D2 | B3LYP/6-311++G(2d,p)+SDD (Ir)//B3LYP/6-31G(d)+LANL2DZ (Ir) |
| D3 | SMD$_{THF}$/B3LYP/6-31G(d)+LANL2DZ (Ir)//B3LYP/6-31G(d)+LANL2DZ (Ir) |
| D4 | IEF-PCM$_{THF}$/B3LYP/6-31G(d)+LANL2DZ (Ir)//B3LYP/6-31G(d)+LANL2DZ (Ir) |
| D5 | SMD$_{THF}$/B3LYP/6-311++G(2d,p)+SDD (Ir)//B3LYP/6-31G(d)+LANL2DZ (Ir) |
| D6 | IEF-PCM$_{THF}$/B3LYP/6-311++G(2d,p)+SDD (Ir)//B3LYP/6-31G(d)+LANL2DZ (Ir) |

**Figure *37*** Low energy outer-sphere transition states (TS) calculated at various theory levels for the oxidative addition step involving *N*,*N*-dimethylbenzamide (**23a**) and Ir$^{III}$(**L27**)(Bpin)$_3$ (*o* = *ortho*, *m* = *meta*). The carbonyl (CO···π) and *N*-methyl ($CH_3$···π) interactions between the substrate and the bipyridine ligand are depicted as red and gray dashed lines, respectively. For clarity, non-reactive hydrogens have been omitted. The relative activation barriers for the *ortho* and *meta* reaction pathways ($\Delta\Delta G^{\ddagger}_{o-m} = \Delta G^{\ddagger}_{o} - \Delta G^{\ddagger}_{m}$) are given in kcal mol$^{-1}$. Negative and positive $\Delta\Delta G^{\ddagger}_{o-m}$ values indicate a preference for the *ortho* and *meta* pathways, respectively.

USC UNIVERSIDADE DE SANTIAGO DE COMPOSTELA

Through an extensive benchmarking (Table *20*), we found that the best correlation between computed and experimental regioselectivities, for all the studied ligands (**bipy**, **L27**, **L46** and **L47**) was achieved with the M06 functional, a large basis set without diffuse functions (6-311G(2d,p) and the SDD effective core potential for Ir, implicit solvation corrections (SMD behaving slightly better for selectivities and PCM giving activation barriers closer to the experimental values) and quasi-harmonic approximations to enthalpy and entropy (Table *20*, methods A7 and A8).

**Table *20*** Theoretical ratios of the *ortho* (*o*) and *meta* (*m*) borylation products predicted from the Boltzmann distribution at 25 ºC of the energies of all outer-sphere transition states (TS) calculated at different theory levels for the oxidative addition step between *N*,*N*-dimethylbenzamide (**23a**) and $Ir^{III}$(ligand)$(Bpin)_3$ (ligand = **bipy**, **L27**, **L46** and **L47**).

| | Method A1 | | | Method A5 | | | Method A6 | | | Method A7 | | | Method A8 | | | Method A9 | | | Method A10 | | |
|---|---|---|---|---|---|---|---|---|---|---|---|---|---|---|---|---|---|---|---|---|---|
| | H | G | $G_{QH}$ | H | G | $G_{QH}$ | H | G | $G_{QH}$ | H | G | $G_{QH}$ | H | G | $G_{QH}$ | H | G | $G_{QH}$ | H | G | $G_{QH}$ |
| **bipy_TS_*o*** | 99 | 35 | 71 | 44 | 0 | 1 | 75 | 1 | 5 | 77 | 1 | 6 | 92 | 5 | 19 | 96 | 11 | 36 | 99 | 35 | 70 |
| **bipy_TS_*m*** | 1 | 65 | 29 | 56 | 100 | 99 | 25 | 99 | 95 | 23 | 99 | 94 | 8 | 95 | 81 | 4 | 89 | 64 | 1 | 65 | 30 |
| **L27_TS_*o*** | 100 | 99 | 100 | 82 | 15 | 37 | 95 | 44 | 72 | 96 | 59 | 81 | 99 | 86 | 95 | 98 | 86 | 95 | 100 | 96 | 99 |
| **L27_TS_*m*** | 0 | 1 | 0 | 17 | 66 | 47 | 5 | 47 | 23 | 4 | 33 | 15 | 1 | 12 | 5 | 2 | 14 | 5 | 0 | 4 | 1 |
| **L46_TS_*o*** | 99 | 78 | 87 | 46 | 6 | 10 | 76 | 18 | 30 | 76 | 21 | 31 | 92 | 49 | 62 | 99 | 88 | 92 | 100 | 97 | 98 |
| **L46_TS_*m*** | 1 | 21 | 13 | 53 | 76 | 84 | 24 | 66 | 66 | 24 | 72 | 67 | 8 | 46 | 37 | 1 | 12 | 8 | 0 | 3 | 2 |
| **L47_TS_*o*** | 99 | 77 | 93 | 59 | 2 | 7 | 83 | 7 | 25 | 84 | 7 | 26 | 95 | 26 | 60 | 98 | 47 | 79 | 99 | 80 | 94 |
| **L47_TS_*m*** | 1 | 23 | 7 | 41 | 98 | 93 | 17 | 93 | 75 | 16 | 93 | 73 | 5 | 74 | 40 | 2 | 53 | 21 | 1 | 20 | 6 |

**Method A1**: M06/6-31G(d)+LANL2DZ(Ir).
**Method A5**: $SMD_{THF}$/M06/6-311++G(2d,p)+SDD(Ir)//M06/6-31G(d)+LANL2DZ(Ir).
**Method A6**: IEF-$PCM_{THF}$/M06/6-311++G(2d,p)+SDD(Ir)//M06/6-31G(d)+LANL2DZ(Ir).
**Method A7**: $SMD_{THF}$/M06/6-311G(2d,p)+SDD(Ir)//M06/6-31G(d)+LANL2DZ(Ir).
**Method A8**: IEF-$PCM_{THF}$/M06/6-311G(2d,p)+SDD(Ir)//M06/6-31G(d)+LANL2DZ(Ir).
**Method A9**: $SMD_{THF}$/ωB97x-D/6-311G(d,p)+SDD(Ir)//M06/6-31G(d)+LANL2DZ(Ir).
**Method A10**: IEF-$PCM_{THF}$/ωB97x-D/6-311G(d,p)+SDD(Ir)//M06/6-31G(d)+LANL2DZ(Ir).

Using this methodology, we observed highly significant and conserved trends, particularly regarding the regioselectivity of the oxidative addition reaction. Notably, only ligand **L27** exhibited a clear and strong preference for oxidative addition at the *ortho* position compared to *meta* or *para* positions (calculated *o*:*m* ratio = 81:15). In contrast, the isomeric trifluromethylated ligands **L46** (calculated *o*:*m* ratio = 31:67) and **L47** (calculated *o*:*m* ratio = 26:73) showed a predominant preference for the *meta*-borylation. Similarly, for the unsubstituted bipyridine **bipy** *meta*-borylation was heavily favored (calculated *o*:*m* ratio = 6:94). Overall, these results are in complete agreement with the observed experimental selectivities.

USC UNIVERSIDADE DE SANTIAGO DE COMPOSTELA

The analysis of non-covalent interactions in key structures using NCIPLOT [116] (Figure *38*), revealed that the *ortho* preference in the case of the ligand **L27** stems from the presence of an extensive network of attractive interactions in the transition state (TS) between the carbonyl group of the benzamide substrate and the $CF_3$-pyridine ring of ligand **L27**. These interactions are notably absent in the *meta* TS, where only a small interaction is observed between the N–Me group of the amide and the ligand. Additionally, in the *ortho*-TS, weak attractive interactions are identified between the methyl groups of the substrate's amide and the $CF_3$ group on the ligand, contributing to TS stabilization and the observed *ortho*-selectivity (Figure *38*).

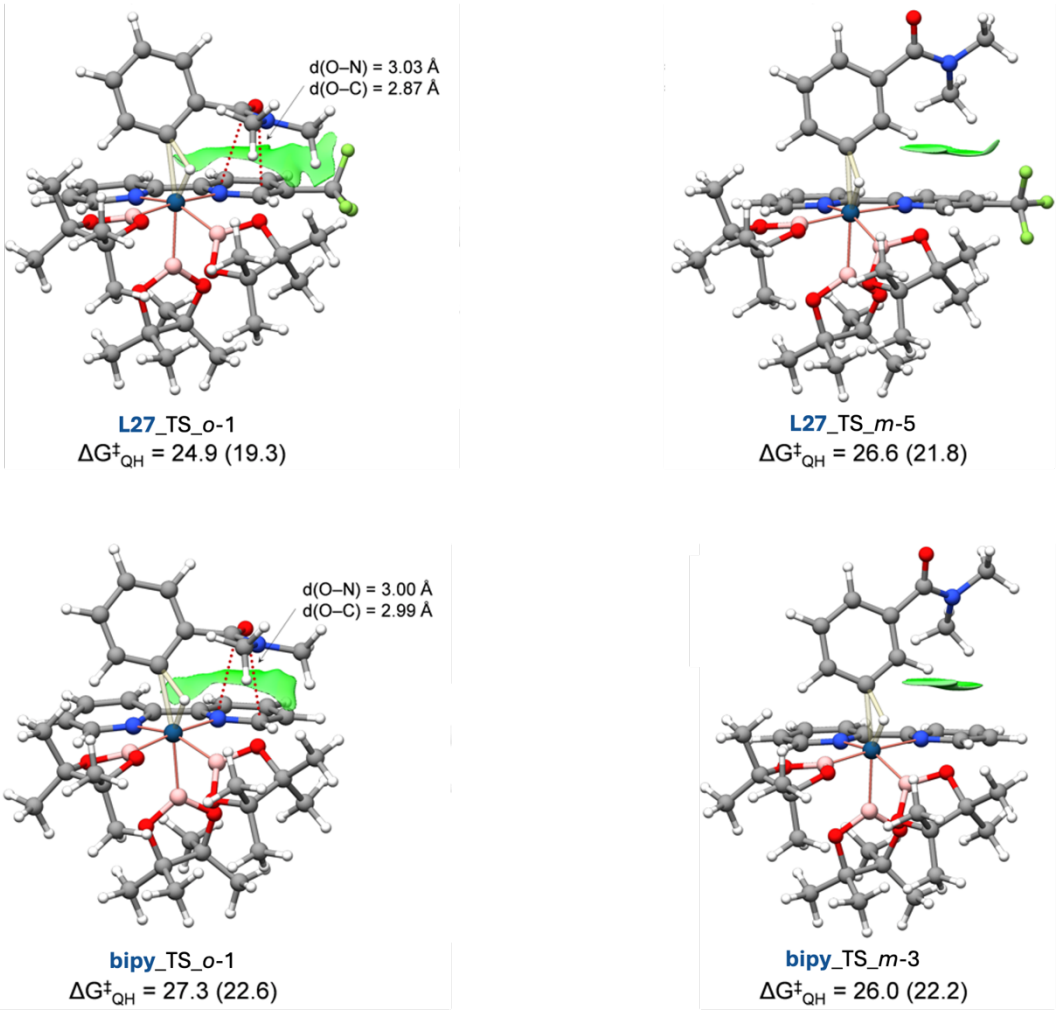



**Figure *38*** Substrate-ligand non-covalent interactions (NCI) occurring in low energy outer-sphere transition states (TS) calculated for the oxidative addition step between *N,N*-dimethylbenzamide (**23a**) and $Ir^{III}$(ligand)$(Bpin)_3$ (ligand = **bipy** and **L27**; *o* = *ortho*, *m* = *meta*). Activation free energies ($\Delta G^{\ddagger}_{QH}$) calculated with $SMD_{THF}$ and $IEF\text{-}PCM_{THF}$ (in parentheses) and M06/6-311G(2d,p)+SDD(Ir)//M06/6-31G(d)+LANL2DZ(Ir) are given in kcal $mol^{-1}$. Metal-ligand and breaking/forming C–H, Ir–C and Ir–H bonds are represented as pale red and yellow lines, respectively. Contacts between the substrate carbonyl O and bipyridine N and C atoms are represented as red dashed lines. Note the larger extension of van der Waals NCI in the *ortho* transition states.

USC UNIVERSIDADE DE SANTIAGO DE COMPOSTELA

In contrast, analysis of the same TS with the unmodified bipyridine ligand **bipy** (Figure *38*) shows significantly weaker interactions. This difference helps explain the reduced *ortho*-selectivity observed with **bipy**, as the non-covalent interactions are much less pronounced than those driving the *ortho* preference with **L27**.

These interactions were further confirmed through a quantum theory of atoms in molecules (QTAIM,[117] Figure *39*) analysis. In the *ortho* transition state (TS), bond paths were identified between the carbonyl group of the benzamide and the $CF_3$-substitutde pyridine ring, along with a bond critical point (BCP), indicating a strong interaction that contributes to the stabilization of the *ortho* TS.

In contrast, these bond paths and BCPs were absent in the *meta* TS, further supporting the idea that the non-covalent interactions between the carbonyl group and the $CF_3$-pyridine ring play a crucial role in driving the regioselectivity toward *ortho* borylation.

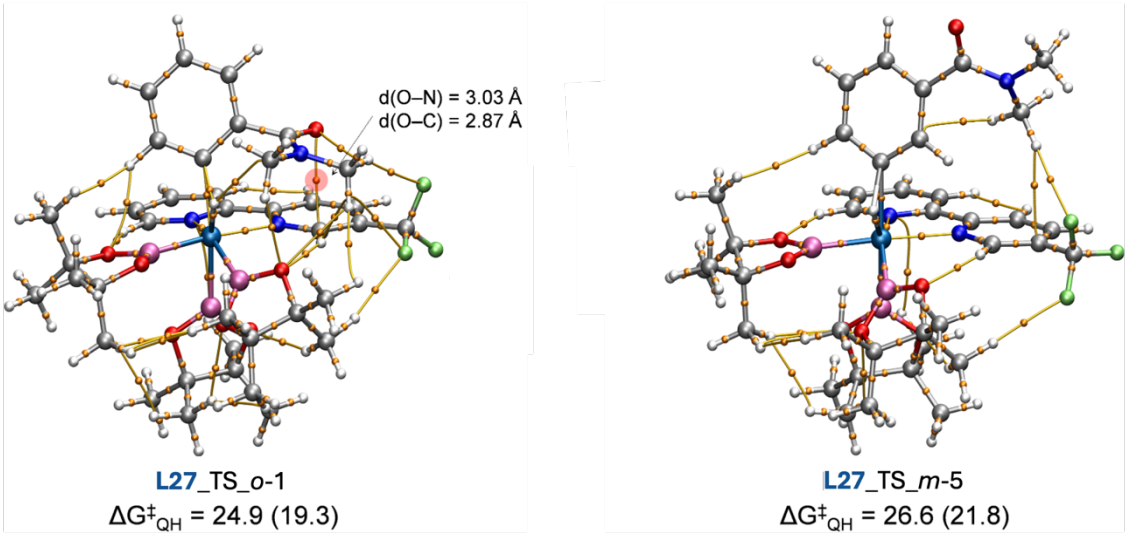



**Figure *39*** Bond critical points (BCP) (3,-1) determined from topology analysis of the electron density in low energy outer-sphere transition states (TS) calculated for the oxidative addition step between *N*,*N*-dimethylbenzamide (**23a**) and $Ir^{III}$(ligand)$(Bpin)_3$ (ligand = **L27**; *o* = *ortho*, *m* = *meta*). Activation free energies ($\Delta G^{‡}_{QH}$) calculated with $SMD_{THF}$ and IEF-$PCM_{THF}$ (in parentheses) and M06/6-311G(2d,p)+SDD(Ir)//M06/6-31G(d)+LANL2DZ(Ir) are given in kcal $mol^{-1}$. The BCP between the substrate carbonyl O and bipyridine N or C atoms in the *ortho* transition states are highlighted with a red circle.

Energy Decomposition Analysis (GSK-EDA,[121] Figure *40*) for the *ortho* and *meta* C–H activation TS allowed for a breakdown of the total interaction energy between the amide and (5-trifluoromethyl)pyridine fragments. The analysis revealed that the attractive interactions, both polar and dispersive, are significantly stronger in the *ortho* borylation TS with **L27**. This higher total interaction energy reinforces the hypothesis that these non-covalent interactions, including polar and dispersive forces, contribute to stabilizing the *ortho* TS over the *meta* one when using ligand **L27**.

USC UNIVERSIDADE DE SANTIAGO DE COMPOSTELA

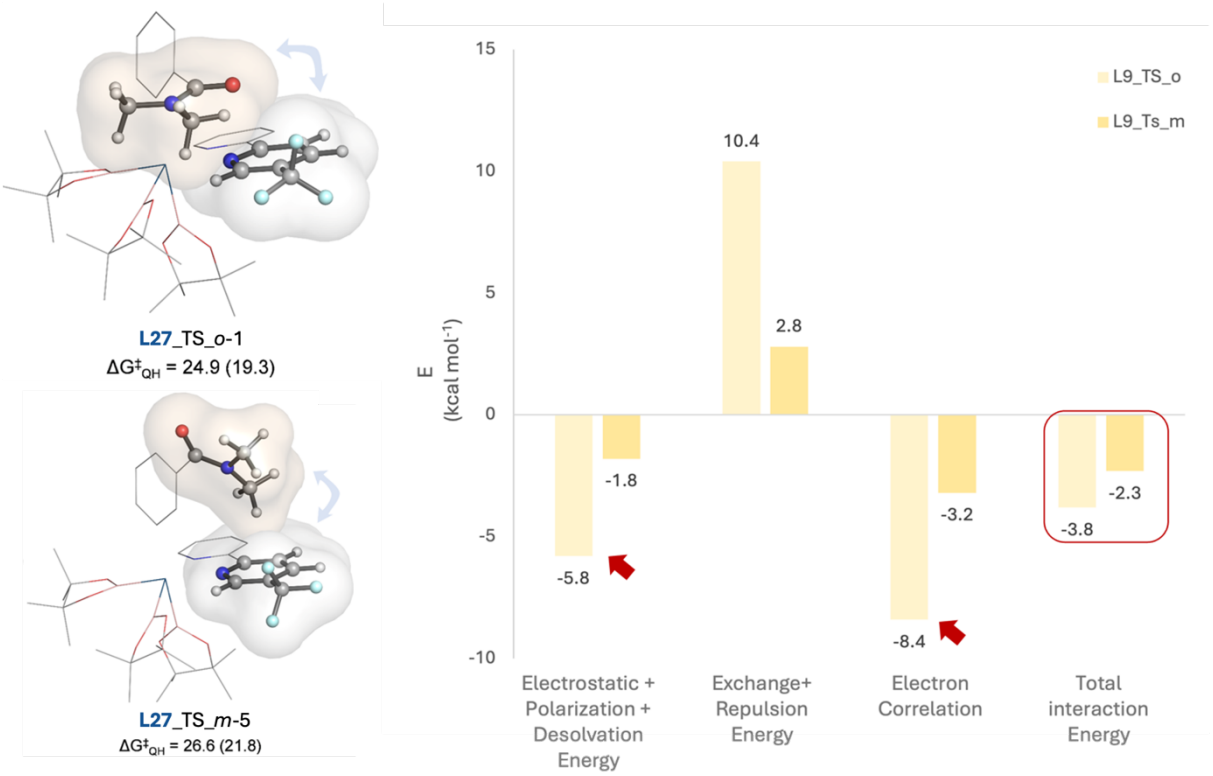



**Figure *40*** Generalized Kohn-Sham Energy Decomposition Analysis (GKS-EDA of the low energy outer-sphere transition states (TS) calculated for the oxidative addition step between *N*,*N*-dimethylbenzamide (**23a**) and $Ir^{III}$(ligand)$(Bpin)_3$ (ligand = **bipy** and **L27**; *o* = *ortho*, *m* = *meta*). Activation free energies ($\Delta G^{\ddagger}_{QH}$) calculated with $SMD_{THF}$ and $IEF\text{-}PCM_{THF}$ (in parentheses) and M06/6-311G(2d,p)+SDD(Ir)//M06/6-31G(d)+LANL2DZ(Ir) are given in kcal $mol^{-1}$.In the graphs, different contributions to the total interaction energy between the *N*,*N*-dimethylformamide and (5-trifluoromethyl)pyridine fragments are shown. Contributions related to the polar character of the interactions (electrostatic, polarization and desolvation) have been added together for clarity. The electron correlation component implicitly accounts for dispersion. The larger values for the attractive interactions (both polar and dispersion) occurring in the *ortho* borylation TS with ligand **L27**, resulting in a larger total interaction energy, are highlighted with red arrows.

Furthermore, natural bond order (NBO)[119] analysis (Figure *41*) provided significant insights into donor-acceptor interactions between the donor (occupied) orbitals on the carbonyl oxygen of the benzamide and the acceptor (unoccupied) orbitals on the pyridine ring of the bipyridine ligands. The $n_{CO} \rightarrow \pi^*_{C=N}$ interaction was more pronounced in the *ortho* TS for **L27** due to the electron-withdrawing nature of the $CF_3$ group, which shortened the distances between the carbonyl oxygen (CO) and the pyridine nitrogen (CN) in the *ortho* transition state of **L27** (**L27**_TS_o) compared to **bipy** (**bipy**_TS_o). This shortening reflects a stronger interaction in **L27**, leading to greater stabilization of the *ortho* TS. Moreover, the electron-withdrawing effect of the $CF_3$ group in **L27** caused a reversal in the direction of electron density donation, from the bipyridine-to-carbonyl seen in **bipy** to carbonyl-to-bipyridine in **L27.**

USC UNIVERSIDADE DE SANTIAGO DE COMPOSTELA

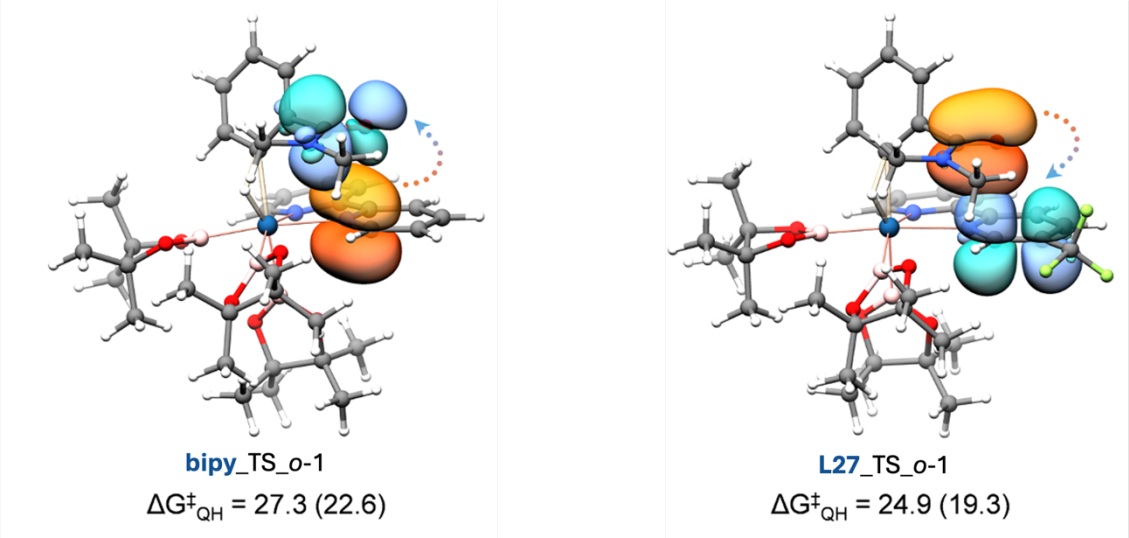



**Figure *41*** Natural Bond Orbital (NBO) analysis of the low energy outer-sphere transition states (TS) calculated for the *ortho* oxidative addition step between *N*,*N*-dimethylbenzamide (**23a**) and $Ir^{III}$(ligand)$(Bpin)_3$ (ligand = **bipy** and **L27**; *o* = *ortho*). Activation free energies ($DG^{‡}_{QH}$) calculated using $SMD_{THF}$ and $IEFPCM_{THF}$ (in parentheses) and M06/6-311G(2d,p)+SDD(Ir)//M06/6-31G(d)+LANL2DZ(Ir) are given in kcal $mol^{-1}$. The NBO orbitals involved in the interactions (donor in orange-red, acceptor in blue-green) are shown as semi-transparent surfaces (isovalue = 0.5). The direction of electron density donation is represented with gradient-colored dashed arrows.

In addition to the unusual substrate-bipyridine interactions, our calculations uncovered a notable enthalpy-entropy interplay influencing regioselectivity. Specifically, in all examined cases, entropy consistently opposes and occasionally even dominates over enthalpy as the key factor in determining regioselectivity. (See experimental information) This enthalpy-entropy compensation has a profound effect on the overall activation free energies ($\Delta\Delta G^{‡}$), significantly impacting both the direction and the extent of regioselectivity. Interestingly, this phenomenon, although well-documented in certain enzymatic processes,[129] appears to be relatively unexplored in the context of organometallic reactions.

## 7.2.4 Conclusions

In summary, we have discovered that the introduction of $CF_3$ groups at the 5-position of bipyridine ligands (Ligands **L27** and **L28**), induces a complete shift in regioselectivity in the iridium- catalyzed borylations of benzamides, changing the reaction preference from the typical *meta/para* obtained with **bipy**, to *ortho*. The presence of a carbonyl-containing directing group, such as an amide, ester, ketone, or even a sulfonamide, is crucial for for reactivity, and ensures an excellent chemo and regioselectivity even in polysubstituted and heteroaromatic substrates. This represents a substantial advantage with respect to other methods based on different ligand systems.

[129] Åqvist, J.; Kazemi, M.; Isaksen, G. V.; Brandsdal, B. O. *Acc. Chem. Res.* **2017,** *50,* 199–207.

Experimental data, along with DFT calculations for both $CF_3$-containing and non-$CF_3$ ligands support a canonical Ir(III)/Ir(V) mechanism where the rate-determining step is the C–H activation. The calculations reveal that the regioselectivity is governed by a delicate balance between enthalpic and entropic factors. While the *ortho* position is typically disfavored with standard 2,2'-bipyridine due to steric and entropic penalties, the 5-$CF_3$-substituted ligands **L27** and **L28** introduce significant enthalpic stabilization. This is attributed to unusual non-covalent, dispersion interactions between the benzamide group from the substrate and the polarized bypiridine ring(s).

These non-covalent interactions, which have rarely been considered in similar contexts, should be taken into account in the future for designing and optimizing other types of chemical reactions.

USC
UNIVERSIDADE DE SANTIAGO DE COMPOSTELA

## 7.3 Ir-catalyzed selective borylation of $Csp^3$–H bonds in methylamides

### 7.3.1 Introduction

As commented in the introduction, the borylation of aliphatic C($sp^3$)–H bonds represents an ongoing, highly relevant challenge in metal-catalyzed C–H functionalizations. Progress in this matter has been slower than in the case of aromatic systems, but recent years have witnessed significant advances that are summarized in the introduction of this PhD manuscript.

Part of the work in this area has been focused on the borylation of C($sp^3$)–H bonds in aliphatic amides, owing to the pharmacological relevance of α-amidoboronic acids, and their potential for further modification.[130] Therefore, Senmiao Xu's group introduced a family of chiral bidentate compounds (CBL) with a diaminoboronate core that can behave as L–X ligands (Figure *42*, **A**).[95] In this work they also include a few examples for the synthesis of α-amidoboronates.

In 2019, Maleczka Jr.'s group reported another L–X ligand capable of selectively performing N–Me borylation on alkyl amides. This system relied on a commercially available quinoline silane moiety, which enabled regioselective functionalization of N–Me bonds, though with a rather limited substrate scope. (Figure *42*, **B**).[94] Building on this work, Clark's group in 2021 developed an N-Si-based ligands derived from picoline, which broadened the substrate scope reported by Maleczka, enabling the application of N–Me borylation to a wider range of amides (Figure *42*, **C**).[93]

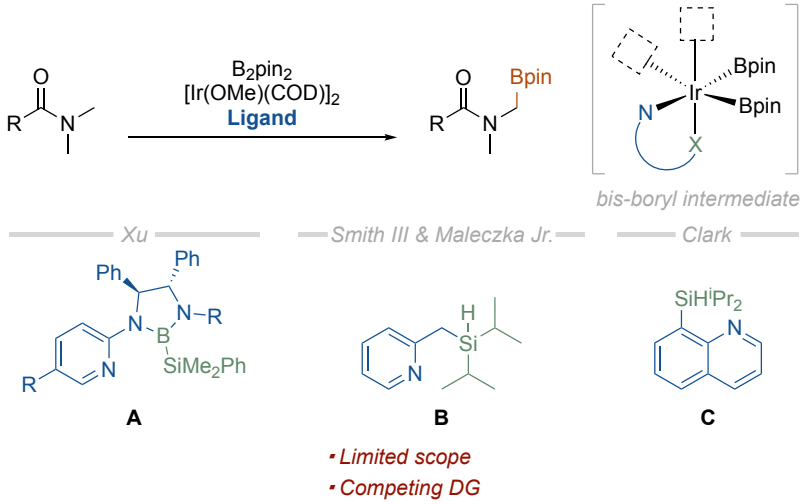



**Figure *42*** Previous research on C($sp^3$)-H borylations of *N*-methylamides.

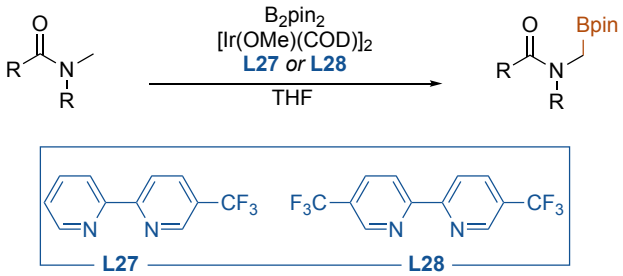
[130] a) Adams, J.; Behnke, M.; Chen, S.; Cruickshank, A. A.; Dick, L. R.; Grenier, L.; Klunder, J. M.; Ma, Y.; Plamondon, L.; Stein, R. L. *Bioorg. Med. Chem. Lett.* **1998,** *8,* 333–338., c) Hecker; Reddy; Totrov; Hirst; Lomovskaya; Griffith; King; Tsivkovski; Sun; Sabet; Tarazi; Clifton; Atkins; Raymond; Potts; Abendroth; Boyer; Loutit; Morgan; Durso; Dudley *J. Med. Chem.* **2015,** *58,* 3682–3692., b) Matteson, D. S. *Med. Res. Rev.,* **2007,** *28,* 233–246.

However, these efforts have been largely limited to a small set of tertiary amides, and present poor functional group tolerance. A critical element for the success of these N-methylamide borylations has been the use of monoanionic bidentate ligands (L–X), which lead to iridium bis-boryl intermediates. These intermediates create two vacant sites at the metal center: one for coordinating the carbonyl of the amide and the other for C–H activation.

As extensively discussed in the previous chapter, we have demonstrated that L–L-bipyridine-type ligands can facilitate the *ortho*-borylation of benzamides when $CF_3$ substituents are present at the 5-position. Our studies suggested that the *ortho*-regiocontrol in aromatic precursors originates from unusual non-covalent, dispersion interactions between the benzamide group of the substrate and the polarized ring(s) of the bipyridine ligand. Therefore, it was intriguing to know whether similar interactions could also be harnessed for promoting the borylation of C($sp^3$)–H bonds.

## 7.3.2 Objectives

In particular, we first aimed at the methyl borylation of non-aromatic alkylamides, as this would represent the first reported regioselective C–H borylation in alkylamides using an L–L type ligand. At the outset, we anticipated that the borylation would occur at the N-methyl group, but it was not clear if the any of the previously prepared ligands could lead to sufficiently reactive iridium catalysts, and which would be the selectivity of the processes.




**Scheme *74*** Objective for the $sp^3$ borylation of N-Me alkylamides.

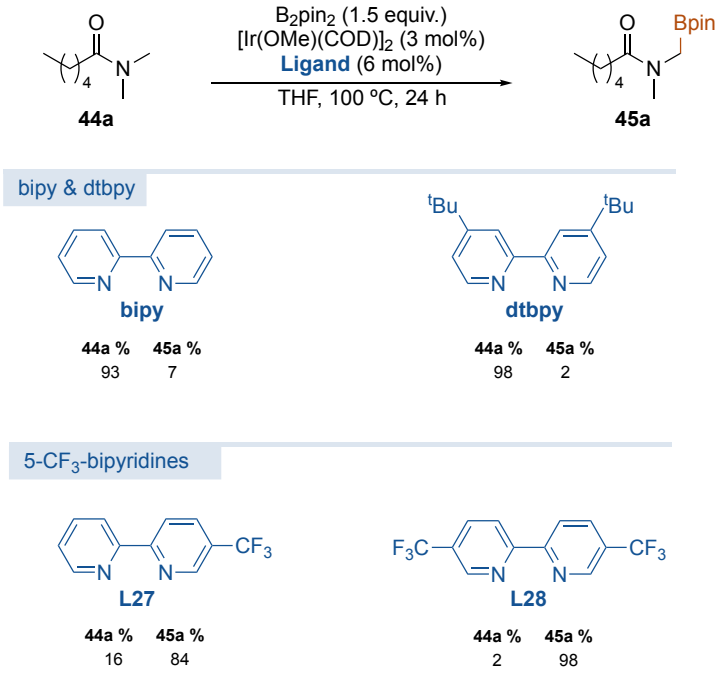
## 7.3.3 Results and discussion

### *7.3.3.1 Reaction discovery, optimization and scope*

The investigation began with a screening of our library of bipyridine ligands for the borylation of N,N-dimethylhexanamide (**44a**), to assess their effectiveness in promoting the reaction.

As anticipated, heating hexanamide **44a** at 100 °C in presence of catalytic amounts of $[Ir(OMe)COD]_2$, $B_2pin_2$ as the boron source, and the common ligands **bipy** or **dtbpy**, resulted in very low conversion to the desired product **45a**, with starting material to product ratios of 93:7 and 98:2 respectively (Scheme 75).

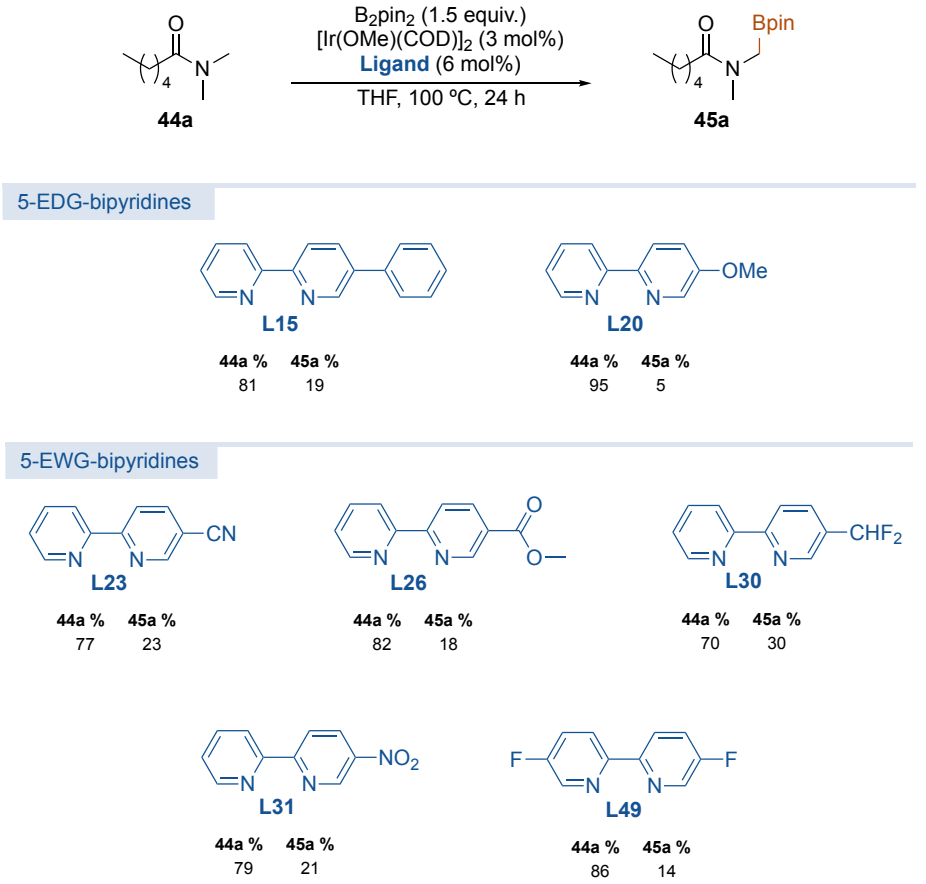
Gratifyingly, using our previous privileged ligand, **L27** resulted in a substantial increase in the desired reactivity. It yielded the α-amidomethylboronate ester **45a** with a 16/84 ratio of **44a** to **45a**. The symmetrical disubstituted ligand, **L28,** exhibited even greater reactivity, providing a 2/98 ratio of **44a** to **45a** overnight, and leading to a 96% isolated yield of **45a** (Scheme 75).




**Scheme 75** Ligand screening for the catalytic borylation of alkyl CH bonds. Note: Ratio of starting material and product was analyzed by GC-MS.

At this point it was pertinent to screen other ligands to know if the presence of $CF_3$ groups in 5 position of pyridines was essential for the observed reactivity, so to get further insight into the reaction we tested several bipyridine ligands. 2.2'-bipyridine ligands with an EDG at the 5-position such as a 5-phenyl substituent (**L15**) gave a 81:19 ratio of starting material and borylated product, while with a -OMe group (**L20**) we observed loss of reactivity (95:5 ratio) (Scheme 76).

Ligands with EWG substituents such as -CN (**L23**), $CO_2Me$ (**L26**), $CHF_2$ (**L30**) and -$NO_2$ (**L31**) at the 5-position led to 20-30% of the borylated product. A 5,5'-difluorobipyridine also yielded moderate conversion, with a 86:14 ratio of starting material to product (**L49**) (Scheme 76).



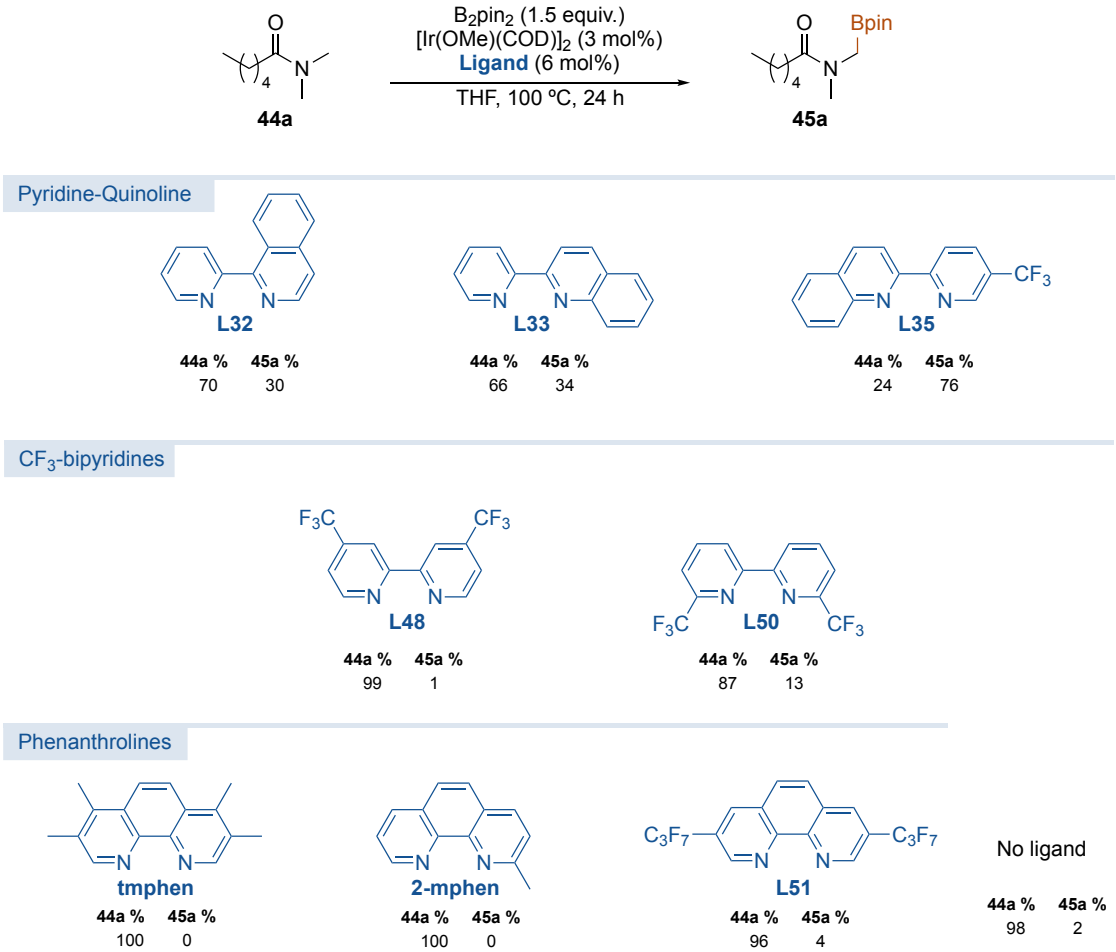

**Scheme 76** 5- substituted bipyridine ligand screening for the catalytic borylation of alkyl CH bonds. Note: Ratio of starting material and product was analyzed by GC-MS.

Quinoline-pyridine ligands like **L32** and **L33** led to moderate yields of approximately 30%. Gratifyingly, incorporating a -$CF_3$ group at the 5 position of the pyridine ring (**L35**) improved the yield significantly, with a 76% conversion to the expected product (Scheme 77).

More significantly, as in the case of the aromatic borylations, shifting the $CF_3$ substitution to other positions of the bipyridine such as 4- (**L48**) or 6- (**L50**) positions did not improve the ratio between starting material and borylated product compared to the unsubstituted **bipy** (Scheme 77).

Finally, we also evaluated phenanthroline ligands, such as **tmphen**, **2-mphen**, and **L51** which have been successful in hydrocarbon borylation reactions.[88, 90] Surprisingly, no conversion was observed in our system, and instead, by-products from the borylation of THF were detected by GC-MS. We also confirmed that the presence of a ligand is essential for the reaction, as no conversion was observed in the absence of a ligand (Scheme 77).

USC UNIVERSIDADE DE SANTIAGO DE COMPOSTELA

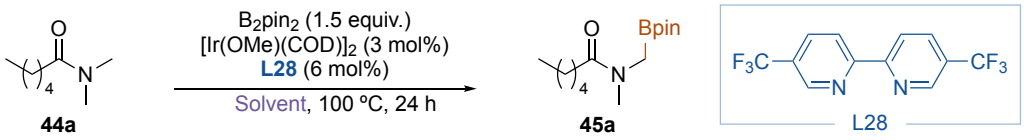



**Scheme 77** Ligand screening for the catalytic borylation of alkyl CH bonds. Note: Ratio of starting material and product was analyzed by GC-MS.

A solvent screening using the best-performing ligand (**L28**) indicated that ethereal solvents, particularly THF, were optimal for achieving higher conversions. In contrast, strongly coordinating solvents such as NMP or MeCN failed to promote any measurable conversion (Table *21*).

USC UNIVERSIDADE DE SANTIAGO DE COMPOSTELA

**Table *21*** Solvent screening for the borylation of **44a** using **L28** as ligand.




| Solvent | Ratio 44a:45a | Solvent | Ratio 44a:45a |
|---|---|---|---|
| THF | 0:100 | NMP | 100:0 |
| 2-MeTHF | 40:60 | *p*-Xylene | 31:69 |
| 1,2-DME | 37:63 | 1,2-DCE | 100:0 |
| 2,2,4-Trimethylpentane | 10:90 | 1,4-Dioxane | 81:19 |
| Methyl-$^{t}$Butylether | 0:100 | MeCN | 100:0 |
| 1,3-Dioxolane | 83:17 | Heptane | 16:84 |
| Cyclopentyl-Methylether | 35:65 | Decahydronaphtalene | 5:95 |
| Cyclooctane | 36:64 | Isopropylcyclohexane | 6:94 |
| Di-$^{n}$Butylether | 4:96 | $^{t}$Butylcyclohexane | 10:90 |
| $^{t}$Amyl-Methylether | 0:100 | | |

Note: Ratio of starting material and product was analyzed by GC-MS.

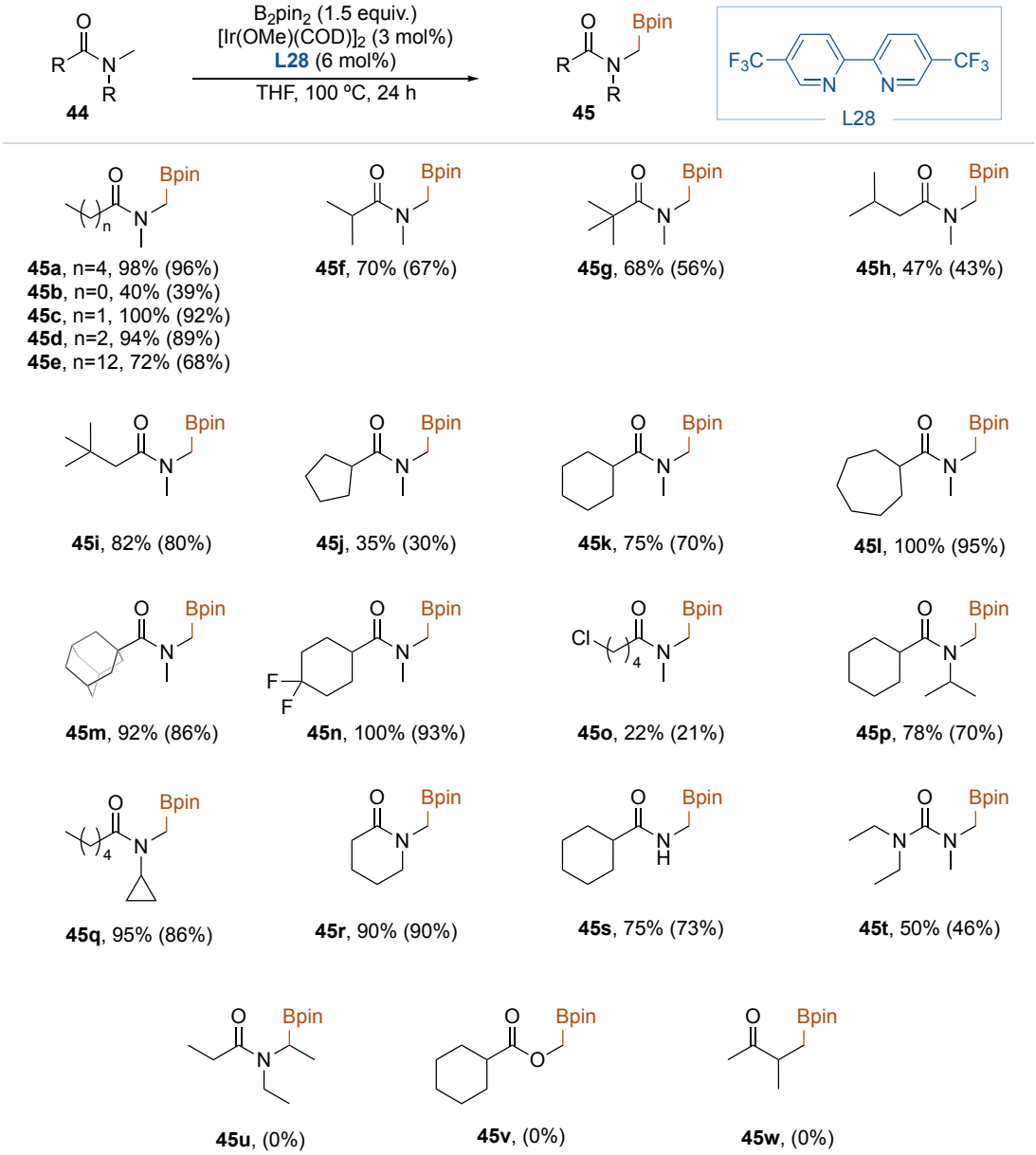
In summary, the screening process revealed that the most effective system encompasses Ir(OMe)(COD)]$_2$ (3 mol%), **L28** (6 mol%), 1.5 equivalents of $B_2pin_2$, and 1 equivalent of the N-methylamide substrate in THF (0.2 M). While initial reactions were conducted over 24 h, we later found that under optimal conditions, full conversion is achieved within 4 h. Using these optimal conditions, we were able to isolate the desired borylated amide **45a** in 96% yield.

With the optimized conditions in hand, we investigated the scope of the reaction. Gratifyingly, a wide range of N-methylamides successfully participated in the process, exhibiting excellent regioselectivity to yield monoborylated N-methyl products (Scheme *78*). The reaction proved effective across substrates with varying alkyl chain lengths, so that products **45a-45e** (**45e** being a myristic acid derivative) were obtained with moderate to good yields. Furthermore, the introduction of diverse bulky groups did not compromise the reaction's efficiency, as demonstrated by the successful synthesis of **45f-45i**, highlighting the steric tolerance of the reaction.

The selective formation of **45f** is particularly significant, as the precursor presents two topologically similar methyl groups, yet only the N–Me undergoes borylation. This result is in consonance with a computational calculation using IEFPCM$_{THF}$/M06/6-311G(2d,p)+SDD(Ir)//M06/6 31G(d) +LANL2DZ(Ir) at 25 °C , on the energetic requirements of the C–H oxidative addition either at the terminal -Me group and at the N–Me position. This study, included in the supporting information, revealed that the activation of the N–Me group is favored by 3.5 kcal mol$^{-1}$.

The reaction seamlessly accommodated cyclic alkyl amides of various ring sizes, ranging from 5 to 7 members, including adamantane (**45j**-**45m**). Notably, the borylation

process demonstrates a tolerance for halogens, as evidenced by the successful synthesis of **45n** and **45o** without any significant side-reaction. In substrates where both a methyl group and a distinct alkyl group were present as amide substituents, the catalyst exhibited remarkable regioselectivity towards the N-methyl position, as demonstrated in the synthesis of the isopropyl derivative **45p** or the cyclopropyl **45q**. Furthermore, cyclic amides, were also effective substrates, exemplified in the synthesis of the 6-membered methyl borylated lactam **45r**.




**Scheme *78*** Scope in the borylation of a variety of N-methylamides using ligand **L28**.Note: $^1$H-NMR yield using $CH_2Br_2$ as IS, isolated yields reported in parentheses.

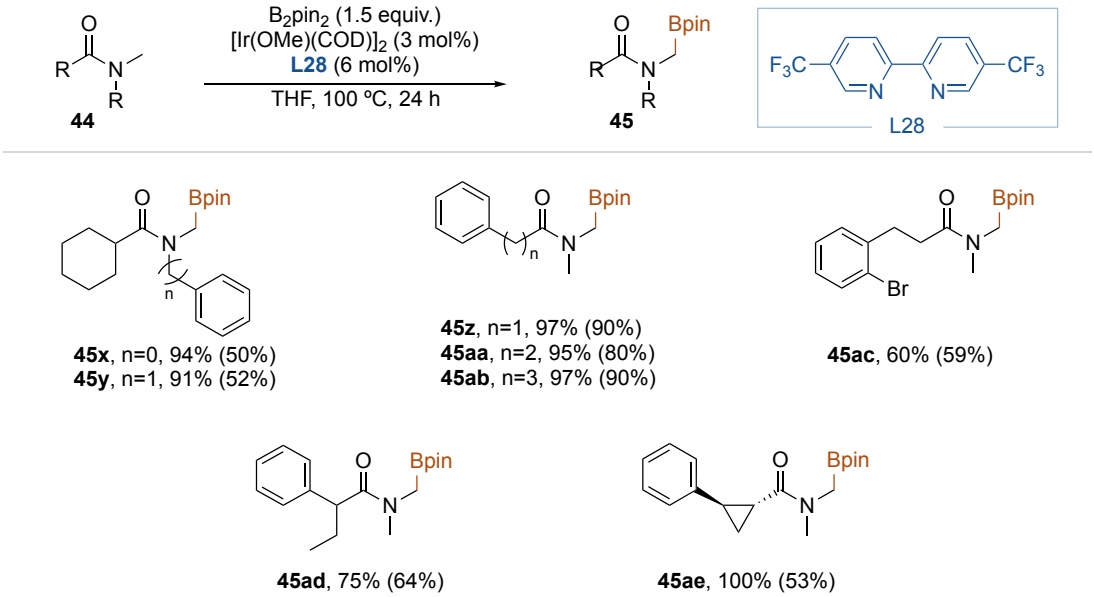
The robustness of the reaction was further demonstrated by its successful extension to secondary amides, with cyclohexylamide **45s** being obtained in good yield. Similarly, the borylated urea derivative **45t** was obtained with satisfactory yields, and

notably, no borylated side-products were observed in the ethyl substituents of the urea (Scheme *78*).

However, several substrates exhibited no observable reactivity under the optimized conditions. Specifically, attempts to activate methylene bonds to give product **45u** were unsuccessful, resulting in the recovery of the starting material. This lack of reactivity can be attributed to the higher BDE of the C–H bond in N–ethyl vs. N–methyl groups. This was corroborated by computational experiments in which the calculated activation energy for the activation of **44u** was 2 kcal $mol^{-1}$ higher than the energy required for the C–H activation of **44a** (See experimental section). Similar outcomes were observed with other carbonyl-containing moieties, such as esters or ketones were no formation of products **45v** and **45w** was detected.

Considering the well-established activity of iridium-based borylation catalysts towards C($sp^2$)–H bonds, we were prompted to evaluate the chemoselectivity of the process in the presence of aromatic rings. Gratifyingly, we observed an exceptional level of selectivity towards the N-methyl position in a variety of precursors equipped with aryl rings. Both N-phenylmethyl and N-benzylmethyl amides underwent successful borylation, yielding exclusively the corresponding products **45x** and **5y**. Aromatic rings could be incorporated into the alkyl chain, even when bearing halogen substituents, resulting in the synthesis of products **45z**-**45ad** in excellent yields (Scheme *79*).

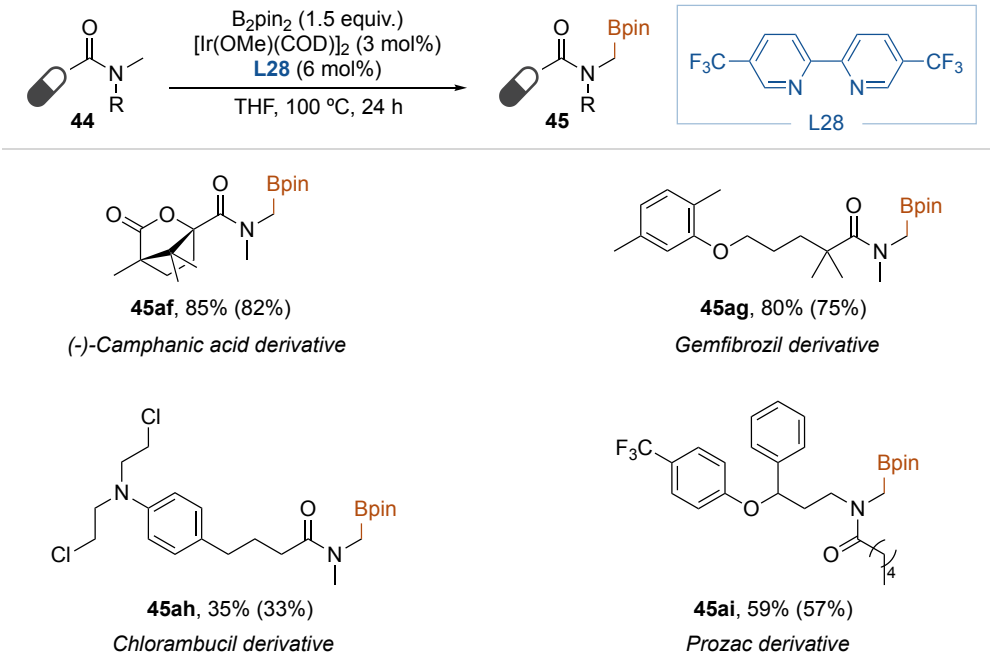
The catalytic system also demonstrated remarkable tolerance towards strained cycles, such as cyclopropanes, resulting in the successful synthesis of product **45ae**.




**Scheme *79*** Borylation of N-methylamides containing aromatic moieties. Note: $^1$H-NMR yield using $CH_2Br_2$ as IS, isolated yields reported in parentheses.

Substrates with more complex structures, such as those depicted in Scheme *80*, were borylated with exceptional yields, leading to the expected borylated derivatives of

several established bioactive compounds (**45af**-**45ai**). This highlights the versatility of the reaction and underscores its significant potential for broad application in medicinal chemistry.




**Scheme *80*** Borylation of more complex substrates. Note: $^{1}$H-NMR yield using $CH_2Br_2$ as IS, isolated yield reported in parentheses.

### *7.3.3.2 Mechanistic insights*

Once we established the broad scope of the reaction, it became essential to gain insights into the origin of the enhanced reactivity observed with ligand **L28**. Towards this end, we conducted a comprehensive quantum mechanical analysis of the reaction mechanism.

We focused on the borylation reaction of N,N-dimethylhexylamide (**44a**), using both the standard 2,2'-bipyridine ligand and the 5-$CF_3$-bipyridine ligands (**L27** and **L28**). This model substrate was chosen to closely represent the catalytic system used in our experimental optimization studies. However, the use of an aliphatic chain introduced additional complexity due to the large number of conformers and rotamers that the chain can adopt.

To address this complexity and evaluate as many structures as possible, we utilized a Conformer–Rotamer Ensemble Sampling Tool (CREST). CREST allowed us to generate, sort, and rank all the possible conformers and rotamers efficiently. Once the ensemble of structures was obtained, we optimized the geometries using Gaussian16 to identify the final stationary points, ensuring that we captured the low-energy conformations relevant to the reaction mechanism (Figure *43*).

USC UNIVERSIDADE DE SANTIAGO DE COMPOSTELA

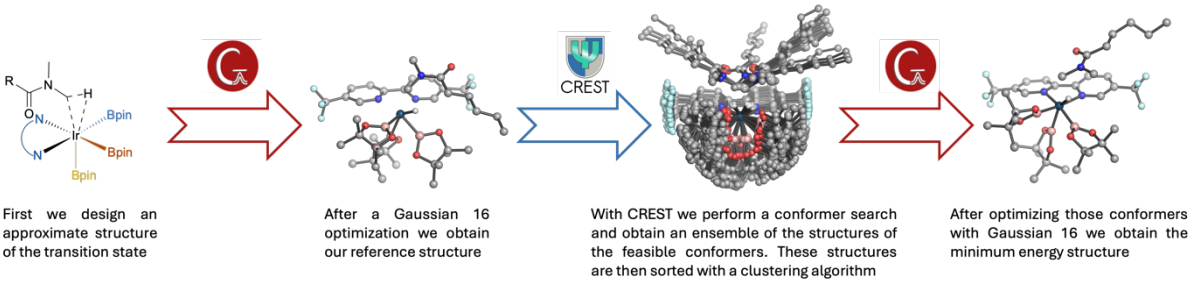



**Figure *43*** Workflow for conformational sampling and posterior optimization of conformers using CREST and Gaussian 16.

Using this methodology for each stationary point, we ensured the calculation of the minimum energy pathway for the C–H borylation reaction. We computed the energy profiles for the reaction using **bipy** and our key trifluoromethylated ligands **L27** and **L28** as reference ligands, with N,N-dimethylhexanamide serving as the model substrate. Several theory levels were employed, however, at this initial stage of the discussion, we will focus on the results obtained with IEFPCM$_{THF}$/M06/6-311G(2d,p)+SDD(Ir)//M06/6 31G(d) +LANL2DZ(Ir) at 25 °C.

Like in the previous project, we first considered the possibility that the better reactivity observed with 5-$CF_3$ ligands could be attributed to the reaction proceeding through an alternative mechanism to the classical Ir(III)/Ir(V) cycle. One hypothesis we considered was the involvement of an Ir(I)/Ir(III) cycle. However, this pathway was quickly dismissed due to the high energy required to access the Ir(I) intermediate, which is primarily due to the highly unfavorable release of $B_2pin_2$ from the 16-electron active catalyst (Figure *44*, formation of Ir(Bpin) intermediate).

Another alternative mechanism we explored is the decoordination of one pyridine ring from the bipyridine ligand, followed by rollover cyclometalation to form a C–N bidentate ligand. However, this pathway was quickly discarded based on the NMR and HRMS experiments described earlier in Figure *34*. These experiments indicated that the Ir and the **L28** ligand are coordinated via the N atoms of the ligand and no cyclometalation was observed even when $B_2pin_2$ was added.

Additionally, the cyclometalation step for this possible pathway presented significantly high activation energies (Figure *44*). Moreover, the energy barriers for decoordination of one of the pyridine moieties was similar for both ligands **bipy** and **L28**, indicating that this process is not the source of the increased reactivity observed with **L28**. The pathway with **bipy** is detailed in the experimental section.

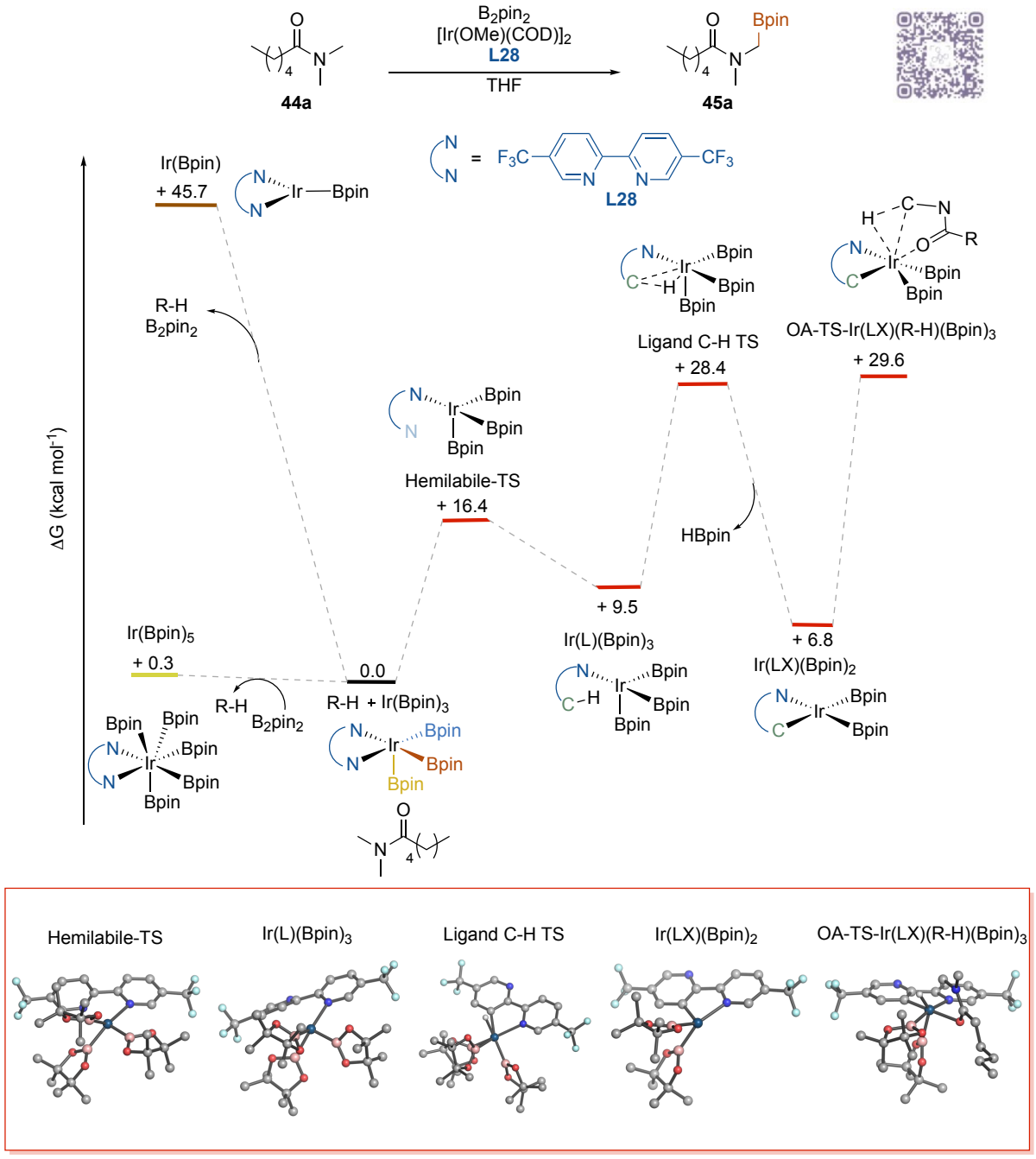



**Figure *44*** Minimum energy pathways (MEP) calculated with IEF-PCM$_{THF}$/M06/6-311G(2d,p)+SDD(Ir)//M06/6-31G(d)+LANL2DZ(Ir) for the oxidative addition step between *N*,*N*-dimethylhexylamide (**44a**) and Ir$^{III}$(**L28**)(Bpin)$_3$. Several mechanisms are compared: the canonical Ir(III) → Ir(V) involving a 16 e$^-$ active catalyst (Ir(Bpin)$_3$), an alternative Ir(I) → Ir(III) mechanism involving a 14 e$^-$ active catalyst (Ir(Bpin)) after $B_2pin_2$ cleavage and a mechanism involving the de-coordination of one pyridine ring followed via a rollover cyclometalation to form a L–X ligand which would be the active catalyst (Ir(LX)(Bpin)$_2$) in this scenario. Free energies relative to (Ir(Bpin)$_3$+R–H) ($\Delta G_{QH}$ in kcal mol$^{-1}$). Non-reactive hydrogens have been omitted for clarity. To see an interactive model of the calculated structures visit https://danielmarcosatanes.github.io/DMA_thesis-viewer/ or scan the QR code.

To gain deeper insights into the factors contributing to the enhanced reactivity of **L28** we computed the energy diagram for the reaction of **44a** and compared it with that obtained by using **bipy** and **L27**.

The profile of the endergonic oxidative addition step using **L28** and **bipy** is depicted in Figure *45*. The energy barriers for this step varied among the ligands, aligning with the experimental evidence. The more favorable C–H activation occurred when using **L28** as the ligand ($\Delta G^{\ddagger}$ of 24.3 kcal $mol^{-1}$), followed by **L27** ($\Delta G^{\ddagger}$ of 26.6 kcal $mol^{-1}$), and the least favorable reaction with **bipy** ($\Delta G^{\ddagger}$ of 27.3 kcal $mol^{-1}$). Although the differences are not high, qualitatively they fit well with the reactivity trend observed.

USC
UNIVERSIDADE DE SANTIAGO DE COMPOSTELA

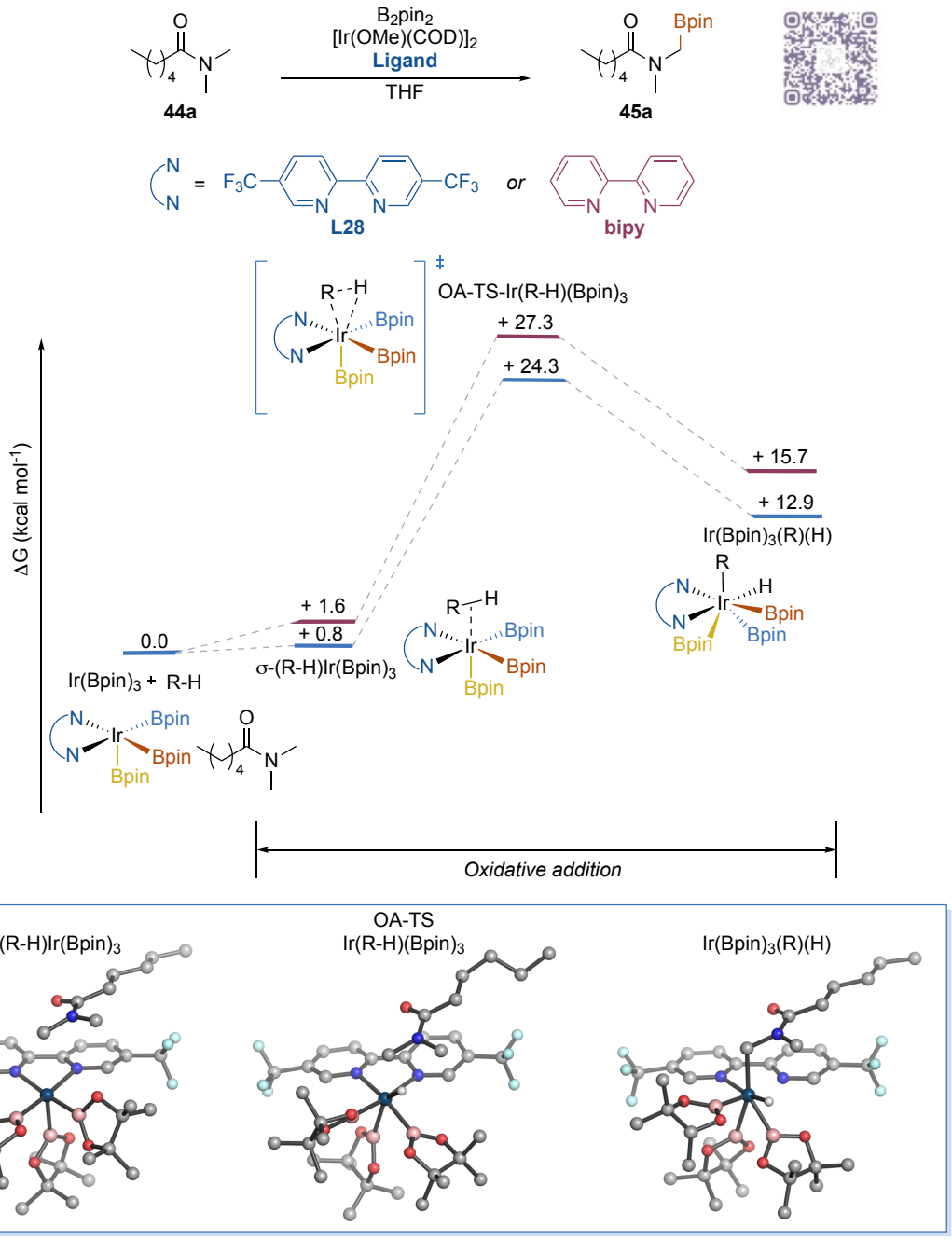



**Figure** ***45*** Minimum energy pathways (MEP) calculated with IEF-PCM$_{THF}$/M06/6-311G(2d,p)+SDD(Ir)//M06/6-31G(d)+LANL2DZ(Ir) for the oxidative addition step of *N*,*N*-dimethylhexylamide (**44a**) to Ir$^{III}$(**L28**)(Bpin)$_3$ (blue lines)or Ir$^{III}$(**bipy**)(Bpin)$_3$ (purple lines). Free energies relative to each lowest energy structure (Ir(Bpin)$_3$+R–H) ($\Delta G_{QH}$ in kcal mol$^{-1}$). Non-reactive hydrogens have been omitted for clarity. The calculated activation energy for the C–H activation is 3 kcal mol$^{-1}$ higher when using **bipy** as a ligand compared to **L28**, ($\Delta G^{\ddagger}_{bipy}$=27.3 kcal mol$^{-}$1 vs $\Delta G^{\ddagger}_{L28}$=24.3 kcal mol$^{-1}$). To see an interactive model of the calculated structures visit https://danielmarcosatanes.github.io/DMA_thesis-viewer/ or scan the QR code.

The intermediate resulting from this OA step can evolve to the product in different ways. Initially, we explored the feasibility of a direct reductive elimination from the intermediate Ir(Bpin)$_3$(R)(H) obtained above, with ligand **L28**. However, this pathway was

calculated to have a substantial intrinsic activation barrier of around 19 kcal mol$^{-1}$ [RE-TS-Ir(Bpin)$_3$(R)(H)], with a transition state located 32.3 kcal mol$^{-1}$ above the starting reactants

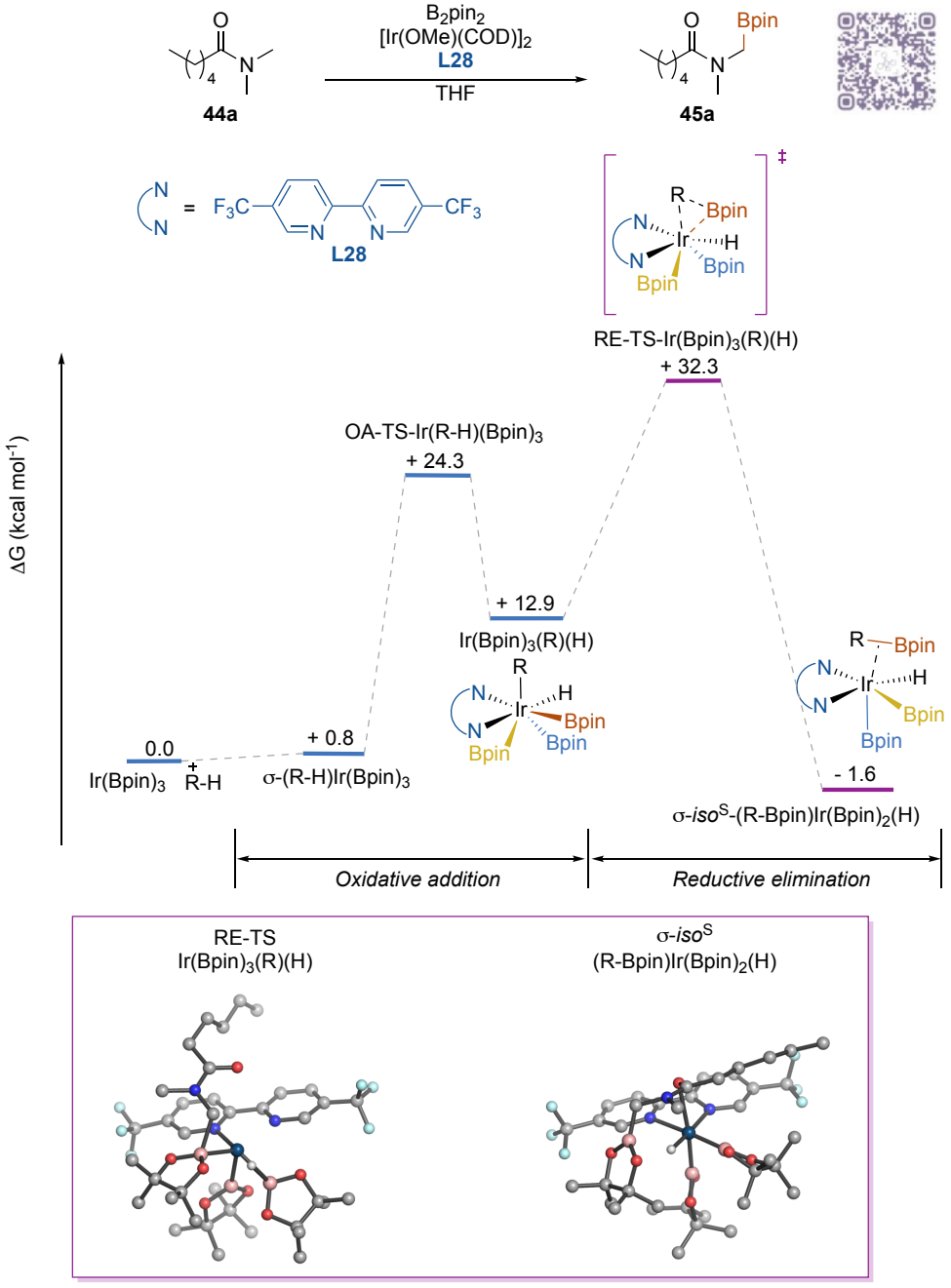



**Figure *46*** Minimum energy pathways (MEP) calculated with IEF-PCM$_{THF}$/M06/6-311G(2d,p)+SDD(Ir)//M06/6-31G(d)+LANL2DZ(Ir) for the direct reductive elimination step from intermediate Ir(Bpin)$_3$(R)(H). Free energies relative to structure (Ir(Bpin)$_3$+R–H) ($\Delta G_{QH}$ in kcal mol$^{-1}$). Non-reactive hydrogens have been omitted for clarity. To see an interactive model of the calculated structures visit https://danielmarcosatanes.github.io/DMA_thesis-viewer/ or scan the QR code.

This high energy barrier raised doubts on whether the turnover-limiting step of the reaction would be the OA or the RE, therefore we performed an experimental calculation of the KIE.

Parallel competition experiments with **44a** and its deuterated equivalent, determining a KIE value of 1.9, which is in line with previously reported values for similar C($sp^3$)–H activations and suggests that the C–H activation is the turnover limiting step (Figure *47*).[88]

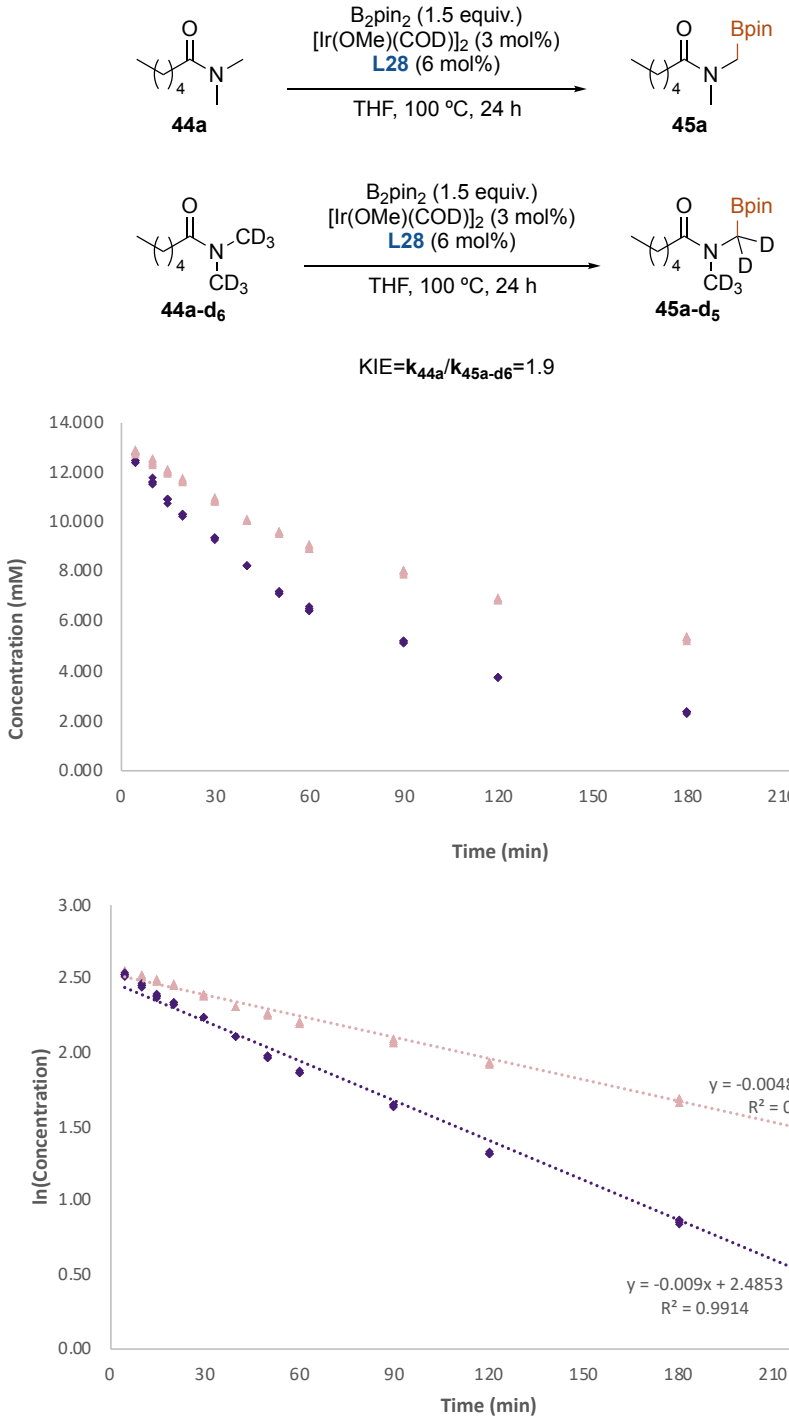



**Figure *47*** Kinetic isotope effect (KIE) determined from parallel reactions of substrates **44a** and **44a-$d_6$** Reaction of **44a** (purple markers) or **44a-$d_6$** (pink markers) and $B_2pin_2$ catalyzed by the combination of $[Ir(OMe)(COD)]_2$ and 5,5'-bis-$CF_3$-bipyridine ligand **L28**.

Given this experimental evidence, we assessed alternative computational pathways after the oxidative addition step, drawing inspiration from isomerization processes proposed in computational studies of related borylations with other substrates and ligands.

One potential pathway involves an isomerization similar to that suggested by Hartwig's group, which entails a hydride migration via a pentagonal bipyramidal structure to give intermediate *isom*$^{H}$-TS-Ir(Bpin)$_3$(R)(H).[90] Such rearrangement places the hydrogen atom nearly coplanar with two boryl groups and the ligand, although at a significant energy cost ($\Delta G^{\ddagger}$= 30.5 kcal mol$^{-1}$) (Figure *48*).

USC
UNIVERSIDADE DE SANTIAGO DE COMPOSTELA

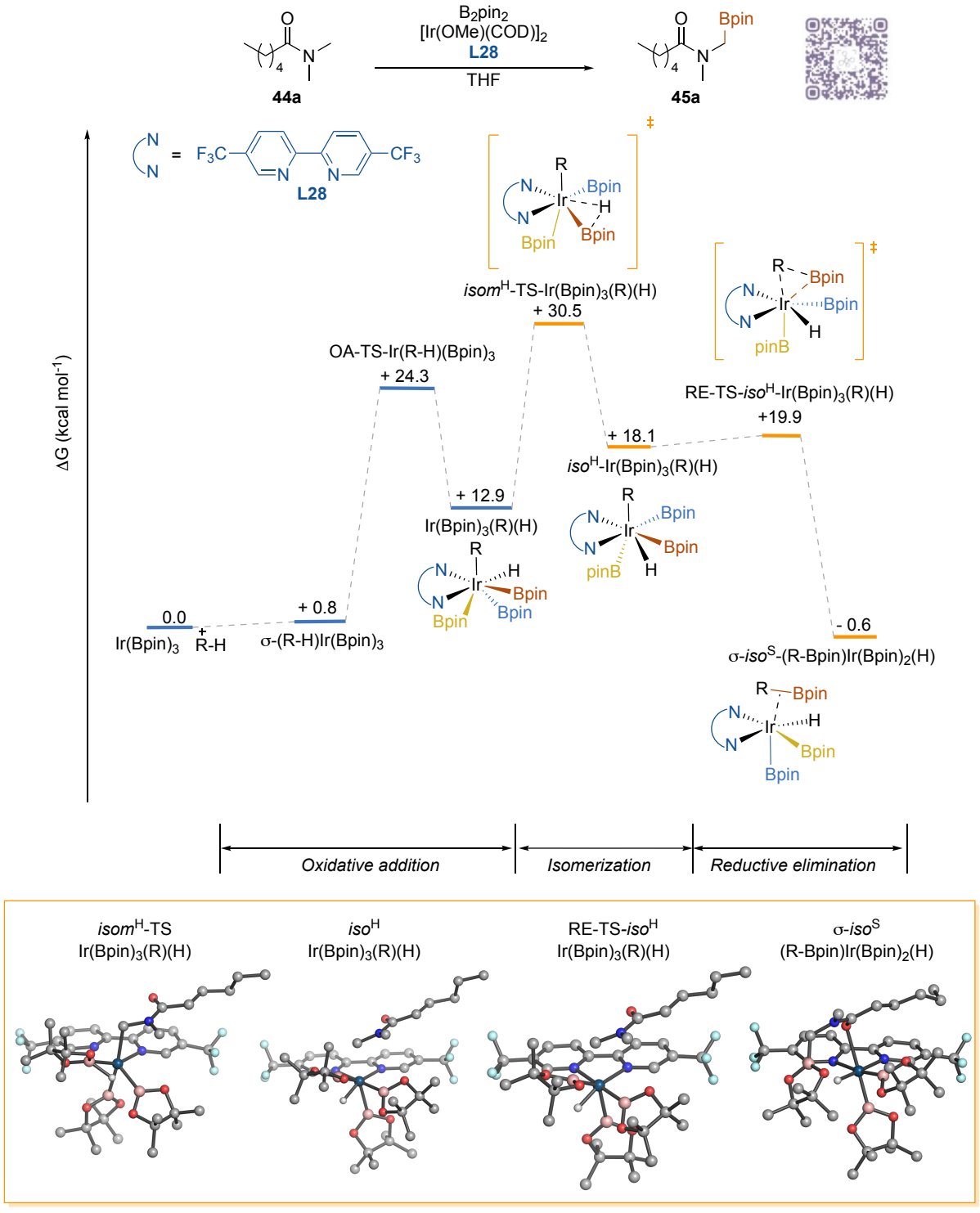



**Figure *48*** Minimum energy pathways (MEP) calculated with IEF-PCM$_{THF}$/M06/6-311G(2d,p)+SDD(Ir)//M06/6-31G(d)+LANL2DZ(Ir) for the isomerization pathway analogous to the one described by Hartwig and coworkers between *N*,*N*-dimethylhexylamide (**44a**) and Ir$^{III}$(**L28**)(Bpin)$_3$. Free energies relative to structure (Ir(Bpin)$_3$+R–H) ($\Delta G_{QH}$ in kcal mol$^{-1}$). Non-reactive hydrogens have been omitted for clarity. To see an interactive model of the calculated structures visit https://danielmarcosatanes.github.io/DMA_thesis-viewer/ or scan the QR code.

USC UNIVERSIDADE DE SANTIAGO DE COMPOSTELA

The high energy barrier for this isomerization prompted us to explore alternative pathways, so we investigated another isomerization pathway similar to the one proposed by Sakaki and colleagues in the borylation of THF.[131]

This pathway involves the repositioning of the two boryl groups situated below the ligand plane, and an alteration in the geometry of the complex, transitioning from one distorted pentagonal bipyramidal structure to another. In $Ir(Bpin)_3(R)(H)$, the axial positions of the pentagonal bipyramidal structure are occupied by one of the N atoms of the ligand and a boryl group (Bpin in orange in Figure *49*).

Conversely, in $iso^S$-$Ir(Bpin)_3(R)(H)$, the axial positions are taken up by the hydride ligand and the other N atom of the ligand. This isomerization exhibits by far the lowest activation energy ($\Delta G^{\ddagger}$= 19.9 kcal $mol^{-1}$) among the three possible pathways after the C–H activation, and yields a complex ($iso^S$-$Ir(Bpin)_3(R)(H)$,) that can undergo an easy reductive elimination via transition state RE-TS-$iso^S$-$Ir(Bpin)_3(R)(H)$.

USC UNIVERSIDADE DE SANTIAGO DE COMPOSTELA

[131] Zhong, R.; Sakaki, S. *J. Am. Chem. Soc.* **2019,** *141,* 9854–9866.

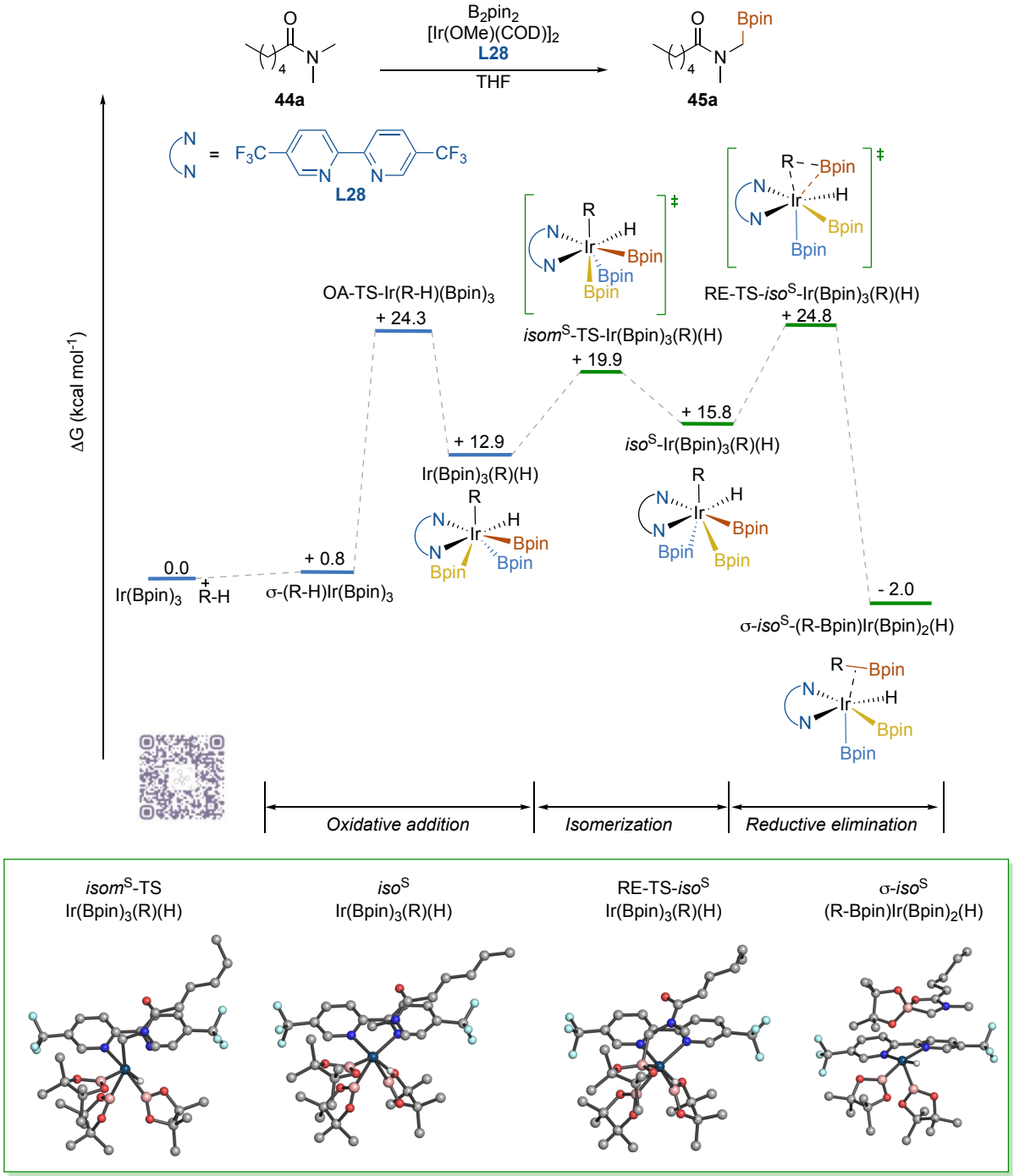






**Figure *49*** Minimum energy pathways (MEP) calculated with IEF-PCM$_{THF}$/M06/6-311G(2d,p)+SDD(Ir)//M06/6-31G(d)+LANL2DZ(Ir) for the isomerization pathway analogous to the one described by Sakaki and coworkers between *N*,*N*-dimethylhexylamide (**44a**) and Ir$^{III}$(**L28**)(Bpin)$_3$. Free energies relative to structure (Ir(Bpin)$_3$+R–H) ($\Delta G_{QH}$ in kcal mol$^{-1}$). Non-reactive hydrogens have been omitted for clarity. To see an interactive model of the calculated structures visit https://danielmarcosatanes.github.io/DMA_thesis-viewer/ or scan the QR code.

Ultimately, the catalyst undergoes turnover with $B_2pin_2$ to regenerate the Ir(Bpin)$_3$ complex, (see the whole pathway with ligand **L28** in Figure *50*). The whole profiles with ligands **bipy** and **L27** are depicted in Figure *51* and Figure *52*.

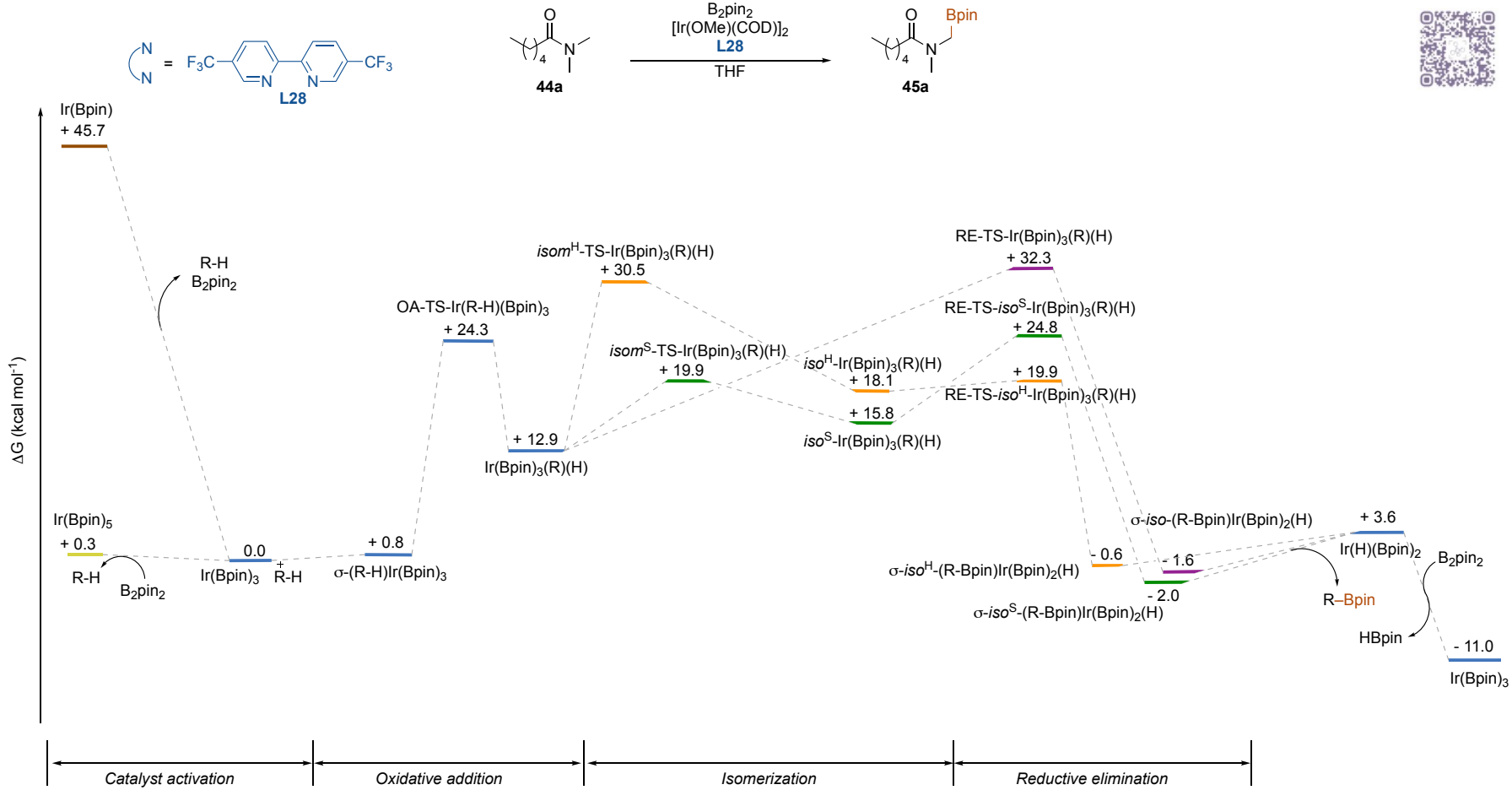



**Figure *50*** Minimum energy pathways (MEP) calculated with IEF-PCM$_{THF}$/M06/6-311G(2d,p)+SDD(Ir)//M06/6-31G(d)+LANL2DZ(Ir) for borylation reaction between *N*,*N*-dimethylhexylamide (**44a**) and Ir$^{III}$(**L28**)(Bpin)$_3$. Free energies relative to structure (Ir(Bpin)$_3$+R–H) ($\Delta G_{QH}$ in kcal mol$^{-1}$). To see an interactive model of the calcul ated structures visit https://danielmarcosatanes.github.io/DMA_thesis-viewer/ or scan the QR code.

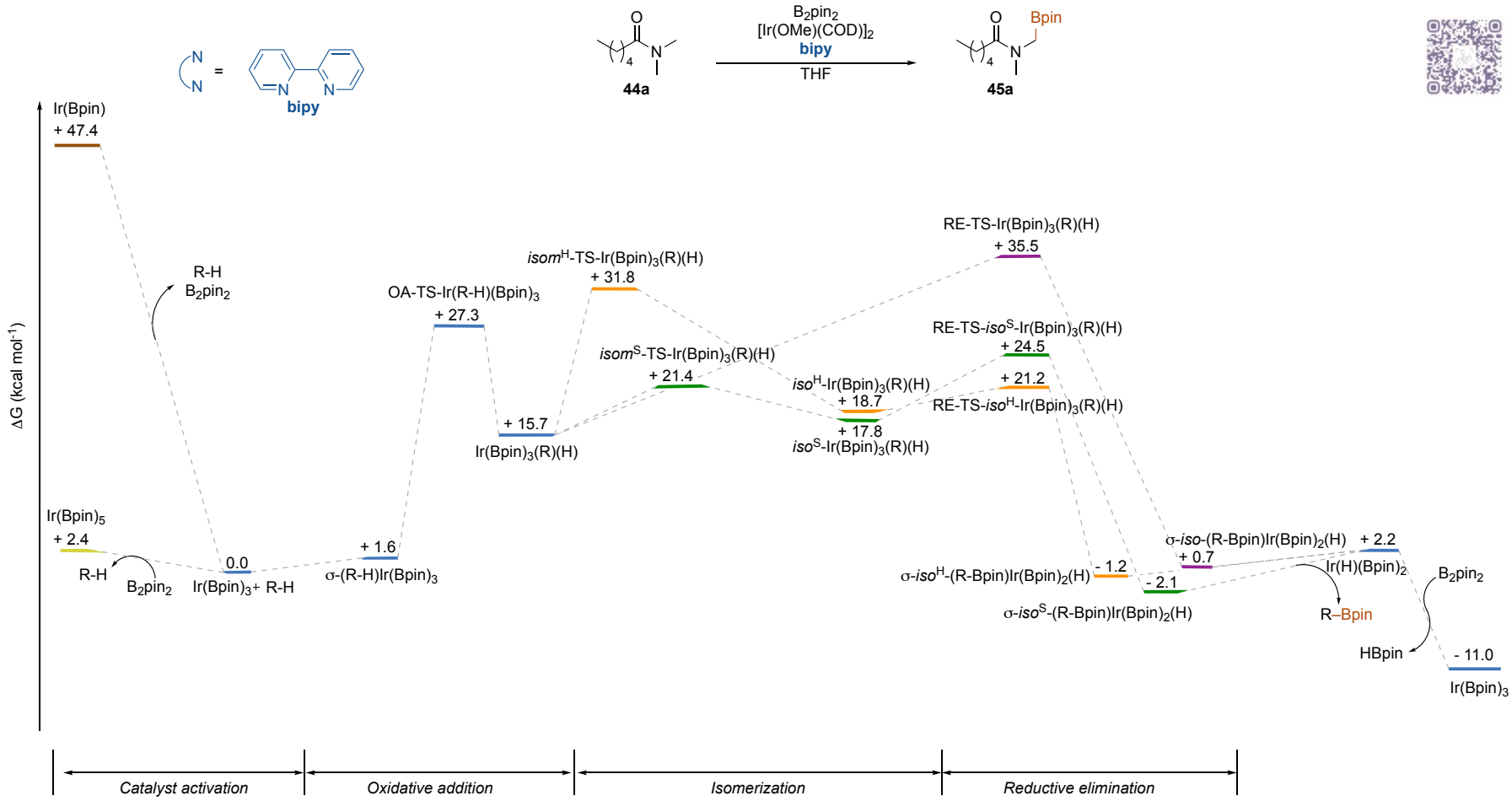



**Figure *51*** Minimum energy pathways (MEP) calculated with IEF-PCM$_{THF}$/M06/6-311G(2d,p)+SDD(Ir)//M06/6-31G(d)+LANL2DZ(Ir) for borylation reaction between *N*,*N*-dimethylhexylamide (**44a**) and Ir$^{III}$(**bipy**)(Bpin)$_3$. Free energies relative to structure (Ir(Bpin)$_3$+R–H) ($\Delta G_{QH}$ in kcal mol$^{-1}$). To see an interactive model of the calculated structures visit https://danielmarcosatanes.github.io/DMA_thesis-viewer/ or scan the QR code.

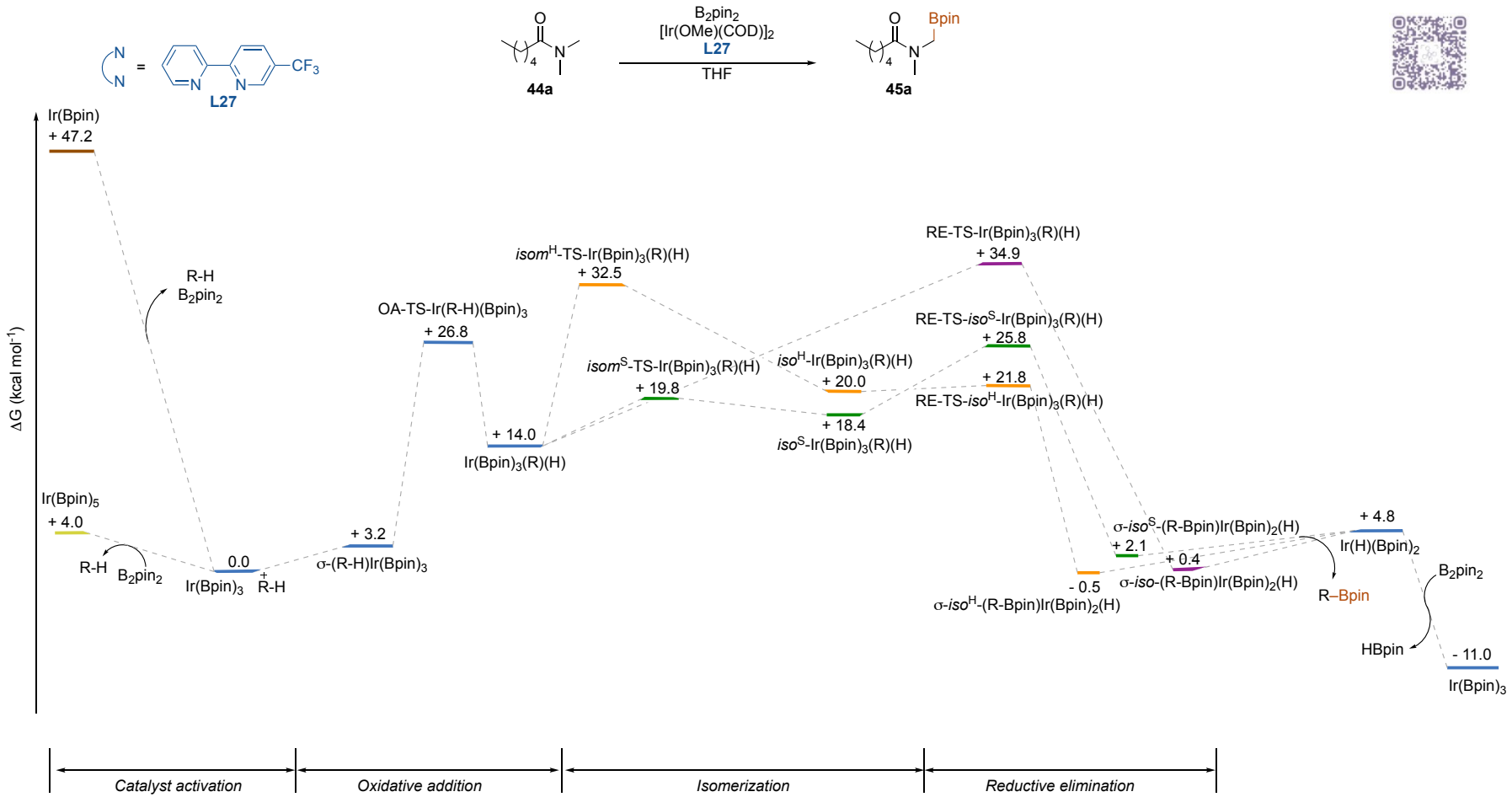



**Figure *52*** Minimum energy pathways (MEP) calculated with IEF-PCM$_{THF}$/M06/6-311G(2d,p)+SDD(Ir)//M06/6-31G(d)+LANL2DZ(Ir) for borylation reaction between *N*,*N*-dimethylhexylamide (**44a**) and Ir$^{III}$(**L27**)(Bpin)$_3$. Free energies relative to structure (Ir(Bpin)$_3$+R–H) ($\Delta G_{QH}$ in kcal mol$^{-1}$). To see an interactive model of the calculated structures visit https://danielmarcosatanes.github.io/DMA_thesis-viewer/ or scan the QR code.

To further validate this computational study, we calculated a similar reaction profile using the conformationally less problematic substrate N,N-dimethylpropylamide (**44c**). The results were com*para*ble to those obtained with N,N-dimethylhexanamide (**44a**), particularly in terms of the activation barriers for the various reaction steps (Figure *53* and Figure *54*). This consistency across different substrates further supports the conclusion that the enhanced reactivity observed with the 5-$CF_3$ ligand (**L28**) can be attributed to a lower activation barrier for the C–H activation step.

USC
UNIVERSIDADE DE SANTIAGO DE COMPOSTELA

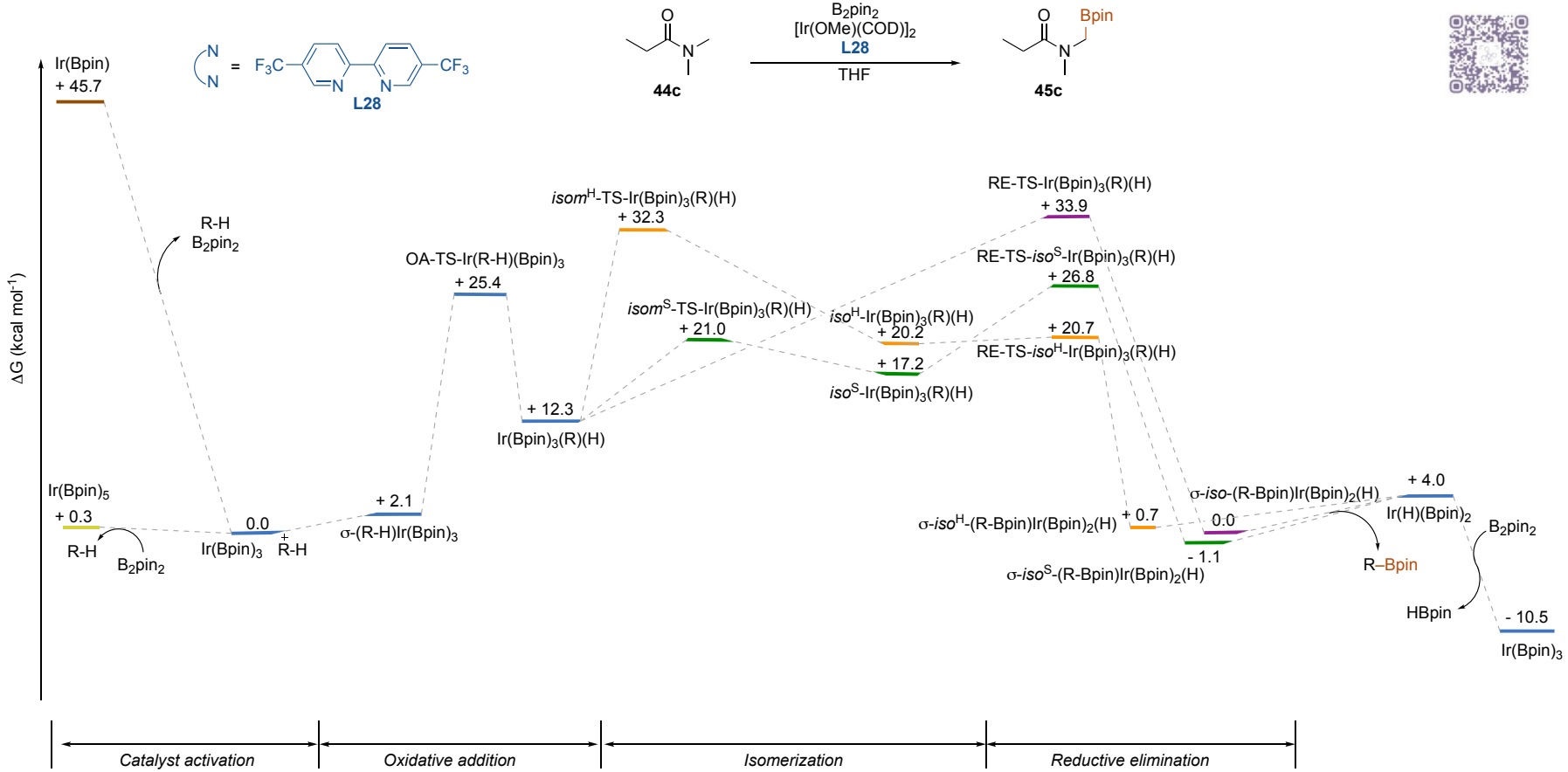



**Figure *53*** Minimum energy pathways (MEP) calculated with IEF-PCM$_{THF}$/M06/6-311G(2d,p)+SDD(Ir)//M06/6-31G(d)+LANL2DZ(Ir) for borylation reaction between *N*,*N*-dimethylhexylamide (**44c**) and Ir$^{III}$(**L28**)(Bpin)$_3$. Free energies relative to structure (Ir(Bpin)$_3$+R–H) ($\Delta G_{QH}$ in kcal mol$^{-1}$). To see an interactive model of the calculated structures visit https://danielmarcosatanes.github.io/DMA_thesis-viewer/ or scan the QR code.

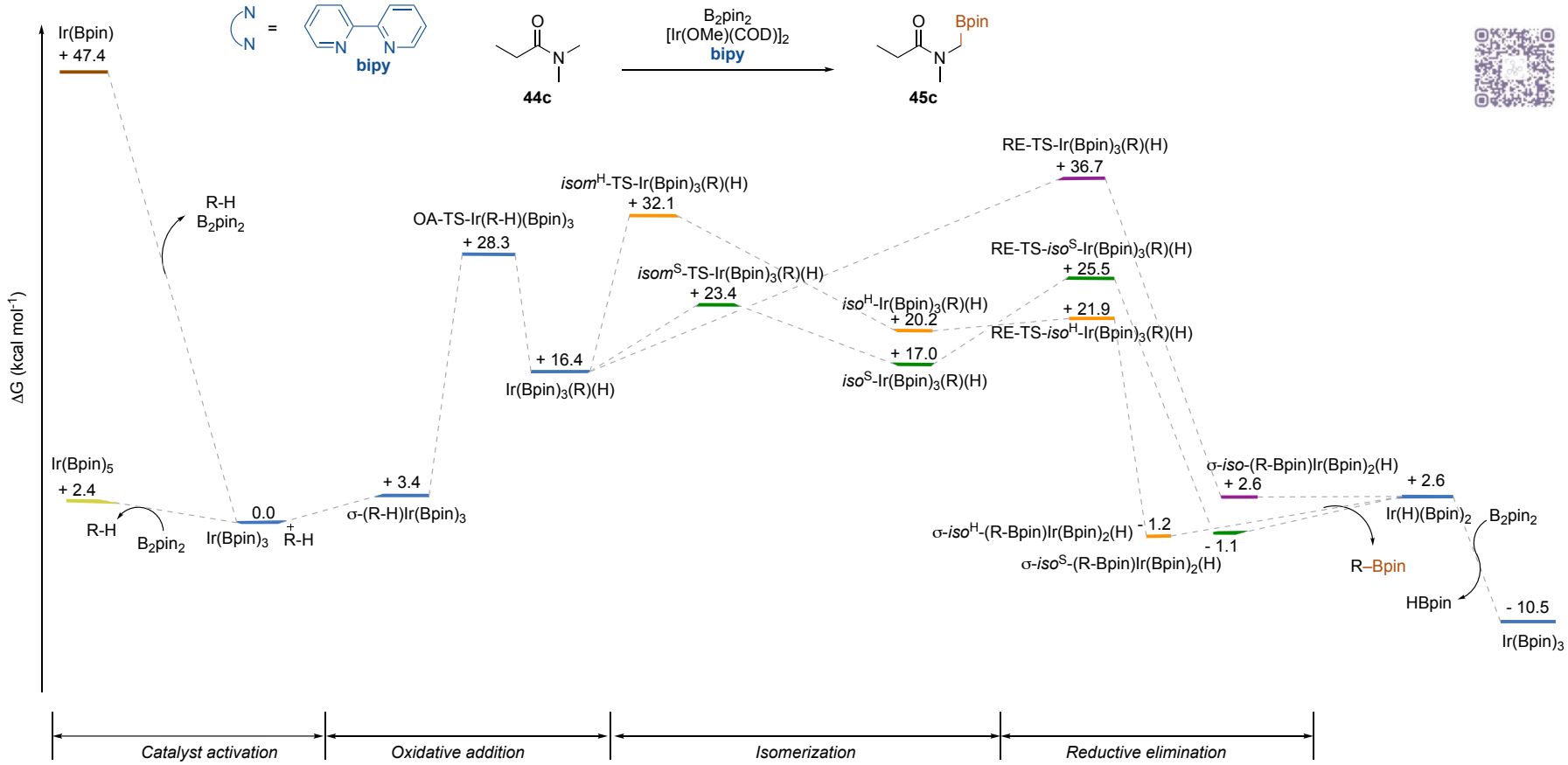



**Figure *54*** Minimum energy pathways (MEP) calculated with IEF-PCM$_{THF}$/M06/6-311G(2d,p)+SDD(Ir)//M06/6-31G(d)+LANL2DZ(Ir) for borylation reaction between *N*,*N*-dimethylhexylamide (**44c**) and Ir$^{III}$(**bipy**)(Bpin)$_3$. Free energies relative to structure (Ir(Bpin)$_3$+R–H) ($\Delta G_{QH}$ in kcal mol$^{-1}$). To see an interactive model of the calculated structures visit https://danielmarcosatanes.github.io/DMA_thesis-viewer/ or scan the QR code.

Overall, the calculations indicate the differences in reactivity when using bis-$CF_3$ ligand **L28** or **bipy** stem from the C–H activation step. These differences cannot be solely attributed to the electronic effects of the trifluoromethyl groups as other $CF_3$ containing ligands, such as **L48** and **L50**, exhibited low conversions.

A close inspection of the transition state structures with ligands **bipy** and **L28** reveals notable geometric distinctions. The more distinctive feature pertains to the orientation of the carbonyl moiety of the amide. In the lowest-energy conformer of the transition state with **bipy**, the carbonyl is oriented toward one of the boryl groups and away from the ligand. Conversely, with **L28**, the carbonyl is positioned above one of the pyridine rings of the ligand, in a conformation similar to that previously reported by our group for the *ortho*-borylation of benzamides.[132]

This strongly implies that outer-sphere interactions between the substrate and the ligand in the oxidative addition transition state play a pivotal role, facilitating the reaction when employing **L28**. In collaboration with the group of Dr. Gonzalo Jiménez Osés, we performed a non-covalent interaction analysis (NCIPLOT)[116] (Figure *55*) which unveiled an extended network of attractive interactions between the carbonyl group of the alkyl amide and the $CF_3$-pyridine ring of ligand **L28**. In contrast, the analysis of the transition state with **bipy** revealed minimal interaction between substrate and ligand.

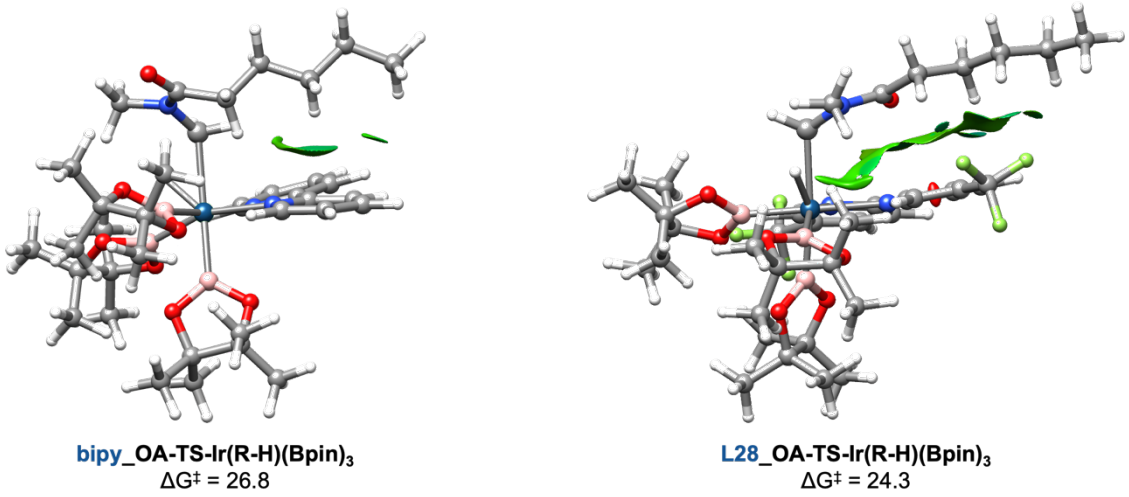



**Figure *55*** Substrate-ligand non-covalent interactions (NCI) occurring in the lowest energy outer-sphere transition states (TS) calculated with IEF-$PCM_{THF}$/M06/6-311G(2d,p)+SDD(Ir)//M06/6-31G(d)+LANL2DZ(Ir) for the oxidative addition step between **44a** and $Ir^{III}$(ligand)$(Bpin)_3$ (ligand = **bipy** (left) and **L28** (right)). Note the larger extension of van der Waals NCI in the transition state with ligand **L28**. Non-reacting hydrogens have been omitted for clarity.

These interactions were further confirmed through a quantum theory of atoms in molecules (QTAIM)[117] analysis (Figure *56*). In the transition state (TS) with ligand **L28**, bond

[132] Marcos-Atanes, D.; Vidal, C.; Navo, C. D.; Peccati, F.; Jiménez-Osés, G.; Mascareñas, J. L. *Angew. Chem. Int. Ed.* **2023,** *62,* e202214510.

paths were identified between the carbonyl group of the benzamide and the $CF_3$-substituted pyridine ring, along with a bond critical point (BCP), indicating a strong interaction that contributes to the stabilization of the TS. Additionally, some interactions were also detected between the alkyl chain of the substrate and the -$CF_3$ group in the ligand

In contrast, these bond paths and BCPs were absent in the TS with **bipy**, further supporting the idea that the non-covalent interactions between the carbonyl group and the $CF_3$-pyridine ring play a crucial role in driving the reactivity

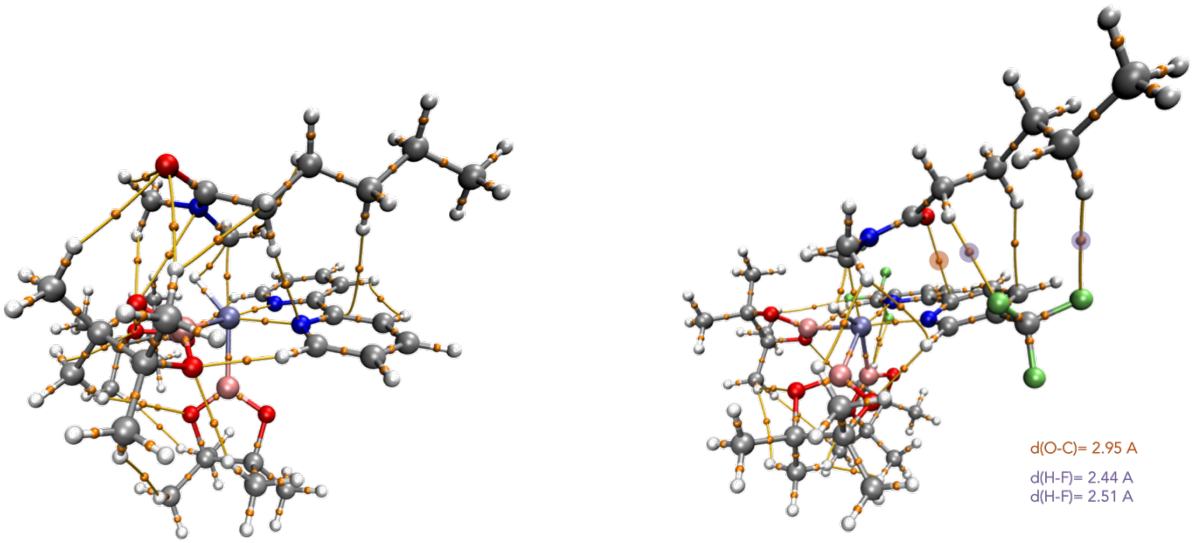



**Figure *56*** Bond critical points (BCP) (3,-1) determined from topology analysis of the electron density in low energy outer-sphere transition states (TS) calculated for the oxidative addition step between **44a** and $Ir^{III}$(ligand)$(Bpin)_3$ (ligand = **bipy** (left) and **L28** (right)). The BCP between the substrate carbonyl O and bipyridine N or C atoms in the C–H activation transition states is highlighted with an orange circle, the BCP between the substrate H atoms and the ligand F atoms are highlighted with a purple circle.

Energy Decomposition Analysis (GSK-EDA,[121] Figure *57*) enabled the breakdown of the total interaction energy between the amide and (5-trifluoromethyl)pyridine fragments. The analysis revealed that the attractive interactions, both polar and dispersive, are significantly stronger in the borylation transition state (TS) with **L28** compared to the **bipy** TS. This higher total interaction energy supports the hypothesis that these non-covalent interactions, including polar and dispersive forces, contribute to stabilizing the C–H activation when using $CF_3$-substituted bipyridines.

USC UNIVERSIDADE DE SANTIAGO DE COMPOSTELA

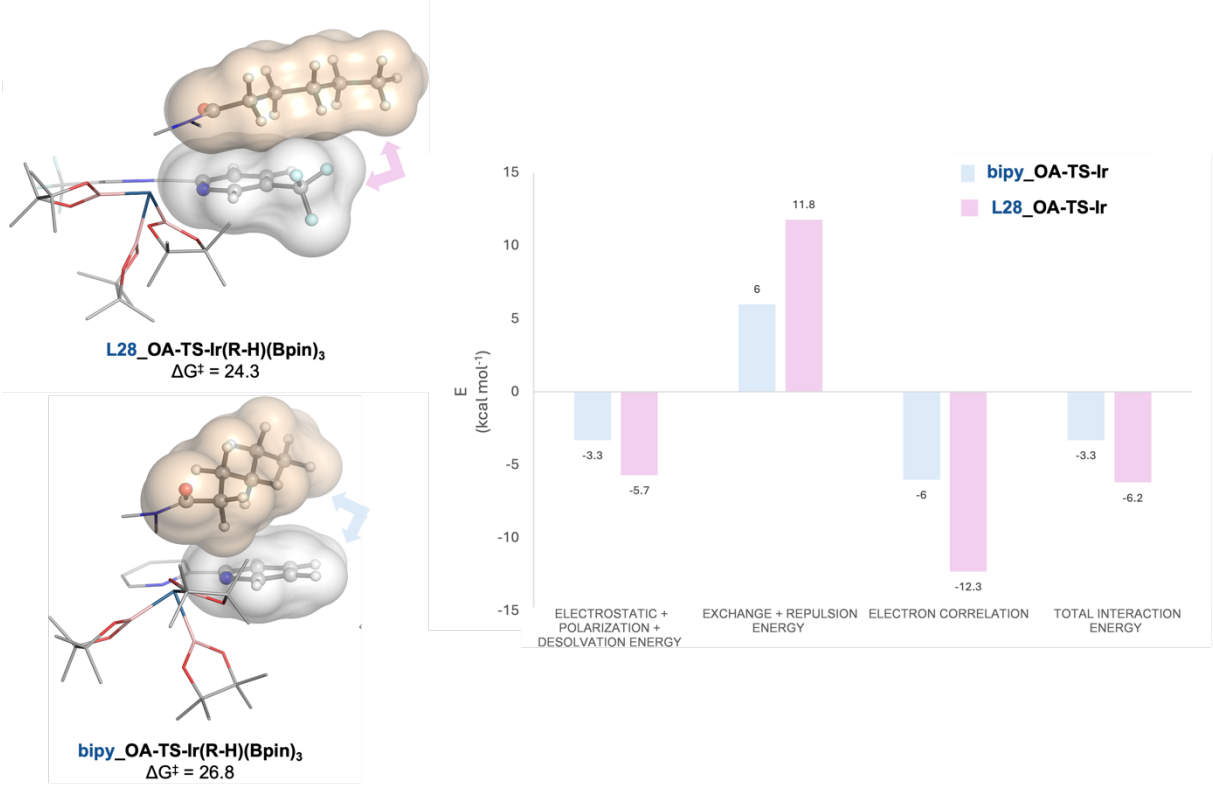



**Figure *57*** Generalized Kohn-Sham Energy Decomposition Analysis (GKS-EDA of the low energy outer-sphere transition states (TS) calculated for the oxidative addition step between N,N-dimethylhexanamide (**23a**) and $Ir^{III}$(ligand)$(Bpin)_3$ (ligand = **bipy** and **L28**). Activation free energies ($\Delta G^{‡}$) calculated with $IEFPCM_{THF}$/M06/6-311G(d,p);SDD(Ir)]//M06/6-31G(d);LANL2DZ(Ir), are given in kcal $mol^{-1}$. In the graphs, different contributions to the total interaction energy between the n- hexanamide and (5-trifluoromethyl)pyridine fragments are shown. Contributions related to the polar character of the interactions (electrostatic, polarization and desolvation) have been added together for clarity. The electron correlation component implicitly accounts for dispersion.

While pinpointing the exact nature of these interactions (dispersive and/or electrostatic) remains challenging, we propose that donor-acceptor $n_{CO} \rightarrow \pi^*_{C=N}$ contacts are particularly relevant, similar as the ones proposed previously by our group in the case of aromatic amides. The electron-withdrawing effect of the trifluoromethyl substituent in **L28** enhances the strength of outer-sphere substrate-catalyst interactions, which is crucial for the observed increase in reactivity.

To further substantiate our findings, we conducted additional computational studies employing various DFT methods (Table *22*). Functionals incorporating dispersion corrections for single-point energy calculations consistently aligned with experimental observations, clearly indicating that the C–H activation step has a lower energy barrier with **L28** compared to **L27** and **bipy**. Notably, single-point energy calculations using B3LYP (without dispersion correction) erroneously predicted a lower energy barrier for **bipy** relative to **L27** and **L28**, contradicting experimental data. These discrepancies underscore the critical importance of including dispersion corrections for accurately modeling the catalytic system and assessing non-covalent interactions in the transition

state. Such interactions are pivotal in reducing the energy barrier for the reaction involving **L28**.

**Table *22*** ΔG barriers for the C-H activation step of **44a** using **bipy**, **L27** and **L28** with different DFT methods and bases

| Method | bipy | 5-$CF_3$-Bipy (L27) | 5, 5'-$CF_3$-Bipy (L28) |
|---|---|---|---|
| M06/6-31g(d)+LANL2DZ(Ir) | 23.58 | 22.61 | 20.71 |
| M06/6-311g(2dp)+SDD(Ir)//IEFPCM | 27.30 | 26.79 | 24.34 |
| M06/6-311++g(2dp)+SDD(Ir)//SMD | 31.14 | 31.12 | 29.04 |
| M06/6-311++g(2dp)+SDD(Ir)//IEFPCM | 28.58 | 29.60 | 26.91 |
| M06/6-311++g(2dp)+SDD(Ir)//SMD | 32.68 | 34.03 | 31.48 |
| B3LYP/6-311g(2dp)+SDD(Ir)//IEFPCM | 47.77 | 47.85 | 45.10 |
| B3LYP/6-311g(2dp)+SDD(Ir)//SMD | 48.60 | 52.44 | 49.70 |
| B3LYP/6-311++g(2dp)+SDD(Ir)//IEFPCM | 46.49 | 50.46 | 47.52 |
| B3LYP/6-311++g(2dp)+SDD(Ir)//SMD | 50.48 | 55.13 | 52.15 |
| B3LYP-D3BJ/6-311g(2dp)+SDD(Ir)//IEFPCM | 22.08 | 23.19 | 20.82 |
| B3LYP-D3BJ/6-311g(2dp)+SDD(Ir)//SMD | 25.99 | 27.62 | 25.43 |
| B3LYP-D3BJ/6-311++g(2dp)+SDD(Ir)//IEFPCM | 23.87 | 26.47 | 23.24 |
| B3LYP-D3BJ/6-311++g(2dp)+SDD(Ir)//SMD | 27.87 | 31.02 | 27.87 |
| B3PW91-D3/6-311g(2dp)+SDD(Ir)//IEFPCM | 16.60 | 17.30 | 15.30 |
| B3PW91-D3/6-311g(2dp)+SDD(Ir)//SMD | 20.46 | 21.69 | 19.88 |
| B3PW91-D3/6-311++g(2dp)+SDD(Ir)//IEFPCM | 22.72 | 19.90 | 17.18 |
| B3PW91-D3/6-311++g(2dp)+SDD(Ir)//SMD | 21.92 | 24.35 | 21.78 |
| PBE0-D3BJ/def2-TZVPD+def2-QZVPD(Ir)//IEFPCM | 36.47 | 40.68 | 37.37 |
| PBE0-D3BJ/def2-TZVPD+def2-QZVPD(Ir)//SMD | 40.51 | 45.45 | 42.12 |
| wB97x-D/6-311g(2dp)+SDD(Ir)//IEFPCM | 32.71 | 20.92 | 18.71 |
| wB97x-D/6-311g(2dp)+SDD(Ir)//SMD | 24.33 | 25.34 | 23.33 |
| wB97x-D/6-311++g(2dp)+SDD(Ir)//IEFPCM | 21.70 | 23.62 | 20.67 |
| wB97x-D/6-311++g(2dp)+SDD(Ir)//SMD | 25.94 | 28.11 | 25.32 |

### 7.3.4 Conclusions

We have discovered that the incorporation of $CF_3$ groups in the 5 position of bipyridine ligands enables highly selective N-methyl borylations across a diverse range of alkyl N-methylamides, with exceptional chemoselectivities. This discovery is particularly significant, as the parent bipyridine (**bipy**) fails to yield any product under identical reaction conditions.

Computational studies involving both $CF_3$ and non-$CF_3$ containing ligands provide support for a canonical Ir(III)/Ir(V) mechanism, where the rate-determining step involves

USC UNIVERSIDADE DE SANTIAGO DE COMPOSTELA

C–H activation followed by an isomerization process, involving the repositioning of the two boryl groups before reductive elimination.

Non-covalent interactions between the polarized ring of the bipyridine ligand and the carbonyl group of the alkyl amide seem to play a crucial role in stabilizing the C–H activation transition state, thereby facilitating the progression of the reaction. The importance of these dispersion-driven non-covalent interactions, although rarely considered, should be acknowledged for future investigations across various chemical reactions.

USC
UNIVERSIDADE DE SANTIAGO DE COMPOSTELA

# 8 Conclusions

USC
UNIVERSIDADE
DE SANTIAGO
DE COMPOSTELA

# Conclusions

The work of this PhD thesis has allowed to discover two new types of chemo- and regioselective iridium-catalyzed borylation reactions, one for the borylation of aromatic amides and other for the N-methyl borylation of aliphatic amides. Experimental and computational mechanistic studies suggest that the controlled reactivity and excellent selectivity stems from the existence of unconventional dispersion non-covalent interactions between the substrate and designed $CF_3$-containing bipyridine ligands.

The initial work described in section 7.1 deals with the synthesis of bifunctional bipyridine ligands designed to explore the potential of hydrogen bonding for the borylation of distal phenyl rings in biphenyl amides. Despite inconsistent outcomes with ligands featuring urea, thiourea, and squaramide recognition sites, this research allowed to discover bipyridine ligands that provide *ortho*-borylated products.

These findings were key for the research described in section 7.2, that allowed to discover that bipyridine ligands bearing $CF_3$ groups at the 5-position enable the *ortho* borylation of benzamides, a transformation unattainable with conventional 2,2'-bipyridine ligands. Experimental observations, supported by DFT calculations, highlighted the crucial role of non-covalent, dispersion interactions for such selective orientation.

These ligands also enable an impressive reactivity for selective N-methyl borylations across a diverse range of alkyl N-methylamides described in section 7.3. This exceptional chemoselectivity was further demonstrated by the fact that under identical reaction conditions, the parent bipyridine ligands produced no detectable products. This unique reactivity was attributed again to non-covalent interactions between the substrate and the $CF_3$ containing ligands, as supported by DFT studies. This work highlights the versatility of $CF_3$-substituted ligands in facilitating challenging transformations where traditional bipyridine ligands are ineffective.

USC
UNIVERSIDADE DE SANTIAGO DE COMPOSTELA

# 9 Bibliography

USC
UNIVERSIDADE
DE SANTIAGO
DE COMPOSTELA

# Bibliography

To facilitate an easy reading of this thesis manuscript, bibliographic references have been included as footnotes in each page.

USC
UNIVERSIDADE DE SANTIAGO DE COMPOSTELA

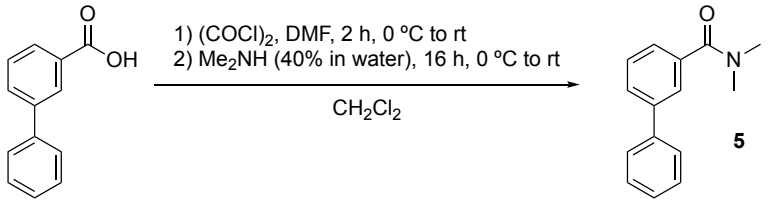
# 10 Experimental section

USC
UNIVERSIDADE
DE SANTIAGO
DE COMPOSTELA

# 10.1 Experimental procedures for section 7.1.

## 10.1.1 Synthesis of substrates

### *10.1.1.1 Preparation of N,N-dimethyl-[1,1'-biphenyl]-3-carboxamide (5)*

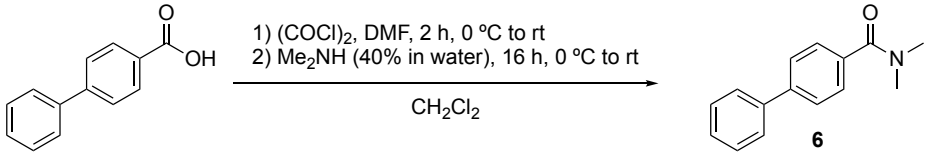



Prepared following an adapted procedure:[133] To a solution of biphenyl-3-carboxylic acid (1 g, 5.0 mmol, 1.0 equiv.) in $CH_2Cl_2$ (20 mL) at room temperature, oxalyl chloride $(COCl)_2$ (0.649 mL, 7.5 mmol, 1.5 equiv.) and DMF (5 drops) were carefully added in that order. The reaction mixture was stirred at room temperature for 2 h. After that time, the mixture was cooled down to 0 ºC and $Me_2NH$ (40% w/w in water; 2.5 mL, 20.0 mmol, 4.0 equiv.) was added dropwise. The reaction mixture was stirred continuously at room temperature overnight.

The reaction was then quenched with water and organic materials were extracted twice with $CH_2Cl_2$, washed first with 1.0 M aqueous HCl solution followed by a second wash with saturated aqueous $NaHCO_3$ solution and brine. The organic fraction was dried over $MgSO_4$ and the solvent was removed in vacuo to obtain the N,N-dimethyl-[1,1'-biphenyl]-3-carboxamide in a 87% yield (990 g) as a pale yellow oil.

**$^1$H NMR** (600.1318 MHz, $CDCl_3$) δ 7.65 – 7.57 (m, 4H), 7.51 – 7.43 (m, 3H), 7.39 (ddd, *J* = 7.4, 2.8, 1.4 Hz, 2H), 3.14 (s, 3H), 3.01 (s, 3H).
**$^{13}$C NMR** (100.63 MHz, $CDCl_3$) δ 171.58 (CO), 141.21 (C, Ar), 140.20 (C, Ar), 136.49 (C, Ar), 128.95 (CH, Ar), 128.90 (CH, Ar), 128.33 (CH, Ar), 127.67 (CH, Ar), 127.14 (CH, Ar), 125.84 (CH, Ar), 125.69 (CH, Ar), 39.76 (N-$CH_3$), 35.38 (N-$CH_3$).
**$^{15}$N NMR** (40.55 MHz, $CDCl_3$) δ 103.59
**HRMS (ESI)**. Calculated for $C_{15}H_{16}NO^+$: 226.1226 Obtained: 226.1221

### *10.1.1.2 Preparation of N,N-dimethyl-[1,1'-biphenyl]-4-carboxamide (6)*




Prepared following an adapted procedure:[133] To a solution of [1,1'-biphenyl]-4-carboxylic acid (1.98 g, 10.0 mmol, 1.0 equiv.) in $CH_2Cl_2$ (40 mL) at room temperature, oxalyl chloride $(COCl)_2$ (1.30 mL, 15.0 mmol, 1.5 equiv.) and DMF (5 drops) were carefully

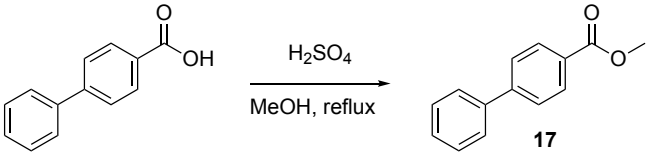
[133] Chan, G. H.; Ong, D. Y.; Yen, Z.; Chiba, S. *Helv. Chim. Acta* **2018,** *101,* e1800049.

added in that order. The reaction mixture was stirred at room temperature for 2 h. After that time, the mixture was cooled down to 0 ºC and $Me_2NH$ (40% w/w in water; 5.06 mL, 40.0 mmol, 4.0 equiv.) was added dropwise. The reaction mixture was stirred continuously at room temperature overnight.

The reaction was then quenched with water and organic materials were extracted twice with $CH_2Cl_2$, washed first with 1.0 M aqueous HCl solution followed by a second wash with saturated aqueous $NaHCO_3$ solution and brine. The organic fraction was dried over $MgSO_4$ and the solvent was removed in vacuo to obtain the *N,N*-dimethyl-[1,1'-biphenyl]-4-carboxamide in a 87% yield (1.96 g) as a white solid.

**$^1$H NMR** (600.1318 MHz, $CDCl_3$) δ 7.64 – 7.58 (m, 4H), 7.52 – 7.48 (m, 2H), 7.45 (t, 2H), 7.39 – 7.35 (m, 1H), 3.13 (s, 3H), 3.04 (s, 3H).
**$^{13}$C NMR** (100.63 MHz, $CDCl_3$) δ 171.58 (CO), 142.56 (C, Ar), 140.48 (C, Ar), 135.23 (C, Ar), 129.00 (CH, Ar), 127.86 (CH, Ar), 127.79 (CH, Ar), 127.28 (CH, Ar), 127.18 (CH, Ar), 39.78 (N-$CH_3$), 35.54 (N-$CH_3$).
**$^{15}$N NMR** (40.55 MHz, $CDCl_3$) δ 102.11
**HRMS (ESI)**. Calculated for $C_{15}H_{16}NO^+$: 226.1226 Obtained: 226.1230

### *10.1.1.3 Preparation of methyl [1,1'-biphenyl]-4-carboxylate (17)*



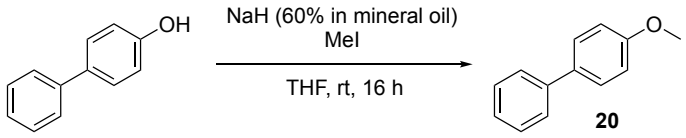

**17**

In a round-bottom flask equipped with a stirring bar, [1,1'-biphenyl]-4-carboxylic acid (5 g, 25.2 mmol, 1.0 equiv.) is dissolved in MeOH (30.0 mL), and $H_2SO_4$ (3.2 mL, 60.7 mmol, 2.4 equiv.) is added. The resulting solution is heated under reflux for 5 hours. The reaction mixture is then allowed to cool, the resulting white solid is filtered, and the product is washed three times with hexane, obtaining the expected product 17 in 90% yield (4.8 g).

**$^1$H NMR** (400.16 MHz, $CDCl_3$) δ 8.15 – 8.09 (m, 2H), 7.69 – 7.65 (m, 2H), 7.65 – 7.60 (m, 2H), 7.51 – 7.44 (m, 2H), 7.43 – 7.37 (m, 1H), 3.95 (s, 3H).
**$^{13}$C NMR** (100.63 MHz, $CDCl_3$) δ 167.07 (CO), 145.70 (C, Ar), 140.07 (C, Ar), 130.19 (CH, Ar), 129.01 (CH, Ar), 128.98 (C, Ar), 128.23 (CH, Ar), 127.36 (CH, Ar), 127.12 (CH, Ar), 52.19 (O-$CH_3$).
**HRMS (ESI).** Calculated for $C_{14}H_{13}O_2^+$: 213.091006 Obtained: 213.090988

USC UNIVERSIDADE DE SANTIAGO DE COMPOSTELA

#### *10.1.1.4 Preparation of 4-methoxy-1,1'-biphenyl (20)*



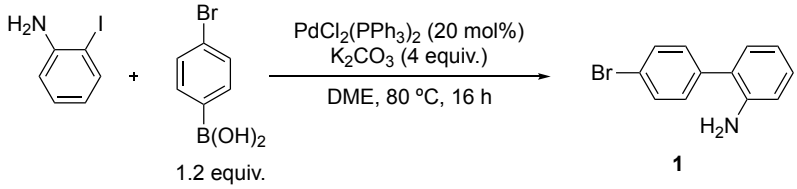

*p*-phenyl phenol (0.5 g, 2.9 mmo, 1.0 equiv.) is dissolved in dry THF (10.0 mL). Sodium hydride (60% dispersion in mineral oil, 3.5 mmol, 1.2 equiv.) is added to the solution in one portion. The mixture is stirred at room temperature for 1 hour, then methyl iodide (0.2 mL, 3.2 mmol, 1.1 equiv.) is added. Stirring is maintained at rt for 16 hours.

After that time, the reaction is quenched with water and NaOH (50 mL) and filtered through water and DCM (500 mL, 1:1, v/v). The organic phase is se*para*ted, washed with brine, and dried with $NaSO_4$. After concentrating under reduced pressure, the product is purified by column chromatography on silica gel with Hexane/EtOAc (3:1), yielding the desired product in 76% yield (411 mg).

**$^1$H NMR** (400.16 MHz, $CDCl_3$) δ 7.64 (td, *J* = 8.6, 1.8 Hz, 4H), 7.50 (t, *J* = 7.7 Hz, 2H), 7.43 – 7.35 (m, 1H), 7.09 – 7.03 (m, 2H), 3.91 (s, 3H).
**$^{13}$C NMR** (100.63 MHz, $CDCl_3$) δ 159.26 (C, Ar), 140.90 (C, Ar), 133.83 (C, Ar), 128.83 (CH, Ar), 128.23 (CH, Ar), 126.81 (CH, Ar), 126.75 (CH, Ar), 114.31 (CH, Ar), 55.36 (-O-$CH_3$).
**HRMS (ESI).** Calculated for $C_{13}H_{13}O^+$: 185.096091 Obtained: 185.096117

### 10.1.2 Ligand synthesis

#### *10.1.2.1 Preparation of 4'-bromo-[1,1'-biphenyl]-2-amine (1)*




To a dry Schlenk flask, 2-iodoaniline (1.1 g, 5.0 mmol, 1.0 equiv.) and (4-bromophenyl)boronic acid (1.2 g, 6.0 mmol, 1.2 equiv.) were added. The flask was evacuated and backfilled with pure $N_2$ three times. DME (5.0 mL) and a 2 M deoxygenated aqueous solution of $K_2CO_3$ (20.0 mL) were added via syringe, and the mixture was stirred for 30 minutes at room temperature under an $N_2$ atmosphere. To the stirred mixture, $PdCl_2(PPh_3)_2$ (70 mg, 0.1 mmol, 0.02 equiv.) in DME (10.0 mL) was added via syringe at room temperature, and the mixture was stirred at 80 ºC for 12 hours under $N_2$ atmosphere (monitored by TLC).

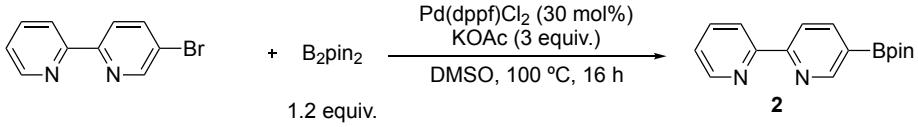
Once the reaction was complete, the mixture was cooled to room temperature and diluted with EtOAc (20.0 mL). The aqueous layer was extracted with EtOAc (20.0 mL x 3) and the combined organic phases were dried over anhydrous $MgSO_4$. The solvent was removed under reduced pressure, and the residue was purified by column

USC UNIVERSIDADE DE SANTIAGO DE COMPOSTELA

chromatography on silica gel using a 30:1 mixture of Hexane/EtOAc as the eluent to afford 744 mg of 4'-bromo-[1,1'-biphenyl]-2-amine (60% yield)

**$^1$H NMR** (400.16 MHz, $CDCl_3$) δ 7.61 – 7.55 (m, 2H), 7.38 – 7.32 (m, 2H), 7.18 (ddd, *J* = 8.0, 7.3, 1.6 Hz, 1H), 7.10 (dd, *J* = 7.6, 1.6 Hz, 1H), 6.84 (td, *J* = 7.4, 1.2 Hz, 1H), 6.77 (dd, *J* = 8.0, 1.2 Hz, 1H), 3.56 (s, 2H).
**$^{13}$C NMR** (100.63 MHz, $CDCl_3$) δ 143.42 (C, Ar), 138.51 (C, Ar), 132.06 (CH, Ar), 130.93 (CH, Ar), 130.38 (CH, Ar), 128.98 (CH, Ar), 126.43 (C, Ar), 121.35 (C, Ar), 118.94 (CH, Ar), 115.89 (CH, Ar).
**HRMS (ESI).** Calculated for $C_{12}H_{11}BrN^+$: 248.006938 Obtained: 248.007400

### *10.1.2.2 Preparation of 5-(4,4,5,5-tetramethyl-1,3,2-dioxaborolan-2-yl)-2,2'-bipyridine (2)*

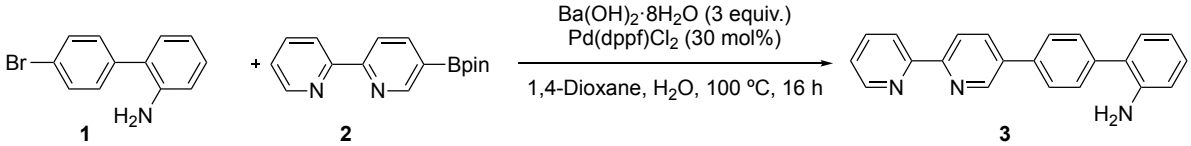



Prepared following and adapted procedure:[72] To a solution of 5-bromo-2,2'-bipyridine (0.8 g, 3.4 mmol, 1.0 equiv.) in DMSO (10.0 mL) were added KOAc (1.0 g, 10.2 mmol, 3.0 equiv.), $PdCl_2$(dppf) (75.4 mg, 0.1 mmol, 3.0 mol%), and $B_2pin_2$ (1.0 g, 4.1 mmol, 1.2 equiv.). The mixture was stirred at 100 ºC for 18 hours.

After cooling to room temperature, the mixture was filtered through Celite, and the eluent was extracted with $CH_2Cl_2$. The solvent was evaporated in vacuo, and then hexane and water were added to the residue. The mixture was extracted with hexane (3 × 30.0 mL), and the solvent was removed under reduced pressure. 5-(4,4,5,5-Tetramethyl-1,3,2-dioxaborolan-2-yl)-2,2'-bipyridine was obtained as a pale yellow solid (911 mg, 95%).

**$^1$H NMR** (400.16 MHz, $CDCl_3$) δ 8.99 (dd, *J* = 1.8, 1.0 Hz, 1H), 8.71 – 8.64 (m, 1H), 8.45 – 8.41 (m, 1H), 8.36 (dd, *J* = 7.9, 1.0 Hz, 1H), 8.18 (dd, *J* = 7.9, 1.8 Hz, 1H), 7.80 (ddd, *J* = 8.0, 7.5, 1.8 Hz, 1H), 7.29 (ddd, *J* = 7.5, 4.8, 1.2 Hz, 1H), 1.35 (s, 12H).
**$^{13}$C NMR** (100.63 MHz, $CDCl_3$) δ 158.07 (C, Ar), 156.18 (C, Ar), 155.15 (CH, Ar), 149.31 (CH, Ar), 143.40 (CH, Ar), 137.04 (CH, Ar), 124.05 (CH, Ar), 121.69 (CH, Ar), 120.32 (CH, Ar), 84.32 (C), 24.98 ($CH_3$).
**$^{11}$B NMR** (128.39 MHz, $CDCl_3$) δ 30.75.
**HRMS (ESI).** Calculated for $C_{16}H_{20}BN_2O_2^+$: 283.161235 Obtained: 283.161733

### *10.1.2.3 Preparation of 4'-([2,2'-bipyridin]-5-yl)-[1,1'-biphenyl]-2-amine (3)*




To a solution of 5-(4,4,5,5-tetramethyl-1,3,2-dioxaborolan-2-yl)-2,2'-bipyridine (227.4 mg, 0.8 mmol, 1.0 equiv.) in dioxane (1.3 mL), $PdCl_2$(dppf) (59.0 mg, 0.081 mmol,

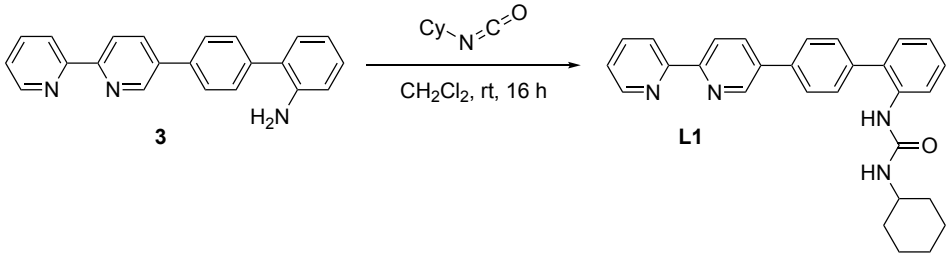
USC UNIVERSIDADE DE SANTIAGO DE COMPOSTELA

10 mol%), $H_2O$ (0.4 mL), $Ba(OH)_2 \cdot 8H_2O$ (724.2 mg, 2.4 mmol, 3.0 equiv.), and **1** (200 mg, 0.8 mmol, 1.0 equiv.) were added. The mixture was stirred at 100 ºC for 24 hours.

After cooling to room temperature, the mixture was filtered through Celite. The eluent was extracted with ethyl acetate (3 × 50 mL), and the organic layer was dried over $Na_2SO_4$. The mixture was filtered, the solvent was removed under reduced pressure, and the residue was purified by column chromatography on silica gel deactivated with 5% $Et_3N$ in hexane (Rf = 0.32 eluent: hexane/EtOAc = 5/1) to afford 142 mg of 4'-([2,2'-bipyridin]-5-yl)-[1,1'-biphenyl]-2-amine (55% yield).

**$^1$H NMR** (400.16 MHz, $CDCl_3$) δ 8.98 (dd, *J* = 2.4, 0.9 Hz, 1H), 8.74 – 8.69 (m, 1H), 8.51 (dd, *J* = 8.2, 0.9 Hz, 1H), 8.46 (dd, *J* = 8.0, 1.1 Hz, 1H), 8.08 (dd, *J* = 8.3, 2.4 Hz, 1H), 7.85 (td, *J* = 7.7, 1.8 Hz, 1H), 7.78 – 7.71 (m, 2H), 7.64 – 7.58 (m, 2H), 7.34 (ddd, *J* = 7.6, 4.8, 1.2 Hz, 1H), 7.23 – 7.16 (m, 2H), 6.86 (td, *J* = 7.4, 1.1 Hz, 1H), 6.83 – 6.78 (m, 1H), 3.31 (s, 2H).
**$^{13}$C NMR** (100.63 MHz, $CDCl_3$) δ 155.89 (C, Ar), 155.02 (C, Ar), 149.35 (CH, Ar), 147.65 (CH, Ar), 143.69 (C, Ar), 139.73 (C, Ar), 137.21 (CH, Ar), 136.44 (C, Ar), 136.22 (C, Ar), 135.32 (CH, Ar), 130.54 (CH, Ar), 129.99 (CH, Ar), 128.92 (CH, Ar), 127.60 (CH, Ar), 126.95 (C, Ar), 123.91 (CH, Ar), 121.29 (CH, Ar), 121.27 (CH, Ar), 118.93 (CH, Ar), 115.90 (CH, Ar).
**HRMS (ESI).** Calculated for $C_{22}H_{18}N_3^+$: 324.149524 Obtained: 324.150158

### *10.1.2.4 Preparation of 1-(4'-([2,2'-bipyridin]-5-yl)-[1,1'-biphenyl]-2-yl)-3-cyclohexylurea (L1)*

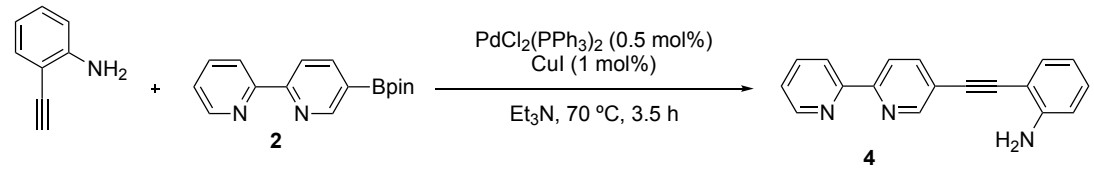



A mixture of **3** (100 mg, 0.3 mmol, 1.0 equiv.) and cyclohexylisocyanate (0.06 mL, 0.5 mmol, 1.5 equiv.) in dichloromethane (1.0 mL) was stirred at room temperature for 24 hours. The solvent was removed, and the residue was purified by recrystallization with DCM/Hexane to obtain 100 mg of the desired product (72% yield).

**$^1$H NMR** (400.16 MHz, DMSO-$d_6$) δ 9.10 (d, *J* = 2.4 Hz, 1H), 8.76 – 8.69 (m, 1H), 8.51 (d, *J* = 8.3 Hz, 1H), 8.45 (d, *J* = 7.9 Hz, 1H), 8.32 (dd, *J* = 8.3, 2.4 Hz, 1H), 8.02 – 7.91 (m, 4H), 7.55 – 7.46 (m, 3H), 7.38 (s, 1H), 7.29 (ddd, *J* = 8.4, 7.3, 1.7 Hz, 1H), 7.20 (dd, *J* = 7.6, 1.7 Hz, 1H), 7.07 (td, *J* = 7.4, 1.3 Hz, 1H), 6.55 (d, *J* = 7.7 Hz, 1H), 3.44 – 3.38 (m, 1H), 1.77 (dd, *J* = 13.1, 3.8 Hz, 2H), 1.68 – 1.59 (m, 2H), 1.51 (dt, *J* = 12.8, 4.0 Hz, 1H), 1.30 – 1.23 (m, 2H), 1.09 (ddd, *J* = 13.0, 10.2, 3.4 Hz, 3H).
**$^{13}$C NMR** (100.63 MHz, DMSO-$d_6$) δ 154.85 (CO), 154.73 (C, Ar), 154.17 (C, Ar), 149.38 (CH, Ar), 147.22 (CH, Ar), 138.90 (C, Ar), 137.42 (CH, Ar), 136.90 (C, Ar), 135.47 (C, Ar), 135.19 (C, Ar), 135.06 (CH, Ar), 131.16 (C, Ar), 130.13 (CH, Ar), 129.99 (CH, Ar), 127.89 (CH, Ar), 127.12 (CH, Ar), 124.25 (CH, Ar), 122.32 (CH, Ar), 121.90 (CH, Ar), 120.59 (CH, Ar), 120.45 (CH, Ar), 47.79 (CH), 32.97 ($CH_2$), 25.25 ($CH_2$), 24.36 ($CH_2$).

**HRMS (ESI).** Calculated for $C_{29}H_{29}N_4O^+$: 449.233588 Obtained: 449.234209

### *10.1.2.5 Preparation of 2-([2,2'-bipyridin]-5-ylethynyl)aniline (4)*




Prepared following an adapted procedure:[72] $PdCl_2(PPh_3)_2$ (7.5 mg, 0.011 mmol, 0.5 mol%.) and CuI (4.1 mg, 0.021 mmol, 1 mol%) were added to a solution of 5-bromo-2,2'-bipyridine (500.0 mg, 2.1 mmol, 1.0 equiv.) in $Et_3N$ (5.3 mL), and the mixture was stirred at room temperature for about 15 minutes. 2-Ethynylaniline (0.3 mL, 2.6 mmol, 1.2 equiv.) was added to the mixture, and the reaction was stirred at room temperature while monitored by TLC.

After 3.5 hours, the white precipitate was filtered through a Celite pad and the filtrate was concentrated under reduced pressure. $H_2O$ (20.0 mL) was added to the residue, and the products were extracted with diethyl ether (3 × 20.0 mL). The combined organic layer were washed with saturated aqueous NaCl solution, dried over anhydrous $Na_2SO_4$, filtered, and concentrated under reduced pressure. The crude product was purified by column chromatography (hexane/ethyl acetate = 3/1) to give 301 mg of 2-([2,2'-bipyridin]-5-ylethynyl)aniline (52% yield).

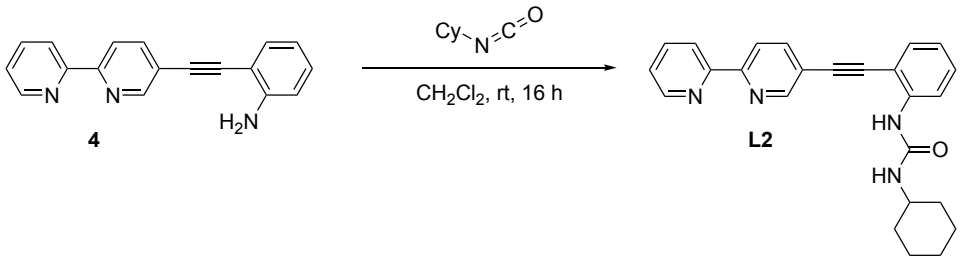
**$^1$H NMR** (400.16 MHz, $CDCl_3$) δ 8.84 – 8.77 (m, 1H), 8.73 – 8.67 (m, 1H), 8.41 (ddd, *J* = 8.3, 2.4, 1.0 Hz, 2H), 7.92 (dd, *J* = 8.3, 2.2 Hz, 1H), 7.82 (td, *J* = 7.7, 1.8 Hz, 1H), 7.40 (dd, *J* = 7.9, 1.6 Hz, 1H), 7.31 (ddd, *J* = 7.5, 4.8, 1.2 Hz, 1H), 7.21 – 7.14 (m, 1H), 6.74 (ddd, *J* = 7.5, 3.6, 2.4 Hz, 2H), 4.03 (s, 2H).

**$^{13}$C NMR** (100.63 MHz, $CDCl_3$) δ 155.54 (C, Ar), 154.80 (C, Ar), 151.51 (CH, Ar), 149.36 (CH, Ar), 148.08, 139.24 (CH, Ar), 137.13 (CH, Ar), 132.45 (CH, Ar), 130.44 (CH, Ar), 124.05 (CH, Ar), 121.48 (CH, Ar), 120.51 (C, Ar), 120.49 (CH, Ar), 118.19 (CH, Ar), 114.60 (CH, Ar), 107.28 (C, Ar), 91.75 (C), 90.37 (C).

**HRMS (ESI).** Calculated for $C_{18}H_{14}N_3^+$: 272.118224 Obtained: 272.118225

USC UNIVERSIDADE DE SANTIAGO DE COMPOSTELA

### *10.1.2.6 Preparation of 1-(2-([2,2'-bipyridin]-5-ylethynyl)phenyl)-3-cyclohexylurea (L2)*




A mixture of **4** (83.9 mg, 0.3 mmol, 1.0 equiv.) and cyclohexylisocyanate (0.06 mL, 0.5 mmol, 1.5 equiv.) in dichloromethane (1.0 mL) was stirred at room temperature for 24 hours.

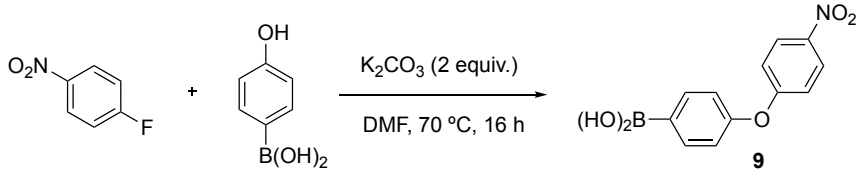
The solvent was removed, and the residue was purified by recrystallization with DCM/Hexane to obtain 94 mg of the desired product (79% yield).

**$^{1}$H NMR** (400.16 MHz, DMSO-$d_6$) δ 8.95 (s, 1H), 8.72 (s, 1H), 8.45 (dd, *J* = 17.6, 8.1 Hz, 2H), 8.23 – 8.14 (m, 2H), 7.99 (t, *J* = 7.8 Hz, 1H), 7.95 (s, 1H), 7.51 (dd, *J* = 7.7, 1.6 Hz, 2H), 7.34 (ddd, *J* = 8.7, 7.3, 1.6 Hz, 1H), 7.11 (d, *J* = 7.6 Hz, 1H), 6.98 (td, *J* = 7.5, 1.2 Hz, 1H), 3.49 (dp, *J* = 10.5, 3.5 Hz, 1H), 1.90 – 1.82 (m, 2H), 1.69 (dt, *J* = 12.9, 3.9 Hz, 3H), 1.57 (ddd, *J* = 16.7, 8.2, 4.2 Hz, 2H), 1.33 – 1.26 (m, 3H).

**$^{13}$C NMR** (100.63 MHz, DMSO-$d_6$) δ 156.60 (CO), 154.36 (C, Ar), 153.91 (C, Ar), 151.66 (CH, Ar), 149.48 (CH, Ar), 141.37 (C, Ar), 139.71 (C, Ar), 137.47 (CH, Ar), 132.32 (CH, Ar), 129.95 (CH, Ar), 124.57 (CH, Ar), 121.23 (CH, Ar), 120.84 (CH, Ar), 119.95 (CH, Ar), 118.96 (CH, Ar), 109.78 (C, Ar), 92.05 (C), 89.71 (C), 47.99 (CH), 33.00 ($CH_2$), 25.24 ($CH_2$), 24.50 ($CH_2$).

**HRMS (ESI).** Calculated for $C_{25}H_{25}N_4O^+$: 397.202288 Obtained: 397.202609

### *10.1.2.7 Preparation of (4-(4-nitrophenoxy)phenyl)boronic acid (9)*



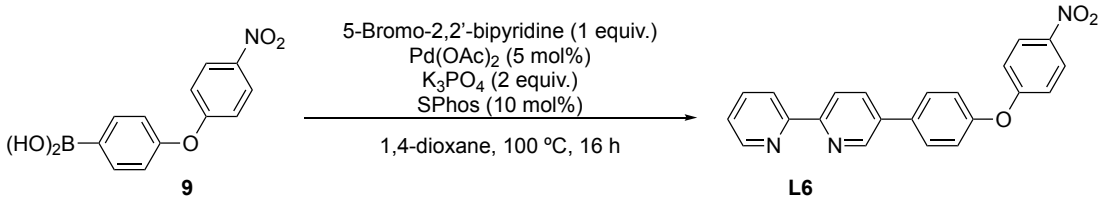

Prepared following an adated procedure:[134] To a solution of 1-fluoro-4-nitrobenzene (511 mg, 3.6 mmol, 1.0 equiv.) in dry DMF (20 mL) was added $K_2CO_3$ (1g, 7.2 mml, 2.0 equiv.) and aryl alcohol (600 mg, 4.3 mmol, 1.2 equiv.). The mixture was stirred at 70 ºC for 17 hours.

After that time, the solution was poured into water, and the mixture was extracted three times with ethyl acetate. After drying over anhydrous $MgSO_4$, the solvents were removed under reduced pressure. The residue was purified by flash column chromatography on silica gel to obtain 854 mg of the desired product (91% yield).

[134] Stockwell, B. R.; Dixon, S. J.; Skouta, R. .,WO 2015/051149 A1

**$^1$H NMR** (400.16 MHz, $CDCl_3$) δ 8.29 (d, *J* = 8.2 Hz, 2H), 8.28 – 8.23 (m, 2H), 7.21 (d, *J* = 8.2 Hz, 2H), 7.12 (d, *J* = 9.2 Hz, 2H).
**$^{13}$C NMR** (100.63 MHz, $CDCl_3$) δ 162.50 (C, Ar), 159.14 (C, Ar), 143.34 (C, Ar), 138.17 (CH, Ar), 126.18 (CH, Ar), 119.70 (CH, Ar), 118.16 (CH, Ar).
**$^{11}$B NMR** (128.39 MHz, $CDCl_3$) δ 29.32.
**HRMS (ESI).** Calculated for $C_{12}H_{10}BNNaO_5^+$: 282.054423 Obtained: 282.054370

### *10.1.2.8 Preparation of 5-(4-(4-nitrophenoxy)phenyl)-2,2'-bipyridine (L6)*

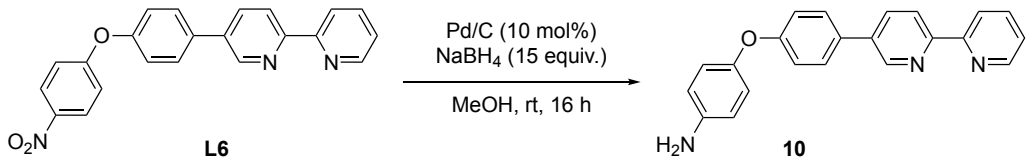



To a dry Schlenk flask equipped with a stir bar were added $Pd(OAc)_2$ (12 mg, 0.05 mmol, 5 mol %), SPhos (43 mg, 0.1 mmol, 10 mol %), 5-bromo-2,2'-bipyridine (250 mg, 1 mmol, 1 equiv.), **9** (413 mg, 1.6 mmol, 1.5 equiv.), and $K_3PO_4$ (451 mg, 2.1, 2 equiv. mmol). The mixture was dissolved in 1,4-dioxane (5 mL) and heated at 100 ºC overnight.

After cooling to room temperature, the solution was poured into water and the products were extracted with ethyl acetate, dried over $MgSO_4$, filtered through Celite, and concentrated to dryness. The residue was purified by column chromatography on silica gel, eluting with ethyl acetate to obtain 360 mg of the desired product (92% yield).

**$^1$H NMR** (400.16 MHz, $CDCl_3$) δ 8.93 (d, *J* = 2.5 Hz, 1H), 8.73 – 8.70 (m, 1H), 8.47 (dd, *J* = 22.0, 8.1 Hz, 2H), 8.26 – 8.21 (m, 2H), 8.04 (dd, *J* = 8.3, 2.2 Hz, 1H), 7.95 – 7.85 (m, 2H), 7.75 – 7.67 (m, 2H), 7.22 (dd, *J* = 8.5, 1.6 Hz, 2H), 7.12 – 7.07 (m, 2H).
**$^{13}$C NMR** (100.63 MHz, $CDCl_3$) δ 163.05 (C, Ar), 155.23 (C, Ar), 150.34 (C, Ar), 149.30 (C, Ar), 149.20 (CH, Ar), 147.52 (CH, Ar), 139.67 (C, Ar), 137.50 (CH, Ar), 136.54 (C, Ar), 135.39 (CH, Ar), 129.13 (CH, Ar), 126.16 (CH, Ar), 126.04 (CH, Ar), 124.09 (CH, Ar), 121.47 (CH, Ar), 121.44 (C, Ar), 121.19 (CH, Ar), 117.57 (CH, Ar).
**HRMS (ESI).** Calculated for $C_{22}H_{16}N_3O_3^+$: 370.118618 Obtained: 370.119144

### *10.1.2.9 Preparation of 4-(4-([2,2'-bipyridin]-5-yl)phenoxy)aniline (10)*

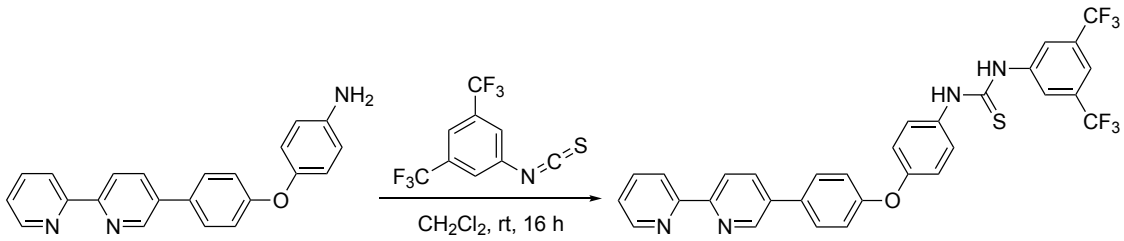



**L6** (400 mg, 1.1 mmol, 1 equiv.) was dissolved in methanol (44 mL). The solution was degassed by bubbling argon through it for 30 minutes, then palladium on activated carbon (10%) (115 mg, 0.1 mmol, 10 mol%) was added. The solution was cooled in an ice bath, and while vigorously stirring, sodium borohydride (615 mg, 16 mmol, 15 equiv.) was added portionwise.

After the addition was complete, the ice bath was removed, and the solution was stirred at room temperature for 5 hours. The catalyst was filtered off with a Celite bed, and the filtrate was concentrated in vacuo. Water (100 mL) was added to the residue, which was then extracted with DCM. The organic layer was dried over anhydrous $MgSO_4$ and evaporated to ontain 280 mg of the desired product (76% yield)

**$^1$H NMR** (400.16 MHz, $CDCl_3$) δ 8.88 (dd, *J* = 2.4, 0.8 Hz, 1H), 8.69 (ddd, *J* = 4.8, 1.8, 0.9 Hz, 1H), 8.43 (ddd, *J* = 8.4, 7.6, 0.9 Hz, 2H), 8.01 – 7.94 (m, 1H), 7.82 (td, *J* = 7.8, 1.8 Hz, 1H), 7.59 – 7.54 (m, 2H), 7.31 (ddd, *J* = 7.6, 4.9, 1.2 Hz, 1H), 7.04 (d, *J* = 9.0 Hz, 2H), 6.92 (d, *J* = 8.7 Hz, 2H), 6.71 (d, *J* = 8.7 Hz, 2H), 3.49 (s, 2H).
**$^{13}$C NMR** (100.63 MHz, $CDCl_3$) δ 159.52 (C, Ar), 156.03 (C, Ar), 154.57 (C, Ar), 149.34 (CH, Ar), 148.23 (C, Ar), 147.42 (CH, Ar), 143.18 (C, Ar), 137.10 (CH, Ar), 136.14 (C, Ar), 134.95 (CH, Ar), 131.38 (C, Ar), 128.37 (CH, Ar), 123.76 (CH, Ar), 121.48 (CH, Ar), 121.16 (CH, Ar), 121.14 (CH, Ar), 117.75 (CH, Ar), 116.42 (CH, Ar).
**HRMS (ESI).** Calculated for $C_{22}H_{18}N_3O^+$: 340.144439 Obtained: 340.144701

### *10.1.2.10 Preparation of 1-(4-(4-([2,2'-bipyridin]-5-yl)phenoxy)phenyl)-3-(3,5-bis(trifluoromethyl)phenyl)thiourea (L3)*



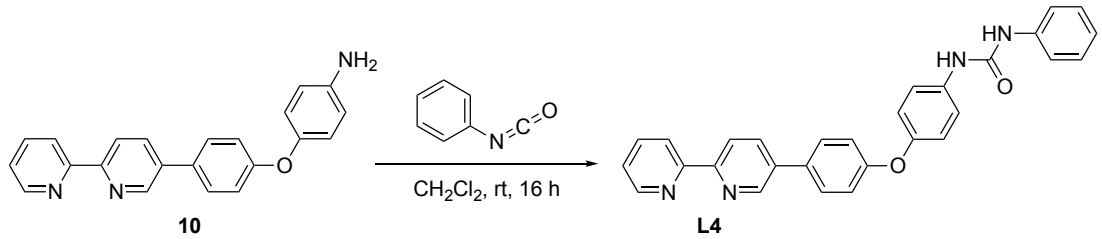

**10** **L3**

A mixture of **10** (50 mg, 0.15 mmol, 1.0 equiv.) and the corresponding isothiocyanate (80 mg, 0.3 mmol, 2 equiv.) in dichloromethane (2.0 mL) was stirred at room temperature for 24 hours. The solvent was removed, and the residue was purified by recrystallization with DCM/Hexane to obtain 71 mg of the desired product (79% yield).

**$^1$H NMR** (400.16 MHz, DMSO-$d_6$) δ 10.29 (s, 1H), 10.19 (s, 1H), 9.02 (dd, *J* = 2.4, 0.8 Hz, 1H), 8.71 (ddd, *J* = 4.8, 1.8, 0.9 Hz, 1H), 8.50 – 8.40 (m, 2H), 8.25 (dd, *J* = 5.0, 2.0 Hz, 3H), 8.02 – 7.92 (m, 1H), 7.86 (d, *J* = 8.7 Hz, 2H), 7.83 – 7.78 (m, 2H), 7.51 – 7.47 (m, 2H), 7.14 (dd, *J* = 17.5, 8.8 Hz, 4H).
**$^{13}$C NMR** (100.63 MHz, DMSO-$d_6$) δ 179.98, 157.30, 154.94, 153.88, 153.51, 149.38, 147.10, 141.86, 137.34, 136.16, 134.96, 134.84, 134.43, 131.71, 129.99 (q, *J* = 32.7 Hz), 128.59, 126.26, 124.17, 123.59 (d, *J* = 3.2 Hz), 123.24 (q, *J* = 274.1 Hz), 120.40 (d, *J* = 7.3 Hz), 119.40, 118.86, 117.06.
**$^{19}$F NMR** (376.46 MHz, DMSO-$d_6$) δ -61.49.
**HRMS (ESI).** Calculated for $C_{17}H_{12}F_3N_2^+$: 611.133478 Obtained: 611.133735

USC UNIVERSIDADE DE SANTIAGO DE COMPOSTELA

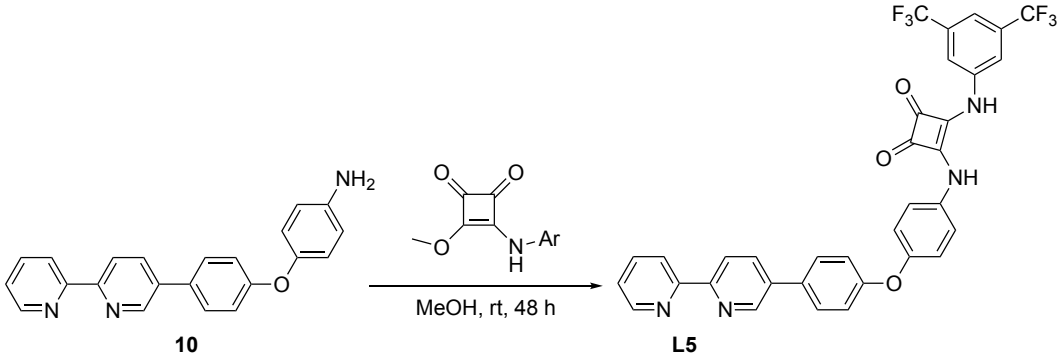
*10.1.2.11 Preparation of 1-(4-(4-([2,2'-bipyridin]-5-yl)phenoxy)phenyl)-3-phenylurea (L4)*




A mixture of **10** (50 mg, 0.13 mmol, 1.0 equiv.) and phenylisocyanate (0.03 mL, 0.3 mmol, 2 equiv.) in dichloromethane (2.0 mL) was stirred at room temperature for 24 hours. The solvent was removed, and the residue was purified by recrystallization with DCM/Hexane to obtain 46 mg of the desired product (68% yield).

**$^{1}$H NMR** (400.16 MHz, DMSO-$d_6$) δ 9.00 (s, 1H), 8.70 (d, *J* = 23.4 Hz, 4H), 8.44 (s, 2H), 8.23 (s, 1H), 7.97 (t, *J* = 7.7 Hz, 1H), 7.82 (d, *J* = 8.2 Hz, 2H), 7.52 (d, *J* = 8.6 Hz, 2H), 7.46 (d, *J* = 8.1 Hz, 2H), 7.29 (d, *J* = 7.7 Hz, 2H), 7.12 – 7.06 (m, 4H), 6.97 (t, *J* = 7.4 Hz, 1H).
**$^{13}$C NMR** (100.63 MHz, DMSO-$d_6$) δ 158.22 (CO), 154.90 (C, Ar), 153.73 (C, Ar), 152.59 (C, Ar), 150.14 (C, Ar), 149.29 (CH, Ar), 146.99 (CH, Ar), 139.71 (C, Ar), 137.32 (CH, Ar), 136.10 (C, Ar), 134.70 (CH, Ar), 131.03 (C, Ar), 128.75 (CH, Ar), 128.47 (CH, Ar), 127.87 (C, Ar), 124.13 (CH, Ar), 121.77 (CH, Ar), 120.41 (CH, Ar), 120.17 (CH, Ar), 119.92 (CH, Ar), 118.17 (CH, Ar), 117.97 (CH, Ar).
**HRMS (ESI).** Calculated for $C_{29}H_{23}N_4O_2^+$: 459.181552 Obtained: 459.181853

*10.1.2.12 Preparation of 3-((4-(4-([2,2'-bipyridin]-5-yl)phenoxy)phenyl)amino)-4-((3,5-bis(trifluoromethyl)phenyl)amino)cyclobut-3-ene-1,2-dione (L5)*



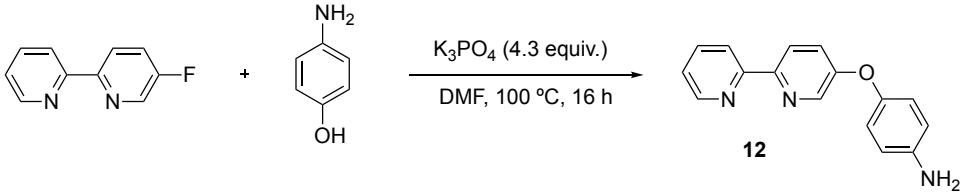

To a solution of **10** (50 mg, 0.15 mmol, 1 equiv.) in MeOH (0.5 mL), was added 3-((3,5-bis(trifluoromethyl)phenyl)amino)-4-methoxycyclobut-3-ene-1,2-dione (50 mg, 1.15 mml, 1 equiv.) at room temperature. The mixture was stirred at room temperature for 2 days.

After that time, the reaction mixture was then filtered, and the collected solid was washed with MeOH. The resulting white solid was dried under vacuum to obtain 86 mg of the desired compound (90% yield).

USC UNIVERSIDADE DE SANTIAGO DE COMPOSTELA

**$^{1}$H NMR** (400.16 MHz, DMSO-$d_6$, 333 K) δ 9.00 (d, *J* = 2.4 Hz, 1H), 8.71 (d, *J* = 4.7 Hz, 1H), 8.44 (dd, *J* = 14.4, 8.2 Hz, 2H), 8.21 (dd, *J* = 8.3, 2.3 Hz, 1H), 8.06 (s, 3H), 7.95 (td, *J* = 7.7, 1.8 Hz, 1H), 7.86 – 7.81 (m, 2H), 7.67 (s, 1H), 7.49 (dd, *J* = 8.7, 1.9 Hz, 2H), 7.46 (d, *J* = 6.1 Hz, 1H), 7.18 – 7.04 (m, 5H).
**$^{13}$C NMR** (100.63 MHz, DMSO-$d_6$, 333 K) δ 182.80 (CO), 181.98 (CO), 166.50 , 164.42, 157.35, 154.86, 153.78, 152.14, 149.04, 146.77, 140.89, 136.91, 134.76, 134.45, 134.22, 131.40, 131.09 (q, *J* = 33.1 Hz, C, Ar), 128.23, 123.74, 122.63 (q, *J* = 270.4 Hz, $CF_3$), 120.58, 120.19 (d, *J* = 6.6 Hz, CH, Ar), 119.88, 118.46 (d, *J* = 3.6 Hz, CH, Ar), 118.37, 116.01, 114.90.
**$^{19}$F NMR** (376.46 MHz, DMSO-$d_6$, 333 K) δ -61.76.
**HRMS (ESI).** Calculated for $C_{34}H_{21}F_6N_4O_3^+$: 647.151236 Obtained: 647.151212

### *10.1.2.13 Preparation of 4-([2,2'-bipyridin]-5-yloxy)aniline (12)*




**12**

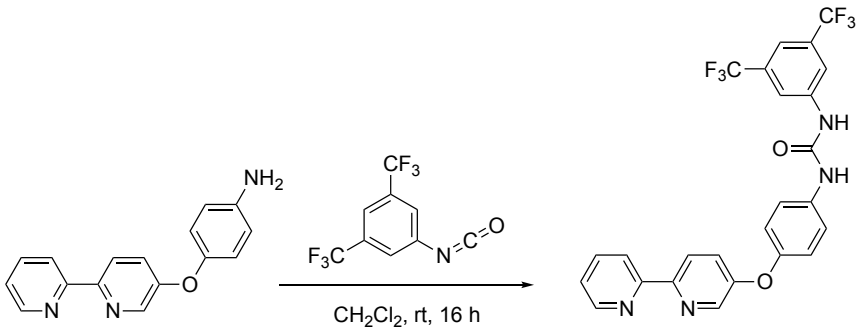
5-fluoro-2,2'-bipyridine (200 mg, 1.1 mmol, 1 equiv.) and 4-aminophenol (138 mg, 1.2 mmol, 1.1 equiv.) were dissolved in DMF (6 mL). To the mixture, $K_2CO_3$ (174 mg, 1.2 mmol, 1.1 equiv.) was added and the reaction was heated at reflux for 12 h.

After cooling to room temperature, $H_2O$ was poured into the mixture and extracted with EtOAc. The combined organic layers were washed with saturated aqueous NaCl solution, dried over anhydrous $MgSO_4$, filtered, and concentrated under reduced pressure. The crude product was purified by column chromatography to obtain 142 mg of the desired product (42% yield).

**$^{1}$H NMR** (400.16 MHz, $CDCl_3$) δ 8.63 (ddd, *J* = 4.8, 1.8, 0.9 Hz, 1H), 8.41 – 8.37 (m, 1H), 8.34 – 8.27 (m, 2H), 7.78 (td, *J* = 7.7, 1.8 Hz, 1H), 7.29 (dd, *J* = 8.8, 2.9 Hz, 1H), 7.26 (td, *J* = 4.9, 2.4 Hz, 1H), 6.94 – 6.88 (m, 2H), 6.70 (d, *J* = 8.7 Hz, 2H), 3.33 (s, 2H).
**$^{13}$C NMR** (100.63 MHz, $CDCl_3$) δ 155.96 (C, Ar), 155.91 (C, Ar), 150.09 (C, Ar), 149.16 (CH, Ar), 147.67 (C, Ar), 143.57 (C, Ar), 139.39 (CH, Ar), 137.06 (CH, Ar), 124.42 (CH, Ar), 123.25 (CH, Ar), 121.89 (CH, Ar), 121.23 (CH, Ar), 120.76 (CH, Ar), 116.45 (CH, Ar).
**HRMS (ESI).** Calculated for $C_{16}H_{14}N_3O^+$: 264.113139 Obtained: 264.113154

USC UNIVERSIDADE DE SANTIAGO DE COMPOSTELA

*10.1.2.14 Preparation of 1-(4-([2,2'-bipyridin]-5-yloxy)phenyl)-3-(3,5-bis(trifluoromethyl)phenyl)urea (L7)*

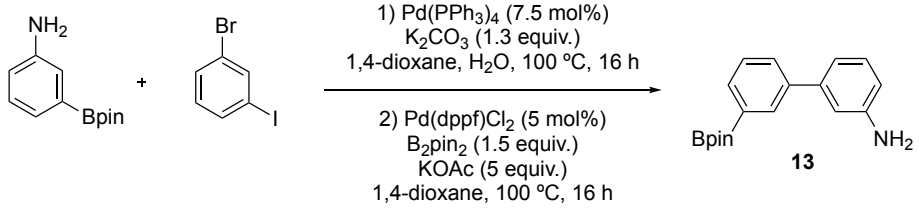



**12** **L7**

A mixture of **12** (44 mg, 0.16 mmol, 1.0 equiv.) and the corresponding isocyanate (58 µL, 0.3 mmol, 2 equiv.) in dichloromethane (1.0 mL) was stirred at room temperature for 24 hours. The solvent was removed, and the residue was purified by recrystallization with DCM/Hexane to obtain 59 mg of the desired product (80% yield).

**$^{1}$H NMR** (400.16 MHz, DMSO-$d_6$) δ 9.84 (s, 1H), 9.56 (s, 1H), 9.18 (s, 1H), 8.68 (d, *J* = 4.9 Hz, 1H), 8.48 (d, *J* = 2.9 Hz, 1H), 8.39 (d, *J* = 3.7 Hz, 1H), 8.17 (s, 1H), 8.14 (s, 1H), 8.02 (t, *J* = 7.7 Hz, 1H), 7.70 (s, 1H), 7.64 (s, 1H), 7.57 (d, *J* = 8.9 Hz, 2H), 7.50 (d, *J* = 5.7 Hz, 1H), 7.15 (d, *J* = 8.8 Hz, 2H).
**$^{13}$C NMR** (100.63 MHz, DMSO-$d_6$) δ 152.54, 150.17, 148.72, 147.38, 143.19, 141.90, 141.33, 139.60, 138.43, 135.84, 132.57, 131.37, 130.91, 130.58, 125.25, 124.68, 121.97, 120.77, 120.52, 120.07, 118.58, 117.93.
**$^{19}$F NMR** (376.46 MHz, DMSO-$d_6$) δ -61.62
**HRMS (ESI).** Calculated for $C_{25}H_{17}F_6N_4O_2^+$: 519.125021 Obtained: 519.125009

*10.1.2.15 Preparation of 3'-(4,4,5,5-tetramethyl-1,3,2-dioxaborolan-2-yl)-[1,1'-biphenyl]-3-amine (13)*




**13**

Step 1:

In a Schlenk flask equipped with a stirring bar, $Pd(PPh_3)_4$ (289.8 mg, 0.3 mmol, 0.1 equiv.), $K_2CO_3$ (820.1 mg, 5.9 mmol, 1.3 equiv.), 3-(4,4,5,5-tetramethyl-1,3,2-dioxaborolan-2-yl)aniline (1.0 g, 4.6 mmol, 1.0 equiv.), and 1-bromo-2-iodobenzene (582 µL, 4.6 mmol, 1.0 equiv.) were added. Subsequently, 90 mL of a 1,4-dioxane/$H_2O$ mixture (5:1) were added. The reaction mixture was heated to 100 ºC and stirred at the same temperature for 16 hours, with progress monitored by TLC.

USC UNIVERSIDADE DE SANTIAGO DE COMPOSTELA

After that time, the reaction was cooled to room temperature, filtered, and extracted with EtOAc (3 × 30 mL). The organic phase was dried over $MgSO_4$. Finally, the solvent was evaporated under reduced pressure, and the residue was purified by column chromatography on silica gel (Hexane/EtOAc 30:1 to 10:1). This afforded 3.3 g of the desired product as a brown oil (90% yield).

**$^1$H NMR** (400.16 MHz, $CDCl_3$) δ 7.75 (q, J = 1.8 Hz, 1H), 7.51 (t, J = 9.0 Hz, 2H), 7.36 – 7.25 (m, 2H), 7.00 (d, J = 7.9 Hz, 1H), 6.95 – 6.90 (m, 1H), 6.76 (d, J = 7.6 Hz, 1H).
**$^{13}$C NMR** (100.63 MHz, $CDCl_3$) δ 146.72 (C, Ar), 143.66 (C, Ar), 141.09 (C, Ar), 130.31 (CH, Ar), 130.29 (CH, Ar), 130.28 (CH, Ar), 129.99 (CH, Ar), 125.86 (CH, Ar), 122.90 (C, Ar), 117.86 (CH, Ar), 114.88(CH, Ar), 113.99 (CH, Ar).
**HRMS (ESI).** Calculated for $C_{12}H_{11}BrN^+$: 248.0069 Obtained: 248.0063

Step 2:

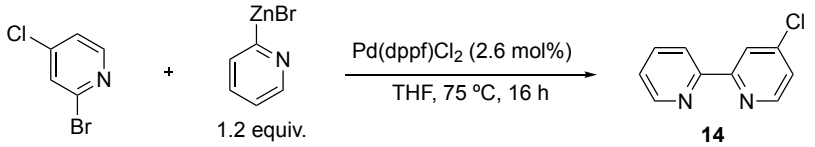
In a dry Schlenk flask equipped with a magnetic stir bar, $Pd(dppf)Cl_2$ (119.4 mg, 0.1 mmol, 0.05 equiv.), KOAc (1.4 g, 14.1 mmol, 5.0 equiv.), $B_2pin_2$ (1.1 g, 4.2 mmol, 1.5 equiv.), and 3'-bromo-[1,1'-biphenyl]-4-amine (700 mg, 2.8 mmol, 1.0 equiv.) were added. The flask was subjected to vacuum-$N_2$ cycles, and under a positive nitrogen flow, dry dioxane (8.0 mL) was added. The resulting mixture was heated to 100 ºC and stirred for 16 hours at the same temperature.

After this period, the reaction was cooled to room temperature and quenched with $H_2O$, then it was extracted with EtOAc (3 × 20 mL). The organic phase was dried over anhydrous $MgSO_4$. The solvent was evaporated under reduced pressure, and the crude product was purified by column chromatography on silica gel (Hexane/EtOAc from 30:1 to 10:1). This yielded the desired product in 83% yield.

**$^1$H NMR** (400.16 MHz, $CDCl_3$) δ 8.02 (s, 1H), 7.78 (d, *J* = 7.3 Hz, 1H), 7.66 (d, *J* = 7.7 Hz, 1H), 7.42 (dt, *J* = 7.7, 4.5 Hz, 1H), 7.21 (dt, *J* = 7.7, 4.4 Hz, 1H), 7.04 (d, *J* = 7.8 Hz, 1H), 6.97 (s, 1H), 6.68 (d, *J* = 7.9 Hz, 1H), 1.36 (d, *J* = 2.9 Hz, 12H).
**$^{13}$C NMR** (100.63 MHz, $CDCl_3$) δ 146.50 (C, Ar), 142.49 (C, Ar), 140.77 (C, Ar), 133.78 (CH, Ar), 133.60 (CH, Ar), 130.10 (CH, Ar), 129.72 (CH, Ar), 128.21 (CH, Ar), 118.12 (CH, Ar), 114.32 (CH, Ar), 114.30 (CH, Ar), 83.99 (C), 25.03 ($CH_3$).
**$^{11}$B NMR** (128.39 MHz, $CDCl_3$) δ 30.99.
**HRMS (ESI).** Calculated for $C_{18}H_{23}BNO_2^+$: 296.1816 Obtained: 296.1814

USC UNIVERSIDADE DE SANTIAGO DE COMPOSTELA

*10.1.2.16 Preparation of 4-chloro-2,2'-bipyridine (14)*

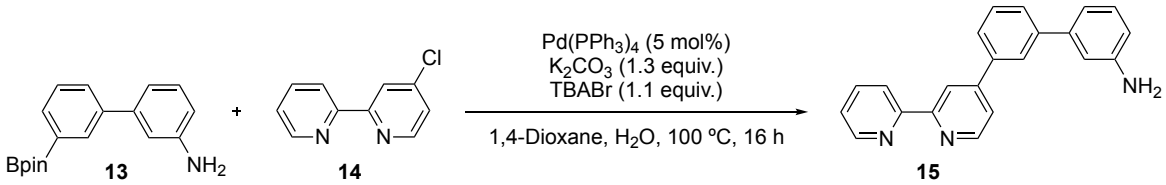



Prepared using an adapted procedure:[135] Under a nitrogen ($N_2$) atmosphere, Pd(dppf)$Cl_2$ (98.6 mg, 0.1 mmol, 0.03 equiv.) and 2-bromo-4-chloropyridine (4.4 mmol, 1.0 equiv.) were added to a dry round-bottom flask. Then, 2-pyridylzinc bromide in THF (10.6 mL, 5.3 mmol, 1.2 equiv.) was added, and the mixture was heated to 75 ºC and stirred at the same temperature for 18 hours.

After this period, the reaction was poured into a saturated 1:1 EDTA/$Na_2CO_3$ solution (500 mL), and the mixture was stirred until the white solid formed turned completely yellow. DCM was added to the mixture to dissolve the yellow solid and the aqueous phase was extracted with DCM (3 × 100 mL). The organic phase was dried over anhydrous $Na_2SO_4$ and the solvent was evaporated under reduced pressure. This yielded 400 mg of the desired product (51% yield).

**$^1$H NMR** (400.16 MHz, $CDCl_3$) δ 8.71 – 8.66 (m, 1H), 8.60 – 8.53 (m, 1H), 8.46 (t, *J* = 2.4 Hz, 1H), 8.40 (d, *J* = 8.0 Hz, 1H), 7.83 (t, *J* = 7.6 Hz, 1H), 7.38 – 7.29 (m, 2H).
**$^{13}$C NMR** (100.63 MHz, $CDCl_3$) δ 157.71 (C, Ar), 154.94 (C, Ar), 150.12 (CH, Ar), 149.36 (CH, Ar), 145.45 (C, Ar), 137.28 (CH, Ar), 124.47 (CH, Ar), 124.07 (CH, Ar), 121.70 (CH, Ar), 121.55 (CH, Ar).
**HRMS (ESI).** Calculated for $C_{10}H_8ClN_2^+$: 191.0371 Obtained: 191.0368

*10.1.2.17 Preparation of 3'-([2,2'-bipyridin]-4-yl)-[1,1'-biphenyl]-3-amine (15)*




In a Schlenk flask equipped with a stirring bar, Pd($PPh_3$)$_4$ (19.6 mg, 0.017 mmol, 0.050 equiv.), $K_2CO_3$ (60.9 mg, 0.440 mmol, 1.3 equiv.), 3'-(4,4,5,5-tetramethyl-1,3,2-dioxoborolan-2-yl)-[1,1'-biphenyl]-3-amine (100 mg, 0.339 mmol, 1.0 equiv.), TBABr (16) (120.1 mg, 0.373 mmol, 1.1 equiv.), and **14** (64.6 mg, 0.339 mmol, 1.0 equiv.) were added. The flask was subjected to cycles of vacuum-$N_2$, and a deoxygenated mixture of 1,4-dioxane (3.4 mL) and $H_2O$ (0.2 ml) was added to the Schlenk flask.

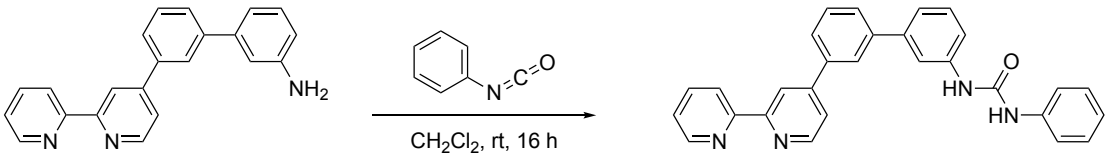
The resulting mixture was heated to 100 ºC and stirred at the same temperature for 16 hours. After this period, the reaction was quenched with water and the mixture was cooled to room temperature and. Then, the mixture was extracted with EtOAc (3 × 30 mL), and the organic phase was dried over anhydrous $MgSO_4$. The solvent was removed under

[135] a) Kim, S.; Rieke, R. D. *Tetrahedron* **2010,** *66,* 3135–3146., b) Wang; Shaffer; Manbeck; Polyansky; Concepcion *ACS Catal.* **2020,** *10,* 580–585.

reduced pressure, and the crude product was purified by column chromatography (DCM/MeOH from 0% to 10%). The desired product was obtained as a yellow oil (166.0 mg, 67% yield).

**$^{1}$H NMR** (400.16 MHz, $CDCl_3$) δ 8.74 (dd, *J* = 5.1, 0.8 Hz, 1H), 8.72 (dd, *J* = 1.9, 0.8 Hz, 2H), 8.46 (dt, *J* = 8.0, 1.1 Hz, 1H), 7.95 – 7.91 (m, 1H), 7.84 (td, *J* = 7.7, 1.8 Hz, 1H), 7.72 (ddd, *J* = 7.7, 1.9, 1.1 Hz, 1H), 7.64 (ddd, *J* = 7.7, 1.8, 1.2 Hz, 1H), 7.59 (dd, *J* = 5.1, 1.9 Hz, 1H), 7.54 (t, *J* = 7.7 Hz, 1H), 7.33 (ddd, *J* = 7.5, 4.8, 1.2 Hz, 1H), 7.26 (t, *J* = 7.8 Hz, 1H), 7.05 (ddd, *J* = 7.6, 1.7, 1.0 Hz, 1H), 6.97 (t, *J* = 2.0 Hz, 1H), 6.72 (ddd, *J* = 7.9, 2.4, 1.0 Hz, 1H), 3.82 (s, 2H).
**$^{13}$C NMR** (100.63 MHz, $CDCl_3$) δ 156.83 (C, Ar), 156.29 (C, Ar), 149.81 (CH, Ar), 149.56 (C, Ar), 149.32 (CH, Ar), 146.99 (C, Ar), 142.49 (C, Ar), 142.08 (C, Ar), 138.89 (C, Ar), 137.11 (CH, Ar), 129.94 (CH, Ar), 129.48 (CH, Ar), 127.96 (CH, Ar), 126.17 (CH, Ar), 126.12 (CH, Ar), 123.95 (CH, Ar), 121.88 (CH, Ar), 121.46 (CH, Ar), 119.31 (CH, Ar), 117.87 (CH, Ar), 114.56 (CH, Ar), 114.09 (CH, Ar).
**HRMS (ESI).** Calculated for $C_{22}H_{17}N_3^+$: 324.1500 Obtained: 324.1493

### *10.1.2.18 Preparation of 1-(3'-([2,2'-bipyridin]-4-yl)-[1,1'-biphenyl]-3-yl)-3-phenylurea (L8)*



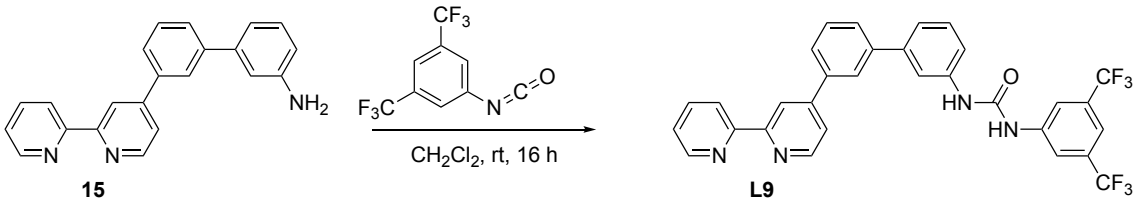

**15** **L8**

To a solution of **15** (50.0 mg, 0.2 mmol, 1.0 equiv.) in DCM (2.3 mL), phenylisocyanate (34.0 µL, 0.3 mmol, 2.0 equiv.) was added. The mixture was stirred at room temperature for 16 hours. After this period, the crude product was purified by recrystallization in DCM/Hexane, obtaining 44 mg of the desired product in 65% yield.

**$^{1}$H NMR** (400.16 MHz, DMSO-$d_6$) δ 8.80 (q, *J* = 3.4 Hz, 2H), 8.73 (s, 3H), 8.50 – 8.42 (m, 1H), 8.01 (d, *J* = 17.5 Hz, 2H), 7.88 (d, *J* = 6.3 Hz, 3H), 7.77 (d, *J* = 8.1 Hz, 1H), 7.47 (d, *J* = 7.7 Hz, 5H), 7.41 (s, 1H), 7.31 – 7.25 (m, 3H), 6.97 (t, *J* = 8.3 Hz, 1H).
**$^{13}$C NMR** (100.63 MHz, DMSO-$d_6$) δ 155.92 (C, Ar), 155.06 (C, Ar), 152.42 (CO), 149.76 (CH, Ar), 149.02 (CH, Ar), 148.06 (C, Ar), 141.24 (C, Ar), 140.20 (C, Ar), 140.13 (C, Ar), 139.42 (C, Ar), 138.00 (C, Ar), 136.99 (CH, Ar), 129.67 (CH, Ar), 129.13 (CH, Ar), 128.44 (CH, Ar), 127.40 (CH, Ar), 125.79 (CH, Ar), 124.85 (CH, Ar), 123.96 (CH, Ar), 121.66 (CH, Ar), 121.53 (CH, Ar), 120.48 (CH, Ar), 120.39 (CH, Ar), 118.22 (CH, Ar), 117.66 (CH, Ar), 117.59 (CH, Ar), 116.66 (CH, Ar).
**HRMS (ESI).** Calculated for $C_{29}H_{22}N_4O^+$: 443.1866 Obtained: 443.1862

USC UNIVERSIDADE DE SANTIAGO DE COMPOSTELA

*10.1.2.19 Preparation of 1-(3'-([2,2'-bipyridin]-4-yl)-[1,1'-biphenyl]-3-yl)-3-(3,5-bis(trifluoromethyl)phenyl)urea (L9)*




**15** **L9**

To a solution of **15** (50 mg, 0.155 mmol, 1.0 equiv.) in DCM (2.3 mL), the corresponding isocyanate (53 µL, 0.309 mmol, 2.0 equiv.) was added. The mixture was stirred at room temperature for 16 hours. After this period, the crude product was purified by recrystallization in DCM/hexane, obtaining 38 mg of the desired product (53% yield).

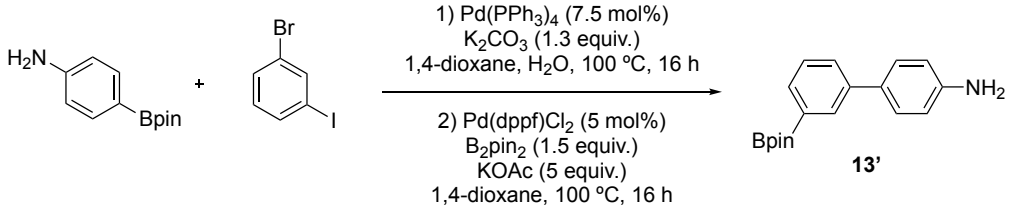
**$^{1}$H NMR** (400.16 MHz, DMSO-$d_6$) δ 9.46 (s, 1H), 9.11 (s, 1H), 8.78 (dd, *J* = 5.1, 0.8 Hz, 1H), 8.72 (dd, *J* = 2.0, 0.8 Hz, 2H), 8.45 (dt, *J* = 8.0, 1.1 Hz, 1H), 8.16 – 8.14 (m, 2H), 8.03 (t, *J* = 1.8 Hz, 1H), 8.00 – 7.96 (m, 1H), 7.88 (td, *J* = 2.6, 1.5 Hz, 3H), 7.86 (dd, *J* = 1.9, 1.1 Hz, 1H), 7.77 (ddd, *J* = 7.8, 1.8, 1.1 Hz, 1H), 7.70 – 7.63 (m, 2H), 7.53 (ddd, *J* = 5.4, 3.4, 2.1 Hz, 1H), 7.48 (ddd, *J* = 7.5, 4.7, 1.2 Hz, 1H), 7.46 – 7.44 (m, 2H).

**$^{13}$C NMR** (100.63 MHz, DMSO-$d_6$) δ 156.00 (C, Ar), 155.12 (C, Ar), 152.52 (CO), 150.05 (CH, Ar), 149.28 (CH, Ar), 148.22 (C, Ar), 141.84 (C, Ar), 141.27 (C, Ar), 140.45 (C, Ar), 139.66 (C, Ar), 138.16 (C, Ar), 137.37 (CH, Ar), 130.70 (C, Ar, q, *J* = 32.6 Hz), 127.74 (CH, Ar), 126.16 (CH, Ar), 125.15 (CH, Ar), 124.66 (CH, Ar), 123.30 (C, q, *J* = 272.7 Hz) 121.95 (CH, Ar), 121.90 (CH, Ar), 121.36 (CH, Ar) , 120.69 (CH, Ar), 118.42 (CH, Ar), 118.07 (CH, Ar), 118.05 (CH, Ar, q, *J* = 3.6 Hz),117.99 (CH, Ar), 117.83 (CH, Ar), 114.42 (CH, Ar, q, *J* = 4.2 Hz).

**$^{19}$F NMR** (376.46 MHz, DMSO-$d_6$) δ -61.40.

**HRMS (ESI).** Calculated for $C_{31}H_{21}F_6N_4O^+$: 579.1627 Obtained: 579.1614

*10.1.2.20 Preparation of 3'-(4,4,5,5-tetramethyl-1,3,2-dioxaborolan-2-yl)-[1,1'-biphenyl]-4-amine (13')*




**13'**

Step 1:

In a Schlenk flask equipped with a magnetic stir bar, $Pd(PPh_3)_4$ (263 mg, 0.2 mmol, 0.05 equiv.), $K_2CO_3$ (820 mg, 5.9 mmol, 1.3 equiv.), 4-(4,4,5,5-tetramethyl-1,3,2-dioxaborolan-2-yl)aniline (1 g, 4.5 mmol, 1 equiv.), and 1-bromo-2-iodobenzene (582 µL, 4. mmol, 1 equiv.) were added. Subsequently, 90 mL of a 1,4-dioxane/$H_2O$ mixture (5:1) were added. The reaction mixture was heated to 100 ºC and stirred at the same temperature for 16 hours, with progress monitored by TLC.

After this time the reaction was cooled to room temperature and water was added. The mixture was filtered and extracted with EtOAc (3 x 30 mL). The combined organic phases were dried over $MgSO_4$. Finally, the solvent was removed under reduced pressure, and the residue was purified by column chromatography on silica gel using a gradient of Hexane/EtOAc from 70:30 to 50:50. The product was obtained as a brown oil (730 mg, 57% yield).

**$^1$H NMR** (400.16 MHz, $CDCl_3$) δ 8.02 – 7.96 (m, 1H), 7.72 (dt, *J* = 7.3, 1.2 Hz, 1H), 7.64 (ddd, *J* = 7.8, 2.1, 1.3 Hz, 1H), 7.48 – 7.44 (m, 2H), 7.41 (ddd, *J* = 7.8, 7.3, 0.6 Hz, 1H), 6.80 – 6.75 (m, 2H), 1.36 (s, 12H).
**$^{13}$C NMR** (100.63 MHz, $CDCl_3$) δ 145.49 (C, Ar), 140.54 (C, Ar), 132.90 (CH, Ar), 132.87 (CH, Ar), 131.93 (C, Ar), 129.44 (CH, Ar), 128.26 (CH, Ar), 128.22 (CH, Ar), 115.68 (CH, Ar), 83.94 (C), 25.02 ($CH_3$).
**HRMS (ESI).** Calculated for $C_{18}H_{23}BNO_2^+$: 296.1820 Obtained: 296.1815

Step 2:

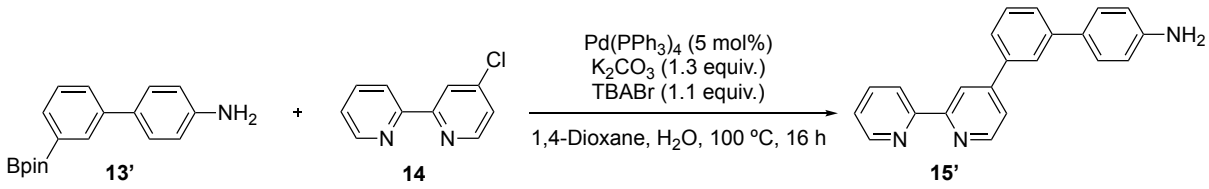
In a dry Schlenk flask equipped with a magnetic stir bar, $Pd(dppf)Cl_2$ (119.4 mg, 0.1 mmol, 0.05 equiv.), KOAc (1.38 g, 14.1 mmol, 5.0 equiv.), $B_2pin_2$ (12) (1.07 g, 4.2 mmol, 1.5 equiv.), and 3'-bromo-[1,1'-biphenyl]-4-amine (700 mg, 2.8 mmol, 1.0 equiv.) were added. The flask was subjected to vacuum-$N_2$ cycles, and under a nitrogen flow, dry 1,4-dioxane (3.5 mL) was added. The resulting mixture was stirred at 100 ºC for 16 hours.

After this time the reaction was cooled to room temperature and water was added. The mixture was extracted with EtOAc (3 × 20 mL), the organic phase was dried over $MgSO_4$, and the solvent was evaporated under reduced pressure. The crude product was purified by column chromatography on silica gel (Hexane/EtOAc from 95:5 to 70:30). This yielded 400 mg of the desired product as a black oil (62% yield).

**$^1$H NMR** (400.16 MHz, $CDCl_3$) δ 8.02 – 7.96 (m, 1H), 7.72 (dt, *J* = 7.3, 1.2 Hz, 1H), 7.64 (ddd, *J* = 7.8, 2.1, 1.3 Hz, 1H), 7.48 – 7.44 (m, 2H), 7.41 (ddd, *J* = 7.8, 7.3, 0.6 Hz, 1H), 6.80 – 6.75 (m, 2H), 1.36 (s, 12H).
**$^{13}$C NMR** (100.63 MHz, $CDCl_3$) δ 145.49 (C, Ar), 140.54 (C, Ar), 132.90 (CH, Ar), 132.87 (CH, Ar), 131.93 (C, Ar), 129.44 (CH, Ar), 128.26 (CH, Ar), 128.22 (CH, Ar), 115.68 (CH, Ar), 83.94 (C), 25.02 ($CH_3$).
**HRMS (ESI).** Calculated for $C_{18}H_{23}BNO_2^+$: 296.1820 Obtained: 296.1815

USC UNIVERSIDADE DE SANTIAGO DE COMPOSTELA

*10.1.2.21 Preparation of 3'-([2,2'-bipyridin]-4-yl)-[1,1'-biphenyl]-4-amine (15')*

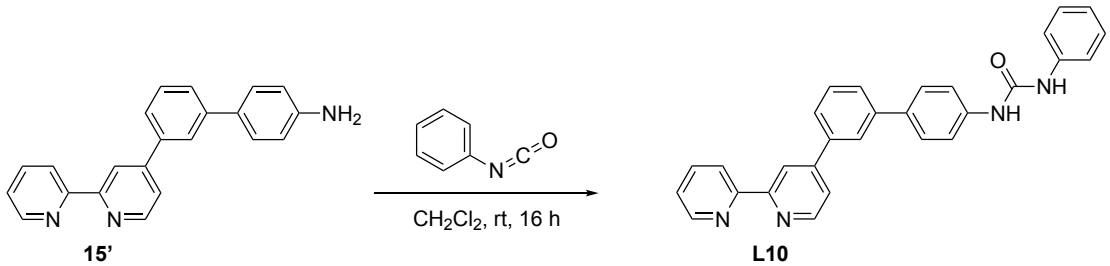



In a Schlenk flask equipped with a stirring bar, $Pd(PPh_3)_4$ (19.6 mg, 0.017 mmol, 0.050 equiv.), $K_2CO_3$ (60.9 mg, 0.4 mmol, 1.3 equiv.), 3'-(4,4,5,5-tetramethyl-1,2,3-dioxaborolan-2-yl)-[1,1'-biphenyl]-4-amine (100 mg, 0.3 mmol, 1.0 equiv.), TBABr (16) (120.1 mg, 0.4 mmol, 1.1 equiv.), and **14** (64.6 mg, 0.3 mmol, 1.0 equiv.) were added. The flask was subjected to three cycles of vacuum-$N_2$, a deoxygenated mixture of 1,4-dioxane (3.4 mL) and $H_2O$ (0.2 ml), was added to the Schlenk flask. The resulting mixture was heated to 100 ºC and stirred at the same temperature for 16 hours.

After this time the reaction was cooled to room temperature and water was added. The mixture was extracted with EtOAc (3 × 20 mL), and the organic phase was dried over anhydrous $MgSO_4$. The solvent was removed under reduced pressure, and the crude product was purified by column chromatography ($CH_2Cl_2$/MeOH from 0% to 10%). The desired product was obtained as a yellow oil (56.6 mg, 51% yield).

**$^1$H NMR** (400.16 MHz, $CDCl_3$) δ 8.74 (dd, *J* = 5.1, 0.8 Hz, 1H), 8.72 (ddt, *J* = 4.0, 2.1, 1.1 Hz, 2H), 8.46 (dt, *J* = 8.0, 1.1 Hz, 1H), 7.91 – 7.89 (m, 1H), 7.84 (ddd, *J* = 8.0, 7.5, 1.8 Hz, 1H), 7.66 (ddd, *J* = 7.6, 1.9, 1.2 Hz, 1H), 7.63 – 7.57 (m, 2H), 7.53 (dd, *J* = 7.7, 0.5 Hz, 1H), 7.51 – 7.47 (m, 2H), 7.33 (ddd, *J* = 7.5, 4.8, 1.2 Hz, 1H), 6.81 – 6.77 (m, 2H).
**$^{13}$C NMR** (100.63 MHz, $CDCl_3$) δ 156.79 (C, Ar), 156.33 (C, Ar), 149.79 (C, Ar), 149.77 (CH, Ar), 149.33 (CH, Ar), 146.34 (C, Ar), 142.23 (C, Ar), 138.94 (C, Ar), 137.10 (CH, Ar), 131.13 (C, Ar), 129.50 (CH, Ar), 128.32 (CH, Ar), 127.27 (CH, Ar), 125.40 (CH, Ar), 125.25 (CH, Ar), 123.93 (CH, Ar), 121.93 (CH, Ar), 121.46 (CH, Ar), 119.35 (CH, Ar), 115.56 (CH, Ar).
**HRMS (ESI).** Calculated for $C_{22}H_{17}N_3^+$: 324.1495 Obtained: 324.1493

*10.1.2.22 Preparation of (L10)*

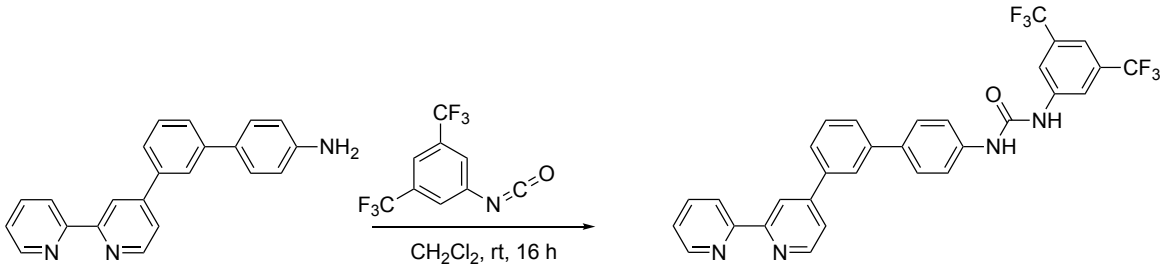



To a solution of **15'** (50.0 mg, 0.2 mmol, 1.0 equiv.) in DCM (2.3 mL), was added phenylisocyanate (34.0 µL, 0.3 mmol, 2.0 equiv.) The mixture was stirred at room temperature for 16 hours. After this period, the product was purified by recrystallization in DCM/hexane, obtaining 21 mg of the desired product (30% yield).

USC UNIVERSIDADE DE SANTIAGO DE COMPOSTELA

**$^{1}$H NMR** (400.16 MHz, DMSO-$d_6$) δ 8.78 (d, *J* = 5.1 Hz, 1H), 8.73 (d, *J* = 3.8 Hz, 3H), 8.60 (s, 1H), 8.46 (d, *J* = 7.9 Hz, 1H), 8.09 – 8.03 (m, 1H), 7.98 (td, *J* = 7.7, 1.7 Hz, 1H), 7.86 (dd, *J* = 5.1, 1.9 Hz, 1H), 7.82 – 7.71 (m, 4H), 7.68 – 7.56 (m, 3H), 7.54 – 7.42 (m, 3H), 7.34 – 7.26 (m, 2H), 6.99 (tt, *J* = 7.3, 1.2 Hz, 1H).
**$^{13}$C NMR** (100.63 MHz, DMSO-$d_6$) δ 155.87 (C, Ar), 155.10 (C, Ar), 152.27 (CO), 149.69 (CH, Ar), 149.01 (CH, Ar), 148.17 (C, Ar), 140.77 (C, Ar), 139.41 (C, Ar), 139.36 (C, Ar), 137.95 (C, Ar), 136.96 (CH, Ar), 132.94 (C, Ar), 129.56 (CH, Ar), 128.45 (CH, Ar), 128.43 (CH, Ar), 127.03 (CH, Ar), 126.85 (CH, Ar), 125.07 (CH, Ar), 124.36 (CH, Ar), 123.93 (CH, Ar), 121.66 (CH, Ar), 121.56 (CH, Ar), 120.48 (CH, Ar), 118.43 (CH, Ar), 118.17 (CH, Ar), 117.70 (CH, Ar).
**HRMS (ESI).** Calculated for $C_{29}H_{22}N_4O^+$: 443.1866 Obtained: 443.1863

### *10.1.2.23 Preparation of 1-(3'-([2,2'-bipyridin]-4-yl)-[1,1'-biphenyl]-4-yl)-3-(3,5-bis(trifluoromethyl)phenyl)urea (L11)*



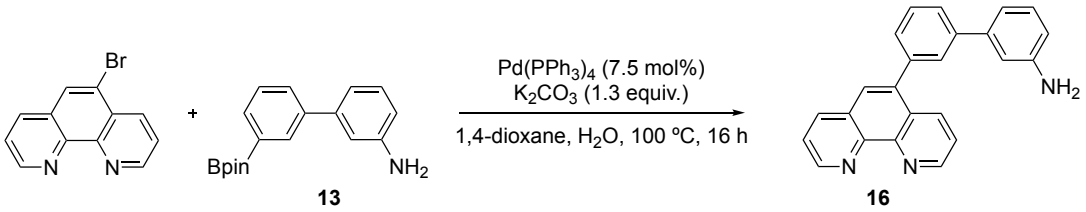

**15'** **L11**

To a solution of **15'** (50 mg, 0.155 mmol, 1.0 equiv.) in DCM (2.3 mL),was added the corresponding isocyanate (53 µL, 0.309 mmol, 2.0 equiv.). The mixture was stirred at room temperature for 16 hours. After this period, the product was purified by recrystallization in DCM/hexane, obtaining 38 mg of the desired product in (53% yield).

**$^{1}$H NMR** (400.16 MHz, DMSO-$d_6$) δ 9.44 (s, 1H), 9.15 (s, 1H), 8.78 (dd, *J* = 5.1, 0.8 Hz, 1H), 8.74 – 8.71 (m, 2H), 8.45 (dt, *J* = 8.0, 1.1 Hz, 1H), 8.16 – 8.14 (m, 2H), 8.06 (t, *J* = 1.8 Hz, 1H), 8.01 – 7.96 (m, 1H), 7.89 (dd, *J* = 5.1, 1.9 Hz, 1H), 7.82 – 7.75 (m, 4H), 7.65 – 7.60 (m, 4H), 7.49 (ddd, *J* = 7.5, 4.8, 1.2 Hz, 1H).
**$^{13}$C NMR** (100.63 MHz, DMSO-$d_6$) δ 155.85 (C, Ar), 155.05 (C, Ar), 152.44 (CO), 152.38 (CH, Ar), 149.95 (CH, Ar), 149.27 (CH, Ar), 148.43 (C, Ar), 141.82 (C, Ar), 141.31 (C, Ar), 140.81 (C, Ar), 138.89 (C, Ar), 138.09 (C, Ar), 137.43 (CH, Ar), 133.74 (CH, Ar), 130.71 (C, Ar, q, *J* = 32.7 Hz), 129.91 (CH, Ar), 127.25 (CH, Ar), 125.52 (CH, Ar), 124.71 (CH, Ar), 123.26 (C, q, *J* = 272.8 Hz), 124.36 (CH, Ar), 121.96 (CH, Ar), 120.74 (CH, Ar), 119.17 (CH, Ar), 118.65 (CH, Ar, d, *J* = 3.6 Hz), 118.02 (CH, Ar, d, *J* = 4.2 Hz), 117.92 (CH, Ar), 115.08 (CH, Ar, dt *J* = 7.5, 3.6 Hz), 114.40 (CH, Ar, q, *J* = 5.3 Hz).
**$^{19}$F NMR** (376.46 MHz, DMSO-$d_6$) δ -61.63.
**HRMS (ESI).** Calculated for $C_{31}H_{21}F_6N_4O^+$: 579.1633 Obtained: 579.1614

USC UNIVERSIDADE DE SANTIAGO DE COMPOSTELA

*10.1.2.24 Preparation of 3'-(1,10-phenanthrolin-5-yl)-[1,1'-biphenyl]-3-amine (16)*



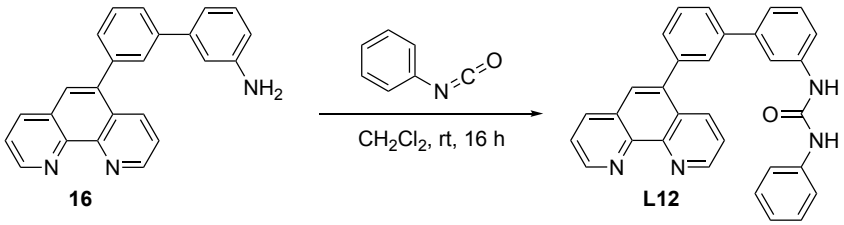

In a Schlenk flask equipped with a stirring bar, $Pd(dppf)Cl_2$ (21.5 mg, 0.03 mmol, 0.075 equiv.), $K_2CO_3$ (60.9 mg, 0.4 mmol, 1.3 equiv.), 3'-(4,4,5,5-tetramethyl-1,3,2-dioxaborolan-2-yl)-[1,1'-biphenyl]-3-amine (100 mg, 0.3 mmol, 1.0 equiv.), and 5-bromo-1,10-phenanthroline (87.8 mg, 0.3 mmol, 1.0 equiv.) were added. Then, 90 mL of a 1,4-dioxane/$H_2O$ mixture (5:1) was added. The resulting mixture was heated to 100 ºC and stirred at the same temperature while the reaction progress was monitored by TLC.

Afterward, water was added to the mixture and, after it cooled down to room temperature, it was extracted with EtOAc (3 × 30.mL). The organic phase was dried over anhydrous $MgSO_4$. Finally, the solvent was removed, and the crude product was purified by column chromatography on silica gel (DCM/(MeOH, $NH_4OH$ 10%) from 30:1 to 10:1). The desired product was obtained as a brown oil in 90% yield.

**$^1$H NMR** (400.16 MHz, $CDCl_3$) δ 9.22 (ddd, J = 4.3, 1.8, 0.7 Hz, 2H), 8.35 (dd, J = 8.4, 1.7 Hz, 1H), 8.27 (dd, J = 8.1, 1.8 Hz, 1H), 7.80 (s, 1H), 7.73 (dt, J = 1.8, 1.0 Hz, 1H), 7.67 (dd, J = 8.0, 4.3 Hz, 1H), 7.60 (ddd, J = 8.4, 4.5, 2.5 Hz, 2H), 7.51 – 7.48 (m, 1H), 7.43 – 7.37 (m, 1H), 7.28 – 7.23 (m, 1H), 7.06 (ddd, J = 7.7, 1.7, 1.0 Hz, 1H), 6.98 (t, J = 2.0 Hz, 1H), 6.71 (ddd, J = 7.9, 2.4, 1.0 Hz, 1H), 2.00 (s, 2H).

**$^{13}$C NMR** (100.63 MHz, $CDCl_3$) δ 150.46 (CH, Ar), 150.26 (CH, Ar), 147.03 (C, Ar), 146.59 (C, Ar), 145.96 (C, Ar), 141.96 (C, Ar), 139.40 (C, Ar), 139.03 (C, Ar), 136.13 (CH, Ar), 131.83 (CH, Ar), 131.80 (CH, Ar), 131.49 (CH, Ar), 131.39 (CH, Ar), 130.02 (C, Ar), 129.11 (CH, Ar), 128.94 (CH, Ar), 128.82 (CH, Ar), 128.49 (CH, Ar), 128.37 (CH, Ar), 128.26 (CH, Ar), 128.09 (CH, Ar), 126.89 (C, Ar), 126.70 (C, Ar), 123.54 (CH, Ar), 123.04 (CH, Ar), 117.80 (CH, Ar), 114.58 (CH, Ar), 113.98 (CH, Ar).
**HRMS (ESI).** Calculated for $C_{24}H_{18}N_3^+$: 348.1495 Obtained: 348.1489

*10.1.2.25 Preparation of 1-(3'-(1,10-phenanthrolin-5-yl)-[1,1'-biphenyl]-3-yl)-3-phenylurea (L12)*



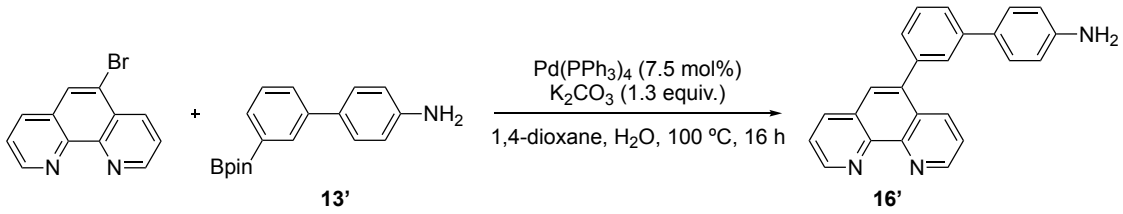

To a solution of **16** (67.9 mg, 0.2 mmol, 1.0 equiv.) in DCM (3.0 mL) was added phenylisocyanate (46.6 mg, 0.4 mmol, 2.0 equiv.) at room temperature. The mixture was

USC UNIVERSIDADE DE SANTIAGO DE COMPOSTELA

stirred at this temperature for 16 hours. After this period, the crude product was purified by recrystallization in DCM/Hexane, yielding the desired product in 89% yield.

**$^1$H NMR** (400.16 MHz, DMSO-$d_6$) δ 9.14 (td, *J* = 4.5, 1.7 Hz, 2H), 8.69 (s, 1H), 8.60 (s, 1H), 8.52 (dd, *J* = 8.1, 1.8 Hz, 1H), 8.32 (dd, *J* = 8.4, 1.7 Hz, 1H), 8.04 (s, 1H), 7.90 (s, 1H), 7.80 (dd, *J* = 4.1, 1.9 Hz, 3H), 7.78 – 7.73 (m, 1H), 7.70 (t, *J* = 7.9 Hz, 1H), 7.58 (dd, *J* = 7.6, 1.5 Hz, 1H), 7.47 – 7.43 (m, 3H), 7.40 – 7.38 (m, 1H), 7.26 (t, *J* = 7.9 Hz, 3H), 7.00 – 6.93 (m, 1H).
**$^{13}$C NMR** (100.63 MHz, DMSO-$d_6$) δ 152.41 (CO), 149.77 (CH, Ar), 149.44 (CH, Ar), 145.68 (C, Ar), 144.99 (C, Ar), 140.60 (C, Ar), 140.17 (C, Ar), 140.15 (C, Ar), 139.40 (C, Ar), 138.87 (C, Ar), 137.72 (C, Ar), 135.95 (CH, Ar), 133.67 (CH, Ar), 129.11 (CH, Ar), 129.01 (CH, Ar), 128.69 (CH, Ar), 128.53 (CH, Ar), 128.42 (CH, Ar), 127.74 (CH, Ar), 127.66 (C, Ar), 127.06 (C, Ar), 126.58 (CH, Ar), 126.06 (CH, Ar), 123.29 (CH, Ar), 122.96 (CH, Ar), 121.63 (CH, Ar), 120.30 (CH, Ar), 118.19 (CH, Ar), 118.09 (CH, Ar), 117.54 (CH, Ar), 116.63 (CH, Ar).
**HRMS (ESI).** Calculated for $C_{31}H_{23}N_4O^+$: 467.1866 Obtained: 467.1860

### *10.1.2.26 Preparation of 3'-(1,10-phenanthrolin-5-yl)-[1,1'-biphenyl]-4-amine (16')*



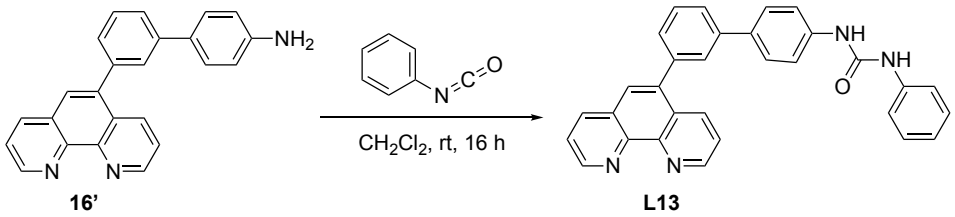

In a Schlenk flask equipped with a stirring bar, Pd(dppf)$Cl_2$ (58.0 mg, 0.07 mmol, 0.075 equiv.), $K_2CO_3$ (164.0 mg, 1.2 mmol, 1.3 equiv.), 3'-(4,4,5,5-tetramethyl-1,3,2-dioxaborolan-2-yl)-[1,1'-biphenyl]-4-amine (269.5 mg, 0.9 mmol, 1.0 equiv.), and 5-bromo-1,10-phenanthroline (236.5 mg, 0.9 mmol, 1.0 equiv.) were added. Then, 90 mL of a 1,4-dioxane/$H_2O$ mixture (5:1) was added. The resulting mixture was heated to 100 ºC and stirred at the same temperature while the reaction progress was monitored by TLC.

Afterward, water was added to the mixture and, after it cooled down to room temperature, it was extracted with EtOAc (3 × 30 mL). The organic phase was dried over anhydrous $MgSO_4$. Finally, the solvent was removed, and the crude product was purified by column chromatography on silica gel (DCM/(MeOH, $NH_4OH$ 10%) from 30:1 to 10:1). The product was obtained as a brown oil in 84% yield.

**$^1$H NMR** (400.16 MHz, $CDCl_3$) δ 9.23 (dt, *J* = 4.4, 1.4 Hz, 2H), 8.37 (dd, *J* = 8.4, 1.7 Hz, 1H), 8.28 (dd, *J* = 8.1, 1.8 Hz, 1H), 7.81 (s, 1H), 7.71 – 7.65 (m, 3H), 7.63 – 7.54 (m, 2H), 7.49 (d, *J* = 8.5 Hz, 2H), 7.43 (dt, *J* = 7.5, 1.4 Hz, 1H), 6.82 – 6.74 (m, 2H), 1.98 (s, 2H).
**$^{13}$C NMR** (100.63 MHz, $CDCl_3$) δ 150.32 (CH, Ar), 150.16 (CH, Ar), 146.36 (C, Ar), 146.29 (C, Ar), 145.65 (C, Ar), 141.73 (C, Ar), 139.31 (C, Ar), 136.30 (CH, Ar), 135.03 (CH, Ar), 130.95 (CH, Ar), 129.13 (CH, Ar), 128.33 (CH, Ar), 128.25 (CH, Ar), 128.21 (CH, Ar), 128.05 (C, Ar), 127.96 (CH, Ar), 126.62 (CH, Ar), 126.17 (CH, Ar), 123.59 (CH, Ar), 123.10 (CH, Ar), 115.61 (CH, Ar).
**HRMS (ESI).** Calculated for $C_{24}H_{18}N_3^+$: 348.1495 Obtained: 348.1486

USC UNIVERSIDADE DE SANTIAGO DE COMPOSTELA

*10.1.2.27 Preparation of 1-(3'-(1,10-phenanthrolin-5-yl)-[1,1'-biphenyl]-4-yl)-3-phenylurea (L13)*




**16'** **L13**

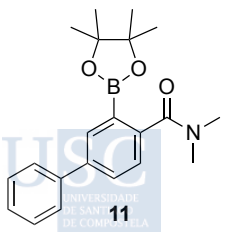
To a solution of **16'** (73.5 mg, 0.2 mmol, 1.0 equiv.) in dichloromethane (3.2 mL) was added phenylisocyanate (50.4 mg, 0.4 mmol, 2.0 equiv.) at room temperature. The mixture was stirred at this temperature for 16 hours. After this period, the crude product was purified by recrystallization in DCM/Hexane, yielding the desired product in 81% yield.

**$^{1}$H NMR** (400.16 MHz, DMSO-$d_6$) δ 9.14 (td, *J* = 4.2, 1.7 Hz, 2H), 8.72 (s, 1H), 8.62 (s, 1H), 8.51 (dd, *J* = 8.1, 1.8 Hz, 1H), 8.32 (dd, *J* = 8.3, 1.7 Hz, 1H), 8.03 (s, 1H), 7.84 – 7.78 (m, 3H), 7.76 (dd, *J* = 9.1, 4.9 Hz, 1H), 7.71 (d, *J* = 8.7 Hz, 2H), 7.65 (t, *J* = 7.6 Hz, 1H), 7.61 – 7.56 (m, 2H), 7.55 – 7.50 (m, 1H), 7.49 – 7.44 (m, 2H), 7.28 (dd, *J* = 8.5, 7.3 Hz, 2H), 7.01 – 6.94 (m, 1H).
**$^{13}$C NMR** (100.63 MHz, DMSO-$d_6$) δ 152.28 (CO), 149.74 (CH, Ar), 149.41 (CH, Ar), 145.69 (C, Ar), 144.98 (C, Ar), 140.18 (C, Ar), 139.43 (C, Ar), 139.33 (C, Ar), 138.83 (C, Ar), 137.87 (C, Ar), 135.94 (CH, Ar), 133.72 (CH, Ar), 132.95 (C, Ar), 128.92 (CH, Ar), 128.45 (CH, Ar), 128.00 (CH, Ar), 127.69 (C, Ar), 127.27 (CH, Ar), 127.10 (C, Ar), 126.97 (CH, Ar), 126.55 (CH, Ar), 125.53 (CH, Ar), 123.28 (CH, Ar), 122.95 (CH, Ar), 121.65 (CH, Ar), 118.44, (CH, Ar), 118.16 (CH, Ar).
**HRMS (ESI).** Calculated for $C_{31}H_{23}N_4O^+$: 467.1866 Obtained: 467.1858

## 10.1.3 General borylation procedure

In a sealed tube $[Ir(COD)(OMe)]_2$ (0.008 mmol, 3 mol%.), $B_2pin_2$ (0.375 mmol, 1.5 equiv.), and ligand (0.015 mmol, 6 mol%) were added. The tube was evacuated and refilled with $N_2$ three times, then under a positive flow of $N_2$, dry THF (1.25 mL) and substrate (0.250 mmol, 1.0 equiv.) were added. The tube was then sealed and heated for the specified time. After that, volatiles were removed under vacuum and $CH_2Br_2$ (internal standard) was added, the yield was determined by $^{1}$H NMR spectroscopy. To isolate the product, the solvent was removed under reduced pressure, and the residue was purified by column chromatography on silica gel.

*10.1.3.1 N,N-dimethyl-3-(4,4,5,5-tetramethyl-1,3,2-dioxaborolan-2-yl)-[1,1'-biphenyl]-4-carboxamide (11)*




**11**

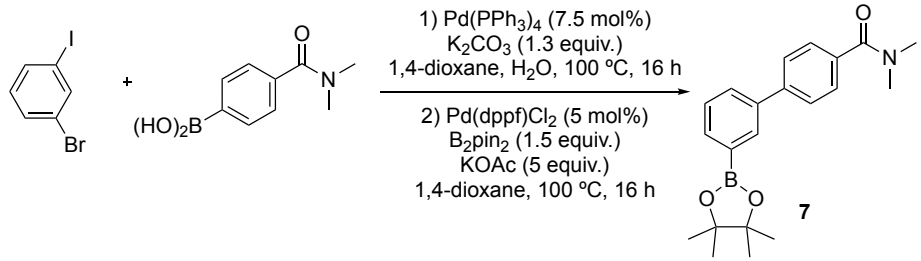
Following the general procedure: **6** (56.3mg, 0.250 mmol, 1.0 equiv.), $[Ir(COD)(OMe)]_2$ (5 mg, 0.008 mmol, 3 mol%.), $B_2pin_2$ (95.2 mg, 0.375 mmol, 1.5 equiv.), **L4** (3.8 mg, 0.015 mmol, 6 mol%.) in THF (1.25 mL) were heated at 65 °C for 16 h. The crude mixture was purified by

column chromatography (Hex/EtOAc 20% to Hex/EtOAc 80%) to obtain 80 mg (92% yield) of **11** as a brown oil.

**$^{1}$H NMR** (600.1318 MHz, $CDCl_3$, 258 K) δ 7.99 (d, *J* = 1.8 Hz, 1H), 7.65 – 7.59 (m, 3H), 7.52 – 7.40 (m, 3H), 7.38 – 7.32 (m, 1H), 3.20 (s, 3H), 3.05 (s, 3H), 1.32 (s, 12H).
**$^{13}$C NMR** (100.63 MHz, $CDCl_3$, 258 K) δ 172.41 (CO), 142.10 (C, Ar), 140.29 (C, Ar), 138.57 (C, Ar), 132.70 (CH, Ar), 129.06 (CH, Ar), 128.75 (CH, Ar), 127.65 (CH, Ar), 127.29 (CH, Ar), 126.12 (CH, Ar), 82.74 (C), 39.46 (N-$CH_3$), 36.74 (N-$CH_3$), 25.05 ($CH_3$).
**$^{11}$B NMR** (128.39 MHz, $CDCl_3$) δ 26.52.
**HRMS (ESI).** Calculated for $C_{21}H_{26}BNNaO_3^+$: 374.18980 Obtained: 374.18989

## 10.1.4 Synthesis of borylated products

### *10.1.4.1 Preparation of N,N-dimethyl-3'-(4,4,5,5-tetramethyl-1,3,2-dioxaborolan-2-yl)-[1,1'-biphenyl]-4-carboxamide (7)*




Step1:

In a Schlenk flask equipped with a magnetic stirrer, $Pd(PPh_3)_4$ (149.7 mg, 0.13 mmol, 0.05 equiv.), $K_2CO_3$ (465.4 mg, 3.4 mmol, 1.3 equiv.), (4-(dimethylcarbamoyl)phenyl)boronic acid (500 mg, 2.5 mmol, 1 equiv.), and 1-bromo-3-iodobenzene (330 µL, 2.6 mmol, 1 equiv.) were added. Next, 90 mL of a 1,4-dioxane/$H_2O$ mixture (5:1 ratio) was added. The resulting mixture was heated up to 100 ºC and stirred at the same temperature for 16 hours, with the reaction monitored by TLC.

After this period, water was added to the mixture and, after it cooled down to room temperature, it was filtered and extracted with EtOAc (3 x 30 mL). The organic phase was dried with $MgSO_4$. Finally, the solvent was removed under reduced pressure, and the crude product was purified by column chromatography on silica gel (Hexane/EtOAc from 90:10 to 40:60), obtaining the desired product in a 65% yield.

**$^{1}$H NMR** (400.16 MHz, $CDCl_3$) δ 7.72 (t, *J* = 1.8 Hz, 1H), 7.64 – 7.55 (m, 2H), 7.55 – 7.46 (m, 4H), 7.33 (t, *J* = 7.8 Hz, 1H), 3.13 (s, 3H), 3.04 (s, 3H).
**$^{13}$C NMR** (100.63 MHz, $CDCl_3$) δ 171.32 (CO), 142.32 (C, Ar), 140.85 (C, Ar), 135.44 (C, Ar), 130.69 (CH, Ar), 130.53 (CH, Ar), 130.17 (CH, Ar), 127.82 (CH, Ar), 127.17 (CH, Ar), 125.86 (CH, Ar), 122.98 (C, Ar), 39.83 (N-$CH_3$), 35.49 (N-$CH_3$).
**HRMS (ESI).** Calculated for $C_{15}H_{15}BrNO^+$: 304.0332 Obtained: 304.0330

USC DE SANTIAGO DE COMPOSTELA

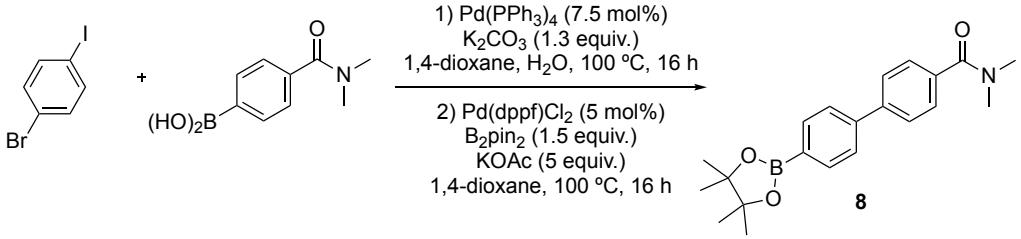
Step 2:

In a Schlenk flask equipped with a magnetic stir bar, $Pd(dppf)Cl_2$ (27.8 mg, 0.03 mmol, 0.05 equiv.), KOAc (322.6 mg, 3.3 mmol, 5.0 equiv.), $B_2pin_2$ (12) (250.4 mg, 1.0 mmol, 1.5 equiv.), and 3'-bromo-N,N-dimethyl-[1,1'-biphenyl]-4-carboxamide (200 mg, 0.7 mmol, 1 equiv.) were added. The flask was subjected to vacuum-$N_2$ cycles, and once under an inert atmosphere, 1.4-dioxane (1.0 mL) was added. The resulting solution was heated up to 100 ºC and stirred at the same temperature for 16 hours.

After this period, water was added to the mixture and, after it cooled down to room temperature, it was filtered and extracted with EtOAc (3 x 20 mL). The organic phase is dried over $MgSO_4$. Finally, the solvent is evaporated under reduced pressure, and the crude product is purified by column chromatography on silica gel (Hexane/EtOAc, from 80:20 to 20:80), obtaining the desired product in 85% yield.

**$^1$H NMR** (400.16 MHz, $CDCl_3$) δ 8.03 (d, *J* = 2.1 Hz, 1H), 7.82 – 7.78 (m, 1H), 7.71 – 7.68 (m, 1H), 7.67 – 7.64 (m, 2H), 7.48 (d, *J* = 8.3 Hz, 2H), 7.25 (d, *J* = 1.0 Hz, 1H), 3.13 (s, 3H), 3.02 (s, 3H), 1.35 (s, 12H).
**$^{13}$C NMR** (100.63 MHz, $CDCl_3$) δ 171.70 (CO), 142.35 (C, Ar), 139.66 (C, Ar), 134.79 (C, Ar), 134.19 (CH, Ar), 133.53 (CH, Ar), 130.15 (CH, Ar), 129.00 (C, Ar), 128.45 (CH, Ar), 127.68 (CH, Ar), 127.27 (CH, Ar), 84.08 (C), 39.87 (N-CH3), 35.56 (N-CH3), 24.96 (CH3).
**$^{11}$B NMR** (128.39 MHz, $CDCl_3$) δ 31.16.
**HRMS (ESI).** Calculated for $C_{21}H_{27}BNO_3^+$: 352.2082 Obtained: 352.2083

### *10.1.4.2 Preparation of N,N-dimethyl-4'-(4,4,5,5-tetramethyl-1,3,2-dioxaborolan-2-yl)-[1,1'-biphenyl]-4-carboxamide (8)*




Step 1:

In a Schlenk flask equipped with a magnetic stir bar, $Pd(PPh_3)_4$ (149.7 mg, 0.1 mmol, 0.05 equiv.), $K_2CO_3$ (465.4 mg, 3.4 mmol, 1.3 equiv.), (4-(dimethylcarbamoyl)phenyl)boronic acid (500 mg, 2.6 mmol, 1 equiv.), and 1-bromo-2-iodobenzene (330 µL, 2.6 mmol, 1 equiv.) were added. Then, 90 mL of a 1,4-dioxane/$H_2O$ mixture (5:1) were added. The resulting mixture was heated up to 100 ºC and stirred at the same temperature for 16 hours, monitored by TLC.

USC UNIVERSIDADE DE SANTIAGO DE COMPOSTELA

After this period, water was added to the mixture and, after it cooled down to room temperature, it was filtered and extracted with EtOAc (3 x 30 mL). The organic phase is dried over $MgSO_4$. Finally, the solvent is evaporated under reduced pressure, and the crude product is purified by column chromatography on silica gel (Hexane/EtOAc, from 90:10 to 30:70), obtaining the desired product in 73% yield.

**$^1$H NMR** (400.16 MHz, $CDCl_3$) δ 7.62 – 7.54 (m, 4H), 7.54 – 7.42 (m, 4H), 3.09 (d, *J* = 37.5 Hz, 6H).
**$^{13}$C NMR** (100.63 MHz, $CDCl_3$) δ 171.38 (CO), 141.17 (C, Ar), 139.15 (C, Ar), 135.21 (C, Ar), 132.03 (CH, Ar), 128.82 (CH, Ar), 127.86 (CH, Ar), 126.98 (CH, Ar), 122.11 (C, Ar), 39.85 (N-$CH_3$), 35.51 (N-$CH_3$).
**HRMS (ESI).** Calculated for $C_{15}H_{15}BrNO^+$: 304.0332 Obtained: 304.0332

Step 2:

In a Schlenk flask equipped with a magnetic stir bar, $Pd(dppf)Cl_2$ (27.8 mg, 0.03 mmol, 0.05 equiv.), KOAc (322.6 mg, 3.3 mmol, 5.0 equiv.), $B_2pin_2$ (12) (250.4 mg, 1.0 mmol, 1.5 equiv.), and 4'-bromo-N,N-dimethyl-[1,1'-biphenyl]-4-carboxamide (200 mg, 0.7 mmol, 1 equiv.) were added. The flask was subjected to vacuum-$N_2$ cycles, and once under an inert atmosphere, dry 1,4-dioxane (1 mL) was added. The resulting solution was heated up to 100 ºC and stirred at the same temperature for 16 hours.

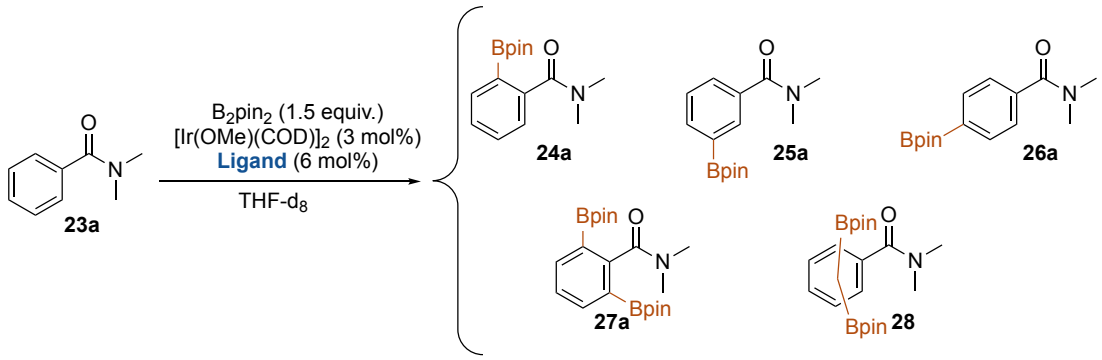
After this period, water was added to the mixture and, after it cooled down to room temperature, it was filtered and extracted with EtOAc (3 x 30 mL). The organic phase is dried over $MgSO_4$. Finally, the solvent is evaporated under reduced pressure, and the crude product is purified by column chromatography on silica gel (Hexane/EtOAc, from 0 to 100%), obtaining the desired product in 88% yield.

**$^1$H NMR** (400.16 MHz, $CDCl_3$) δ 7.77 – 7.73 (m, 1H), 7.63 – 7.58 (m, 1H), 7.51 – 7.45 (m, 2H), 7.43 (d, *J* = 2.1 Hz, 2H), 7.38 (d, *J* = 1.2 Hz, 1H), 7.37 (dd, *J* = 3.0, 1.3 Hz, 1H), 3.14 (s, 3H), 3.04 (s, 3H), 1.20 (d, *J* = 1.5 Hz, 12H).
**$^{13}$C NMR** (100.63 MHz, $CDCl_3$) δ 171.90 (CO), 146.68 (C, Ar), 144.50 (C, Ar), 134.90 (C, Ar), 134.50 (C, Ar), 130.48 (CH, Ar), 129.18 (CH, Ar), 126.81 (CH, Ar), 83.94 (C), 39.81 (N-$CH_3$), 35.53 (N-$CH_3$), 24.65 ($CH_3$).
**$^{11}$B NMR** (128.39 MHz, $CDCl_3$) δ 32.01.
**HRMS (ESI).** Calculated for $C_{21}H_{27}BNO_3^+$: 352.2082 Obtained: 352.2083

USC UNIVERSIDADE DE SANTIAGO DE COMPOSTELA

## 10.2 Experimental procedures for section 7.2

### 10.2.1 Kinetic studies at different temperatures




An NMR tube equipped with a screw-cap and septum was charged with $B_2pin_2$ (38.1mg, 0.15 mmol, 1.5 equiv.) and dissolved with 100 mL of THF-$d_8$. To that solution were added 100 μL of a solution 0.03 M of $[Ir(COD)(OMe)]_2$ in THF-$d_8$ (2 mg, 0.003 mmol, 0.03 equiv.) and 100 μL of a solution 0.06 M of **bipy**, **L27** or **L47** in THF-$d_8$ (0.06 mmol, 0.06 equiv.). The contents were thoroughly mixed for 1 minute while observing a color change from light yellow to dark brown. After that time, 200 μL of a solution 0.5 M of **23a** in THF-$d_8$ (14.9 mg, 0.1 mmol, 1 equiv.) and 0.05 M of 1,3,5-Trimethoxybenzene in THF-$d_8$ (1.7 mg, 0.01 mmol, 0.1 equiv.) as internal standard were added. The tube was then closed and inserted into a heated NMR probe at the corresponding temperature.

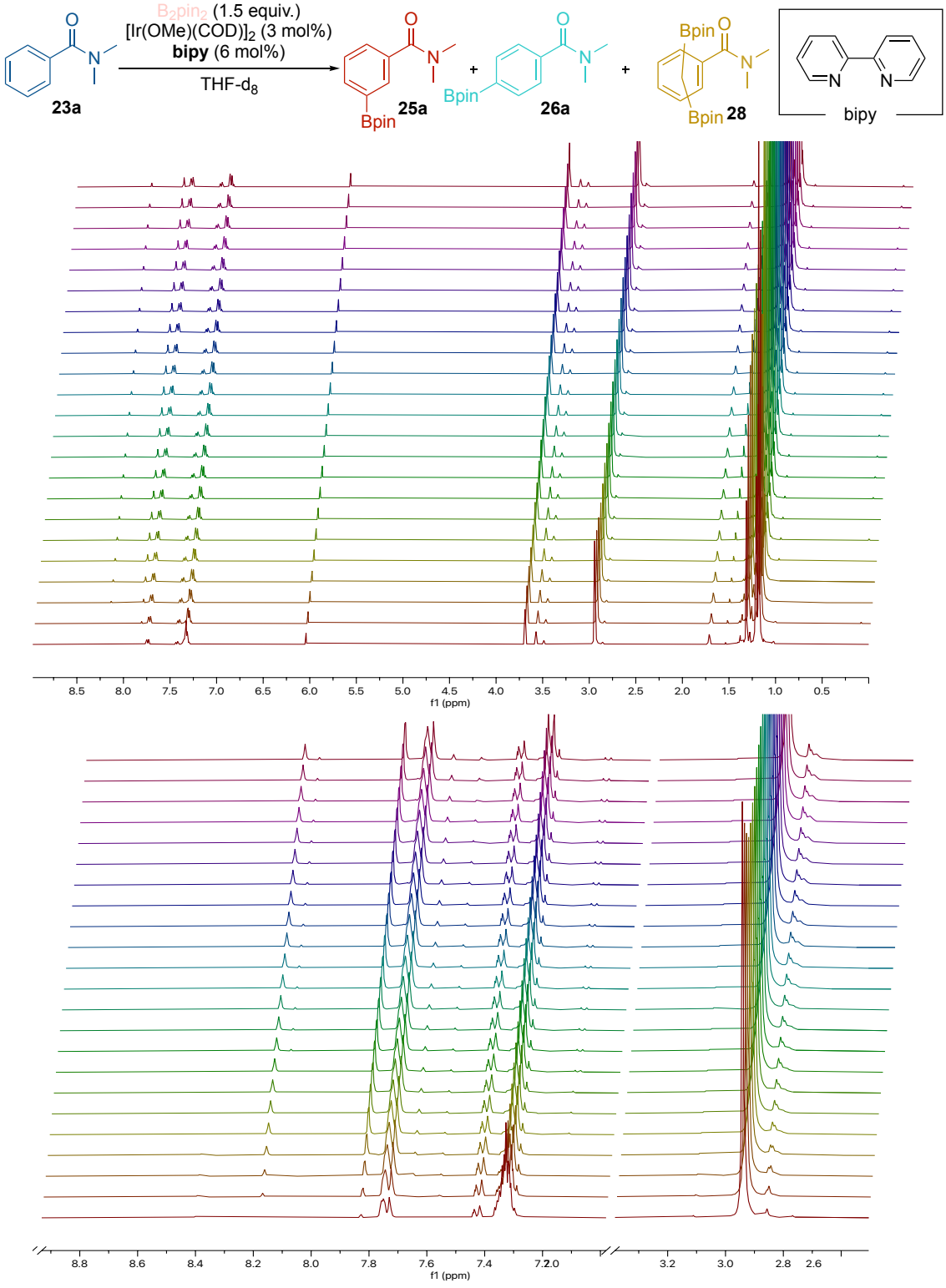
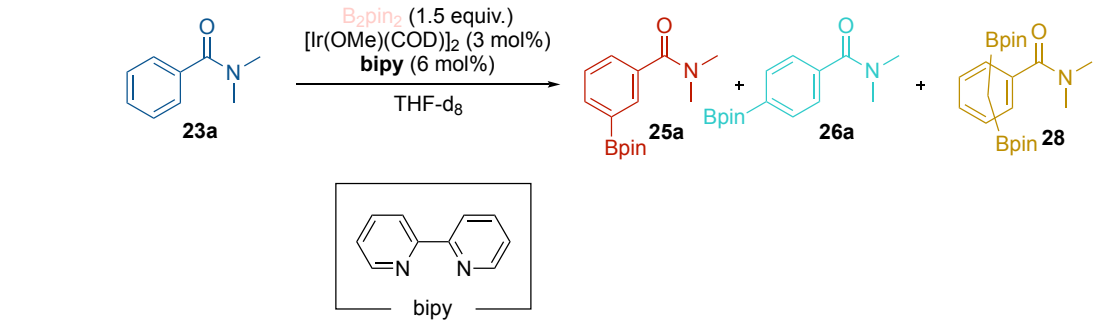



***Figure* 58** Example of spectra recorded while following the borylation reaction of **23a** using **bipy** as ligand. Reaction progression goes from front to bottom. Full NMR spectra (top) and cropped spectra to show the aromatic and N-$Me_2$ region (bottom). It can be observed the disappearance of the broad signal at 7.3 ppm corresponding to the substrate **23a** and the appearance of signals at 7.44 ppm corresponding to **25a** and at 7.75 ppm corresponding to **25a** and **26a**. This spectra correspond to the reaction at 65ºC.



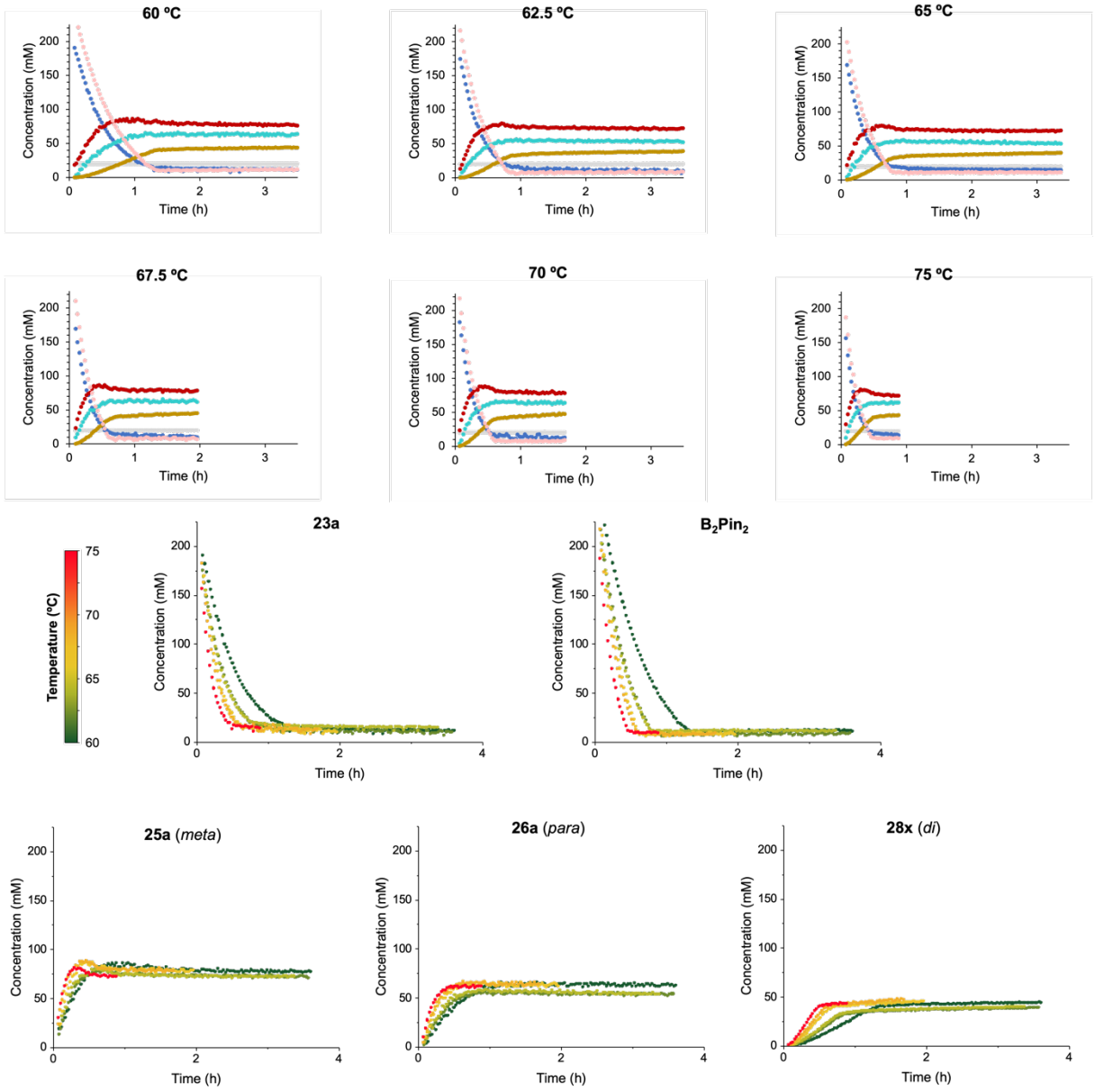




**Figure *59*** profiles of the borylation reaction of benzamide **23a** with $B_2Pin_2$ catalyzed by $[Ir(OMe)(COD)]_2$ in the presence of ligand **bipy** at different temperatures.

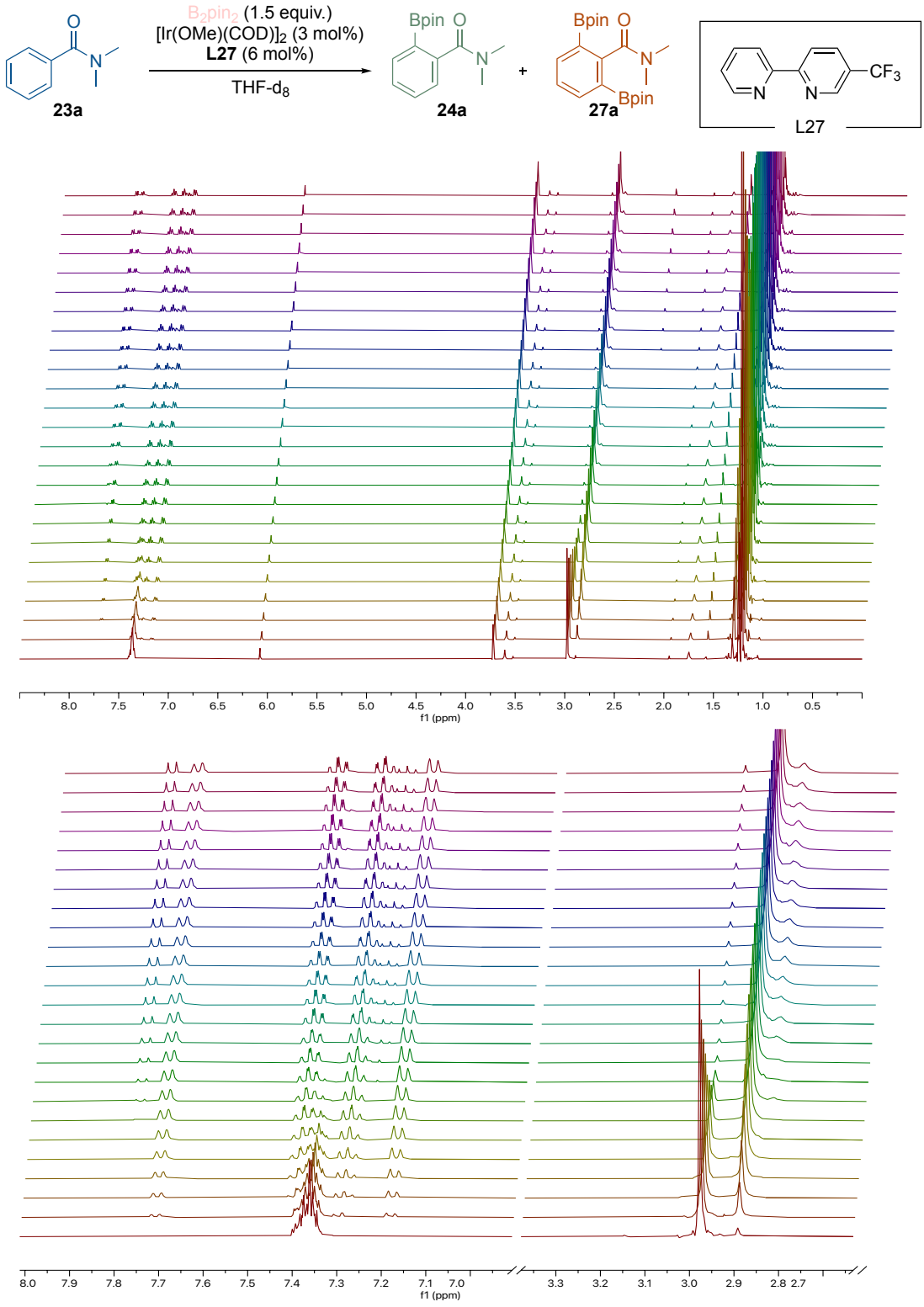



**Figure 60** Example of spectra recorded while following the borylation reaction of **23a** using **L27** as ligand. Reaction progression goes from front to bottom. Full NMR spectra (top) and cropped spectra to show the aromatic and N-$Me_2$ region (bottom). It can be observed the disappearance of the broad signal at 7.3 ppm corresponding to the substrate **23a** and the appearance of signals at 7.69 ppm and 7.15 ppm corresponding to **24a**, additionally the signal at 2.99 ppm corresponds to **23a** and the signal at 2.89 pppm corresponds to **25a**. This spectra correspond to the reaction at 65ºC.

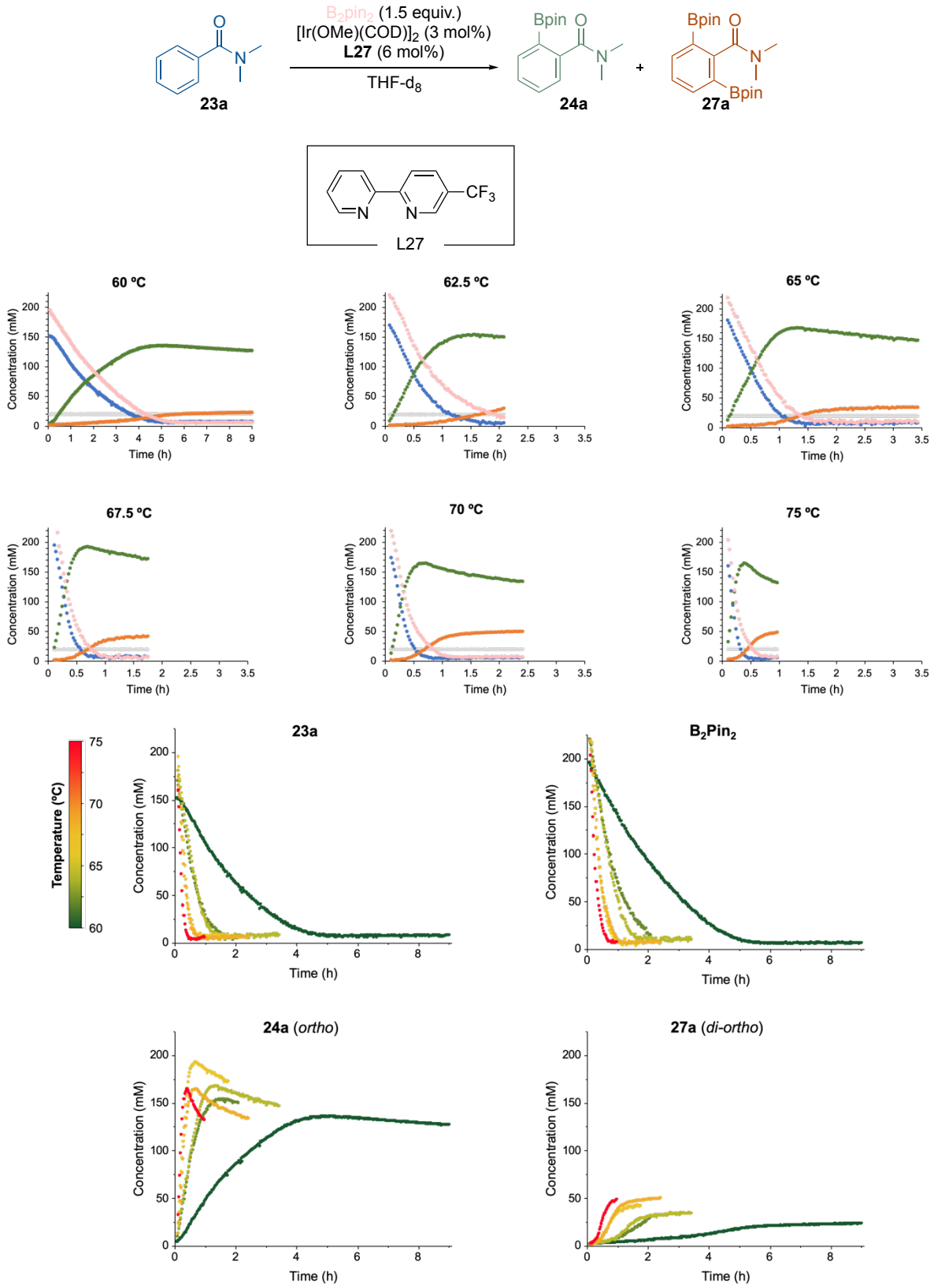



**Figure *61*** Kinetic profiles of the borylation reaction of benzamide **23a** with $B_2Pin_2$ catalyzed by $[Ir(OMe)(COD)]_2$ in the presence of ligand **L27** at different temperatures**.**

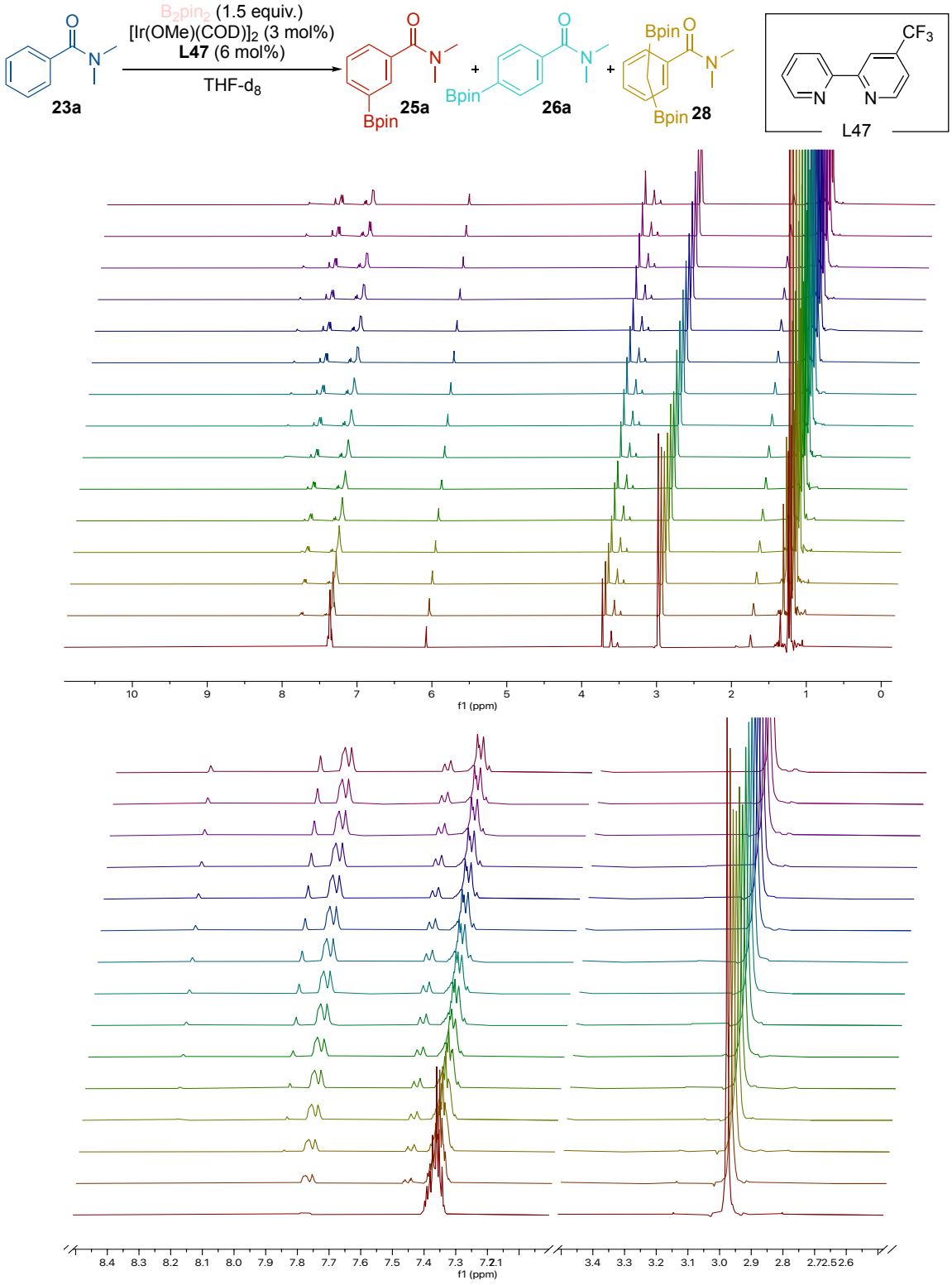



**Figure 62** Example of spectra recorded while following the borylation reaction of **23a** using **L47** as ligand. Reaction progression goes from front to bottom. Full NMR spectra (top) and cropped spectra to show the aromatic and N-$Me_2$ region (bottom). It can be observed the disappearance of the broad signal at 7.3 ppm corresponding to the substrate **23a** and the appearance of signals at 7.44 ppm corresponding to **25a** and at 7.75 ppm corresponding to **25a** and **26a**. This spectra correspond to the reaction at 65ºC.

USC UNIVERSIDADE DE SANTIAGO DE COMPOSTELA

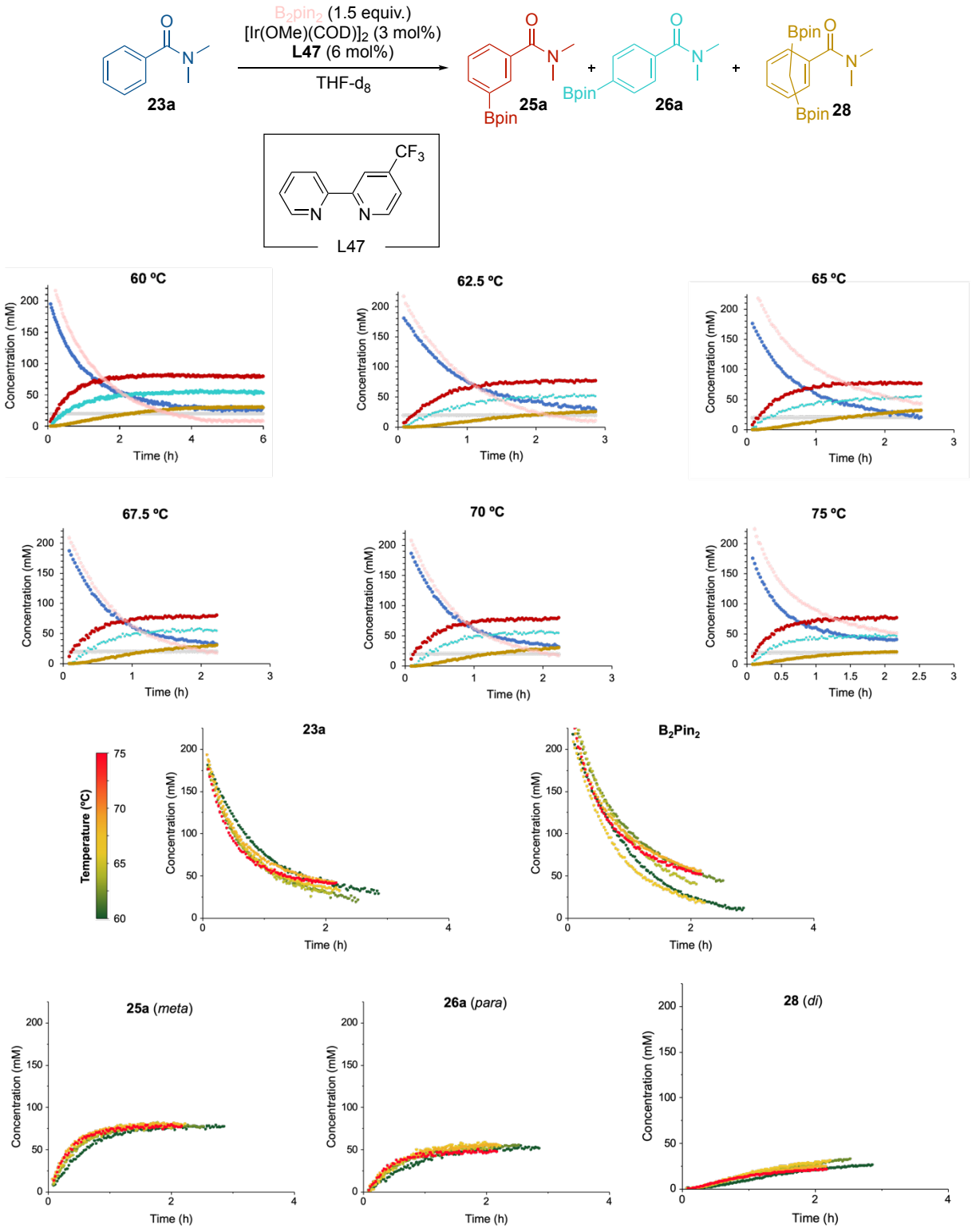



**Figure 63** Kinetic profiles of the borylation reaction of benzamide **23a** with $B_2Pin_2$ catalyzed by $[Ir(OMe)(COD)]_2$ in the presence of ligand **L47** at different temperatures.

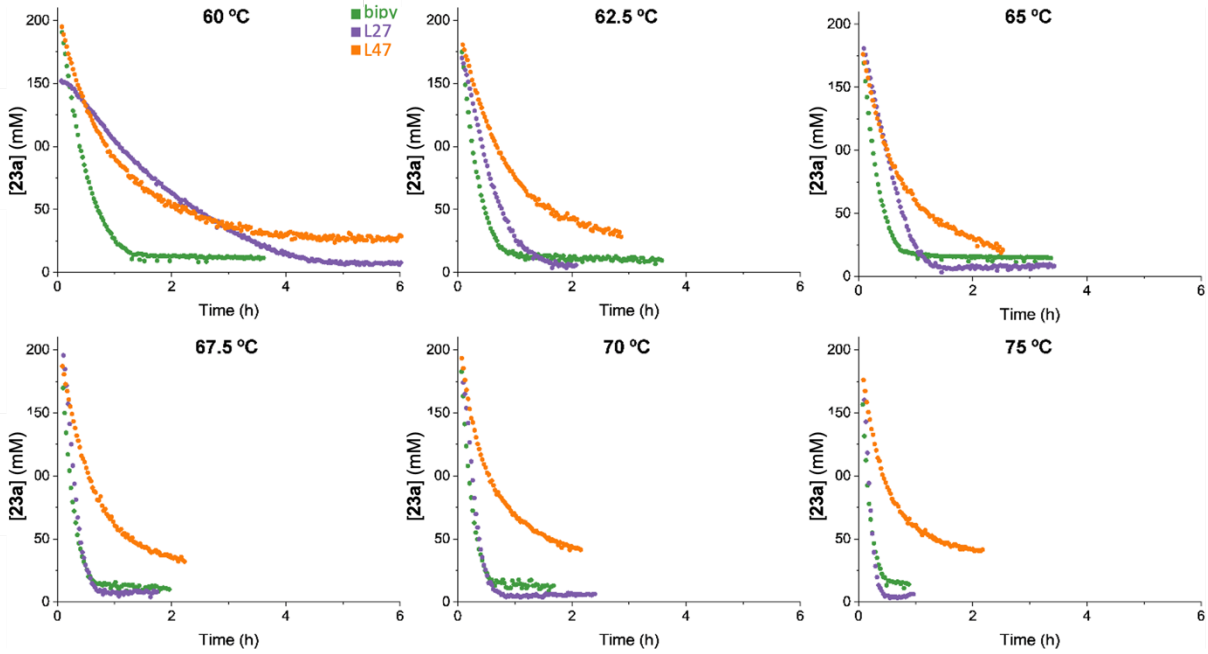
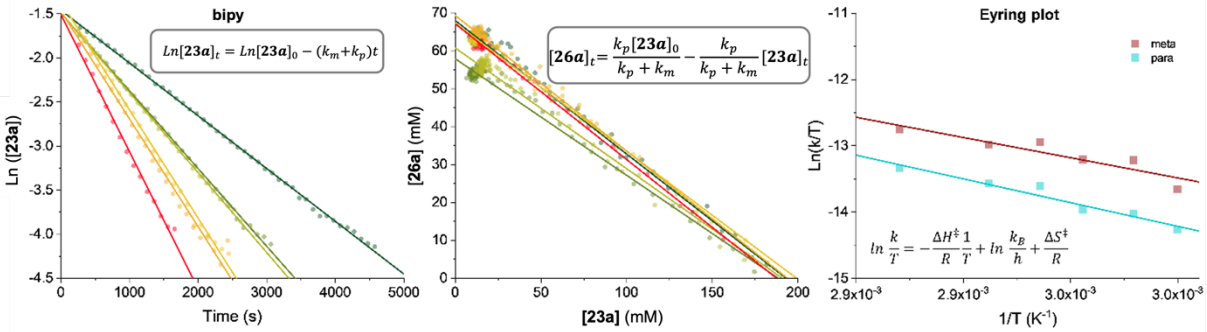



**Figure *64*** Com*para*tive time courses for the conversion of benzamide **23a** with $B_2pin_2$ catalyzed by $[Ir(OMe)(COD)]_2$ in the presence of ligands **bipy**, **L27** and **L47** at different temperatures.

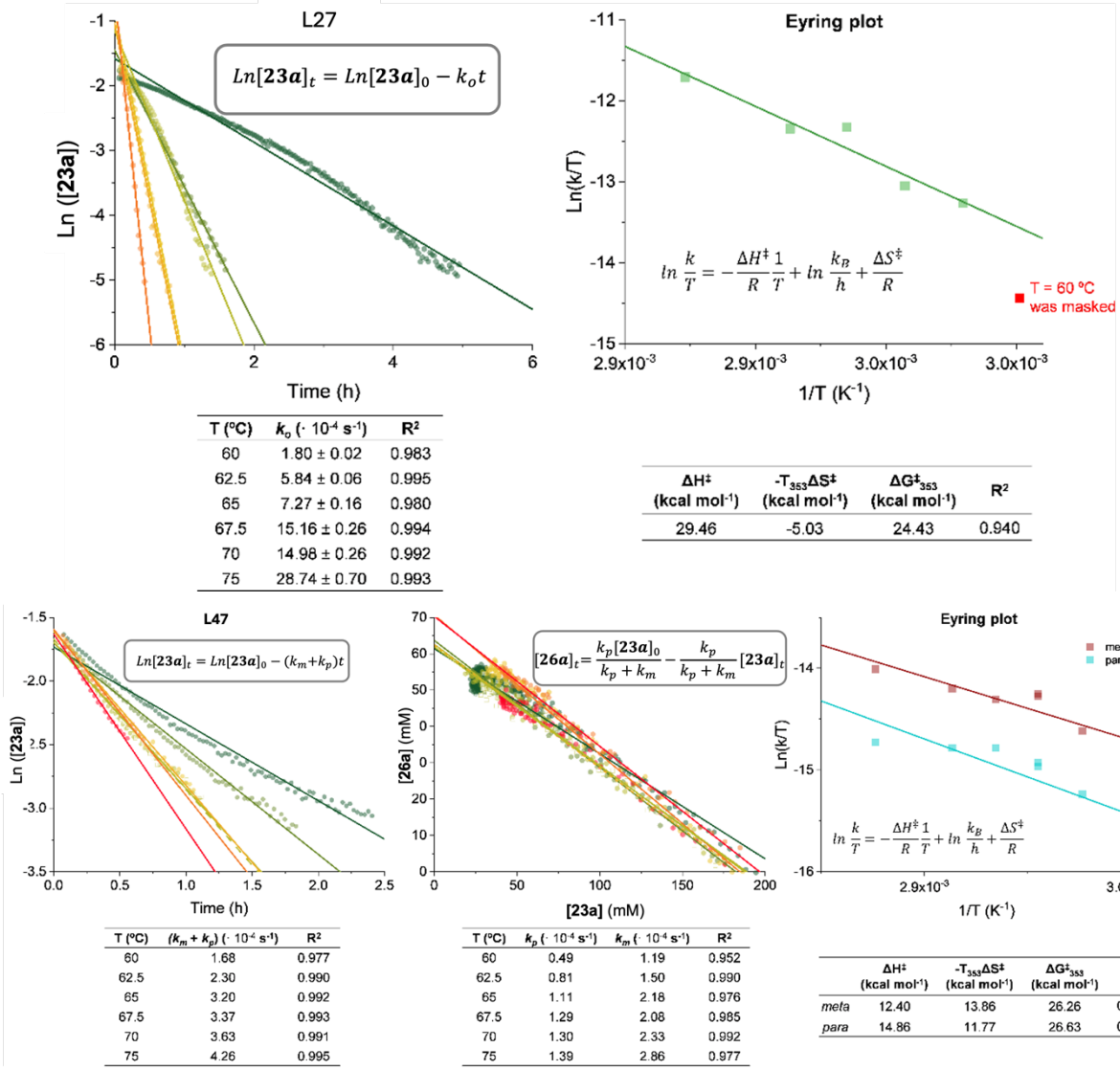
## 10.2.2 Eyring plots and activation *para*meters




| T (°C) | $(k_m + k_p)$ ($\cdot 10^{-4}$ s$^{-1}$) | $R^2$ |
|---|---|---|
| 60 | 5.99 ± 0.03 | 0.999 |
| 62.5 | 8.81 ± 0.07 | 0.998 |
| 65 | 9.07 ± 0.05 | 0.999 |
| 67.5 | 12.27 ± 0.19 | 0.995 |
| 70 | 12.23 ± 0.31 | 0.997 |
| 75 | 15.57 ± 0.36 | 0.993 |

| T (°C) | $k_p$ ($\cdot 10^{-4}$ s$^{-1}$) | $k_m$ ($\cdot 10^{-4}$ s$^{-1}$) | $R^2$ |
|---|---|---|---|
| 60 | 2.11 | 3.88 | 0.988 |
| 62.5 | 2.69 | 6.06 | 0.978 |
| 65 | 2.89 | 6.18 | 0.961 |
| 67.5 | 4.15 | 8.12 | 0.986 |
| 70 | 4.38 | 7.85 | 0.990 |
| 75 | 5.58 | 9.99 | 0.995 |

| | $\Delta H^{\ddagger}$ (kcal mol$^{-1}$) | $-T_{353}\Delta S^{\ddagger}$ (kcal mol$^{-1}$) | $\Delta G^{\ddagger}_{353}$ (kcal mol$^{-1}$) | $R^2$ |
|---|---|---|---|---|
| *meta* | 12.11 | 13.30 | 25.41 | 0.840 |
| *para* | 14.23 | 11.58 | 25.80 | 0.946 |




| T (°C) | $k_o$ (· 10$^{-4}$ s$^{-1}$) | R² |
|---|---|---|
| 60 | 1.80 ± 0.02 | 0.983 |
| 62.5 | 5.84 ± 0.06 | 0.995 |
| 65 | 7.27 ± 0.16 | 0.980 |
| 67.5 | 15.16 ± 0.26 | 0.994 |
| 70 | 14.98 ± 0.26 | 0.992 |
| 75 | 28.74 ± 0.70 | 0.993 |

| ΔH‡ (kcal mol$^{-1}$) | -T$_{353}$ΔS‡ (kcal mol$^{-1}$) | ΔG‡$_{353}$ (kcal mol$^{-1}$) | R² |
|---|---|---|---|
| 29.46 | -5.03 | 24.43 | 0.940 |

| T (°C) | $(k_m + k_p)$ (· 10$^{-4}$ s$^{-1}$) | R² |
|---|---|---|
| 60 | 1.68 | 0.977 |
| 62.5 | 2.30 | 0.990 |
| 65 | 3.20 | 0.992 |
| 67.5 | 3.37 | 0.993 |
| 70 | 3.63 | 0.991 |
| 75 | 4.26 | 0.995 |

| T (°C) | $k_p$ (· 10$^{-4}$ s$^{-1}$) | $k_m$ (· 10$^{-4}$ s$^{-1}$) | R² |
|---|---|---|---|
| 60 | 0.49 | 1.19 | 0.952 |
| 62.5 | 0.81 | 1.50 | 0.990 |
| 65 | 1.11 | 2.18 | 0.976 |
| 67.5 | 1.29 | 2.08 | 0.985 |
| 70 | 1.30 | 2.33 | 0.992 |
| 75 | 1.39 | 2.86 | 0.977 |

| | ΔH‡ (kcal mol$^{-1}$) | -T$_{353}$ΔS‡ (kcal mol$^{-1}$) | ΔG‡$_{353}$ (kcal mol$^{-1}$) | R² |
|---|---|---|---|---|
| *meta* | 12.40 | 13.86 | 26.26 | 0.825 |
| *para* | 14.86 | 11.77 | 26.63 | 0.719 |

**Figure 65** Eyring plots and activation *para*meters derived for the borylation reactions of benzamide **23a** catalyzed by [Ir(OMe)(COD)]$_2$ in the presence of ligands **bipy** (top), **L27** (middle) and **L47** (bottom).

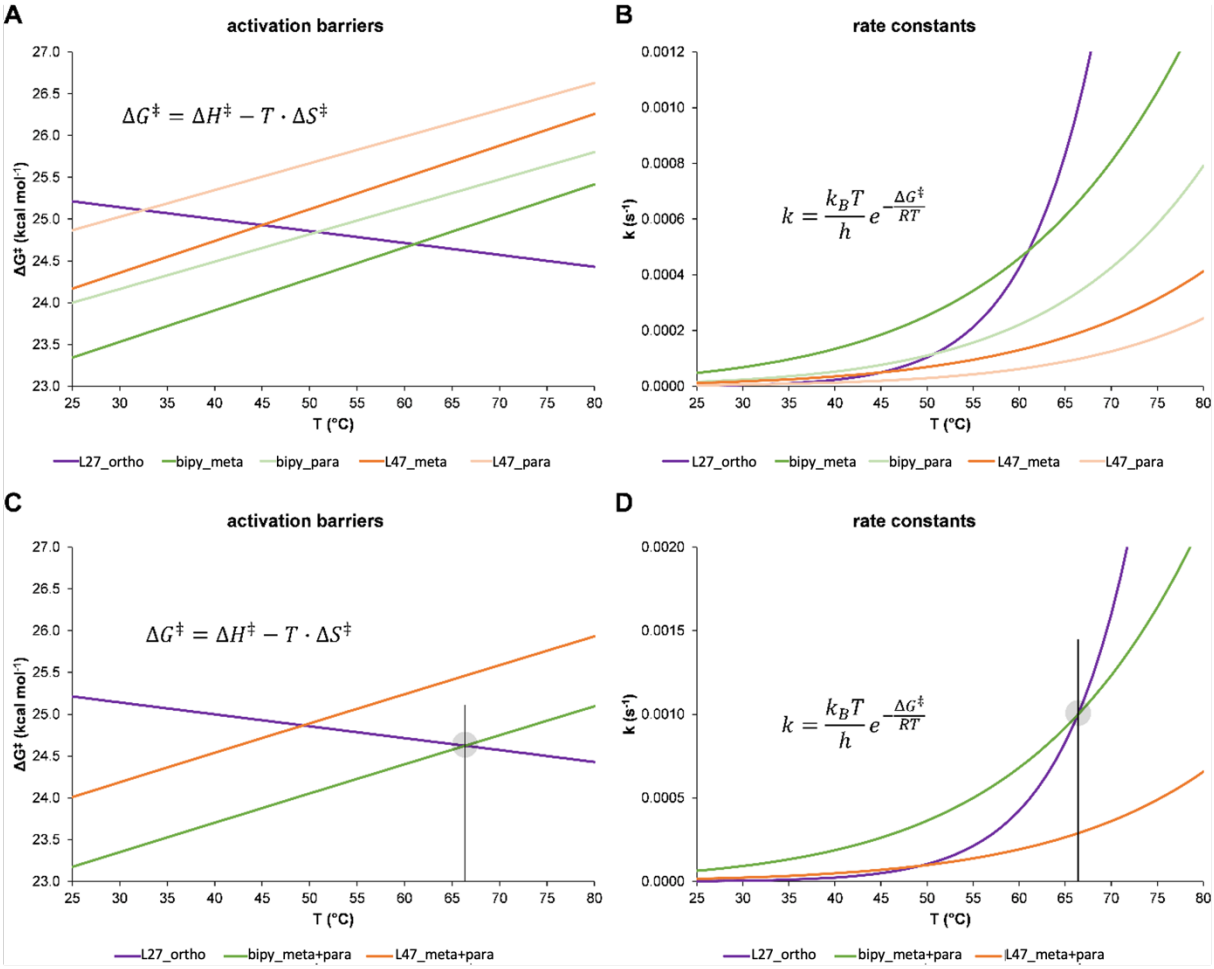



**Figure 66 A)** Activation free energies ($\Delta G^{\ddagger}$) and **B)** reaction rate constants (k) calculated as a function of temperature for the *ortho*, *meta* and *para* borylation reactions of benzamide **23a** catalyzed by $[Ir(OMe)(COD)]_2$ in the presence of ligands **bipy**, **L27** and **L47**. **(C,D)** The same *para*meters but combining the *meta* and *para* reaction pathways for ligands **bipy** and **L47**. The temperature at which the global reaction rates with ligands **bipy** and **L27** are equal (around 66 °C) is marked with a vertical line.

### 10.2.3 NMR and HRMS studies of $[Ir(COD)Cl]_2$ and L28 complexes

#### *10.2.3.1 NMR and HRMS experiments*

An NMR tube equipped with a screw-cap and septum was charged with either **L28** (top spectra), **L28** (2 equiv.) and $[Ir(COD)Cl]_2$ (1 equiv.) (middle spectra) or **L28** (2 equiv.) and $[Ir(COD)Cl]_2$ (1 equiv.) and $B_2pin_2$ (1.5 equiv.) (bottom spectra). The tubes were evacuated and refilled with Ar 3 times and the solids were dissolved in dry $CDCl_3$ (0.5 mL). Those tubes were heated up to 55 ºC and the reactions were monitored until no evolution was observed by NMR spectra.

The HRMS spectra samples were prepared by taking an aliquot from the correponding NMR tubes after no evolution was observed. The aliquot was diluted with dry THF and injected into a SOLARIX XR FT-ICR-MS 7T spectrometer. The fact that we can observe the $M^+$ ion of our compound even without any ionization agent included in the sprayed solution indicates that we have successfully obtained a cationic complex.

USC UNIVERSIDADE DE SANTIAGO DE COMPOSTELA

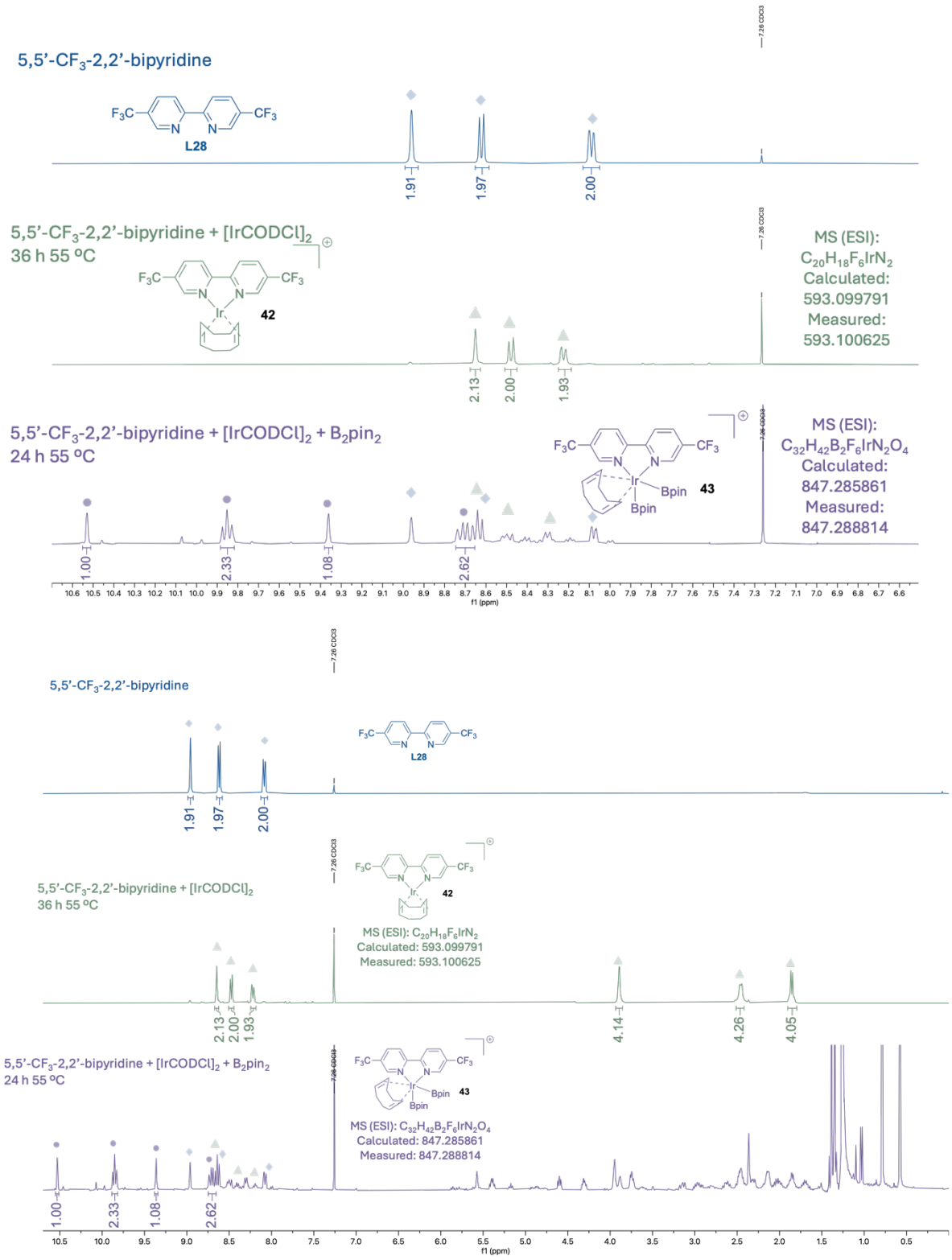
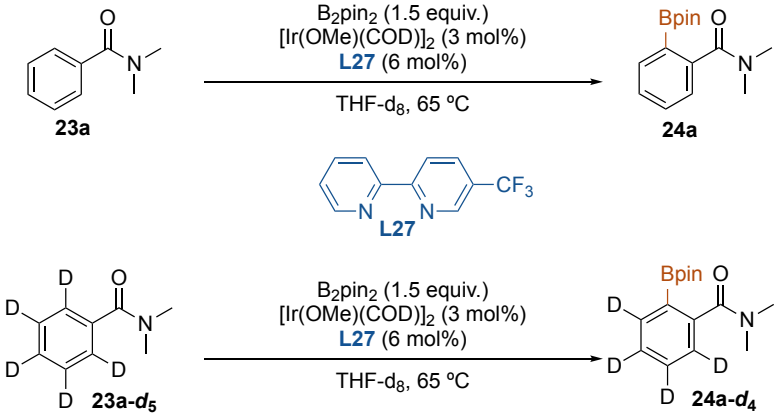



**Figure 67** NMR and HRMS studies on the formation of complex **42** and **43**. Expansion of the aromatic region (top) and full NMR spectra (bottom). Blue markers correspond to signals for **L28**, green markers to signals from complex **42** and purple markers to signals from complex **43**.

## 10.2.4 Kinetic Isotopic Effects (KIE)

### *10.2.4.1 Parallel experiments*




An NMR tube equipped with a screw-cap and septum was charged with $B_2pin_2$ (38.1mg, 0.15 mmol, 1.5 equiv.) and dissolved with 100 µL of THF-$d_8$. To that solution were added 100 µL of a solution 0.03 M of $[Ir(COD)(OMe)]_2$ in THF-$d_8$ (2 mg, 0.003 mmol, 0.03 equiv.) and 100 µL of a solution 0.06 M of **L27** in THF-$d_8$ (1.3 mg, 0.06 mmol, 0.06 equiv.). The contents were thoroughly mixed for 1 minute while observing a color change from light yellow to dark brown. After that time, 200 µL of a solution 0.5 M of **1a** in THF-$d_8$ (14.9 mg, 0.1 mmol, 1 equiv.) or **1a-d5** in THF-$d_8$ (15.4 mg, 0.1 mmol, 1 equiv.) and 0.05 M of 1,3,5-Trimethoxybenzene in THF-$d_8$ (1.7 mg, 0.01 mmol, 0.1 equiv.) as internal standard were added. The tube was then closed and inserted into a heated NMR probe at 65 ºC.

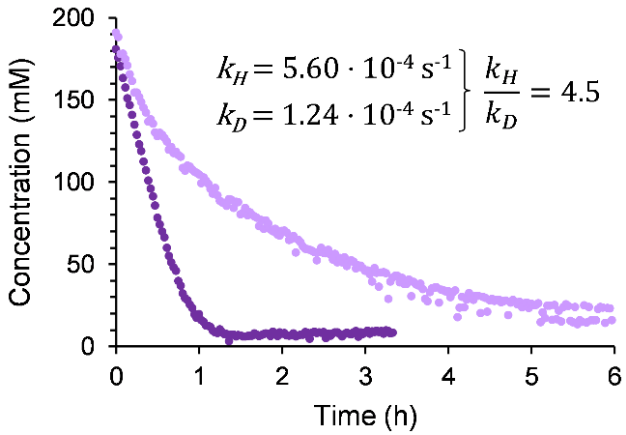
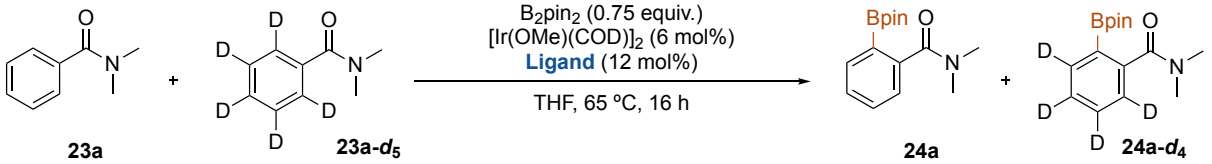



**Figure *68*** Kinetic isotope effect (KIE) determined from parallel reactions of substrates **23a** (in dark purple) and **23a-*d*$_5$** (in light purple) with ligand **L27**

### *10.2.4.2 Intermolecular competitive experiments*




**23a** **23a-*d*$_5$** **24a** **24a-*d*$_4$**

In a sealed tube $[Ir(COD)(OMe)]_2$ (5.0 mg, 0.008 mmol, 6 mol%), $B_2pin_2$ (23.8 mg, 0.094 mmol, 0.75 equiv.), and **L27** (3.4 mg, 0.015 mmol, 12 mol%) or **bipy** (2.3 mg, 0.015 mmol, 12 mol%) were added. The tube was evacuated and refilled with $N_2$ three times, then under a positive flow of $N_2$, were added dry THF (1.25 mL) and **23a** (18.6 mg, 0.125 mmol, 1.0 equiv.) and **23a-*d*$_5$** (19.3 mg, 0.125 mmol, 1.0 equiv.) were added. The tube was then sealed and heated at 65 °C overnight. The rection mixture was diluted with $CH_2Cl_2$ and subjected to GC/MS analysis (Column: 30 m HP-5MS; method: Initial temperature = 70 °C for 3 min, then 30 °C/min to 300 °C and hold for 8 min). The kinetic isotope effect was calculated by taking the ratios of the $[M+H]^+$ mass peak for protiated and deuterated products.

**Table *23*** Kinetic isotope effect (KIE) determined from competitive reactions of substrates **23a** and **23a-*d*$_5$** with ligands **bipy** and **L27**

| | **bipy** | **L27** |
|---|---|---|
| **KIE** | 3.44 | 2.47 |

### *10.2.4.3 Calculated kinetic isotopic effects*

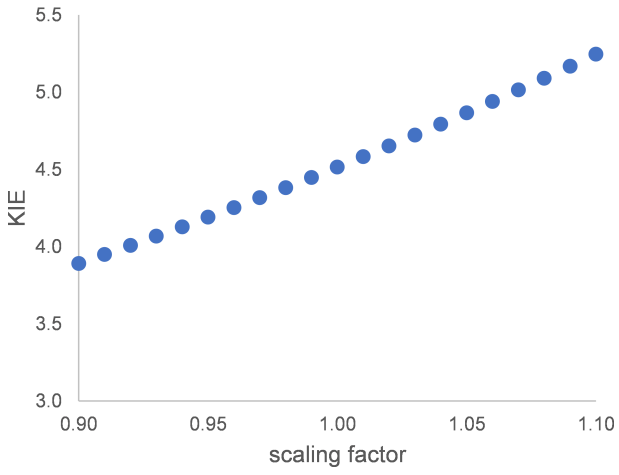
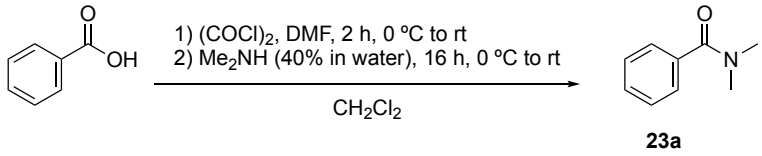



**Figure *69*** $^2D/^1H$ Kinetic isotopic effects (KIE) calculated at 298 K with M06/6-31G(d)+LANL2DZ(Ir) for the oxidative addition step between *N*,*N*-dimethylbenzamide (**23a**) and $Ir^{III}$(**L27**)$(Bpin)_3$ (*o* = *ortho* pathway), using different scaling factors for vibrational frequencies.

USC UNIVERSIDADE DE SANTIAGO DE COMPOSTELA

## 10.2.5 Synthesis of substrates

### *10.2.5.1 Preparation of N,N-dimethylbenzamide (23a)*



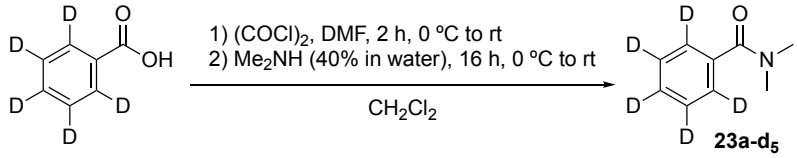

**23a**

Prepared following an adapted procedure:[133] To a solution of benzoic acid (1.22 g, 10.0 mmol, 1.0 equiv.) in $CH_2Cl_2$ (40 mL) at room temperature, oxalyl chloride $(COCl)_2$ (1.30 mL, 15.0 mmol, 1.5 equiv.) and DMF (5 drops) were carefully added in that order. The reaction mixture was stirred at room temperature for 2 h. After that time, the mixture was cooled down to 0 °C and $Me_2NH$ (40% w/w in water; 5.06 mL, 40.0 mmol, 4.0 equiv.) was added dropwise. The reaction mixture was stirred continuously at room temperature overnight.

The reaction was then quenched with water and organic materials were extracted twice with $CH_2Cl_2$, washed first with 1.0 M aqueous HCl solution followed by a second wash with saturated aqueous $NaHCO_3$ solution and brine. The organic fraction was dried over $MgSO_4$ and the solvent was removed in vacuo to obtain the *N,N*-dimethylbenzamide in a 83% yield (1.23 g) as a transparent oil that solidifies in the freezer as a white solid.

**$^1$H NMR** (400.16 MHz, $CDCl_3$, 258 K) δ 7.45 – 7.36 (m, 5H), 3.12 (s, 3H), 2.99 (s, 3H).
**$^{13}$C NMR** (100.63 MHz, $CDCl_3$, 258 K) δ 171.75 (CO), 136.04 (C, Ar), 129.69 (CH, Ar), 128.47 (CH, Ar), 127.09 (CH, Ar), 39.80 (N–$CH_3$), 35.43 (N–$CH_3$).
**$^{15}$N NMR** (40.55 MHz, $CDCl_3$, 258 K) δ 103.14.
**HRMS (ESI)**. Calculated for $C_9H_{12}NO^+$: 150.0913 Obtained: 150.0923

### *10.2.5.2 Preparation of N,N-dimethylbenzamide-$d_5$ (23a-$d_5$)*




**23a-$d_5$**

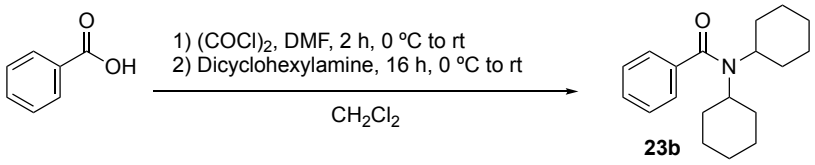
Prepared following an adapted procedure:[133] To a solution of benzoic acid-$d_5$ (255 mg, 2.0 mmol, 1.0 equiv.) in $CH_2Cl_2$ (8 mL) at room temperature, oxalyl chloride $(COCl)_2$ (0.25 mL, 3.0 mmol, 1.5 equiv.) and DMF (5 drops) were carefully added in that order. The reaction mixture was stirred at room temperature for 2 h. After that time, the mixture was cooled down to 0 °C and $Me_2NH$ (40% w/w in water; 1.0 mL, 8.0 mmol, 4.0 equiv.) was added dropwise. The reaction mixture was stirred continuously at room temperature overnight.

The reaction was then quenched with water and organic materials were extracted twice with $CH_2Cl_2$, washed first with 1.0 M aqueous HCl solution followed by a second wash with saturated aqueous $NaHCO_3$ solution and brine. The organic fraction was dried

over $MgSO_4$ and the solvent was removed in vacuo to obtain the *N,N*-dimethylbenzamide-$d_5$ in a 78% yield (240 mg) as a white solid.

**$^1$H NMR** (400.16 MHz, $CDCl_3$, 258 K) δ 3.09 (s, 3H), 2.96 (s, 3H).
**$^2$H NMR** (61 MHz, $CD_3COCD_3$) δ 7.46 (s, 5D).
**$^{13}$C NMR** (100.63 MHz, $CDCl_3$, 258 K) δ 171.64 (CO), 135.71 (C, Ar), 129.08 (CD, Ar, t, *J* = 23.9 Hz), 127.84 (CD, Ar, t, *J* = 24.1 Hz), 126.59 (CD, Ar, t, *J* = 24.1 Hz), 39.70 (N–$CH_3$), 35.32 (N–$CH_3$).
**$^{15}$N NMR** (40.55 MHz, $CDCl_3$, 258 K) δ 103.14.
**HRMS (ESI)**. Calculated for $C_9H_7D_5NO^+$: 155.1227 Obtained: 155.1229

### *10.2.5.3 Preparation of N,N-dicyclohexylbenzamide (23b)*




**23b**

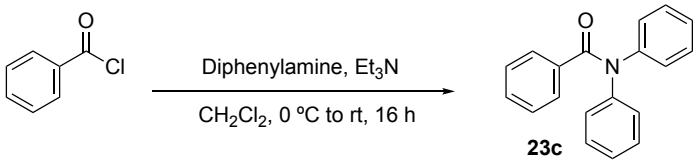
Prepared following an adapted procedure:[133] To a solution of benzoic acid (1.22 g, 10.0 mmol, 1.0 equiv.) in $CH_2Cl_2$ (40 mL) at room temperature, oxalyl chloride $(COCl)_2$ (1.30 mL, 15.0 mmol, 1.5 equiv.) and DMF (5 drops) were carefully added in that order. The reaction mixture was stirred at room temperature for 2 h. After that time, the mixture was cooled down to 0 °C and dicyclohexylamine (7.95 mL, 40.0 mmol, 4.0 equiv.) was added dropwise. The reaction mixture was stirred continuously at room temperature overnight.

The reaction was then quenched with water and organic materials were extracted twice with $CH_2Cl_2$, washed first with 1.0 M aqueous HCl solution followed by a second wash with saturated aqueous $NaHCO_3$ solution and brine. The organic fraction was dried over $MgSO_4$ and the solvent was removed in vacuo to obtain the *N,N*-dicyclohexylbenzamide in a 81% yield (2.32 g) as a white solid.

**$^1$H NMR** (400.16 MHz, $CDCl_3$, 258 K) δ 7.42 – 7.32 (m, 3H), 7.32 – 7.27 (m, 2H), 3.34 (tt, *J* = 12.0, 3.4 Hz, 1H), 2.99 (t, *J* = 12.1 Hz, 1H), 2.70 – 2.38 (m, 1H), 1.84 – 1.45 (m, 13H), 1.29 – 1.19 (m, 3H), 1.05 – 0.91 (m, 3H).
**$^{13}$C NMR** (100.63 MHz, $CDCl_3$, 258 K) δ 171.49 (CO), 138.50 (C, Ar), 128.83 (CH, Ar), 128.53 (CH, Ar), 125.58 (CH, Ar), 59.84 (N–CH), 56.17 (N–CH), 31.10 ($CH_2$), 29.88 ($CH_2$), 26.63 ($CH_2$), 25.49 ($CH_2$), 25.28 ($CH_2$), 25.05 ($CH_2$).
**$^{15}$N NMR** (40.55 MHz, $CDCl_3$, 258 K) δ 142.93
**HRMS (ESI)**. Calculated for $C_{19}H_{28}NO^+$: 286.2165 Obtained: 286.2160

USC UNIVERSIDADE DE SANTIAGO DE COMPOSTELA

### *10.2.5.4 Preparation of N,N-diphenylbenzamide (23c)*



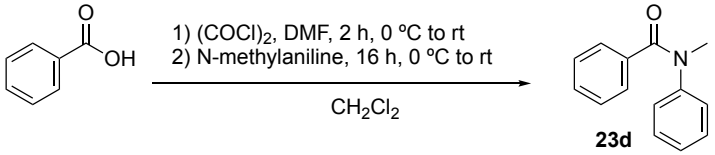

**23c**

Prepared following an adapted procedure:[136] A solution of diphenylamine (930 mg, 5.5 mmol, 1.1 equiv.) and triethylamine (0.76 mL, 5.5 mmol, 1.1 equiv.) in $CH_2Cl_2$ (10 mL) was cooled to 0 °C. To this mixture, benzoyl chloride (0.58 mL, 5.0 mmol, 1.0 equiv.) was added dropwise. The reaction mixture was stirred continuously at room temperature overnight.

The reaction was then quenched with water and organic materials were extracted twice with $CH_2Cl_2$, washed first with 1.0 M aqueous HCl solution followed by a second wash with saturated aqueous $NaHCO_3$ solution and brine. The organic fraction was dried over $MgSO_4$ and the solvent was removed in vacuo to obtain the *N*-benzoyl piperidine in a 79% yield (1.08 g) as a off-white solid.

**$^1$H NMR** (400.16 MHz, $CDCl_3$, 258K) δ 7.48 – 7.44 (m, 2H), 7.32 – 7.26 (m, 5H), 7.26 – 7.09 (m, 8H).
**$^{13}$C NMR** (100.63 MHz, $CDCl_3$, 258K) δ 170.78 (CO), 144.00 (C, Ar), 136.18 (C, Ar), 130.30 (CH, Ar), 129.29 (CH, Ar), 129.23 (CH, Ar), 127.99 (CH, Ar), 127.61 (CH, Ar), 126.47 (CH, Ar).
**$^{15}$N NMR** (40.55 MHz, $CDCl_3$) δ 147.25
**HRMS (ESI)**. Calculated for $C_{19}H_{16}NO^+$: 274.1226 Obtained: 274.1223

### *10.2.5.5 Preparation of N-methyl-N-phenylbenzamide (23d)*




**23d**

Prepared following an adapted procedure:[133] To a solution of benzoic acid (500 mg, 4.0 mmol, 1.0 equiv.) in $CH_2Cl_2$ (15 mL) at room temperature, oxalyl chloride $(COCl)_2$ (0.527 mL, 6.1 mmol, 1.5 equiv.) and DMF (5 drops) were carefully added in that order. The reaction mixture was stirred at room temperature for 2 h. After that time, the mixture was cooled down to 0 °C and *N*-methylaniline (4.43 mL, 16.0 mmol, 4.0 equiv.) was added dropwise. The reaction mixture was stirred continuously at room temperature overnight.

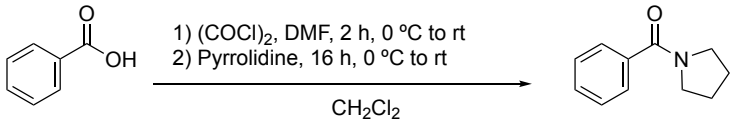
The reaction was then quenched with water and organic materials were extracted twice with $CH_2Cl_2$, washed first with 1.0 M aqueous HCl solution followed by a second wash with saturated aqueous $NaHCO_3$ solution and brine. The organic fraction was dried over $MgSO_4$ and the solvent was removed in vacuo to obtain the *N*-methyl-*N*-phenylbenzamide in an 86% yield (744 mg) as a white solid.

USC UNIVERSIDADE DE SANTIAGO DE COMPOSTELA

[136] Sitte, N. A.; Bursch, M.; Grimme, S.; Paradies, J. *J. Am. Chem. Soc.* **2019,** *141,* 159–162.

**$^{1}$H NMR** (400.16 MHz, $CDCl_3$, 258 K) δ 7.37 – 7.07 (m, 8H), 7.02 (d, *J* = 6.9 Hz, 2H), 3.49 (s, 3H).
**$^{13}$C NMR** (100.63 MHz, $CDCl_3$, 258 K) δ 170.79 (CO), 144.70 (C, Ar), 135.60 (C, Ar), 129.73 (CH, Ar), 129.20 (CH, Ar), 128.76 (CH, Ar), 127.80 (CH, Ar), 126.90 (CH, Ar), 126.56 (CH, Ar), 38.48 (N–$CH_3$).
**$^{15}$N NMR** (40.55 MHz, $CDCl_3$, 258 K) δ 125.69
**HRMS (ESI).** Calculated for $C_{14}H_{14}NO^+$: 212.1070 Obtained: 212.1067

### *10.2.5.6 Preparation of phenyl(pyrrolidin-1-yl)methanone (23e)*



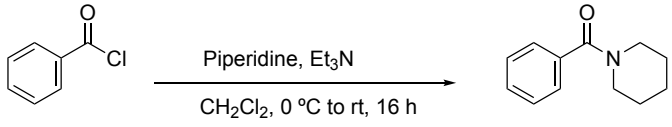

**23e**

Prepared following an adapted procedure:[133] To a solution of benzoic acid (500 mg, 4.0 mmol, 1.0 equiv.) in $CH_2Cl_2$ (10 mL) at room temperature, oxalyl chloride $(COCl)_2$ (0.527 mL, 6.1 mmol, 1.5 equiv.) and DMF (5 drops) were carefully added in that order. The reaction mixture was stirred at room temperature for 2 h. After that time, the mixture was cooled down to 0 °C and pyrrolidine (1.35 mL, 16.0 mmol, 4.0 equiv.) was added dropwise. The reaction mixture was stirred continuously at room temperature overnight.

The reaction was then quenched with water and organic materials were extracted twice with $CH_2Cl_2$, washed first with 1.0 M aqueous HCl solution followed by a second wash with saturated aqueous $NaHCO_3$ solution and brine. The organic fraction was dried over $MgSO_4$ and the solvent was removed in vacuo to obtain the *N*-Benzoylpyrrolidine in a 51% yield (367 mg) as a transparent oil.

**$^{1}$H NMR** (400.16 MHz, $CDCl_3$) δ 7.55 – 7.47 (m, 2H), 7.43 – 7.35 (m, 3H), 3.62 (t, *J* = 7.0 Hz, 2H), 3.42 (t, *J* = 6.6 Hz, 2H), 1.95 (p, *J* = 6.7, 2H), 1.86 (p, *J* = 6.6 Hz, 2H).
**$^{13}$C NMR** (100.63 MHz, $CDCl_3$) δ 169.84 (CO), 136.84 (C, Ar), 129.95 (CH, Ar), 128.32 (CH, Ar), 127.08 (CH, Ar), 49.83 (N–$CH_2$), 46.31 (N–$CH_2$), 26.42 ($CH_2$), 24.53 ($CH_2$).
**$^{15}$N NMR** (40.55 MHz, $CDCl_3$) δ 129.76
**HRMS (ESI)**. Calculated for $C_{11}H_{14}NO^+$: 176.1070 Obtained: 176.1068

### *10.2.5.7 Preparation of phenyl(piperidin-1-yl)methanone (23f)*




**23f**

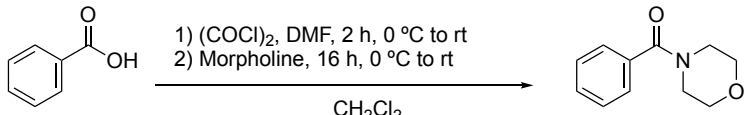
Prepared following an adapted procedure:[136] A solution of piperidine (0.54 mL, 5.5 mmol, 1.1 equiv.) and triethylamine (0.76 mL, 5.5 mmol, 1.1 equiv.) in $CH_2Cl_2$ (10 mL) was cooled to 0 °C. To this mixture, benzoyl chloride (0.58 mL, 5.0 mmol, 1.0 equiv.) was added dropwise. The reaction mixture was stirred continuously at room temperature overnight.

USC UNIVERSIDADE DE SANTIAGO DE COMPOSTELA

The reaction was then quenched with water and organic materials were extracted twice with $CH_2Cl_2$, washed first with 1.0 M aqueous HCl solution followed by a second wash with saturated aqueous $NaHCO_3$ solution and brine. The organic fraction was dried over $MgSO_4$ and the solvent was removed in vacuo to obtain the *N*-benzoyl piperidine in a 99% yield (940 mg) as a white solid.

**$^1$H NMR** (400.16 MHz, $CDCl_3$) δ 7.41 – 7.36 (m, 5H), 3.70 (t, *J* = 6.8, 5.4 Hz, 2H), 3.33 (t, *J* = 7.0, 5.3 Hz, 2H), 1.70 – 1.61 (m, 4H), 1.55 – 1.45 (m, 2H).
**$^{13}$C NMR** (100.63 MHz, $CDCl_3$) δ 170.38 (CO), 136.22 (C, Ar), 129.50 (CH, Ar), 128.54 (CH, Ar), 126.77 (CH, Ar), 48.82 (N–$CH_2$), 43.08 (N–$CH_2$), 26.53 ($CH_2$), 25.62 ($CH_2$), 24.55 ($CH_2$).
**$^{15}$N NMR** (40.55 MHz, $CDCl_3$) δ 124.95
**HRMS (ESI)**. Calculated for $C_{12}H_{16}NO^+$: 190.1226 Obtained: 190.1225

### *10.2.5.8 Preparation of morpholino(phenyl)methanone (23g)*




**23g**

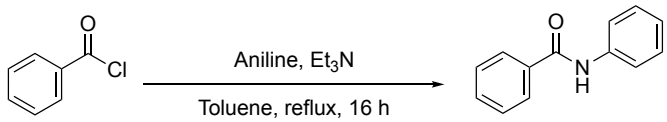
Prepared following an adapted procedure:[133] To a solution of benzoic acid (611 mg, 5.0 mmol, 1.0 equiv.) in $CH_2Cl_2$ (20 mL) at room temperature, oxalyl chloride $(COCl)_2$ (0.65 mL, 7.5 mmol, 1.5 equiv.) and DMF (5 drops) were carefully added in that order. The reaction mixture was stirred at room temperature for 2 h. After that time, the mixture was cooled down to 0 °C and morpholine (1.74 mL, 20.0 mmol, 4.0 equiv.) was added dropwise. The reaction mixture was stirred continuously at room temperature overnight.

The reaction was then quenched with water and organic materials were extracted twice with $CH_2Cl_2$, washed first with 1.0 M aqueous HCl solution followed by a second wash with saturated aqueous $NaHCO_3$ solution and brine. The organic fraction was dried over $MgSO_4$ and the solvent was removed in vacuo to obtain the morpholino(phenyl)methanone in a 99% yield (950 mg) as a white solid.

**$^1$H NMR** (400.16 MHz, $CDCl_3$, 258 K) δ 7.44 – 7.37 (m, 5H), 3.80 (m, 4H), 3.62 (dd, *J* = 5.6, 4.0 Hz, 2H), 3.46 (dd, *J* = 5.6, 4.0 Hz, 2H).
**$^{13}$C NMR** (100.63 MHz, $CDCl_3$, 258 K) δ 170.52 (CO), 134.99 (C, Ar), 130.06 (CH, Ar), 128.70 (CH, Ar), 127.10 (CH, Ar), 66.97 ($CH_2$), 66.89 ($CH_2$), 48.18 ($CH_2$), 42.42 ($CH_2$).
**$^{15}$N NMR** (40.55 MHz, $CDCl_3$, 258 K) δ 116.12
**HRMS (ESI)**. Calculated for $C_{11}H_{14}NO_2^+$: 192.1019 Obtained: 192.1016

USC UNIVERSIDADE DE SANTIAGO DE COMPOSTELA

### *10.2.5.9 Preparation of N-phenylbenzamide (23i)*

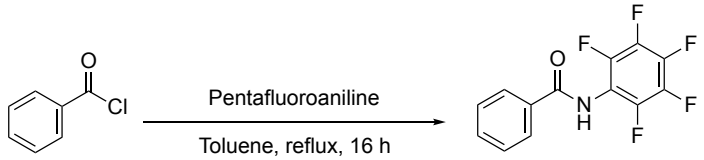



**23i**

Prepared following an adapted procedure:[137] Benzoyl chloride (0.29 mL, 2.5 mmol, 1.0 equiv.) was added to a stirring solution of aniline (0.25 mL, 2.75 mmol, 1.1 equiv.) in toluene (10 mL). The reaction mixture was stirred continuously under reflux overnight. After cooling to room temperature, the white precipitate was filtered off, washed with cold water, and recrystallized from EtOAc/hexane (1:10) to give the desired product **23i** in 93% yield (460 mg) as a grey solid.

**$^{1}$H NMR** (400.16 MHz, $CDCl_3$) δ 8.03 (s, 1H), 7.90 – 7.82 (m, 2H), 7.69 – 7.63 (m, 2H), 7.58 – 7.53 (m, 1H), 7.50 – 7.43 (m, 2H), 7.40 – 7.35 (m, 2H), 7.21 – 7.12 (m, 1H).
**$^{13}$C NMR** (100.63 MHz, $CDCl_3$) δ 166.05 (CO), 137.78 (C, Ar), 134.78 (C, Ar), 132.05 (CH, Ar), 129.21 (CH, Ar), 128.89 (CH, Ar), 127.09 (CH, Ar), 124.66 (CH, Ar), 120.14 (CH, Ar).
**$^{15}$N NMR** (40.55 MHz, $CDCl_3$) δ 127.24
**HRMS (ESI).** Calculated for $C_{13}H_{12}NO^+$: 198.0913 Obtained: 198.0911

### *10.2.5.10 Preparation of N-(perfluorophenyl)benzamide (23j)*




**23j**

Prepared following an adapted procedure:[137] Benzoyl chloride (0.29 mL, 2.5 mmol, 1.0 equiv.) was added to a stirring solution of 2,3,4,5,6-pentafluoroaniline (503.5 mg, 2.75 mmol, 1.1 equiv.) in toluene (10 mL). The reaction mixture was stirred continuously under reflux overnight. After cooling to room temperature, the white precipitate was filtered off, washed with cold water, and recrystallized from EtOAc/hexane (1:10) to give the desired product **23j** in 38% yield (274 mg) as an off-white solid.

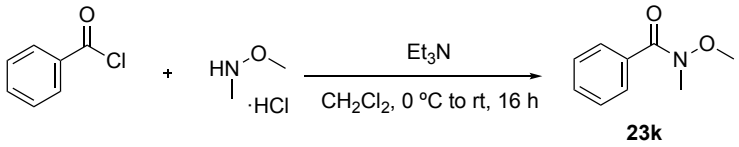
**$^{1}$H NMR** (400.16 MHz, $CDCl_3$, 313 K) δ 7.90 (dd, *J* = 8.3, 1.4 Hz, 2H), 7.61 (tt, *J* = 7.4, 7.4, 1.6 Hz, 1H), 7.55 – 7.45 (m, 3H).
**$^{13}$C NMR** (100.63 MHz, $CDCl_3$, 313 K) δ 165.80 (CO), 144.54 (CF, Ar, dq, *J* = 12.1, 4.2 Hz), 142.04 (CF, Ar, dq, *J* = 12.6, 4.3 Hz), 141.62 (CF, Ar, tt, *J* = 13.3, 4.4 Hz), 139.64 – 138.90 (CF, Ar, m), 137.10 – 136.57 (CF, Ar, m), 133.00 (CH, Ar), 132.66 (C, Ar), 129.10 (CH, Ar), 127.80 (CH, Ar), 112.33 (CN, Ar, td, *J* = 14.9, 4.1 Hz).
**$^{19}$F NMR** (376.46 MHz, $CDCl_3$) δ -144.79 – -144.95 (m), -156.69 (t, *J* = 21.2 Hz), -162.46 (tt, *J* = 19.5, 4.5 Hz).

[137] Lu, Y.; Wang, H.; Spangler, J. E.; Chen, K.; Cui, P.; Zhao, Y.; Sun, W.; Yu, J. *Chem. Sci.* **2015,** *6,* 1923–1927.

USC UNIVERSIDADE DE SANTIAGO DE COMPOSTELA

**$^{15}$N NMR** (40.55 MHz, $CDCl_3$, 313 K) δ 96.16
**HRMS (ESI).** Calculated for $C_{13}H_7F_5NO^+$: 288.0442 Obtained: 288.0440

### *10.2.5.11 Preparation of N-methoxy-N-methylbenzamide (23k)*



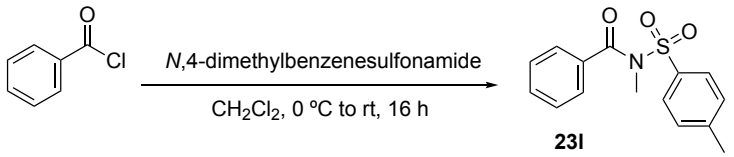

**23k**

Prepared following an adapted procedure:[136] A solution of *N*-methoxy-*N*-methylamine hydrochloride (1.21 g, 5.0 mmol, 1.0 equiv.) and triethylamine (1.39 mL, 10 mmol, 2.0 equiv.) in $CH_2Cl_2$ (10 mL) was cooled to 0 °C. To this mixture, benzoyl chloride (0.58 mL, 5.0 mmol, 1.0 equiv.) was added dropwise. The reaction mixture was stirred continuously at room temperature overnight.

The reaction was then quenched with water and organic materials were extracted twice with $CH_2Cl_2$, washed first with 1.0 M aqueous HCl solution followed by a second wash with saturated aqueous $NaHCO_3$ solution and brine. The organic fraction was dried over $MgSO_4$ and the solvent was removed in vacuo to obtain the desired product in 81% yield (669 mg) as a colorless oil.

**$^1$H NMR** (400.16 MHz, $CDCl_3$, 258 K) δ 7.65 (d, *J* = 7.4 Hz, 2H), 7.51 – 7.35 (m, 3H), 3.53 (s, 3H), 3.36 (s, 3H).
**$^{13}$C NMR** (100.63 MHz, $CDCl_3$, 258 K) δ 169.87 (CO), 133.77(C, Ar), 130.70 (CH, Ar), 128.10 (CH, Ar), 61.17 (O–$CH_3$), 33.16 (N–$CH_3$).
**$^{15}$N NMR** (40.55 MHz, $CDCl_3$, 258 K) δ 186.22
**HRMS (ESI)**. Calculated for $C_9H_{12}NO_2^+$: 166.0863 Obtained: 166.0862

### *10.2.5.12 Preparation of N-methyl-N-tosylbenzamide (23l)*




**23l**

Prepared following an adapted procedure:[138] A solution of *N*,4-dimethylbenzenesulfonamide (1.01 g, 5.5 mmol, 1.1 equiv.) and triethylamine (0.76 mL, 5.5 mmol, 1.1 equiv.) in $CH_2Cl_2$ (10 mL) was cooled to 0 °C. To this mixture, benzoyl chloride (0.58 mL, 5.0 mmol, 1.0 equiv.) was added dropwise. The reaction mixture was stirred continuously at room temperature overnight.

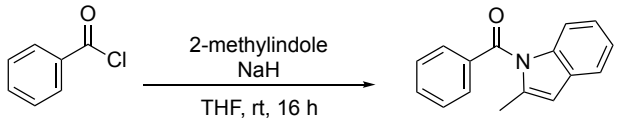
The reaction was then quenched with water and organic materials were extracted twice with $CH_2Cl_2$, washed first with 1.0 M aqueous HCl solution followed by a second

[138] Shi, S.; Szostak, M. *Chem. Eur. J.* **2016,** *22,* 10420–10424.

wash with saturated aqueous $NaHCO_3$ solution and brine. The organic fraction was dried over $MgSO_4$ and the solvent was removed in vacuo to obtain the desired product in a 62% yield (902 mg) as a white solid.

**$^1$H NMR** (400.16 MHz, $CDCl_3$) δ 7.92 – 7.84 (m, 2H), 7.59 – 7.48 (m, 3H), 7.47 – 7.37 (m, 2H), 7.35 (dd, *J* = 8.7, 0.7 Hz, 2H), 3.29 (s, 3H), 2.44 (s, 3H).
**$^{13}$C NMR** (100.63 MHz, $CDCl_3$) δ 171.61 (CO), 145.06 (C, Ar), 135.25 (C, Ar), 134.57 (C, Ar), 132.11 (CH, Ar), 129.75 (CH, Ar), 128.61 (CH, Ar), 128.55 (CH, Ar), 128.43 (CH, Ar), 35.78 (N–$CH_3$), 21.81 ($CH_3$).
**$^{15}$N NMR** (40.55 MHz, $CDCl_3$) δ 153.17
**HRMS (ESI)**. Calculated for $C_{15}H_{17}NO_3S^+$: 290.0845 Obtained: 290.0845

### *10.2.5.13 Preparation of (2-methyl-1H-indol-1-yl)(phenyl)methanone (23m)*




**23m**

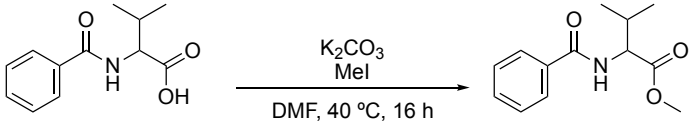
Prepared following an adapted procedure:[139] A stirred solution of 2-methylindole (524 mg, 4.0 mmol, 1.0 equiv.) in dry THF (10 mL) was cooled down to 0 °C and NaH (60% dispersion in mineral oil, 192 mg, 4.8 mmol, 1.2 equiv.) was added in portions and the mixture was allowed to warm to room temperature. After 30 min, the reaction was cooled down to 0 °C and benzoyl chloride (0.92 mL, 8.0 mmol, 2.0 equiv.) was added dropwise. The reaction was stirred at room temperature overnight. After that time, water (10 mL) was added, and the mixture was extracted with $CH_2Cl_2$ (3 x 20 mL). The combined organic layers were dried over $MgSO_4$ and the volatiles were removed under reduced pressure. The residue was purified by colum chromatography (pentane/$Et_2O$ 20/1) to afford the desired compound in a 37% yield (349 mg) as an off-white solid.

**$^1$H NMR** (400.16 MHz, $CDCl_3$) δ 7.75 (dd, *J* = 8.4, 1.3 Hz, 2H), 7.69 – 7.63 (m, 1H), 7.55 – 7.49 (m, 3H), 7.19 (ddd, *J* = 7.7, 6.7, 1.5 Hz, 1H), 7.09 – 7.00 (m, 2H), 6.47 (d, *J* = 1.1 Hz, 1H), 2.45 (d, *J* = 1.2 Hz, 3H).
**$^{13}$C NMR** (100.63 MHz, $CDCl_3$) δ 170.02 (CO), 138.03 (C, Pyrrole), 136.92 (C, Ar), 135.18 (C, Ar), 133.05 (C, Ar), 129.76 (CH, Ar), 129.43 (CH, Ar), 128.81 (CH, Ar), 122.62 (CH, Ar), 122.60 (CH, Ar), 119.83 (CH, Ar), 114.33 (CH, Ar), 108.62 (CH, Pyrrole), 16.05 ($CH_3$).
**$^{15}$N NMR** (40.55 MHz, $CDCl_3$) δ 176.20
**HRMS (ESI)**. Calculated for $C_{16}H_{14}NO^+$: 236.1070 Obtained: 236.1067

USC UNIVERSIDADE

[139] Ramella; He; Daniliuc; Studer *Org. Lett.* **2015,** *17,* 664–667.

*10.2.5.14 Preparation of methyl benzoylvalinate (23n)*



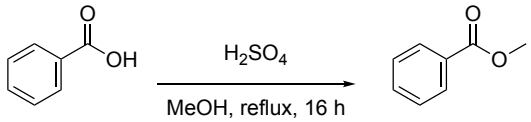

**23n**

Prepared following an adapted procedure:[140] In a 25 mL round-bottom flask equipped with a magnetic stirring bar, the *N*-benzoyl-*DL*-valine (221 mg, 1 mmol, 1.0 equiv.), $K_2CO_3$ (276 mg, 2 mmol, 2 equiv.) and DMF (2 mL) were added. Then, methyl iodide (0.075 mL, 1.2 mmol, 1.2 equiv.) was added and the reaction mixture was heated at 40 °C overnight.

Upon completion, the reaction crude was diluted with water and $Et_2O$. The organic phase was washed with water, saturated $K_2CO_3$ and brine, then it was dried over $MgSO_4$, and evaporated to dryness to afford the desired compound as a white solid in a 67% yield (158 mg).

**$^1$H NMR** (400.16 MHz, $CDCl_3$, 258 K) δ 7.85 – 7.77 (m, 2H), 7.58 – 7.49 (m, 1H), 7.51 – 7.42 (m, 2H), 6.69 (d, *J* = 8.7 Hz, 1H), 4.80 (dd, *J* = 8.7, 4.8 Hz, 1H), 3.78 (s, 3H), 2.28 (pd, *J* = 6.9, 4.8 Hz, 1H), 0.98 (dd, *J* = 13.3, 6.9 Hz, 6H).
**$^{13}$C NMR** (100.63 MHz, $CDCl_3$, 258 K) δ 172.82 (CO), 167.41 (CO), 134.33 (C, Ar), 131.88 (CH, Ar), 128.77 (CH, Ar), 127.19 (CH, Ar), 57.54 (N–CH), 52.40 (O–$CH_3$), 31.81 (CH), 19.14 ($CH_3$), 18.10 ($CH_3$).
**$^{15}$N NMR** (40.55 MHz, $CDCl_3$) δ 108.26
**HRMS (ESI).** Calculated for $C_{13}H_{18}NO_3^+$: 236.1281 Obtained: 236.1278

*10.2.5.15 Preparation of methyl benzoate (23o)*




**23o**

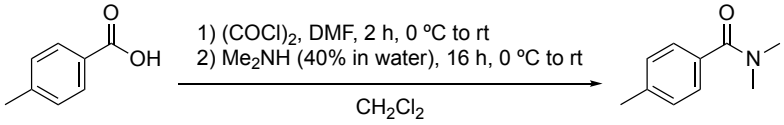
Benzoic acid (1.20 g, 10 mmol, 1.0 equiv.) was dissolved in MeOH (20 mL), and 98% sulfuric acid (0.54 mL, 10 mmol, 1.0 equiv.) was added. The mixture was heated to reflux 16 h. After that time the reaction solution was cooled to room temperature and concentrated in vacuo. The resulting crude residue was dissolved in a sat. $NaHCO_3$ solution and extracted with $CH_2Cl_2$. The combined organic layers were washed with brine, dried over $MgSO_4$, and concentrated to afford the methyl benzoate in 99% yield (1.3 g) as a colorless oil.

**$^1$H NMR** (400.16 MHz, $CDCl_3$) δ 8.04 (dd, *J* = 8.2, 1.4 Hz, 2H), 7.55 (ddt, *J* = 8.0, 6.9, 1.3 Hz, 1H), 7.43 (tt, *J* = 6.8, 1.3 Hz, 2H), 3.91 (s, 3H).

[140] Ticconi, B.; Colcerasa, A.; Stefano, S. D.; Lanzalunga, O.; Lapi, A.; Mazzonna, M.; Olivo, G. *RSC Adv.* **2018,** *8,* 19144–19151.

**$^{13}$C NMR** (100.63 MHz, $CDCl_3$) δ 167.21 (CO), 133.01 (C, Ar), 130.27 (CH, Ar), 129.67 (CH, Ar), 128.46 (CH, Ar), 52.19 (O–$CH_3$).
**HRMS (ESI)**. Calculated for $C_8H_9O_2^+$: 137.0597 Obtained: 137.0597

### *10.2.5.16 Preparation of N,N-4-trimethylbenzamide (23aa)*



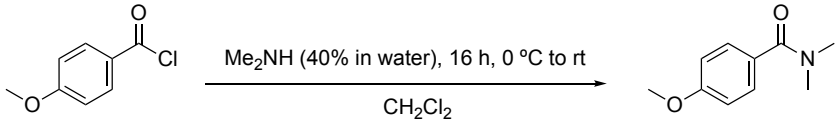

**23aa**

Prepared following an adapted procedure:[133] To a solution of *p*-toluic acid (681 mg, 5.0 mmol, 1.0 equiv.) in $CH_2Cl_2$ (20 mL) at room temperature, oxalyl chloride $(COCl)_2$ (0.643 mL, 7.5 mmol, 1.5 eq) and DMF (5 drops) were carefully added in that order. The reaction mixture was stirred at room temperature for 2 h. After that time, the mixture was cooled down to 0 ºC and $Me_2NH$ (40% w/w in water; 2.5 mL, 20.0 mmol, 4.0 equiv.) was added dropwise. The reaction mixture was stirred continuously at room temperature overnight.

The reaction was then quenched with water and organic materials were extracted twice with $CH_2Cl_2$, washed first with 1.0 M aqueous HCl solution followed by a second wash with saturated aqueous $NaHCO_3$ solution and brine. The organic fraction was dried over $MgSO_4$ and the solvent was removed in vacuo to obtain the *N,N*-4-trimethylbenzamide in a 73% yield (594 mg) as a white solid.

**$^1$H NMR** (400.16 MHz, $CDCl_3$, 258 K) δ 7.31 (d, *J* = 7.8 Hz, 2H), 7.19 (d, *J* = 7.8 Hz, 2H), 3.04 (s, 6H), 2.37 (s, 3H).
**$^{13}$C NMR** (100.63 MHz, $CDCl_3$, 258 K) δ 172.00 (CO), 139.81 (C, Ar), 133.31 (C, Ar), 129.05 (CH, Ar), 127.33 (CH, Ar), 37.73 (N–$CH_3$), 37.17 (N–$CH_3$), 21.50 ($CH_3$).
**$^{15}$N NMR** (40.55 MHz, $CDCl_3$) δ 102.64
**HRMS (ESI)**. Calculated for $C_{10}H_{14}NO^+$: 164.1070 Obtained: 164.1073

### *10.2.5.17 Preparation of 4-methoxy-N,N-dimethylbenzamide (23ab)*




**23ab**

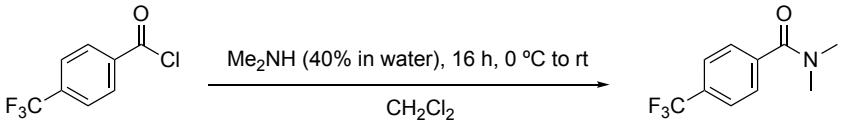
Prepared following an adapted procedure:[133] To a solution of 4-methoxybenzoyl chloride (426 mg, 2.5 mmol, 1.0 equiv.) in $CH_2Cl_2$ (20 mL), $Me_2NH$ (40% w/w in water; 2.5 mL, 20.0 mmol, 4.0 equiv.) was added dropwise at 0 ºC. The reaction mixture was stirred continuously at room temperature for 2 h.

The reaction was then quenched with water and organic materials were extracted twice with $CH_2Cl_2$, washed first with 1.0 M aqueous HCl solution followed by a second

wash with saturated aqueous $NaHCO_3$ solution and brine. The organic fraction was dried over $MgSO_4$ and the solvent was removed in vacuo to obtain the 4-methoxy-*N,N*-dimethylbenzamide in a 71% yield (320 mg) as a orange solid.

**$^1$H NMR** (400.16 MHz, $CDCl_3$, 258 K) δ 7.35 (d, *J* = 8.7 Hz, 2H), 6.84 (d, *J* = 8.7 Hz, 2H), 3.76 (s, 3H), 3.03 (s, 3H), 2.97 (s, 3H).
**$^{13}$C NMR** (100.63 MHz, $CDCl_3$, 258 K) δ 171.42 (CO), 160.27 (C, Ar), 129.08 (CH, Ar), 127.87 (C, Ar), 113.29 (CH, Ar), 55.27 (O–$CH_3$), 39.86 (N–$CH_3$), 35.47 (N–$CH_3$).
**$^{15}$N NMR** (40.55 MHz, $CDCl_3$) δ 101.92
**HRMS (ESI)**. Calculated for $C_{10}H_{14}NO_2^+$: 180.1019 Obtained: 180.1021

### *10.2.5.18 Preparation of N,N-dimethyl-4-(trifluoromethyl)benzamide (23ac)*




**23ac**

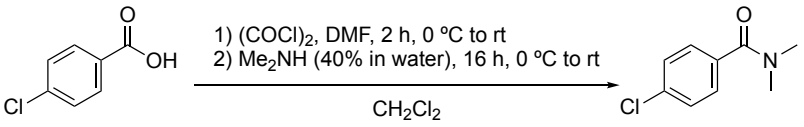
Prepared following an adapted procedure:[133] A solution of 4-(trifluoromethyl)benzoyl chloride (1.04 g, 5.0 mmol, 1.0 equiv.) in $CH_2Cl_2$ (20 mL) was cooled to 0 °C. To this mixture, $Me_2NH$ (40% w/w in water; 2.5 mL, 20.0 mmol, 4.0 equiv.) was added dropwise. The reaction mixture was stirred continuously at room temperature overnight.

The reaction was then quenched with water and organic materials were extracted twice with $CH_2Cl_2$, washed first with 1.0 M aqueous HCl solution followed by a second wash with saturated aqueous $NaHCO_3$ solution and brine. The organic fraction was dried over $MgSO_4$ and the solvent was removed in vacuo to obtain the *N,N*-dimethyl-4-(trifluoromethyl)benzamide in a 97% yield (532 mg) as a white solid.

**$^1$H NMR** (400.16 MHz, $CDCl_3$, 258 K) δ 7.72 – 7.62 (m, 2H), 7.56 – 7.48 (m, 2H), 3.12 (s, 3H), 2.96 (s, 3H).
**$^{13}$C NMR** (100.63 MHz, $CDCl_3$, 258 K) δ 170.21 (CO), 139.69 (C, Ar), 131.34 (C, Ar, q, *J* = 32.6 Hz), 127.40 (CH, Ar), 125.63 (CH, Ar, q, *J* = 3.8 Hz), 123.76 ($CF_3$, q, *J* = 272.4 Hz), 39.56 (N–$CH_3$), 35.34 (N–$CH_3$).
**$^{19}$F NMR** (376.46 MHz, $CDCl_3$, 258 K) δ -62.91.
**$^{15}$N NMR** (40.55 MHz, $CDCl_3$) δ 103.91
**HRMS (ESI)**. Calculated for $C_{10}H_{11}F_3NO^+$: 218.0787 Obtained: 218.0785

USC UNIVERSIDADE DE SANTIAGO DE COMPOSTELA

### *10.2.5.19 Preparation of 4-chloro-N,N-dimethylbenzamide (23ad)*



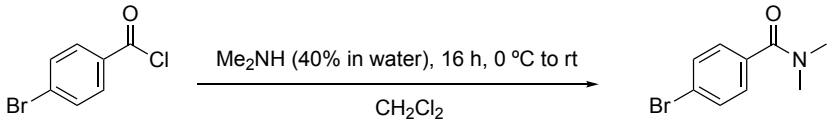

**23ad**

Prepared following an adapted procedure:[133] To a solution of 4-chlorobenzoic acid (391 mg, 2.5 mmol, 1.0 equiv.) in $CH_2Cl_2$ (10 mL) at room temperature, oxalyl chloride $(COCl)_2$ (0.322 mL, 3.75 mmol, 1.5 equiv.) and DMF (5 drops) were carefully added in that order. The reaction mixture was stirred at room temperature for 2 h. After that time, the mixture was cooled down to 0 °C and $Me_2NH$ (40% w/w in water; 1.25 mL, 10.0 mmol, 4.0 equiv.) was added dropwise. The reaction mixture was stirred continuously at room temperature overnight.

The reaction was then quenched with water and organic materials were extracted twice with $CH_2Cl_2$, washed first with 1.0 M aqueous HCl solution followed by a second wash with saturated aqueous $NaHCO_3$ solution and brine. The organic fraction was dried over $MgSO_4$ and the solvent was removed in vacuo to obtain the 4-chloro-*N,N*-dimethylbenzamide in a 83% yield (384 mg) as a white solid.

**$^1$H NMR** (400.16 MHz, $CDCl_3$, 258 K) δ 7.35 (s, 4H), 3.07 (s, 3H), 2.95 (s, 3H).
**$^{13}$C NMR** (100.63 MHz, $CDCl_3$, 258 K) δ 170.55 (CO), 135.46 (C, Ar), 134.29 (C, Ar), 128.63 (CH, Ar), 39.69 (N–$CH_3$), 35.43 (N–$CH_3$).
**$^{15}$N NMR** (40.55 MHz, $CDCl_3$) δ 103.38
**HRMS (ESI)**. Calculated for $C_9H_{10}ClNO^+$: 184.0524 Obtained: 184.0522

### *10.2.5.20 Preparation of 4-bromo-N,N-dimethylbenzamide (23ae)*




**23ae**

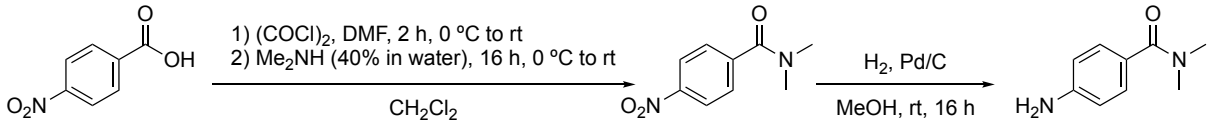
Prepared following an adapted procedure:[133] To a solution of 4-bromobenzoyl chloride (1.09 g, 5.0 mmol, 1.0 equiv.) in $CH_2Cl_2$ (20 mL) at 0 °C $Me_2NH$ (40% w/w in water; 2.5 mL, 20.0 mmol, 4.0 equiv.) was added dropwise. The reaction mixture was stirred continuously at room temperature overnight.

The reaction was then quenched with water and organic materials were extracted twice with $CH_2Cl_2$, washed first with 1.0 M aqueous HCl solution followed by a second wash with saturated aqueous $NaHCO_3$ solution and brine. The organic fraction was dried over $MgSO_4$ and the solvent was removed in vacuo to obtain the 4-bromo-*N,N*-dimethylbenzamide in a 77% yield (886 mg) as a white solid.

**$^1$H NMR** (400.16 MHz, $CDCl_3$, 258 K) δ 7.50 (ddd, *J* = 8.6, 2.7, 2.1 Hz, 2H), 7.27 (ddd, *J* = 8.6, 2.7, 2.0 Hz, 2H), 3.06 (s, 3H), 2.94 (s, 3H).

**$^{13}$C NMR** (100.63 MHz, $CDCl_3$, 258 K) δ 170.53 (CO), 134.73 (C, Ar), 131.52 (CH, Ar), 128.80 (CH, Ar), 123.79 (C, Ar), 39.65 (N–$CH_3$), 35.38 (N–$CH_3$).
**$^{15}$N NMR** (40.55 MHz, $CDCl_3$, 258 K) δ 103.43
**HRMS (ESI).** Calculated for $C_9H_{11}BrNO^+$: 228.0019 Obtained: 228.0013

### *10.2.5.21 Preparation of 4-amino-N,N-dimethylbenzamide (23ag)*




*Step 1*

Prepared following an adapted procedure:[133] To a solution of 4-nitrobenzoic acid (1.67 g, 10.0 mmol, 1.0 equiv.) in $CH_2Cl_2$ (40 mL) at room temperature, oxalyl chloride $(COCl)_2$ (1.30 mL, 15.0 mmol, 1.5 equiv.) and DMF (5 drops) were carefully added in that order. The reaction mixture was stirred at room temperature for 2 h. After that time, the mixture was cooled down to 0 °C and $Me_2NH$ (40% w/w in water; 5.06 mL, 40.0 mmol, 4.0 equiv.) was added dropwise. The reaction mixture was stirred continuously at room temperature overnight.

The reaction was then quenched with water and organic materials were extracted twice with $CH_2Cl_2$, washed first with 1.0 M aqueous HCl solution followed by a second wash with saturated aqueous $NaHCO_3$ solution and brine. The organic fraction was dried over $MgSO_4$ and the solvent was removed in vacuo to obtain the *N,N*-dimethyl-4-nitro benzamide in a 63% yield (1.23 g) as a yellow solid.

**$^{1}$H NMR** (400.16 MHz, $CDCl_3$, 258 K) δ 8.24 (d, *J* = 8.9 Hz, 2H), 7.56 (d, *J* = 8.8 Hz, 2H), 3.09 (s, 3H), 2.93 (s, 3H).
**$^{13}$C NMR** (100.63 MHz, $CDCl_3$, 258 K) δ 169.18 (CO), 147.85 (C, Ar), 142.27 (C, Ar), 128.04 (CH, Ar), 123.79 (CH, Ar), 39.37 (N–$CH_3$), 35.27 (N–$CH_3$).
**$^{15}$N NMR** (40.55 MHz, $CDCl_3$, 258 K) δ 167.92, 104.82.
**HRMS (ESI)**. Calculated for $C_9H_{11}N_2O_3^+$: 195.0764 Obtained: 195.0763

*Step 2*

Prepared following an adapted procedure:[141] To a 100 mL round-bottom flask equipped with a teflon septum and a magnetic stir bar, the *N,N*-dimethyl-4-nitrobenzamide (500 mg, 2.5 mmol, 1.0 equiv.) and Pd/C (50 mg, 10% w/w, 0.5 mmol, 10 mol%) were added.

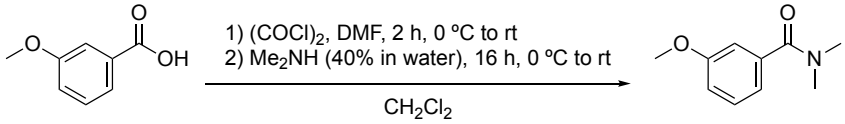
The flask was purged with a stream of $N_2$ and MeOH (30 mL) was added to the flask via a syringe. The reaction mixture was degassed with $N_2$ and $H_2$ was bubbled trough the solution using a balloon. After being stirred for 16 h at room temperature, the mixture was

[141] Ide, T.; Barham, J. P.; Fujita, M.; Kawato, Y.; Egami, H.; Hamashima, Y. *Chem. Sci.* **2018,** *9,* 8453–8460.

filtered through a pad of Celite and the filtrate was concentrated in vacuo giving the in 95% yield (403 mg) as a white solid.

**$^{1}$H NMR** (400.16 MHz, $CDCl_3$, 258 K) δ 7.24 (d, *J* = 8.6 Hz, 1H), 6.61 (d, *J* = 8.6 Hz, 1H), 3.84 (bs, 2H), 3.03 (s, 3H), 3.00 (s, 3H).
**$^{13}$C NMR** (100.63 MHz, $CDCl_3$, 258 K) δ 172.00 (CO), 147.83 (C, Ar), 129.33 (CH, Ar), 125.29 (C, Ar), 114.20 (CH, Ar), 40.12 (N–$CH_3$), 35.69 (N–$CH_3$).
**$^{15}$N NMR** (40.55 MHz, $CDCl_3$, 258 K) δ 100.96, 58.5
**HRMS (ESI)**. Calculated for $C_9H_{13}N_2O^+$: 165.1022 Obtained: 165.1023

### *10.2.5.22 Preparation of 3-methoxy-N,N-dimethylbenzamide (23ah)*




**23ah**

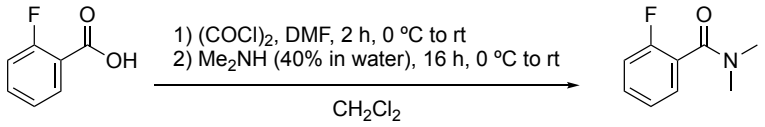
Prepared following an adapted procedure:[133] To a solution of 3-methoxybenzoic acid (761 mg, 5.0 mmol, 1.0 equiv.) in $CH_2Cl_2$ (20 mL) at room temperature, oxalyl chloride $(COCl)_2$ (0.643 mL, 7.5 mmol, 1.5 equiv.) and DMF (5 drops) were carefully added in that order. The reaction mixture was stirred at room temperature for 2 h. After that time, the mixture was cooled down to 0 °C and $Me_2NH$ (40% w/w in water; 2.5 mL, 20.0 mmol, 4.0 equiv.) was added dropwise. The reaction mixture was stirred continuously at room temperature overnight.

The reaction was then quenched with water and organic materials were extracted twice with $CH_2Cl_2$, washed first with 1.0 M aqueous HCl solution followed by a second wash with saturated aqueous $NaHCO_3$ solution and brine. The organic fraction was dried over $MgSO_4$ and the solvent was removed in vacuo to obtain the 3-methoxy-*N,N*-dimethylbenzamide in a 97% yield (870 g) as an orange oil.

**$^{1}$H NMR** (400.16 MHz, $CDCl_3$, 258 K) δ 7.33 – 7.27 (m, 1H), 6.98 – 6.90 (m, 3H), 3.81 (s, 3H), 3.10 (s, 3H), 2.97 (s, 3H).
**$^{13}$C NMR** (100.63 MHz, $CDCl_3$, 258 K) δ 171.37 (CO), 159.22 (C, Ar), 137.27 (C, Ar), 129.52 (CH, Ar), 119.03 (CH, Ar), 115.34 (CH, Ar), 111.95 (CH, Ar), 55.32 (O–$CH_3$), 39.65 (N–$CH_3$), 35.28 (N–$CH_3$).
**$^{15}$N NMR** (40.55 MHz, $CDCl_3$, 258 K) δ 103.34
**HRMS (ESI)**. Calculated for $C_{10}H_{14}NO_2^+$: 180.1019 Obtained: 180.1016

USC UNIVERSIDADE DE SANTIAGO DE COMPOSTELA

*10.2.5.23 Preparation of 2-fluoro-N,N-dimethylbenzamide (23aj)*



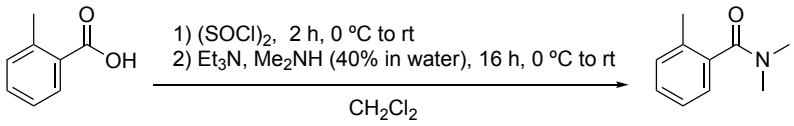

**23aj**

Prepared following an adapted procedure:[133] To a solution of 2-fluorobenzoic acid (1.40 g, 10.0 mmol, 1.0 equiv.) in $CH_2Cl_2$ (20 mL) at room temperature, oxalyl chloride $(COCl)_2$ (1.3 mL, 15.0 mmol, 1.5 equiv.) and DMF (5 drops) were carefully added in that order. The reaction mixture was stirred at room temperature for 2 h. After that time, the mixture was cooled down to 0 °C and $Me_2NH$ (40% w/w in water; 5 mL, 40.0 mmol, 4.0 equiv.) was added dropwise. The reaction mixture was stirred continuously at room temperature overnight.

The reaction was then quenched with water and organic materials were extracted twice with $CH_2Cl_2$, washed first with 1.0 M aqueous HCl solution followed by a second wash with saturated aqueous $NaHCO_3$ solution and brine. The organic fraction was dried over $MgSO_4$ and the solvent was removed in vacuo to obtain the 3-bromo-*N,N*-4-trimethylbenzamide in a 58% yield (972 mg) as a transparent oil.

**$^1$H NMR** (400.16 MHz, $CDCl_3$, 258 K) δ 7.38 – 7.21 (m, 2H), 7.13 (td, *J* = 7.5, 1.1 Hz, 1H), 7.01 (ddd, *J* = 9.8, 8.8, 1.1 Hz, 1H), 3.05 (s, 3H), 2.86 (d, *J* = 1.7 Hz, 3H).
**$^{13}$C NMR** (100.63 MHz, $CDCl_3$, 258 K) δ 166.62 (CO), 157.79 (d, *J* = 247.6 Hz, CF, Ar), 131.21 (d, *J* = 8.0 Hz, CH, Ar), 128.83 (d, *J* = 3.8 Hz, CH, Ar), 124.58 (d, *J* = 3.4 Hz, CH, Ar), 124.10 (d, *J* = 17.7 Hz, C, Ar), 115.59 (d, *J* = 21.4 Hz, CH, Ar), 38.31 (d, *J* = 2.7 Hz, N–$CH_3$), 34.81 (N–$CH_3$).
**$^{19}$F NMR** (376.46 MHz, $CDCl_3$, 258 K) δ -115.28.
**$^{15}$N NMR** (40.55 MHz, $CDCl_3$, 258K) δ 107.49
**HRMS (ESI)**. Calculated for $C_9H_{11}FNO^+$: 168.0819 Obtained: 168.0818

*10.2.5.24 Preparation of N,N-2-trimethylbenzamide (23ak)*




**23ak**

Prepared following an adapted procedure:[133] To a solution of 2-methylbenzoic acid (340 mg, 2.5 mmol, 1.0 equiv.) in $CH_2Cl_2$ (20 mL) at 0 °C, $SOCl_2$ (0.27 mL, 3.75 mmol, 1.5 equiv.) was carefully added. The reaction mixture was stirred at room temperature for 2 h. After that time, the mixture was cooled down to 0 °C and $Et_3N$ (1.04 mL, 7.50 mmol, 3 equiv.) and $Me_2NH$ (40% w/w in water; 0.38 mL, 3.0 mmol, 1.2 equiv.) were added dropwise. The reaction mixture was stirred continuously at room temperature overnight.

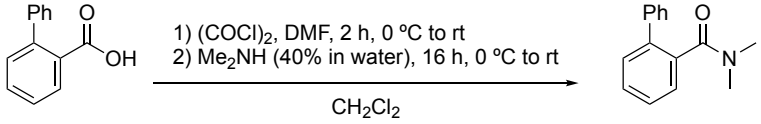
The reaction was then quenched with water and organic materials were extracted twice with $CH_2Cl_2$, washed first with 1.0 M aqueous HCl solution followed by a second

USC DE SANTIAGO DE COMPOSTELA

wash with saturated aqueous $NaHCO_3$ solution and brine. The organic fraction was dried over $MgSO_4$ and the solvent was removed in vacuo to obtain the *N,N*-2-trimethylbenzamide in a 92% yield (375 mg) as a colorless oil.

**$^1$H NMR** (400.16 MHz, $CDCl_3$, 258 K) δ 7.30 – 7.21 (m, 1H), 7.24 – 7.12 (m, 3H), 3.13 (s, 3H), 2.83 (s, 3H), 2.27 (s, 3H).
**$^{13}$C NMR** (100.63 MHz, $CDCl_3$, 258 K) δ 171.59 (CO), 136.44 (C, Ar), 133.84 (C, Ar), 130.34 (CH, Ar), 128.82 (CH, Ar), 126.02 (CH, Ar), 125.71 (CH, Ar), 38.50 (N–$CH_3$), 34.59 (N–$CH_3$), 19.02 ($CH_3$).
**$^{15}$N NMR** (40.55 MHz, $CDCl_3$) δ 106.17
**HRMS (ESI).** Calculated for $C_{11}H_{14}NO^+$: 164.1070 Obtained: 164.1071

### *10.2.5.25 Preparation of N,N-dimethyl-[1,1'-biphenyl]-2-carboxamide (23al)*



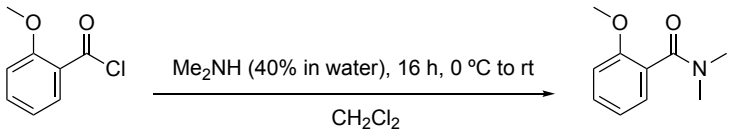

**23al**

Prepared following an adapted procedure:[133] To a solution of [1,1'-biphenyl]-2-carboxylic acid (991 mg, 5.0 mmol, 1.0 equiv.) in $CH_2Cl_2$ (20 mL) at room temperature, oxalyl chloride $(COCl)_2$ (0.643 mL, 7.5 mmol, 1.5 equiv.) and DMF (5 drops) were carefully added in that order. The reaction mixture was stirred at room temperature for 2 h. After that time, the mixture was cooled down to 0 °C and $Me_2NH$ (40% w/w in water; 2.5 mL, 20.0 mmol, 4.0 equiv.) was added dropwise. The reaction mixture was stirred continuously at room temperature overnight.

The reaction was then quenched with water and organic materials were extracted twice with $CH_2Cl_2$, washed first with 1.0 M aqueous HCl solution followed by a second wash with saturated aqueous $NaHCO_3$ solution and brine. The organic fraction was dried over $MgSO_4$ and the solvent was removed in vacuo to obtain the N,N-dimethyl-[1,1'-biphenyl]-2-carboxamide in a 72% yield (811 mg) as a pale yellow oil.

**$^1$H NMR** (400.16 MHz, $CDCl_3$, 258 K) δ 7.51 – 7.32 (m, 9H), 2.85 (s, 3H), 2.37 (s, 3H).
**$^{13}$C NMR** (100.63 MHz, $CDCl_3$, 258 K) δ 171.50 (CO), 139.79 (C, Ar), 138.57 (C, Ar), 135.38 (C, Ar), 129.57 (CH, Ar), 129.40 (CH, Ar), 128.54 (CH, Ar), 128.45 (CH, Ar), 127.92 (CH, Ar), 127.73 (CH, Ar), 127.47 (CH, Ar), 38.13 (N–$CH_3$), 34.68 (N–$CH_3$).
**HRMS (ESI).** Calculated for $C_{15}H_{15}NNaO^+$: 248.10458 Obtained: 248.10520

### *10.2.5.26 Preparation of 2-methoxy-N,N-dimethylbenzamide (23am)*




**23am**

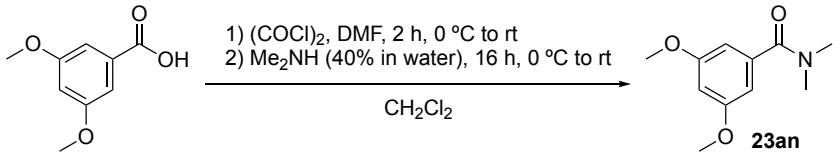
Prepared following an adapted procedure:[133] To a solution of 2-methoxybenzoyl chloride (0.74 mL, 5.0 mmol, 1.0 equiv.) in $CH_2Cl_2$ (10 mL) at 0 °C $Me_2NH$ (40% w/w in

water; 2.5 mL, 20.0 mmol, 4.0 equiv.) was added dropwise. The reaction mixture was stirred continuously at room temperature overnight.

The reaction was then quenched with water and organic materials were extracted twice with $CH_2Cl_2$, washed first with 1.0 M aqueous HCl solution followed by a second wash with saturated aqueous $NaHCO_3$ solution and brine. The organic fraction was dried over $MgSO_4$ and the solvent was removed in vacuo to obtain the 2-methoxy-N,N-dimethylbenzamide in a 83% yield (743 mg) as a transparent oil.

**$^1$H NMR** (400.16 MHz, $CDCl_3$, 258 K) δ 7.27 (ddd, *J* = 8.3, 7.4, 1.8 Hz, 1H), 7.16 (dd, *J* = 7.4, 1.7 Hz, 1H), 6.90 (td, *J* = 7.4, 0.9 Hz, 1H), 6.84 (dd, *J* = 8.4, 1.0 Hz, 1H), 3.75 (s, 3H), 3.05 (s, 3H), 2.78 (s, 3H).
**$^{13}$C NMR** (100.63 MHz, $CDCl_3$, 258 K) δ 169.27 (CO), 154.82 (C, Ar), 130.20 (CH, Ar), 127.50 (CH, Ar), 125.55 (C, Ar), 120.57 (CH, Ar), 110.46 (CH, Ar), 55.29 (O–$CH_3$), 38.22 (N–$CH_3$), 34.55 (N–$CH_3$).
**HRMS (ESI).** Calculated for $C_{10}H_{14}NO_2^+$: 180.10191 Obtained: 180.10202

### *10.2.5.27 Preparation of 3,5-dimethoxy-N,N-dimethylbenzamide (23an)*



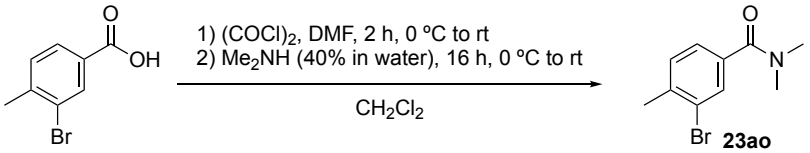

Prepared following an adapted procedure:[133] To a solution of 3,5-dimethoxybenzoic acid (455 mg, 2.5 mmol, 1.0 equiv.) in $CH_2Cl_2$ (10 mL) at room temperature, oxalyl chloride $(COCl)_2$ (0.32 mL, 3.75 mmol, 1.5 equiv.) and DMF (5 drops) were carefully added in that order. The reaction mixture was stirred at room temperature for 2 h. After that time, the mixture was cooled down to 0 °C and $Me_2NH$ (40% w/w in water; 1.25 mL, 10.0 mmol, 4.0 equiv.) was added dropwise. The reaction mixture was stirred continuously at room temperature overnight.

The reaction was then quenched with water and organic materials were extracted twice with $CH_2Cl_2$, washed first with 1.0 M aqueous HCl solution followed by a second wash with saturated aqueous $NaHCO_3$ solution and brine. The organic fraction was dried over $MgSO_4$ and the solvent was removed in vacuo to obtain the 3,5-dimethoxy-*N,N*-dimethylbenzamide in a 90% yield (475 mg) as an off-white solid.

**$^1$H NMR** (400.16 MHz, $CDCl_3$, 258 K) δ 6.51 (d, *J* = 2.3 Hz, 2H), 6.45 (t, *J* = 2.3 Hz, 1H), 3.78 (s, 6H), 3.08 (s, 3H), 2.96 (s, 3H).
**$^{13}$C NMR** (100.63 MHz, $CDCl_3$, 258 K) δ 171.31 (CO), 160.54 (C, Ar), 138.01 (C, Ar), 104.56 (CH, Ar), 101.31 (CH, Ar), 55.56 (O–$CH_3$), 39.67 (N–$CH_3$), 35.31 (N–$CH_3$).
**$^{15}$N NMR** (40.55 MHz, $CDCl_3$) δ 103.47
**HRMS (ESI)**. Calculated for $C_{11}H_{16}NO_3^+$: 210.1125 Obtained: 210.1122

USC UNIVERSIDADE DE SANTIAGO DE COMPOSTELA

*10.2.5.28 Preparation of 3-bromo-N,N-4-trimethylbenzamide (23ao)*

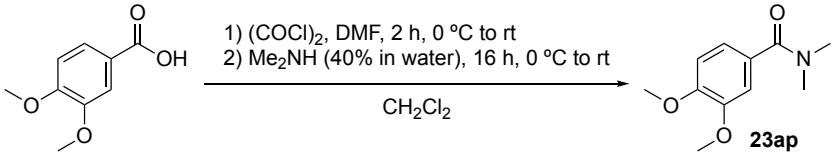



Prepared following an adapted procedure:[133] To a solution of 3-bromo-4-methylbenzoic acid (1.07 g, 5.0 mmol, 1.0 equiv.) in $CH_2Cl_2$ (20 mL) at room temperature, oxalyl chloride $(COCl)_2$ (0.64 mL, 7.5 mmol, 1.5 equiv.) and DMF (5 drops) were carefully added in that order. The reaction mixture was stirred at room temperature for 2 h. After that time, the mixture was cooled down to 0 °C and $Me_2NH$ (40% w/w in water; 2.5 mL, 20.0 mmol, 4.0 equiv.) was added dropwise. The reaction mixture was stirred continuously at room temperature overnight.

The reaction was then quenched with water and organic materials were extracted twice with $CH_2Cl_2$, washed first with 1.0 M aqueous HCl solution followed by a second wash with saturated aqueous $NaHCO_3$ solution and brine. The organic fraction was dried over $MgSO_4$ and the solvent was removed in vacuo to obtain the 3-bromo-*N,N*-4-trimethylbenzamide in a 58% yield (712 mg) as a brown solid.

**$^1$H NMR** (400.16 MHz, $CDCl_3$, 258 K) δ 7.57 (s, 1H), 7.24 (d, *J* = 1.0 Hz, 2H), 3.07 (s, 3H), 2.97 (s, 3H), 2.37 (s, 3H).
**$^{13}$C NMR** (100.63 MHz, $CDCl_3$, 258 K) δ 170.05 (CO), 139.60 (C, Ar), 135.06 (C, Ar), 130.88 (CH, Ar), 130.68 (CH, Ar), 126.03 (CH, Ar), 124.75 (C, Ar), 39.74 (N–$CH_3$), 35.44 (N–$CH_3$), 23.09 ($CH_3$).
**$^{15}$N NMR** (40.55 MHz, $CDCl_3$) δ 103.45
**HRMS (ESI).** Calculated for $C_{10}H_{13}BrNO^+$: 242.0175 Obtained: 242.0172

*10.2.5.29 Preparation of 3,4-dimethoxy-N,N-dimethylbenzamide (23ap)*




Prepared following an adapted procedure:[133] To a solution of 3,4-dimethoxybenzoic acid (911 mg, 5.0 mmol, 1.0 equiv.) in $CH_2Cl_2$ (20 mL) at room temperature, oxalyl chloride $(COCl)_2$ (0.64 mL, 7.5 mmol, 1.5 equiv.) and DMF (5 drops) were carefully added in that order. The reaction mixture was stirred at room temperature for 2 h. After that time, the mixture was cooled down to 0 °C and $Me_2NH$ (40% w/w in water; 2.5 mL, 20.0 mmol, 4.0 equiv.) was added dropwise. The reaction mixture was stirred continuously at room temperature overnight.

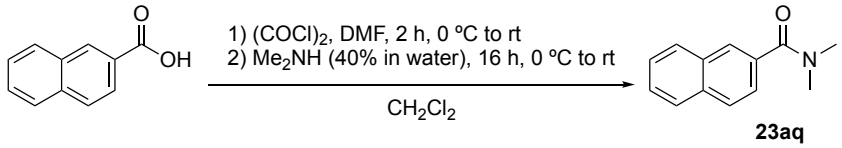
The reaction was then quenched with water and organic materials were extracted twice with $CH_2Cl_2$, washed first with 1.0 M aqueous HCl solution followed by a second wash with saturated aqueous $NaHCO_3$ solution and brine. The organic fraction was dried

USC UNIVERSIDADE DE SANTIAGO DE COMPOSTELA

over $MgSO_4$ and the solvent was removed in vacuo to obtain the 3,4-dimethoxy-*N,N*-dimethylbenzamide in a 87% yield (910 mg) white solid.

**$^1$H NMR** (400.16 MHz, $CDCl_3$, 258 K) δ 6.86 – 6.79 (m, 2H), 6.69 (d, *J* = 8.1 Hz, 1H), 3.72 (s, 6H), 2.91 (s, 3H), 2.86 (s, 3H).
**$^{13}$C NMR** (100.63 MHz, $CDCl_3$, 258 K) δ 171.02 (CO), 149.27 (C, Ar), 147.97 (C, Ar), 127.73 (C, Ar), 119.76 (CH, Ar), 109.89 (CH, Ar), 109.49 (CH, Ar), 55.54 (O–$CH_3$), 55.47 (O–$CH_3$), 39.58 (N–$CH_3$), 35.16 (N–$CH_3$).
**$^{15}$N NMR** (40.55 MHz, $CDCl_3$) δ 102.03
**HRMS (ESI).** Calculated for $C_{11}H_{16}NO_3^+$: 210.1125 Obtained: 210.1127

### *10.2.5.30 Preparation of N,N-dimethyl-2-naphthamide (23aq)*




**23aq**

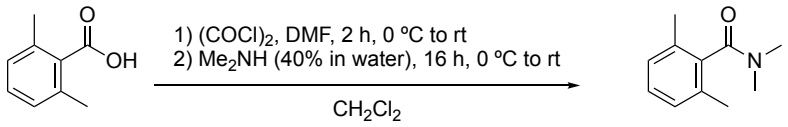
Prepared following an adapted procedure:[133] To a solution of 2-naphtoic acid (861 mg, 5.0 mmol, 1.0 equiv.) in $CH_2Cl_2$ (20 mL) at room temperature, oxalyl chloride $(COCl)_2$ (0.64 mL, 7.5 mmol, 1.5 equiv.) and DMF (5 drops) were carefully added in that order. The reaction mixture was stirred at room temperature for 2 h. After that time, the mixture was cooled down to 0 °C and $Me_2NH$ (40% w/w in water; 2.5 mL, 20.0 mmol, 4.0 equiv.) was added dropwise. The reaction mixture was stirred continuously at room temperature overnight.

The reaction was then quenched with water and organic materials were extracted twice with $CH_2Cl_2$, washed first with 1.0 M aqueous HCl solution followed by a second wash with saturated aqueous $NaHCO_3$ solution and brine. The organic fraction was dried over $MgSO_4$ and the solvent was removed in vacuo to obtain the *N,N*-dimethyl-2-naphthamide in a 80% yield (803 mg) as an off-white solid.

**$^1$H NMR** (400.16 MHz, $CDCl_3$, 258 K) δ 7.93 – 7.90 (m, 1H), 7.90 – 7.83 (m, 3H), 7.57 – 7.48 (m, 3H), 3.16 (s, 3H), 3.02 (s, 3H).
**$^{13}$C NMR** (100.63 MHz, $CDCl_3$, 258 K) δ 171.67 (CO), 133.43 (C, Ar), 133.29 (C, Ar), 132.44 (C, Ar), 128.39 (CH, Ar), 128.25 (CH, Ar), 127.78 (CH, Ar), 127.03 (CH, Ar), 126.86 (CH, Ar), 126.66 (CH, Ar), 124.38 (CH, Ar), 39.81 (N–$CH_3$), 35.46 (N–$CH_3$).
**$^{15}$N NMR** (40.55 MHz, $CDCl_3$, 258 K) δ 103.42
**HRMS (ESI).** Calculated for $C_{10}H_{14}NO^+$: 200.1070 Obtained: 200.1069

USC UNIVERSIDADE DE SANTIAGO DE COMPOSTELA

*10.2.5.31 Preparation of 2,6-dimethyl-N,N-dimethylbenzamide (23ar)*



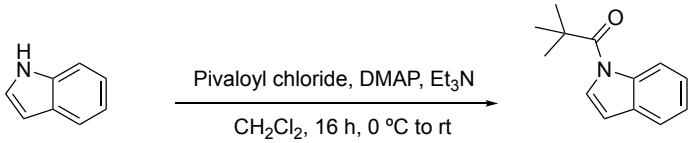

**23ar**

Prepared following an adapted procedure:[133] To a solution of 2,6-dimethylbenzoic acid (380 mg, 2.5 mmol, 1.0 equiv.) in $CH_2Cl_2$ (10 mL) at room temperature, oxalyl chloride $(COCl)_2$ (0.32 mL, 3.75 mmol, 1.5 equiv.) and DMF (5 drops) were carefully added in that order. The reaction mixture was stirred at room temperature for 2 h. After that time, the mixture was cooled down to 0 °C and $Me_2NH$ (40% w/w in water; 1.3 mL, 10.0 mmol, 4.0 equiv.) was added dropwise. The reaction mixture was stirred continuously at room temperature overnight.

The reaction was then quenched with water and organic materials were extracted twice with $CH_2Cl_2$, washed first with 1.0 M aqueous HCl solution followed by a second wash with saturated aqueous $NaHCO_3$ solution and brine. The organic fraction was dried over $MgSO_4$ and the solvent was removed in vacuo to obtain the 2,6-dimethyl-*N*,*N*-dimethylbenzamide in a 85% yield (375 mg) as a white solid.

**$^1$H NMR** (400.16 MHz, $CDCl_3$, 258 K) δ 7.14 (t, *J* = 7.5 Hz, 1H), 7.02 (d, *J* = 7.7 Hz, 1H), 3.16 (s, 3H), 2.81 (s, 3H), 2.22 (s, 6H).
**$^{13}$C NMR** (100.63 MHz, $CDCl_3$, 258 K) δ 171.46 (CO), 136.38 (C), 133.44 (C), 128.37 (CH, Ar), 127.53 (CH, Ar), 37.62 (N–$CH_3$), 34.27 (N–$CH_3$), 19.12 ($CH_3$).
**HRMS (ESI).** Calculated for $C_{11}H_{16}NO^+$: 178.1226 Obtained: 178.1227

*10.2.5.32 Preparation of 1-(1H-indol-1-yl)-2,2-dimethylpropan-1-one (23r)*




**23r**

Prepared following an adapted procedure:[142] To a solution of indole (1.17 g, 10.0 mmol, 1.0 equiv.), DMAP (122 mg, 1.0 mmol, 0.1 equiv.) and $Et_3N$ (2.1 mL, 2.1 mmol, 1.5 equiv.) in $CH_2Cl_2$ (18 mL) at 0 ºC, pivaloyl chloride (1.5 mL, 12.0 mmol, 1.2 equiv.) was added dropwise. The solution was stirred for 16 hours at room temperature.

After this time, the reaction mixture was evaporated to dryness under reduced pressure. The crude was portioned between $Et_2O$ and saturated aqueous $NH_4Cl$. The two layers were se*para*ted and the aqueous layer was extracted with $Et_2O$. The combined organic layers were washed with brine, dried over anhydrous $MgSO_4$ and evaporated to

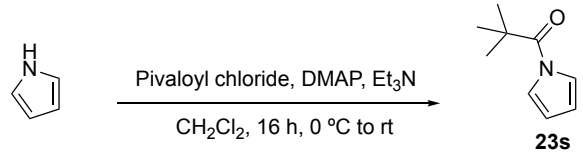
USC UNIVERSIDADE DE SANTIAGO DE COMPOSTELA

[142] Xie; Yang; Zhou; Li; Wang; Tan; An; Guo *Org. Lett.* **2010,** *12,* 1564–1567.

dryness. The crude was purified by column chromatography (Hex to Hex/EtOAc 60%) to afford the *N*-pivaloyl indole as a white solid in an 91% yield (1.84 g).

**$^{1}$H NMR** (400.16 MHz, $CDCl_3$, 258 K) δ 8.54 (dd, *J* = 8.4, 1.0 Hz, 1H), 7.76 (d, *J* = 3.8 Hz, 1H), 7.58 (ddd, *J* = 7.7, 1.4, 0.7 Hz, 1H), 7.37 (ddd, *J* = 8.5, 7.2, 1.4 Hz, 1H), 7.31 (s, 1H), 6.65 (dd, *J* = 3.9, 0.8 Hz, 1H), 1.52 (s, 9H).
**$^{13}$C NMR** (100.63 MHz, $CDCl_3$, 258 K) δ 177.22 (CO), 136.88 (C), 129.51 (C), 125.78 (CH), 125.22 (CH), 123.66 (CH), 120.60 (CH), 117.45 (CH), 108.36 (CH), 41.36 (C), 28.82 ($CH_3$).
**$^{15}$N NMR** (40.55 MHz, $CDCl_3$) δ 174.36.
**HRMS (ESI).** Calculated for $C_9H_{13}NO^+$: 202.1226 Obtained: 202.1225

### *10.2.5.33 Preparation of 2,2-dimethyl-1-(1H-pyrrol-1-yl)propan-1-one (23s)*



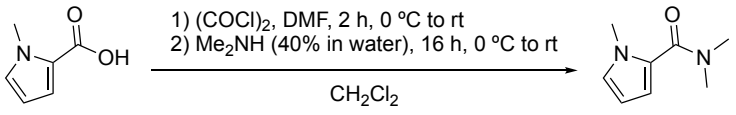

**23s**

Prepared following an adapted procedure:[142] To a solution of pyrrole (0.347 L 5.0 mmol, 1.0 equiv.), DMAP (61 mg, 1.0 mmol, 0.1 equiv.) and $Et_3N$ (1.0 mL, 7.5 mmol, 1.5 equiv.) in $CH_2Cl_2$ (3 mL) at 0 ºC, pivaloyl chloride (0.92 mL, 7.5 mmol, 1.5 equiv.) was added dropwise. The solution was stirred for 16 hours at room temperature.

After this time, the reaction mixture was evaporated to dryness under reduced pressure. The crude was portioned between $Et_2O$ and saturated aqueous $NH_4Cl$. The two layers were se*para*ted and the aqueous layer was extracted with $Et_2O$. The combined organic layers were washed with brine, dried over anhydrous $MgSO_4$ and evaporated to dryness. The crude was purified by column chromatography (Hex to Hex/EtOAc 60%) to afford the *N*-pivaloyl pyrrole as a transparent oil in an 50% yield (372 mg).

**$^{1}$H NMR** (400.16 MHz, $CDCl_3$, 258 K) δ 7.45 (dd, *J* = 4.8, 2.5 Hz, 2H), 6.26 (dd, *J* = 4.8, 2.4 Hz, 2H), 1.45 (s, 9H).
**$^{13}$C NMR** (100.63 MHz, $CDCl_3$, 258 K) δ 176.00 (CO), 120.71 (CH, Pyrrole), 112.02 (CH, Pyrrole), 40.74 (C), 28.66 ($CH_3$).
**$^{15}$N NMR** (40.55 MHz, $CDCl_3$, 298 K) δ 193.55
**HRMS (ESI).** Calculated for $C_9H_{13}NO^+$: 152.1070 Obtained: 152.1070

### *10.2.5.34 Preparation of N,N,1-trimethyl-1H-pyrrole-2-carboxamide (23t)*




**23t**

Prepared following an adapted procedure:[133] To a solution of 1-Methyl-2-pyrrolecarboxylic acid (0.626 g, 5.0 mmol, 1 equiv.) in $CH_2Cl_2$ (20 mL) at room temperature, oxalyl chloride $(COCl)_2$ (0.64 mL, 7.5 mmol, 1.5 equiv.) and DMF (5 drops)

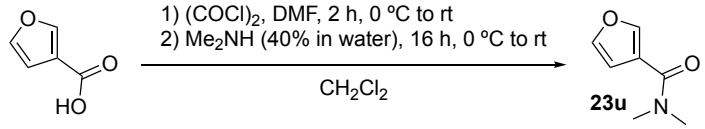
USC UNIVERSIDADE

were carefully added in that order. The reaction mixture was stirred at room temperature for 2 h. After that time, the mixture was cooled down to 0 °C and $Me_2NH$ (40 w/w% in water; 2.5 mL, 20.0 mmol, 4 equiv.) was added dropwise. The reaction mixture was stirred continuously at room temperature overnight.

The reaction was then quenched with water and organic materials were extracted twice with $CH_2Cl_2$, washed first with 1.0 M aqueous HCl solution followed by a second wash with saturated aqueous $NaHCO_3$ solution and brine. The organic fraction was dried over $MgSO_4$ and the solvent was removed in vacuo to obtain the *N,N*,1-trimethyl-1H-pyrrole-2-carboxamide in a 75% yield (570 mg) as a brown oil.

**$^1$H NMR** (400.16 MHz, $CDCl_3$, 258 K) δ 6.68 (ddd, *J* = 2.6, 1.7, 0.4 Hz, 1H), 6.37 (dd, *J* = 3.8, 1.7 Hz, 1H), 6.06 (dd, *J* = 3.8, 2.6 Hz, 1H), 3.77 (d, *J* = 0.4 Hz, 3H), 3.22 (s, 3H), 3.04 (s, 3H).
**$^{13}$C NMR** (100.63 MHz, $CDCl_3$, 258 K) δ 163.95 (CO), 126.29 (CH, Pyrrole), 124.86 (C, Pyrrole), 113.53 (CH, Pyrrole), 106.54 (CH, Pyrrole), 39.96 (N–$CH_3$), 36.07 (N–$CH_3$), 35.41 (N–$CH_3$).
**$^{15}$N NMR** (40.55 MHz, $CDCl_3$, 258 K) δ 100.95, 154.69
**HRMS (ESI).** Calculated for $C_8H_{13}N_2O^+$: 153.1022 Obtained: 153.1022

### *10.2.5.35 Preparation of N,N-dimethylfuran-3-carboxamide (23u)*



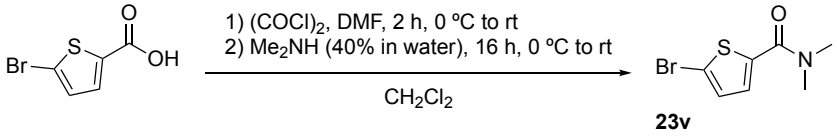

Prepared following an adapted procedure:[133] To a solution of 3-furoic acid (0.506 g, 5.0 mmol, 1 equiv.) in $CH_2Cl_2$ (20 mL) at room temperature, were added carefully $(COCl)_2$ (0.64 mL, 7.5 mmol, 1.5 equiv.) and DMF (5 drops) in that order. The reaction mixture was stirred at room temperature for 2 h. After that time, the mixture was cooled down to 0 ºC and $Me_2NH$ (40 w/w% in water; 2.5 mL, 20.0 mmol, 4 equiv.) was added dropwise. The reaction mixture was stirred continuously at room temperature overnight.

The reaction was then quenched with water and organic materials were extracted twice with $CH_2Cl_2$, washed first with 1.0 M aqueous HCl solution followed by a second wash with saturated aqueous $NaHCO_3$ solution and brine. The organic fraction was dried over $MgSO_4$ and the solvent was removed in vacuo to obtain the N,N-dimethylfuran-2-carboxamide in a 45% yield (471 mg) as a white solid.

**$^1$H NMR** (400.16 MHz, $CDCl_3$, 258 K) δ 7.69 (dd, *J* = 1.5, 0.8 Hz, 1H), 7.38 (t, *J* = 2.0 Hz, 1H), 6.57 (dd, *J* = 1.9, 0.9 Hz, 1H), 3.12 (s, 3H), 3.03 (s, 3H).
**$^{13}$C NMR** (100.63 MHz, $CDCl_3$, 258 K) δ 164.81 (CO), 143.60 (CH, Furane), 142.70 (CH, Furane), 121.12 (C, Furane), 110.43 (CH, Furane), 39.06 (N–$CH_3$), 35.66 (N–$CH_3$).
**$^{15}$N NMR** (40.55 MHz, $CDCl_3$) δ 102.97
**HRMS (ESI).** Calculated for $C_7H_{10}NO_2^+$: 140.0706 Obtained: 140.0706

USC UNIVERSIDADE DE SANTIAGO DE COMPOSTELA

*10.2.5.36 Preparation of 5-bromo-N,N-dimethylthiophene-2-carboxamide (23v)*



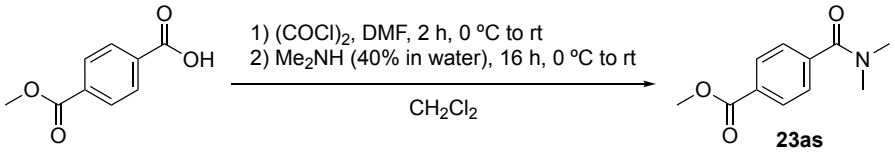

**23v**

Prepared following an adapted procedure:[133] To a solution of 5-bromothiophene-2-carboxylic acid (1.0 g, 5.0 mmol, 1.0 equiv.) in $CH_2Cl_2$ (20 mL) at room temperature, oxalyl chloride $(COCl)_2$ (0.64 mL, 7.5 mmol, 1.5 equiv.) and DMF (5 drops) were carefully added in that order. The reaction mixture was stirred at room temperature for 2 h. After that time, the mixture was cooled down to 0 °C and $Me_2NH$ (40% w/w in water; 2.5 mL, 20.0 mmol, 4.0 equiv.) was added dropwise. The reaction mixture was stirred continuously at room temperature overnight.

The reaction was then quenched with water and organic materials were extracted twice with $CH_2Cl_2$, washed first with 1.0 M aqueous HCl solution followed by a second wash with saturated aqueous $NaHCO_3$ solution and brine. The organic fraction was dried over $MgSO_4$ and the solvent was removed in vacuo to obtain the 5-bromo-N,N-dimethylthiophene-2-carboxamide in a 73% yield (854 mg) as a white solid.

**$^1$H NMR** (400.16 MHz, $CDCl_3$, 258 K) δ 7.12 (d, *J* = 3.9 Hz, 1H), 7.01 (d, *J* = 3.9 Hz, 1H), 3.26 (s, 3H), 3.09 (s, 3H).
**$^{13}$C NMR** (100.63 MHz, $CDCl_3$, 258 K) δ 163.15 (CO), 139.52 (C, Thiophene), 129.88 (CH, Tiophene), 129.85 (CH, Tiophene), 117.20 (C, Tiophene), 39.73 (N–$CH_3$), 36.71 (N–$CH_3$).
**$^{15}$N NMR** (40.55 MHz, $CDCl_3$) δ 101.58
**HRMS (ESI)**. Calculated for $C_7H_9BrNOS^+$: 233.9583 Obtained: 233.9579

*10.2.5.37 Preparation of methyl 4-(dimethylcarbamoyl)benzoate (23as)*




**23as**

Prepared following an adapted procedure:[133] To a solution of mono-methyl terephthalate (901 mg, 5.0 mmol, 1.0 equiv.) in $CH_2Cl_2$ (20 mL) at room temperature, oxalyl chloride $(COCl)_2$ (0.64 mL, 7.5 mmol, 1.5 eq) and DMF (5 drops) were carefully added in that order. The reaction mixture was stirred at room temperature for 2 h. After that time, the mixture was cooled down to 0 °C and $Me_2NH$ (40% w/w in water; 2.5 mL, 20.0 mmol, 4.0 equiv.) was added dropwise. The reaction mixture was stirred continuously at room temperature overnight.

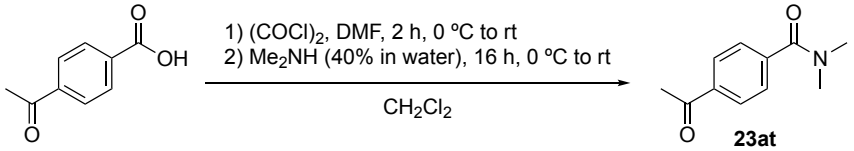
The reaction was then quenched with water and organic materials were extracted twice with $CH_2Cl_2$, washed first with 1.0 M aqueous HCl solution followed by a second wash with saturated aqueous $NaHCO_3$ solution and brine. The organic fraction was dried

USC UNIVERSIDADE DE SANTIAGO DE COMPOSTELA

over $MgSO_4$ and the solvent was removed in vacuo to obtain the methyl 4-(dimethylcarbamoyl)benzoate in a 86% yield (896 mg) as a white solid.

**$^1$H NMR** (400.16 MHz, $CDCl_3$, 258 K) δ 8.07 (d, *J* = 8.5 Hz, 2H), 7.48 (d, *J* = 8.6 Hz, 2H), 3.93 (s, 3H), 3.12 (s, 3H), 2.96 (s, 3H).
**$^{13}$C NMR** (100.63 MHz, $CDCl_3$, 258 K) δ 170.68 (CO), 166.59 (CO), 140.45 (C, Ar), 130.79 (C, Ar), 129.82 (CH, Ar), 127.09 (CH, Ar), 52.65 (O–$CH_3$), 39.60 (N–$CH_3$), 35.38 (N–$CH_3$).
**$^{15}$N NMR** (40.55 MHz, $CDCl_3$, 258 K) δ 103.96
**HRMS (ESI)**. Calculated for $C_{11}H_{14}NO_3^+$: 208.0968 Obtained: 208.0968

### *10.2.5.38 Preparation of 4-acetyl-N,N-dimethylbenzamide (23at)*



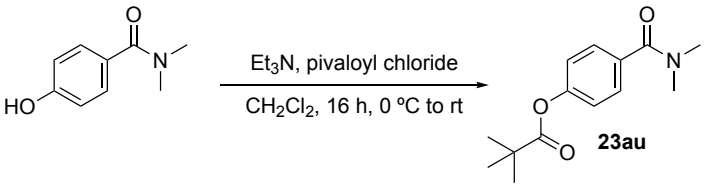

Prepared following an adapted procedure:[133] To a solution of 4-acetylbenzoic acid (410 mg, 2.5 mmol, 1.0 equiv.) in $CH_2Cl_2$ (10 mL) at room temperature, oxalyl chloride $(COCl)_2$ (0.32 mL, 3.75 mmol, 1.5 equiv.) and DMF (5 drops) were carefully added in that order. The reaction mixture was stirred at room temperature for 2 h. After that time, the mixture was cooled down to 0 °C and $Me_2NH$ (40% w/w in water; 1.26 mL, 10.0 mmol, 4.0 equiv.) was added dropwise. The reaction mixture was stirred continuously at room temperature overnight.

The reaction was then quenched with water and organic materials were extracted twice with $CH_2Cl_2$, washed first with 1.0 M aqueous HCl solution followed by a second wash with saturated aqueous $NaHCO_3$ solution and brine. The organic fraction was dried over $MgSO_4$ and the solvent was removed in vacuo to obtain the 4-acetyl-*N,N*-dimethylbenzamide in a 85% yield (406 mg) as a white solid.

**$^1$H NMR** (400.16 MHz, $CDCl_3$, 258 K) δ 7.91 (d, *J* = 8.5 Hz, 2H), 7.42 (d, *J* = 8.5 Hz, 2H), 3.03 (s, 3H), 2.88 (s, 3H), 2.55 (s, 3H).
**$^{13}$C NMR** (100.63 MHz, $CDCl_3$, 258 K) δ 197.78 (CO), 170.32 (CO), 140.37 (CH, Ar), 137.09 (CH, Ar), 128.36 (C, Ar), 127.08 (C, Ar), 39.35 (N–$CH_3$), 35.12 (N–$CH_3$), 26.93 ($CH_3$).
**$^{15}$N NMR** (40.55 MHz, $CDCl_3$, 258 K) δ 104.23
**HRMS (ESI)**. Calculated for $C_{11}H_{14}NO_2^+$:192.10191 Obtained: 192.10189

USC UNIVERSIDADE DE SANTIAGO DE COMPOSTELA

*10.2.5.39 Preparation of 4-(dimethylcarbamoyl)phenyl pivalate (23au)*

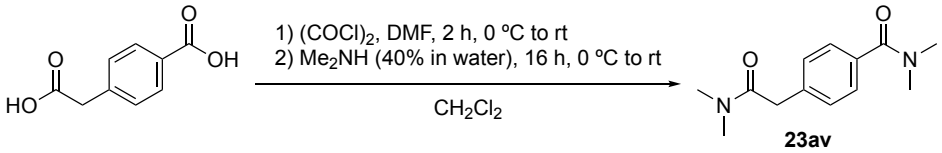



Prepared following an adapted procedure:[143] To a solution of 4-hydroxy-*N,N*-dimethylbenzamide (200 mg, 1.2 mmol, 1.0 equiv.) and $Et_3N$ (0.18 mL, 1.3 mmol, 1.1 equiv.) in $CH_2Cl_2$ (6 mL) at 0 °C was added pivaloyl chloride (0.15 mL, 1.0 mmol, 1.0 equiv.) dropwise. The reaction mixture was stirred continuously at room temperature overnight.

The reaction was then quenched with water and organic materials were extracted twice with $CH_2Cl_2$, washed first with 1.0 M aqueous HCl solution followed by a second wash with saturated aqueous $NaHCO_3$ solution and brine. The organic fraction was dried over $MgSO_4$ and the solvent was removed in vacuo to obtain the 4-(dimethylcarbamoyl)phenyl pivalate in a 82% yield (247 mg) as a white solid.

**$^1$H NMR** (400.16 MHz, $CDCl_3$, 258 K) δ 7.45 (d, *J* = 8.5 Hz, 2H), 7.08 (d, *J* = 8.6 Hz, 2H), 3.10 (s, 3H), 3.00 (s, 3H), 1.34 (s, 9H).
**$^{13}$C NMR** (100.63 MHz, $CDCl_3$, 258 K) δ 177.19 (CO), 170.94 (CO), 151.77 (C, Ar), 133.32 (C, Ar), 128.63 (CH, Ar), 121.67 (CH, Ar), 39.86 (N–$CH_3$), 39.15 (C), 35.54 (N–$CH_3$), 27.12 ($CH_3$).
**$^{15}$N NMR** (40.55 MHz, $CDCl_3$, 258 K) δ 103.18
**HRMS (ESI)**. Calculated for $C_{14}H_{20}NO_3^+$:250.1438 Obtained: 250.1436.

*10.2.5.40 Preparation of 4-(2-(dimethylamino)-2-oxoethyl)-N,N-dimethylbenzamide (23av)*




Prepared following an adapted procedure:[133] To a solution of 4-(carboxymethyl)benzoic acid (900 mg, 5.0 mmol, 1.0 equiv.) in $CH_2Cl_2$ (20 mL) at room temperature, oxalyl chloride $(COCl)_2$ (1.0 mL, 12.5 mmol, 2.5 equiv.) and DMF (5 drops) were carefully added in that order. The reaction mixture was stirred at room temperature for 2 h. After that time, the mixture was cooled down to 0 °C and $Me_2NH$ (40% w/w in water; 2.5 mL, 20.0 mmol, 4.0 equiv.) was added dropwise. The reaction mixture was stirred continuously at room temperature overnight.

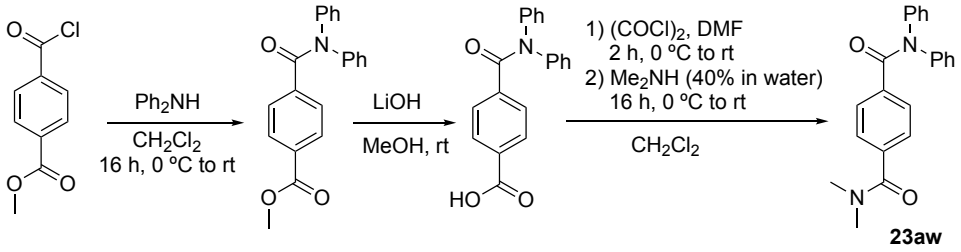
The reaction was then quenched with water and organic materials were extracted twice with $CH_2Cl_2$, washed first with 1.0 M aqueous HCl solution followed by a second wash with saturated aqueous $NaHCO_3$ solution and brine. The organic fraction was dried

[143] Gu, Y.; Martín, R. *Angew. Chem. Int. Ed.* **2017,** *56,* 3187–3190.

over $MgSO_4$ and the solvent was removed in vacuo to obtain the 4-(2-(dimethylamino)-2-oxoethyl)-*N,N*-dimethylbenzamide in a 35% yield (416 mg) as a white solid.

**$^1$H NMR** (400.16 MHz, $CDCl_3$, 258 K) δ 7.36 (d, *J* = 8.3 Hz, 2H), 7.26 (d, *J* = 8.3 Hz, 2H), 3.72 (s, 2H), 3.08 (s, 3H), 2.98 (s, 3H), 2.97 (s, 3H), 2.94 (s, 3H).
**$^{13}$C NMR** (100.63 MHz, $CDCl_3$, 258 K) δ 171.46 (CO), 170.71 (CO), 136.52 (C, Ar), 134.44 (C, Ar), 128.83 (CH, Ar), 127.48 (CH, Ar), 40.77 ($CH_2$), 39.78 (N–$CH_3$), 37.82 (N–$CH_3$), 35.70 (N–$CH_3$), 35.39 (N–$CH_3$).
**$^{15}$N NMR** (40.55 MHz, $CDCl_3$, 258 K) δ 102.05, 102.30
**HRMS (ESI)**. Calculated for $C_{13}H_{19}N_2O_2^+$:235.14410 Obtained: 235.14422

### *10.2.5.41 Preparation of N$^1$,N$^1$-dimethyl-N$^4$,N$^4$-diphenylterephthalamide (23aw)*




*Step 1*

Prepared following an adapted procedure:[136] A solution of $Ph_2NH$ (4.2 g, 10.0 mmol, 2.0 equiv.) and triethylamine (0.76 mL, 5.5 mmol, 1.1 equiv.) in $CH_2Cl_2$ (10 mL) was cooled to 0 °C. To this mixture, methyl 4-chlorocarbonylbenzoate (993 mg, 5.0 mmol, 1.0 equiv.) was added carefully. The reaction mixture was stirred continuously at room temperature overnight.

The reaction was then quenched with water and organic materials were extracted twice with $CH_2Cl_2$, washed first with 1.0 M aqueous HCl solution followed by a second wash with saturated aqueous $NaHCO_3$ solution and brine. The organic fraction was dried over $MgSO_4$ and the solvent was removed in vacuo to obtain the methyl 4-(diphenylcarbamoyl)benzoate in a 45% yield (750 mg) as a pale yelow solid.

**$^1$H NMR** (400.16 MHz, $CDCl_3$, 258 K) δ 7.88 (d, *J* = 8.7 Hz, 2H), 7.50 (d, *J* = 8.7 Hz, 1H), 7.29 (t, *J* = 7.5 Hz, 4H), 7.23 – 7.11 (m, 6H), 3.88 (s, 3H).
**$^{13}$C NMR** (100.63 MHz, $CDCl_3$, 258 K) δ 169.77 (CO), 166.46 (CO), 143.41 (C, Ar), 140.56 (C, Ar), 131.30 (C, Ar), 129.35 (CH, Ar), 129.27 (CH, Ar), 129.08 (CH, Ar), 127.55 (CH, Ar), 126.83 (CH, Ar), 52.43 (O–$CH_3$).
**HRMS (ESI).** Calculated for $C_{21}H_{18}NO_3^+$: 332.12812 Obtained: 332.12836

*Step 2*

Methyl 4-(diphenylcarbamoyl)benzoate (300 mg, 0.9 mmol, 1 equiv.) was dissolved in MeOH (6 mL). To that solution, LiOH (217 mg, 9 mmol, 10 equiv.) was added and the dissolved mixture was stirred for 1 hour at room temperature.

USC UNIVERSIDADE DE SANTIAGO DE COMPOSTELA

After that time, the solvent was removed under vacuum. The residue was dissolved in water and poured into a beaker. The product was precipitated by titrating the solution with concentrated HCl until the pH reached 3. Then the aqueous mixture was extracted with DCM and the combined organic fractions were dried over MgSO4 and the solvent was removed in vacuo to obtain 4-(diphenylcarbamoyl)benzoic acid as a white powder in a 70% yield (200 mg).

**$^{1}$H NMR** (400.16 MHz, $CDCl_3$, 318K) δ 7.93 (d, *J* = 8.4 Hz, 2H), 7.53 (d, *J* = 8.5 Hz, 2H), 7.30 (t, *J* = 7.7 Hz, 4H), 7.24 – 7.12 (m, 6H).
**$^{13}$C NMR** (100.63 MHz, CDCl3, 318K) δ 169.87 (CO), 169.66 (CO), 143.48 (C, Ar), 141.55 (C, Ar), 130.38 (C, Ar), 129.92 (CH, Ar), 129.42 (CH, Ar), 129.19 (CH, Ar), 127.63 (CH, Ar), 126.95 (CH, Ar).
**HRMS (ESI)**. Calculated for $C_{20}H_{16}NO_3^+$: 318.11247 Obtained: 318.11269

*Step 3*

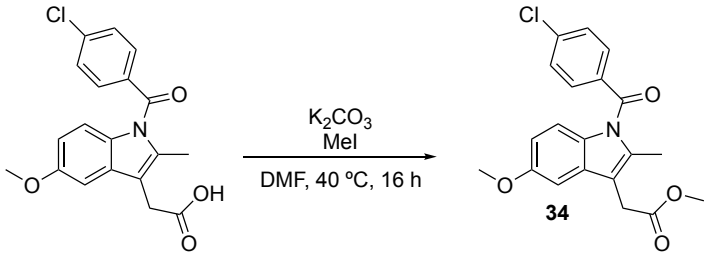
Prepared following an adapted procedure:[133] To a solution of 4-(diphenylcarbamoyl)benzoic acid (200 mg, 0.6 mmol, 1.0 equiv.) in $CH_2Cl_2$ (2.5 mL) at room temperature, oxalyl chloride $(COCl)_2$ (81 mL, 0.94 mmol, 1.5 equiv.) and DMF (5 drops) were carefully added in that order. The reaction mixture was stirred at room temperature for 2 h. After that time, the mixture was cooled down to 0 °C and $Me_2NH$ (40% w/w in water; 0.32 mL, 2.5 mmol, 4.0 equiv.) was added dropwise. The reaction mixture was stirred continuously at room temperature overnight.

The reaction was then quenched with water and organic materials were extracted twice with $CH_2Cl_2$, washed first with 1.0 M aqueous HCl solution followed by a second wash with saturated aqueous $NaHCO_3$ solution and brine. The organic fraction was dried over $MgSO_4$ and the solvent was removed in vacuo to obtain the $N^1$,$N^1$-dimethyl-$N^4$,$N^4$-diphenylterephthalamide in a 83% yield (182 mg) as a white solid.

**$^{1}$H NMR** (400.16 MHz, $CDCl_3$, 318K) δ 7.29 (d, *J* = 8.3 Hz, 2H), 7.26 – 6.67 (m, 12H), 2.87 (s, 3H), 2.69 (s, 3H).
**$^{13}$C NMR** (100.63 MHz, CDCl3, 318K) δ 170.77 (CO), 169.97 (CO), 143.25 (C, Ar), 137.55 (C, Ar), 137.06 (C, Ar), 129.36 (CH, Ar), 129.29 (CH, Ar), 128.05 (C, Ar), 127.18 (CH, Ar), 126.80 (CH, Ar), 126.75 (CH, Ar), 39.59 (N–$CH_3$), 35.41 (N–$CH_3$).
**HRMS (ESI)**. Calculated for $C_{22}H_{20}N_2NaO_2^+$: 367.14170 Obtained: 367.14195

USC UNIVERSIDADE DE SANTIAGO DE COMPOSTELA

*10.2.5.42 Preparation of methyl 2-(1-(4-chlorobenzoyl)-5-methoxy-2-methyl-1H-indol-3-yl)acetate (34)*

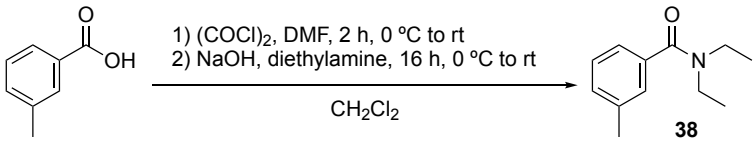



Prepared following an adapted procedure:[140] To a 25 mL round-bottom flask equipped with a magnetic stirring bar, the indomethacine (715 mg, 2.0 mmol, 1.0 equiv.), $K_2CO_3$ (552 mg, 4.0 mmol, 2.0 equiv.) and DMF (4 mL) were added. Then, methyl iodide (0.15 mL, 2.4 mmol, 1.2 equiv.) was added and the reaction mixture was heated at 40 °C overnight.

Upon completion, the reaction crude was diluted with water and $Et_2O$. The organic phase was washed with water, saturated $K_2CO_3$ and brine, then it was dried over $MgSO_4$, and evaporated to dryness to afford the desired compound as an off-white solid in a 88% yield (665 mg).

**$^1$H NMR** (400.16 MHz, $CDCl_3$, 258 K) δ 7.66 (d, *J* = 8.6 Hz, 2H), 7.47 (d, *J* = 8.5 Hz, 2H), 6.96 (d, *J* = 2.5 Hz, 1H), 6.86 (d, *J* = 9.0 Hz, 1H), 6.67 (dd, *J* = 9.0, 2.5 Hz, 1H), 3.84 (d, *J* = 1.0 Hz, 3H), 3.70 (d, *J* = 1.0 Hz, 3H), 3.67 (s, 2H), 2.39 (s, 3H).
**$^{13}$C NMR** (100.63 MHz, $CDCl_3$, 258 K) δ 171.47 (CO), 168.43 (CO), 156.20 (C, Ar), 139.40 (C, Ar), 136.11 (C, Ar), 134.05 (C, Ar), 131.32 (CH, Ar), 130.94 (C, Ar), 130.79 (C, Ar), 129.26 (CH, Ar), 115.09 (CH, Ar), 112.64 (C, Ar), 111.75 (CH, Ar), 101.46 (CH, Ar), 55.86 (O–$CH_3$), 52.30 (O–$CH_3$), 30.28 ($CH_2$), 13.46 ($CH_3$).
**HRMS (ESI).** Calculated for $C_{20}H_{19}ClNO_4^+$:372.0997 Obtained: 372.0996

*10.2.5.43 Preparation of N,N-diethyl-3-methylbenzamide (38)*




Prepared following an adapted procedure:[133] To a solution of 3-methylbenzoic acid (340 mg, 2.5 mmol, 1.0 equiv.) in $CH_2Cl_2$ (10 mL) at room temperature, oxalyl chloride $(COCl)_2$ (0.32 mL, 3.75 mmol, 1.5 equiv.) and DMF (5 drops) were carefully added in that order. The reaction mixture was stirred at room temperature for 2 h. After that time, the mixture was added to a stirred solution of NaOH (220 mg, 5.5 mmol, 2.2 equiv.) and Diethylamine (1 mL, 10 mmol, 4 equiv.) in water (5 ml). The reaction mixture was stirred continuously at room temperature overnight.

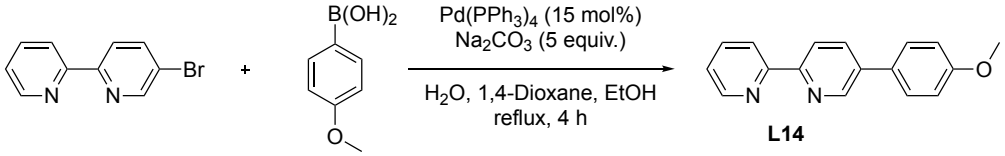
The reaction was then quenched with water and organic materials were extracted twice with $CH_2Cl_2$, washed first with 1.0 M aqueous HCl solution followed by a second

wash with saturated aqueous $NaHCO_3$ solution and brine. The organic fraction was dried over $MgSO_4$ and the solvent was removed in vacuo to obtain the *N*,*N*-diethyl-3-methylbenzamide (350 mg, 73% yield) as a transparent oil.

**$^1$H NMR** (400.16 MHz, $CDCl_3$, 258 K) δ 7.35 (t, *J* = 7.8 Hz, 1H), 7.31 – 7.19 (m, 3H), 3.61 (q, *J* = 7.1 Hz, 2H), 3.31 (q, *J* = 7.1 Hz, 2H), 2.44 (s, 3H), 1.31 (t, *J* = 7.1 Hz, 3H), 1.18 (t, *J* = 7.1 Hz, 3H).
**$^{13}$C NMR** (100.63 MHz, $CDCl_3$, 258 K) δ 171.56 (CO), 138.38 (C, Ar), 136.99 (C, Ar), 129.85 (CH, Ar), 128.32 (CH, Ar), 126.82 (CH, Ar), 122.97 (CH, Ar), 43.21 (N–$\underline{C}H_2$–$CH_3$), 39.00 (N–$\underline{C}H_2$–$CH_3$), 21.56 (Ar–$CH_3$), 14.30 ($CH_2$–$\underline{C}H_3$), 12.96 ($CH_2$–$\underline{C}H_3$).
**HRMS (ESI)**. Calculated for $C_{12}H_{18}NO^+$: 192.1383 Obtained: 192.1380

## 10.2.6 Ligand synthesis

### *10.2.6.1 Preparation of 5-(4-methoxyphenyl)-2,2'-bipyridine (L14)*




Prepared following an adapted procedure:[144] 5-bromo-2,2'-bipyridine (500 mg, 2.1 mmol, 1.0 equiv.), boronic acid (323 mg, 2.1 mmol, 1.0 equiv.), $Pd(PPh_3)_4$ (369 mg, 0.3 mmol, 15 mol%), and $Na_2CO_3$ (1.12 g, 10.6 mmol, 5 equiv.) were added into a two-necked flask quipped with a reflux condenser. After addition of degassed 1,4-dioxane (10.0 mL, 0.2 M), EtOH (7.0 mL, 0.3 M), and water (7.0 mL, 0.3 M), the mixture was refluxed for 4 h.

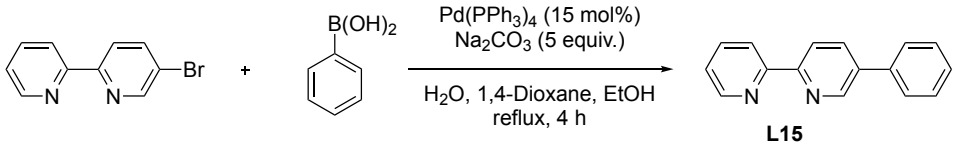
The reaction mixture was cooled to room temperature and extracted with EtOAc. The organic phase was se*para*ted and washed with water and dried over anhydrous $MgSO_4$. The mixture was filtered, the solvent was removed under vacuum and the mixture was purified by column chromatography on silica gel (Hex/EtOAc 10% to Hex/EtOAc 50%) to afford 5-(4-methoxyphenyl)-2,2'-bipyridine (98.12 mg, 88% yield) as a white solid.

**$^1$H NMR** (400.16 MHz, $CDCl_3$) δ 8.92 (dd, *J* = 2.4, 0.8 Hz, 1H), 8.73 (ddd, *J* = 4.9, 1.8, 0.9 Hz, 1H), 8.53 (ddd, *J* = 8.1, 7.4, 0.9 Hz, 2H), 8.04 (dd, *J* = 8.3, 2.4 Hz, 1H), 7.90 (ddd, *J* = 8.0, 7.5, 1.8 Hz, 1H), 7.66 – 7.55 (m, 2H), 7.37 (ddd, *J* = 7.5, 4.9, 1.2 Hz, 1H), 7.08 – 7.00 (m, 2H), 3.88 (s, 3H).
**$^{13}$C NMR** (100.63 MHz, $CDCl_3$) δ 160.23 (C, Ar), 148.85 (CH, Ar), 146.83 (CH, Ar), 137.86 (CH, Ar), 136.77 (C, Ar), 135.45 (CH, Ar), 129.63 (C, Ar), 128.36 (CH, Ar), 124.08 (CH, Ar), 121.71 (CH, Ar), 121.66 (CH, Ar), 114.84 (CH, Ar), 55.57 (O–$CH_3$).
**$^{15}$N NMR** (40.55 MHz, $CDCl_3$) δ 298.43
**HRMS (ESI).** Calculated for $C_{17}H_{15}N_2O^+$: 263.1179 Obtained: 263.1179

USC UNIVERSIDADE DE SANTIAGO DE COMPOSTELA

[144] Zeng, J.; Naito, M.; Torigoe, T.; Yamanaka, M.; Kuninobu, Y. *Org. Lett.* **2020,** *22,* 3485–3489.

*10.2.6.2 Preparation of 5-phenyl-2,2'-bipyridine (L15)*

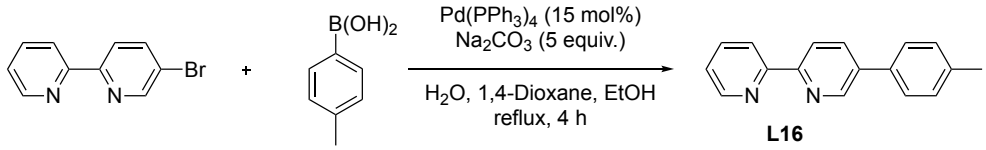



Prepared following an adapted procedure:[144] 5-bromo-2,2'-bipyridine (100 mg, 0.42 mmol, 1.0 equiv.), boronic acid (52 mg, 0.42 mmol, 1.0 equiv.), $Pd(PPh_3)_4$ (73.7 mg, 0.06 mmol, 15 mol%), and $Na_2CO_3$ (227 mg, 2.1 mmol, 5.0 equiv.) were added into a two-necked flask quipped with a reflux condenser. After addition of degassed 1,4-dioxane (2.0 mL, 0.2 M), EtOH (1.2 mL, 0.3 M), and water (1.2 mL, 0.3 M), the mixture was refluxed for 4 h.

The reaction mixture was cooled to room temperature and extracted with EtOAc. The organic phase was se*para*ted and washed with water and dried over anhydrous $MgSO_4$. The mixture was filtered, the solvent was removed under vacuum and the mixture was purified by column chromatography on silica gel to afford 5-phenyl-2,2'-bipyridine (126 mg, 85% yield) as a white solid.

**$^1$H NMR** (400.16 MHz, $CDCl_3$) δ 8.95 (dd, *J* = 2.4, 0.8 Hz, 1H), 8.73 (ddd, *J* = 4.9, 1.8, 0.9 Hz, 1H), 8.55 (dd, *J* = 8.3, 0.8 Hz, 1H), 8.51 (dt, *J* = 8.0, 1.1 Hz, 1H), 8.07 (dd, *J* = 8.3, 2.4 Hz, 1H), 7.89 (ddd, *J* = 8.0, 7.5, 1.8 Hz, 1H), 7.68 – 7.64 (m, 2H), 7.54 – 7.48 (m, 2H), 7.46 – 7.41 (m, 1H), 7.37 (ddd, *J* = 7.5, 4.9, 1.2 Hz, 1H).
**$^{13}$C NMR** (100.63 MHz, $CDCl_3$) δ 155.22 (C, Ar), 154.08 (C, Ar), 148.91 (CH, Ar), 147.50 (CH, Ar), 137.78 (CH, Ar), 137.44 (C, Ar), 137.02 (C, Ar), 135.82(CH, Ar), 129.32 (CH, Ar), 128.54 (CH, Ar), 127.25 (CH, Ar), 124.11 (CH, Ar), 121.65 (CH, Ar), 121.59 (CH, Ar).
**$^{15}$N NMR** (40.55 MHz, $CDCl_3$) δ 301.57
**HRMS (ESI)**. Calculated for $C_{16}H_{13}N_2^+$: 233.1073 Obtained: 233.1074

*10.2.6.3 Preparation of 5-(p-tolyl)-2,2'-bipyridine (L16)*




Prepared following an adapted procedure:[144] 5-bromo-2,2'-bipyridine (150 mg, 0.64 mmol, 1 eq.), boronic acid (86.7 mg, 0.64 mmol, 1 eq.), $Pd(PPh_3)_4$ (110.5 mg, 0.1 mmol, 15 mol%), and $Na_2CO_3$ (340 mg, 3.2 mmol, 5 eq.) were added into a two-necked flask equipped with a reflux condenser. After addition of degassed 1,4-dioxane (3 ml, 0.2 M), EtOH (1.8 ml, 0.3 M), and water (1.8 ml, 0.3M), the mixture was refluxed for 4 h.

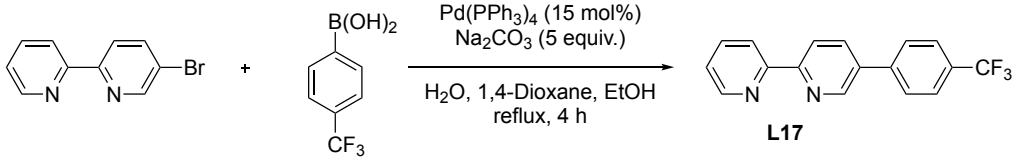
The reaction mixture was cooled to room temperature and extracted with EtOAc (2 x 20 mL). The organic phase was se*para*ted and washed with $H_2O$ (30 mL) and dried over anhydrous $MgSO_4$. The mixture was filtered, the solvent was removed under vacuum and

USC UNIVERSIDADE DE SANTIAGO DE COMPOSTELA

the mixture was purified by column chromatography on silica gel. To afford 5-(p-tolyl)-2,2'-bipyridine (102 mg, 65 % yield) as a white solid.

**$^{1}$H NMR** (400.16 MHz, $CDCl_3$) δ 8.94 (d, *J* = 2.3 Hz, 1H), 8.77 – 8.69 (m, 1H), 8.54 (dd, *J* = 10.2, 8.1 Hz, 2H), 8.07 (dd, *J* = 8.3, 2.3 Hz, 1H), 7.90 (td, *J* = 7.8, 1.8 Hz, 1H), 7.56 (d, *J* = 8.1 Hz, 2H), 7.38 (ddd, *J* = 7.6, 4.8, 1.2 Hz, 1H), 7.35 – 7.28 (m, 2H), 2.43 (s, 3H).
**$^{13}$C NMR** (100.63 MHz, $CDCl_3$) δ 155.01 (C, Ar), 153.49 (C, Ar), 148.84 (CH, Ar), 147.15 (CH, Ar), 138.66 (C, Ar), 137.89 (CH, Ar), 137.09 (C, Ar), 135.76 (CH, Ar), 134.38 (C, Ar), 130.07 (CH, Ar), 127.08 (CH, Ar), 124.13 (CH, Ar), 121.72 (CH, Ar), 21.35 ($CH_3$).
**HRMS (ESI)**. Calculated for $C_{17}H_{15}N_2^+$: 247.1230 Obtained: 247.1226

### *10.2.6.4 Preparation of 5-(4-(trifluoromethyl)phenyl)-2,2'-bipyridine (L17)*



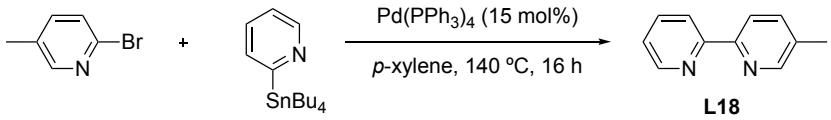

Prepared following an adapted procedure:[144] 5-bromo-2,2'-bipyridine (150 mg, 0.64 mmol, 1.0 equiv.), boronic acid (121 mg, 0.64 mmol, 1.0 equiv.), $Pd(PPh3)_4$ (110 mg, 0.09 mmol, 15 mol%), and $Na_2CO_3$ (340 mg, 3.2 mmol, 5.0 equiv.) were added into a two-necked flask quipped with a reflux condenser. After addition of degassed 1,4-dioxane (3.0 mL, 0.2 M), EtOH (1.8 mL, 0.3 M), and water (1.8 mL, 0.3 M), the mixture was refluxed for 4 h.

The reaction mixture was cooled to room temperature and extracted with EtOAc. The organic phase was se*para*ted and washed with water and dried over anhydrous $MgSO_4$. The mixture was filtered, the solvent was removed under vacuum and the mixture was purified by column chromatography on silica gel (Hex/EtOAc 10% to Hex/EtOAc 30%) to afford 5-(4-(trifluoromethyl)phenyl)-2,2'-bipyridine (92.5 mg, 48% yield) as a white solid.

**$^{1}$H NMR** (400.16 MHz, $CDCl_3$) δ 8.95 (dd, *J* = 2.4, 0.8 Hz, 1H), 8.75 (ddd, *J* = 4.9, 1.8, 0.9 Hz, 1H), 8.61 (dd, *J* = 8.3, 0.8 Hz, 1H), 8.52 (dt, *J* = 8.0, 1.1 Hz, 1H), 8.08 (dd, *J* = 8.3, 2.4 Hz, 1H), 7.92 (ddd, *J* = 8.0, 7.5, 1.8 Hz, 1H), 7.77 (s, 4H), 7.41 (ddd, *J* = 7.5, 4.9, 1.2 Hz, 1H).
**$^{13}$C NMR** (100.63 MHz, $CDCl_3$) δ 154.93 (C, Ar), 154.80 (C, Ar), 148.72 (CH, Ar), 147.75 (CH, Ar), 141.07 (C, Ar), 138.10 (CH, Ar), 135.88 (CH, Ar), 135.61 (C, Ar), 130.57 (q, *J* = 32.6 Hz, C, Ar), 127.59 (CH, Ar), 126.27 (q, *J* = 3.8 Hz, CH, Ar), 124.37 (CH, Ar), 124.21 (q, *J* = 272.1 Hz, $CF_3$), 121.85 (CH, Ar), 121.72 (CH, Ar).
**$^{19}$F NMR** (376.46 MHz, $CDCl_3$) δ -62.60.
**$^{15}$N NMR** (40.55 MHz, $CDCl_3$) δ 305.00
**HRMS (ESI).** Calculated for $C_{17}H_{12}F_3N_2^+$: 301.0947 Obtained: 301.0944

USC UNIVERSIDADE DE SANTIAGO DE COMPOSTELA

### *10.2.6.5 Preparation of 5-methyl-2,2'-bipyridine (L18)*

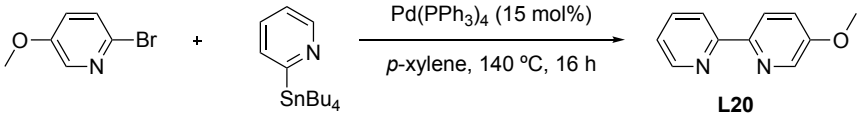



**L18**

Prepared following an adapted procedure:[145] 2-(tributylstannyl)pyridine (0.35 mL, 0.92 mL, 1.0 equiv.), 2-bromo-5-methylpyridine (211 mg, 1.2 mmol, 1.3 equiv.) and $Pd(PPh_3)_4$ (74.7 mg, 0.06 mmol, 7 mol%) were sequentially added to degassed *p*-xylene (8.0 mL, 0.1 M). The mixture was stirred for 13 h at 120 °C under an argon atmosphere. Then, the solution was poured onto 2.0 M aq. KOH (50 mL) and vigorously stirred for 15 min. The phases were se*para*ted, and the aqueous phase extracted with toluene. The combined organic layers were washed with 0.5 M EDTA solution (pH = 7), dried over anhydrous $MgSO_4$, filtrated and evaporated. The mixture was purified by column chromatography on silica gel (Hex/$Et_2O$ 5% to Hex/$Et_2O$ 30%) to afford 5-methyl-2,2'-bipyridine (466 mg, 91% yield) as a colorless oil.

**$^1$H NMR** (400.16 MHz, $CDCl_3$) δ 8.66 (ddd, *J* = 4.8, 1.9, 1.0 Hz, 1H), 8.50 (d, *J* = 2.6 Hz, 1H), 8.36 (dd, *J* = 8.0, 1.1 Hz, 1H), 8.29 (d, *J* = 8.1 Hz, 1H), 7.79 (td, *J* = 7.7, 1.8 Hz, 1H), 7.65 – 7.59 (m, 1H), 7.33 – 7.25 (m, 1H), 2.38 (d, *J* = 2.2 Hz, 3H).
**$^{13}$C NMR** (100.63 MHz, $CDCl_3$) δ 156.15 (C, Ar), 153.52 (C, Ar), 149.60 (CH, Ar), 149.16 (CH, Ar), 137.77 (CH, Ar), 137.11 (CH, Ar), 133.66 (C, Ar), 123.58 (CH, Ar), 121.02 (CH, Ar), 120.84 (CH, Ar), 18.47 ($CH_3$).
**$^{15}$N NMR** (40.55 MHz, $CDCl_3$) δ 304.98
**HRMS (ESI).** Calculated for $C_{11}H_{10}N_2^+$: 171.09167 Obtained: 171.09169

### *10.2.6.6 Preparation of 5-methoxy-2,2'-bipyridine (L20)*




**L20**

Prepared following an adapted procedure:[145] 2-(tributylstannyl)pyridine (0.52 mL, 1.38 mmol, 1.3 eq.), 2-bromo-5-methoxypyridine (200 mg, 1.1 mmol, 1.0 eq.) and $Pd(PPh_3)_4$ (122.5 mg, 0.1 mmol, 10 mol%) were sequentially added to degassed p-xylene (33 mL, 0.03 M). The mixture was stirred for 16 h at 140 °C under an argon atmosphere.

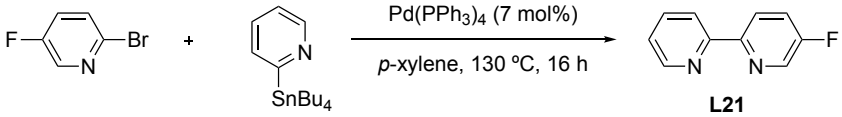
Then, the solution was poured onto 2.0 M aq. KOH (50 mL) and vigorously stirred for 15 min. The phases were se*para*ted, and the aqueous phase extracted with toluene. The combined organic layers were washed with 0.5 M EDTA solution (pH=7), dried over anhydrous $MgSO_4$, filtrated and evaporated. The mixture was purified by column chromatography on silica gel (Hex/$Et_2O$ 5% to Hex/$Et_2O$ 30%) to afford 5-methoxy-2,2'-bipyridine (168 mg, 85% yield) as a colorless oil.

USC UNIVERSIDADE

[145] Heller; Schubert *J. Org. Chem.* **2002,** *67,* 8269–8272.

**$^{1}$H NMR** (400.16 MHz, $CDCl_3$) δ 8.61 (ddd, *J* = 4.8, 1.8, 0.9 Hz, 1H), 8.36 – 8.27 (m, 3H), 7.75 (ddd, *J* = 8.0, 7.5, 1.8 Hz, 1H), 7.28 (dd, *J* = 8.7, 3.0 Hz, 1H), 7.22 (ddd, *J* = 7.5, 4.9, 1.2 Hz, 1H), 3.87 (s, 3H).
**$^{13}$C NMR** (100.63 MHz, $CDCl_3$) δ 156.18 (C, Ar), 155.97 (C, Ar), 148.96 (CH, Ar), 148.80 (C, Ar), 137.05 (CH, Ar), 137.04 (CH, Ar), 123.01 (CH, Ar), 121.82 (CH, Ar), 120.97 (CH, Ar), 120.54 (CH, Ar), 55.73 (O-$CH_3$).
**$^{15}$N NMR** (40.55 MHz, $CDCl_3$) δ 308.74
**HRMS (ESI)**. Calculated for $C_{11}H_{11}N_2O^+$: 187.0866 Obtained: 187.0866

### *10.2.6.7 Preparation of 5-fluoro-2,2'-bipyridine (L21)*

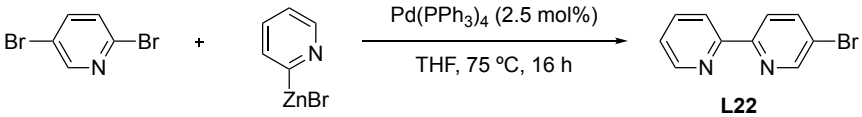


**L21**

Prepared following an adapted procedure:[145] 2-(tributylstannyl)pyridine (0.35 mL, 0.92 mL, 1.0 equiv.), 2-bromo-5-fluoropyridine (211 mg, 1.2 mmol, 1.3 equiv.) and $Pd(PPh_3)_4$ (74.7 mg, 0.06 mmol, 7 mol%) were sequentially added to degassed *p*-xylene (8.0 mL, 0.1 M). The mixture was stirred for 13 h at 130 °C under an argon atmosphere. Then, the solution was poured onto 2.0 M aq. KOH (50 mL) and vigorously stirred for 15 min. The phases were se*para*ted, and the aqueous phase extracted with toluene. The combined organic layers were washed with 0.5 M EDTA solution (pH = 7), dried over anhydrous $MgSO_4$, filtrated and concentrated under reduced pressure. The mixture was purified by column chromatography on silica gel (Hex/$Et_2O$ 5%) to afford 5-fluoro-2,2'-bipyridine (104 mg, 65% yield) as a white solid.

**$^{1}$H NMR** (400.16 MHz, $CDCl_3$) δ 8.67 (ddd, *J* = 4.8, 1.9, 0.9 Hz, 1H), 8.52 (d, *J* = 2.9 Hz, 1H), 8.51 – 8.46 (m, 1H), 8.37 (dt, *J* = 8.1, 1.1 Hz, 1H), 7.85 (ddd, *J* = 8.0, 7.5, 1.8 Hz, 1H), 7.53 (ddd, *J* = 8.8, 8.1, 2.9 Hz, 1H), 7.33 (ddd, *J* = 7.5, 4.9, 1.2 Hz, 1H).
**$^{13}$C NMR** (100.63 MHz, $CDCl_3$) δ 160.08 (d, *J* = 258.0 Hz, CF), 155.01 (C, Ar), 152.02 (C, Ar), 148.83 (CH, Ar), 137.65 (CH, Ar), 137.57 (d, *J* = 24.2 Hz, CH, Ar), 123.88 (CH, Ar), 123.83 (d, *J* = 18.3 Hz, CH, Ar), 122.68 (d, *J* = 4.7 Hz, CH, Ar), 121.29 (CH, Ar).
**$^{19}$F NMR** (376.46 MHz, $CDCl_3$) δ -126.80.
**$^{15}$N NMR** (40.55 MHz, $CDCl_3$) δ 313.10
**HRMS (ESI).** Calculated for $C_{1o}H_8FN_2^+$: 175.0666 Obtained: 175.0667

### *10.2.6.8 Preparation of 5-bromo-2,2'-bipyridine (L22)*



**L22**

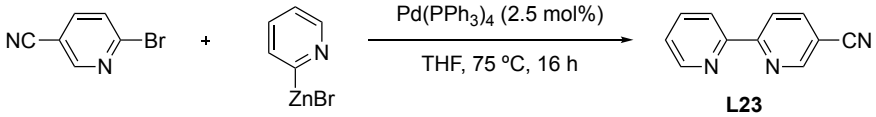
Prepared following an adapted procedure:[135] Under a nitrogen atmosphere, $Pd(PPh_3)_4$ (243 mg, 0.2 mmol, 2.5 mol%) and 2,5-dibromopyridine (1.89 g, 8.0 mmol, 1.0 equiv.) were added to a dry two-neck round-bottom flask and cooled to 0 °C. Upon

USC UNIVERSIDADE DE SANTIAGO DE COMPOSTELA

addition of 2-pyridylzinc bromide in THF 0.5 M (19.2 mL, 9.6 mmol, 1.2 equiv.) the reaction mixture turned brown in color. The mixture was stirred overnight at 75 °C under an inert atmosphere during which time a white precipitate formed. Subsequently, the reaction mixture was poured into saturated aqueous solution of 1:1 EDTA/$Na_2CO_3$ (500 mL) and the mixture was stirred until the white solid turned completely yellow. The aqueous suspension was extracted with dichloromethane (3 x 100 mL), the combined organic layers were dried over anhydrous $MgSO_4$ and the solvent was evaporated under reduced pressure. The mixture was purified by column chromatography on silica gel (Hex/$Et_2O$ 5%) to afford 5-fluoro-2,2'-bipyridine (1.43 g, 76% yield) as a white solid.

**$^1$H NMR** (400.16 MHz, $CDCl_3$) δ 8.71 (dd, *J* = 2.4, 0.8 Hz, 1H), 8.67 (ddd, *J* = 4.9, 1.8, 0.9 Hz, 1H), 8.38 (dt, *J* = 8.0, 1.0 Hz, 1H), 8.34 (dd, *J* = 8.5, 0.8 Hz, 1H), 7.93 (dd, *J* = 8.5, 2.4 Hz, 1H), 7.83 (ddd, *J* = 8.0, 7.5, 1.8 Hz, 1H), 7.33 (ddd, *J* = 7.5, 4.8, 1.2 Hz, 1H).
**$^{13}$C NMR** (100.63 MHz, $CDCl_3$) δ 155.08 (C, Ar), 154.38 (C, Ar), 150.37 (CH, Ar), 149.09 (CH, Ar), 139.67 (CH, Ar), 137.46 (CH, Ar), 124.19 (CH, Ar), 122.58 (CH, Ar), 121.41 (C, Ar), 121.26 (CH, Ar).
**$^{15}$N NMR** (40.55 MHz, $CDCl_3$) δ 311.68
**HRMS (ESI)**. Calculated for $C_{10}H_8BrN_2^+$: 234.9865 Obtained: 234.9863

### *10.2.6.9 Preparation of [2,2'-bipyridine]-5-carbonitrile (L23)*




**L23**

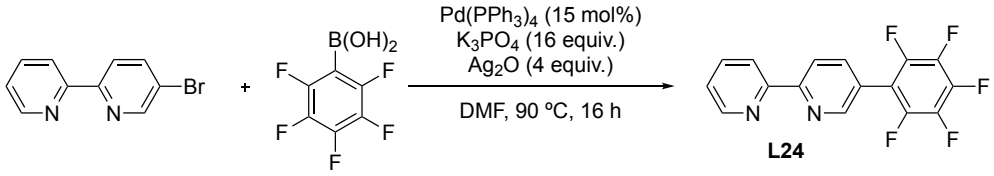
Prepared following an adapted procedure:[135] Under a nitrogen atmosphere, $Pd(PPh_3)_4$ (60.8 mg, 0.05 mmol, 2.5 mol%) and 2-bromo-5-(cyano)pyridine (366 mg, 2.0 mmol, 1.0 equiv.) were added to a dry two-neck round-bottom flask and cooled to 0 °C. Upon addition of 2-pyridylzinc bromide in THF 0.5 M (4.8 mL, 2.4 mmol, 1.2 equiv.) the reaction mixture turned brown in color. The mixture was stirred overnight at 75 °C under an inert atmosphere during which time a white precipitate formed. Subsequently, the reaction mixture was poured into saturated aqueous solution of 1:1 EDTA/$Na_2CO_3$ (50 mL), and the mixture was stirred until the white solid turned completely yellow. The aqueous suspension was extracted with dichloromethane (3 x 100 mL), the combined organic layers were dried over anhydrous $MgSO_4$ and the solvent was evaporated under reduced pressure. The mixture was purified by column chromatography on silica gel (Hex/$Et_2O$ 15%) to afford [2,2'-bipyridine]-5-carbonitrile (195 mg, 54% yield) as a white solid.

**$^1$H NMR** (400.16 MHz, $CDCl_3$) δ 8.95 (dd, *J* = 2.4, 0.8 Hz, 1H), 8.73 (ddd, *J* = 4.9, 1.8, 0.9 Hz, 1H), 8.55 (dd, *J* = 8.3, 0.8 Hz, 1H), 8.51 (dt, *J* = 8.0, 1.1 Hz, 1H), 8.07 (dd, *J* = 8.3, 2.4 Hz, 1H), 7.89 (ddd, *J* = 8.0, 7.5, 1.8 Hz, 1H), 7.68 – 7.64 (m, 2H), 7.54 – 7.48 (m, 2H), 7.46 – 7.41 (m, 1H), 7.37 (ddd, *J* = 7.5, 4.9, 1.2 Hz, 1H).

USC UNIVERSIDADE DE SANTIAGO DE COMPOSTELA

**$^{13}$C NMR** (100.63 MHz, $CDCl_3$) δ 158.80 (C, Ar), 154.01 (C, Ar), 152.11 (CH, Ar), 149.35 (CH, Ar), 140.28 (CH, Ar), 137.73 (CH, Ar), 125.23 (CH, Ar), 122.34, (CH, Ar) 121.04 (CH, Ar), 117.03 (C, Ar), 109.69 (C, Ar).
**$^{15}$N NMR** (40.55 MHz, $CDCl_3$) δ 308.52
**HRMS (ESI)**. Calculated for $C_{11}H_8N_3^+$: 182.07127 Obtained: 182.07125

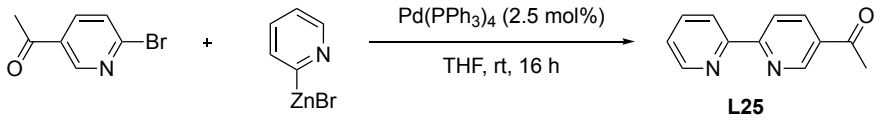
### *10.2.6.10 Preparation of 5-(perfluorophenyl)-2,2'-bipyridine (L24)*




Prepared following an adapted procedure:[146] 5-bromo-2,2'-bipyridine (100 mg, 0.42 mmol, 1.0 equiv.), pentafluorophenylboronic acid (90 mg, 0.42 mmol, 1.0 equiv.), $Pd(PPh_3)_4$ (78 mg, 15 mol%), $Ag_2O$ (394 mg, 1.7 mmol, 4.0 equiv.) and $K_3PO_4$ (1,44 g, 6.8 mmol, 16.0 equiv.) were added into a 25 mL two-necked flask. After addition of DMF (8.5 mL, 0.05 M) the reaction was heated at 90°C overnight. After that time, the reaction mixture was cooled to room temperature, water was added and the mixture was extracted with EtOAc (2 x 20 mL). The organic phase was se*para*ted and washed with $H_2O$ (30 mL) and dried over anhydrous $MgSO_4$. The mixture was filtered, the solvent was removed under vacuum and the mixture was purified by column chromatography on silica gel (Hex/$Et_2O$ 15%) to afford 5-(perfluorophenyl)-2,2'-bipyridine (87 mg, 64% yield) as a white solid.

**$^1$H NMR** (400.16 MHz, $CDCl_3$) δ 8.79 – 8.73 (m, 2H), 8.64 (d, *J* = 8.3 Hz, 1H), 8.51 (dt, *J* = 7.9, 1.1 Hz, 1H), 7.98 – 7.87 (m, 2H), 7.41 (ddd, *J* = 7.5, 4.8, 1.2 Hz, 1H).
**$^{13}$C NMR** (100.63 MHz, $CDCl_3$) δ 155.80 (C, Ar), 154.78 (C, Ar), 150.03 (CH, Ar), 148.76 (CH, Ar), 144.49 (d, *J* = 249.1 Hz, CF, Ar), 141.21 (d, *J* = 255.7 Hz, CF, Ar), 138.77 (CH, Ar), 138.18 (d, *J* = 252.6 Hz, CF, Ar), 138.12 (CH, Ar), 124.62 (CH, Ar), 123.34 (C, Ar), 121.97 (CH, Ar), 121.43 (CH, Ar), 112.60 (C, Ar).
**$^{19}$F NMR** (376.46 MHz, $CDCl_3$) δ -142.25 – -143.11 (m), -153.34 (t, *J* = 21.0 Hz), -161.08 (td, *J* = 22.2, 8.1 Hz).
**HRMS (ESI)**. Calculated for $C_{16}H_8F_5N_2^+$: 323.0602 Obtained: 323.0598

### *10.2.6.11 Preparation of 1-([2,2'-bipyridin]-5-yl)ethan-1-one (L25)*



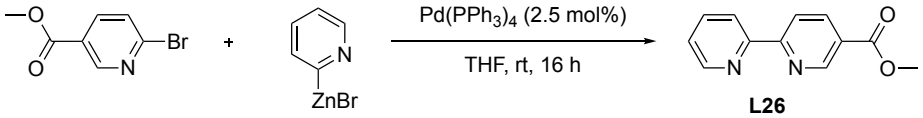

Prepared following an adapted procedure:[135] Under a nitrogen atmosphere, $Pd(PPh_3)_4$ (38 mg, 0.03 mmol, 2.5 mol%) and 5-Acetyl-2-bromopyridine (250 mg, 1.1

[146] Liu, C.; Han, N.; Song, X.; Qiu, J. *Eur. J. Org. Chem.* **2010,** *2010,* 5548–5551.

mmol, 1 eq.) were added to a dry two-neck round-bottom flask and cooled to 0 ºC. Upon addition of 2-pyridylzinc bromide (3 ml, 1.5 mmol, 1.2 eq) in THF (0.5M) the reaction mixture turned brown in color. The mixture was stirred overnight at rt under an inert atmosphere during which time a white precipitate formed. Subsequently, the reaction mixture was poured into saturated aqueous solution of 1:1 EDTA/$Na_2CO_3$ (500 mL), and the mixture was stirred until the white solid turned completely yellow. The aqueous suspension was extracted with dichloromethane (3 x 100 mL), the combined organic layers were dried over anhydrous sodium sulphate and the solvent was evaporated under reduced pressure. The mixture was purified by column chromatography on silica gel (Hex/$Et_2O$ 10%) to afford 1-([2,2'-bipyridin]-5-yl)ethan-1-one (225 mg, 91% yield) as a white solid.

**$^1$H NMR** (400.16 MHz, $CDCl_3$) δ 9.23 (d, *J* = 2.3 Hz, 1H), 8.75 (d, *J* = 4.2 Hz, 1H), 8.62 (d, *J* = 8.0 Hz, 1H), 8.53 (d, *J* = 7.9 Hz, 1H), 8.37 (dd, *J* = 8.3, 2.3 Hz, 1H), 7.92 (td, *J* = 7.8, 1.8 Hz, 1H), 7.43 (ddd, *J* = 7.6, 4.9, 1.2 Hz, 1H), 2.68 (s, 3H).
**$^{13}$C NMR** (100.63 MHz, $CDCl_3$) δ 196.65 (CO), 158.63 (C, Ar), 154.50 (C, Ar), 149.70 (CH, Ar), 148.91 (CH, Ar), 138.08 (CH, Ar), 136.93 (CH, Ar), 132.21 (C, Ar), 124.93 (CH, Ar), 122.52 (CH, Ar), 121.35 (CH, Ar), 27.01 ($CH_3$).
**HRMS (ESI)**. Calculated for $C_{12}H_{11}N_2O^+$: 199.0866 Obtained: 199.0865

### *10.2.6.12 Preparation of methyl [2,2'-bipyridine]-5-carboxylate (L26)*




**L26**

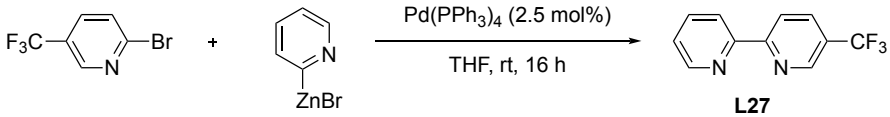
Prepared following an adapted procedure:[135] Under a nitrogen atmosphere, $Pd(PPh_3)_4$ (35.2 mg, 0.03 mmol, 2.5 mol%) and Methyl 6-bromonicotinate (250 mg, 1.1 mmol, 1 eq.) were added to a dry two-neck round-bottom flask and cooled to 0 ºC. Upon addition of 2-pyridylzinc bromide (2.8 ml, 1.4 mmol, 1.2 eq) in THF (0.5M) the reaction mixture turned brown in color. The mixture was stirred overnight at rt under an inert atmosphere during which time a white precipitate formed. Subsequently, the reaction mixture was poured into saturated aqueous solution of 1:1 EDTA/$Na_2CO_3$ (500 mL), and the mixture was stirred until the white solid turned completely yellow. The aqueous suspension was extracted with dichloromethane (3 x 100 mL), the combined organic layers were dried over anhydrous sodium sulphate and the solvent was evaporated under reduced pressure. The mixture was purified by column chromatography on silica gel (Hex/$Et_2O$ 10%) to afford methyl [2,2'-bipyridine]-5-carboxylate (215 mg, 87% yield) as a white solid.

**$^1$H NMR** (400.16 MHz, $CDCl_3$) δ 9.31 – 9.25 (m, 1H), 8.74 (d, *J* = 4.9 Hz, 1H), 8.59 (d, *J* = 8.0 Hz, 1H), 8.53 (dt, *J* = 8.0, 1.1 Hz, 1H), 8.43 (dd, *J* = 8.3, 2.2 Hz, 1H), 7.92 (td, *J* = 7.8, 1.8 Hz, 1H), 7.42 (ddd, *J* = 7.6, 4.8, 1.2 Hz, 1H), 3.98 (s, 3H).

USC UNIVERSIDADE DE SANTIAGO DE COMPOSTELA

**$^{13}$C NMR** (100.63 MHz, $CDCl_3$) δ 165.83 (CO), 158.64 (C, Ar), 154.62 (C, Ar), 150.66 (CH, Ar), 148.87 (CH, Ar), 138.39 (CH, Ar), 138.05 (CH, Ar), 126.08 (C, Ar), 124.86 (CH, Ar), 122.47 (CH, Ar), 121.05 (CH, Ar), 52.61 (O-$CH_3$).
**HRMS (ESI).** Calculated for $C_{12}H_{11}N_2O_2^+$: 215.0815 Obtained: 215.0813

### *10.2.6.13 Preparation of 5-(trifluoromethyl)-2,2'-bipyridine (L27)*



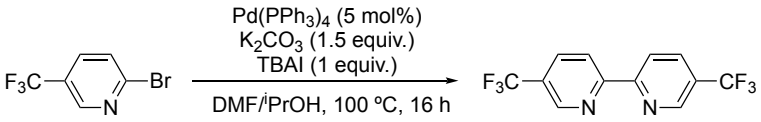

**L27**

Prepared following an adapted procedure:[135] Under a nitrogen atmosphere, $Pd(PPh_3)_4$ (134.6 mg, 0.1 mmol, 2.5 mol%) and 2-bromo-5-(trifluoromethyl)pyridine (1.0 g, 4.4 mmol, 1.0 equiv.) were added to a dry two-neck round-bottom flask and cooled to 0 °C. Upon addition of 2-pyridylzinc bromide in THF 0.5 M (10.62 mL, 5.3 mmol, 1.2 equiv.) the reaction mixture turned brown in color. The mixture was stirred overnight at 75 °C under an inert atmosphere during which time a white precipitate formed. Subsequently, the reaction mixture was poured into saturated aqueous solution of 1:1 EDTA/$Na_2CO_3$ (500 mL), and the mixture was stirred until the white solid turned completely yellow. The aqueous suspension was extracted with dichloromethane (3 x 100 mL), the combined organic layers were dried over anhydrous sodium sulphate and the solvent was evaporated under reduced pressure. The mixture was purified by column chromatography on silica gel (Hex/$Et_2O$ 2.5% to Hex/$Et_2O$ 5%) to afford 5-(trifluoromethyl)-2,2'-bipyridine (807 mg, 81% yield) as a white solid.

**$^{1}$H NMR** (400.16 MHz, $CDCl_3$) δ 8.93 (dt, *J* = 2.4, 0.9 Hz, 1H), 8.71 (ddd, *J* = 4.8, 1.8, 0.9 Hz, 1H), 8.58 (dt, *J* = 8.4, 0.8 Hz, 1H), 8.47 (dt, *J* = 8.0, 1.1 Hz, 1H), 8.05 (ddq, *J* = 8.4, 2.2, 0.7 Hz, 1H), 7.87 (ddd, *J* = 8.0, 7.5, 1.8 Hz, 1H), 7.38 (ddd, *J* = 7.5, 4.8, 1.2 Hz, 1H).
**$^{13}$C NMR** (100.63 MHz, $CDCl_3$) δ 159.08 (C, Ar), 154.65 (C, Ar), 149.31 (CH, Ar), 146.28 (q, *J* = 4.1 Hz, CH, Ar), 137.53 (CH, Ar), 134.25 (q, *J* = 3.5 Hz, CH, Ar), 126.50 (q, *J* = 33.1 Hz, C, Ar), 124.82 (CH, Ar), 123.81 (q, *J* = 272.5 Hz, $CF_3$), 121.96 (CH, Ar), 120.90 (CH, Ar).
**$^{19}$F NMR** (376.46 MHz, $CDCl_3$) δ -62.35.
**$^{15}$N NMR** (40.55 MHz, $CDCl_3$) δ 307.82
**HRMS (ESI)**. Calculated for $C_{11}H_8F_3N_2^+$: 225.0634 Obtained: 225.0632

USC UNIVERSIDADE DE SANTIAGO DE COMPOSTELA

*10.2.6.14 Preparation of 5,5'-bis(trifluoromethyl)-2,2'-bipyridine (L28)*



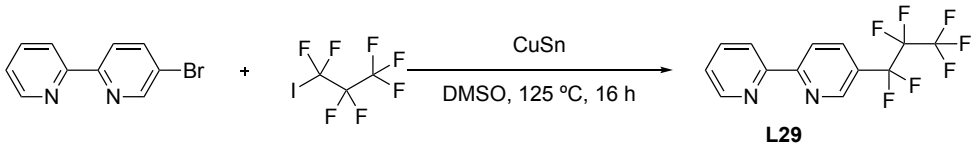

**L28**

Prepared following an adapted procedure:[147] To a round-bottom flask charged with a magnetic stir bar were added, $Pd(OAc)_2$ (99.3 mg, 0.4 mmol, 5 mol%), TBAI (3.3 g, 8.8 mmol, 1 equiv.) and $K_2CO_3$ (1.8 g, 1.3 mmol, 1.5 eq.). The flask was then evacuated and backfilled with $N_2$ three times. To this flask were added 2-bromo-5-(trifluoromethyl)pyridine (2 g, 8.8 mmol, 1 equiv.), $^{i}$PrOH (1.5 mL, 6.5 M) and DMF (30 mL, 0.3 M) and the reaction was heated at 100 °C for 24 h.

The reaction mixture was then cooled to room temperature and filtered, washing the solid copiously with EtOAc. The organic liquids were extracted three times with 40 mL of 10% (w/w) aqueous LiCl. The aqueous layer was backwashed once with EtOAc (50 mL) and the combined organic fractions were finally washed with water (40 mL) and brine (40 mL) before drying over $MgSO_4$. Following removal of the solvent in vacuo, the crude residue was purified by silica gel chromatography (gradient from 100% hexane to 5% EtOAc/hexane) to afford 5,5'-bis(trifluoromethyl)-2,2'-bipyridine (1.2 g, 99% yield) as a white solid.

**$^{1}$H NMR** (400.16 MHz, $CDCl_3$) δ 8.96 (s, 2H), 8.62 (d, *J* = 8.3 Hz, 2H), 8.08 (dd, *J* = 8.3, 1.5 Hz, 2H).
**$^{13}$C NMR** (100.63 MHz, $CDCl_3$) δ 157.83 (C, Ar), 146.46 (q, *J* = 4.0 Hz, CH, Ar), 134.52 (q, *J* = 3.5 Hz, CH, Ar), 127.32 (q, *J* = 33.0 Hz, C, Ar), 123.65 (q, *J* = 272.4 Hz, $CF_3$), 121.46 (CH, Ar).
**$^{19}$F NMR** (376.46 MHz, $CDCl_3$) δ -62.45.
**$^{15}$N NMR** (40.55 MHz, $CDCl_3$) δ 309.64.
**HRMS (ESI)**. Calculated for $C_{12}H_7F_6N_2^+$: 293.050794 Obtained: 293.051312

*10.2.6.15 Preparation of 5-(perfluoropropyl)-2,2'-bipyridine (L29)*




**L29**

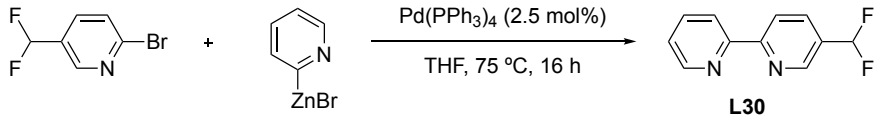
Prepared following an adapted procedure:[148] Perfluoropropyl iodide (134 μl, 0.9 mmol, 1.1 equiv.) was added to a well-stirred mixture of Copper-tin alloy (341 mg, 1.9 mmol, 2.2 equiv.), 5-bromo-2,2'-bipyridine (200 mg, 0.8 mmol, 1 equiv.) and DMSO (2 ml, 0.4 M) under a nitrogen atmosphere and the reaction was heated at 125° C for 4 h.

[147] Miller, D. C.; Ganley, J. M.; Musacchio, A. J.; Sherwood, T. C.; Ewing, W. R.; Knowles, R. R. *J. Am. Chem. Soc.* **2019,** *141,* 16590–16594.
[148] Chen, G. J.; Tamborski, C. *J. Fluorine Chem.* **1990,** *46,* 137–159.

The reaction mixture was cooled to room temperature, diethyl ether (10 ml) and water (6 ml) were slowly added. The mixture was stirred and then centrifuged. The aqueous and organic layers were decanted from the solid This solid was washed with additional diethyl ether (2 x 40 ml) The ether extracts and the previous organic layer were combined, and repeatedly treated with an aqueous ammonium hydroxide solution until no blue color in the aqueous layer was noted. The ether layer was se*para*ted and dried over anhydrous $MgSO_4$. The mixture was filtered, the solvent was removed under vacuum and the mixture was purified by column chromatography on silica gel to afford 5-(perfluoropropyl)-2,2'-bipyridine (113 mg, 41% yield) as a white solid.

**$^1$H NMR** (400.16 MHz, $CDCl_3$) δ 8.86 (d, *J* = 1.6 Hz, 1H), 8.69 (ddd, *J* = 4.8, 1.8, 0.9 Hz, 1H), 8.57 (dd, *J* = 8.4, 0.9 Hz, 1H), 8.46 (dt, *J* = 8.0, 1.1 Hz, 1H), 7.98 (dd, *J* = 8.4, 2.3 Hz, 1H), 7.81 (td, *J* = 7.7, 1.8 Hz, 1H), 7.33 (ddd, *J* = 7.5, 4.8, 1.2 Hz, 1H).
**$^{13}$C NMR** (100.63 MHz, $CDCl_3$) δ 159.53 (C, Ar), 154.74 (C, Ar), 149.53 (CH, Ar), 147.41 (t, *J* = 6.9 Hz, CH, Ar), 137.19 (CH, Ar), 135.59 (t, *J* = 6.1 Hz, CH, Ar), 124.78 (CH, Ar), 121.84 (CH, Ar), 120.66 (CH, Ar), 118.08 (qt, *J* = 287.7, 34.7 Hz, $–CF_2–\underline{\mathbf{C}}F_2–CF_3$), 115.03 (tt, *J* = 257.6, 32.3 Hz, $–\underline{\mathbf{C}}F_2–CF_2–CF_3$), 108.73 (tq, *J* = 265.6, 38.0 Hz, $–CF_2–CF_2–\underline{\mathbf{C}}F_3$).
**$^{19}$F NMR** (376.46 MHz, $CDCl_3$) δ -80.02 (t, *J* = 9.8 Hz), -112.44 – -112.60 (m), -126.51 (t, *J* = 4.5, 3.9 Hz).
**HRMS (ESI)**. Calculated for $C_{13}H_8F_7N_2^+$: 325.0570 Obtained: 325.0565

### *10.2.6.16 Preparation of 5-(difluoromethyl)-2,2'-bipyridine (L30)*



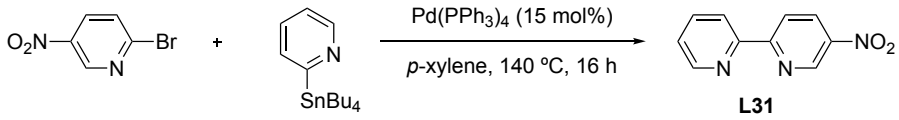

**L30**

Prepared following an adapted procedure:[135] Under a nitrogen atmosphere, $Pd(PPh_3)_4$ (14.6 mg, 0.01 mmol, 2.5 mol%) and 2-bromo-5(difluoromethyl)pyridine (100 mg, 4.4 mmol, 1 equiv.) were added to a dry two-neck round-bottom flask and cooled to 0 °C. Upon addition of 2-pyridylzinc bromide in THF 0.5 M (1. 2 ml, 0.5 mmol, 1.2 eq) the reaction mixture turned brown in color. The mixture was stirred overnight at 75 °C under an inert atmosphere during which time a white precipitate formed. Then, the reaction mixture was poured into saturated aqueous solution of 1:1 EDTA/$Na_2CO_3$ (50 mL), and the mixture was stirred until the white solid turned completely yellow. The aqueous suspension was extracted with dichloromethane (3 x 100 mL), the combined organic layers were dried over anhydrous sodium sulphate and the solvent was evaporated under reduced pressure. The mixture was purified by column chromatography on silica gel (Hex/$Et_2O$ 15%) to afford 5-(difluoromethyl)-2,2'-bipyridine (181 mg, 76% yield) as a white solid.

**$^1$H NMR** (400.16 MHz, $CDCl_3$) δ 8.86 – 8.79 (m, 1H), 8.73 (ddd, *J* = 4.9, 1.8, 0.9 Hz, 1H), 8.60 (dd, *J* = 8.2, 1.0 Hz, 1H), 8.49 (d, *J* = 8.0 Hz, 1H), 7.99 (ddt, *J* = 8.3, 1.6, 0.5 Hz, 1H), 7.91 (td, *J* = 7.8, 1.8 Hz, 1H), 7.41 (ddd, *J* = 7.5, 4.9, 1.2 Hz, 1H), 6.78 (t, *J* = 55.8 Hz, 1H).

**$^{13}$C NMR** (100.63 MHz, $CDCl_3$) δ 157.60 (C, Ar), 154.73 (C, Ar), 148.82 (CH, Ar), 146.91 (t, *J* = 6.7 Hz, CH, Ar), 138.04 (CH, Ar), 134.63 (t, *J* = 5.4 Hz, CH, Ar), 130.24 (t, *J* = 23.0 Hz, C, Ar), 124.70 (CH, Ar), 122.09 (CH, Ar), 121.34 (CH, Ar), 113.56 (t, *J* = 239.5 Hz, $CHF_2$).
**$^{19}$F NMR** (376.46 MHz, $CDCl_3$) δ -112.41
**HRMS (ESI)**. Calculated for $C_{11}H_9F_2N_2^+$: 207.0728 Obtained: 207.0725

### *10.2.6.17 Preparation of 5-nitro-2,2'-bipyridine (L31)*

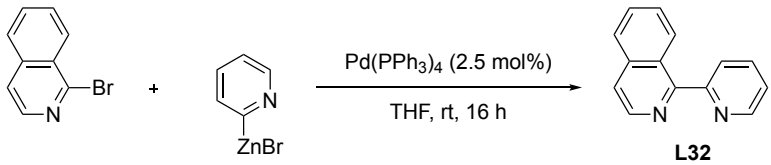



**L31**

Prepared following an adapted procedure:[145] 2-(tributylstannyl)pyridine (1 mL, 2.7 mmol, 1.1 eq.), 2-bromo-5-nitropyridine (500 mg, 2.5 mmol, 1.0 eq.) and $Pd(PPh3)_4$ (93.3 mg, 0.1 mmol, 5 mol%) were sequentially added to degassed THF (4 mL, 0.6 M). The mixture was stirred for 16 h at 140 ºC under an argon atmosphere. Then, the solution was poured onto 2.0 M aq. KOH (50 mL) and vigorously stirred for 15 min. The phases were se*para*ted, and the aqueous phase extracted with $CH_2Cl_2$. The combined organic layers were washed with 0.5 M EDTA solution (pH = 7), dried over anhydrous $MgSO_4$, filtrated and evaporated. The mixture was purified by column chromatography on silica gel (Hex/$Et_2O$ 5% to Hex/$Et_2O$ 30%) to afford 5-nitro-2,2'-bipyridine (391 mg, 79% yield).

**$^1$H NMR** (400.16 MHz, $CDCl_3$) δ 9.48 (dd, *J* = 2.6, 0.7 Hz, 1H), 8.74 (ddd, *J* = 4.8, 1.8, 0.9 Hz, 1H), 8.68 (dd, *J* = 8.8, 0.7 Hz, 1H), 8.59 (dd, *J* = 8.8, 2.6 Hz, 1H), 8.53 (dt, *J* = 8.0, 1.1 Hz, 1H), 7.90 (ddd, *J* = 8.0, 7.5, 1.8 Hz, 1H), 7.43 (ddd, *J* = 7.6, 4.8, 1.2 Hz, 1H).
**$^{13}$C NMR** (100.63 MHz, $CDCl_3$) δ 160.81 (C, Ar), 153.83 (C, Ar), 149.56 (CH, Ar), 144.92 (CH, Ar), 144.21 (C, Ar), 137.64 (CH, Ar), 132.20 (CH, Ar), 125.38 (CH, Ar), 122.68 (CH, Ar), 121.35. (CH, Ar)
**$^{15}$N NMR** (40.55 MHz, $CDCl_3$) δ 309.83
**HRMS (ESI)**. Calculated for $C_{10}H_8N_3O_2^+$: 202.0611 Obtained: 202.0611

### *10.2.6.18 Preparation of 1-(pyridin-2-yl)isoquinoline (L32)*



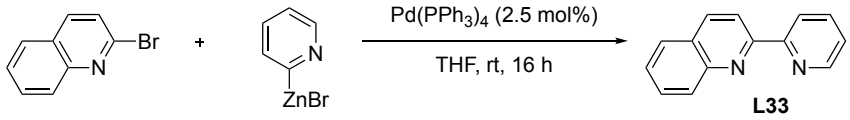

**L32**

Prepared following an adapted procedure:[135] Under a nitrogen atmosphere, $Pd(PPh_3)_4$ (33.6 mg, 0.03 mmol, 2.5 mol%) and 1-bromo-isoquinoline (230 mg, 1.1 mmol, 1 eq.) were added to a dry two-neck round-bottom flask and cooled to 0 ºC. Upon addition of 2-pyridylzinc bromide (2.7 ml, 1.3 mmol, 1.2 eq) in THF (0.5M) the reaction mixture turned brown in color. The mixture was stirred overnight at room temperature under an inert atmosphere, during which time a white precipitate formed. Then, the reaction mixture was poured into saturated aqueous solution of 1:1 EDTA/$Na_2CO_3$ (500 mL), and the mixture was stirred until the white solid turned completely yellow. The aqueous

suspension was extracted with dichloromethane (3 x 100 mL), the combined organic layers were dried over anhydrous sodium sulphate and the solvent was evaporated under reduced pressure. The mixture was purified by column chromatography on silica gel (Tol/AcOEt 10%) to afford 1-(pyridin-2-yl)isoquinoline (117 mg, 51% yield) as a white solid.

**$^{1}$H NMR** (400.16 MHz, $CDCl_3$) δ 8.80 (ddd, *J* = 4.9, 1.8, 1.0 Hz, 1H), 8.63 (d, *J* = 5.7 Hz, 1H), 8.60 (dd, *J* = 8.6, 1.1 Hz, 1H), 8.01 (dt, *J* = 8.1, 1.1 Hz, 1H), 7.95 – 7.87 (m, 2H), 7.77 – 7.69 (m, 2H), 7.61 (ddd, *J* = 8.3, 6.8, 1.3 Hz, 1H), 7.42 (ddd, *J* = 7.5, 4.9, 1.3 Hz, 1H).
**$^{13}$C NMR** (100.63 MHz, $CDCl_3$) δ 157.91 (C, Ar), 157.53 (C, Ar), 148.87 (CH, Ar), 141.52 (CH, Ar), 137.38 (C, Ar), 137.19 (CH, Ar), 130.50 (CH, Ar), 127.98 (CH, Ar), 127.96 (CH, Ar), 127.07 (CH, Ar), 126.72 (C, Ar), 125.47 (CH, Ar), 123.54 (CH, Ar), 121.55 (CH, Ar).
**$^{15}$N NMR** (40.55 MHz, $CDCl_3$) δ 301.34
**HRMS (ESI)**. Calculated for $C_{14}H_{11}N_2^+$: 207.0917 Obtained: 207.0912

### *10.2.6.19 Preparation of 2-(pyridin-2-yl)quinoline (L33)*



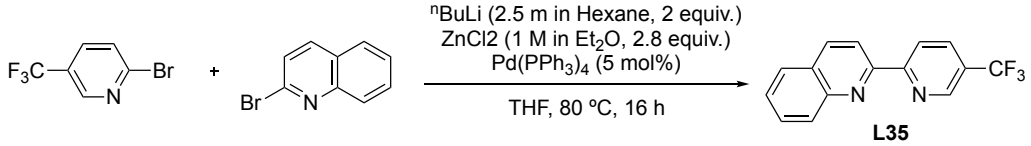

**L33**

Prepared following an adapted procedure:[135] Under a nitrogen atmosphere, $Pd(PPh_3)_4$ (33.6 mg, 0.03 mmol, 2.5 mol%) and 2-bromo-quinoline (230 mg, 1.1 mmol, 1 eq.) were added to a dry two-neck round-bottom flask and cooled to 0 ºC. Upon addition of 2-pyridylzinc bromide (2.7 ml, 1.3 mmol, 1.2 eq) in THF (0.5M) the reaction mixture turned brown in color. The mixture was stirred overnight at rt under an inert atmosphere during which time a white precipitate formed. Then, the reaction mixture was poured into saturated aqueous solution of 1:1 EDTA/$Na_2CO_3$ (500 mL), and the mixture was stirred until the white solid turned completely yellow. The aqueous suspension was extracted with dichloromethane (3 x 100 mL), the combined organic layers were dried over anhydrous sodium sulphate and the solvent was evaporated under reduced pressure. The mixture was purified by column chromatography on silica gel (Hex/$Et_2O$ 10%) to afford 2-(pyridin-2-yl)quinoline (177 mg, 77% yield) as a white solid.

**$^{1}$H NMR** (400.16 MHz, $CDCl_3$) δ 8.75 (ddd, *J* = 4.8, 1.8, 0.9 Hz, 1H), 8.67 (dt, *J* = 8.0, 1.1 Hz, 1H), 8.57 (d, *J* = 8.6 Hz, 1H), 8.29 (dd, *J* = 8.7, 0.8 Hz, 1H), 8.21 (dd, *J* = 8.6, 1.0 Hz, 1H), 7.87 (dtd, *J* = 8.1, 7.4, 1.6 Hz, 2H), 7.74 (ddd, *J* = 8.4, 6.9, 1.5 Hz, 1H), 7.56 (ddd, *J* = 8.1, 6.9, 1.2 Hz, 1H), 7.37 (ddd, *J* = 7.5, 4.8, 1.2 Hz, 1H).
**$^{13}$C NMR** (100.63 MHz, $CDCl_3$) δ 156.22 (C, Ar), 156.09 (C, Ar), 149.22 (CH, Ar), 147.88 (C, Ar), 137.22 (CH, Ar), 137.12 (CH, Ar), 129.82 (CH, Ar), 129.79 (CH, Ar), 128.36 (C, Ar), 127.75 (CH, Ar), 126.97 (CH, Ar), 124.24 (CH, Ar), 122.08 (CH, Ar), 119.11 (CH, Ar).
**$^{15}$N NMR** (40.55 MHz, $CDCl_3$) δ 299.91, 305.98
**HRMS (ESI).** Calculated for $C_{14}H_{11}N_2^+$: 207.0917 Obtained: 207.0916

USC UNIVERSIDADE DE SANTIAGO DE COMPOSTELA

*10.2.6.20 Preparation of 2-(5-(trifluoromethyl)pyridin-2-yl)quinoline (L35)*



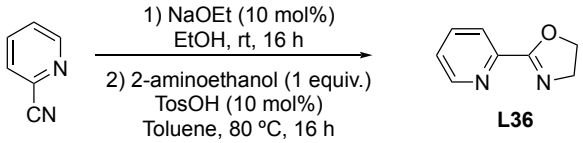

**L35**

Prepared following an adapted procedure:[135] To a solution of *n*BuLi (0.8 mL, 2 mmol, 2 equiv.) in dry THF (5.0 mL) at −78 °C, a solution of 2-bromoquinoline (228.9 mg, 1.1 mmol, 1.1 equiv.) in dry THF (5.0 mL) was added dropwise. The mixture was kept stirring for 30 min at −78 °C and then $ZnCl_2$ (1.0 M in diethyl ether) (2.8 mL, 2.8 mmol, 2.8 equiv.) was added. The temperature was warmed up to 0 °C for 1 h and then to room temperature for 2 h more. After this time, the reaction mixture was cooled again to 0 °C and a solution of 2-bromo-5-(trifluoromethyl)pyridine (226.0 mg, 1 mmol, 1 equiv.) and $Pd(PPh_3)_4$ (57.8 mg, 0.05 mmol, 5 mol%) in dry THF (3.7 mL) was added. After 1 h at 0 °C, the reaction mixture was warmed up and heated at reflux for 16h while observing the formation of a bright yellow precipitate. The solution was cooled to rt, poured into saturated aqueous solution of 1:1 EDTA/$Na_2CO_3$ and stirred for 30 min.

The aqueous suspension was extracted with dichloromethane (3 x 100 mL), the combined organic layers were dried over anhydrous magnesium sulphate and the solvent was evaporated under reduced pressure. The residue was purified by flash colum chromatography on silica gel (Hex/$Et_2O$ 10%) to afford 2-(5-(trifluoromethyl)pyridin-2-yl)quinoline (123 mg, 45% yield) as a white solid.

**$^1$H NMR** (400.16 MHz, $CDCl_3$) δ 8.99 (s, 0H), 8.84 (d, *J* = 8.4 Hz, 1H), 8.61 (d, *J* = 8.6 Hz, 1H), 8.33 (d, *J* = 8.6 Hz, 1H), 8.22 (d, *J* = 8.5 Hz, 1H), 8.10 (dd, *J* = 8.3, 2.5 Hz, 1H), 7.89 (d, *J* = 8.1 Hz, 1H), 7.77 (ddd, *J* = 8.5, 6.8, 1.5 Hz, 1H), 7.60 (ddd, *J* = 8.1, 6.8, 1.2 Hz, 1H).
**$^{13}$C NMR** (100.63 MHz, $CDCl_3$) δ 159.40 (C, Ar), 154.71 (C, Ar), 147.90 (C, Ar), 146.26 (q, *J* = 4.2 Hz, CH, Ar), 137.40 (CH, Ar), 134.19 (q, *J* = 3.5 Hz, CH, Ar), 130.11 (CH, Ar), 129.99 (CH, Ar), 128.73 (C, Ar), 127.84 (CH, Ar), 127.56 (CH, Ar), 126.74 (q, *J* = 33.3 Hz, C, Ar), 123.86 (q, *J* = 272.4 Hz, $CF_3$), 121.65 (CH, Ar), 119.23 (CH, Ar).
**$^{19}$F NMR** (376.46 MHz, $CDCl_3$) δ -62.32.
**HRMS (ESI).** Calculated for $C_{15}H_{10}F_3N_2^+$: 275.0791 Obtained: 275.0788

*10.2.6.21 Preparation of 2-(pyridin-2-yl)-4,5-dihydrooxazole (L36)*




**L36**

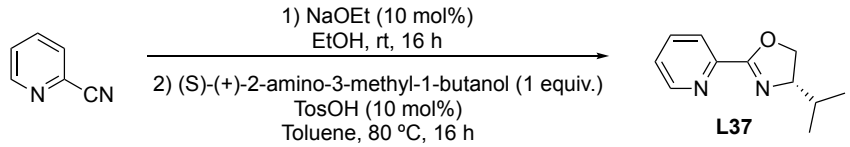
To a solution of pyridine-2-carbonitrile (200 mg, 1.9 mmol, 1 equiv.) in anhydrous ethanol (6.5 mL, 0.3 M), NaOEt (13 mg, 0.2 mmol, 10 mol%) was added in one portion. The reaction mixture was stirred at room temperature overnight. The solvent was removed under vacuum, and the resulting residue was partitioned with ethyl acetate and water.

The combined organic layers were dried over $MgSO_4$, filtered, and concentrated under vacuum.

The crude product was dissolved in toluene (4 mL, 0.5 M), to which 2-aminoethanol (0.1 mL, 1.9 mmol, 1 equiv.) and TosOH (36.5 mg, 0.2 mmol, 10 mol%) were added. The reaction mixture was heated at 80°C overnight. The reaction was quenched with water, and extracted with ethyl acetate. The combined organic layers were dried over $MgSO_4$, filtered, and concentrated under vacuum. The crude product was purified by column chromatography on silica gel (Hex to Hex/EtOAC 2:8) to afford 2-(pyridin-2-yl)-4,5-dihydrooxazole (192 mg, 68% yield).

**$^1$H NMR** (400.16 MHz, $CDCl_3$) δ 8.68 (ddd, *J* = 4.8, 1.8, 0.9 Hz, 1H), 8.02 (dt, *J* = 7.9, 1.1 Hz, 1H), 7.76 (td, *J* = 7.7, 1.8 Hz, 1H), 7.38 (ddd, *J* = 7.6, 4.8, 1.2 Hz, 1H), 4.55 – 4.47 (m, 2H), 4.15 – 4.07 (m, 2H).
**$^{13}$C NMR** (100.63 MHz, $CDCl_3$) δ 163.96 (C, Ar), 149.78 (CH, Ar), 146.77 (C), 136.77 (CH, Ar), 125.66 (CH, Ar), 123.89 (CH, Ar), 68.30 ($CH_2$), 55.18 ($CH_2$).
**$^{15}$N NMR** (40.55 MHz, $CDCl_3$) δ 309.23, 104.36
**HRMS (ESI)**. Calculated for $C_8H_9N_2O^+$: 149.0709 Obtained: 149.0711

### *10.2.6.22 Preparation of (S)-4-isopropyl-2-(pyridin-2-yl)-4,5-dihydrooxazole (L37)*




**L37**

To a solution of pyridine-2-carbonitrile (200 mg, 1.9 mmol, 1 equiv.) in anhydrous ethanol (6.5 mL, 0.3 M), NaOEt (13 mg, 0.2 mmol, 10 mol%) was added in one portion. The reaction mixture was stirred at room temperature overnight. The solvent was removed under vacuum, and the resulting residue was partitioned with ethyl acetate and water. The combined organic layers were dried over $MgSO_4$, filtered, and concentrated under vacuum.

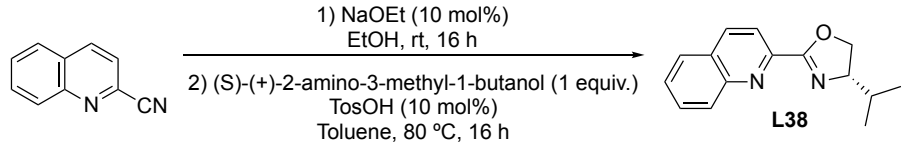
The crude product was dissolved in toluene (4 mL, 0.5 M), to which (S)-(+)-2-Amino-3-methyl-1-butanol (198 mg, 1.9 mmol, 1 equiv.) and TosOH (36.5 mg, 0.2 mmol, 10 mol%) were added. The reaction mixture was heated at 80°C overnight. The reaction was quenched with water, and extracted with ethyl acetate. The combined organic layers were dried over $MgSO_4$, filtered, and concentrated under vacuum. The crude product was purified by column chromatography on silica gel (Hex to Hex/EtOAC 2:8) to afford (S)-4-isopropyl-2-(pyridin-2-yl)-4,5-dihydrooxazole (155 mg, 42% yield).

**$^1$H NMR** (400.16 MHz, $CDCl_3$) δ 8.70 (ddd, *J* = 4.8, 1.8, 0.9 Hz, 1H), 8.05 (dt, *J* = 7.9, 1.1 Hz, 1H), 7.77 (td, *J* = 7.8, 1.8 Hz, 1H), 7.38 (ddd, *J* = 7.6, 4.8, 1.2 Hz, 1H), 4.54 – 4.47 (m, 1H), 4.24 – 4.18 (m, 1H), 4.18 – 4.11 (m, 1H), 1.95 – 1.85 (m, 1H), 1.05 (d, *J* = 6.7 Hz, 3H), 0.94 (d, *J* = 6.8 Hz, 3H).

USC UNIVERSIDADE DE SANTIAGO DE COMPOSTELA

**$^{13}$C NMR** (100.63 MHz, $CDCl_3$) δ 162.68 (C, Ar), 149.84 (CH, Ar), 146.95 (C), 136.74 (CH, Ar), 125.61 (CH, Ar), 124.02 (CH, Ar), 73.03 (CH), 70.88 ($CH_2$), 32.87 (CH), 19.19 ($CH_3$), 18.30 ($CH_3$).
**$^{15}$N NMR** (40.55 MHz, $CDCl_3$) δ 309.04, 151.08
**HRMS (ESI)**. Calculated for $C_{11}H_{15}N_2O^+$: 191.1179 Obtained: 191.1178

### *10.2.6.23 Preparation of (S)-4-isopropyl-2-(quinolin-2-yl)-4,5-dihydrooxazole (L38)*



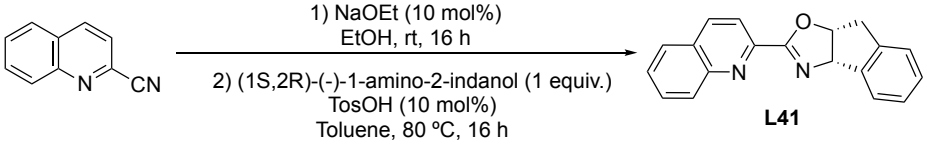
**L38**

To a solution of Quinoline-2-carbonitrile (100 mg, 0.6 mmol, 1 equiv.) in anhydrous ethanol (2.2 mL, 0.3 M), NaOEt (4.4 mg, 0.06 mmol, 10 mol%) was added in one portion. The reaction mixture was stirred at room temperature overnight. The solvent was removed under vacuum, and the resulting residue was partitioned with ethyl acetate and water. The combined organic layers were dried over $MgSO_4$, filtered, and concentrated under vacuum.

The crude product was dissolved in toluene (1.3 mL, 0.5 M), to which (S)-(+)-2-Amino-3-methyl-1-butanol (67 mg, 0.6 mmol, 1 equiv.) and TosOH (12.3 mg, 0.06 mmol, 10 mol%) were added. The reaction mixture was heated at 80°C overnight. The reaction was quenched with water, and extracted with ethyl acetate. The combined organic layers were dried over $MgSO_4$, filtered, and concentrated under vacuum. The crude product was purified by column chromatography on silica gel (Hex to Hex/EtOAC 2:8) to afford (S)-4-isopropyl-2-(quinolin-2-yl)-4,5-dihydrooxazole (86 mg, 55% yield).

**$^{1}$H NMR** (400.16 MHz, $CDCl_3$) δ 8.32 – 8.25 (m, 1H), 8.24 – 8.18 (m, 2H), 7.85 (ddd, *J* = 8.1, 1.5, 0.7 Hz, 1H), 7.75 (ddd, *J* = 8.4, 6.9, 1.5 Hz, 1H), 7.60 (ddd, *J* = 8.1, 6.9, 1.2 Hz, 1H), 4.59 (dd, *J* = 9.7, 8.3 Hz, 1H), 4.31 (t, *J* = 8.3 Hz, 1H), 4.23 (ddd, *J* = 9.7, 8.3, 6.3 Hz, 1H), 1.94 (dq, *J* = 13.4, 6.7 Hz, 1H), 1.08 (d, *J* = 6.7 Hz, 3H), 0.97 (d, *J* = 6.8 Hz, 3H).
**$^{13}$C NMR** (100.63 MHz, $CDCl_3$) δ 162.98 (C, Ar), 147.69 (C, Ar), 147.07 (C, Ar), 136.83 (CH, Ar), 130.50 (CH, Ar), 130.15 (CH, Ar), 128.87 (C), 128.02 (CH, Ar), 127.66 (CH, Ar), 121.01 (CH, Ar), 73.10 (CH), 71.15 ($CH_2$), 32.95 (CH), 19.22 ($CH_3$), 18.34 ($CH_3$).
**HRMS (ESI)**. Calculated for $C_{15}H_{17}N_2O^+$: 241.1335 Obtained: 241.1332

### *10.2.6.24 Preparation of (3aS,8aR)-2-(quinolin-2-yl)-3a,8a-dihydro-8H-indeno[1,2-d]oxazole (L41)*



**L41**

To a solution of quinoline-2-carbonitrile (100 mg, 0.6 mmol, 1 equiv.) in anhydrous ethanol (2.2 mL, 0.3 M), NaOEt (4.4 mg, 0.06 mmol, 10 mol%) was added in one portion.

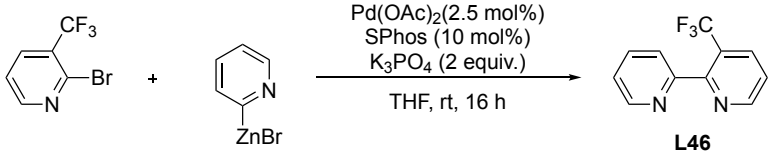
USC UNIVERSIDADE DE SANTIAGO DE COMPOSTELA

The reaction mixture was stirred at room temperature overnight. The solvent was removed under vacuum, and the resulting residue was partitioned with ethyl acetate and water. The combined organic layers were dried over $MgSO_4$, filtered, and concentrated under vacuum.

The crude product was dissolved in toluene (1.3 mL, 0.5 M), to which (1S,2R)-(-)-1-amino-2-indanol (97 mg, 0.6 mmol, 1 equiv.) and TosOH (12.3 mg, 0.06 mmol, 10 mol%) were added. The reaction mixture was heated at 80°C overnight. The reaction was quenched with water, and extracted with ethyl acetate. The combined organic layers were dried over $MgSO_4$, filtered, and concentrated under vacuum. The crude product was purified by column chromatography on silica gel (Hex to Hex/EtOAC 2:8) to afford of (3aS,8aR)-2-(quinolin-2-yl)-3a,8a-dihydro-8H-indeno[1,2-d]oxazole (166 mg, 89% yield).

**$^1$H NMR** (400.16 MHz, $CDCl_3$) δ 8.35 – 8.22 (m, 3H), 7.85 (ddd, *J* = 8.2, 1.5, 0.7 Hz, 1H), 7.76 (ddd, *J* = 8.5, 6.9, 1.5 Hz, 1H), 7.71 (s, 1H), 7.62 (ddd, *J* = 8.1, 6.9, 1.2 Hz, 1H), 7.34 – 7.28 (m, 3H), 5.93 (d, *J* = 8.0 Hz, 1H), 5.76 (dt, *J* = 8.2, 4.2 Hz, 1H), 3.60 (d, *J* = 4.3 Hz, 2H).
**$^{13}$C NMR** (100.63 MHz, $CDCl_3$) δ 164.41, 159.85, 147.71, 139.81, 137.12, 130.56, 130.40, 129.13, 129.08, 128.50, 127.89, 127.73, 126.08, 125.55, 121.40, 39.81.
**HRMS (ESI)**. Calculated for $C_{19}H_{15}N_2O^+$: 287.1179 Obtained: 287.1176

### *10.2.6.25 Preparation of 3-(trifluoromethyl)-2,2'-bipyridine (L46)*



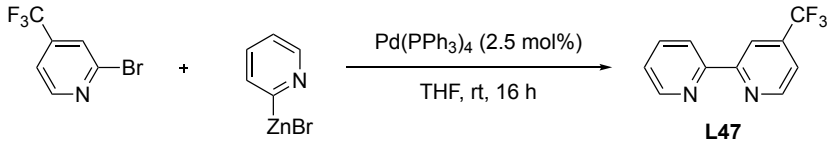

**L46**

Prepared following an adapted procedure:[135] Under a nitrogen atmosphere, $Pd(OAc)_2$ (12.4 mg, 0.05 mmol, 5 mol%), SPhos (45.4 mg, 0.1 mmol, 10 mol%), $K_3PO_4$ (469 mg, 2.2 mmol, 2 equiv.) and 2-bromo-3(trifluoromethyl)pyridine (250 mg, 1.1 mmol, 1 equiv.) were added to a dry two-neck round-bottom flask and cooled to 0 ºC. Upon addition of 2-pyridylzinc bromide (2.7 ml, 1.3 mmol, 1.2 equiv.) in THF (0.5M) the reaction mixture turned brown in color. The mixture was stirred overnight at rt under an inert atmosphere during which time a white precipitate formed. Subsequently, the reaction mixture was poured into saturated aqueous solution of 1:1 EDTA/$Na_2CO_3$ (500 mL), and the mixture was stirred until the white solid turned completely yellow. The aqueous suspension was extracted with dichloromethane (3 x 100 mL), the combined organic layers were dried over anhydrous sodium sulphate and the solvent was evaporated under reduced pressure. The mixture was purified by column chromatography on silica gel (Hex/$Et_2O$ 5%) to afford 3-(trifluoromethyl)-2,2'-bipyridine (202 mg, 81% yield) as a white solid.

USC UNIVERSIDADE DE SANTIAGO DE COMPOSTELA

**$^{1}$H NMR** (400.16 MHz, $CDCl_3$) δ 8.86 (dd, *J* = 4.8, 1.6 Hz, 1H), 8.76 – 8.69 (m, 1H), 8.12 (dd, *J* = 8.0, 1.6 Hz, 1H), 7.83 (td, *J* = 7.7, 1.8 Hz, 1H), 7.71 – 7.64 (m, 1H), 7.48 (ddd, *J* = 8.0, 4.8, 0.9 Hz, 1H), 7.38 (ddd, *J* = 7.6, 4.9, 1.2 Hz, 1H).
**$^{13}$C NMR** (100.63 MHz, $CDCl_3$) δ 156.84 (C, Ar) , 156.55 (C, Ar), 151.93 (CH, Ar), 149.05 (CH, Ar), 136.71 (CH, Ar), 135.42 (q, *J* = 4.9 Hz, CH, Ar), 125.57 (q, *J* = 32.7 Hz, C, Ar), 123.86 (CH, Ar), 123.74 (CH, Ar), 123.57 (q, *J* = 273.3 Hz, $CF_3$), 122.92 (CH, Ar).
**$^{19}$F NMR** (376.46 MHz, $CDCl_3$) δ -57.74.
**HRMS (ESI).** Calculated for $C_{11}H_8F_3N_2^+$: 225.0634 Obtained: 225.0629

### *10.2.6.26 Preparation of 4-(trifluoromethyl)-2,2'-bipyridine (L47)*



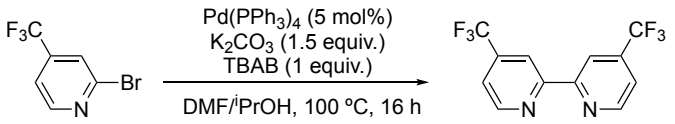
**L47**

Prepared following an adapted procedure:[135] Under a nitrogen atmosphere, $Pd(PPh_3)_4$ (33.6 mg, 0.03 mmol, 2.5 mol%) and 2-bromo-4(trifluoromethyl)pyridine (250 mg, 1.1 mmol, 1 equiv.) were added to a dry two-neck round-bottom flask and cooled to 0 ºC. Upon addition of 2-pyridylzinc bromide (2.7 ml, 1.3 mmol, 1.2 eq) in THF (0.5M) the reaction mixture turned brown in color. The mixture was stirred overnight at rt under an inert atmosphere during which time a white precipitate formed. Subsequently, the reaction mixture was poured into saturated aqueous solution of 1:1 EDTA/$Na_2CO_3$ (500 mL), and the mixture was stirred until the white solid turned completely yellow. The aqueous suspension was extracted with dichloromethane (3 x 100 mL), the combined organic layers were dried over anhydrous sodium sulphate and the solvent was evaporated under reduced pressure. The mixture was purified by column chromatography on silica gel (Hex/$Et_2O$ 5%) to afford 4-(trifluoromethyl)-2,2'-bipyridine (196 mg, 79% yield) as a white solid.

**$^{1}$H NMR** (400.16 MHz, $CDCl_3$) δ 8.85 (d, *J* = 5.0 Hz, 1H), 8.71 (s, 2H), 8.45 (d, *J* = 8.0 Hz, 1H), 7.86 (t, *J* = 7.8 Hz, 1H), 7.53 (d, *J* = 5.0 Hz, 1H), 7.38 (t, *J* = 6.3 Hz, 1H).
**$^{13}$C NMR** (100.63 MHz, $CDCl_3$) δ 157.40(C, Ar), 154.65(C, Ar), 150.24 (CH, Ar), 149.26 (CH, Ar), 139.56 (q, J = 33.5 Hz, C, Ar), 124.74 (CH, Ar), 123.09 (q, J = 273.3 Hz, CF3), 121.62 (CH, Ar), 119.44 (q, J = 3.5 Hz, CH, Ar), 117.27 (q, J = 3.7 Hz, CH, Ar).
**$^{19}$F NMR** (376.46 MHz, $CDCl_3$) δ -64.78.
**$^{15}$N NMR** (40.55 MHz, $CDCl_3$) δ 315.69
**HRMS (ESI).** Calculated for $C_{11}H_8F_3N_2^+$: 225.0634 Obtained: 225.0632

USC UNIVERSIDADE DE SANTIAGO DE COMPOSTELA

*10.2.6.27 Preparation of 4,4'-bis(trifluoromethyl)-2,2'-bipyridine (L48)*



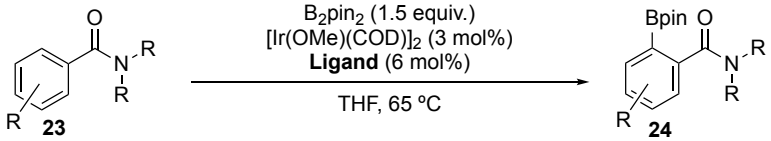

**L48**

To a round-bottom flask charged with a magnetic stir bar were added, $Pd(OAc)_2$ (25 mg, 0.11 mmol, 5 mol%), TBAB (709 mg, 2.2 mmol, 1 eq.) and $K_2CO_3$ (456 mg, 3.3 mmol, 1.5 eq.). The flask was then evacuated and backfilled with $N_2$ three times. To this flask were added 2-bromo-4-(trifluoromethyl)pyridine (497 mg, 2.2 mmol, 1 eq.), $^{i}$PrOH (0.34 mL, 6.5 M) and DMF (7.5 ml, 0.3 M) and the reaction was heated at 100 °C for 24 h.

The reaction mixture was then cooled to room temperature and filtered, washing the solid copiously with EtOAc. The organic liquids were extracted three times with 40 mL of 10% (w/w) aqueous LiCl. The aqueous layer was backwashed once with EtOAc (50 mL) and the combined organic fractions were finally washed with water (40 mL) and brine (40 mL) before drying over $MgSO_4$. Following removal of the solvent in vacuo, the crude residue was purified by silica gel chromatography (gradient from 100% hexane to 5% EtOAc/hexane) to afford 4,4'-bis(trifluoromethyl)-2,2'-bipyridine (292 mg, 90% yield) as a white solid.

**$^{1}$H NMR** (400.16 MHz, $CDCl_3$) δ 8.88 (dt, *J* = 5.0, 0.7 Hz, 1H), 8.76 – 8.70 (m, 1H), 7.58 (ddd, *J* = 5.1, 1.7, 0.8 Hz, 1H).
**$^{13}$C NMR** (100.63 MHz, $CDCl_3$) δ 156.19 (C, Ar), 150.40 (CH, Ar), 139.81 (C, Ar, q, *J* = 34.3 Hz), 122.98 ($CF_3$, q, *J* = 273.3 Hz), 120.08 (CH, Ar, q, *J* = 3.4 Hz), 117.34 (CH, Ar, q, *J* = 3.7 Hz).
**$^{19}$F NMR** (376.46 MHz, $CDCl_3$) δ -64.87.
**$^{15}$N NMR** (40.55 MHz, $CDCl_3$) δ 316.03
**HRMS (ESI)**. Calculated for $C_{12}H_7F_6N_2^+$: 293.0508 Obtained: 293.0508

## 10.2.7 General Procedure for *ortho*-Borylation




**23** **24**

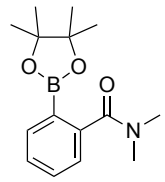
Following an adapted procedure:[149] In a sealed tube $[Ir(COD)(OMe)]_2$ (0.008 mmol, 3 mol%.), $B_2pin_2$ (0.375 mmol, 1.5 equiv.), and ligand (0.015 mmol, 6 mol%) were added. The tube was evacuated and refilled with $N_2$ three times, then under a positive flow of $N_2$, dry THF (1.25 mL) and substrate (0.250 mmol, 1.0 equiv.) were added. The tube was then sealed and heated for the specified time. After that, volatiles were removed under vacuum and $CH_2Br_2$ (internal standard) was added, the yield was determined by $^{1}$H NMR

USC UNIVERSIDADE DE SANTIAGO DE COMPOSTELA

[149] Murphy, J. M.; Liao, X.; Hartwig, J. F. *J. Am. Chem. Soc.* **2007,** *129,* 15434–15435.

spectroscopy. To isolate the product, the solvent was removed under reduced pressure, and the residue was purified by column chromatography on silica gel.

### *10.2.7.1 N,N-dimethyl-2-(4,4,5,5-tetramethyl-1,3,2-dioxaborolan-2-yl)benzamide (24a)*

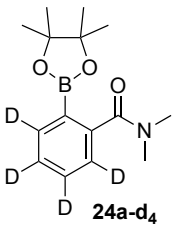


**24a**

Following the general procedure: **23a** (37.3 mg, 0.250 mmol, 1.0 equiv.), $[Ir(COD)(OMe)]_2$ (5 mg, 0.008 mmol, 3 mol%.), $B_2pin_2$ (95.2 mg, 0.375 mmol, 1.5 equiv.), **L27** (3.4 mg, 0.015 mmol, 6 mol%.) in THF (1.25 mL) were heated at 65 °C for 1.5 h. The crude mixture was purified by column chromatography (Hex/EtOAc 20% to Hex/EtOAc 80%) to obtain 57 mg (83% yield) of **24a** as a white solid.

**$^1$H NMR** (400.16 MHz, $CDCl_3$, 258 K) δ 7.76 (dd, J = 6.9, 1.9 Hz, 1H), 7.45 – 7.39 (m, 1H), 7.38 (dd, J = 7.2, 1.5 Hz, 1H), 7.34 (dd, J = 7.2, 1.7 Hz, 1H), 3.14 (s, 3H), 2.92 (s, 3H), 1.28 (s, 12H).
**$^{13}$C NMR** (100.63 MHz, $CDCl_3$, 258 K) δ 172.53 (CO), 140.58 (C, Ar), 134.37 (CH, Ar), 130.63 (CH, Ar), 129.16 (CH, Ar), 125.56 (CH, Ar), 83.02 (C), 39.35 (N–$CH_3$), 36.22 (N–$CH_3$), 24.98 ($CH_3$).
**$^{11}$B NMR** (128.39 MHz, $CDCl_3$, 258K) δ 27.53.
**HRMS (ESI).** Calculated for $C_{15}H_{23}BNO_3^+$: 276.17655 Obtained: 276.17622

### *10.2.7.2 N,N-dimethyl-2-(4,4,5,5-tetramethyl-1,3,2-dioxaborolan-2-yl)benzamide-3,4,5,6-$d_4$ (24a-$d_4$)*



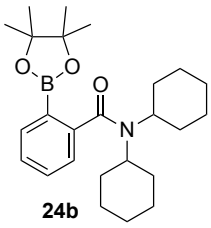
**24a-$d_4$**

Following the general procedure: **23a-$d_5$** (38.6 mg, 0.250 mmol, 1.0 equiv.), $[Ir(COD)(OMe)]_2$ (5 mg, 0.008 mmol, 3 mol%), $B_2pin_2$ (95.2 mg, 0.375 mmol, 1.5 equiv.), **L27** (3.4 mg, 0.015 mmol, 6 mol%) in THF (1.25 mL) were heated at 65 °C for 1.5 h. The crude mixture was purified by column chromatography (Hex/EtOAc 20% to Hex/EtOAc 80%) to obtain 33 mg (48% yield) of **24a-$d_4$** as a white solid.

**$^1$H NMR** (400.16 MHz, $CDCl_3$, 258 K) δ 3.14 (s, 3H), 2.92 (s, 3H), 1.29 (s, 12H).
**$^2$H NMR** (61 MHz, $(CD_3)_2CO$) δ 7.77 (s, 1H), 7.53 (s, 1H), 7.43 (s, 1H), 7.29 (s, 1H).
**$^{13}$C NMR** (100.63 MHz, $CDCl_3$, 258 K) δ 172.54 (CO), 140.51 (C, Ar), 133.96 (CD, Ar, t, *J* = 24.1 Hz), 130.12 (CD, Ar, t, *J* = 24.1, 23.2 Hz), 128.61 (CD, Ar, t, *J* = 23.7, 22.6 Hz), 125.16 (CD, Ar, t, *J* = 24.1, 22.1 Hz), 83.02 (C), 39.34 (N–$CH_3$), 36.19 (N–$CH_3$), 24.98 ($CH_3$).
**$^{11}$B NMR** (128.39 MHz, $CDCl_3$, 258K) δ 27.27.
**HRMS (ESI).** Calculated for $C_{15}H_{19}D_4BNO_3^+$: 280.20166 Obtained: 280.20196

USC UNIVERSIDADE DE SANTIAGO DE COMPOSTELA

### *10.2.7.3 N,N-dicyclohexyl-2-(4,4,5,5-tetramethyl-1,3,2-dioxaborolan-2-yl)benzamide (24b)*

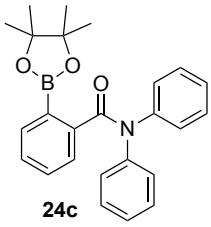


**24b**

Following the general procedure: **23b** (71.4 mg, 0.250 mmol, 1.0 equiv.), $[Ir(COD)(OMe)]_2$ (5 mg, 0.008 mmol, 3 mol%.), $B_2pin_2$ (95.2 mg, 0.375 mmol, 1.5 equiv.), **L27** (3.4 mg, 0.015 mmol, 6 mol%) in THF (1.25 mL) were heated at 65 °C for 24 h. The crude mixture was purified by column chromatography (Hex/EtOAc 20% to Hex/EtOAc 80%) to obtain 100 mg (98% yield) of **24b** as a white solid.

**$^1$H NMR** (400.16 MHz, $CDCl_3$, 258 K) δ 7.74 (d, J = 6.8 Hz, 1H), 7.39 – 7.27 (m, 2H), 7.15 (d, J = 7.2 Hz, 1H), 3.35 (t, J = 12.0 Hz, 1H), 3.01 (t, J = 10.6 Hz, 1H), 2.61 (s, 2H), 1.85 – 1.73 (m, 3H), 1.72 – 1.53 (m, 7H), 1.53 – 1.36 (m, 4H), 1.27 (s, 12H), 1.07 – 0.84 (m, 4H).
**$^{13}$C NMR** (100.63 MHz, $CDCl_3$, 258 K) δ 171.62 (CO), 143.31 (C, Ar), 134.79 (CH, Ar), 130.21 (CH, Ar), 128.06 (CH, Ar), 124.39 (CH, Ar), 83.11 (C), 59.60 (N–CH), 56.28 (N–CH), 30.33 ($CH_2$), 29.57 ($CH_2$), 26.51 ($CH_2$), 25.40 ($CH_2$), 25.21 ($CH_2$), 25.06 ($CH_2$), 24.91 ($CH_3$).
**$^{11}$B NMR** (128.39 MHz, $CDCl_3$, 258K) δ 29.09.
**HRMS (ESI)**. Calculated for $C_{25}H_{38}BNNaO_3^+$: 434.28370 Obtained: 434.28373

### *10.2.7.4 N,N-diphenyl-2-(4,4,5,5-tetramethyl-1,3,2-dioxaborolan-2-yl)benzamide (24c)*

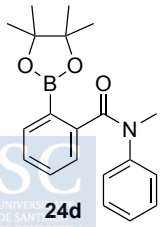


**24c**

Following the general procedure: **23c** (68.3 mg, 0.250 mmol, 1.0 equiv.), $[Ir(COD)(OMe)]_2$ (5 mg, 0.008 mmol, 3 mol%), $B_2pin_2$ (95.2 mg, 0.375 mmol, 1.5 equiv.), **L27** (3.4 mg, 0.015 mmol, 6 mol%) in THF (1.25 mL) were heated at 80 °C for 24 h. The crude mixture was purified by column chromatography (Hex/EtOAc 20% to Hex/EtOAc 80%) to obtain 85 mg (85% yield) of **24c** as an off-white solid.

**$^1$H NMR** (400.16 MHz, $CDCl_3$, 258 K) δ 7.65 – 7.61 (m, 1H), 7.42 (d, *J* = 20.3 Hz, 3H), 7.30 – 7.00 (m, 10H), 1.35 (s, 12H).
**$^{13}$C NMR** (100.63 MHz, $CDCl_3$, 258 K) δ 171.78 (CO), 143.12 (C, Ar), 142.10 (C, Ar), 134.55 (CH, Ar), 129.93 (CH, Ar), 128.98 (CH, Ar), 128.72 (C, Ar), 128.58 (CH, Ar), 127.41 (CH, Ar), 126.86 (CH, Ar), 126.57 (CH, Ar), 83.83 (C), 25.06 ($CH_3$).
**$^{11}$B NMR** (128.39 MHz, $CDCl_3$, 258K) δ 29.57.
**HRMS (ESI)**. Calculated for $C_{25}H_{26}BNNaO_3^+$: 422.18980 Obtained: 422.19019

### *10.2.7.5 N-methyl-N-phenyl-2-(4,4,5,5-tetramethyl-1,3,2-dioxaborolan-2-yl)benzamide (24d)*



**24d**

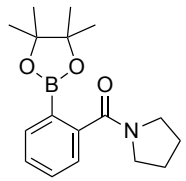
Following the general procedure: **23d** (52.8 mg, 0.250 mmol, 1.0 equiv.), $[Ir(COD)(OMe)]_2$ (5 mg, 0.008 mmol, 3 mol%), $B_2pin_2$ (95.2 mg, 0.375 mmol, 1.5 equiv.), **L27** (3.4 mg, 0.015 mmol, 6 mol%) in THF (1.25 mL) were heated at 65 °C for 1.5 h. The crude mixture was purified by column

USC UNIVERSIDADE DE SANTIAGO DE COMPOSTELA

chromatography (Hex/EtOAc 20% to Hex/EtOAc 80%) to obtain 62 mg (74% yield) of **24d** as a white solid.

**$^1$H NMR** (400.16 MHz, $CDCl_3$, 258 K) δ 7.62 (dt, *J* = 7.3, 1.0 Hz, 1H), 7.49 – 7.43 (m, 3H), 7.31 (td, *J* = 7.3, 0.9 Hz, 1H), 7.24 (dt, *J* = 4.4, 1.5 Hz, 2H), 6.87 (ddd, *J* = 8.5, 7.4, 1.2 Hz, 1H), 5.99 (dd, *J* = 8.1, 1.0 Hz, 1H), 3.61 (s, 3H), 1.36 (s, 12H).
**$^{13}$C NMR** (100.63 MHz, $CDCl_3$, 258 K) δ 171.96 (CO), 141.74 (C, Ar), 134.01 (C, Ar), 132.19 (CH, Ar), 131.08 (CH, Ar), 130.43 (CH, Ar), 129.42 (CH, Ar), 127.64 (CH, Ar), 126.90 (CH, Ar), 126.19 (CH, Ar), 81.08 (C), 41.56 (N–$CH_3$), 25.23 ($CH_3$).
**$^{11}$B NMR** (128.39 MHz, $CDCl_3$, 258K) δ 17.90.
**HRMS (ESI).** Calculated for $C_{20}H_{24}BNNaO_3^+$: 360.17415 Obtained: 360.17532

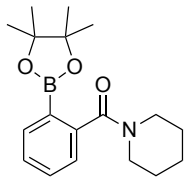
### *10.2.7.6 Pyrrolidin-1-yl(2-(4,4,5,5-tetramethyl-1,3,2-dioxaborolan-2-yl)phenyl)methanone (24e)*


**24e**

Following the general procedure: **23e** (43.8 mg, 0.250 mmol, 1.0 equiv.), $[Ir(COD)(OMe)]_2$ (5 mg, 0.008 mmol, 3 mol%), $B_2pin_2$ (95.2 mg, 0.375 mmol, 1.5 equiv.), **L27** (3.4 mg, 0.015 mmol, 6 mol%) in THF (1.25 mL) were heated at 65 °C for 4 h. The crude mixture was purified by column chromatography (Hex/EtOAc 20% to Hex/EtOAc 80%) to obtain 59 mg (78% yield) of **24e** as a colorless oil.

**$^1$H NMR** (400.16 MHz, $CDCl_3$, 258 K) δ 7.74 (d, *J* = 7.2 Hz, 1H), 7.63 (d, *J* = 7.9 Hz, 1H), 7.53 (td, *J* = 7.3, 0.8 Hz, 1H), 7.34 (td, *J* = 7.6, 1.2 Hz, 1H), 3.93 (q, *J* = 6.5 Hz, 4H), 2.15 (p, *J* = 6.8 Hz, 2H), 1.98 (p, *J* = 6.8 Hz, 2H), 1.35 (s, 12H).
**$^{13}$C NMR** (100.63 MHz, $CDCl_3$, 258 K) δ 170.33 (CO), 133.77 (C, Ar), 133.06 (CH, Ar), 131.41 (CH, Ar), 128.19 (CH, Ar), 125.15 (CH, Ar), 81.07 (C), 50.01 (N–$CH_2$), 48.95 (N–$CH_2$), 26.48 ($CH_2$), 25.19 ($CH_3$), 23.75 ($CH_2$).
**$^{11}$B NMR** (128.39 MHz, $CDCl_3$, 258K) δ 15.39
**HRMS (ESI).** Calculated for $C_{17}H_{24}BNNaO_3^+$: 324.17414 Obtained: 324.17458

### *10.2.7.7 Piperidin-1-yl(2-(4,4,5,5-tetramethyl-1,3,2-dioxaborolan-2-yl)phenyl)methanone (24f)*


**24f**

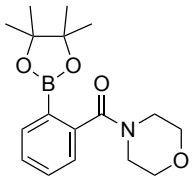
Following the general procedure: **23f** (47.3 mg, 0.250 mmol, 1.0 equiv.), $[Ir(COD)(OMe)]_2$ (5 mg, 0.008 mmol, 3 mol%.), $B_2pin_2$ (95.2 mg, 0.375 mmol, 1.5 equiv.), **L27** (3.4 mg, 0.015 mmol, 6 mol%) in THF (1.25 mL) were heated at 65 °C for 1.5 h. The crude mixture was purified by column chromatography (Hex/EtOAc 20% to Hex/EtOAc 80%) to obtain 75 mg (95% yield) of **24f** as a white solid.

**$^1$H NMR** (400.16 MHz, $CDCl_3$, 258 K) δ 7.78 (dd, *J* = 7.4, 1.3 Hz, 1H), 7.42 (td, *J* = 7.5, 1.4 Hz, 1H), 7.33 (td, *J* = 7.5, 1.1 Hz, 1H), 7.25 – 7.19 (m, 1H), 3.69 (t, *J* = 5.3 Hz, 2H), 3.14 (dd, *J* = 6.6, 4.5 Hz, 2H), 1.73 – 1.56 (m, 4H), 1.52 – 1.40 (m, 2H), 1.28 (s, 12H)

USC UNIVERSIDADE DE SANTIAGO DE COMPOSTELA

**$^{13}$C NMR** (100.63 MHz, $CDCl_3$, 258 K) δ 170.92 (CO), 142.35(C, Ar), 135.32 (CH, Ar), 131.09 (CH, Ar), 128.12 (CH, Ar), 125.36 (CH, Ar), 83.72 (C), 48.33 (N–$CH_2$), 42.85 (N–$CH_2$), 25.57 ($CH_2$), 25.02 ($CH_2$), 24.91 ($CH_3$).
**$^{11}$B NMR** (128.39 MHz, $CDCl_3$) δ 30.25
**HRMS (ESI).** Calculated for $C_{18}H_{26}BNNaO_3^+$: 338.18979 Obtained: 338.18899

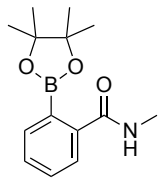
### *10.2.7.8 Morpholino(2-(4,4,5,5-tetramethyl-1,3,2-dioxaborolan-2-yl)phenyl)methanone (24g)*


**24g**

Following the general procedure: **23g** (47.3 mg, 0.250 mmol, 1.0 equiv.), $[Ir(COD)(OMe)]_2$ (5 mg, 0.008 mmol, 3 mol%), $B_2pin_2$ (95.2 mg, 0.375 mmol, 1.5 equiv.), **L27** (3.4 mg, 0.015 mmol, 6 mol%) in THF (1.25 mL) were heated at 65 °C for 1.5 h. The crude mixture was purified by column chromatography (Hex/EtOAc 20% to Hex/EtOAc 80%) to obtain 66 mg (83% yield) of **24g** as a white solid.

**$^{1}$H NMR** (400.16 MHz, $CDCl_3$, 258 K) δ 7.78 (dd, *J* = 7.4, 1.3 Hz, 1H), 7.45 (td, *J* = 7.6, 1.4 Hz, 1H), 7.34 (td, *J* = 7.5, 1.2 Hz, 1H), 7.22 (dt, *J* = 7.5, 1.0 Hz, 1H), 3.77 (s, 4H), 3.57 (dd, *J* = 5.6, 4.1 Hz, 2H), 3.17 (dd, *J* = 5.5, 4.1 Hz, 2H), 1.29 (s, 12H).
**$^{13}$C NMR** (100.63 MHz, $CDCl_3$, 258 K) δ 171.30 (CO), 142.02 (C, Ar), 135.60 (CH, Ar), 131.42 (CH, Ar), 128.21 (CH, Ar), 125.37 (CH, Ar), 84.02 (C), 66.37 (O–$CH_2$), 66.28 (O–$CH_2$), 47.46 (N–$CH_2$), 41.87 (N–$CH_2$), 24.92 ($CH_3$).
**$^{11}$B NMR** (128.39 MHz, $CDCl_3$, 258 K) δ 29.64
**HRMS (ESI).** Calculated for $C_{17}H_{24}BNNaO_4^+$: 340.16906 Obtained: 340.16827

### *10.2.7.9 N-methyl-2-(4,4,5,5-tetramethyl-1,3,2-dioxaborolan-2-yl)benzamide (24h)*

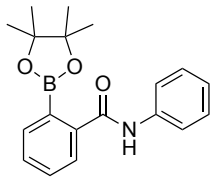

**24h**

Following the general procedure: **23h** (33.8 mg, 0.250 mmol, 1.0 equiv.), $[Ir(COD)(OMe)]_2$ (5 mg, 0.008 mmol, 3 mol%), $B_2pin_2$ (95.2 mg, 0.375 mmol, 1.5 equiv.), **L27** (3.4 mg, 0.015 mmol, 6 mol%) in THF (1.25 mL) were heated at 80 °C for 4 h. The crude mixture was purified by column chromatography (Hex/EtOAc 20% to Hex/EtOAc 80%) to obtain 57 mg (87% yield) of **24h** as a white solid.

**$^{1}$H NMR** (400.16 MHz, $CDCl_3$, 258 K) δ 10.41 (s, 1H), 7.83 (d, *J* = 7.8 Hz, 1H), 7.61 (d, *J* = 7.2 Hz, 1H), 7.41 (td, *J* = 7.3, 0.8 Hz, 1H), 7.12 (td, *J* = 7.5, 1.1 Hz, 1H), 2.38 (d, *J* = 4.6 Hz, 3H), 1.33 (s, 12H).
**$^{13}$C NMR** (100.63 MHz, $CDCl_3$, 258 K) δ 172.48 (CO), 133.04 (CH, Ar), 132.43 (C, Ar), 129.89 (CH, Ar), 127.35 (CH, Ar), 123.39 (CH, Ar), 80.78 (C), 27.26 (N–$CH_3$), 25.28 ($CH_3$).
**$^{11}$B NMR** (128.39 MHz, $CDCl_3$, 258 K) δ 15.30
**HRMS (ESI)**. Calculated for $C_{14}H_{20}BNNaO_3^+$: 284.14284 Obtained: 284.14315

USC UNIVERSIDADE DE SANTIAGO DE COMPOSTELA

*10.2.7.10 N-phenyl-2-(4,4,5,5-tetramethyl-1,3,2-dioxaborolan-2-yl)benzamide (24i)*

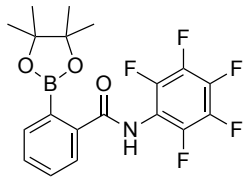


**24i**

Following the general procedure: **23i** (49.3 mg, 0.250 mmol, 1.0 equiv.), $[Ir(COD)(OMe)]_2$ (5 mg, 0.008 mmol, 3 mol%), $B_2pin_2$ (95.2 mg, 0.375 mmol, 1.5 equiv.), **L27** (3.4 mg, 0.015 mmol, 6 mol%) in THF (1.25 mL) were heated at 80 °C for 24 h. The crude mixture was purified by column chromatography (Hex/EtOAc 20% to Hex/EtOAc 80%) to obtain 67 mg (83% yield) of **24i** as an off-white solid.

**$^1$H NMR** (400.16 MHz, $CDCl_3$, 258 K) δ 10.50 (s, 1H), 8.61 (d, *J* = 8.4 Hz, 1H), 8.07 – 7.95 (m, 2H), 7.84 – 7.72 (m, 1H), 7.59 – 7.42 (m, 4H), 7.09 (t, *J* = 7.3 Hz, 1H), 1.41 (s, 12H).
**$^{13}$C NMR** (100.63 MHz, $CDCl_3$, 258 K) δ 165.36 (CO), 144.24 (C, Ar), 136.02 (CH, Ar), 134.54 (C, Ar), 132.78 (CH, Ar), 131.98 (CH, Ar), 128.60 (CH, Ar), 127.37 (CH, Ar), 123.46 (CH, Ar), 118.85 (CH, Ar), 84.32 (C), 25.13 ($CH_3$).
**$^{11}$B NMR** (128.39 MHz, $CDCl_3$, 258 K) δ 29.87
**HRMS (ESI)**. Calculated for $C_{19}H_{22}BNNaO_3^+$: 346.15849 Obtained: 346.15904

*10.2.7.11 N-(perfluorophenyl)-2-(4,4,5,5-tetramethyl-1,3,2-dioxaborolan-2-yl)benzamide (24j)*



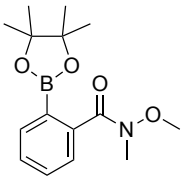
**24j**

Following the general procedure: **23j** (71.8 mg, 0.250 mmol, 1.0 equiv.), $[Ir(COD)(OMe)]_2$ (5 mg, 0.008 mmol, 3 mol%), $B_2pin_2$ (95.2 mg, 0.375 mmol, 1.5 equiv.), **L27** (3.4 mg, 0.015 mmol, 6 mol%) in THF (1.25 mL) were heated at 80 °C for 24 h. The crude mixture was purified by column chromatography (Hex/EtOAc 20% to Hex/EtOAc 80%) to obtain 42 mg (41% yield) of **24j** as a off-white solid.

**$^1$H NMR** (400.16 MHz, $CDCl_3$, 258 K) δ 8.76 (s, 1H), 7.87 (dd, *J* = 7.8, 1.2 Hz, 1H), 7.68 (dd, *J* = 7.2, 1.5 Hz, 1H), 7.50 (dtd, *J* = 19.4, 7.4, 1.4 Hz, 2H), 1.34 (s, 12H).
**$^{13}$C NMR** (100.63 MHz, $CDCl_3$, 258 K) δ 167.26 (CO), 144.40 – 143.96 (CF, Ar, m), 141.68 (CF, Ar, h, *J* = 4.5 Hz), 141.40 – 140.90 (CF, Ar, m), 139.37 – 138.24 (CF, Ar, m), 136.76 (C, Ar), 136.68 – 135.98 (CF, Ar, m), 134.17 (CH, Ar), 131.46 (CH, Ar), 130.12 (CH, Ar), 127.53 (CH, Ar), 112.04 (CF, Ar, td, *J* = 14.6, 14.2, 3.8 Hz), 84.62 (C), 24.71 ($CH_3$).
**$^{11}$B NMR** (128.39 MHz, $CDCl_3$, 258 K) δ 31.34.
**$^{19}$F NMR** (376.46 MHz, $CDCl_3$, 258 K) δ -144.06 – -144.21 (m), -157.18 (t, *J* = 21.5 Hz), -162.58 (dd, *J* = 21.6, 16.2 Hz).
**HRMS (ESI)**. Calculated for $C_{19}H_{17}BF_5NNaO_3^+$: 436.11139 Obtained: 436.11185

USC UNIVERSIDADE DE SANTIAGO DE COMPOSTELA

### *10.2.7.12 N-methoxy-N-methyl-2-(4,4,5,5-tetramethyl-1,3,2-dioxaborolan-2-yl)benzamide (24k)*

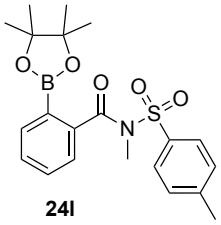


**24k**

Following the general procedure: **23k** (41.3 mg, 0.250 mmol, 1.0 equiv.), $[Ir(COD)(OMe)]_2$ (5 mg, 0.008 mmol, 3 mol%), $B_2pin_2$ (95.2 mg, 0.375 mmol, 1.5 equiv.), **L27** (3.4 mg, 0.015 mmol, 6 mol%) in THF (1.25 mL) were heated at 65 °C for 2 h. The crude mixture was purified by column chromatography (Hex/EtOAc 50% to EtOAc) to obtain 60 mg (83% yield) of **24k** as an off-white solid.

**$^1$H NMR** (400.16 MHz, $CDCl_3$, 258 K) δ 7.71 (dd, *J* = 12.4, 7.4 Hz, 2H), 7.48 (t, *J* = 7.4 Hz, 1H), 7.42 (d, *J* = 7.5 Hz, 1H), 3.58 (s, 3H), 3.47 (s, 3H), 1.33 (s, 12H).
**$^{13}$C NMR** (100.63 MHz, $CDCl_3$, 258 K) δ 171.48 (CO), 135.77 (C, Ar), 132.37 (CH, Ar), 131.37 (CH, Ar), 129.60 (CH, Ar), 126.72 (CH, Ar), 82.37 (C), 61.50 (N–$CH_3$), 34.40 (O–$CH_3$), 25.15 ($CH_3$).
**$^{11}$B NMR** (128.39 MHz, $CDCl_3$, 258 K) δ 21.76
**HRMS (ESI).** Calculated for $C_{15}H_{22}BNNaO_4^+$: 314.15341 Obtained: 314.15358

### *10.2.7.13 N-methyl-2-(4,4,5,5-tetramethyl-1,3,2-dioxaborolan-2-yl)-N-tosylbenzamide (24l)*

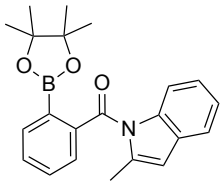


**24l**

Following the general procedure: **23l** (72.3 mg, 0.250 mmol, 1.0 equiv.), $[Ir(COD)(OMe)]_2$ (5 mg, 0.008 mmol, 3 mol%), $B_2pin_2$ (95.2 mg, 0.375 mmol, 1.5 equiv.), **L27** (3.4 mg, 0.015 mmol, 6 mol%) in THF (1.25 mL) were heated at 65 °C for 24 h. The crude mixture was purified by column chromatography (Hex/EtOAc 20% to Hex/EtOAc 80%) to obtain 78 mg (75% yield) of **24l** as a white solid.

**$^1$H NMR** (400.16 MHz, $CDCl_3$, 258 K) δ 7.73 – 7.71 (m, 1H), 7.69 (d, *J* = 8.4 Hz, 2H), 7.40 – 7.34 (m, 2H), 7.23 (dd, *J* = 7.9, 1.8 Hz, 2H), 7.17 – 7.12 (m, 1H), 3.20 (s, 3H), 2.37 (s, 3H), 1.15 (s, 12H).
**$^{13}$C NMR** (100.63 MHz, $CDCl_3$, 258 K) δ 171.80 (CO), 144.72 (C, Ar), 141.38 (C, Ar), 135.57 (C, Ar), 134.82 (CH, Ar), 130.56 (CH, Ar), 129.49 (CH, Ar), 129.24 (CH, Ar), 128.33 (CH, Ar), 126.16 (CH, Ar), 84.22 (C), 34.63 (N–$CH_3$), 24.61 ($CH_3$), 21.76 ($CH_3$).
**$^{11}$B NMR** (128.39 MHz, $CDCl_3$, 258 K) δ 31.30.
**HRMS (ESI).** Calculated for $C_{21}H_{26}BNNaO_5S^+$: 438.15170 Obtained: 438.15231

### *10.2.7.14 (2-methyl-1H-indol-1-yl)(2-(4,4,5,5-tetramethyl-1,3,2-dioxaborolan-2-yl)phenyl)methanone (24m)*



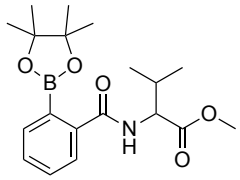
**24m**

Following the general procedure: **23m** (58.8 mg, 0.250 mmol, 1.0 equiv.), $[Ir(COD)(OMe)]_2$ (5 mg, 0.008 mmol, 3 mol%), $B_2pin_2$ (95.2 mg, 0.375 mmol, 1.5 equiv.), **L27** (3.4 mg, 0.015 mmol, 6 mol%) in THF (1.25 mL) were heated at 65 °C for 24 h. The crude mixture was purified by column chromatography (Hex/EtOAc 20% to Hex/EtOAc 80%) to obtain 66 mg (73% yield) of **24m** as a white solid.

USC UNIVERSIDADE DE SANTIAGO DE COMPOSTELA

**$^{1}$H NMR** (400.16 MHz, $CDCl_3$, 258 K) δ 7.83 (ddd, *J* = 7.2, 1.4, 0.8 Hz, 1H), 7.67 – 7.54 (m, 3H), 7.39 (ddd, *J* = 7.8, 1.3, 0.7 Hz, 1H), 7.12 – 7.07 (m, 1H), 6.96 (ddd, *J* = 8.5, 7.2, 1.3 Hz, 1H), 6.75 (dd, *J* = 8.4, 0.9 Hz, 1H), 6.40 – 6.35 (m, 1H), 2.35 (d, *J* = 1.2 Hz, 3H), 1.00 (s, 6H), 0.88 (s, 6H).
**$^{13}$C NMR** (100.63 MHz, $CDCl_3$, 258 K) δ 171.18 (CO), 142.19 (C, Ar), 138.70 (C, Ar), 136.85 (C, Ar), 135.18 (CH, Ar), 131.51 (CH, Ar), 130.44 (CH, Ar), 129.70 (C, Ar), 128.05 (CH, Ar), 122.87 (CH, Ar), 122.70 (CH, Ar), 119.43 (CH, Ar), 114.88 (CH, Ar), 108.99 (CH, Ar), 84.01 (C), 24.40 ($CH_3$), 24.19 ($CH_3$), 16.72 ($CH_3$).
**$^{11}$B NMR** (128.39 MHz, $CDCl_3$, 258 K) δ 31.05
**HRMS (ESI).** Calculated for $C_{22}H_{24}BNNaO_3^+$: 384.17415 Obtained: 384.17497

### *10.2.7.15 Methyl (2-(4,4,5,5-tetramethyl-1,3,2-dioxaborolan-2-yl)benzoyl)valinate (24n)*

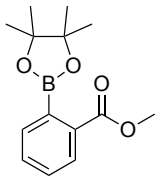


**24n**

Following the general procedure: **23n** (58.8 mg, 0.250 mmol, 1.0 equiv.), $[Ir(COD)(OMe)]_2$ (5 mg, 0.008 mmol, 3 mol%), $B_2pin_2$ (95.2 mg, 0.375 mmol, 1.5 equiv.), **L27** (3.4 mg, 0.015 mmol, 6 mol%) in THF (1.25 mL) were heated at 80 °C for 24 h. The crude mixture was purified by column chromatography (Hex/EtOAc 20% to Hex/EtOAc 80%) to obtain 51 mg (57% yield) of **24n** as a white solid.

**$^{1}$H NMR** (400.16 MHz, $CDCl_3$, 258 K) δ 7.60 (d, *J* = 6.8 Hz, 2H), 7.49 (t, *J* = 7.3 Hz, 1H), 7.37 (t, *J* = 7.4 Hz, 1H), 7.11 (d, *J* = 8.6 Hz, 1H), 4.82 (dd, *J* = 8.5, 4.4 Hz, 1H), 3.77 (s, 3H), 2.35 – 2.20 (m, 1H), 1.35 (s, 6H), 1.34 (s, 6H), 0.95 (dd, *J* = 17.2, 6.7 Hz, 6H).
**$^{13}$C NMR** (100.63 MHz, $CDCl_3$, 258 K) δ172.34 (CO), 169.62 (CO), 135.65 (C, Ar), 132.15 (CH, Ar), 131.95 (CH, Ar), 128.69 (CH, Ar), 123.56 (CH, Ar), 82.75 (C), 58.10 (N–CH), 52.76 (O–$CH_3$), 31.85 ($\underline{CH}$–$(CH_3)_2$), 25.12 ($CH_3$), 24.74 ($CH_3$), 19.09 (CH–$(\underline{CH_3})_2$), 17.98 (CH–$(\underline{CH_3})_2$).
**$^{11}$B NMR** (128.39 MHz, $CDCl_3$, 258 K) δ 22.33.
**HRMS (ESI).** Calculated for $C_{19}H_{28}BNNaO_5^+$: 384.19527 Obtained: 384.19530

### *10.2.7.16 Methyl 2-(4,4,5,5-tetramethyl-1,3,2-dioxaborolan-2-yl)benzoate (24o)*

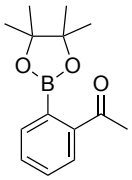


**24o**

Following the general procedure: **23o** (34.0 mg, 0.250 mmol, 1.0 equiv.), $[Ir(COD)(OMe)]_2$ (5 mg, 0.008 mmol, 3 mol%), $B_2pin_2$ (95.2 mg, 0.375 mmol, 1.5 equiv.), **L28** (4.4 mg, 0.015 mmol, 0.06 equiv.) in THF (1.25 mL) were heated at 100 °C for 1 h. The crude mixture was purified by column chromatography (Hex/EtOAc 20% to Hex/EtOAc 80%) to obtain 42 mg (64% yield) of **24o** as a colorless oil.

**$^{1}$H NMR** (400.16 MHz, $CDCl_3$, 258 K) δ 7.94 (ddd, *J* = 7.8, 1.2, 0.7 Hz, 1H), 7.58 – 7.45 (m, 2H), 7.42 (ddd, *J* = 7.8, 7.1, 1.7 Hz, 1H), 3.91 (s, 3H), 1.42 (s, 12H).
**$^{13}$C NMR** (100.63 MHz, $CDCl_3$, 258 K) δ 168.63 (CO), 132.85 (C, Ar), 132.14 (CH, Ar), 131.99 (CH, Ar), 129.08 (CH, Ar), 128.77 (CH, Ar), 84.15 (C), 52.66 (O–$CH_3$), 24.88 ($CH_3$).
**$^{11}$B NMR** (128.39 MHz, $CDCl_3$, 258 K) δ 32.14.
**HRMS (ESI).** Calculated for $C_{14}H_{19}BNaO_4^+$: 285.12686 Obtained: 285.12736

*10.2.7.17 1-(2-(4,4,5,5-tetramethyl-1,3,2-dioxaborolan-2-yl)phenyl)ethan-1-one (24p)*

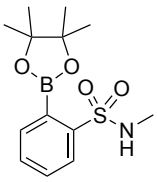


**24p**

Following the general procedure: **23p** (30.0 mg, 0.250 mmol, 1.0 equiv.), $[Ir(COD)(OMe)]_2$ (5 mg, 0.008 mmol, 3 mol%), $B_2pin_2$ (95.2 mg, 0.375 mmol, 1.5 equiv.), **L27** (3.4 mg, 0.015 mmol, 6 mol%) in THF (1.25 mL) were heated at 80 °C for 1.5 h. The crude mixture was purified by column chromatography (Hex to Hex/EtOAc 40%) to obtain 50 mg (81% yield) of **24p** as a colorless oil.

**$^1$H NMR** (400.16 MHz, $CDCl_3$, 258 K) δ 7.85 (dd, *J* = 7.8, 0.7 Hz, 1H), 7.60 – 7.49 (m, 2H), 7.44 (ddd, *J* = 7.8, 7.1, 1.6 Hz, 1H), 2.62 (s, 3H), 1.44 (s, 12H).
**$^{13}$C NMR** (100.63 MHz, $CDCl_3$, 258 K) δ 200.26 (CO), 139.97 (C, Ar), 132.86 (CH, Ar), 132.07 (CH, Ar), 129.04 (CH, Ar), 128.73 (CH, Ar), 83.79 (C), 25.64 ($CH_3$), 24.94 ($CH_3$).
**$^{11}$B NMR** (128.39 MHz, $CDCl_3$, 258 K) δ 31.81
**HRMS (ESI).** Calculated for $C_{14}H_{19}BNaO_3^+$: 269.13195 Obtained: 269.13216

*10.2.7.18 N,4-dimethyl-2-(4,4,5,5-tetramethyl-1,3,2-dioxaborolan-2-yl)benzenesulfonamide (24q)*

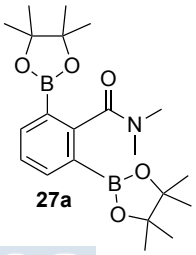


**24q**

Following the general procedure: **23q** (46.3 mg, 0.250 mmol, 1.0 equiv.), $[Ir(COD)(OMe)]_2$ (5 mg, 0.008 mmol, 3 mol%), $B_2pin_2$ (95.2 mg, 0.375 mmol, 1.5 equiv.), **L27** (3.4 mg, 0.015 mmol, 6 mol%) in THF (1.25 mL) were heated at 65 °C for 24 h. The crude mixture was purified by column chromatography (Hex/EtOAc 20% to Hex/EtOAc 80%) to obtain 77 mg (99% yield) of **24q** as a white solid.

**$^1$H NMR** (400.16 MHz, $CDCl_3$, 258 K) δ 7.82 (d, J = 7.9 Hz, 1H), 7.55 (d, J = 1.8 Hz, 1H), 7.31 (ddd, J = 7.9, 1.9, 0.9 Hz, 1H), 5.78 (q, J = 5.4 Hz, 1H), 2.55 (d, J = 5.4 Hz, 3H), 2.39 (s, 3H), 1.38 (s, 12H).
**$^{13}$C NMR** (100.63 MHz, $CDCl_3$, 258 K) δ 142.34 (C, Ar), 138.84 (C, Ar), 136.21 (CH, Ar), 130.63 (CH, Ar), 128.87 (CH, Ar), 85.22 (C), 29.69 (N–$CH_3$), 24.72 ($CH_3$), 21.43 (Ar–$CH_3$).
**$^{11}$B NMR** (128.39 MHz, $CDCl_3$, 258 K) δ 31.79
**HRMS (ESI).** Calculated for $C_{14}H_{22}BNNaO_4S^+$: 334.12548 Obtained: 334.12569

*10.2.7.19 N,N-dimethyl-2,6-bis(4,4,5,5-tetramethyl-1,3,2-dioxaborolan-2-yl)benzamide (27a)*



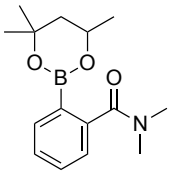
**27a**

Following the general procedure: **23a** (37.3 mg, 0.250 mmol, 1.0 equiv.), $[Ir(COD)(OMe)]_2$ (5 mg, 0.008 mmol, 3 mol%), $B_2pin_2$ (158.7 mg, 0.375 mmol, 1.5 equiv.), **L28** (4.4 mg, 0.015 mmol, 0.06 equiv.) in THF (1.25 mL) were heated at 65 °C for 1.5 h. The crude mixture was purified by column chromatography (Hex/EtOAc 20% to Hex/EtOAc 80%) to obtain 99 mg (99% yield) of **27a** as a white solid.

USC UNIVERSIDADE DE SANTIAGO DE COMPOSTELA

**$^1$H NMR** (400.16 MHz, $CDCl_3$, 258 K) δ 7.82 (d, *J* = 7.5 Hz, 2H), 7.30 (t, *J* = 7.5 Hz, 1H), 3.02 (s, 3H), 2.69 (s, 3H), 1.26 (s, 24H).
**$^{13}$C NMR** (100.63 MHz, $CDCl_3$, 258 K) δ 172.18 (CO), 149.10 (C, Ar), 137.92 (CH, Ar), 126.83 (CH, Ar), 125.41 (CB, Ar), 83.73 (C), 38.91 (N–$CH_3$), 34.43 (N–$CH_3$), 24.81 ($CH_3$).
**$^{11}$B NMR** (128.39 MHz, $CDCl_3$, 258 K) δ 31.65
**HRMS (ESI).** Calculated for $C_{21}H_{33}B_2NNaO_5^+$: 424.2444 Obtained: 424.2444

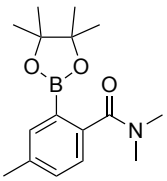
### *10.2.7.20 N,N-dimethyl-2-(4,4,6-trimethyl-1,3,2-dioxaborinan-2-yl)benzamide (29a)*


**29a**

Following the general procedure: **23a** (37.3 mg, 0.250 mmol, 1.0 equiv.), $[Ir(COD)(OMe)]_2$ (5 mg, 0.008 mmol, 3 mol%), $B_2hex_2$ (95.2 mg, 0.375 mmol, 1.5 equiv.), **L27** (3.4 mg, 0.015 mmol, 6 mol%) in THF (1.25 mL) were heated at 65 °C for 24 h. The crude mixture was purified by column chromatography (Hex/EtOAc 20% to Hex/EtOAc 80%) to obtain 62 mg (91% yield) of **29a** as a white solid.

**$^1$H NMR** (400.16 MHz, $CDCl_3$, 258 K) δ 7.81 (ddd, *J* = 7.4, 1.5, 0.6 Hz, 1H), 7.40 (td, *J* = 7.5, 1.5 Hz, 1H), 7.32 (td, *J* = 7.5, 1.3 Hz, 1H), 7.18 (ddd, *J* = 7.5, 1.3, 0.6 Hz, 1H), 4.30 (dqd, *J* = 12.1, 6.1, 2.8 Hz, 1H), 3.09 (s, 3H), 2.76 (s, 3H), 1.84 (dd, *J* = 13.9, 2.9 Hz, 1H), 1.56 (dd, *J* = 14.0, 11.6 Hz, 1H), 1.32 (s, 6H), 1.28 (d, *J* = 6.1 Hz, 3H).
**$^{13}$C NMR** (100.63 MHz, $CDCl_3$, 258 K) δ 173.59 (CO), 142.45 (C, Ar), 134.64 (CH, Ar), 130.47 (CH, Ar), 127.73 (CH, Ar), 125.52 (CH, Ar), 71.26 (C), 65.11 (CH), 45.55 ($CH_2$), 39.10 (N–$CH_3$), 34.76 (N–$CH_3$), 31.31 ($CH_3$), 28.17 ($CH_3$), 23.33 ($CH_3$).
**$^{11}$B NMR** (128.39 MHz, $CDCl_3$, 258 K) δ 27.15
**HRMS (ESI).** Calculated for $C_{15}H_{22}BNNaO_3^+$: 298.15849 Obtained: 298.15900

### *10.2.7.21 N,N,4-trimethyl-2-(4,4,5,5-tetramethyl-1,3,2-dioxaborolan-2-yl)benzamide (24aa)*

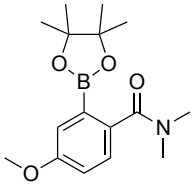

**24aa**

Following the general procedure: **23aa** (40.8 mg, 0.250 mmol, 1.0 equiv.), $[Ir(COD)(OMe)]_2$ (5 mg, 0.008 mmol, 3 mol%), $B_2pin_2$ (95.2 mg, 0.375 mmol, 1.5 equiv.), **L27** (3.4 mg, 0.015 mmol, 6 mol%) in THF (1.25 mL) were heated at 65 °C for 2 h. The crude mixture was purified by column chromatography (Hex/EtOAc 20% to Hex/EtOAc 80%) to obtain 58 mg (80% yield) of **24aa** as a white solid.

**$^1$H NMR** (400.16 MHz, $CDCl_3$, 258 K) δ 7.54 (s, 1H), 7.31 (d, *J* = 7.9 Hz, 1H), 7.15 (dd, *J* = 8.1, 1.8 Hz, 1H), 3.17 (s, 3H), 3.05 (s, 3H), 2.31 (s, 3H), 1.28 (s, 12H).
**$^{13}$C NMR** (100.63 MHz, $CDCl_3$, 258 K) δ 172.56 (CO), 140.33 (C, Ar), 135.65 (C, Ar), 133.97 (CH, Ar), 130.50 (CH, Ar), 125.58 (CH, Ar), 82.14 (C), 39.44 (N–$CH_3$), 37.32 (N–$CH_3$), 25.05 ($CH_3$), 21.41 ($CH_3$).
**$^{11}$B NMR** (128.39 MHz, $CDCl_3$, 258 K) δ 23.55.
**HRMS (ESI)**. Calculated for $C_{16}H_{24}BNNaO_3^+$: 312.17414 Obtained: 312.17414

USC UNIVERSIDADE DE SANTIAGO DE COMPOSTELA

### *10.2.7.22 4-methoxy-N,N-dimethyl-2-(4,4,5,5-tetramethyl-1,3,2-dioxaborolan-2-yl)benzamide (24ab)*

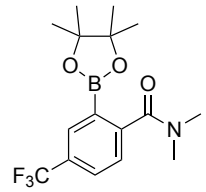


**24ab**

Following the general procedure: **23ab** (44.8 mg, 0.250 mmol, 1.0 equiv.), $[Ir(COD)(OMe)]_2$ (5 mg, 0.008 mmol, 3 mol%), $B_2pin_2$ (95.2 mg, 0.375 mmol, 1.5 equiv.), **L27** (3.4 mg, 0.015 mmol, 6 mol%) in THF (1.25 mL) were heated at 65 °C for 1.25 h. The crude mixture was purified by column chromatography (Hex/EtOAc 20% to EtOAc) to obtain 52 mg (69% yield) of **24ab** as a yellowish solid.

**$^1$H NMR** (400.16 MHz, $CDCl_3$, 258 K) δ 7.53 (d, *J* = 8.7 Hz, 1H), 7.17 (d, *J* = 2.6 Hz, 1H), 6.76 (dd, *J* = 8.7, 2.5 Hz, 1H), 3.83 (s, 3H), 3.36 (s, 3H), 3.30 (s, 3H), 1.29 (s, 12H).
**$^{13}$C NMR** (100.63 MHz, $CDCl_3$, 258 K) δ 171.95 (CO), 162.79 (CO, Ar), 127.54 (CH, Ar), 125.89 (C, Ar), 115.54 (CH, Ar), 114.13 (CH, Ar), 80.57 (C), 55.31 (O–$CH_3$), 39.86 (N–$CH_3$), 25.26 ($CH_3$).
**$^{11}$B NMR** (128.39 MHz, $CDCl_3$, 258 K) δ 15.38.
**HRMS (ESI)**. Calculated for $C_{16}H_{24}BNNaO_4^+$: 328.16906 Obtained: 328.16902

### *10.2.7.23 N,N-dimethyl-2-(4,4,5,5-tetramethyl-1,3,2-dioxaborolan-2-yl)-4-(trifluoromethyl)benzamide (24ac)*

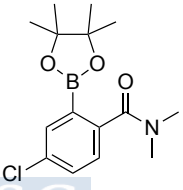


**24ac**

Following the general procedure: **23ac** (54.3 mg, 0.250 mmol, 1.0 equiv.), $[Ir(COD)(OMe)]_2$ (5 mg, 0.008 mmol, 3 mol%), $B_2pin_2$ (95.2 mg, 0.375 mmol, 1.5 equiv.), **L27** (3.4 mg, 0.015 mmol, 6 mol%) in THF (1.25 mL) were heated at 65 °C for 1 h. The crude mixture was purified by column chromatography (Hex/EtOAc 20% to Hex/EtOAc 80%) to obtain 51 mg (60% yield) of **24ac** as a white solid.

**$^1$H NMR** (400.16 MHz, $CDCl_3$, 258 K) δ 8.04 (d, *J* = 1.8 Hz, 1H), 7.69 (ddd, *J* = 8.0, 1.9, 0.8 Hz, 1H), 7.43 (dt, *J* = 8.0, 0.7 Hz, 1H), 3.12 (s, 3H), 2.85 (s, 3H), 1.30 (s, 12H).
**$^{13}$C NMR** (100.63 MHz, $CDCl_3$, 258 K) δ 171.24 (CO), 145.19 (C, Ar), 131.76 (CH, Ar, q, *J* = 3.7 Hz), 130.38 (C, Ar, q, *J* = 32.5 Hz), 127.89 (CH, Ar, q, *J* = 3.7 Hz), 125.99 (CH, Ar), 123.72 ($CF_3$, q, *J* = 271.8 Hz), 83.92 (C), 39.17 (N–$CH_3$), 35.55 (N–$CH_3$), 24.96 ($CH_3$).
**$^{11}$B NMR** (128.39 MHz, $CDCl_3$, 258 K) δ 28.89
**$^{19}$F NMR** (376.46 MHz, $CDCl_3$, 258 K) δ -62.77.
**HRMS (ESI).** Calculated for $C_{16}H_{21}BF_3NNaO_3^+$: 366.14588 Obtained: 366.14587

### *10.2.7.24 4-chloro-N,N-dimethyl-2-(4,4,5,5-tetramethyl-1,3,2-dioxaborolan-2-yl)benzamide (24ad)*



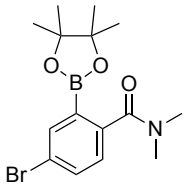
**24ad**

Following the general procedure: **23ad** (45.9 mg, 0.250 mmol, 1.0 equiv.), $[Ir(COD)(OMe)]_2$ (5 mg, 0.008 mmol, 3 mol%), $B_2pin_2$ (95.2 mg, 0.375 mmol, 1.5 equiv.), **L27** (3.4 mg, 0.015 mmol, 6 mol%) in THF (1.25 mL) were heated at 65 °C for 2 h. The crude mixture was purified by column chromatography (Hex/EtOAc 20% to Hex/EtOAc 80%) to obtain 42 mg (54% yield) of **24ad** as a white solid.

USC DE COMPOSTELA

**$^1$H NMR** (400.16 MHz, $CDCl_3$, 258 K) δ 7.70 (d, *J* = 2.0 Hz, 1H), 7.39 (d, *J* = 8.2 Hz, 1H), 7.34 (dd, *J* = 8.3, 2.1 Hz, 1H), 3.20 (s, 3H), 3.09 (s, 3H), 1.29 (s, 12H).
**$^{13}$C NMR** (100.63 MHz, $CDCl_3$, 258 K) δ 171.55 (CO), 136.94 (C, Ar), 136.41 (C, Ar), 133.37 (CH, Ar), 129.85 (CH, Ar), 127.11 (CH, Ar), 82.52 (C), 39.59 (N–$CH_3$), 37.66 (N–$CH_3$), 25.05 ($CH_3$).
**$^{11}$B NMR** (128.39 MHz, $CDCl_3$) δ 23.27
**HRMS (ESI).** Calculated for $C_{15}H_{22}BClNO_3^+$: 310.13758 Obtained: 310.73764

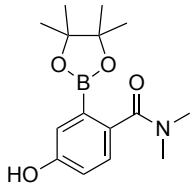
### *10.2.7.25 4-bromo-N,N-dimethyl-2-(4,4,5,5-tetramethyl-1,3,2-dioxaborolan-2-yl)benzamide (24ae)*


**24ae**

Following the general procedure: **23ae** (57.0 mg, 0.250 mmol, 1.0 equiv.), $[Ir(COD)(OMe)]_2$ (5 mg, 0.008 mmol, 3 mol%), $B_2pin_2$ (95.2 mg, 0.375 mmol, 1.5 equiv.), **L27** (3.4 mg, 0.015 mmol, 6 mol%) in THF (1.25 mL) were heated at 65 °C for 24 h. The crude mixture was purified by column chromatography (Hex/EtOAc 20% to Hex/EtOAc 80%) to obtain 73 mg (83% yield) of **24ae** as a white solid.

**$^1$H NMR** (400.16 MHz, $CDCl_3$, 258 K) δ 7.87 (d, *J* = 2.0 Hz, 1H), 7.51 (dd, *J* = 8.3, 2.1 Hz, 1H), 7.31 (d, *J* = 8.3 Hz, 1H), 3.20 (s, 3H), 3.08 (s, 3H), 1.29 (s, 12H).
**$^{13}$C NMR** (100.63 MHz, $CDCl_3$, 258 K) δ 171.65 (CO), 137.07 (C, Ar), 136.42 (CH, Ar), 132.85 (CH, Ar), 127.30 (CH, Ar), 125.71 (C, Ar), 82.65 (C), 39.59 (N–$CH_3$), 37.57 (N–$CH_3$), 25.04 ($CH_3$).
**$^{11}$B NMR** (128.39 MHz, $CDCl_3$, 258 K) δ 23.01
**HRMS (ESI).** Calculated for $C_{15}H_{21}BBrNNaO_3^+$: 376.0691 Obtained: 376.06090

### *10.2.7.26 4-hydroxy-N,N-dimethyl-2-(4,4,5,5-tetramethyl-1,3,2-dioxaborolan-2-yl)benzamide (24af)*

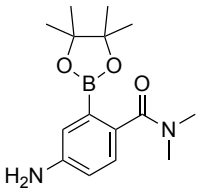

**24af**

Following the general procedure: **23af** (41.3 mg, 0.250 mmol, 1.0 equiv.), $[Ir(COD)(OMe)]_2$ (5 mg, 0.008 mmol, 3 mol%), $B_2pin_2$ (95.2 mg, 0.375 mmol, 1.5 equiv.), **L27** (3.4 mg, 0.015 mmol, 6 mol%) in THF (1.25 mL) were heated at 80 °C for 24 h. The crude mixture was purified by column chromatography (Hex/EtOAc 50% to EtOAc/MeOH 10%) to obtain 40 mg (55% yield) of **24af** as a white solid.

**$^1$H NMR** (400.16 MHz, $CDCl_3$, 258 K) δ 7.38 (d, *J* = 8.6 Hz, 1H), 7.30 (s, 1H), 6.45 (d, *J* = 7.9 Hz, 1H), 3.38 (s, 3H), 3.31 (s, 3H), 1.39 (s, 12H).
**$^{13}$C NMR** (100.63 MHz, $CDCl_3$, 258 K) δ 172.05 (CO), 161.84 (C, Ar), 127.96 (CH, Ar), 122.99 (C, Ar), 118.71 (CH, Ar), 115.82 (CH, Ar), 80.50 (C), 40.68 (N–$CH_3$), 39.93 (N–$CH_3$), 25.34 ($CH_3$).
**$^{11}$B NMR** (128.39 MHz, MeOD, 258K) δ 14.34.
**HRMS (ESI)**. Calculated for $C_{15}H_{23}BNO_4^+$: 292.17146 Obtained: 292.17174

USC UNIVERSIDADE DE SANTIAGO DE COMPOSTELA

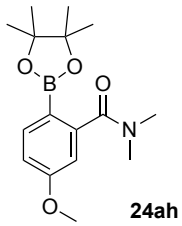
### *10.2.7.27 4-amino-N,N-dimethyl-2-(4,4,5,5-tetramethyl-1,3,2-dioxaborolan-2-yl)benzamide (24ag)*


**24ag**

Following the general procedure: **23ag** (41.1 mg, 0.250 mmol, 1.0 equiv.), $[Ir(COD)(OMe)]_2$ (5 mg, 0.008 mmol, 3 mol%), $B_2pin_2$ (95.2 mg, 0.375 mmol, 1.5 equiv.), **L27** (3.4 mg, 0.015 mmol, 6 mol%) in THF (1.25 mL) were heated at 80 °C for 1.5 h. The crude mixture was purified by column chromatography (Hex/EtOAc 50% to EtOAc/MeOH 10%) to obtain 31 mg (43% yield) of **24ag** as a white solid.

**$^1$H NMR** (400.16 MHz, $CDCl_3$, 318 K) δ 7.28 (d, *J* = 8.4 Hz, 1H), 7.05 (d, *J* = 2.2 Hz, 1H), 6.68 (dd, *J* = 8.3, 2.4 Hz, 1H), 3.17 (s, 6H), 1.32 (s, 12H).
**$^{13}$C NMR** (100.63 MHz, $CDCl_3$, 318 K) δ 172.58 (CO), 152.78 (C, Ar), 131.35 (C, Ar), 127.56 (CH, Ar), 119.89 (CH, Ar), 116.64 (CH, Ar), 81.98 (C), 38.85 (N–$CH_3$), 25.37 ($CH_3$).
**HRMS (ESI).** Calculated for $C_{15}H_{24}BN_2O_3^+$: 291.18745 Obtained: 291.18750

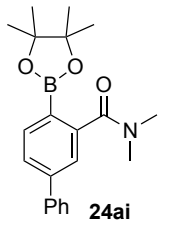
### *10.2.7.28 5-methoxy-N,N-dimethyl-2-(4,4,5,5-tetramethyl-1,3,2-dioxaborolan-2-yl)benzamide (2ah)*


**24ah**

Following the general procedure: **23ah** (44.8 mg, 0.250 mmol, 1.0 equiv.), $[Ir(COD)(OMe)]_2$ (5 mg, 0.008 mmol, 3 mol%), $B_2pin_2$ (95.2 mg, 0.375 mmol, 1.5 equiv.), **L27** (3.4 mg, 0.015 mmol, 6 mol%) in THF (1.25 mL) were heated at 65 °C for 2 h. The crude mixture was purified by column chromatography (Hex/EtOAc 20% to EtOAc) to obtain 65 mg (85% yield) of **2ah** were obtained as a colorless oil.

**$^1$H NMR** (400.16 MHz, $CDCl_3$, 258 K) δ 7.73 (d, *J* = 8.3 Hz, 1H), 6.87 (dd, *J* = 8.3, 2.4 Hz, 1H), 6.80 (d, *J* = 2.5 Hz, 1H), 3.81 (s, 3H), 3.08 (s, 3H), 2.76 (s, 3H), 1.28 (s, 12H).
**$^{13}$C NMR** (100.63 MHz, $CDCl_3$, 258 K) δ 172.29 (CO), 161.94(C, Ar), 144.73 (C, Ar) , 137.38 (CH, Ar), 113.88 (CH, Ar), 110.85 (CH, Ar), 83.55 (C), 55.38 (O–$CH_3$), 39.13 (N–$CH_3$), 34.94 (N–$CH_3$), 24.95 ($CH_3$).
**$^{11}$B NMR** (128.39 MHz, $CDCl_3$, 258 K) δ 30.46.
**HRMS (ESI).** Calculated for $C_{16}H_{24}BNNaO_4^+$: 328.16906 Obtained: 328.16947.

### *10.2.7.29 N,N-dimethyl-4-(4,4,5,5-tetramethyl-1,3,2-dioxaborolan-2-yl)-[1,1'-biphenyl]-3-carboxamide (24ai)*


**24ai**

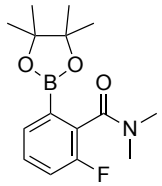
Following the general procedure: **5** (56.3 mg, 0.250 mmol, 1.0 equiv.), $[Ir(COD)(OMe)]_2$ (5 mg, 0.008 mmol, 3 mol%), $B_2pin_2$ (95.2 mg, 0.375 mmol, 1.5 equiv.), **L27** (3.4 mg, 0.015 mmol, 6 mol%) in THF (1.25 mL) were heated at 65 °C for 1.5 h. The crude mixture was purified by column chromatography (Hex/EtOAc 20% to Hex/EtOAc 80%) to obtain 57 mg (65% yield) of **24ai** were obtained as a pale yellow oil.

**$^1$H NMR** (400.16 MHz, $CDCl_3$, 258 K) δ 7.36 (dd, *J* = 7.4, 1.1 Hz, 1H), 7.33 – 7.27 (m, 1H), 6.99 (dd, *J* = 8.2, 1.1 Hz, 1H), 3.79 (s, 3H), 3.08 (s, 3H), 2.74 (s, 3H), 1.27 (s, 12H).

USC UNIVERSIDADE

**$^{13}$C NMR** (100.63 MHz, $CDCl_3$, 258 K) δ 170.03 (CO), 154.58 (C, Ar), 131.66 (C, Ar), 129.13 (CH, Ar), 127.31 (CH, Ar), 113.61 (CH, Ar), 83.81 (C), 55.69 (O–$CH_3$), 38.59 (N–$CH_3$), 34.61 (N–$CH_3$), 24.89 ($CH_3$).
**$^{11}$B NMR** (128.39 MHz, $CDCl_3$, 258K) δ 30.37
**HRMS (ESI).** Calculated for $C_{16}H_{24}BNNaO_4^+$: 328.16906 Obtained: 328.16962

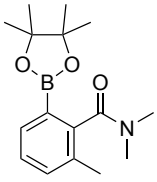
### *10.2.7.30 2-fluoro-N,N-dimethyl-6-(4,4,5,5-tetramethyl-1,3,2-dioxaborolan-2-yl)benzamide (24aj)*


**24aj**

Following the general procedure: **23aj** (41.8 mg, 0.250 mmol, 1.0 equiv.), $[Ir(COD)(OMe)]_2$ (5 mg, 0.008 mmol, 3 mol%), $B_2pin_2$ (95.2 mg, 0.375 mmol, 1.5 equiv.), **L27** (3.4 mg, 0.015 mmol, 6 mol%) in THF (1.25 mL) were heated at 80 °C for 1.5 h. The crude mixture was purified by column chromatography (Hex/EtOAc 20% to Hex/EtOAc 80%) to obtain 68 mg (93% yield) of **24aj** as a colorless oil.

**$^1$H NMR** (400.16 MHz, $CDCl_3$, 258 K) δ 7.56 (dd, *J* = 7.4, 1.1 Hz, 1H), 7.33 (ddd, *J* = 8.3, 7.3, 5.3 Hz, 1H), 7.16 (ddd, *J* = 9.3, 8.3, 1.1 Hz, 1H), 3.08 (s, 3H), 2.80 (s, 3H), 1.28 (s, 12H).
**$^{13}$C NMR** (100.63 MHz, $CDCl_3$, 258 K) δ 167.50 (CO), 157.70 (CF, Ar, d, *J* = 246.6 Hz), 131.17 (CH, Ar, d, *J* = 3.3 Hz), 129.94 (CH, Ar, d, *J* = 7.3 Hz), 129.91 (C, Ar, d, *J* = 17.6 Hz), 118.64 (CH, Ar, d, *J* = 21.3 Hz), 84.16 (C), 38.70 (N–$CH_3$), 34.76 (N–$CH_3$), 24.77 ($CH_3$).
**$^{11}$B NMR** (128.39 MHz, $CDCl_3$, 258 K) δ 22.46
**$^{19}$F NMR** (376.46 MHz, $CDCl_3$, 258 K) δ -117.49.
**HRMS (ESI).** Calculated for $C_{15}H_{21}BFNNaO_3^+$: 316.14907 Obtained: 316.14939.

### *10.2.7.31 N,N,2-trimethyl-6-(4,4,5,5-tetramethyl-1,3,2-dioxaborolan-2-yl)benzamide (24ak)*

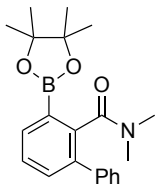

**24ak**

Following the general procedure: **23ak** (40.8 mg, 0.250 mmol, 1.0 equiv.), $[Ir(COD)(OMe)]_2$ (5 mg, 0.008 mmol, 3 mol%), $B_2pin_2$ (95.2 mg, 0.375 mmol, 1.5 equiv.), **L27** (3.4 mg, 0.015 mmol, 6 mol%) in THF (1.25 mL) were heated at 80 °C for 24 h. The crude mixture was purified by column chromatography (Hex/EtOAc 20% to Hex/EtOAc 80%) to obtain 57 mg (79% yield) of **24ak** as a colorless oil.

**$^1$H NMR** (400.16 MHz, $CDCl_3$, 258 K) δ 7.63 (dd, *J* = 7.1, 1.2 Hz, 1H), 7.28 (dd, *J* = 7.8, 0.8 Hz, 1H), 7.24 (d, *J* = 7.3 Hz, 1H), 3.09 (s, 3H), 2.72 (s, 3H), 2.26 (s, 3H), 1.29 (s, 12H).
**$^{13}$C NMR** (100.63 MHz, $CDCl_3$, 258 K) δ 172.08 (CO), 142.50 (C, Ar), 133.21 (CH, Ar), 133.16 (C, Ar), 133.07 (CH, Ar), 127.78 (CH, Ar), 83.77 (C), 38.54 (N–$CH_3$), 34.53 (N–$CH_3$), 24.91 ($CH_3$), 19.09 ($CH_3$).
**$^{11}$B NMR** (128.39 MHz, $CDCl_3$, 258 K) δ 30.65
**HRMS (ESI).** Calculated for $C_{16}H_{24}BNNaO_3^+$: 312.17414 Obtained: 312.17412

USC UNIVERSIDADE DE SANTIAGO DE COMPOSTELA

### *10.2.7.32 N,N-dimethyl-3-(4,4,5,5-tetramethyl-1,3,2-dioxaborolan-2-yl)-[1,1'-biphenyl]-2-carboxamide (24al)*

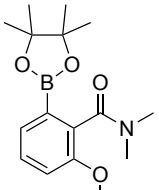


**24al**

Following the general procedure: **23al** (56.3 mg, 0.250 mmol, 1.0 equiv.), $[Ir(COD)(OMe)]_2$ (5 mg, 0.008 mmol, 3 mol%), $B_2pin_2$ (95.2 mg, 0.375 mmol, 1.5 equiv.), **L27** (3.4 mg, 0.015 mmol, 6 mol%) in THF (1.25 mL) were heated at 80 °C for 24 h. The crude mixture was purified by column chromatography (Hex/EtOAc 20% to Hex/EtOAc 80%) to obtain 62 mg (71% yield) of **24al** as a colorless oil.

**$^1$H NMR** (400.16 MHz, $CDCl_3$, 258 K) δ 7.71 (dd, *J* = 6.2, 2.5 Hz, 1H), 7.46 – 7.23 (m, 7H), 2.76 (s, 3H), 2.44 (s, 3H), 1.24 (s, 13H).
**$^{13}$C NMR** (100.63 MHz, $CDCl_3$, 258 K) δ 171.24 (CO), 141.40 (C, Ar), 140.03 (C, Ar), 137.85 (C, Ar), 134.20 (CH, Ar), 132.40 (CH, Ar), 128.61 (CH, Ar), 128.16 (CH, Ar), 128.02 (CH, Ar), 127.33 (CH, Ar), 83.86 (C), 38.25 (N–$CH_3$), 34.33 (N–$CH_3$), 24.80 ($CH_3$).
**HRMS (ESI).** Calculated for $C_{21}H_{26}BNNaO_3^+$: 374.18980 Obtained: 374.19017

### *10.2.7.33 2-methoxy-N,N-dimethyl-6-(4,4,5,5-tetramethyl-1,3,2-dioxaborolan-2-yl)benzamide (24am)*

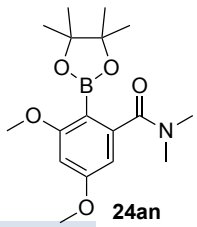


**24am**

Following the general procedure: **23am** (44.8 mg, 0.250 mmol, 1.0 equiv.), $[Ir(COD)(OMe)]_2$ (5 mg, 0.008 mmol, 3 mol%), $B_2pin_2$ (95.2 mg, 0.375 mmol, 1.5 equiv.), **L27** (3.4 mg, 0.015 mmol, 6 mol%) in THF (1.25 mL) were heated at 80 °C for 24 h. The crude mixture was purified by column chromatography (Hex/EtOAc 20% to Hex/EtOAc 80%) to obtain 46 mg (60% yield) of **24am** as a colorless oil.

**$^1$H NMR** (400.16 MHz, $CDCl_3$, 258 K) δ 7.36 (dd, *J* = 7.4, 1.1 Hz, 1H), 7.33 – 7.27 (m, 1H), 6.99 (dd, *J* = 8.2, 1.1 Hz, 1H), 3.79 (s, 3H), 3.08 (s, 3H), 2.74 (s, 3H), 1.27 (s, 12H).
**$^{13}$C NMR** (100.63 MHz, $CDCl_3$, 258 K) δ 170.03 (CO), 154.58 (C, Ar), 131.66 (C, Ar), 129.13 (CH, Ar), 127.31 (CH, Ar), 113.61 (CH, Ar), 83.81 (C), 55.69 (O–$CH_3$), 38.59 (N–$CH_3$), 34.61 (N–$CH_3$), 24.89 ($CH_3$).
**$^{11}$B NMR** (128.39 MHz, $CDCl_3$, 258 K) δ 30.72
**HRMS (ESI).** Calculated for $C_{16}H_{24}BNNaO_4^+$: 328.16906 Obtained: 328.16962

### *10.2.7.34 3,5-dimethoxy-N,N-dimethyl-2-(4,4,5,5-tetramethyl-1,3,2-dioxaborolan-2-yl)benzamide (24an)*



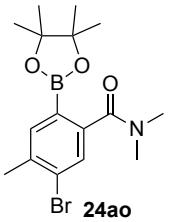
**24an**

Following the general procedure: **23an** (52.3 mg, 0.250 mmol, 1.0 equiv.), $[Ir(COD)(OMe)]_2$ (5 mg, 0.008 mmol, 3 mol%), $B_2pin_2$ (95.2 mg, 0.375 mmol, 1.5 equiv.), **L27** (3.4 mg, 0.015 mmol, 6 mol%) in THF (1.25 mL) were heated at 65 °C for 24 h. The crude mixture was purified by column chromatography (Hex/EtOAc 20% to EtOAc) to obtain 74 mg (88% yield) of **24an** as an off-white solid.

USC UNIVERSIDADE DE SANTIAGO DE COMPOSTELA

**$^1$H NMR** (400.16 MHz, $CDCl_3$, 258 K) δ 6.42 (d, *J* = 2.0 Hz, 1H), 6.36 (d, *J* = 2.0 Hz, 1H), 3.77 (s, 3H), 3.74 (s, 3H), 3.06 (s, 2H), 2.93 (s, 2H), 1.27 (s, 12H).
**$^{13}$C NMR** (100.63 MHz, $CDCl_3$, 258 K) δ 172.04 (CO), 164.50 (CO, Ar), 162.17 (CO, Ar), 143.04 (C, Ar), 102.08 (CH, Ar), 98.46 (CH, Ar), 82.96 (C), 55.68 ($O–CH_3$), 55.44 ($O–CH_3$), 39.39 ($N–CH_3$), 35.84 ($N–CH_3$), 24.84 ($CH_3$).
**HRMS (ESI).** Calculated for $C_{17}H_{26}BNNaO_5^+$: 358.17962 Obtained: 358.17974

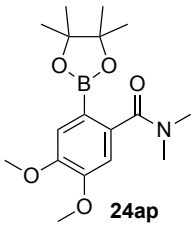
### *10.2.7.35 5-bromo-N,N,4-trimethyl-2-(4,4,5,5-tetramethyl-1,3,2-dioxaborolan-2-yl)benzamide (24ao)*


**24ao**

Following the general procedure: **23ao** (60.5 mg, 0.250 mmol, 1.0 equiv.), $[Ir(COD)(OMe)]_2$ (5 mg, 0.008 mmol, 3 mol%), $B_2pin_2$ (95.2 mg, 0.375 mmol, 1.5 equiv.), **L27** (3.4 mg, 0.015 mmol, 6 mol%) in THF (1.25 mL) were heated at 80 °C for 24 h. The crude mixture was purified by column chromatography (Hex/EtOAc 20% to Hex/EtOAc 80%) to obtain 41 mg (45% yield) of **24ao** as a brown solid.

**$^1$H NMR** (400.16 MHz, $CDCl_3$, 258 K) δ 7.62 (s, 1H), 7.52 (s, 1H), 3.13 (s, 3H), 2.93 (s, 3H), 2.37 (s, 3H), 1.29 (s, 12H).
**$^{13}$C NMR** (100.63 MHz, $CDCl_3$, 258 K) δ 171.01 (CO), 139.86 (C, Ar), 139.01 (C, Ar), 136.64 (CH, Ar), 129.49 (CH, Ar), 127.72 (C, Ar), 83.32 (C), 39.36 ($N–CH_3$), 36.17 ($N–CH_3$), 24.98 ($CH_3$), 22.85 ($CH_3$).
**HRMS (ESI)**. Calculated for $C_{16}H_{23}BBrNNaO_3^+$: 390.08466 Obtained: 390.08563

### *10.2.7.36 4,5-dimethoxy-N,N-dimethyl-2-(4,4,5,5-tetramethyl-1,3,2-dioxaborolan-2-yl)benzamide (24ap)*

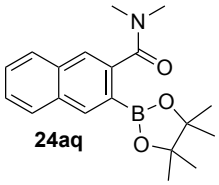

**24ap**

Following the general procedure: **23ap** (52.3 mg, 0.250 mmol, 1.0 equiv.), $[Ir(COD)(OMe)]_2$ (5 mg, 0.008 mmol, 3 mol%), $B_2pin_2$ (95.2 mg, 0.375 mmol, 1.5 equiv.), **L27** (3.4 mg, 0.015 mmol, 6 mol%) in THF (1.25 mL) were heated at 65 °C for 2 h. The crude mixture was purified by column chromatography (Hex/EtOAc 20% to EtOAc) to obtain 78 mg (93% yield) of **24ap** as a white solid.

**$^1$H NMR** (400.16 MHz, $CDCl_3$, 258 K) δ 7.16 (s, 1H), 6.82 (s, 1H), 3.89 (s, 3H), 3.82 (s, 3H), 3.08 (s, 3H), 2.89 (s, 3H), 1.24 (s, 12H).
**$^{13}$C NMR** (100.63 MHz, $CDCl_3$, 258 K) δ 172.26 (CO), 150.28 (CO, Ar), 149.05 (CO, Ar), 133.73 (C, Ar), 115.30 (CH, Ar), 108.37 (CH, Ar), 82.77 (C), 55.83 ($O–CH_3$), 55.81($O–CH_3$), 39.25 ($N–CH_3$), 36.15 ($N–CH_3$), 24.93 ($CH_3$).
**$^{11}$B NMR** (128.39 MHz, $CDCl_3$, 258 K) δ 27.31.
**HRMS (ESI).** Calculated for $C_{17}H_{26}BNNaO_5^+$: 358.17962 Obtained: 358.17957

USC UNIVERSIDADE DE SANTIAGO DE COMPOSTELA

### *10.2.7.37 N,N-dimethyl-1-(4,4,5,5-tetramethyl-1,3,2-dioxaborolan-2-yl)-2-naphthamide (24aq)*

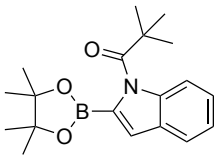


**24aq**

Following the general procedure: **23aq** (49.8 mg, 0.250 mmol, 1.0 equiv.), $[Ir(COD)(OMe)]_2$ (5 mg, 0.008 mmol, 3 mol%), $B_2pin_2$ (95.2 mg, 0.375 mmol, 1.5 equiv.), **L27** (3.4 mg, 0.015 mmol, 6 mol%) in THF (1.25 mL) were heated at 65 °C for 2 h. The crude mixture was purified by column chromatography (Hex/EtOAc 20% to Hex/EtOAc 80%) to obtain 71 mg (87% yield) of **24aq** as a white solid.

**$^1$H NMR** (400.16 MHz, $CDCl_3$, 258 K) δ 8.34 (s, 1H), 7.87 – 7.84 (m, 1H), 7.81 – 7.78 (m, 2H), 7.52 – 7.48 (m, 2H), 3.15 (s, 3H), 2.87 (s, 3H), 1.33 (s, 12H).
**$^{13}$C NMR** (100.63 MHz, $CDCl_3$, 258 K) δ 172.49 (CO), 137.87 (C, Ar), 136.40 (CH, Ar), 133.96 (C, Ar), 132.61 (C, Ar), 128.41 (CH, Ar), 128.04 (CH, Ar), 127.52 (CH, Ar), 126.84 (CH, Ar), 125.04 (CH, Ar), 83.44 (C), 39.30 (N–$CH_3$), 35.63 (N–$CH_3$), 24.97 ($CH_3$).
**$^{11}$B NMR** (128.39 MHz, $CDCl_3$, 258 K) δ 29.48
**HRMS (ESI)**. Calculated for $C_{19}H_{24}BNNaO_3^+$: 348.17415 Obtained: 348.17406

### *10.2.7.38 2,2-dimethyl-1-(2-(4,4,5,5-tetramethyl-1,3,2-dioxaborolan-2-yl)-1H-indol-1-yl)propan-1-one (24r)*

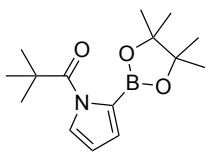


**24r**

Following the general procedure: **23r** (50.3 mg, 0.250 mmol, 1.0 equiv.), $[Ir(COD)(OMe)]_2$ (5 mg, 0.008 mmol, 3 mol%), $B_2pin_2$ (95.2 mg, 0.375 mmol, 1.5 equiv.), **L27** (3.4 mg, 0.015 mmol, 6 mol%) in THF (1.25 mL) were heated at 65 °C for 24 h. The crude mixture was purified by column chromatography (Hex/EtOAc 20% to EtOAc) to obtain 77 mg (94% yield) of **24r**as a white solid.

**$^1$H NMR** (400.16 MHz, $CDCl_3$, 258 K) δ 8.40 (dd, *J* = 7.0, 1.2 Hz, 1H), 8.05 (s, 1H), 7.93 (dd, *J* = 6.3, 1.3 Hz, 1H), 7.32 – 7.20 (m, 2H), 1.45 (s, 9H), 1.29 (s, 12H).
**$^{13}$C NMR** (100.63 MHz, $CDCl_3$, 258 K) δ 177.59 (CO), 137.44 (C, Ar), 134.65 (CH, Ar), 132.25 (C, Ar), 125.10 (CH, Ar), 123.83 (CH, Ar), 122.22 (CH, Ar), 116.99 (CH, Ar), 83.49 (C), 41.50 (C), 28.70 ($CH_3$), 24.92 ($CH_3$).
**$^{11}$B NMR** (128.39 MHz, $CDCl_3$, 258 K) δ 30.66
**HRMS (ESI)**. Calculated for $C_{19}H_{26}BNNaO_3^+$: 350.18979 Obtained: 350.18997

### *10.2.7.39 2,2-dimethyl-1-(2-(4,4,5,5-tetramethyl-1,3,2-dioxaborolan-2-yl)-1H-pyrrol-1-yl)propan-1-one (24s)*



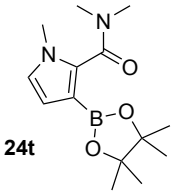
**24s**

Following the general procedure: **23s** (37.8 mg, 0.250 mmol, 1.0 equiv.), $[Ir(COD)(OMe)]_2$ (5 mg, 0.008 mmol, 3 mol%), $B_2pin_2$ (95.2 mg, 0.375 mmol, 1.5 equiv.), **L27** (3.4 mg, 0.015 mmol, 6 mol%) in THF (1.25 mL) were heated at 80 °C for 1 h. The crude mixture was purified by column chromatography (Hex/EtOAc 20% to EtOAc) to obtain 37 mg (54% yield) of **24s** as a transparent oil.

USC DE COMPOSTELA

**$^1$H NMR** (400.16 MHz, $CDCl_3$, 258 K) δ 7.38 (dd, *J* = 3.2, 1.2 Hz, 1H), 6.42 (dd, *J* = 3.1, 1.1 Hz, 1H), 6.28 (t, *J* = 3.1 Hz, 1H), 1.42 (s, 9H), 1.37 (s, 12H).
**$^{13}$C NMR** (100.63 MHz, $CDCl_3$, 258 K) δ 176.83 (CO), 122.02 (CH), 118.42 (CH), 114.01 (CH), 83.74 (C), 39.97 (C), 28.47 ($CH_3$), 24.79 ($CH_3$).
**HRMS (ESI)**. Calculated for $C_{15}H_{24}BNNaO_3^+$: 300.17414 Obtained: 300.17425

### *10.2.7.40 N,N,1-trimethyl-3-(4,4,5,5-tetramethyl-1,3,2-dioxaborolan-2-yl)-1H-pyrrole-2-carboxamide (24t)*

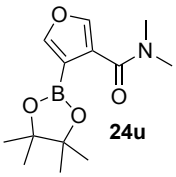


**24t**

Following the general procedure: **23t** (38.0 mg, 0.250 mmol, 1.0 equiv.), $[Ir(COD)(OMe)]_2$ (5 mg, 0.008 mmol, 3 mol%), $B_2pin_2$ (95.2 mg, 0.375 mmol, 1.5 equiv.), **L28** (4.4 mg, 0.015 mmol, 6 mol%) in THF (1.25 mL) were heated at 80 °C for 24 h. The crude mixture was purified by column chromatography (Hex/EtOAc 20% to EtOAc) to obtain 50 mg (72% yield) of **24t** as a brown oil.

**$^1$H NMR** (400.16 MHz, $CDCl_3$, 258 K) δ 6.71 (d, *J* = 3.8 Hz, 1H), 6.32 (d, *J* = 3.8 Hz, 1H), 3.91 (s, 3H), 3.15 (s, 3H), 3.08 (s, 3H), 1.30 (s, 12H).
**$^{13}$C NMR** (100.63 MHz, $CDCl_3$, 258 K) δ 164.25 (CO), 131.12 (C), 119.92 (CH), 112.17 (CH), 83.51 (C), 39.75 (N–$CH_3$), 35.29 (N–$CH_3$), 35.20 (N–$CH_3$), 24.81 ($CH_3$).
**$^{11}$B NMR** (128.39 MHz, $CDCl_3$, 258 K) δ 22.19
**HRMS (ESI)**. Calculated for $C_{14}H_{23}BN_2NaO_3^+$: 301.16939 Obtained: 301.16965

### *10.2.7.41 N,N-dimethyl-4-(4,4,5,5-tetramethyl-1,3,2-dioxaborolan-2-yl)furan-3-carboxamide (24u)*



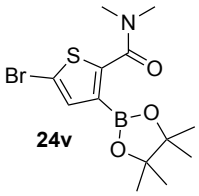
**24u**

Following the general procedure: **23u** (34.8 mg, 0.250 mmol, 1.0 equiv.), $[Ir(COD)(OMe)]_2$ (5 mg, 0.008 mmol, 3 mol%), $B_2pin_2$ (95.2 mg, 0.375 mmol, 1.5 equiv.), **L27** (3.4 mg, 0.015 mmol, 6 mol%) in THF (1.25 mL) were heated at 65 °C for 15 min. The crude mixture was purified by column chromatography (Hex/EtOAc 20% to EtOAc) to obtain 55 mg (84% yield) of **24u** as a brown oil.

**$^1$H NMR** (400.16 MHz, $CDCl_3$, 258 K) δ 7.94 (d, *J* = 0.7 Hz, 1H), 7.20 (d, *J* = 0.7 Hz, 1H), 3.14 (s, 3H), 3.06 (s, 3H), 1.33 (s, 12H).
**$^{13}$C NMR** (100.63 MHz, $CDCl_3$, 258 K) δ 164.59 (CO), 148.91 (CH), 123.03 (CH), 122.06 (C), 84.72 (C), 39.23 (N–$CH_3$), 35.78 (N–$CH_3$), 24.77 ($CH_3$).
**$^{11}$B NMR** (128.39 MHz, $CDCl_3$, 258 K) δ 27.48
**HRMS (ESI)**. Calculated for $C_{13}H_{20}BNNaO_4^+$: 288.13776 Obtained: 288.13801

USC UNIVERSIDADE DE SANTIAGO DE COMPOSTELA

### *10.2.7.42 5-bromo-N,N-dimethyl-3-(4,4,5,5-tetramethyl-1,3,2-dioxaborolan-2-yl)thiophene-2-carboxamide (24v)*

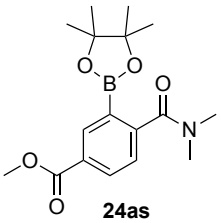


**24v**

Following the general procedure: **23v** (58.5 mg, 0.250 mmol, 1.0 equiv.), $[Ir(COD)(OMe)]_2$ (5 mg, 0.008 mmol, 3 mol%), $B_2pin_2$ (95.2 mg, 0.375 mmol, 1.5 equiv.), **L27** (3.4 mg, 0.015 mmol, 6 mol%) in THF (1.25 mL) were heated at 80 °C for 24 h. The crude mixture was purified by column chromatography (Hex/EtOAc 20% to EtOAc) to obtain 26 mg (30% yield) of **24v** as a white solid.

**$^1$H NMR** (400.16 MHz, $CDCl_3$, 258 K) δ 7.34 (s, 1H), 3.29 (s, 3H), 3.08 (s, 4H), 1.33 (s, 12H).
**$^{13}$C NMR** (100.63 MHz, $CDCl_3$, 258 K) δ 175.77 (CO), 135.07 (CH), 133.30 (C), 84.22 (C), 31.36 (N–$CH_3$), 29.86 (N–$CH_3$), 24.88 ($CH_3$).
**$^{11}$B NMR** (128.39 MHz, $CDCl_3$, 258 K) δ 28.59.
**HRMS (ESI)**. Calculated for $C_{13}H_{19}BNNaO_3S^+$: 382.02543 Obtained: 382.02579

### *10.2.7.43 Methyl 4-(dimethylcarbamoyl)-3-(4,4,5,5-tetramethyl-1,3,2-dioxaborolan-2-yl)benzoate (24as)*

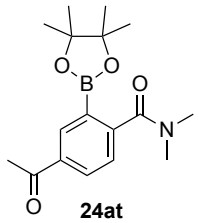


**24as**

Following the general procedure: **23as** (51.8 mg, 0.250 mmol, 1.0 equiv.), $[Ir(COD)(OMe)]_2$ (5 mg, 0.008 mmol, 3 mol%), $B_2pin_2$ (95.2 mg, 0.375 mmol, 1.5 equiv.), **L27** (3.4 mg, 0.015 mmol, 6 mol%) in THF (1.25 mL) were heated at 65 °C for 2 h. The crude mixture was purified by column chromatography (Hex/EtOAc 20% to EtOAc) to obtain 80 mg (96% yield) of **24as** as a white solid.

**$^1$H NMR** (400.16 MHz, $CDCl_3$, 258 K) δ 8.42 (d, *J* = 1.5 Hz, 1H), 8.10 (dd, *J* = 8.0, 1.8 Hz, 1H), 7.37 (d, *J* = 7.9 Hz, 1H), 3.89 (s, 3H), 3.09 (s, 3H), 2.79 (s, 3H), 1.28 (s, 12H).
**$^{13}$C NMR** (100.63 MHz, $CDCl_3$, 258 K) δ 171.58 (CO), 166.63 (CO), 146.30 (C, Ar), 136.17 (CH, Ar), 132.29 (CH, Ar), 129.65 (C, Ar), 125.74 (CH, Ar), 83.81 (C), 52.45 (O–$CH_3$), 39.07 (N–$CH_3$), 35.31 (N–$CH_3$), 24.93 ($CH_3$).
**$^{11}$B NMR** (128.39 MHz, $CDCl_3$, 258 K) δ 29.23
**HRMS (ESI)**. Calculated for $C_{17}H_{24}BNNaO_5^+$: 356.16397 Obtained: 356.16389

### *10.2.7.44 4-acetyl-N,N-dimethyl-2-(4,4,5,5-tetramethyl-1,3,2-dioxaborolan-2-yl)benzamide (24at)*



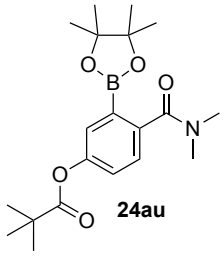
**24at**

Following the general procedure: **23at** (47.8 mg, 0.250 mmol, 1.0 equiv.), $[Ir(COD)(OMe)]_2$ (5 mg, 0.008 mmol, 3 mol%), $B_2pin_2$ (95.2 mg, 0.375 mmol, 1.5 equiv.), **L27** (3.4 mg, 0.015 mmol, 6 mol%) in THF (1.25 mL) were heated at 65 °C for 1.5 h. The crude mixture was purified by column chromatography (Hex/EtOAc 20% to EtOAc) to obtain 65 mg (82% yield) of **24at** as a white solid.

**$^1$H NMR** (400.16 MHz, $CDCl_3$, 258 K) δ 8.33 (d, *J* = 1.8 Hz, 1H), 8.05 (dd, *J* = 8.0, 1.9 Hz, 1H), 7.42 (d, *J* = 8.0 Hz, 1H), 3.12 (s, 3H), 2.84 (s, 3H), 2.65 (s, 3H), 1.30 (s, 12H).

**$^{13}$C NMR** (100.63 MHz, $CDCl_3$, 258 K) δ 198.34 (CO), 171.56 (CO), 145.86 (C, Ar), 136.39 (C, Ar), 135.12 (CH, Ar), 130.73 (CH, Ar), 126.02 (CH, Ar), 83.80 (C), 39.14 (N–$CH_3$), 35.55 (N–$CH_3$), 27.20 ($CH_3$), 25.00 ($CH_3$).
**$^{11}$B NMR** (128.39 MHz, $CDCl_3$, 258 K) δ 27.87
**HRMS (ESI)**. Calculated for $C_{17}H_{24}BNNaO_4^+$: 340.16906 Obtained: 340.16938.

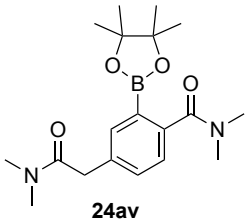
### *10.2.7.45 4-(dimethylcarbamoyl)-3-(4,4,5,5-tetramethyl-1,3,2-dioxaborolan-2-yl)phenyl pivalate (24au)*


**24au**

Following the general procedure: **23au** (62.3 mg, 0.250 mmol, 1.0 equiv.), $[Ir(COD)(OMe)]_2$ (5 mg, 0.008 mmol, 3 mol%), $B_2pin_2$ (95.2 mg, 0.375 mmol, 1.5 equiv.), **L27** (3.4 mg, 0.015 mmol, 6 mol%) in THF (1.25 mL) were heated at 65 °C for 1.5 h. The crude mixture was purified by column chromatography (Hex/EtOAc 20% to EtOAc/MeOH 10%) to obtain 87 mg (93% yield) of **24au** as a white solid.

**$^1$H NMR** (400.16 MHz, $CDCl_3$, 258 K) δ 7.44 (d, *J* = 8.3 Hz, 1H), 7.40 (d, *J* = 1.8 Hz, 1H), 7.12 (d, *J* = 7.4 Hz, 1H), 3.19 (s, 3H), 3.05 (s, 3H), 1.31 (s, 9H), 1.29 (s, 12H).
**$^{13}$C NMR** (100.63 MHz, $CDCl_3$, 258 K) δ 176.95 (CO), 171.89 (CO), 152.09 (C, Ar), 136.32 (C, Ar), 127.05 (CH, Ar), 126.37 (CH, Ar), 123.51 (CH, Ar), 83.05 (C), 39.63 (N–$CH_3$), 39.11 (CH), 37.22 (N–$CH_3$), 27.11 ($CH_3$), 25.02 ($CH_3$).
**$^{11}$B NMR** (128.39 MHz, $CDCl_3$, 258 K) δ 22.83
**HRMS (ESI)**. Calculated for $C_{20}H_{30}BNNaO_5^+$: 398.21092 Obtained: 398.21132.

### *10.2.7.46 4-(2-(dimethylamino)-2-oxoethyl)-N,N-dimethyl-2-(4,4,5,5-tetramethyl-1,3,2-dioxaborolan-2-yl)benzamide (24av)*

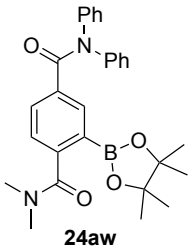

**24av**

Following the general procedure: **23av** (58.6 mg, 0.250 mmol, 1.0 equiv.), $[Ir(COD)(OMe)]_2$ (5 mg, 0.008 mmol, 3 mol%), $B_2pin_2$ (95.2 mg, 0.375 mmol, 1.5 equiv.), **L27** (3.4 mg, 0.015 mmol, 6 mol%) in THF (1.25 mL) were heated at 65 °C for 1.5 h. The crude mixture was purified by column chromatography (Hex/EtOAc 20% to Hex/EtOAc 80%) to obtain 73 mg (81% yield) of **24av** as a white solid.

**$^1$H NMR** (400.16 MHz, $CDCl_3$, 258 K) δ 7.62 (d, *J* = 1.2 Hz, 1H), 7.34 (dd, *J* = 7.9, 1.9 Hz, 1H), 7.22 (d, *J* = 7.8 Hz, 1H), 3.70 (s, 2H), 2.97 (s, 6H), 2.94 (s, 6H), 1.28 (s, 12H).
**$^{13}$C NMR** (100.63 MHz, $CDCl_3$, 258 K) δ 172.50 (CO), 170.80 (CO), 141.28 (C, Ar), 135.57 (C, Ar), 135.26 (CH, Ar), 131.29 (CH, Ar), 126.05 (CH, Ar), 83.70 (C), 40.76 ($CH_2$), 37.86 (N–$CH_3$), 35.73 (N–$CH_3$), 25.05 ($CH_3$).
**$^{11}$B NMR** (128.39 MHz, $CDCl_3$, 258 K) δ 25.78.
**HRMS (ESI)**. Calculated for $C_{19}H_{29}BN_2NaO_4^+$: 383.21126 Obtained: 383.21125.

USC UNIVERSIDADE DE SANTIAGO DE COMPOSTELA

*10.2.7.47 $N^1$,$N^1$-dimethyl-$N^4$,$N^4$-diphenyl-2-(4,4,5,5-tetramethyl-1,3,2-dioxaborolan-2-yl)terephthalamide (24aw)*

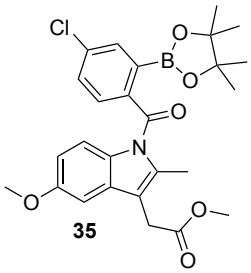


**24aw**

Following the general procedure: **23aw** (86.1 mg, 0.250 mmol, 1.0 equiv.), $[Ir(COD)(OMe)]_2$ (5 mg, 0.008 mmol, 3 mol%), $B_2pin_2$ (95.2 mg, 0.375 mmol, 1.5 equiv.), **L27** (3.4 mg, 0.015 mmol, 6 mol%) in THF (1.25 mL) were heated at 65 °C for 24 h. The crude mixture was purified by column chromatography (Hex/EtOAc 20% to Hex/EtOAc 80%) to obtain 87 mg (74% yield) of **24aw** as a white solid.

**$^1$H NMR** (400.16 MHz, $CDCl_3$, 323 K) δ 7.92 (d, *J* = 1.3 Hz, 1H), 7.51 (dd, *J* = 7.9, 1.9 Hz, 1H), 7.33 – 7.25 (m, 3H), 7.21 – 7.13 (m, 8H), 7.10 (d, *J* = 7.9 Hz, 2H), 2.89 (s, 6H), 1.27 (s, 12H).
**$^{13}$C NMR** (100.63 MHz, $CDCl_3$, 258 K) δ 171.67 (CO), 169.96 (CO), 143.17 (C, Ar), 135.89 (CH, Ar), 131.71 (CH, Ar), 129.34 (CH, Ar), 129.16 (C, Ar), 126.83 (C, Ar), 126.64 (CH, Ar), 125.26 (CH, Ar), 83.57 (C), 39.11 (N–$CH_3$), 35.61 (N–$CH_3$), 24.95($CH_3$).
**$^{11}$B NMR** (128.39 MHz, $CDCl_3$, 258 K) δ 27.89
**HRMS (ESI)**. Calculated for $C_{16}H_{24}BNNaO_4^+$: 493.22691 Obtained: 493.22707

*10.2.7.48 Methyl 2-(1-(4-chloro-2-(4,4,5,5-tetramethyl-1,3,2-dioxaborolan-2-yl)benzoyl)-5-methoxy-2-methyl-1H-indol-3-yl)acetate (35).*



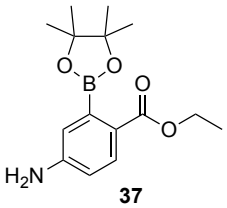
**35**

Following the general procedure: **34** (93 mg, 0.250 mmol, 1.0 equiv.), $[Ir(COD)(OMe)]_2$ (5 mg, 0.008 mmol, 3 mol%), $B_2pin_2$ (95.2 mg, 0.375 mmol, 1.5 equiv.), **L27** (3.4 mg, 0.015 mmol, 6 mol%) in THF (1.25 mL) were heated at 65 °C for 24 h. The crude mixture was purified by column chromatography (Hex/EtOAc 20% to Hex/EtOAc 80%) to obtain 112 mg (90% yield) of **35** as an off-white solid.

**$^1$H NMR** (400.16 MHz, $CDCl_3$, 258 K) δ 7.78 (d, *J* = 2.1 Hz, 1H), 7.56 (dd, *J* = 8.2, 2.1 Hz, 1H), 7.51 (d, *J* = 8.2 Hz, 1H), 6.89 (d, *J* = 2.4 Hz, 1H), 6.65 (d, *J* = 9.1 Hz, 1H), 6.60 (dd, *J* = 9.1, 2.4 Hz, 1H), 3.79 (s, 3H), 3.65 (s, 3H), 3.63 (s, 2H), 2.32 (s, 3H), 0.98 (s, 12H).
**$^{13}$C NMR** (100.63 MHz, $CDCl_3$, 258 K) δ 171.42 (CO), 169.52 (CO), 155.74 (C, Ar), 140.37 (C, Ar), 136.76 (C, Ar), 136.54 (C, Ar), 135.03 (CH, Ar), 131.42 (CH, Ar), 130.84 (C, Ar), 130.42 (C, Ar), 129.68 (CH, Ar), 115.46 (CH, Ar), 112.43 (C, Ar), 111.24 (CH, Ar), 100.94 (CH, Ar), 84.39 (C), 55.59 (O–$CH_3$), 52.28 (O–$CH_3$), 30.12 ($CH_2$), 24.31 ($CH_3$), 13.98 ($CH_3$).
**$^{11}$B NMR** (128.39 MHz, $CDCl_3$, 258 K) δ 29.56
**HRMS (ESI)**. Calculated for $C_{26}H_{29}BClNNaO_6^+$: 520.16687 Obtained: 520.16732.

USC UNIVERSIDADE DE SANTIAGO DE COMPOSTELA

*10.2.7.49 Ethyl 4-amino-2-(4,4,5,5-tetramethyl-1,3,2-dioxaborolan-2-yl)benzoate (37)*

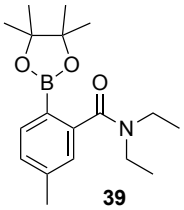


**37**

Following the general procedure: Benzocaine (**36**) (41.3 mg, 0.250 mmol, 1.0 equiv.), $[Ir(COD)(OMe)]_2$ (5 mg, 0.008 mmol, 3 mol%), $B_2pin_2$ (95.2 mg, 0.375 mmol, 1.5 equiv.), **L28** (4.4 mg, 0.015 mmol, 0.06 equiv.) in THF (1.25 mL) were heated at 100 °C for 1 h. The crude mixture was purified by column chromatography (Hex/EtOAc 20% to Hex/EtOAc 80%) to obtain 39 mg (53% yield) of **37** as an off-white solid.

**$^1$H NMR** (400.16 MHz, $CDCl_3$, 258K) δ 7.75 (d, *J* = 8.4 Hz, 1H), 6.66 (d, *J* = 2.4 Hz, 1H), 6.57 (dd, *J* = 8.5, 2.5 Hz, 1H), 4.31 (d, *J* = 7.1 Hz, 1H), 1.40 (s, 12H), 1.33 (t, *J* = 7.1 Hz, 3H).
**$^{13}$C NMR** (100.63 MHz, $CDCl_3$, 258K) δ 168.04 (CO), 149.95 (C, Ar), 130.82 (CH, Ar), 123.22 (C, Ar), 117.60 (CH, Ar), 114.25 (CH, Ar), 83.94(C), 60.68 (O–$CH_2$), 24.97 ($CH_3$), 14.53 ($CH_3$).
**$^{11}$B NMR** (128.39 MHz, $CDCl_3$, 258 K) δ 33.16
**HRMS (ESI).** Calculated for $C_{15}H_{22}BNNaO_4^+$: 314.15341 Obtained: 314.15363.

*10.2.7.50 N,N-diethyl-5-methyl-2-(4,4,5,5-tetramethyl-1,3,2-dioxaborolan-2-yl)benzamide (39)*



**39**

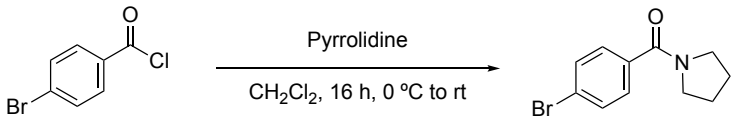
Following the general procedure: **38** (47.8 mg, 0.250 mmol, 1.0 equiv.), $[Ir(COD)(OMe)]_2$ (5 mg, 0.008 mmol, 3 mol%), $B_2pin_2$ (95.2 mg, 0.375 mmol, 1.5 equiv.), **L27** (3.4 mg, 0.015 mmol, 0.06 equiv.) in THF (1.25 mL) were heated at 100 °C for 2 h. The crude mixture was purified by column chromatography (Hex/EtOAc 20% to Hex/EtOAc 80%) to obtain 58 mg (73% yield) of **39** as an off-white solid.

**$^1$H NMR** (400.16 MHz, $CDCl_3$, 258K) δ 7.69 (d, *J* = 7.6 Hz, 1H), 7.16 (ddd, *J* = 7.6, 1.7, 0.8 Hz, 1H), 7.07 (dd, *J* = 1.6, 0.8 Hz, 1H), 3.55 (q, *J* = 7.1 Hz, 2H), 3.16 (q, *J* = 7.1 Hz, 2H), 2.34 (s, 3H), 1.27 (s, 15H), 1.02 (t, *J* = 7.1 Hz, 3H).
**$^{13}$C NMR** (100.63 MHz, $CDCl_3$, 258K) δ 171.89 (CO), 142.69 (C, Ar), 141.22 (C, Ar), 135.36 (CH, Ar), 128.97 (CH, Ar), 126.10 (CH, Ar), 83.42 (C), 42.79 (N–$CH_2$–$CH_3$), 39.31 (N–$\underline{C}H_2$–$CH_3$), 24.91 ($CH_3$), 21.81 (Ar–$CH_3$), 13.76 ($CH_2$–$\underline{C}H_3$), 12.48 ($CH_2$–$\underline{C}H_3$).
**$^{11}$B NMR** (128.39 MHz, $CDCl_3$, 258 K) δ 29.33
**HRMS (ESI).** Calculated for $C_{18}H_{28}BNNaO_3^+$: 340.20578 Obtained: 340.20568

USC UNIVERSIDADE DE SANTIAGO DE COMPOSTELA

## 10.2.8 Pre*para*tion of fungicide 41

### *10.2.8.1 Synthesis of (4-bromophenyl)(pyrrolidin-1-yl)methanone (40)*



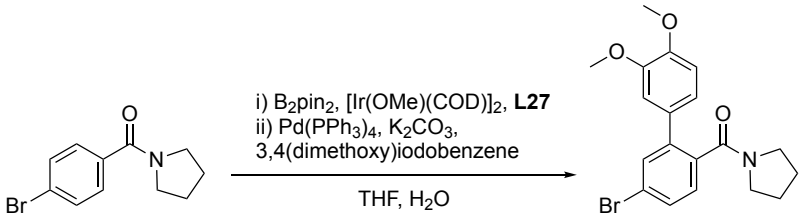

**40**

To a solution of 4-bromobenzoyl chloride (1.097 g, 5.0 mmol, 1.0 equiv.) in $CH_2Cl_2$ (20 mL) at 0 °C was added pyrrolidine (4.1 mL, 20.0 mmol, 4.0 equiv.) dropwise. The reaction mixture was stirred continuously at room temperature overnight.

The reaction was then quenched with water and organic materials were extracted twice with $CH_2Cl_2$, washed first with 1.0 M aqueous HCl solution followed by a second wash with saturated aqueous $NaHCO_3$ solution and brine. The organic fraction was dried over $MgSO_4$ and the solvent was removed in vacuo to obtain the 4-(4-bromophenyl)(pyrrolidin-1-yl)methanone in a 90% yield (1.143 g) as a white solid.

**$^1$H NMR** (400.16 MHz, $CDCl_3$, 258 K) δ 7.53 (d, *J* = 8.6 Hz, 2H), 7.40 (d, *J* = 8.6 Hz, 2H), 3.61 (t, *J* = 7.0 Hz, 2H), 3.41 (t, *J* = 6.6 Hz, 2H), 1.97 (tt, *J* = 7.6, 5.8 Hz, 2H), 1.92 – 1.85 (m, 2H).
**$^{13}$C NMR** (100.63 MHz, $CDCl_3$, 258 K) δ 168.74 (CO), 135.74 (C, Ar), 131.53 (CH, Ar), 128.93 (CH, Ar), 124.25(C, Ar), 49.85 ($CH_2$), 46.46 ($CH_2$), 26.51 ($CH_2$), 24.55 ($CH_2$).
**HRMS (ESI).** Calculated for $C_{11}H_{13}BrNO^+$: 254.0175 Obtained: 254.0180

### *10.2.8.2 Synthesis of (5-bromo-3',4'-dimethoxy-[1,1'-biphenyl]-2-yl)(pyrrolidin-1-yl)methanone (41)*




**40** **41**

To a sealed tube $[Ir(COD)(OMe)]_2$ (0.008 mmol, 3 mol%), $B_2pin_2$ (0.375 mmol, 1.5 equiv.), and **L27** (0.015 mmol, 6 mol%) were added. The tube was evacuated and refilled with $N_2$ three times, then under a positive flow of $N_2$, dry THF (1.25 mL) and **40** (0.250 mmol, 1.0 equiv.) were added. The tube was then sealed and heated at 65 °C for 1.5 h. After that time the reaction mixture was cooled to room temperature and $H_2O$ was added under a positive flow of $N_2$. Then the mixture was degassed via freeze-thaw (5 cycles) and $Pd(PPh_3)_4$, $K_2CO_3$ and 3,4-(dimethoxy)iodobenzene were added under a positive flow of $N_2$. The reaction was heated at 100 °C overnight.

After cooling to room temperature, the reaction mixture was diluted with EtOAc (10 mL) and extracted $H_2O$ (10 mL) and brine (10 mL). The organic layer was concentrated under reduced pressure. The residue was purified by column chromatography on silica

USC UNIVERSIDADE DE SANTIAGO DE COMPOSTELA

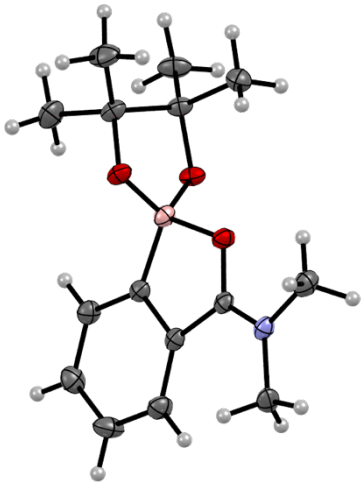
gel (Hex/EtOAc 50% to EtOAc/MeOH 10%) to give the product **41** (47 mg, 48% yield) as a white solid.

**$^{1}$H NMR** (400.16 MHz, $CDCl_3$, 258 K) δ 7.57 (d, *J* = 2.0 Hz, 1H), 7.48 (dd, *J* = 8.1, 2.0 Hz, 1H), 7.27 (d, *J* = 7.9 Hz, 1H), 7.07 (d, *J* = 2.1 Hz, 1H), 7.02 (dd, *J* = 8.2, 2.1 Hz, 1H), 6.89 (d, *J* = 8.3 Hz, 1H), 3.90 (s, 3H), 3.89 (s, 3H), 3.40 (t, *J* = 7.1 Hz, 2H), 2.76 (t, *J* = 6.7 Hz, 2H), 1.67 (t, *J* = 8.1, 6.6 Hz, 2H), 1.52 (t, *J* = 6.7 Hz, 2H).
**$^{13}$C NMR** (100.63 MHz, $CDCl_3$, 258 K) δ 169.08 (CO), 149.36 (C, Ar), 149.16 (C, Ar), 140.29 (C, Ar), 135.85 (C, Ar), 132.26 (CH, Ar), 131.57 (C, Ar), 130.44 (CH, Ar), 128.96 (CH, Ar), 123.33 (C, Ar), 120.94 (CH, Ar), 112.08 (CH, Ar), 111.52 (CH, Ar), 56.30 (O–$CH_3$), 56.12 (O–$CH_3$), 47.63 (N–$CH_2$), 45.64 (N–$CH_2$), 25.74 ($CH_2$), 24.34 ($CH_2$).
**HRMS (ESI)**. Calculated for $C_{19}H_{20}BBrNNaO_3^+$: 412.05188 Obtained: 412.05198.

USC
UNIVERSIDADE DE SANTIAGO DE COMPOSTELA

## 10.2.9 Crystallographic data

### *10.2.9.1 X-Ray structure of 24a*



CCDC 2095587 contains the supplementary crystallographic data for **24a**

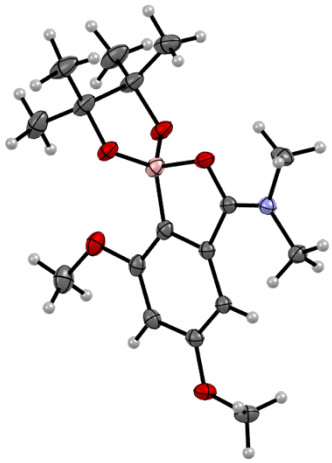
These data can be obtained free of charge via *www.ccdc.cam.ac.uk/conts/retrieving.html* (or from the Cambridge Crystallographic Data Centre, 12 Union Road, Cambridge CB21EZ, UK; fax: (+44)1223-336-033; or *deposit@ccdc.cam.ac.uk*).

**Table *24*** Crystal data and structure refine for compound ***24a***

Molecular Formula = $C_{15}H_{22}BNO_3$
Mr = 275.14
*Ortho*rhombic, Pna21
a = 15.4272 (8) Å
b = 27.6198 (14) Å
c = 7.1168 (4) Å
V = 3032.4 (3) Å3
Z = 8
F(000) = 1184
Dx = 1.205 Mg m−3
Cu Kα radiation, λ = 1.54178 Å
Cell *para*meters from 9829 reflections
θ = 3.3–78.9°
μ = 0.66 mm−1
T = 100 K
Prism, clear colorless
0.43 × 0.07 × 0.05 mm

USC UNIVERSIDADE DE SANTIAGO DE COMPOSTELA

### *10.2.9.2 X-Ray structure of 24an*



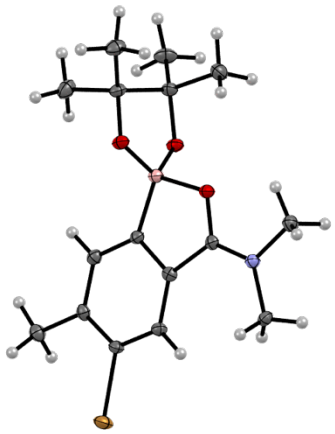
CCDC 2095584 contains the supplementary crystallographic data for **24an**

These data can be obtained free of charge via *www.ccdc.cam.ac.uk/conts/retrieving.html* (or from the Cambridge Crystallographic Data Centre, 12 Union Road, Cambridge CB21EZ, UK; fax: (+44)1223-336-033; or *deposit@ccdc.cam.ac.uk*).

**Table *25*** Crystal data and structure refine for compound **24an**

Molecular Formula = $C_{17}H_{26}BNO_5 \cdot H_2O$
Mr = 353.21
Monoclinic, P21/n
a = 7.0679 (2) Å
b = 23.8611 (7) Å
c = 11.2533 (3) Å
β = 97.9404 (12)°
V = 1879.65 (9) Å3
Z = 4
F(000) = 760
Dx = 1.248 Mg m−3
Cu Kα radiation, λ = 1.54178 Å
Cell *para*meters from 9957 reflections
θ = 5.4–79.1°
μ = 0.76 mm−1
T = 100 K
Needle, clear colorless
0.62 × 0.17 × 0.05 mm

### *10.2.9.3 X-Ray structure of 24ao*



CCDC *2095495* contains the supplementary crystallographic data for **24ao**

These data can be obtained free of charge via *www.ccdc.cam.ac.uk/conts/retrieving.html* (or from the Cambridge Crystallographic Data Centre, 12 Union Road, Cambridge CB21EZ, UK; fax: (+44)1223-336-033; or *deposit@ccdc.cam.ac.uk*).

**Table *26*** Crystal data and structure refine for compound **24ao**

Molecular Formula = C16H23BBrNO3
Mr = 368.07
Monoclinic, P21/n
a = 7.3498 (6) Å
b = 21.3668 (16) Å
c = 10.9096 (7) Å
β = 101.352 (3)°
V = 1679.7 (2) Å3
Z = 4
F(000) = 760
Dx = 1.455 Mg m−3
Mo Kα radiation, λ = 0.71073 Å
Cell *para*meters from 9203 reflections
θ = 2.7–30.2°
μ = 2.46 mm−1
T = 100 K
Plate, clear colorless
0.24 × 0.17 × 0.05 mm

## 10.3 Computational analysis for section 7.2

### 10.3.1 Calculated structures for borylation pre-catalytic species

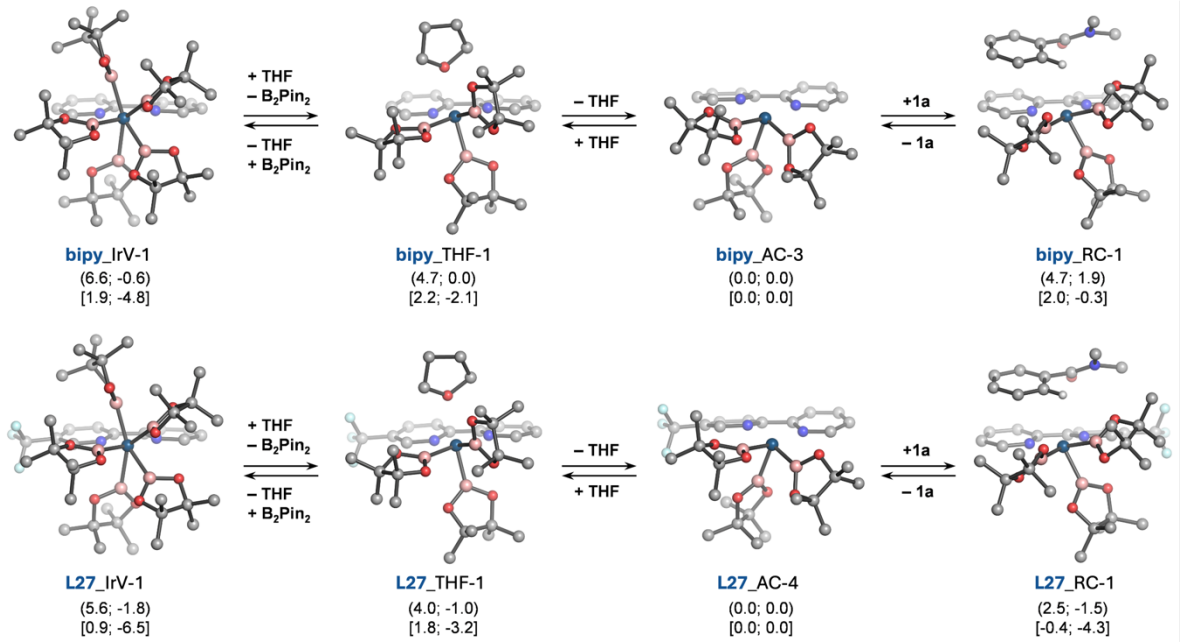



**Figure *70*** Pre-catalytic $Ir^{V}(Bpin)_5$, $Ir^{III}(THF)(Bpin)_3$, active catalyst (AC), and out-sphere reactive complexes (RC) calculated for ligands **bipy** and **L27**. Non-reactive hydrogens have been omitted for clarity. Free energies relative to the lowest energy Ir(III) active catalyst ($\Delta G_{QH}$ in kcal $mol^{-1}$) calculated with $SMD_{THF}$ and IEF-$PCM_{THF}$/M06/6-311++G(2d,p)+SDD(Ir)//M06/6-31G(d)+LANL2DZ(Ir) are given in parentheses, and with $SMD_{THF}$ and IEF-$PCM_{THF}$/M06/6-311G(2d,p)+SDD(Ir)//M06/6-31G(d)+LANL2DZ(Ir) in brackets, respectively

## 10.3.2 Calculated structures for benzamide borylation with Ir(I) catalysts

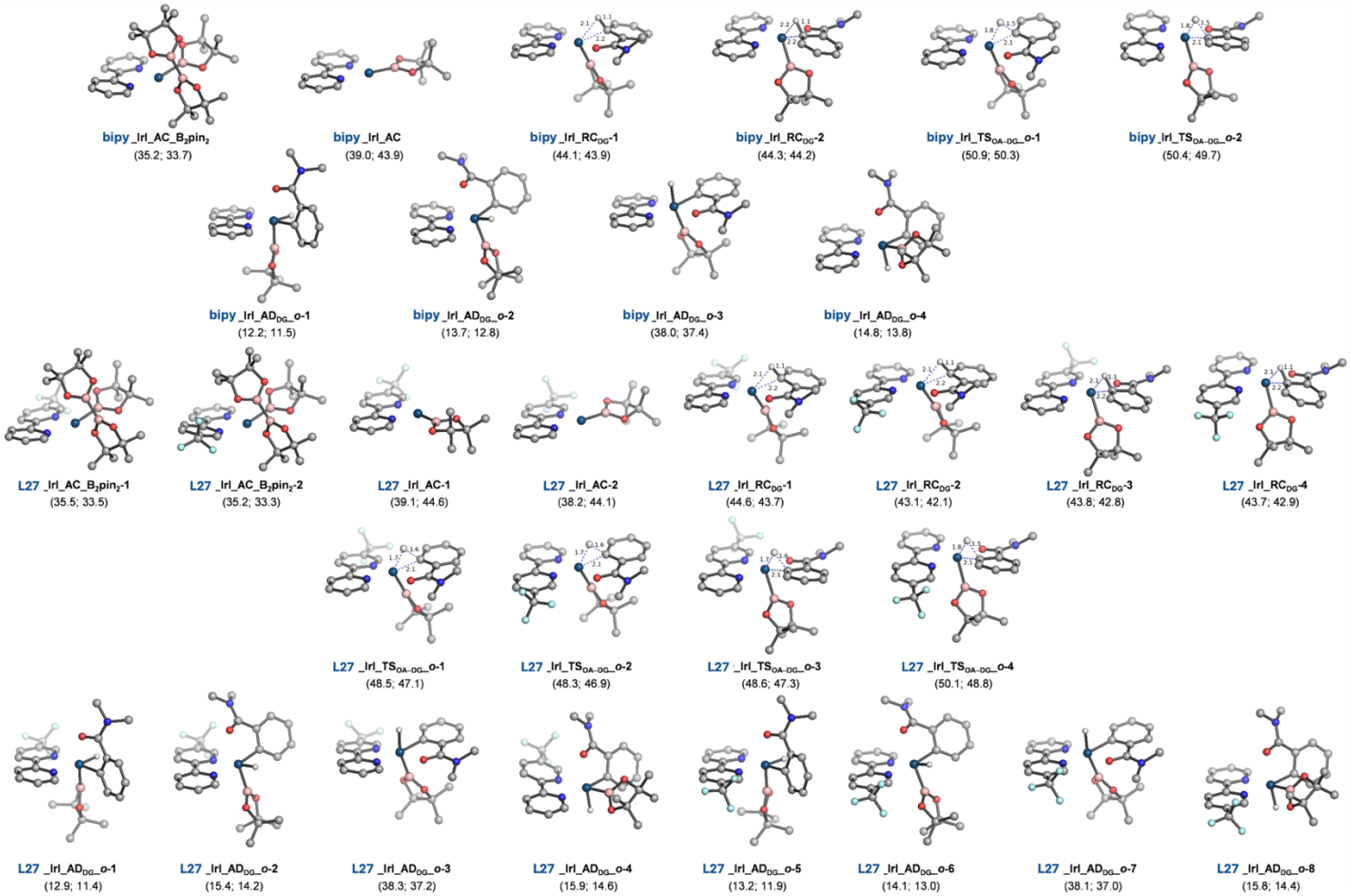
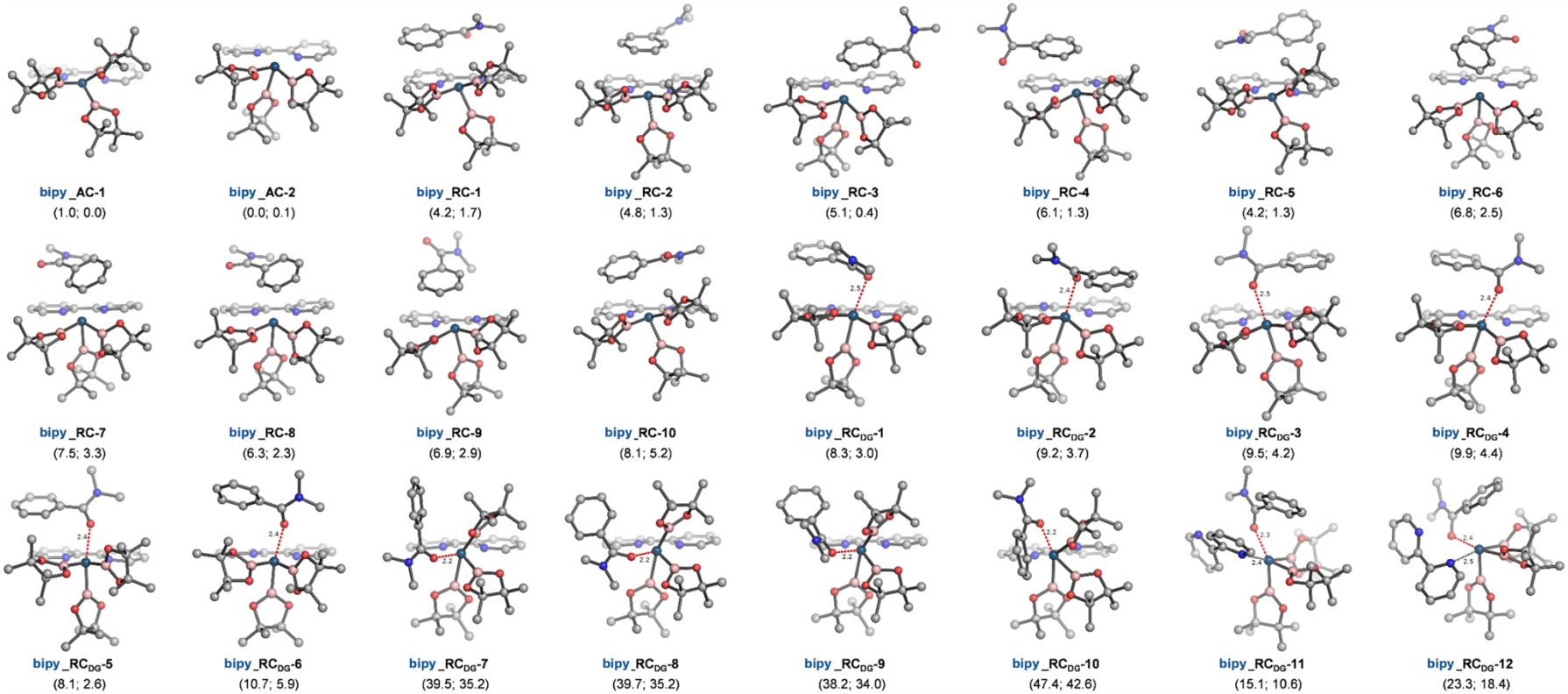



**Figure *71*** Active catalyst (AC), directing-group reactive complexes ($RC_{DG}$) and directing-group transition states ($TS_{DG}$) calculated for the oxidative addition step between *N*,*N*-dimethylbenzamide (**23a**) and $Ir^{I}$(**bipy**)$(Bpin)_3$ or $Ir^{I}$(**L27**)$(Bpin)_3$ (*o* = *ortho*, *m* = *meta*, *p* = *para*). Non-reactive hydrogens have been omitted for clarity. Free energies relative to the lowest energy Ir(III) active catalyst ($\Delta G_{QH}$ in kcal $mol^{-1}$) calculated with $SMD_{THF}$ and IEF-$PCM_{THF}$/M06/6-311++G(2d,p)+SDD(Ir)//M06/6-31G(d)+LANL2DZ(Ir) are given in parentheses.

## 10.3.3 Calculated structures for benzamide borylation with ligand bipy and Ir(III) catalyst



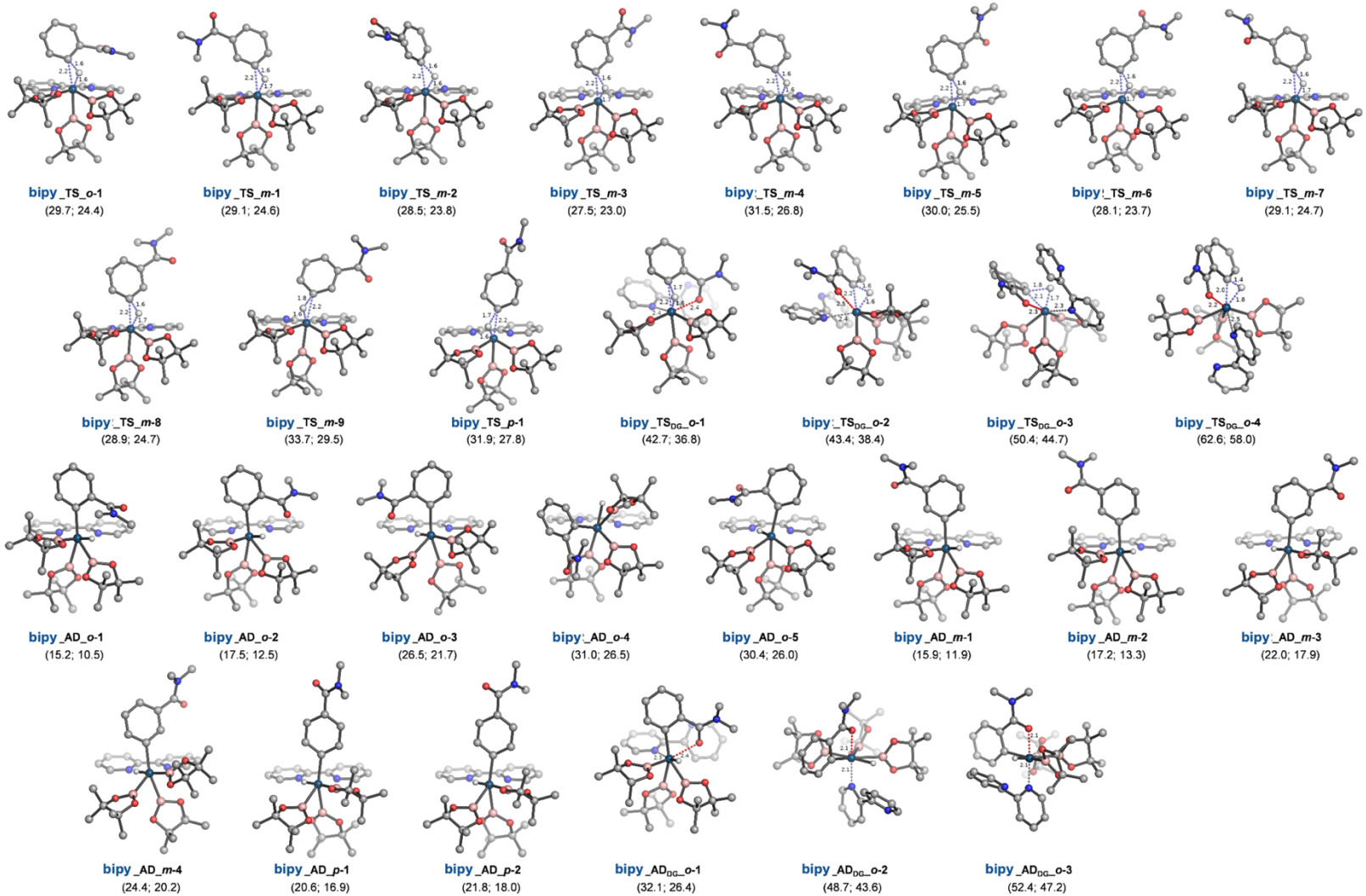



**Figure *72*** Active catalyst (AC), outer-sphere (RC) and directing-group ($RC_{DG}$) reactive complexes, outer-sphere (TS) and directing-group ($TS_{DG}$) transition states and outer-sphere (AD) and directing-group ($AD_{DG}$) reaction adducts calculated for the oxidative addition step between *N*,*N*-dimethylbenzamide (**23a**) and $Ir^{III}$(**bipy**)$(Bpin)_3$ (*o* = *ortho*, *m* = *meta*, *p* = *para*). Non-reactive hydrogens have been omitted for clarity. Free energies relative to the lowest energy active catalyst (AC) ($\Delta G_{QH}$ in kcal $mol^{-1}$) calculated with $SMD_{THF}$ and $IEF\text{-}PCM_{THF}$/M06/6-311++G(2d,p)+SDD(Ir)//M06/6-31G(d)+LANL2DZ(Ir) are given in parentheses.

## 10.3.4 Calculated structures for benzamide borylation with ligand L27 and Ir(III) catalyst

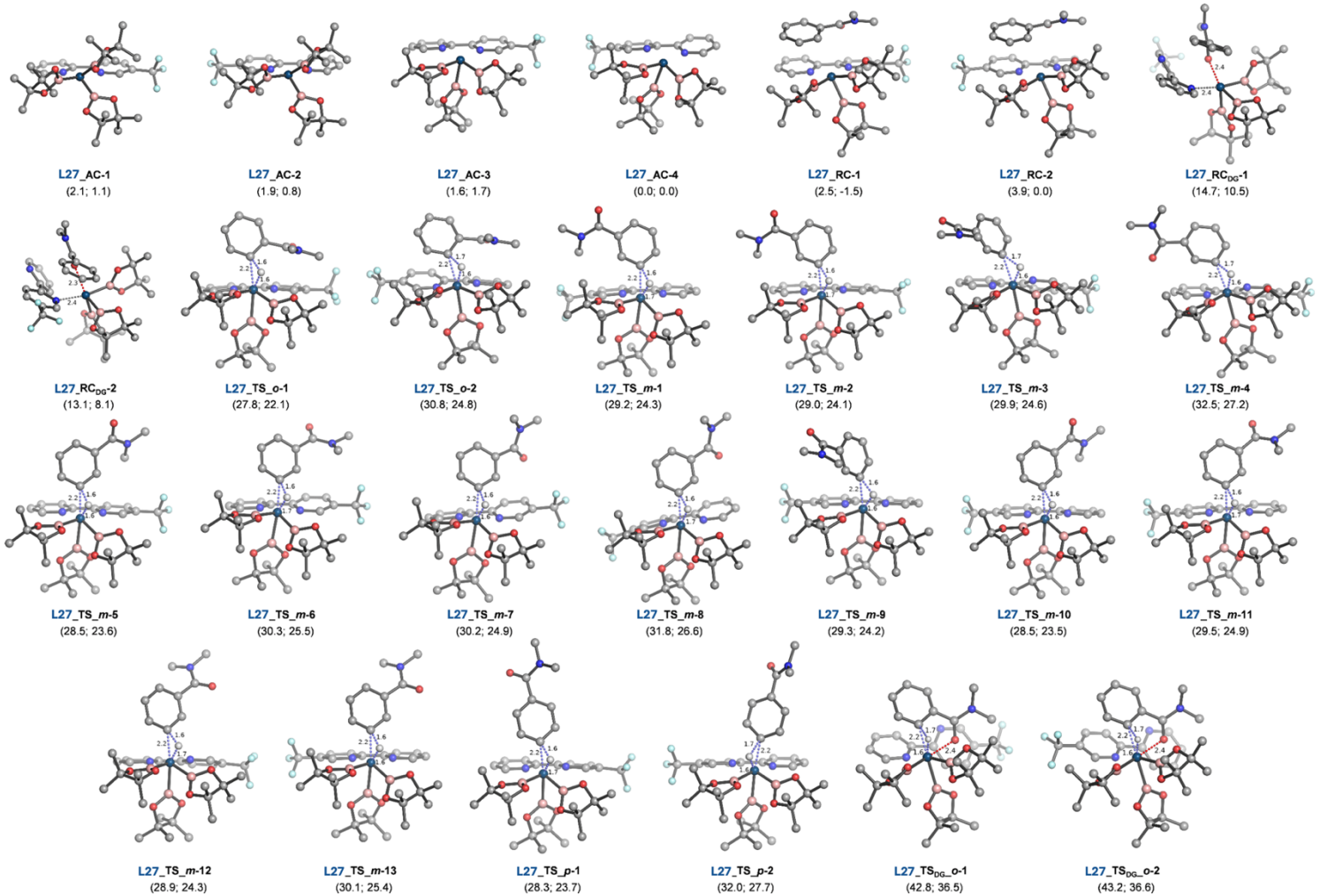
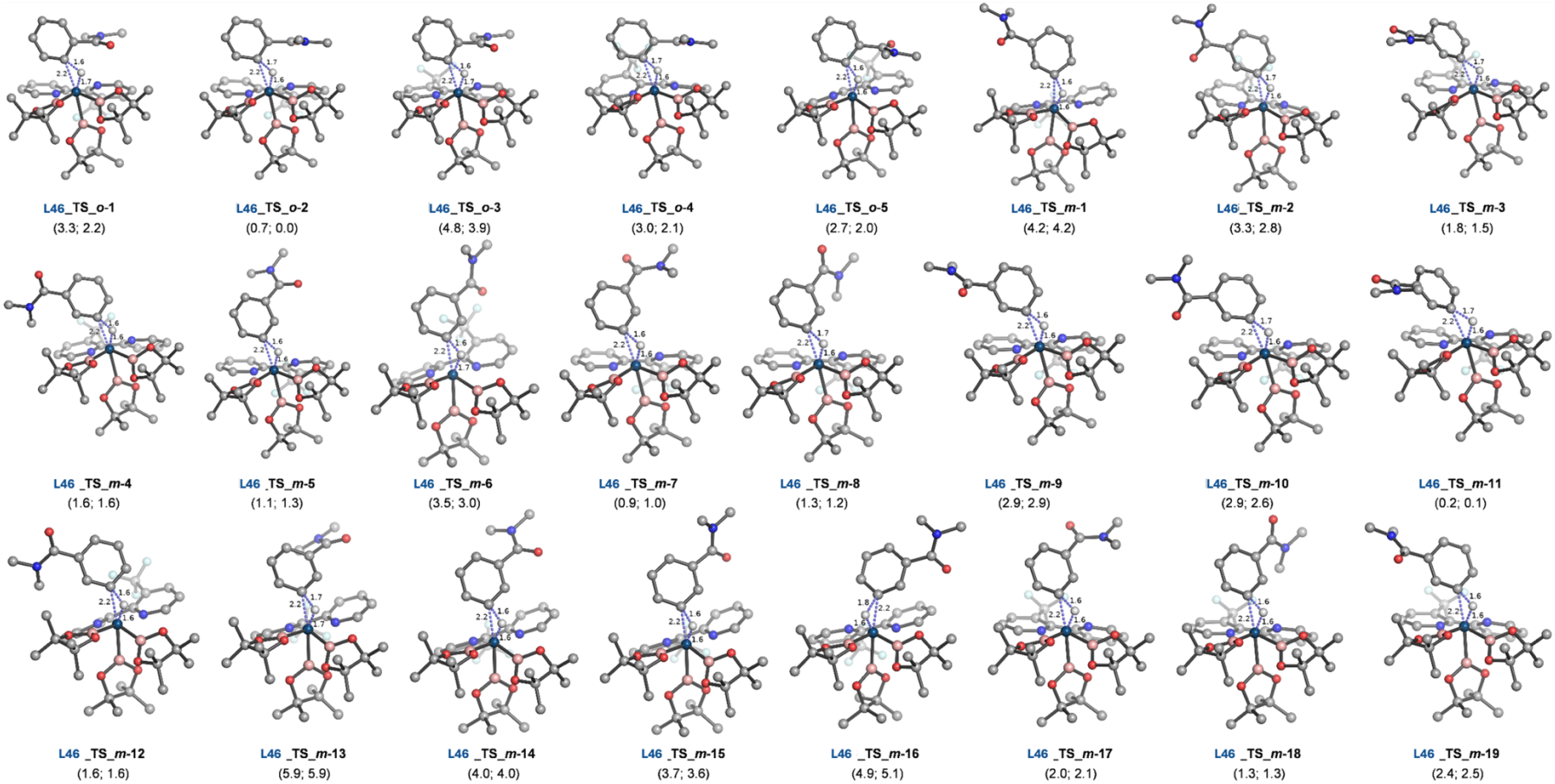



**Figure *73*** Active catalyst (AC), outer-sphere (RC) and directing-group ($RC_{DG}$) reactive complexes, outer-sphere (TS) and directing-group ($TS_{DG}$) transition states calculated for the oxidative addition step between *N*,*N*-dimethylbenzamide (**23a**) and $Ir^{III}$(L**27**)$(Bpin)_3$ (*o* = *ortho*, *m* = *meta*, *p* = *para*). Non-reactive hydrogens have been omitted for clarity. Free energies relative to the lowest energy active catalyst (AC) ($\Delta G_{QH}$ in kcal $mol^{-1}$) calculated with $SMD_{THF}$ and IEF-$PCM_{THF}$/M06/6-311++G(2d,p)+SDD(Ir)//M06/6-31G(d)+LANL2DZ(Ir) are given in parentheses.

## 10.3.5 Calculated structures for benzamide borylation with ligand L46 and Ir(III) catalyst



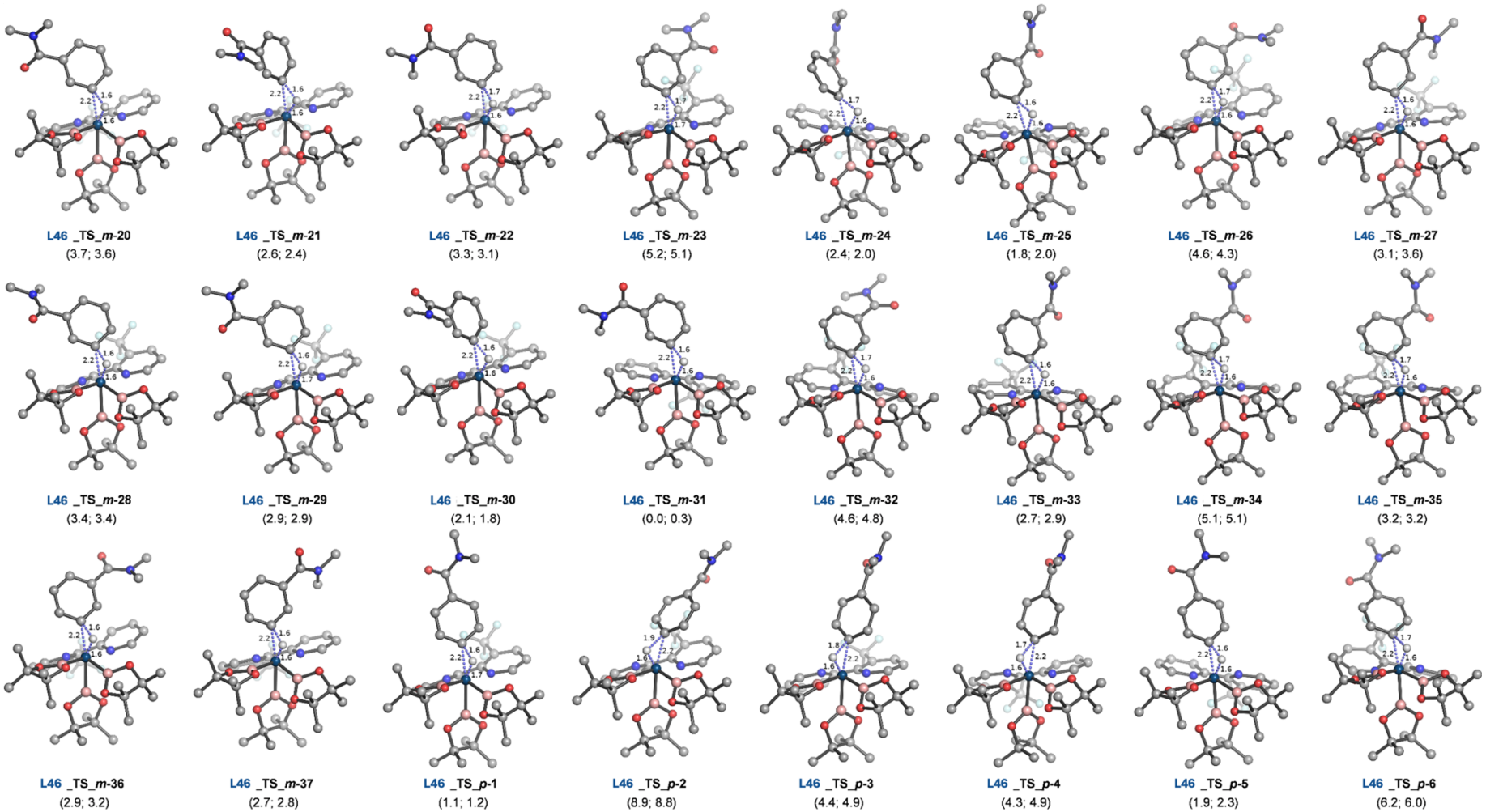



**Figure *74*** Outer-sphere transition states (TS) calculated for the oxidative addition step between *N*,*N*-dimethylbenzamide (**23a**) and $Ir^{III}$(**L46**)$(Bpin)_3$ (*o* = *ortho*, *m* = *meta*, *p* = *para*). Non-reactive hydrogens have been omitted for clarity. Relative activation free energies ($\Delta\Delta G^{\ddagger}_{QH}$ in kcal $mol^{-1}$) calculated with $SMD_{THF}$ and IEF-$PCM_{THF}$/M06/6-311++G(2d,p)+SDD(Ir)//M06/6-31G(d)+LANL2DZ(Ir) are given in parentheses.

## 10.3.6 Calculated structures for benzamide borylation with ligand L47 and Ir(III) catalyst

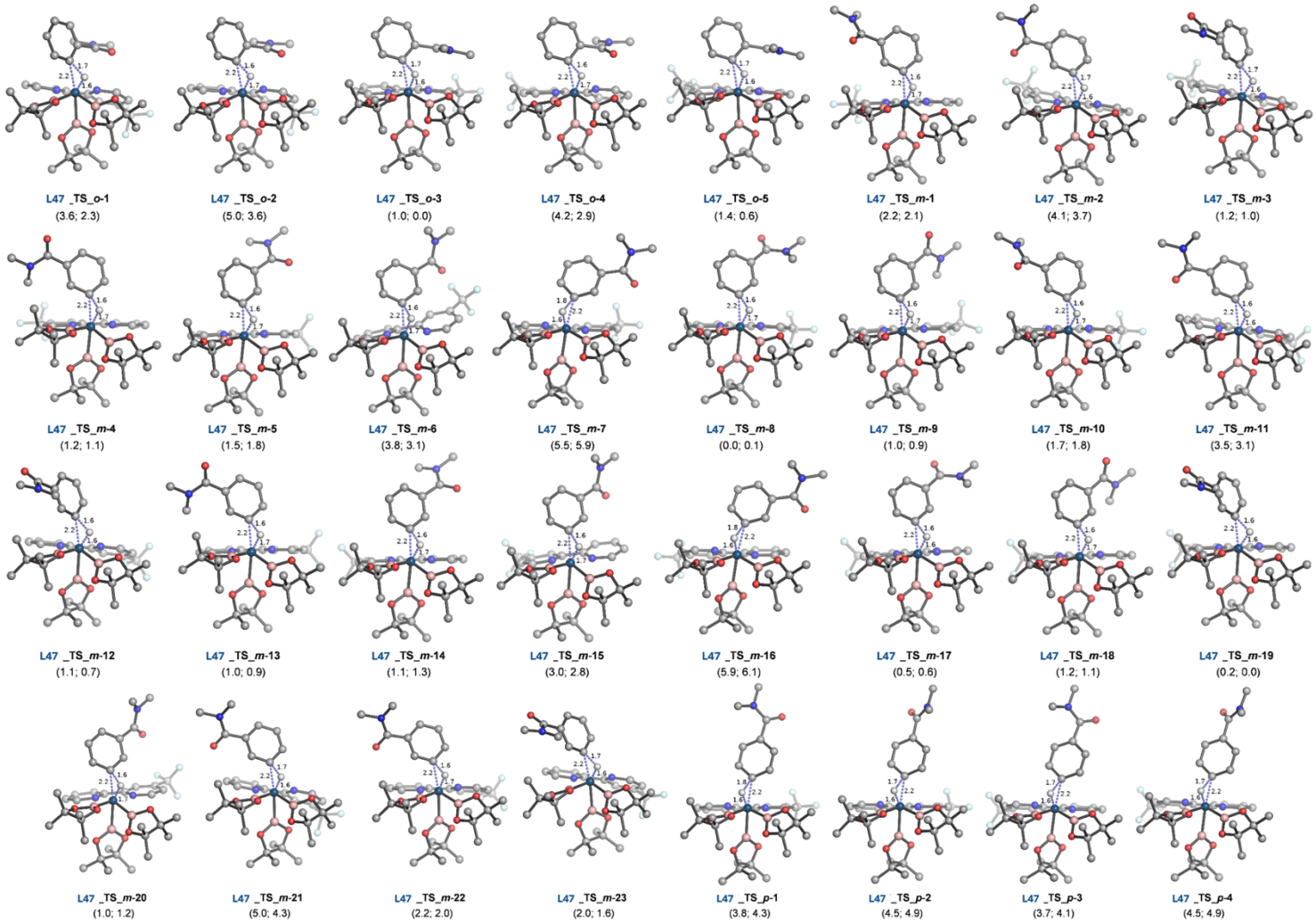



**Figure *75*** Outer-sphere transition states (TS) calculated for the oxidative addition step between *N*,*N*-dimethylbenzamide (**23a**) and $Ir^{III}$(**L47**)$(Bpin)_3$ (*o* = *ortho*, *m* = *meta*, *p* = *para*). Non-reactive hydrogens have been omitted for clarity. Relative activation free energies ($\Delta\Delta G^{\ddagger}_{QH}$ in kcal $mol^{-1}$) calculated with $SMD_{THF}$ and IEF-$PCM_{THF}$/M06/6-311++G(2d,p)+SDD(Ir)//M06/6-31G(d)+LANL2DZ(Ir) are given in parentheses.

### 10.3.7 Quantum theory of atoms in molecules (QTAIM) analysis

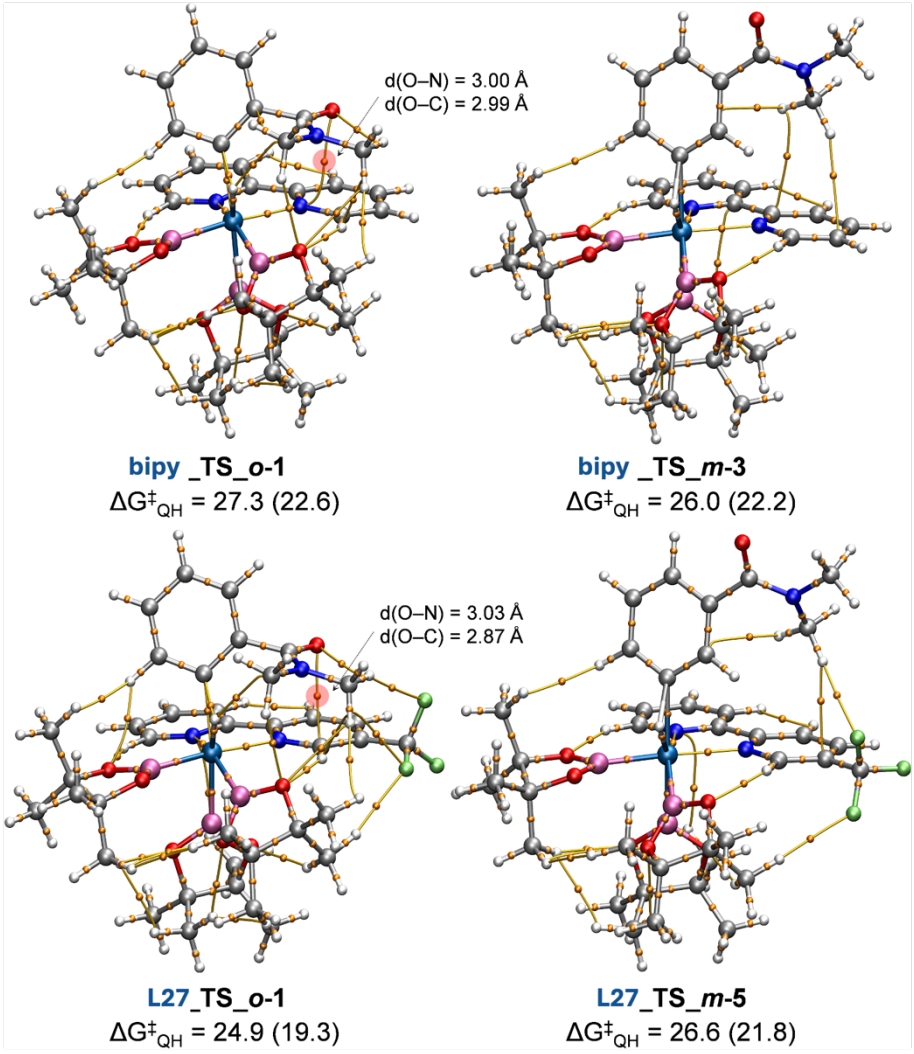



**Figure *76*** Bond critical points (BCP) (3,-1) determined from topology analysis of the electron density in low energy outer-sphere transition states (TS) calculated for the oxidative addition step between *N*,*N*-dimethylbenzamide (23a) and $Ir^{III}$(ligand)$(Bpin)_3$ (ligand = **bipy** and **L27**; *o* = *ortho*, *m* = *meta*). Activation free energies ($\Delta G^{\ddagger}_{QH}$) calculated with $SMD_{THF}$ and $IEF\text{-}PCM_{THF}$ (in parentheses) and M06/6-311G(2d,p)+SDD(Ir)//M06/6-31G(d)+LANL2DZ(Ir) are given in kcal $mol^{-1}$. The BCP between the substrate carbonyl O and bipyridine N or C atoms in the *ortho* transition states are highlighted with a red circle. Contacts between the substrate carbonyl O and bipyridine N and C atoms are represented as red dashed lines.

**Table *27*** Topological *para*meters of electron density at bond critical points (BCP) calculated for outer-sphere transition state **bipy** _TS_*o*-1. Values corresponding to the BCP between the substrate carbonyl O and bipyridine N atom (CO···$N_{bipy}$) are highlighted in red.

| | **C···H** (breaking bond) | **Ir···C** (forming bond) | **Ir···H** (forming bond) | **CO···$N_{bipy}$** (NCI) |
|---|---|---|---|---|
| **Density of all electrons: ρ(r)** | **0.0867** | **0.0924** | **0.1219** | **0.0099** |
| **Laplacian of electron density: $\nabla^2\rho(r)$** | 0.0432 | 0.1690 | 0.1270 | 0.0347 |
| **Lagrangian kinetic energy: G(r)** | 0.0363 | 0.0729 | 0.0813 | 0.0076 |
| **Potential energy density: V(r)** | –0.0619 | –0.1049 | –0.1327 | –0.0065 |
| **Total electronic energy density: H(r) = G(r) + V(r)** | –0.0255 | –0.0320 | –0.0514 | 0.0011 |
| **–G(r)/V(r)** | **0.5872** | **0.6952** | **0.6124** | **1.1692** |

**Table *28*** Topological *para*meters of electron density at bond critical points (BCP) calculated for outer-sphere transition state **bipy** _TS_*m*-3.

| | **C···H** (breaking bond) | **Ir···C** (forming bond) | **Ir···H** (forming bond) | **$CH_3$···$C_{bipy}$** (NCI) | **$CH_3$···$C_{bipy}$** (NCI) |
|---|---|---|---|---|---|
| **Density of all electrons: ρ(r)** | **0.0912** | **0.0967** | **0.1206** | **0.0032** | **0.0054** |
| **Laplacian of electron density: $\nabla^2\rho(r)$** | 0.0355 | 0.1742 | 0.1303 | 0.0108 | 0.0163 |
| **Lagrangian kinetic energy: G(r)** | 0.0372 | 0.0768 | 0.0810 | 0.0021 | 0.0032 |
| **Potential energy density: V(r)** | –0.0655 | –0.1114 | –0.1313 | –0.0015 | –0.0024 |
| **Total electronic energy density: H(r) = G(r) + V(r)** | –0.0283 | –0.0347 | –0.0503 | 0.0006 | 0.0008 |
| **–G(r)/V(r)** | **0.5678** | **0.6889** | **0.6170** | **1.4192** | **1.3436** |

**Table *29*** Topological *para*meters of electron density at bond critical points (BCP) calculated for outer-sphere transition state L**27**_TS_*o*-1. Values corresponding to the BCP between the substrate carbonyl O and bipyridine C atom (CO···$C_{bipy}$) are highlighted in red.

| | **C···H** (breaking bond) | **Ir···C** (forming bond) | **Ir···H** (forming bond) | **CO···$C_{bipy}$** (NCI) | **$CH_3$···$F_3C_{bipy}$** (NCI) | **$CH_3$···$F_3C_{bipy}$** (NCI) |
|---|---|---|---|---|---|---|
| **Density of all electrons: ρ(r)** | **0.0886** | **0.0919** | **0.1213** | **0.0118** | **0.0038** | **0.0066** |
| **Laplacian of electron density: $\nabla^2\rho(r)$** | 0.0390 | 0.1698 | 0.1289 | 0.0406 | 0.0191 | 0.0310 |
| **Lagrangian kinetic energy: G(r)** | 0.0364 | 0.0728 | 0.0814 | 0.0091 | 0.0036 | 0.0063 |
| **Potential energy density: V(r)** | –0.0631 | –0.1044 | –0.1324 | –0.0081 | –0.0024 | –0.0048 |
| **Total electronic energy density: H(r) = G(r) + V(r)** | –0.0267 | –0.0316 | –0.0510 | 0.0010 | 0.0012 | 0.0015 |
| **–G(r)/V(r)** | **0.5771** | **0.6971** | **0.6146** | **1.1301** | **1.4756** | **1.3015** |

**Table *30*** Topological *para*meters of electron density at bond critical points (BCP) calculated for outer-sphere transition state **L27**_TS_*m*-5.

| | **C···H** (breaking bond) | **Ir···C** (forming bond) | **Ir···H** (forming bond) | **$CH_3$···$C_{bipy}$** (NCI) | **$CH_3$···$F_3C_{bipy}$** (NCI) |
|---|---|---|---|---|---|
| **Density of all electrons: ρ(r)** | **0.0913** | **0.0963** | **0.1213** | **0.0064** | **0.0053** |
| **Laplacian of electron density: $\nabla^2\rho(r)$** | 0.0363 | 0.1752 | 0.1300 | 0.0199 | 0.0246 |
| **Lagrangian kinetic energy: G(r)** | 0.0374 | 0.0768 | 0.0815 | 0.0039 | 0.0048 |
| **Potential energy density: V(r)** | –0.0657 | –0.1112 | –0.1323 | –0.0029 | –0.0035 |
| **Total electronic energy density: H(r) = G(r) + V(r)** | –0.0283 | –0.0344 | –0.0508 | 0.0010 | 0.0013 |
| **–G(r)/V(r)** | **0.5690** | **0.6905** | **0.6158** | **1.3626** | **1.3793** |

USC UNIVERSIDADE DE SANTIAGO DE COMPOSTELA

### 10.3.8 Natural Bond Orbital (NBO) analysis

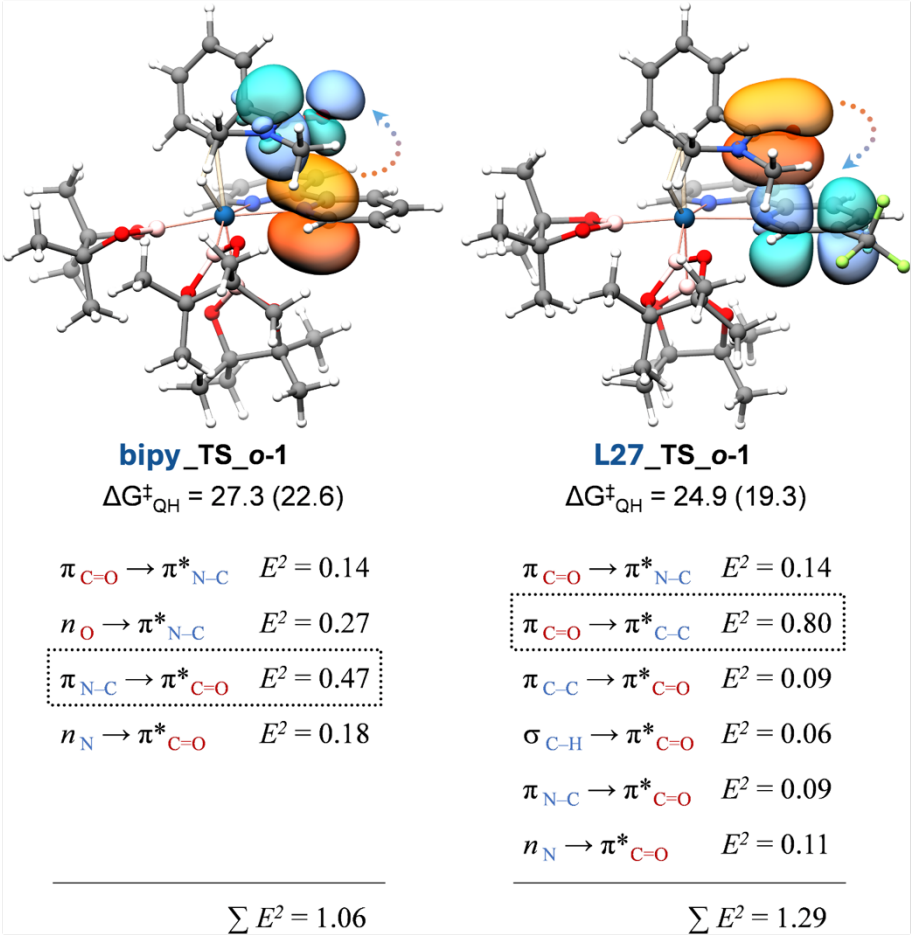



**Figure *77*** Natural Bond Orbital (NBO) analysis of the low energy outer-sphere transition states (TS) calculated for the *ortho* oxidative addition step between *N*,*N*-dimethylbenzamide (**23a**) and $Ir^{III}$(ligand)$(Bpin)_3$ (ligand = **bipy** and **L27**; *o* = *ortho*). Activation free energies ($\Delta G^{\ddagger}_{QH}$) calculated with $SMD_{THF}$ and IEF-$PCM_{THF}$ (in parentheses) and M06/6-311G(2d,p)+SDD(Ir)//M06/6-31G(d)+LANL2DZ(Ir) are given in kcal $mol^{-1}$. Attractive interactions between donor (i.e. occupied) and acceptor (i.e. unoccupied) orbitals at the benzamide substrate (atoms in red) and bipyridine ligand (atoms in blue), as well as their second-order perturbation energies ($E^2$ in kcal $mol^{-1}$) are shown. The aggregated energies of these interactions are shown as $\sum E^2$. The most favorable interaction for each structure is highlighted with a dashed box and the NBO orbitals involved in these interactions (donor in orange-red, acceptor in blue-green) are shown as semi-transparent surfaces (isovalue = 0.5). The direction of electron density donation is represented with gradient-colored dashed arrows. Note the change of the electron density donation from bipyridine-to-carbonyl in bipy to carbonyl-to-bipyridine with **L27** due to the electron-withdrawing effect of the $CF_3$ group.

### 10.3.9 Energy Decomposition Analysis (EDA)

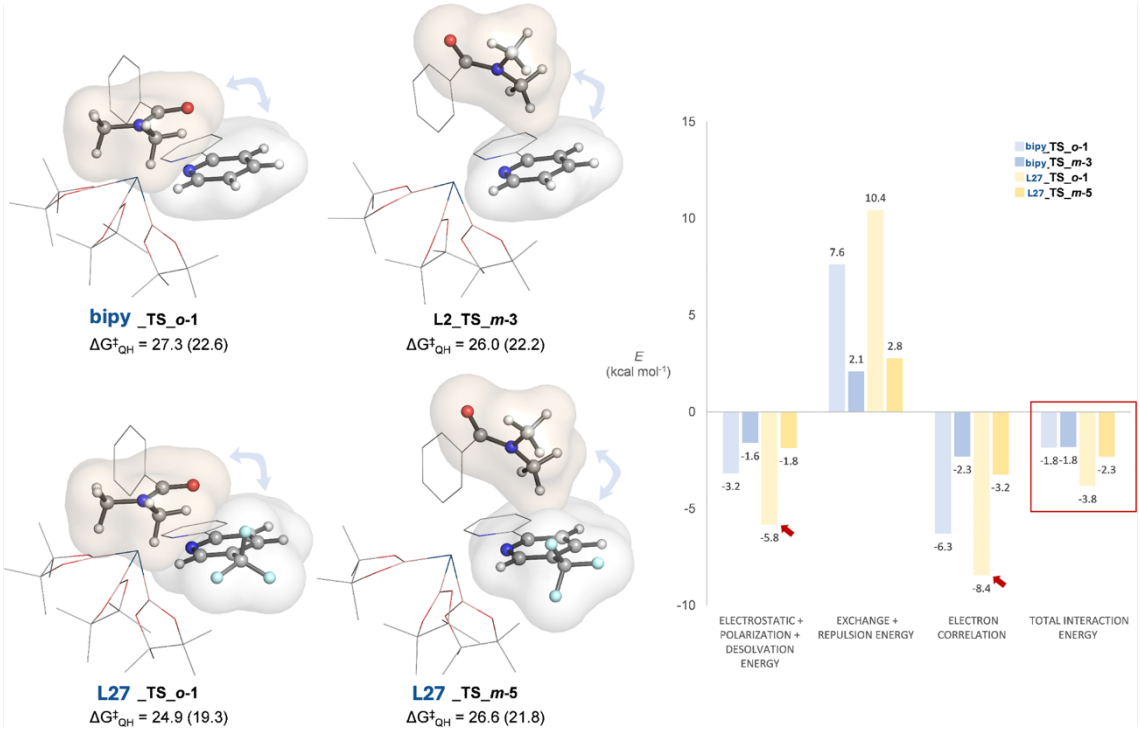



**Figure *78*** Generalized Kohn-Sham Energy Decomposition Analysis (GKS-EDA of the low energy outer-sphere transition states (TS) calculated for the oxidative addition step between *N*,*N*-dimethylbenzamide (**23a**) and $Ir^{III}$(ligand)$(Bpin)_3$ (ligand = **bipy** and **L27**; *o* = *ortho*, *m* = *meta*). Activation free energies ($\Delta G^{\ddagger}_{QH}$) calculated with $SMD_{THF}$ and $IEF\text{-}PCM_{THF}$ (in parentheses) and M06/6-311G(2d,p)+SDD(Ir)//M06/6-31G(d)+LANL2DZ(Ir) are given in kcal $mol^{-1}$. In the graphs, different contributions to the total interaction energy between the *N*,*N*-dimethylformamide and (5-trifluoromethyl)pyridine fragments are shown. Contributions related to the polar character of the interactions (electrostatic, polarization and desolvation) have been added together for clarity. The electron correlation component implicitly accounts for dispersion. The larger values for the attractive interactions (both polar and dispersion) occurring in the *ortho* borylation TS with ligand **L27**, resulting in a larger total interaction energy, are highlighted with red arrows.

### 10.3.10 Enthalpy-entropy compensation including quasiharmonic approximations to enthalpy and entropy




**Figure *79*** Relative activation enthalpies ($\Delta\Delta H^{\ddagger}_{QH}$), entropies ($-T\cdot\Delta\Delta S^{\ddagger}_{QH}$) and free energies ($\Delta\Delta G^{\ddagger}_{QH}$) for the *ortho* and *meta* reaction pathways derived from the lowest energy outer-sphere transition states (TS) calculated with $SMD_{THF}$/M06/6-311G(2d,p)+SDD(Ir)//M06/6-31G(d)+LANL2DZ(Ir) for the oxidative addition step between *N*,*N*-dimethylbenzamide (**23a**) and $Ir^{III}$(ligand)$(Bpin)_3$ (ligand = **bipy**, **L27**, **L46** and **L47**). Quasiharmonic approximations to enthalpy and entropy were either excluded (left) or included (right). Regioselectivity is defined as $\Delta\Delta E^{\ddagger}o\text{-}m = \Delta E^{\ddagger}o - \Delta E^{\ddagger}m$ (E = H, –T·S or G). Negative and positive values indicate a preference for the *ortho* and *meta* pathways, respectively. In all cases entropy (i.e. TS 'tightness') opposes and often supersedes enthalpy (i.e. TS 'strength') in terms of calculated regioselectivity.

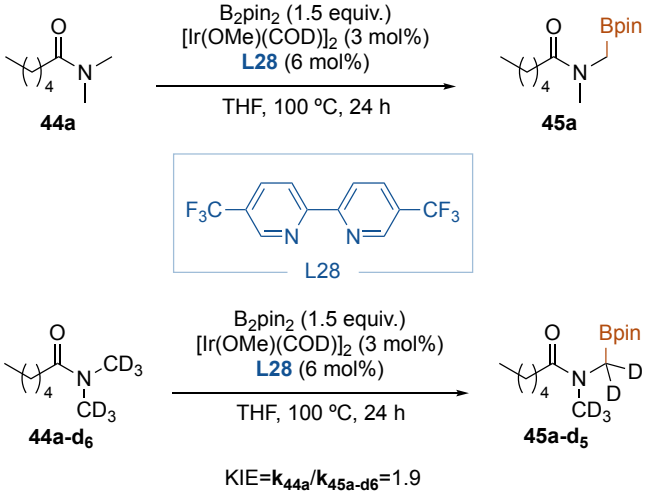
Enthalpy-entropy compensation is perfect in ligand **L46** ($\Delta\Delta G^{\ddagger}_{o\text{-}m} \approx 0$). and larger in ligands bipy and **L47**, for which regioselectivity is calculated to be entropy-driven (i.e. $-T\cdot\Delta\Delta S^{\ddagger}$ dominates over $\Delta\Delta H^{\ddagger}$). In contrast, for the *ortho*-directing $CF_3$-containing ligand L27, the underlying non-covalent interactions between substrate and the ligand are intense, and therefore the *ortho*-regioselectivity is enthalpy-driven.

These results suggest that in the tighter *ortho* TS there is a larger reduction of the reactants' translational and rotational degrees of freedom (larger entropic penalty) than in the looser *meta* TS. This is reflected by the systematic appearance of larger-amplitude normal modes (i.e. low frequency vibrations) in *meta* TS than in *ortho* TS, which in turn translate into larger $-T\cdot\Delta\Delta S^{\ddagger}$ values. Importantly, this enthalpy-entropy compensation trend was maintained when applying quasiharmonic approximations to both enthalpy and entropy, which aim at mitigating the well-documented inadequacy of the rigid rotor harmonic oscillator (RRHO) approach to calculating low frequency vibrations

# 10.4 Experimental procedures for section 7.3

## 10.4.1 Kinetic Isotope effects (KIE)

### *10.4.1.1 Parallel experiments*




KIE=$k_{44a}/k_{45a\text{-}d6}$=1.9

In a sealed tube [Ir(COD)(OMe)]$_2$ (5.0 mg, 0.008 mmol, 3 mol%.) and $B_2pin_2$ (95.2 mg 0.375 mmol, 1.5 equiv.) were added. The tube was evacuated and refilled with $N_2$ three times, then under a positive flow of $N_2$ the solids were dissolved in dry THF (1 mL). To that solution were added 125 µL of a solution 0.12 M of **L28** in THF (4.4 mg, 0.015 mmol, 6 mol%) and 125 µL of a solution 2 M of **44a** (35.8 mg, 0.250 mmol, 1.0 equiv.) or **44a-d$_6$** (37.3 mg, 0.250 mmol, 1.0 equiv.) in THF. The tube was then closed and heated at 100 ºC for the amount of time necessary.

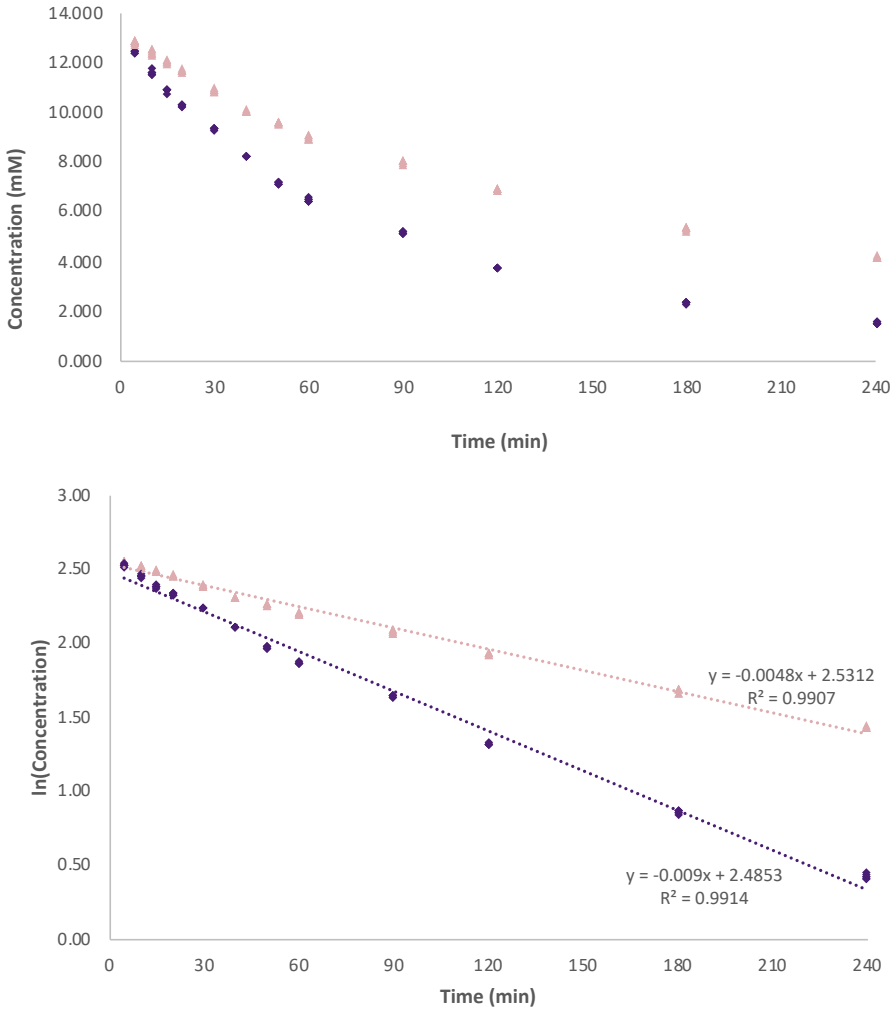



**Figure *80*** Profile of the reaction of 44a (purple markers) or 44a-$d_6$ (pink markers) and $B_2pin_2$ catalyzed by the combination of $[Ir(OMe)(COD)]_2$ and 5,5'-bis-$CF_3$-bipyridine ligand L28. The values of the slopes for the reaction of 1a and 1a-$d_6$ were $-9 \times 10^{-3}$ and $-4.8 \times 10^{-3}$ respectively, resulting in a KIE of 1.9.

### *10.4.1.2 Calculated kinetic isotopic effects*

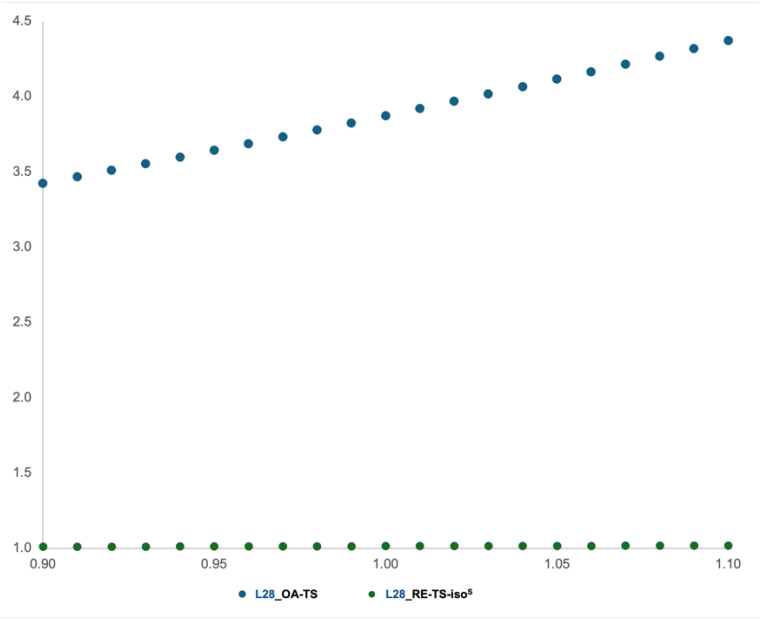
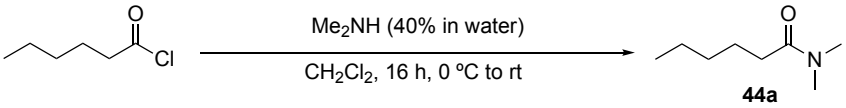



**Figure *81*** $^{2}D/^{1}H$ Kinetic isotopic effects (KIE) calculated at 298 K with M06/6-31G(d); LANL2DZ(Ir) for the oxidative addition (in blue) and reductive elimination (in green) steps in the borylation of *N*,*N*-dimethylhexanamide (**23a**) catalyzed by $Ir^{III}$(**L28**)$(Bpin)_3$, using different scaling factors for vibrational frequencies.

## 10.4.2 Synthesis of substrates

### *10.4.2.1 Preparation of N,N-dimethylhexanamide (44a)*

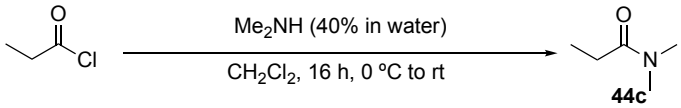



Prepared following an adapted procedure:[133] To a solution of hexanoyl chloride (0.70 mL, 5.0 mmol, 1 equiv.) in $CH_2Cl_2$ (10 mL) at 0 ºC, was added dropwise $Me_2NH$ (40 w/w% in water; 2.5 mL, 20.0 mmol, 4 equiv.). The reaction mixture was stirred continuously at room temperature overnight.

The reaction was then quenched with water and the mixture was extracted twice with $CH_2Cl_2$, then, the combined organic fractions were washed first with 1M aqueous HCl solution followed by a second wash with saturated aqueous $NaHCO_3$ solution and finally washed with brine. The organic fraction was dried over $MgSO_4$ and the solvent was removed in vacuo to obtain the *N,N*- dimethylhexanamide in a 92% yield (659 mg).

**$^1$H NMR** (400.16 MHz, $CDCl_3$, 258 K) δ 2.97 (s, 3H), 2.90 (s, 3H), 2.31 – 2.23 (m, 2H), 1.57 (dt, *J* = 15.4, 7.5 Hz, 2H), 1.26 (q, *J* = 2.7 Hz, 4H), 0.84 (t, *J* = 6.8 Hz, 3H).
**$^{13}$C NMR** (100.63 MHz, $CDCl_3$, 258 K) δ 173.43 (CO), 37.41 (N-$CH_3$), 35.37 (N-$CH_3$), 33.47 ($CH_2$), 31.67 ($CH_2$), 24.94 ($CH_2$), 22.60 ($CH_2$), 14.16 ($CH_3$).
**$^{15}$N NMR** (40.55 MHz, $CDCl_3$, 258 K) δ 100.54
**HRMS (ESI)**. Calculated for $C_8H_{18}NO^+$: 144.1383 Obtained: 144.1383

### *10.4.2.2 Preparation of N,N-dimethylpropionamide (44c)*



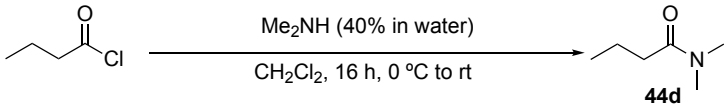

Prepared following an adapted procedure:[133] To a solution of propionyl chloride (0.44 mL, 5.0 mmol, 1 equiv.) in $CH_2Cl_2$ (20 mL) at 0 ºC, was added dropwise $Me_2NH$ (40 w/w% in water; 2.5 mL, 20.0 mmol, 4 equiv.). The reaction mixture was stirred continuously at room temperature overnight.

The reaction was then quenched with water and the mixture was extracted twice with $CH_2Cl_2$, then, the combined organic fractions were washed first with 1M aqueous HCl solution followed by a second wash with saturated aqueous $NaHCO_3$ solution and finally washed with brine. The organic fraction was dried over $MgSO_4$ and the solvent was removed in vacuo to obtain the N,N-dimethylpropionamide in a 68% yield (343 mg).

**$^1$H NMR** (400.16 MHz, $CDCl_3$, 258 K) δ 2.98 (s, 3H), 2.92 (s, 3H), 2.32 (q, *J* = 7.5 Hz, 2H), 1.10 (t, *J* = 7.5 Hz, 3H).
**$^{13}$C NMR** (100.63 MHz, $CDCl_3$, 258 K) δ 173.97 (CO), 37.22 (N-$CH_3$), 35.45 (N-$CH_3$), 26.66 ($CH_2$), 9.47 ($CH_3$).
**$^{15}$N NMR** (40.55 MHz, $CDCl_3$, 258 K) δ 99.90

**HRMS (ESI)**. Calculated for $C_5H_{12}NO^+$: 102.0913 Obtained: 102.0916

*10.4.2.3 Preparation of N,N-dimethylbutyramide (44d)*



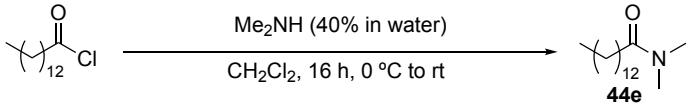

**44d**

Prepared following an adapted procedure:[133] To a solution of butyryl chloride (0.52 mL, 5.0 mmol, 1 equiv.) in $CH_2Cl_2$ (20 mL) at 0 ºC, was added dropwise $Me_2NH$ (40 w/w% in water; 2.5 mL, 20.0 mmol, 4 equiv.). The reaction mixture was stirred continuously at room temperature overnight.

The reaction was then quenched with water and the mixture was extracted twice with $CH_2Cl_2$, then, the combined organic fractions were washed first with 1M aqueous HCl solution followed by a second wash with saturated aqueous $NaHCO_3$ solution and finally washed with brine. The organic fraction was dried over $MgSO_4$ and the solvent was removed in vacuo to obtain the *N,N*-dimethylbutyramide in a 67% yield (385 mg).

**$^1$H NMR** (400.16 MHz, $CDCl_3$, 258 K) δ 2.97 (s, 3H), 2.90 (s, 3H), 2.31 – 2.22 (m, 2H), 1.60 (dq, *J* = 14.8, 7.4 Hz, 2H), 0.91 (t, *J* = 7.4 Hz, 3H).
**$^{13}$C NMR** (100.63 MHz, $CDCl_3$, 258 K) δ 173.25 (CO), 37.39 (N-$CH_3$), 35.39 ($CH_2$), 35.35 (N-$CH_3$), 18.61 ($CH_2$), 14.14 ($CH_2$).
**HRMS (ESI)**. Calculated for $C_6H_{14}NO^+$: 116.10699 Obtained: 116.10708

*10.4.2.4 Preparation of N,N-dimethylmyristoylamide (44e)*




**44e**

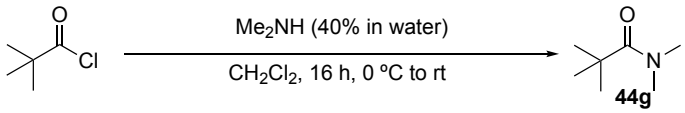
Prepared following an adapted procedure:[133] To a solution of myristoyl chloride (0.93 mL, 3.4 mmol, 1 equiv.) in $CH_2Cl_2$ (20 mL) at 0 ºC, were added dropwise $Me_2NH$ (40 w/w% in water; 0.6 mL, 5.1 mmol, 1.5 equiv.) and triethylamine (1.4 mL, 10.2 mmol, 3 equiv.). The reaction mixture was stirred continuously at room temperature overnight.

The reaction was then quenched with water and the mixture was extracted twice with $CH_2Cl_2$, then, the combined organic fractions were washed first with 1M aqueous HCl solution followed by a second wash with saturated aqueous $NaHCO_3$ solution and finally washed with brine. The organic fraction was dried over $MgSO_4$ and the solvent was removed in vacuo to obtain the *N,N*-dimethylmyristoylamide in a 86% yield (749 mg).

**$^1$H NMR** (400.16 MHz, $CDCl_3$, 258 K) δ 3.01 (s, 3H), 2.95 (s, 3H), 2.37 – 2.25 (m, 2H), 1.66 – 1.53 (m, 2H), 1.27 (s, 6H), 1.21 (s, 14H), 0.91 – 0.80 (m, 3H).
**$^{13}$C NMR** (100.63 MHz, $CDCl_3$, 258 K) δ 173.74 (CO), 37.57 (N-$CH_3$), 35.57 (N-$CH_3$), 33.52 ($CH_2$), 32.05 ($CH_2$), 29.83 ($CH_2$), 29.81 ($CH_2$), 29.78 ($CH_2$), 29.67 ($CH_2$), 29.63 ($CH_2$), 29.61 ($CH_2$), 29.55 ($CH_2$), 25.34 ($CH_2$), 22.87 ($CH_2$), 14.40 ($CH_3$).
**HRMS (ESI)**. Calculated for $C_{16}H_{34}NO^+$: 256.26349 Obtained: 256.26423

USC UNIVERSIDADE DE SANTIAGO DE COMPOSTELA

### *10.4.2.5 Preparation of N,N-dimethylpivalamide (44g)*

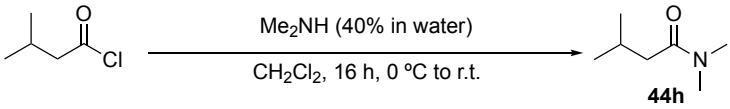



Prepared following an adapted procedure:[133] To a solution of pivaloyl chloride (0.61 mL, 5.0 mmol, 1 equiv.) in $CH_2Cl_2$ (20 mL) at 0 ºC, was added dropwise $Me_2NH$ (40 w/w% in water; 2.5 mL, 20.0 mmol, 4 equiv.). The reaction mixture was stirred continuously at room temperature overnight.

The reaction was then quenched with water and the mixture was extracted twice with $CH_2Cl_2$, then, the combined organic fractions were washed first with 1M aqueous HCl solution followed by a second wash with saturated aqueous $NaHCO_3$ solution and finally washed with brine. The organic fraction was dried over $MgSO_4$ and the solvent was removed in vacuo to obtain the *N,N*-dimethylpivalamide in a 66% yield (426 mg).

**$^1$H NMR** (400.16 MHz, $CDCl_3$, 258 K) δ 3.09 (s, 3H), 2.93 (s, 3H), 1.25 (s, 9H).
**$^{13}$C NMR** (100.63 MHz, $CDCl_3$, 258 K) δ 177.61 (CO), 38.76 (N-$CH_3$), 38.63 (C), 38.07 (N-$CH_3$), 28.16 ($CH_3$).
**$^{15}$N NMR** (40.55 MHz, $CDCl_3$, 258 K) δ 134.18
**HRMS (ESI)**. Calculated for $C_7H_{16}NO^+$: 130.1226 Obtained: 130.1226

### *10.4.2.6 Preparation of N,N,3-trimethylbutanamide (44h)*



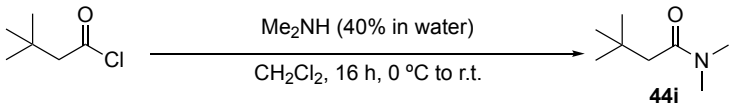

Prepared following an adapted procedure:[133] To a solution of 3-methylbutanoyl chloride (0.61 mL, 5.0 mmol, 1 equiv.) in $CH_2Cl_2$ (20 mL) at 0 ºC, was added dropwise $Me_2NH$ (40 w/w% in water; 2.5 mL, 20.0 mmol, 4 equiv.). The reaction mixture was stirred continuously at room temperature overnight.

The reaction was then quenched with water and the mixture was extracted twice with $CH_2Cl_2$, then, the combined organic fractions were washed first with 1M aqueous HCl solution followed by a second wash with saturated aqueous $NaHCO_3$ solution and finally washed with brine. The organic fraction was dried over $MgSO_4$ and the solvent was removed in vacuo to obtain the *N,N,3*-trimethylbutanamide in a 64% yield (413 mg).

**$^1$H NMR** (400.16 MHz, $CDCl_3$, 258 K) δ 2.98 (s, 3H), 2.91 (s, 3H), 2.16 (d, *J* = 6.5 Hz, 2H), 2.08 (ddd, *J* = 12.8, 7.9, 6.4 Hz, 1H), 0.91 (d, *J* = 6.5 Hz, 6H).
**$^{13}$C NMR** (100.63 MHz, $CDCl_3$, 258 K) δ 172.79 (CO), 42.06 ($CH_2$), 37.63 (N-$CH_3$), 35.38 (N-$CH_3$), 25.67 (CH), 22.78 ($CH_3$).
**$^{15}$N NMR** (40.55 MHz, $CDCl_3$, 258 K) δ 101.56
**HRMS (ESI)**. Calculated for $C_7H_{15}NO^+$: 130.1226 Obtained: 130.1228

USC UNIVERSIDADE DE SANTIAGO DE COMPOSTELA

*10.4.2.7 Preparation of N,N,3,3-tetramethylbutanamide (44i)*



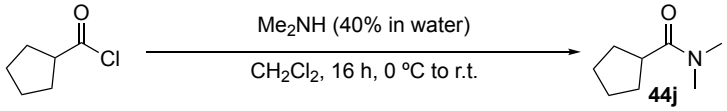

**44i**

Prepared following an adapted procedure:[133] To a solution of pivaloyl chloride (0.61 mL, 5.0 mmol, 1 equiv.) in $CH_2Cl_2$ (20 mL) at 0 ºC, was added dropwise $Me_2NH$ (40 w/w% in water; 2.5 mL, 20.0 mmol, 4 equiv.). The reaction mixture was stirred continuously at room temperature overnight.

The reaction was then quenched with water and the mixture was extracted twice with $CH_2Cl_2$, then, the combined organic fractions were washed first with 1M aqueous HCl solution followed by a second wash with saturated aqueous $NaHCO_3$ solution and finally washed with brine. The organic fraction was dried over $MgSO_4$ and the solvent was removed in vacuo to obtain the *N,N*-dimethylpivalamide in a 66% yield (426 mg).

**$^1$H NMR** (400.16 MHz, $CDCl_3$, 258 K) δ 3.09 (s, 3H), 2.93 (s, 3H), 1.25 (s, 9H).
**$^{13}$C NMR** (100.63 MHz, $CDCl_3$, 258 K) δ 177.61 (CO), 38.76 (N-$CH_3$), 38.63 (C), 38.07 (N-$CH_3$), 28.16 ($CH_3$).
**HRMS (ESI)**. Calculated for $C_7H_{16}NO^+$: 130.1226 Obtained: 130.1226

*10.4.2.8 Preparation of N,N-dimethylcyclopentanecarboxamide (44j)*




**44j**

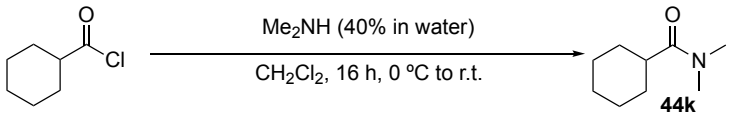
Prepared following an adapted procedure:[133] To a solution of cyclopentanecarbonyl chloride (0.41 mL, 3.4 mmol, 1 equiv.) in $CH_2Cl_2$ (20 mL) at 0 ºC, were added dropwise $Me_2NH$ (40 w/w% in water; 0.8 mL, 6.8 mmol, 2 equiv.) and triethylamine (1.4 mL, 10.2 mmol, 3 equiv.). The reaction mixture was stirred continuously at room temperature overnight.

The reaction was then quenched with water and the mixture was extracted twice with $CH_2Cl_2$, then, the combined organic fractions were washed first with 1M aqueous HCl solution followed by a second wash with saturated aqueous $NaHCO_3$ solution and finally washed with brine. The organic fraction was dried over $MgSO_4$ and the solvent was removed in vacuo to obtain the *N,N*-dimethylcyclopentanecarboxamide in a 92% yield (440 mg).

**$^1$H NMR** (400.16 MHz, $CDCl_3$, 258 K) δ 3.03 (s, 3H), 2.92 (s, 3H), 2.86 (q, *J* = 7.9 Hz, 1H), 1.86 – 1.63 (m, 6H), 1.59 – 1.45 (m, 2H).
**$^{13}$C NMR** (100.63 MHz, $CDCl_3$, 258 K) δ 176.31 (CO), 41.11 (CH), 37.29 (N-$CH_3$), 35.68 (N-$CH_3$), 29.96 ($CH_2$), 26.04 ($CH_2$).
**HRMS (ESI)**. Calculated for $C_8H_{16}NO^+$: 142.12264 Obtained: 142.12257

USC UNIVERSIDADE DE SANTIAGO DE COMPOSTELA

*10.4.2.9 Preparation of N,N-dimethylcyclohexanecarboxamide (44k)*

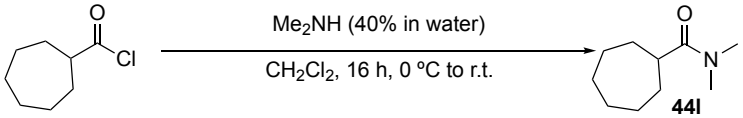



Prepared following an adapted procedure:[133] To a solution of cyclohexanecarbonyl chloride (0.67 mL, 5.0 mmol, 1 equiv.) in $CH_2Cl_2$ (20 mL) at 0 ºC, was added dropwise $Me_2NH$ (40 w/w% in water; 2.5 mL, 20.0 mmol, 4 equiv.). The reaction mixture was stirred continuously at room temperature overnight.

The reaction was then quenched with water and the mixture was extracted twice with $CH_2Cl_2$, then, the combined organic fractions were washed first with 1M aqueous HCl solution followed by a second wash with saturated aqueous $NaHCO_3$ solution and finally washed with brine. The organic fraction was dried over $MgSO_4$ and the solvent was removed in vacuo to obtain the *N,N*-dimethylcyclohexanecarboxamide in a 73% yield (566 mg).

**$^1$H NMR** (400.16 MHz, $CDCl_3$, 258 K) δ 2.99 (s, 3H), 2.87 (s, 3H), 2.43 (tt, *J* = 11.7, 3.3 Hz, 1H), 1.77 – 1.58 (m, 5H), 1.41 (qd, *J* = 12.1, 3.0 Hz, 2H), 1.28 – 1.08 (m, 3H).
**$^{13}$C NMR** (100.63 MHz, $CDCl_3$, 258 K) δ 176.15 (CO), 40.46 (CH), 37.11 (N-$CH_3$), 35.45 (N-$CH_3$), 28.97 ($CH_2$), 25.75($CH_2$), 25.70($CH_2$).
**$^{15}$N NMR** (40.55 MHz, $CDCl_3$, 258 K) δ 98.98
**HRMS (ESI)**. Calculated for $C_9H_{18}NO^+$: 156.13829 Obtained: 156.13832

*10.4.2.10 Preparation of N,N-dimethylcycloheptanecarboxamide (44l)*




Prepared following an adapted procedure:[133] To a solution of cycloheptanecarbonyl chloride (546 mg, 3.4 mmol, 1 equiv.) in $CH_2Cl_2$ (20 mL) at 0 ºC, was added dropwise $Me_2NH$ (40 w/w% in water; 1.7 mL, 13.6 mmol, 4 equiv.). The reaction mixture was stirred continuously at room temperature overnight.

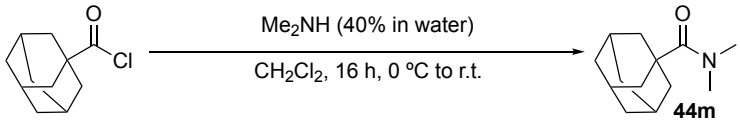
The reaction was then quenched with water and the mixture was extracted twice with $CH_2Cl_2$, then, the combined organic fractions were washed first with 1M aqueous HCl solution followed by a second wash with saturated aqueous $NaHCO_3$ solution and finally washed with brine. The organic fraction was dried over $MgSO_4$ and the solvent was removed in vacuo to obtain the *N,N*-dimethylcycloheptanecarboxamide in a 86% yield (496 mg).

**$^1$H NMR** (400.16 MHz, $CDCl_3$, 258 K) δ 3.01 (s, 3H), 2.90 (s, 3H), 2.61 (ddt, *J* = 11.6, 9.9, 3.6 Hz, 1H), 1.79 – 1.68 (m, 4H), 1.67 – 1.56 (m, 2H), 1.55 – 1.46 (m, 4H), 1.46 – 1.33 (m, 2H).
**$^{13}$C NMR** (100.63 MHz, $CDCl_3$, 258 K) δ 177.46 (CO), 41.60 (CH), 37.34 (N-$CH_3$), 35.57 (N-$CH_3$), 31.01 ($CH_2$), 28.03 ($CH_2$), 26.68 ($CH_2$).

USC DE COMPOSTELA

**HRMS (ESI)**. Calculated for $C_{10}H_{20}NO^+$: 170.15394 Obtained: 170.15392

*10.4.2.11 Preparation of N,N-dimethyladamantane-1-carboxamide (44m)*

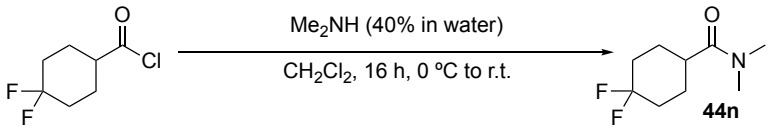



Prepared following an adapted procedure:[133] To a solution of adamantane-1-carbonyl chloride (678 mg, 3.4 mmol, 1 equiv.) in $CH_2Cl_2$ (20 mL) at 0 ºC, were added dropwise $Me_2NH$ (40 w/w% in water; 0.6 mL, 5.1 mmol, 1.5 equiv.) and triethylamine (1.4 mL, 10.2 mmol, 3 equiv.). The reaction mixture was stirred continuously at room temperature overnight.

The reaction was then quenched with water and the mixture was extracted twice with $CH_2Cl_2$, then, the combined organic fractions were washed first with 1M aqueous HCl solution followed by a second wash with saturated aqueous $NaHCO_3$ solution and finally washed with brine. The organic fraction was dried over $MgSO_4$ and the solvent was removed in vacuo to obtain the *N,N*-dimethyladamantane-1-carboxamide in a 83% yield (587 mg).

**$^1$H NMR** (400.16 MHz, $CDCl_3$, 258 K) δ 3.05 (s, 6H), 2.02 (s, 3H), 1.98 (d, *J* = 2.9 Hz, 6H), 1.68 (d, *J* = 2.0 Hz, 7H).
**$^{13}$C NMR** (100.63 MHz, $CDCl_3$, 258 K) δ 177.05 (CO), 41.40 (C), 38.66 (N-$CH_3$), 38.57 ($CH_2$), 36.54 ($CH_2$), 28.32 (CH).
**HRMS (ESI)**. Calculated for $C_{13}H_{22}NO^+$: 208.16959 Obtained: 208.16997

*10.4.2.12 Preparation of 4,4-difluoro-N,N-dimethylcyclohexane-1-carboxamide (44n)*




Prepared following an adapted procedure:[133] To a solution of 4,4-difluorocyclohexane-1-carbonyl chloride (620 mg, 3.4 mmol, 1 equiv.) in $CH_2Cl_2$ (20 mL) at 0 ºC, was added dropwise $Me_2NH$ (40 w/w% in water; 1.7 mL, 13.6 mmol, 4 equiv.). The reaction mixture was stirred continuously at room temperature overnight.

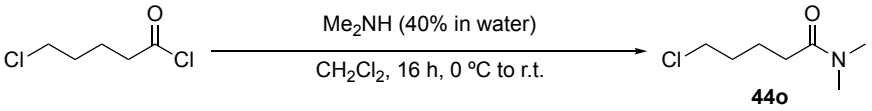
The reaction was then quenched with water and the mixture was extracted twice with $CH_2Cl_2$, then, the combined organic fractions were washed first with 1M aqueous HCl solution followed by a second wash with saturated aqueous $NaHCO_3$ solution and finally washed with brine. The organic fraction was dried over $MgSO_4$ and the solvent was removed in vacuo to obtain the 4,4-difluoro-*N,N*-dimethylcyclohexane-1-carboxamide in a 77% yield (503 mg).

**$^1$H NMR** (400.16 MHz, $CDCl_3$, 258 K) δ 3.05 (s, 3H), 2.93 (s, 3H), 2.61 – 2.52 (m, 1H), 2.23 – 2.10 (m, 2H), 1.88 – 1.63 (m, 6H).

USC DE SANTIAGO DE COMPOSTELA

**$^{13}$C NMR** (100.63 MHz, $CDCl_3$, 258 K) δ 174.21 (d, *J* = 2.0 Hz), 122.88 (t, *J* = 241.1 Hz), 38.14, 37.27, 35.66, 33.34 – 32.51 (m), 25.40 (d, *J* = 9.6 Hz).
**$^{19}$F NMR** (376.46 MHz, $CDCl_3$, 258 K) δ -92.31 (d, *J* = 236.4 Hz), -100.83 (d, *J* = 236.2 Hz).
**HRMS (ESI)**. Calculated for $C_9H_{15}F_2NO^+$: 192.11945 Obtained: 192.11943

*10.4.2.13 Preparation of 5-chloro-N,N-dimethylpentanamide (44o)*



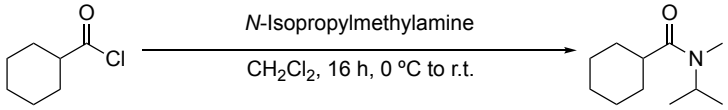
**44o**

Prepared following an adapted procedure:[133] To a solution of 5-chloropentanoyl chloride (0.32 mL, 2.5 mmol, 1 equiv.) in $CH_2Cl_2$ (20 mL) at 0 ºC, was added dropwise $Me_2NH$ (40 w/w% in water; 1.3 mL, 10.0 mmol, 4 equiv.). The reaction mixture was stirred continuously at room temperature overnight.

The reaction was then quenched with water and the mixture was extracted twice with $CH_2Cl_2$, then, the combined organic fractions were washed first with 1M aqueous HCl solution followed by a second wash with saturated aqueous $NaHCO_3$ solution and finally washed with brine. The organic fraction was dried over $MgSO_4$ and the solvent was removed in vacuo to obtain the 5-chloro-*N*,*N*-dimethylpentanamide in a 40% yield (164 mg).

**$^{1}$H NMR** (400.16 MHz, $CDCl_3$, 258 K) δ 3.55 (t, *J* = 6.3 Hz, 2H), 2.99 (s, 3H), 2.92 (s, 3H), 2.33 (t, *J* = 7.1 Hz, 2H), 1.86 – 1.69 (m, 4H).
**$^{13}$C NMR** (100.63 MHz, $CDCl_3$, 258 K) δ 172.49 (CO), 45.06 ($CH_2$), 37.34 (N-$CH_3$), 35.45 (N-$CH_3$), 32.44 ($CH_2$), 32.10 ($CH_2$), 22.32 ($CH_2$).
**HRMS (ESI)**. Calculated for $C_7H_{14}ClNO^+$: 164.08367 Obtained: 164.08380

*10.4.2.14 Preparation of N-isopropyl-N-methylcyclohexanecarboxamide (44p)*



**44p**

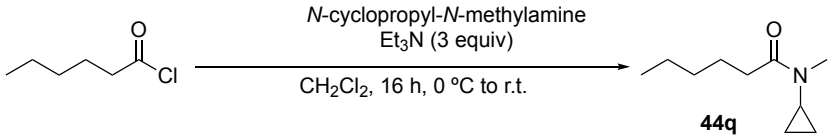
Prepared following an adapted procedure:[133] To a solution of cyclohexanecarbonyl chloride (0.70 mL, 5.0 mmol, 1 equiv.) in $CH_2Cl_2$ (20 mL) at 0 ºC, was added dropwise *N*-Isopropylmethylamine (2.1 mL, 20.0 mmol, 4 equiv.). The reaction mixture was stirred continuously at room temperature overnight.

The reaction was then quenched with water and the mixture was extracted twice with $CH_2Cl_2$, then, the combined organic fractions were washed first with 1M aqueous HCl solution followed by a second wash with saturated aqueous $NaHCO_3$ solution and finally washed with brine. The organic fraction was dried over $MgSO_4$ and the solvent was removed in vacuo to obtain the *N*-isopropyl-*N*-methylcyclohexanecarboxamide in a 79% yield (724 mg).

USC UNIVERSIDADE DE SANTIAGO DE COMPOSTELA

**$^{1}$H NMR** (400.16 MHz, $CDCl_3$, 258 K) δ 4.86 (p, *J* = 6.8 Hz, 0.5H), 4.09 (p, *J* = 6.6 Hz, 0.5H), 2.80 (s, 1.5H), 2.71 (s, 1.5H), 2.50 – 2.33 (m, 1H), 1.78 – 1.72 (m, 2H), 1.72 – 1.59 (m, 3H), 1.46 (td, *J* = 12.2, 3.9 Hz, 2H), 1.20 (d, *J* = 8.2 Hz, 3H), 1.15 (d, *J* = 6.6 Hz, 3H), 1.02 (d, *J* = 6.8 Hz, 3H).
**$^{13}$C NMR** (100.63 MHz, $CDCl_3$, 258 K) δ 175.62 (CO), 47.29 (N-CH), 43.32 (N-CH), 41.23 (CH), 40.72 (CH), 29.58 ($CH_2$), 28.97 ($CH_2$), 27.96 (N-$CH_3$), 26.06 (N-$CH_3$), 25.87 ($CH_2$), 25.85 ($CH_2$), 25.77 ($CH_2$), 20.81 ($CH_3$), 19.50 ($CH_3$).
**$^{15}$N NMR** (40.55 MHz, $CDCl_3$, 258 K) δ 123.03
**HRMS (ESI)**. Calculated for $C_{11}H_{22}NO^+$: 184.1696 Obtained: 184.1691

### *10.4.2.15 Preparation of N-cyclopropyl-N-methylhexanamide (44q)*



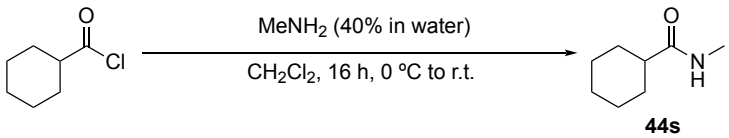

**44q**

Prepared following an adapted procedure:[133] To a solution of hexanoyl chloride (0.21 mL, 1.5 mmol, 1 equiv.) in $CH_2Cl_2$ (20 mL) at 0 ºC, were added *N*-cyclopropyl-*N*-methylamine hydrochloride (1.6 g, 6.0 mmol, 4 equiv.) and triethylamine (0.8 mL, 6.0 mmol, 4 equiv.). The reaction mixture was stirred continuously at room temperature overnight.

The reaction was then quenched with water and the mixture was extracted twice with $CH_2Cl_2$, then, the combined organic fractions were washed first with 1M aqueous HCl solution followed by a second wash with saturated aqueous $NaHCO_3$ solution and finally washed with brine. The organic fraction was dried over $MgSO_4$ and the solvent was removed in vacuo to obtain the *N*-cyclopropyl-*N*-methylhexanamide in a 55% yield (270 mg).

**$^{1}$H NMR** (400.16 MHz, $CDCl_3$, 258 K) δ 2.89 (s, 3H), 2.65 (dt, *J* = 7.1, 3.4 Hz, 1H), 2.49 (t, *J* = 7.7 Hz, 2H), 1.61 (p, *J* = 7.4 Hz, 2H), 1.29 (d, *J* = 3.7 Hz, 4H), 0.93 – 0.80 (m, 5H), 0.70 (dd, *J* = 4.1, 2.0 Hz, 2H).
**$^{13}$C NMR** (100.63 MHz, $CDCl_3$, 258 K) δ 176.51 (CO), 34.29 (N-$CH_3$), 34.08 ($CH_2$), 31.83 ($CH_2$), 31.29 (CH), 25.01 ($CH_2$), 22.72 ($CH_2$), 14.24 ($CH_3$), 9.25 ($CH_2$).
**HRMS (ESI)**. Calculated for $C_{10}H_{20}NO^+$: 170.15394 Obtained: 170.15408

### *10.4.2.16 Preparation of N-methylcyclohexanecarboxamide (44s)*




**44s**

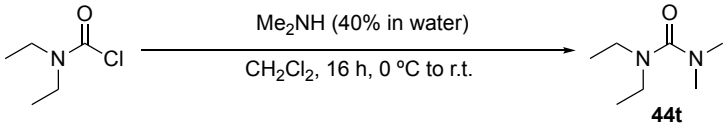
Prepared following an adapted procedure:[133] To a solution of cyclohexanecarbonyl chloride (0.67mL, 5.0 mmol, 1 equiv.) in $CH_2Cl_2$ (20 mL) at 0 ºC, was added dropwise $MeNH_2$ (40 w/w% in water; 1.8 mL, 20.0 mmol, 4 equiv.). The reaction mixture was stirred continuously at room temperature overnight.

USC UNIVERSIDADE DE SANTIAGO DE COMPOSTELA

The reaction was then quenched with water and the mixture was extracted twice with $CH_2Cl_2$, then, the combined organic fractions were washed first with 1M aqueous HCl solution followed by a second wash with saturated aqueous $NaHCO_3$ solution and finally washed with brine. The organic fraction was dried over $MgSO_4$ and the solvent was removed in vacuo to obtain the *N*-methylcyclohexanecarboxamide in a 40% yield (276 mg).

**$^1$H NMR** (400.16 MHz, $CDCl_3$, 258 K) δ 5.93 (s, 1H), 2.79 (d, *J* = 4.8 Hz, 3H), 2.08 (tt, *J* = 12.0, 3.4 Hz, 1H), 1.87 – 1.79 (m, 2H), 1.79 – 1.71 (m, 2H), 1.68 – 1.60 (m, 1H), 1.39 (qd, *J* = 12.1, 3.1 Hz, 2H), 1.28 – 1.13 (m, 3H).
**$^{13}$C NMR** (100.63 MHz, $CDCl_3$, 258 K) δ 177.30 (CO), 45.45 (N-$CH_3$), 29.60 ($CH_2$), 26.45 (CH), 25.71 ($CH_2$), 25.66 ($CH_2$).
**$^{15}$N NMR** (40.55 MHz, $CDCl_3$, 258 K) δ 101.07
**HRMS (ESI)**. Calculated for $C_8H_{16}NO^+$: 142.1226 Obtained: 142.1229

### *10.4.2.17 Preparation of 1,1-diethyl-3,3-dimethylurea (44t)*



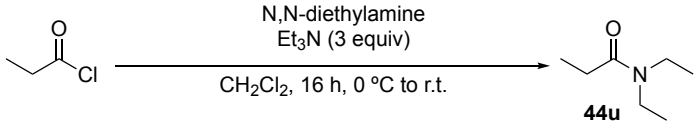

**44t**

Prepared following an adapted procedure:[133] To a solution of diethylcarbamic chloride (0.43 mL, 3.4 mmol, 1 equiv.) in $CH_2Cl_2$ (20 mL) at 0 ºC, were added dropwise $Me_2NH$ (40 w/w% in water; 0.6 mL, 5.1 mmol, 1.5 equiv.) and triethylamine (1.4 mL, 10.2 mmol, 3 equiv.). The reaction mixture was stirred continuously at room temperature overnight.

The reaction was then quenched with water and the mixture was extracted twice with $CH_2Cl_2$, then, the combined organic fractions were washed first with 1M aqueous HCl solution followed by a second wash with saturated aqueous $NaHCO_3$ solution and finally washed with brine. The organic fraction was dried over $MgSO_4$ and the solvent was removed in vacuo to obtain the 1,1-diethyl-3,3-dimethylurea in a 55% yield (270 mg).

**$^1$H NMR** (400.16 MHz, $CDCl_3$, 300 K) δ 2.93 (q, *J* = 7.1 Hz, 4H), 2.56 (s, 6H), 0.87 (t, *J* = 7.1 Hz, 6H).
**$^{13}$C NMR** (100.63 MHz, $CDCl_3$, 300 K) δ 164.83 (CO), 41.62 (N-$CH_2$), 38.32 (N-$CH_3$), 12.86 ($CH_3$).
**HRMS (ESI)**. Calculated for $C_7H_{17}N_2O^+$: 145.13354 Obtained: 145.13366

### *10.4.2.18 Preparation of N,N-diethylpropionamide (44u)*



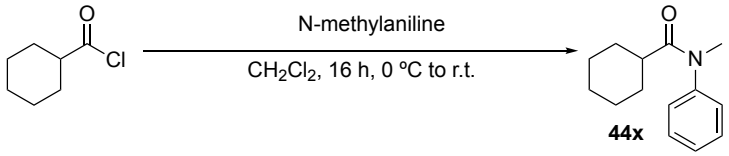

**44u**

Prepared following an adapted procedure:[133] To a solution of propionyl chloride (0.29 mL, 3.4 mmol, 1 equiv.) in $CH_2Cl_2$ (20 mL) at 0 ºC, were added dropwise $Et_2NH$ (0.5 mL, 5.1 mmol, 1.5 equiv.) and triethylamine (1.4 mL, 10.2 mmol, 3 equiv.). The reaction mixture was stirred continuously at room temperature overnight.

The reaction was then quenched with water and the mixture was extracted twice with $CH_2Cl_2$, then, the combined organic fractions were washed first with 1M aqueous HCl solution followed by a second wash with saturated aqueous $NaHCO_3$ solution and finally washed with brine. The organic fraction was dried over $MgSO_4$ and the solvent was removed in vacuo to obtain the *N,N*-diethylpropionamide in a 66% yield (290 mg).

**$^1$H NMR** (400.16 MHz, $CDCl_3$, 258 K) δ 3.35 (q, *J* = 7.1 Hz, 2H), 3.28 (q, *J* = 7.1 Hz, 2H), 2.33 (q, *J* = 7.4 Hz, 2H), 1.18 – 1.07 (m, 9H).
**$^{13}$C NMR** (100.63 MHz, $CDCl_3$, 258 K) δ 173.09 (CO), 41.81 (N-$CH_2$), 40.05 (N-$CH_2$), 26.28 ($CH_2$), 14.29 ($CH_3$), 13.18 ($CH_3$), 9.78 ($CH_3$).
**HRMS (ESI)**. Calculated for $C_7H_{16}NO^+$: 130.12264 Obtained: 130.12272

### *10.4.2.19 Preparation of N-methyl-N-phenylcyclohexanecarboxamide (44x)*



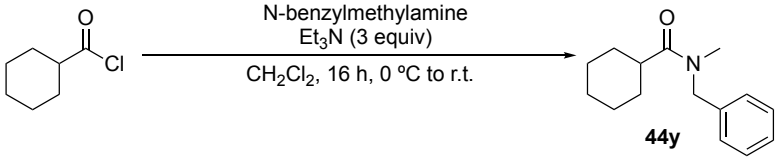

**44x**

Prepared following an adapted procedure:[133] To a solution of cyclohexanecarbonyl chloride (0.70 mL, 5.0 mmol, 1 equiv.) in $CH_2Cl_2$ (20 mL) at 0 ºC, was added dropwise *N*-Methylaniline (2.2 mL, 20.0 mmol, 4 equiv.). The reaction mixture was stirred continuously at room temperature overnight.

The reaction was then quenched with water and the mixture was extracted twice with $CH_2Cl_2$, then, the combined organic fractions were washed first with 1M aqueous HCl solution followed by a second wash with saturated aqueous $NaHCO_3$ solution and finally washed with brine. The organic fraction was dried over $MgSO_4$ and the solvent was removed in vacuo to obtain the *N-methyl-N*-phenylcyclohexanecarboxamide in a 89% yield (965 mg).

**$^1$H NMR** (400.16 MHz, $CDCl_3$, 258 K) δ 7.46 – 7.39 (m, 2H), 7.38 – 7.31 (m, 1H), 7.19 – 7.12 (m, 2H), 3.22 (s, 3H), 2.13 (tt, *J* = 11.9, 3.3 Hz, 1H), 1.62 (d, *J* = 10.1 Hz, 4H), 1.50 (td, *J* = 12.5, 2.9 Hz, 3H), 1.22 – 1.06 (m, 1H), 0.99 – 0.84 (m, 2H).
**$^{13}$C NMR** (100.63 MHz, $CDCl_3$, 258 K) δ 176.59 (CO), 143.94 (C, Ar), 129.81 (CH, Ar), 127.82 (CH, Ar), 127.21 (CH, Ar), 41.16 (CH), 37.51 (N-$CH_3$), 29.34 ($CH_2$), 25.49 ($CH_2$), 25.40 ($CH_2$).
**$^{15}$N NMR** (40.55 MHz, $CDCl_3$, 258 K) δ 124.10
**HRMS (ESI)**. Calculated for $C_{14}H_{20}NO^+$: 218.1539 Obtained: 218.1539

### *10.4.2.20 Preparation of N-benzyl-N-methylcyclohexanecarboxamide (44y)*




**44y**

USC DE COMPOSTELA

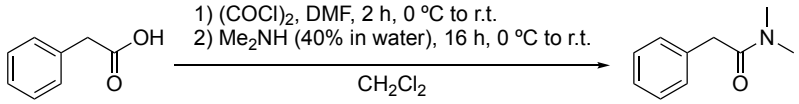
Prepared following an adapted procedure:[133] To a solution of cyclohexanecarbonyl chloride (0.45 mL, 3.4 mmol, 1 equiv.) in $CH_2Cl_2$ (5 mL) at 0 ºC, were added dropwise *N*-

Benzylmethylamine (0.88 mL, 6.8 mmol, 2 equiv.) and triethylamine (0.71 mL, 5.1 mmol, 1.5 equiv.). The reaction mixture was stirred continuously at room temperature overnight.

The reaction was then quenched with water and the mixture was extracted twice with $CH_2Cl_2$, then, the combined organic fractions were washed first with 1M aqueous HCl solution followed by a second wash with saturated aqueous $NaHCO_3$ solution and finally washed with brine. The organic fraction was dried over $MgSO_4$ and the solvent was removed in vacuo to obtain the *N*-benzyll-*N*-methylcyclohexanecarboxamide in a 87% yield (686 mg).

**$^1$H NMR** (400.16 MHz, $CDCl_3$, 258 K) δ 7.40 – 7.34 (m, 1H), 7.34 – 7.25 (m, 2H), 7.23 – 7.18 (m, 1H), 7.17 – 7.12 (m, 1H), 4.58 (s, 1H), 4.57 (s, 1H), 2.94 (s, 1.5H), 2.90 (s, 1.5H), 2.58 – 2.44 (m, 1H), 1.83 – 1.49 (m, 7H), 1.24 (dt, *J* = 23.3, 10.6 Hz, 3H).
**$^{13}$C NMR** (100.63 MHz, $CDCl_3$, 258 K) δ 176.94 (CO), 176.38 (CO), 137.51 (C, Ar), 136.79 (C, Ar), 128.94 (CH, Ar), 128.60 (CH, Ar), 127.84 (CH, Ar), 127.58 (CH, Ar), 127.25 (CH, Ar), 126.18 (CH, Ar), 52.92 ($CH_2$), 50.52 ($CH_2$), 40.68 (CH), 40.55 (CH), 34.69 (N-$CH_3$), 33.90 (N-$CH_3$), 29.57 ($CH_2$), 29.10 ($CH_2$), 25.83 ($CH_2$), 25.78 ($CH_2$), 25.72 ($CH_2$), 25.66 ($CH_2$).
**HRMS (ESI)**. Calculated for $C_{15}H_{22}NO^+$: 232.16959 Obtained: 232.16981

### *10.4.2.21 Preparation of N,N-dimethyl-2-phenylacetamide (44z)*




**44z**

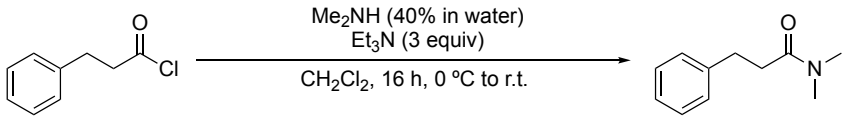
Prepared following an adapted procedure:[133] To a solution of 2-phenylacetic acid (680.7 mg, 5.0 mmol, 1 equiv.) in $CH_2Cl_2$ (20 mL) at room temperature, were added carefully $(COCl)_2$ (0.64 mL, 7.5 mmol, 1.5 equiv.) and DMF (5 drops) in that order. The reaction mixture was stirred at room temperature for 2 h. After that time, the mixture was cooled down to 0 ºC and $Me_2NH$ (40 w/w% in water; 2.5 mL, 20.0 mmol, 4 equiv.) was added dropwise. The reaction mixture was stirred continuously at room temperature overnight.

The reaction was then quenched with water and the mixture was extracted twice with $CH_2Cl_2$, then, the combined organic fractions were washed first with 1M aqueous HCl solution followed by a second wash with saturated aqueous $NaHCO_3$ solution and finally washed with brine. The organic fraction was dried over $MgSO_4$ and the solvent was removed in vacuo to obtain the *N,N*-dimethyl-2-phenylacetamide in a 94% yield (767 mg).

**$^1$H NMR** (400.16 MHz, $CDCl_3$, 258 K) δ 7.35 – 7.29 (m, 2H), 7.27 – 7.22 (m, 3H), 3.73 (s, 2H), 2.99 (s, 3H), 2.96 (s, 3H).
**$^{13}$C NMR** (100.63 MHz, $CDCl_3$, 258 K) δ 171.21 (CO), 134.84 (C, Ar), 128.73 (CH, Ar), 128.70 (CH, Ar), 126.77 (CH, Ar), 40.98 ($CH_2$), 37.82 (N-$CH_3$), 35.69 (N-$CH_3$).
**$^{15}$N NMR** (40.55 MHz, $CDCl_3$, 258 K) δ 101.91
**HRMS (ESI)**. Calculated for $C_{10}H_{14}NO^+$: 164. 1070 Obtained: 164. 1070

USC UNIVERSIDADE DE SANTIAGO DE COMPOSTELA

*10.4.2.22 Preparation of N,N-dimethyl-3-phenylpropanamide (44aa)*



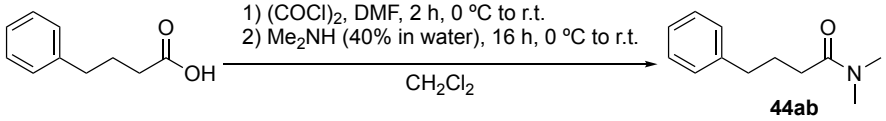

**44aa**

Prepared following an adapted procedure:[133] To a solution of 3-phenylpropanoyl chloride (0.5 mL, 3.4 mmol, 1 equiv.) in $CH_2Cl_2$ (20 mL) at 0 ºC, were added dropwise $Me_2NH$ (40 w/w% in water; 0.9 mL, 6.8 mmol, 2 equiv.) and triethylamine (1.4 mL, 10.2 mmol, 3 equiv.). The reaction mixture was stirred continuously at room temperature overnight.

The reaction was then quenched with water and the mixture was extracted twice with $CH_2Cl_2$, then, the combined organic fractions were washed first with 1M aqueous HCl solution followed by a second wash with saturated aqueous $NaHCO_3$ solution and finally washed with brine. The organic fraction was dried over $MgSO_4$ and the solvent was removed in vacuo to obtain the *N,N*-dimethyl-3-phenylpropanamide in a 98% yield (595 mg).

**$^1$H NMR** (400.16 MHz, $CDCl_3$, 258 K) δ 7.33 – 7.27 (m, 2H), 7.25 – 7.19 (m, 3H), 2.94 (d, *J* = 8.9 Hz, 8H), 2.64 – 2.58 (m, 2H).
**$^{13}$C NMR** (100.63 MHz, $CDCl_3$, 258 K) δ 172.21 (CO), 141.39 (C, Ar), 128.49 (CH, Ar), 128.46 (CH, Ar), 126.12 (CH, Ar), 37.21 ($CH_2$), 35.51 (N-$CH_3$), 35.46 ($CH_2$), 31.28 (N-$CH_3$).
**$^{15}$N NMR** (40.55 MHz, $CDCl_3$, 258 K) δ 100.72
**HRMS (ESI)**. Calculated for $C_{11}H_{16}NO^+$: 178.122641 Obtained: 178.122724

*10.4.2.23 Preparation of N,N-dimethyl-4-phenylbutanamide (44ab)*




**44ab**

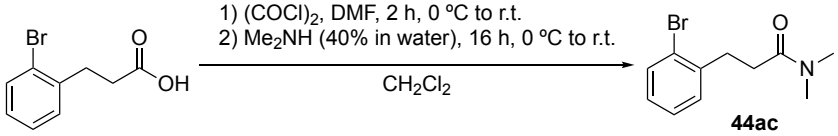
Prepared following an adapted procedure:[133] To a solution of 4-phenylbutanoic acid (1.0 g, 6.0 mmol, 1 equiv.) in $CH_2Cl_2$ (25 mL) at room temperature, were added carefully $(COCl)_2$ (0.78 mL, 9.1 mmol, 1.5 equiv.) and DMF (5 drops) in that order. The reaction mixture was stirred at room temperature for 2 h. After that time, the mixture was cooled down to 0 ºC and $Me_2NH$ (40 w/w% in water; 3.1 mL, 24.4 mmol, 4 equiv.) was added dropwise. The reaction mixture was stirred continuously at room temperature overnight.

The reaction was then quenched with water and the mixture was extracted twice with $CH_2Cl_2$, then, the combined organic fractions were washed first with 1M aqueous HCl solution followed by a second wash with saturated aqueous $NaHCO_3$ solution and finally washed with brine. The organic fraction was dried over $MgSO_4$ and the solvent was removed in vacuo to obtain the *N,N*-dimethyl-4-phenylbutanamide in a 89% yield (1 g).

USC UNIVERSIDADE DE SANTIAGO DE COMPOSTELA

**$^{1}$H NMR** (400.16 MHz, $CDCl_3$, 258 K) δ 7.33 – 7.26 (m, 2H), 7.22 – 7.16 (m, 3H), 2.93 (s, 6H), 2.66 (t, *J* = 7.6 Hz, 2H), 2.34 – 2.28 (m, 2H), 1.95 (ddd, *J* = 15.2, 8.2, 6.9 Hz, 2H).
**$^{13}$C NMR** (100.63 MHz, $CDCl_3$, 258 K) δ 172.84 (CO), 141.77 (C, Ar), 128.50 (CH, Ar), 128.34 (CH, Ar), 125.85 (CH, Ar), 37.27 (N-$CH_3$), 35.38 (N-$CH_3$), 35.26 ($CH_2$), 32.49 ($CH_2$), 26.57 ($CH_2$).
**$^{15}$N NMR** (40.55 MHz, $CDCl_3$, 258 K) δ 100.62
**HRMS (ESI)**. Calculated for $C_{12}H_{17}NNaO^+$: 214.120235 Obtained: 214.120347

*10.4.2.24 Preparation of 3-(2-bromophenyl)-N,N-dimethylpropanamide (44ac)*



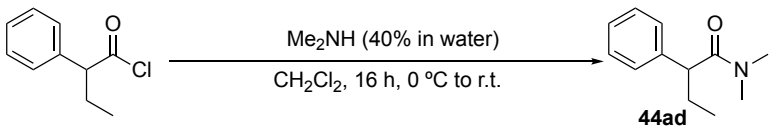
**44ac**

Prepared following an adapted procedure:[133] To a solution of 3-(2-bromophenyl)propanoic acid (572 mg, 2.5 mmol, 1 equiv.) in $CH_2Cl_2$ (20 mL) at room temperature, were added carefully $(COCl)_2$ (0.32 mL, 3.75 mmol, 1.5 equiv.) and DMF (5 drops) in that order. The reaction mixture was stirred at room temperature for 2 h. After that time, the mixture was cooled down to 0 ºC and $Me_2NH$ (40 w/w% in water; 1.3 mL, 10.0 mmol, 4 equiv.) was added dropwise. The reaction mixture was stirred continuously at room temperature overnight.

The reaction was then quenched with water and the mixture was extracted twice with $CH_2Cl_2$, then, the combined organic fractions were washed first with 1M aqueous HCl solution followed by a second wash with saturated aqueous $NaHCO_3$ solution and finally washed with brine. The organic fraction was dried over $MgSO_4$ and the solvent was removed in vacuo to obtain the 3-(2-bromophenyl)-*N*,*N*-dimethylpropanamide in a 80% yield (515 mg).

**$^{1}$H NMR** (400.16 MHz, $CDCl_3$, 258 K) δ 7.56 (d, *J* = 7.9 Hz, 1H), 7.30 (dt, *J* = 14.9, 7.5 Hz, 2H), 7.12 (t, *J* = 7.6 Hz, 1H), 3.09 (t, *J* = 8.1 Hz, 2H), 2.99 (d, *J* = 1.6 Hz, 6H), 2.65 (t, *J* = 8.1 Hz, 2H).
**$^{13}$C NMR** (100.63 MHz, $CDCl_3$, 258 K) δ 172.05 (CO), 140.56 (C, Ar), 132.78 (CH, Ar), 130.98 (CH, Ar), 128.10 (CH, Ar), 127.74 (CH, Ar), 124.31 (C, Ar), 37.35 (N-$CH_3$), 35.56 (N-$CH_3$), 33.52 ($CH_2$), 32.03 ($CH_2$).
**HRMS (ESI)**. Calculated for $C_{11}H_{14}BrNONa^+$: 278.01510 Obtained: 278.01516

*10.4.2.25 Preparation of N,N-dimethyl-2-phenylbutanamide (44ad)*



**44ad**

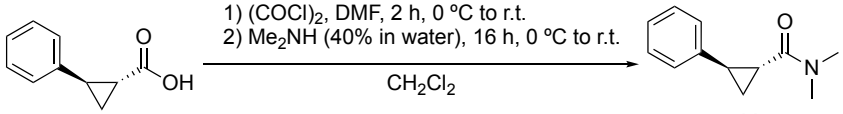
Prepared following an adapted procedure:[133] To a solution of 2-phenylbutanoyl chloride (0.57 mL, 3.4 mmol, 1 equiv.) in $CH_2Cl_2$ (20 mL) at 0 ºC, were added dropwise $Me_2NH$ (40 w/w% in water; 0.6 mL, 5.1 mmol, 1.5 equiv.) and triethylamine (1.4 mL, 10.2 mmol, 3 equiv.). The reaction mixture was stirred continuously at room temperature overnight.

UNIVERSIDADE DE SANTIAGO DE COMPOSTELA

The reaction was then quenched with water and the mixture was extracted twice with $CH_2Cl_2$, then, the combined organic fractions were washed first with 1M aqueous HCl solution followed by a second wash with saturated aqueous $NaHCO_3$ solution and finally washed with brine. The organic fraction was dried over $MgSO_4$ and the solvent was removed in vacuo to obtain the *N,N*-dimethyl-2-phenylbutanamide in a 76% yield (495 mg).

**$^1$H NMR** (400.16 MHz, $CDCl_3$, 258 K) δ 7.34 – 7.27 (m, 4H), 7.24 (m, 1H), 3.58 (t, *J* = 7.3 Hz, 1H), 2.94 (s, 6H), 2.14 – 2.00 (m, 1H), 1.78 – 1.65 (m, 1H), 0.84 (t, *J* = 7.4 Hz, 3H).
**$^{13}$C NMR** (100.63 MHz, $CDCl_3$, 258 K) δ 173.25 (CO), 140.01 (C, Ar), 128.74 (CH, Ar), 127.99 (CH, Ar), 126.88 (CH, Ar), 50.59 (CH), 37.28 (N-$CH_3$), 35.96 (N-$CH_3$), 28.17 ($CH_2$), 12.62 ($CH_3$).
**HRMS (ESI)**. Calculated for $C_{12}H_{18}NO^+$: 192.13829 Obtained: 192.13860

*10.4.2.26 Preparation of (1R,2R)-N,N-dimethyl-2-phenylcyclopropane-1-carboxamide (44ae)*




**44ae**

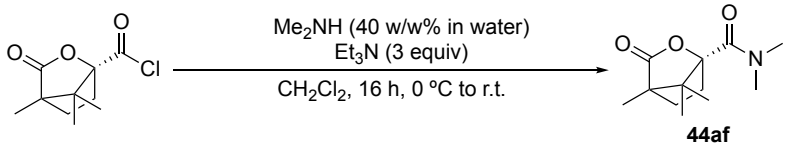
Prepared following an adapted procedure:[133] To a solution of (1*R*,2*R*)-2-phenylcyclopropane-1-carboxylic acid (500 mg, 3.0 mmol, 1 equiv.) in $CH_2Cl_2$ (20 mL) at room temperature, were added carefully $(COCl)_2$ (0.39 mL, 4.6 mmol, 1.5 equiv.) and DMF (5 drops) in that order. The reaction mixture was stirred at room temperature for 2 h. After that time, the mixture was cooled down to 0 ºC and $Me_2NH$ (40 w/w% in water; 1.6 mL, 12.3 mmol, 4 equiv.) was added dropwise. The reaction mixture was stirred continuously at room temperature overnight.

The reaction was then quenched with water and the mixture was extracted twice with $CH_2Cl_2$, then, the combined organic fractions were washed first with 1M aqueous HCl solution followed by a second wash with saturated aqueous $NaHCO_3$ solution and finally washed with brine. The organic fraction was dried over $MgSO_4$ and the solvent was removed in vacuo to obtain the *N,N*-dimethyl-2-phenylacetamide in a 91% yield (530 mg).

**$^1$H NMR** (400.16 MHz, $CDCl_3$, 258 K) δ 7.32 – 7.27 (m, 2H), 7.25 – 7.16 (m, 1H), 7.14 – 7.09 (m, 2H), 3.12 (s, 3H), 3.00 (s, 2H), 2.47 (ddd, *J* = 9.0, 6.3, 4.1 Hz, 1H), 2.00 (ddd, *J* = 8.2, 5.3, 4.2 Hz, 1H), 1.65 (ddd, *J* = 9.0, 5.3, 4.3 Hz, 1H), 1.29 (ddd, *J* = 8.2, 6.3, 4.3 Hz, 1H).
**$^{13}$C NMR** (100.63 MHz, $CDCl_3$, 258 K) δ 172.04 (CO), 141.08 (C, Ar), 128.51 (CH, Ar), 126.25 (CH, Ar), 125.98 (CH, Ar), 37.50 (N-$CH_3$), 36.05 (N-$CH_3$), 25.69 (CH), 23.39 (CH), 16.72 ($CH_2$).
**HRMS (ESI)**. Calculated for $C_{12}H_{16}NO^+$: 190.12264 Obtained: 190.12265

USC UNIVERSIDADE DE SANTIAGO DE COMPOSTELA

*10.4.2.27 Preparation of (1S)-N,N,4,7,7-pentamethyl-3-oxo-2-oxabicyclo[2.2.1]heptane-1-carboxamide (44af)*



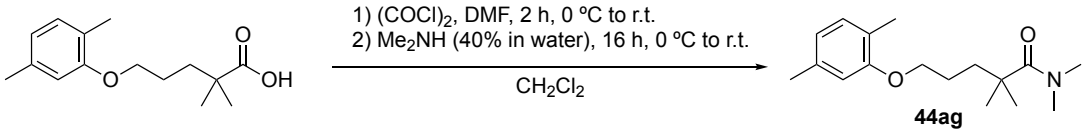

**44af**

Prepared following an adapted procedure:[133] To a solution of (1S)-4,7,7-trimethyl-3-oxo-2-oxabicyclo[2.2.1]heptane-1-carbonyl chloride (500 mg, 2.3 mmol, 1 equiv.) in $CH_2Cl_2$ (20 mL) at 0 ºC, were added dropwise $Me_2NH$ (40 w/w% in water; 1.2 mL, 9.2 mmol, 4 equiv.) and triethylamine (0.9 mL, 6.9 mmol, 3 equiv.). The reaction mixture was stirred continuously at room temperature overnight.

The reaction was then quenched with water and the mixture was extracted twice with $CH_2Cl_2$, then, the combined organic fractions were washed first with 1M aqueous HCl solution followed by a second wash with saturated aqueous $NaHCO_3$ solution and finally washed with brine. The organic fraction was dried over $MgSO_4$ and the solvent was removed in vacuo to obtain the (1*S*)-*N*,*N*,4,7,7-pentamethyl-3-oxo-2-oxabicyclo[2.2.1]heptane-1-carboxamide in a 37% yield (191 mg).

**$^1$H NMR** (400.16 MHz, $CDCl_3$, 258 K) δ 3.19 (s, 3H), 2.97 (s, 3H), 2.36 (ddd, *J* = 13.6, 10.8, 4.3 Hz, 1H), 2.06 (ddd, *J* = 13.7, 9.3, 4.5 Hz, 1H), 1.91 (ddd, *J* = 13.1, 10.9, 4.5 Hz, 1H), 1.69 (ddd, *J* = 13.4, 9.3, 4.3 Hz, 1H), 1.17 – 1.13 (m, 3H), 1.08 (s, 3H), 0.99 (s, 3H).
**$^{13}$C NMR** (100.63 MHz, $CDCl_3$, 258 K) δ 179.28 (CO), 166.79 (CO), 92.60 (C), 55.18 (C), 53.81 (C), 38.09 (N-$CH_3$), 37.02 (N-$CH_3$), 30.88 ($CH_2$), 29.17 ($CH_2$), 17.80 ($CH_3$), 16.84 ($CH_3$), 9.77 ($CH_3$).
**HRMS (ESI)**. Calculated for $C_{12}H_{20}NO_3^+$: 226.14377 Obtained: 226.14372

*10.4.2.28 Preparation of 5-(2,5-dimethylphenoxy)-N,N,2,2-tetramethylpentanamide (44ag)*




**44ag**

Prepared following an adapted procedure:[133] To a solution of Gemfibrozil (625 mg, 2.5 mmol, 1 equiv.) in $CH_2Cl_2$ (20 mL) at room temperature, were added carefully $(COCl)_2$ (0.32 mL, 3.75 mmol, 1.5 equiv.) and DMF (5 drops) in that order. The reaction mixture was stirred at room temperature for 2 h. After that time, the mixture was cooled down to 0 ºC and $Me_2NH$ (40 w/w% in water; 1.3 mL, 10.0 mmol, 4 equiv.) was added dropwise. The reaction mixture was stirred continuously at room temperature overnight.

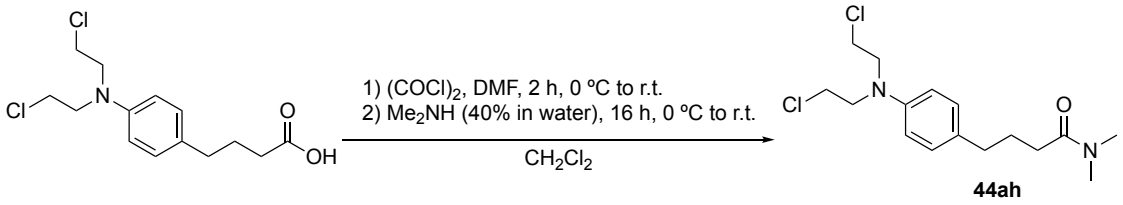
The reaction was then quenched with water and the mixture was extracted twice with $CH_2Cl_2$, then, the combined organic fractions were washed first with 1M aqueous HCl solution followed by a second wash with saturated aqueous $NaHCO_3$ solution and finally washed with brine. The organic fraction was dried over $MgSO_4$ and the solvent was

USC UNIVERSIDADE DE SANTIAGO DE COMPOSTELA

removed in vacuo to obtain the 5-(2,5-dimethylphenoxy)-*N*,*N*,2,2-tetramethylpentanamide in a 40% yield (277 mg).

**$^{1}$H NMR** (400.16 MHz, $CDCl_3$, 258 K) δ 7.01 (d, *J* = 7.4 Hz, 1H), 6.66 (d, *J* = 7.5 Hz, 1H), 6.60 (s, 1H), 3.92 (t, *J* = 5.7 Hz, 2H), 3.15 (s, 3H), 2.96 (s, 3H), 2.30 (s, 3H), 2.15 (s, 3H), 1.86 – 1.68 (m, 4H), 1.30 (s, 6H).
**$^{13}$C NMR** (100.63 MHz, $CDCl_3$, 258 K) δ 176.63 (CO), 156.75 (C, Ar), 136.66 (C, Ar), 130.27 (CH, Ar), 123.17 (C, Ar), 120.50 (CH, Ar), 111.44 (CH, Ar), 67.44 ($CH_2$), 42.36 (C), 38.28 (N-$CH_3$), 37.01 ($CH_2$), 27.06 ($CH_3$), 25.24 ($CH_2$), 21.61 ($CH_3$), 16.15 ($CH_3$).
**HRMS (ESI)**. Calculated for $C_{17}H_{28}NO_2^+$: 278.21146 Obtained: 278.21189

*10.4.2.29 Preparation of 4-(4-(bis(2-chloroethyl)amino)phenyl)-N,N-dimethylbutanamide (44ah)*



**44ah**

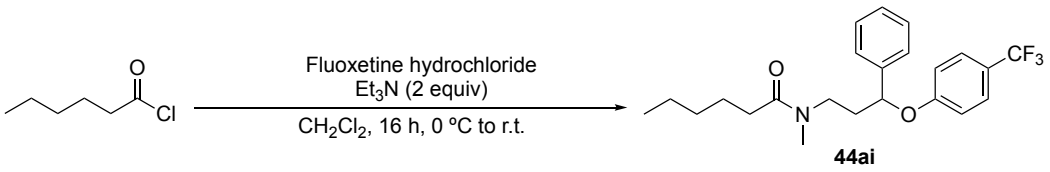
Prepared following an adapted procedure:[133] To a solution of Chlorambucil (304 mg, 1.0 mmol, 1 equiv.) in $CH_2Cl_2$ (20 mL) at room temperature, were added carefully $(COCl)_2$ (0.13 mL, 1.5 mmol, 1.5 equiv.) and DMF (5 drops) in that order. The reaction mixture was stirred at room temperature for 2 h. After that time, the mixture was cooled down to 0 ºC and $Me_2NH$ (40 w/w% in water; 0.5 mL, 4.0 mmol, 4 equiv.) was added dropwise. The reaction mixture was stirred continuously at room temperature overnight.

The reaction was then quenched with water and the mixture was extracted twice with $CH_2Cl_2$, then, the combined organic fractions were washed first with 1M aqueous HCl solution followed by a second wash with saturated aqueous $NaHCO_3$ solution and finally washed with brine. The organic fraction was dried over $MgSO_4$ and the solvent was removed in vacuo to obtain the 4-(4-(bis(2-chloroethyl)amino)phenyl)-*N*,*N*-dimethylbutanamide in a 61% yield (204 mg).

**$^{1}$H NMR** (400.16 MHz, $CDCl_3$, 258 K) δ 7.16 – 7.03 (m, 2H), 6.62 (s, 2H), 3.69 (d, *J* = 6.7 Hz, 4H), 3.66 – 3.56 (m, 4H), 2.97 (d, *J* = 1.1 Hz, 3H), 2.94 (s, 3H), 2.58 (t, *J* = 7.6 Hz, 2H), 2.32 (t, *J* = 7.6 Hz, 2H), 1.90 (p, *J* = 7.6 Hz, 2H).
**$^{13}$C NMR** (100.63 MHz, $CDCl_3$, 258 K) δ 172.98 (CO), 129.86 (CH, Ar), 128.21 (C, Ar), 111.56 (C, Ar), 53.43 ($CH_2$), 40.39 ($CH_2$), 37.41 (N-$CH_3$), 35.49 (N-$CH_3$), 34.25 ($CH_2$), 32.65 ($CH_2$), 26.88 ($CH_2$).
**HRMS (ESI)**. Calculated for $C_{16}H_{25}Cl_2N_2O^+$: 331.13385 Obtained: 331.13397

USC UNIVERSIDADE DE SANTIAGO DE COMPOSTELA

*10.4.2.30 Preparation of N-methyl-N-(3-phenyl-3-(4-(trifluoromethyl)phenoxy)propyl)hexanamide (44ai)*




**44ai**

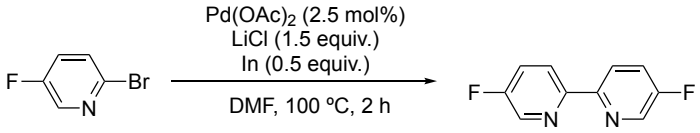
Prepared following an adapted procedure:[133] To a solution of hexanoyl chloride (0.14 mL, 1.0 mmol, 1 equiv.) in $CH_2Cl_2$ (5 mL) at 0 ºC, were added Fluoxetine hydrochloride (345 mg, 1.0 mmol, 1 equiv.) and triethylamine (0.3 mL, 2.0 mmol, 2 equiv.). The reaction mixture was stirred continuously at room temperature overnight.

The reaction was then quenched with water and the mixture was extracted twice with $CH_2Cl_2$, then, the combined organic fractions were washed first with 1M aqueous HCl solution followed by a second wash with saturated aqueous $NaHCO_3$ solution and finally washed with brine. The organic fraction was dried over $MgSO_4$ and the solvent was removed in vacuo to obtain the *N*-methyl-*N*-(3-phenyl-3-(4-(trifluoromethyl)phenoxy)propyl)hexanamide in a 55% yield (216 mg).

**$^1$H NMR** (400.16 MHz, DMSO, 398 K) δ 7.53 (d, *J* = 8.5 Hz, 2H), 7.42 (d, *J* = 8.0 Hz, 2H), 7.36 (t, *J* = 7.6 Hz, 2H), 7.28 (t, *J* = 7.2 Hz, 1H), 7.07 (d, *J* = 8.5 Hz, 2H), 5.43 (dd, *J* = 7.8, 4.8 Hz, 1H), 3.46 (td, *J* = 6.9, 2.0 Hz, 2H), 2.88 (s, 3H), 2.27 – 2.15 (m, 3H), 2.15 – 2.04 (m, 1H), 1.49 (p, *J* = 7.2 Hz, 2H), 1.35 – 1.17 (m, 4H), 0.86 (t, *J* = 6.7 Hz, 3H).
**$^{13}$C NMR** (100.63 MHz, DMSO, 398 K) δ 171.31 (CO), 160.04 (C, Ar), 140.00 (C, Ar), 127.80 (CH, Ar), 127.02 (CH, Ar), 125.94 (q, *J* = 3.9 Hz, CH, Ar), 125.36 (CH, Ar), 123.81 (q, *J* = 270.4 Hz, $CF_3$), 121.28 (q, *J* = 32.2 Hz, C, Ar), 115.79 (CH, Ar), 77.50 (CH), 44.14 ($CH_2$), 35.31 ($CH_2$), 33.29 (N-$CH_3$), 31.77 ($CH_2$), 30.32 ($CH_2$), 23.68 ($CH_2$), 21.02 ($CH_2$), 12.68 ($CH_3$).
**$^{19}$F NMR** (376.46 MHz, $CDCl_3$, 298 K) δ -61.52, -61.61.
**HRMS (ESI)**. Calculated for $C_{23}H_{29}F_3NO_2^+$: 408.21449 Obtained: 408.21456

## 10.4.3 Ligand synthesis

*10.4.3.1 Preparation of 5,5'-difluoro-2,2'-bipyridine (L49)*




A mixture of 2-bromo-5-fluoropyridine (1 g, 5.7 mmol, 1equiv), $Pd(OAc)_2$ (32 mg, 0.14 mmol, 2.5 mol%), LiCl (360 mg, 8.5 mmol, 1.5 equiv.) and indium powder (361 g, 8.5 mmol, 1.5 equiv.) in anhydrous DMF (11.3 mL) was deoxygenated by purging the solution with $N_2$ for 10 minutes. The reaction was then heated to 100 °C for 2 h then cooled to rt and quenched with sat. $NaHCO_3$ (50 mL) and $H_2O$ (100 mL).

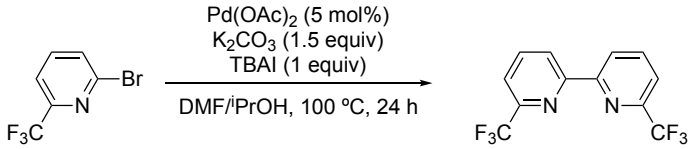
The layers were se*para*ted and the aqueous layer was extracted with EtOAc (3 × 50 mL). The combined organic portions were washed with $H_2O$ (60 mL) then brine (40 mL),

USC DE SANTIAGO DE COMPOSTELA

dried over $MgSO_4$, filtered and concentrated in vacuo. Purification by column chromatography (5% EtOAc in hexane) afforded the title compound (1.72 g, 90%) as a colorless solid.

**$^1$H NMR** (400.16 MHz, $CDCl_3$) δ 8.51 (d, *J* = 2.9 Hz, 2H), 8.41 (dd, *J* = 8.8, 4.4 Hz, 2H), 7.54 (td, *J* = 8.4, 2.9 Hz, 2H).
**$^{13}$C NMR** (100.63 MHz, $CDCl_3$) δ 159.99 (d, *J* = 257.9 Hz, C, Ar), 151.42 (C, Ar), 137.31 (d, *J* = 24.5 Hz, CH, Ar), 124.12 (d, *J* = 18.1 Hz, CH, Ar), 122.49 (d, *J* = 4.7 Hz, CH, Ar).
**$^{19}$F NMR** (376.46 MHz, $CDCl_3$) δ -127.10.
**$^{15}$N NMR** (40.55 MHz, $CDCl_3$) δ 312.04.
**HRMS (ESI)**. Calculated for $C_{10}H_7F_2N_2^+$: 193.057181 Obtained: 193.057206

### *10.4.3.2 Preparation of 6,6'-bis(trifluoromethyl)-2,2'-bipyridine (L50)*



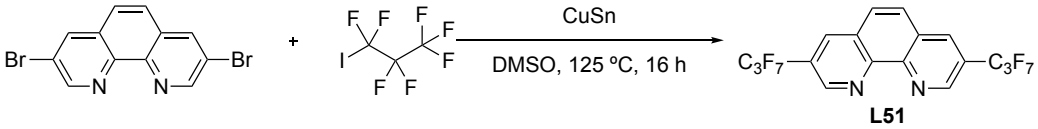

Prepared following an adapted procedure:[147] To a round-bottom flask charged with a magnetic stir bar were added, $Pd(OAc)_2$ (9.9 mg, 0.04 mmol, 5 mol%), TBAI (327 mg, 0.88 mmol, 1 eq.) and $K_2CO_3$ (183 mg, 1.3 mmol, 1.5 eq.). The flask was then evacuated and backfilled with $N_2$ three times. To this flask were added 2-bromo-6-(trifluoromethyl)pyridine (200 mg, 0.88 mmol, 1 eq.), $^i$PrOH (0.1 mL, 6.5 M) and DMF (3 ml, 0.3 M) and the reaction was heated at 100 °C for 24 h.

The reaction mixture was then cooled to room temperature and filtered, washing copiously with EtOAc. The organics were washed three times with 40 mL of 10% (w/w) aqueous LiCl. The aqueous layer was backwashed once with EtOAc (50 mL) and the combined organics washed with water (40 mL) and brine (40 mL) before drying over MgSO4. Following removal of the solvent in vacuo, the crude residue was purified by silica gel chromatography (gradient from 100% hexane to 5% EtOAc/hexane) to afford 6,6'-bis(trifluoromethyl)-2,2'-bipyridine (206 mg, 80% yield) as a white solid.

**$^1$H NMR** (400.16 MHz, $CDCl_3$) δ 8.73 (d, *J* = 8.1 Hz, 1H), 8.03 (td, *J* = 7.9, 0.7 Hz, 2H), 7.74 (dd, *J* = 7.8, 1.0 Hz, 2H).
**$^{13}$C NMR** (100.63 MHz, $CDCl_3$) δ 155.20 (C, Ar), 147.97 (q, *J* = 34.9 Hz, C, Ar), 138.71 (CH, Ar), 124.16 (CH, Ar), 121.61 (q, *J* = 274.3 Hz, $CF_3$), 121.02 (q, *J* = 2.8 Hz, CH, Ar).
**$^{19}$F NMR** (376.46 MHz, $CDCl_3$) δ -68.07.
**HRMS (ESI)**. Calculated for $C_{12}H_7F_6N_2^+$: 293.05079 Obtained: 293.05088

USC UNIVERSIDADE DE SANTIAGO DE COMPOSTELA

### *10.4.3.3 Preparation of 3,8-bis(perfluoropropyl)-1,10-phenanthroline (L51)*



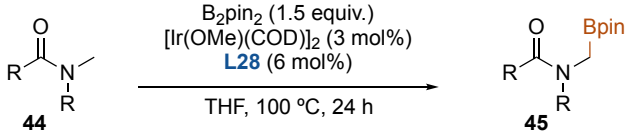

**L51**

Prepared following an adapted procedure:[148] Perfluoropropyl iodide (94 µl, 0.65 mmol, 1.1 equiv.) was added to a well-stirred mixture of Copper-tin alloy (237 mg, 1.3 mmol, 2.2 equiv.), 3,8-dibromo-1,10-phenanthroline (100 mg, 0.3 mmol, 1 equiv.) and DMSO (0.7 ml, 0.4 M) under a nitrogen atmosphere and the reaction was heated at 125° C for 4 h.

The reaction mixture was cooled to room temperature, diethyl ether (10 ml) and water (6 ml) were slowly added. The mixture was stirred and then centrifuged and the aqueous and organic layers were decanted from the solid This solid was washed with additional diethyl ether (2 x 40 ml) The ether extracts and the previous organic layer were combined, and repeatedly treated with an aqueous ammonium hydroxide solution until no blue color in the aqueous layer was noted. The ether layer was se*para*ted and dried over anhydrous $MgSO_4$. The mixture was filtered, the solvent was removed under vacuum and the mixture was purified by column chromatography on silica gel to afford 3,8-bis(perfluoropropyl)-1,10-phenanthroline (85 mg, 56% yield) as a white solid.

**$^1$H NMR** (400.16 MHz, $CDCl_3$) δ 9.37 (s, 2H), 8.59 – 8.53 (m, 2H), 8.03 (s, 2H).
**$^{13}$C NMR** (100.63 MHz, $CDCl_3$) δ 147.74 (dd, *J* = 7.2, 5.2 Hz, CH, Ar), 147.49 (C, Ar), 135.82 (t, *J* = 6.5 Hz, CH, Ar), 128.41 (C, Ar), 128.10 (CH, Ar), 125.14 (t, *J* = 24.5 Hz, C, Ar), 117.99 (qt, *J* = 287.3, 33.8 Hz, $CF_3$–$\underline{C}F_2$–$CF_2$–), 114.88 (tt, *J* = 256.6, 31.7 Hz, $CF_3$–$CF_2$–$\underline{C}F_2$–), 108.76 (tq, *J* = 264.6, 38.2 Hz, $\underline{C}F_3$–$CF_2$–$CF_2$–).
**$^{19}$F NMR** (376.46 MHz, $CDCl_3$) δ -79.71 (t, *J* = 9.8 Hz), -111.83 (q, *J* = 9.8 Hz), -125.90.
**HRMS (ESI).** Calculated for $C_{18}H_7F_{14}N_2^+$: 517.038019 Obtained: 517.038160

## 10.4.4 General procedure for N-Me borylation



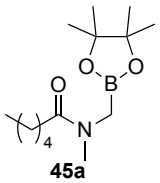

**44** **45**

Following an adapted procedure:[149] In a sealed tube $[Ir(COD)(OMe)]_2$ (5 mg, 0.008 mmol, 3 mol%.), $B_2pin_2$ (95.2 mg, 0.375 mmol, 1.5 equiv.), and **L28** (4.4 mg, 0.015 mmol, 6 mol%) were added. The tube was evacuated and refilled with $N_2$ three times, then under a positive flow of $N_2$, dry THF (1.25 mL) and substrate (0.250 mmol, 1.0 equiv.) were added. The tube was then sealed and heated for the specified time. After that, volatiles were removed under vacuum and $CH_2Br_2$ (internal standard) was added, the yield was determined by $^1$H NMR spectroscopy. To isolate the product, the solvent was removed

USC UNIVERSIDADE DE SANTIAGO DE COMPOSTELA

under reduced pressure, and the residue was purified by column chromatography on silica gel.

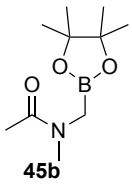
*10.4.4.1 N-methyl-N-((4,4,5,5-tetramethyl-1,3,2-dioxaborolan-2-yl)methyl)hexanamide (45a)*


45a

Following the general procedure: **44a** (35.8 mg, 0.250 mmol, 1.0 eq.), $[Ir(COD)(OMe)]_2$ (5 mg, 0.008 mmol, 3 mol%), $B_2pin_2$ (95.2 mg, 0.375 mmol, 1.5 eq.), **L28** (4.4 mg, 0.015 mmol, 6 mol%) in THF (1.25 mL) were heated at 100 °C for 24 h. The crude mixture was purified by column chromatography (Hex/EtOAc 0% - EtOAc 100% - EtOAc/MeOH 20%) to obtain 65 mg (96% yield) of **45a**.

**$^1$H NMR** (600.1318 MHz, $CDCl_3$, 258 K) δ 3.03 (s, 3H), 2.36 (s, 2H), 2.32 (t, *J* = 7.9 Hz, 2H), 1.64 (dq, *J* = 12.1, 7.5 Hz, 2H), 1.30 (dt, *J* = 7.3, 3.9 Hz, 4H), 1.15 (s, 12H), 0.89 – 0.84 (m, 3H).
**$^{13}$C NMR** (100.63 MHz, $CDCl_3$, 258 K) δ 176.94 (CO), 79.82 (C), 43.78 (N-$CH_2$-B), 35.79 (N-$CH_3$), 31.28 ($CH_2$), 28.42 ($CH_2$), 25.11 ($CH_3$), 24.23 ($CH_2$), 22.27 ($CH_2$), 13.99 ($CH_3$).
**$^{11}$B NMR** (128.39 MHz, $CDCl_3$, 258 K) δ 12.55.
**HRMS (ESI).** Calculated for $C_{14}H_{29}BNO_3^+$: 270.223501 Obtained: 270.223812

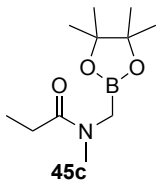
*10.4.4.2 N-methyl-N-((4,4,5,5-tetramethyl-1,3,2-dioxaborolan-2-yl)methyl)acetamide (45b)*


45b

Following the general procedure: **44b** (21.6 mg, 0.250 mmol, 1.0 eq.), $[Ir(COD)(OMe)]_2$ (5 mg, 0.008 mmol, 3 mol%), $B_2pin_2$ (95.2 mg, 0.375 mmol, 1.5 eq.), **L28** (4.4 mg, 0.015 mmol, 6 mol%) in THF (1.25 mL) were heated at 100 °C for 24 h. The crude mixture was purified by column chromatography (Hex/EtOAc 0% - EtOAc 100% - EtOAc/MeOH 20%) to obtain 21 mg (39% yield) of **45b**.

**$^1$H NMR** (600.1318 MHz, $CDCl_3$, 258 K) δ 3.07 (s, 3H), 2.40 (s, 2H), 2.16 – 2.11 (m, 3H), 1.18 (s, 12H).
**$^{13}$C NMR** (100.63 MHz, $CDCl_3$, 258 K) δ 174.56 (CO), 80.20 (C), 43.72 (N-$CH_2$-B), 36.26 (N-$CH_3$), 25.24 ($CH_3$), 15.67 ($CH_3$).
**$^{11}$B NMR** (128.39 MHz, $CDCl_3$, 258 K) δ 12.61.
**HRMS (ESI).** Calculated for $C_{10}H_{20}BNNaO_3^+$: 236.142845 Obtained: 236.142964

*10.4.4.3 N-methyl-N-((4,4,5,5-tetramethyl-1,3,2-dioxaborolan-2-yl)methyl)propionamide (45c)*

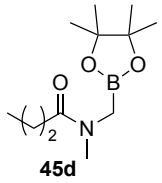

45c

Following the general procedure: **44c** (25.3 mg, 0.250 mmol, 1.0 eq.), $[Ir(COD)(OMe)]_2$ (5 mg, 0.008 mmol, 3 mol%), $B_2pin_2$ (95.2 mg, 0.375 mmol, 1.5 eq.), **L28** (4.4 mg, 0.015 mmol, 6 mol%) in THF (1.25 mL) were heated at 100 °C for 24 h. The crude mixture was purified by column chromatography (Hex/EtOAc 0% - EtOAc 100% - EtOAc/MeOH 20%) to obtain 52 mg (92% yield) of **45c**.

USC UNIVERSIDADE DE SANTIAGO DE COMPOSTELA

**$^{1}$H NMR** (600.1318 MHz, $CDCl_3$, 258 K) δ 3.01 (s, 3H), 2.41 – 2.31 (m, 4H), 1.18 (dd, *J* = 6.1, 1.3 Hz, 3H), 1.14 (s, 12H).
**$^{13}$C NMR** (100.63 MHz, $CDCl_3$, 258 K) δ 177.62 (CO), 80.00 (C), 44.36 (N-$CH_2$-B), 35.60 (N-$CH_3$), 25.17 ($CH_3$), 22.13 ($CH_2$), 8.76 ($CH_3$).
**$^{11}$B NMR** (128.39 MHz, $CDCl_3$, 258 K) δ 12.59
**HRMS (ESI).** Calculated for $C_{11}H_{22}BNNaO_3^+$: 250.158495 Obtained: 250.158519

#### *10.4.4.4 N-methyl-N-((4,4,5,5-tetramethyl-1,3,2-dioxaborolan-2-yl)methyl)butyramide (45d)*

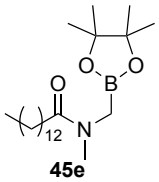


**45d**

Following the general procedure: **44d** (28.8 mg, 0.250 mmol, 1.0 eq.), $[Ir(COD)(OMe)]_2$ (5 mg, 0.008 mmol, 3 mol%), $B_2pin_2$ (95.2 mg, 0.375 mmol, 1.5 eq.), **L28** (4.4 mg, 0.015 mmol, 6 mol%) in THF (1.25 mL) were heated at 100 °C for 24 h. The crude mixture was purified by column chromatography (Hex/EtOAc 0% - EtOAc 100% - EtOAc/MeOH 20%) to obtain 54 mg (89% yield) of **45d**.

**$^{1}$H NMR** (600.1318 MHz, $CDCl_3$, 258 K) δ 3.04 (s, 3H), 2.37 (s, 2H), 2.32 (t, *J* = 7.5 Hz, 2H), 1.69 (h, *J* = 7.4 Hz, 2H), 1.16 (s, 12H), 0.97 (t, *J* = 7.4 Hz, 3H).
**$^{13}$C NMR** (100.63 MHz, $CDCl_3$, 258 K) δ 176.97 (CO), 80.01 (C), 44.20 (N-$CH_2$-B), 35.81 (N-$CH_3$), 30.45 ($CH_2$), 25.25 ($CH_3$), 18.32 ($CH_2$), 13.91 ($CH_3$).
**$^{11}$B NMR** (128.39 MHz, $CDCl_3$, 258 K) δ 12.61
**HRMS (ESI).** Calculated for $C_{12}H_{24}BNNaO_3^+$: 264.174145 Obtained: 264.174192

#### *10.4.4.5 N,2-dimethyl-N-((4,4,5,5-tetramethyl-1,3,2-dioxaborolan-2-yl)methyl)tridecanamide (45e)*

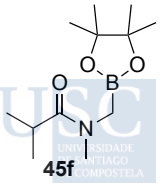


**45e**

Following the general procedure: **44e** (63.9 mg, 0.250 mmol, 1.0 eq.), $[Ir(COD)(OMe)]_2$ (5 mg, 0.008 mmol, 3 mol%), $B_2pin_2$ (95.2 mg, 0.375 mmol, 1.5 eq.), **L28** (4.4 mg, 0.015 mmol, 6 mol%) in THF (1.25 mL) were heated at 100 °C for 24 h. The crude mixture was purified by column chromatography (Hex/EtOAc 0% - EtOAc 100% - EtOAc/MeOH 20%) to obtain 65 mg (68% yield) of **45e**.

**$^{1}$H NMR** (600.1318 MHz, $CDCl_3$, 258 K) δ 3.01 (s, 3H), 2.34 (s, 2H), 2.33 – 2.28 (m, 2H), 1.62 (dq, *J* = 8.8, 7.0 Hz, 2H), 1.21 (s, 20H), 1.14 (s, 12H), 0.87 – 0.80 (m, 3H).
**$^{13}$C NMR** (100.63 MHz, $CDCl_3$, 258 K) δ 177.09 (CO), 79.93 (C), 43.97 (N-$CH_2$-B), 35.76 (N-$CH_3$), 31.97 ($CH_2$), 29.70 ($CH_2$), 29.68 ($CH_2$), 29.61 ($CH_2$), 29.42 ($CH_2$), 29.40 ($CH_2$), 29.24 ($CH_2$), 29.20 ($CH_2$), 28.53 ($CH_2$), 25.20 ($CH_3$), 24.63 ($CH_2$), 22.74 ($CH_2$), 14.17 ($CH_3$).
**$^{11}$B NMR** (128.39 MHz, $CDCl_3$, 258 K) δ 12.62.
**HRMS (ESI).** Calculated for $C_{22}H_{45}BNO_3^+$: 382.348701 Obtained: 382.348974

#### *10.4.4.6 N-methyl-N-((4,4,5,5-tetramethyl-1,3,2-dioxaborolan-2-yl)methyl)isobutyramide (45f)*



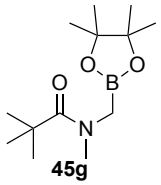
**45f**

Following the general procedure: **44f** (28.8 mg, 0.250 mmol, 1.0 eq.), $[Ir(COD)(OMe)]_2$ (5 mg, 0.008 mmol, 3 mol%), $B_2pin_2$ (95.2 mg, 0.375 mmol, 1.5 eq.), **L28** (4.4 mg, 0.015 mmol, 6 mol%) in THF (1.25 mL) were

heated at 100 °C for 24 h. The crude mixture was purified by column chromatography (Hex/EtOAc 0% - EtOAc 100% - EtOAc/MeOH 20%) to obtain 41 mg (67% yield) of **45f**.

**$^{1}$H NMR** (600.1318 MHz, $CDCl_3$, 258 K) δ 3.04 (s, 3H), 2.73 (p, *J* = 6.8 Hz, 1H), 2.34 (s, 2H), 1.16 (s, 3H), 1.15 (s, 3H), 1.14 (s, 12H).
**$^{13}$C NMR** (100.63 MHz, $CDCl_3$, 258 K) δ 180.32 (CO), 79.91 (C), 44.50 (N-$CH_2$-B), 35.52 (N-$CH_3$), 27.44 (CH), 25.16 ($CH_3$), 18.54 ($CH_3$).
**$^{11}$B NMR** (128.39 MHz, $CDCl_3$, 258 K) δ 12.37
**HRMS (ESI).** Calculated for $C_{12}H_{24}BNNaO_3^+$: 264.174145 Obtained: 264.174077

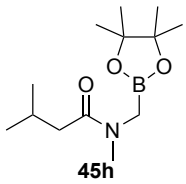
#### *10.4.4.7 N-methyl-N-((4,4,5,5-tetramethyl-1,3,2-dioxaborolan-2-yl)methyl)pivalamide (45g)*




Following the general procedure: **44g** (32.3 mg, 0.250 mmol 1.0 eq.), $[Ir(COD)(OMe)]_2$ (5 mg, 0.008 mmol, 3 mol%), $B_2pin_2$ (95.2 mg, 0.375 mmol, 1.5 eq.), **L28** (4.4 mg, 0.015 mmol, 6 mol%) in THF (1.25 mL) were heated at 100 °C for 24 h. The crude mixture was purified by column chromatography (Hex/EtOAc 0% - EtOAc 100% - EtOAc/MeOH 20%) to obtain 36 mg (56% yield) of **45g**.

**$^{1}$H NMR** (600.1318 MHz, $CDCl_3$, 258 K) δ 3.20 (s, 3H), 2.44 (s, 2H), 1.29 (s, 9H), 1.15 (s, 12H).
**$^{13}$C NMR** (100.63 MHz, $CDCl_3$, 258 K) δ 181.10 (CO), 79.73 (C), 47.02 (N-$CH_2$-B), 37.73 (N-$CH_3$), 35.63 (C), 27.18 ($CH_3$), 25.12 ($CH_3$).
**$^{11}$B NMR** (128.39 MHz, $CDCl_3$, 258 K) δ 11.71.
**HRMS (ESI).** Calculated for $C_{13}H_{26}BNNaO_3^+$: 278.189795 Obtained: 278.190164

#### *10.4.4.8 N,3-dimethyl-N-((4,4,5,5-tetramethyl-1,3,2-dioxaborolan-2-yl)methyl)butanamide (45h)*

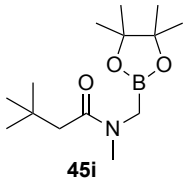



Following the general procedure: **44h** (32.3 mg, 0.250 mmol, 1.0 eq.), $[Ir(COD)(OMe)]_2$ (5 mg, 0.008 mmol, 3 mol%), $B_2pin_2$ (95.2 mg, 0.375 mmol, 1.5 eq.), **L28** (4.4 mg, 0.015 mmol, 6 mol%) in THF (1.25 mL) were heated at 100 °C for 24 h. The crude mixture was purified by column chromatography (Hex/EtOAc 0% - EtOAc 100% - EtOAc/MeOH 20%) to obtain 28 mg (43% yield) of **45h.**

**$^{1}$H NMR** (600.1318 MHz, $CDCl_3$, 258 K) δ 3.07 (s, 3H), 2.39 (s, 2H), 2.25 (d, *J* = 7.6 Hz, 2H), 2.15 (dtd, *J* = 13.1, 6.5, 1.3 Hz, 1H), 1.16 (s, 12H), 0.96 (s, 3H), 0.95 (s, 3H).
**$^{13}$C NMR** (100.63 MHz, $CDCl_3$, 258 K) δ 176.39 (CO), 79.84 (C), 43.89 (N-$CH_2$-B), 36.81 ($CH_2$), 36.12 (N-$CH_3$), 26.08 (CH), 25.14 ($CH_3$), 22.65 ($CH_3$).
**$^{11}$B NMR** (128.39 MHz, $CDCl_3$, 258 K) δ 12.42.
**HRMS (ESI).** Calculated for $C_{13}H_{26}BNNaO_3^+$: 278.189795 Obtained: 278.190334

USC UNIVERSIDADE DE SANTIAGO DE COMPOSTELA

#### *10.4.4.9 N,3,3-trimethyl-N-((4,4,5,5-tetramethyl-1,3,2-dioxaborolan-2-yl)methyl)butanamide (45i)*

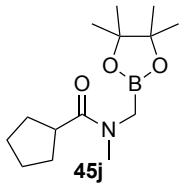


**45i**

Following the general procedure: **44i** (35.8 mg, 0.250 mmol, 1.0 eq.), $[Ir(COD)(OMe)]_2$ (5 mg, 0.008 mmol, 3 mol%), $B_2pin_2$ (95.2 mg, 0.375 mmol, 1.5 eq.), **L28** (4.4 mg, 0.015 mmol, 6 mol%) in THF (1.25 mL) were heated at 100 °C for 24 h. The crude mixture was purified by column chromatography (Hex/EtOAc 0% - EtOAc 100% - EtOAc/MeOH 20%) to obtain 54 mg (80% yield) of **45i**.

**$^1$H NMR** (600.1318 MHz, $CDCl_3$, 258 K) δ 3.08 (s, 3H), 2.38 (s, 2H), 2.29 (s, 2H), 1.14 (s, 12H), 1.01 (s, 9H).
**$^{13}$C NMR** (100.63 MHz, $CDCl_3$, 258 K) δ 175.70 (CO), 79.73 (C), 43.89 (N-$CH_2$-B), 40.45 ($CH_2$), 36.82 (N-$CH_3$), 32.82 (C), 29.83 ($CH_3$), 25.11 ($CH_3$).
**$^{11}$B NMR** (128.39 MHz, $CDCl_3$, 258 K) δ 12.02.
**HRMS (ESI).** Calculated for $C_{14}H_{28}BNNaO_3^+$: 292.205445 Obtained: 292.206017

#### *10.4.4.10 N-methyl-N-((4,4,5,5-tetramethyl-1,3,2-dioxaborolan-2-yl)methyl)cyclopentanecarboxamide (45j)*

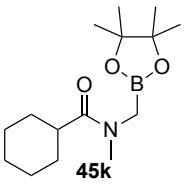


**45j**

Following the general procedure: **44j** (35.2 mg, 0.250 mmol, 1.0 eq.), $[Ir(COD)(OMe)]_2$ (5 mg, 0.008 mmol, 3 mol%), $B_2pin_2$ (95.2 mg, 0.375 mmol, 1.5 eq.), **L28** (4.4 mg, 0.015 mmol, 6 mol%) in THF (1.25 mL) were heated at 100 °C for 24 h. The crude mixture was purified by column chromatography (Hex/EtOAc 0% - EtOAc 100% - EtOAc/MeOH 20%) to obtain 20 mg (30% yield) of **45j**.

**$^1$H NMR** (600.1318 MHz, $CDCl_3$, 258 K) δ 3.06 (s, 3H), 2.82 (p, *J* = 8.1 Hz, 1H), 2.37 (s, 2H), 1.91 – 1.73 (m, 6H), 1.63 – 1.54 (m, 2H), 1.15 (s, 12H).
**$^{13}$C NMR** (100.63 MHz, $CDCl_3$, 258 K) δ 179.77 (CO), 79.77 (C), 44.13 (N-$CH_2$-B), 37.33 (CH), 35.75 ($CH_3$), 29.73 ($CH_2$), 25.90 ($CH_2$), 25.15 ($CH_3$).
**$^{11}$B NMR** (128.39 MHz, $CDCl_3$, 258 K) δ 12.32.
**HRMS (ESI).** Calculated for $C_{14}H_{26}BNNaO_3^+$: 290.189795 Obtained: 290.190580

#### *10.4.4.11 N-methyl-N-((4,4,5,5-tetramethyl-1,3,2-dioxaborolan-2-yl)methyl)cyclohexanecarboxamide (45k)*



**45k**

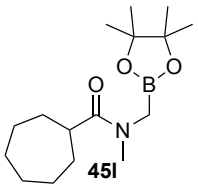
Following the general procedure: **44k** (52.3 mg, 0.250 mmol, 1.0 eq.), $[Ir(COD)(OMe)]_2$ (5 mg, 0.008 mmol, 3 mol%), $B_2pin_2$ (95.2 mg, 0.375 mmol, 1.5 eq.), **L** (4.4 mg, 0.015 mmol, 6 mol%) in THF (1.25 mL) were heated at 100 °C for 24 h. The crude mixture was purified by column chromatography (Hex/EtOAc 0% - EtOAc 100% - EtOAc/MeOH 20%) to obtain 50 mg (70% yield) of **45k**.

**$^1$H NMR** (400.16 MHz, $CDCl_3$, 258 K) δ 3.05 (s, 3H), 2.42 (tt, *J* = 11.6, 3.5 Hz, 1H), 2.35 (s, 2H), 1.83 – 1.66 (m, 5H), 1.61 – 1.49 (m, 2H), 1.27 – 1.23 (m, 3H), 1.16 (s, 12H).

USC UNIVERSIDADE DE SANTIAGO DE COMPOSTELA

**$^{13}$C NMR** (100.63 MHz, $CDCl_3$, 258 K) δ 179.42 (CO), 79.90 (C), 43.93 (N-$CH_2$-B), 37.16 (CH), 35.58, (N-$CH_3$) 28.37 ($CH_2$), 25.50 ($CH_2$), 25.46 ($CH_2$), 25.25 ($CH_3$).
**$^{11}$B NMR** (128.39 MHz, $CDCl_3$, 258 K) δ 12.46.
**HRMS (ESI).** Calculated for $C_{15}H_{29}BNO_3^+$: 282.223501 Obtained: 282.223615

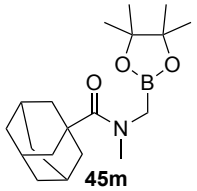
#### *10.4.4.12 N-methyl-N-((4,4,5,5-tetramethyl-1,3,2-dioxaborolan-2-yl)methyl)cycloheptanecarboxamide (45l)*




Following the general procedure: **44l** (42.3 mg, 0.250 mmol, 1.0 eq.), $[Ir(COD)(OMe)]_2$ (5 mg, 0.008 mmol, 3 mol%), $B_2pin_2$ (95.2 mg, 0.375 mmol, 1.5 eq.), **L28** (4.4 mg, 0.015 mmol, 6 mol%) in THF (1.25 mL) were heated at 100 °C for 24 h. The crude mixture was purified by column chromatography (Hex/EtOAc 0% - EtOAc 100% - EtOAc/MeOH 20%) to obtain 70 mg (95% yield) of **45l**.

**$^1$H NMR** (600.1318 MHz, $CDCl_3$, 258 K) δ 3.04 (s, 3H), 2.57 (ddd, *J* = 9.6, 7.5, 3.8 Hz, 1H), 2.33 (s, 2H), 1.82 – 1.65 (m, 6H), 1.52 (t, *J* = 3.8 Hz, 4H), 1.43 – 1.34 (m, 2H), 1.13 (s, 12H).
**$^{13}$C NMR** (100.63 MHz, $CDCl_3$, 258 K) δ 180.34 (CO), 79.72 (C), 43.97 (N-$CH_2$-B), 38.04 (CH), 35.70 ($CH_3$), 30.07 ($CH_2$), 28.09 ($CH_2$), 26.32 ($CH_2$), 25.09 ($CH_3$).
**$^{11}$B NMR** (128.39 MHz, $CDCl_3$, 258 K) δ 12.22.
**HRMS (ESI).** Calculated for $C_{16}H_{30}BNNaO_3^+$: 318.221095 Obtained: 318.221747

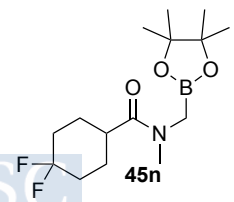
#### *10.4.4.13 (3r,5r,7r)-N-methyl-N-((4,4,5,5-tetramethyl-1,3,2-dioxaborolan-2-yl)methyl)adamantane-1-carboxamide (45m)*




Following the general procedure: **44m** (51.8 mg, 0.250 mmol, 1.0 eq.), $[Ir(COD)(OMe)]_2$ (5 mg, 0.008 mmol, 3 mol%), $B_2pin_2$ (95.2 mg, 0.375 mmol, 1.5 eq.), **L28** (4.4 mg, 0.015 mmol, 6 mol%) in THF (1.25 mL) were heated at 100 °C for 24 h. The crude mixture was purified by column chromatography (Hex/EtOAc 0% - EtOAc 100% - EtOAc/MeOH 20%) to obtain 72 mg (86% yield) of **45m**.

**$^1$H NMR** (600.1318 MHz, $CDCl_3$, 258 K) δ 3.23 (s, 3H), 2.40 (s, 2H), 2.02 – 1.96 (m, 9H), 1.66 (dt, *J* = 6.7, 2.9 Hz, 6H), 1.14 (s, 12H).
**$^{13}$C NMR** (100.63 MHz, $CDCl_3$, 258 K) δ 179.96 (CO), 79.65 (C), 47.30 (N-$CH_2$-B), 38.13 (C), 37.80 (N-$CH_3$), 37.30 ($CH_2$), 36.01 ($CH_2$), 27.60 (CH), 25.10 (N-$CH_3$).
**$^{11}$B NMR** (128.39 MHz, $CDCl_3$, 258 K) δ 11.39.
**HRMS (ESI).** Calculated for $C_{19}H_{32}BNNaO_3^+$: 356.236745 Obtained: 356.238031

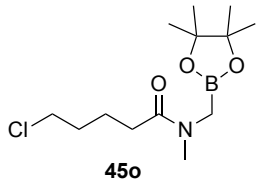
#### *10.4.4.14 4,4-difluoro-N-methyl-N-((4,4,5,5-tetramethyl-1,3,2-dioxaborolan-2-yl)methyl)cyclohexane-1-carboxamide (45n)*




Following the general procedure: **44n** (47.8 mg, 0.250 mmol, 1.0 eq.), $[Ir(COD)(OMe)]_2$ (5 mg, 0.008 mmol, 3 mol%), $B_2pin_2$ (95.2 mg, 0.375 mmol, 1.5 eq.), **L28** (4.4 mg, 0.015 mmol, 6 mol%) in THF (1.25 mL) were heated at 100 °C for 24 h. The crude mixture was purified by column chromatography (Hex/EtOAc 0% - EtOAc 100% - EtOAc/MeOH 20%) to obtain 74 mg (93% yield) of **45n**.

**$^{1}$H NMR** (600.1318 MHz, $CDCl_3$, 258 K) δ 3.08 (s, 3H), 2.55 (dt, *J* = 10.2, 5.3 Hz, 1H), 2.36 (s, 2H), 2.24 – 2.14 (m, 2H), 1.93 – 1.69 (m, 6H), 1.13 (s, 12H).
**$^{13}$C NMR** (100.63 MHz, $CDCl_3$, 258 K) δ 177.56 (CO), 122.23 (t, *J* = 241.3 Hz, $CF_2$), 79.93 (C), 43.80 (N-$CH_2$-B), 35.76 (N-$CH_3$), 34.15 (CH), 32.31 (t, *J* = 24.7 Hz, $CH_2$), 25.10, 24.65 (d, *J* = 10.3 Hz, $CH_2$).
**$^{19}$F NMR** (376.46 MHz, $CDCl_3$, 258 K) δ -93.89 (d, *J* = 237.9 Hz), -100.06 (d, *J* = 237.9 Hz).
**$^{11}$B NMR** (128.39 MHz, $CDCl_3$, 258 K) δ 12.83
**HRMS (ESI).** Calculated for $C_{15}H_{26}BF_2NNaO_3^+$: 340.186601 Obtained: 340.187716

#### *10.4.4.15 5-chloro-N-methyl-N-((4,4,5,5-tetramethyl-1,3,2-dioxaborolan-2-yl)methyl)pentanamide (45o)*

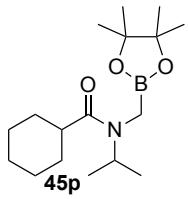


**45o**

Following the general procedure: **44o** (40.9 mg, 0.250 mmol, 1.0 eq.), $[Ir(COD)(OMe)]_2$ (5 mg, 0.008 mmol, 3 mol%), $B_2pin_2$ (95.2 mg, 0.375 mmol, 1.5 eq.), **L28** (4.4 mg, 0.015 mmol, 6 mol%) in THF (1.25 mL) were heated at 100 °C for 24 h. The crude mixture was purified by column chromatography (Hex/EtOAc 0% - EtOAc 100% - EtOAc/MeOH 20%) to obtain 15 mg (21% yield) of **45o**.

**$^{1}$H NMR** (600.1318 MHz, $CDCl_3$, 258 K) δ 3.59 – 3.52 (m, 2H), 3.05 (s, 3H), 2.44 – 2.35 (m, 4H), 1.84 (dq, *J* = 6.6, 3.2 Hz, 4H), 1.17 (s, 12H).
**$^{13}$C NMR** (100.63 MHz, $CDCl_3$, 258 K) δ 176.22 (CO), 79.99 (C), 44.22 ($CH_2$), 43.61 (N-$CH_2$-B), 35.70 (N-$CH_3$), 31.54 ($CH_2$), 27.57 ($CH_2$), 25.12 ($CH_3$), 21.81 ($CH_2$).
**$^{11}$B NMR** (128.39 MHz, $CDCl_3$, 258 K) δ 12.92
**HRMS (ESI).** Calculated for $C_{13}H_{26}BClNO_3^+$: 290.168878 Obtained: 290.168893

#### *10.4.4.16 N-isopropyl-N-((4,4,5,5-tetramethyl-1,3,2-dioxaborolan-2-yl)methyl)cyclohexanecarboxamide (45p)*



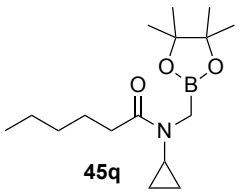
**45p**

Following the general procedure: **44p** (45.8 mg, 0.250 mmol, 1.0 eq.), $[Ir(COD)(OMe)]_2$ (5 mg, 0.008 mmol, 3 mol%), $B_2pin_2$ (95.2 mg, 0.375 mmol, 1.5 eq.), **L28** (4.4 mg, 0.015 mmol, 6 mol%) in THF (1.25 mL) were heated at 100 °C for 24 h. The crude mixture was purified by column chromatography (Hex/EtOAc 0% - EtOAc 100% - EtOAc/MeOH 20%) to obtain 54 mg (70% yield) of **45p.**

**$^{1}$H NMR** (600.1318 MHz, $CDCl_3$, 258 K) δ 4.00 (p, *J* = 6.6 Hz, 1H), 2.42 (tt, *J* = 11.8, 3.5 Hz, 1H), 2.20 (s, 2H), 1.83 – 1.74 (m, 2H), 1.69 (ddd, *J* = 15.2, 7.7, 4.4 Hz, 3H), 1.57 (dt, *J* = 12.4, 6.0 Hz, 2H), 1.24 – 1.20 (m, 3H), 1.18 (s, 6H), 1.16 (s, 12H).
**$^{13}$C NMR** (100.63 MHz, $CDCl_3$, 258 K) δ 178.20 (CO), 79.61 (C), 47.61 (N-CH), 37.27 (CH), 32.93 (N-CH2-B), 28.64 ($CH_2$), 25.42 ($CH_2$), 25.30 ($CH_2$), 20.63 ($CH_3$).
**$^{11}$B NMR** (128.39 MHz, $CDCl_3$, 258 K) δ 12.11
**HRMS (ESI).** Calculated for $C_{17}H_{32}BNNaO_3^+$: 332.236745 Obtained: 332.236742

USC UNIVERSIDADE DE SANTIAGO DE COMPOSTELA

*10.4.4.17 N-cyclopropyl-N-((4,4,5,5-tetramethyl-1,3,2-dioxaborolan-2-yl)methyl)hexanamide (45q)*

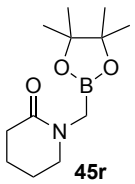


45q

Following the general procedure: **44q** (42.3 mg, 0.250 mmol, 1.0 eq.), $[Ir(COD)(OMe)]_2$ (5 mg, 0.008 mmol, 3 mol%), $B_2pin_2$ (95.2 mg, 0.375 mmol, 1.5 eq.), **L28** (4.4 mg, 0.015 mmol, 6 mol%) in THF (1.25 mL) were heated at 100 °C for 24 h. The crude mixture was purified by column chromatography (Hex/EtOAc 0% - EtOAc 100% - EtOAc/MeOH 20%) to obtain 64 mg (86% yield) of **45q**.

**$^1$H NMR** (600.1318 MHz, $CDCl_3$, 258 K) δ 2.67 (tt, *J* = 7.2, 4.0 Hz, 1H), 2.51 – 2.45 (m, 2H), 2.27 (s, 2H), 1.71 – 1.61 (m, 2H), 1.31 (ddd, *J* = 7.3, 4.3, 3.2 Hz, 4H), 1.14 (s, 12H), 0.90 – 0.81 (m, 5H), 0.77 – 0.71 (m, 2H).
**$^{13}$C NMR** (100.63 MHz, $CDCl_3$, 258 K) δ 179.93 (CO), 79.97 (C), 40.70 (N-$CH_2$-B), 31.45 ($CH_2$), 29.49 ($CH_2$), 29.46 (CH), 25.21 ($CH_3$), 24.14 ($CH_2$), 22.30 ($CH_2$), 13.89 ($CH_3$), 6.97 ($CH_2$).
**$^{11}$B NMR** (128.39 MHz, $CDCl_3$, 258 K) δ 12.77
**HRMS (ESI).** Calculated for $C_{16}H_{30}BNNaO_3^+$: 318.221095 Obtained: 318.221084

*10.4.4.18 1-((4,4,5,5-tetramethyl-1,3,2-dioxaborolan-2-yl)methyl)piperidin-2-one (45r)*

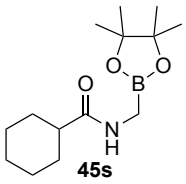


45r

Following the general procedure: **44r** (28.3 mg, 0.250 mmol, 1.0 eq.), $[Ir(COD)(OMe)]_2$ (5 mg, 0.008 mmol, 3 mol%), $B_2pin_2$ (95.2 mg, 0.375 mmol, 1.5 eq.), **L28** (4.4 mg, 0.015 mmol, 6 mol%) in THF (1.25 mL) were heated at 100 °C for 24 h. The crude mixture was purified by column chromatography (Hex/EtOAc 0% - EtOAc 100% - EtOAc/MeOH 20%) to obtain 54 mg (90% yield) of **45r.**

**$^1$H NMR** (600.1318 MHz, $CDCl_3$, 258 K) δ 3.30 (t, *J* = 5.4 Hz, 2H), 2.51 – 2.44 (m, 2H), 2.33 (d, *J* = 1.7 Hz, 2H), 1.84 – 1.75 (m, 4H), 1.17 (s, 12H).
**$^{13}$C NMR** (100.63 MHz, $CDCl_3$, 258 K) δ 174.13 (CO), 80.12 (C), 47.96 ($CH_2$), 42.54 (N-$CH_2$-B), 26.54 ($CH_2$), 25.24 ($CH_2$), 22.12 ($CH_2$), 19.57 ($CH_3$).
**$^{11}$B NMR** (128.39 MHz, $CDCl_3$, 258 K) δ 12.75.
**HRMS (ESI).** Calculated for $C_{12}H_{22}BNNaO_3^+$: 262.158495 Obtained: 262.166977

*10.4.4.19 N-((4,4,5,5-tetramethyl-1,3,2-dioxaborolan-2-yl)methyl)cyclohexanecarboxamide (45s)*



45s

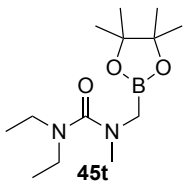
Following the general procedure: **44s** (35.3 mg, 0.250 mmol, 1.0 eq.), $[Ir(COD)(OMe)]_2$ (5 mg, 0.008 mmol, 3 mol%), $B_2pin_2$ (95.2 mg, 0.375 mmol, 1.5 eq.), **L28** (4.4 mg, 0.015 mmol, 6 mol%) in THF (1.25 mL) were heated at 100 °C for 24 h. The crude mixture was purified by column chromatography (Hex/EtOAc 0% - EtOAc 100% - EtOAc/MeOH 20%) to obtain 49 mg (73% yield) of **45s**.

**$^1$H NMR** (600.1318 MHz, $CDCl_3$, 258 K) δ 5.74 (s, 1H), 2.76 (d, *J* = 4.7 Hz, 2H), 2.06 (tt, *J* = 11.8, 3.5 Hz, 1H), 1.85 – 1.72 (m, 4H), 1.67 – 1.60 (m, 1H), 1.46 – 1.32 (m, 2H), 1.22 (d, *J* = 9.3 Hz, 15H).

USC UNIVERSIDADE DE SANTIAGO DE COMPOSTELA

**$^{13}$C NMR** (100.63 MHz, $CDCl_3$, 258 K) δ 177.14 (CO), 82.98 (C), 45.55 (CH), 29.76 ($CH_2$), 25.84 ($CH_2$), 24.62 ($CH_3$).
**$^{11}$B NMR** (128.39 MHz, $CDCl_3$, 258 K) δ 22.19.
**HRMS (ESI).** Calculated for $C_{14}H_{27}BNO_3^+$: 268.207851 Obtained: 268.207982

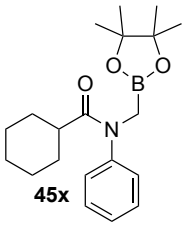
#### *10.4.4.20 1,1-diethyl-3-methyl-3-((4,4,5,5-tetramethyl-1,3,2-dioxaborolan-2-yl)methyl)urea (45t)*




Following the general procedure: **44t** (36.1 mg, 0.250 mmol, 1.0 eq.), $[Ir(COD)(OMe)]_2$ (5 mg, 0.008 mmol, 3 mol%), $B_2pin_2$ (95.2 mg, 0.375 mmol, 1.5 eq.), **L28** (4.4 mg, 0.015 mmol, 6 mol%) in THF (1.25 mL) were heated at 100 °C for 24 h. The crude mixture was purified by column chromatography (Hex/EtOAc 0% - EtOAc 100% - EtOAc/MeOH 20%) to obtain 31 mg (46% yield) of **45t**.

**$^{1}$H NMR** (600.1318 MHz, $CDCl_3$, 258 K) δ 3.25 (q, *J* = 7.1 Hz, 4H), 3.00 (s, 3H), 2.44 (s, 2H), 1.17 (t, *J* = 7.1 Hz, 6H), 1.15 (s, 12H).
**$^{13}$C NMR** (100.63 MHz, $CDCl_3$, 258 K) δ 164.29 (CO), 79.36 (C), 47.92 (N-$CH_2$-B), 43.22 (N-$CH_2$), 38.42 (N-$CH_3$), 25.17 ($CH_3$), 13.61 ($CH_3$).
**$^{11}$B NMR** (128.39 MHz, $CDCl_3$, 258 K) δ 10.91
**HRMS (ESI).** Calculated for $C_{13}H_{27}BN_2NaO_3^+$: 293.200694 Obtained: 293.200933

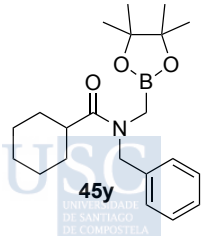
#### *10.4.4.21 N-phenyl-N-((4,4,5,5-tetramethyl-1,3,2-dioxaborolan-2-yl)methyl)cyclohexanecarboxamide (45x)*




Following the general procedure: **44x** (54.3 mg, 0.250 mmol, 1.0 eq.), $[Ir(COD)(OMe)]_2$ (5 mg, 0.008 mmol, 3 mol%), $B_2pin_2$ (95.2 mg, 0.375 mmol, 1.5 eq.), **L28** (4.4 mg, 0.015 mmol, 6 mol%) in THF (1.25 mL) were heated at 100 °C for 24 h. The crude mixture was purified by column chromatography (Hex/EtOAc 0% - EtOAc 100% - EtOAc/MeOH 20%) to obtain 43 mg (50% yield) of **45x.**

**$^{1}$H NMR** (600.1318 MHz, $CDCl_3$, 258 K) δ 7.47 – 7.37 (m, 3H), 7.16 – 7.11 (m, 2H), 2.75 (s, 2H), 2.28 – 2.20 (m, 1H), 1.69 (d, *J* = 11.0 Hz, 4H), 1.62 – 1.52 (m, 3H), 1.27 – 1.22 (m, 3H), 1.21 (s, 12H).
**$^{13}$C NMR** (100.63 MHz, $CDCl_3$, 258 K) δ 180.21 (CO), 139.75 (C, Ar), 130.03 (CH, Ar), 128.78 (CH, Ar), 125.60 (CH, Ar), 80.03 (C), 46.74 (N-$CH_2$-B), 37.48 (CH), 28.74 ($CH_2$), 25.21 ($CH_3$), 25.02 ($CH_2$).
**$^{11}$B NMR** (128.39 MHz, $CDCl_3$, 258 K) δ 12.80.
**HRMS (ESI).** Calculated for $C_{20}H_{31}BNO_3^+$: 344.2392 Obtained: 344.2395

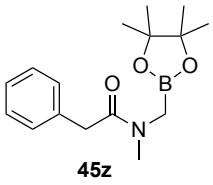
#### *10.4.4.22 N-benzyl-N-((4,4,5,5-tetramethyl-1,3,2-dioxaborolan-2-yl)methyl)cyclohexanecarboxamide (45y)*




Following the general procedure: **44y** (57.8 mg, 0.250 mmol, 1.0 eq.), $[Ir(COD)(OMe)]_2$ (5 mg, 0.008 mmol, 3 mol%), $B_2pin_2$ (95.2 mg, 0.375 mmol, 1.5 eq.), **L28** (4.4 mg, 0.015 mmol, 6 mol%) in THF (1.25 mL) were heated at 100 °C for 24 h. The crude mixture was purified by column chromatography (Hex/EtOAc 0% - EtOAc 100% - EtOAc/MeOH 20%) to obtain 47 mg (52% yield) of **45y**.

**$^{1}$H NMR** (600.1318 MHz, $CDCl_3$, 258 K) δ 7.36 – 7.26 (m, 3H), 7.13 (dd, *J* = 7.9, 1.6 Hz, 2H), 4.52 (s, 2H), 2.55 (tt, *J* = 11.6, 3.4 Hz, 1H), 2.27 (s, 2H), 1.83 – 1.74 (m, 4H), 1.72 – 1.55 (m, 3H), 1.21 (s, 3H), 1.14 (s, 12H).
**$^{13}$C NMR** (100.63 MHz, $CDCl_3$, 258 K) δ 179.87 (CO), 133.95 (C, Ar), 129.06 (CH, Ar), 128.30 (CH, Ar), 127.43 (CH, Ar), 79.83 (C), 52.08 (N-$CH_2$), 41.00 (N-$CH_2$-B), 37.24 (CH), 28.71 ($CH_2$), 25.31 ($CH_2$), 25.27 ($CH_2$), 25.05 ($CH_3$).
**$^{11}$B NMR** (128.39 MHz, $CDCl_3$) δ 12.65.
**HRMS (ESI).** Calculated for $C_{21}H_{33}BNO_3^+$: 358.254801 Obtained: 358.255302

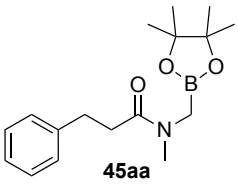
#### *10.4.4.23 N-methyl-2-phenyl-N-((4,4,5,5-tetramethyl-1,3,2-dioxaborolan-2-yl)methyl)acetamide (45z)*


**45z**

Following the general procedure: **44z** (40.8 mg, 0.250 mmol, 1.0 eq.), $[Ir(COD)(OMe)]_2$ (5 mg, 0.008 mmol, 3 mol%), $B_2pin_2$ (95.2 mg, 0.375 mmol, 1.5 eq.), **L28** (4.4 mg, 0.015 mmol, 6 mol%) in THF (1.25 mL) were heated at 100 °C for 24 h. The crude mixture was purified by column chromatography (Hex/EtOAc 0% - EtOAc 100% - EtOAc/MeOH 20%) to obtain 65 mg (90% yield) of **45z** as an off-white solid.

**$^{1}$H NMR** (600.1318 MHz, $CDCl_3$, 258 K) δ 7.33 – 7.26 (m, 3H), 7.22 (ddt, *J* = 7.3, 1.5, 0.7 Hz, 2H), 3.75 (s, 2H), 3.01 (s, 3H), 2.44 – 2.39 (m, 2H), 1.18 (s, 12H).
**$^{13}$C NMR** (100.63 MHz, $CDCl_3$, 258 K) δ 174.96 (CO), 132.07 (C, Ar), 129.13 (CH, Ar), 128.74 (CH, Ar), 127.70 (CH, Ar), 80.19 (C), 43.90 (N-$CH_2$-B), 36.21 (N-$CH_3$), 35.53 ($CH_2$), 25.22 ($CH_3$).
**$^{11}$B NMR** (128.39 MHz, $CDCl_3$, 258 K) δ 13.12.
**HRMS (ESI).** Calculated for $C_{16}H_{24}BNNaO_3^+$: 312.174145 Obtained: 312.174990

#### *10.4.4.24 N-methyl-3-phenyl-N-((4,4,5,5-tetramethyl-1,3,2-dioxaborolan-2-yl)methyl)propanamide (45aa)*

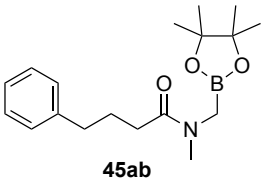

**45aa**

Following the general procedure: **44aa** (44.3 mg, 0.250 mmol, 1.0 eq.), $[Ir(COD)(OMe)]_2$ (5 mg, 0.008 mmol, 3 mol%), $B_2pin_2$ (95.2 mg, 0.375 mmol, 1.5 eq.), **L28** (4.4 mg, 0.015 mmol, 6 mol%) in THF (1.25 mL) were heated at 100 °C for 24 h. The crude mixture was purified by column chromatography (Hex/EtOAc 0% - EtOAc 100% - EtOAc/MeOH 20%) to obtain 61 mg (80% yield) of **45aa**.

**$^{1}$H NMR** (600.1318 MHz, $CDCl_3$, 258 K) δ 7.32 – 7.27 (m, 2H), 7.25 – 7.17 (m, 3H), 3.04 – 2.97 (m, 2H), 2.93 (s, 3H), 2.69 – 2.60 (m, 2H), 2.39 (t, *J* = 0.9 Hz, 2H), 1.21 (s, 12H).
**$^{13}$C NMR** (100.63 MHz, $CDCl_3$, 258 K) δ 176.05 (CO), 139.87 (C, Ar), 128.89 (CH, Ar), 128.46 (CH, Ar), 126.81 (CH, Ar), 80.17 (C), 43.79 (N-$CH_2$-B), 35.70 (N-$CH_3$), 30.89 ($CH_2$), 30.77 ($CH_2$), 25.30 ($CH_3$).
**$^{11}$B NMR** (128.39 MHz, $CDCl_3$, 258 K) δ 12.86.
**HRMS (ESI).** Calculated for $C_{17}H_{26}BNNaO_3^+$: 326.189795 Obtained: 326.190588

USC UNIVERSIDADE DE SANTIAGO DE COMPOSTELA

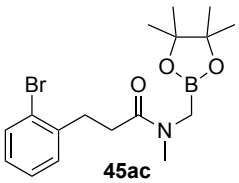
*10.4.4.25 N-methyl-4-phenyl-N-((4,4,5,5-tetramethyl-1,3,2-dioxaborolan-2-yl)methyl)butanamide (45ab)*


45ab

Following the general procedure: **44ab** (47.8 mg, 0.250 mmol, 1.0 eq.), $[Ir(COD)(OMe)]_2$ (5 mg, 0.008 mmol, 3 mol%), $B_2pin_2$ (95.2 mg, 0.375 mmol, 1.5 eq.), **L28** (4.4 mg, 0.015 mmol, 6 mol%) in THF (1.25 mL) were heated at 100 °C for 24 h. The crude mixture was purified by column chromatography (Hex/EtOAc 0% - EtOAc 100% - EtOAc/MeOH 20%) to obtain 71.8 mg (90% yield) of **45ab**.

**$^1$H NMR** (600.1318 MHz, $CDCl_3$, 258 K) δ 7.30 – 7.23 (m, 2H), 7.22 – 7.09 (m, 3H), 2.96 (s, 3H), 2.68 (t, *J* = 7.5 Hz, 2H), 2.37 (s, 2H), 2.36 – 2.25 (m, 3H), 2.00 (tt, *J* = 8.5, 6.9 Hz, 2H), 1.18 (s, 12H).
**$^{13}$C NMR** (100.63 MHz, $CDCl_3$, 258 K) δ 176.71 (CO), 140.83 (C, Ar), 128.61 (CH, Ar), 128.56 (CH, Ar), 126.30 (CH, Ar), 80.08 (C), 43.87 (N-$CH_2$-B), 35.72 (N-$CH_3$), 34.94 ($CH_2$), 27.58 ($CH_2$), 25.92 ($CH_2$), 25.23 ($CH_3$).
**$^{11}$B NMR** (128.39 MHz, $CDCl_3$, 258 K) δ 12.74.
**HRMS (ESI).** Calculated for $C_{18}H_{28}BNNaO_3^+$: 340.205445 Obtained: 340.215715

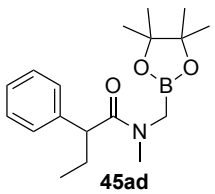
*10.4.4.26 3-(2-bromophenyl)-N-methyl-N-((4,4,5,5-tetramethyl-1,3,2-dioxaborolan-2-yl)methyl)propanamide (45ac)*


45ac

Following the general procedure: **44ac** (64 mg, 0.250 mmol, 1.0 eq.), $[Ir(COD)(OMe)]_2$ (5 mg, 0.008 mmol, 3 mol%), $B_2pin_2$ (95.2 mg, 0.375 mmol, 1.5 eq.), **L28** (4.4 mg, 0.015 mmol, 6 mol%) in THF (1.25 mL) were heated at 100 °C for 24 h. The crude mixture was purified by column chromatography (Hex/EtOAc 0% - EtOAc 100% - EtOAc/MeOH 20%) to obtain 57 mg (59% yield) of **45ac**.

**$^1$H NMR** (600.1318 MHz, $CDCl_3$, 258 K) δ 7.55 (dd, *J* = 8.0, 1.1 Hz, 1H), 7.29 (ddd, *J* = 5.0, 3.5, 1.6 Hz, 2H), 7.12 (ddd, *J* = 7.8, 6.7, 2.4 Hz, 1H), 3.18 – 3.12 (m, 2H), 2.99 (s, 3H), 2.71 (dd, *J* = 8.7, 7.1 Hz, 2H), 2.43 (s, 2H), 1.25 (s, 12H).
**$^{13}$C NMR** (100.63 MHz, $CDCl_3$, 258 K) δ 175.84 (CO), 139.00 (C, Ar), 133.07 (CH, Ar), 131.13 (CH, Ar), 128.74 (CH, Ar), 128.11 (CH, Ar), 124.21 (C, Ar), 80.31 (C), 43.89 (N-$CH_2$-B), 35.79 (N-$CH_3$), 31.45 ($CH_2$), 28.82 ($CH_2$), 25.25 ($CH_3$).
**$^{11}$B NMR** (128.39 MHz, $CDCl_3$, 258 K) δ 13.00
**HRMS (ESI).** Calculated for $C_{17}H_{26}BBrNO_3^+$: 382.118363 Obtained: 382.118276

*10.4.4.27 3-(2-bromophenyl)-N-methyl-N-((4,4,5,5-tetramethyl-1,3,2-dioxaborolan-2-yl)methyl)propanamide (45ad)*

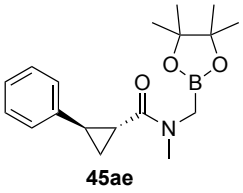

45ad

Following the general procedure: **44ad** (47.8 mg, 0.250 mmol, 1.0 eq.), $[Ir(COD)(OMe)]_2$ (5 mg, 0.008 mmol, 3 mol%), $B_2pin_2$ (95.2 mg, 0.375 mmol, 1.5 eq.), **L28** (4.4 mg, 0.015 mmol, 6 mol%) in THF (1.25 mL) were heated at 100 °C for 24 h. The crude mixture was purified by column chromatography (Hex/EtOAc 0% - EtOAc 100% - EtOAc/MeOH 20%) to obtain 51 mg (64% yield) of **45ad**.

USC UNIVERSIDADE DE SANTIAGO DE COMPOSTELA

**$^{1}$H NMR** (600.1318 MHz, $CDCl_3$, 258 K) δ 7.34 – 7.28 (m, 2H), 7.27 – 7.21 (m, 3H), 3.52 (t, *J* = 7.4 Hz, 1H), 2.92 (s, 3H), 2.41 (d, *J* = 13.8 Hz, 1H), 2.32 (d, *J* = 13.8 Hz, 1H), 2.10 (dt, *J* = 13.8, 7.3 Hz, 1H), 1.82 (dt, *J* = 13.8, 7.4 Hz, 1H), 1.21 (d, *J* = 2.0 Hz, 12H), 0.87 (t, *J* = 7.4 Hz, 3H).
**$^{13}$C NMR** (100.63 MHz, $CDCl_3$, 258 K) δ 177.13 (CO), 137.48 (C, Ar), 129.18 (CH, Ar), 128.02 (CH, Ar), 127.77 (CH, Ar), 80.07 (C), 47.20 (CH), 43.90 (N-$CH_2$-B), 35.73 (N-$CH_3$), 27.48 ($CH_2$), 25.29 ($CH_2$), 24.74 ($CH_3$), 12.03 ($CH_3$).
**$^{11}$B NMR** (128.39 MHz, $CDCl_3$) δ 13.15
**HRMS (ESI).** Calculated for $C_{18}H_{29}BNO_3^+$: 318.223501 Obtained: 318.223326

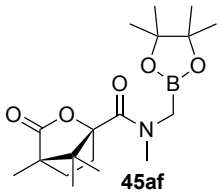
*10.4.4.28 (1R,2R)-N-methyl-2-phenyl-N-((4,4,5,5-tetramethyl-1,3,2-dioxaborolan-2-yl)methyl)cyclopropane-1-carboxamide (45ae)*


45ae

Following the general procedure: **44ae** (47.3 mg, 0.250 mmol, 1.0 eq.), $[Ir(COD)(OMe)]_2$ (5 mg, 0.008 mmol, 3 mol%), $B_2pin_2$ (95.2 mg, 0.375 mmol, 1.5 eq.), **L28** (4.4 mg, 0.015 mmol, 6 mol%) in THF (1.25 mL) were heated at 100 °C for 24 h. The crude mixture was purified by column chromatography (Hex/EtOAc 0% - EtOAc 100% - EtOAc/MeOH 20%) to obtain 42 mg (53% yield) of **45ae**.

**$^{1}$H NMR** (600.1318 MHz, $CDCl_3$, 258 K) δ 7.30 (t, *J* = 7.4 Hz, 3H), 7.14 – 7.09 (m, 2H), 3.14 (s, 3H), 2.80 – 2.74 (m, 1H), 2.43 (s, 2H), 1.85 (dd, *J* = 9.2, 4.8 Hz, 2H), 1.54 (td, *J* = 7.3, 4.6 Hz, 1H), 1.20 – 1.15 (m, 12H).
**$^{13}$C NMR** (100.63 MHz, $CDCl_3$, 258 K) δ 175.47 (CO), 139.25 (C, Ar), 128.75 (CH, Ar), 126.98 (CH, Ar), 126.20 (CH, Ar), 79.92 (C), 44.60 (N-$CH_2$-B), 35.82 (N-$CH_3$), 27.19 (CH), 25.22 ($CH_3$), 19.68 (CH), 17.55 ($CH_2$).
**$^{11}$B NMR** (128.39 MHz, $CDCl_3$, 258 K) δ 12.24
**HRMS (ESI).** Calculated for $C_{18}H_{27}BNO_3^+$: 316.2079 Obtained: 316.2080

*10.4.4.29 (1S)-N,4,7,7-tetramethyl-3-oxo-N-((4,4,5,5-tetramethyl-1,3,2-dioxaborolan-2-yl)methyl)-2-oxabicyclo[2.2.1]heptane-1-carboxamide (45af)*


45af

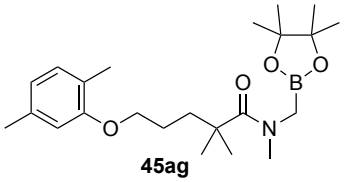
Following the general procedure: **44af** (56.3 mg, 0.250 mmol, 1.0 eq.), $[Ir(COD)(OMe)]_2$ (5 mg, 0.008 mmol, 3 mol%), $B_2pin_2$ (95.2 mg, 0.375 mmol, 1.5 eq.), **L28** (4.4 mg, 0.015 mmol, 6 mol%) in THF (1.25 mL) were heated at 100 °C for 24 h. The crude mixture was purified by column chromatography (Hex/EtOAc 0% - EtOAc 100% - EtOAc/MeOH 20%) to obtain 72 mg (82% yield) of **45af**.

**$^{1}$H NMR** (600.1318 MHz, $CDCl_3$, 258 K) δ 3.27 (s, 3H), 2.52 – 2.40 (m, 3H), 2.00 (ddd, *J* = 13.5, 9.2, 4.5 Hz, 1H), 1.91 (ddd, *J* = 13.1, 10.8, 4.5 Hz, 1H), 1.66 (ddd, *J* = 13.3, 9.2, 4.2 Hz, 1H), 1.12 (d, *J* = 2.1 Hz, 12H), 1.09 (s, 3H), 1.06 (s, 3H), 0.95 (s, 3H).
**$^{13}$C NMR** (100.63 MHz, $CDCl_3$, 258 K) δ 177.71 (CO), 169.58 (CO), 89.88 (C), 80.03 (C), 55.83 (C), 53.85 (C), 45.55 (N-$CH_2$-B), 37.57 (N-$CH_3$), 31.24 ($CH_2$), 25.20 ($CH_2$), 24.87 ($CH_3$), 17.19 ($CH_3$), 16.52 ($CH_3$), 9.62 ($CH_3$).
**$^{11}$B NMR** (128.39 MHz, $CDCl_3$, 258 K) δ 13.61.

USC UNIVERSIDADE DE SANTIAGO DE COMPOSTELA

**HRMS (ESI).** Calculated for $C_{18}H_{30}BNNaO_5^+$: 374.210924 Obtained: 374.212029

*10.4.4.30 (2,5-dimethylphenoxy)-N,2,2-trimethyl-N-((4,4,5,5-tetramethyl-1,3,2-dioxaborolan-2-yl)methyl)pentanamide (45ag)*

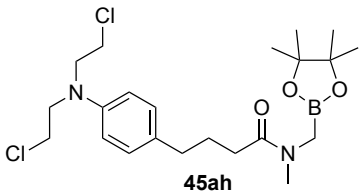


**45ag**

Following the general procedure: **44ag** (69.4 mg, 0.250 mmol, 1.0 eq.), $[Ir(COD)(OMe)]_2$ (5 mg, 0.008 mmol, 3 mol%), $B_2pin_2$ (95.2 mg, 0.375 mmol, 1.5 eq.), **L28** (4.4 mg, 0.015 mmol, 6 mol%) in THF (1.25 mL) were heated at 100 °C for 24 h. The crude mixture was purified by column chromatography (Hex/EtOAc 0% - EtOAc 100% - EtOAc/MeOH 20%) to obtain 75.8 mg (75% yield) of **45ag**.

**$^1$H NMR** (600.1318 MHz, $CDCl_3$, 258 K) δ 7.01 – 6.95 (m, 1H), 6.68 – 6.63 (m, 1H), 6.60 – 6.56 (m, 1H), 3.91 (t, *J* = 5.4 Hz, 2H), 3.21 (s, 3H), 2.47 (s, 2H), 2.29 (s, 3H), 2.13 (s, 3H), 1.87 – 1.75 (m, 4H), 1.33 (s, 6H), 1.17 (s, 12H).
**$^{13}$C NMR** (100.63 MHz, $CDCl_3$, 258 K) δ 180.57 (CO), 156.81 (C, Ar), 136.56 (C, Ar), 130.32 (CH, Ar), 123.34 (C, Ar), 120.82 (CH, Ar), 111.91 (CH, Ar), 79.77 (C), 67.49 (CH2), 47.44 (N-CH2-B), 39.24 (C), 37.44 (N-CH3), 37.35 (CH2), 25.59 (CH3), 25.05 (CH3), 24.91 (CH2), 21.38 (CH3), 15.83 (CH3).
**$^{11}$B NMR** (128.39 MHz, $CDCl_3$, 258 K) δ 12.03
**HRMS (ESI).** Calculated for $C_{23}H_{39}BNO_4^+$: 404.296666 Obtained: 404.296746

*10.4.4.31 4-(4-(bis(2-chloroethyl)amino)phenyl)-N-methyl-N-((4,4,5,5-tetramethyl-1,3,2-dioxaborolan-2-yl)methyl)butanamide (45ah)*

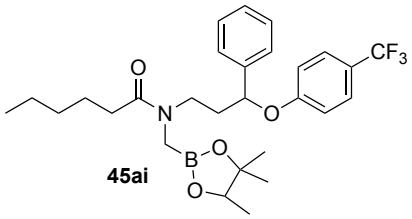


**45ah**

Following the general procedure: **44ah** (82.8 mg, 0.250 mmol, 1.0 eq.), $[Ir(COD)(OMe)]_2$ (5 mg, 0.008 mmol, 3 mol%), $B_2pin_2$ (95.2 mg, 0.375 mmol, 1.5 eq.), **L28** (4.4 mg, 0.015 mmol, 6 mol%) in THF (1.25 mL) were heated at 100 °C for 24 h. The crude mixture was purified by column chromatography (Hex/EtOAc 0% - EtOAc 100% - EtOAc/MeOH 20%) to obtain 38 mg (33% yield) of **45ah**.

**$^1$H NMR** (600.1318 MHz, $CDCl_3$, 258 K) δ 7.04 (d, *J* = 8.6 Hz, 2H), 6.60 (d, *J* = 8.6 Hz, 2H), 3.68 (dd, *J* = 8.1, 6.2 Hz, 4H), 3.64 – 3.57 (m, 4H), 2.98 (s, 3H), 2.57 (t, *J* = 7.5 Hz, 2H), 2.37 (s, 2H), 2.33 (t, *J* = 7.6 Hz, 2H), 2.00 – 1.89 (m, 2H), 1.17 (s, 12H).
**$^{13}$C NMR** (100.63 MHz, $CDCl_3$, 258 K) δ 176.77 (CO), 144.58 (C, Ar), 129.98 (C, Ar), 129.75 (CH, Ar), 112.33 (CH, Ar), 79.99 (C), 53.67 ($CH_2$), 43.87 (N-$CH_2$-B), 40.60 ($CH_2$), 35.73 (N-$CH_3$), 33.86 ($CH_2$), 27.64 ($CH_2$), 26.12 ($CH_2$), 25.25 ($CH_3$).
**$^{11}$B NMR** (128.39 MHz, $CDCl_3$, 258 K) δ 12.95
**HRMS (ESI).** Calculated for $C_{22}H_{36}BCl_2N_2O_3^+$: 457.219055 Obtained: 457.218984

*10.4.4.32 N-(3-phenyl-3-(4-(trifluoromethyl)phenoxy)propyl)-N-((4,4,5,5-tetramethyl-1,3,2-dioxaborolan-2-yl)methyl)hexanamide (45ai)*



**45ai**

Following the general procedure: **44ai** (101.9 mg, 0.250 mmol, 1.0 eq.), $[Ir(COD)(OMe)]_2$ (5 mg, 0.008 mmol, 3 mol%), $B_2pin_2$ (95.2 mg, 0.375 mmol, 1.5 eq.), **L28** (4.4 mg, 0.015 mmol, 6 mol%) in THF (1.25 mL) were heated at 100 °C for 24 h. The crude mixture was purified by column chromatography (Hex/EtOAc 0% - EtOAc 100% - EtOAc/MeOH 20%) to obtain 76.3 mg (57% yield) of **45ai**.

**$^1$H NMR** (600.1318 MHz, $CDCl_3$, 258 K) δ 7.33 (d, *J* = 8.7 Hz, 2H), 7.25 – 7.15 (m, 5H), 6.75 (d, *J* = 8.6 Hz, 2H), 5.02 (dd, *J* = 8.9, 3.8 Hz, 1H), 3.64 (dt, *J* = 13.9, 7.8 Hz, 1H), 3.30 (ddd, *J* = 14.0, 7.4, 4.5 Hz, 1H), 2.37 (d, *J* = 13.5 Hz, 1H), 2.21 – 2.03 (m, 5H), 1.52 – 1.36 (m, 2H), 1.09 (s, 12H), 1.06 – 0.94 (m, 4H), 0.71 (t, *J* = 7.0 Hz, 3H).
**$^{13}$C NMR** (100.63 MHz, $CDCl_3$, 258 K) δ 177.55 (CO), 159.84 (C, Ar), 139.64 (C, Ar), 129.18 (CH, Ar), 128.45 (CH, Ar), 127.04 (q, *J* = 3.7 Hz CH, Ar), 125.62 (CH, Ar), 124.31 (q, *J* = 271.1 Hz, $CF_3$), 123.56 (q, *J* = 32.8 Hz, C, Ar), 115.71 (CH, Ar), 80.07 (C), 76.53 (CH), 44.84 (N-$CH_2$), 40.30 (N-$CH_2$-B), 36.26 ($CH_2$), 31.27 ($CH_2$), 28.44 ($CH_2$), 25.24 ($CH_3$), 25.19 ($CH_3$), 24.41 ($CH_2$), 22.14 ($CH_2$), 13.80 ($CH_3$).
**$^{19}$F NMR** (376.46 MHz, $CDCl_3$, 258 K) δ -61.72.
**$^{11}$B NMR** (128.39 MHz, $CDCl_3$, 258 K) δ 13.10
**HRMS (ESI).** Calculated for $C_{29}H_{40}BF_3NO_4^+$: 534.299700 Obtained: 534.299523

USC UNIVERSIDADE DE SANTIAGO DE COMPOSTELA

## 10.5 Computational analysis for section 7.3

### 10.5.1 Non-Covalent Interactions (NCI) analysis

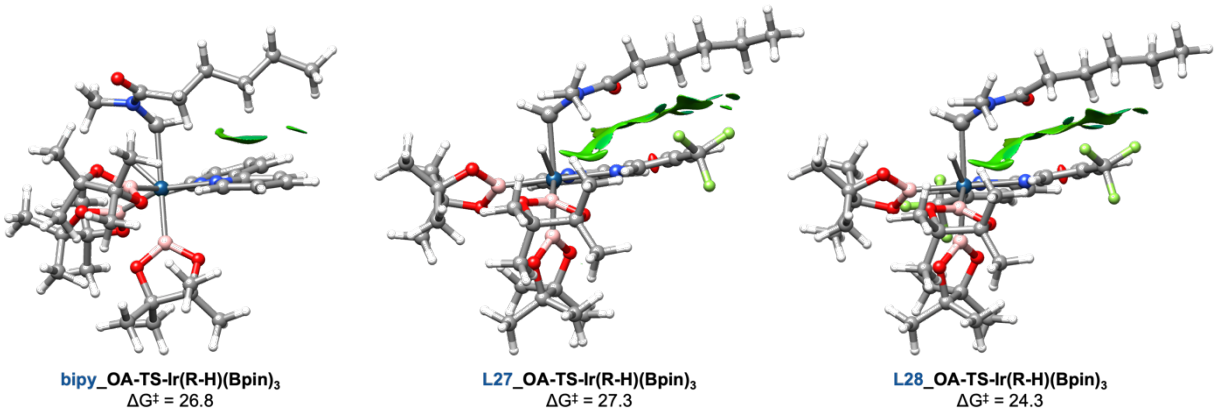



**Figure *82*** Substrate-ligand non-covalent interactions (NCI) occurring in low energy outer-sphere transition states (TS) calculated for the oxidative addition step between *N*,*N*-dimethylhexanamide (1a) and $Ir^{III}$(ligand)$(Bpin)_3$ (ligand = **bipy**, **L27** and **L28**). Activation free energies ($\Delta G^{\ddagger}$) calculated with $SMD_{THF}$/M06/6-311G(d,p);SDD(Ir)]//M06/6-31G(d);LANL2DZ(Ir), are given in kcal $mol^{-1}$. Reduced density gradient (RDG) isosurfaces are plotted at a 0.25 level and color-coded based on sign(λ2)ρ: –3.0 (blue; strong attractive interactions) < 0.0 (green; weak van der Waals interactions) < 3.0 (red; strong repulsive interactions). Note the larger extension of non-covalent interactions in the borylation TS with 5-trifluoromethylated ligands **L27** and **L28**.

USC UNIVERSIDADE DE SANTIAGO DE COMPOSTELA

## 10.5.2 Energy Decomposition Analysis (EDA)

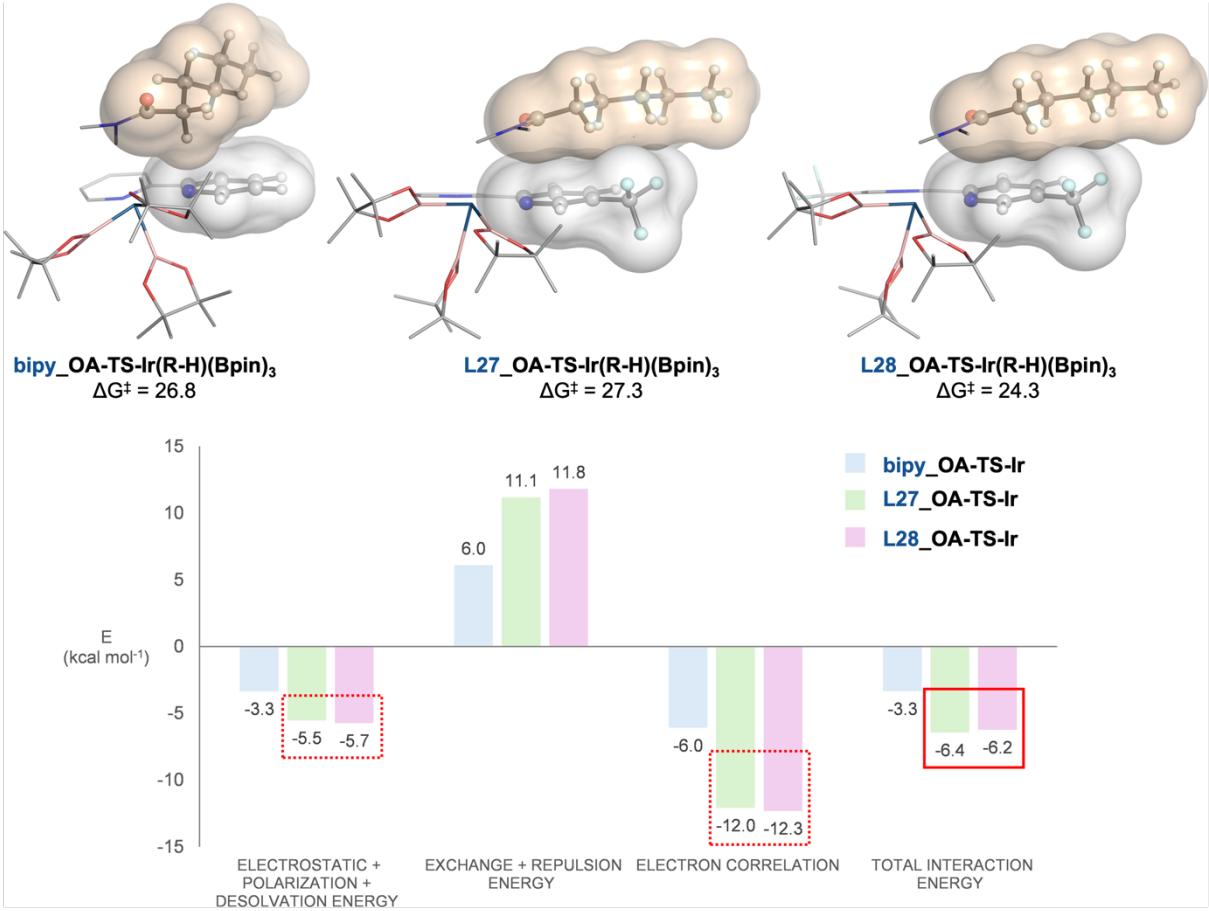



**Figure *83*** Generalized Kohn-Sham Energy Decomposition Analysis (GKS-EDA of the low energy outer-sphere transition states (TS) calculated for the oxidative addition step between *N*,*N*-dimethylhexanamide (1a) and $Ir^{III}$(ligand)$(Bpin)_3$ (ligand = **bipy**, **L27** and **L28**). Activation free energies ($\Delta G^{\ddagger}$) calculated with $SMD_{THF}$/M06/6-311G(d,p);SDD(Ir)]//M06/6-31G(d);LANL2DZ(Ir), are given in kcal $mol^{-1}$. In the graphs, different contributions to the total interaction energy between the *n*- hexanamide and (5-trifluoromethyl)pyridine fragments are shown. Contributions related to the polar character of the interactions (electrostatic, polarization and desolvation) have been added together for clarity. The electron correlation component implicitly accounts for dispersion. The larger values for the attractive interactions (both polar and especially dispersion) occurring in the borylation TS with 5-trifluoromethylated ligands **L27** and **L28**, resulting in a larger total interaction energy, are highlighted with red boxes.

## 10.5.3 Calculated structures for the borylation of 44a with bipy as ligand

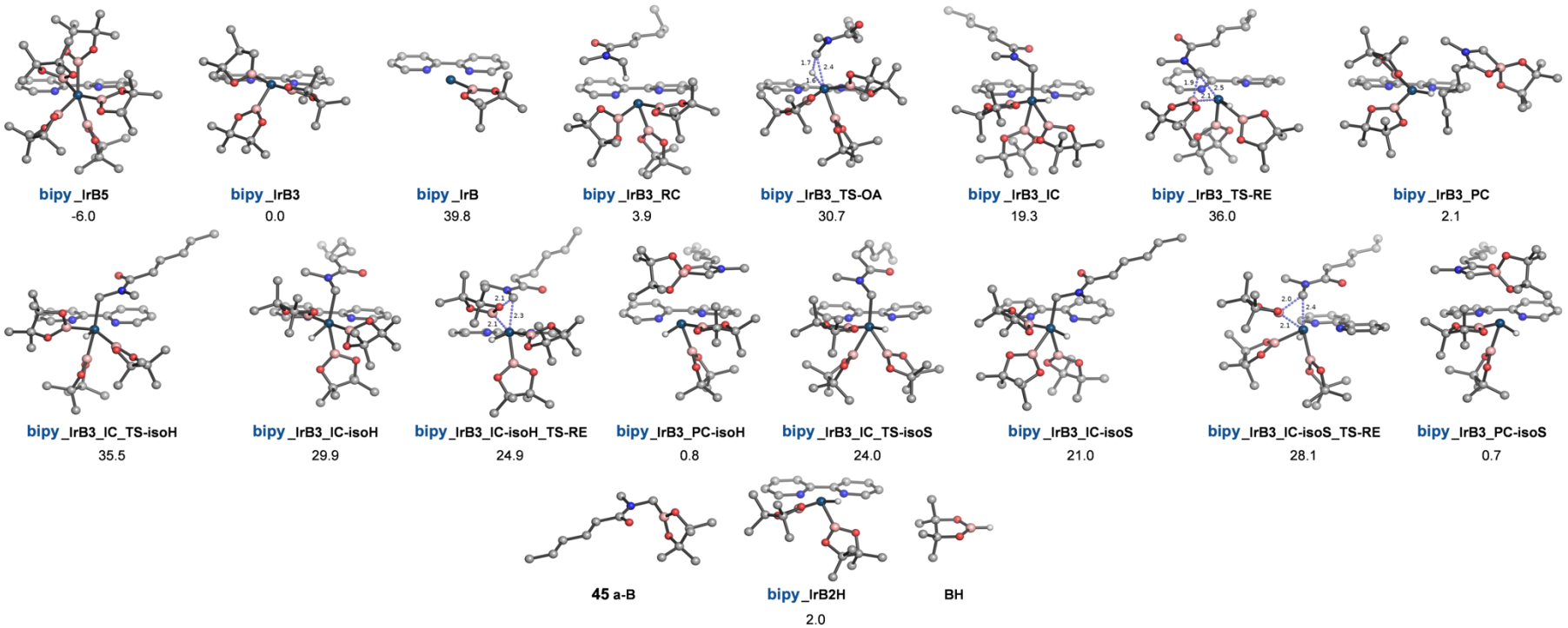



**Figure *84*** Lowest energy conformers calculated with $SMD_{THF}$/M06/6-311G(d,p);SDD(Ir)]//M06/6-31G(d);LANL2DZ(Ir), for the borylation of *N*,*N*-dimethylhexanamide (**44a**) catalyzed by $Ir^{III}$(**bipy**)$(Bpin)_3$. B: Bpin; RC: reactive complex; IC: intermediate complex; PC: product complex. Non-reactive hydrogens have been omitted for clarity. Free energies (ΔG in kcal $mol^{-1}$) relative to the isolated reactants (**bipy**_IrB3 + 44a) are shown.

## 10.5.4 Calculated structures for the borylation of 44a with L27 as ligand

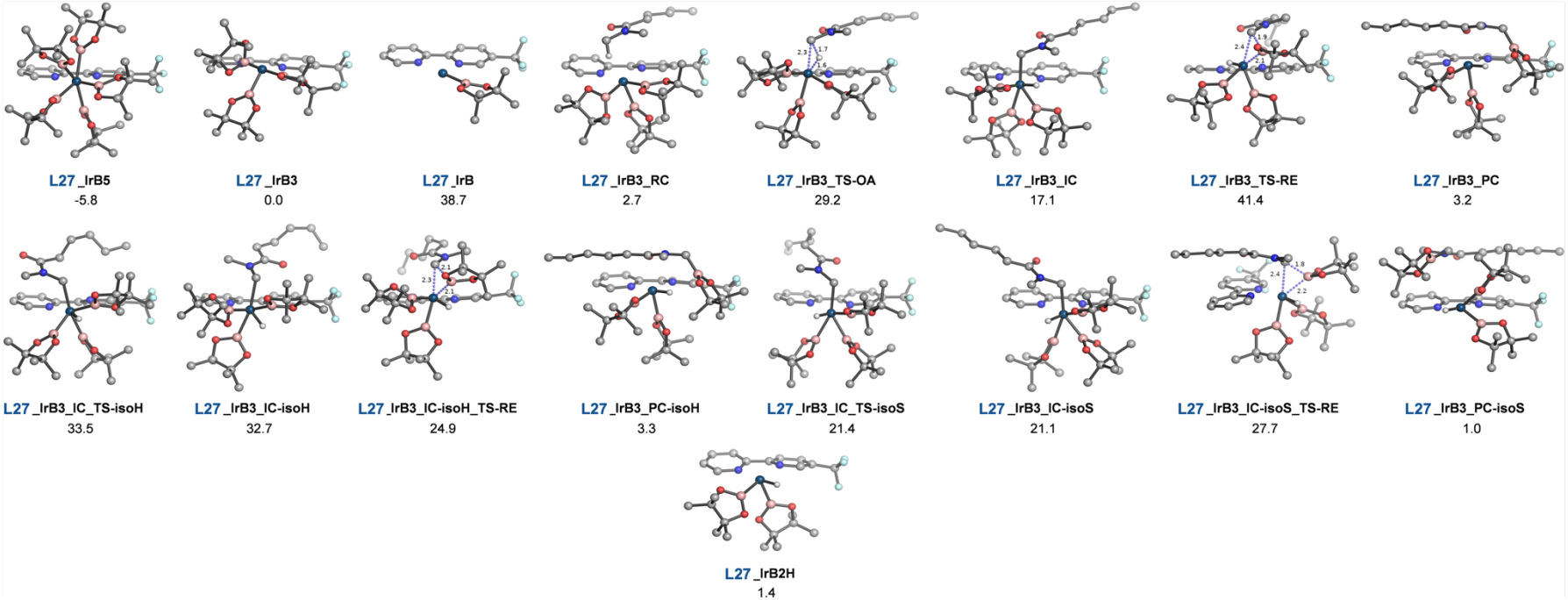



**Figure *85*** Lowest energy conformers calculated with $SMD_{THF}$/M06/6-311G(d,p);SDD(Ir)]//M06/6-31G(d);LANL2DZ(Ir), for the borylation of *N*,*N*-dimethylhexanamide (**44a**) catalyzed by $Ir^{III}$(**L27**)$(Bpin)_3$. B: Bpin; RC: reactive complex; IC: intermediate complex; PC: product complex. Non-reactive hydrogens have been omitted for clarity. Free energies (ΔG in kcal $mol^{-1}$) relative to the isolated reactants (**L27**_IrB3 + **44a**) are shown.

## 10.5.5 Calculated structures for the borylation of 44a with L28 as ligand

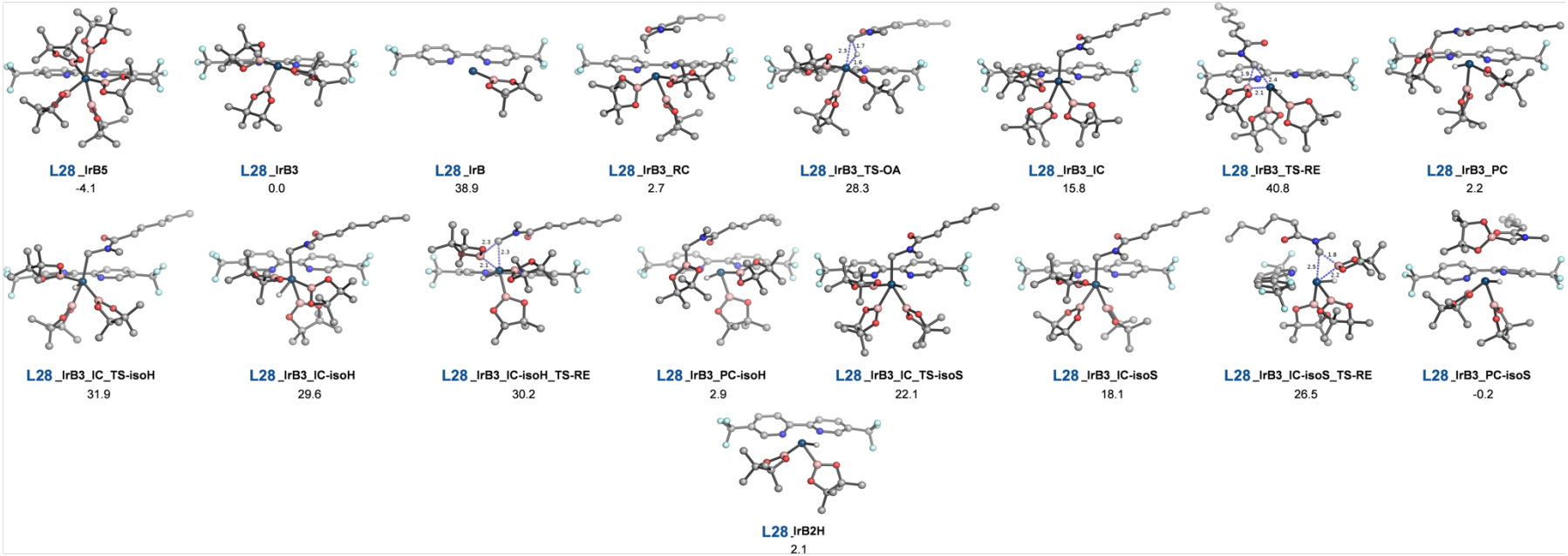



**Figure *86*** Lowest energy conformers calculated with $SMD_{THF}$/M06/6-311G(d,p);SDD(Ir)]//M06/6-31G(d);LANL2DZ(Ir), for the borylation of *N*,*N*-dimethylhexanamide (**44a**) catalyzed by $Ir^{III}$(**L28**)$(Bpin)_3$. B: Bpin; RC: reactive complex; IC: intermediate complex; PC: product complex. Non-reactive hydrogens have been omitted for clarity. Free energies (ΔG in kcal $mol^{-1}$) relative to the isolated reactants (**L28**_IrB3 + **44a**) are shown.

### 10.5.6 Minimum energy pathway (MEP) for *N*,*N*-diethylpropionamide (**44u**) borylation

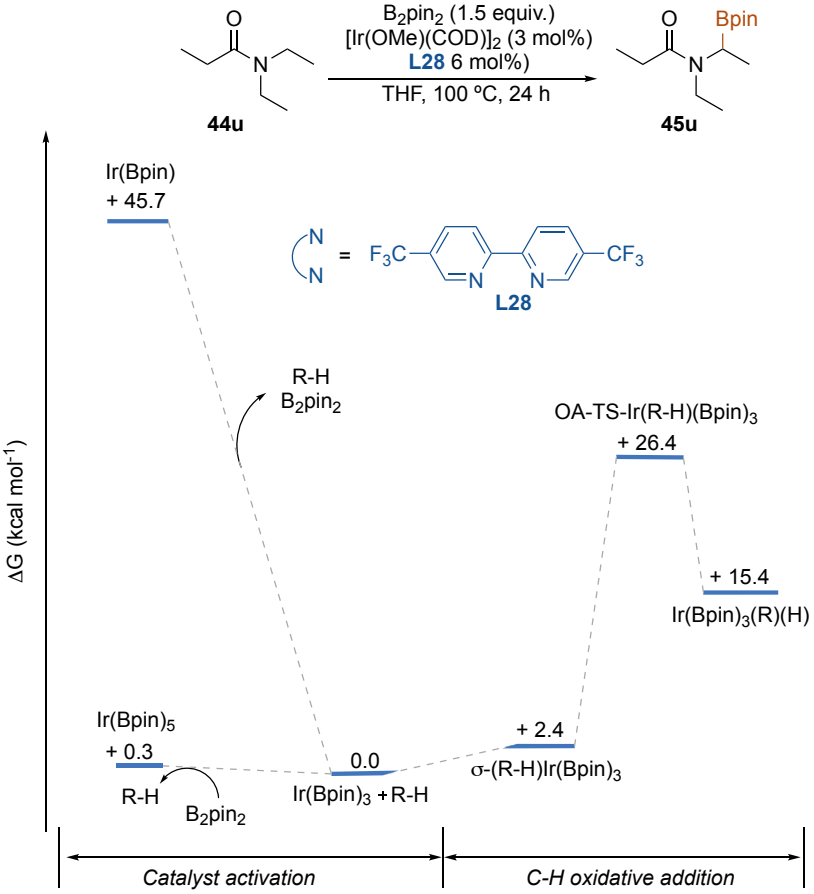



**Figure *87*** Minimum energy pathways (MEP) calculated with IEF-PCM$_{THF}$/M06/6-311G(2d,p)+SDD(Ir)//M06/6-31G(d)+LANL2DZ(Ir) for the oxidative addition step between *N*,*N*-diethylpropionamide (**44u**) and Ir$^{III}$(**L28**)(Bpin)$_3$. Free energies relative to (Ir(Bpin)$_3$+R–H) ($\Delta G_{QH}$ in kcal mol$^{-1}$).

### 10.5.7 Minimum energy pathway (MEP) for *N,N*-dimethylisobutyramide (**44f**) borylation (N-$CH_3$ vs C-$CH_3$ positions)

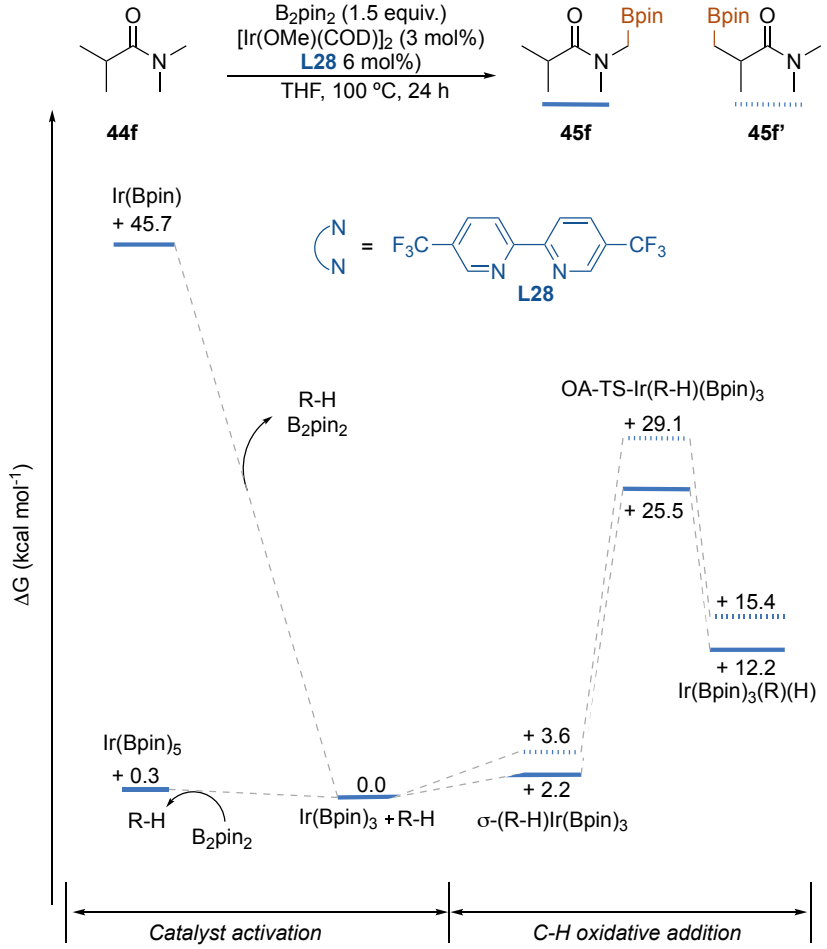



**Figure *88*** Minimum energy pathways (MEP) calculated with IEF-$PCM_{THF}$/M06/6-311G(2d,p)+SDD(Ir)//M06/6-31G(d)+LANL2DZ(Ir) for the oxidative addition step between *N,N*-dimethylisobutyramide (**44f**) and $Ir^{III}$(**L28**)$(Bpin)_3$. C–H activation at the N-$CH_3$ (solid lines) and C-$CH_3$ (dashed lines) positions of **44f** (topologically identical relative to the carbonyl group) are compared. Free energies relative to ($Ir(Bpin)_3$+R–H) ($\Delta G_{QH}$ in kcal $mol^{-1}$).

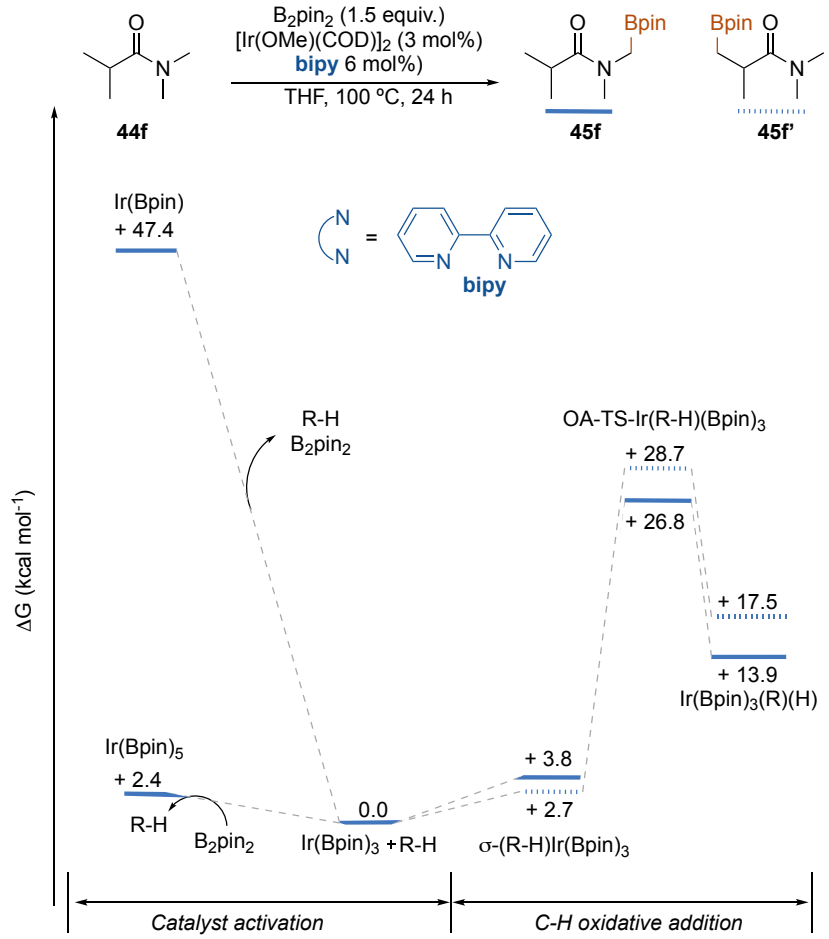



**Figure *89*** Minimum energy pathways (MEP) calculated with IEF-PCM$_{THF}$/M06/6-311G(2d,p)+SDD(Ir)//M06/6-31G(d)+LANL2DZ(Ir) for the oxidative addition step between *N,N*-dimethylisobutyramide (**44f**) and Ir$^{III}$(**bipy**)(Bpin)$_3$. C–H activation at the N-CH$_3$ (solid lines) and C-CH$_3$ (dashed lines) positions of **44f** (topologically identical relative to the carbonyl group) are compared. Free energies relative to (Ir(Bpin)$_3$+R–H) ($\Delta G_{QH}$ in kcal mol$^{-1}$).

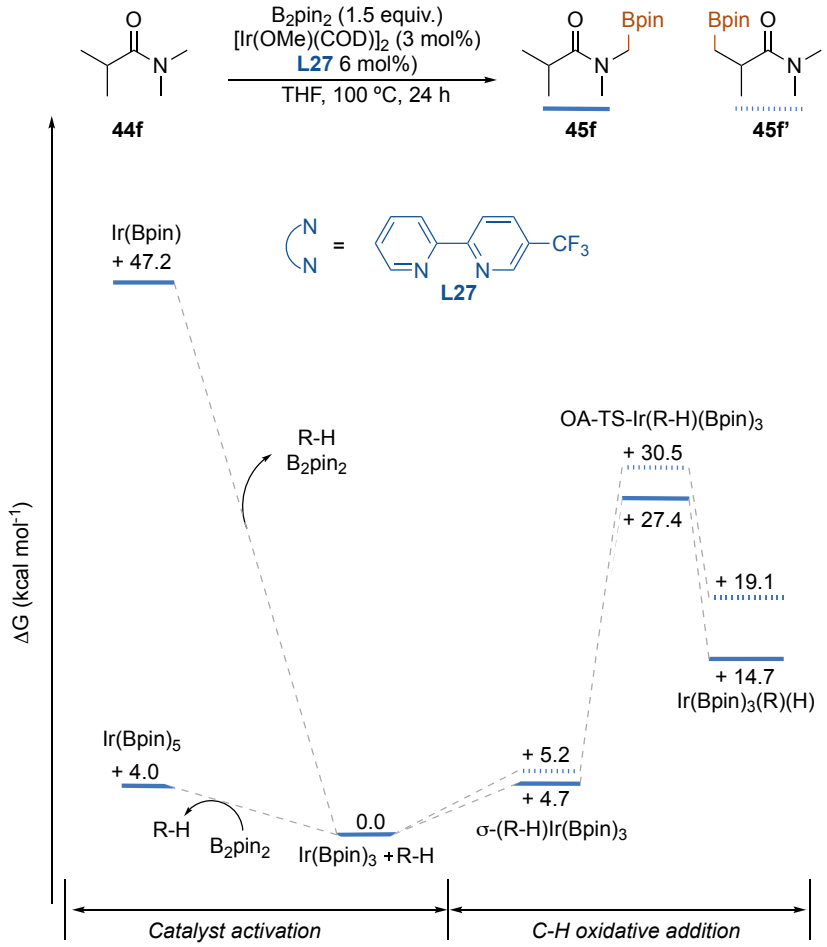



**Figure *90*** Minimum energy pathways (MEP) calculated with IEF-PCM$_{THF}$/M06/6-311G(2d,p)+SDD(Ir)//M06/6-31G(d)+LANL2DZ(Ir) for the oxidative addition step between *N,N*-dimethylisobutyramide (**44f**) and Ir$^{III}$(**L27**)(Bpin)$_3$. C–H activation at the N-CH$_3$ (solid lines) and C-CH$_3$ (dashed lines) positions of **44f** (topologically identical relative to the carbonyl group) are compared. Free energies relative to (Ir(Bpin)$_3$+R–H) ($\Delta G_{QH}$ in kcal mol$^{-1}$).

## 10.5.8 Minimum energy pathway (MEP) for *N,N*-dimethylhexylamide (**44a**) borylation following a rollover cyclometalation mechanism

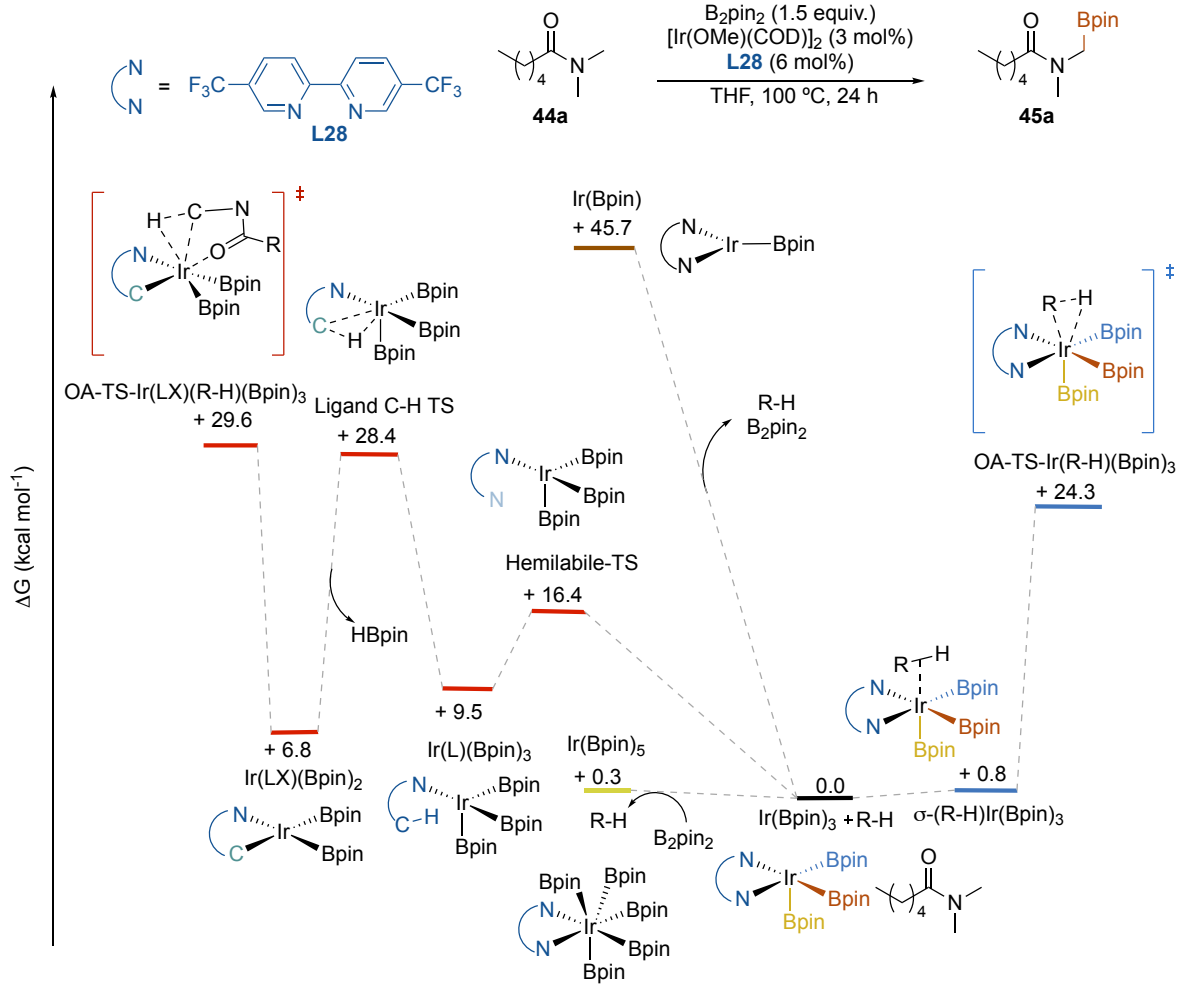



**Figure *91*** Minimum energy pathways (MEP) calculated with IEF-PCM$_{THF}$/M06/6-311G(2d,p)+SDD(Ir)//M06/6-31G(d)+LANL2DZ(Ir) for the oxidative addition step between *N,N*-dimethylhexylamide (**44a**) and Ir$^{III}$(**L28**)(Bpin)$_3$. Several mechanisms are compared: the canonical Ir(III) → Ir(V) involving a 16 e$^-$ active catalyst (Ir(Bpin)$_3$), an alternative Ir(I) → Ir(III) mechanism involving a 14 e$^-$ active catalyst (Ir(Bpin)) after $B_2pin_2$ cleavage and a mechanism involving the de-coordination of one pyridine ring followed via a rollover cyclometalation to form a L–X ligand which would be the active catalyst (Ir(LX)(Bpin)$_2$) in this scenario. Free energies relative to (Ir(Bpin)$_3$+R–H) ($\Delta G_{QH}$ in kcal mol$^{-1}$).

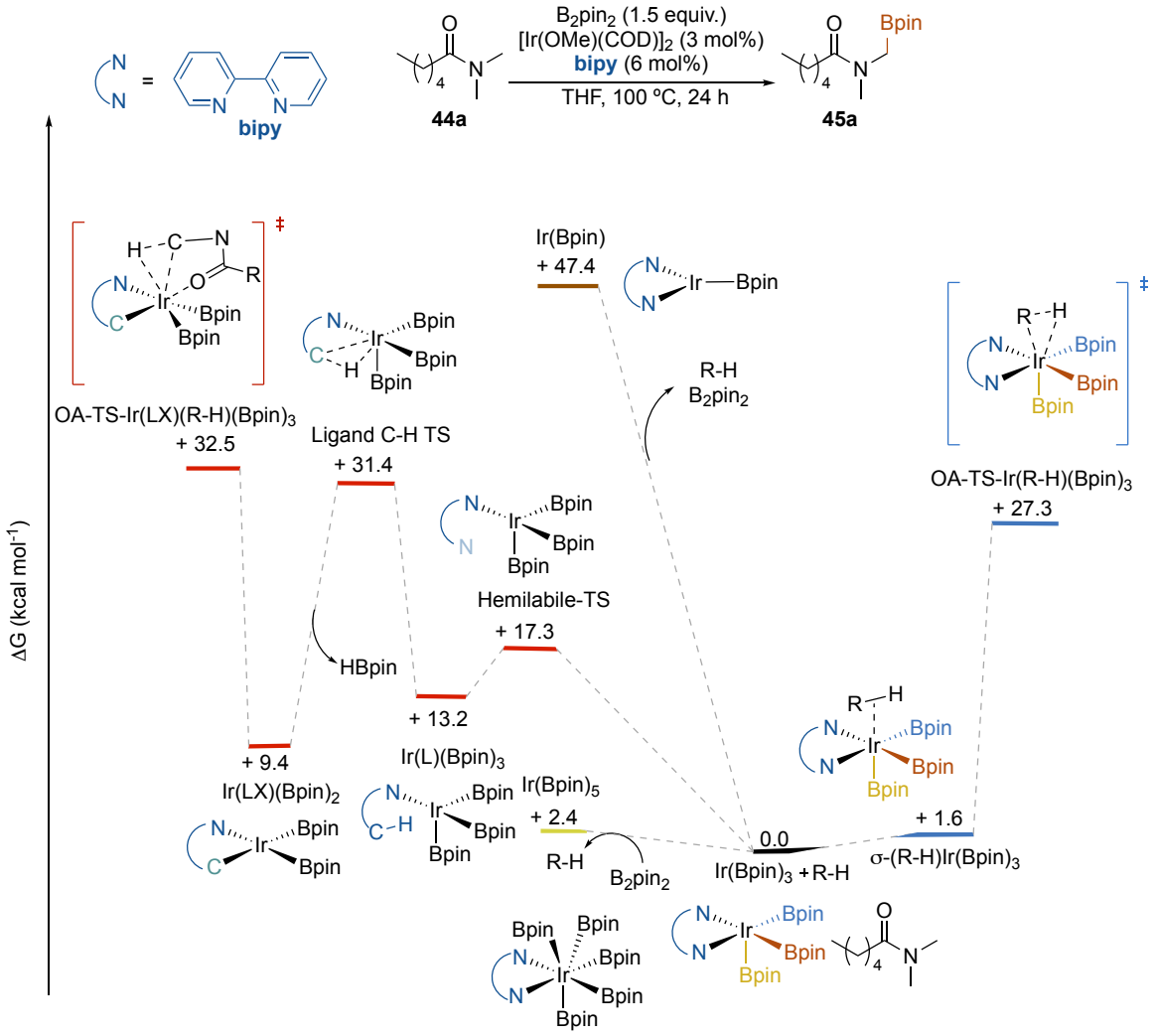



**Figure 92** Minimum energy pathways (MEP) calculated with IEF-PCM$_{THF}$/M06/6-311G(2d,p)+SDD(Ir)//M06/6-31G(d)+LANL2DZ(Ir) for the oxidative addition step between *N*,*N*-dimethylhexylamide (**44a**) and Ir$^{III}$(**bipy**)(Bpin)$_3$. Several mechanisms are compared: the canonical Ir(III) → Ir(V) involving a 16 e$^-$ active catalyst (Ir(Bpin)$_3$), an alternative Ir(I) → Ir(III) mechanism involving a 14 e$^-$ active catalyst (Ir(Bpin)) after $B_2pin_2$ cleavage and a mechanism involving the de-coordination of one pyridine ring followed via a rollover cyclometalation to form a L–X ligand which would be the active catalyst (Ir(LX)(Bpin)$_2$) in this scenario. Free energies relative to (Ir(Bpin)$_3$+R–H) ($\Delta G_{QH}$ in kcal mol$^{-1}$).

## 10.5.9 Calculated structures for borylation pre-catalytic species

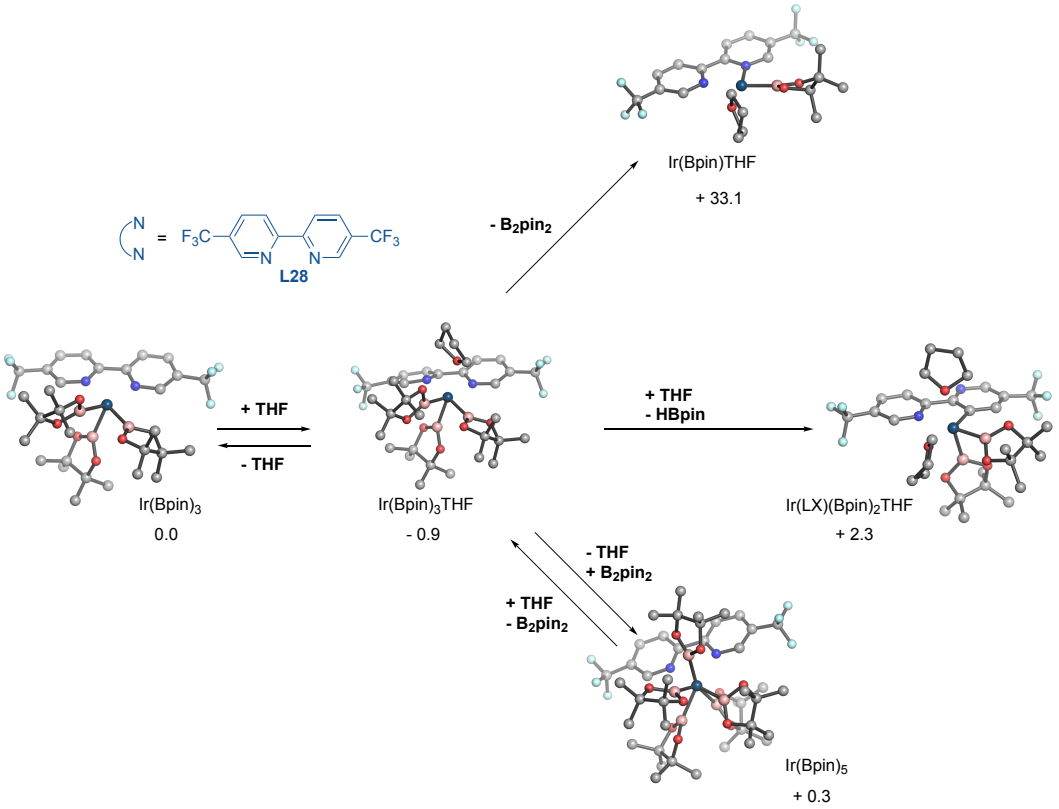



**Figure *93*** Pre-catalytic $Ir^{III}(Bpin)_3$, $Ir^{III}(THF)(Bpin)_3THF$, $Ir^{I}(Bpin)THF$, $Ir^{III}(LX)Bpin_2THF$ and $Ir^{V}(Bpin)_5$, calculated for ligand **L28**. Non-reactive hydrogens have been omitted for clarity. Free energies relative to the $Ir^{III}(Bpin)_3$ intermediate ($\Delta G_{QH}$ in kcal $mol^{-1}$) calculated with IEF-$PCM_{THF}$/M06/6-311G(2d,p)+SDD(Ir)//M06/6-31G(d)+LANL2DZ(Ir)

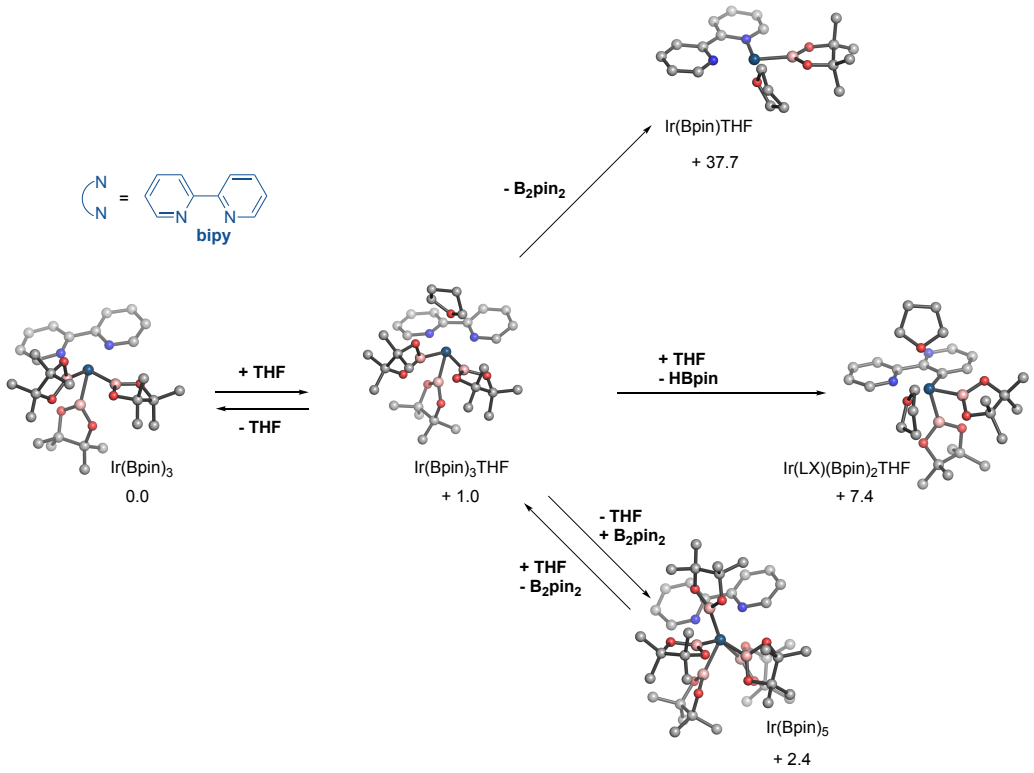



**Figure *94*** Pre-catalytic $Ir^{III}(Bpin)_3$, $Ir^{III}(THF)(Bpin)_3THF$, $Ir^{I}(Bpin)THF$, $Ir^{III}(LX)Bpin_2THF$ and $Ir^{V}(Bpin)_5$, calculated for ligand **bipy**. Non-reactive hydrogens have been omitted for clarity. Free energies relative to the $Ir^{III}(Bpin)_3$ intermediate ($\Delta G_{QH}$ in kcal $mol^{-1}$) calculated with $IEF\text{-}PCM_{THF}$/M06/6-311G(2d,p)+SDD(Ir)//M06/6-31G(d)+LANL2DZ(Ir)

# 11 Annexes

USC
UNIVERSIDADE
DE SANTIAGO
DE COMPOSTELA

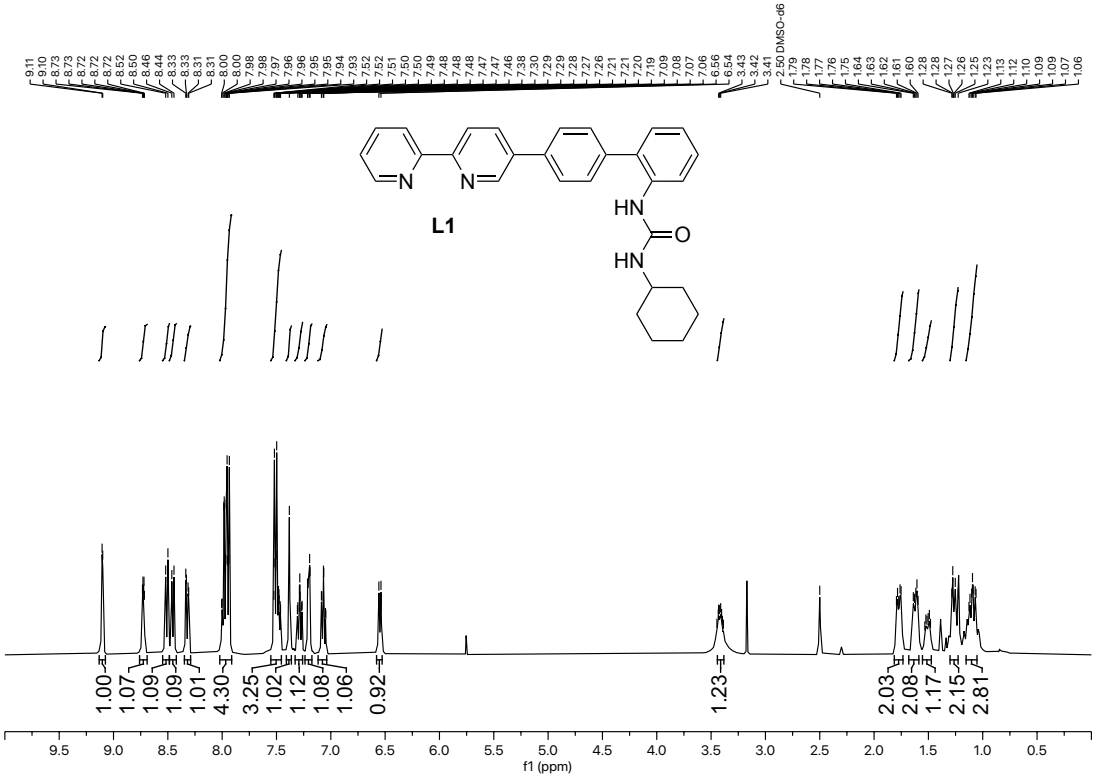
## 11.1 Annex I: Selected NMR spectra

USC
UNIVERSIDADE
DE SANTIAGO
DE COMPOSTELA

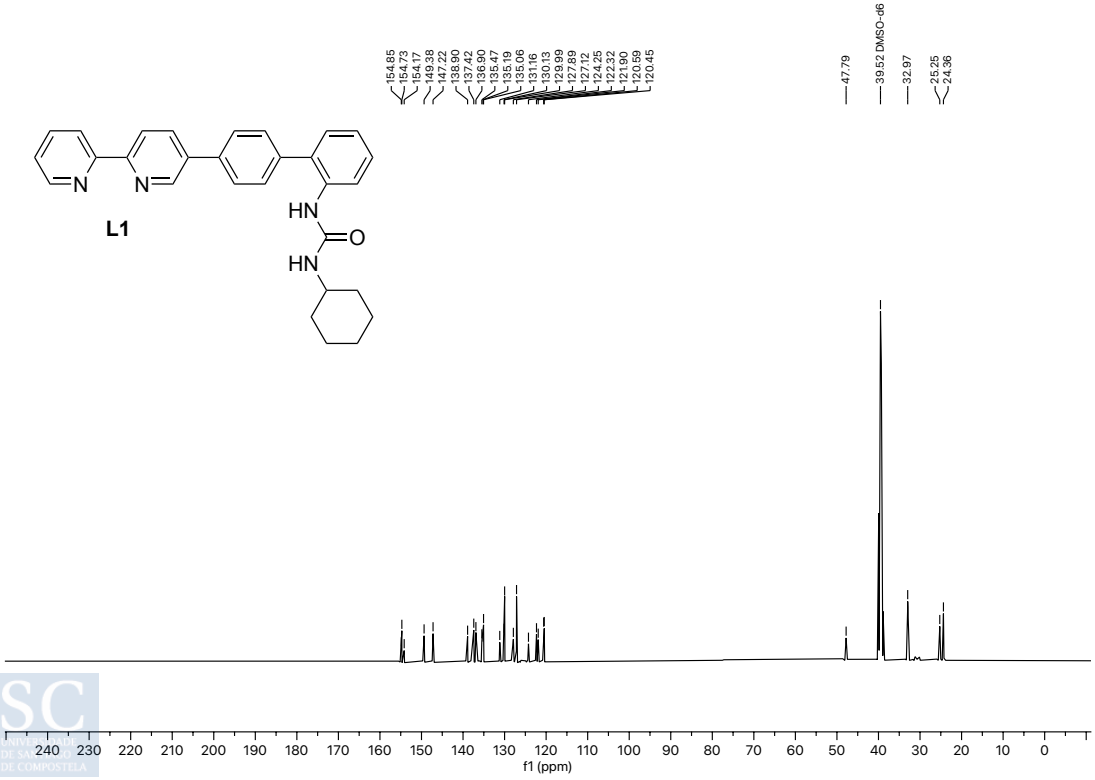
## 11.1.1 Selected spectra for molecules in section 7.1

### *11.1.1.1 Spectra of ligands*

*$^{1}$H NMR 1-(4'-([2,2'-bipyridin]-5-yl)-[1,1'-biphenyl]-2-yl)-3-cyclohexylurea (L1)*

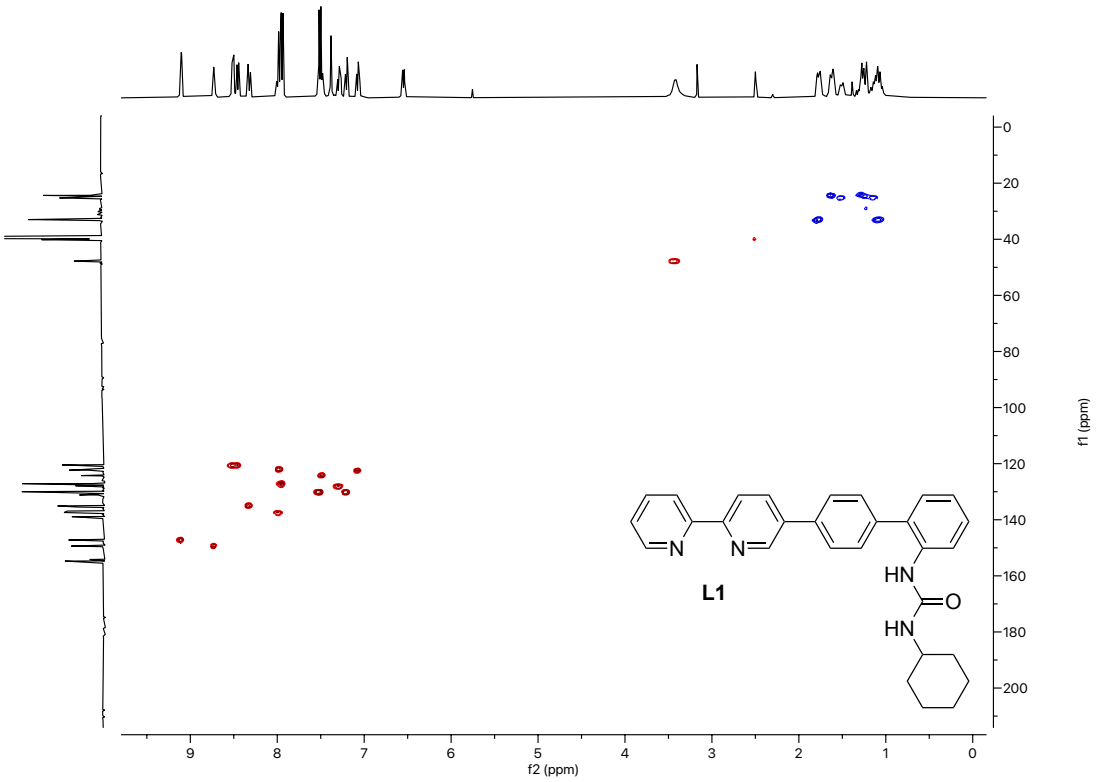



*$^{13}$C NMR 1-(4'-([2,2'-bipyridin]-5-yl)-[1,1'-biphenyl]-2-yl)-3-cyclohexylurea (L1)*

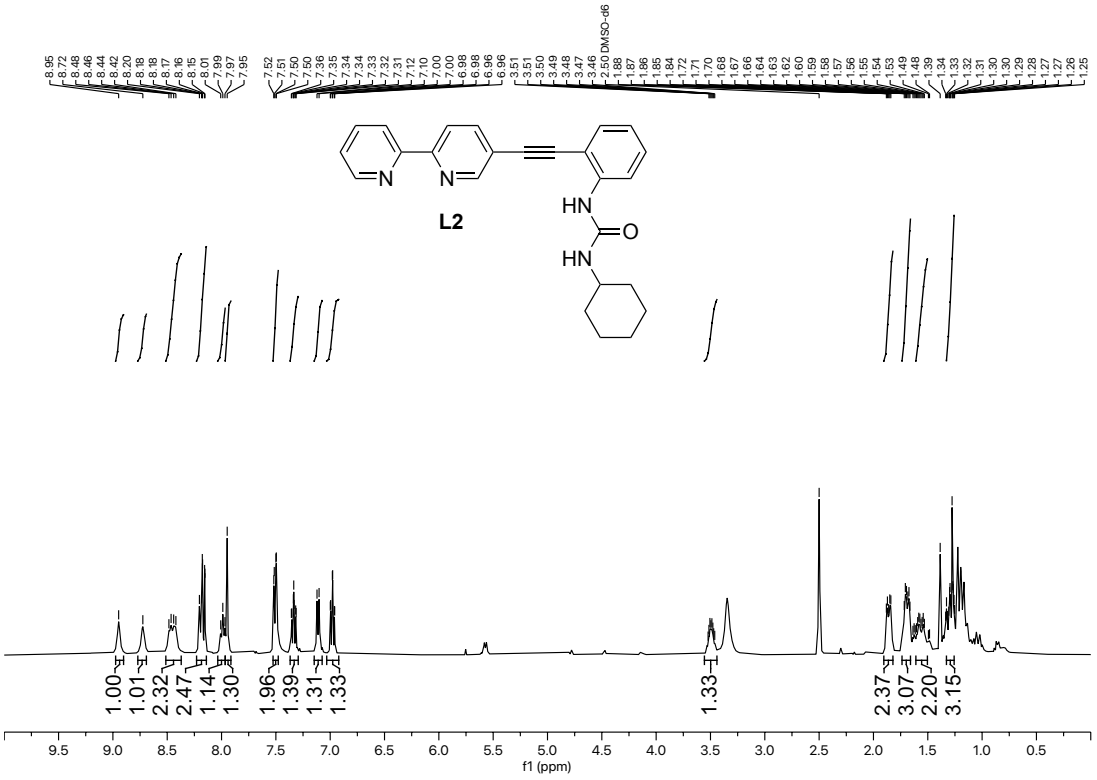



USC UNIVERSIDADE DE SANTIAGO DE COMPOSTELA

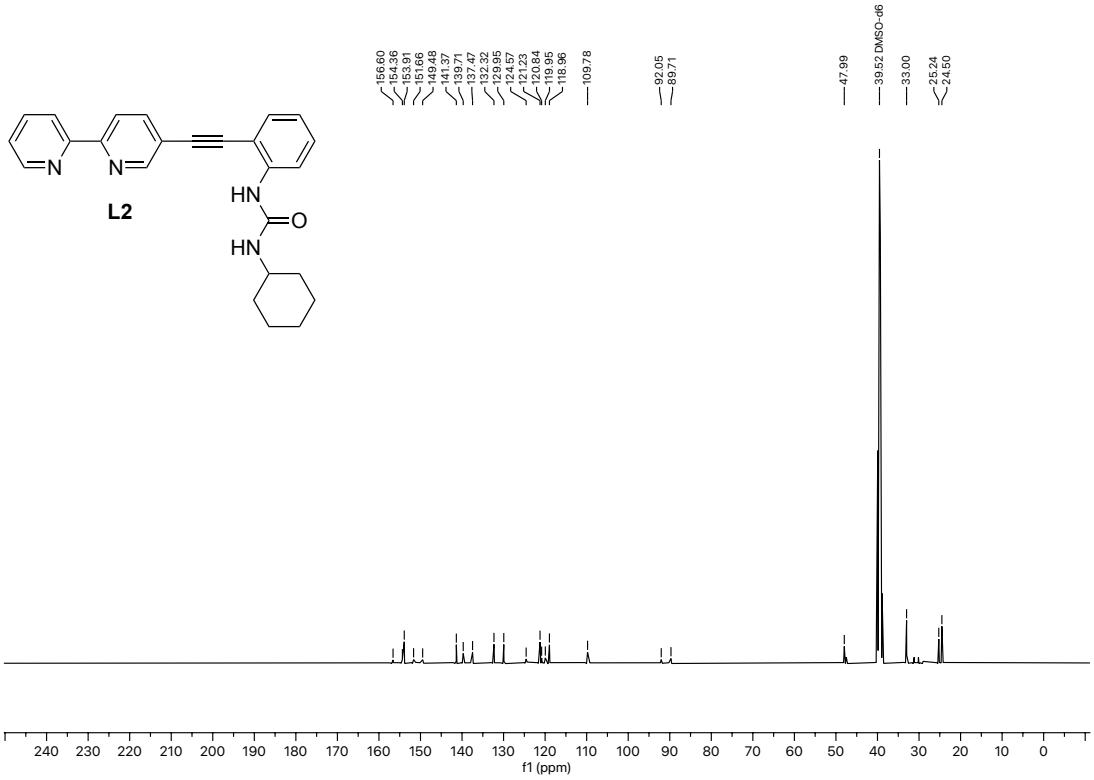
*HSQC NMR 1-(4'-([2,2'-bipyridin]-5-yl)-[1,1'-biphenyl]-2-yl)-3-cyclohexylurea (L1)*



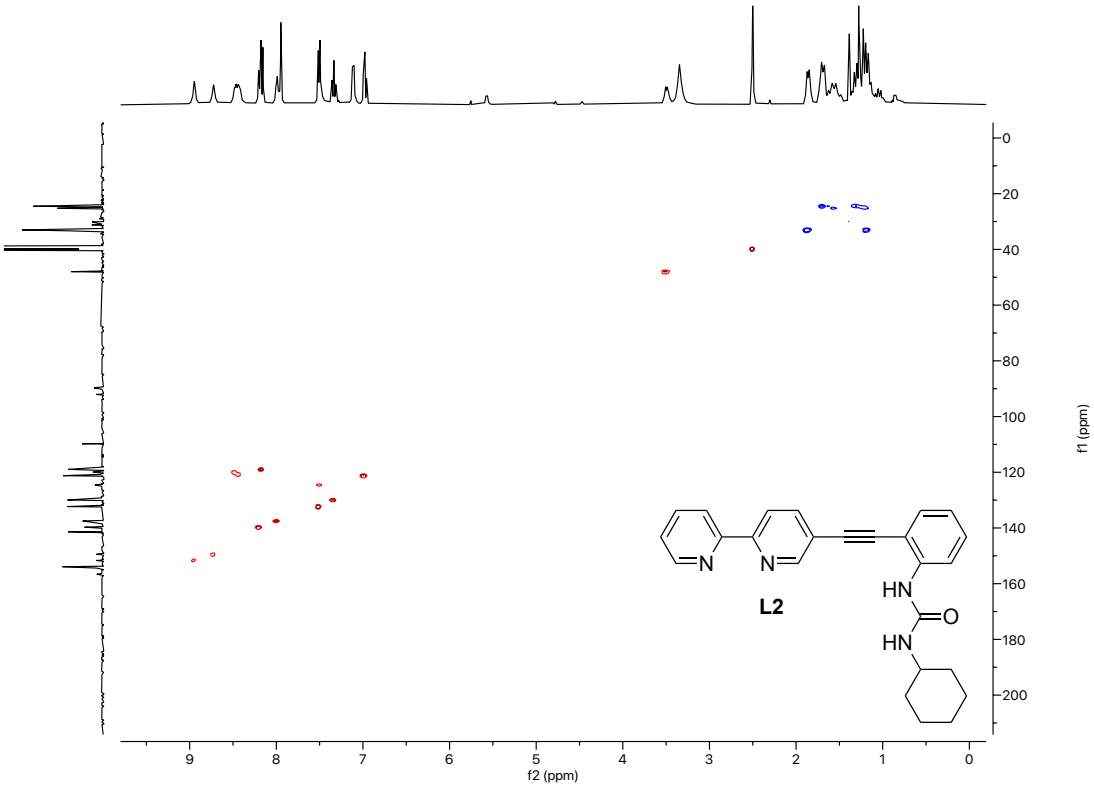

*$^{1}$H NMR 1-(2-([2,2'-bipyridin]-5-ylethynyl)phenyl)-3-cyclohexylurea (L2)*



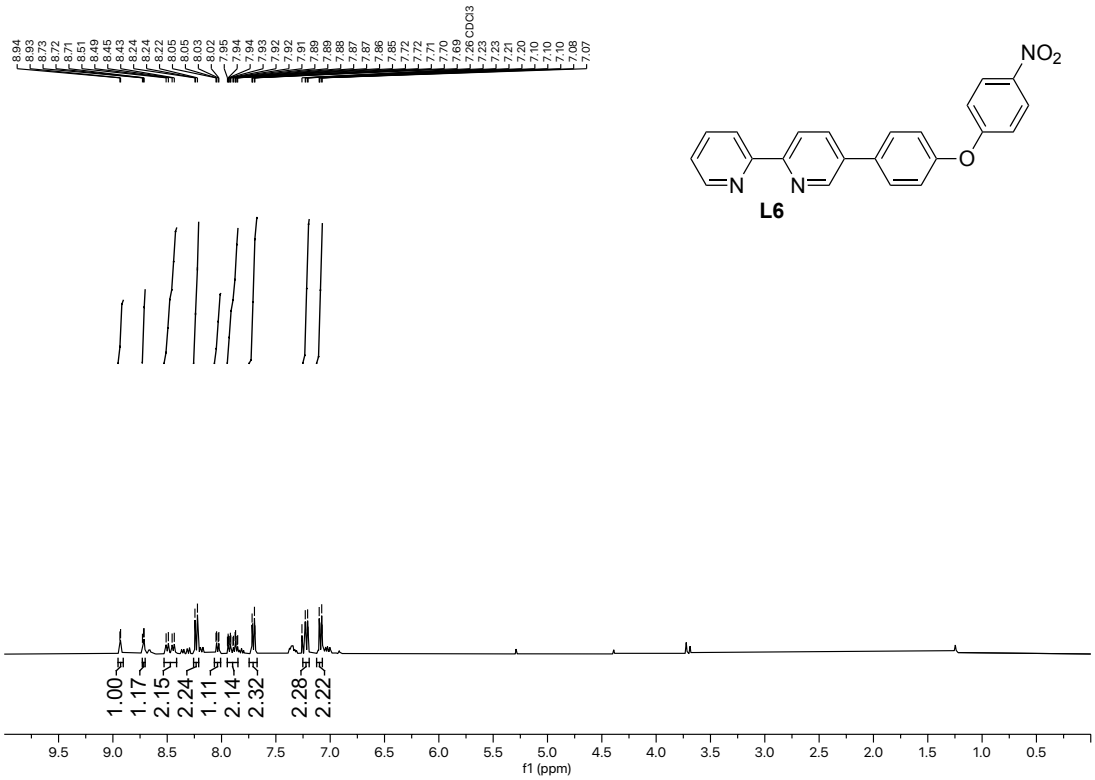
*$^{13}$C NMR 1-(2-([2,2'-bipyridin]-5-ylethynyl)phenyl)-3-cyclohexylurea (L2)*



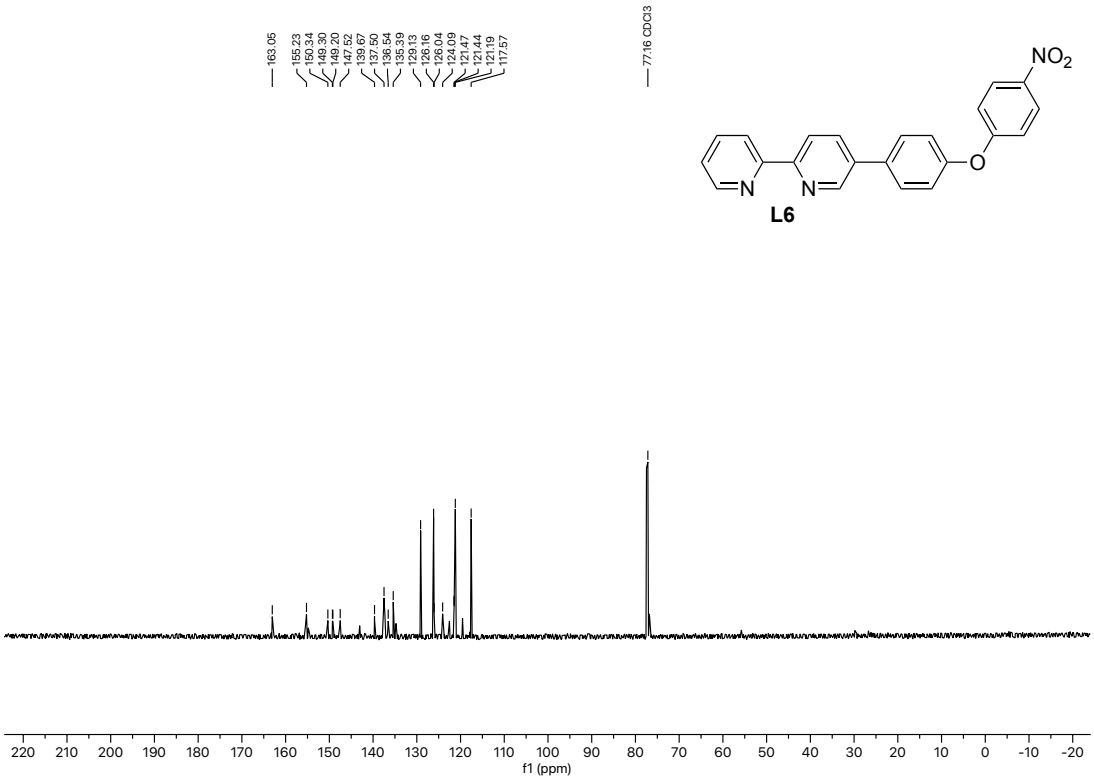

*HSQC NMR 1-(2-([2,2'-bipyridin]-5-ylethynyl)phenyl)-3-cyclohexylurea (L2)*



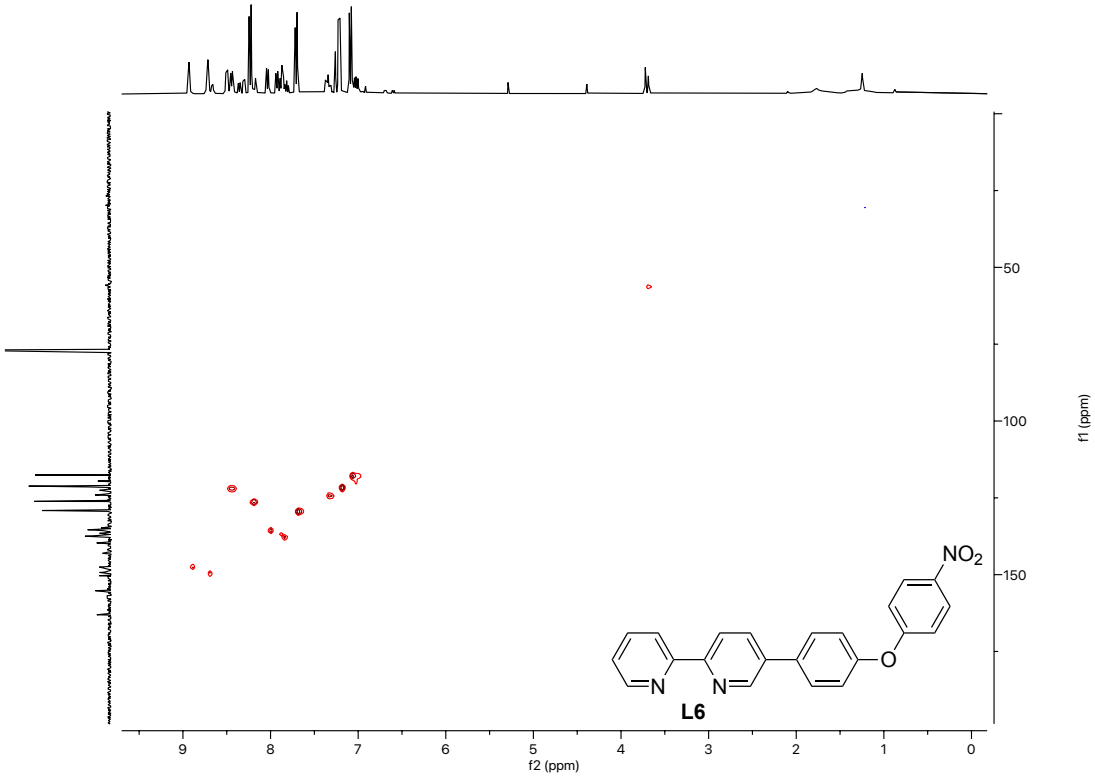
*[1]H NMR 5-(4-(4-nitrophenoxy)phenyl)-2,2'-bipyridine (L6)*



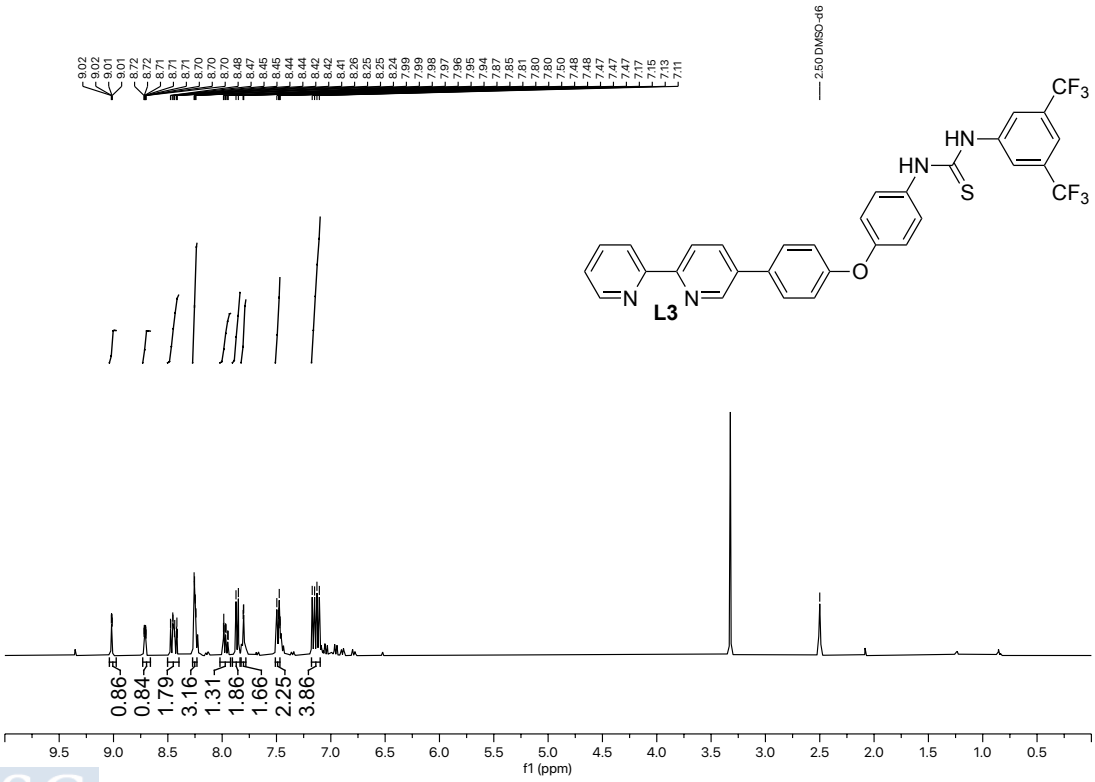

*[13]C NMR 5-(4-(4-nitrophenoxy)phenyl)-2,2'-bipyridine (L6)*



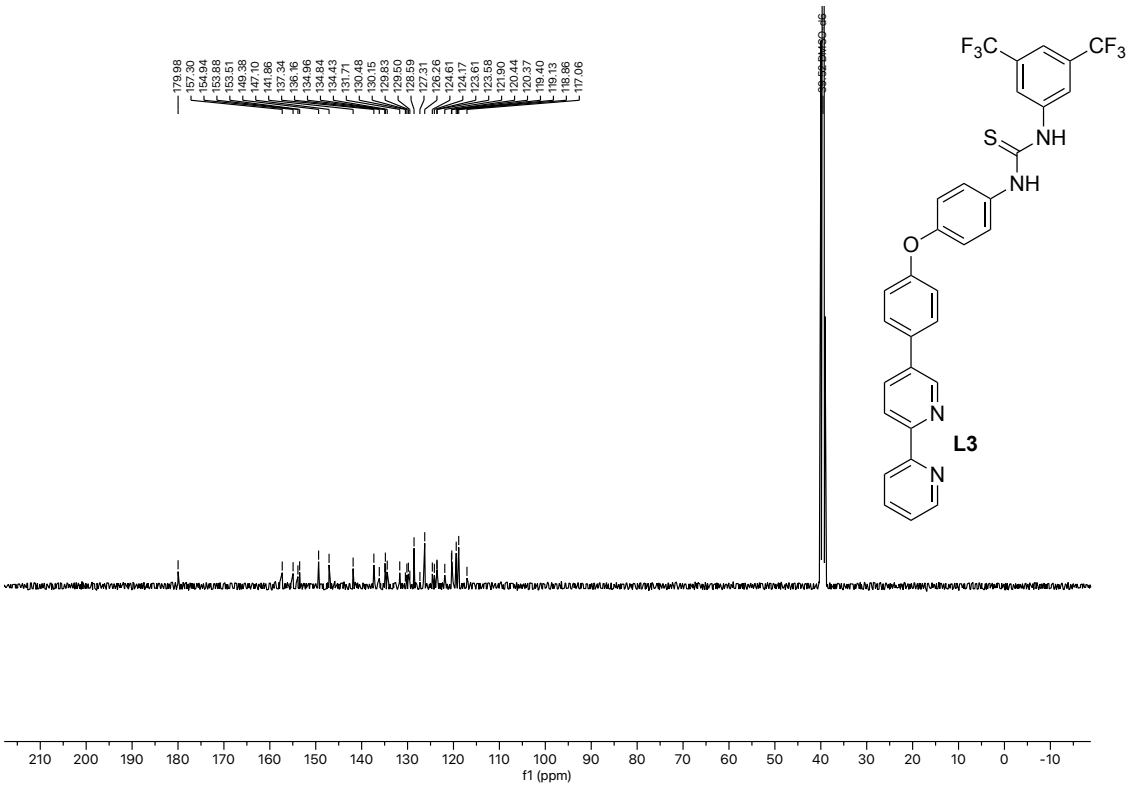
*HSQC NMR 5-(4-(4-nitrophenoxy)phenyl)-2,2'-bipyridine (L6)*



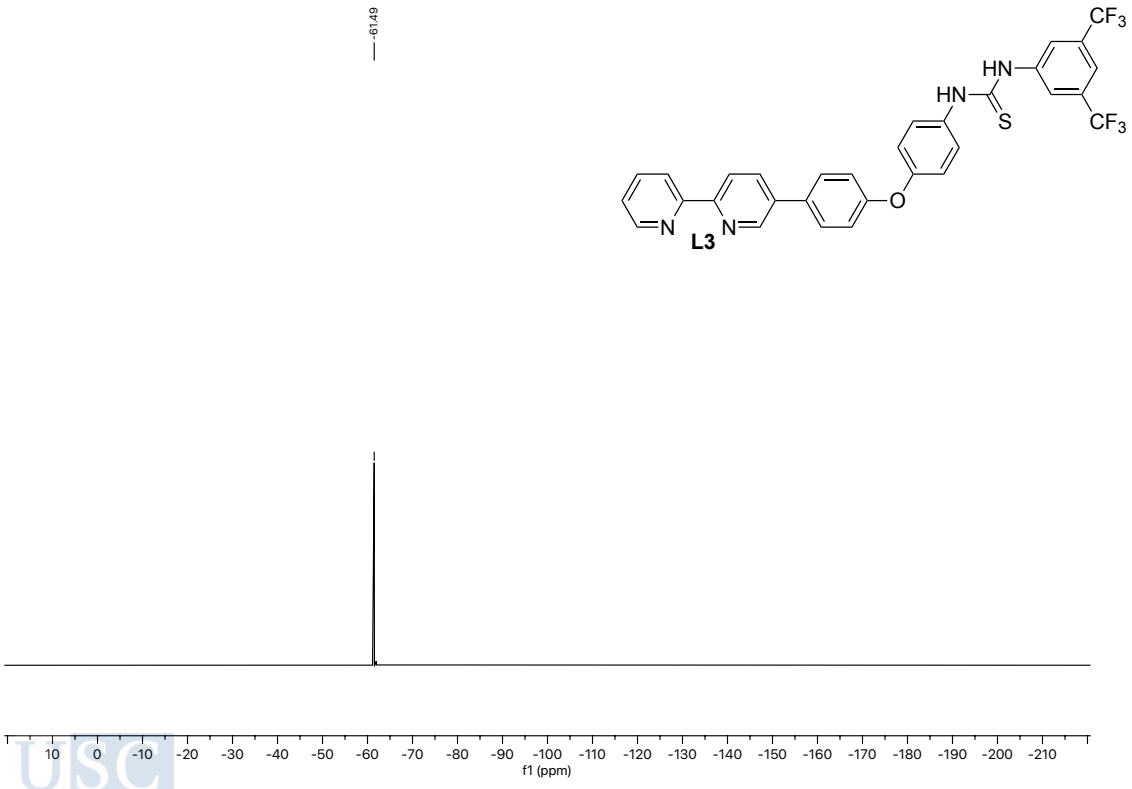

*$^{1}$H NMR 1-(4-(4-([2,2'-bipyridin]-5-yl)phenoxy)phenyl)-3-(3,5-bis(trifluoromethyl)phenyl)thiourea (L3)*



*$^{13}$C NMR 1-(4-(4-([2,2'-bipyridin]-5-yl)phenoxy)phenyl)-3-(3,5-bis(trifluoromethyl)phenyl)thiourea (L3)*

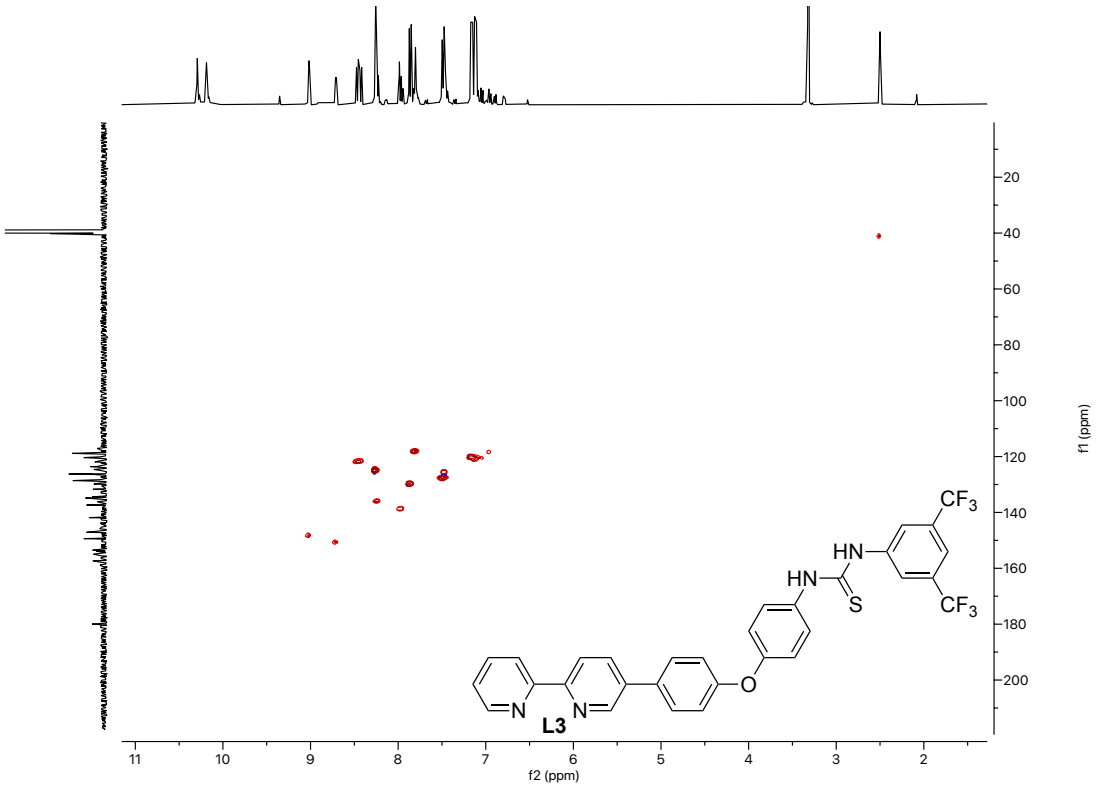



*$^{19}$F NMR 1-(4-(4-([2,2'-bipyridin]-5-yl)phenoxy)phenyl)-3-(3,5-bis(trifluoromethyl)phenyl)thiourea (L3)*

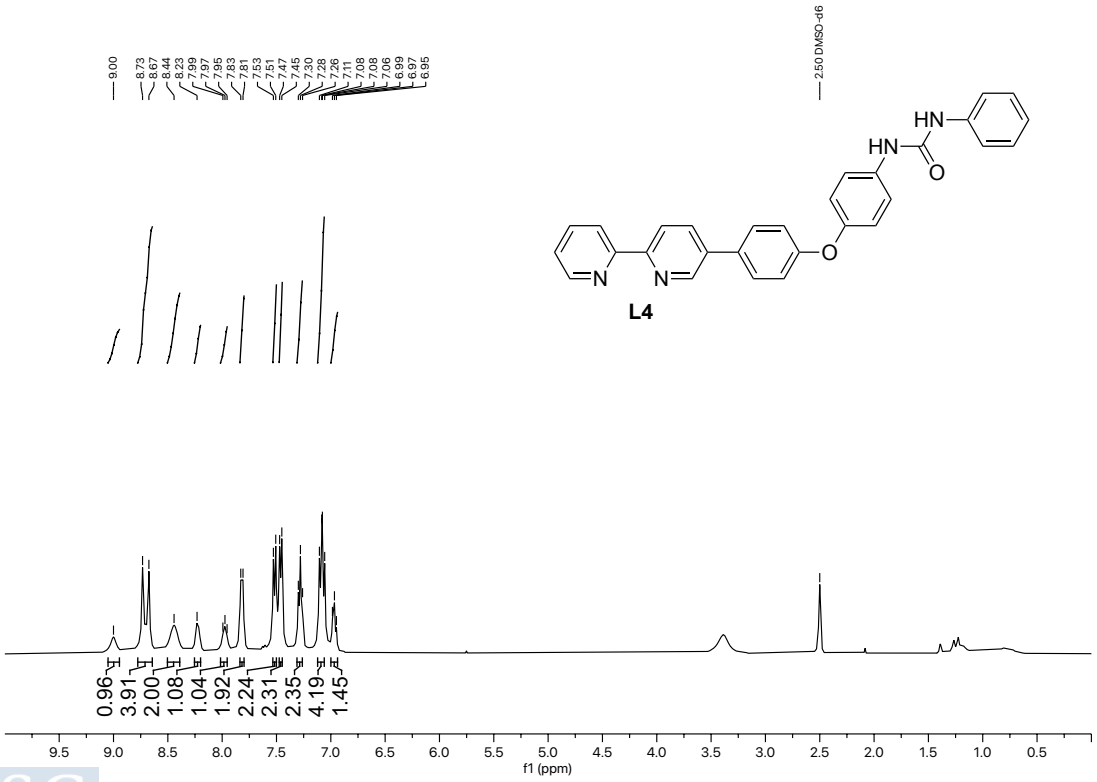



USC UNIVERSIDADE DE SANTIAGO DE COMPOSTELA

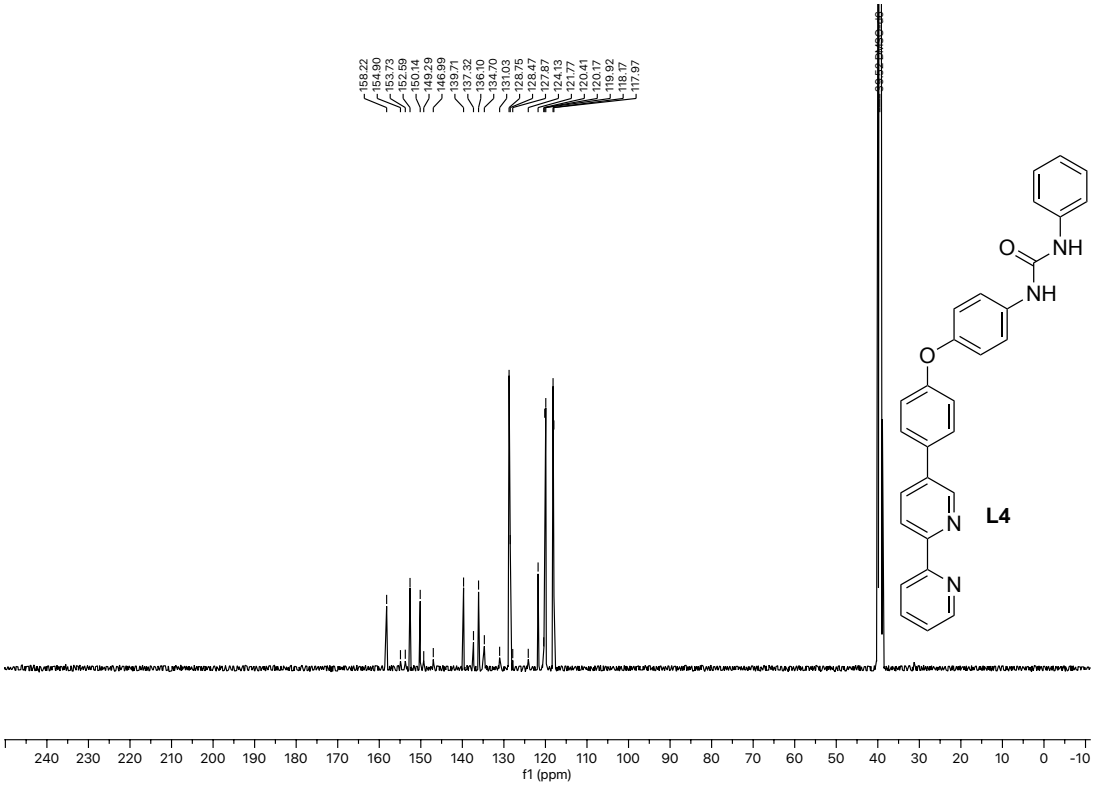
*HSQC NMR 1-(4-(4-([2,2'-bipyridin]-5-yl)phenoxy)phenyl)-3-(3,5-bis(trifluoromethyl)phenyl)thiourea (L3)*



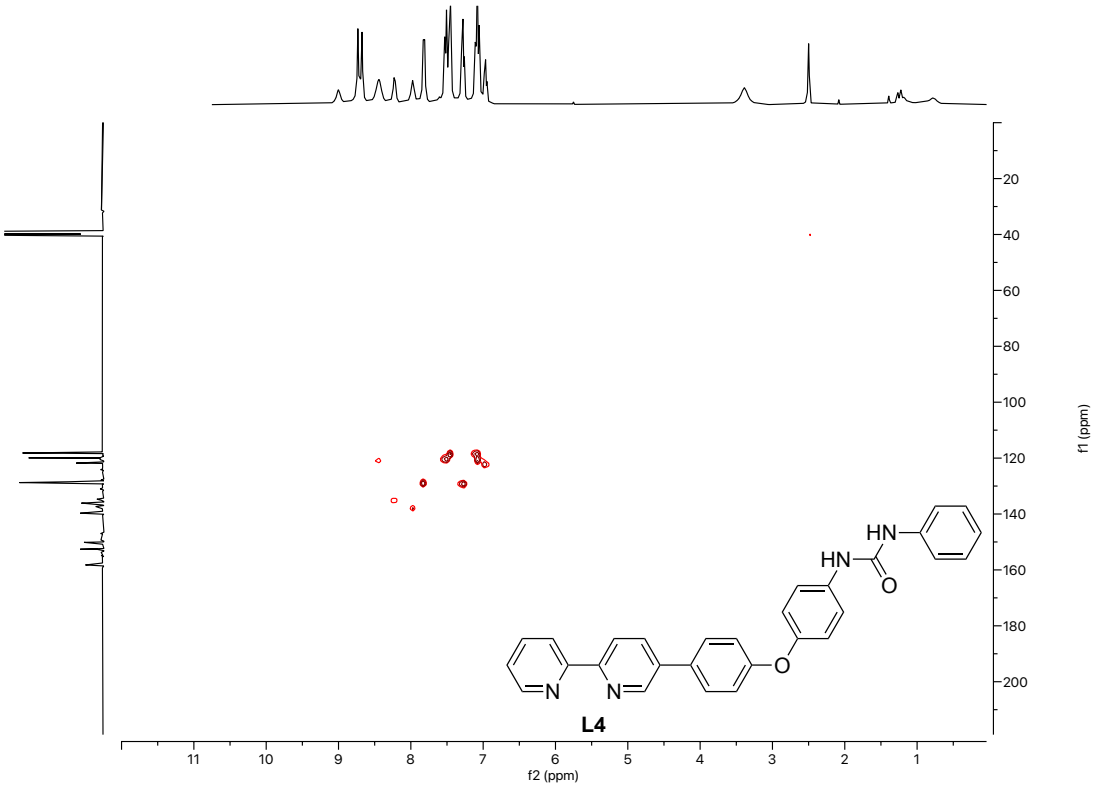

*[1]H NMR 1-(4-(4-([2,2'-bipyridin]-5-yl)phenoxy)phenyl)-3-phenylurea (L4)*



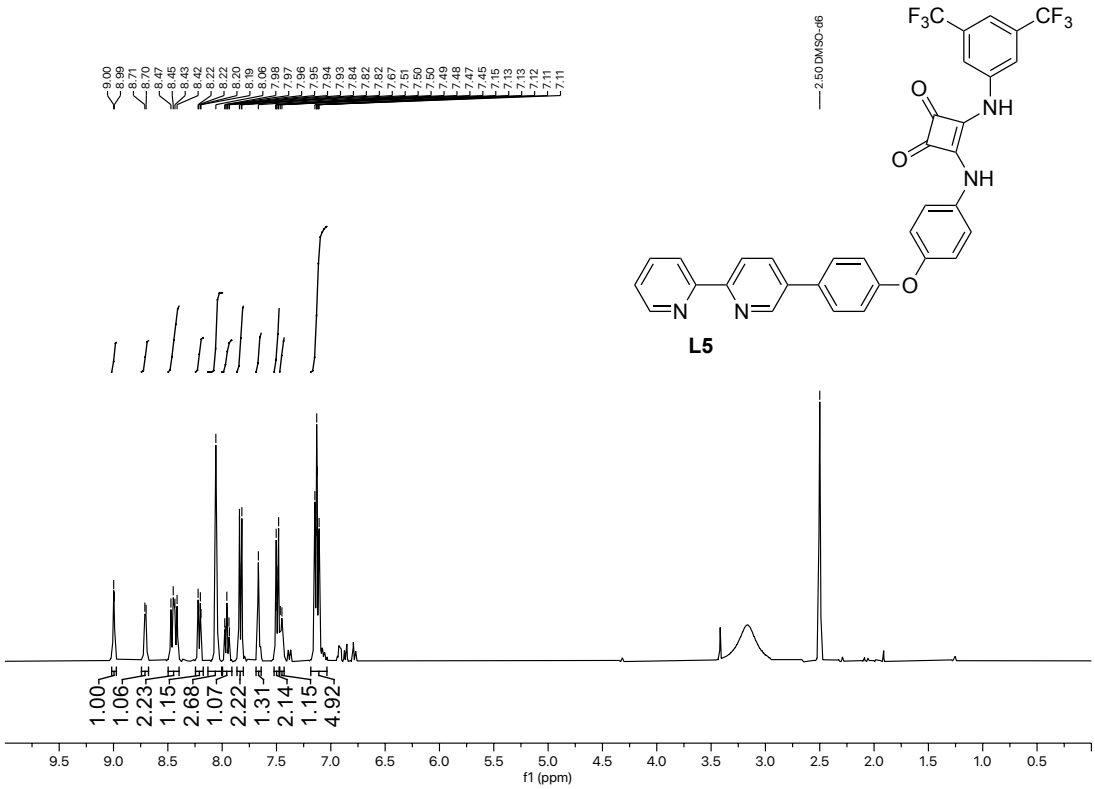
*$^{13}$C NMR 1-(4-(4-([2,2'-bipyridin]-5-yl)phenoxy)phenyl)-3-phenylurea (L4)*



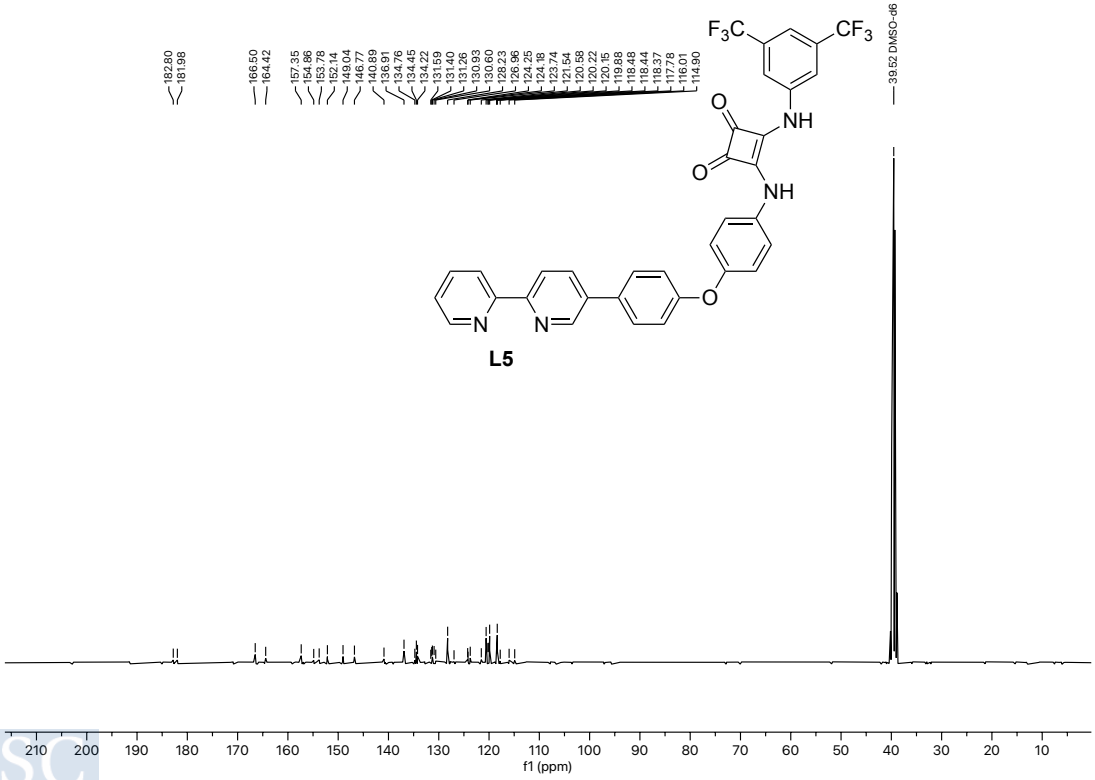

*HSQC NMR 1-(4-(4-([2,2'-bipyridin]-5-yl)phenoxy)phenyl)-3-phenylurea (L4)*



*[1]H NMR 3-((4-(4-([2,2'-bipyridin]-5-yl)phenoxy)phenyl)amino)-4-((3,5-bis(trifluoromethyl)phenyl)amino)cyclobut-3-ene-1,2-dione (L5)*

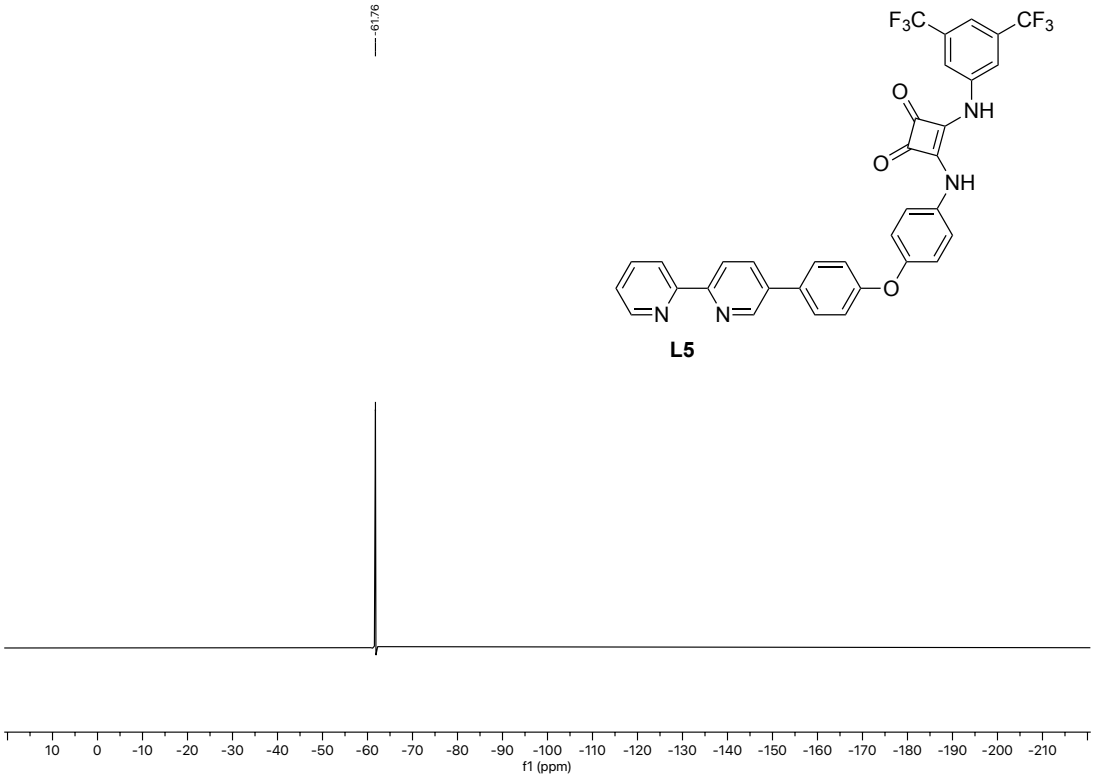



*[13]C NMR 3-((4-(4-([2,2'-bipyridin]-5-yl)phenoxy)phenyl)amino)-4-((3,5-bis(trifluoromethyl)phenyl)amino)cyclobut-3-ene-1,2-dione (L5)*

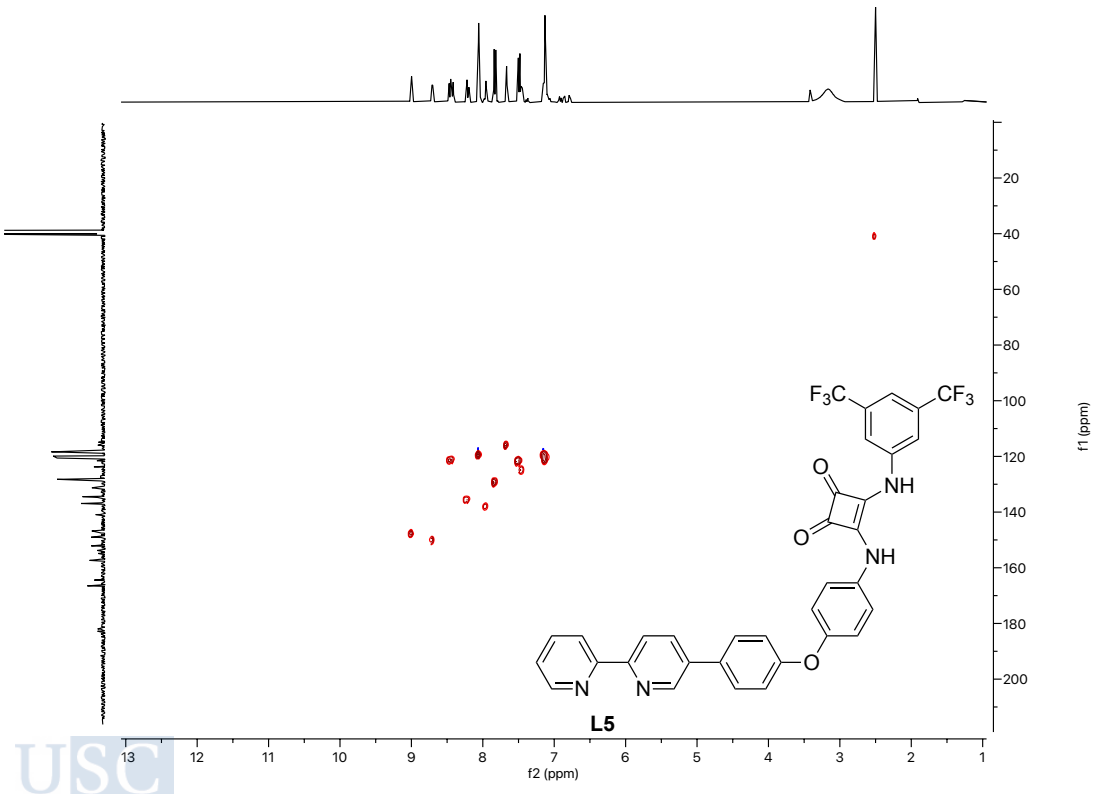



USC UNIVERSIDADE DE SANTIAGO DE COMPOSTELA

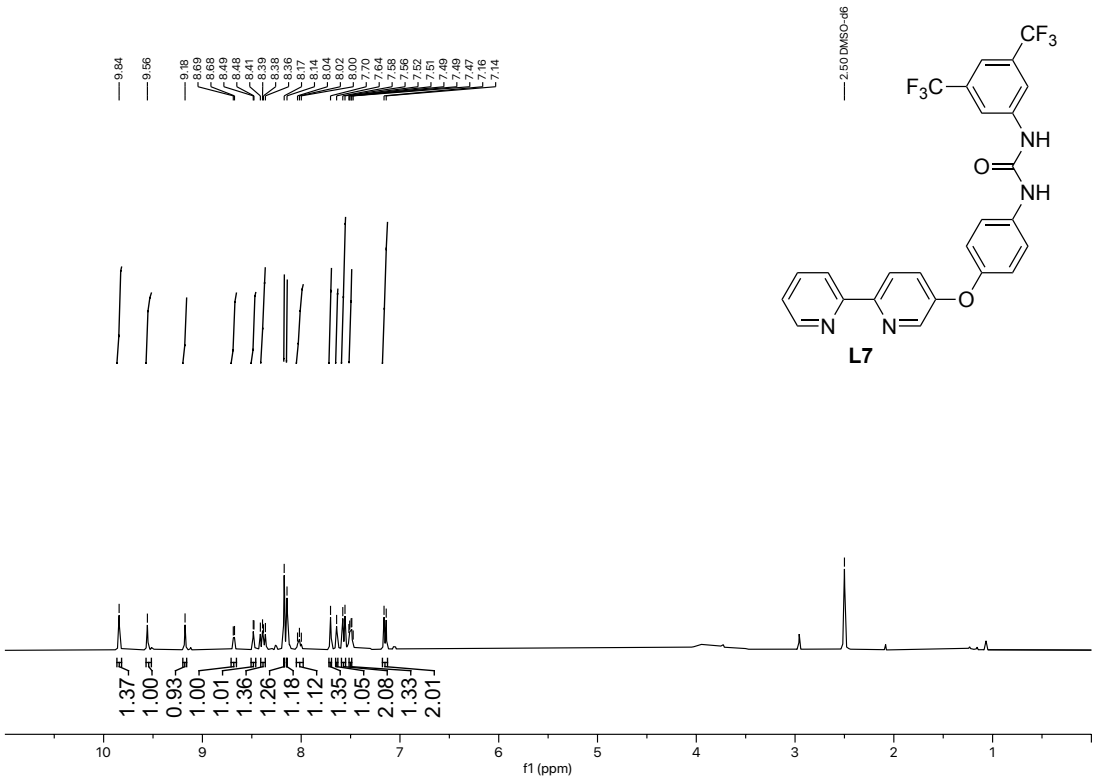
*$^{19}$F NMR 3-((4-(4-([2,2'-bipyridin]-5-yl)phenoxy)phenyl)amino)-4-((3,5-bis(trifluoromethyl)phenyl)amino)cyclobut-3-ene-1,2-dione (L5)*



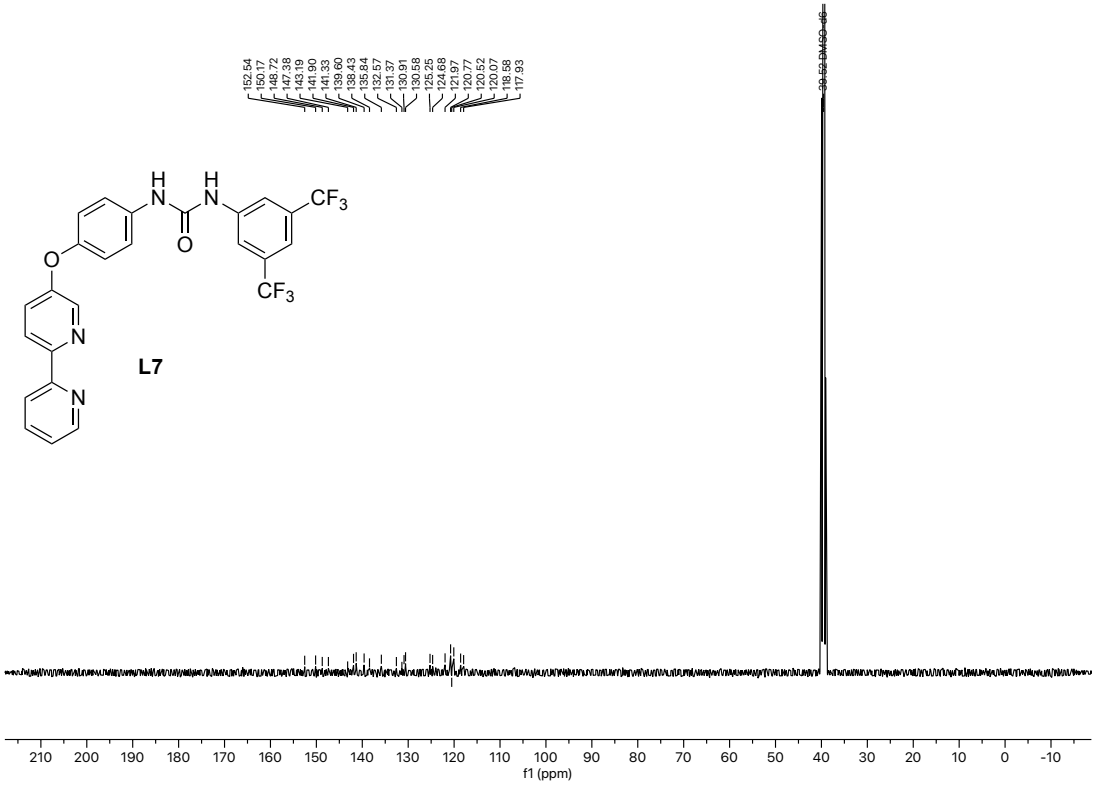

*HSQC NMR 3-((4-(4-([2,2'-bipyridin]-5-yl)phenoxy)phenyl)amino)-4-((3,5-bis(trifluoromethyl)phenyl)amino)cyclobut-3-ene-1,2-dione (L5)*



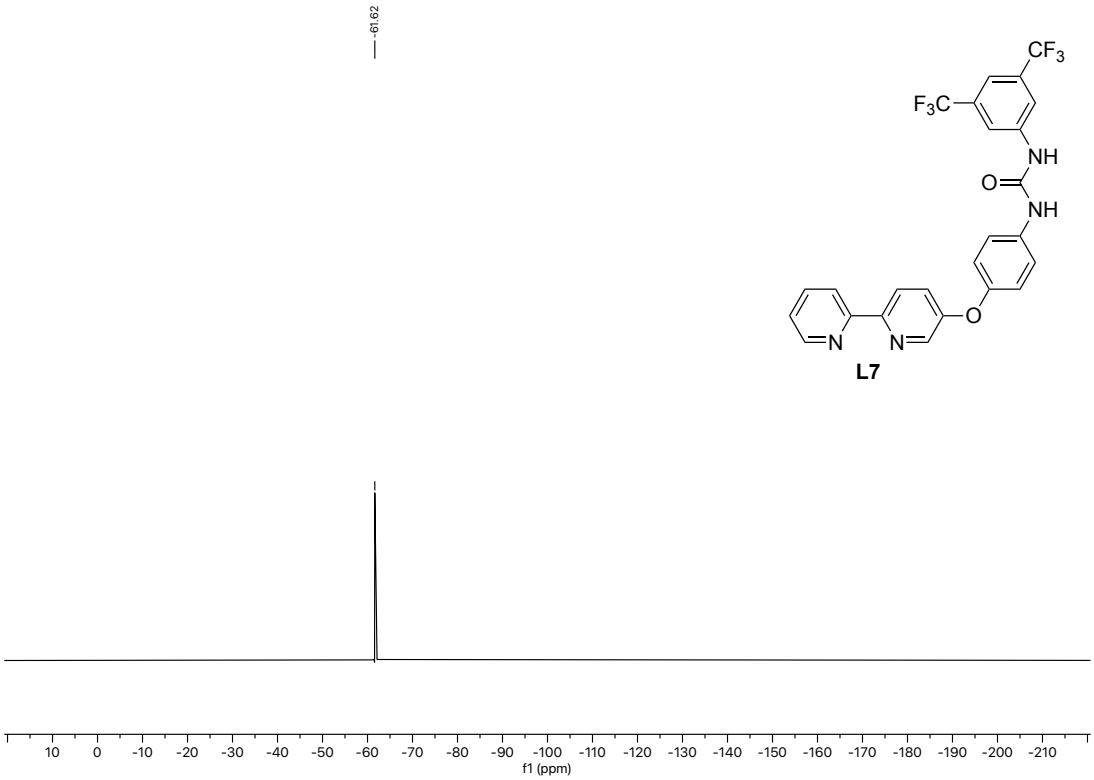
*[1]H NMR 1-(4-([2,2'-bipyridin]-5-yloxy)phenyl)-3-(3,5-bis(trifluoromethyl)phenyl)urea (L7)*



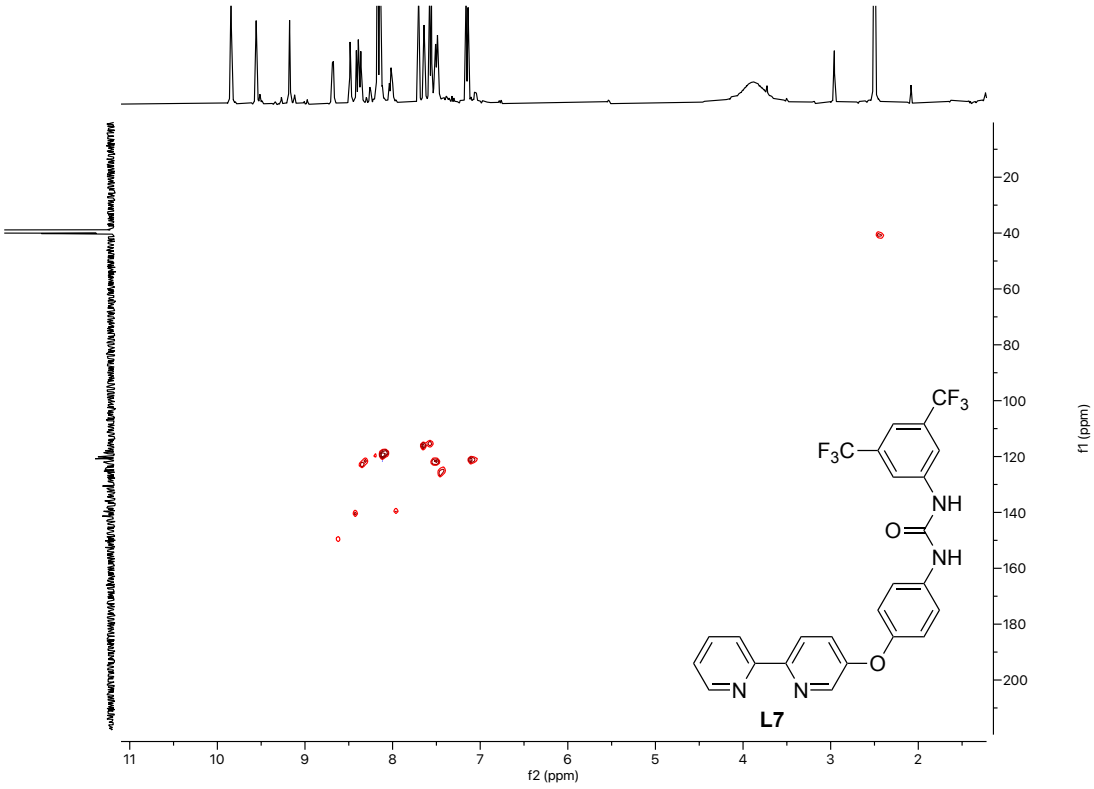

*[13]C NMR 1-(4-([2,2'-bipyridin]-5-yloxy)phenyl)-3-(3,5-bis(trifluoromethyl)phenyl)urea (L7)*



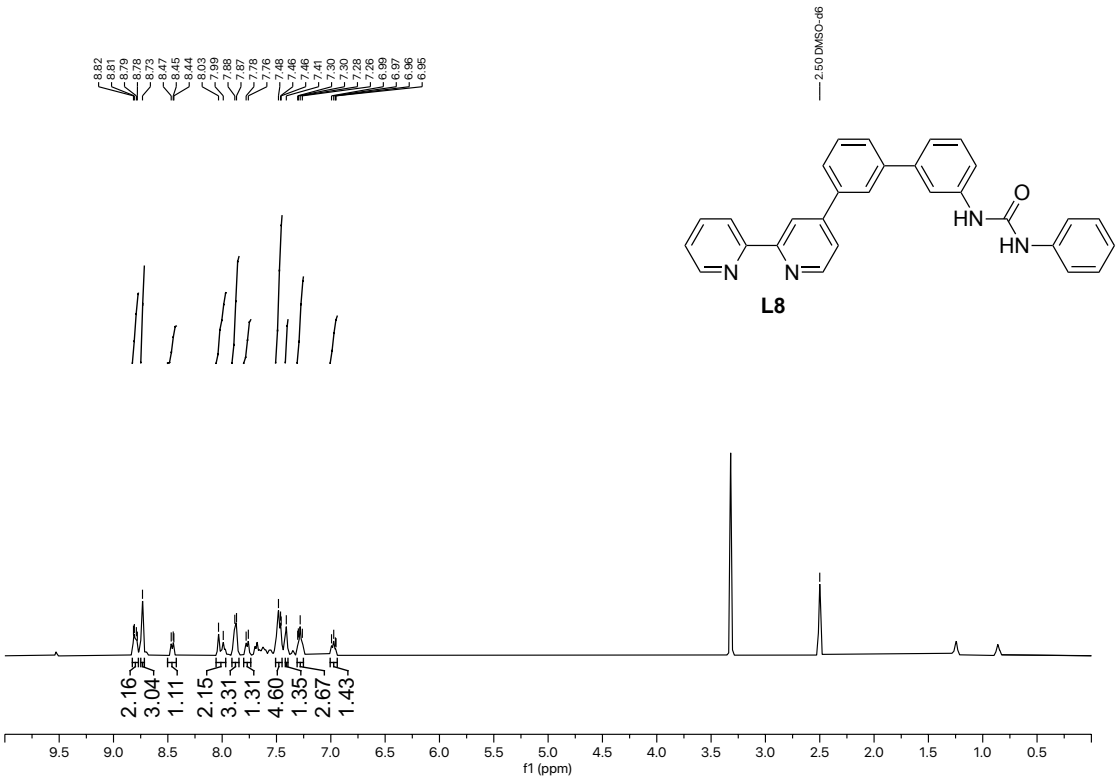
*$^{19}$F NMR 1-(4-([2,2'-bipyridin]-5-yloxy)phenyl)-3-(3,5-bis(trifluoromethyl)phenyl)urea (L7)*



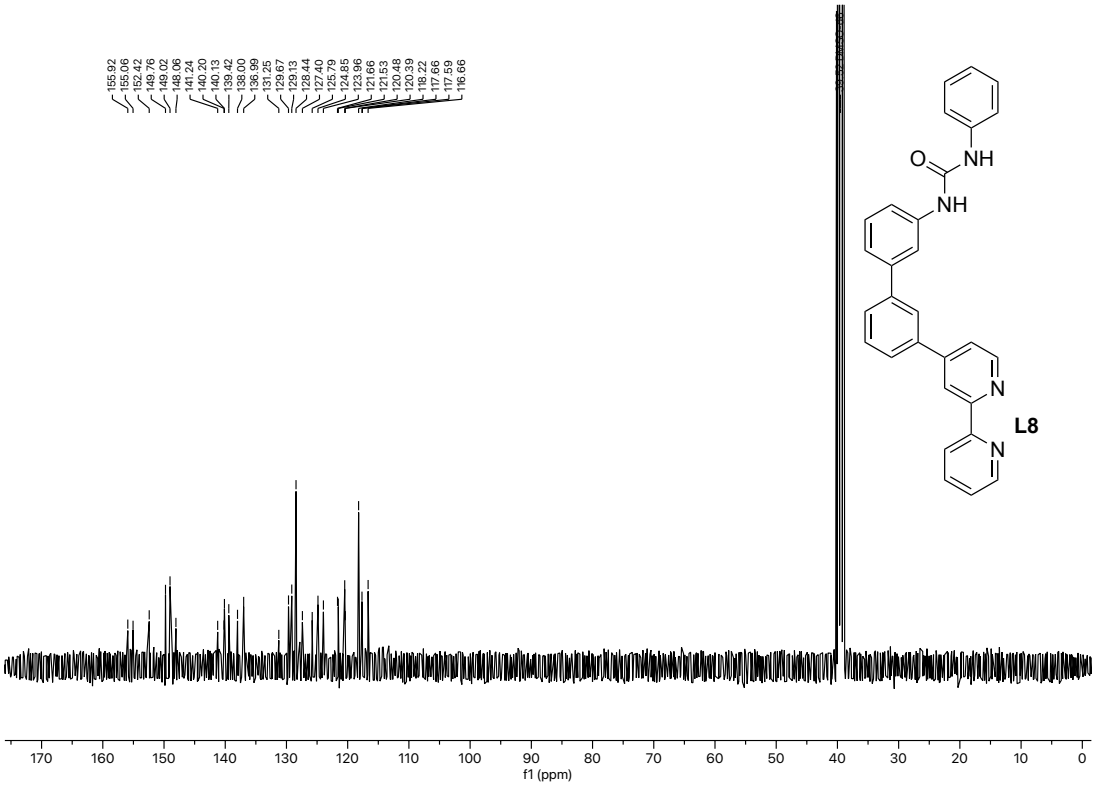

*HSQC NMR 1-(4-([2,2'-bipyridin]-5-yloxy)phenyl)-3-(3,5-bis(trifluoromethyl)phenyl)urea (L7)*



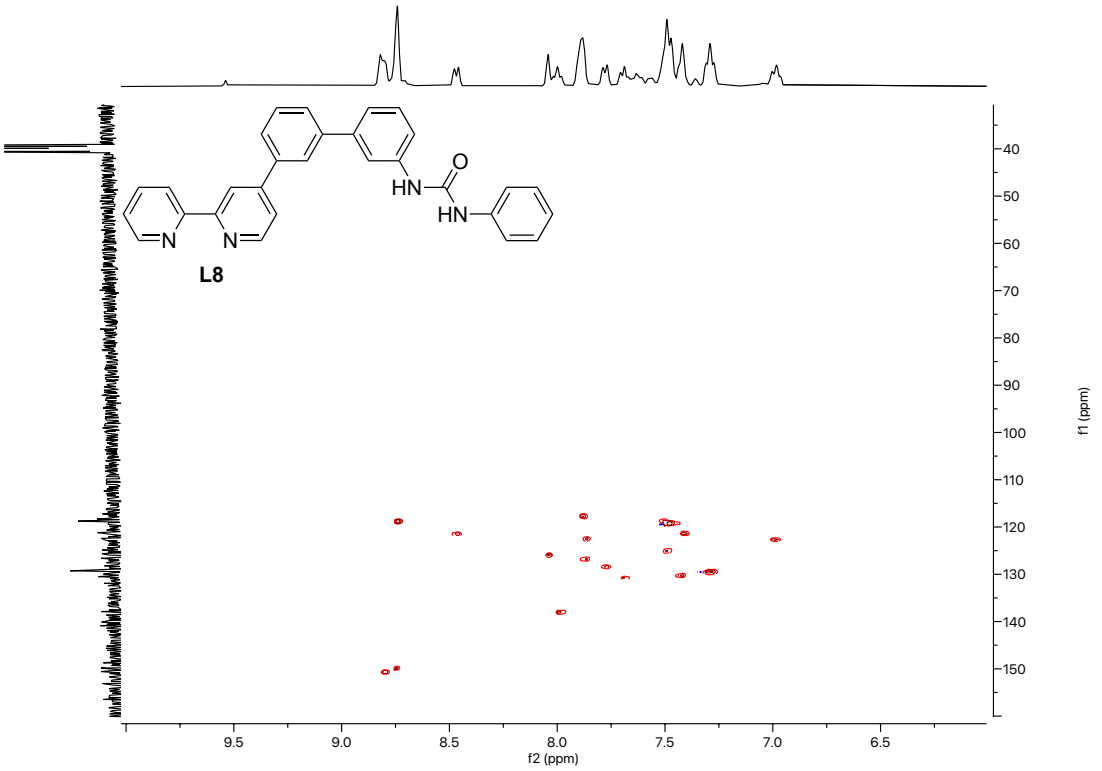
*[1]H NMR 1-(3'-([2,2'-bipyridin]-4-yl)-[1,1'-biphenyl]-3-yl)-3-phenylurea (L8)*



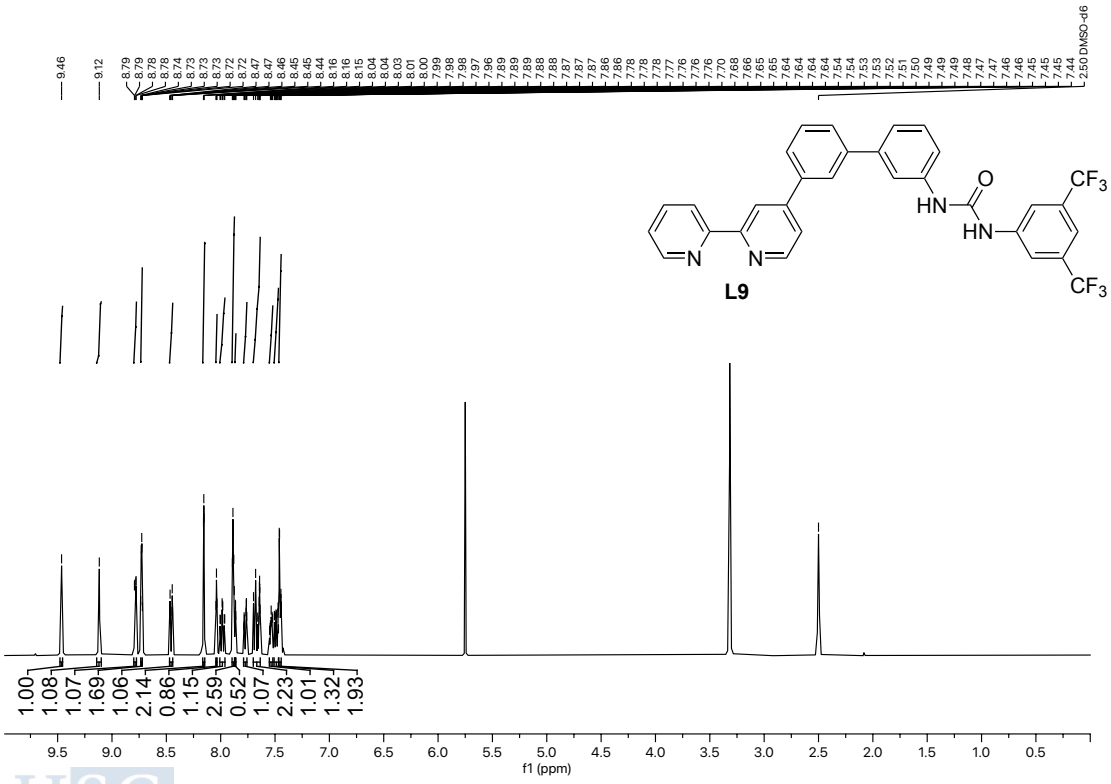

*[13]C NMR 1-(3'-([2,2'-bipyridin]-4-yl)-[1,1'-biphenyl]-3-yl)-3-phenylurea (L8)*



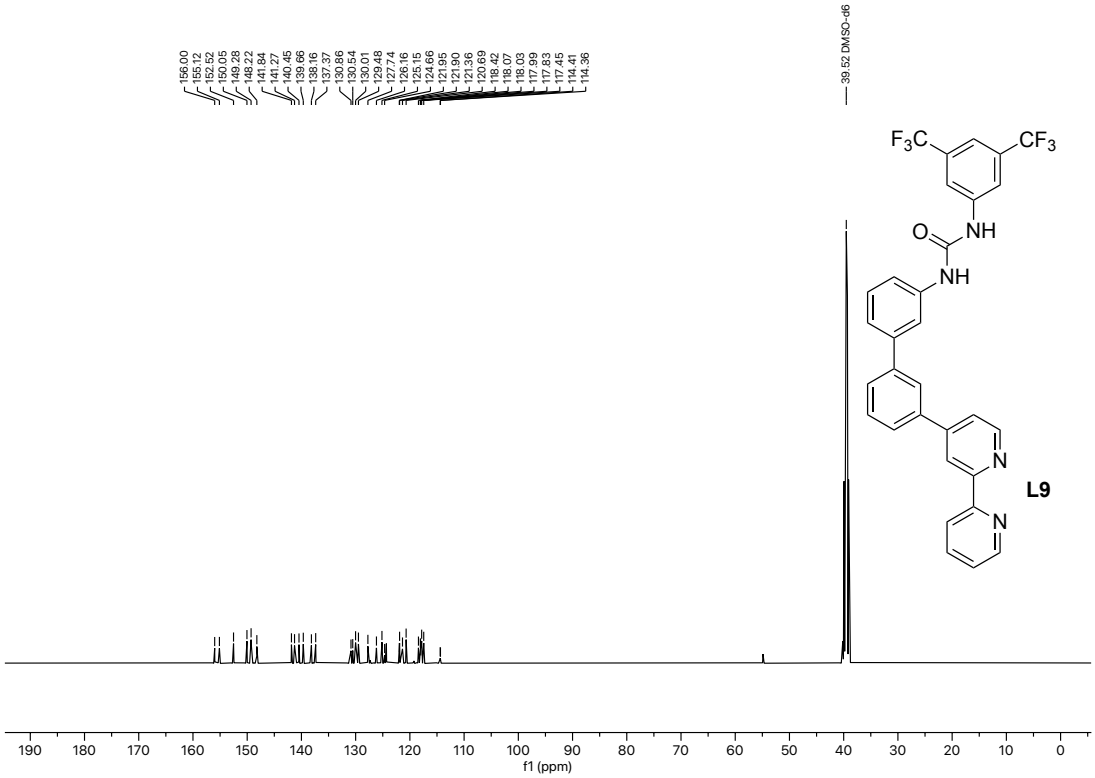
*HSQC NMR 1-(3'-([2,2'-bipyridin]-4-yl)-[1,1'-biphenyl]-3-yl)-3-phenylurea (L8)*



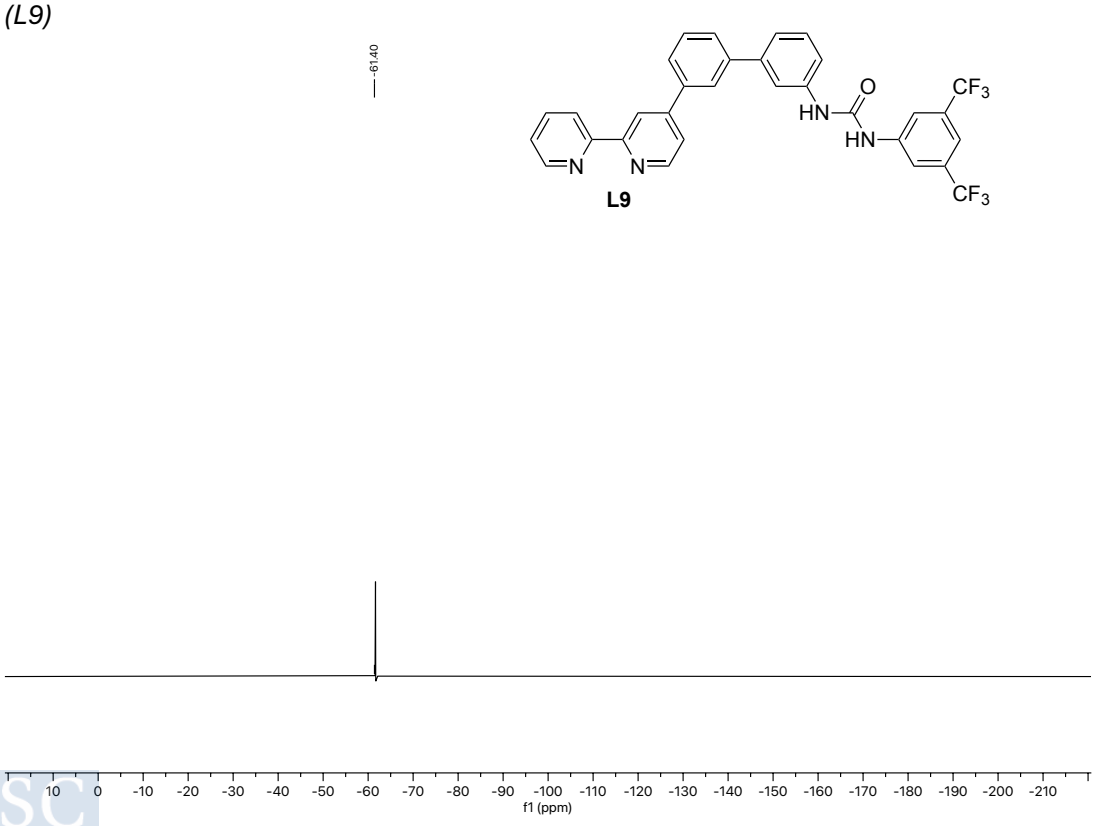

*$^{1}$H NMR 1-(3'-([2,2'-bipyridin]-4-yl)-[1,1'-biphenyl]-3-yl)-3-(3,5-bis(trifluoromethyl)phenyl)urea (L9)*



*$^{13}$C NMR 1-(3'-([2,2'-bipyridin]-4-yl)-[1,1'-biphenyl]-3-yl)-3-(3,5-bis(trifluoromethyl)phenyl)urea (L9)*

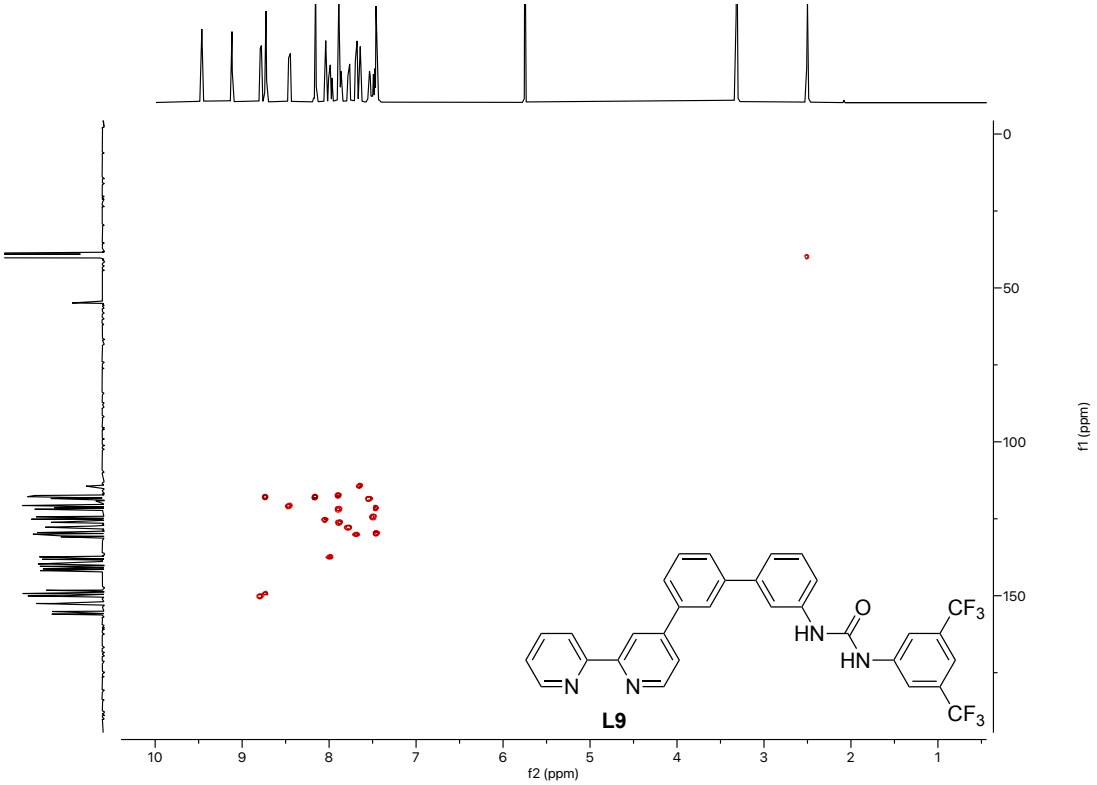



*$^{19}$F NMR 1-(3'-([2,2'-bipyridin]-4-yl)-[1,1'-biphenyl]-3-yl)-3-(3,5-bis(trifluoromethyl)phenyl)urea (L9)*

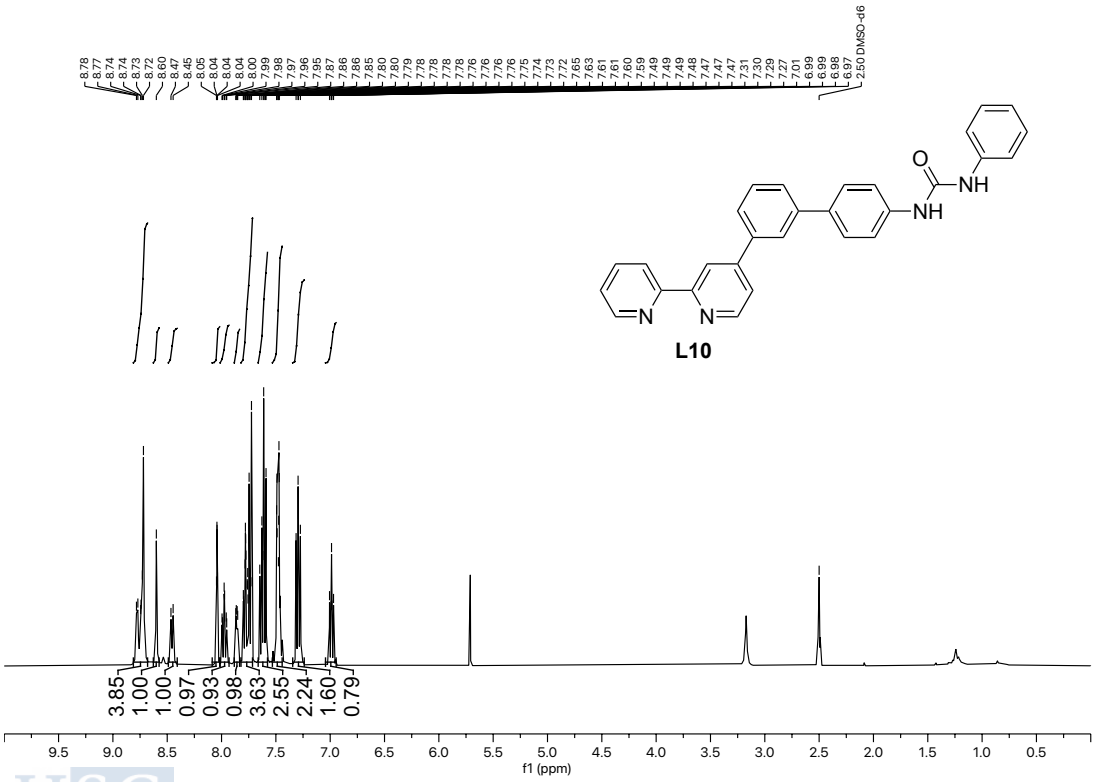



USC UNIVERSIDADE DE SANTIAGO DE COMPOSTELA

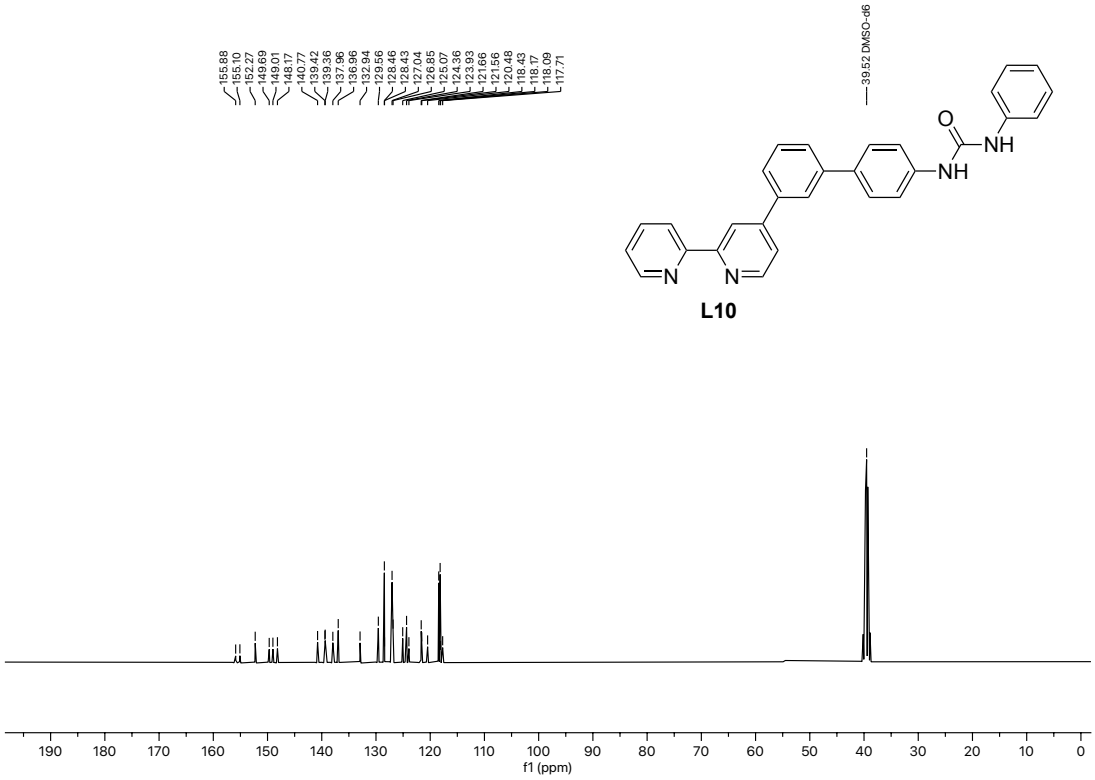
*HSQC NMR 1-(3'-([2,2'-bipyridin]-4-yl)-[1,1'-biphenyl]-3-yl)-3-(3,5-bis(trifluoromethyl)phenyl)urea (L9)*



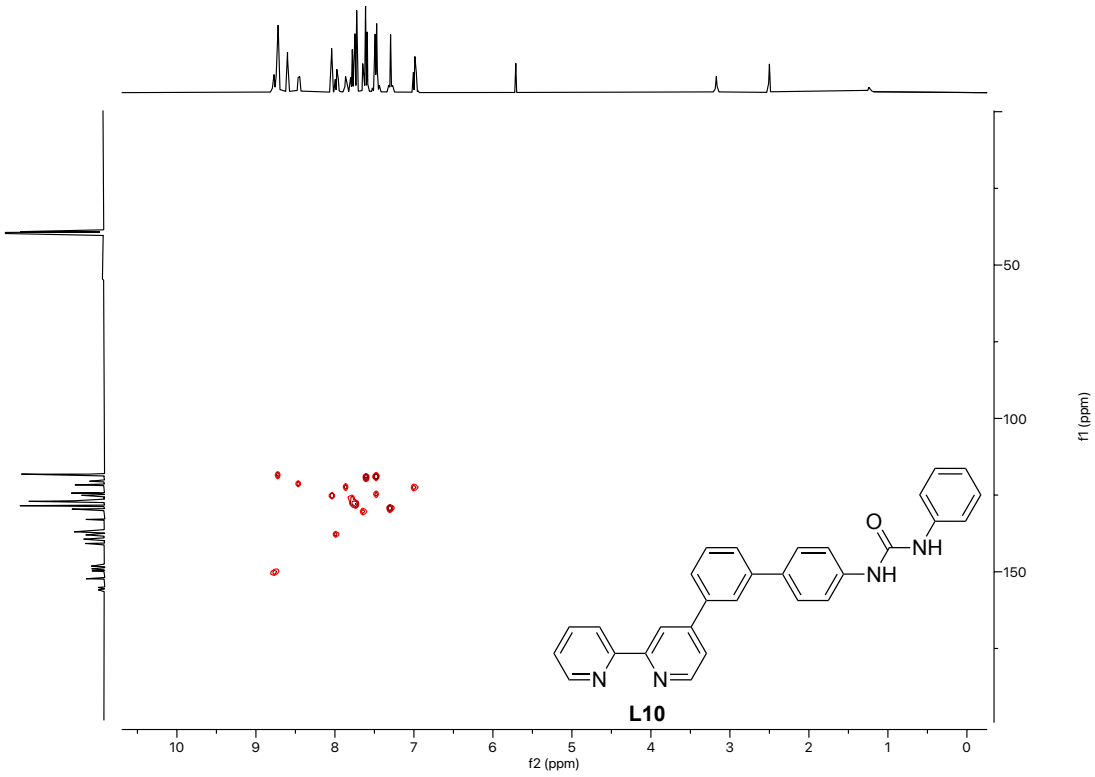

*$^{1}$H NMR 1-(3'-([2,2'-bipyridin]-4-yl)-[1,1'-biphenyl]-4-yl)-3-phenylurea (L10)*



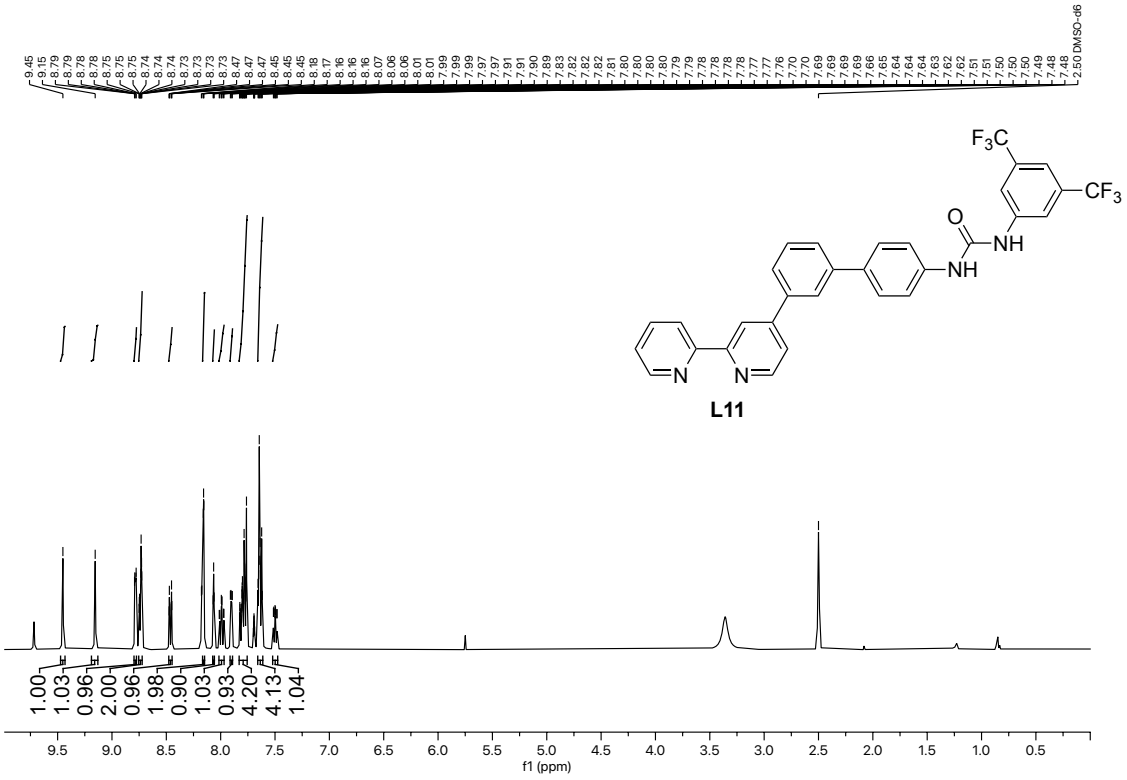
*$^{13}$C NMR 1-(3'-([2,2'-bipyridin]-4-yl)-[1,1'-biphenyl]-4-yl)-3-phenylurea (L10)*



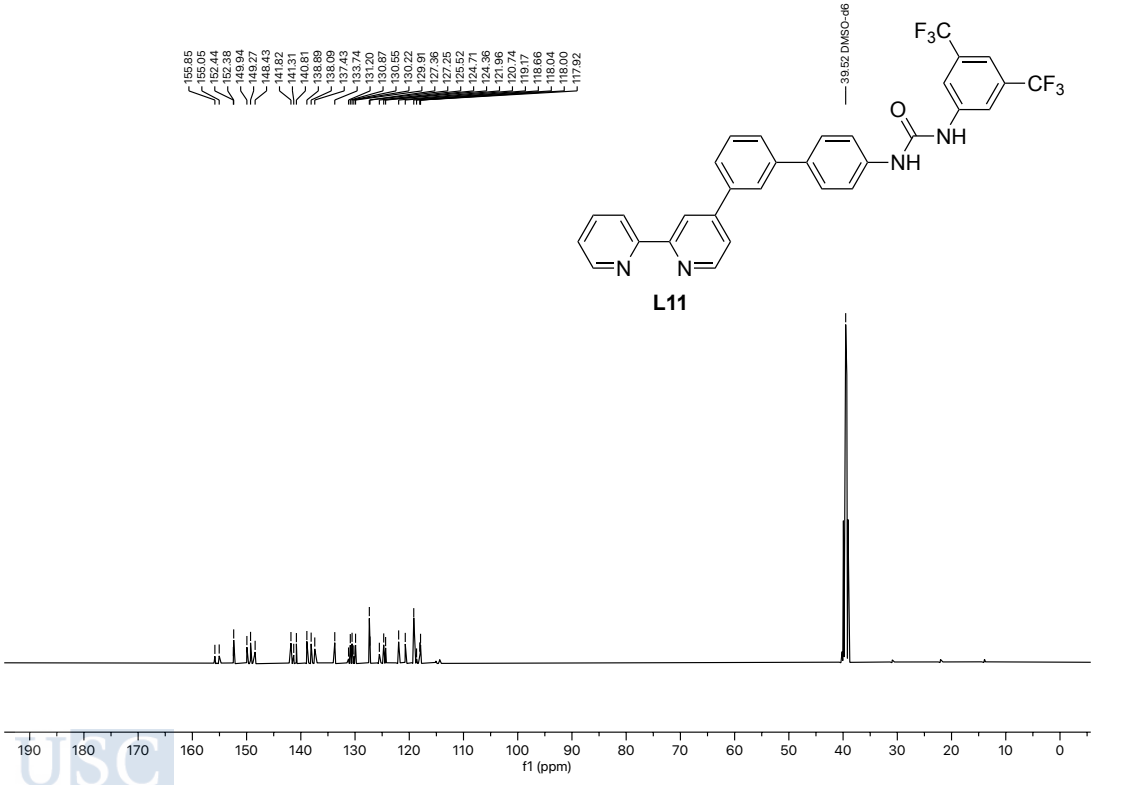

*HSQC NMR 1-(3'-([2,2'-bipyridin]-4-yl)-[1,1'-biphenyl]-4-yl)-3-phenylurea (L10)*



*[1]H NMR 1-(3'-([2,2'-bipyridin]-4-yl)-[1,1'-biphenyl]-4-yl)-3-(3,5-bis(trifluoromethyl)phenyl)urea (L11)*

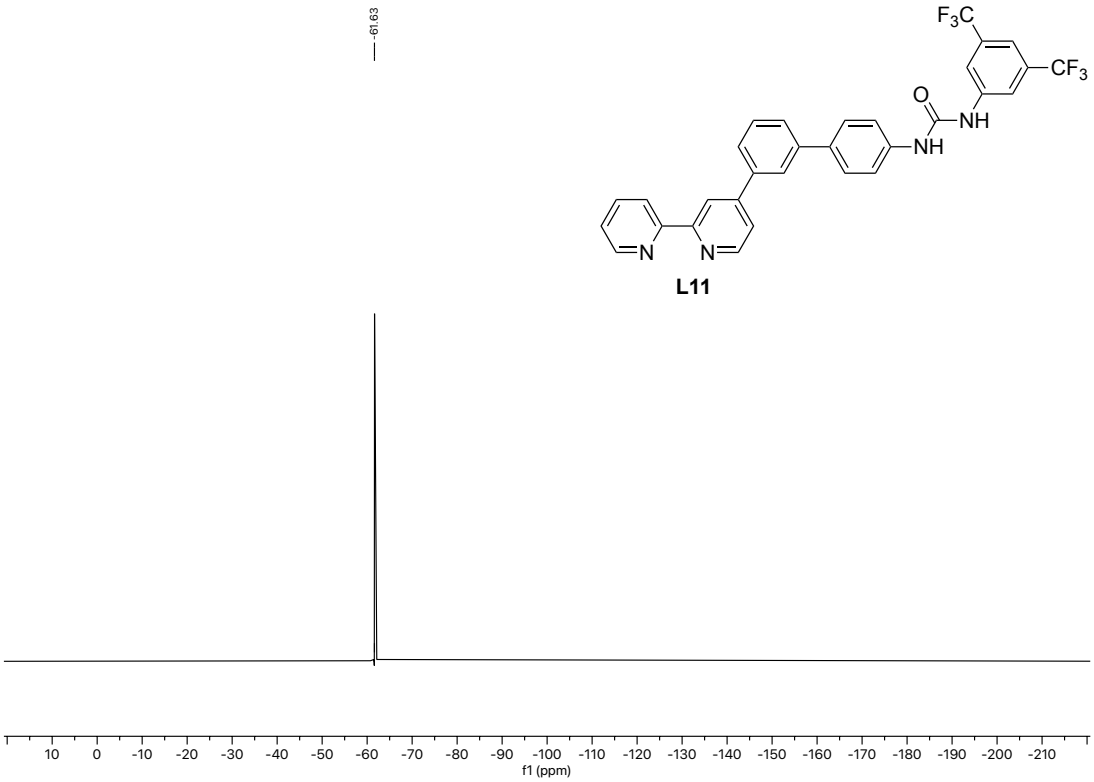



*[13]C NMR 1-(3'-([2,2'-bipyridin]-4-yl)-[1,1'-biphenyl]-4-yl)-3-(3,5-bis(trifluoromethyl)phenyl)urea (L11)*

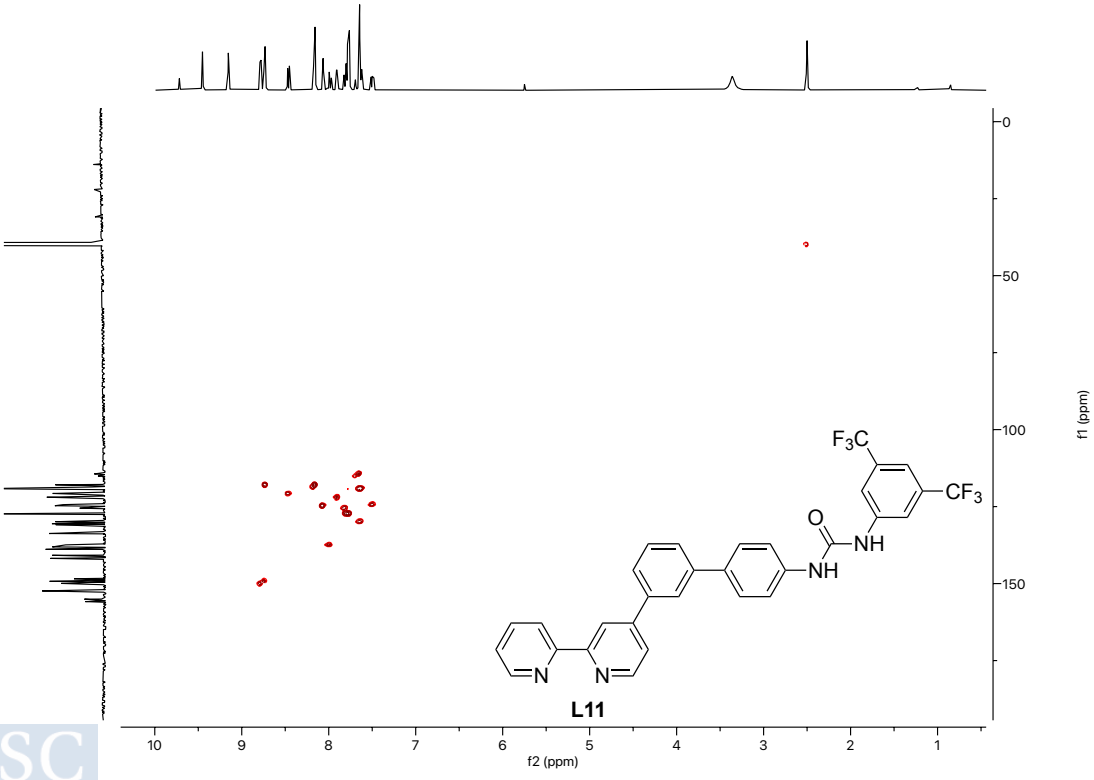



USC UNIVERSIDADE DE SANTIAGO DE COMPOSTELA

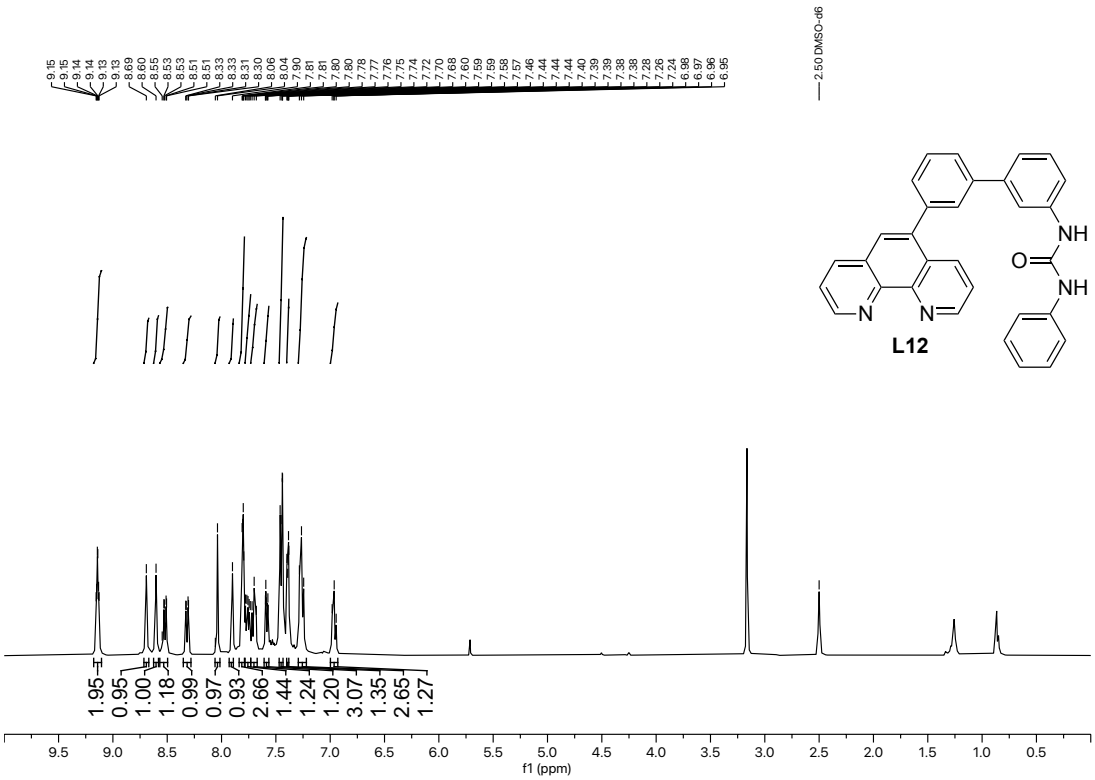
*$^{19}$F NMR 1-(3'-([2,2'-bipyridin]-4-yl)-[1,1'-biphenyl]-4-yl)-3-(3,5-bis(trifluoromethyl)phenyl)urea (L11)*



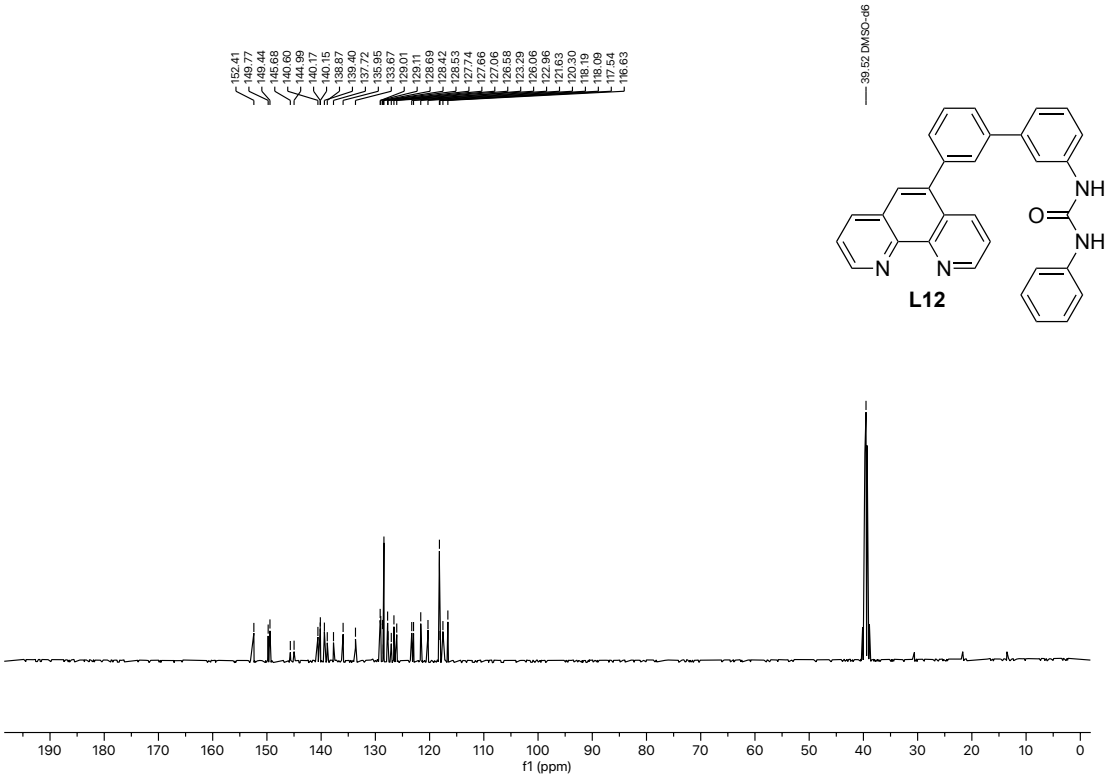

*HSQC NMR 1-(3'-([2,2'-bipyridin]-4-yl)-[1,1'-biphenyl]-4-yl)-3-(3,5-bis(trifluoromethyl)phenyl)urea (L11)*



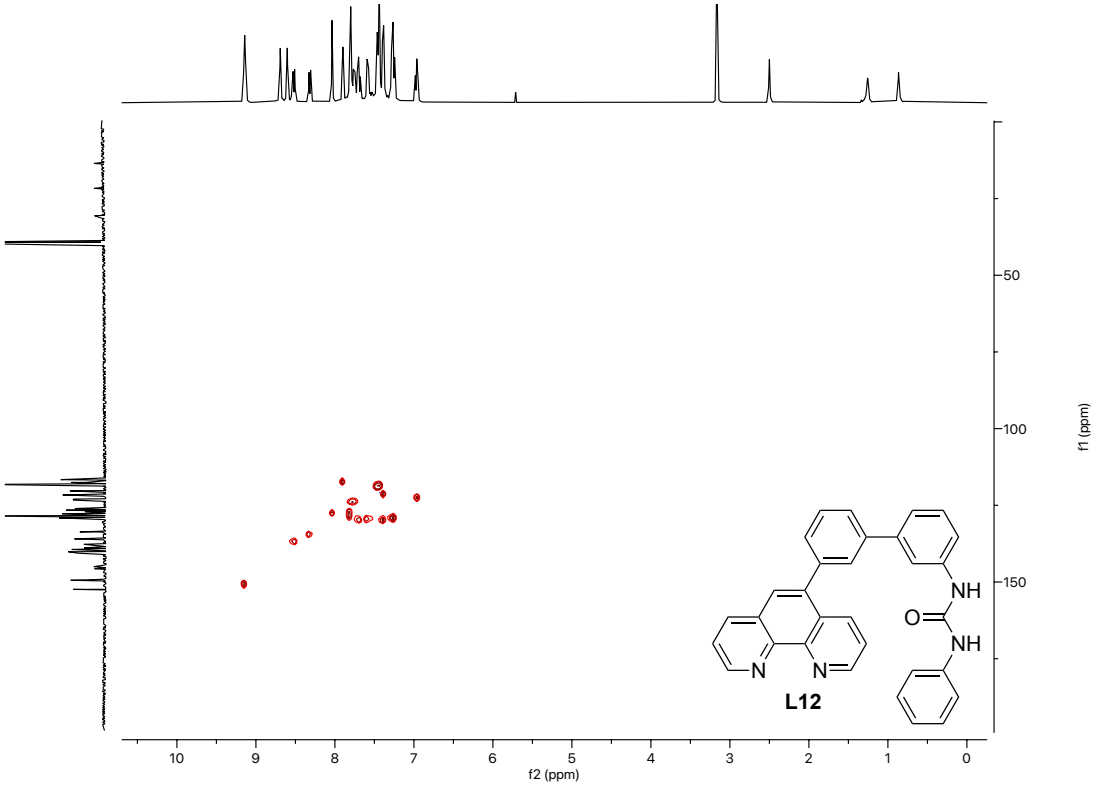
*[1]H NMR 1-(3'-(1,10-phenanthrolin-5-yl)-[1,1'-biphenyl]-3-yl)-3-phenylurea (L12)*



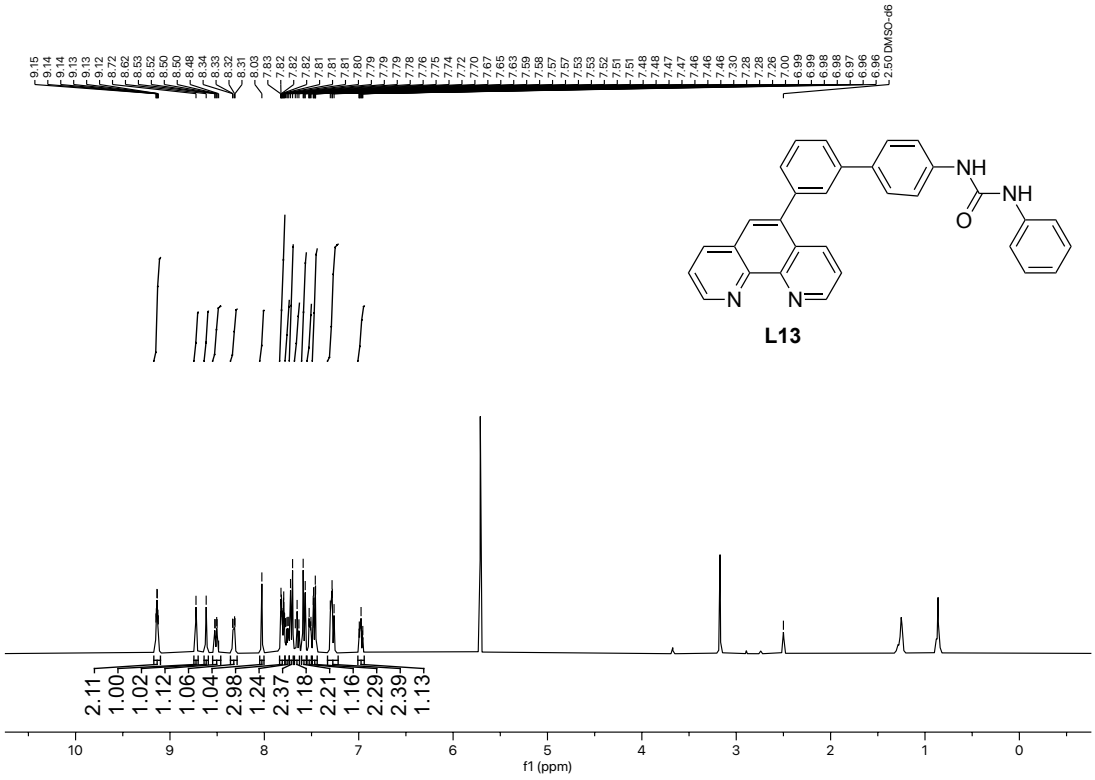

*[13]C NMR 1-(3'-(1,10-phenanthrolin-5-yl)-[1,1'-biphenyl]-3-yl)-3-phenylurea (L12)*



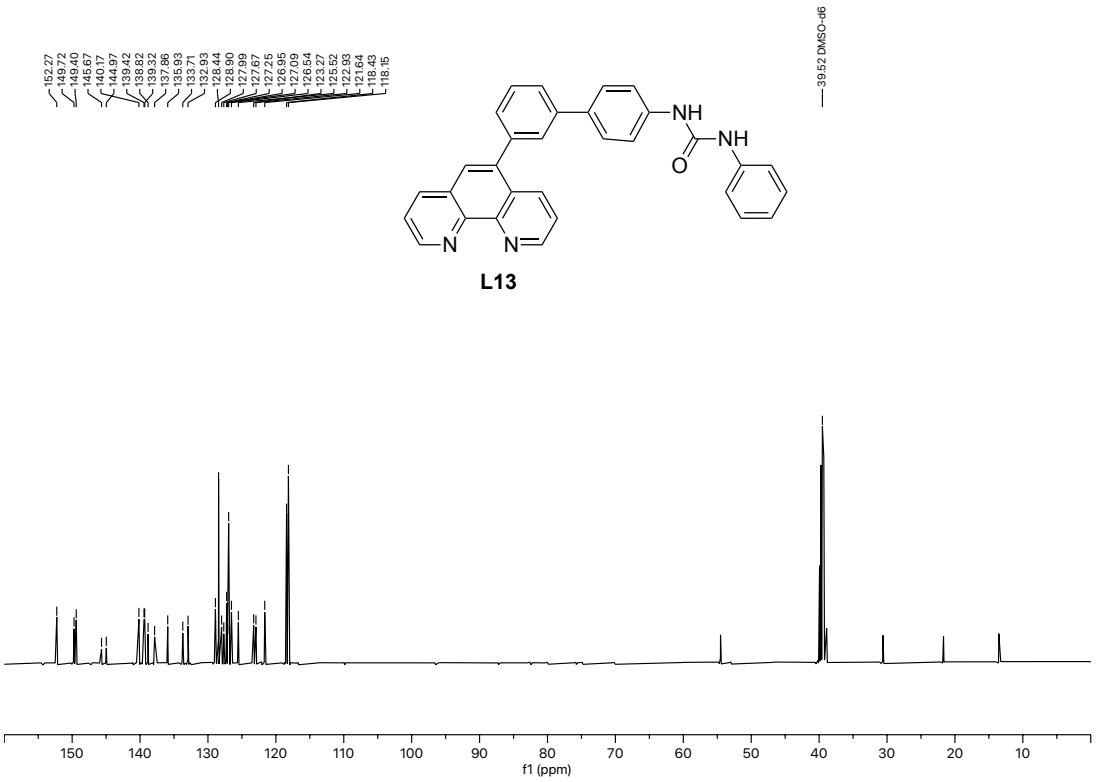
*HSQC NMR 1-(3'-(1,10-phenanthrolin-5-yl)-[1,1'-biphenyl]-3-yl)-3-phenylurea (L12)*



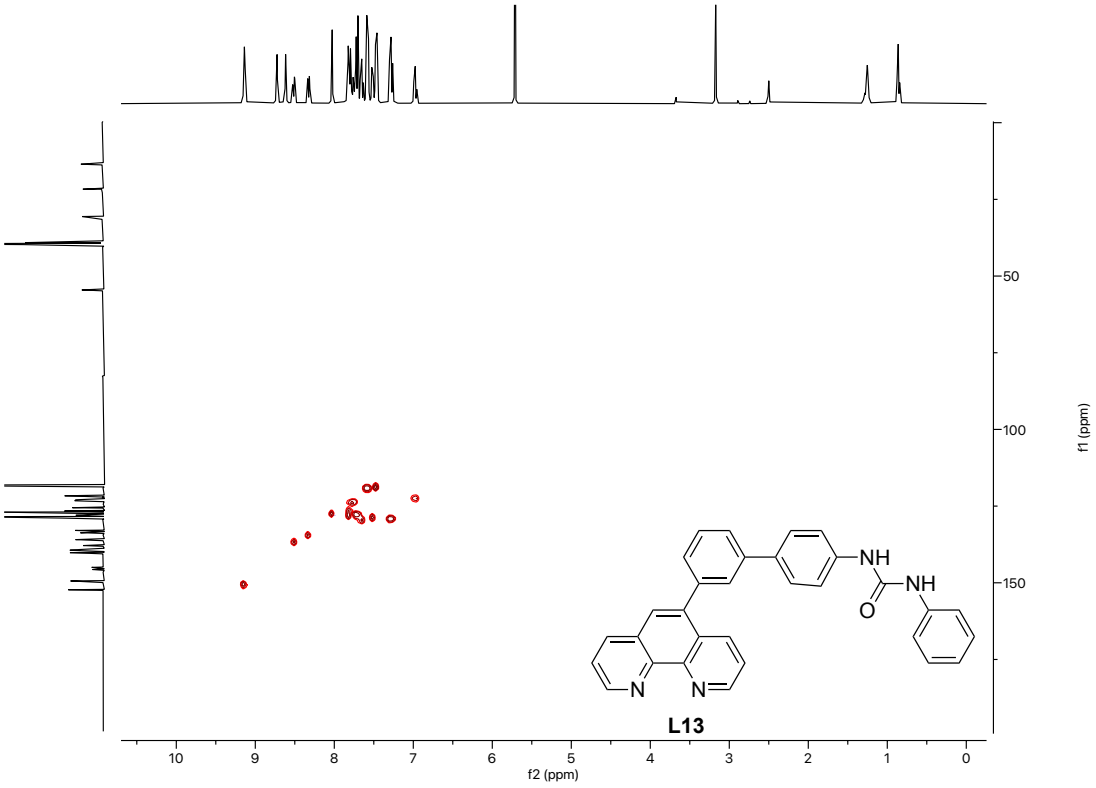

*$^{1}$H NMR 1-(3'-(1,10-phenanthrolin-5-yl)-[1,1'-biphenyl]-4-yl)-3-phenylurea (L13)*



*$^{13}$C NMR 1-(3'-(1,10-phenanthrolin-5-yl)-[1,1'-biphenyl]-4-yl)-3-phenylurea (L13)*

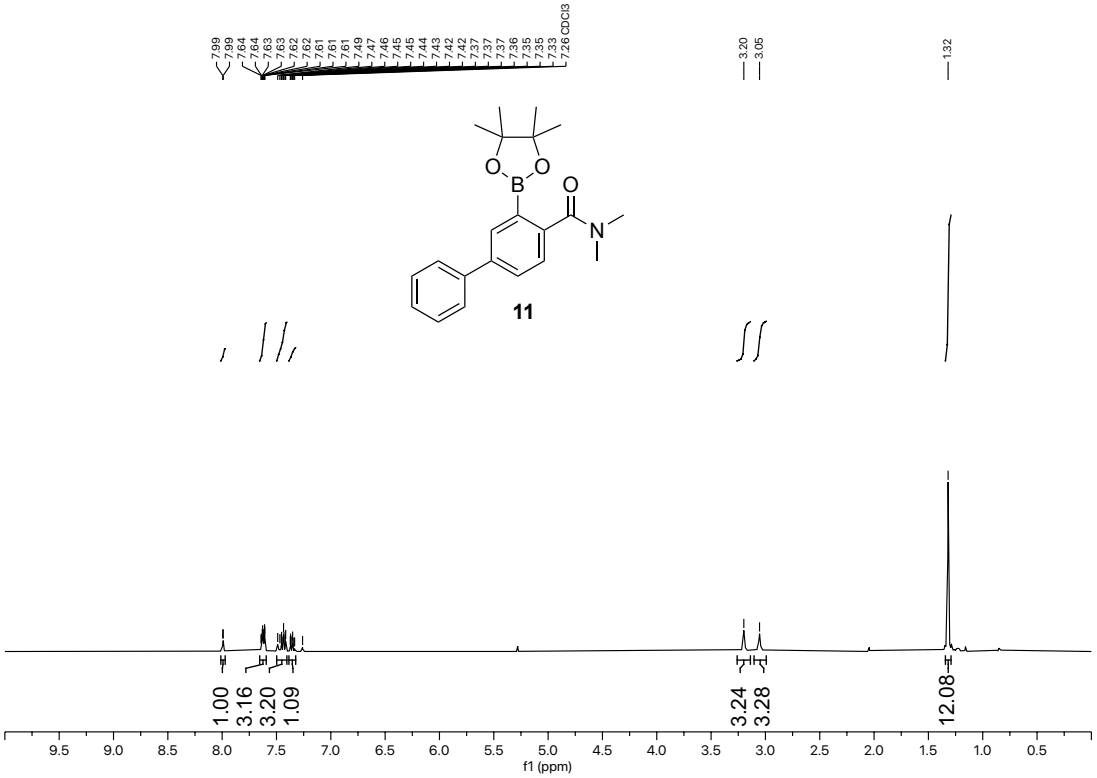



*HSQC NMR 1-(3'-(1,10-phenanthrolin-5-yl)-[1,1'-biphenyl]-4-yl)-3-phenylurea (L13)*

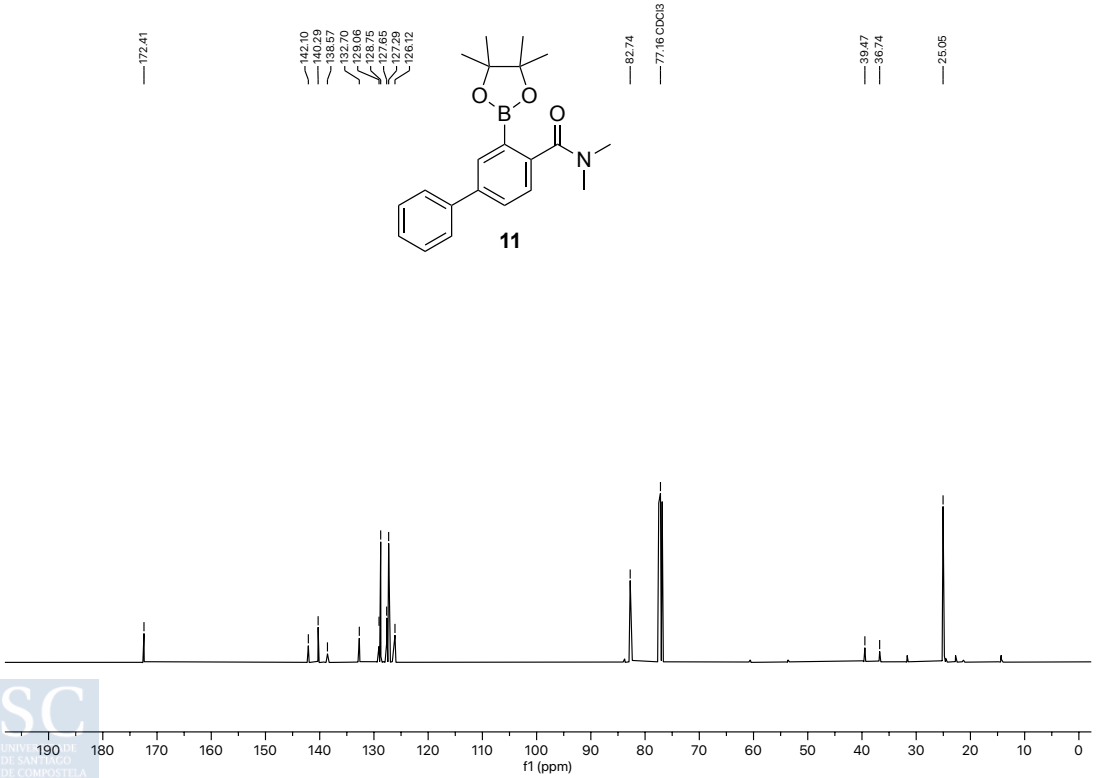


### *11.1.1.2 Spectra of products*

*$^{1}$H NMR N,N-dimethyl-3-(4,4,5,5-tetramethyl-1,3,2-dioxaborolan-2-yl)-[1,1'-biphenyl]-4-carboxamide (11)*

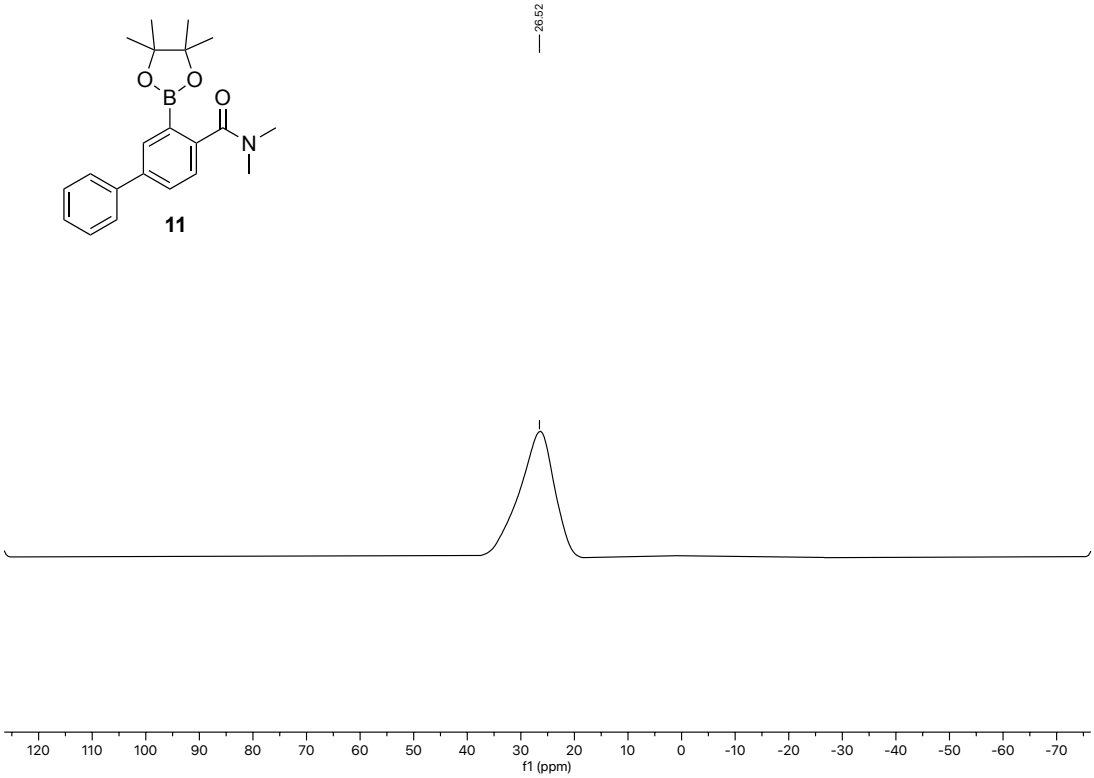



*$^{13}$C NMR N,N-dimethyl-3-(4,4,5,5-tetramethyl-1,3,2-dioxaborolan-2-yl)-[1,1'-biphenyl]-4-carboxamide (11)*

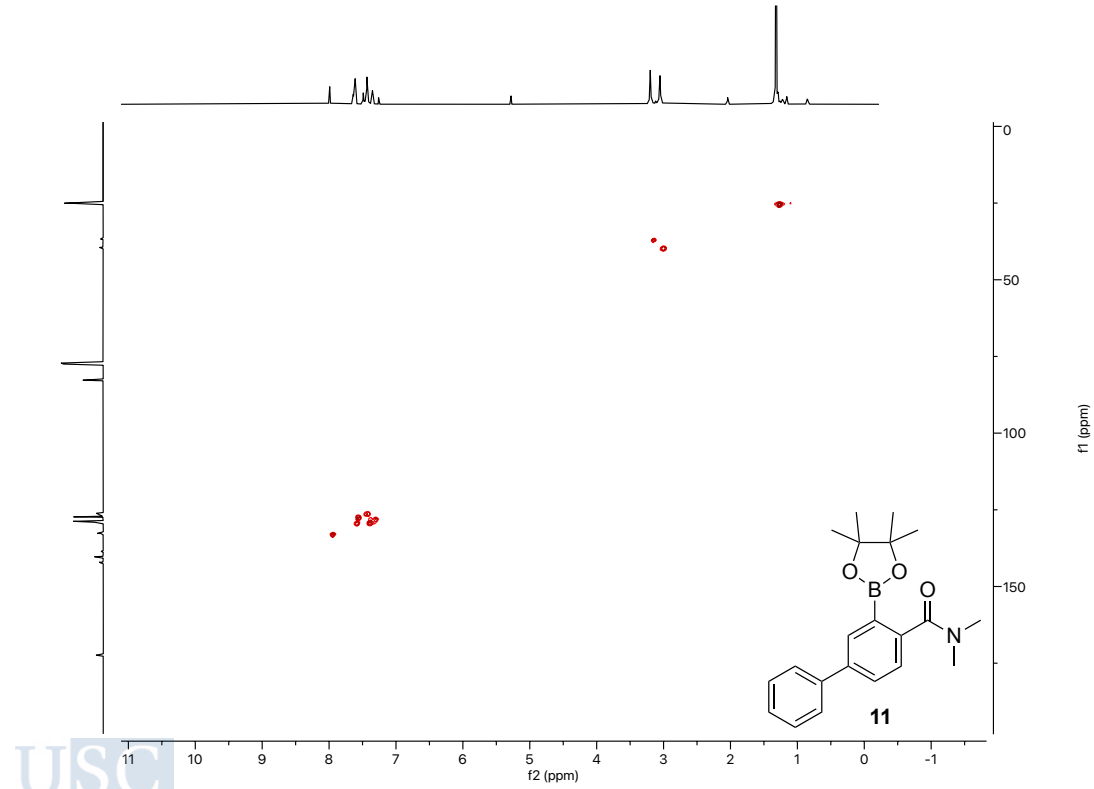



USC UNIVERSIDADE DE SANTIAGO DE COMPOSTELA

*[11]B NMR N,N-dimethyl-3-(4,4,5,5-tetramethyl-1,3,2-dioxaborolan-2-yl)-[1,1'-biphenyl]-4-carboxamide (11)*

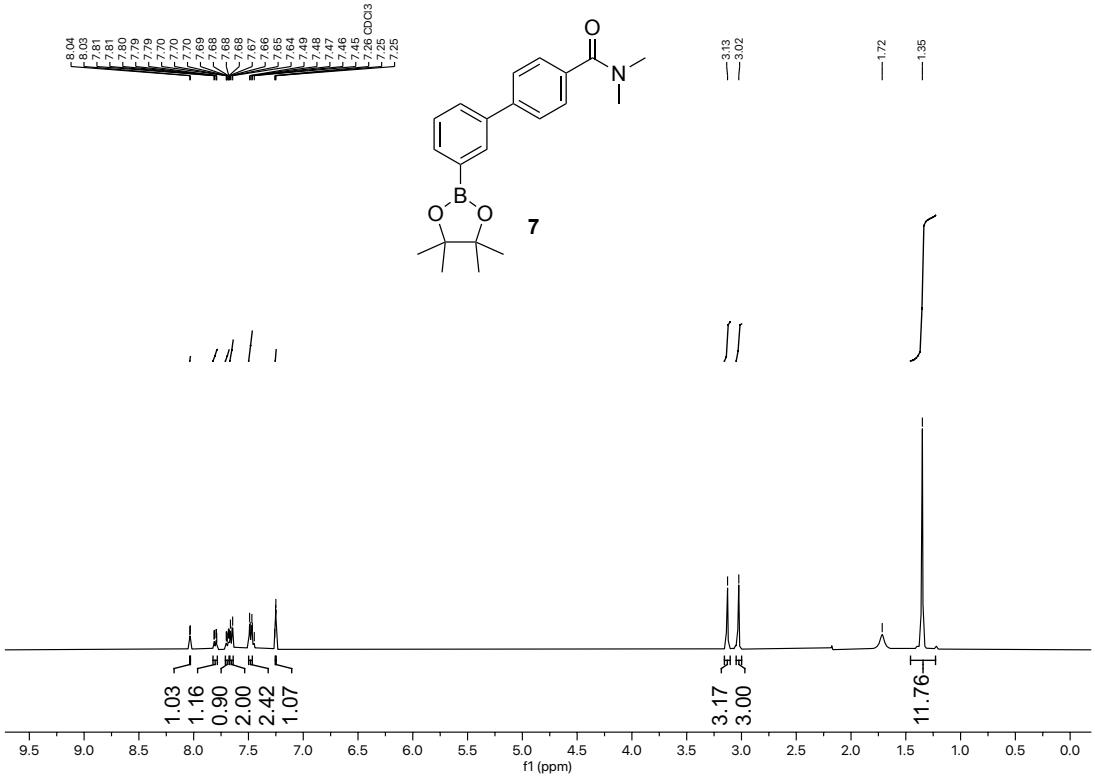



*HSQC NMR N,N-dimethyl-3-(4,4,5,5-tetramethyl-1,3,2-dioxaborolan-2-yl)-[1,1'-biphenyl]-4-carboxamide (11)*

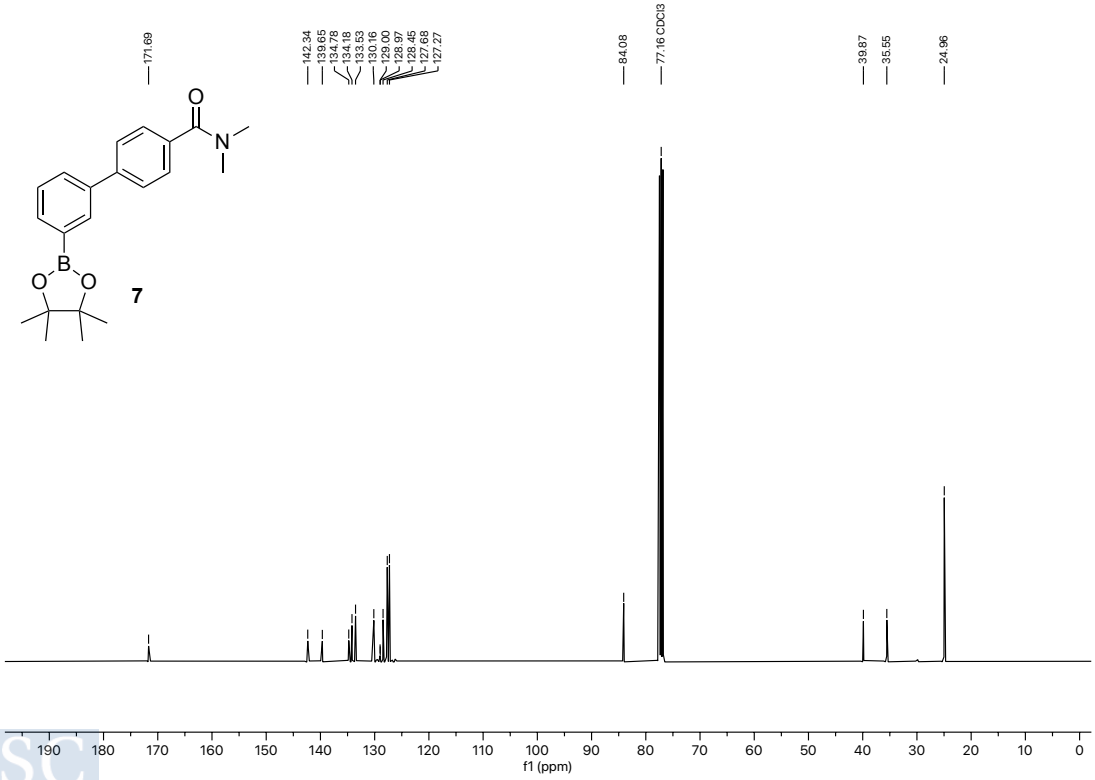



USC UNIVERSIDADE DE SANTIAGO DE COMPOSTELA

*[1]H NMR N,N-dimethyl-3'-(4,4,5,5-tetramethyl-1,3,2-dioxaborolan-2-yl)-[1,1'-biphenyl]-4-carboxamide (7)*

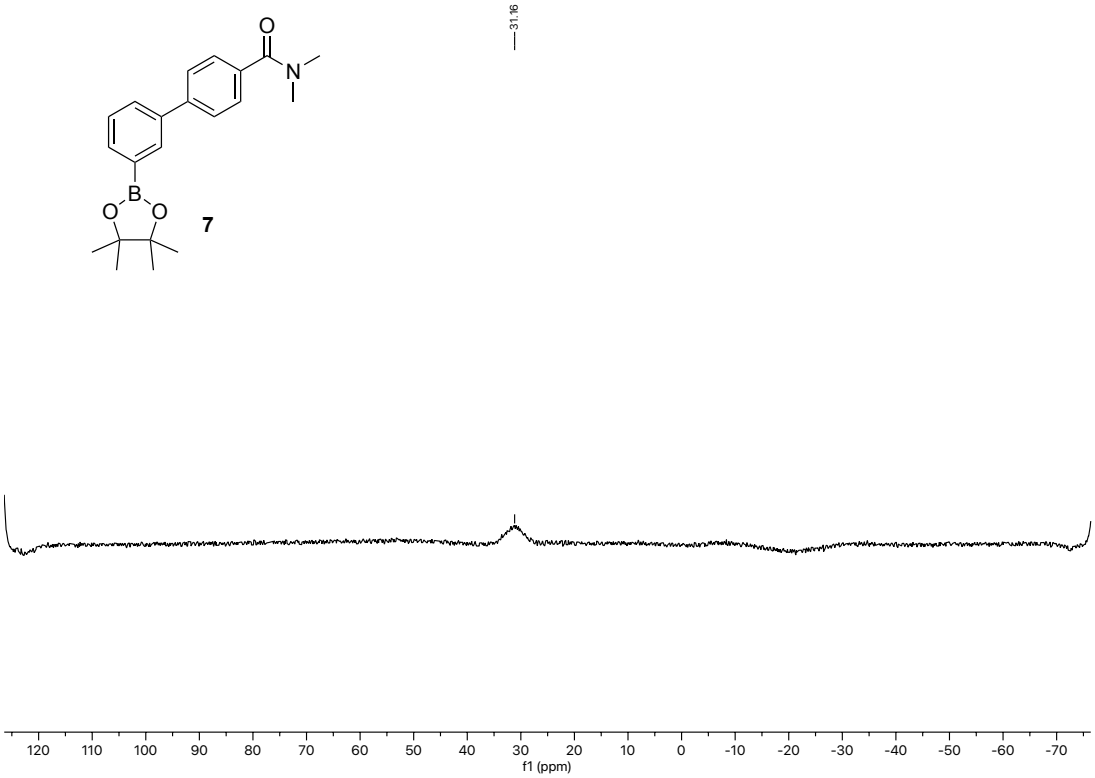



*[13]C NMR N,N-dimethyl-3'-(4,4,5,5-tetramethyl-1,3,2-dioxaborolan-2-yl)-[1,1'-biphenyl]-4-carboxamide (7)*

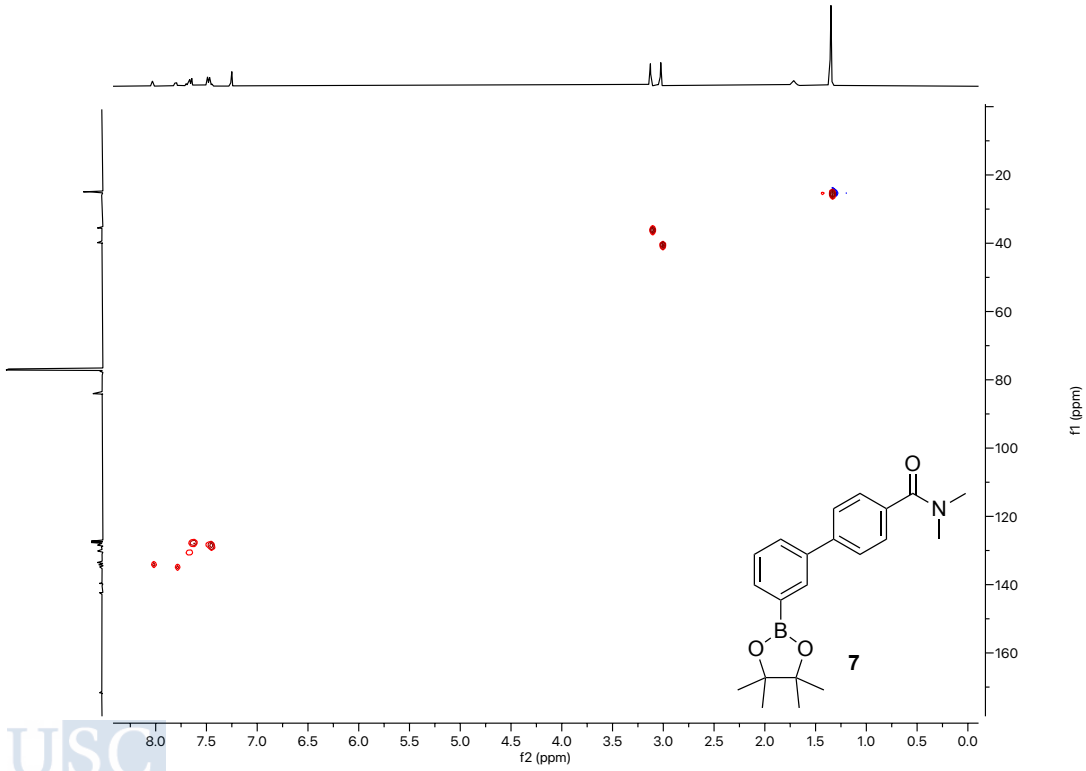



USC UNIVERSIDADE DE SANTIAGO DE COMPOSTELA

*$^{11}$B NMR N,N-dimethyl-3'-(4,4,5,5-tetramethyl-1,3,2-dioxaborolan-2-yl)-[1,1'-biphenyl]-4-carboxamide (7)*

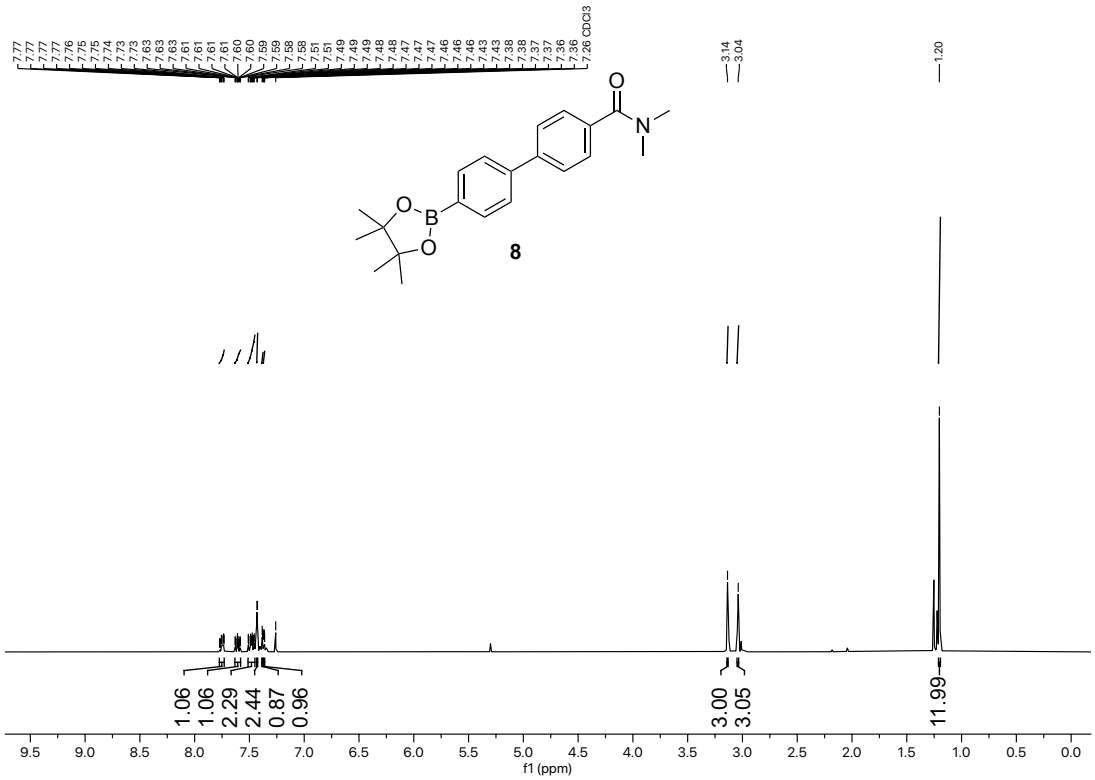



*HSQC NMR N,N-dimethyl-3'-(4,4,5,5-tetramethyl-1,3,2-dioxaborolan-2-yl)-[1,1'-biphenyl]-4-carboxamide (7)*

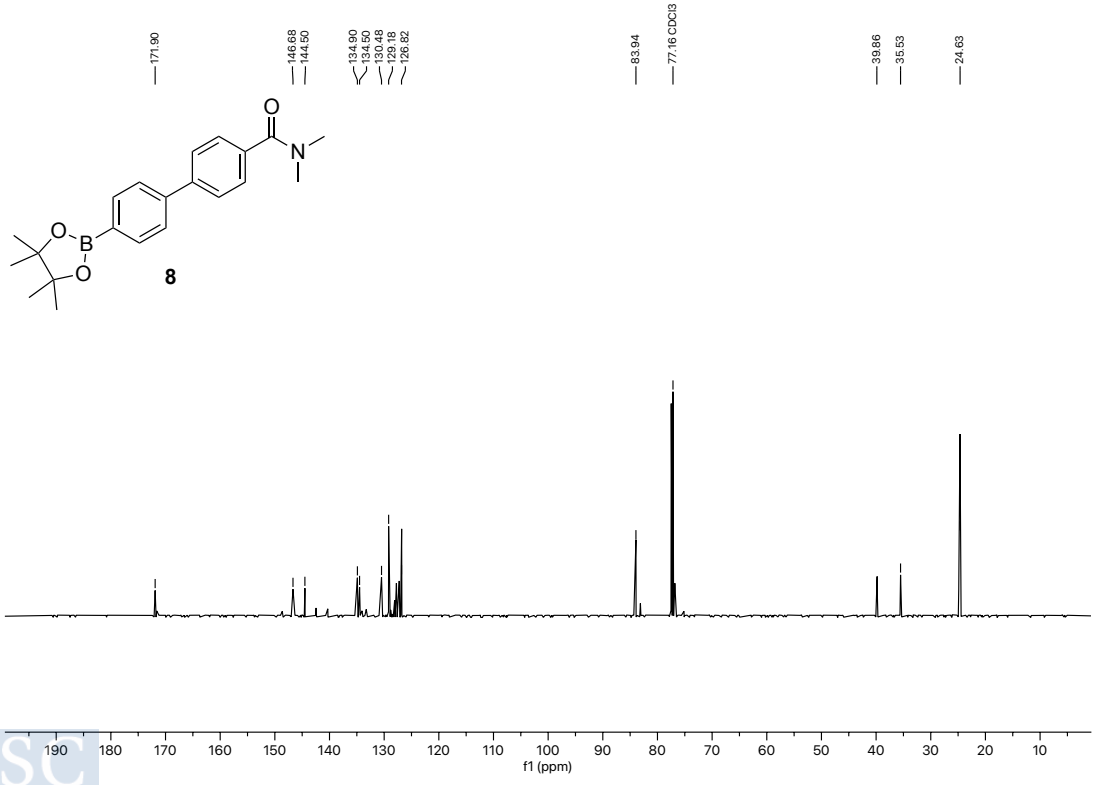



USC UNIVERSIDADE DE SANTIAGO DE COMPOSTELA

*[1]H NMR N,N-dimethyl-4'-(4,4,5,5-tetramethyl-1,3,2-dioxaborolan-2-yl)-[1,1'-biphenyl]-4-carboxamide (8)*

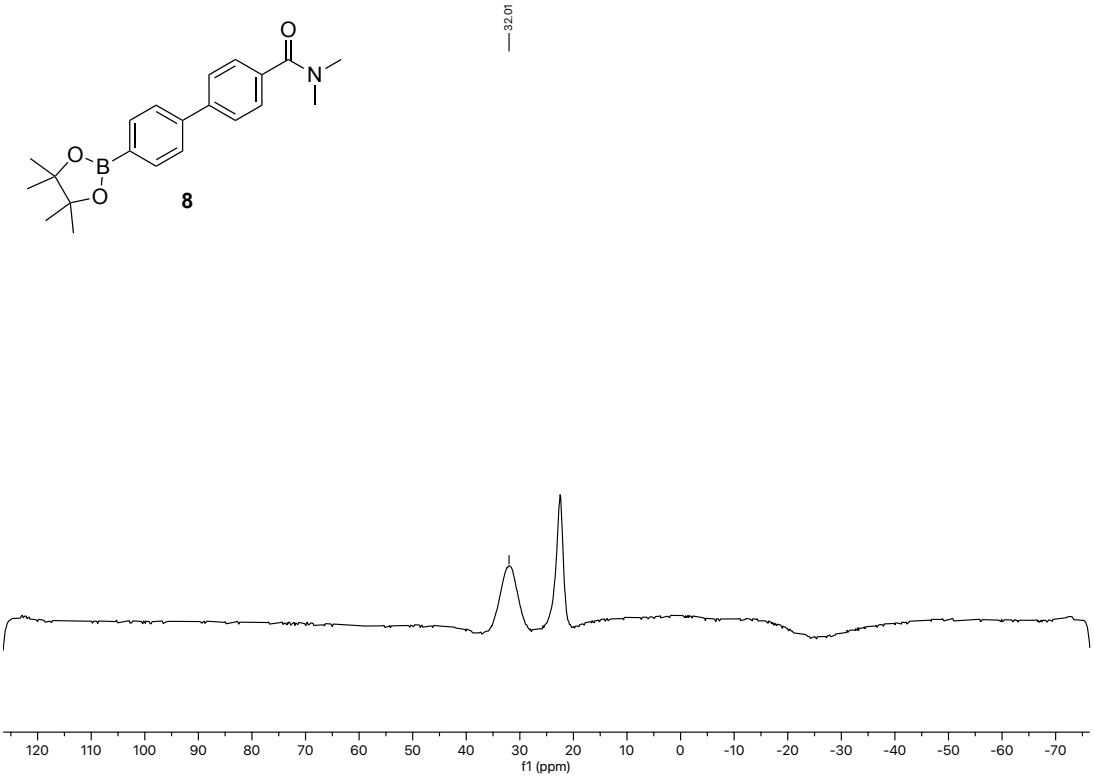



*[13]C NMR N,N-dimethyl-4'-(4,4,5,5-tetramethyl-1,3,2-dioxaborolan-2-yl)-[1,1'-biphenyl]-4-carboxamide (8)*

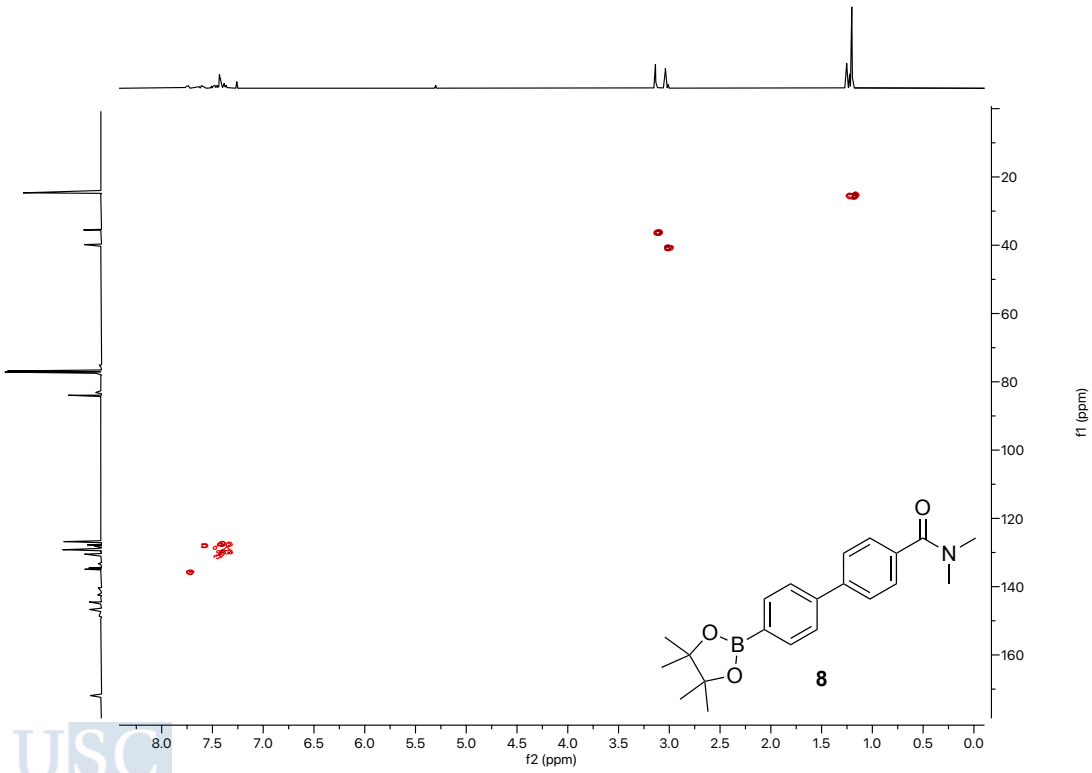



USC UNIVERSIDADE DE SANTIAGO DE COMPOSTELA

*$^{11}$B NMR N,N-dimethyl-4'-(4,4,5,5-tetramethyl-1,3,2-dioxaborolan-2-yl)-[1,1'-biphenyl]-4-carboxamide (8)*



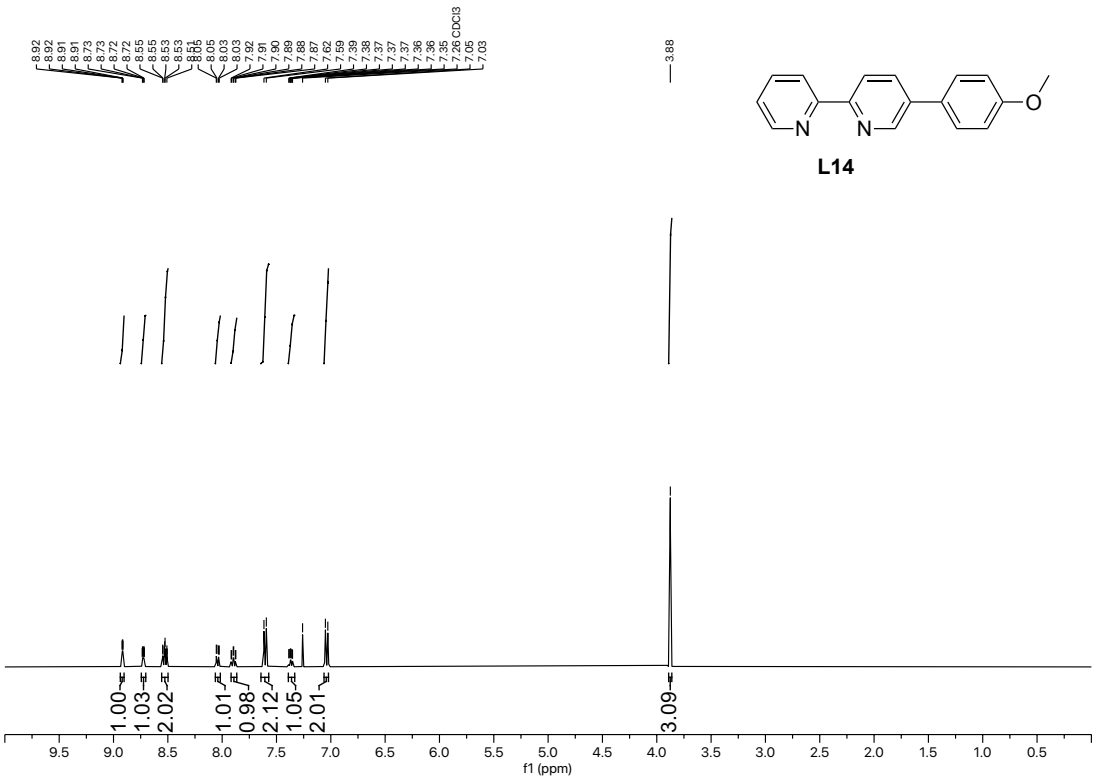

*HSQC NMR N,N-dimethyl-4'-(4,4,5,5-tetramethyl-1,3,2-dioxaborolan-2-yl)-[1,1'-biphenyl]-4-carboxamide (8)*



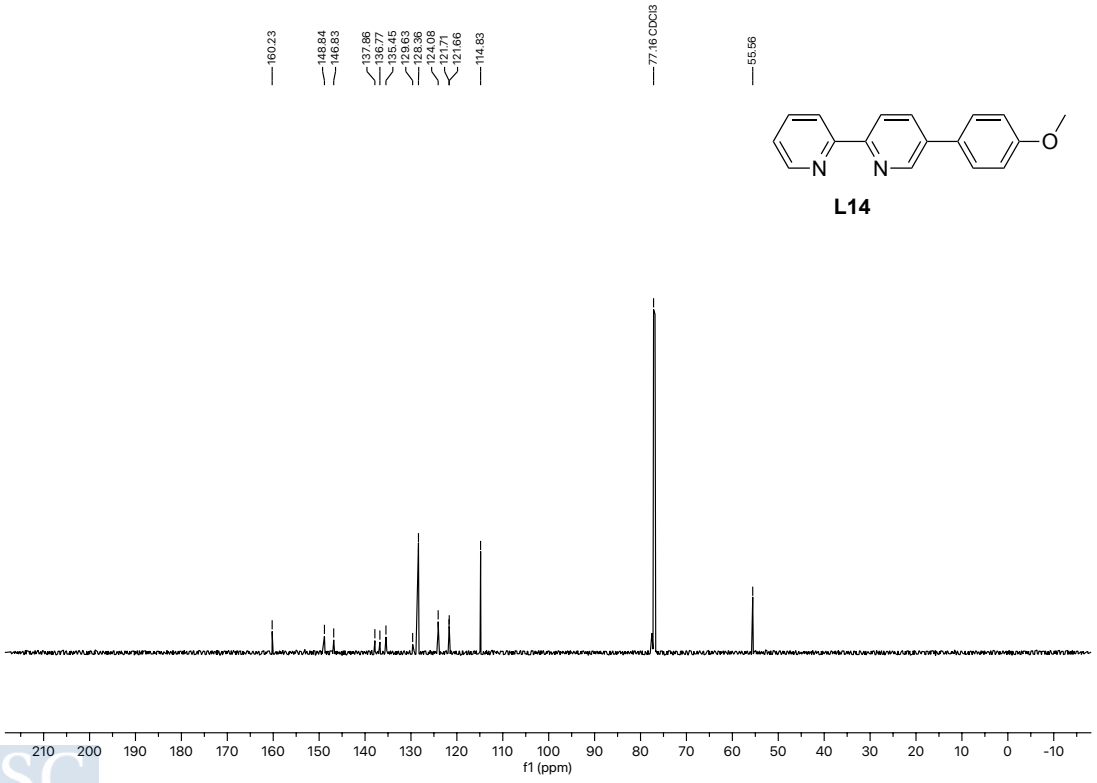

USC UNIVERSIDADE DE SANTIAGO DE COMPOSTELA

## 11.1.2 Selected spectra for molecules in section 7.2

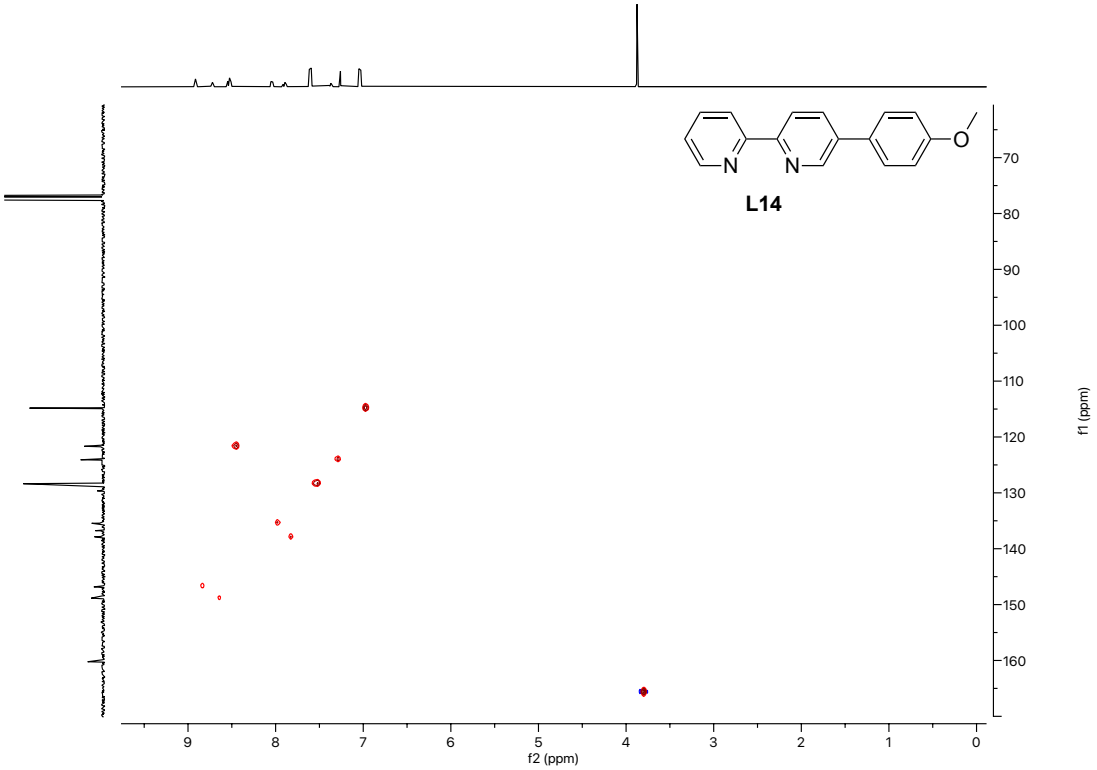
*$^{1}$H NMR 5-(4-methoxyphenyl)-2,2'-bipyridine (L14)*



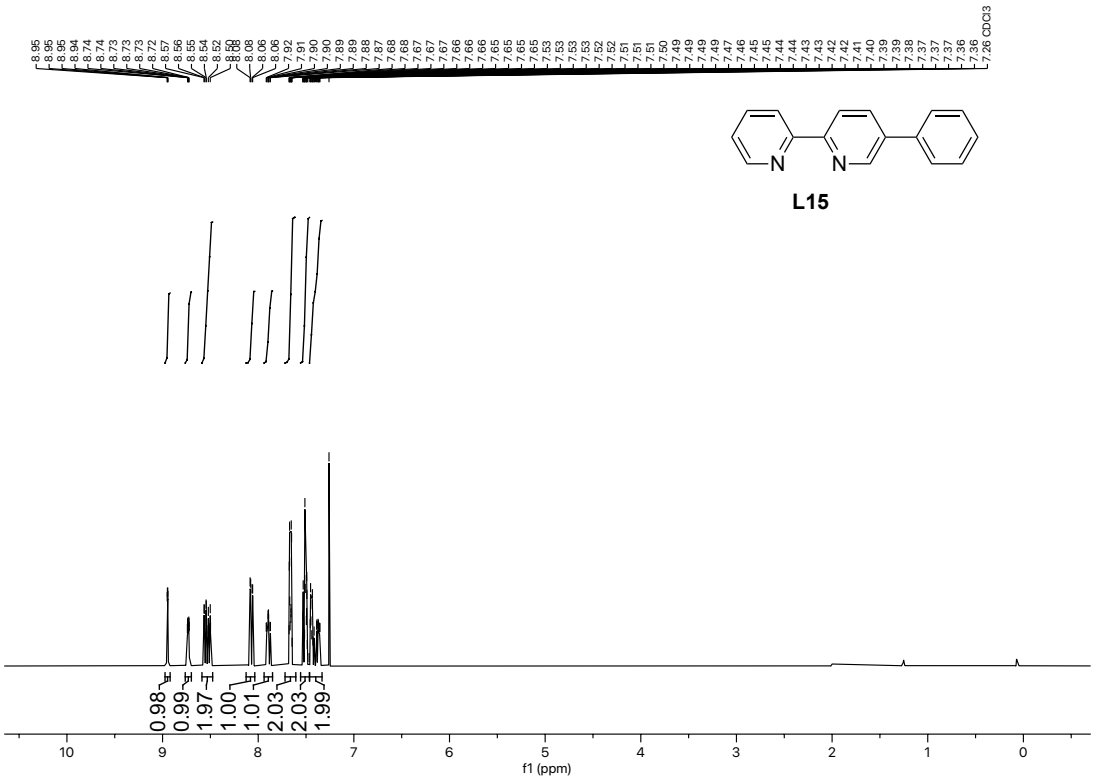

*$^{13}$C NMR 5-(4-methoxyphenyl)-2,2'-bipyridine (L14)*



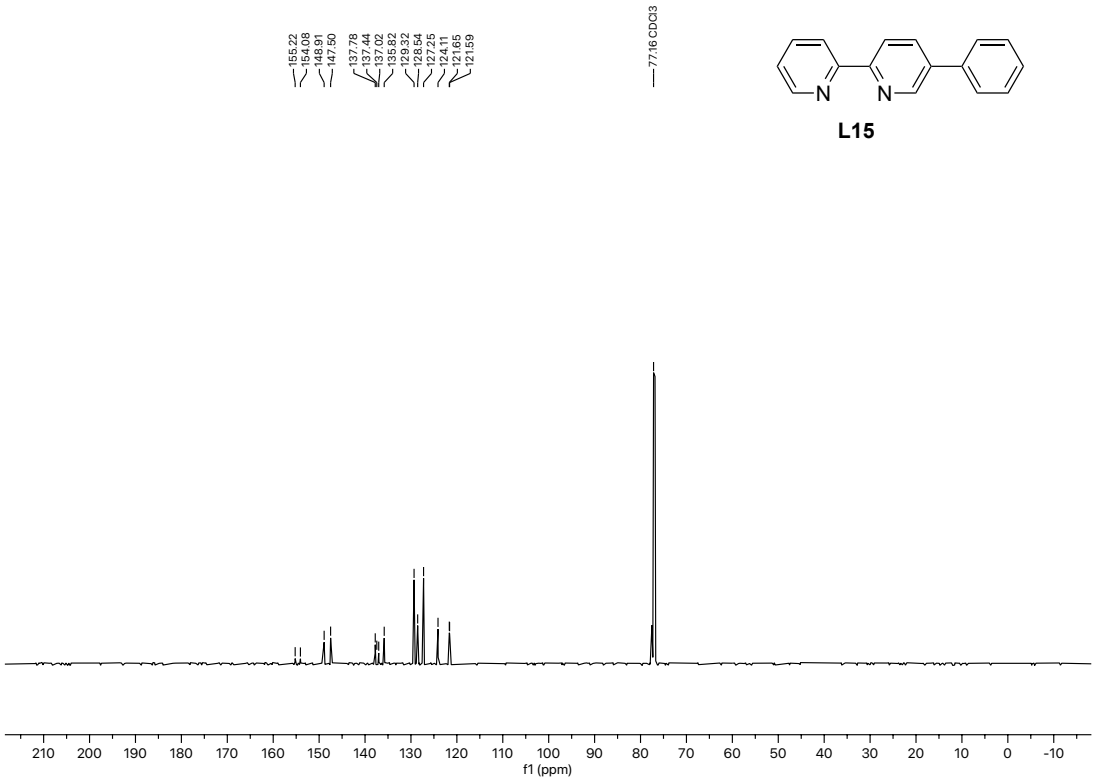
*HSQC NMR 5-(4-methoxyphenyl)-2,2'-bipyridine (L14)*



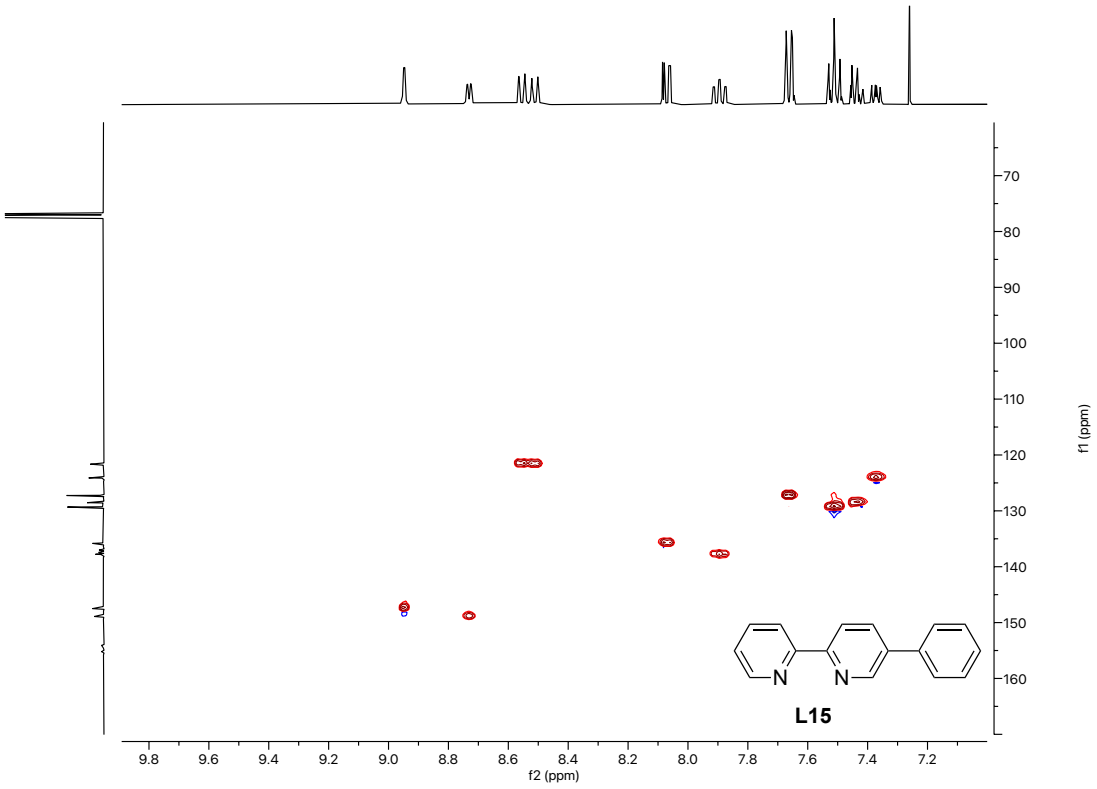

*$^{1}$H NMR 5-phenyl-2,2'-bipyridine (L15)*



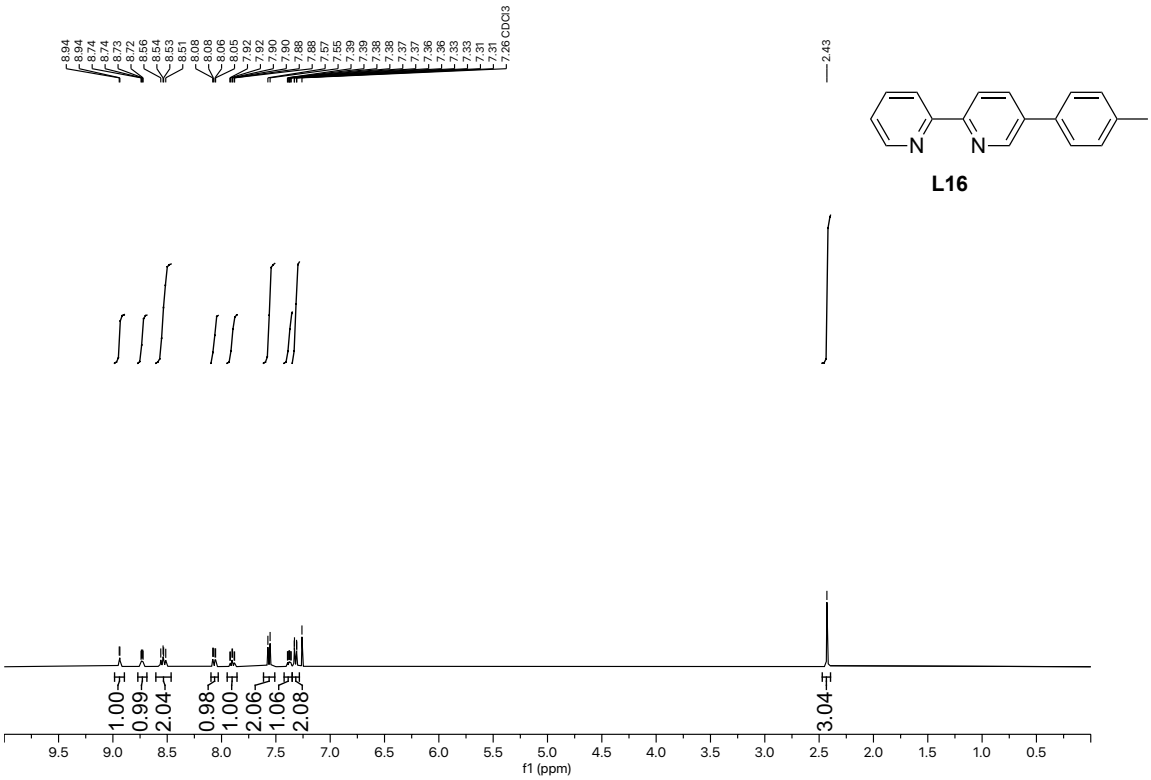
*$^{13}$C NMR 5-phenyl-2,2'-bipyridine (L15)*



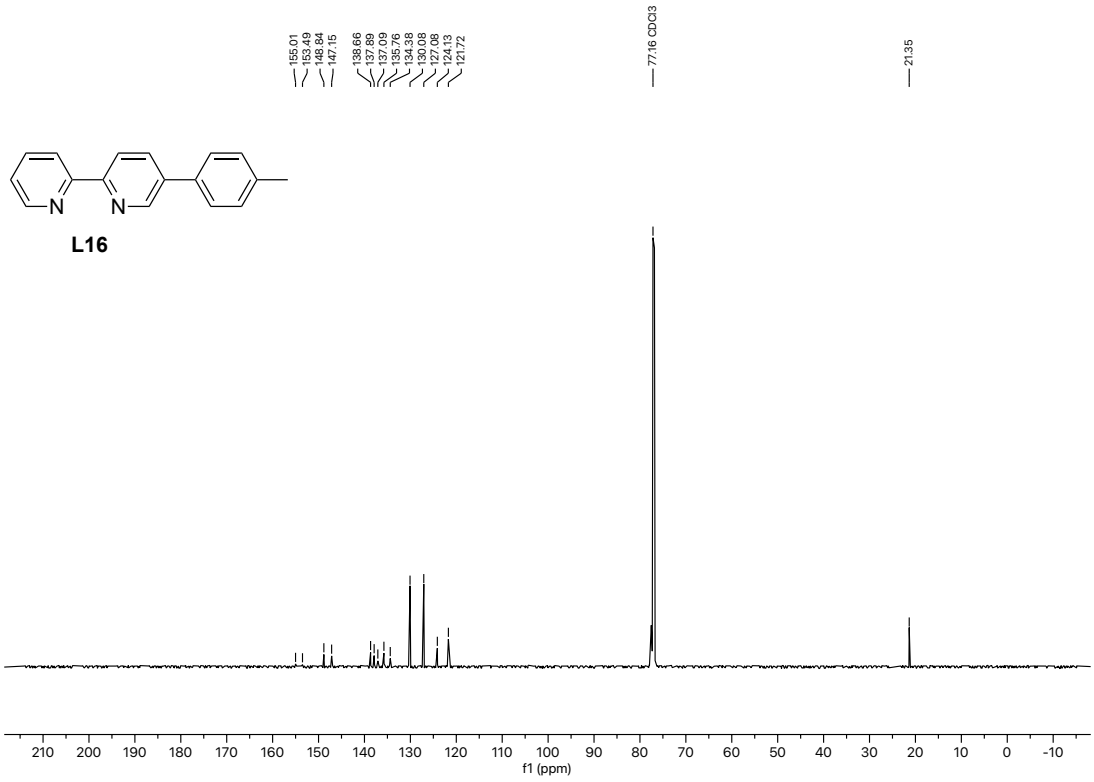

*HSQC NMR 5-phenyl-2,2'-bipyridine (L15)*



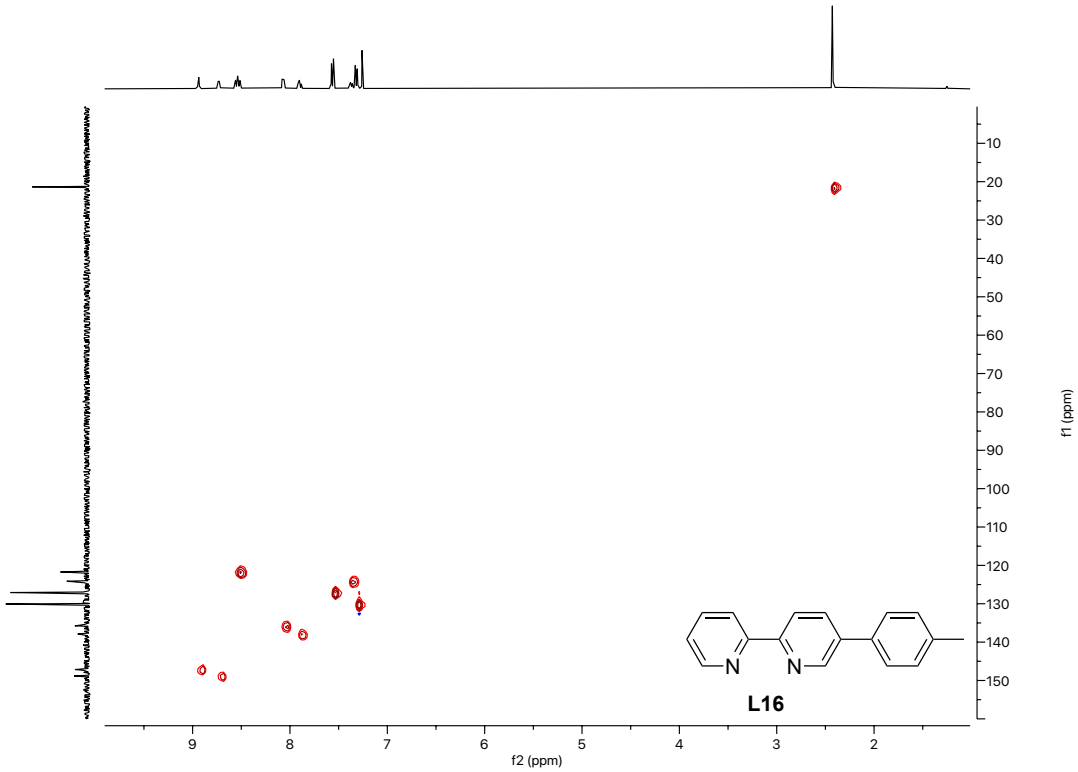
*[1]H NMR 5-(p-tolyl)-2,2'-bipyridine (L16)*



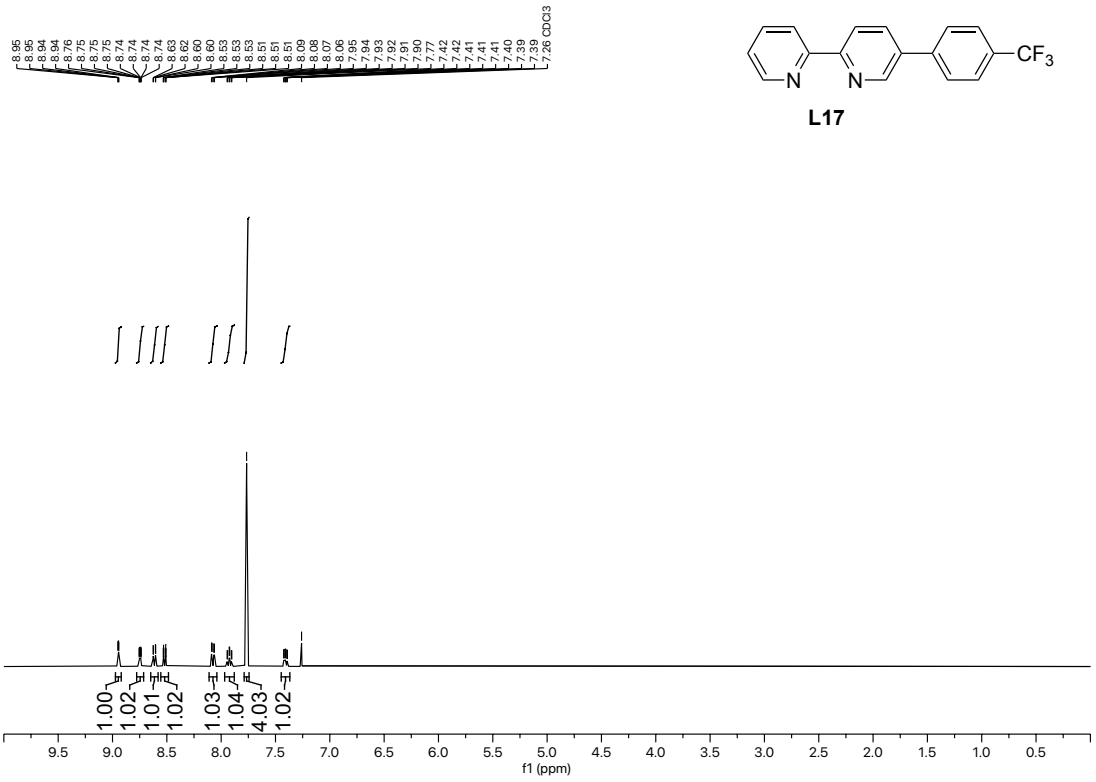

*[13]C NMR 5-(p-tolyl)-2,2'-bipyridine (L16)*



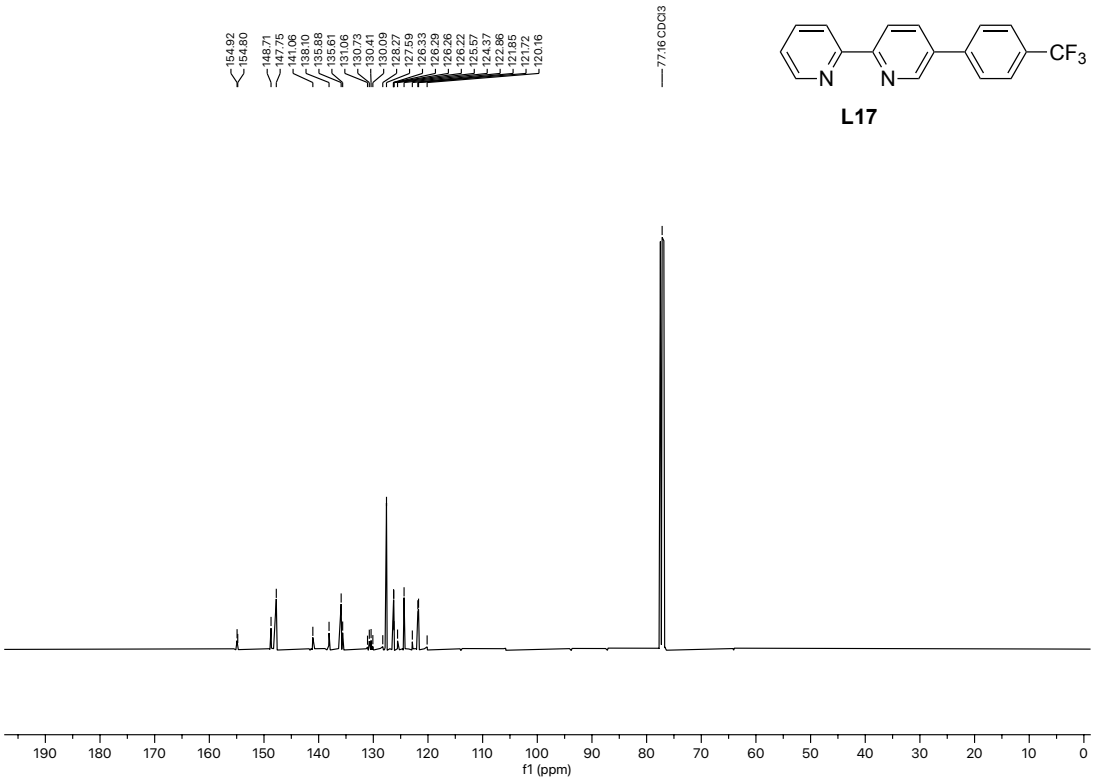
*HSQC NMR 5-(p-tolyl)-2,2'-bipyridine (L16)*




*$^{1}$H NMR 5-(4-(trifluoromethyl)phenyl)-2,2'-bipyridine (L17)*

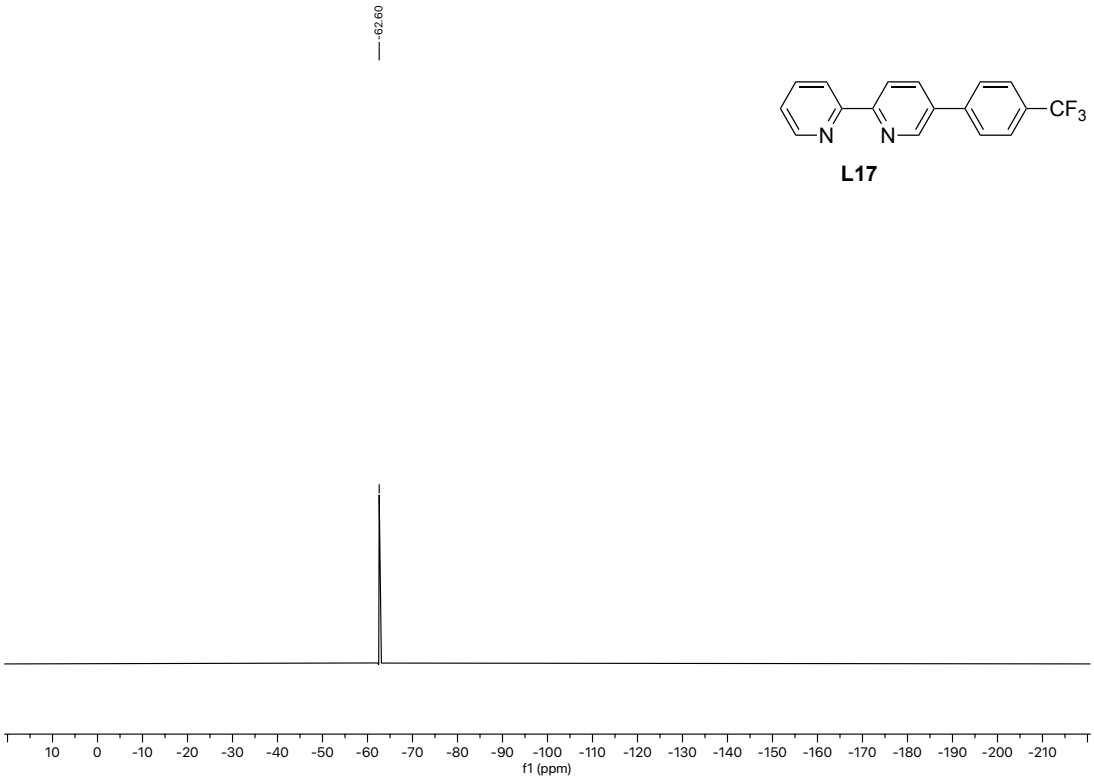


*$^{13}$C NMR 5-(4-(trifluoromethyl)phenyl)-2,2'-bipyridine (L17)*



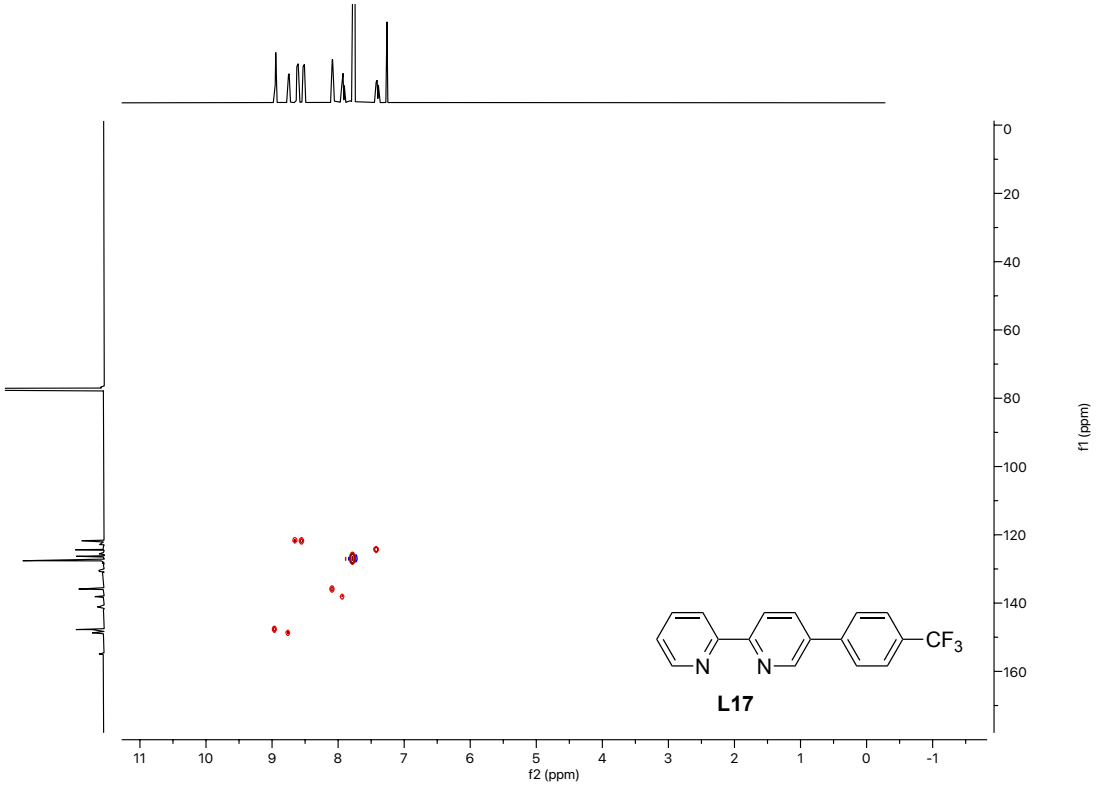

**L17**

*$^{19}$F NMR 5-(4-(trifluoromethyl)phenyl)-2,2'-bipyridine (L17)*

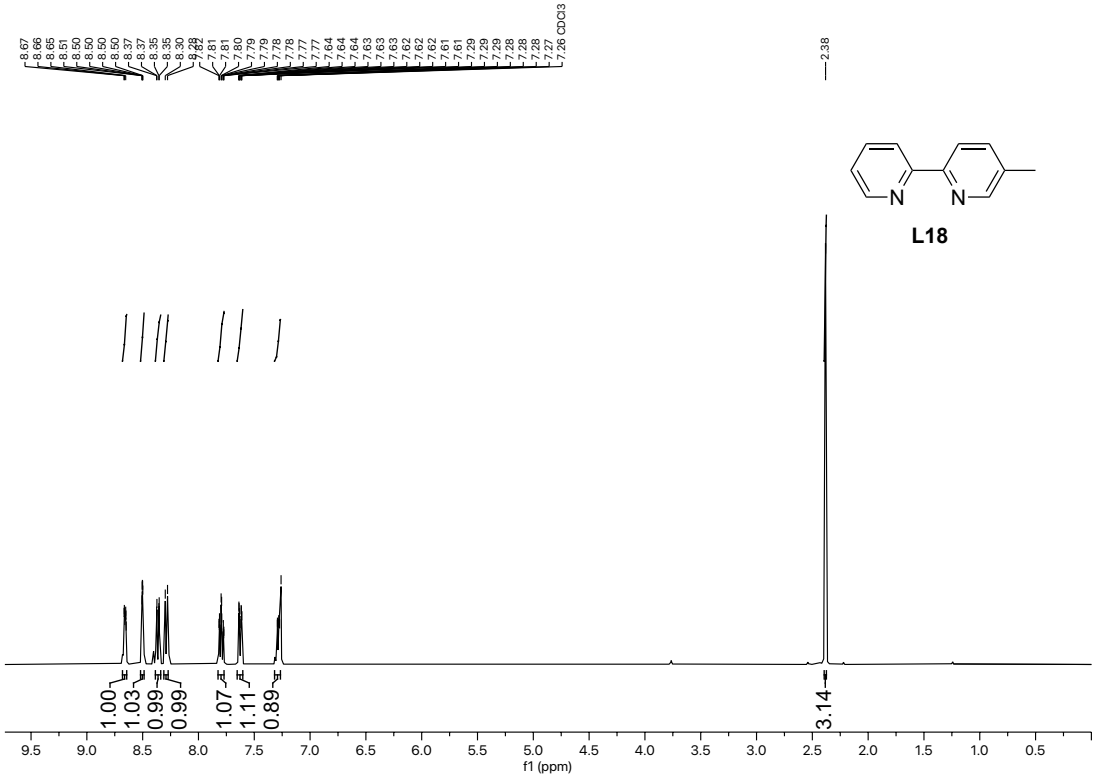



**L17**

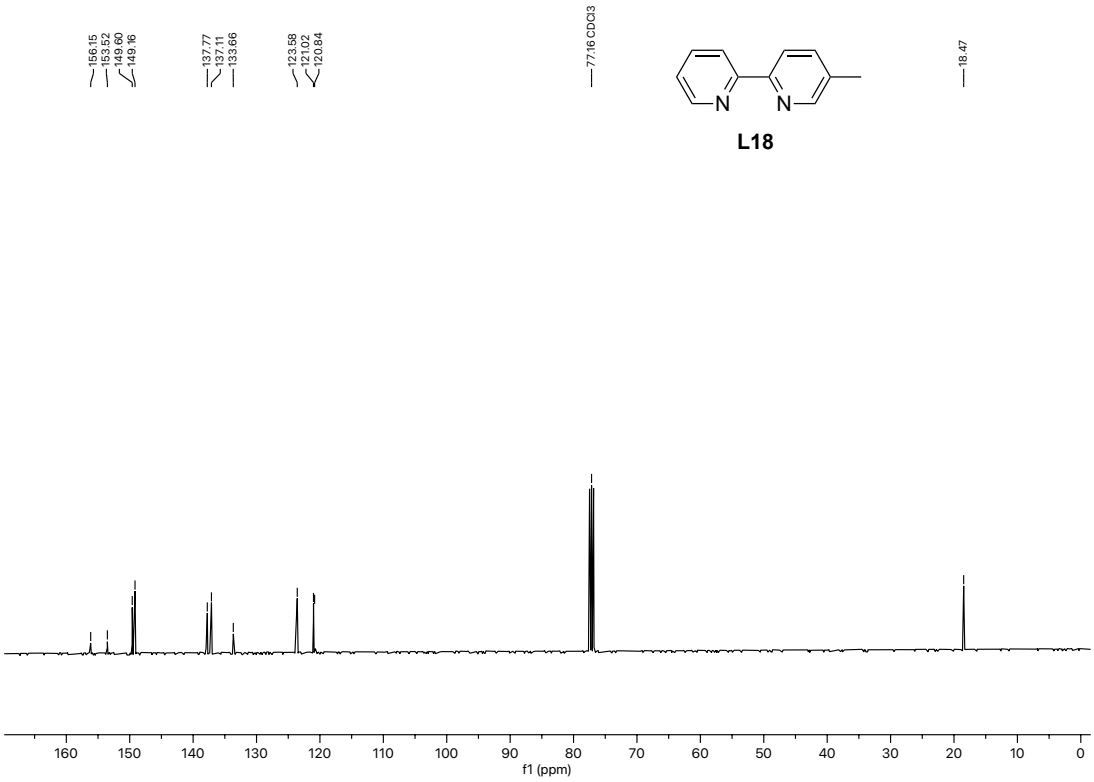
*HSQC NMR 5-(4-(trifluoromethyl)phenyl)-2,2'-bipyridine (L17)*



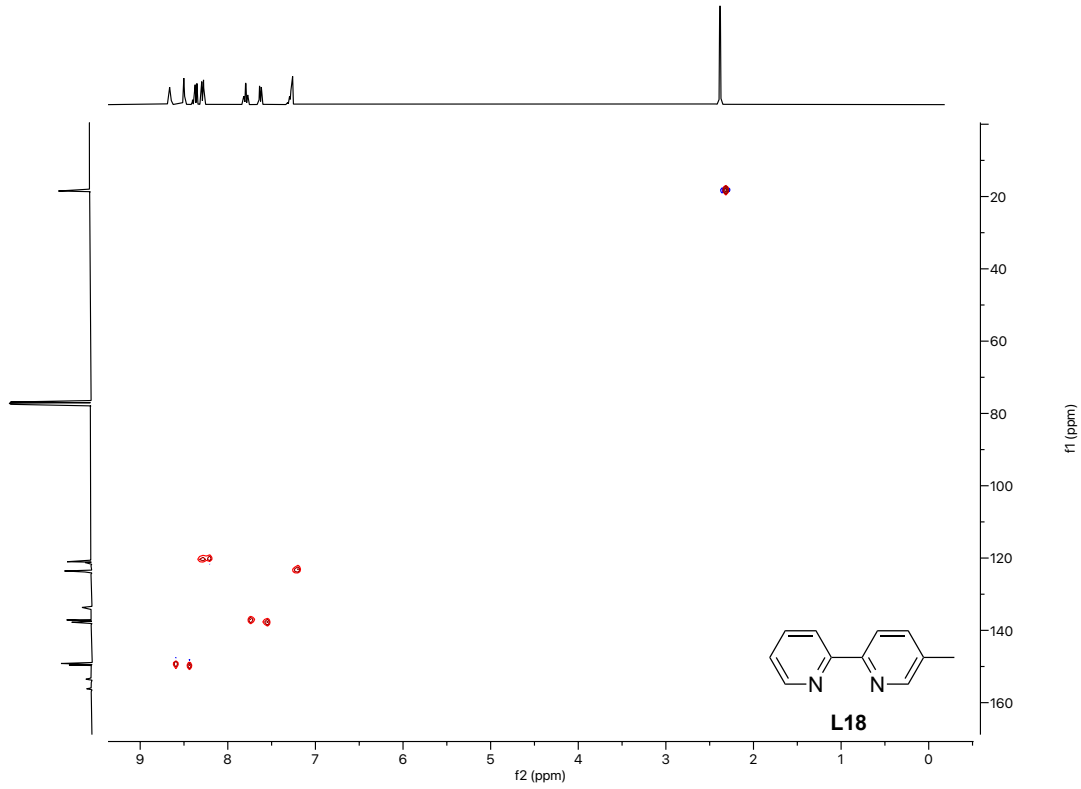

*$^{1}$H NMR 5-methyl-2,2'-bipyridine (L18)*



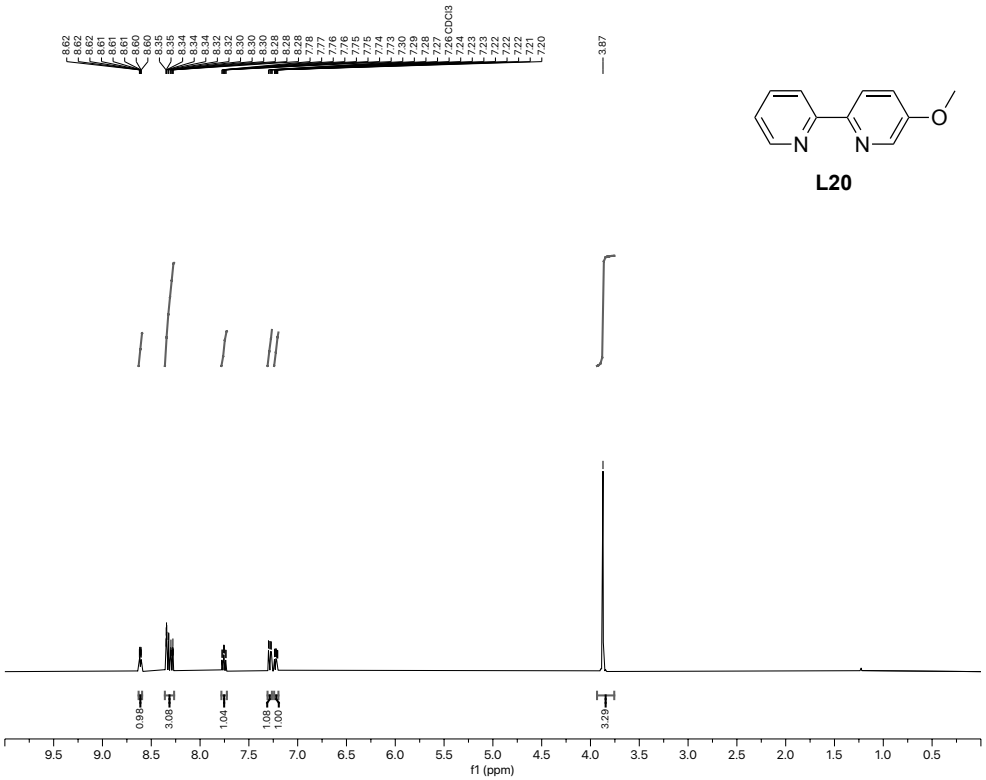
*$^{13}$C NMR 5-methyl-2,2'-bipyridine (L18)*




*HSQC NMR 5-methyl-2,2'-bipyridine (L18)*

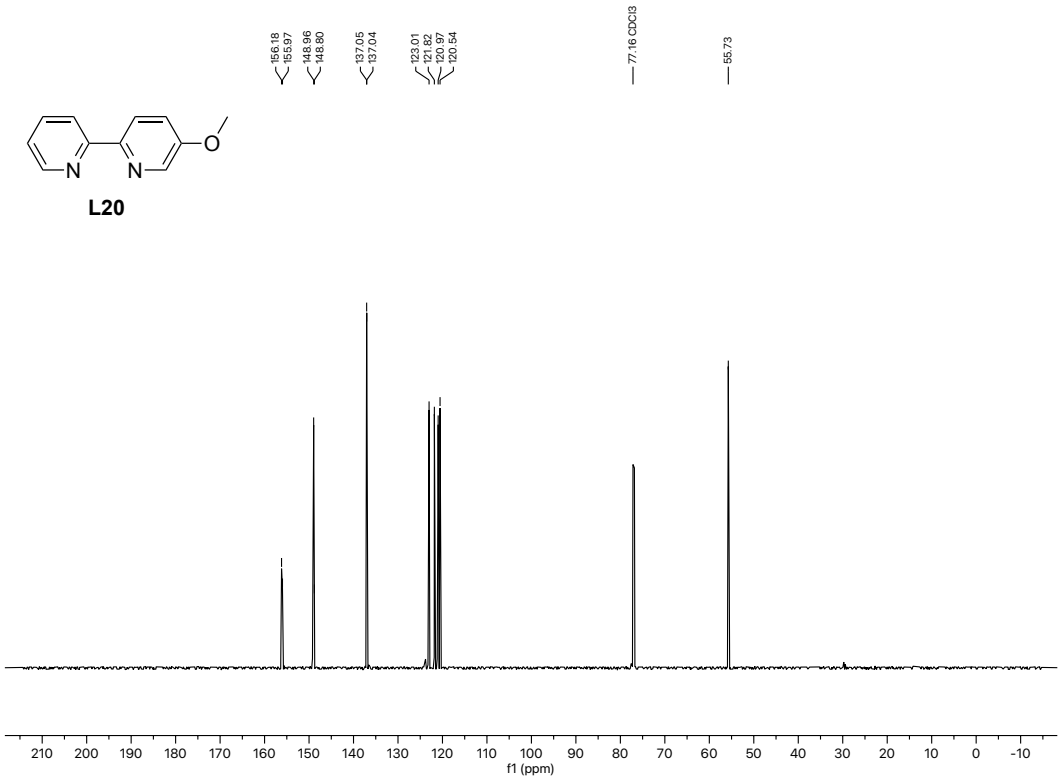


*[1]H NMR 5-methoxy-2,2'-bipyridine (L20)*



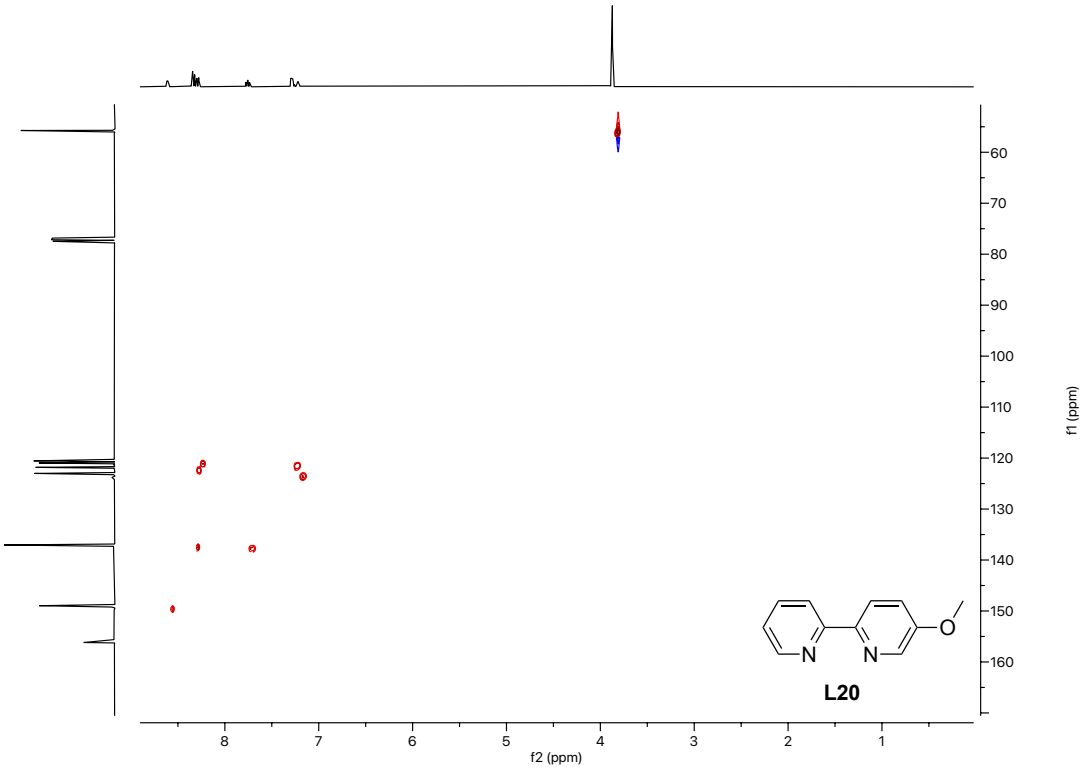

**L20**

*[13]C NMR 5-methoxy-2,2'-bipyridine (L20)*

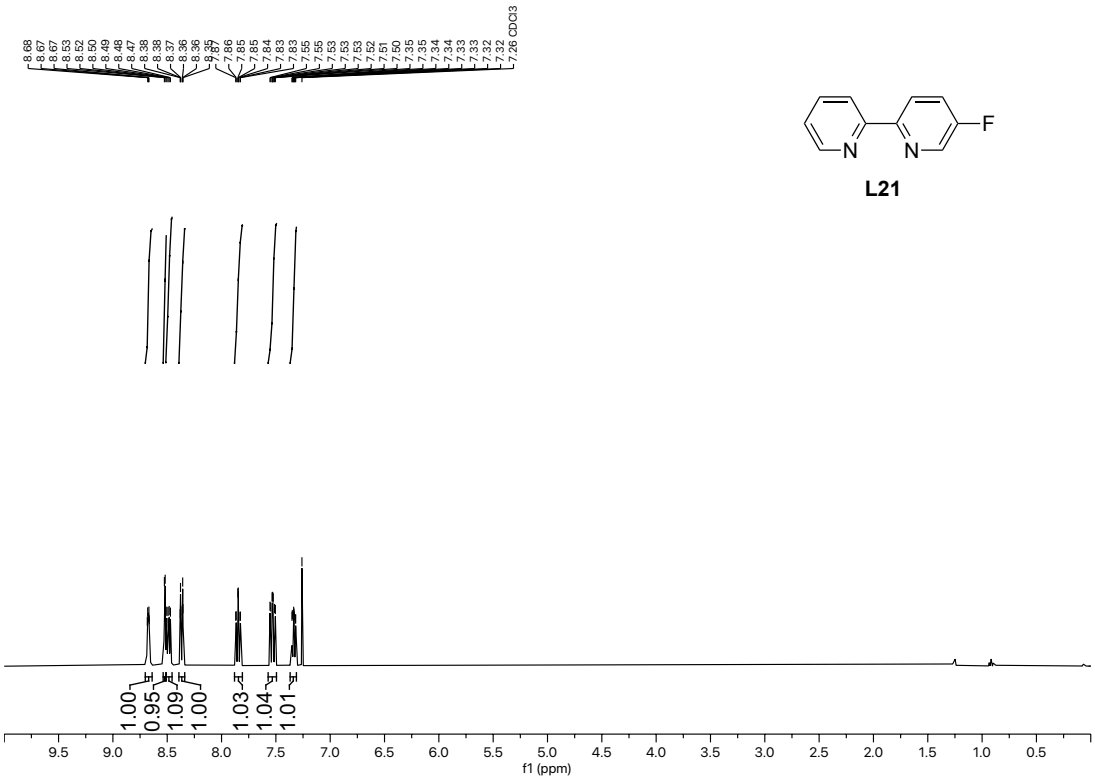



**L20**

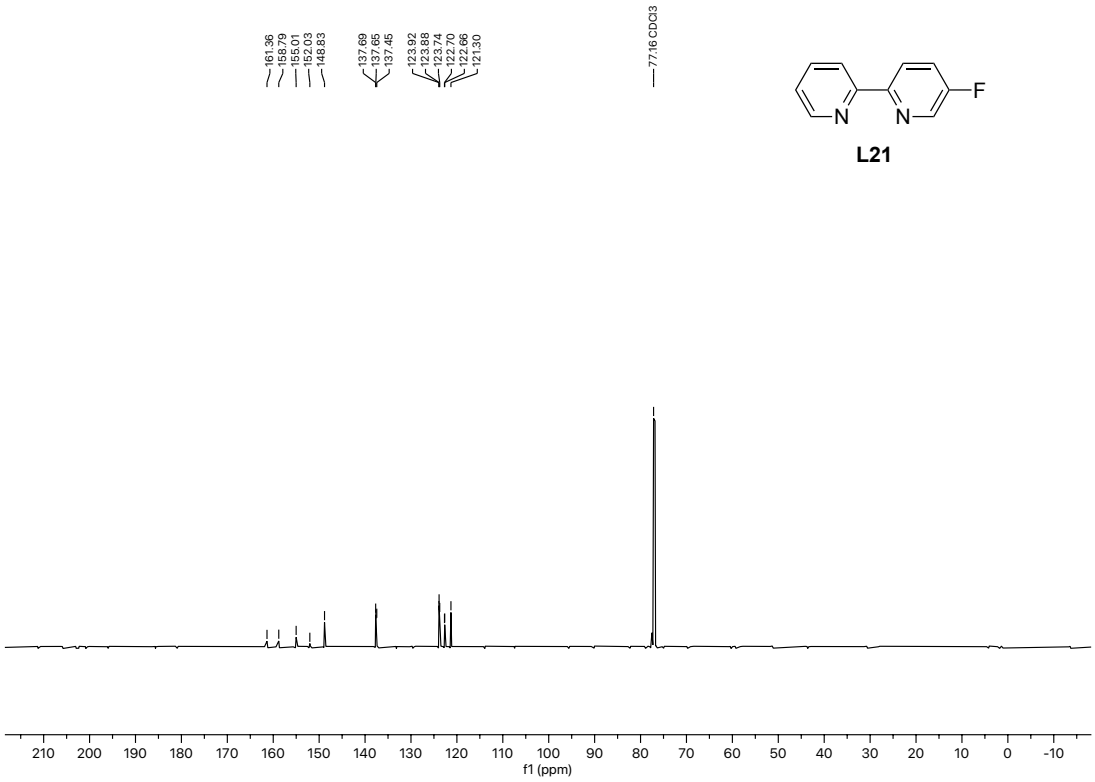
*HSQC NMR 5-methoxy-2,2'-bipyridine (L20)*



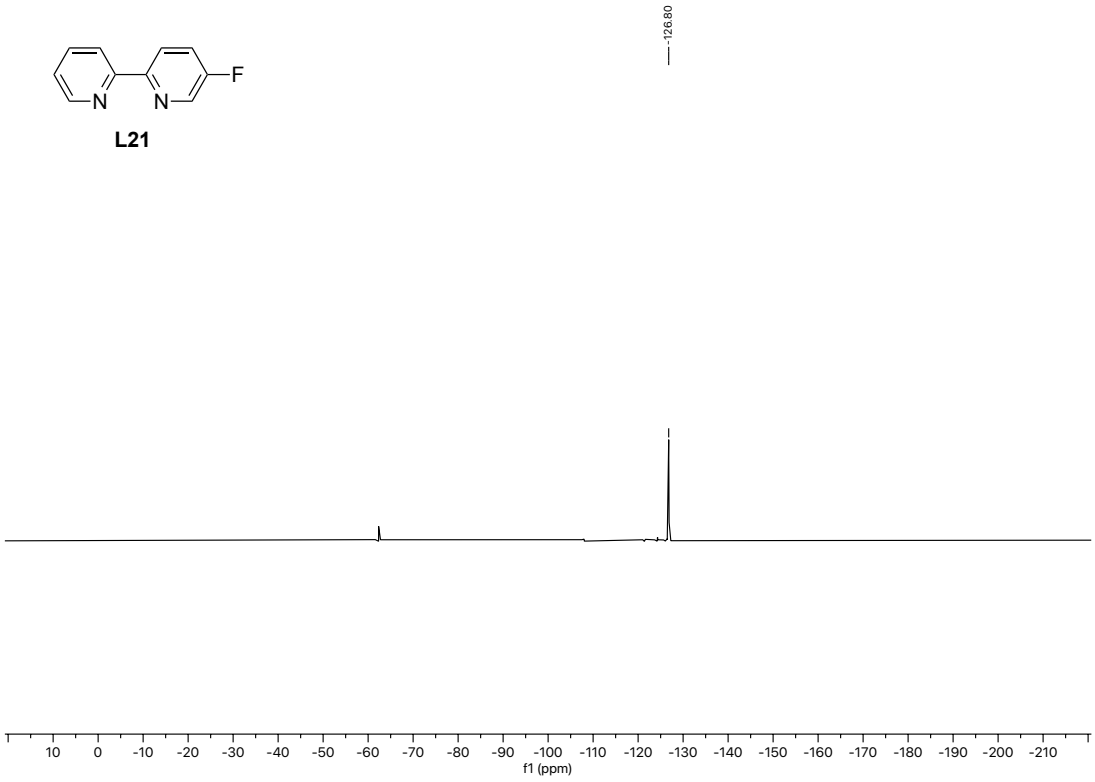

*$^{1}$H NMR 5-fluoro-2,2'-bipyridine (L21)*



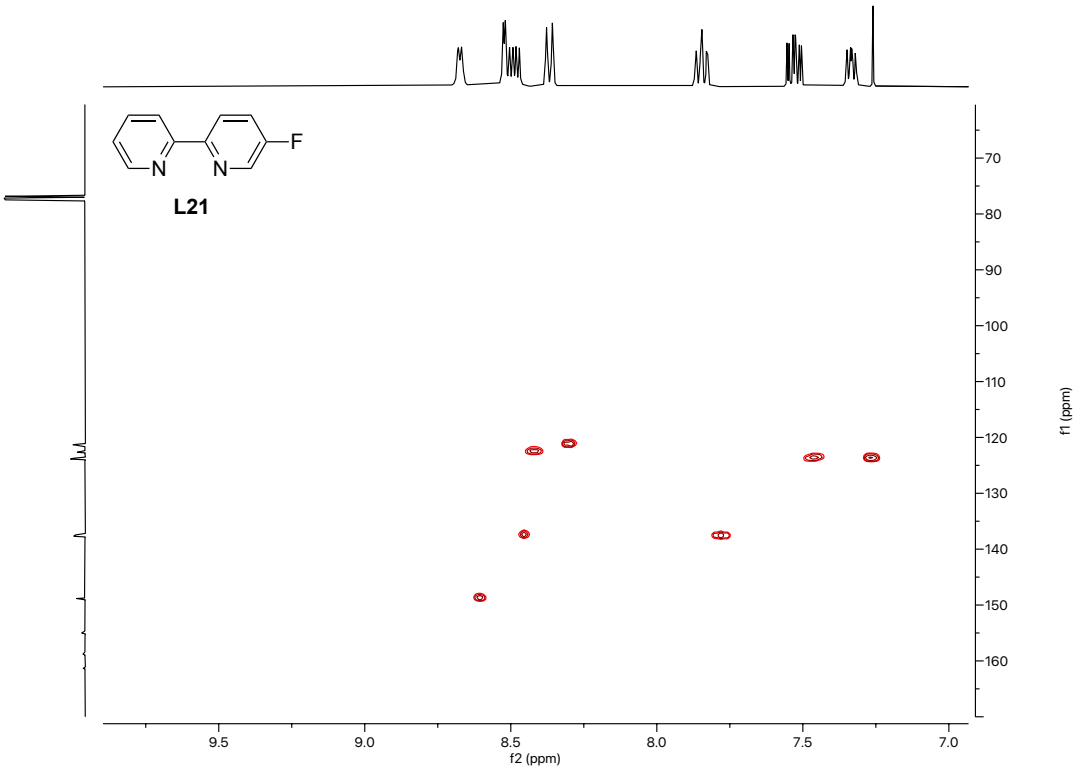
*$^{13}$C NMR 5-fluoro-2,2'-bipyridine (L21)*



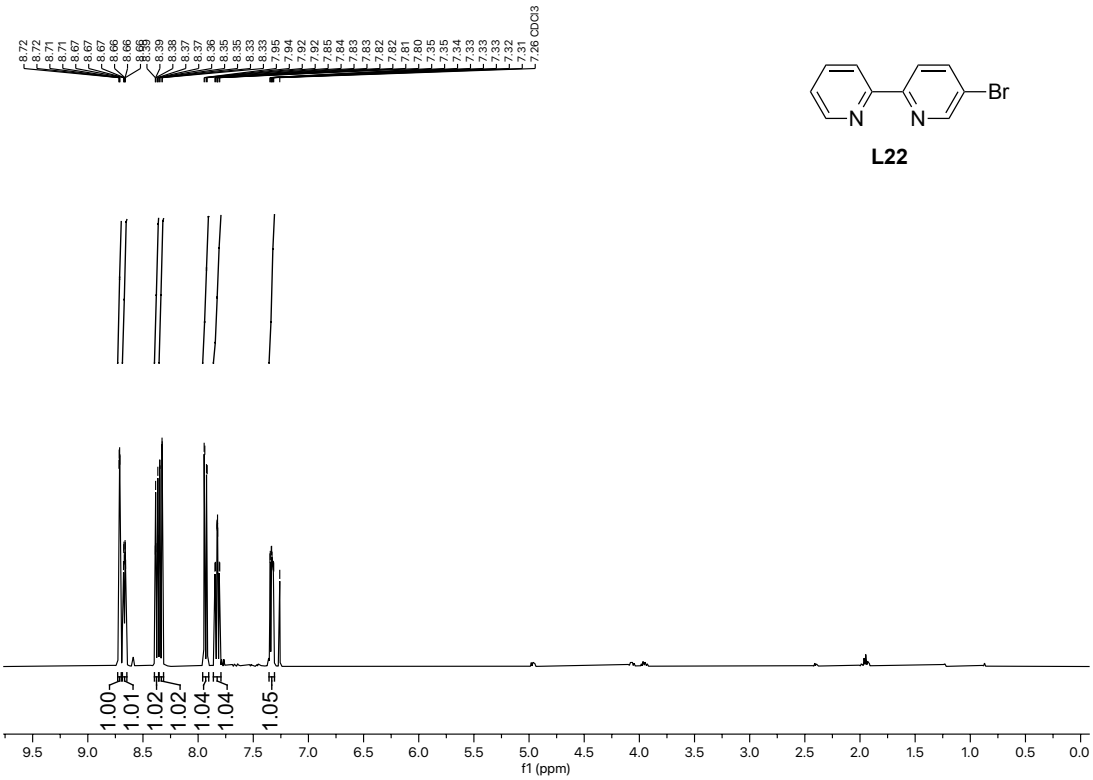

*$^{19}$F NMR 5-fluoro-2,2'-bipyridine (L21)*



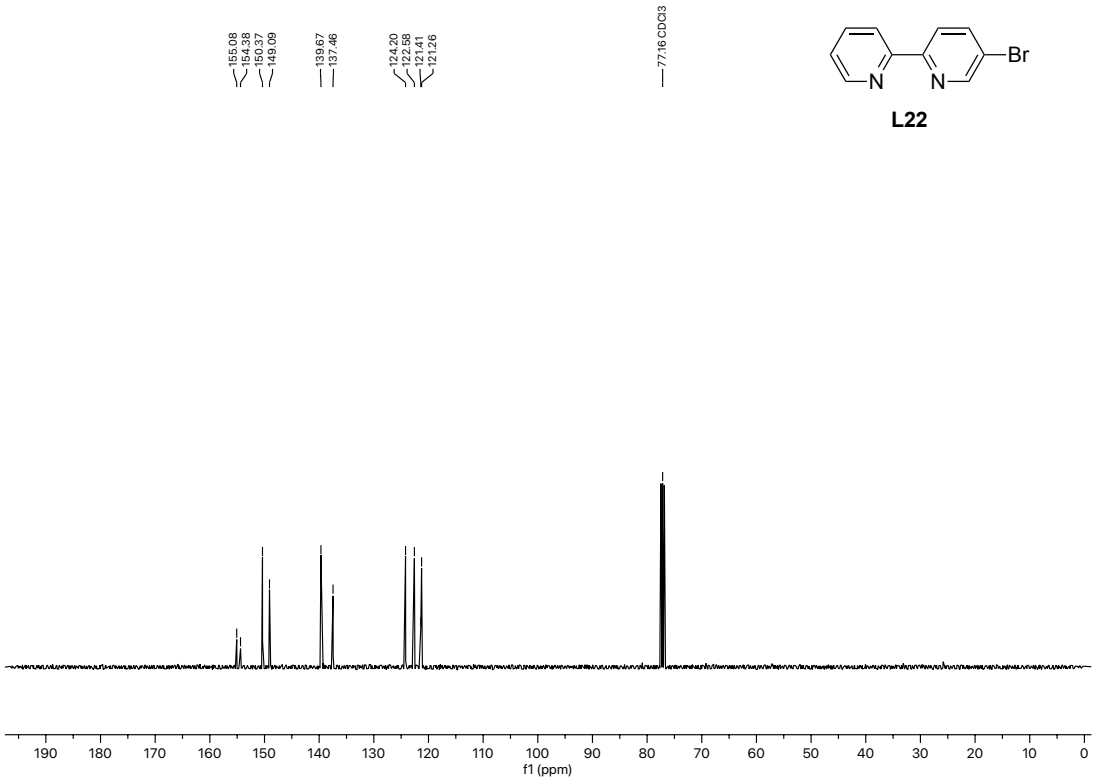
*HSQC NMR 5-fluoro-2,2'-bipyridine (L21)*



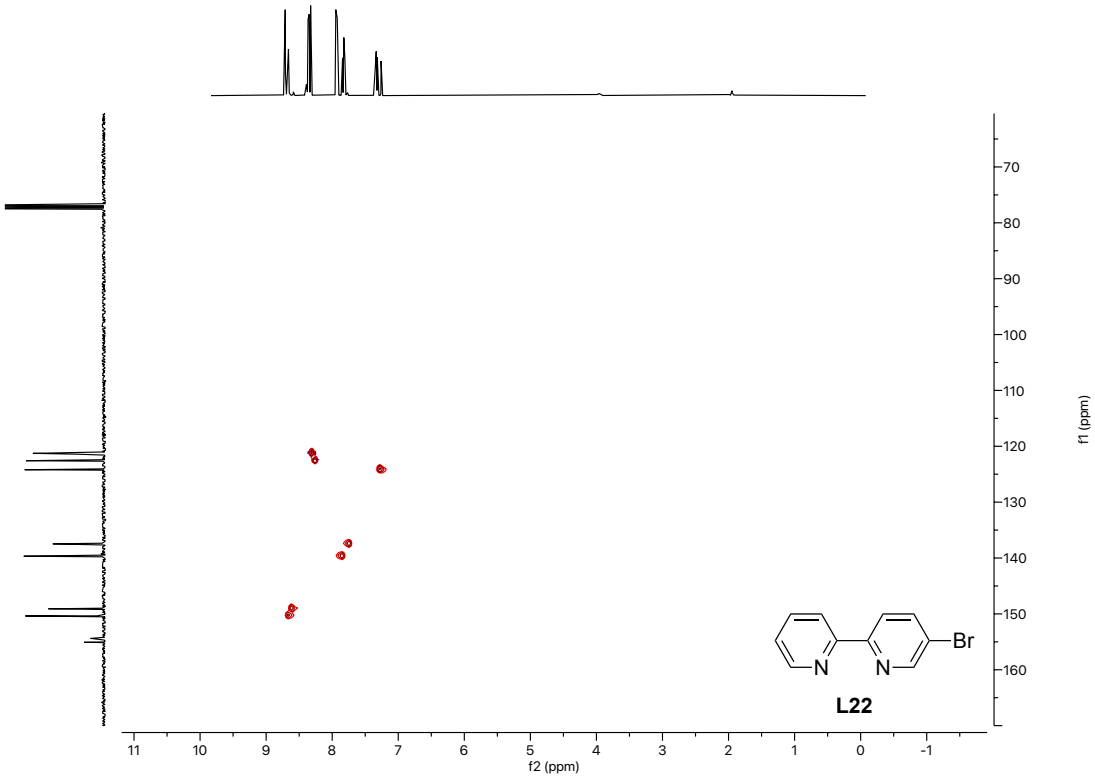

*$^{1}$H NMR 5-bromo-2,2'-bipyridine (L22)*



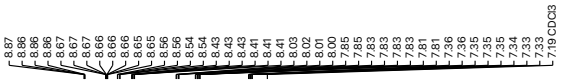
*$^{13}$C NMR 5-bromo-2,2'-bipyridine (L22)*

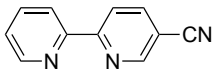



*HSQC NMR 5-bromo-2,2'-bipyridine (L22)*

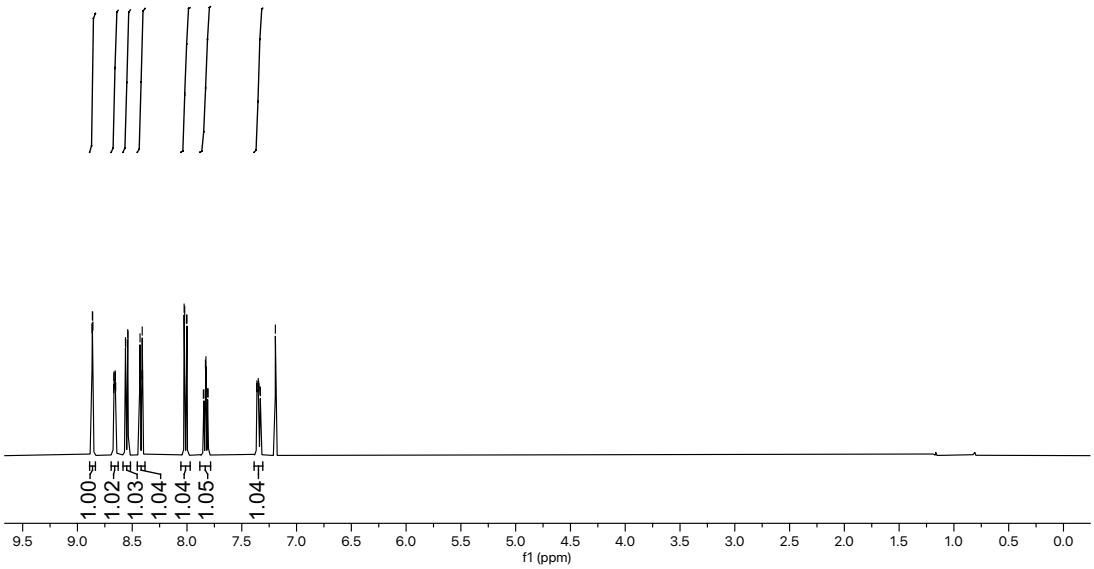


*[1]H NMR [2,2'-bipyridine]-5-carbonitrile (L23)*



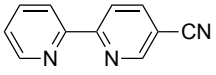




**L23**

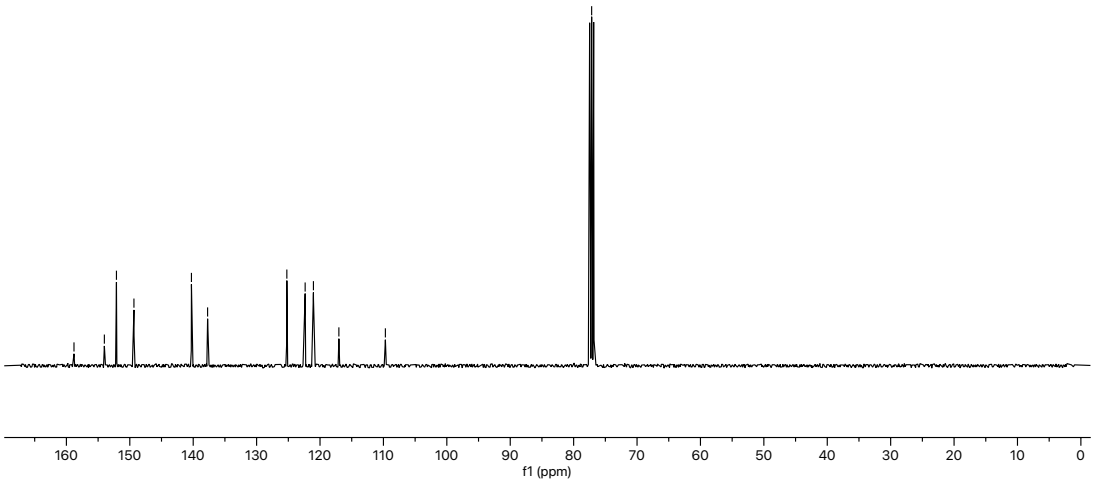



*[13]C NMR [2,2'-bipyridine]-5-carbonitrile (L23)*

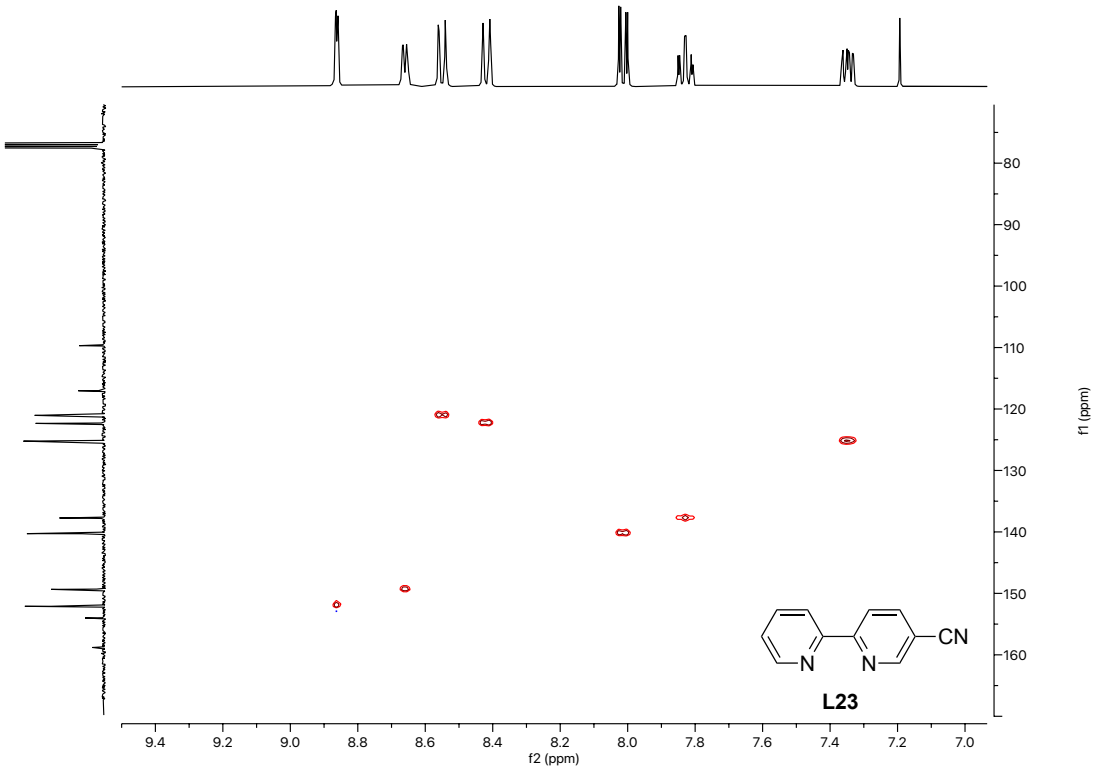


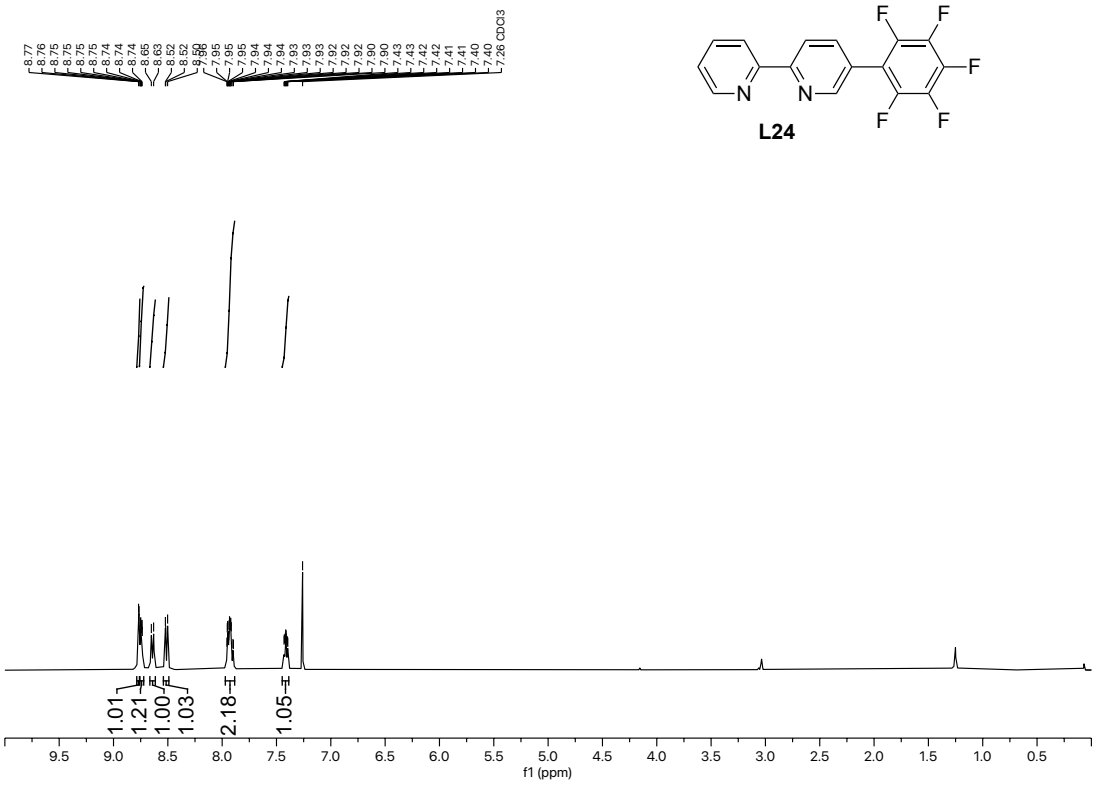

**L23**



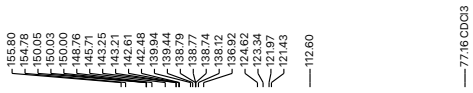
*HSQC NMR [2,2'-bipyridine]-5-carbonitrile (L23)*

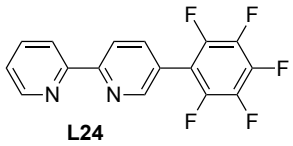



*$^{1}$H NMR 5-(perfluorophenyl)-2,2'-bipyridine (L24)*

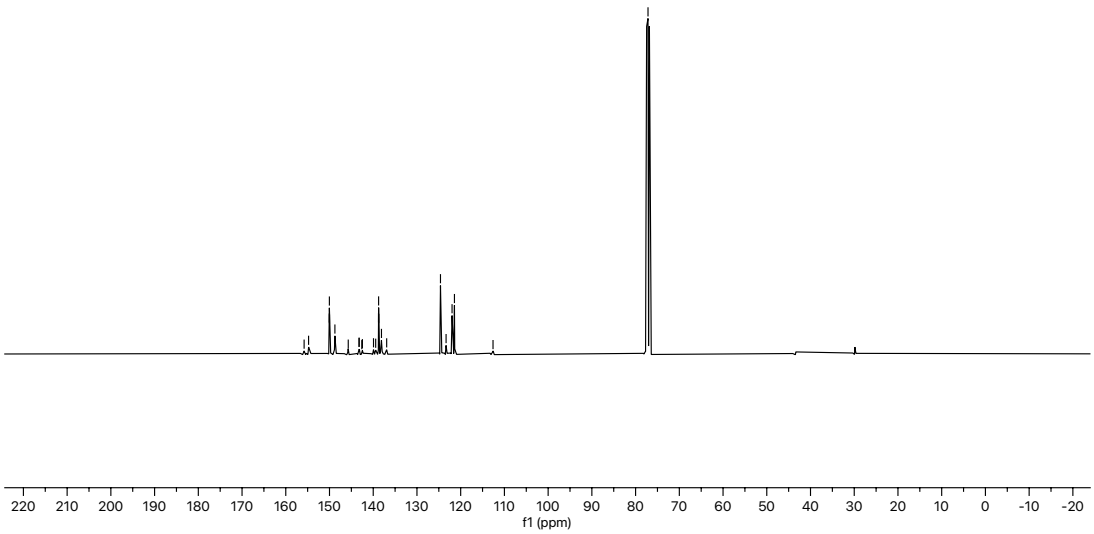


*$^{13}$C NMR 5-(perfluorophenyl)-2,2'-bipyridine (L24)*

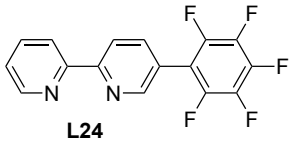


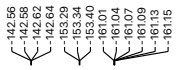

**L24**

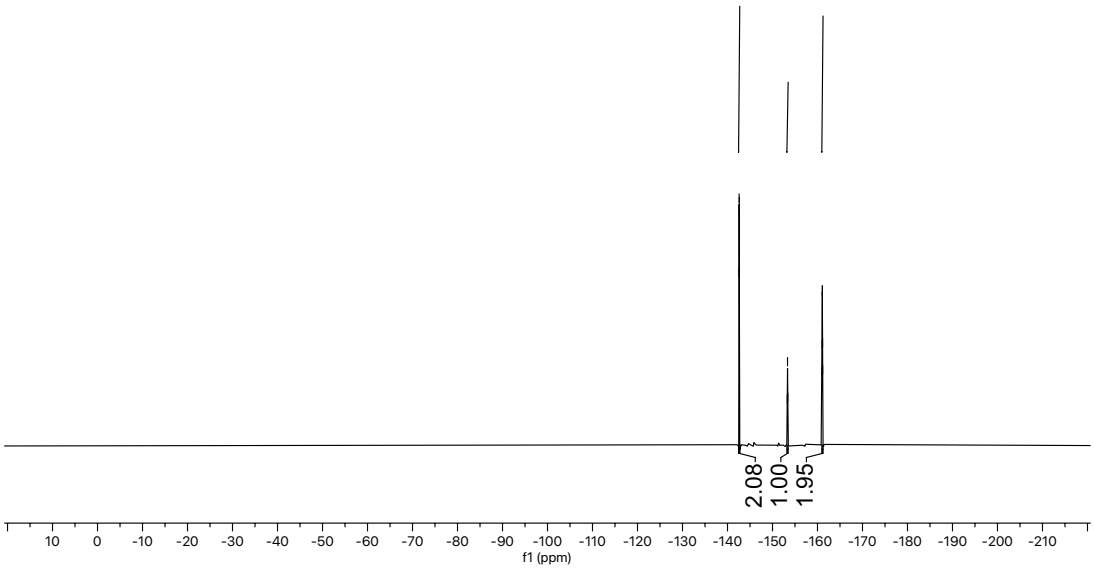



*$^{19}$F NMR 5-(perfluorophenyl)-2,2'-bipyridine (L24)*

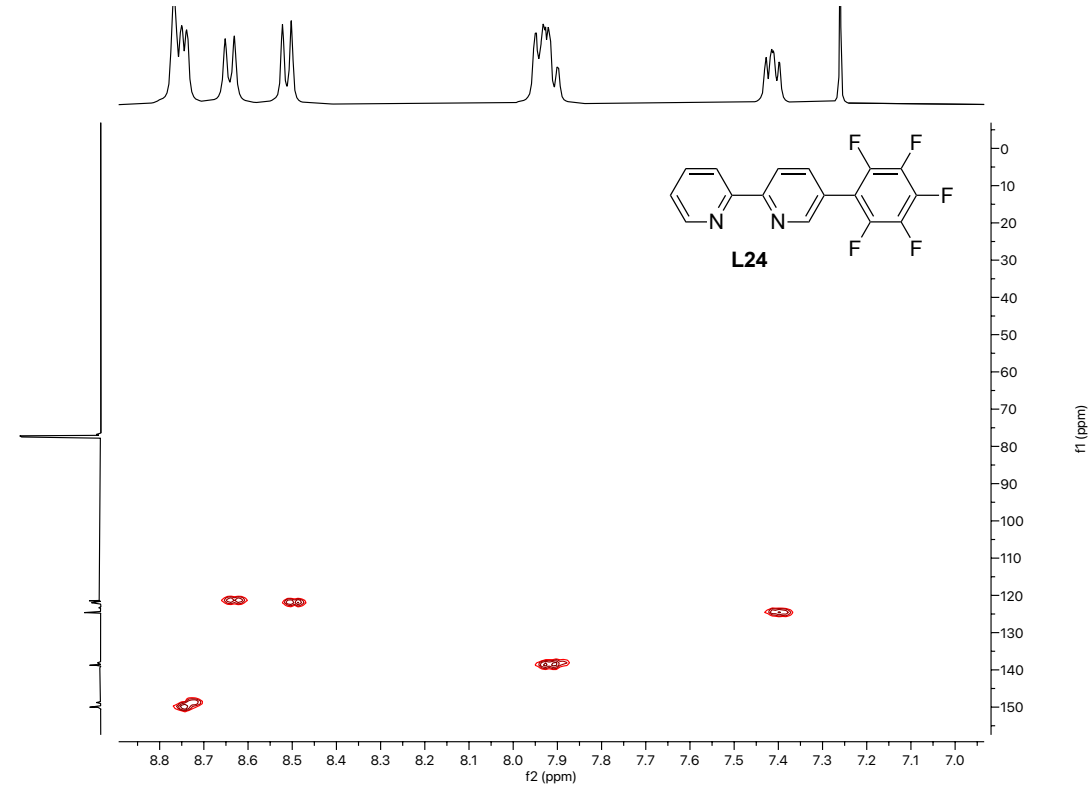



**L24**

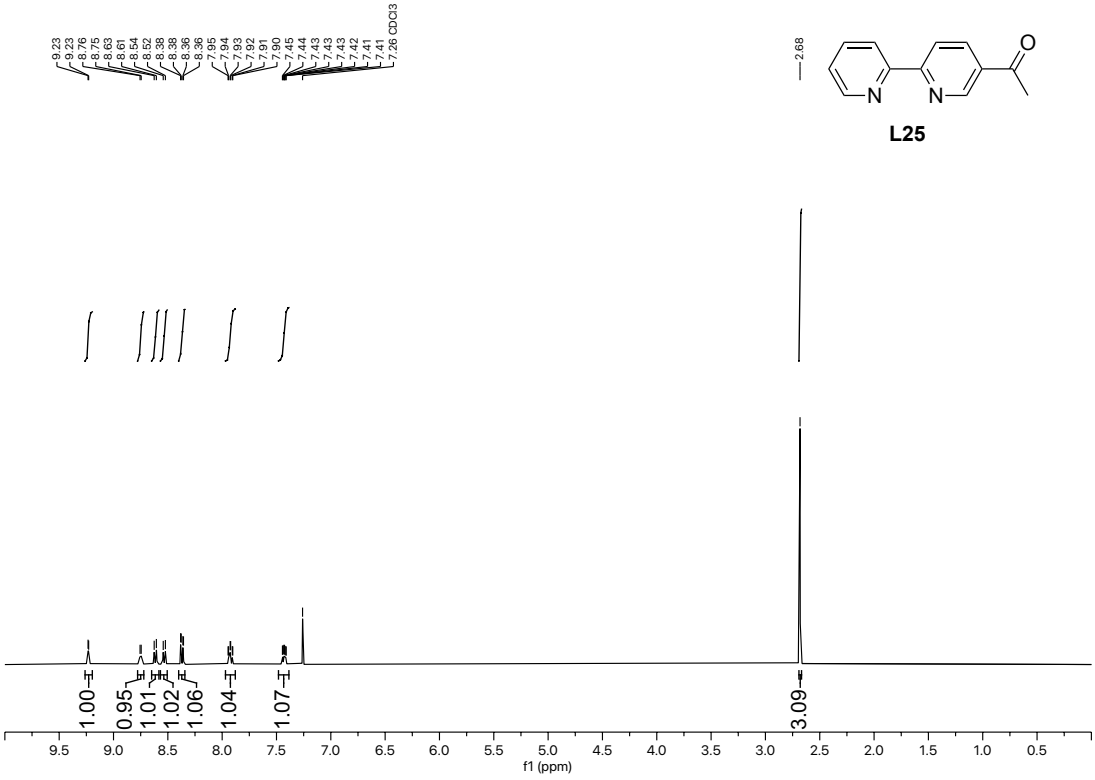


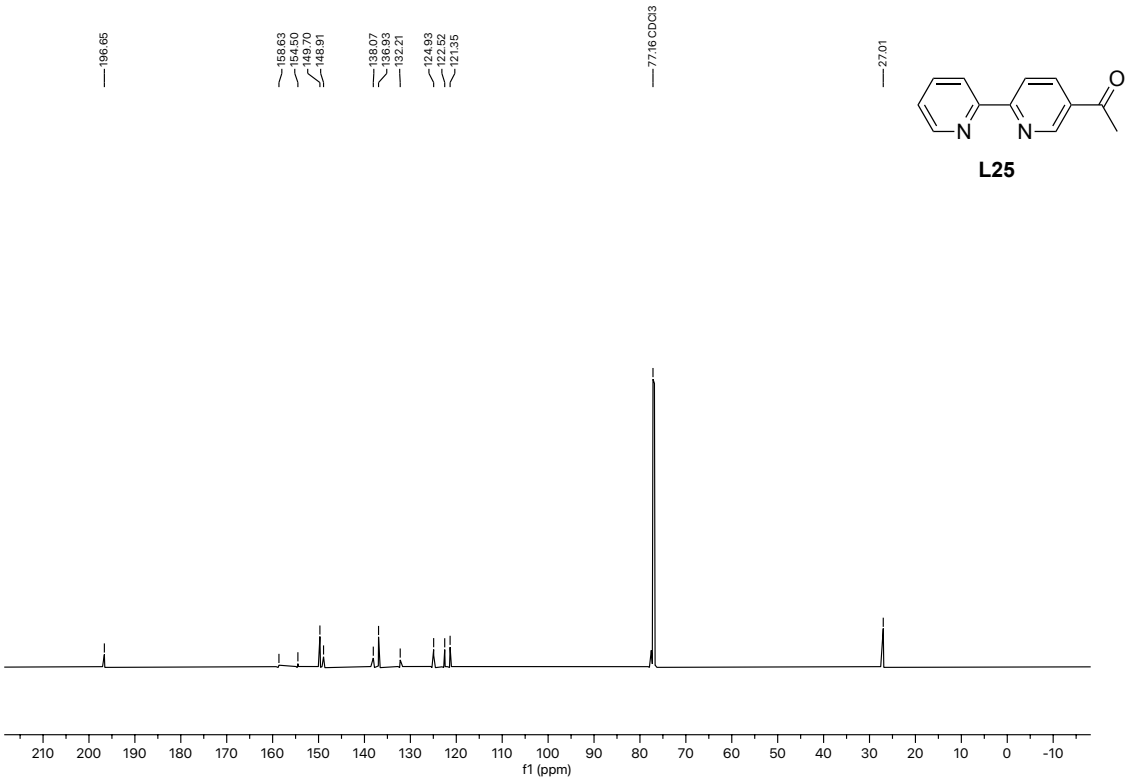
*HSQC NMR 5-(perfluorophenyl)-2,2'-bipyridine (L24)*



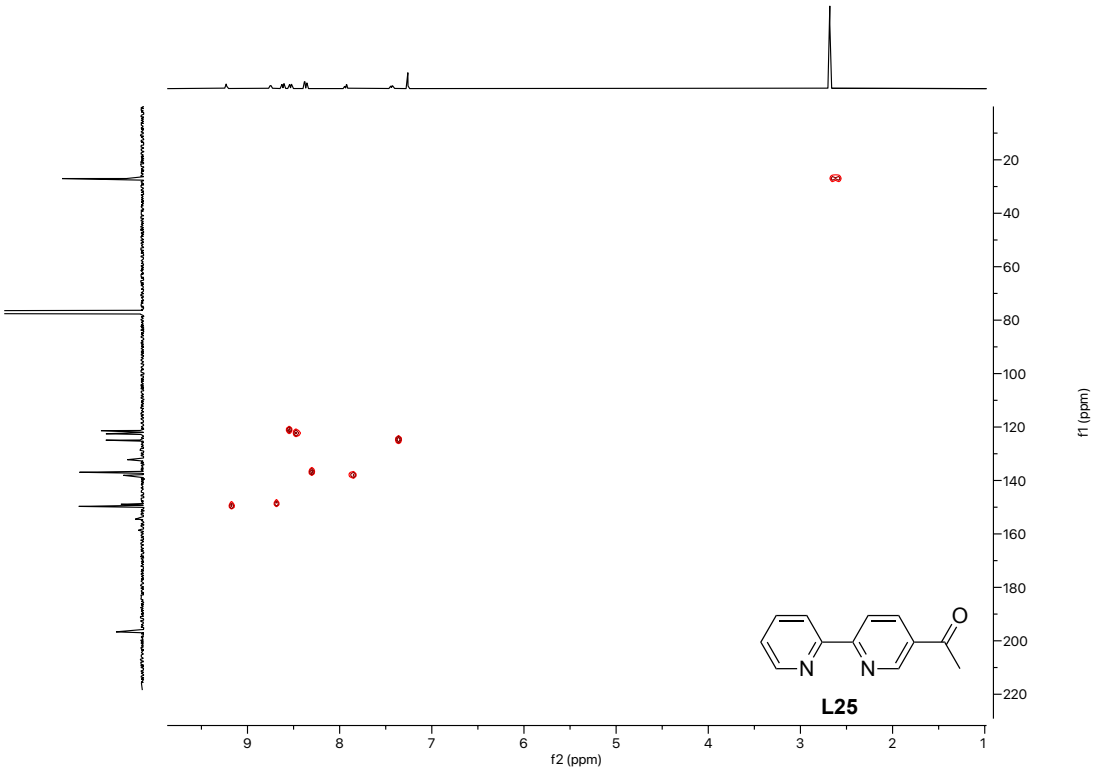

*$^{1}$H NMR 1-([2,2'-bipyridin]-5-yl)ethan-1-one (L25)*



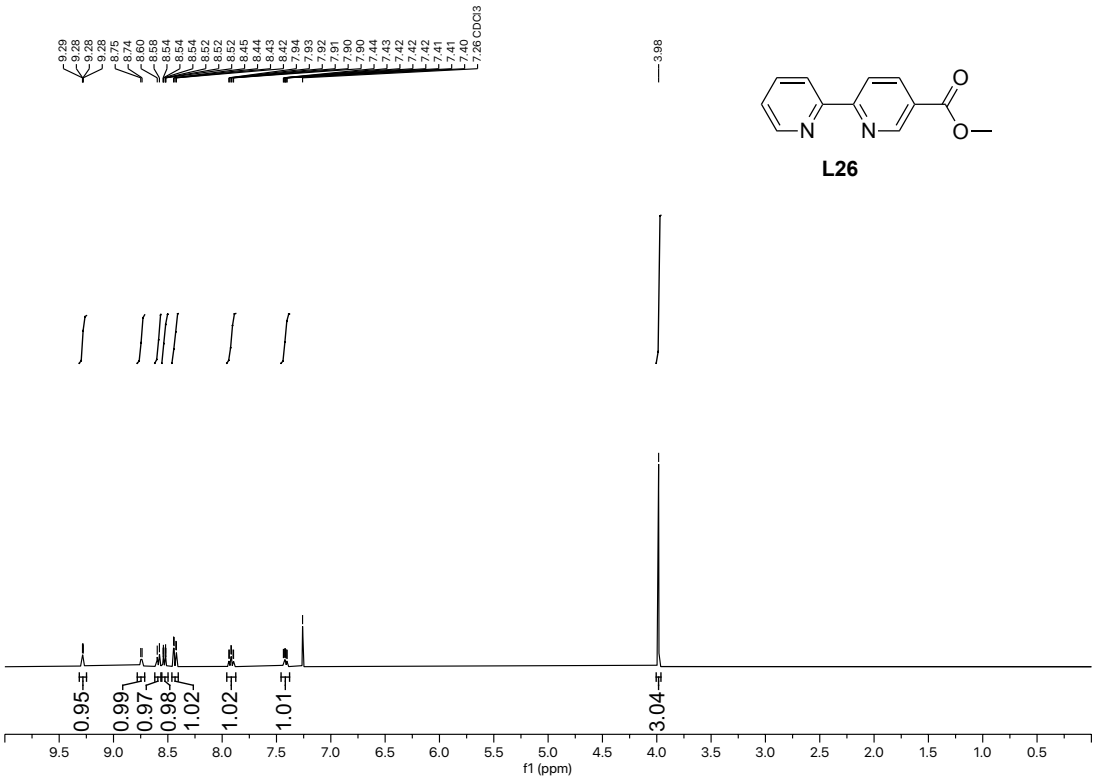
*$^{13}$C NMR 1-([2,2'-bipyridin]-5-yl)ethan-1-one (L25)*




*HSQC NMR 1-([2,2'-bipyridin]-5-yl)ethan-1-one (L25)*

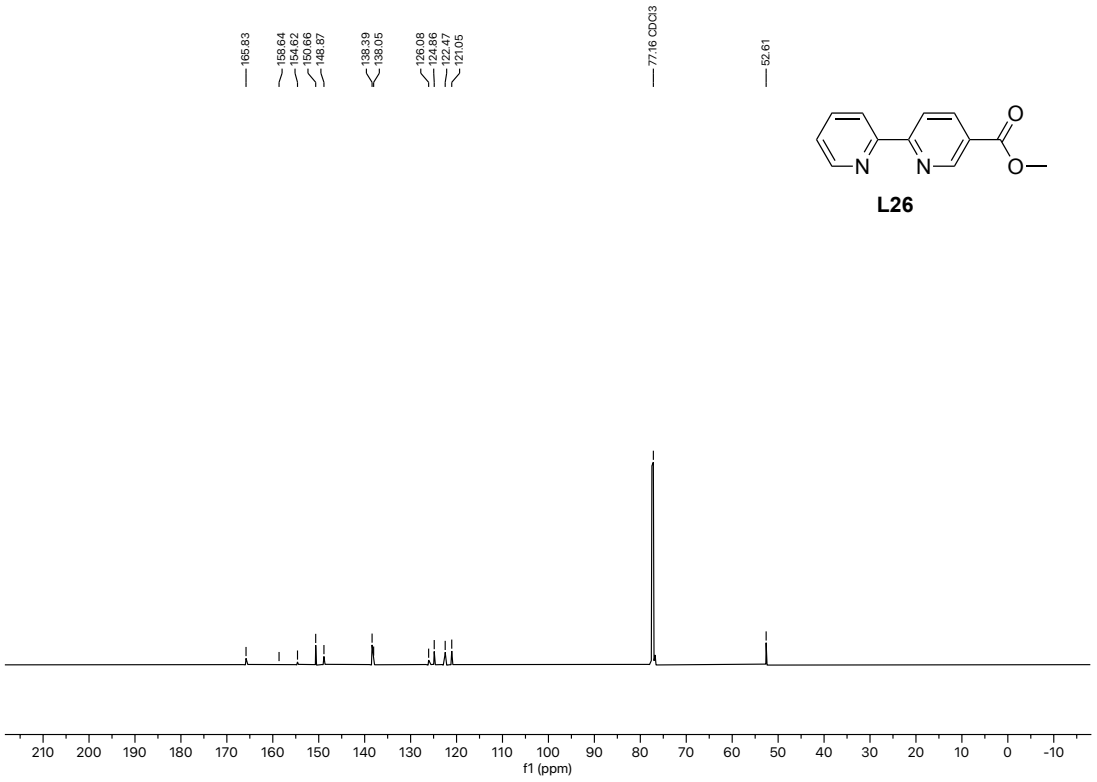


*[1]H NMR methyl [2,2'-bipyridine]-5-carboxylate (L26)*



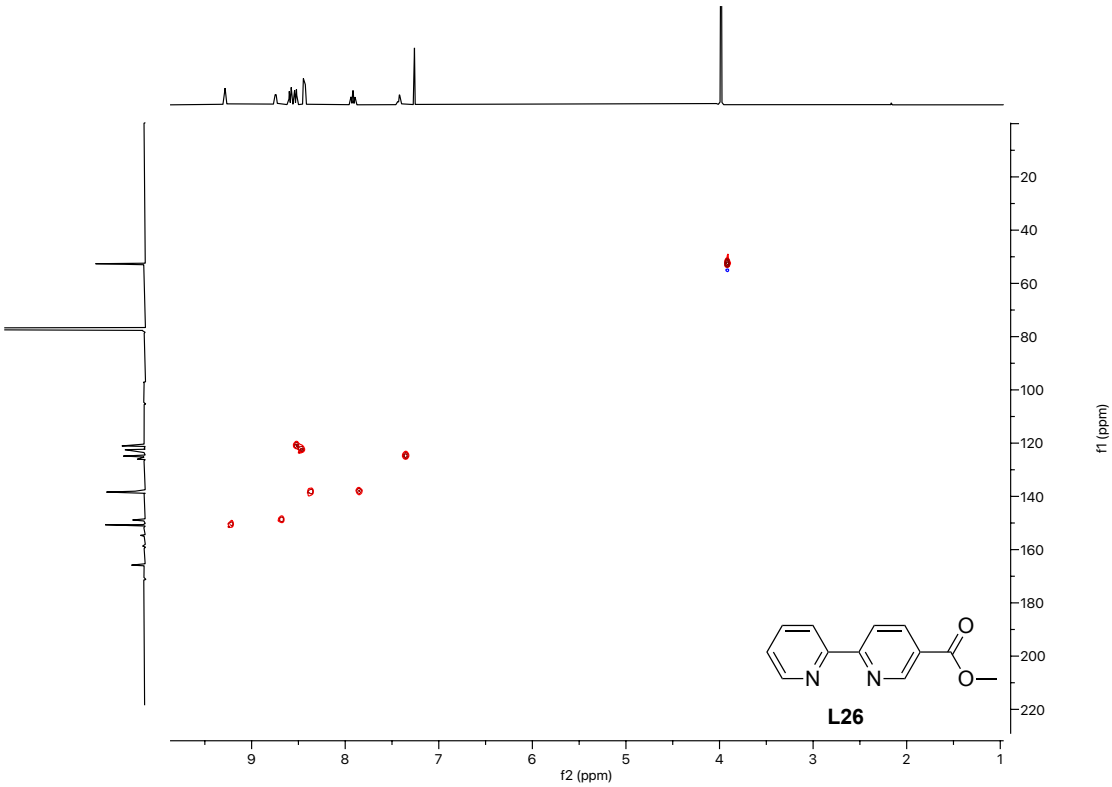

**L26**

*[13]C NMR methyl [2,2'-bipyridine]-5-carboxylate (L26)*

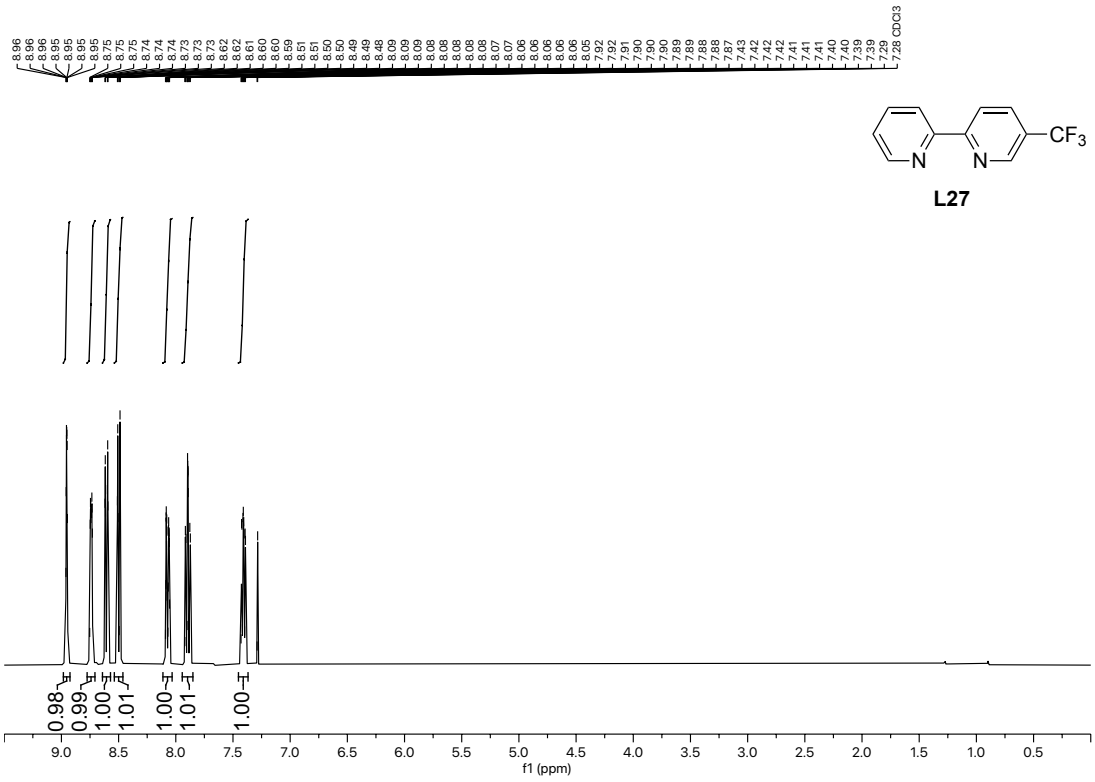



**L26**

*HSQC NMR methyl [2,2'-bipyridine]-5-carboxylate (L26)*

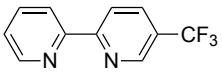



*$^{1}$H NMR 5-(trifluoromethyl)-2,2'-bipyridine (L27)*

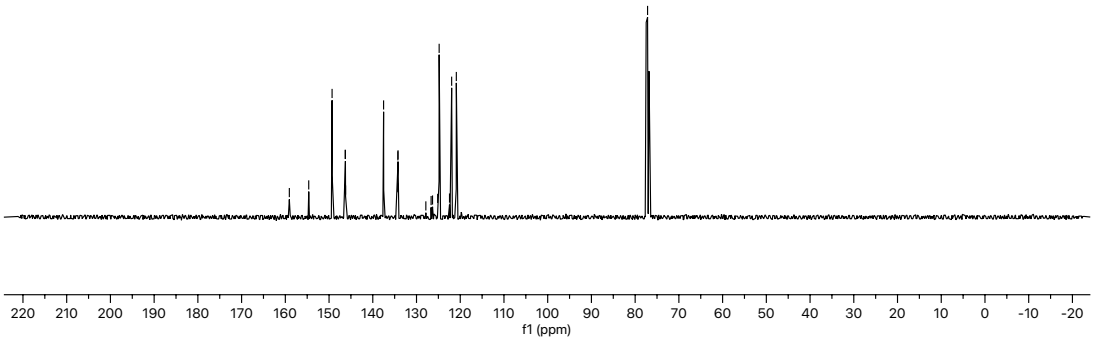


*$^{13}$C NMR 5-(trifluoromethyl)-2,2'-bipyridine (L27)*



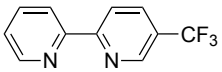




**L27**

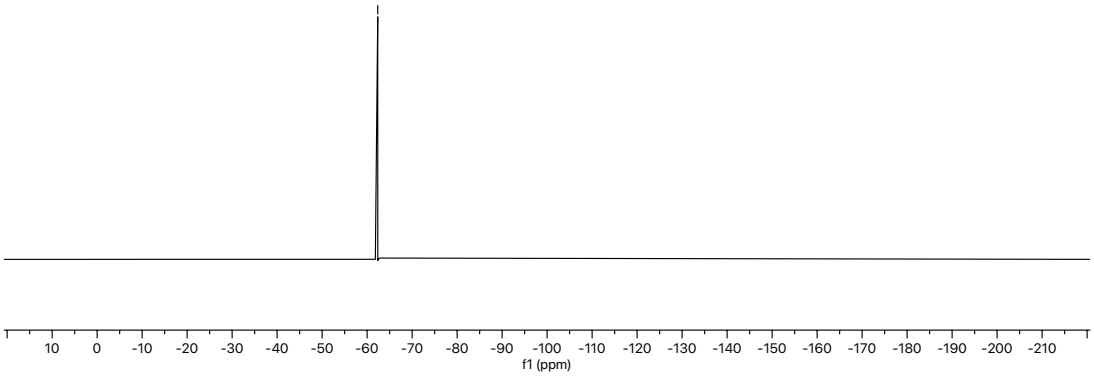



*$^{19}$F NMR 5-(trifluoromethyl)-2,2'-bipyridine (L27)*

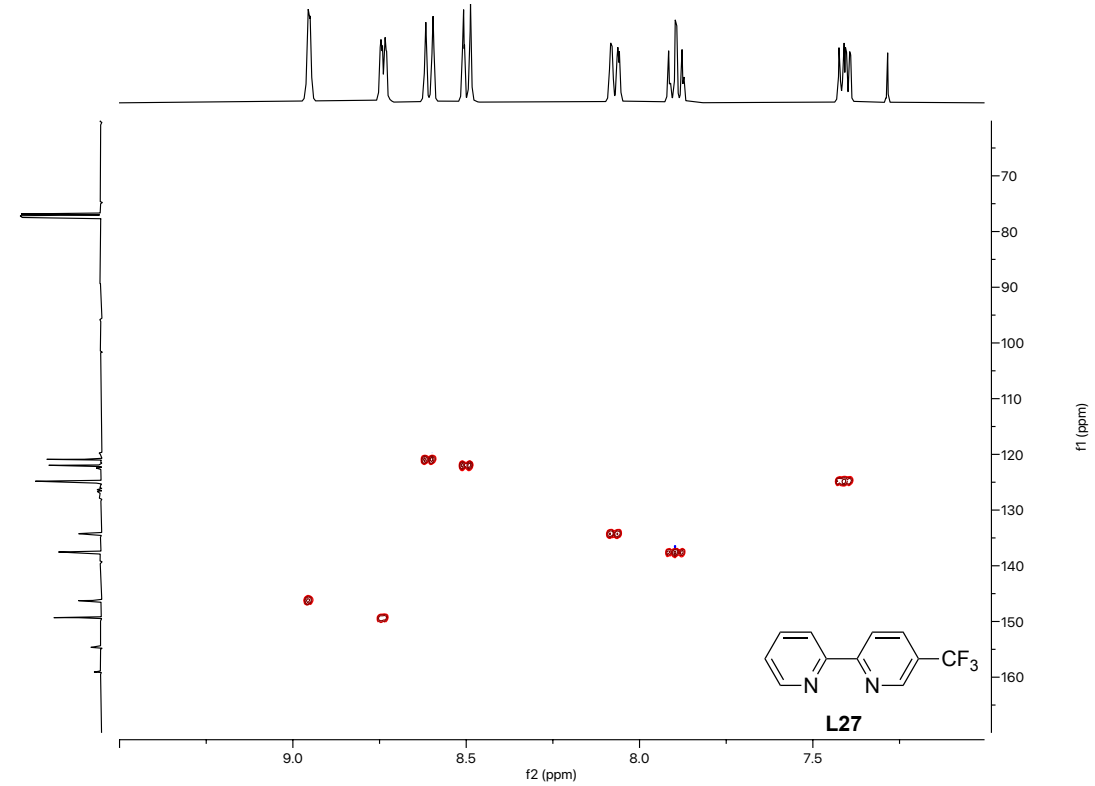


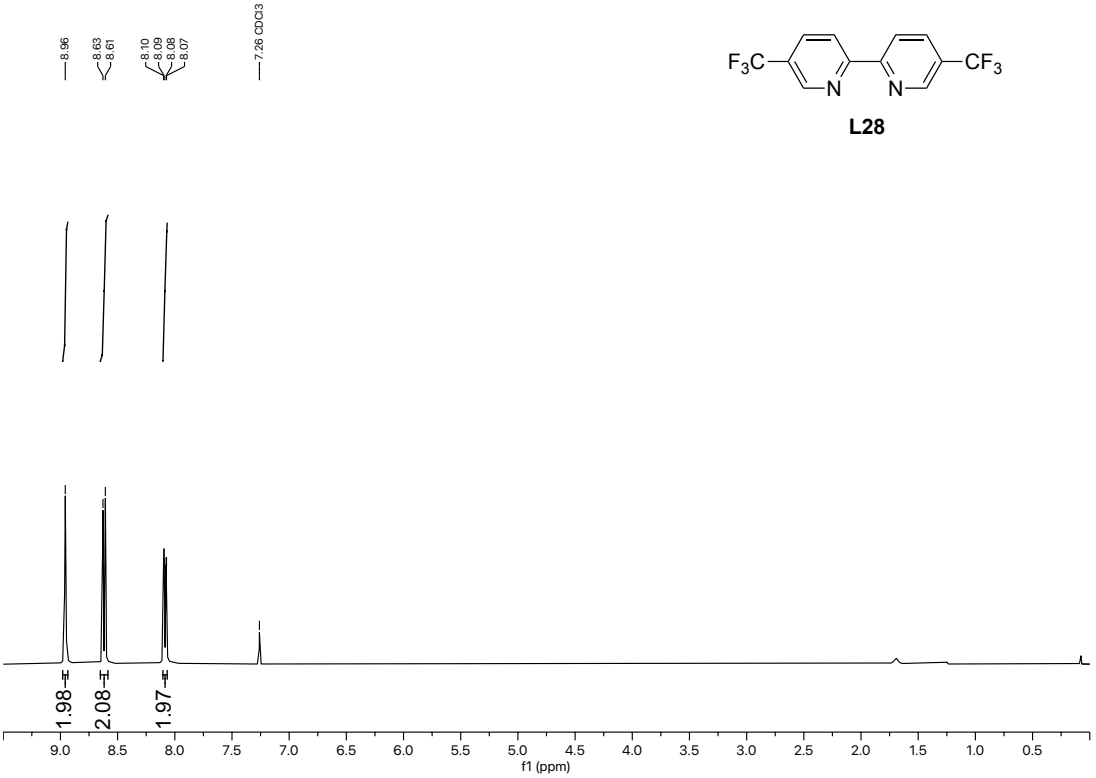

**L27**



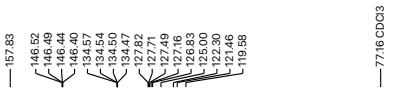
*HSQC NMR 5-(trifluoromethyl)-2,2'-bipyridine (L27)*

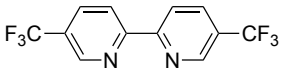



*$^{1}$H NMR 5,5'-bis(trifluoromethyl)-2,2'-bipyridine (L28)*

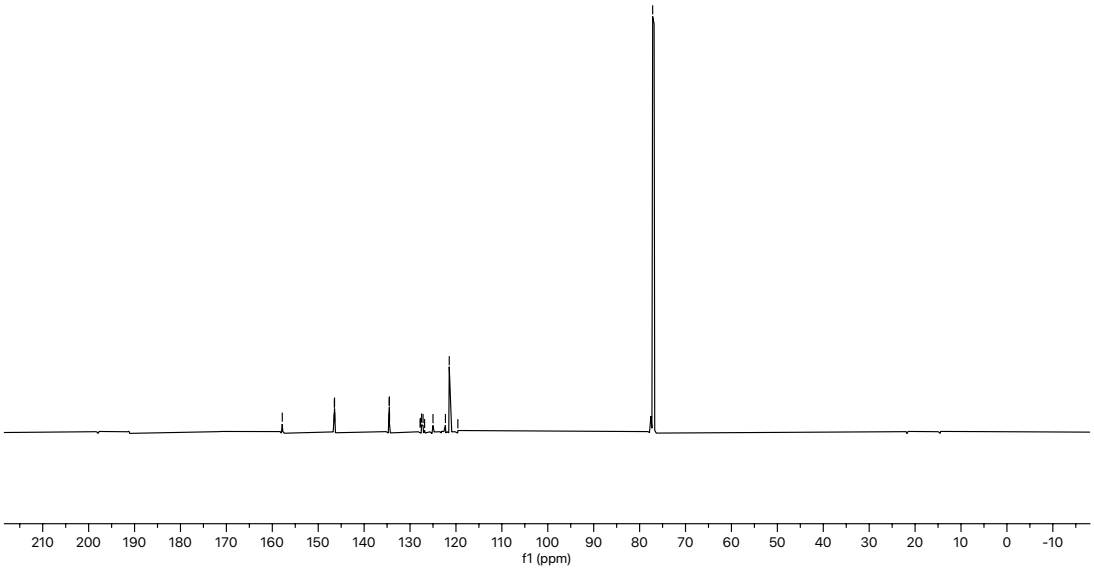


*$^{13}$C NMR 5,5'-bis(trifluoromethyl)-2,2'-bipyridine (L28)*



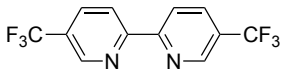




**L28**

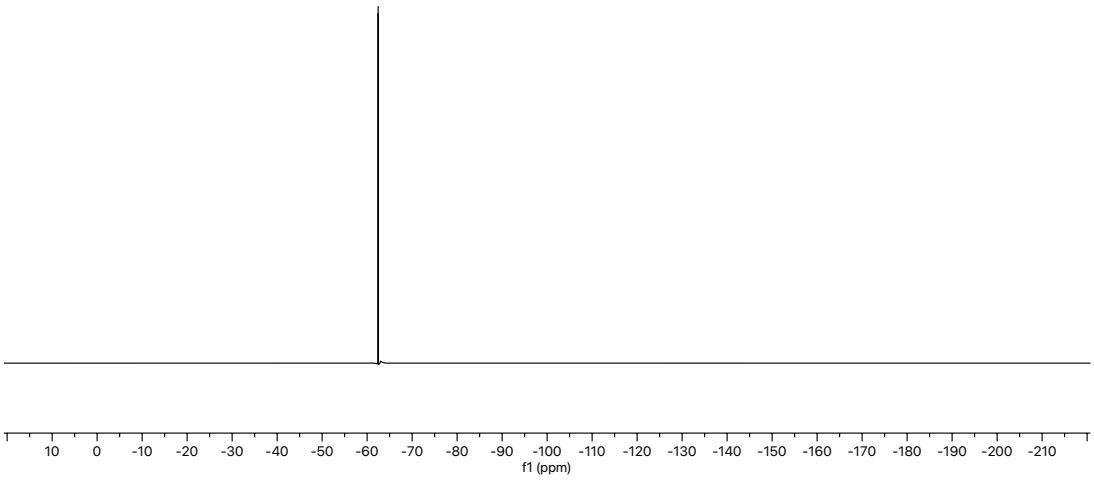



*$^{19}$F NMR 5,5'-bis(trifluoromethyl)-2,2'-bipyridine (L28)*



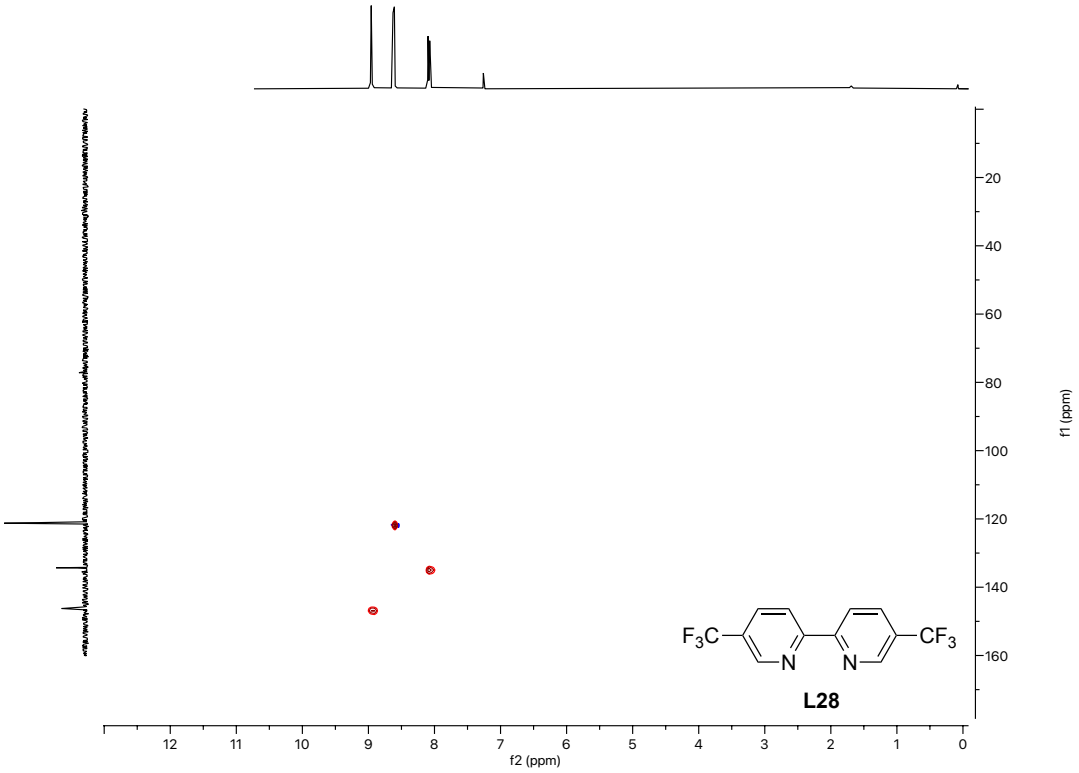




**L28**

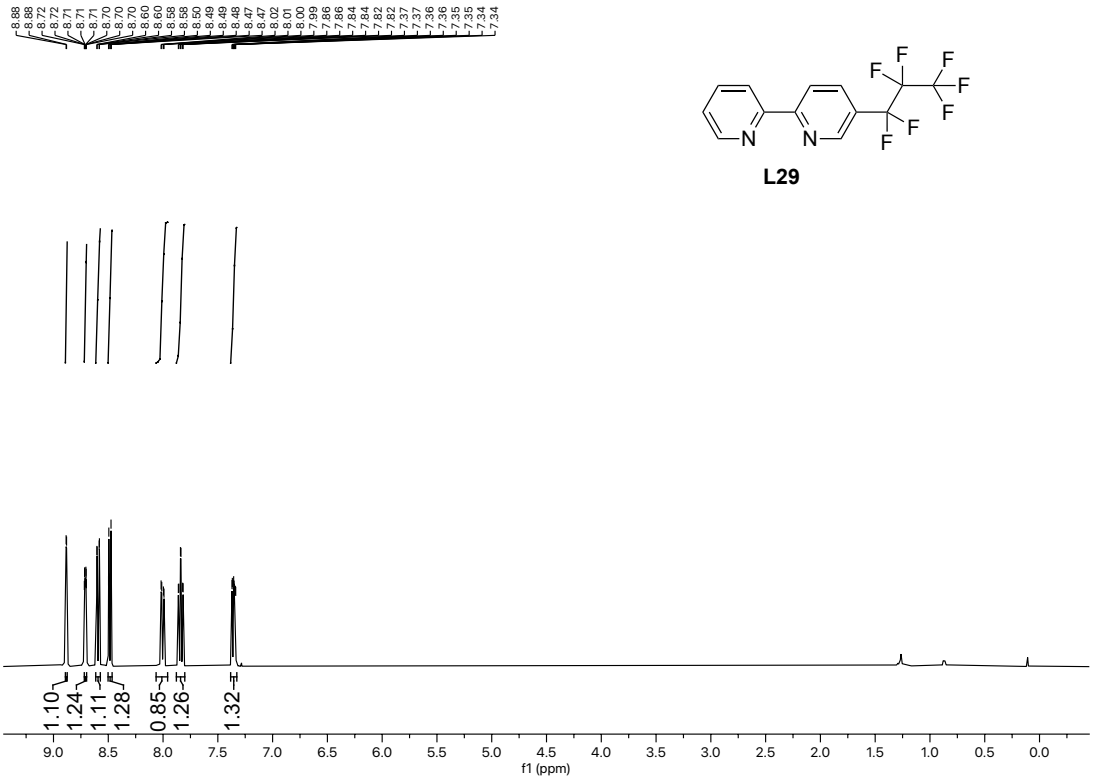



USC
UNIVERSIDADE DE SANTIAGO DE COMPOSTELA

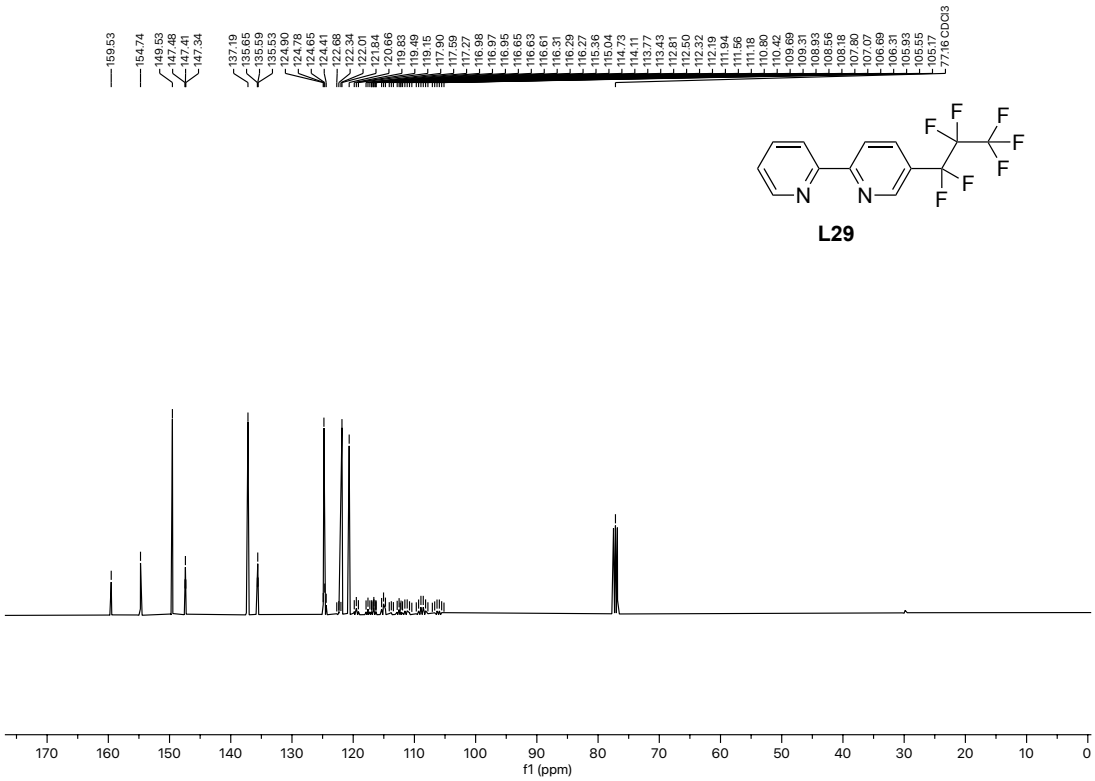
*HSQC NMR 5,5'-bis(trifluoromethyl)-2,2'-bipyridine (L28)*



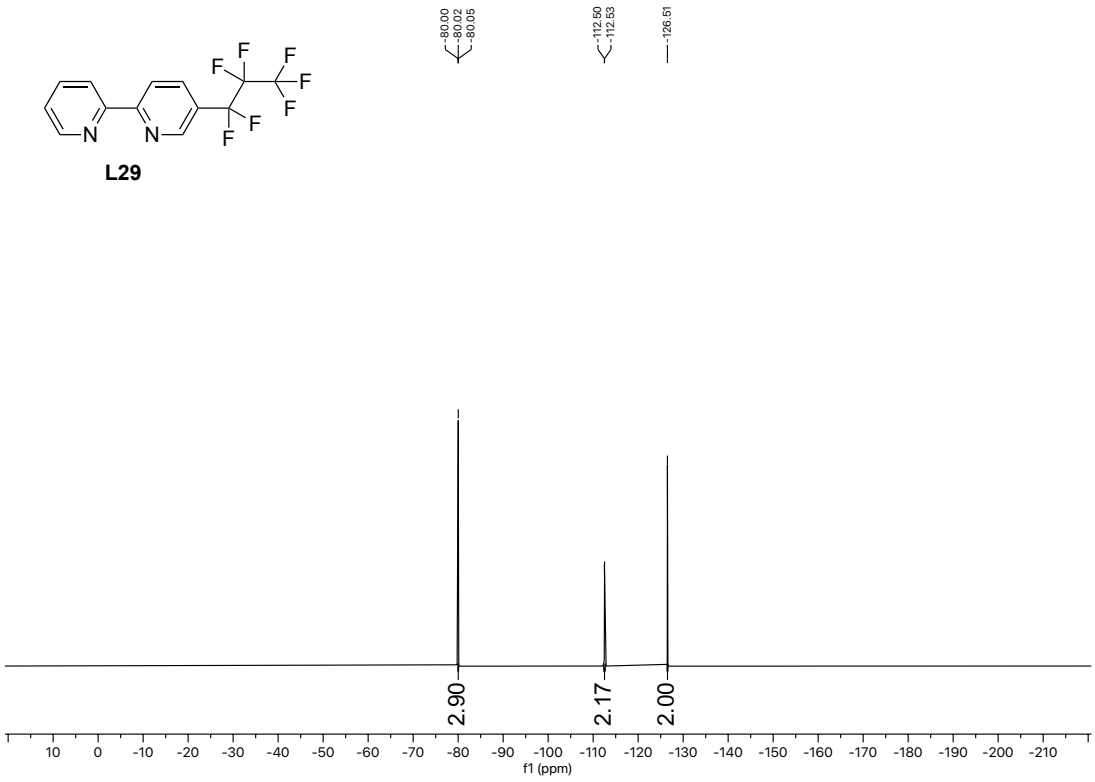

*[1]H NMR 5-(perfluoropropyl)-2,2'-bipyridine (L29)*



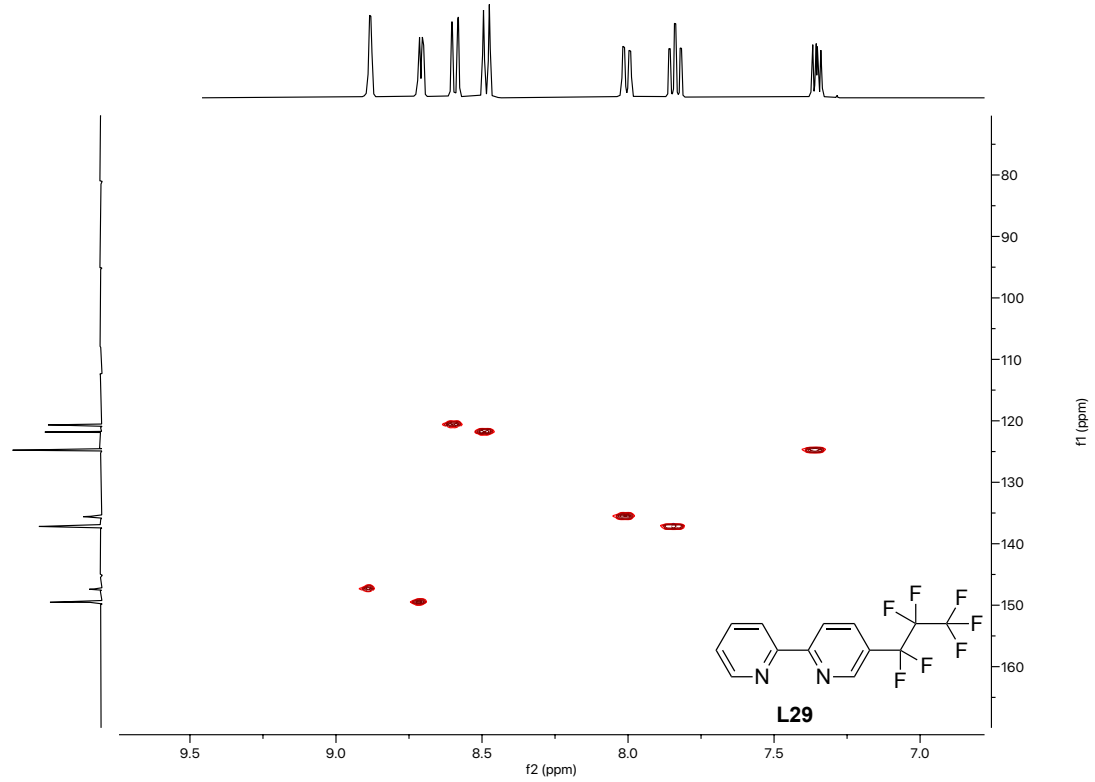
*$^{13}$C NMR 5-(perfluoropropyl)-2,2'-bipyridine (L29)*



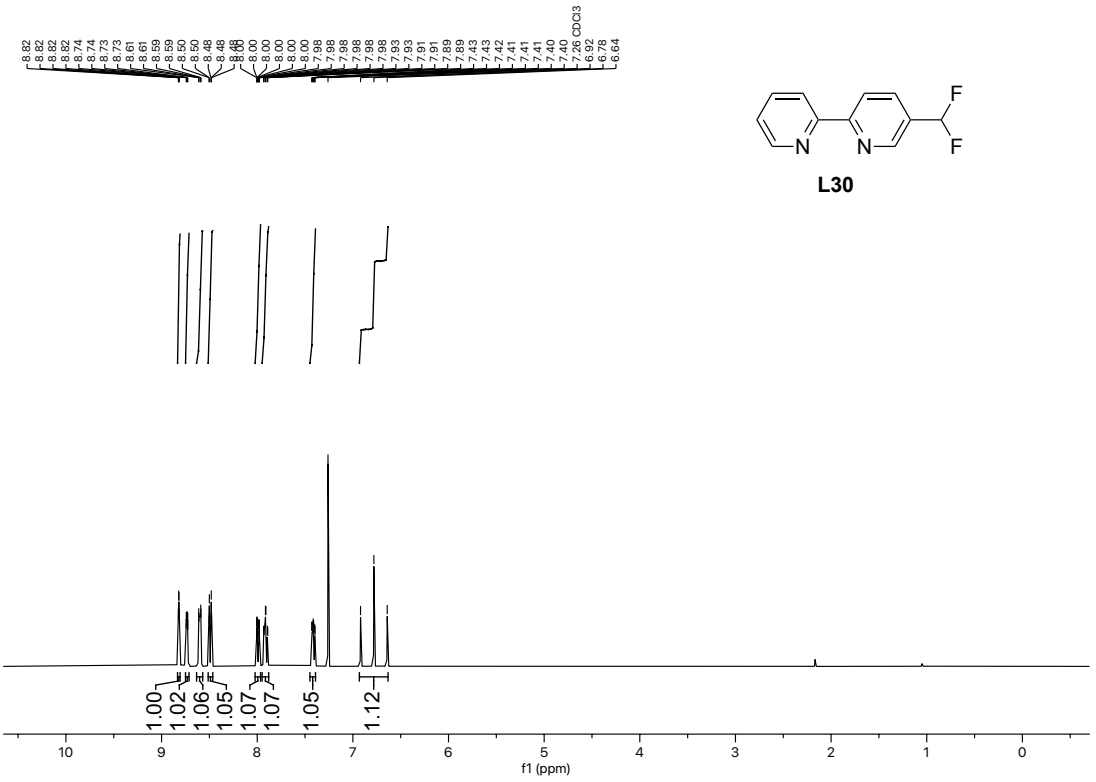

*$^{19}$F NMR 5-(perfluoropropyl)-2,2'-bipyridine (L29)*



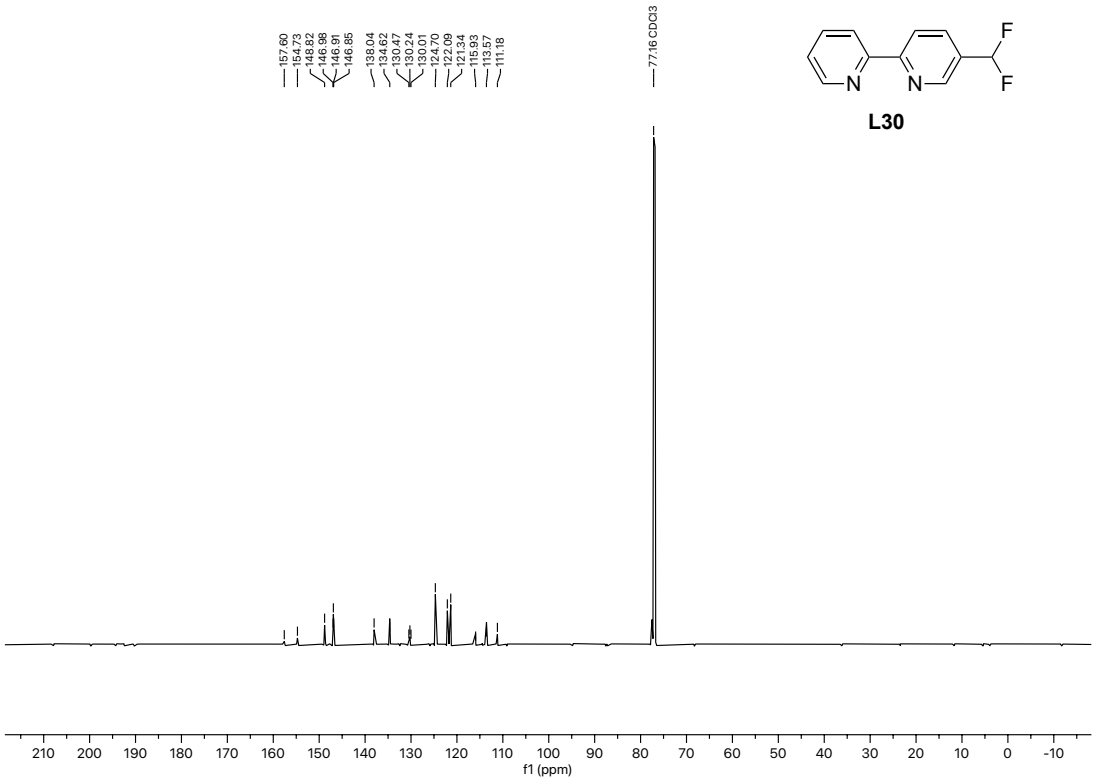
*HSQC NMR 5-(perfluoropropyl)-2,2'-bipyridine (L29)*



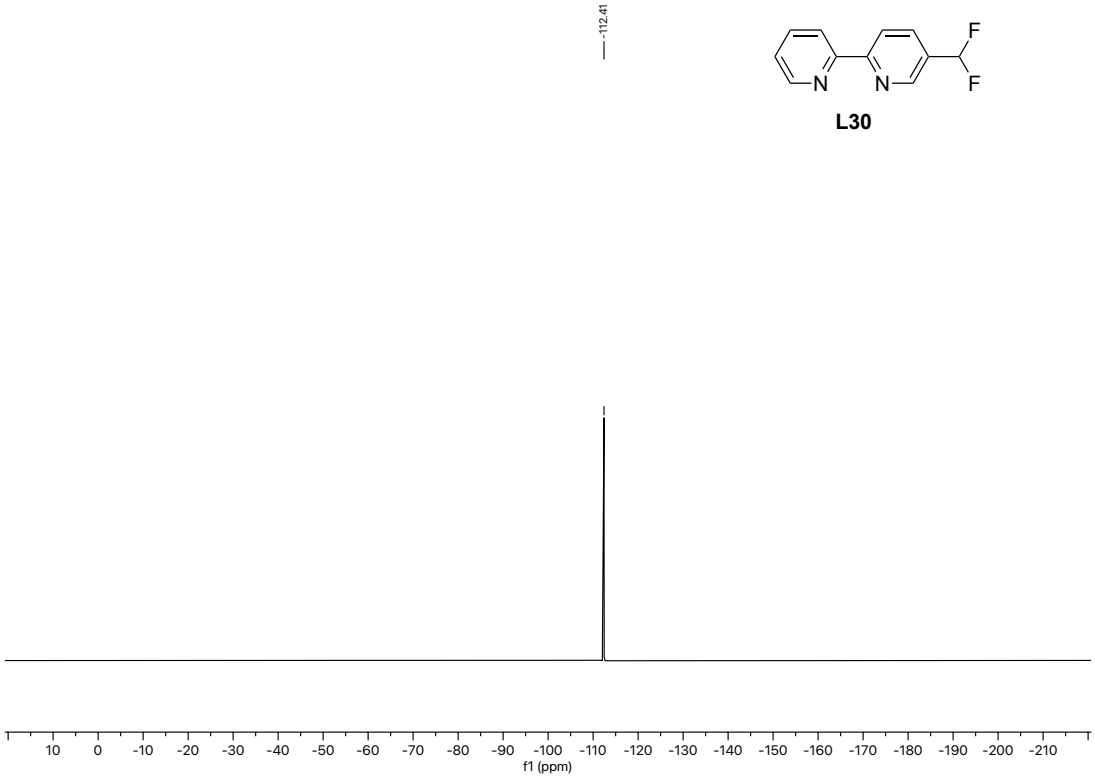

*$^{1}$H NMR 5-(difluoromethyl)-2,2'-bipyridine (L30)*



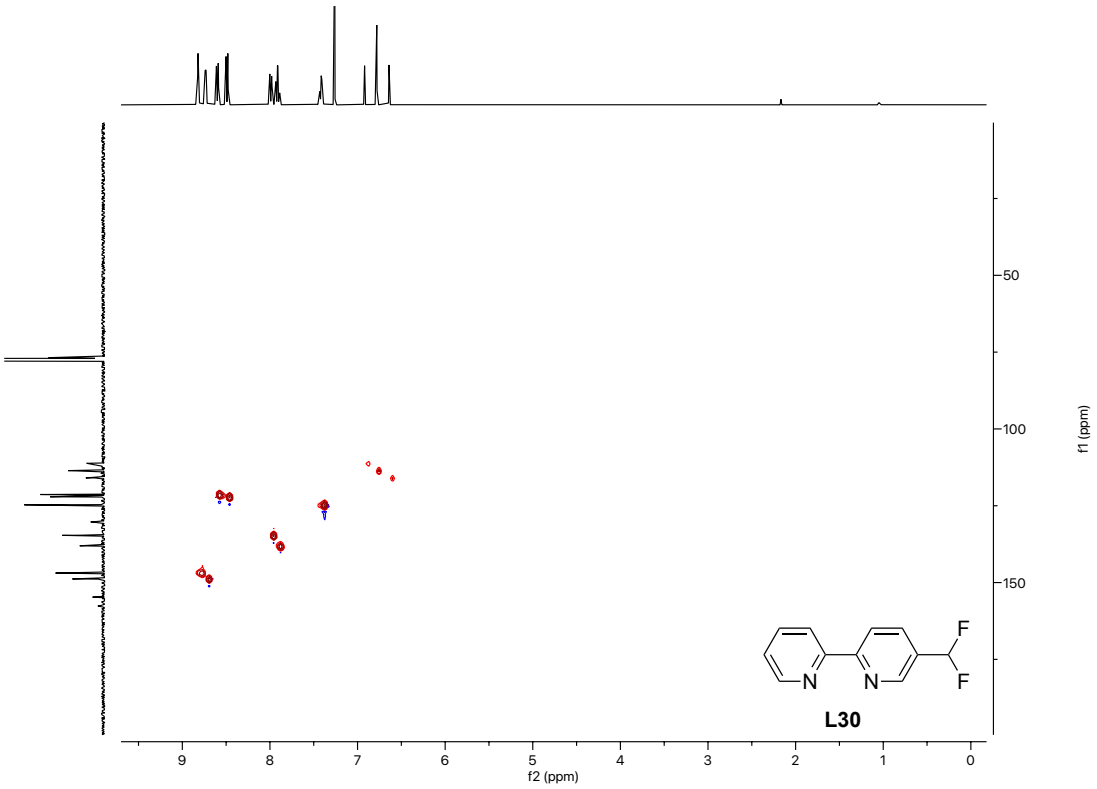
*$^{13}$C NMR 5-(difluoromethyl)-2,2'-bipyridine (L30)*



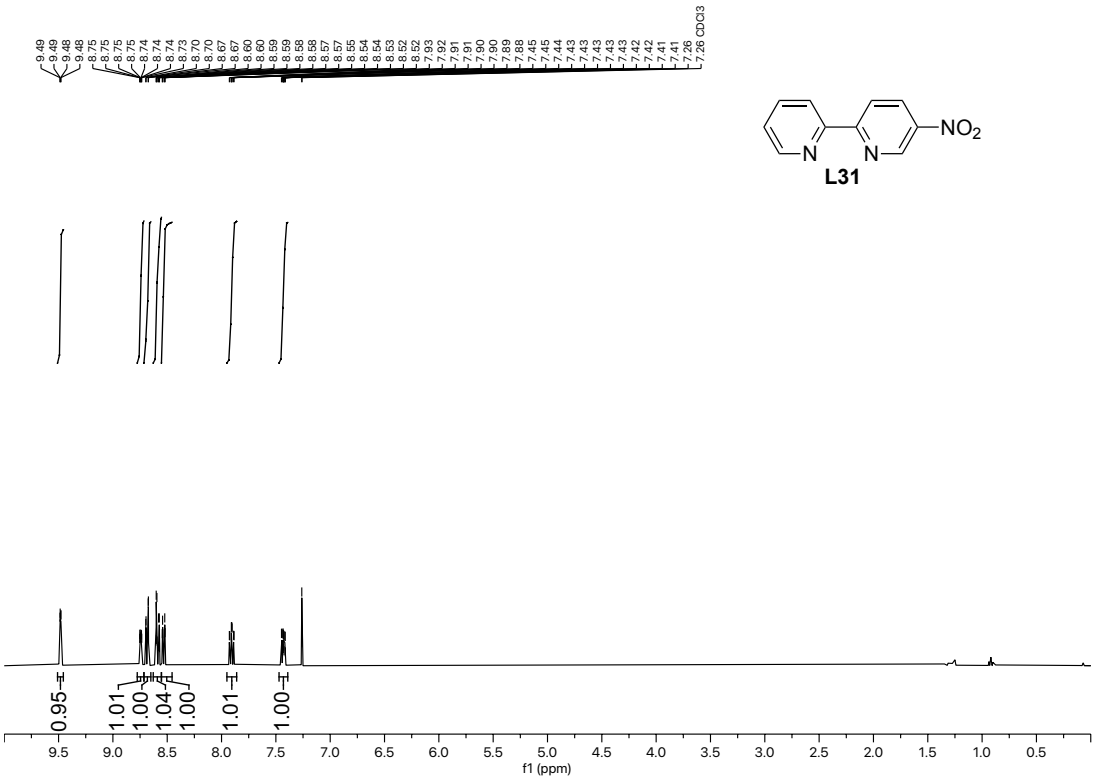

*$^{19}$F NMR 5-(difluoromethyl)-2,2'-bipyridine (L30)*



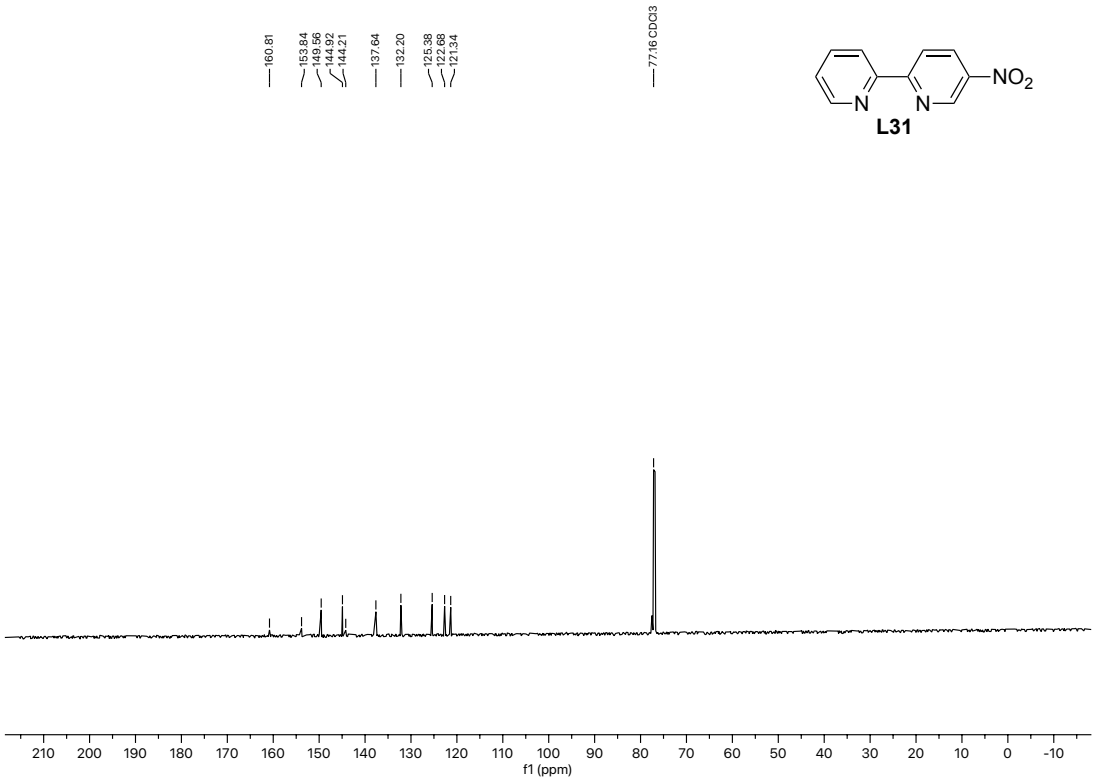
*HSQC NMR 5-(difluoromethyl)-2,2'-bipyridine (L30)*



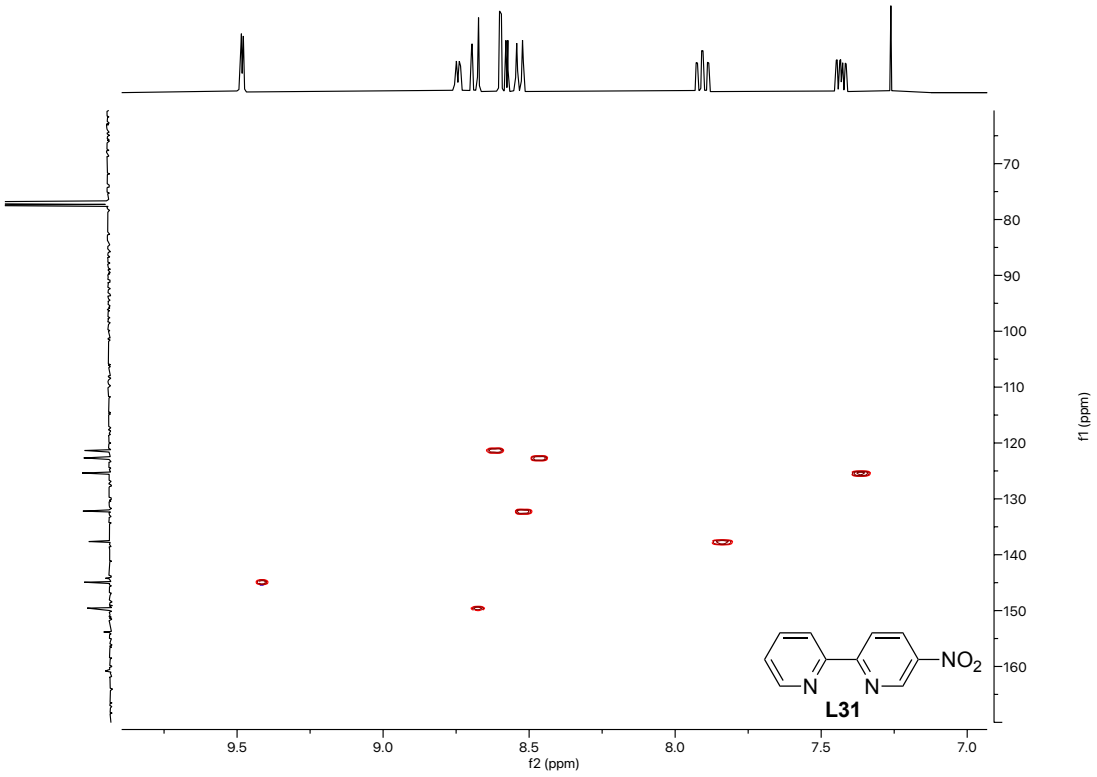

*$^{1}$H NMR 5-nitro-2,2'-bipyridine (L31)*



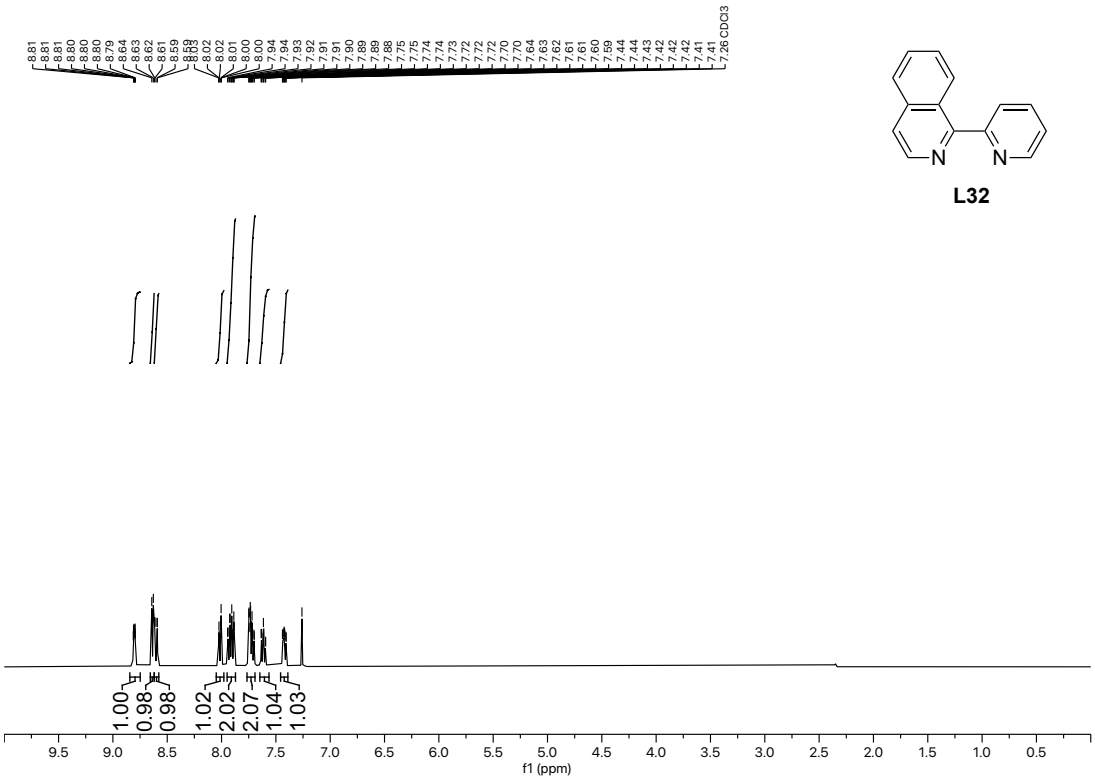
*$^{13}$C NMR 5-nitro-2,2'-bipyridine (L31)*




*HSQC NMR 5-nitro-2,2'-bipyridine (L31)*



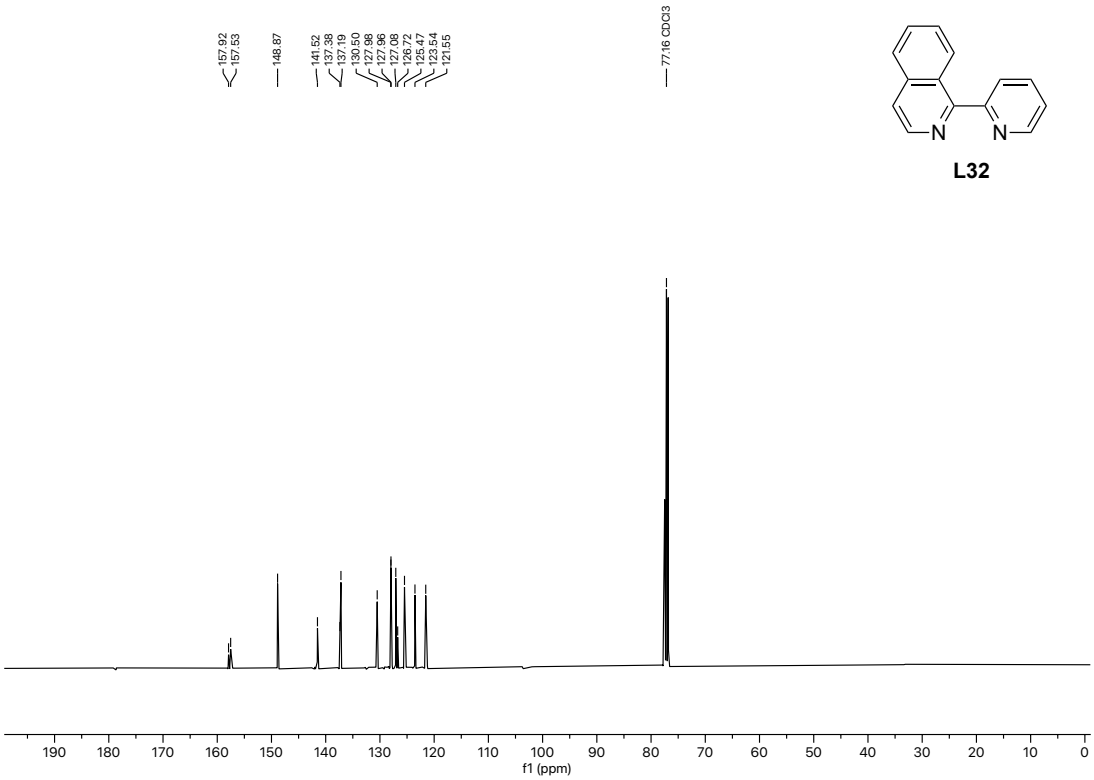
*[1]H NMR 1-(pyridin-2-yl)isoquinoline (L32)*






**L32**

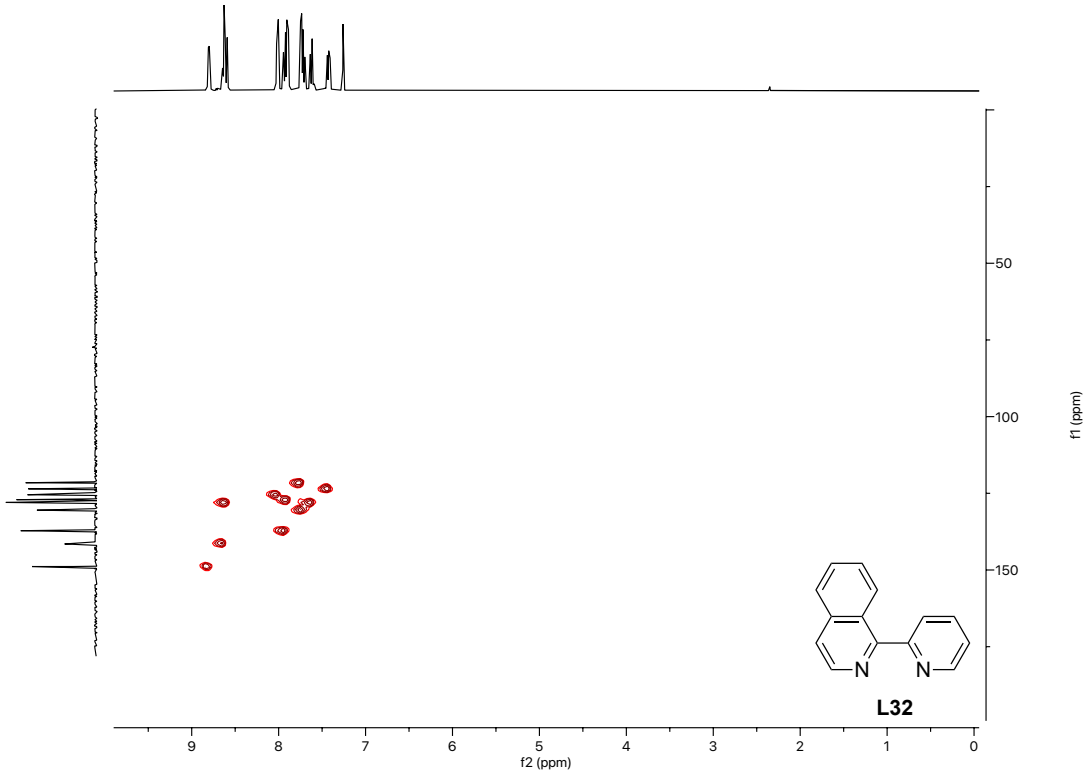
*[13]C NMR 1-(pyridin-2-yl)isoquinoline (L32)*



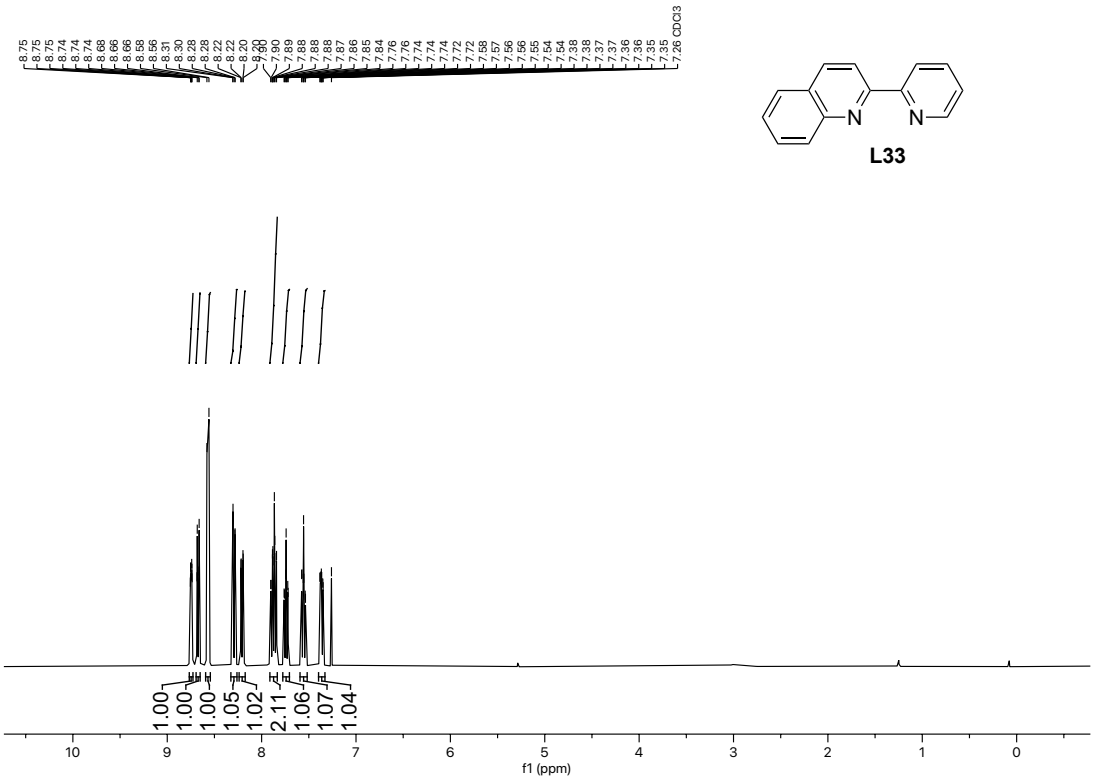



**L32**

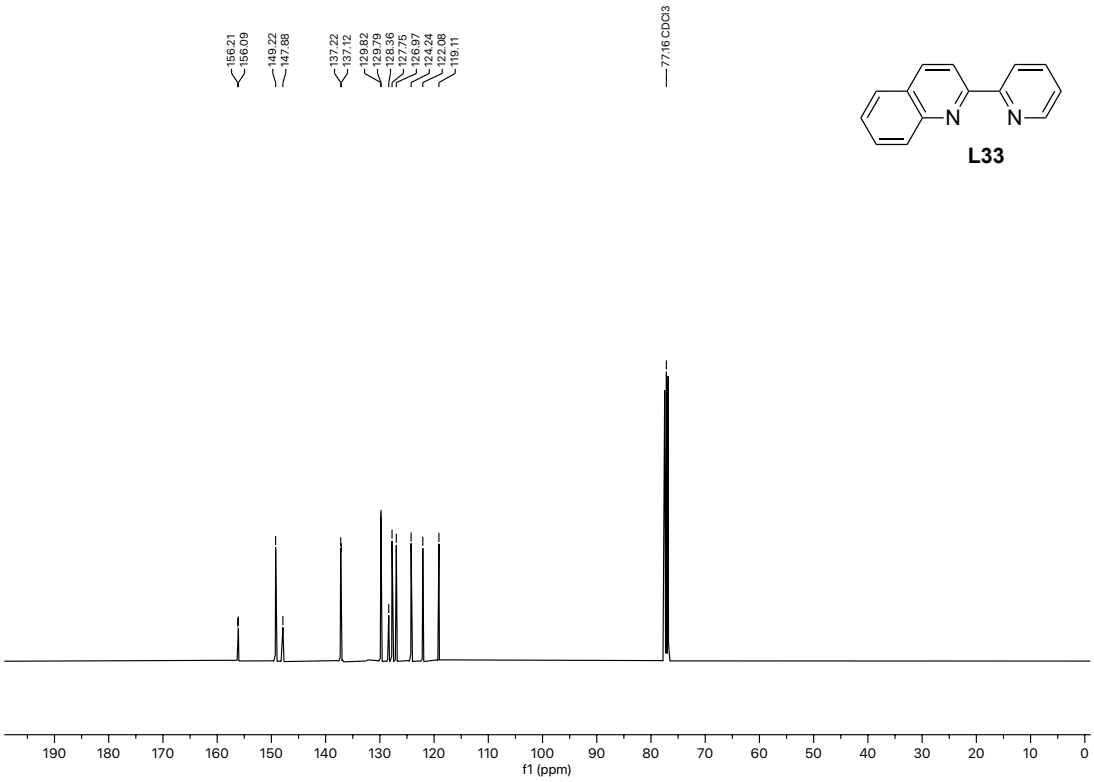
*HSQC NMR 1-(pyridin-2-yl)isoquinoline (L32)*



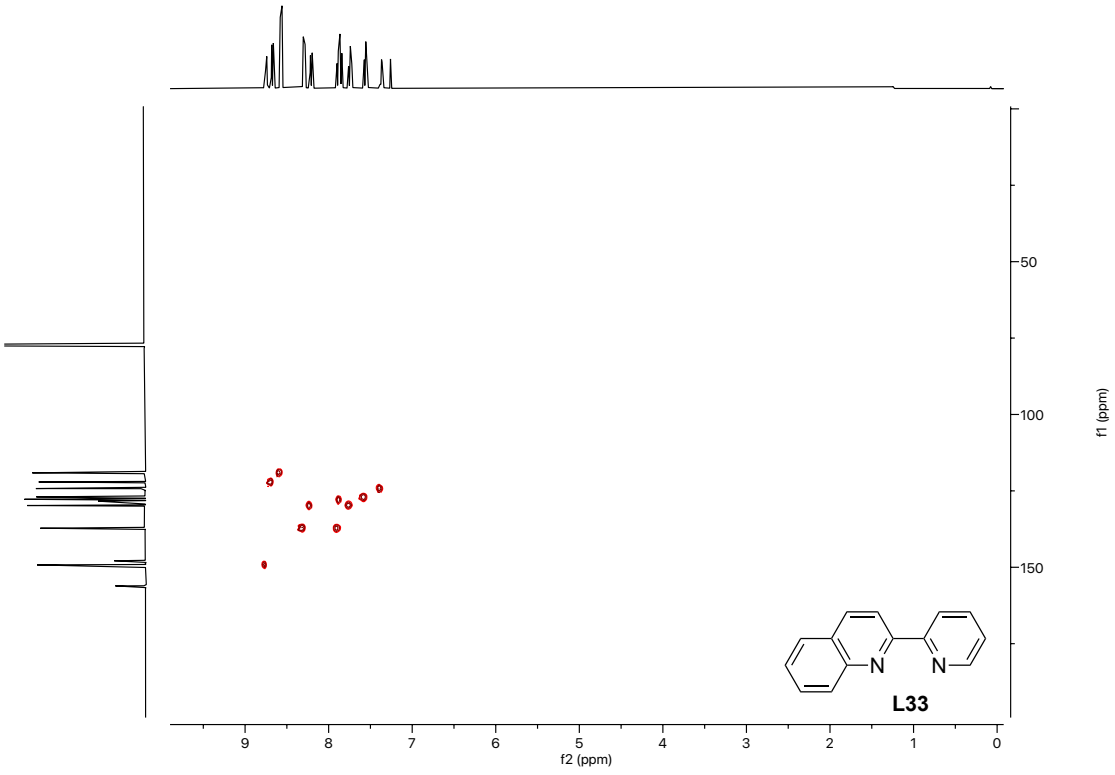

*[1]H NMR 2-(pyridin-2-yl)quinoline (L33)*



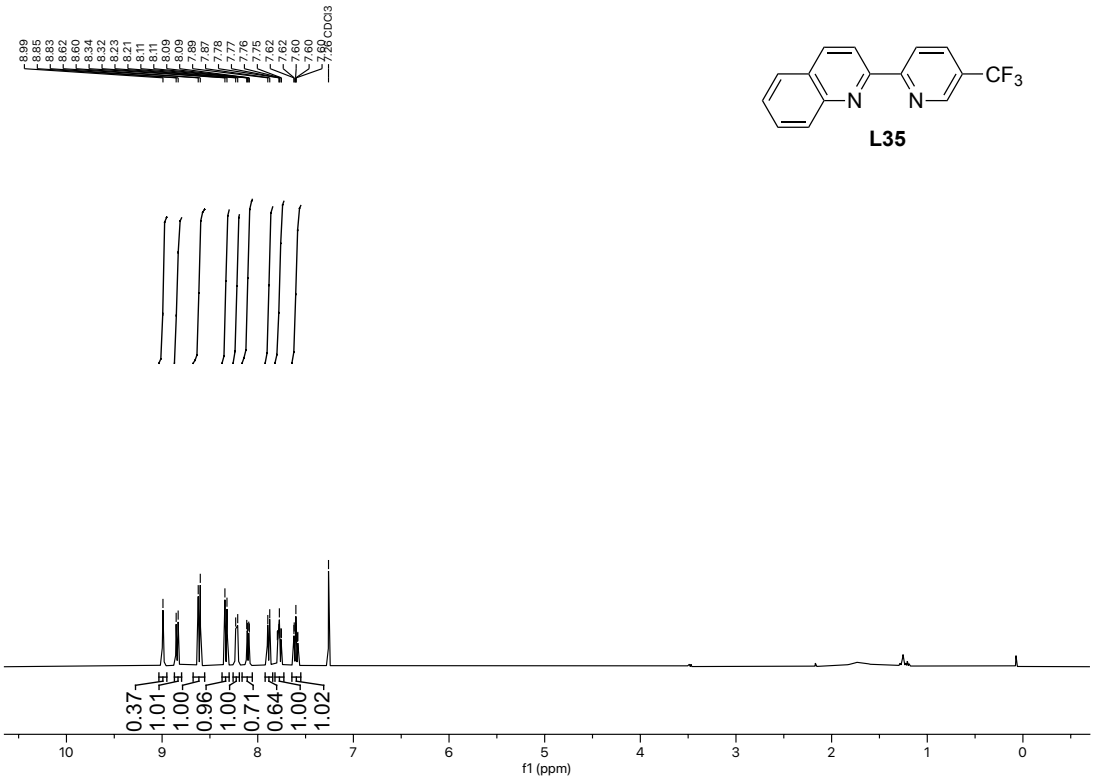
*$^{13}$C NMR 2-(pyridin-2-yl)quinoline (L33)*



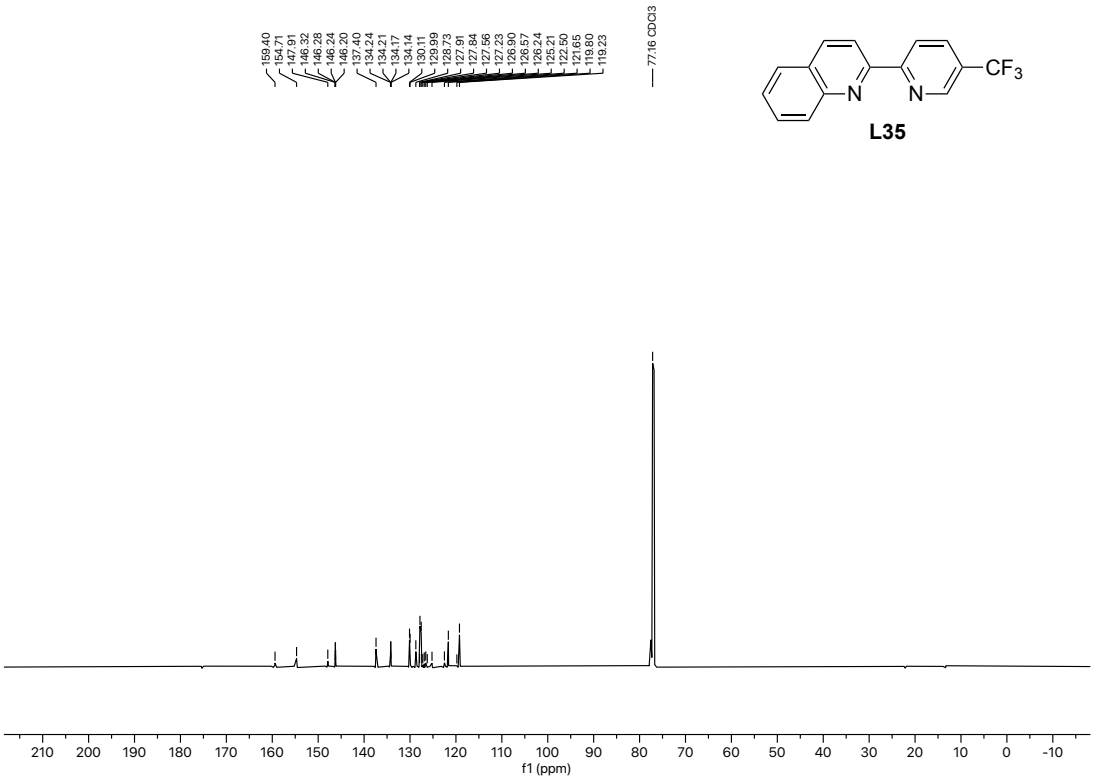

*HSQC NMR 2-(pyridin-2-yl)quinoline (L33)*



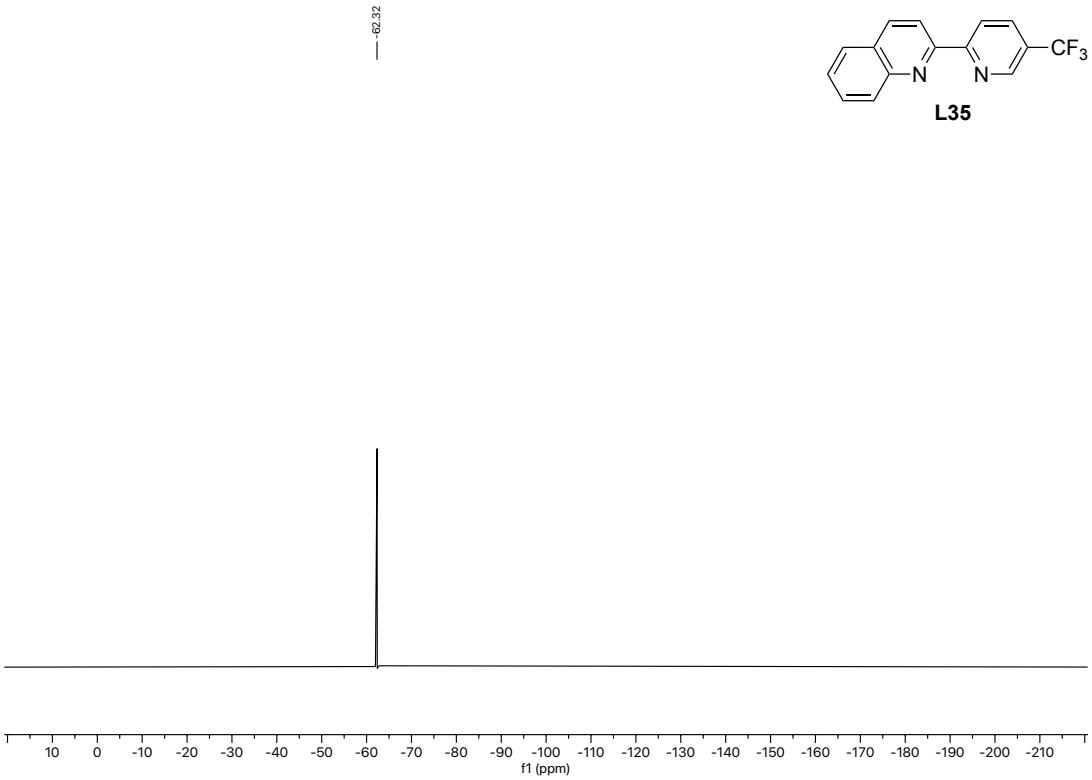
*[1]H NMR 2-(5-(trifluoromethyl)pyridin-2-yl)quinoline (L35)*



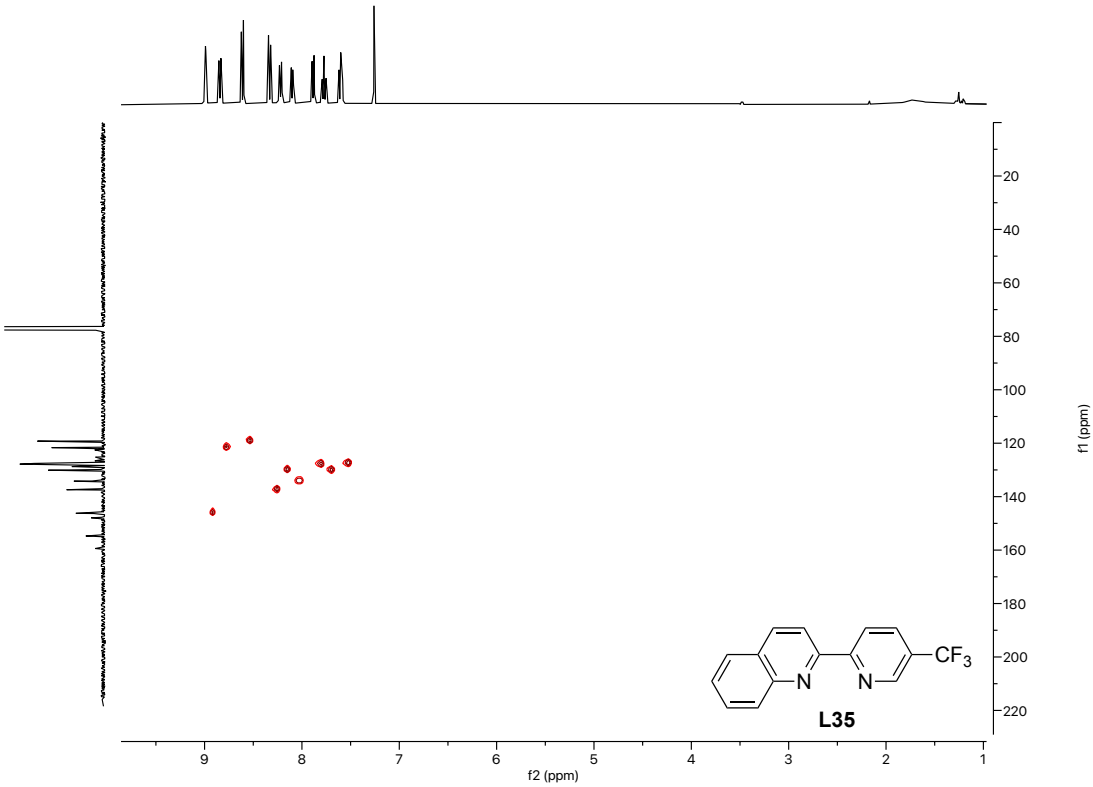

*[13]C NMR 2-(5-(trifluoromethyl)pyridin-2-yl)quinoline (L35)*



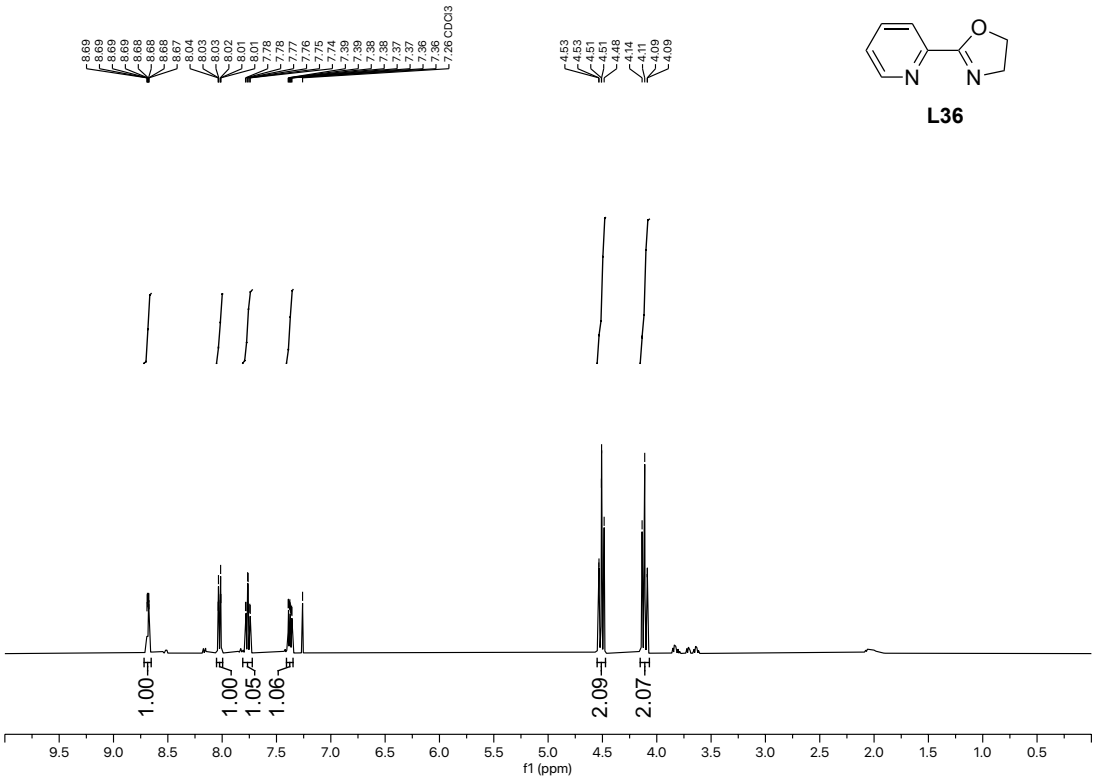
*$^{19}$F NMR 2-(5-(trifluoromethyl)pyridin-2-yl)quinoline (L35)*



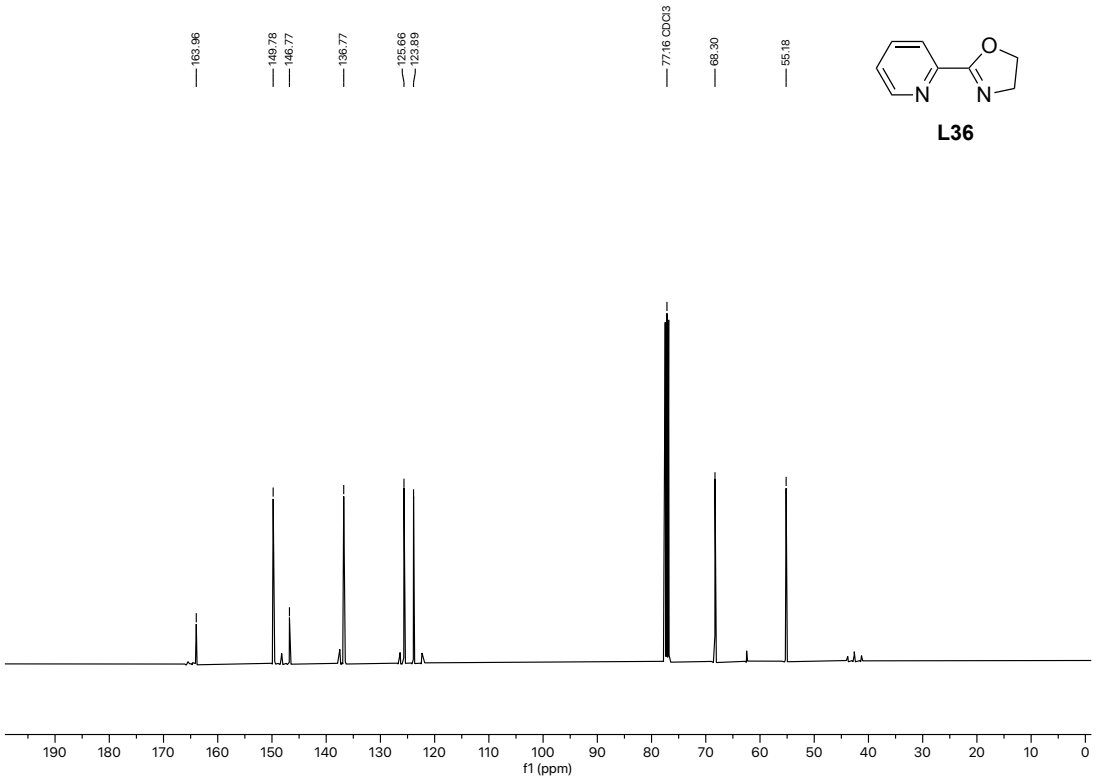

*HSQC NMR 2-(5-(trifluoromethyl)pyridin-2-yl)quinoline (L35)*



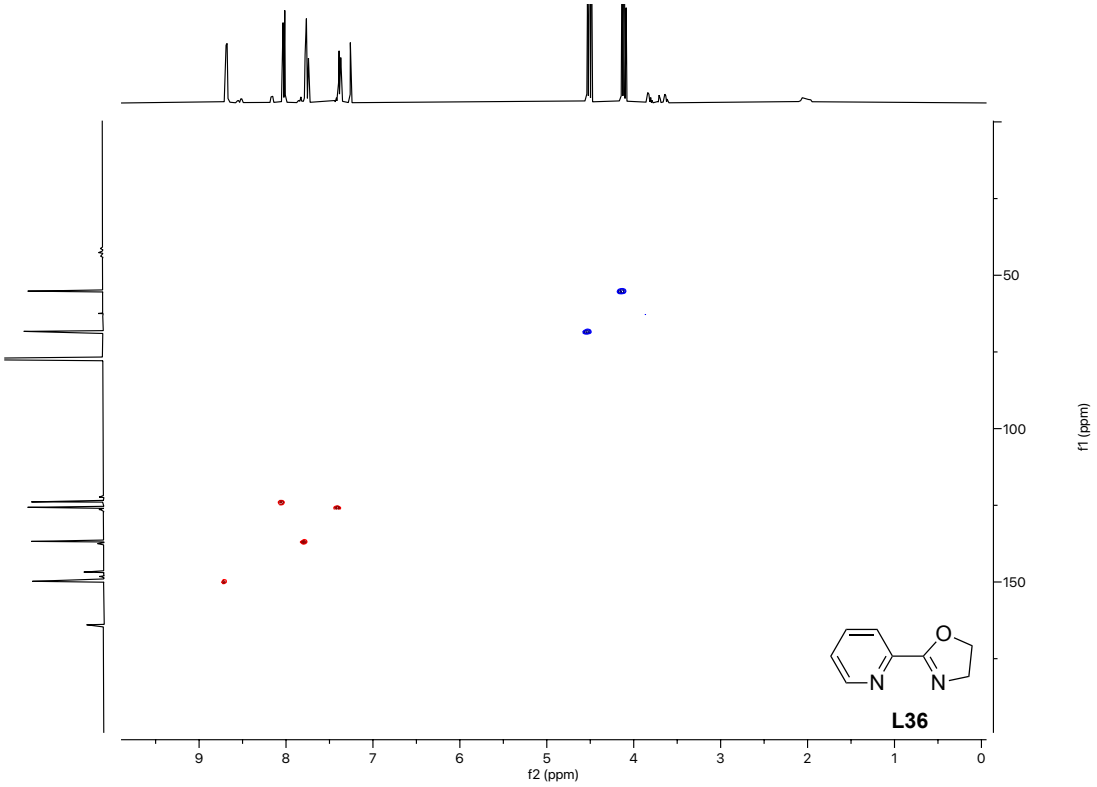
*[1]H NMR 2-(pyridin-2-yl)-4,5-dihydrooxazole (L36)*



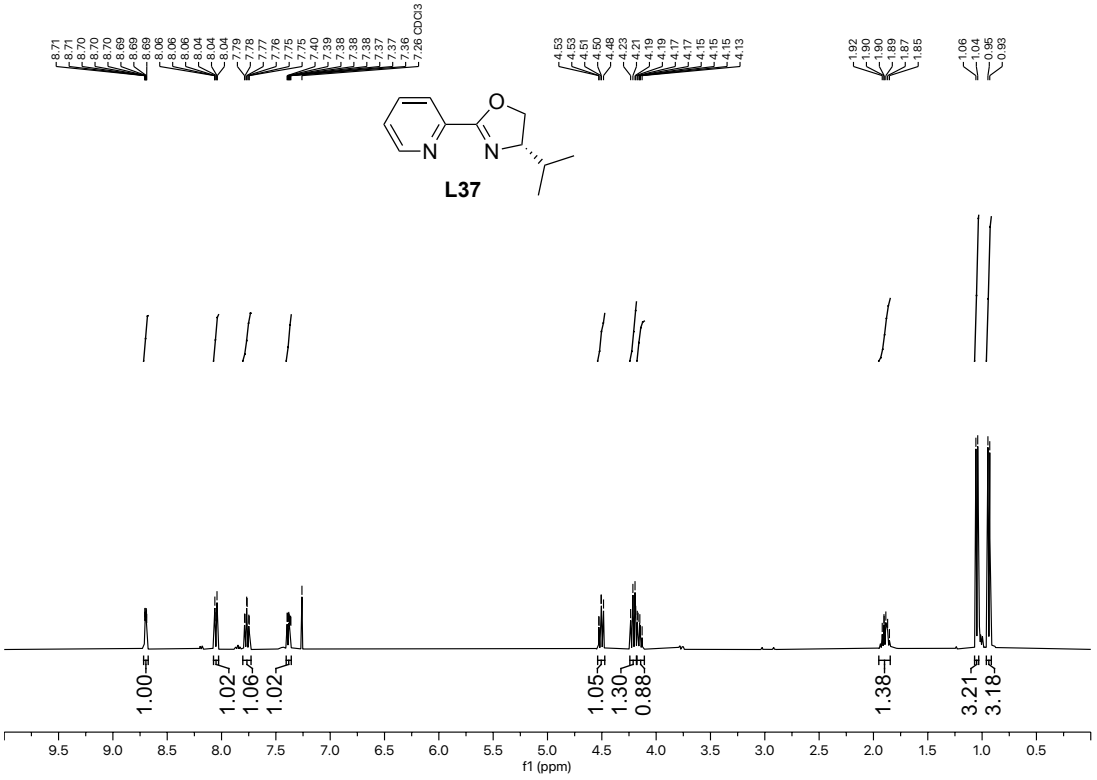

*[13]C NMR 2-(pyridin-2-yl)-4,5-dihydrooxazole (L36)*



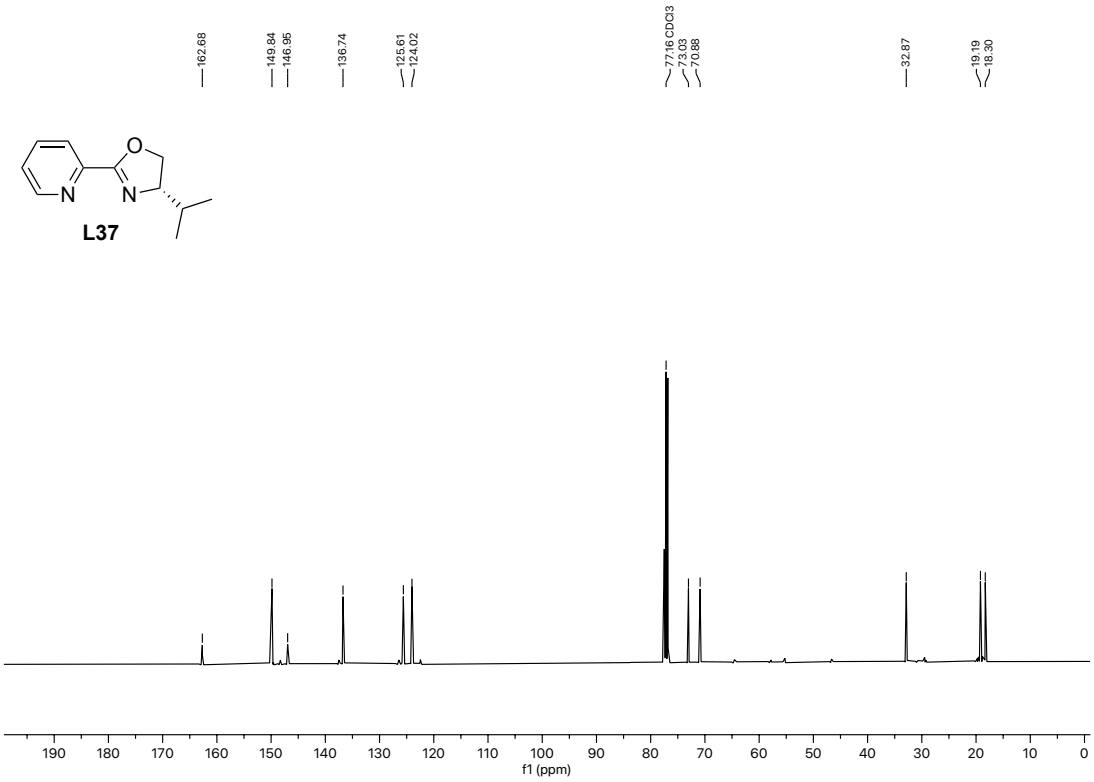
*HSQC NMR 2-(pyridin-2-yl)-4,5-dihydrooxazole (L36)*



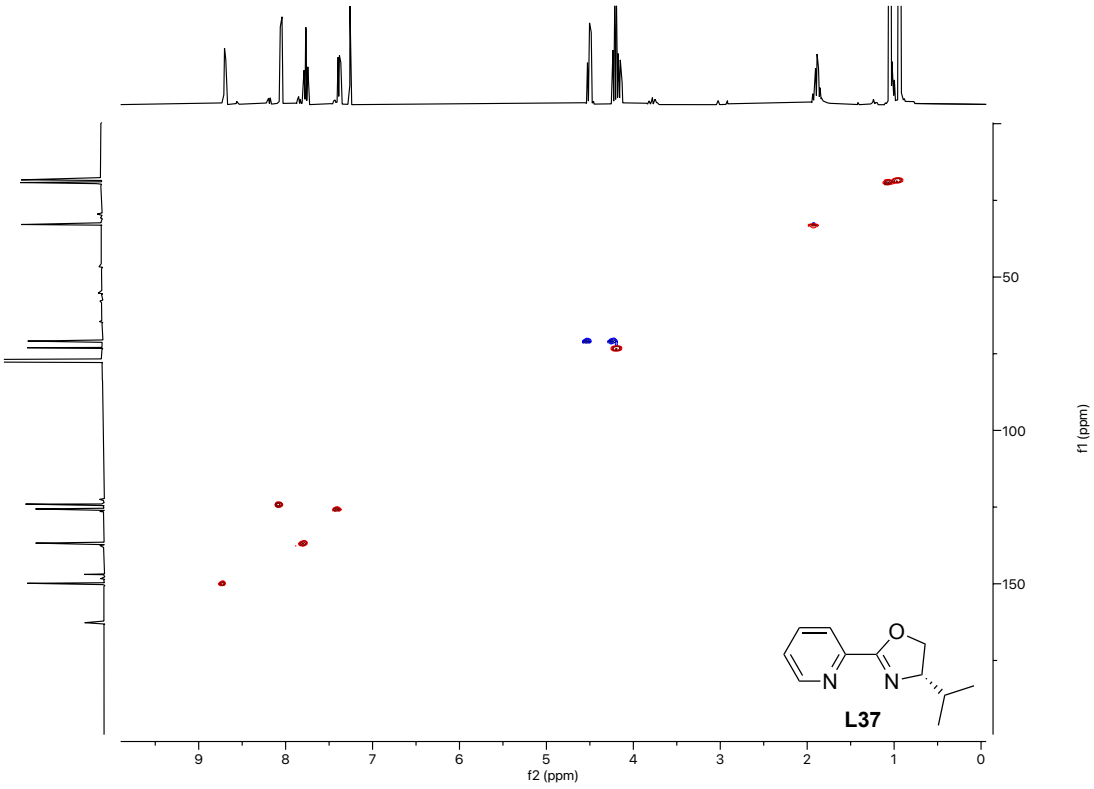

*[1]H NMR (S)-4-isopropyl-2-(pyridin-2-yl)-4,5-dihydrooxazole (L37)*



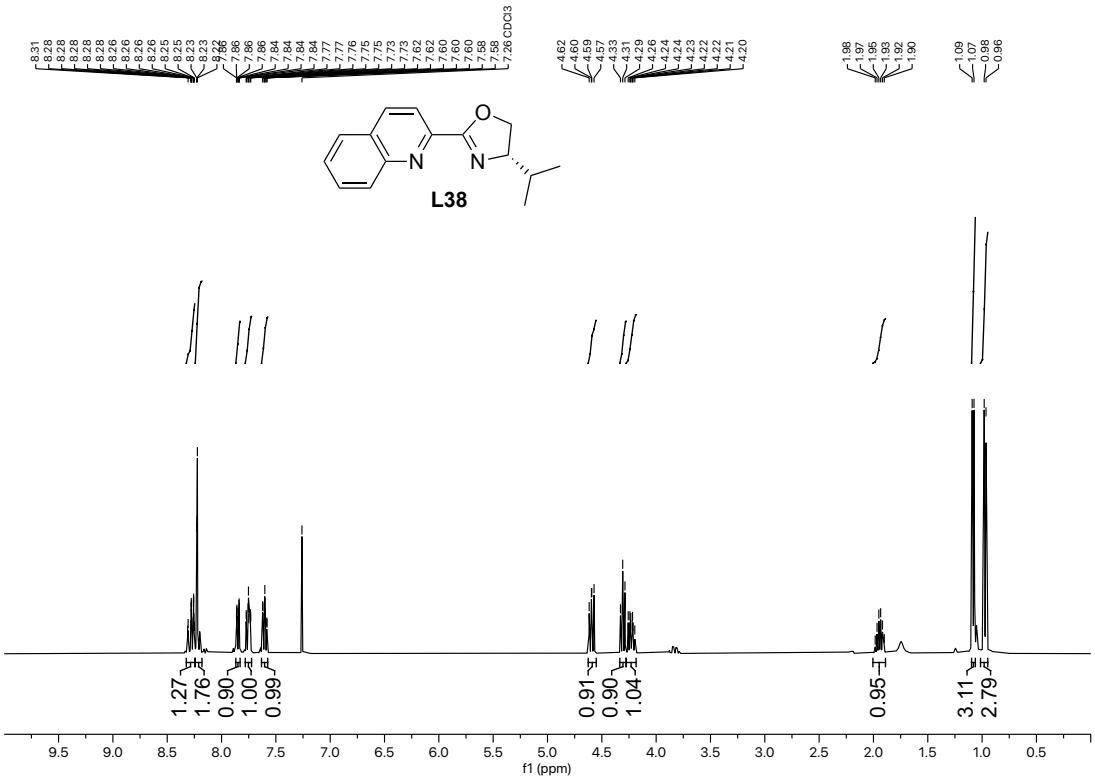
*$^{13}$C NMR (S)-4-isopropyl-2-(pyridin-2-yl)-4,5-dihydrooxazole (L37)*



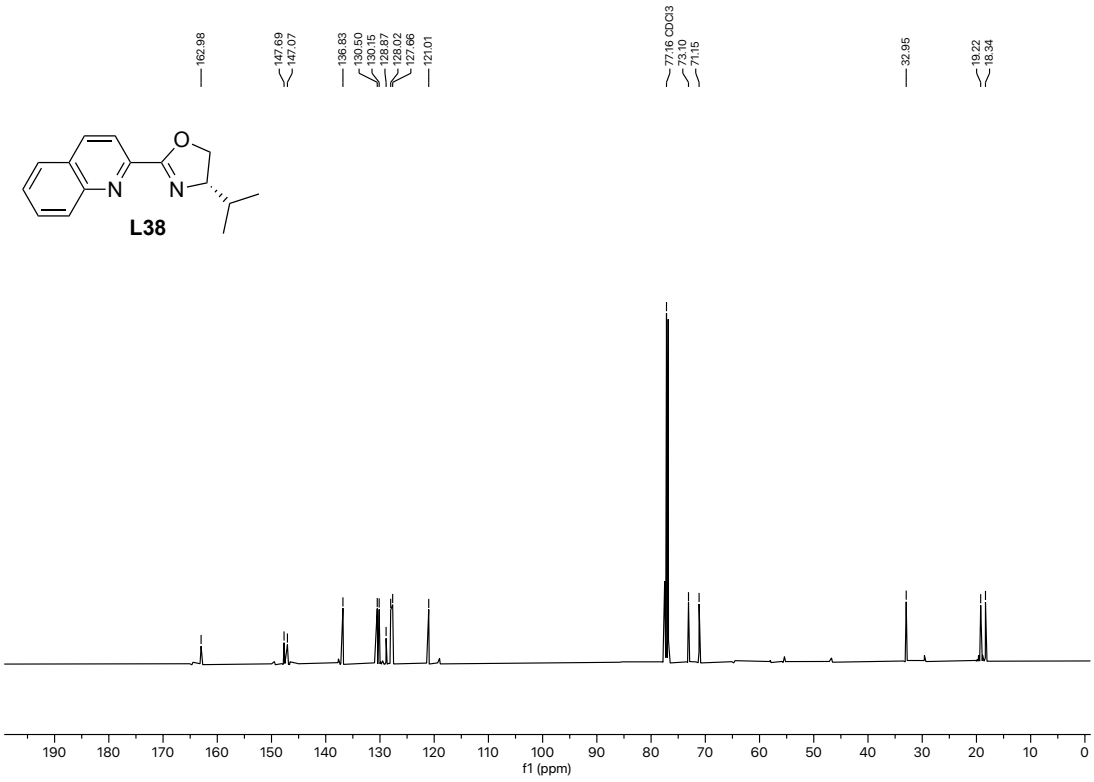

*HSQC NMR (S)-4-isopropyl-2-(pyridin-2-yl)-4,5-dihydrooxazole (L37)*



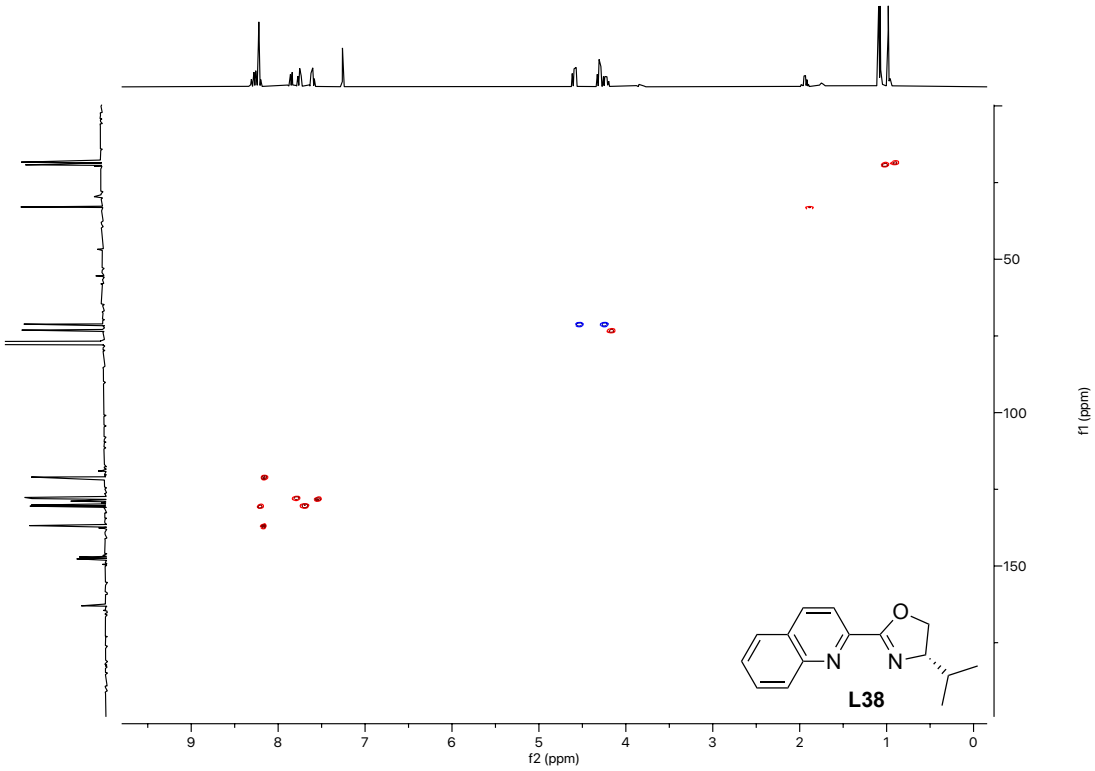
*[1]H NMR (S)-4-isopropyl-2-(quinolin-2-yl)-4,5-dihydrooxazole (L38)*



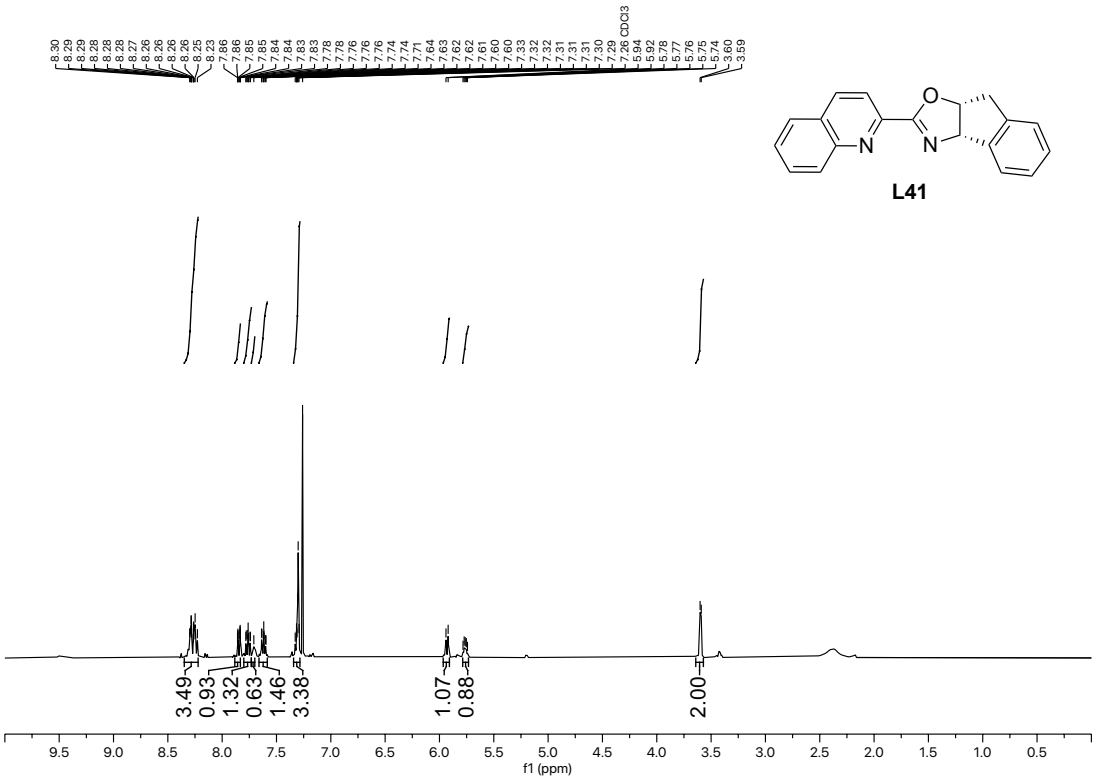

*[13]C NMR (S)-4-isopropyl-2-(quinolin-2-yl)-4,5-dihydrooxazole (L38)*



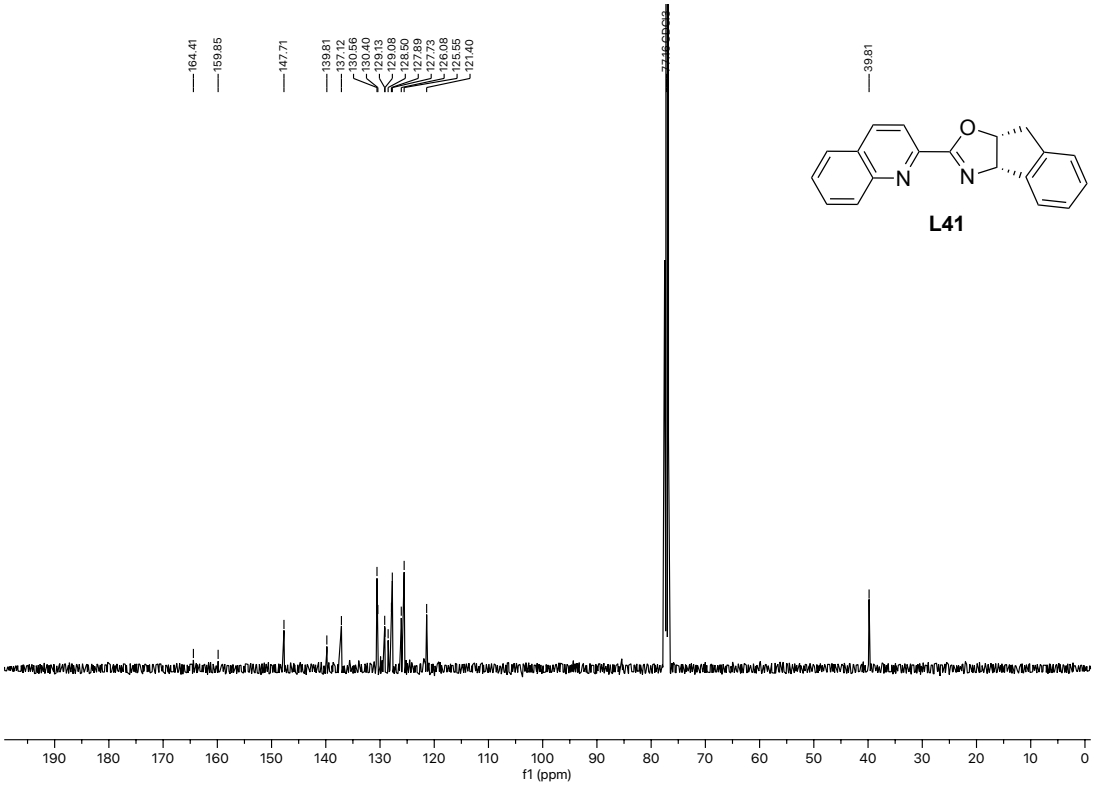
*HSQC NMR (S)-4-isopropyl-2-(quinolin-2-yl)-4,5-dihydrooxazole (L38)*



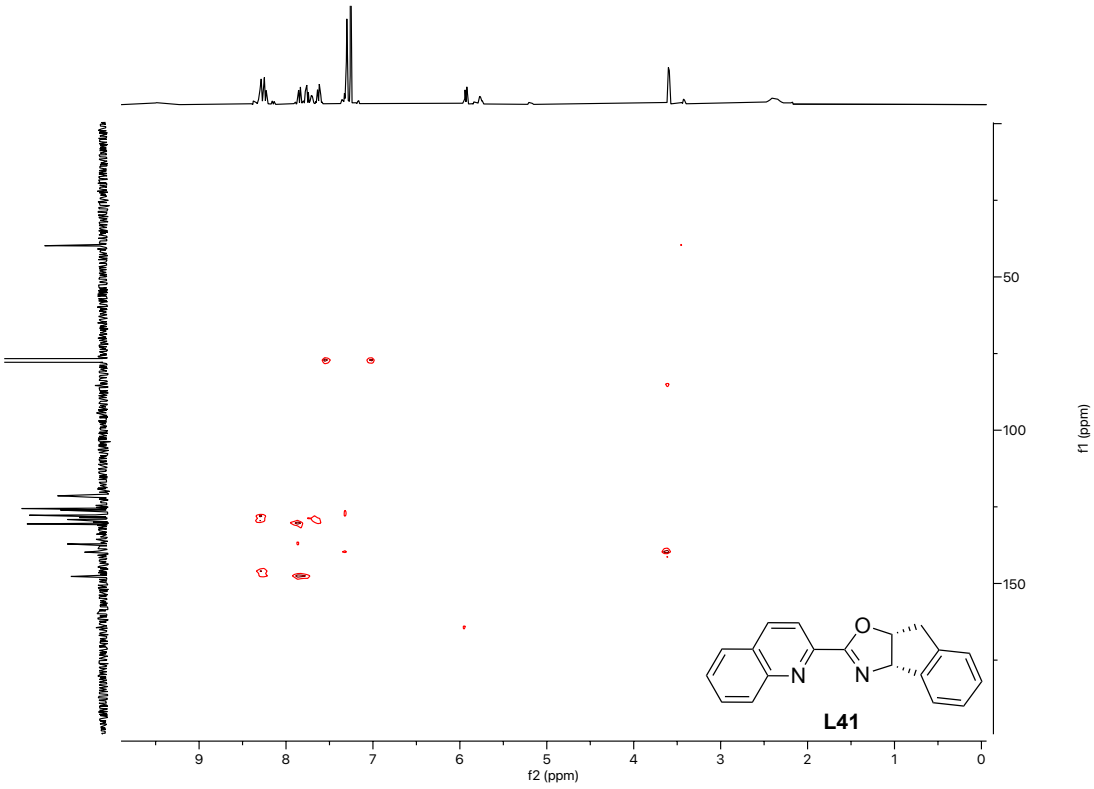

*$^{1}$H NMR (3aS,8aR)-2-(quinolin-2-yl)-3a,8a-dihydro-8H-indeno[1,2-d]oxazole (L41)*



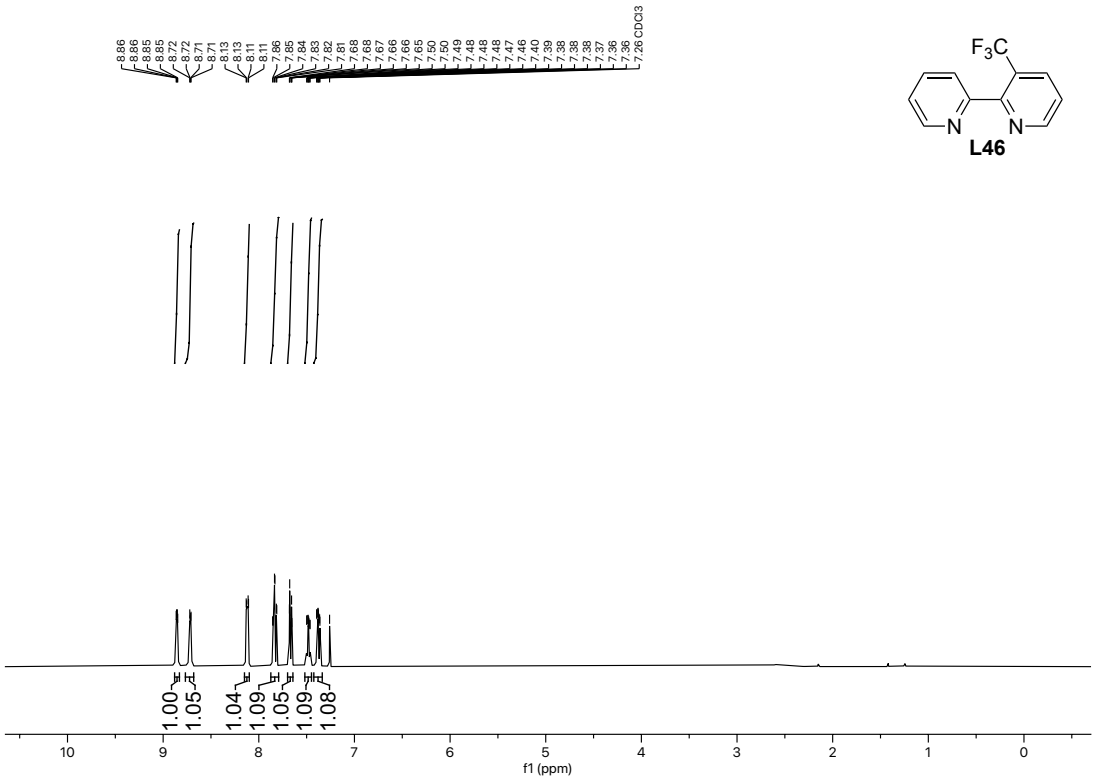
*$^{13}$C NMR (3aS,8aR)-2-(quinolin-2-yl)-3a,8a-dihydro-8H-indeno[1,2-d]oxazole (L41)*



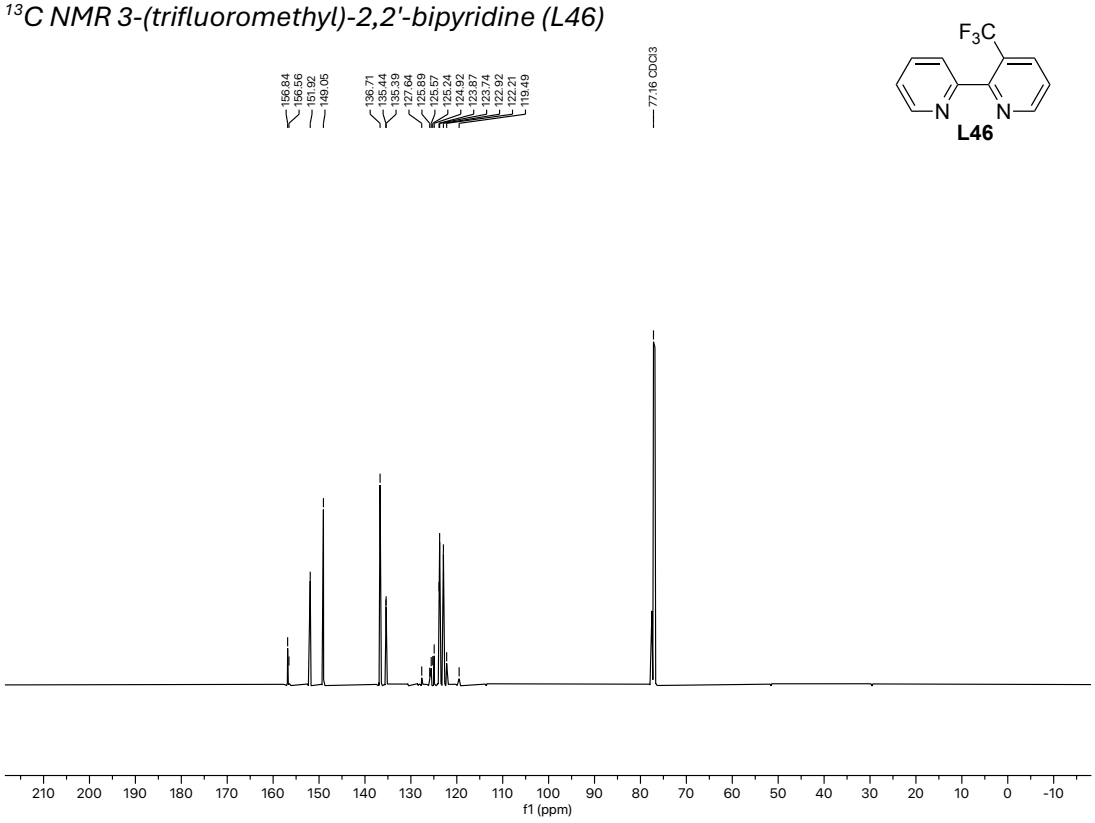

*HSQC NMR (3aS,8aR)-2-(quinolin-2-yl)-3a,8a-dihydro-8H-indeno[1,2-d]oxazole (L41)*



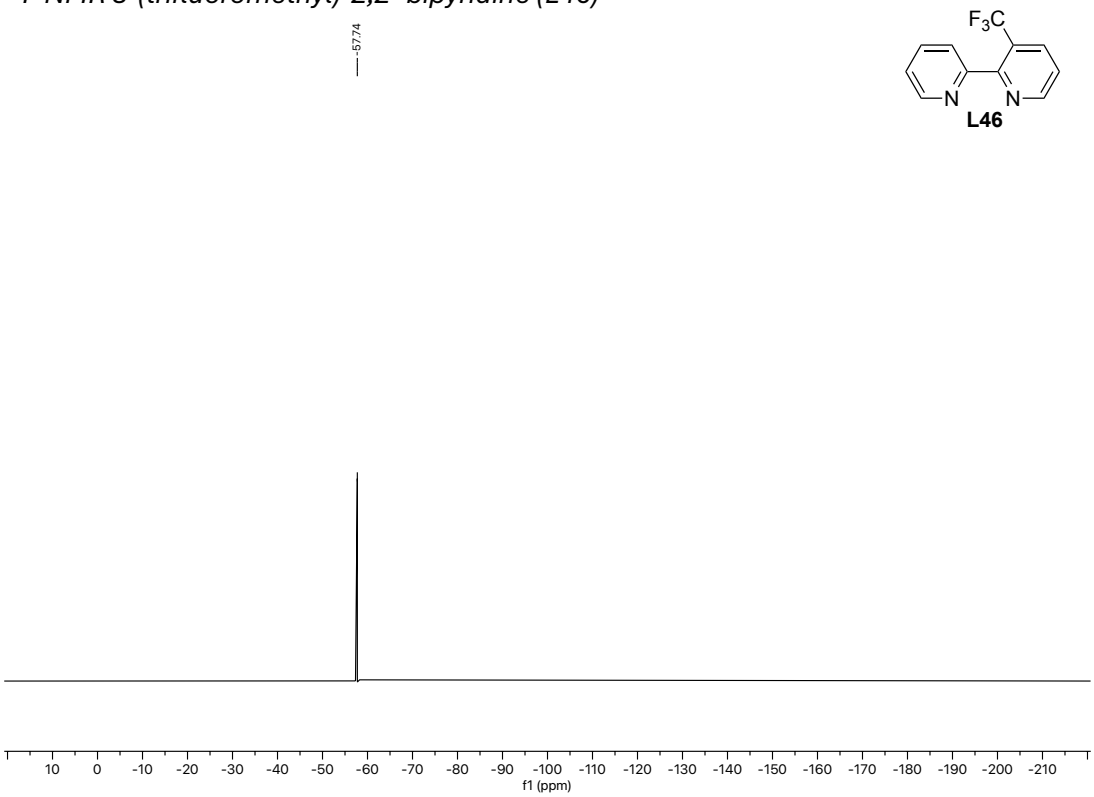
*[1]H NMR 3-(trifluoromethyl)-2,2'-bipyridine (L46)*



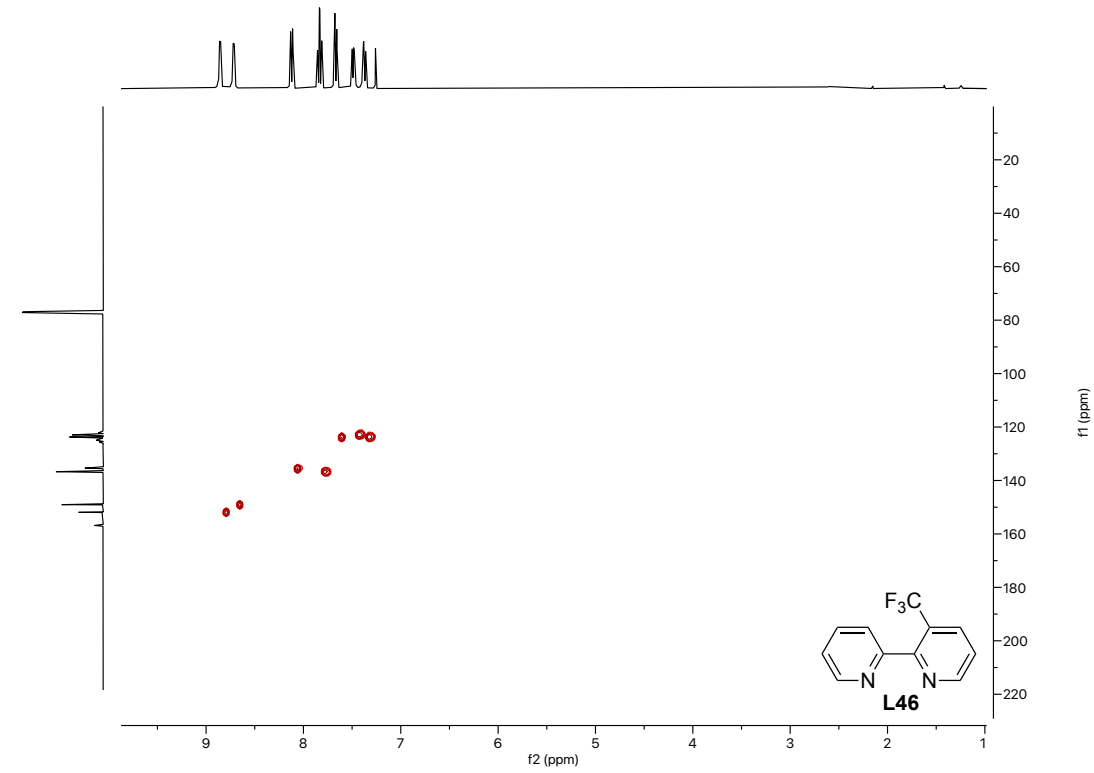

*[13]C NMR 3-(trifluoromethyl)-2,2'-bipyridine (L46)*



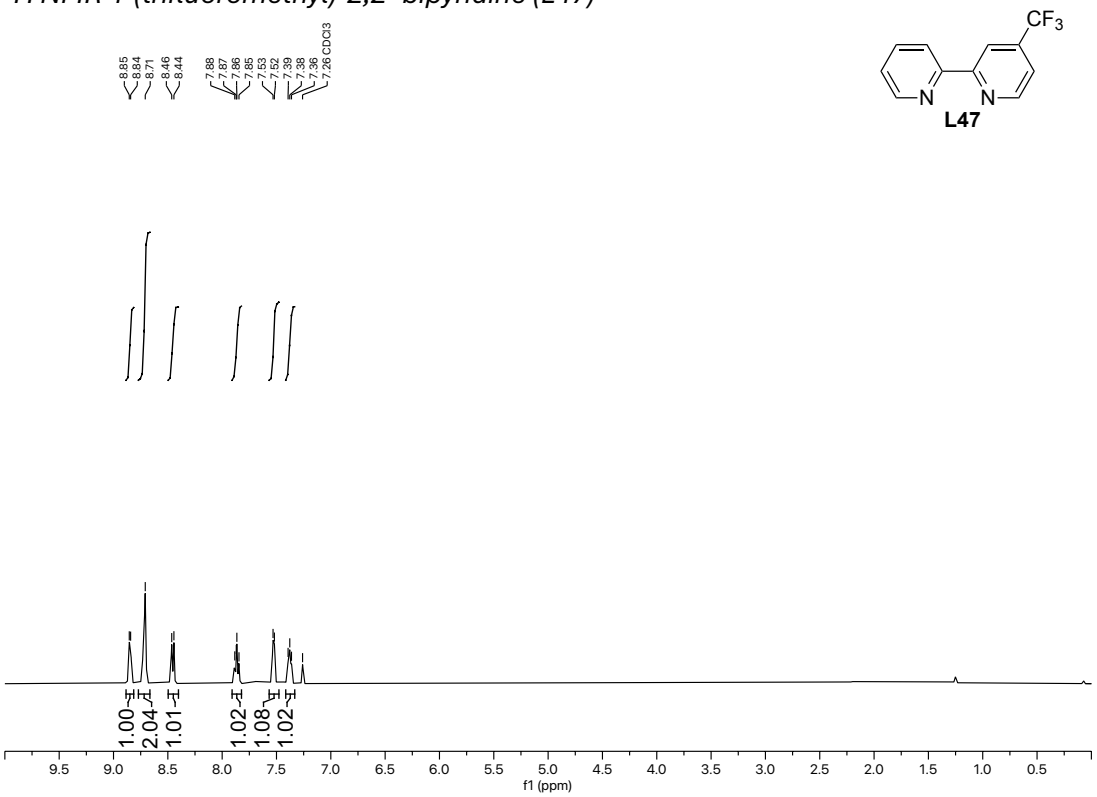
*$^{19}$F NMR 3-(trifluoromethyl)-2,2'-bipyridine (L46)*




*HSQC NMR 3-(trifluoromethyl)-2,2'-bipyridine (L46)*



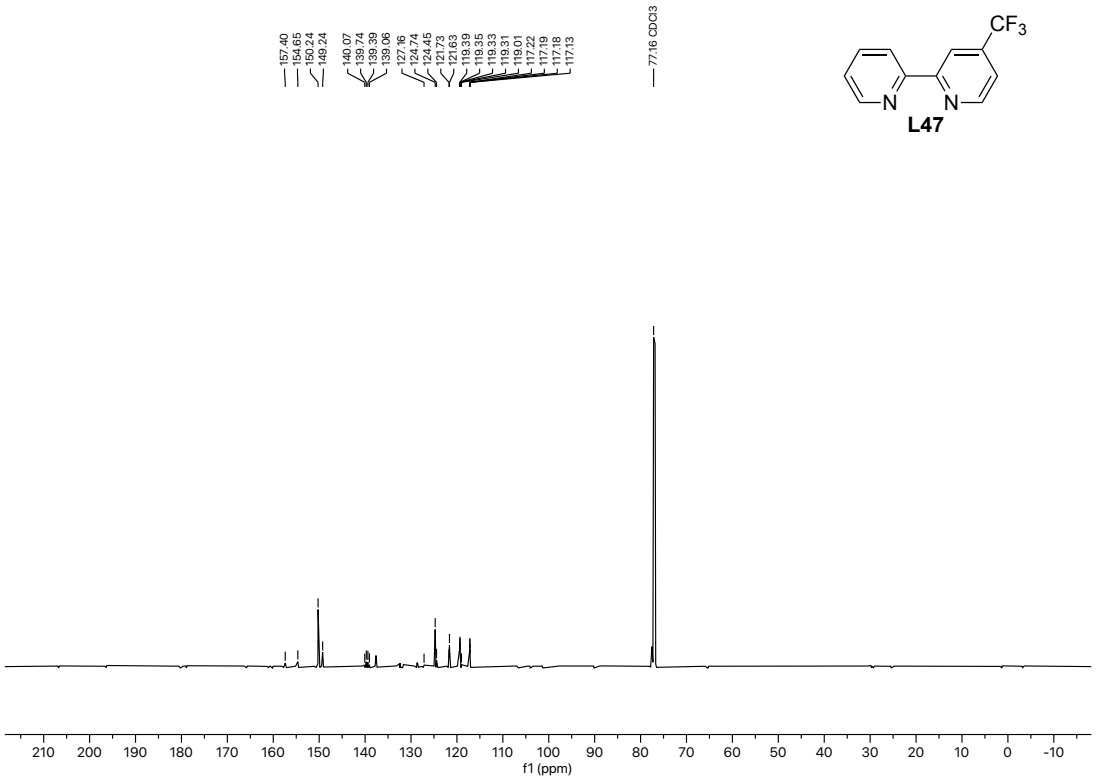
*[1]H NMR 4-(trifluoromethyl)-2,2'-bipyridine (L47)*



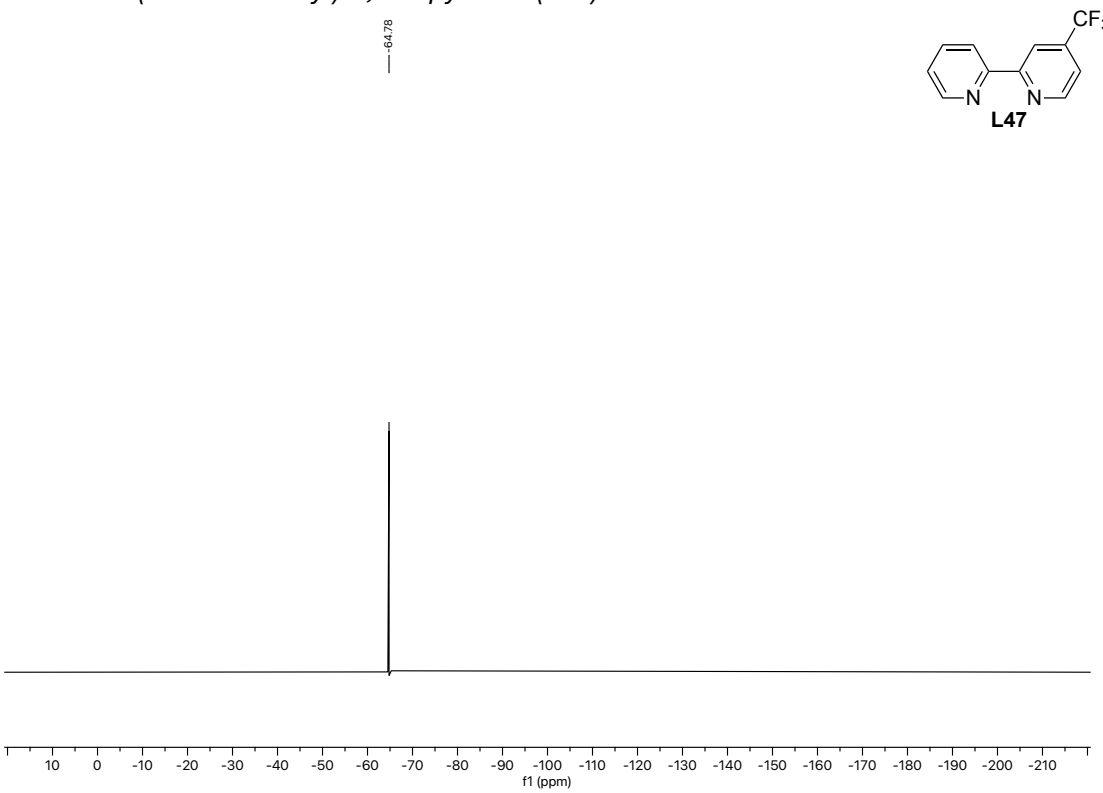




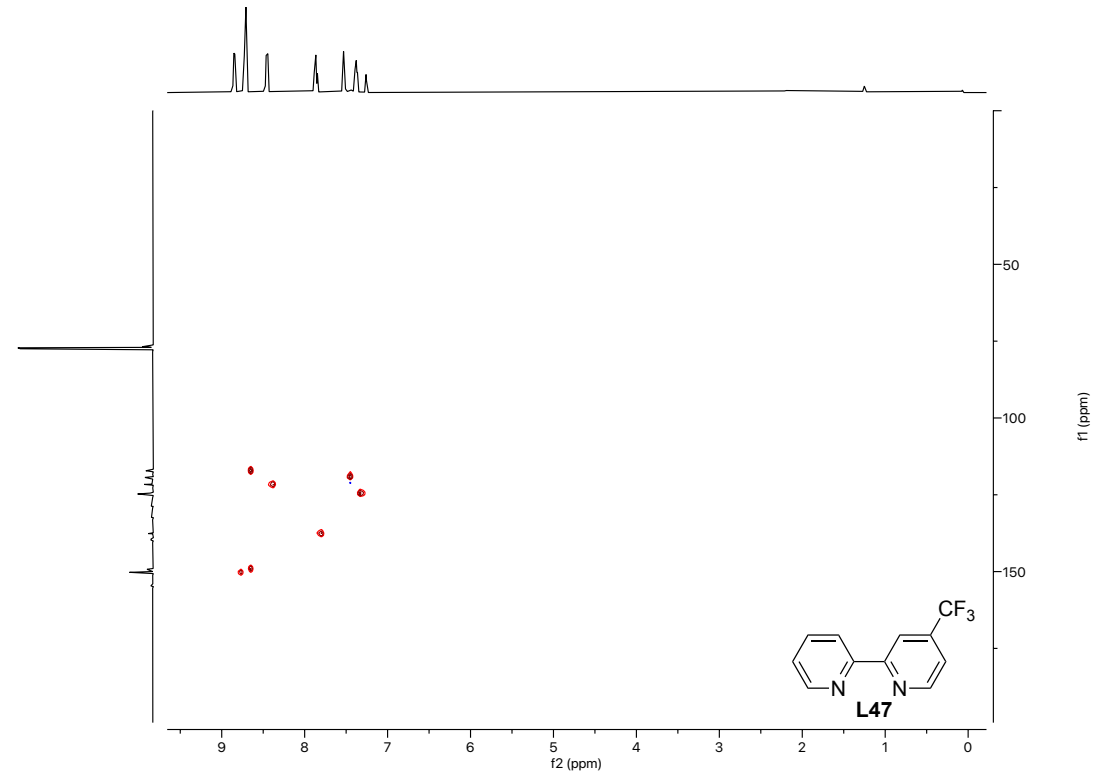
*[13]C NMR 4-(trifluoromethyl)-2,2'-bipyridine (L47)*



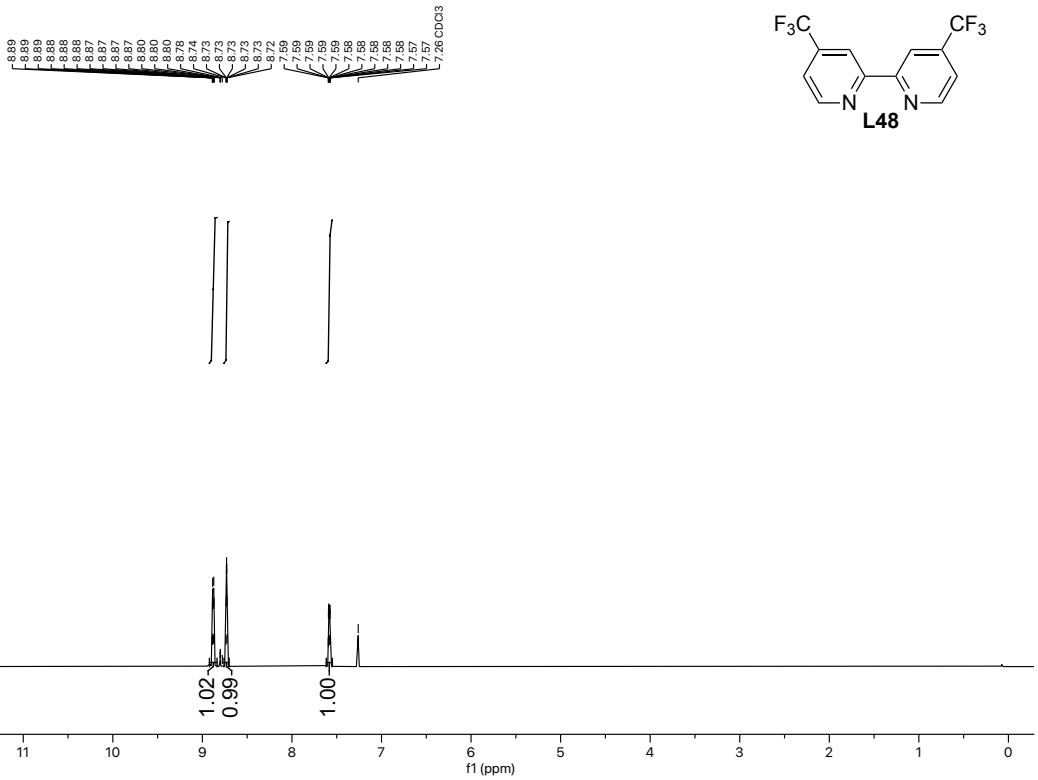
*$^{19}$F NMR 4-(trifluoromethyl)-2,2'-bipyridine (L47)*



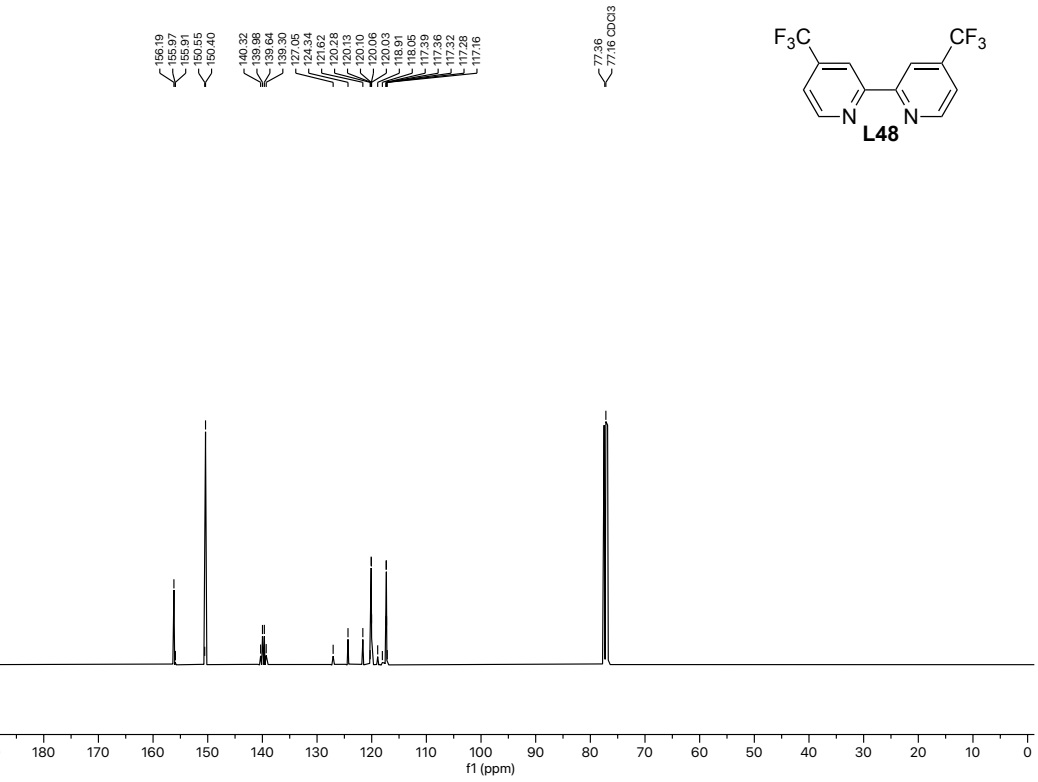

*HSQC NMR 4-(trifluoromethyl)-2,2'-bipyridine (L47)*



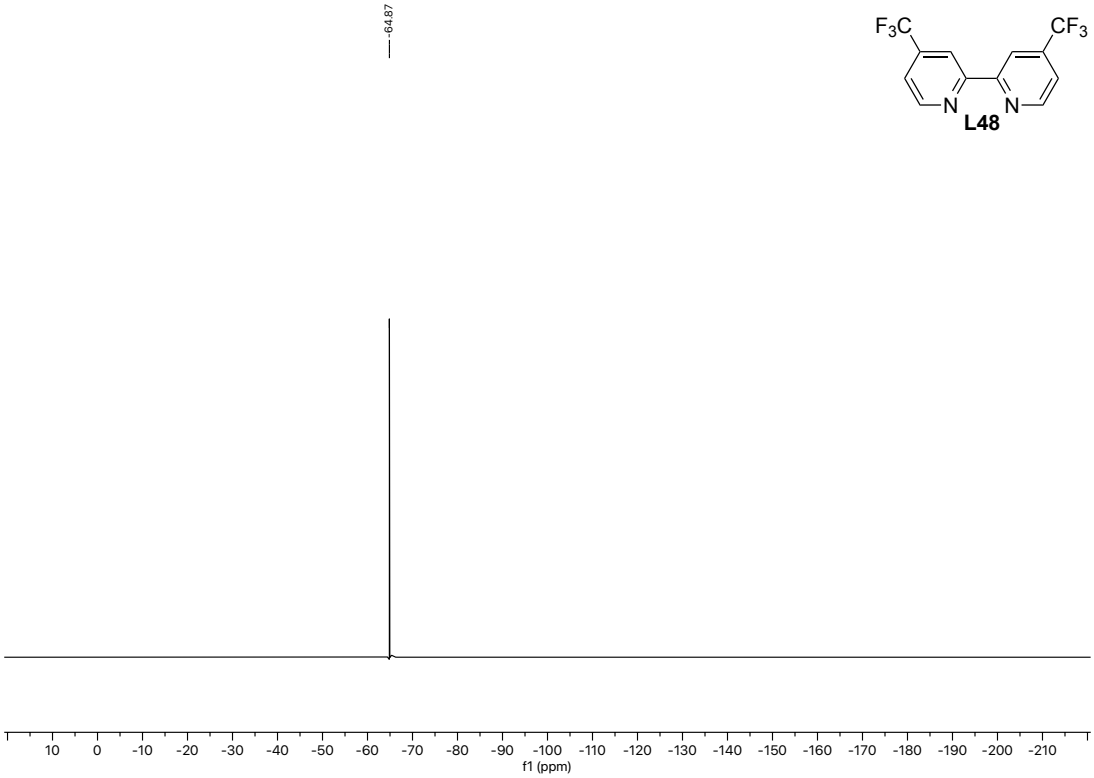
*[1]H NMR 4,4'-bis(trifluoromethyl)-2,2'-bipyridine (L48)*



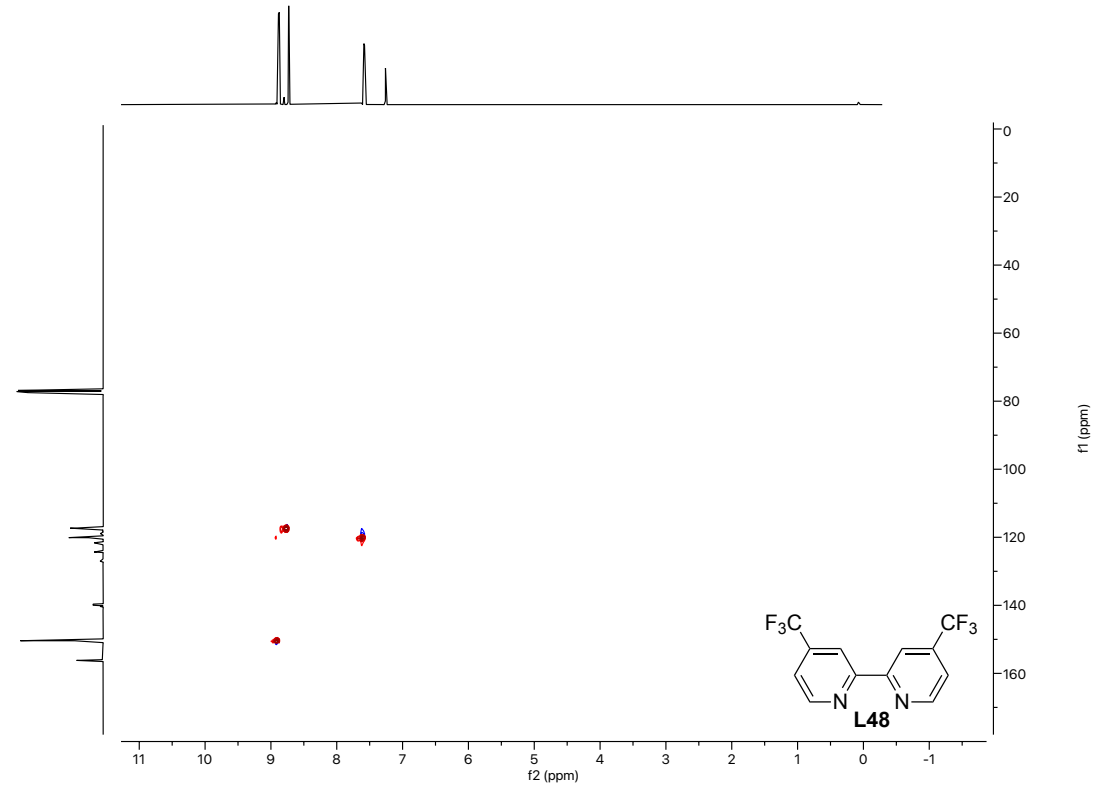

*[13]C NMR 4,4'-bis(trifluoromethyl)-2,2'-bipyridine (L48)*



*$^{19}$F NMR 4,4'-bis(trifluoromethyl)-2,2'-bipyridine (L48)*

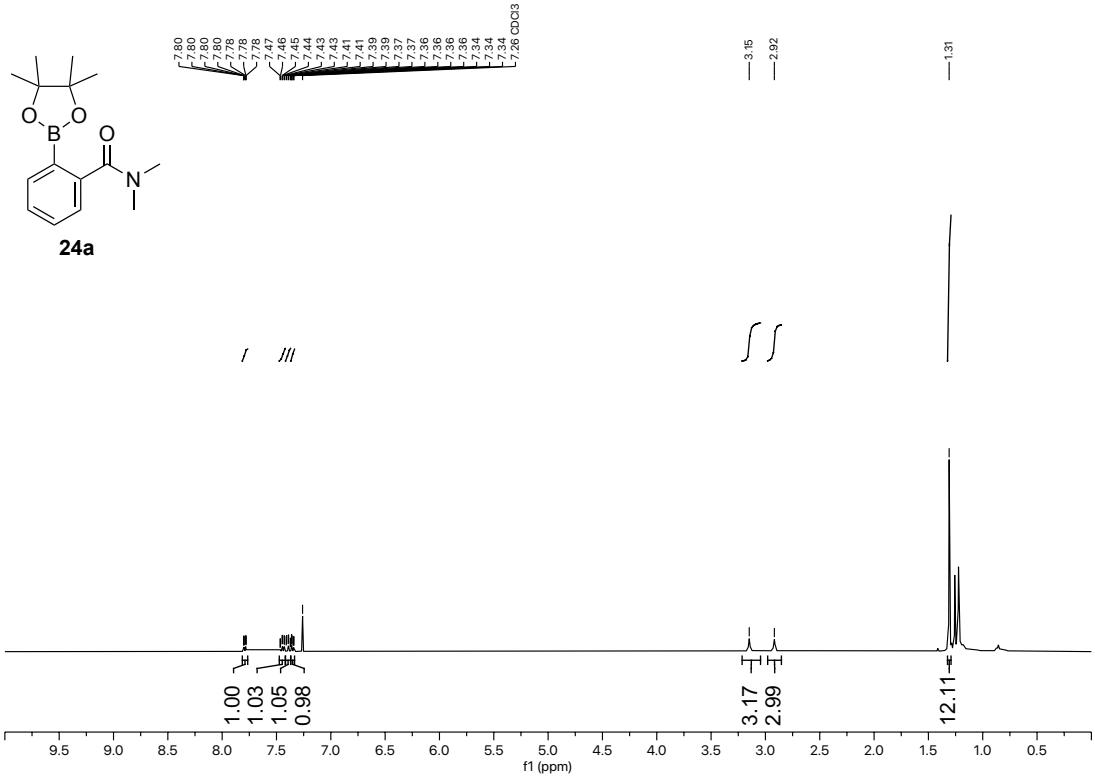



*HSQC NMR 4,4'-bis(trifluoromethyl)-2,2'-bipyridine (L48)*



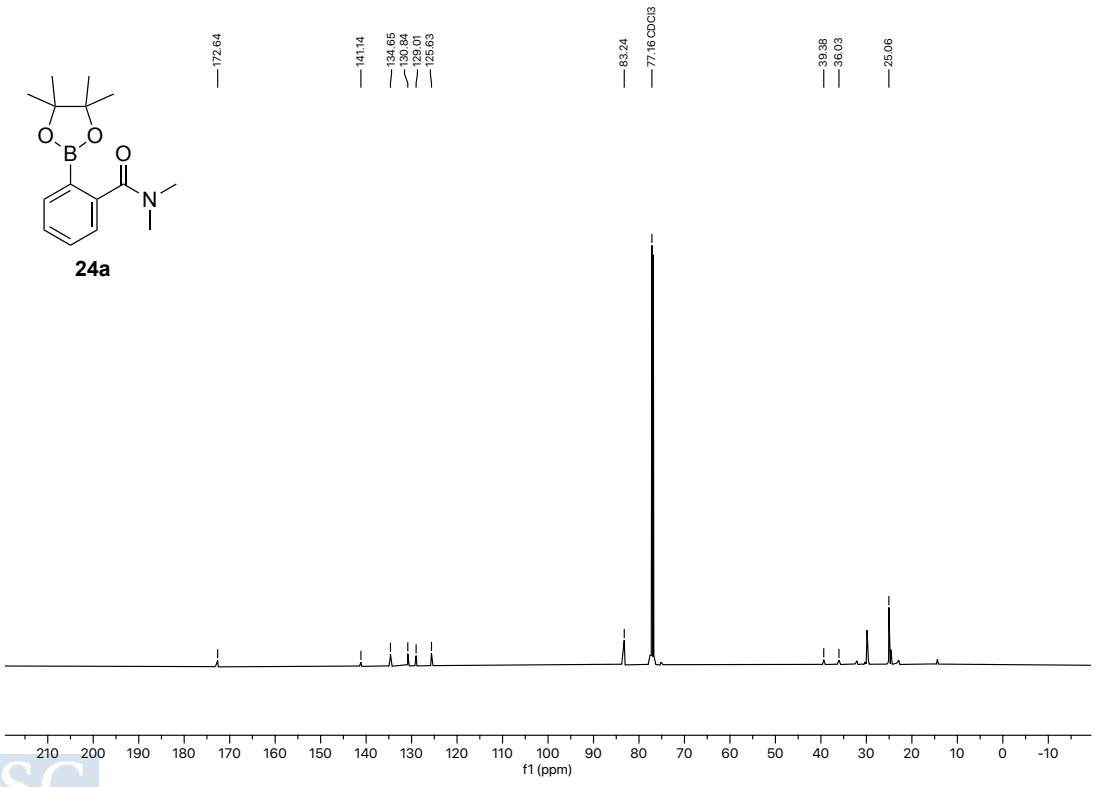
### *11.1.2.1 Selected spectra of products*

*$^{1}$H NMR N,N-dimethyl-2-(4,4,5,5-tetramethyl-1,3,2-dioxaborolan-2-yl)benzamide (24a)*



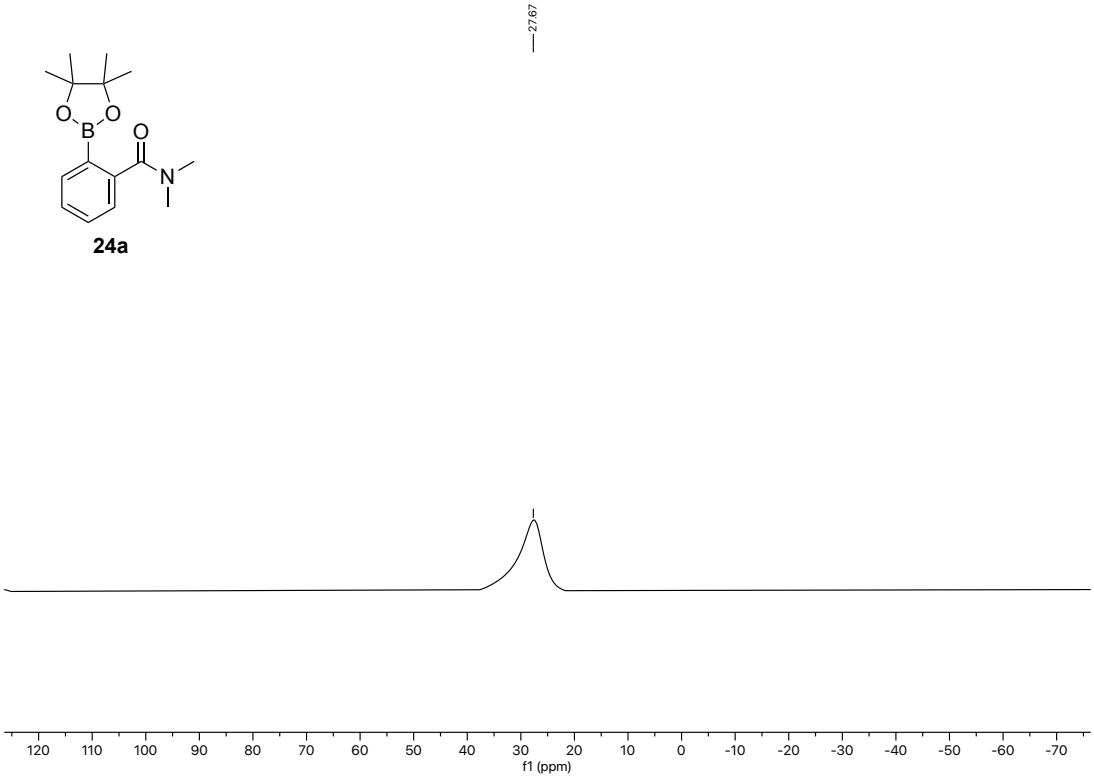

**24a**

*$^{13}$C NMR N,N-dimethyl-2-(4,4,5,5-tetramethyl-1,3,2-dioxaborolan-2-yl)benzamide (24a)*

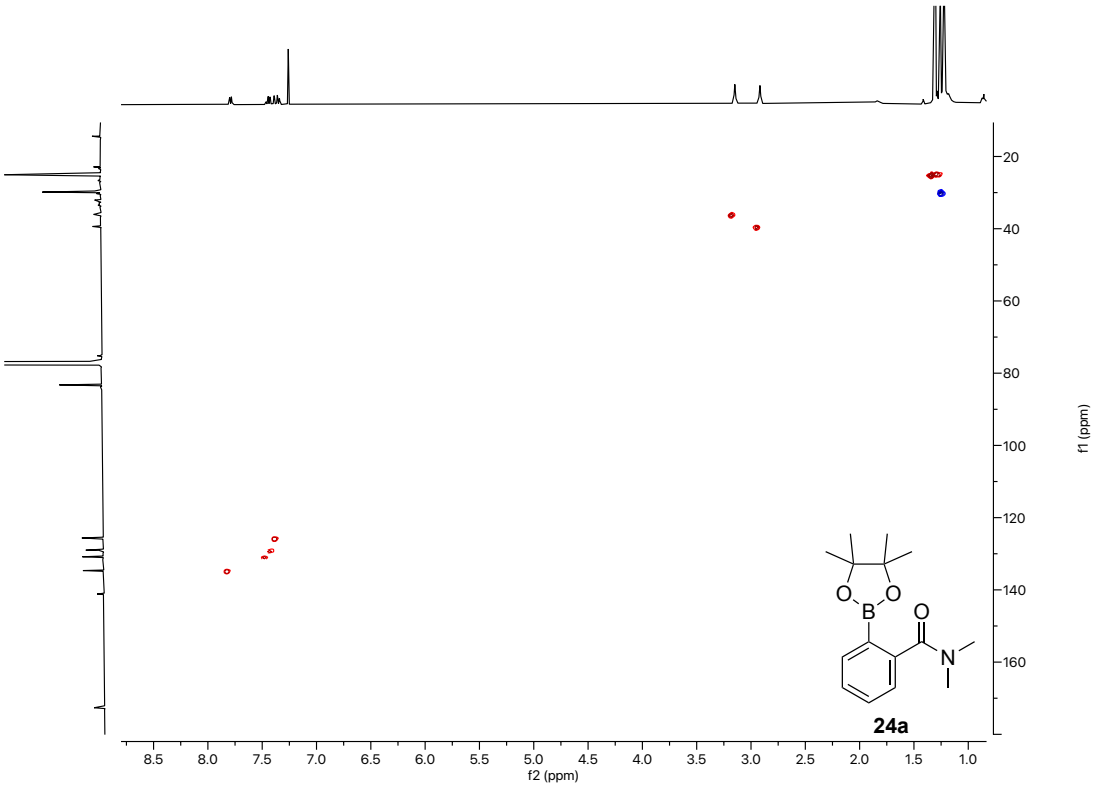



**24a**

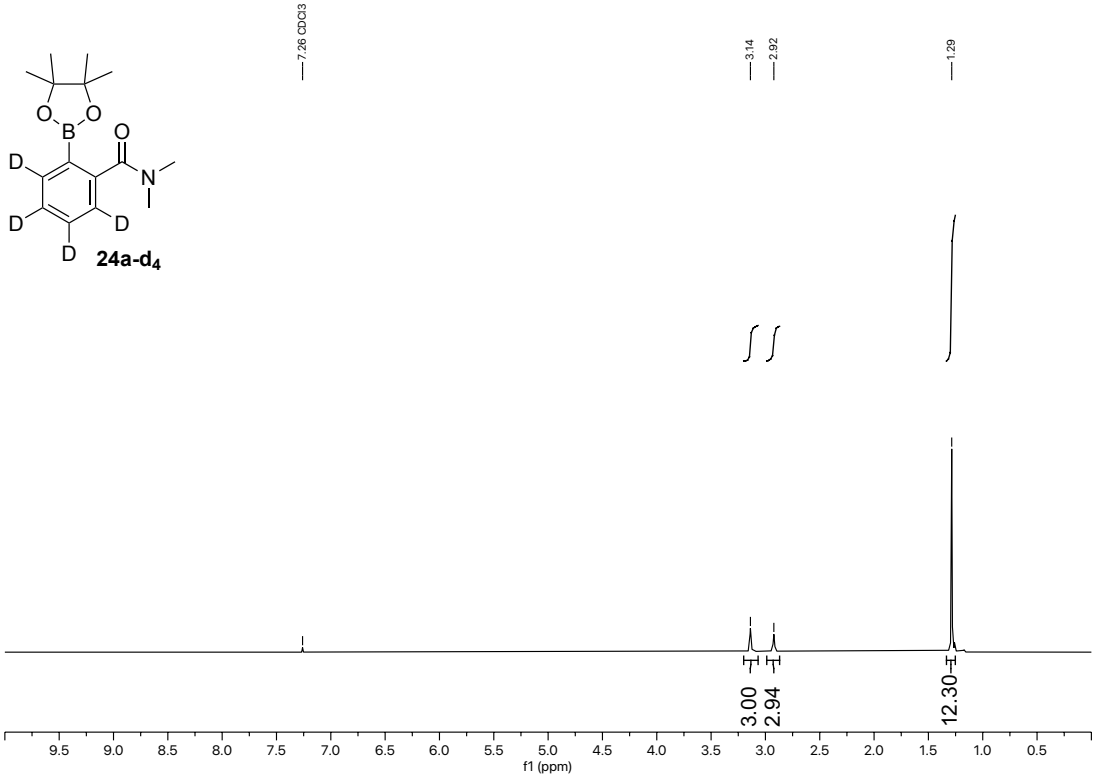
*[11]B NMR N,N-dimethyl-2-(4,4,5,5-tetramethyl-1,3,2-dioxaborolan-2-yl)benzamide (24a)*



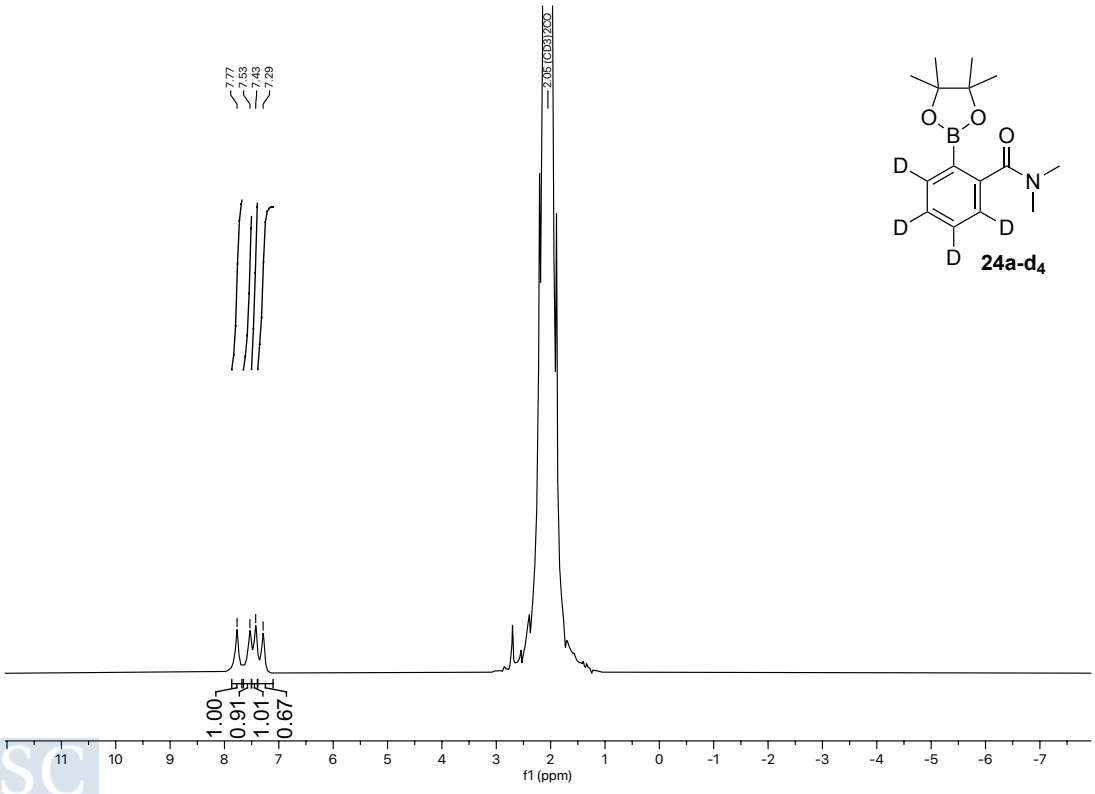

*HSQC NMR N,N-dimethyl-2-(4,4,5,5-tetramethyl-1,3,2-dioxaborolan-2-yl)benzamide (24a)*



*[1]H NMR N,N-dimethyl-2-(4,4,5,5-tetramethyl-1,3,2-dioxaborolan-2-yl)benzamide-3,4,5,6-d4 (24a-d4)*

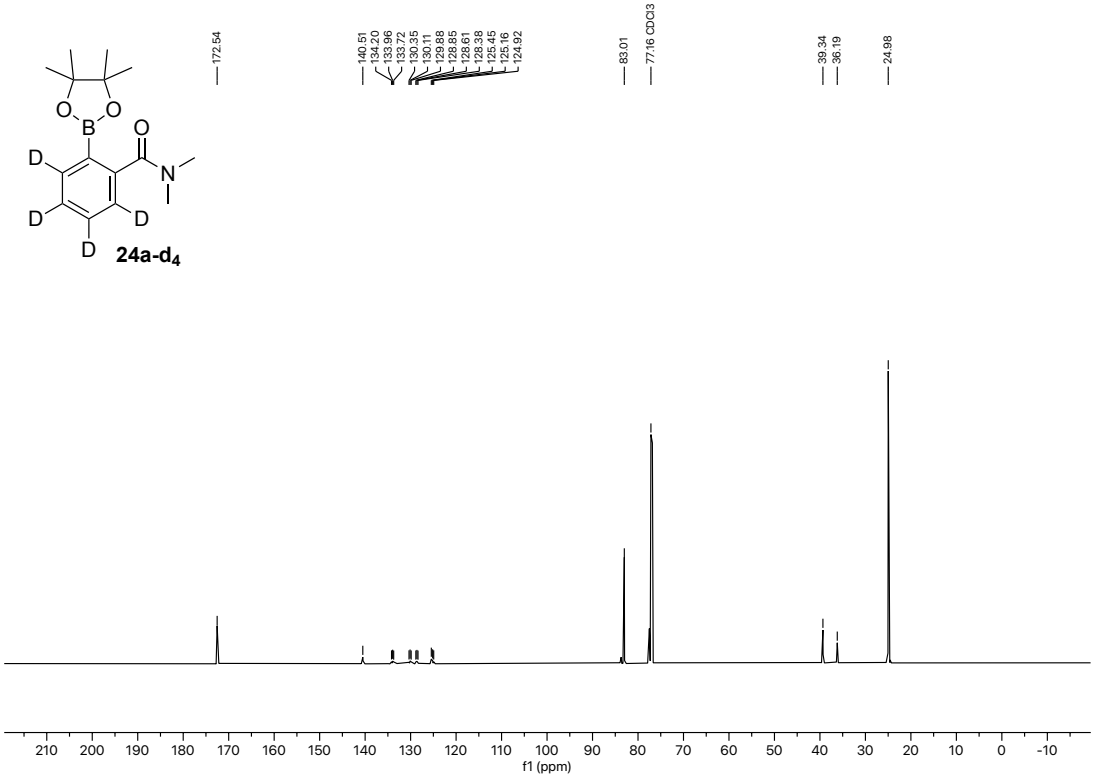



*[2]H NMR N,N-dimethyl-2-(4,4,5,5-tetramethyl-1,3,2-dioxaborolan-2-yl)benzamide-3,4,5,6-d4 (24a-d4)*

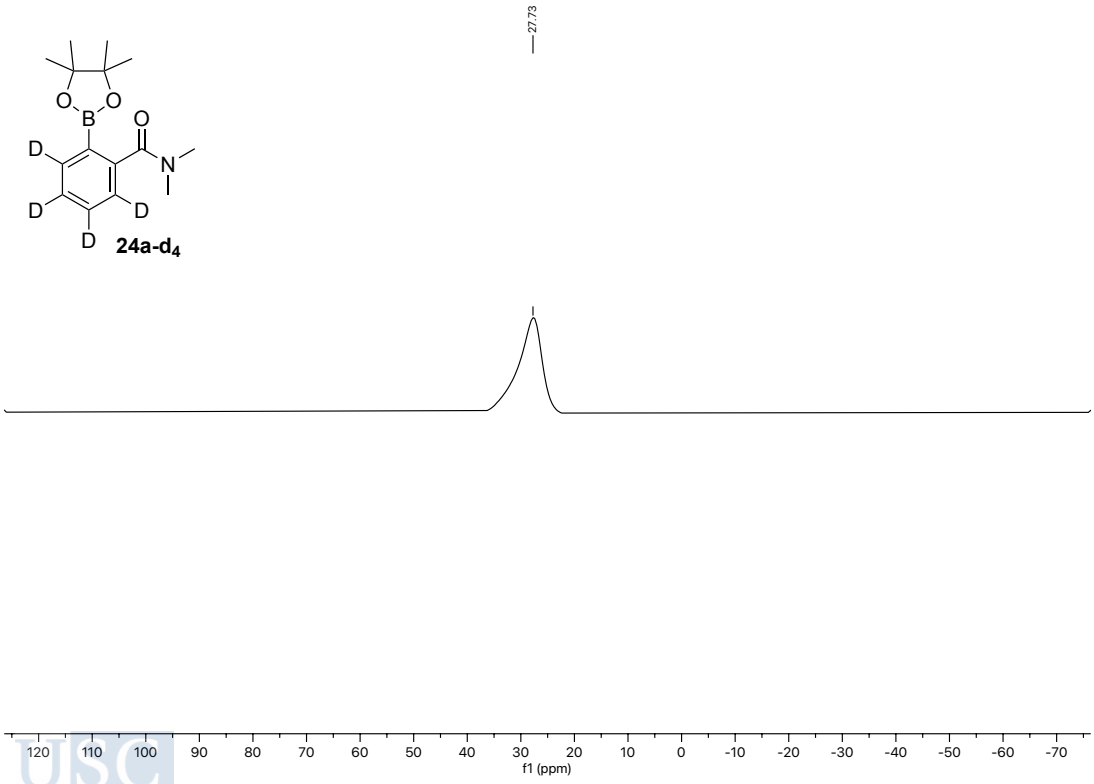



USC UNIVERSIDADE DE SANTIAGO DE COMPOSTELA

*[13]C NMR N,N-dimethyl-2-(4,4,5,5-tetramethyl-1,3,2-dioxaborolan-2-yl)benzamide-3,4,5,6-d4 (24a-d4)*

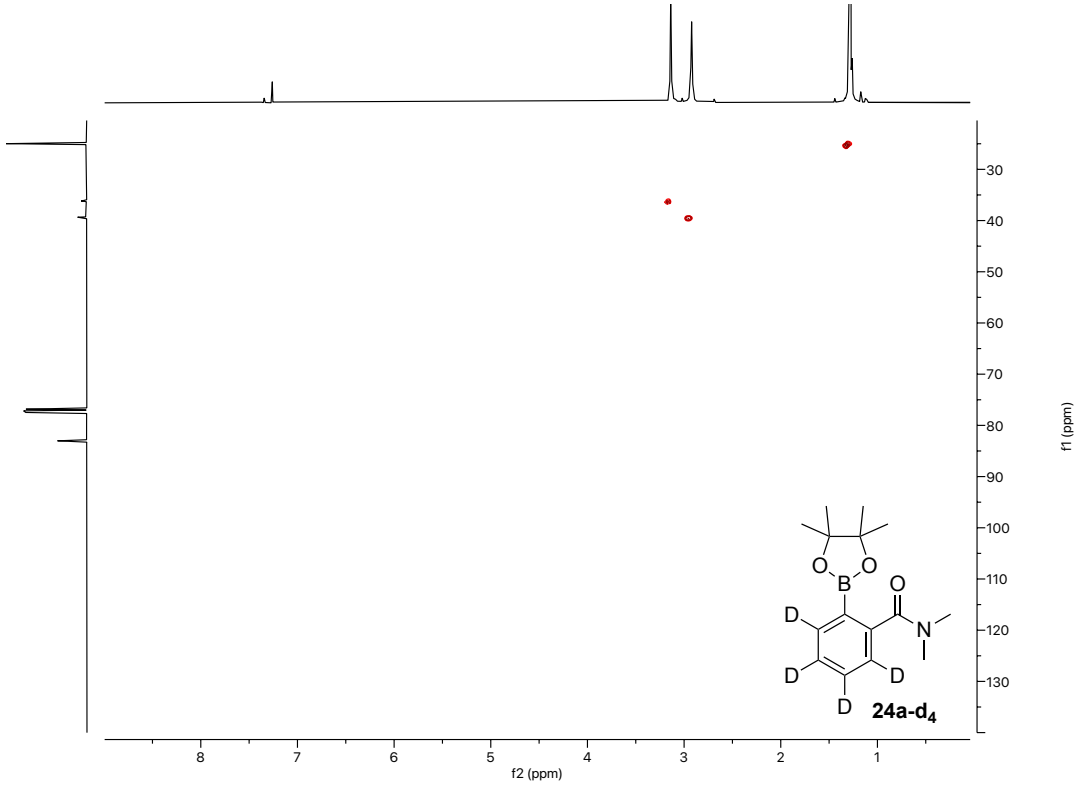



*[11]B NMR N,N-dimethyl-2-(4,4,5,5-tetramethyl-1,3,2-dioxaborolan-2-yl)benzamide-3,4,5,6-d4 (24a-d4)*

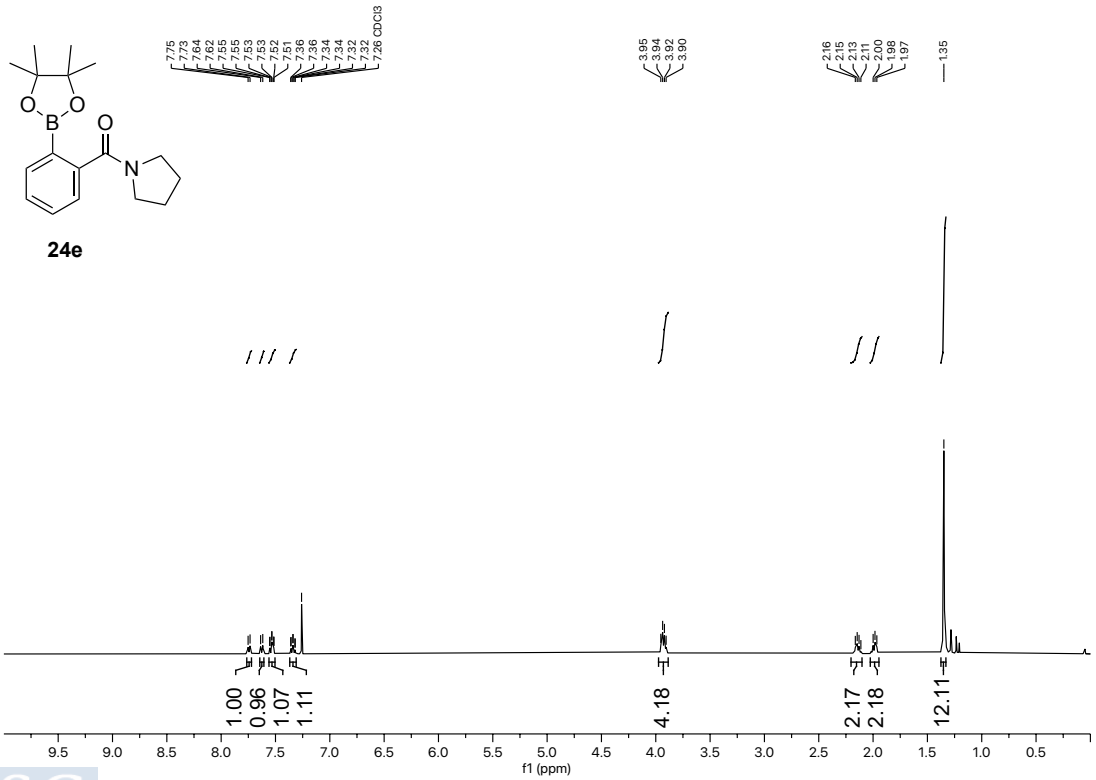



USC UNIVERSIDADE DE SANTIAGO DE COMPOSTELA

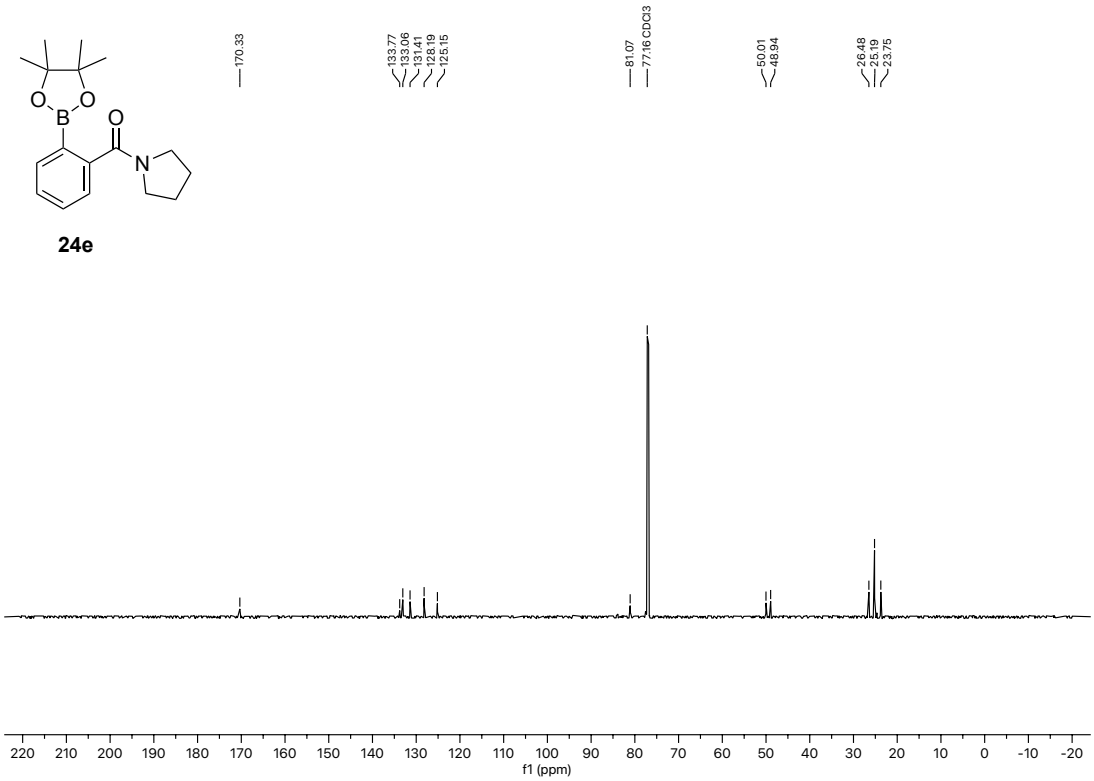
*HSQC NMR N,N-dimethyl-2-(4,4,5,5-tetramethyl-1,3,2-dioxaborolan-2-yl)benzamide-3,4,5,6-d4 (24a-d4)*




*$^{1}$H NMR Pyrrolidin-1-yl(2-(4,4,5,5-tetramethyl-1,3,2-dioxaborolan-2-yl)phenyl)methanone (24e)*

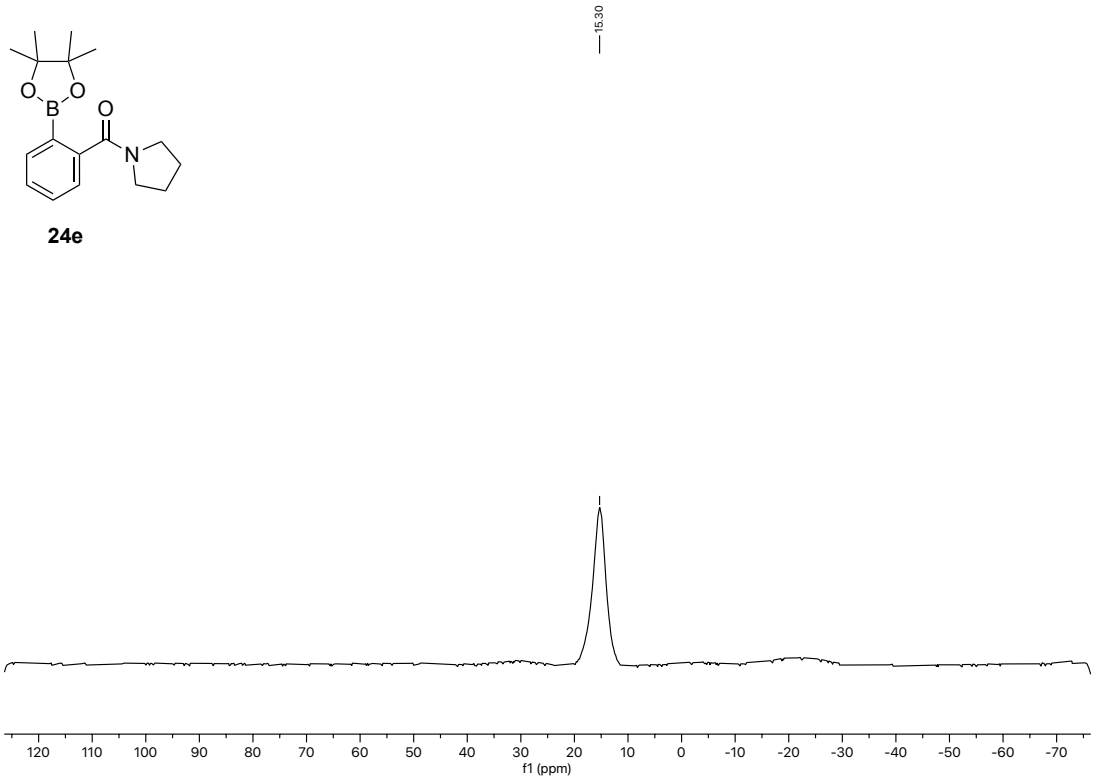


*[13]C NMR Pyrrolidin-1-yl(2-(4,4,5,5-tetramethyl-1,3,2-dioxaborolan-2-yl)phenyl)methanone (24e)*



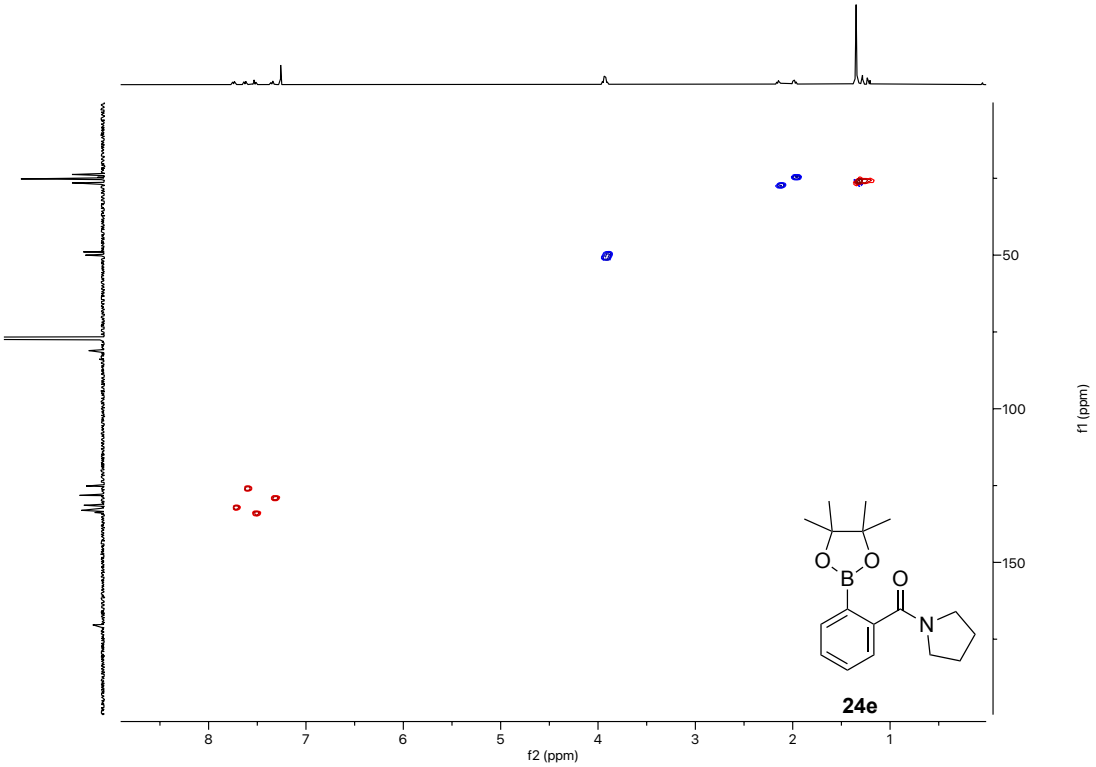

**24e**

*[11]B NMR Pyrrolidin-1-yl(2-(4,4,5,5-tetramethyl-1,3,2-dioxaborolan-2-yl)phenyl)methanone (24e)*

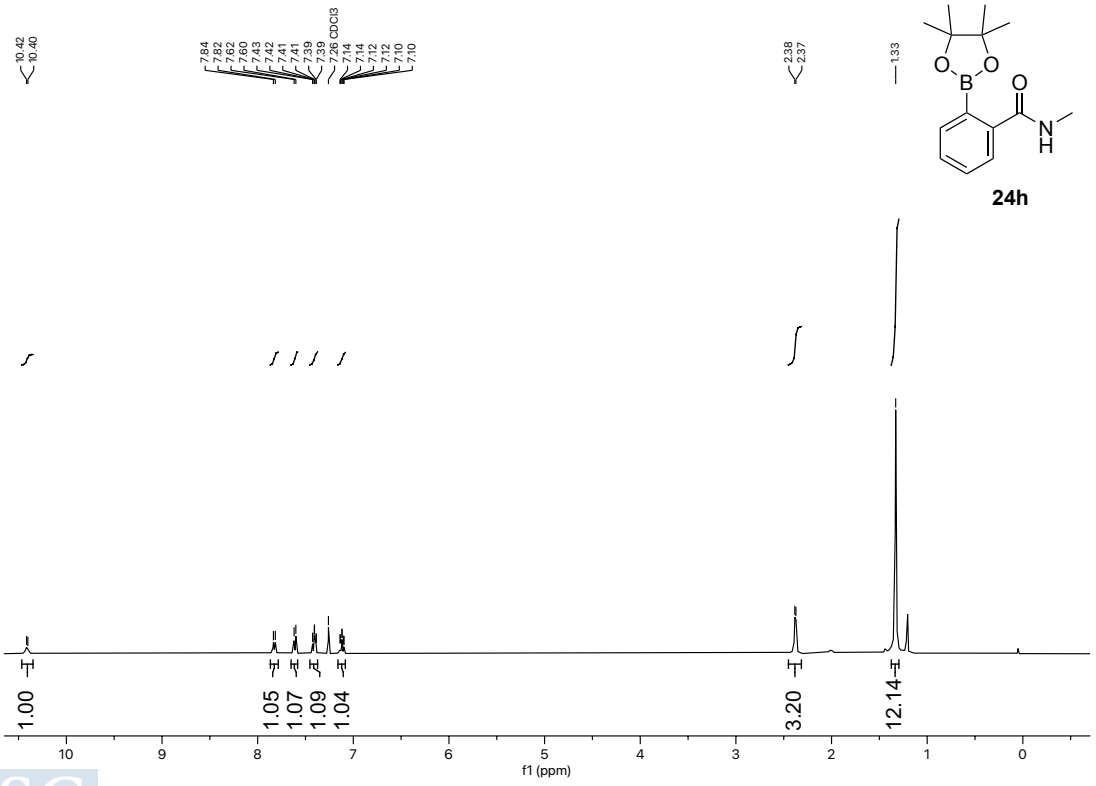



**24e**

*HSQC NMR Pyrrolidin-1-yl(2-(4,4,5,5-tetramethyl-1,3,2-dioxaborolan-2-yl)phenyl)methanone (24e)*



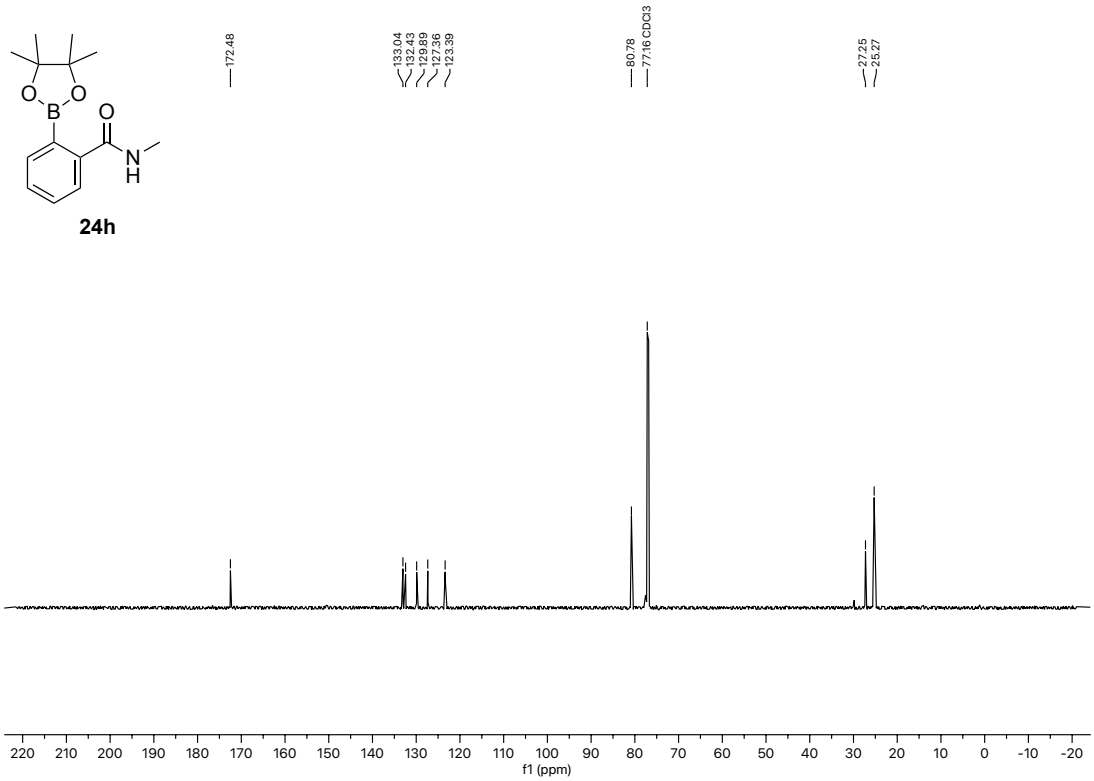

*$^{1}$H NMR N-methyl-2-(4,4,5,5-tetramethyl-1,3,2-dioxaborolan-2-yl)benzamide (24h)*



*$^{13}$C NMR N-methyl-2-(4,4,5,5-tetramethyl-1,3,2-dioxaborolan-2-yl)benzamide (24h)*



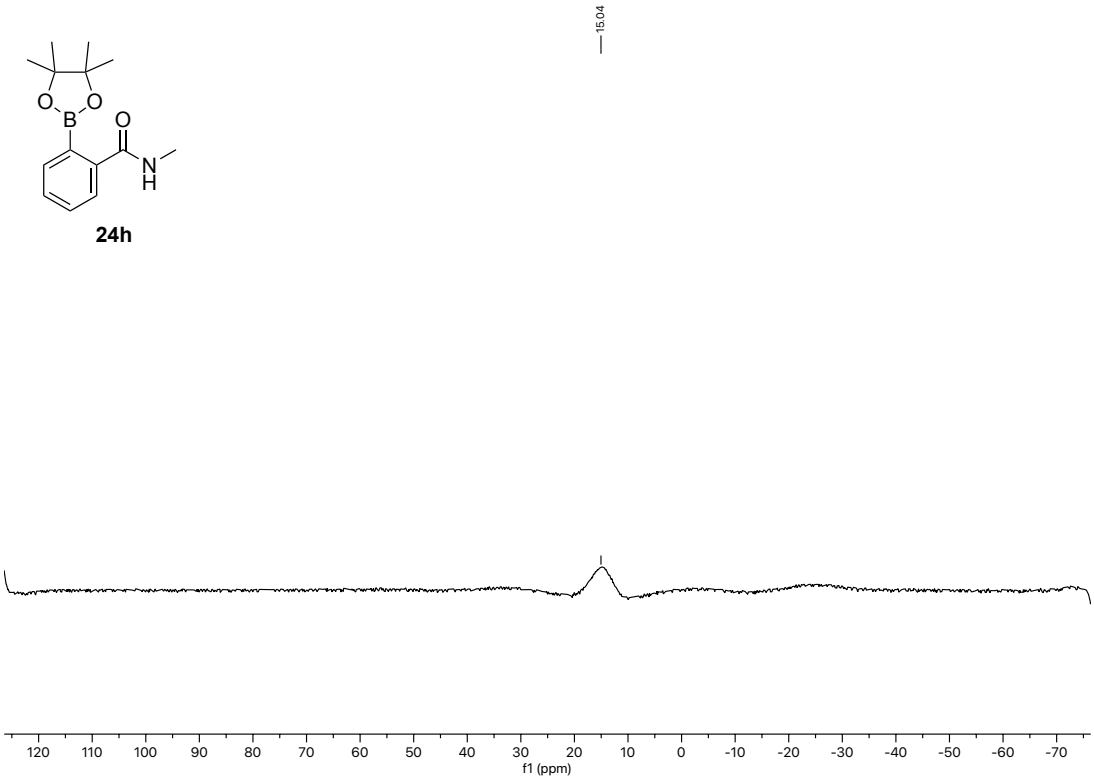
**24h**



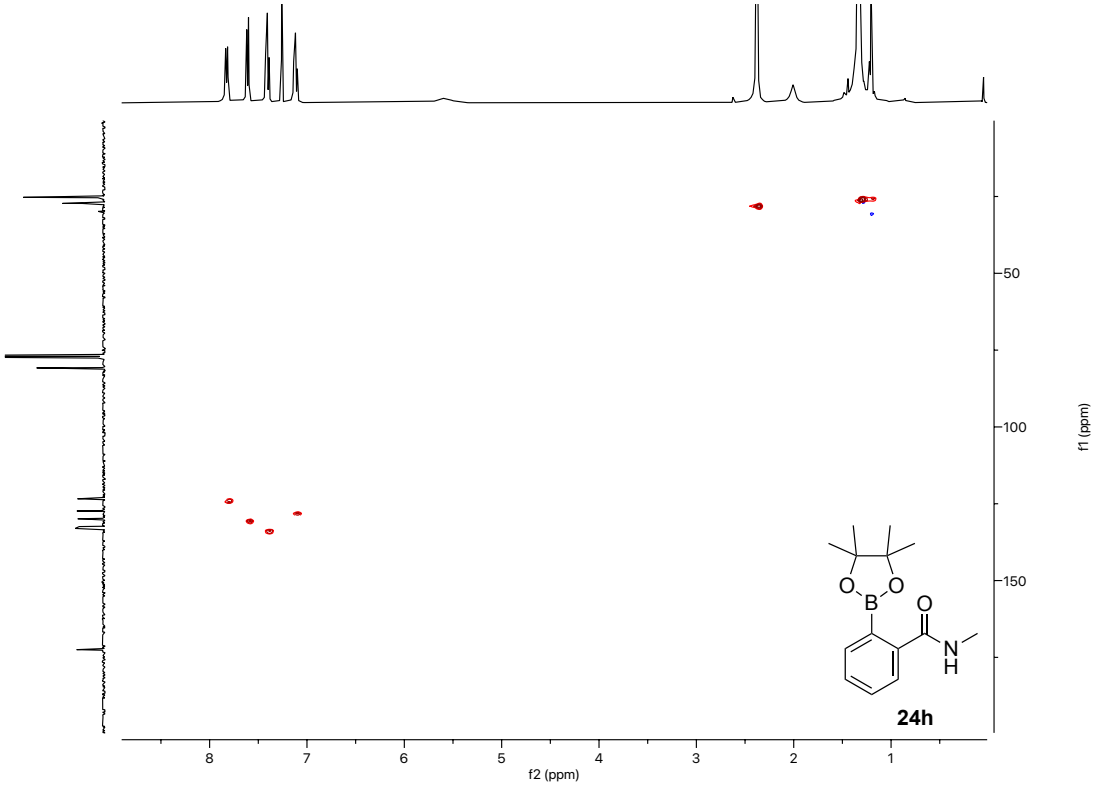

*$^{11}$B NMR N-methyl-2-(4,4,5,5-tetramethyl-1,3,2-dioxaborolan-2-yl)benzamide (24h)*



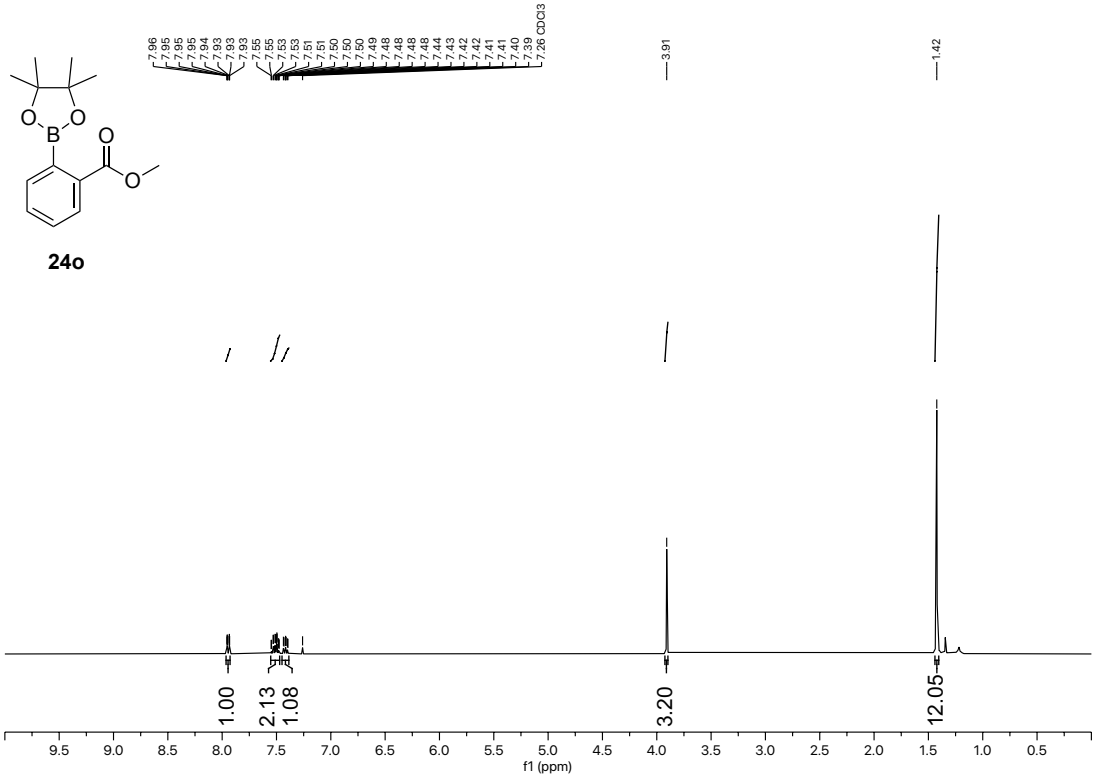
**24h**



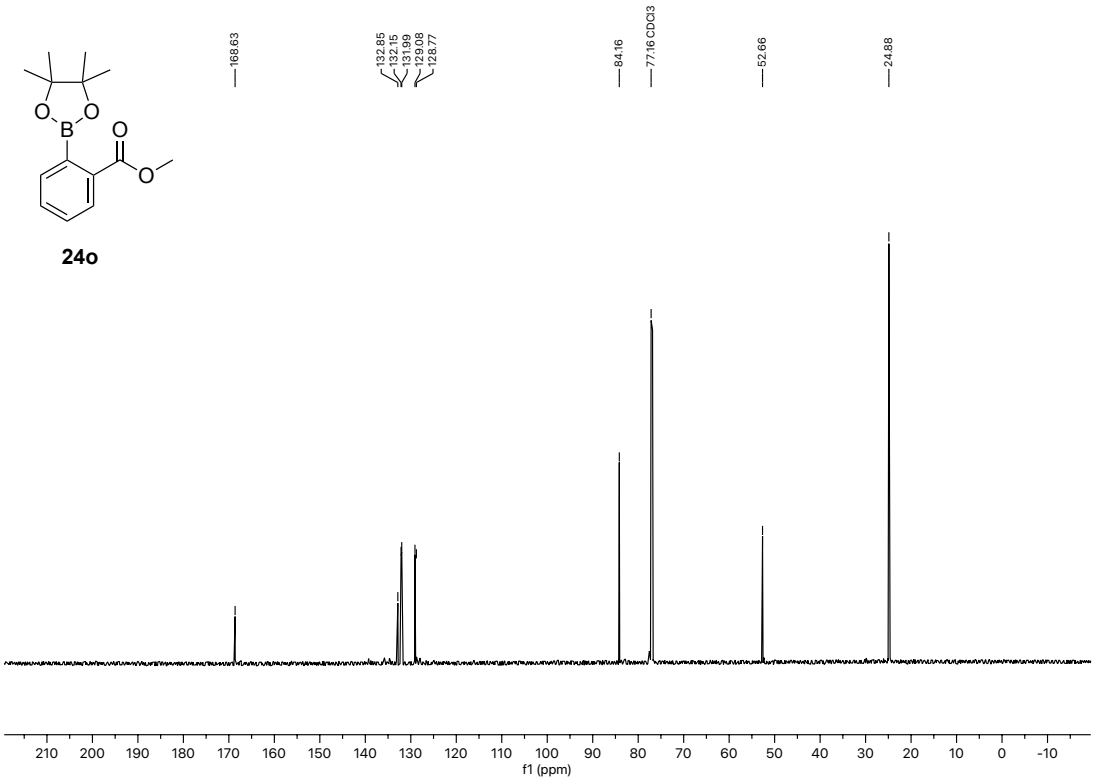
*HSQC NMR N-methyl-2-(4,4,5,5-tetramethyl-1,3,2-dioxaborolan-2-yl)benzamide (24h)*




*$^{1}$H NMR Methyl 2-(4,4,5,5-tetramethyl-1,3,2-dioxaborolan-2-yl)benzoate (24o)*

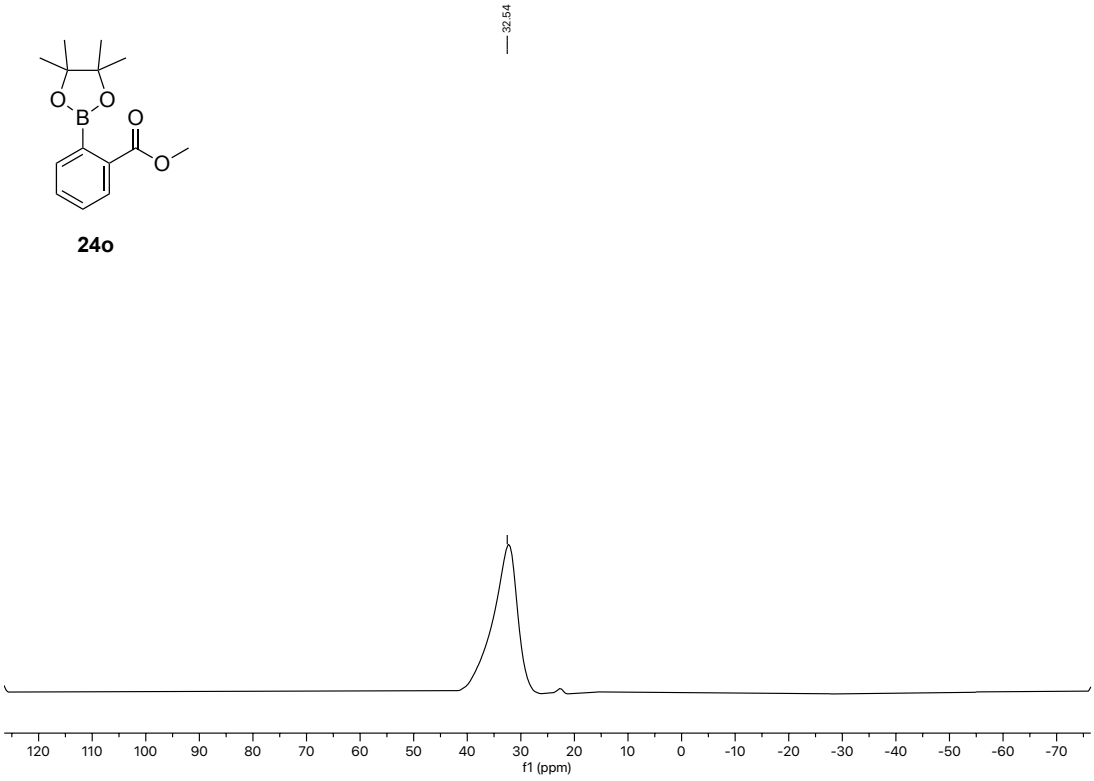


*$^{13}$C NMR Methyl 2-(4,4,5,5-tetramethyl-1,3,2-dioxaborolan-2-yl)benzoate (24o)*



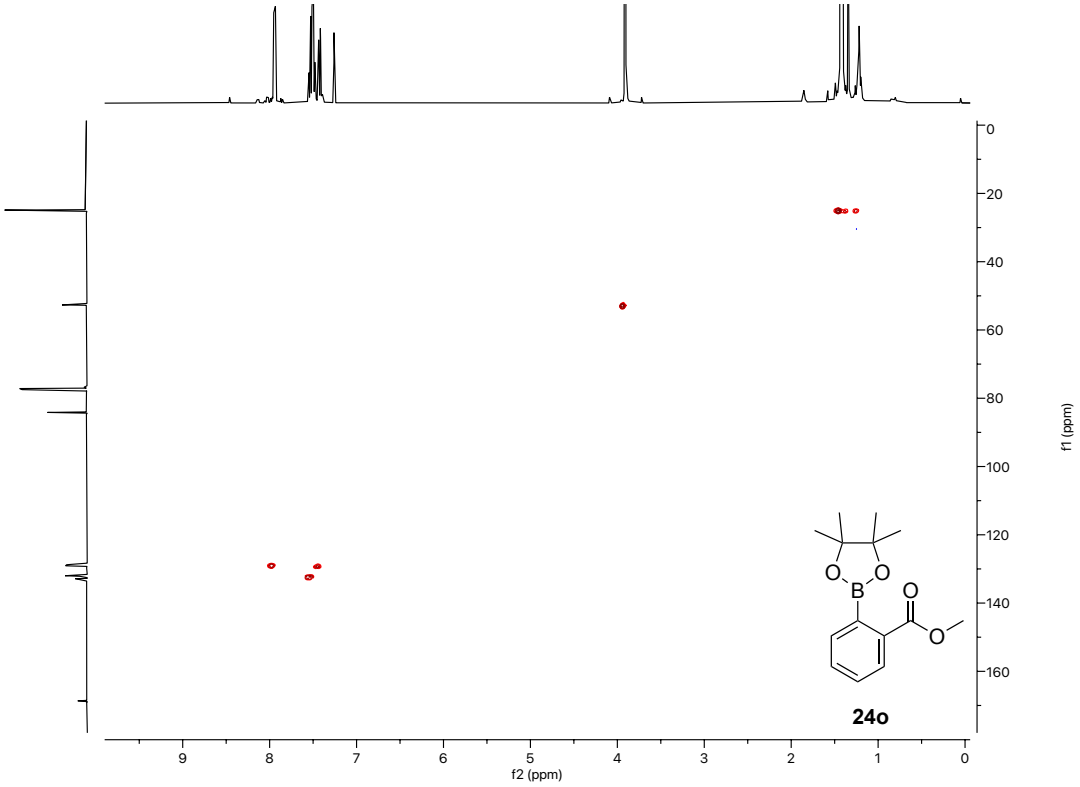

**24o**

*$^{11}$B NMR Methyl 2-(4,4,5,5-tetramethyl-1,3,2-dioxaborolan-2-yl)benzoate (24o)*

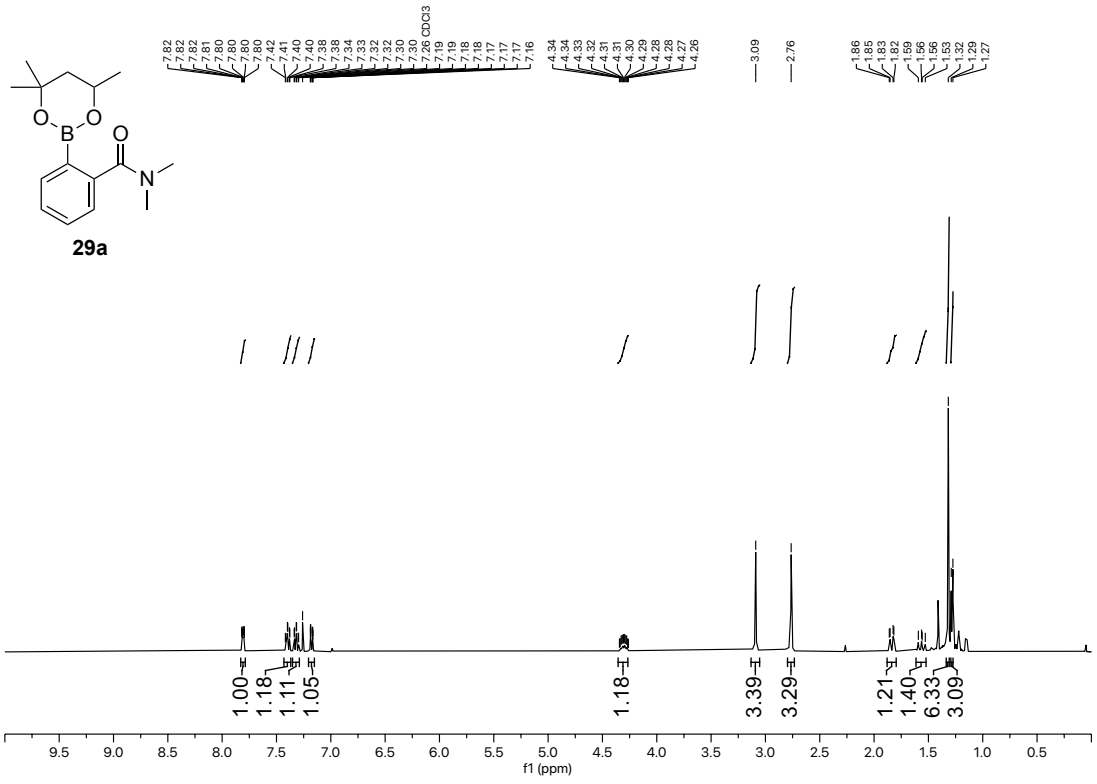



**24o**

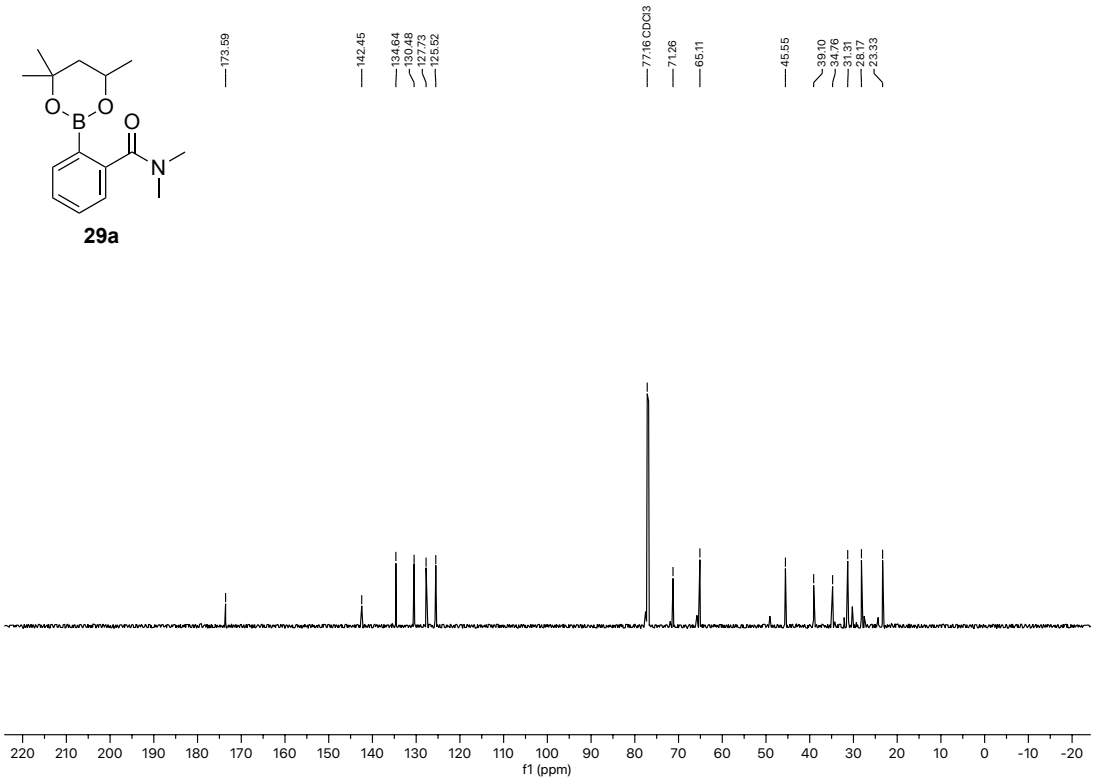
*HSQC NMR Methyl 2-(4,4,5,5-tetramethyl-1,3,2-dioxaborolan-2-yl)benzoate (24o)*




*$^{1}$H NMR N,N-dimethyl-2-(4,4,6-trimethyl-1,3,2-dioxaborinan-2-yl)benzamide (29a)*

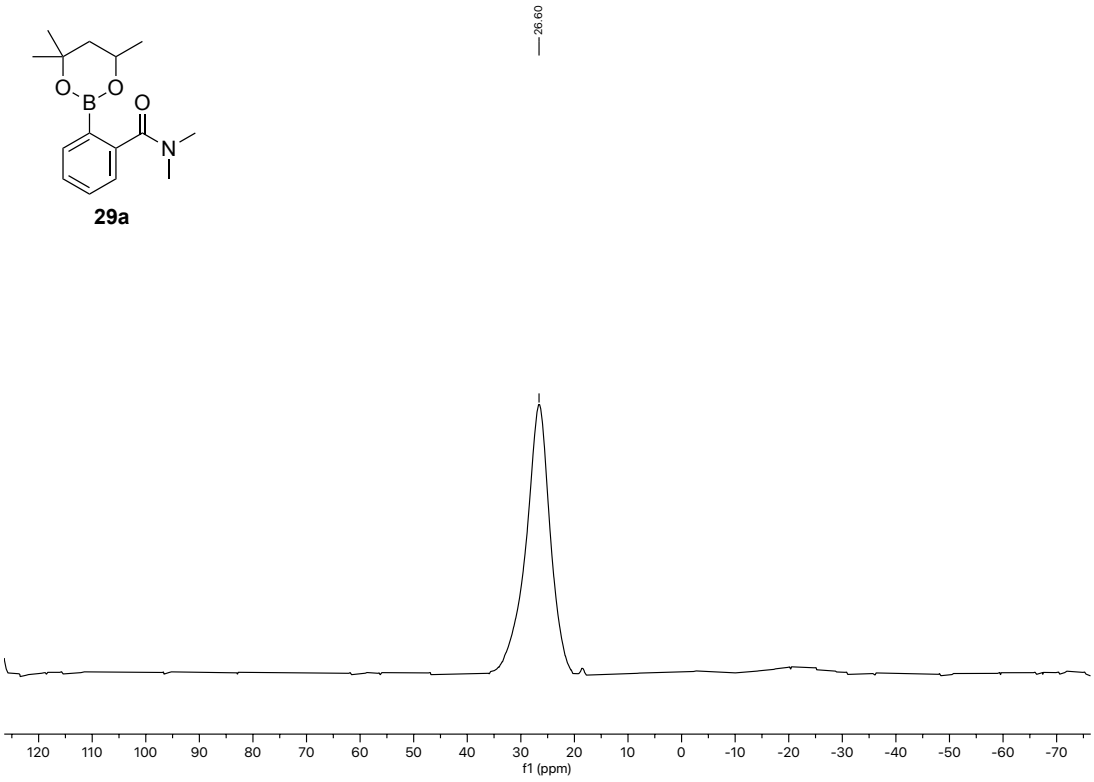


*$^{13}$C NMR N,N-dimethyl-2-(4,4,6-trimethyl-1,3,2-dioxaborinan-2-yl)benzamide (29a)*



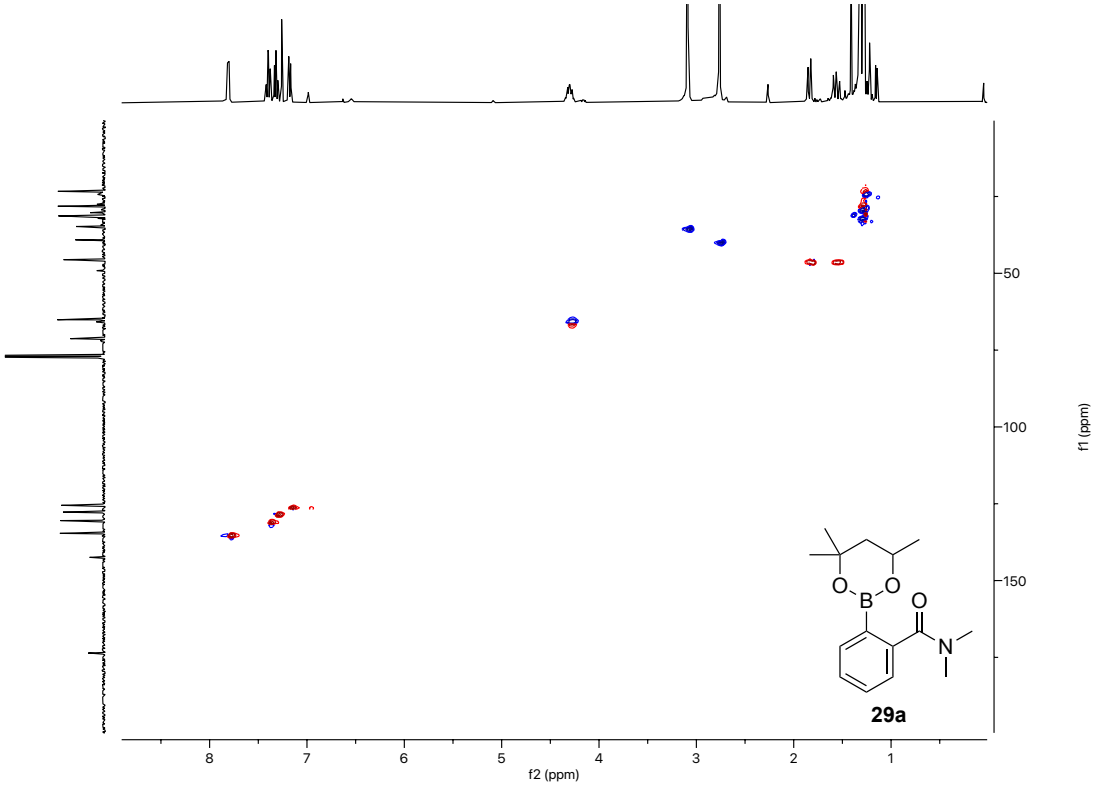

**29a**

*$^{11}$B NMR N,N-dimethyl-2-(4,4,6-trimethyl-1,3,2-dioxaborinan-2-yl)benzamide (29a)*

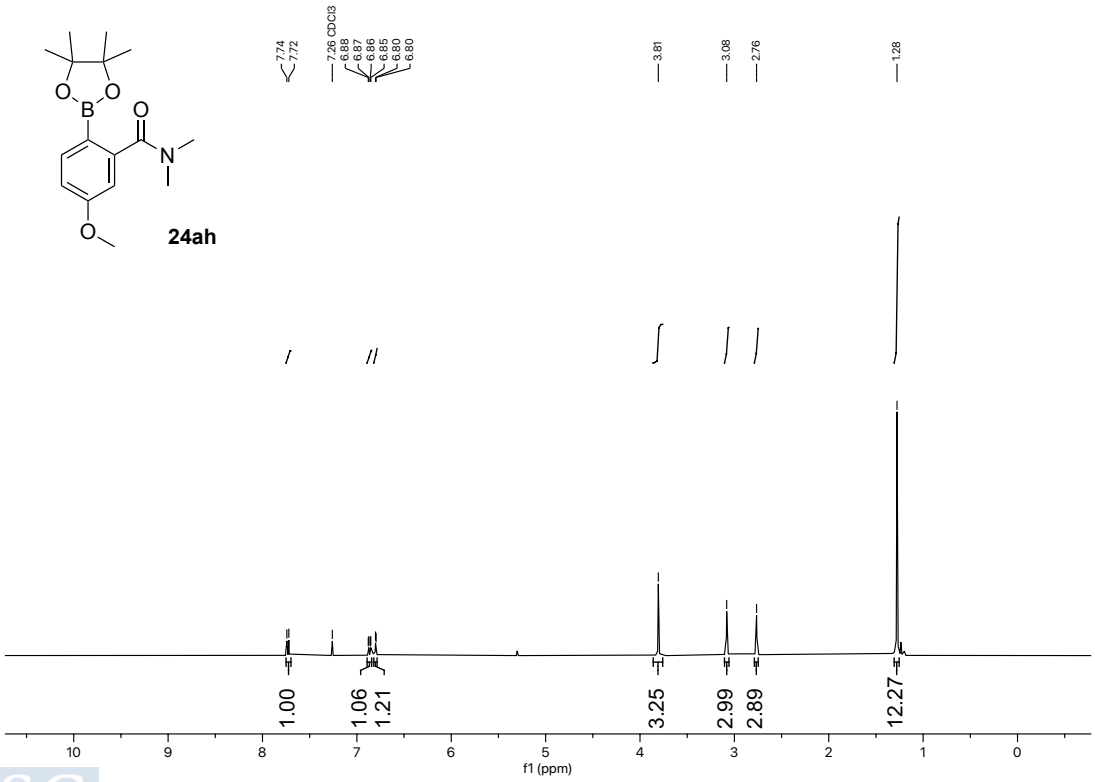



**29a**

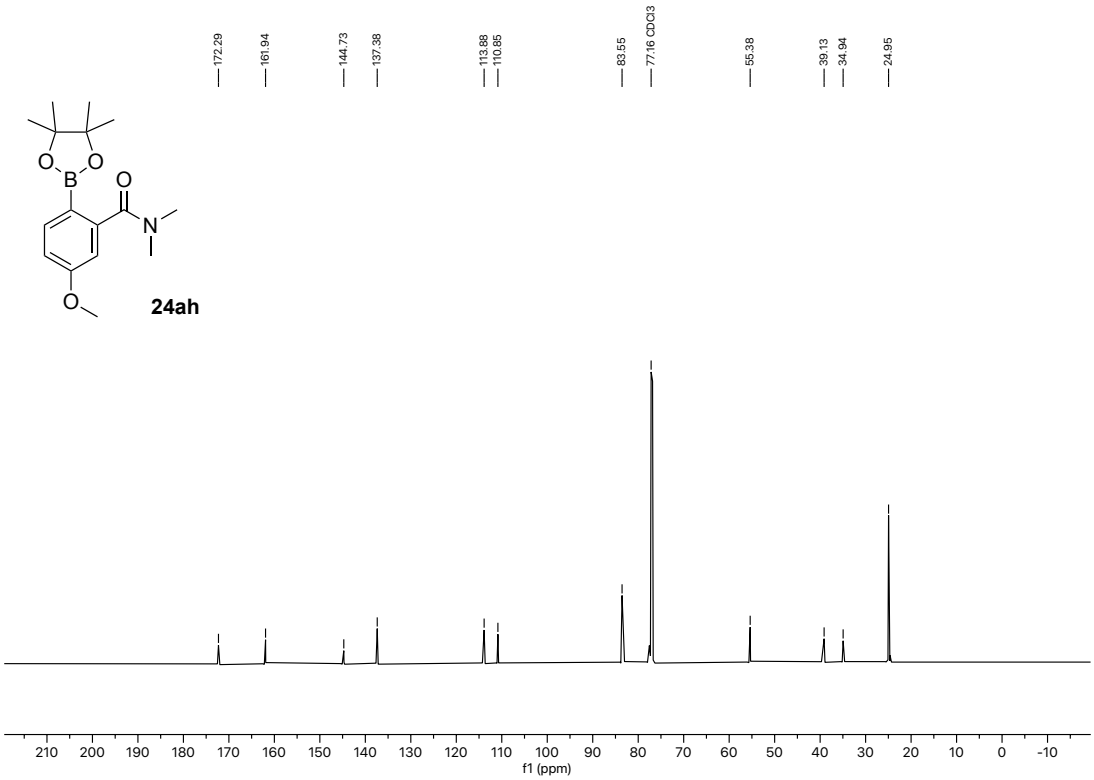
*HSQC NMR N,N-dimethyl-2-(4,4,6-trimethyl-1,3,2-dioxaborinan-2-yl)benzamide (29a)*



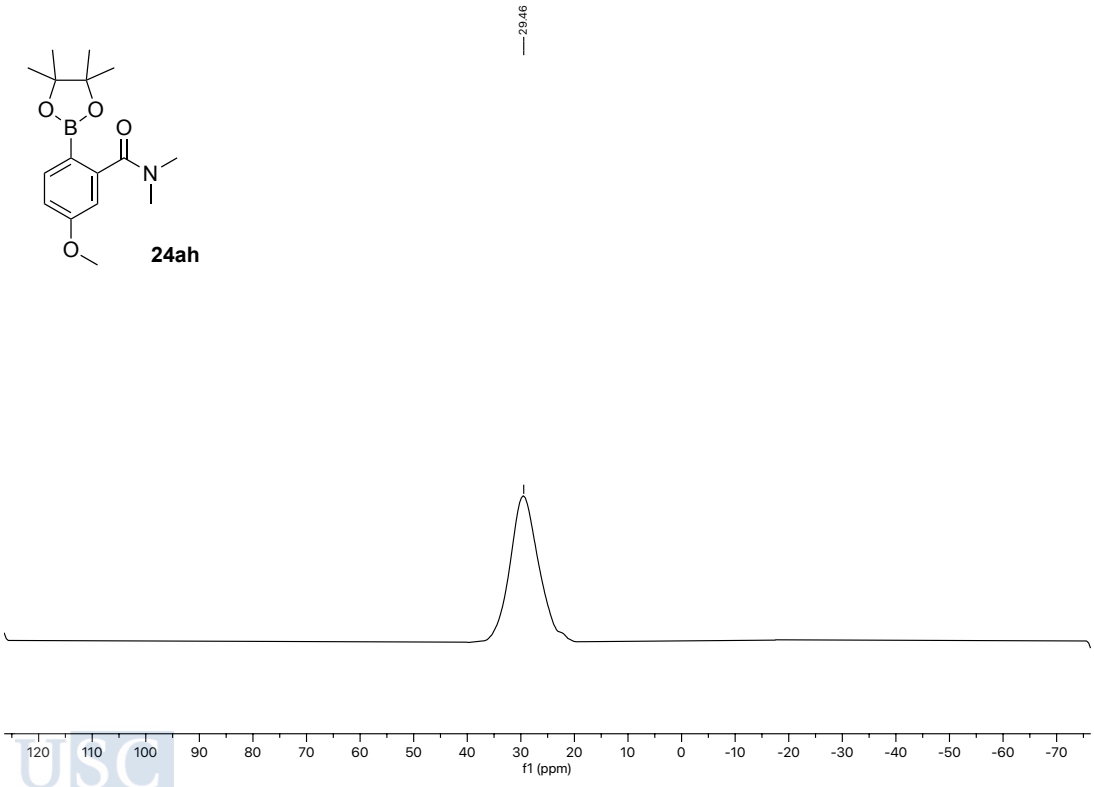

*$^{1}$H NMR 5-methoxy-N,N-dimethyl-2-(4,4,5,5-tetramethyl-1,3,2-dioxaborolan-2-yl)benzamide (24ah)*



*$^{13}$C NMR 5-methoxy-N,N-dimethyl-2-(4,4,5,5-tetramethyl-1,3,2-dioxaborolan-2-yl)benzamide (24ah)*

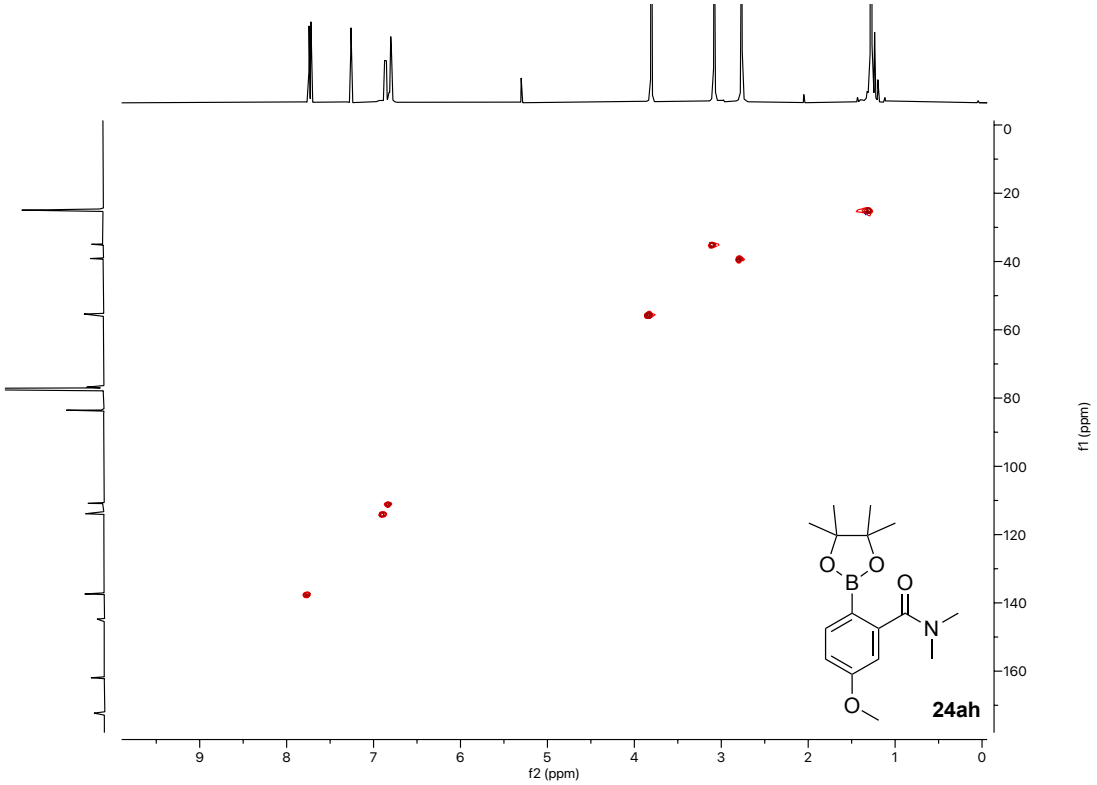



*$^{11}$B NMR 5-methoxy-N,N-dimethyl-2-(4,4,5,5-tetramethyl-1,3,2-dioxaborolan-2-yl)benzamide (24ah)*

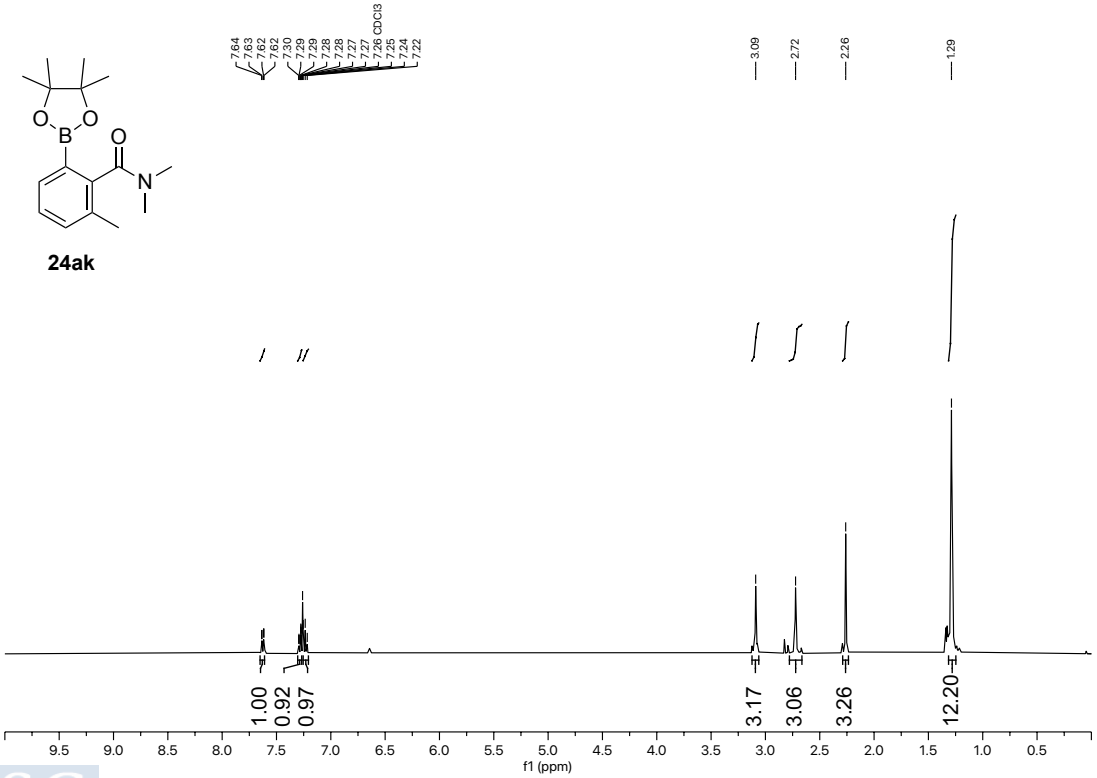



USC UNIVERSIDADE DE SANTIAGO DE COMPOSTELA

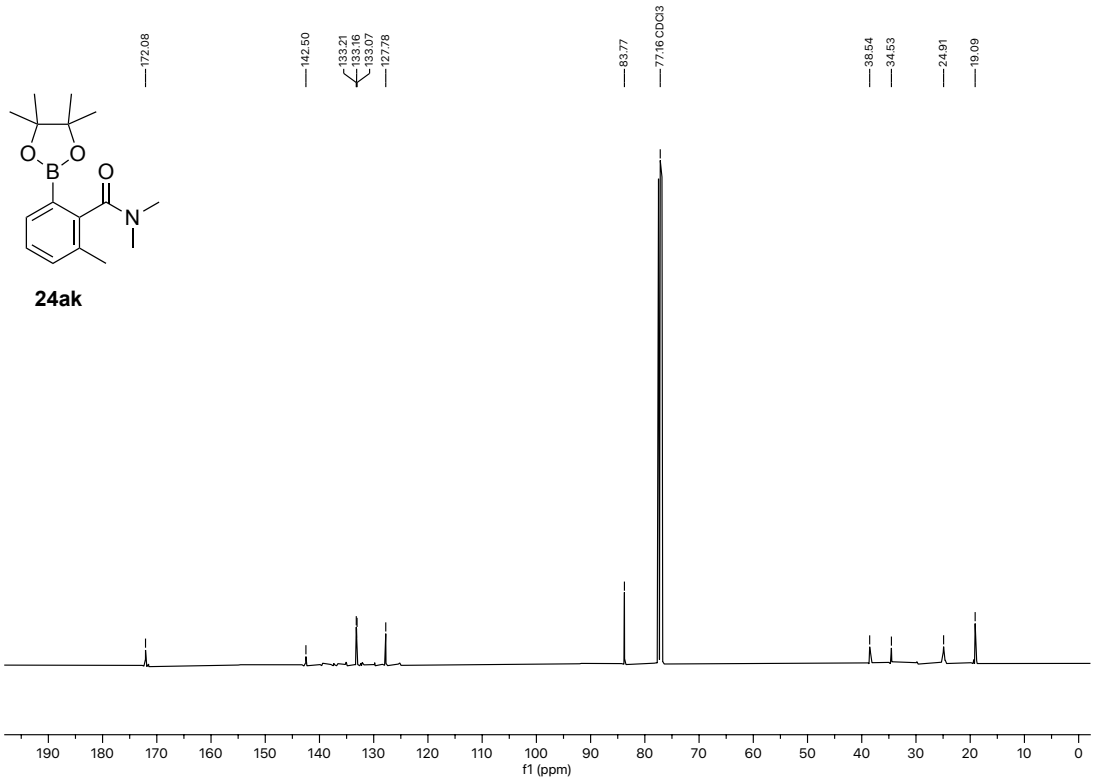
*HSQC NMR 5-methoxy-N,N-dimethyl-2-(4,4,5,5-tetramethyl-1,3,2-dioxaborolan-2-yl)benzamide (24ah)*




*$^{1}$H NMR N,N,2-trimethyl-6-(4,4,5,5-tetramethyl-1,3,2-dioxaborolan-2-yl)benzamide (24ak)*

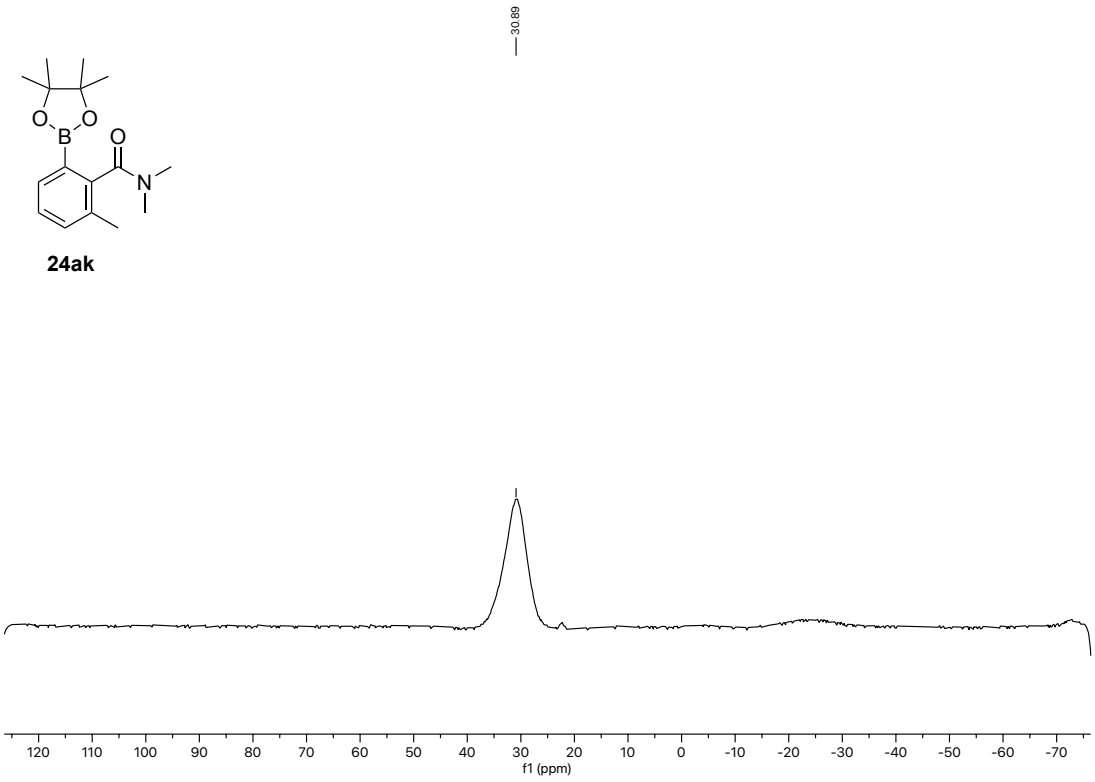


*$^{13}$C NMR N,N,2-trimethyl-6-(4,4,5,5-tetramethyl-1,3,2-dioxaborolan-2-yl)benzamide (24ak)*



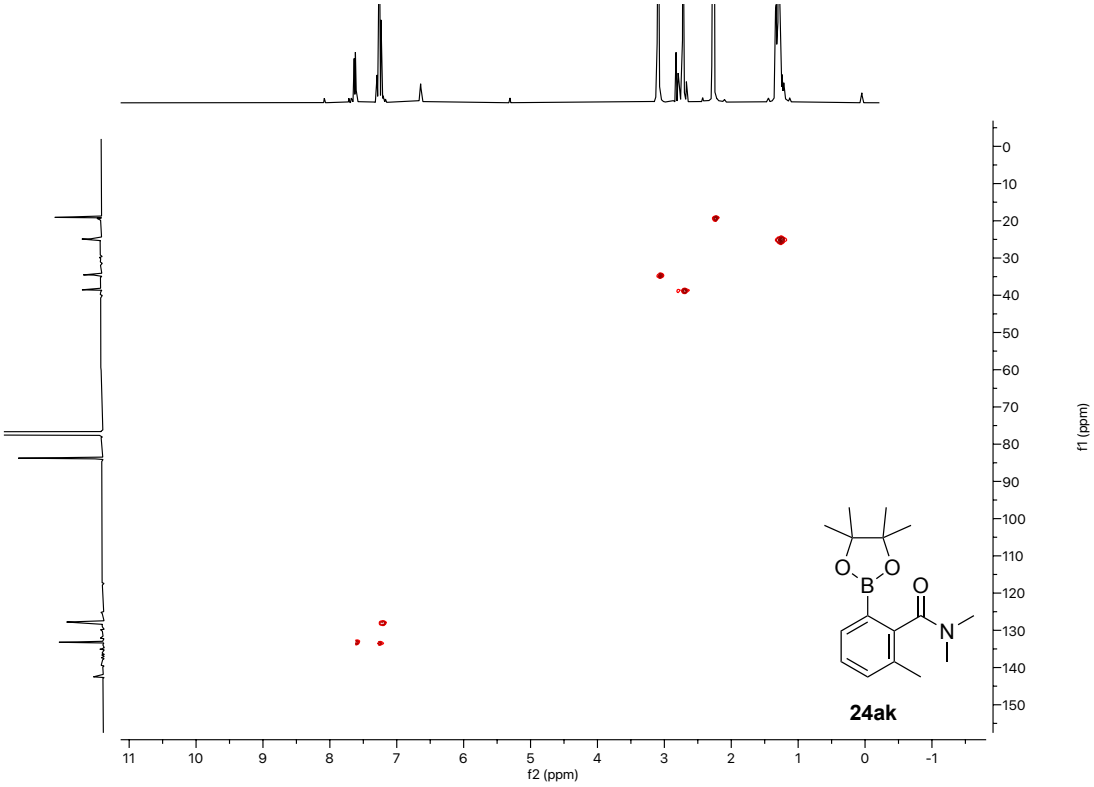

**24ak**

*$^{11}$B NMR N,N,2-trimethyl-6-(4,4,5,5-tetramethyl-1,3,2-dioxaborolan-2-yl)benzamide (24ak)*

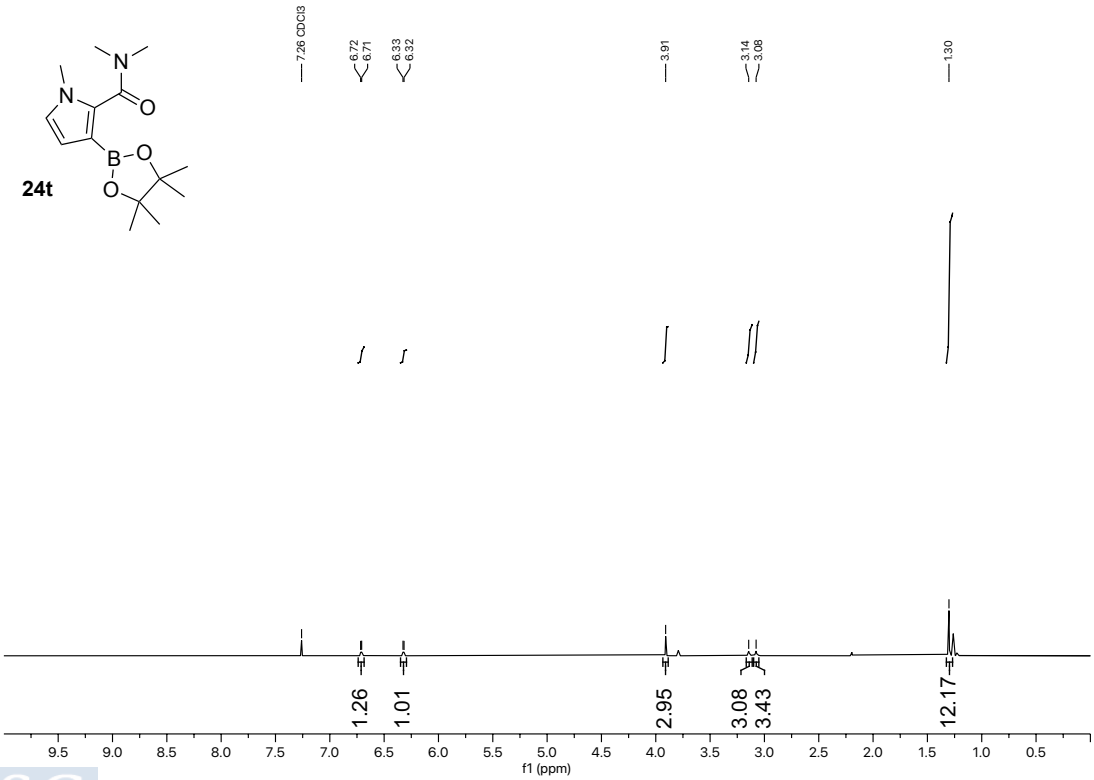



**24ak**

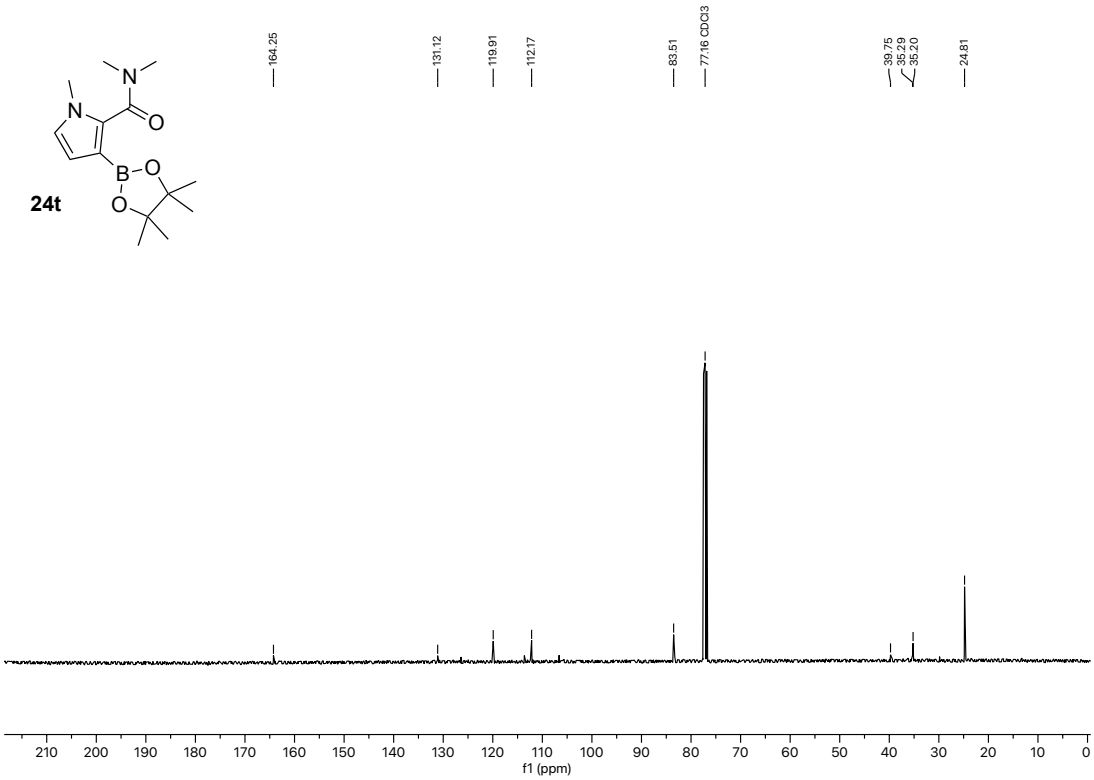
*HSQC NMR N,N,2-trimethyl-6-(4,4,5,5-tetramethyl-1,3,2-dioxaborolan-2-yl)benzamide (24ak)*



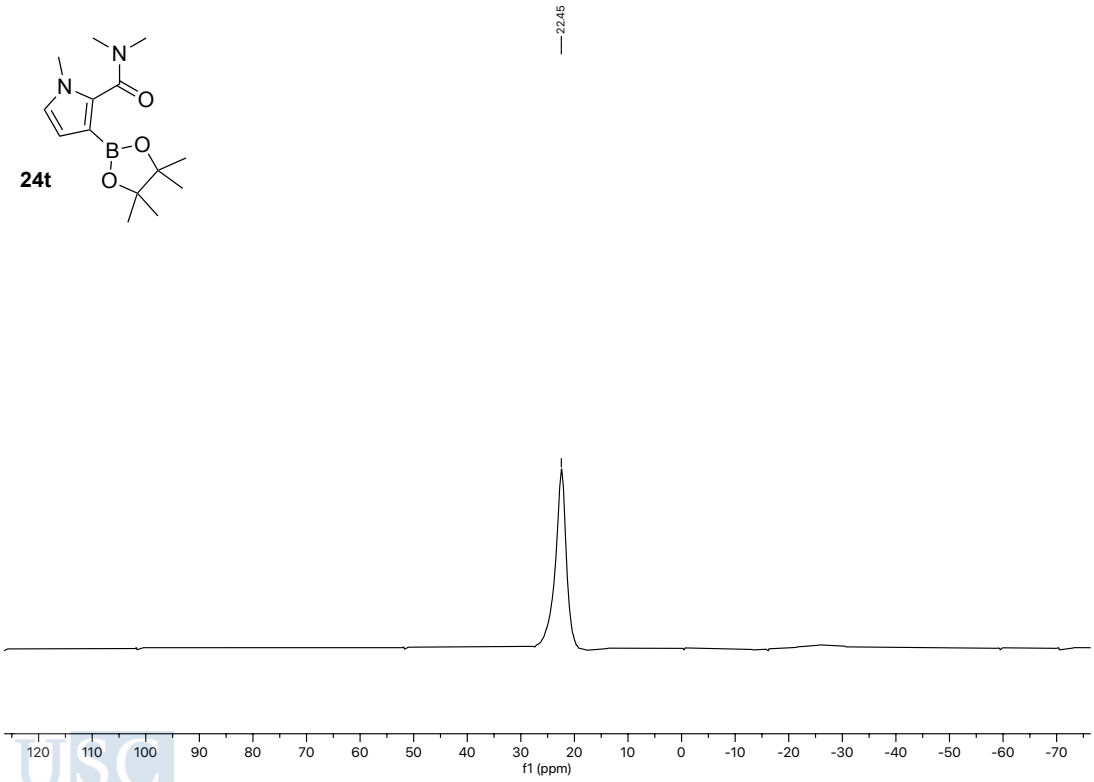

*$^{1}$H NMR N,N,1-trimethyl-3-(4,4,5,5-tetramethyl-1,3,2-dioxaborolan-2-yl)-1H-pyrrole-2-carboxamide (24t)*



*$^{13}$C NMR N,N,1-trimethyl-3-(4,4,5,5-tetramethyl-1,3,2-dioxaborolan-2-yl)-1H-pyrrole-2-carboxamide (24t)*

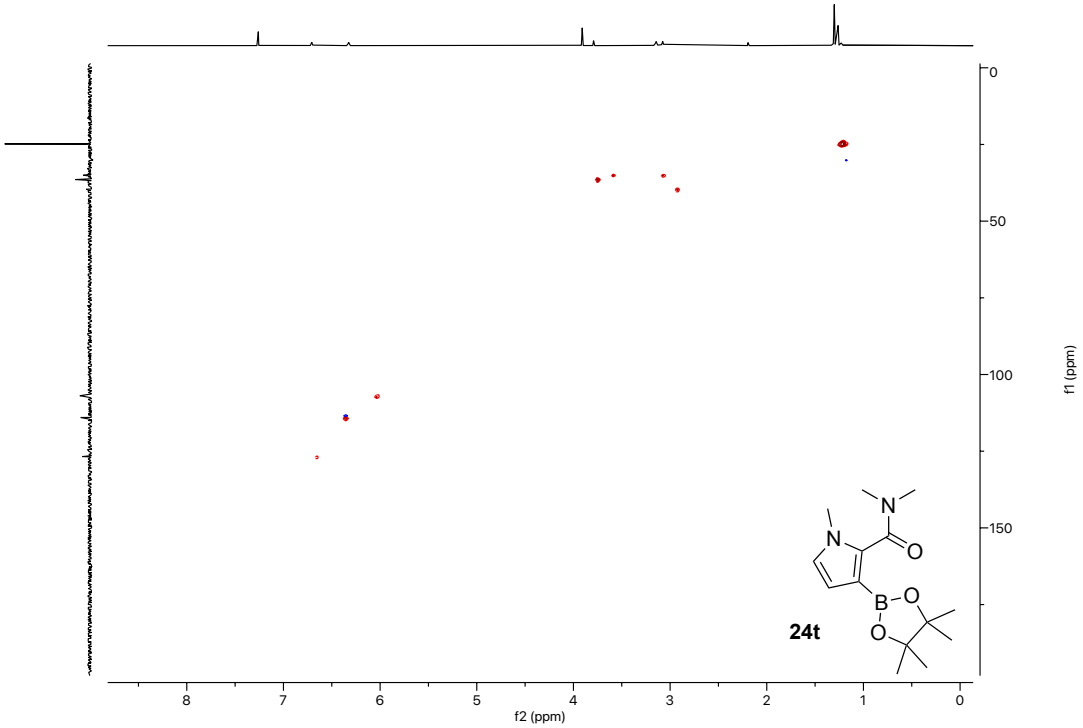



*$^{11}$B NMR N,N,1-trimethyl-3-(4,4,5,5-tetramethyl-1,3,2-dioxaborolan-2-yl)-1H-pyrrole-2-carboxamide (24t)*

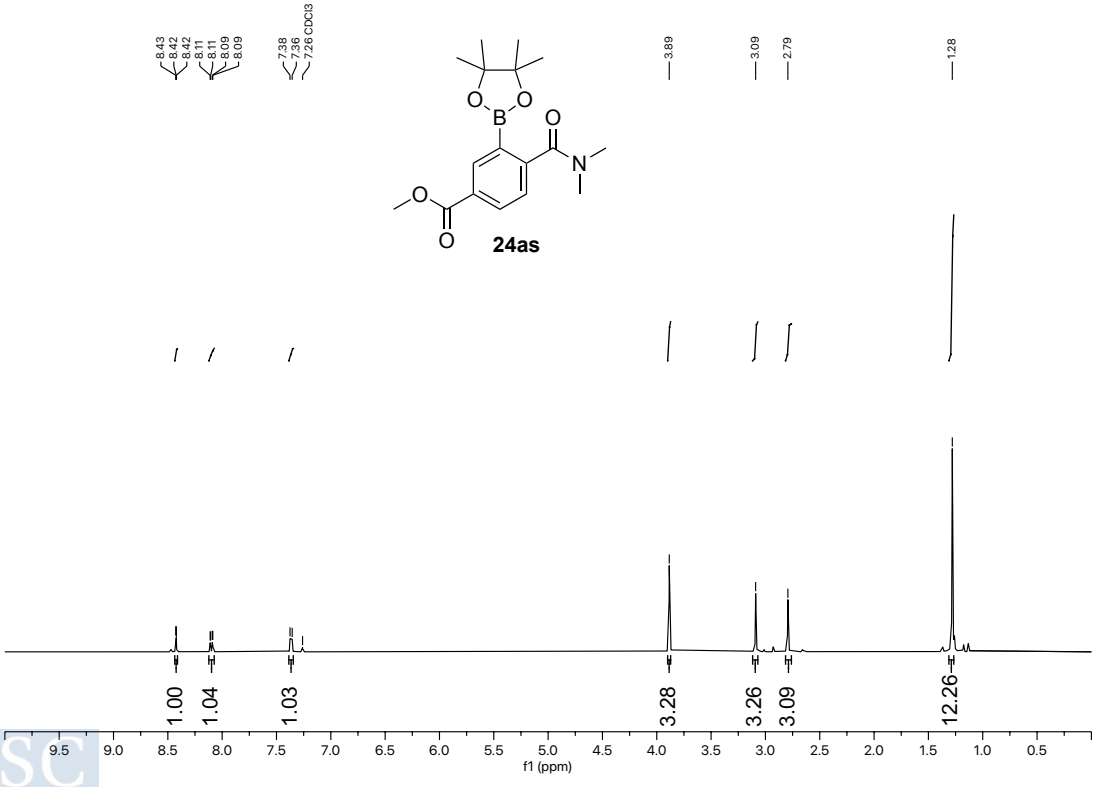



USC UNIVERSIDADE DE SANTIAGO DE COMPOSTELA

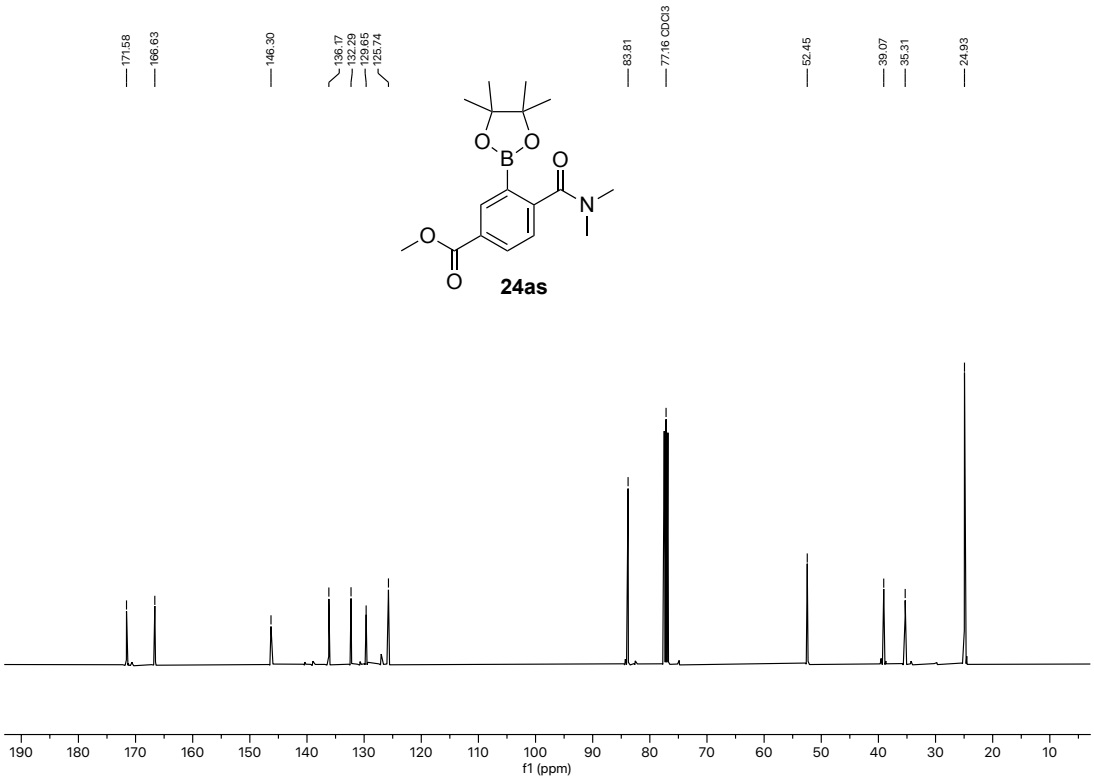
*HSQC NMR N,N,1-trimethyl-3-(4,4,5,5-tetramethyl-1,3,2-dioxaborolan-2-yl)-1H-pyrrole-2-carboxamide (24t)*



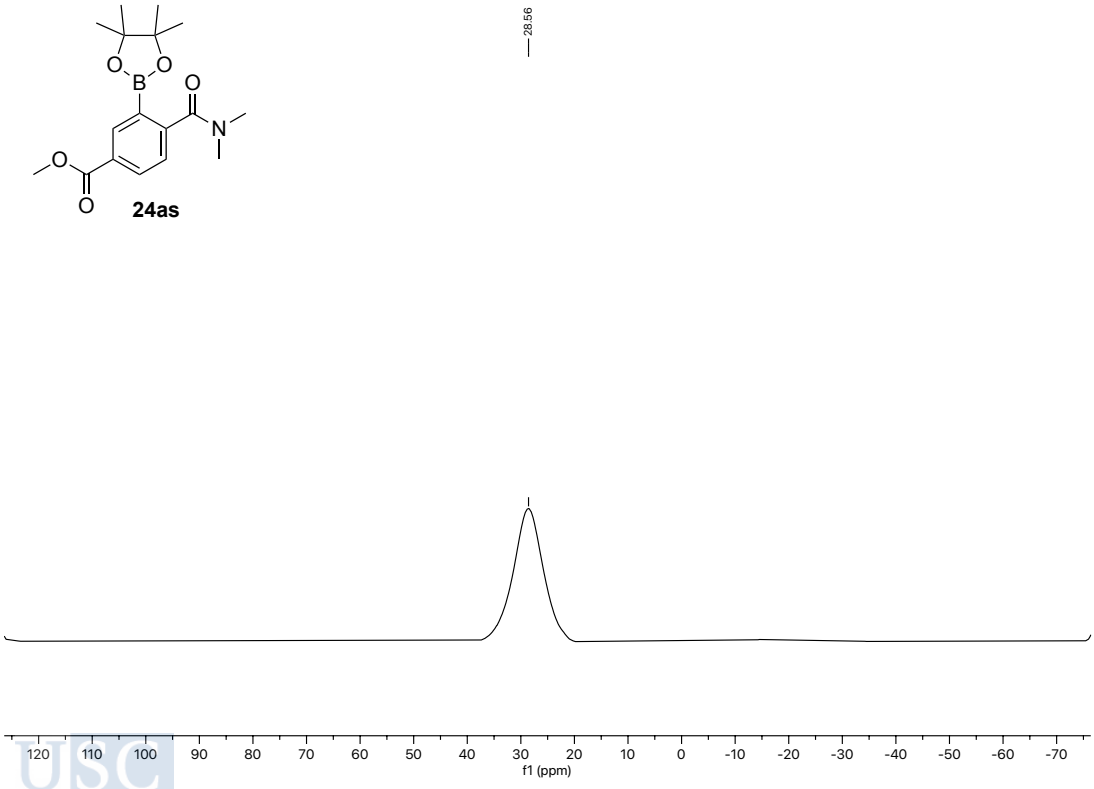

*$^{1}$H NMR Methyl 4-(dimethylcarbamoyl)-3-(4,4,5,5-tetramethyl-1,3,2-dioxaborolan-2-yl)benzoate (24as)*



*[13]C NMR Methyl 4-(dimethylcarbamoyl)-3-(4,4,5,5-tetramethyl-1,3,2-dioxaborolan-2-yl)benzoate (24as)*

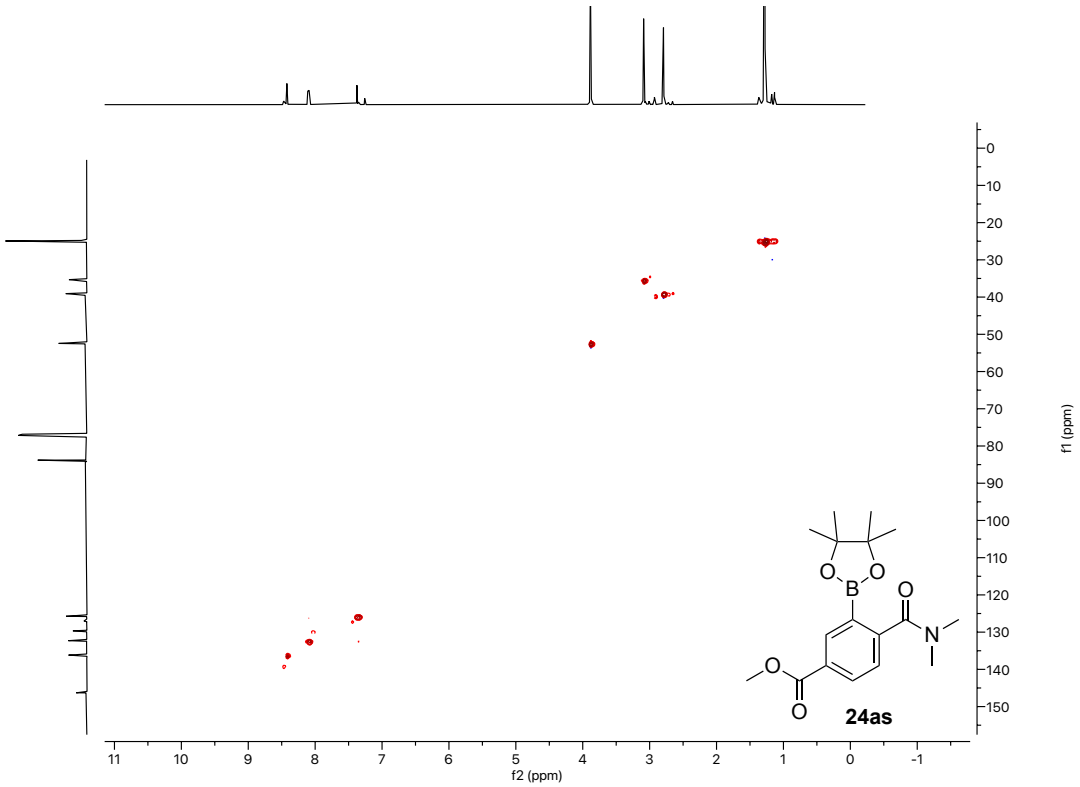



*[11]B NMR Methyl 4-(dimethylcarbamoyl)-3-(4,4,5,5-tetramethyl-1,3,2-dioxaborolan-2-yl)benzoate (24as)*

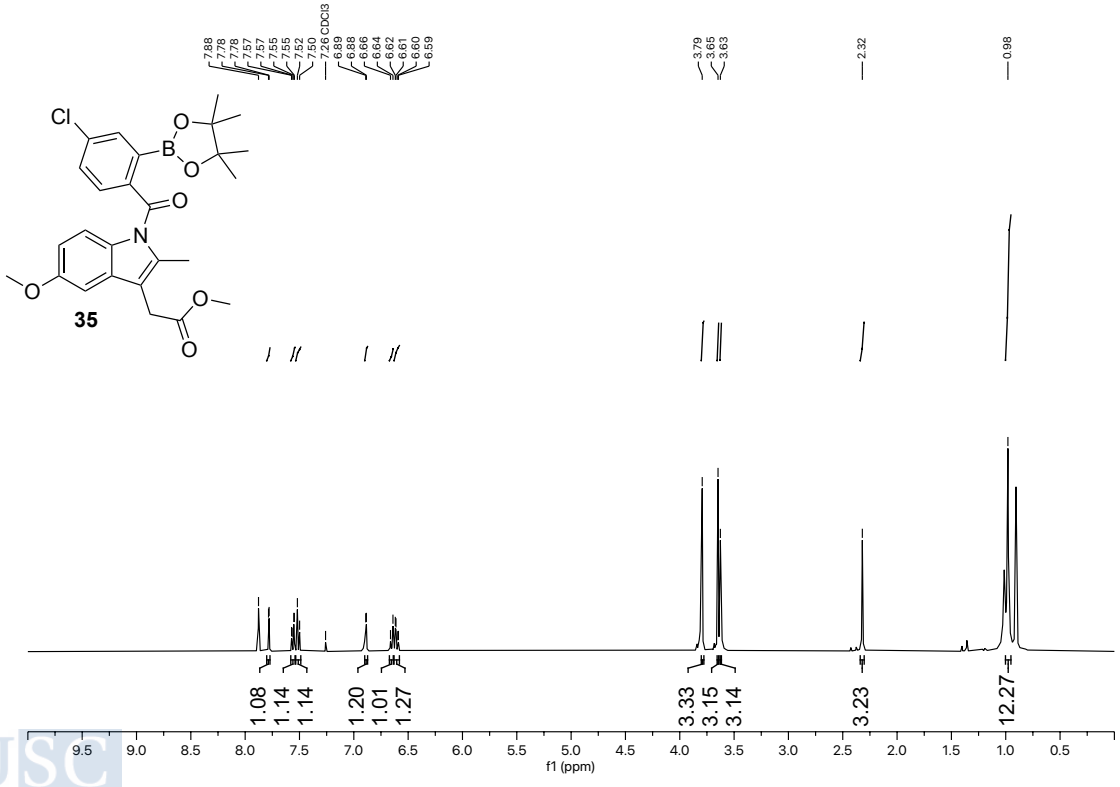



USC UNIVERSIDADE DE SANTIAGO DE COMPOSTELA

*HSQC NMR Methyl 4-(dimethylcarbamoyl)-3-(4,4,5,5-tetramethyl-1,3,2-dioxaborolan-2-yl)benzoate (24as)*

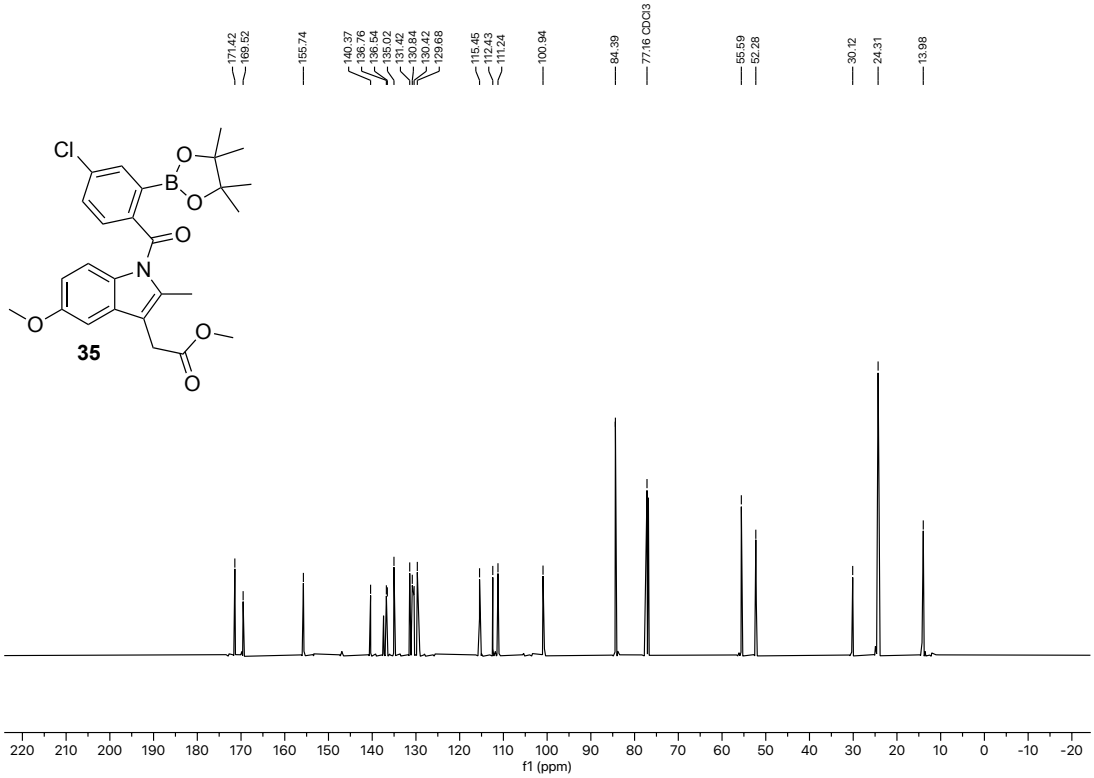



*$^1$H NMR Methyl 2-(1-(4-chloro-2-(4,4,5,5-tetramethyl-1,3,2-dioxaborolan-2-yl)benzoyl)-5-methoxy-2-methyl-1H-indol-3-yl)acetate (35).*

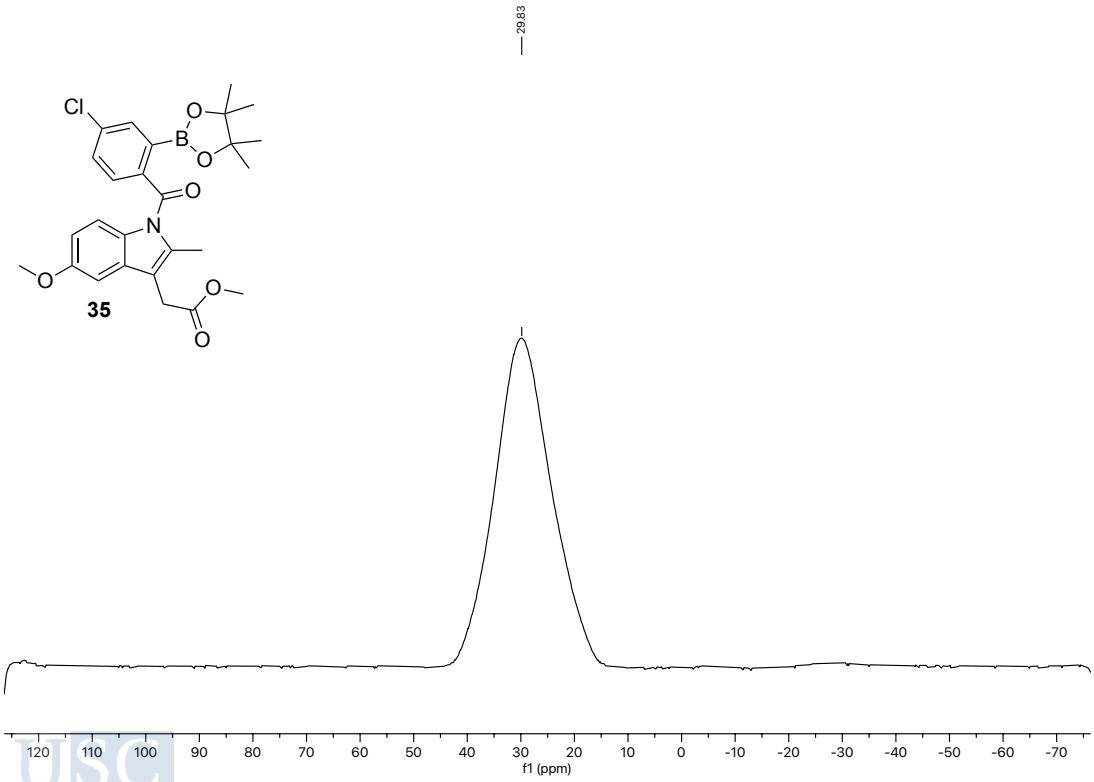



USC UNIVERSIDADE DE SANTIAGO DE COMPOSTELA

*[13]C NMR Methyl 2-(1-(4-chloro-2-(4,4,5,5-tetramethyl-1,3,2-dioxaborolan-2-yl)benzoyl)-5-methoxy-2-methyl-1H-indol-3-yl)acetate (35).*

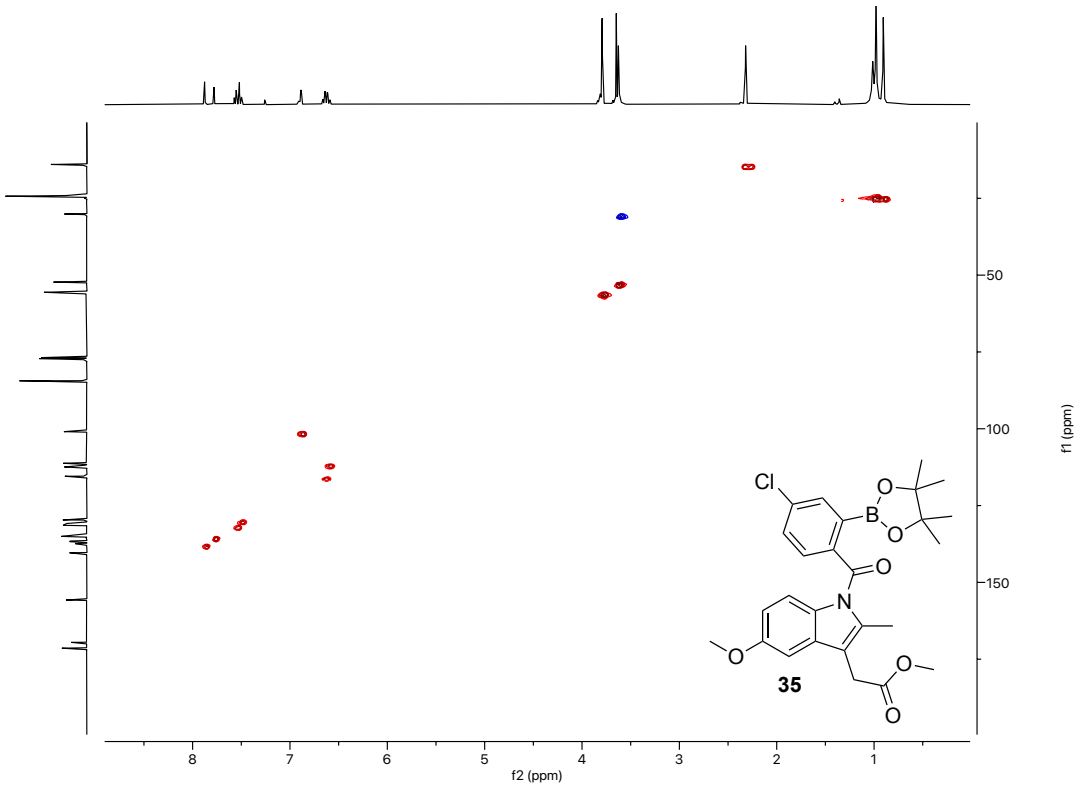



*[11]B NMR Methyl 2-(1-(4-chloro-2-(4,4,5,5-tetramethyl-1,3,2-dioxaborolan-2-yl)benzoyl)-5-methoxy-2-methyl-1H-indol-3-yl)acetate (35).*

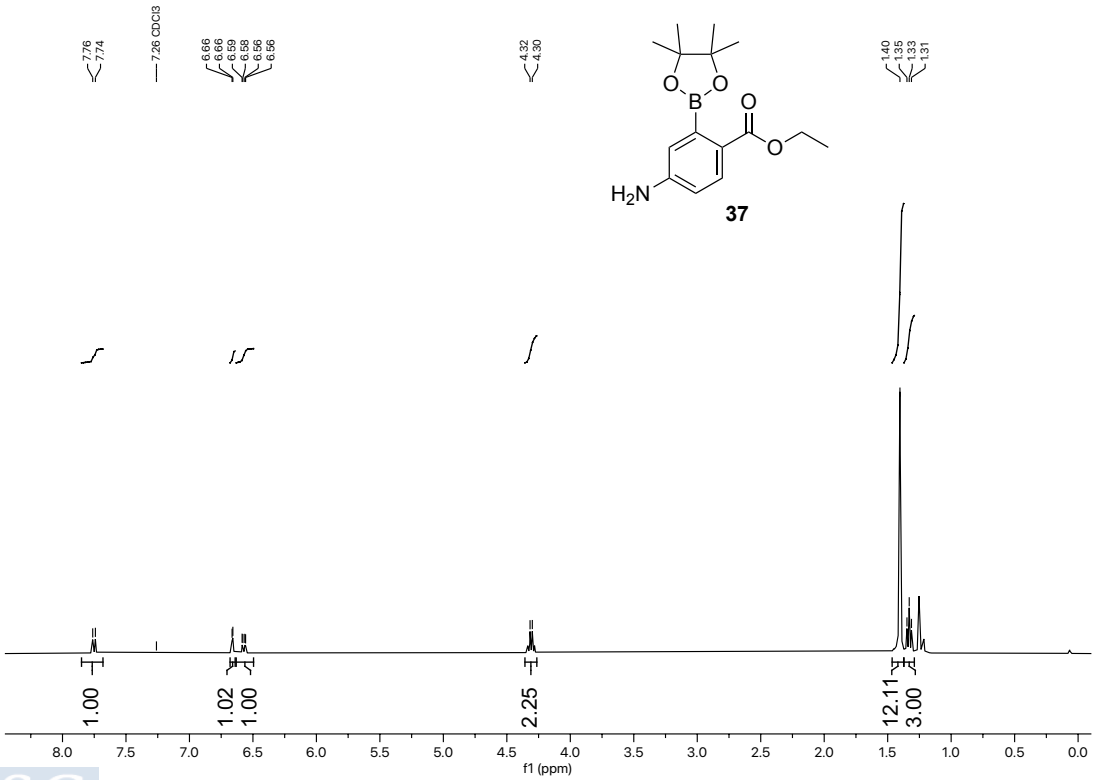



USC
UNIVERSIDADE DE SANTIAGO DE COMPOSTELA

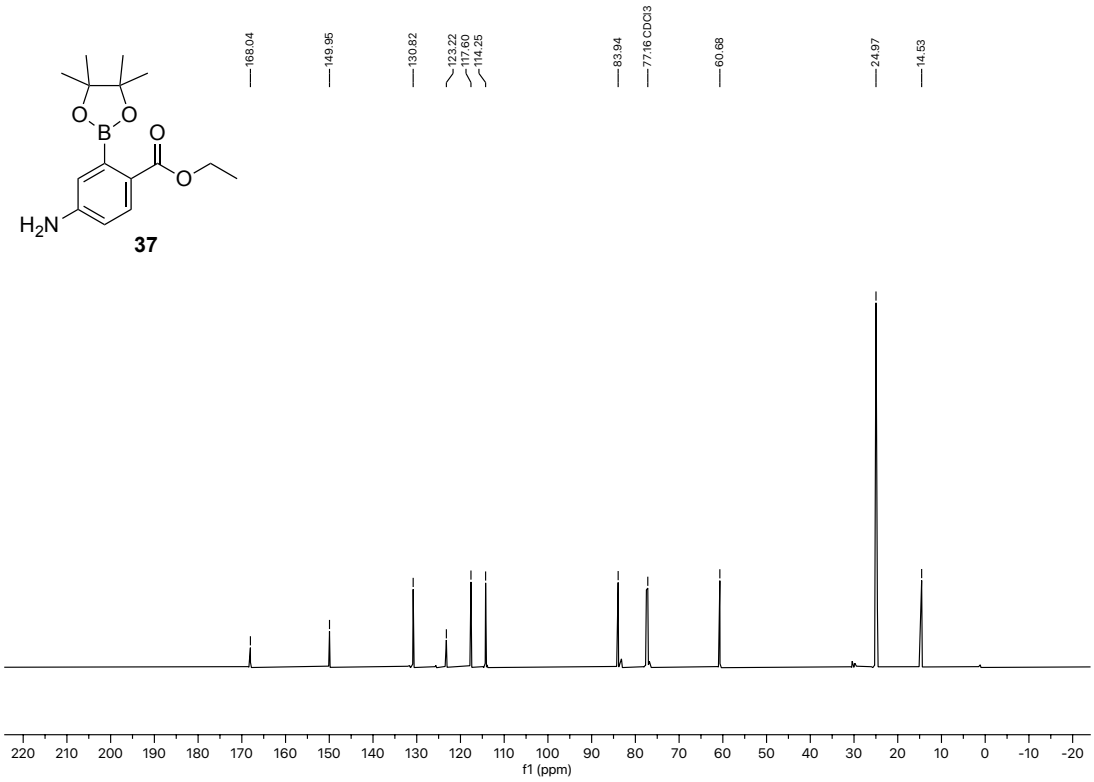
*HSQC NMR Methyl 2-(1-(4-chloro-2-(4,4,5,5-tetramethyl-1,3,2-dioxaborolan-2-yl)benzoyl)-5-methoxy-2-methyl-1H-indol-3-yl)acetate (35).*



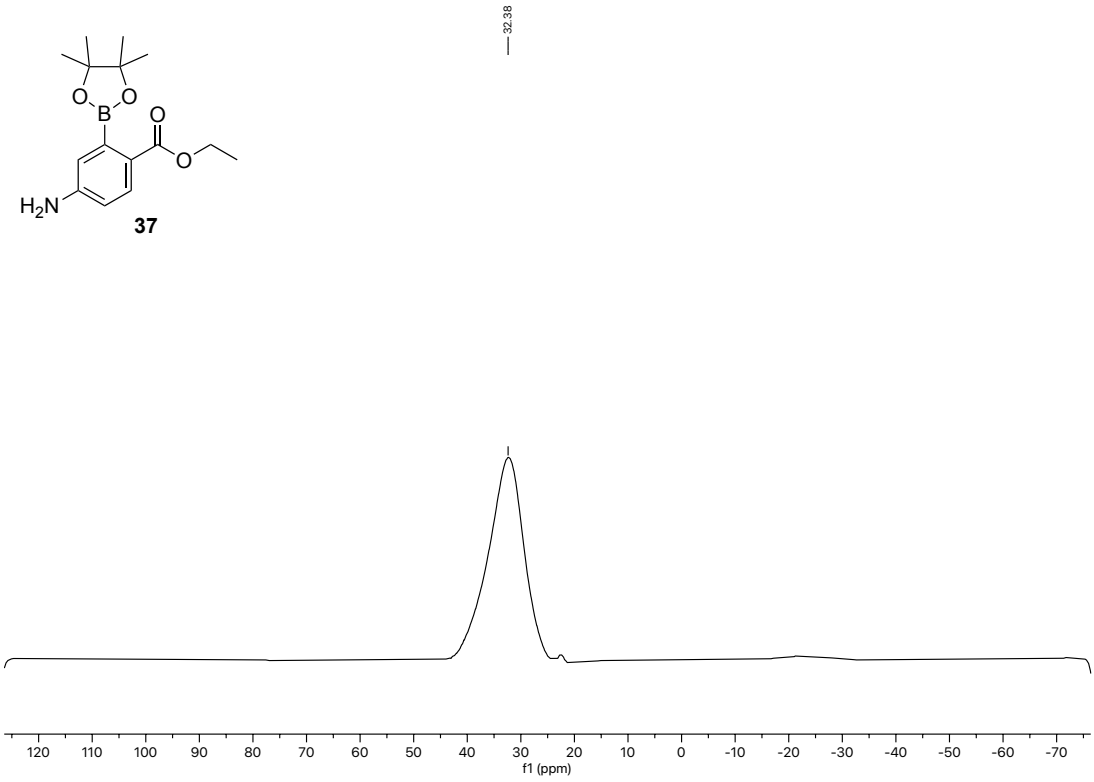

*$^{1}$H NMR Ethyl 4-amino-2-(4,4,5,5-tetramethyl-1,3,2-dioxaborolan-2-yl)benzoate (37)*



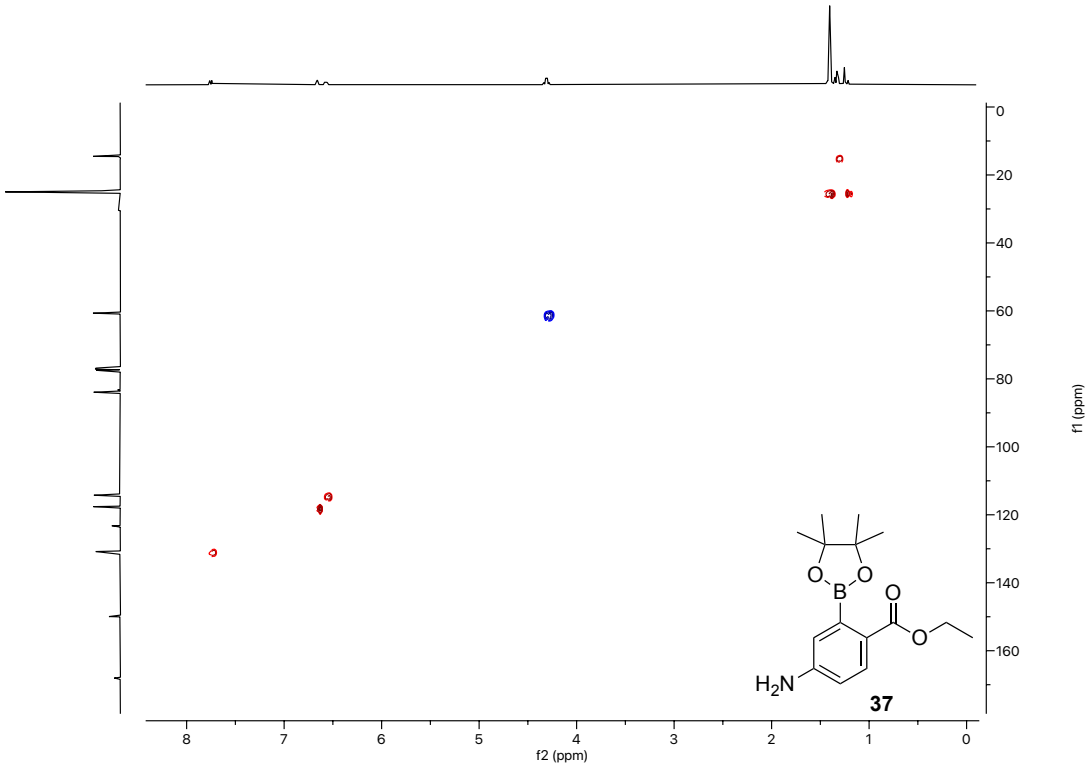
*$^{13}$C NMR Ethyl 4-amino-2-(4,4,5,5-tetramethyl-1,3,2-dioxaborolan-2-yl)benzoate (37)*



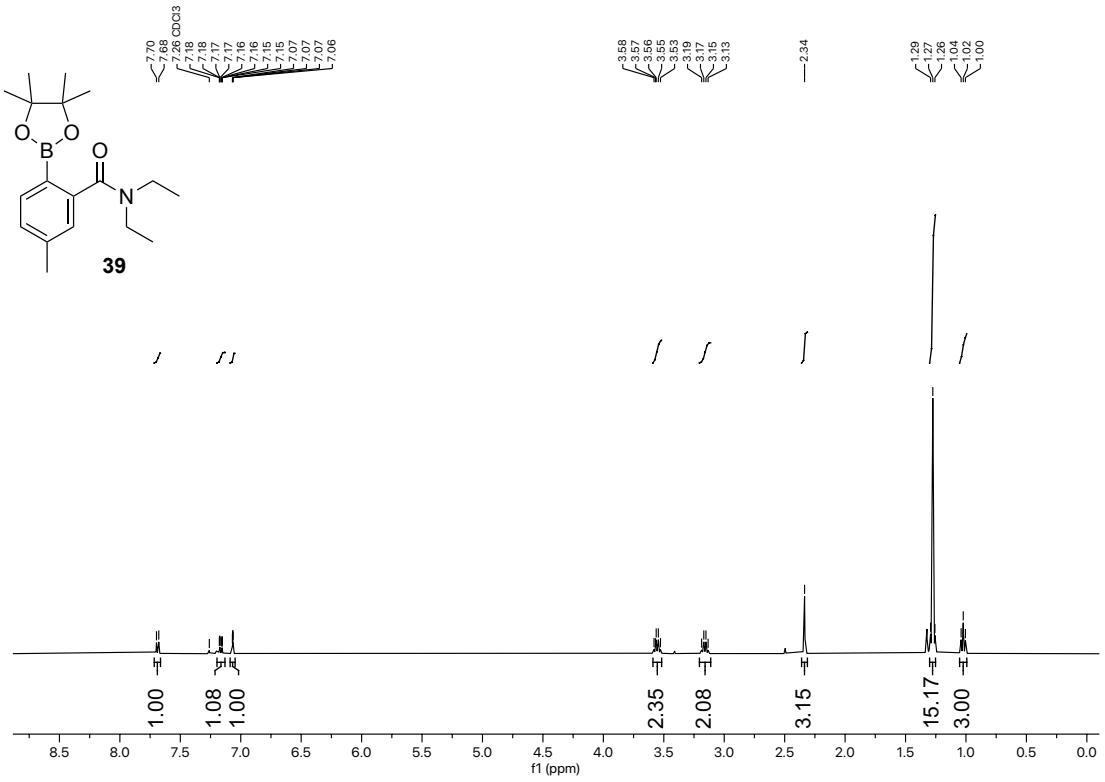

*$^{11}$B NMR Ethyl 4-amino-2-(4,4,5,5-tetramethyl-1,3,2-dioxaborolan-2-yl)benzoate (37)*



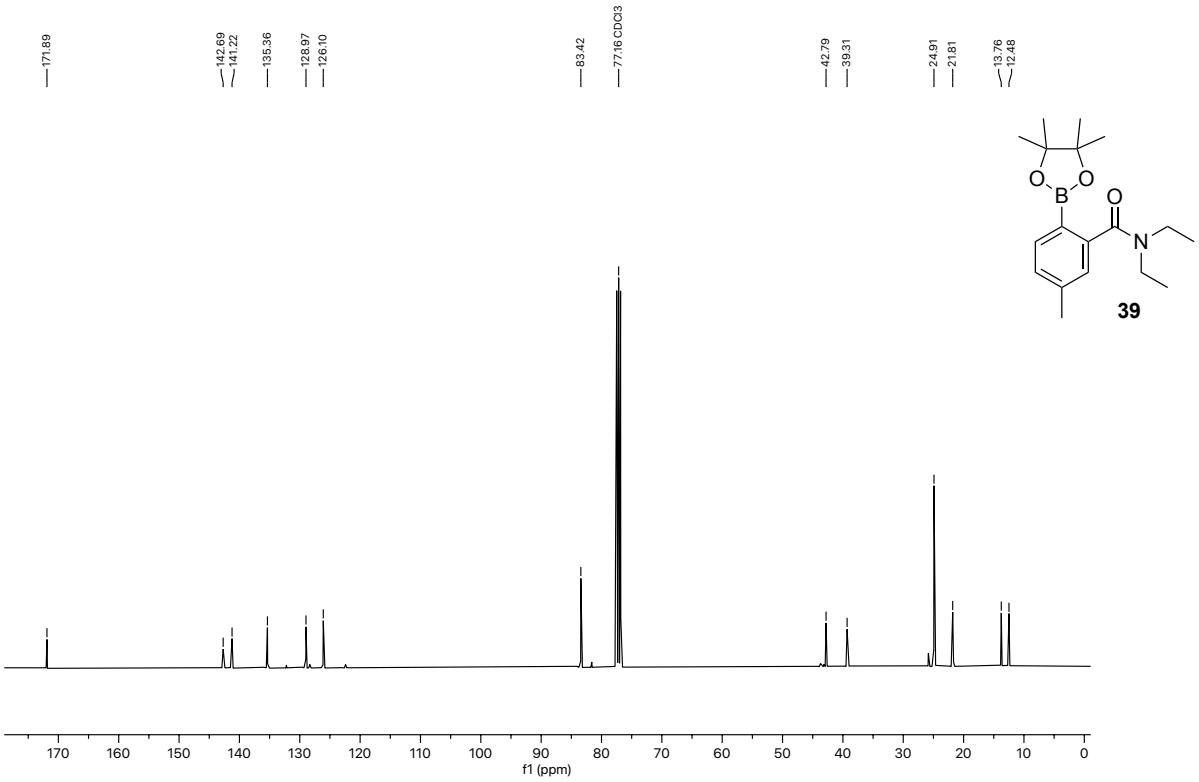
*HSQC NMR Ethyl 4-amino-2-(4,4,5,5-tetramethyl-1,3,2-dioxaborolan-2-yl)benzoate (37)*



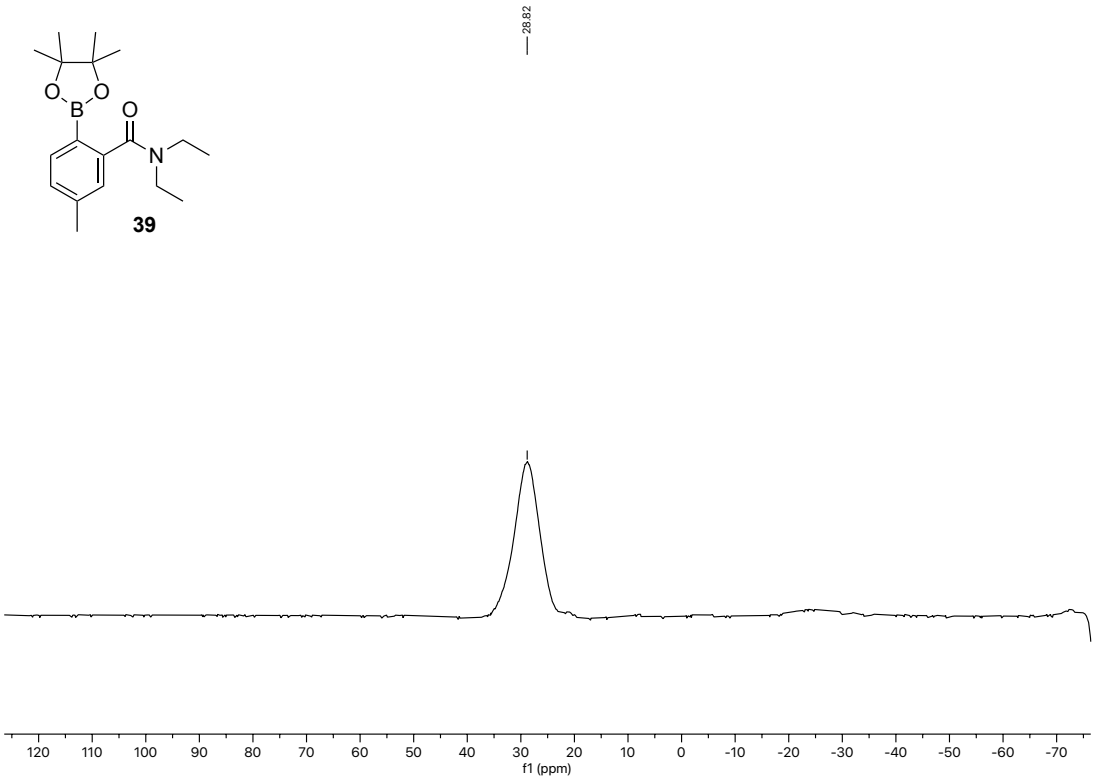

*$^{1}$H NMR N,N-diethyl-5-methyl-2-(4,4,5,5-tetramethyl-1,3,2-dioxaborolan-2-yl)benzamide (39)*



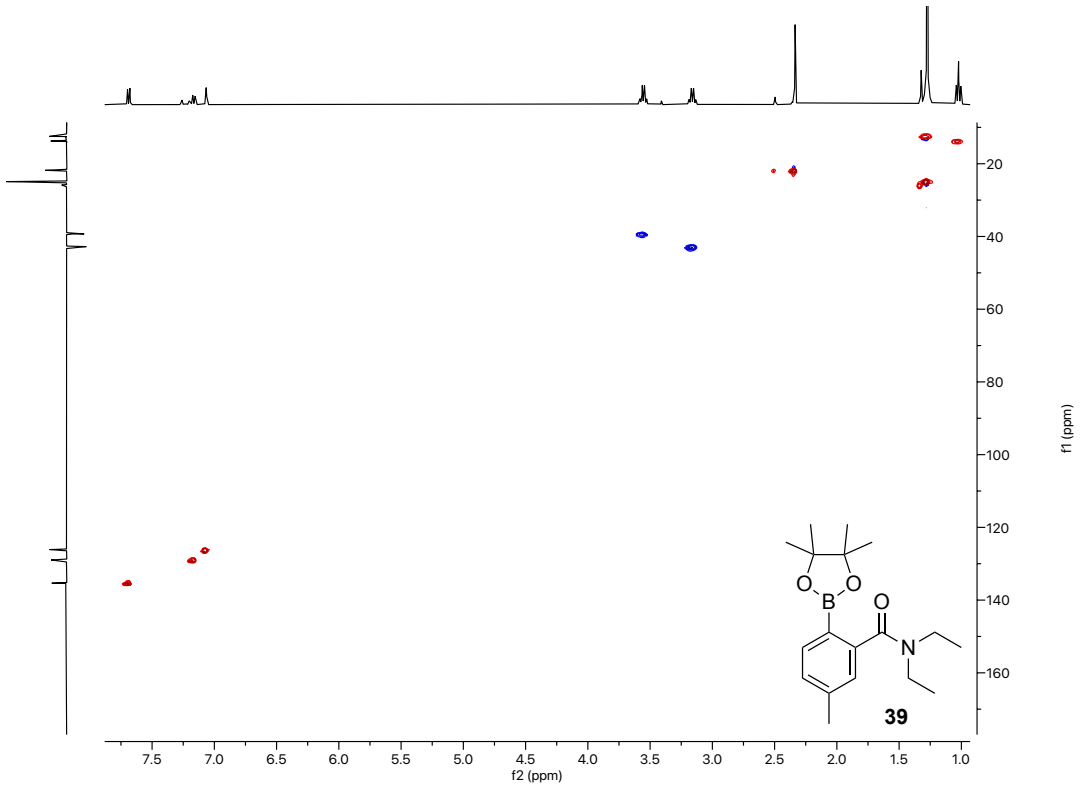
*$^{13}$C NMR N,N-diethyl-5-methyl-2-(4,4,5,5-tetramethyl-1,3,2-dioxaborolan-2-yl)benzamide (39)*



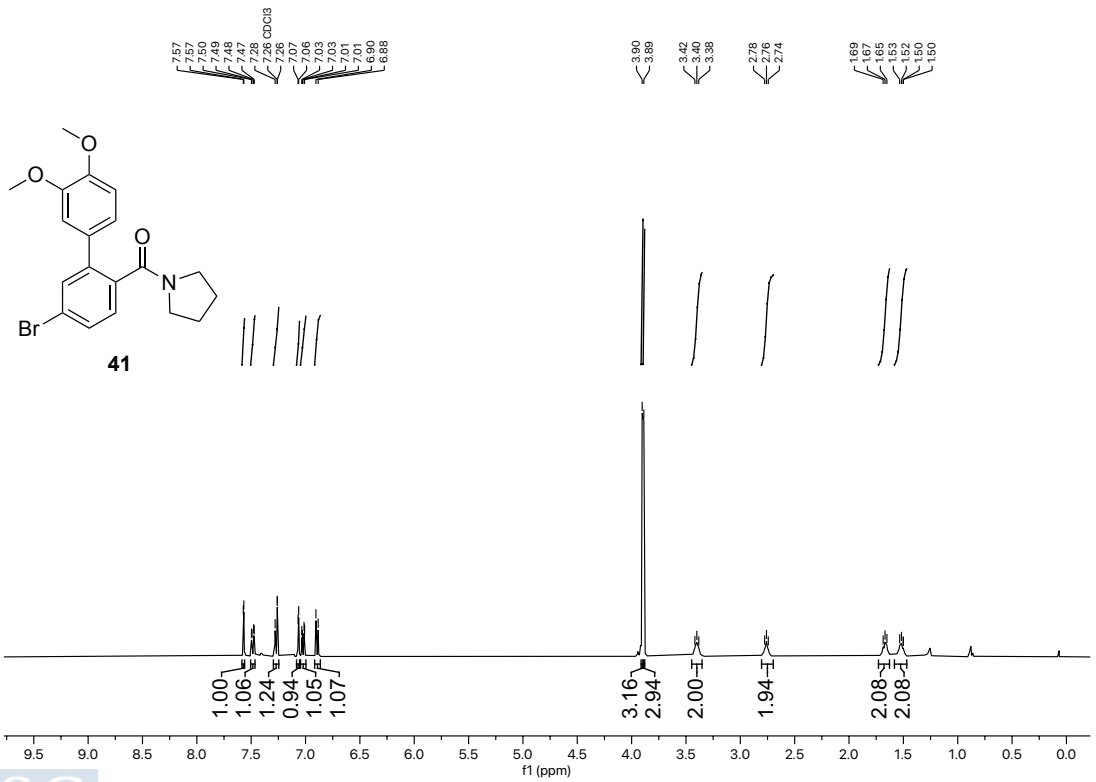

*$^{11}$B NMR N,N-diethyl-5-methyl-2-(4,4,5,5-tetramethyl-1,3,2-dioxaborolan-2-yl)benzamide (39)*



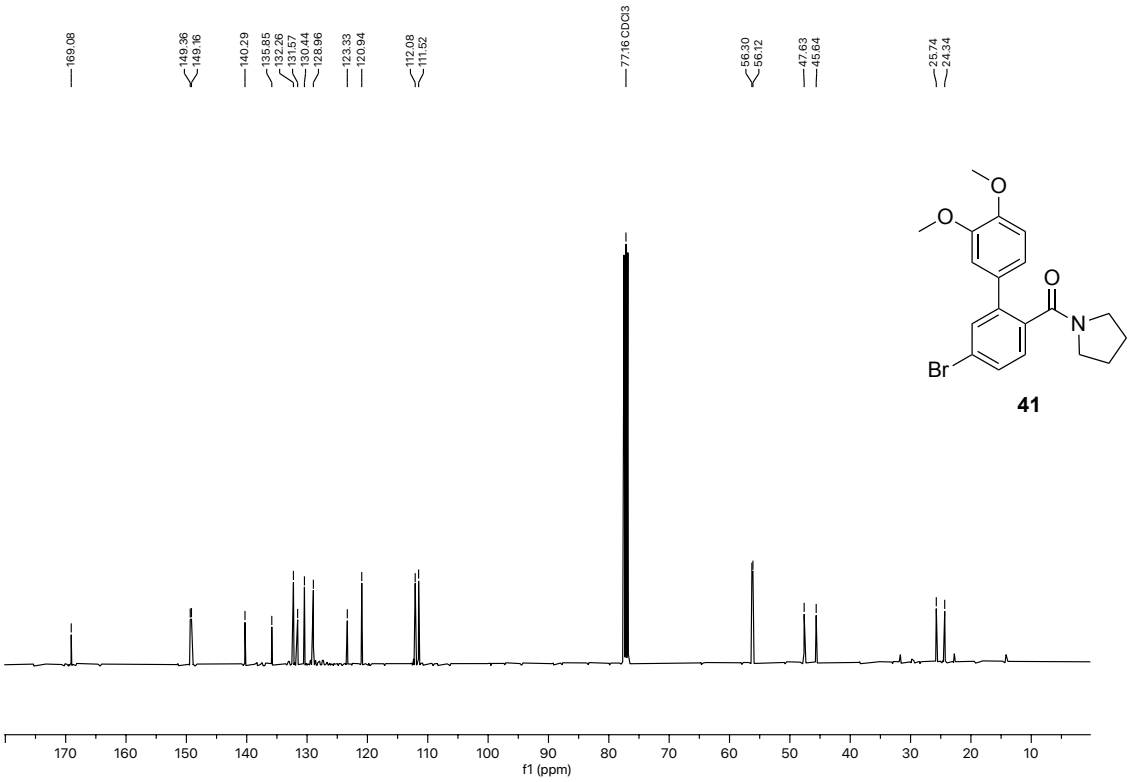
*HSQC NMR N,N-diethyl-5-methyl-2-(4,4,5,5-tetramethyl-1,3,2-dioxaborolan-2-yl)benzamide (39)*



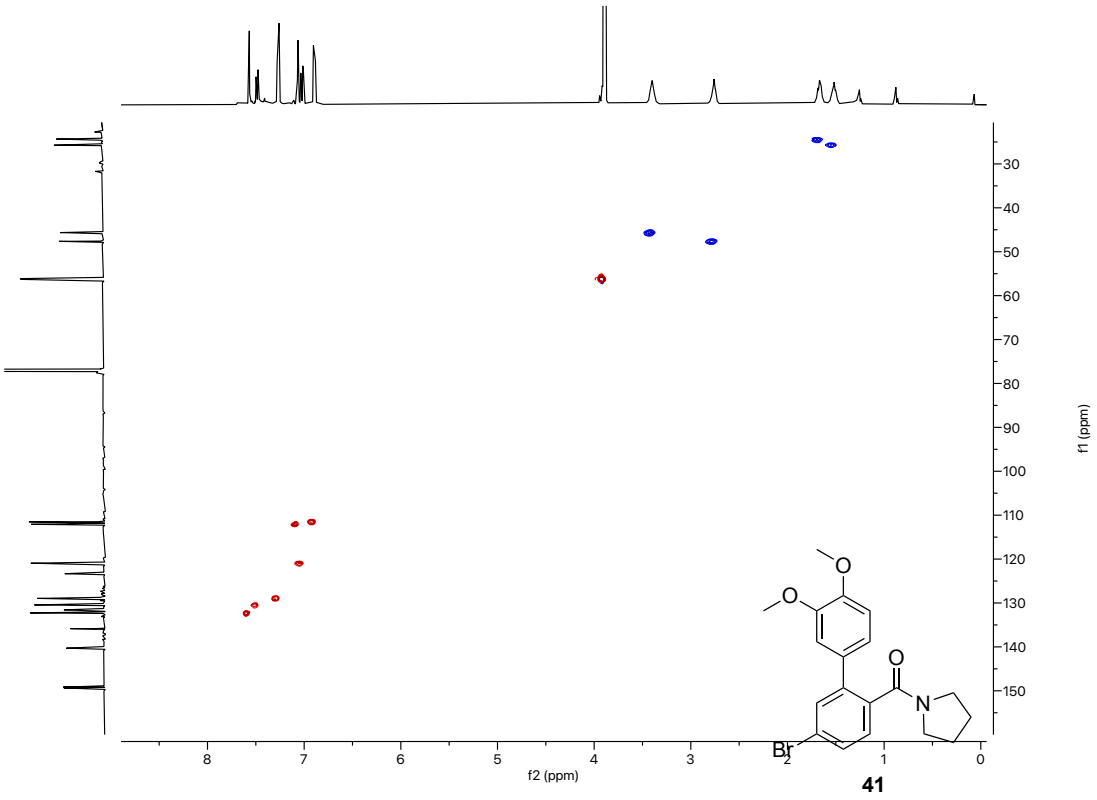

*$^1$H NMR (5-bromo-3',4'-dimethoxy-[1,1'-biphenyl]-2-yl)(pyrrolidin-1-yl)methanone (41)*



*$^{13}$C NMR (5-bromo-3',4'-dimethoxy-[1,1'-biphenyl]-2-yl)(pyrrolidin-1-yl)methanone (41)*



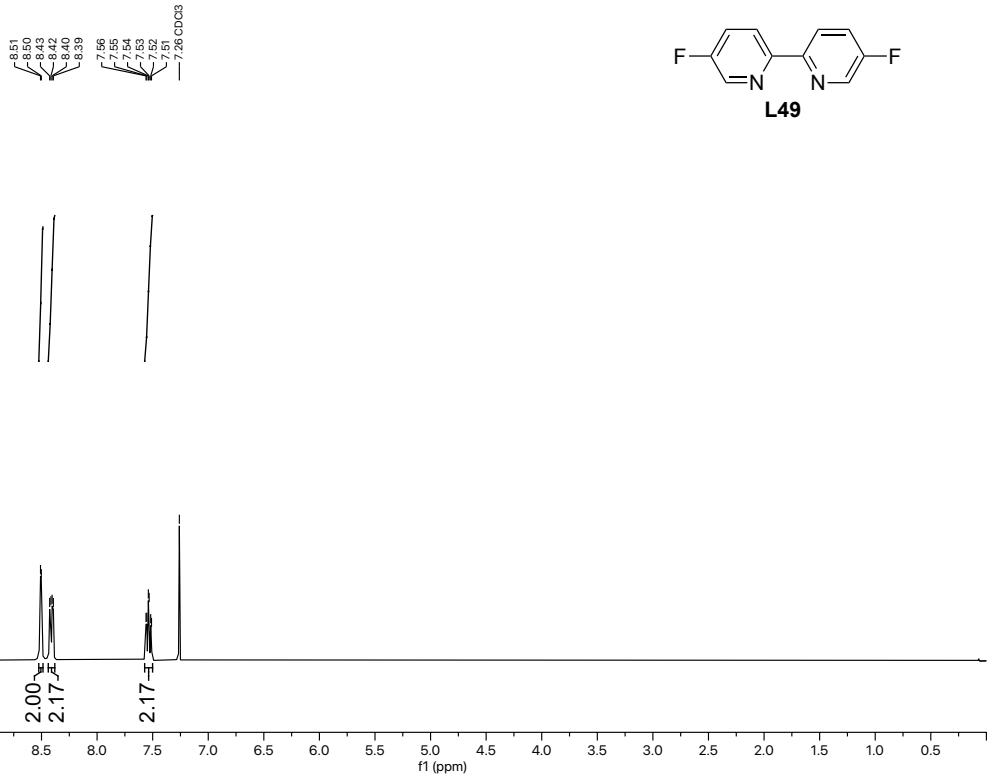

*HSQC NMR (5-bromo-3',4'-dimethoxy-[1,1'-biphenyl]-2-yl)(pyrrolidin-1-yl)methanone (41)*



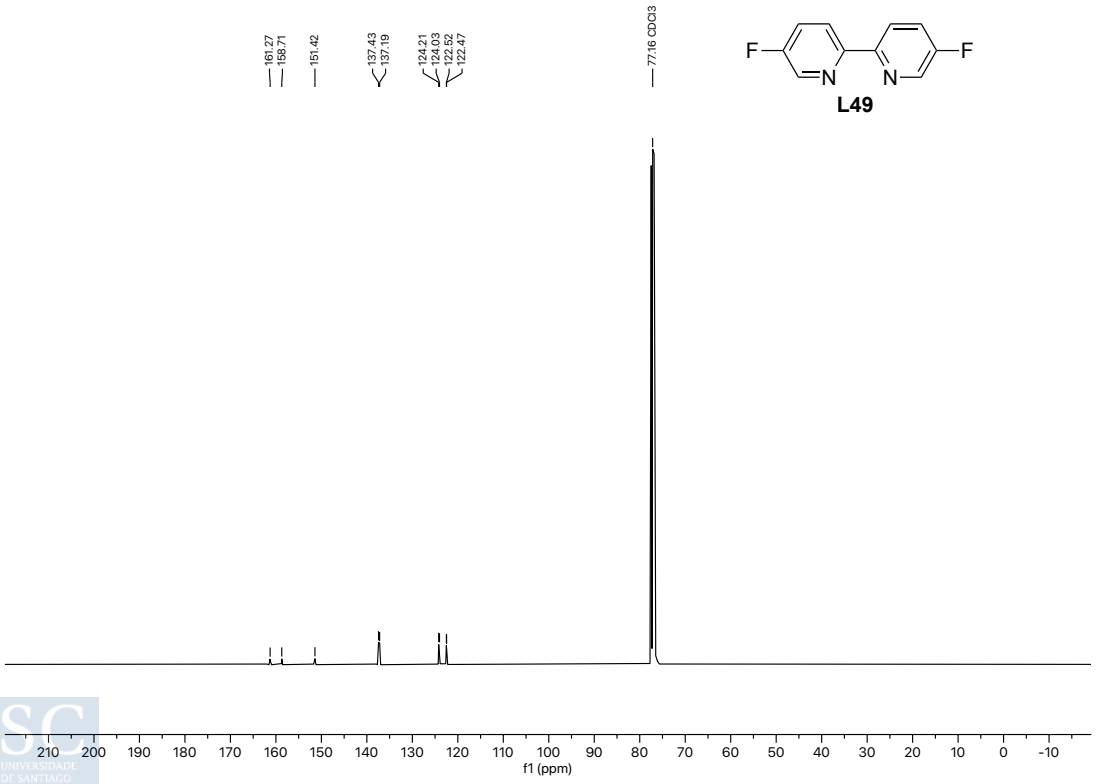
## 11.1.3 Selected spectra for molecules in section 7.3

### *11.1.3.1 Spectra of ligands*

*$^{1}$H NMR 5,5'-difluoro-2,2'-bipyridine (L49)*

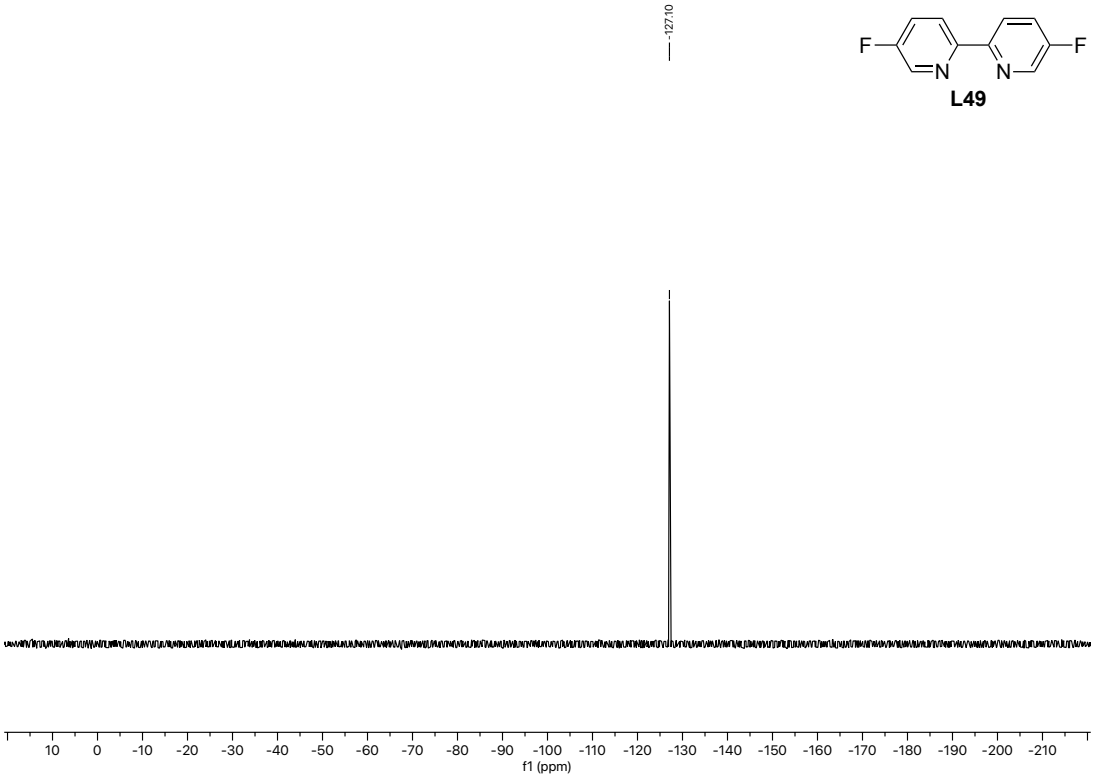



*$^{13}$C NMR 5,5'-difluoro-2,2'-bipyridine (L49)*

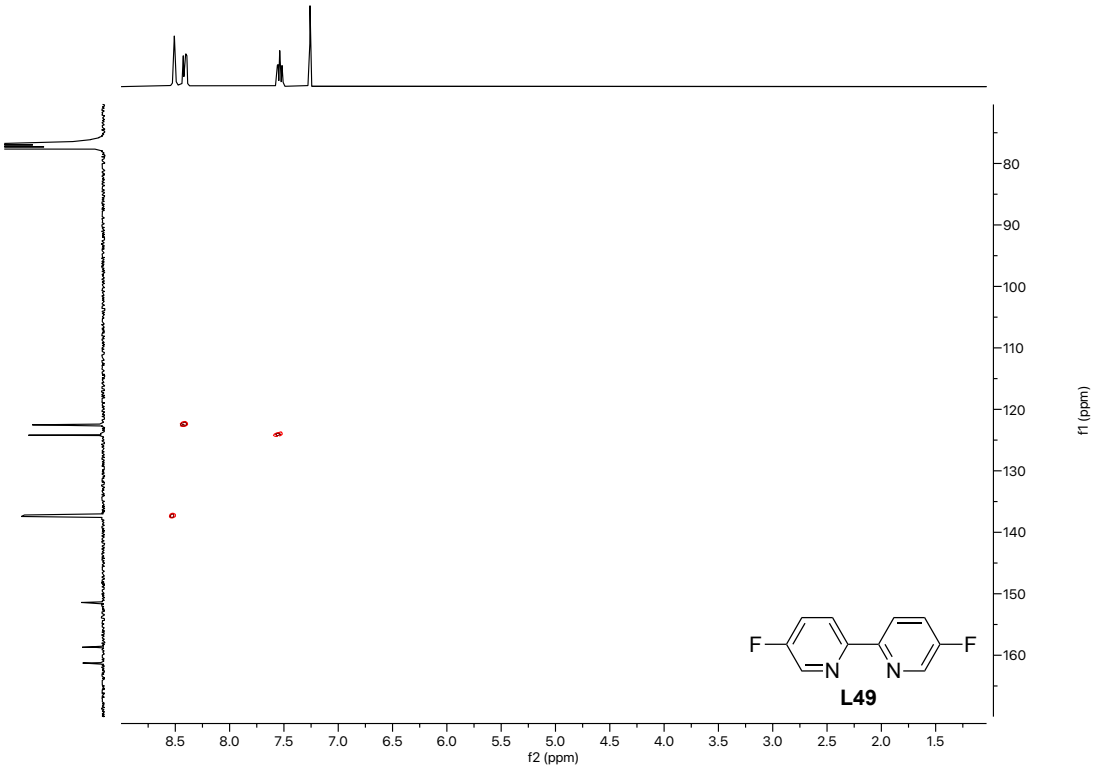



USC UNIVERSIDADE DE SANTIAGO DE COMPOSTELA

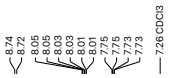
*$^{19}$F NMR 5,5'-difluoro-2,2'-bipyridine (L49)*

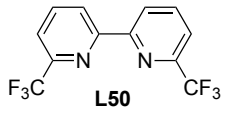


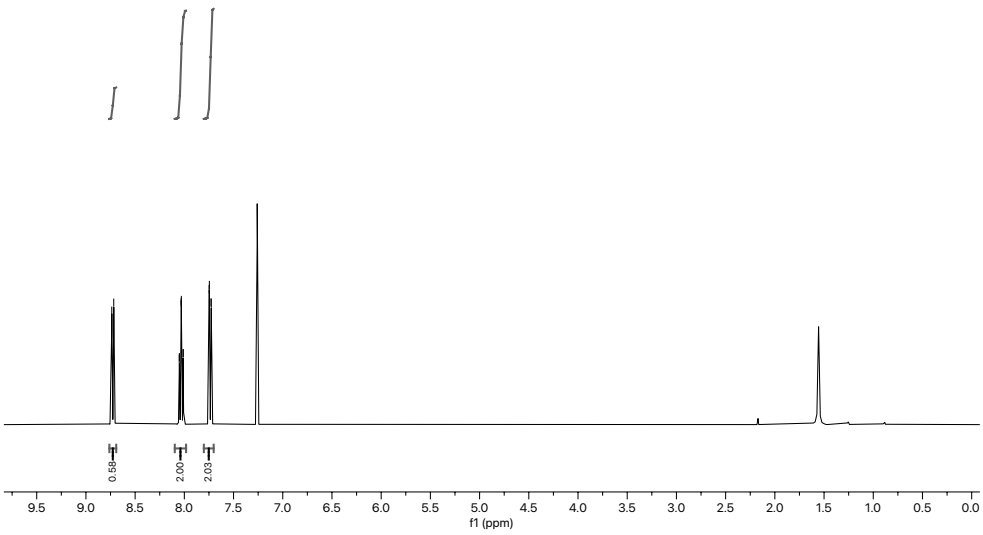

*HSQC NMR 5,5'-difluoro-2,2'-bipyridine (L49)*



*[1]H NMR 6,6'-bis(trifluoromethyl)-2,2'-bipyridine (L50)*

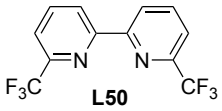


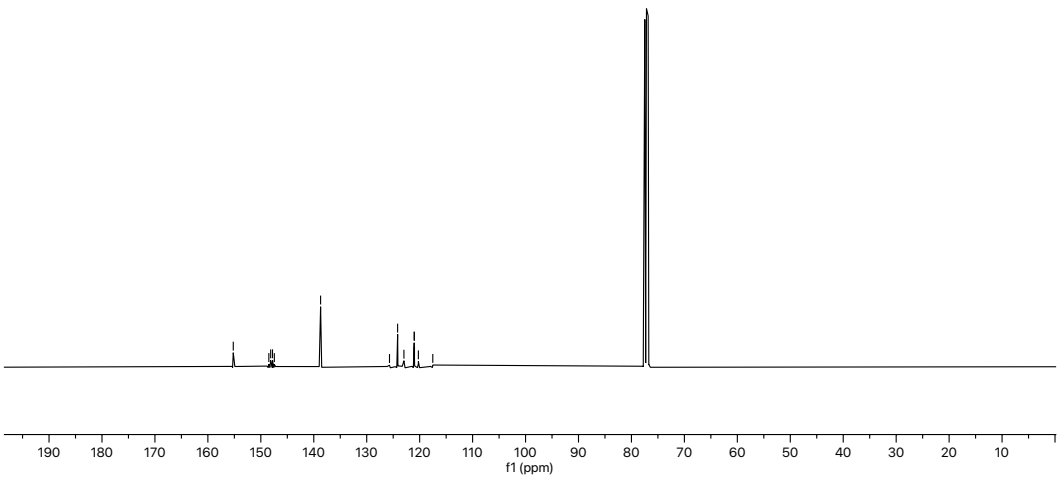



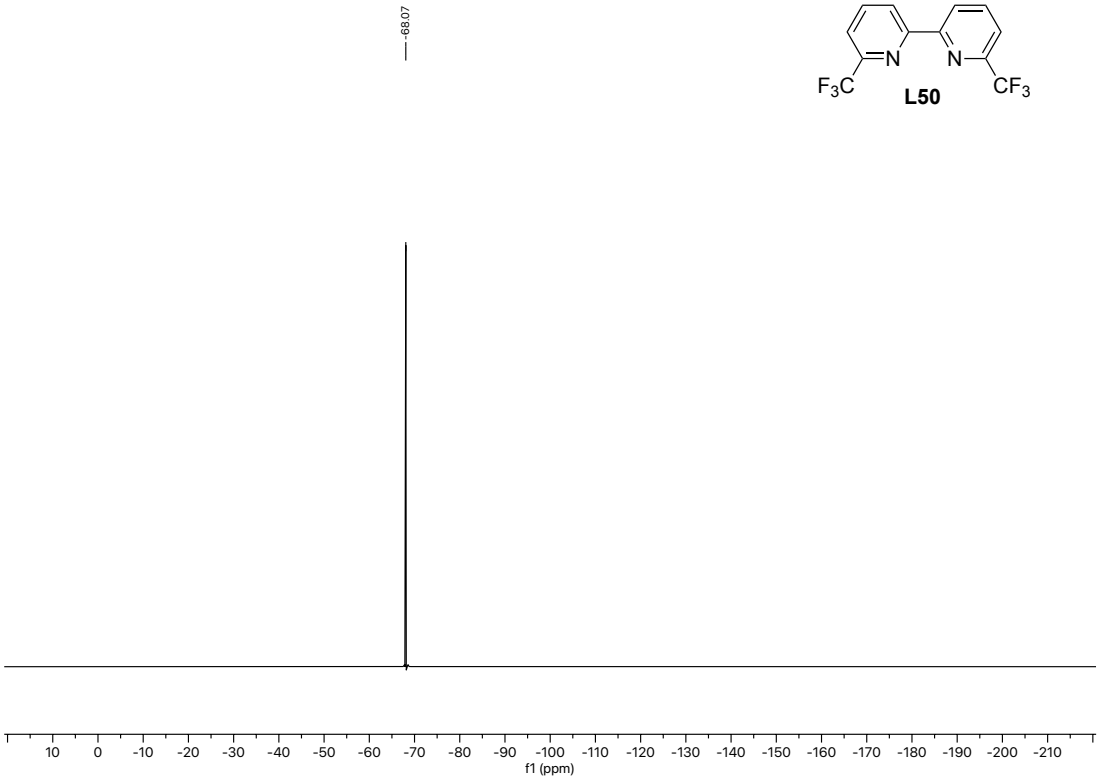

*[13]C NMR 6,6'-bis(trifluoromethyl)-2,2'-bipyridine (L50)*



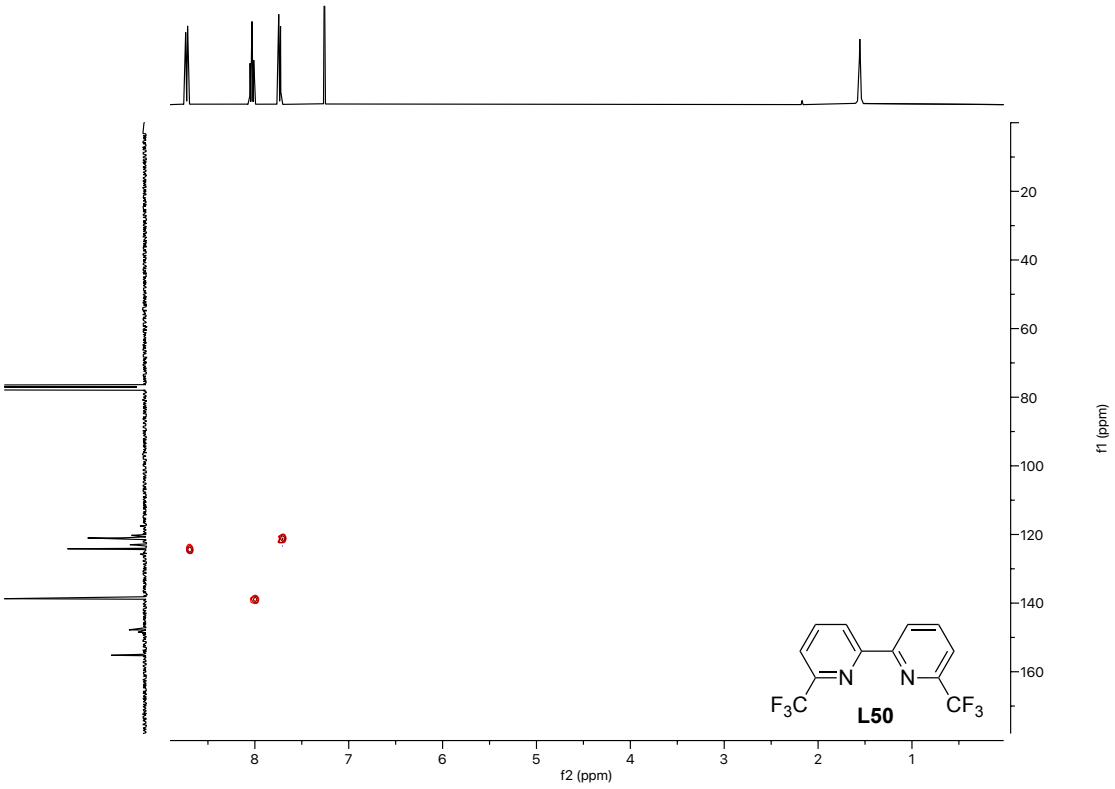



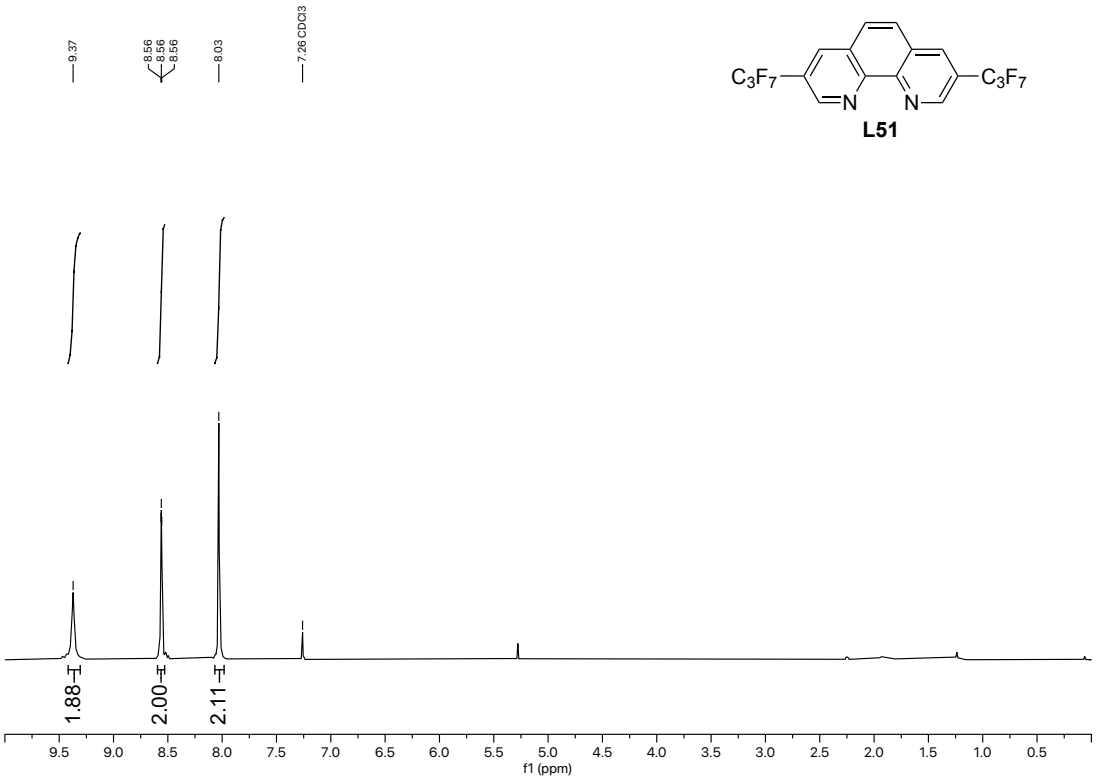
*$^{19}$F NMR 6,6'-bis(trifluoromethyl)-2,2'-bipyridine (L50)*



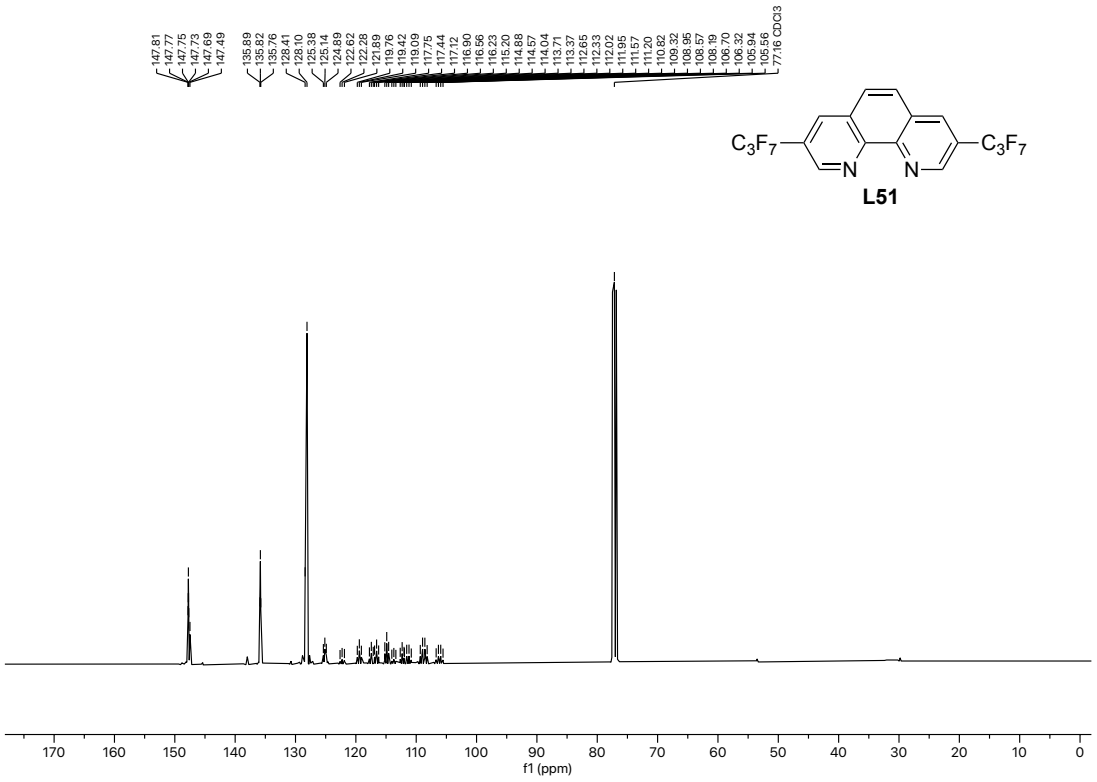

*HSQC NMR 6,6'-bis(trifluoromethyl)-2,2'-bipyridine (L50)*



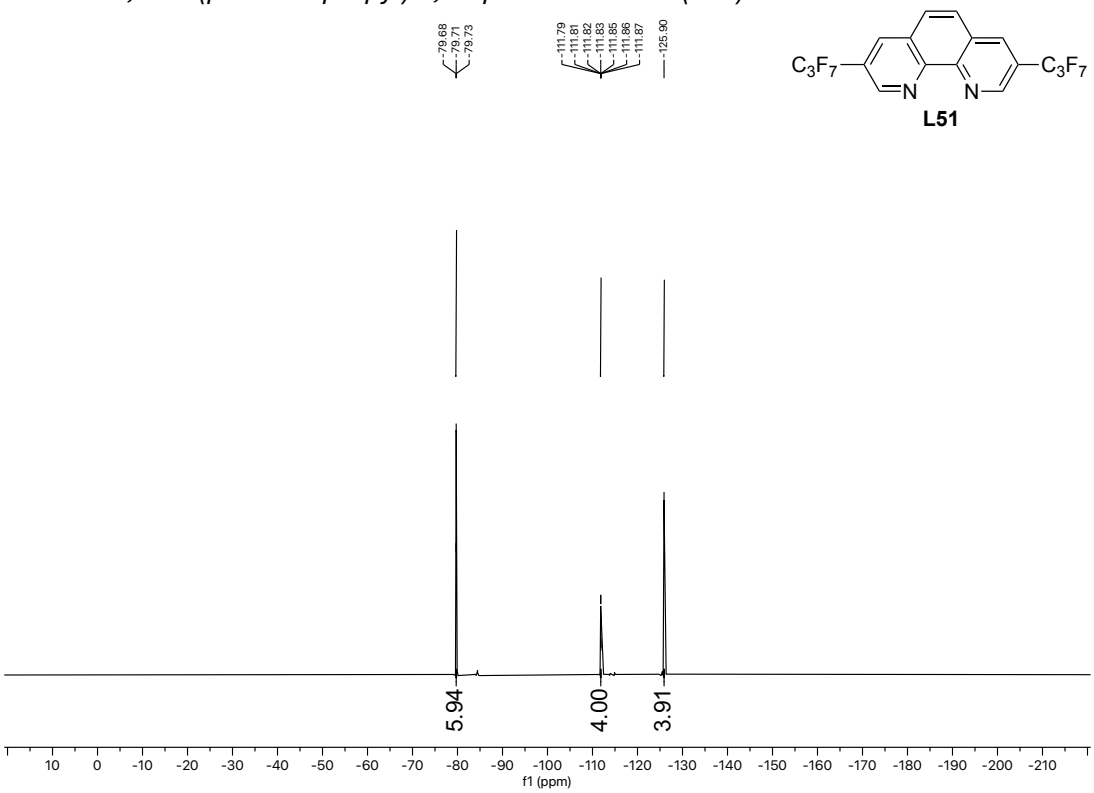
*[1]H NMR 3,8-bis(perfluoropropyl)-1,10-phenanthroline (L51)*



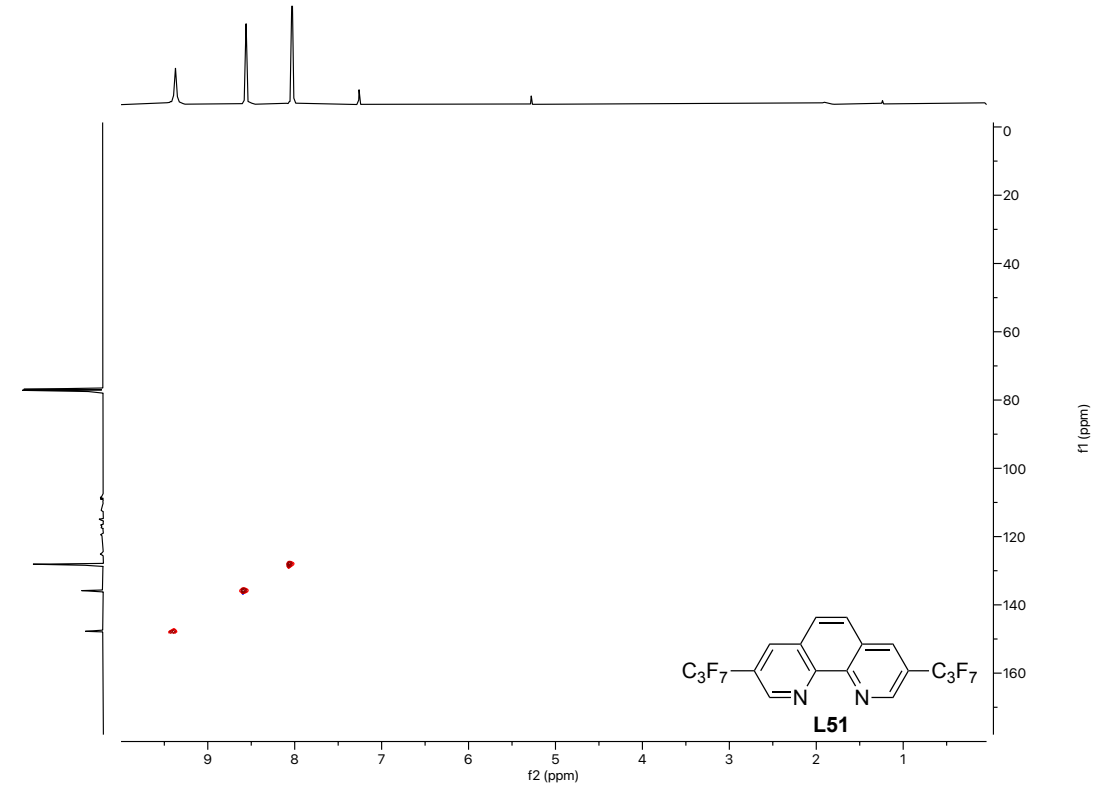

*[13]C NMR 3,8-bis(perfluoropropyl)-1,10-phenanthroline (L51)*



*$^{19}$F NMR 3,8-bis(perfluoropropyl)-1,10-phenanthroline (L51)*

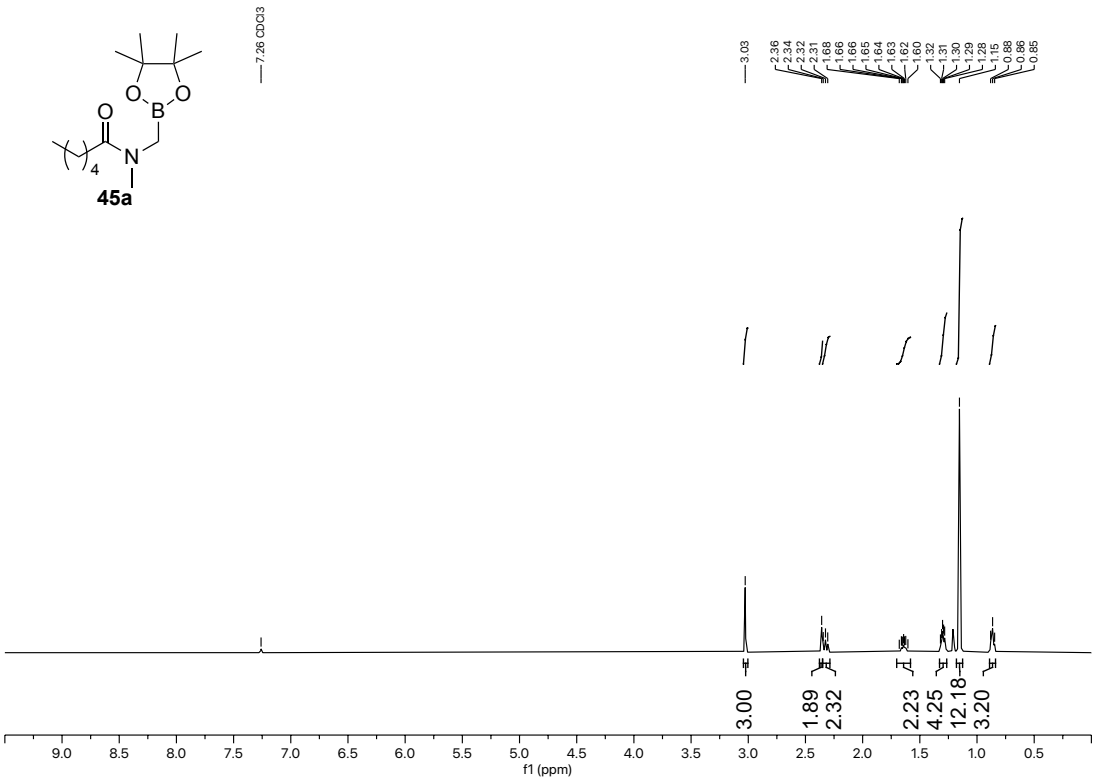



*HSQC NMR 3,8-bis(perfluoropropyl)-1,10-phenanthroline (L51)*

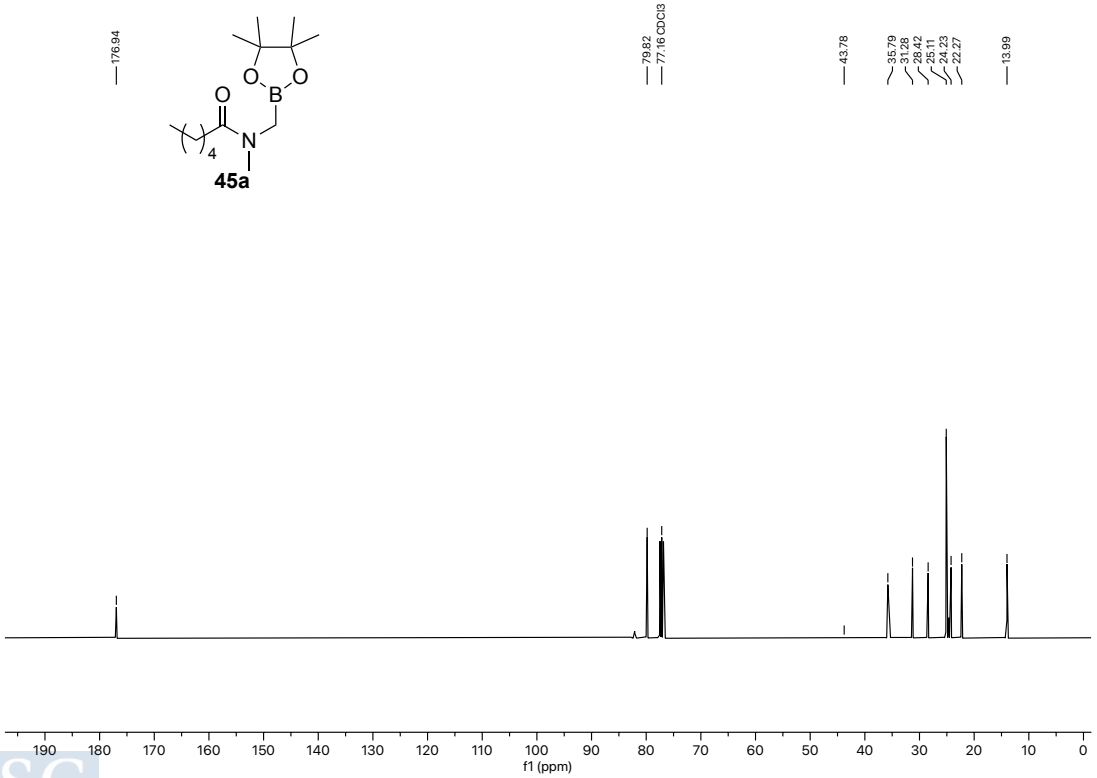


### *11.1.3.2 Selected spectra of products*

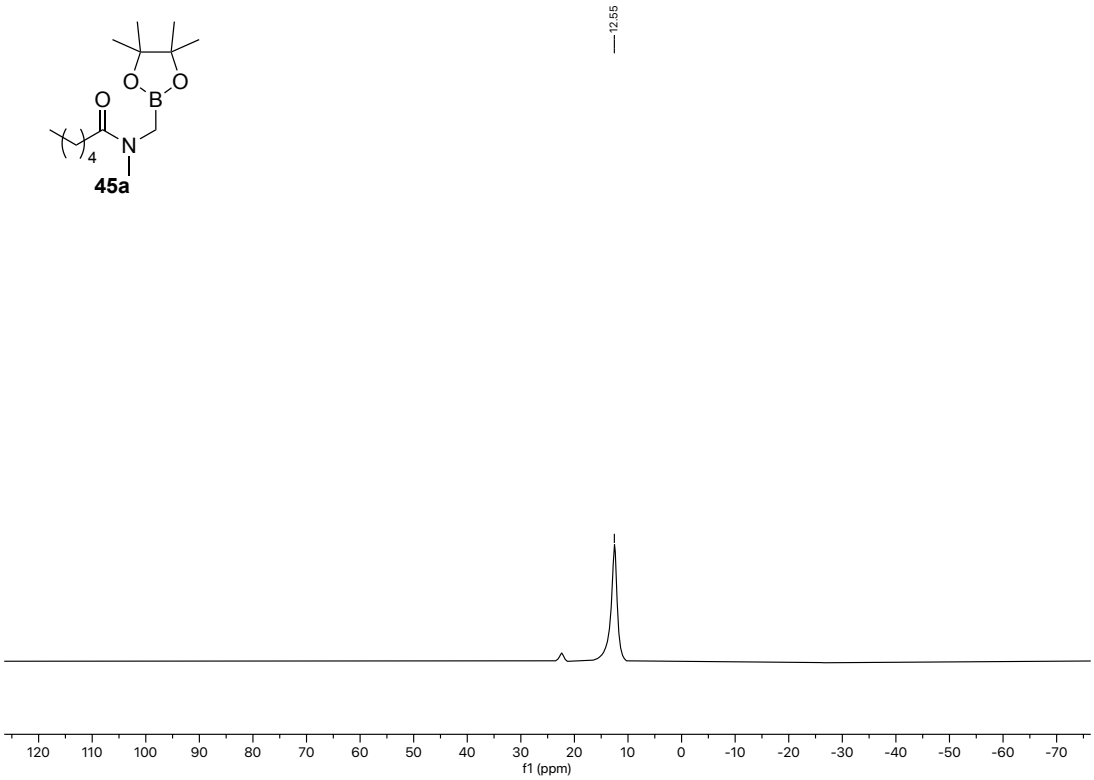
*$^{1}$H NMR N-methyl-N-((4,4,5,5-tetramethyl-1,3,2-dioxaborolan-2-yl)methyl)hexanamide (45a)*



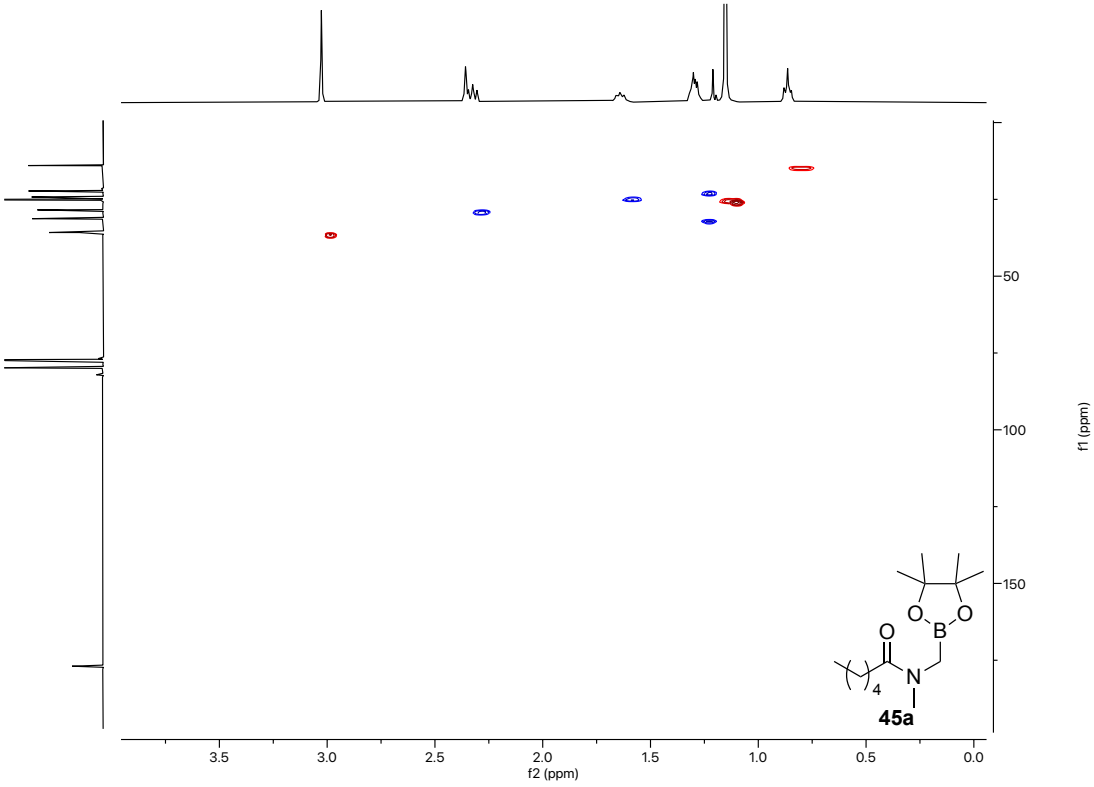

*$^{13}$C NMR N-methyl-N-((4,4,5,5-tetramethyl-1,3,2-dioxaborolan-2-yl)methyl)hexanamide (45a)*



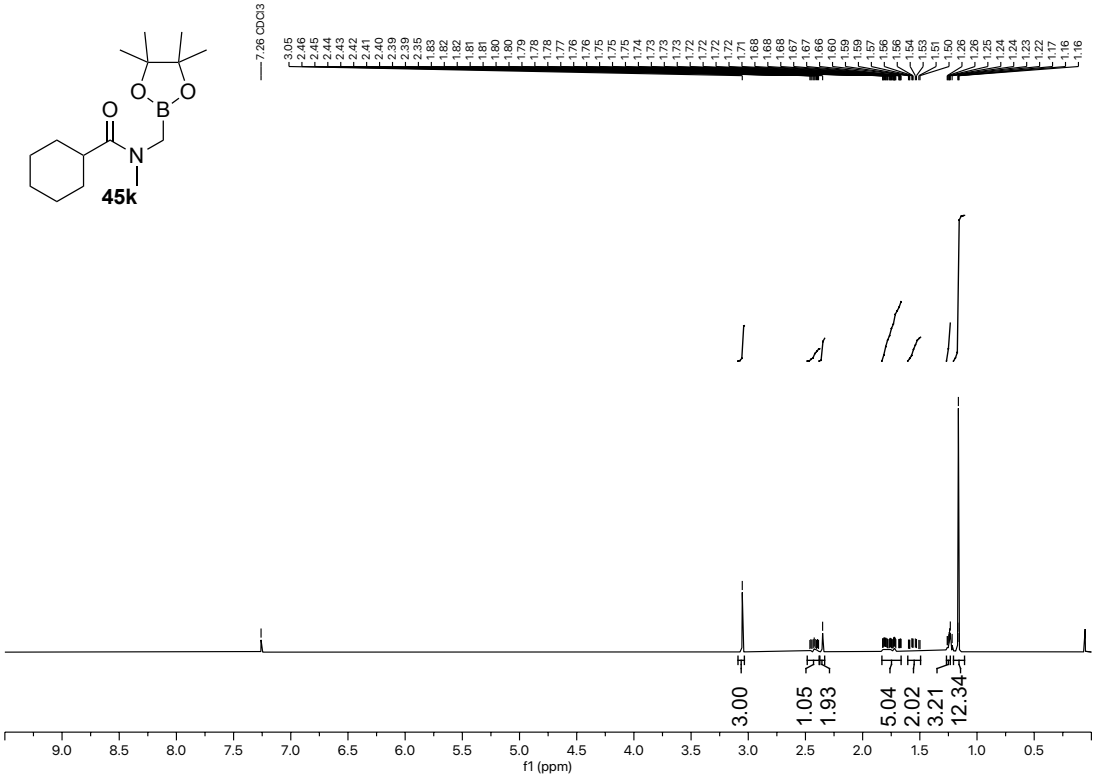
*$^{11}$B NMR N-methyl-N-((4,4,5,5-tetramethyl-1,3,2-dioxaborolan-2-yl)methyl)hexanamide (45a)*



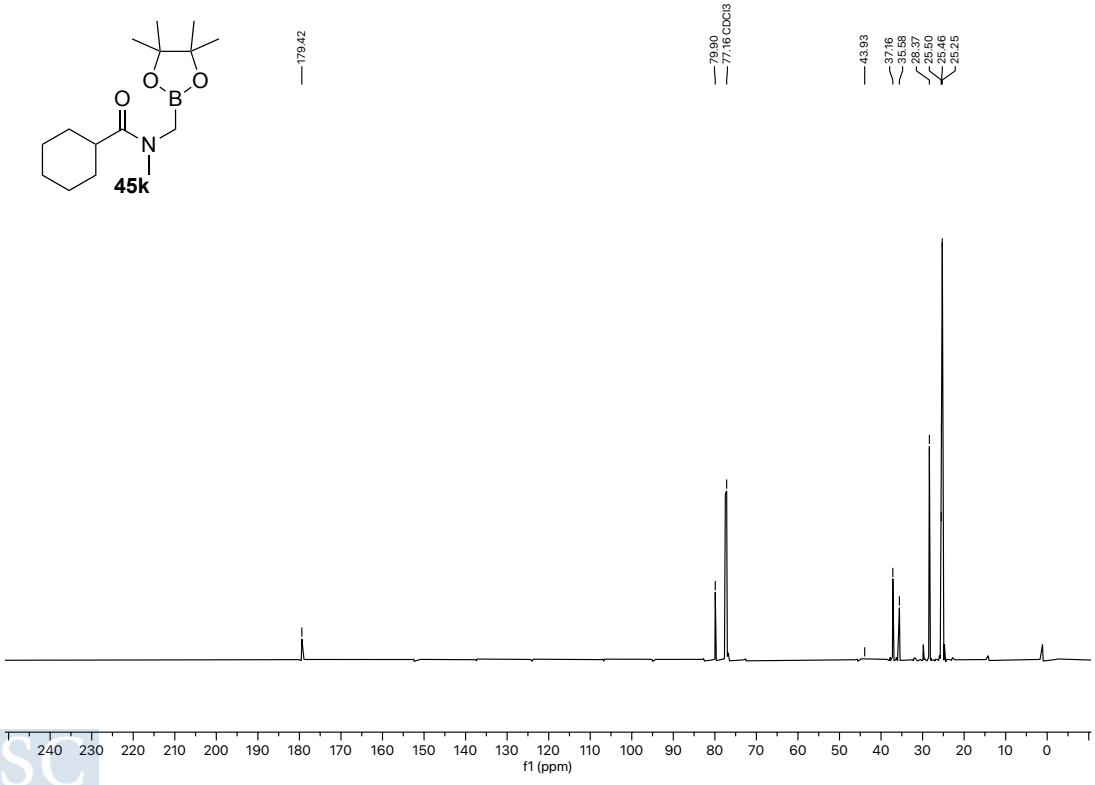

*HSQC NMR N-methyl-N-((4,4,5,5-tetramethyl-1,3,2-dioxaborolan-2-yl)methyl)hexanamide (45a)*



*[1]H NMR N-methyl-N-((4,4,5,5-tetramethyl-1,3,2-dioxaborolan-2-yl)methyl)cyclohexanecarboxamide (45k)*

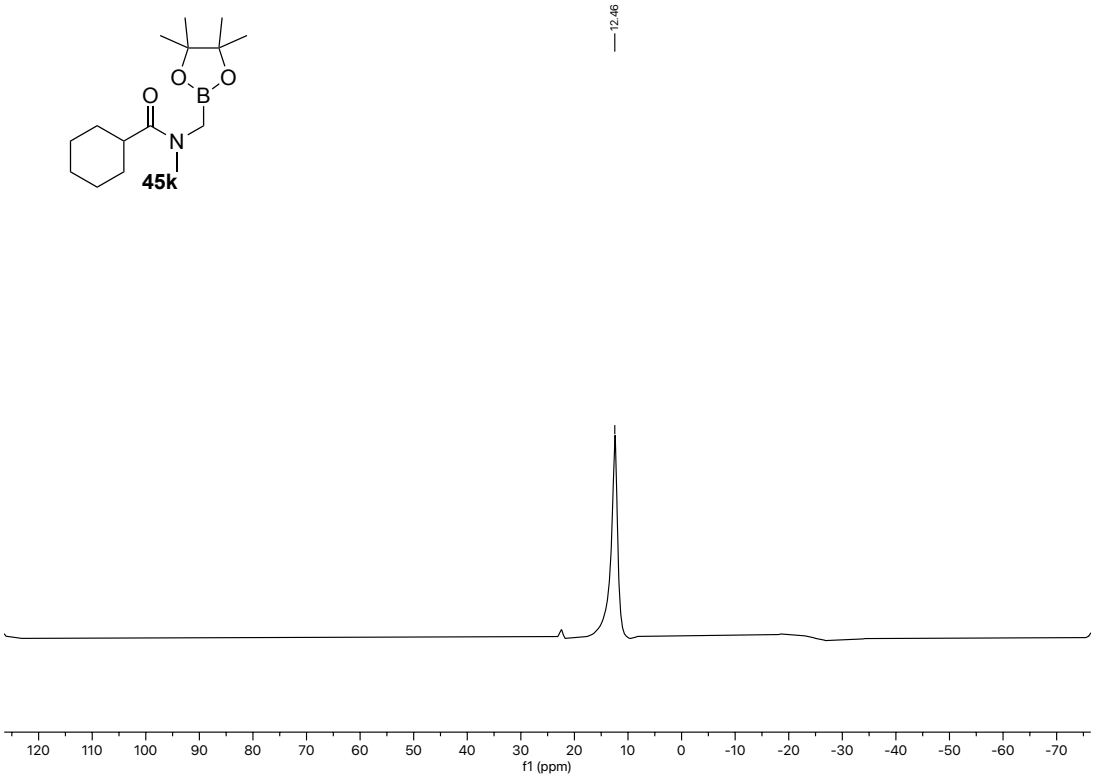



*[13]C NMR N-methyl-N-((4,4,5,5-tetramethyl-1,3,2-dioxaborolan-2-yl)methyl)cyclohexanecarboxamide (45k)*

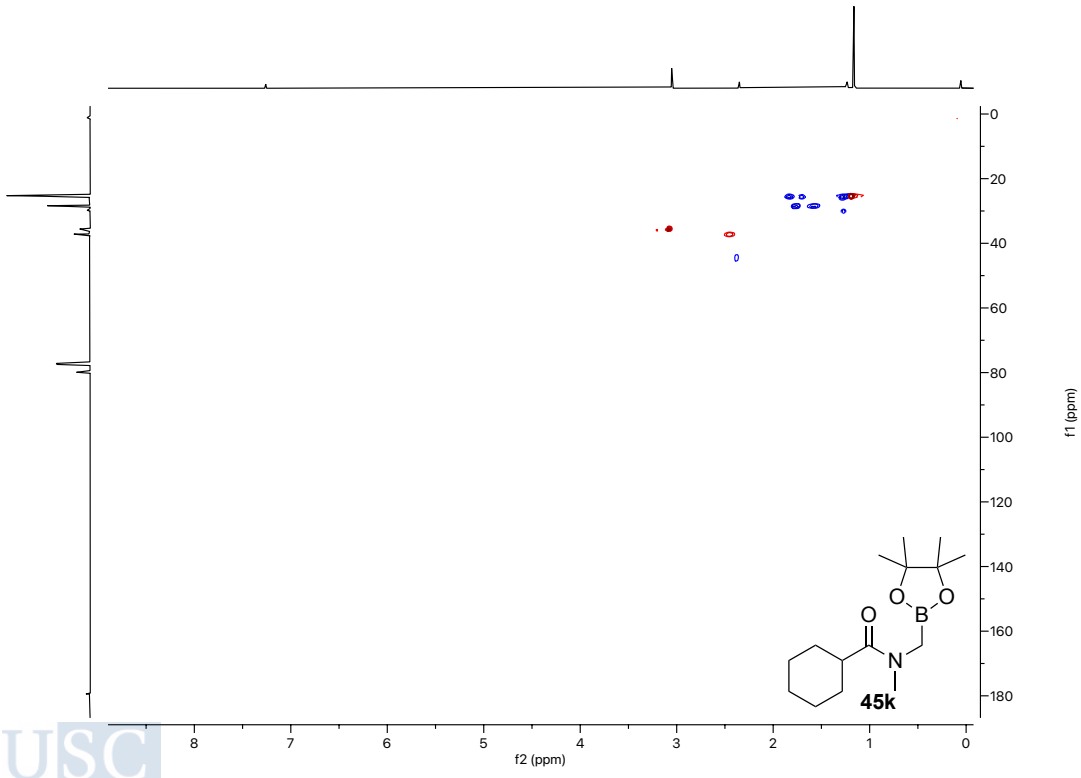



USC UNIVERSIDADE DE SANTIAGO DE COMPOSTELA

*[11]B NMR N-methyl-N-((4,4,5,5-tetramethyl-1,3,2-dioxaborolan-2-yl)methyl)cyclohexanecarboxamide (45k)*

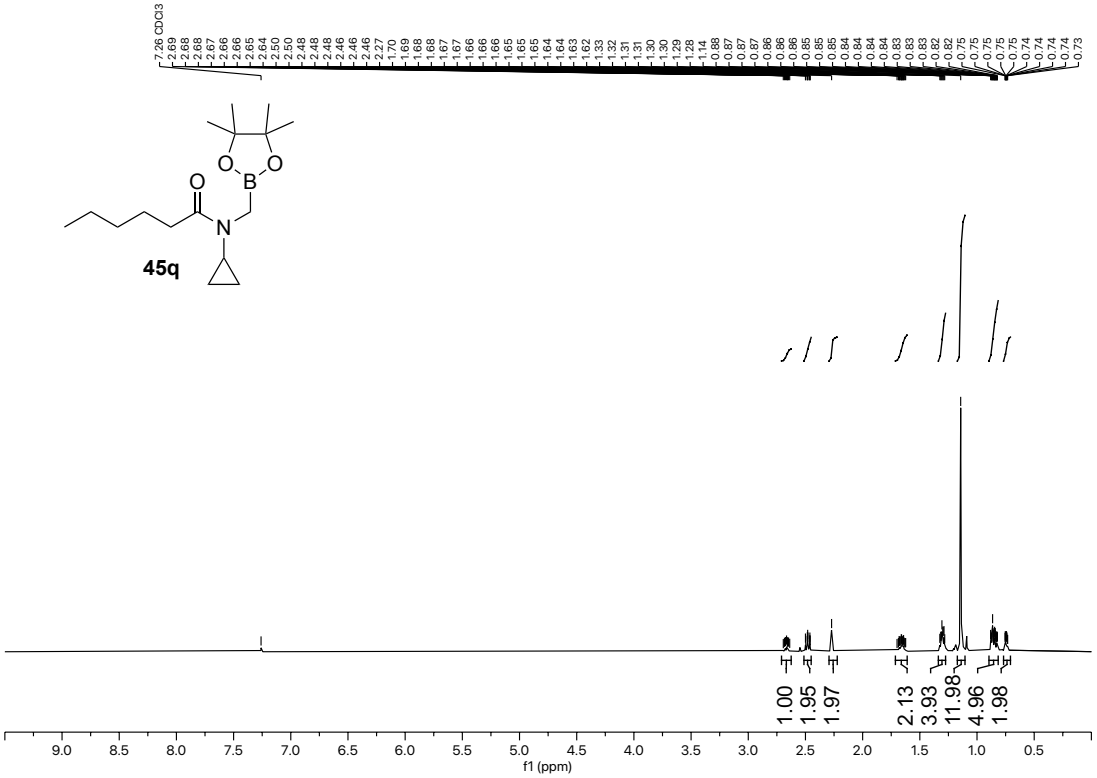



*HSQC NMR N-methyl-N-((4,4,5,5-tetramethyl-1,3,2-dioxaborolan-2-yl)methyl)cyclohexanecarboxamide (45k)*

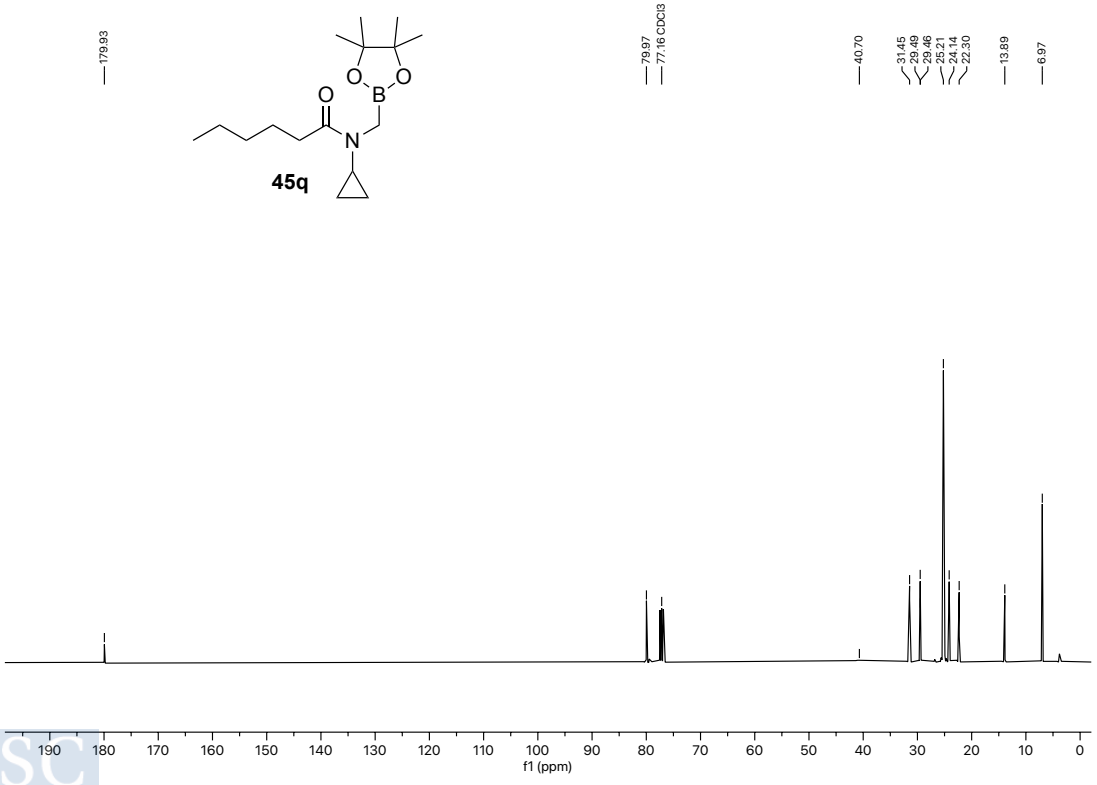



USC UNIVERSIDADE DE SANTIAGO DE COMPOSTELA

*[1]H NMR N-cyclopropyl-N-((4,4,5,5-tetramethyl-1,3,2-dioxaborolan-2-yl)methyl)hexanamide (45q)*

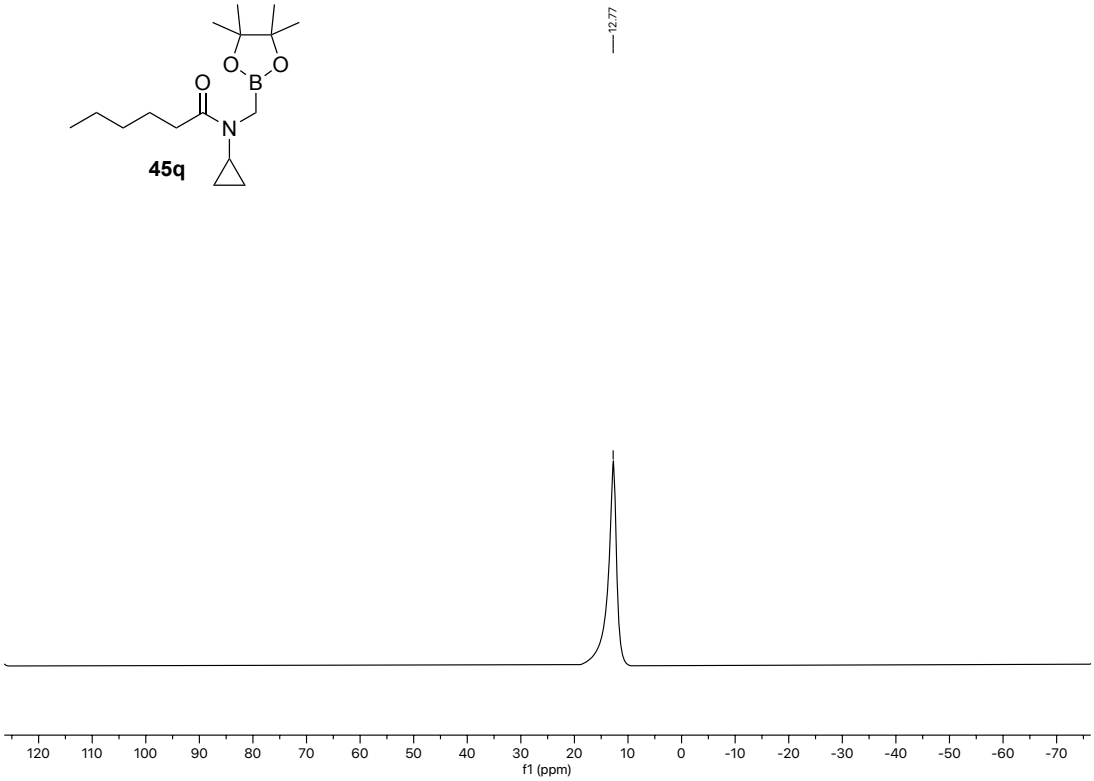



*[13]C NMR N-cyclopropyl-N-((4,4,5,5-tetramethyl-1,3,2-dioxaborolan-2-yl)methyl)hexanamide (45q)*

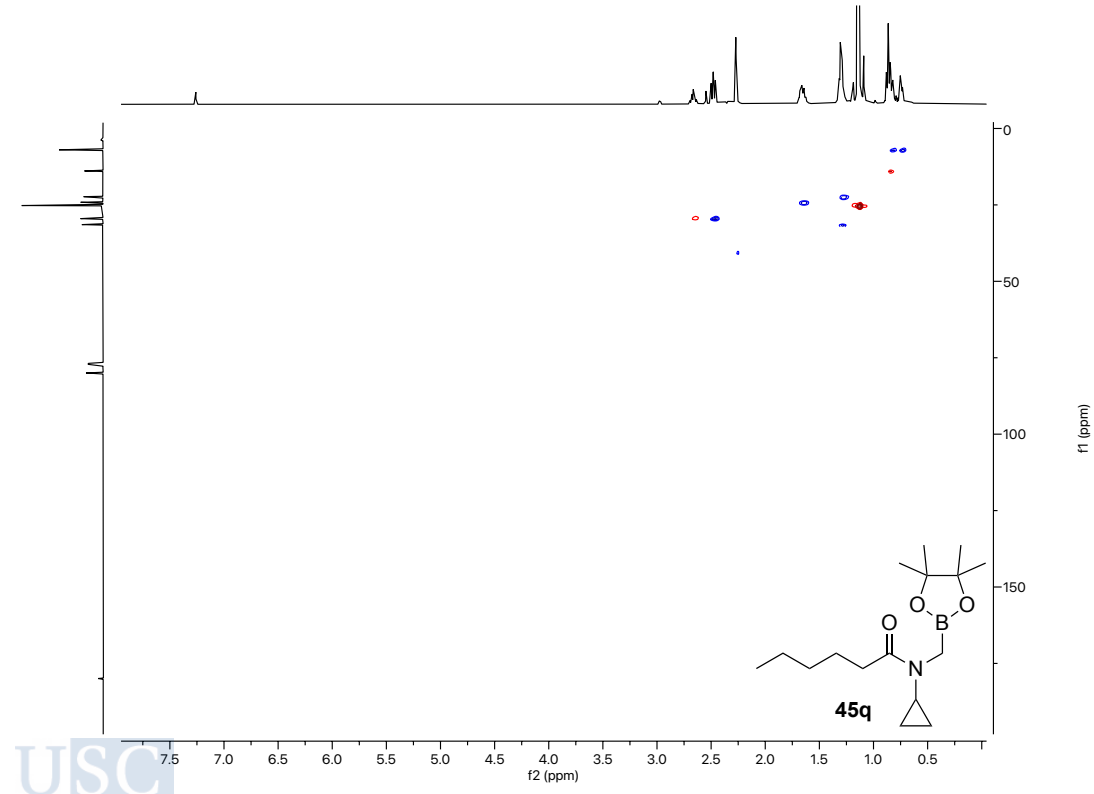


*$^{11}$B NMR N-cyclopropyl-N-((4,4,5,5-tetramethyl-1,3,2-dioxaborolan-2-yl)methyl)hexanamide (45q)*



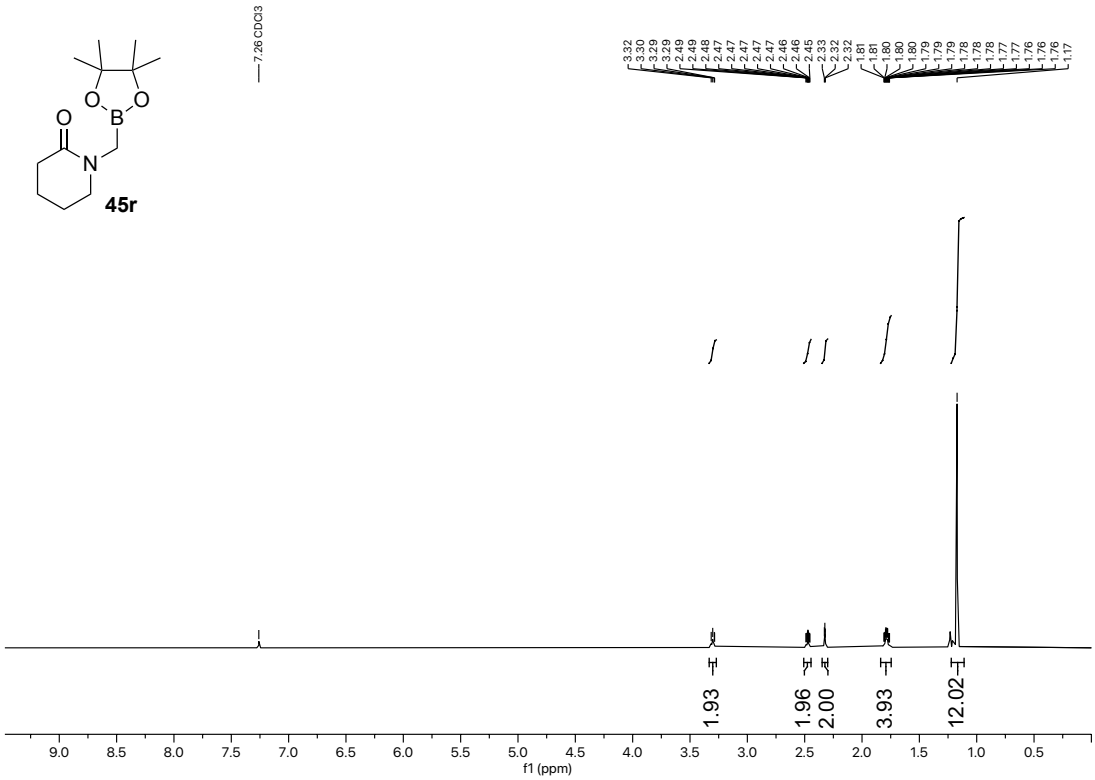




*HSQC NMR N-cyclopropyl-N-((4,4,5,5-tetramethyl-1,3,2-dioxaborolan-2-yl)methyl)hexanamide (45q)*

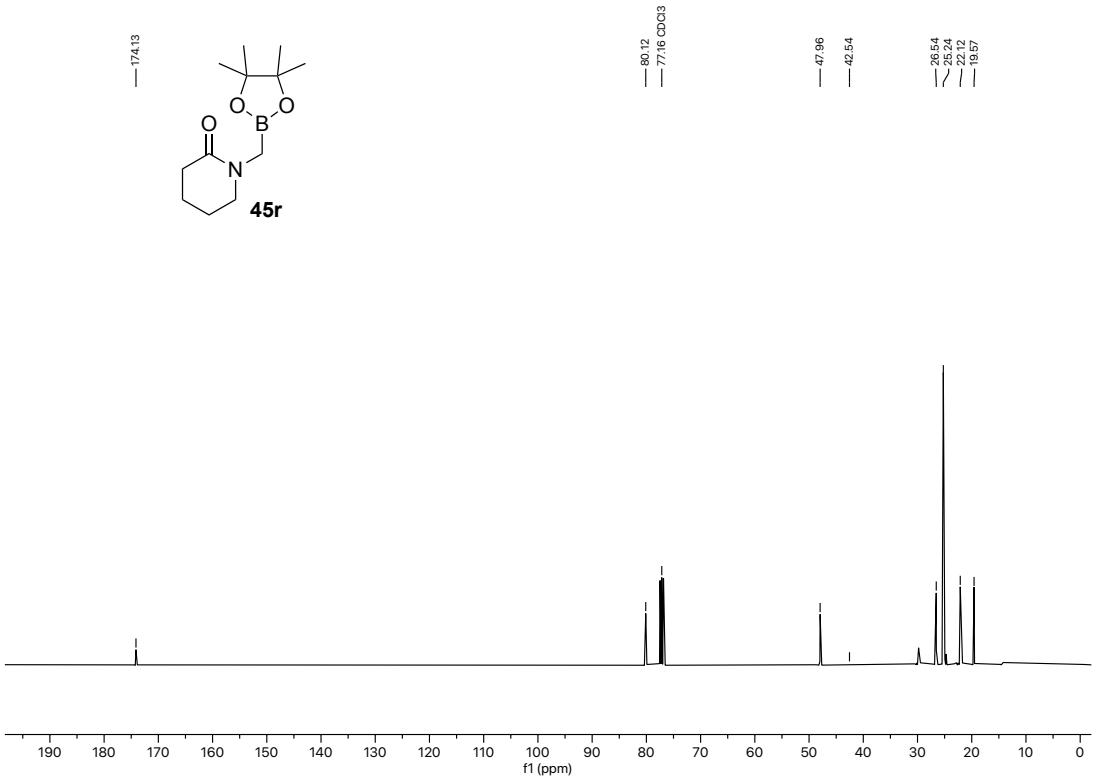



USC UNIVERSIDADE DE SANTIAGO DE COMPOSTELA

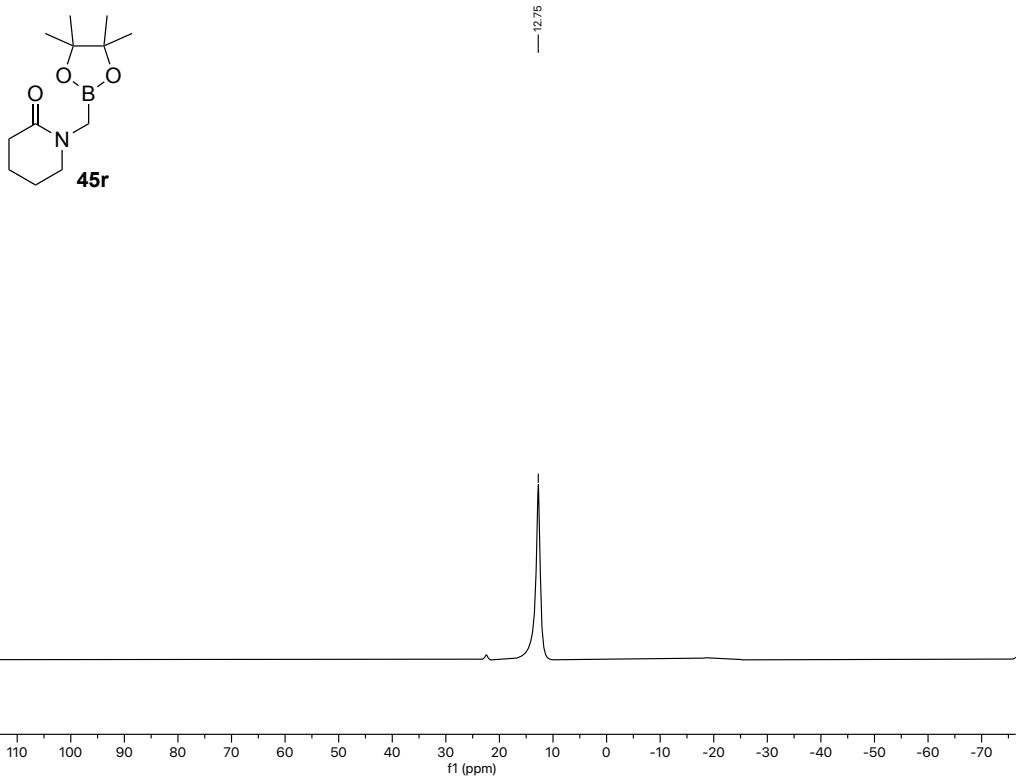
*[1]H NMR 1-((4,4,5,5-tetramethyl-1,3,2-dioxaborolan-2-yl)methyl)piperidin-2-one (45r)*



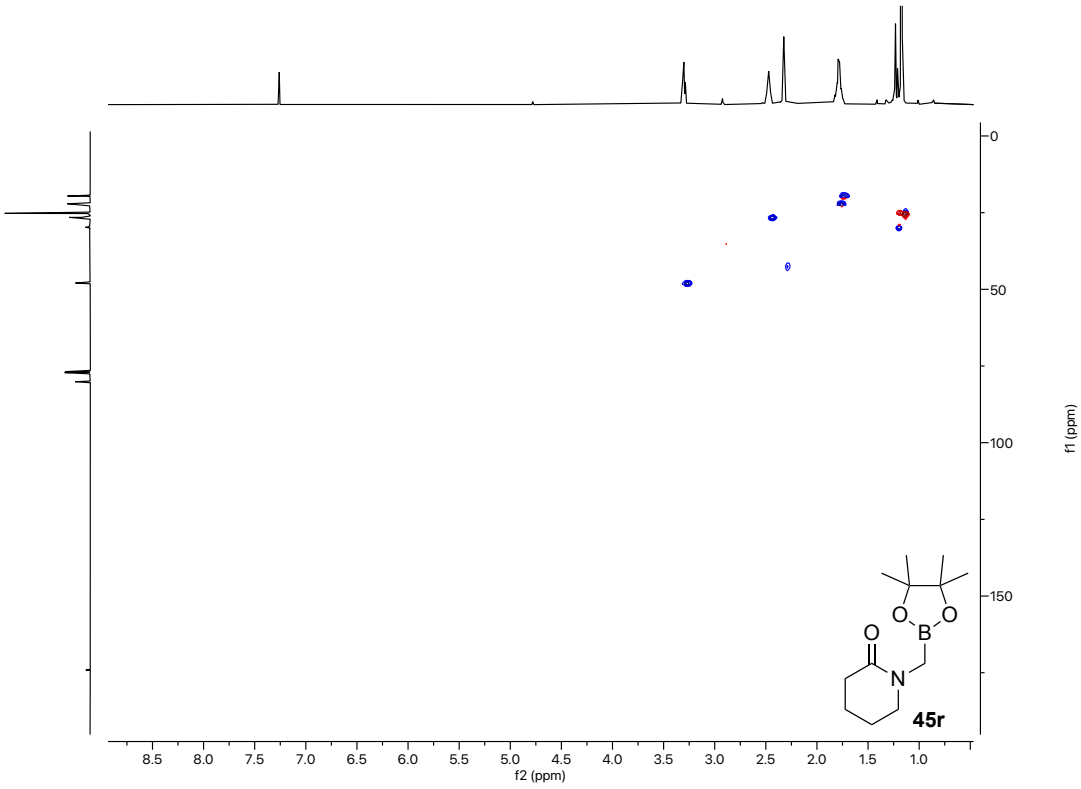

*[13]C NMR 1-((4,4,5,5-tetramethyl-1,3,2-dioxaborolan-2-yl)methyl)piperidin-2-one (45r)*



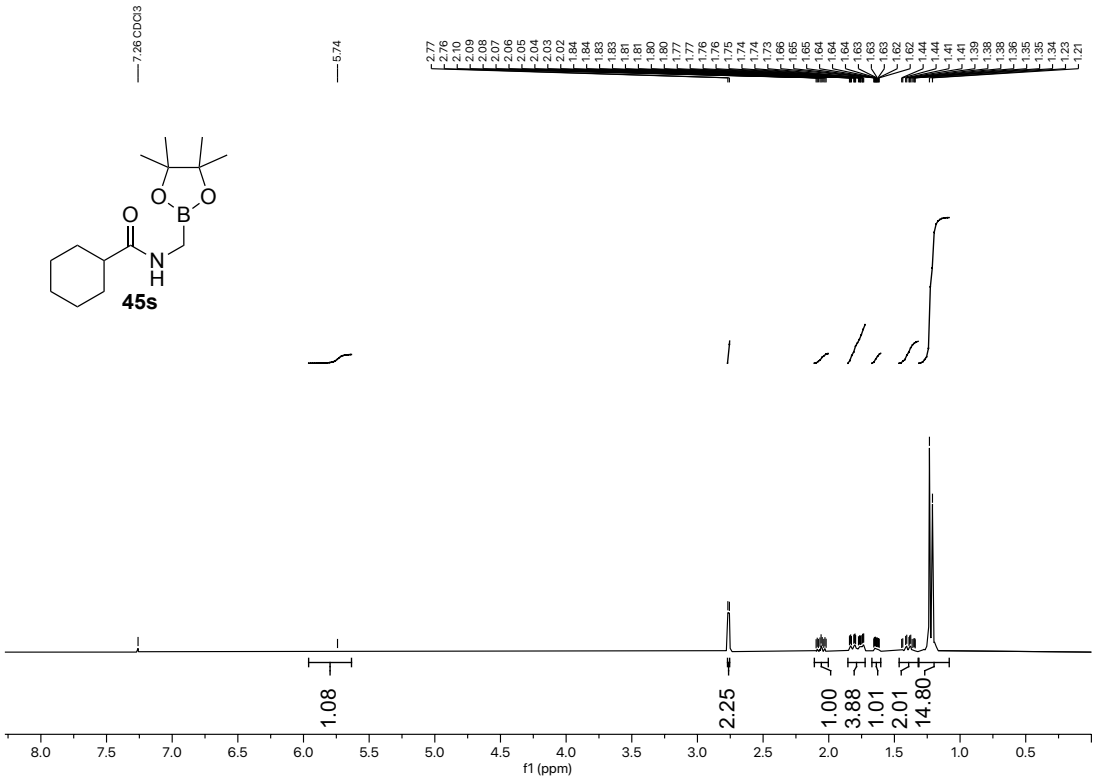
*$^{11}$B NMR 1-((4,4,5,5-tetramethyl-1,3,2-dioxaborolan-2-yl)methyl)piperidin-2-one (45r)*



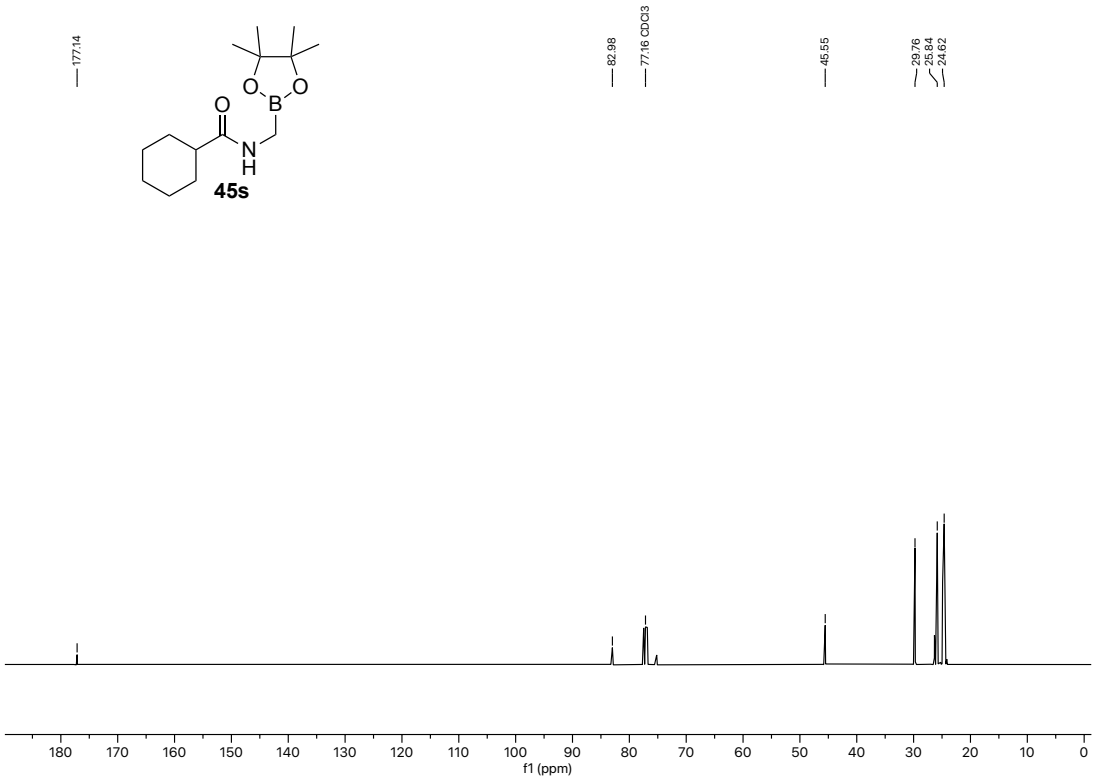

*HSQC NMR 1-((4,4,5,5-tetramethyl-1,3,2-dioxaborolan-2-yl)methyl)piperidin-2-one (45r)*



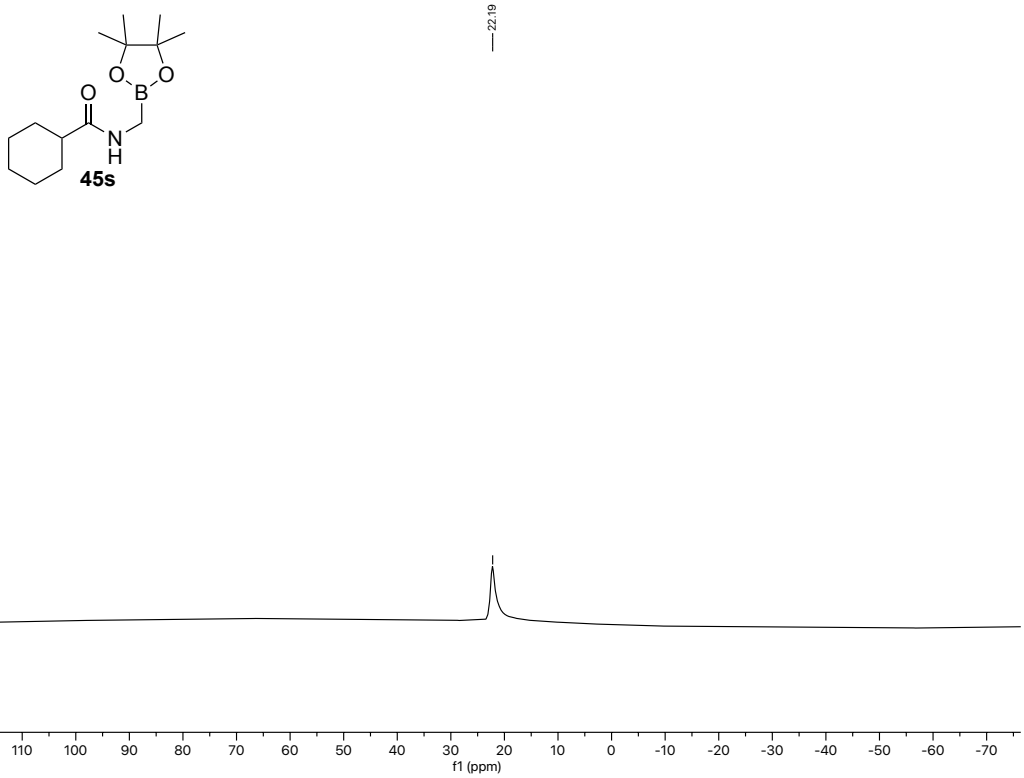
*[1]H NMR N-((4,4,5,5-tetramethyl-1,3,2-dioxaborolan-2-yl)methyl)cyclohexanecarboxamide (45s)*



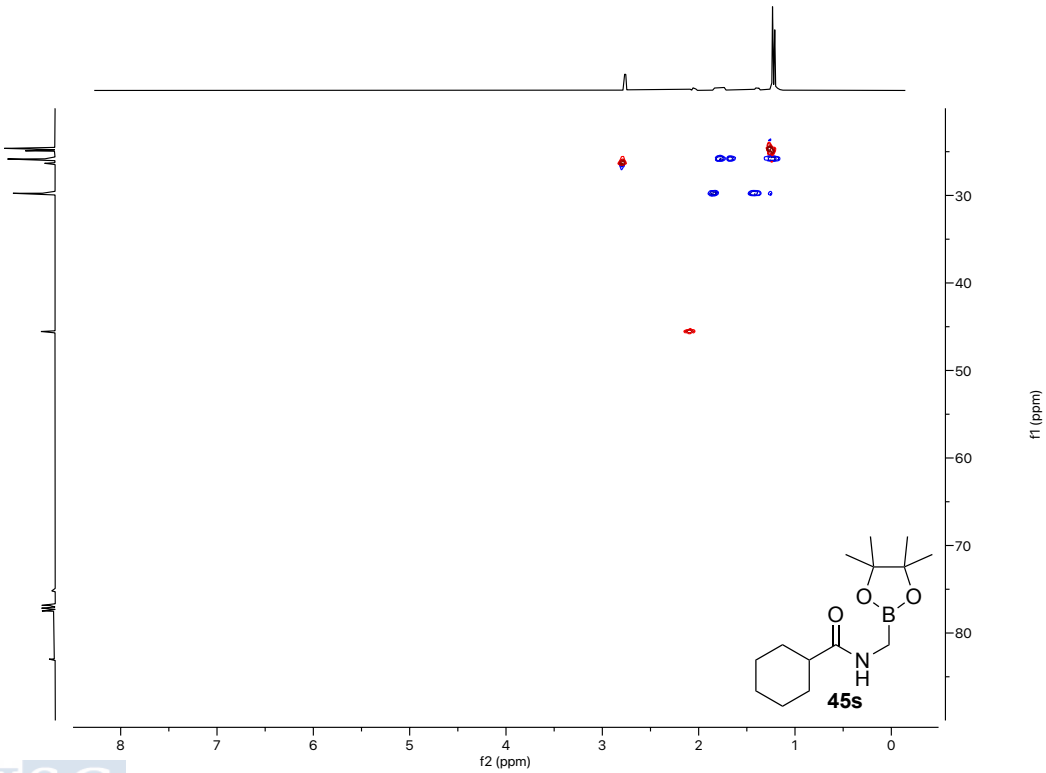

*[13]C NMR N-((4,4,5,5-tetramethyl-1,3,2-dioxaborolan-2-yl)methyl)cyclohexanecarboxamide (45s)*



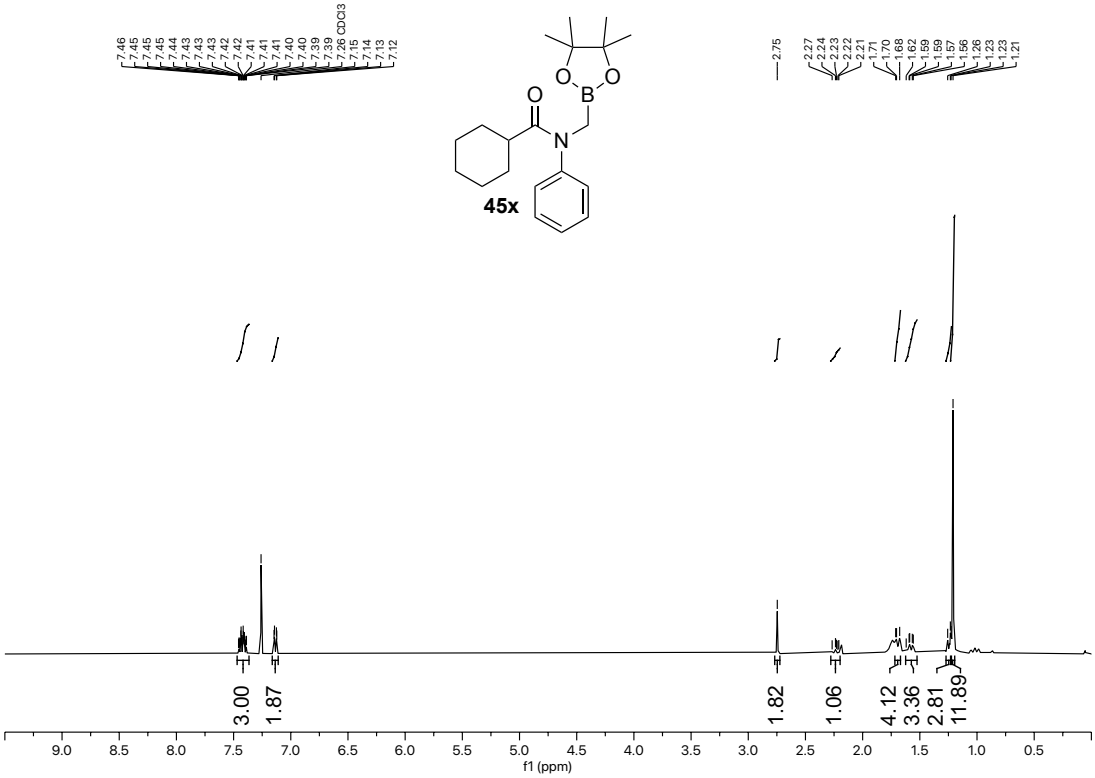
*$^{11}$B NMR N-((4,4,5,5-tetramethyl-1,3,2-dioxaborolan-2-yl)methyl)cyclohexanecarboxamide (45s)*



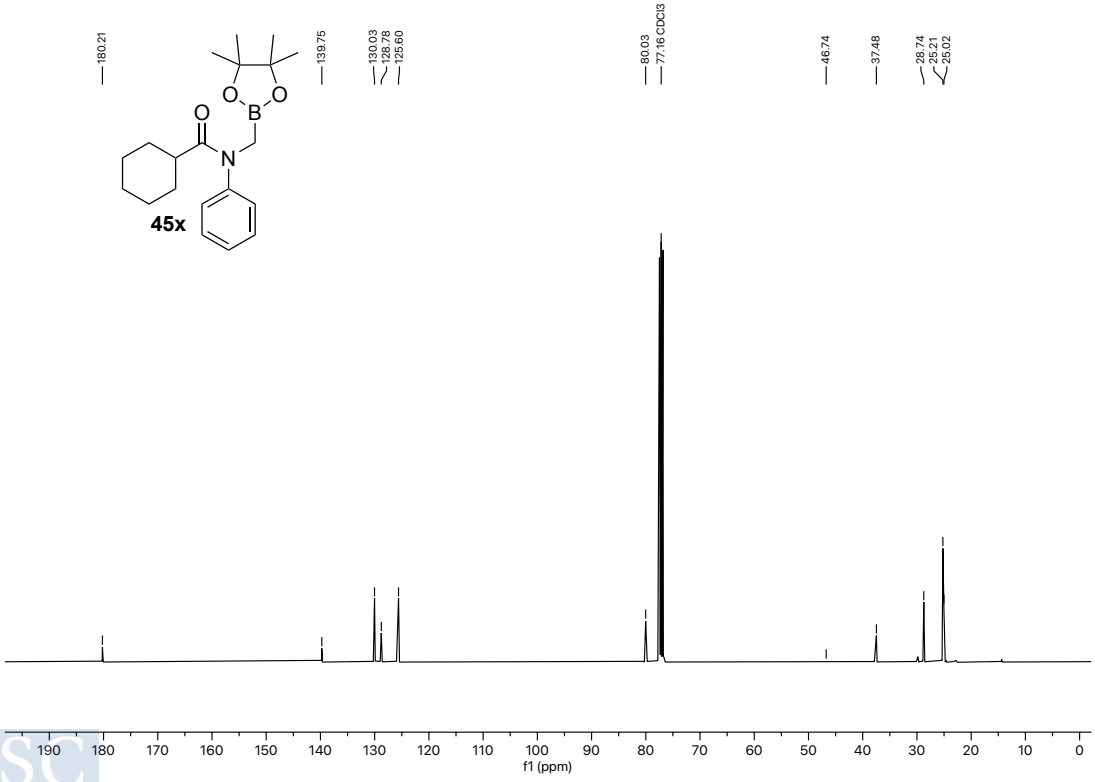

*HSQC NMR N-((4,4,5,5-tetramethyl-1,3,2-dioxaborolan-2-yl)methyl)cyclohexanecarboxamide (45s)*



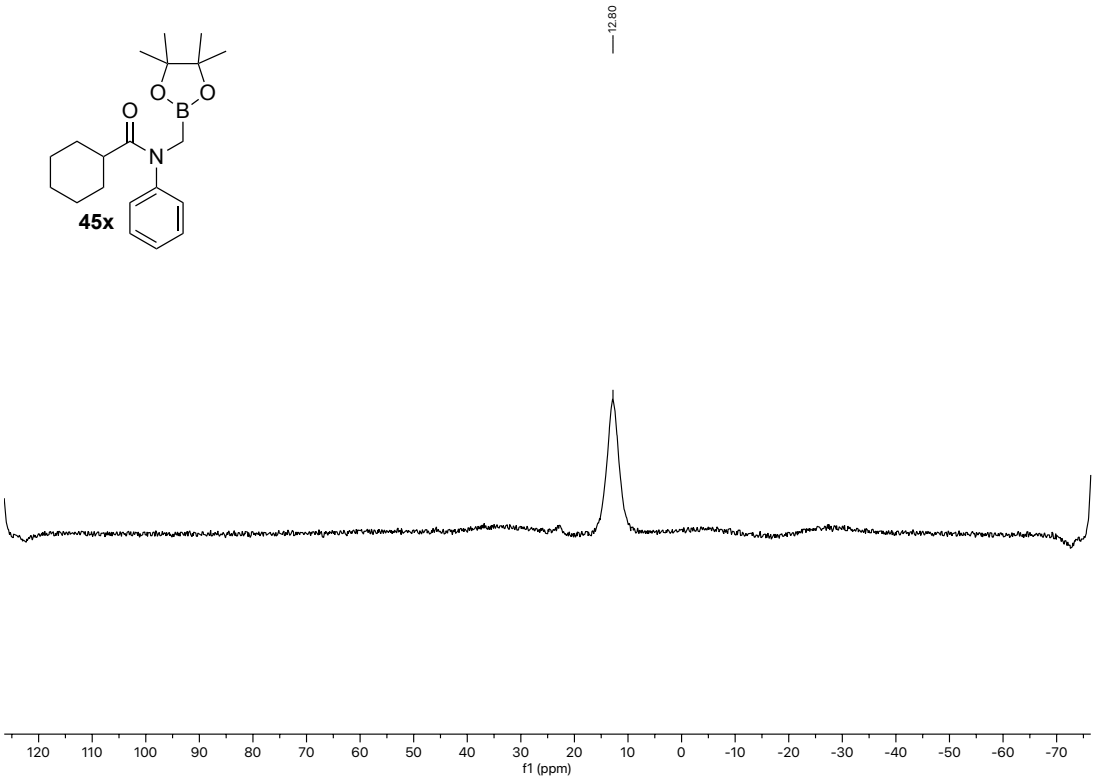
*[1]H NMR N-phenyl-N-((4,4,5,5-tetramethyl-1,3,2-dioxaborolan-2-yl)methyl)cyclohexanecarboxamide (45x)*



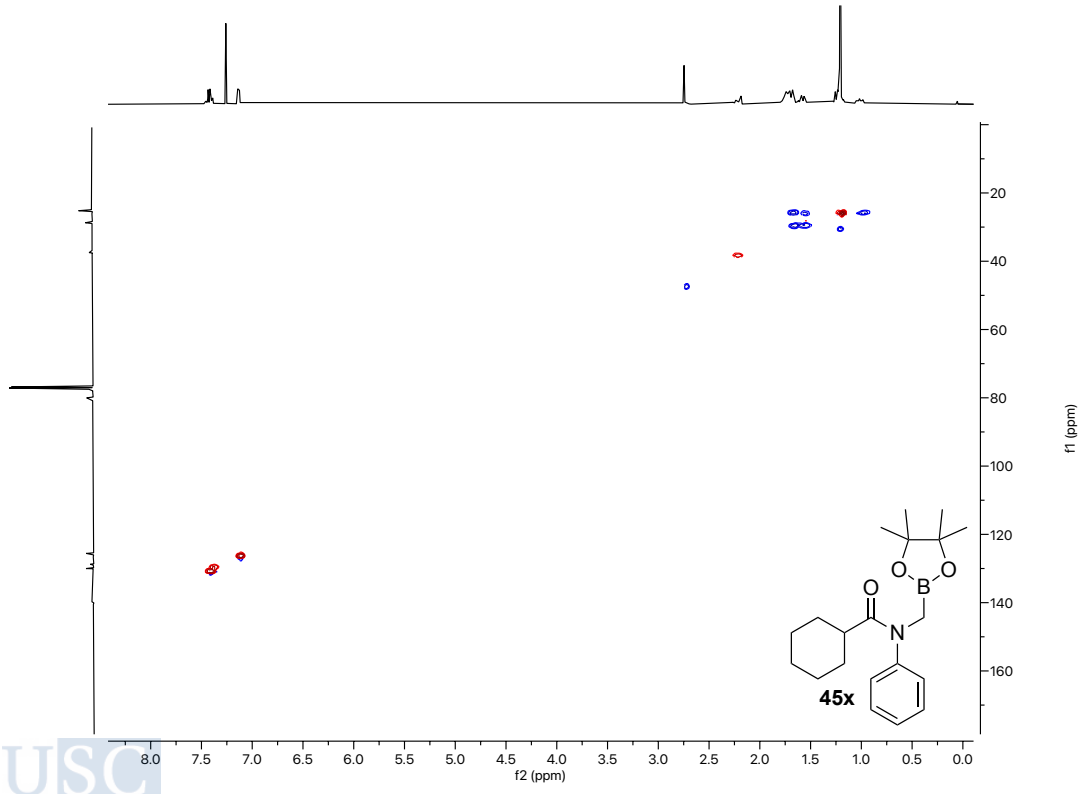

*[13]C NMR N-phenyl-N-((4,4,5,5-tetramethyl-1,3,2-dioxaborolan-2-yl)methyl)cyclohexanecarboxamide (45x)*



*$^{11}$B NMR N-phenyl-N-((4,4,5,5-tetramethyl-1,3,2-dioxaborolan-2-yl)methyl)cyclohexanecarboxamide (45x)*

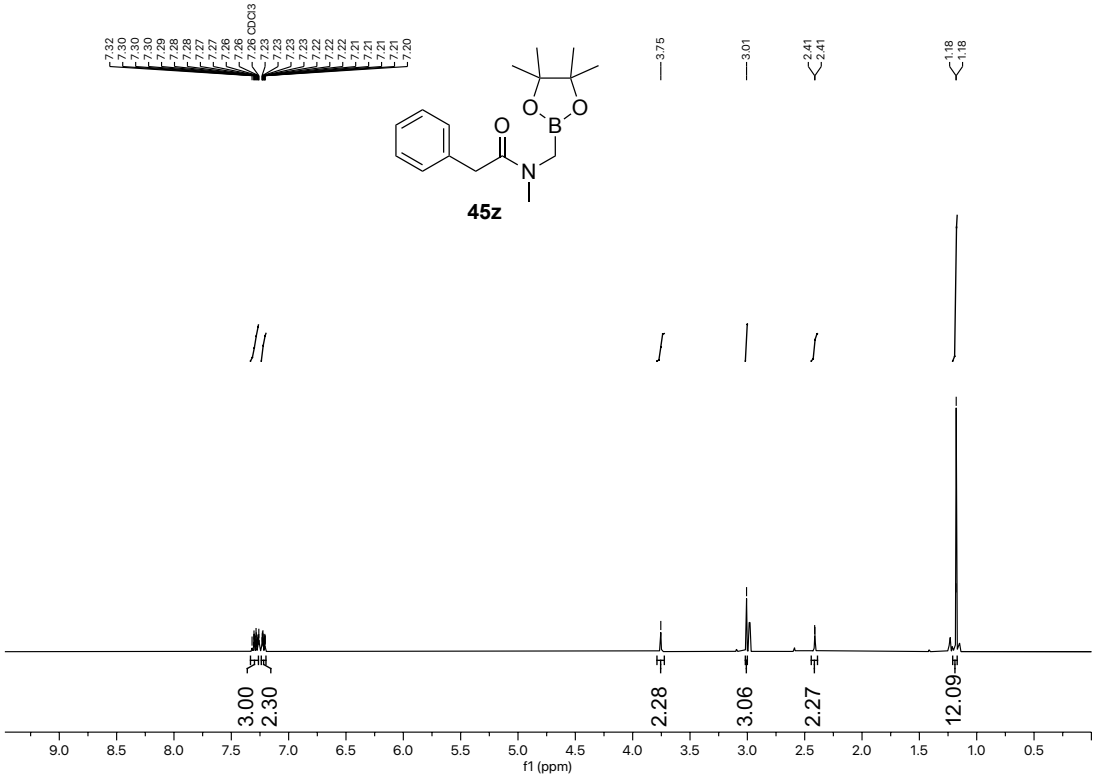



*HSQC NMR N-phenyl-N-((4,4,5,5-tetramethyl-1,3,2-dioxaborolan-2-yl)methyl)cyclohexanecarboxamide (45x)*

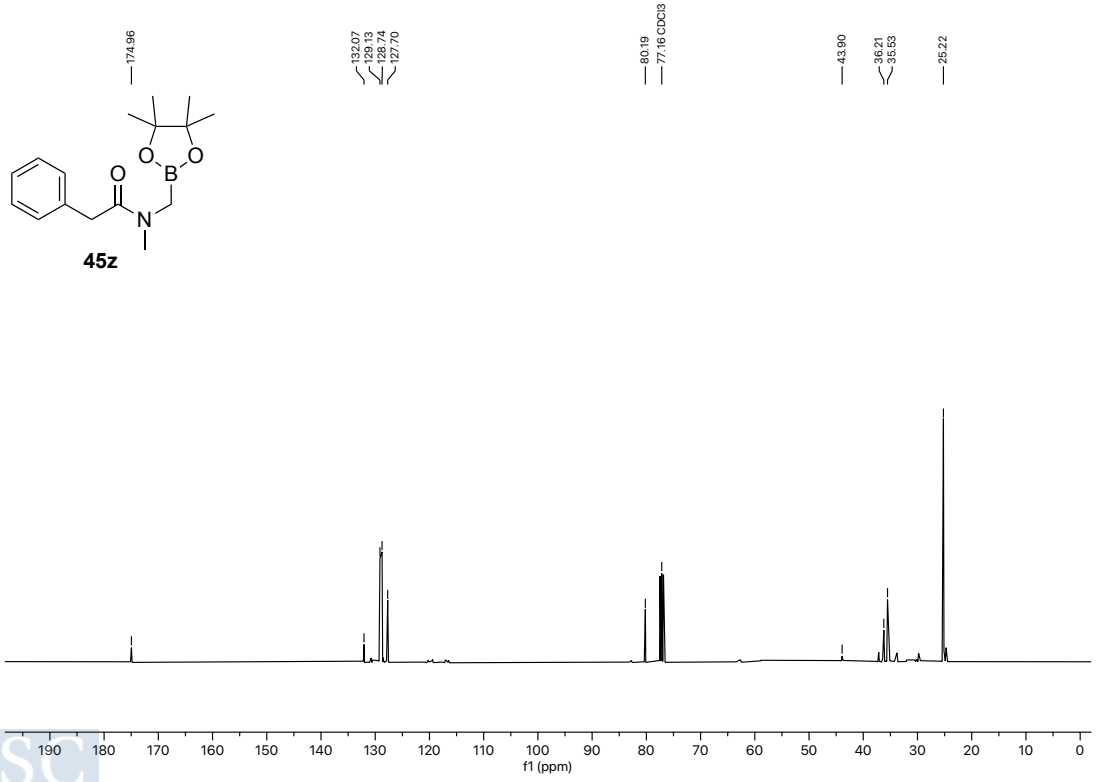



USC UNIVERSIDADE DE SANTIAGO DE COMPOSTELA

*[1]H NMR N-methyl-2-phenyl-N-((4,4,5,5-tetramethyl-1,3,2-dioxaborolan-2-yl)methyl)acetamide (45z)*

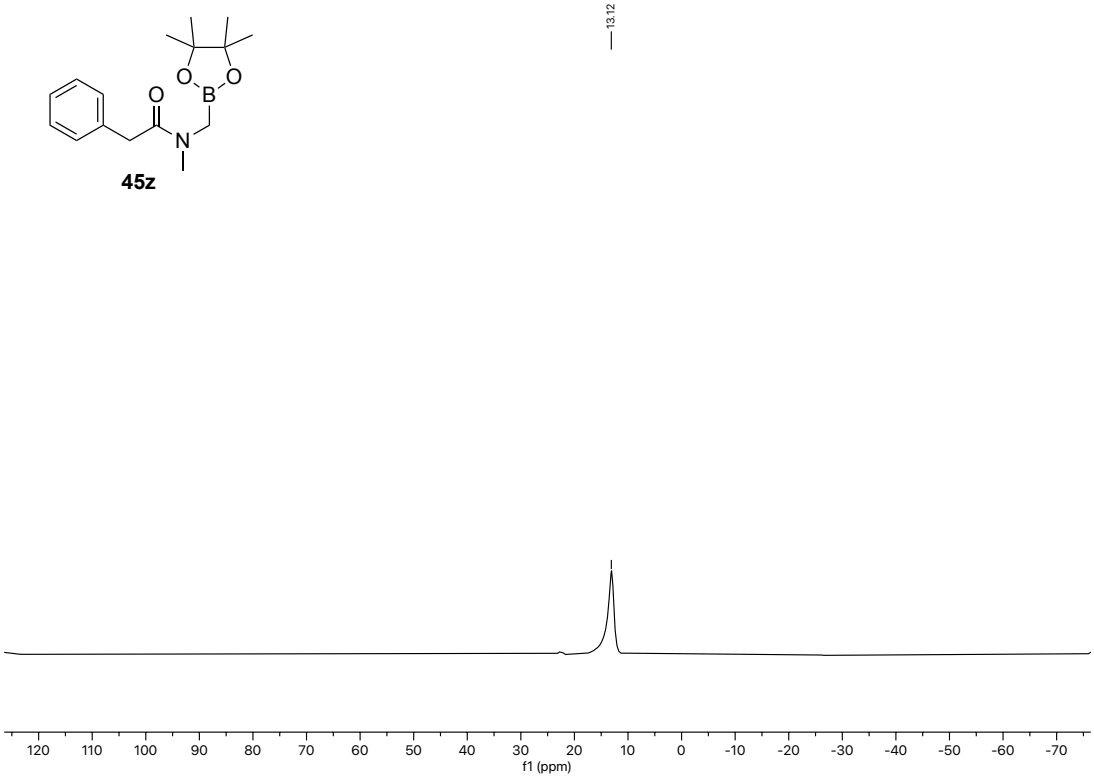



*[13]C NMR N-methyl-2-phenyl-N-((4,4,5,5-tetramethyl-1,3,2-dioxaborolan-2-yl)methyl)acetamide (45z)*

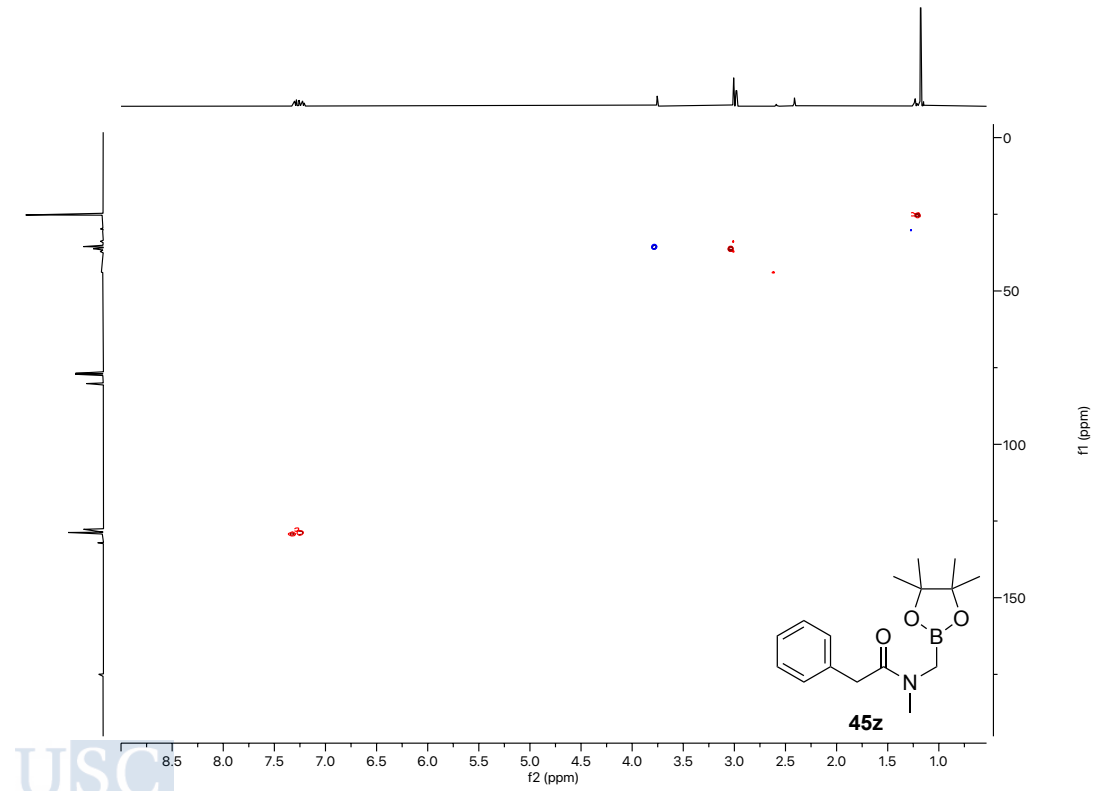



USC UNIVERSIDADE DE SANTIAGO DE COMPOSTELA

*[11]B NMR N-methyl-2-phenyl-N-((4,4,5,5-tetramethyl-1,3,2-dioxaborolan-2-yl)methyl)acetamide (45z)*

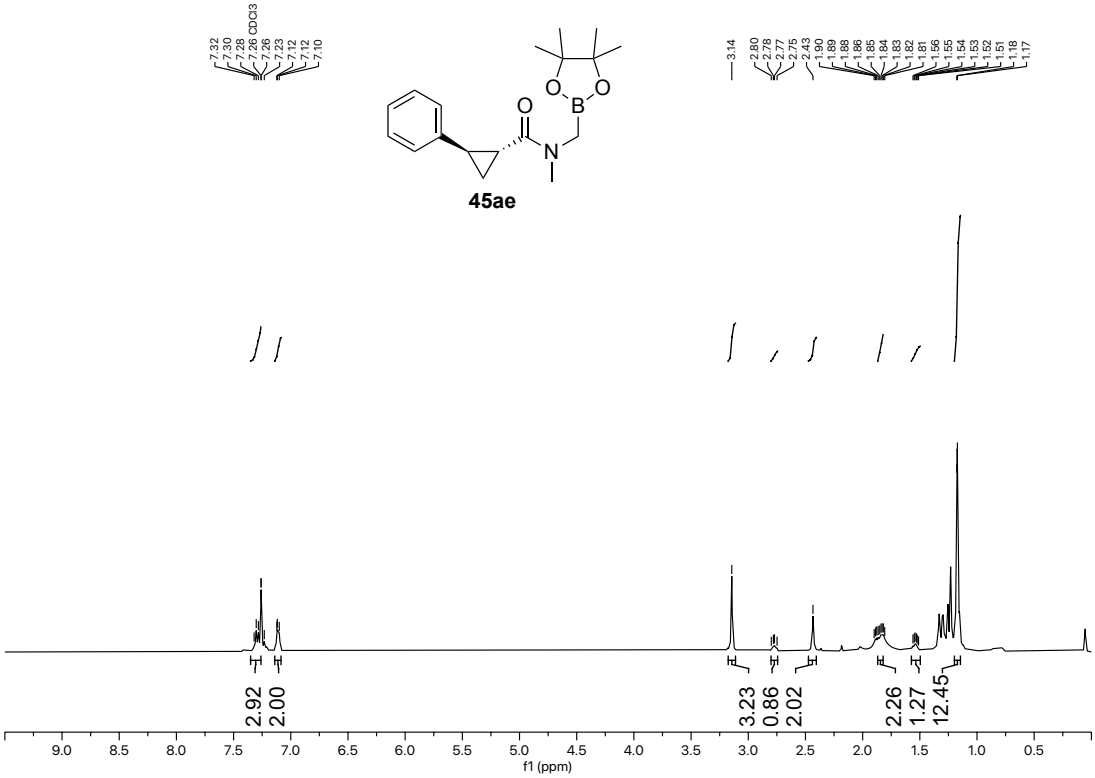



*HSQC NMR N-methyl-2-phenyl-N-((4,4,5,5-tetramethyl-1,3,2-dioxaborolan-2-yl)methyl)acetamide (45z)*

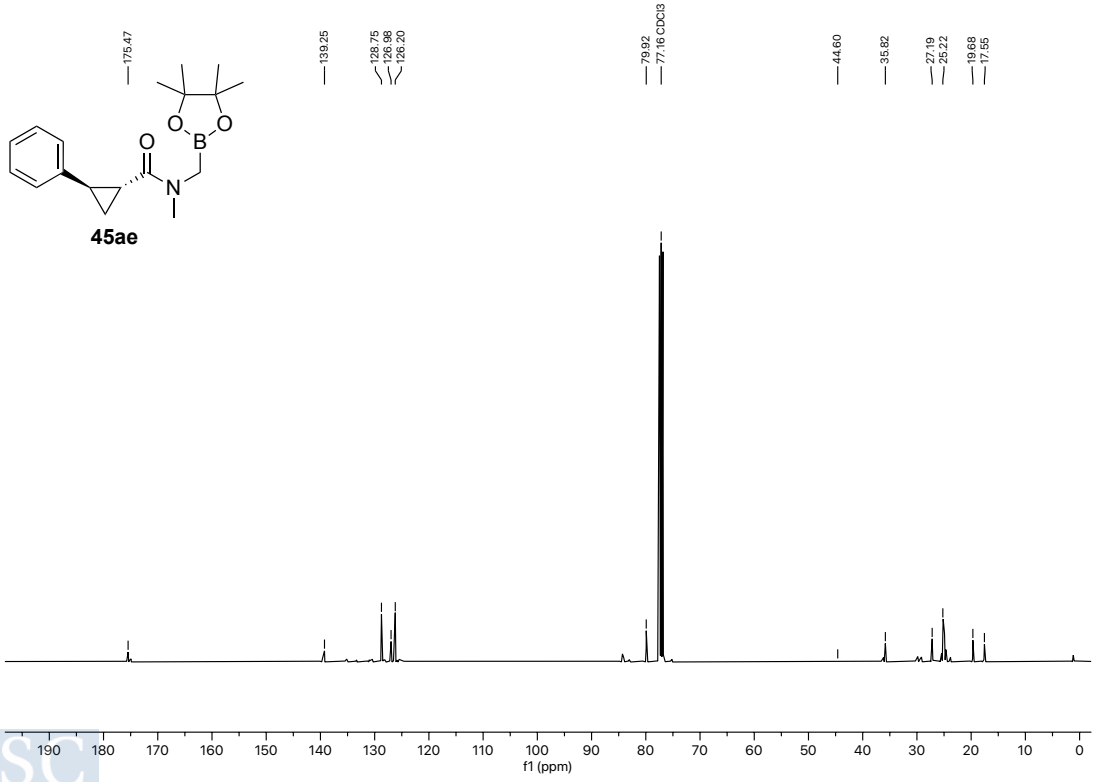



USC UNIVERSIDADE DE SANTIAGO DE COMPOSTELA

*[1]H NMR (1R,2R)-N-methyl-2-phenyl-N-((4,4,5,5-tetramethyl-1,3,2-dioxaborolan-2-yl)methyl)cyclopropane-1-carboxamide (45ae)*

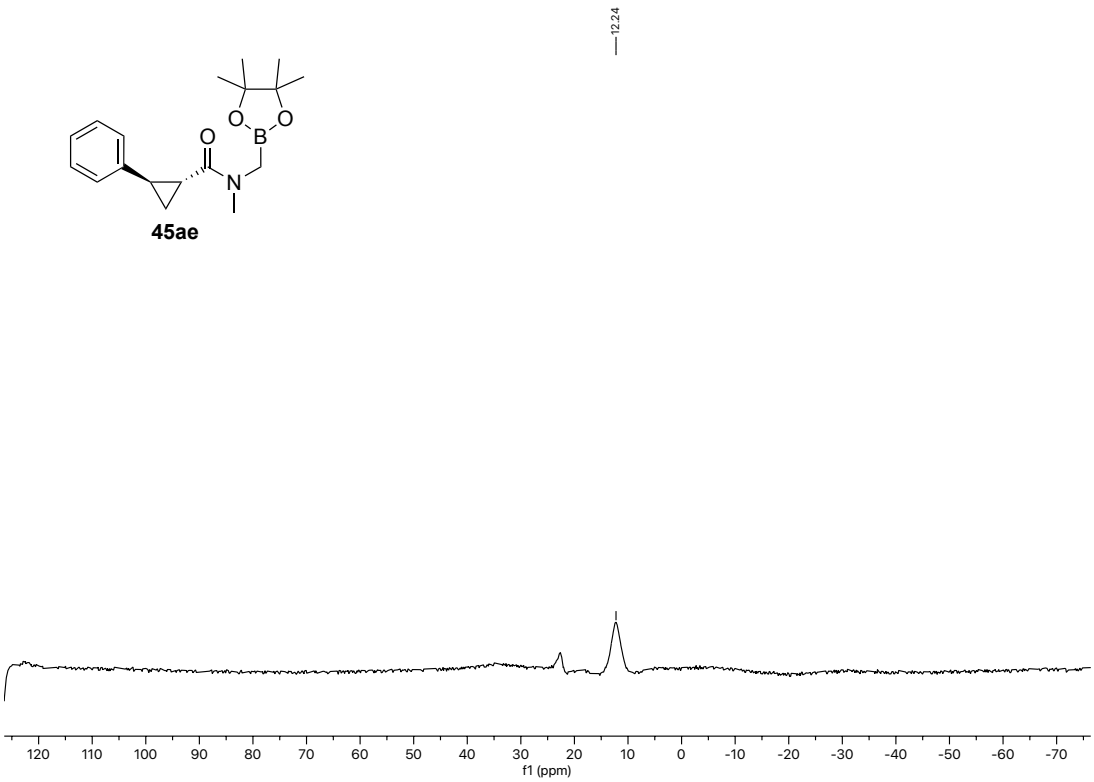



*[13]C NMR (1R,2R)-N-methyl-2-phenyl-N-((4,4,5,5-tetramethyl-1,3,2-dioxaborolan-2-yl)methyl)cyclopropane-1-carboxamide (45ae)*

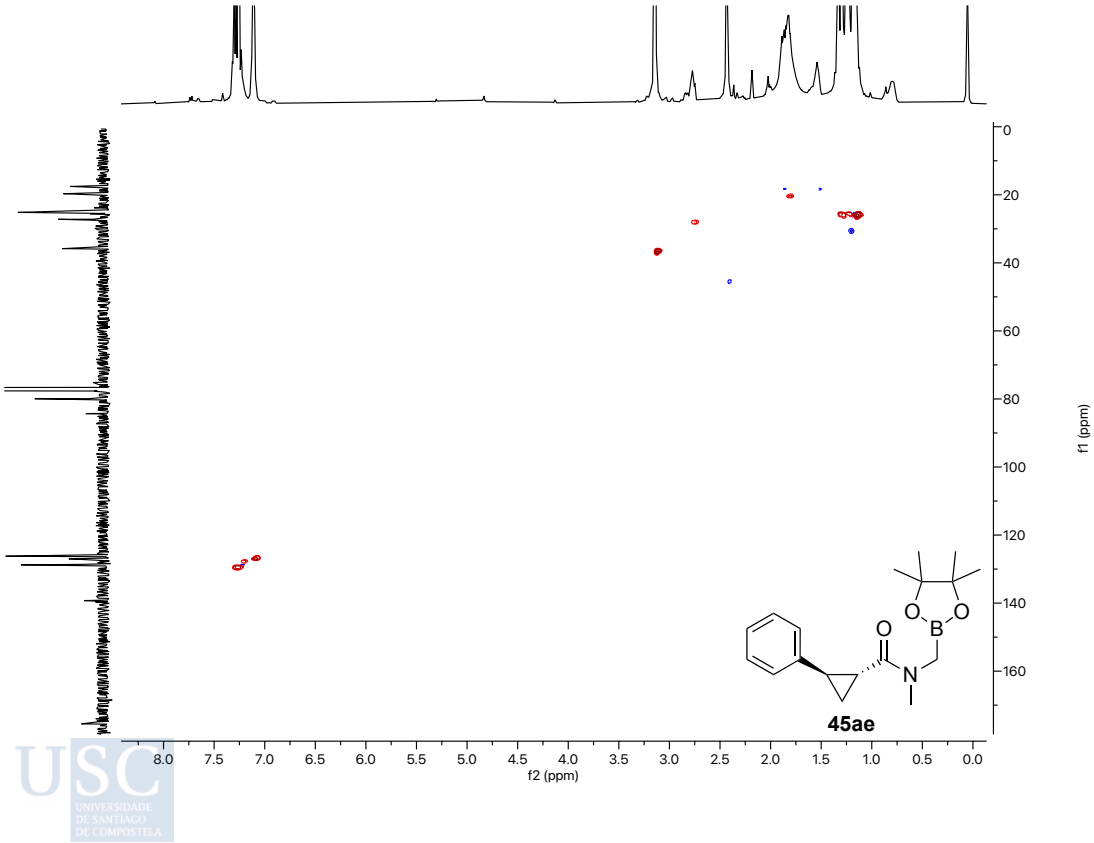


*$^{11}$B NMR (1R,2R)-N-methyl-2-phenyl-N-((4,4,5,5-tetramethyl-1,3,2-dioxaborolan-2-yl)methyl)cyclopropane-1-carboxamide (45ae)*



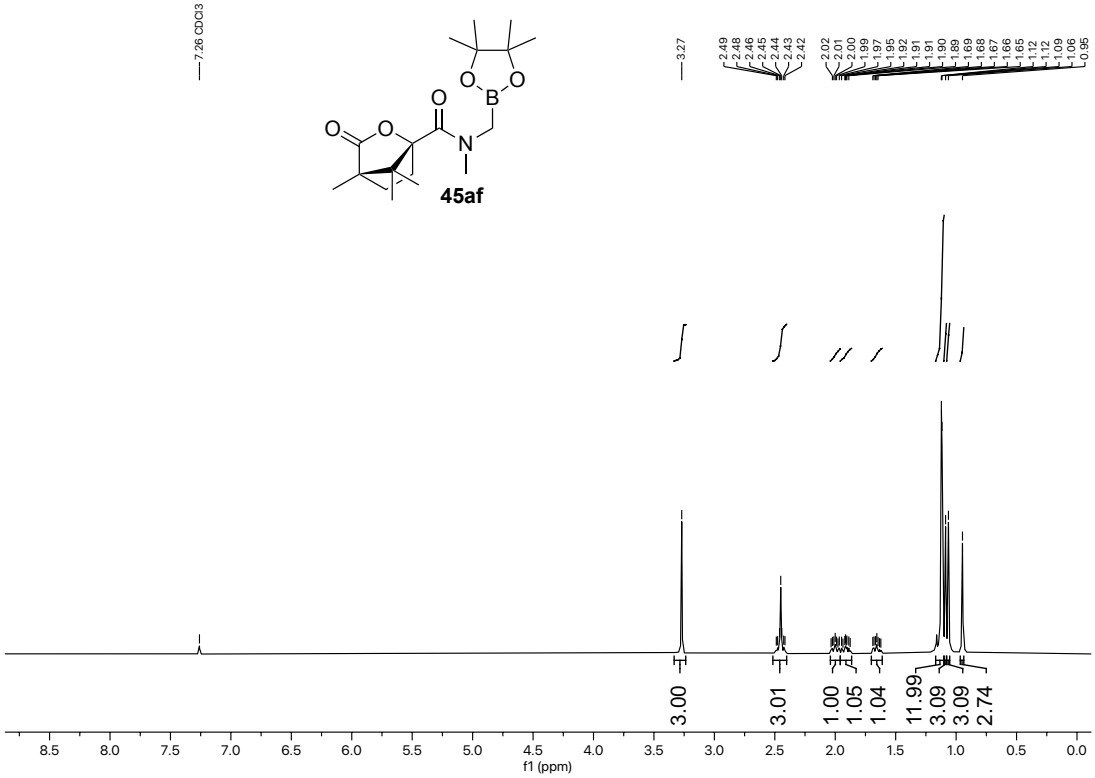




*HSQC NMR (1R,2R)-N-methyl-2-phenyl-N-((4,4,5,5-tetramethyl-1,3,2-dioxaborolan-2-yl)methyl)cyclopropane-1-carboxamide (45ae)*

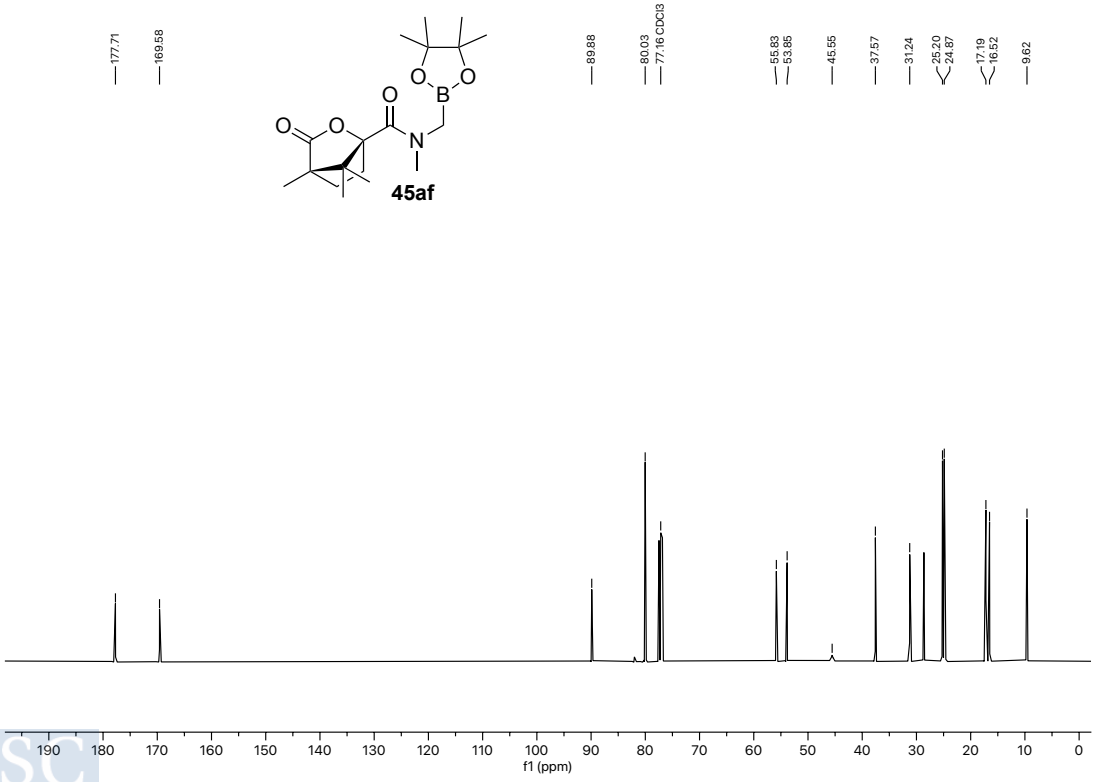



USC UNIVERSIDADE DE SANTIAGO DE COMPOSTELA

*[1]H NMR (1S)-N,4,7,7-tetramethyl-3-oxo-N-((4,4,5,5-tetramethyl-1,3,2-dioxaborolan-2-yl)methyl)-2-oxabicyclo[2.2.1]heptane-1-carboxamide (45af)*

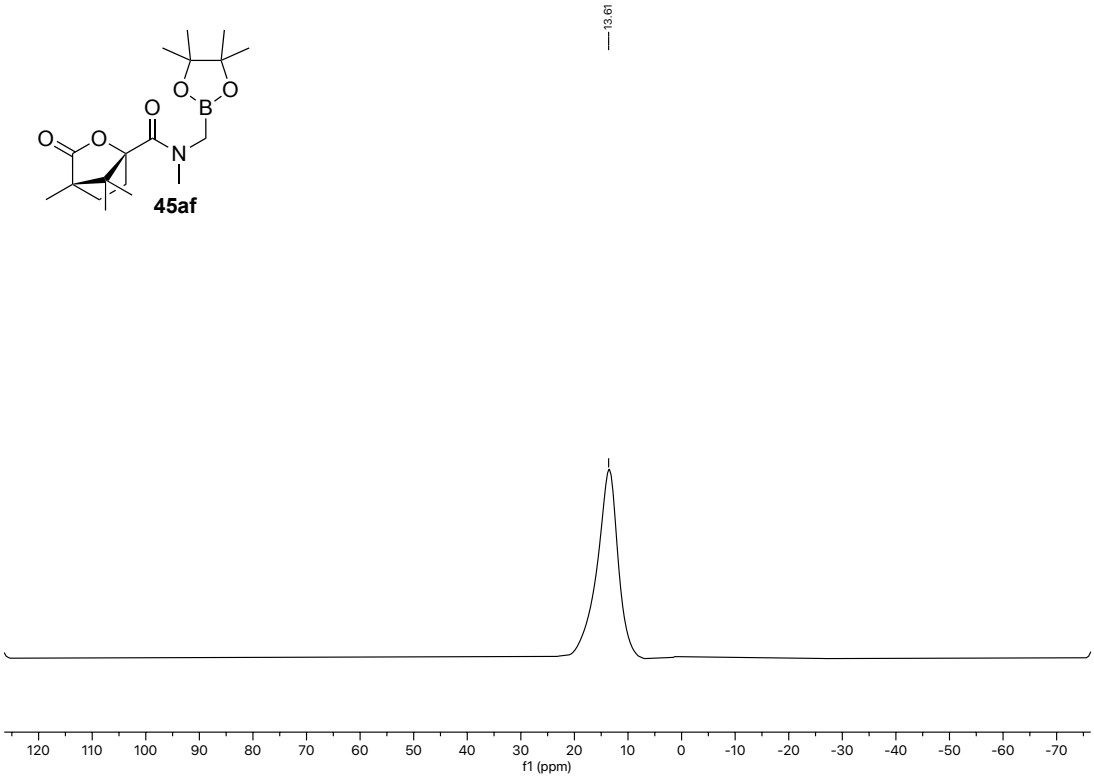



*[13]C NMR (1S)-N,4,7,7-tetramethyl-3-oxo-N-((4,4,5,5-tetramethyl-1,3,2-dioxaborolan-2-yl)methyl)-2-oxabicyclo[2.2.1]heptane-1-carboxamide (45af)*

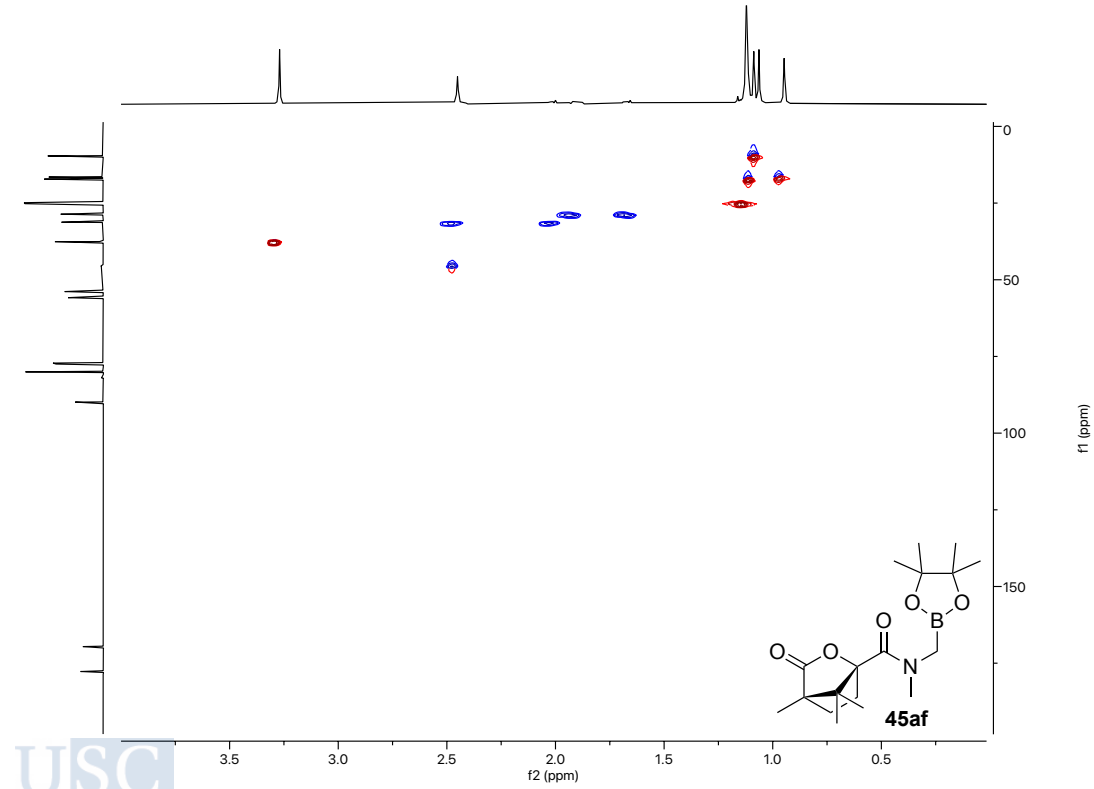



USC UNIVERSIDADE DE SANTIAGO DE COMPOSTELA

*$^{11}$B NMR (1S)-N,4,7,7-tetramethyl-3-oxo-N-((4,4,5,5-tetramethyl-1,3,2-dioxaborolan-2-yl)methyl)-2-oxabicyclo[2.2.1]heptane-1-carboxamide (45af)*

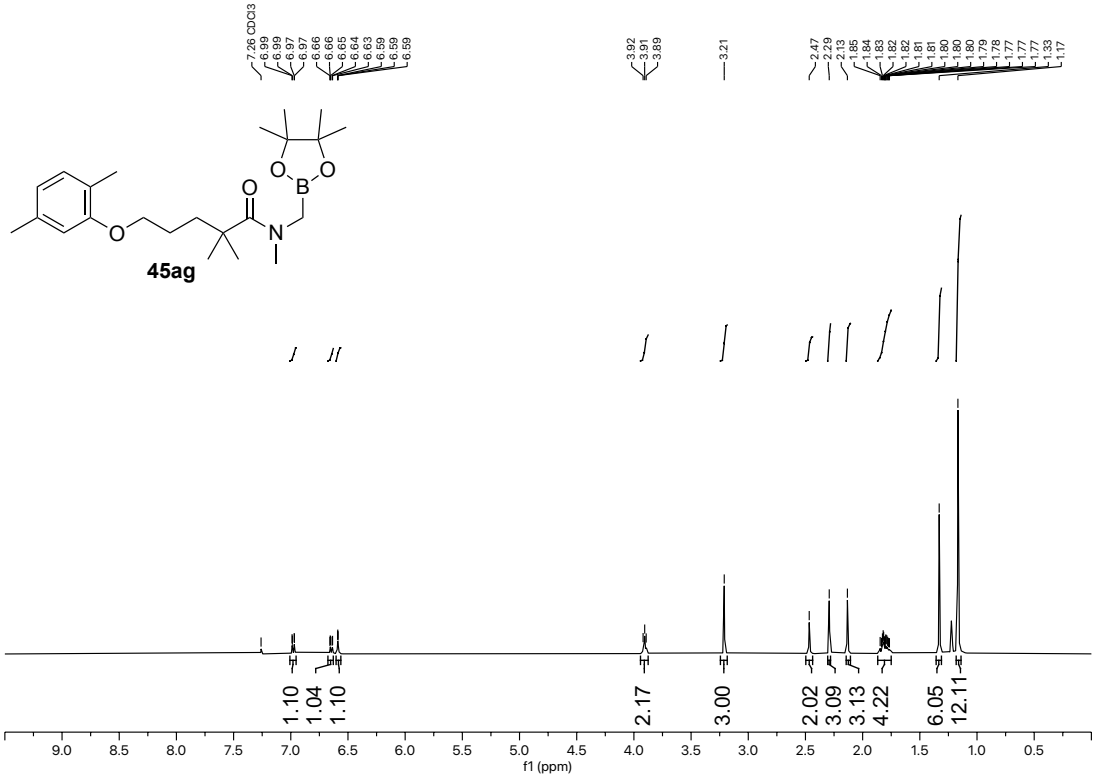



*HSQC NMR (1S)-N,4,7,7-tetramethyl-3-oxo-N-((4,4,5,5-tetramethyl-1,3,2-dioxaborolan-2-yl)methyl)-2-oxabicyclo[2.2.1]heptane-1-carboxamide (45af)*

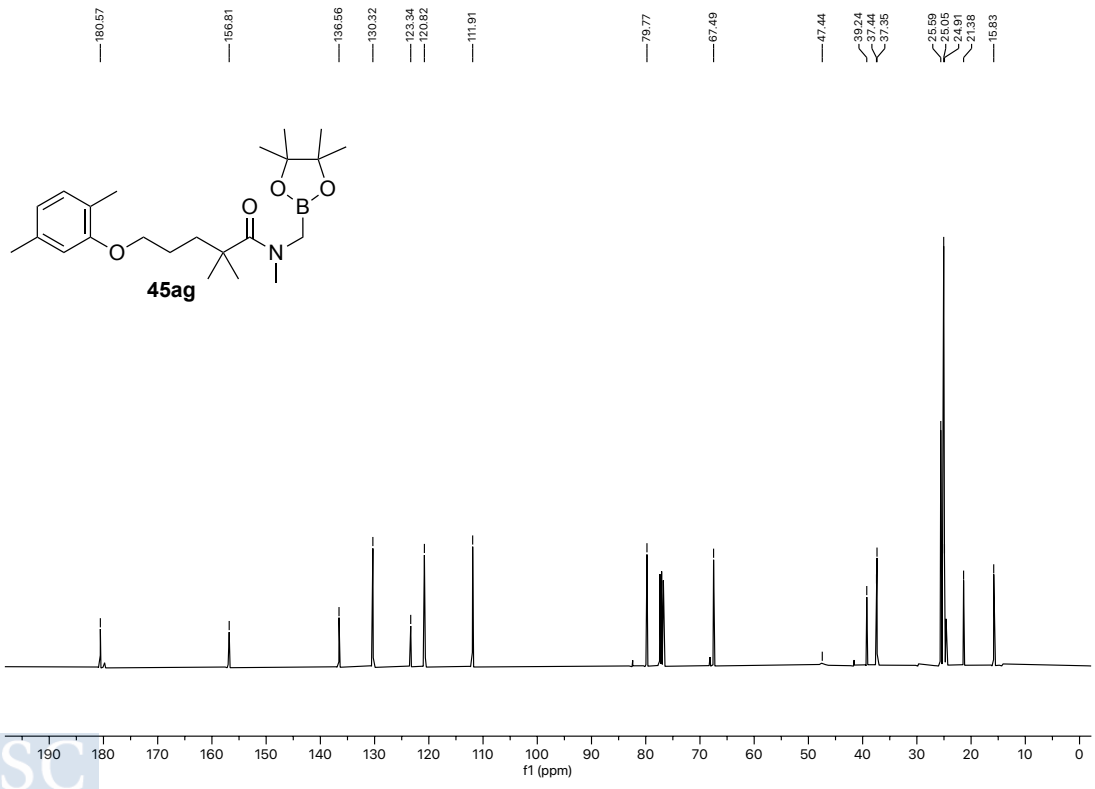



USC UNIVERSIDADE DE SANTIAGO DE COMPOSTELA

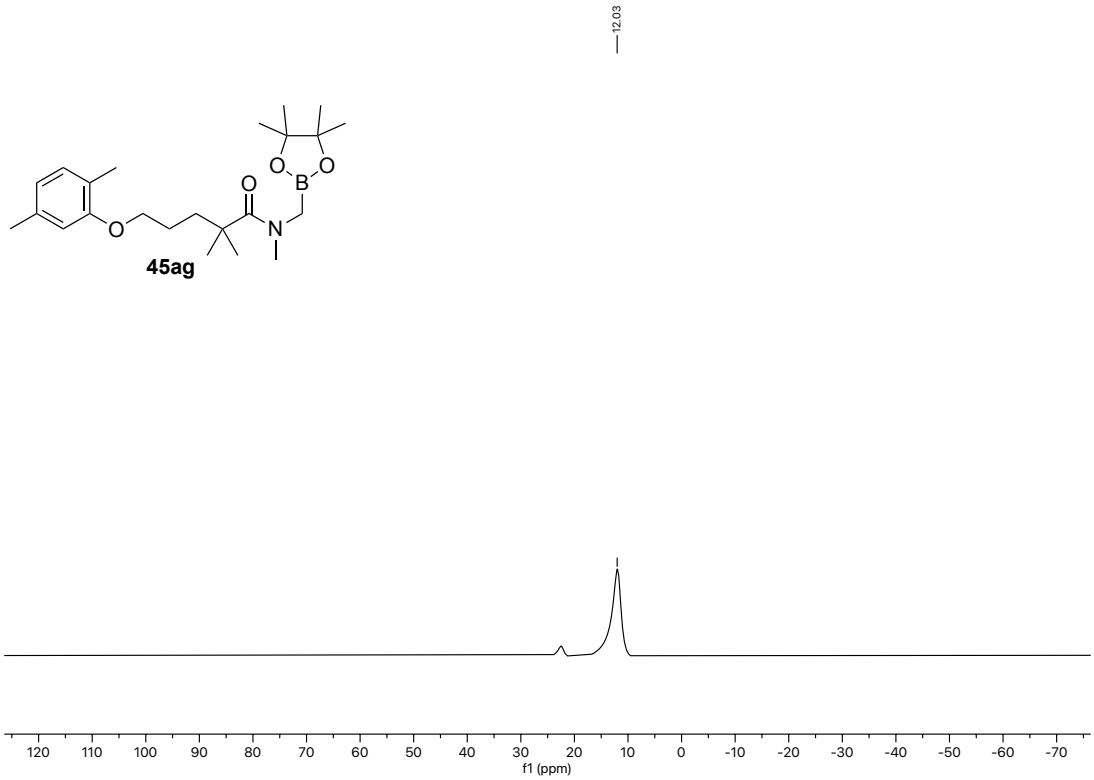
*[1]H NMR (2,5-dimethylphenoxy)-N,2,2-trimethyl-N-((4,4,5,5-tetramethyl-1,3,2-dioxaborolan-2-yl)methyl)pentanamide (45ag)*



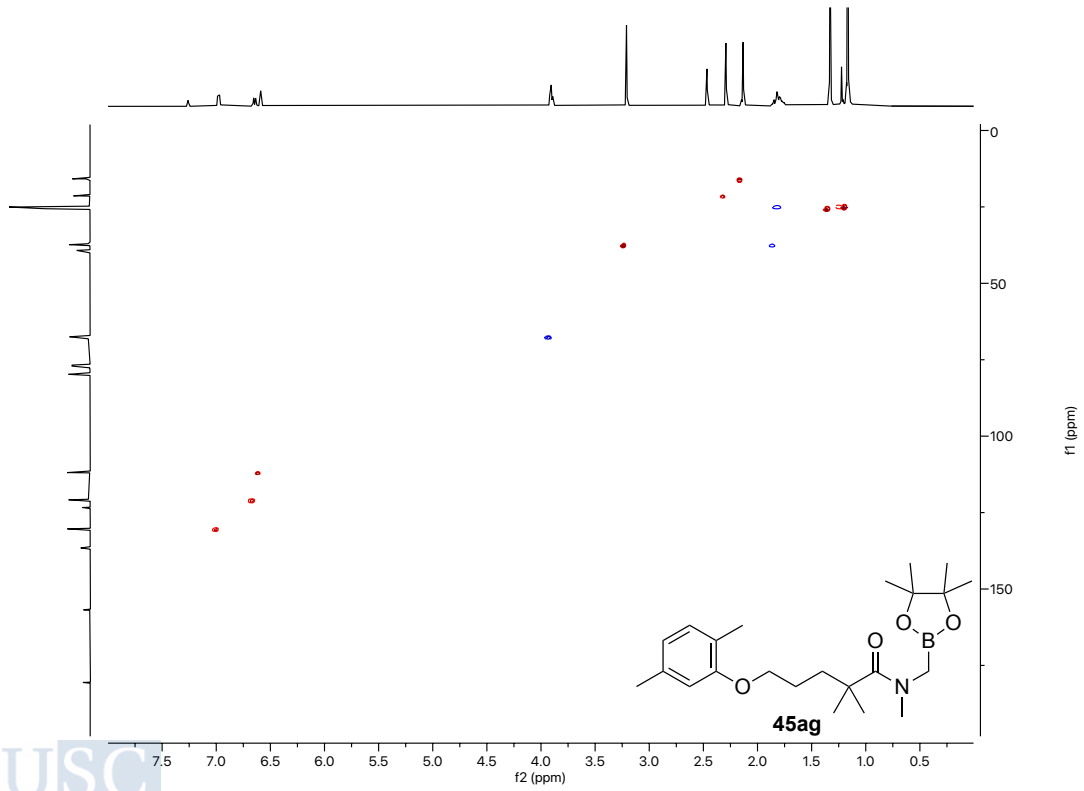

*[13]C NMR (2,5-dimethylphenoxy)-N,2,2-trimethyl-N-((4,4,5,5-tetramethyl-1,3,2-dioxaborolan-2-yl)methyl)pentanamide (45ag)*



*$^{11}$B NMR (2,5-dimethylphenoxy)-N,2,2-trimethyl-N-((4,4,5,5-tetramethyl-1,3,2-dioxaborolan-2-yl)methyl)pentanamide (45ag)*

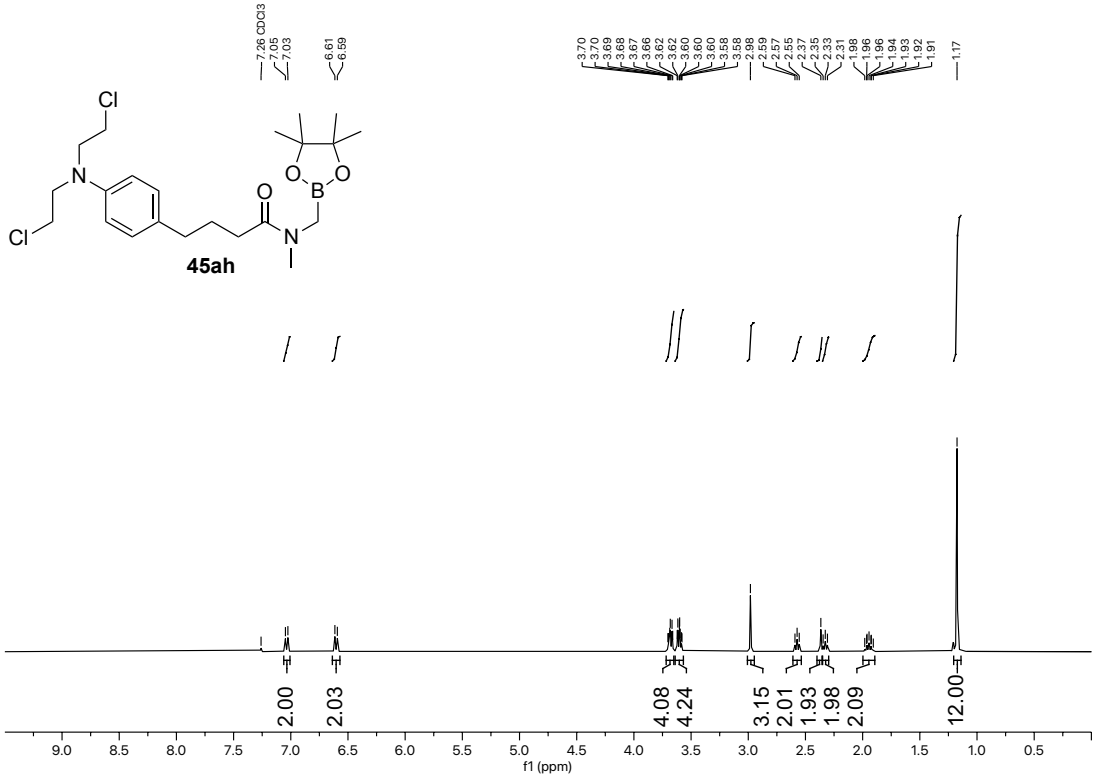



*HSQC NMR (2,5-dimethylphenoxy)-N,2,2-trimethyl-N-((4,4,5,5-tetramethyl-1,3,2-dioxaborolan-2-yl)methyl)pentanamide (45ag)*

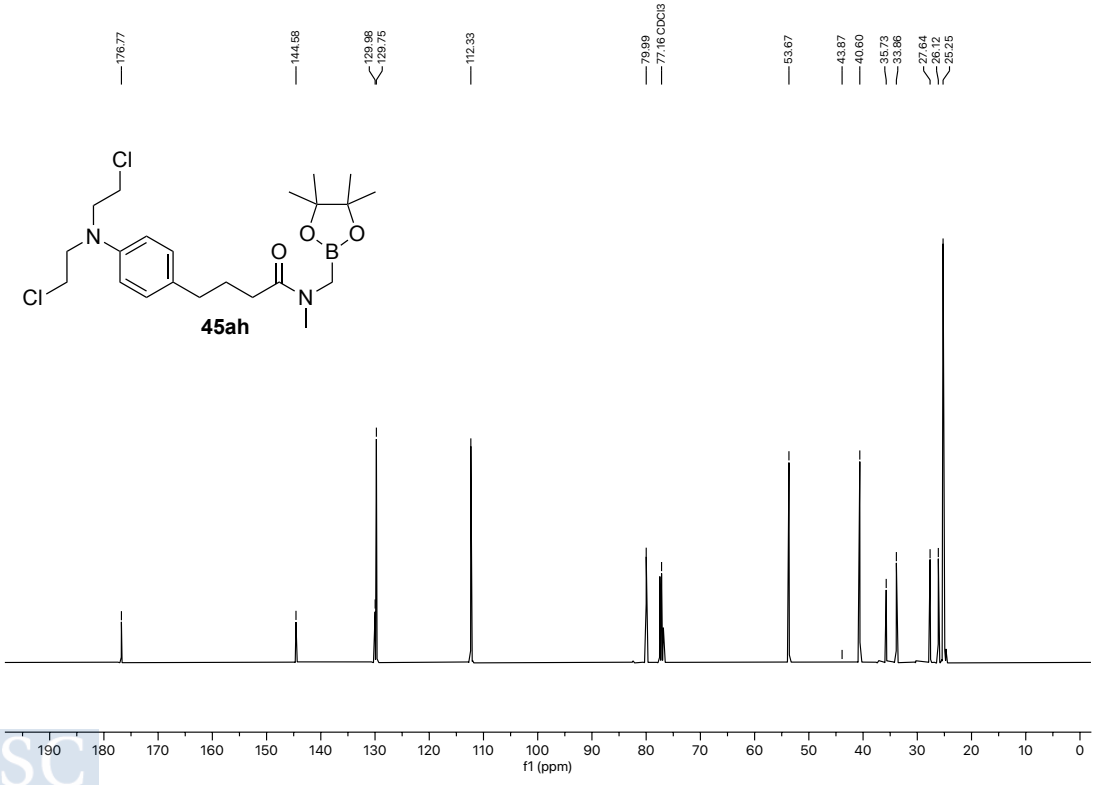



USC UNIVERSIDADE DE SANTIAGO DE COMPOSTELA

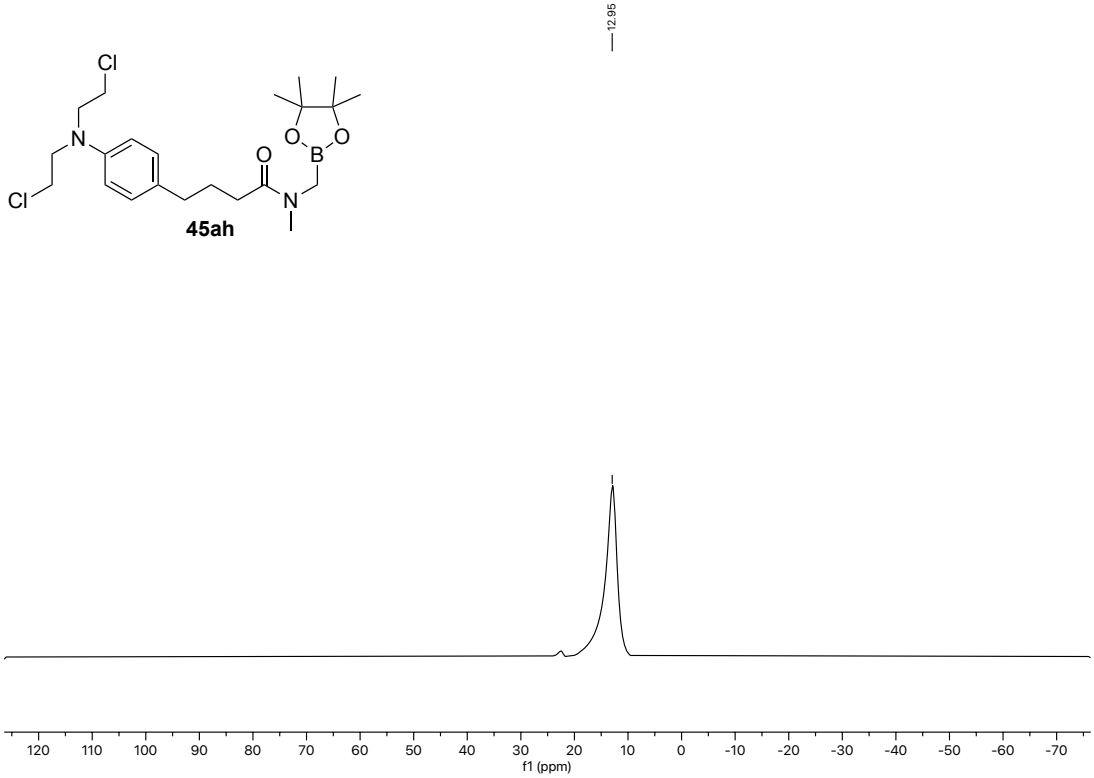
*[1]H NMR 4-(4-(bis(2-chloroethyl)amino)phenyl)-N-methyl-N-((4,4,5,5-tetramethyl-1,3,2-dioxaborolan-2-yl)methyl)butanamide (45ah)*



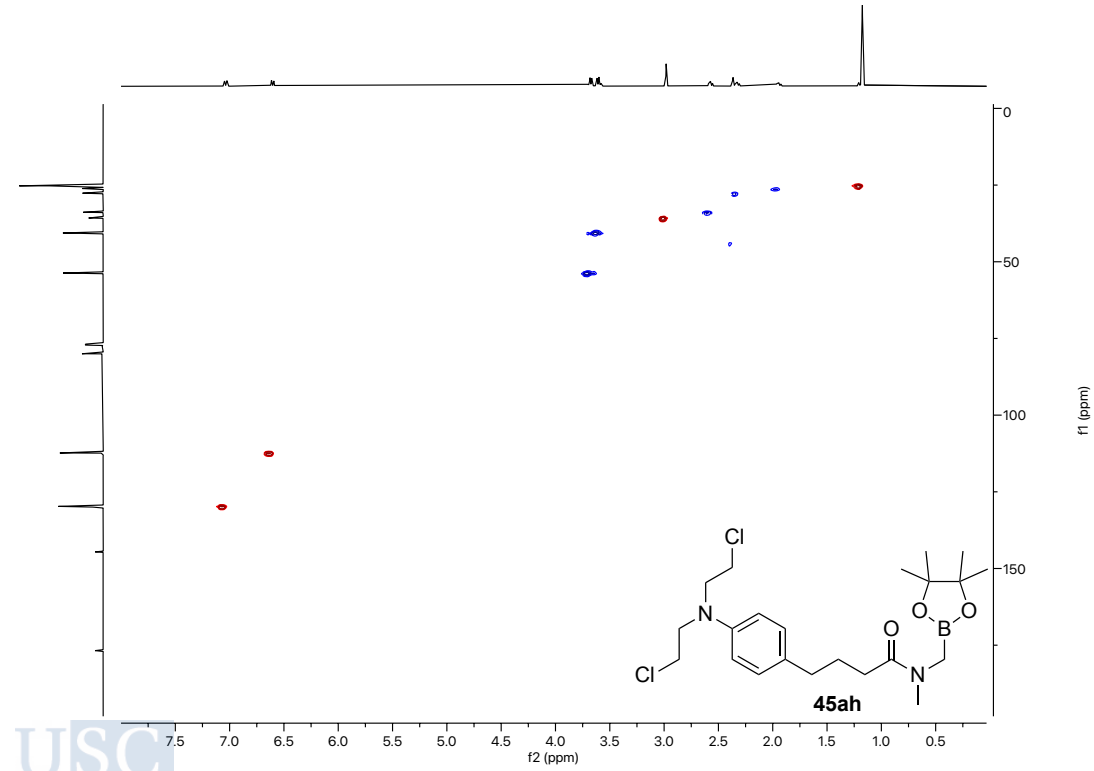

*[13]C NMR 4-(4-(bis(2-chloroethyl)amino)phenyl)-N-methyl-N-((4,4,5,5-tetramethyl-1,3,2-dioxaborolan-2-yl)methyl)butanamide (45ah)*



*$^{11}$B NMR 4-(4-(bis(2-chloroethyl)amino)phenyl)-N-methyl-N-((4,4,5,5-tetramethyl-1,3,2-dioxaborolan-2-yl)methyl)butanamide (45ah)*

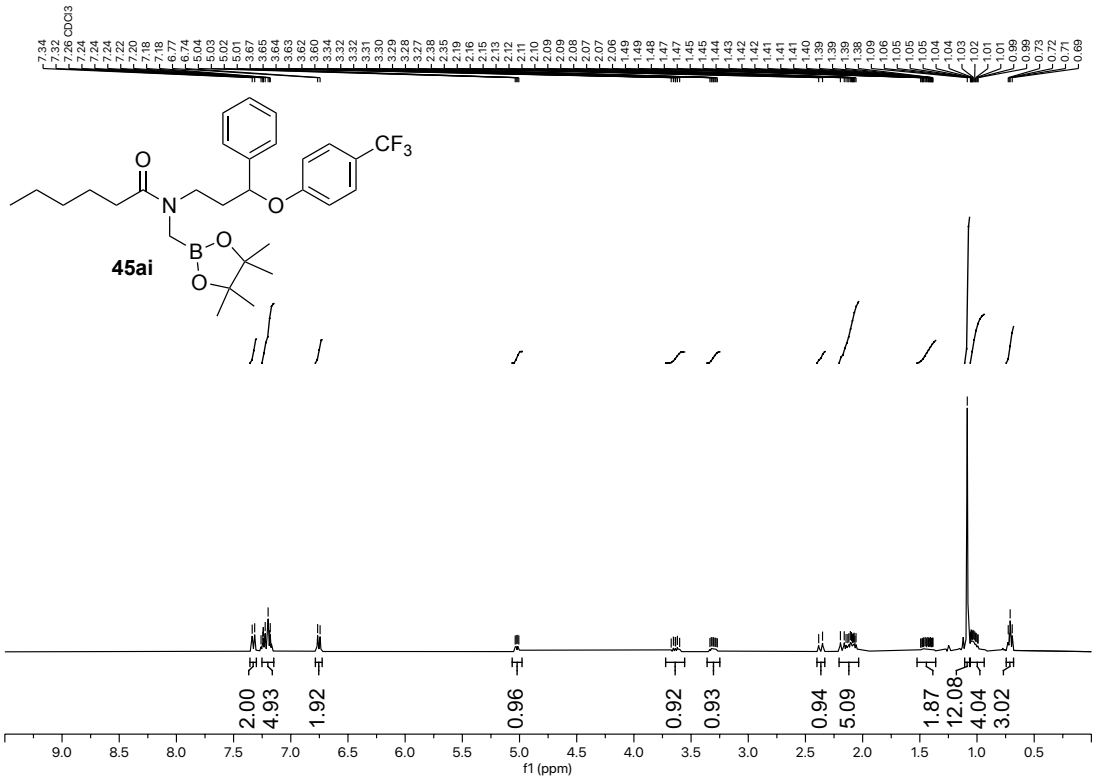



*HSQC NMR 4-(4-(bis(2-chloroethyl)amino)phenyl)-N-methyl-N-((4,4,5,5-tetramethyl-1,3,2-dioxaborolan-2-yl)methyl)butanamide (45ah)*

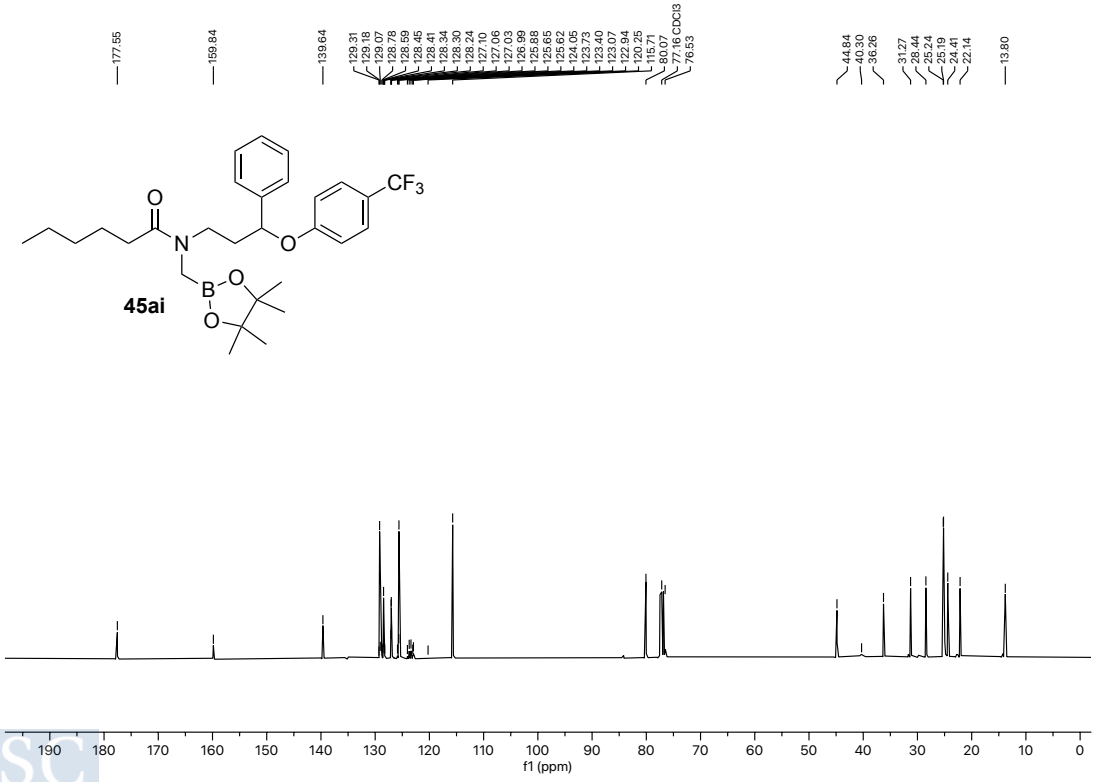



USC UNIVERSIDADE DE SANTIAGO DE COMPOSTELA

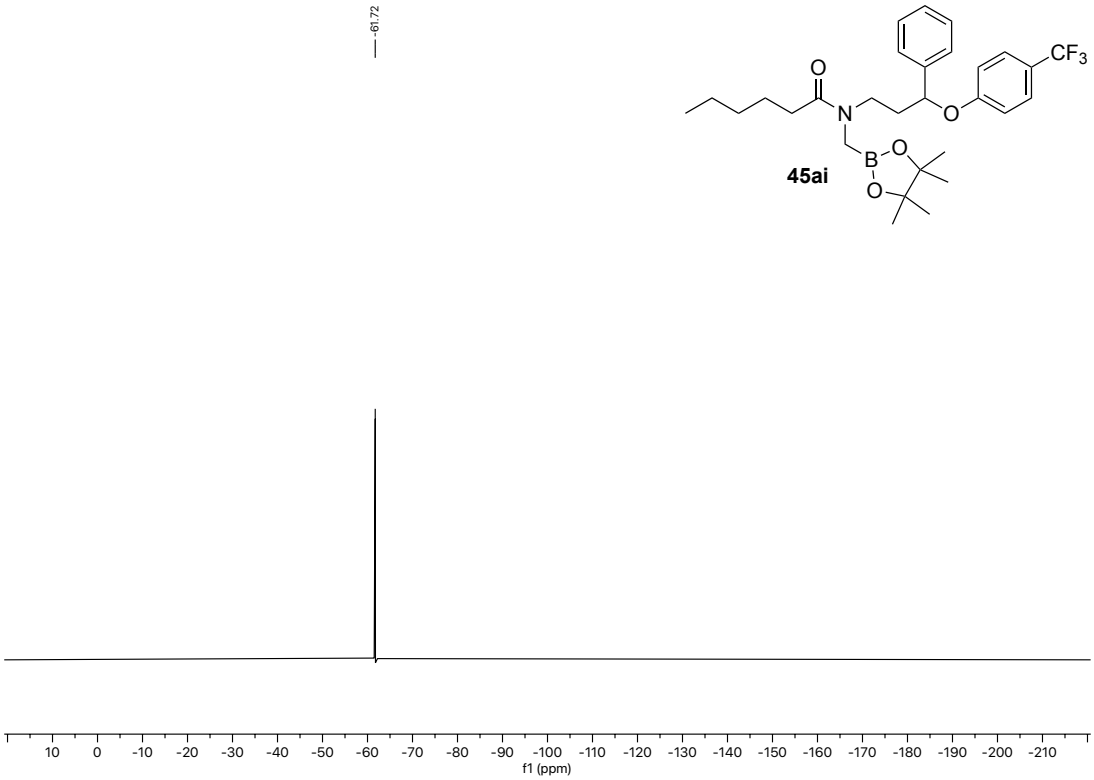
*[1]H NMR N-(3-phenyl-3-(4-(trifluoromethyl)phenoxy)propyl)-N-((4,4,5,5-tetramethyl-1,3,2-dioxaborolan-2-yl)methyl)hexanamide (45ai)*



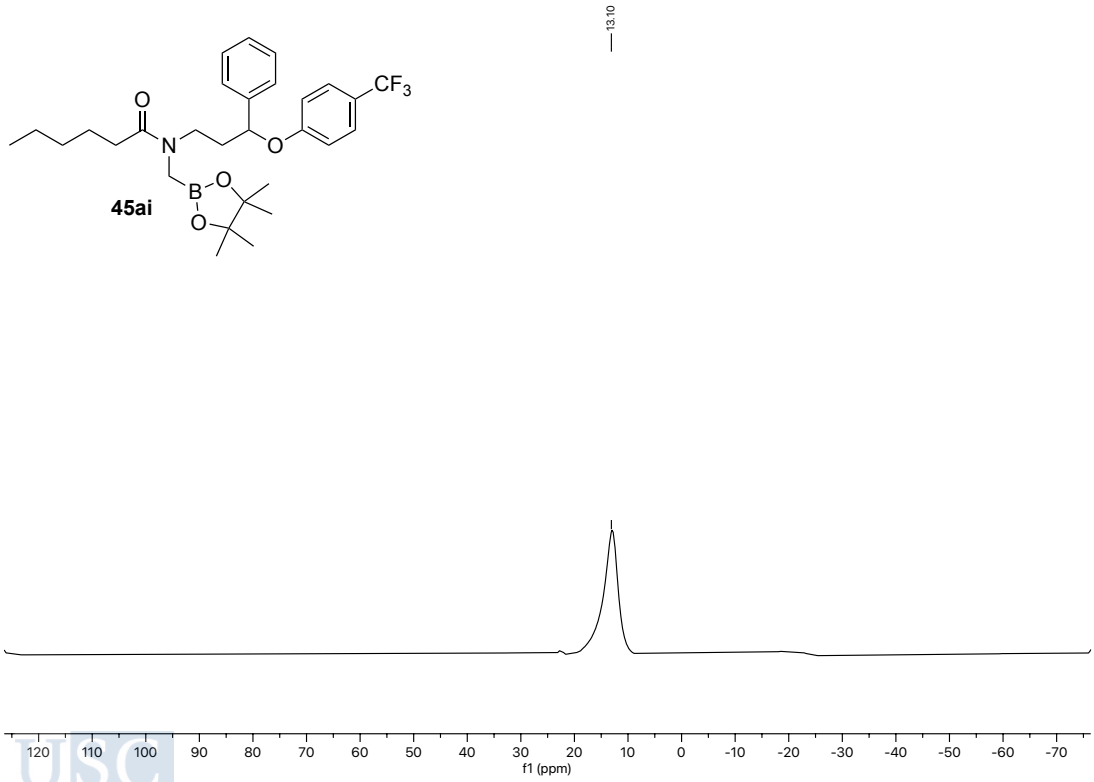

*[13]C NMR N-(3-phenyl-3-(4-(trifluoromethyl)phenoxy)propyl)-N-((4,4,5,5-tetramethyl-1,3,2-dioxaborolan-2-yl)methyl)hexanamide (45ai)*



*[19]F NMR N-(3-phenyl-3-(4-(trifluoromethyl)phenoxy)propyl)-N-((4,4,5,5-tetramethyl-1,3,2-dioxaborolan-2-yl)methyl)hexanamide (45ai)*

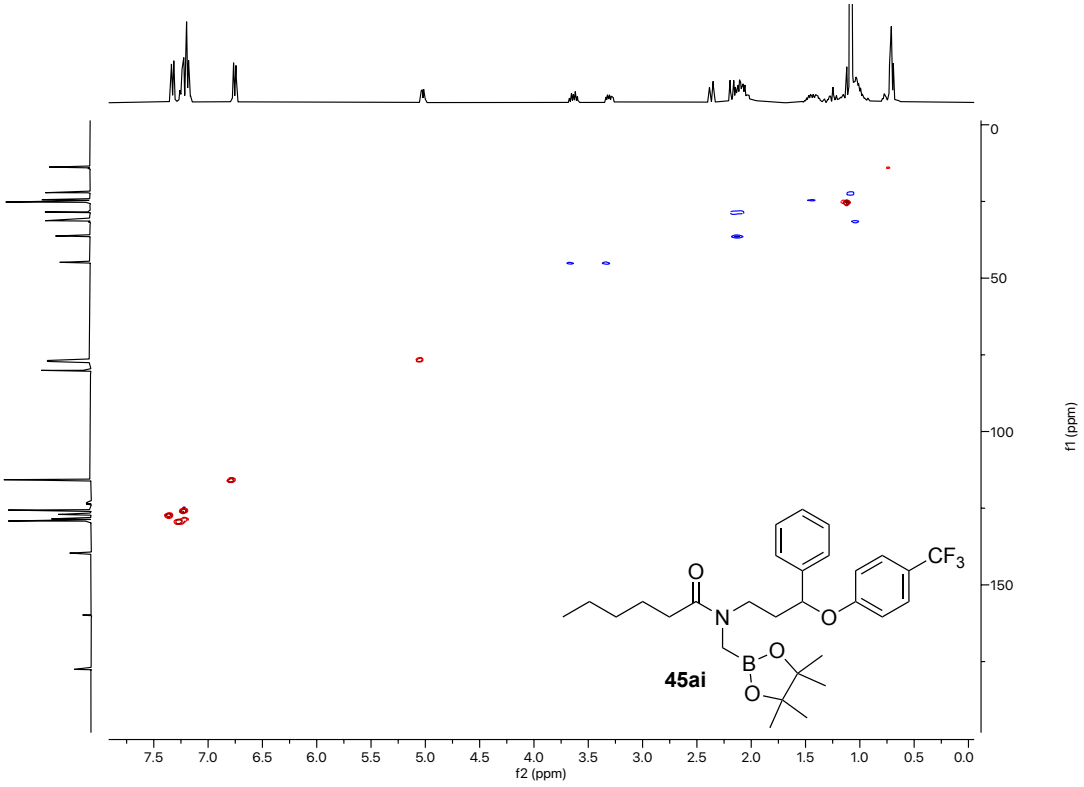



*[11]B NMR N-(3-phenyl-3-(4-(trifluoromethyl)phenoxy)propyl)-N-((4,4,5,5-tetramethyl-1,3,2-dioxaborolan-2-yl)methyl)hexanamide (45ai)*




USC UNIVERSIDADE DE SANTIAGO DE COMPOSTELA

*HSQC NMR N-(3-phenyl-3-(4-(trifluoromethyl)phenoxy)propyl)-N-((4,4,5,5-tetramethyl-1,3,2-dioxaborolan-2-yl)methyl)hexanamide (45ai)*



## 11.2 Annex II: Complete list of NMR spectra

USC
UNIVERSIDADE
DE SANTIAGO
DE COMPOSTELA

# Complete list of NMR spectra

The complete list of NMR spectra can be obtained from the Zenodo repository:

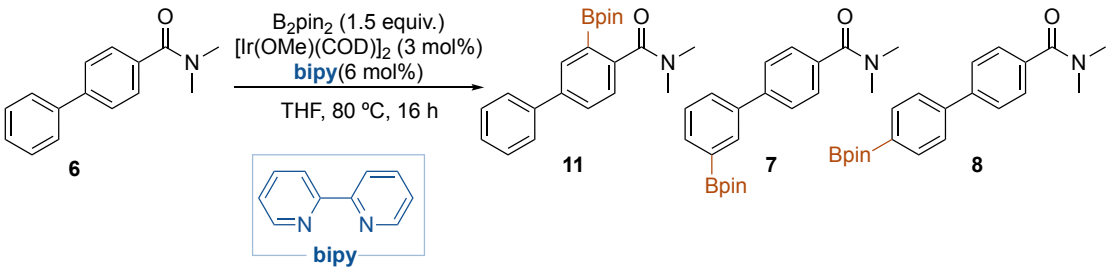
https://doi.org/10.5281/zenodo.14671313

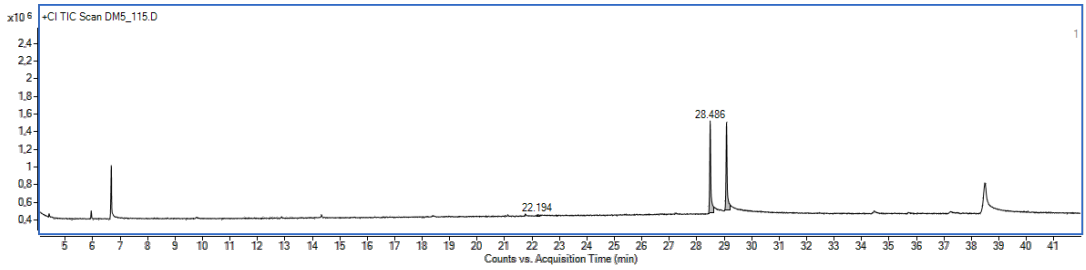
USC UNIVERSIDADE DE SANTIAGO DE COMPOSTELA

## 11.3 Annex III: Selected GC-MS chromatograms

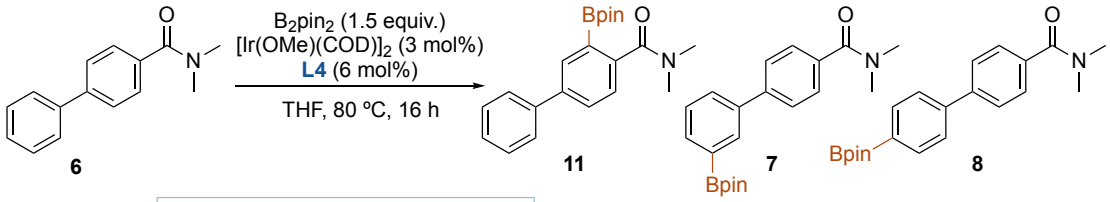
USC
UNIVERSIDADE
DE SANTIAGO
DE COMPOSTELA

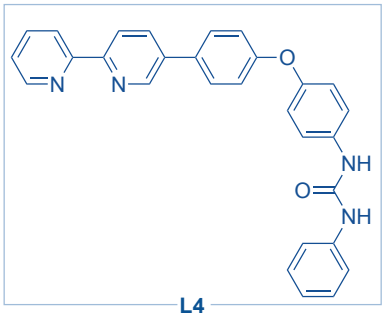
## 11.3.1 Selected GC-MS chromatograms for reactions in section 7.1

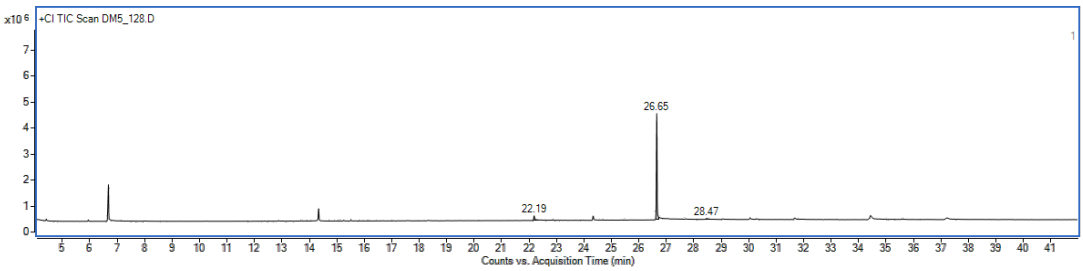


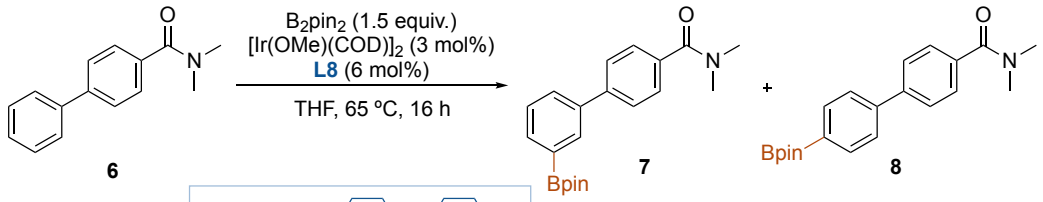

| **RT** (min) | **Area Sum** (%) | **Product** |
|---|---|---|
| 22.19 | 1.5 | 6 |
| 28.49 | 49.5 | 7 |
| 29.08 | 48.9 | 8 |

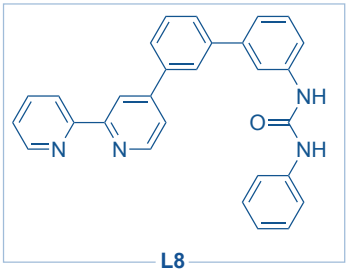


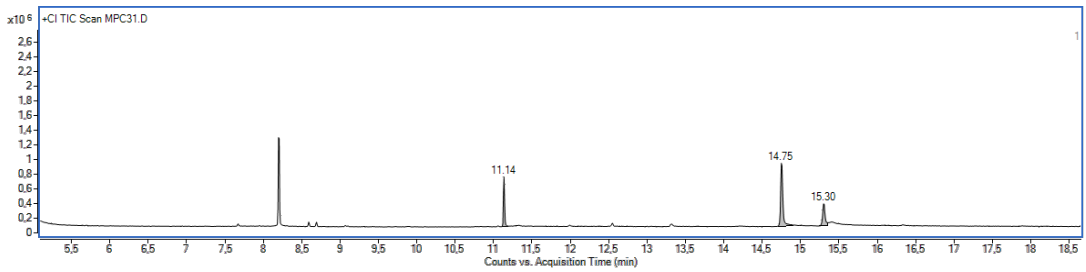



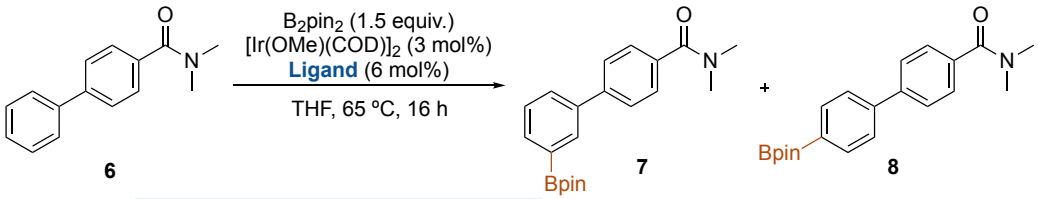

| **RT** (min) | **Area Sum** (%) | **Product** |
|---|---|---|
| 22.19 | 6.2 | 6 |
| 26.65 | 91.9 | 11 |
| 28.47 | 1.9 | 7 |

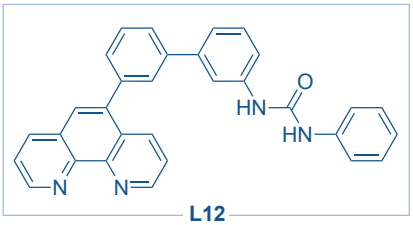


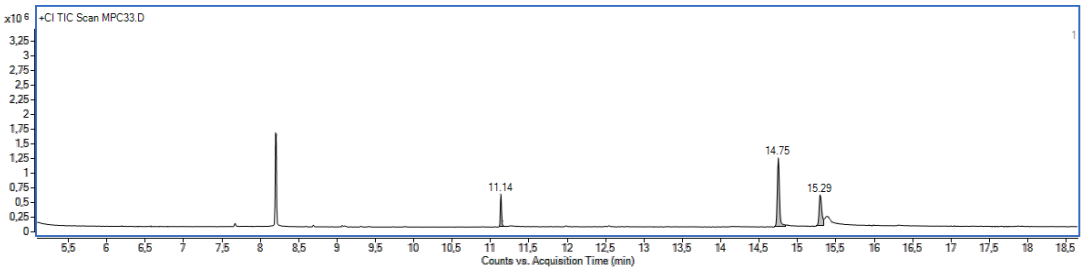




| **RT** (min) | **Area Sum** (%) | **Product** |
|---|---|---|
| 11.14 | 23 | 6 |
| 14.75 | 55.7 | 7 |
| 15.3 | 21.2 | 8 |

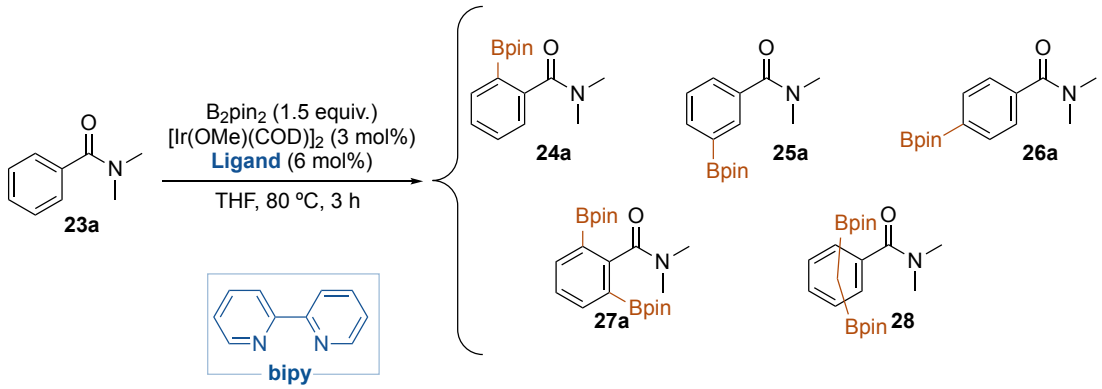


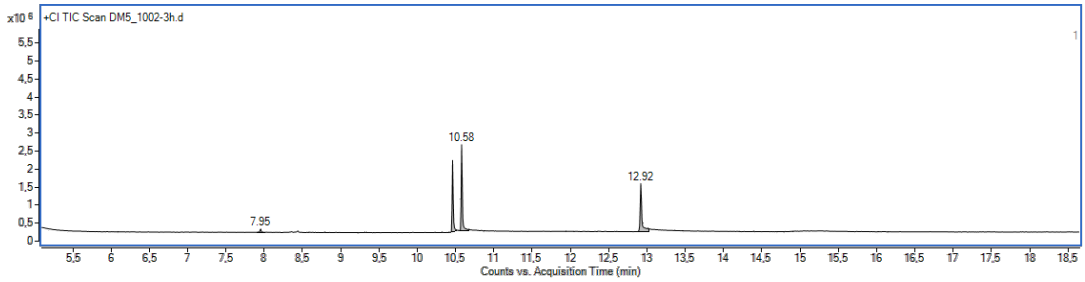



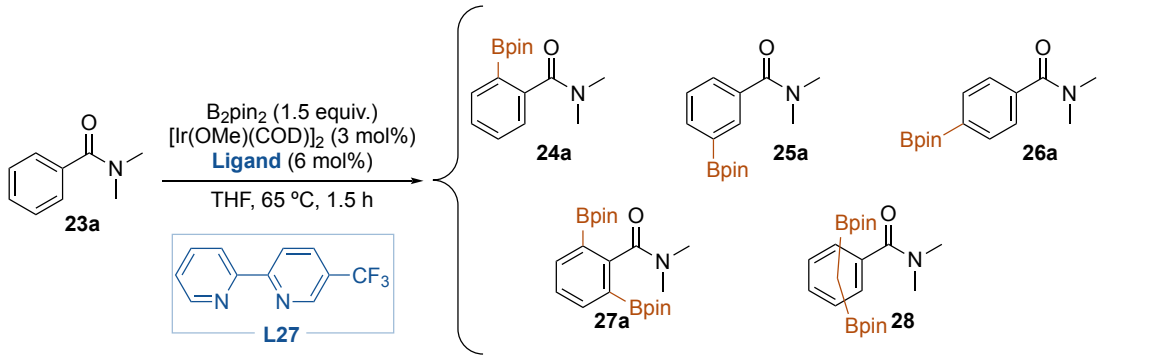

| **RT** (min) | **Area Sum** (%) | **Product** |
|---|---|---|
| 11.14 | 15 | 6 |
| 14.75 | 55.4 | 7 |
| 15.3 | 29.5 | 8 |

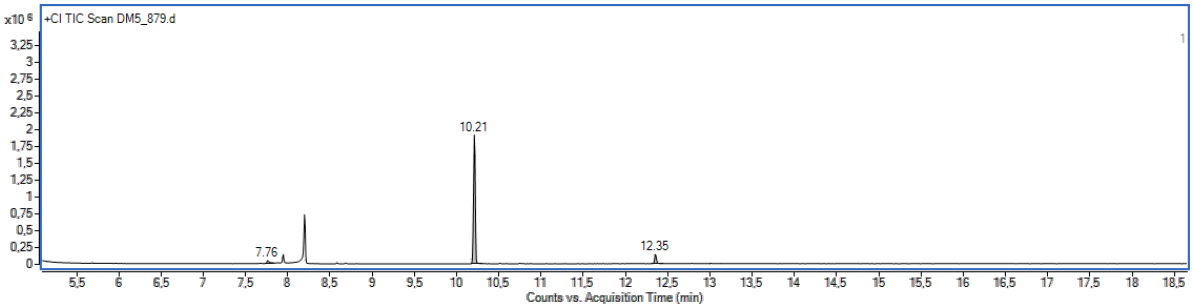
## 11.3.2 Selected GC-MS chromatograms for reactions in section 7.2



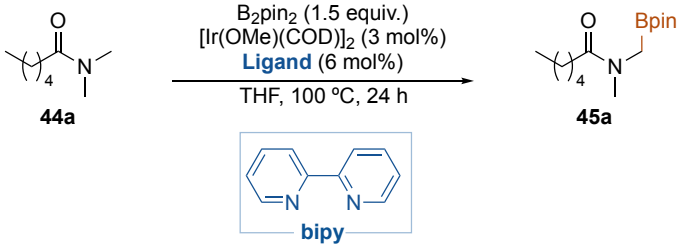

| **RT** (min) | **Area Sum** (%) | **Product** |
|---|---|---|
| 7.9 | 1.9 | 23a |
| 10.4 | 28.5 | 25a |
| 10.5 | 37.5 | 26a |
| 12.9 | 32.1 | 28 |

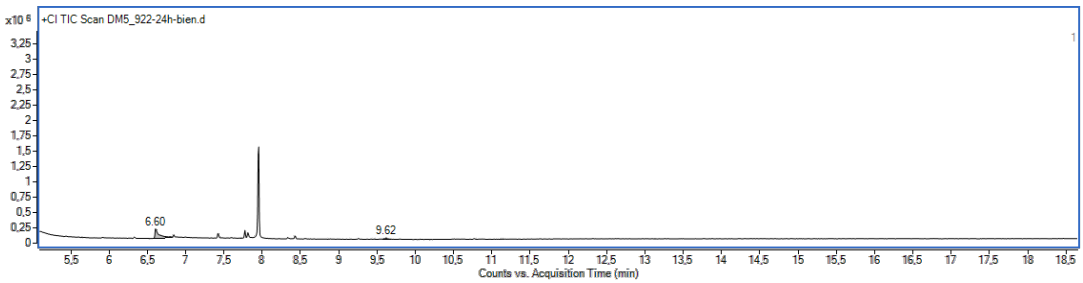


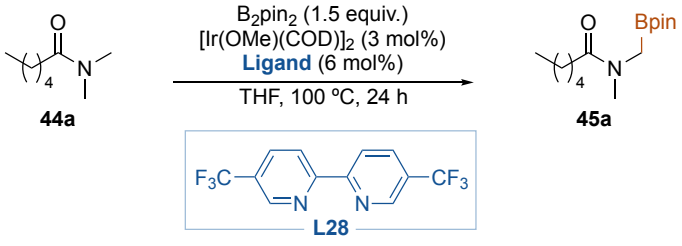

| **RT** (min) | **Area Sum** (%) | **Product** |
|---|---|---|
| 7.7 | 2.9 | 23a |
| 10.2 | 89.9 | 24a |
| 12.3 | 7.1 | 27a |

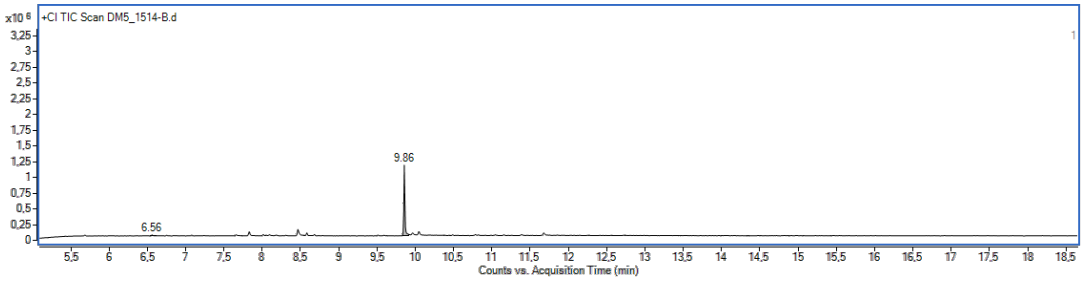
## 11.3.3 Selected GC-MS chromatograms for reactions in section 7.3




| **RT** (min) | **Area Sum** (%) | **Product** |
|---|---|---|
| 6.6 | 91.8 | 44a |
| 9.6 | 8.2 | 45a |




| **RT** (min) | **Area Sum** (%) | **Product** |
|---|---|---|
| 6.6 | 2.1 | 44a |
| 9.6 | 97.8 | 45a |

## 11.4 Annex IV: Exploring 3D models of relevant calculated structures

USC
UNIVERSIDADE
DE SANTIAGO
DE COMPOSTELA

# Exploring 3D models of relevant calculated structures

On the following website and QR code you can find the 3D models of the relevant calculated structures for the different sections of the discussion where you can interact with them (e.g. rotate, distance measurements).

https://danielmarcosatanes.github.io/DMA_thesis-viewer/

## 11.5 Annex V: Relevant calculated structures

USC
UNIVERSIDADE
DE SANTIAGO
DE COMPOSTELA

# Relevant calculated structures

The Gaussian outputs of the relevant calculated structures can be obtained from the Zenodo repository:

https://doi.org/10.5281/zenodo.14671313

USC UNIVERSIDADE DE SANTIAGO DE COMPOSTELA

## 11.6 Annex VI: List of publications

USC
UNIVERSIDADE
DE SANTIAGO
DE COMPOSTELA

# List of publications

Results discussed in section 7.2 have been published in the following journal:

Journal: Angewandte Chemie International Edition

Article title: Iridium-Catalyzed *ortho*-Selective Borylation of Aromatic Amides Enabled by 5-Trifluoromethylated Bipyridine Ligands

Authors: Daniel Marcos-Atanes, Dr. Cristian Vidal, Dr. Claudio D. Navo, Dr. Francesca Peccati, Dr. Gonzalo Jiménez-Osés, Prof. Dr. José L. Mascareñas

Citation: *Angew. Chem. Int. Ed*. **2023**, 62, e202214510*; Angew. Chem*. **2023**, *135*, e202214510.

DOI: 10.1002/anie.202214510

Personal contribution: Experimental procedures, preliminary DFT calculations, results discussion and preliminary manuscript

Journal Information Print Edition ISSN: 1433-7851

Web Edition ISSN: 1521-3773

2 Year Impact Factor 2022-2023: 16.1

Quartile 2023-2024: Q1

USC UNIVERSIDADE DE SANTIAGO DE COMPOSTELA

## 11.7 Annex VII: Copyright permission

USC
UNIVERSIDADE
DE SANTIAGO
DE COMPOSTELA

# Copyright permission



**Iridium-Catalyzed ortho-Selective Borylation of Aromatic Amides Enabled by 5-Trifluoromethylated Bipyridine Ligands**

**Author:** José L. Mascareñas, Gonzalo Jiménez-Osés, Francesca Peccati, et al
**Publication:** Angewandte Chemie International Edition
**Publisher:** John Wiley and Sons
**Date:** Jan 24, 2023

*© 2023 The Authors. Angewandte Chemie International Edition published by Wiley-VCH GmbH*

**Order Completed**

Thank you for your order.

This Agreement between Daniel Marcos Atanes / Universidade de Santiago de COmpostela ("You") and John Wiley and Sons ("John Wiley and Sons") consists of your license details and the terms and conditions provided by John Wiley and Sons and Copyright Clearance Center.

Your confirmation email will contain your order number for future reference.

| | |
|---|---|
| **License Number** | 5915800440403 |
| **License date** | Nov 25, 2024 |

Printable Details

**Licensed Content**

| | |
|---|---|
| **Licensed Content Publisher** | John Wiley and Sons |
| **Licensed Content Publication** | Angewandte Chemie International Edition |
| **Licensed Content Title** | Iridium-Catalyzed ortho-Selective Borylation of Aromatic Amides Enabled by 5-Trifluoromethylated Bipyridine Ligands |
| **Licensed Content Author** | José L. Mascareñas, Gonzalo Jiménez-Osés, Francesca Peccati, et al |
| **Licensed Content Date** | Jan 24, 2023 |
| **Licensed Content Volume** | 62 |
| **Licensed Content Issue** | 18 |
| **Licensed Content Pages** | 10 |

**Order Details**

| | |
|---|---|
| **Type of use** | Dissertation/Thesis |
| **Requestor type** | Author of this Wiley article |
| **Format** | Print and electronic |
| **Portion** | Full article |
| **Will you be translating?** | No |







This Ph.D. thesis explores the role of supramolecular and non-covalent interactions in achieving regioselective C–H borylations within iridium-catalyzed systems.

Initially, a series of bifunctional ligands were designed and synthesized to investigate the potential of hydrogen bonding in directing borylation to distal positions on biphenyl systems. A significant breakthrough was achieved with the development of bipyridine ligands featuring $CF_3$ groups at the 5-position. These ligands induced a remarkable shift in regioselectivity, enabling ortho borylation of benzamides and highly selective N-methyl borylation of alkyl methylamides.

Experimental findings, supported by DFT calculations, underscored the critical role of non-covalent interactions in guiding and favoring the observed reactivity and selectivity.